WOODHEAD PUBLISHING SERIES IN MATERIALS

# ADVANCED POLYMER NANOCOMPOSITES

## SCIENCE, TECHNOLOGY AND APPLICATIONS

Edited by
MD ENAMUL HOQUE
KUMAR RAMAR
AHMED SHARIF

ELSEVIER

# Advanced Polymer Nanocomposites

Woodhead Publishing Series in Materials

# Advanced Polymer Nanocomposites

## Science, Technology and Applications

*Edited by*

***Md Enamul Hoque***

***Kumar Ramar***

***Ahmed Sharif***

ELSEVIER

WP
WOODHEAD
PUBLISHING
An imprint of Elsevier

Woodhead Publishing is an imprint of Elsevier
50 Hampshire Street, 5th Floor, Cambridge, MA 02139, United States
The Boulevard, Langford Lane, Kidlington, OX5 1GB, United Kingdom



**Notices**

Knowledge and best practice in this field are constantly changing. As new research and experience broaden our understanding, changes in research methods, professional practices, or medical treatment may become necessary.

Practitioners and researchers must always rely on their own experience and knowledge in evaluating and using any information, methods, compounds, or experiments described herein. In using such information or methods they should be mindful of their own safety and the safety of others, including parties for whom they have a professional responsibility.

To the fullest extent of the law, neither the Publisher nor the authors, contributors, or editors, assume any liability for any injury and/or damage to persons or property as a matter of products liability, negligence or otherwise, or from any use or operation of any methods, products, instructions, or ideas contained in the material herein.

ISBN: 978-0-12-824492-0 (print)
ISBN: 978-0-323-85287-6 (online)



*Publisher:* Matthew Deans
*Acquisitions Editor:* Gwen Jones
*Editorial Project Manager:* Joshua Mearns
*Production Project Manager:* Surya Narayanan Jayachandran
*Cover Designer:* Matthew Limbert

Typeset by MPS Limited, Chennai, India


# Contents



# List of contributors

**Md. Rubel Alam** Department of Knitwear Manufacturing and Technology, BGMEA University of Fashion and Technology, Dhaka, Bangladesh

**M. Azam Ali** Centre for Bioengineering and Nanomedicine, Faculty of Dentistry, University of Otago, Dunedin, New Zealand

**Kazi Faiza Amin** Department of Materials and Metallurgical Engineering, Bangladesh University of Engineering and Technology (BUET), Dhaka, Bangladesh

**Md Arifuzzaman** Department of Civil and Environmental Engineering, King Faisal University, Al Hofuf, Saudi Arabia

**Asrafuzzaman** Department of Materials Science and Engineering, Rajshahi University of Engineering & Technology (RUET), Rajshahi, Bangladesh

**Yashdi Saif Autul** Department of Mechanical Engineering, Military Institute of Science and Technology (MIST), Dhaka, Bangladesh

**Sitesh C. Bachar** Department of Pharmacy, Faculty of Pharmacy, University of Dhaka, Dhaka, Bangladesh

**Nitesh Dhar Badgayan** Department of Mechanical Engineering, Centurion University of Technology and Management, Bhubaneswar, Odisha, India

**Rachid Bouhfid** Moroccan Foundation for Advanced Science, Innovation and Research (MAScIR), Institute of Nanomaterials and Nanotechnology (NANOTECH), Laboratory of Polymer Processing, Rabat, Morocco

**T. Chai Hua** Institute of Tropical Forestry and Forest Products (INTROP), Serdang, Selangor, Malaysia

**Muhammad Ifaz Shahriar Chowdhury** Department of Mechanical Engineering, Military Institute of Science and Technology (MIST), Dhaka, Bangladesh

**Hamid Essabir** Moroccan Foundation for Advanced Science, Innovation and Research (MAScIR), Institute of Nanomaterials and Nanotechnology (NANOTECH), Laboratory of Polymer Processing, Rabat, Morocco; Mechanic Materials and Composites (MMC), Laboratory of Energy Engineering, Materials and Systems, National School of Applied Sciences of Agadir, Ibn Zohr University, Morocco

**B. Farid** Department of Aerospace Engineering, Faculty of Engineering, Serdang, Selangor, Malaysia

**Syed Waheedullah Ghori** Mechanical Engineering Department, College of Engineering, King Khalid University, Abha, Asir, Saudi Arabia

**Maree L. Gould** Centre for Bioengineering and Nanomedicine, Faculty of Dentistry, University of Otago, Dunedin, New Zealand

**Parul Gupta** Global Institute of Technology & Management, Gurgoan, Haryana, India

**Md Enamul Hoque** Department of Biomedical Engineering, Military Institute of Science and Technology (MIST), Dhaka, Bangladesh

**Habibul Islam** Department of Biomedical Engineering, Military Institute of Science and Technology (MIST), Dhaka, Bangladesh

**Tarikul Islam** Department of Textile Engineering, Jashore University of Science and Technology, Jashore, Bangladesh

**V.M. Ravindra Kumar** Department of Mechanical Engineering, Vellore Institute of Technology - Andhra Pradesh (VIT-AP University), Amaravati, Andhra Pradesh, India

**Kishor Mazumder** Department of Pharmacy, Jashore University of Science and Technology, Jashore, Bangladesh; School of Optometry and Vision Science, UNSW Medicine, University of New South Wales (UNSW), Sydney, NSW, Australia; School of Biomedical Sciences and Graham Centre for Agricultural Innovation, Charles Sturt University, Wagga Wagga, NSW, Australia

**H. Mohit** Department of Mechanical Engineering, Alliance College of Engineering and Design, Alliance University, Karnataka, India

**Ayeman Mazdi Nahin** Department of Materials Science and Engineering, Rajshahi University of Engineering & Technology (RUET), Rajshahi, Bangladesh

**B. Nivedha** Department of Physics, National Institute of Technology, Tiruchirappalli, Tamil Nadu, India

**M. Norkhairunnisa** Institute of Nanoscience and Nanotechnology (ION2), Universiti Putra Malaysia, Serdang, Serdang, Selangor, Malaysia; Department of Aerospace Engineering, Faculty of Engineering, Serdang, Selangor, Malaysia; Aerospace Malaysia Research Center (AMRC), Universiti Putra Malaysia, Serdang, Selangor, Malaysia

**Swapnita Patra** Department of Chemistry, Veer Surendra Sai University of Technology, Burla, Sambalpur, Odisha, India

**Abou el kacem Qaiss** Moroccan Foundation for Advanced Science, Innovation and Research (MAScIR), Institute of Nanomaterials and Nanotechnology (NANOTECH), Laboratory of Polymer Processing, Rabat, Morocco

**Mamun Rabbani** Department of Biomedical Physics and Technology, University of Dhaka, Dhaka, Bangladesh

**Sazedur Rahman** Department of Mechanical and Production Engineering, Ahsanullah University of Science and Technology (AUST), Dhaka, Bangladesh

**Marya Raji** Moroccan Foundation for Advanced Science, Innovation and Research (MAScIR), Institute of Nanomaterials and Nanotechnology (NANOTECH), Laboratory of Polymer Processing, Rabat, Morocco

**Pawan Kumar Rakesh** Department of Mechanical Engineering, National Institute of Technology Uttarakhand, Srinagar Garhwal, Uttarakhand, India

**P. Ramesh** Department of Production Engineering, National Institute of Technology, Tiruchirappalli, Tamil Nadu, India

**Adib Bin Rashid** Department of Industrial and Production Engineering, Military Institute of Science and Technology, Dhaka, Bangladesh

**Md. Reazuddin Repon** ZR Research Institute for Advanced Materials, Sherpur, Bangladesh; Department of Textile Engineering, Khwaja Yunus Ali University, Sirajganj, Bangladesh; Department of Production Engineering, Faculty of Mechanical Engineering and Design, Kaunas University of Technology, Kaunas, Lithuania

**Oishy Roy** Department of Materials and Metallurgical Engineering, Bangladesh University of Engineering and Technology, Dhaka, Bangladesh

**Santosh Kumar Sahu** Department of Mechanical Engineering, Amrita School of Engineering, Amrita Vishwa Vidyapeetham, Bengaluru, Karnataka, India

**M.R. Sanjay** Natural Composites Research Group, Department of Materials and Production Engineering, The Siridhorn International Thai German Graduate School of Engineering, King Mongkut's University of Technology North Bangkok, Bangkok, Thailand

**Carlo Santulli** School of Science and Technology, University of Camerino, Camerino, Italy

**S. Krishna Satya** Department of Mechanical Engineering, Vellore Institute of Technology - Andhra Pradesh (VIT-AP University), Amaravati, Andhra Pradesh, India

**Aungkan Sen** Department of Chemical Engineering and Materials Science, Michigan State University, East Lansing, MI, United States

**Ahmed Sharif** Department of Materials and Metallurgical Engineering, Bangladesh University of Engineering and Technology, Dhaka, Bangladesh

**Suchart Siengchin** Natural Composites Research Group, Department of Materials and Production Engineering, The Siridhorn International Thai German Graduate School of Engineering, King Mongkut's University of Technology North Bangkok, Bangkok, Thailand

**P.S. Rama Sreekanth** Department of Mechanical Engineering, Vellore Institute of Technology - Andhra Pradesh (VIT-AP University), Amaravati, Andhra Pradesh, India

**P. Sri Ram Murthy** Department of Mechanical Engineering, Vellore Institute of Technology - Andhra Pradesh (VIT-AP University), Amaravati, Andhra Pradesh, India

**N.S. Suresh** Department of Electrical and Electronics Engineering, St. Joseph Engineering College, Mangalore, Karnataka, India

**Sarat K. Swain** Department of Chemistry, Veer Surendra Sai University of Technology, Burla, Sambalpur, Odisha, India

**Vineet Tirth** Mechanical Engineering Department, College of Engineering, King Khalid University, Abha, Asir, Saudi Arabia; Research Center for Advanced Materials Science (RCAMS), King Khalid University, Abha, Asir, Saudi Arabia

**Md. Sharjis Ibne Wadud** Department of Biomedical Engineering, Military Institute of Science and Technology (MIST), Dhaka, Bangladesh

**Ch. Sridhar Yesaswi** Department of Mechanical Engineering, Vellore Institute of Technology - Andhra Pradesh (VIT-AP University), Amaravati, Andhra Pradesh, India

# Preface

Polymer is one of the main commercial products that have the greatest impact on the global market. It can be easily synthesized to produce smart materials and the production cost is also lower. However, the polymer is weak in properties. The incorporation of nanomaterials can improve the polymer properties such as tensile strength, impact and scratch resistance, electrical and thermal conductivity, thermal stability, and fire resistance. Polymer nanocomposite is a multiphase solid polymeric material comprising a polymer matrix and a dispersive phase of nanofillers with one, two, or three dimensions of less than 100 nm in scale. The nanocomposites are finding growing applications in industries ranging from sports and leisure to biological, renewable energy, electronics, marine, automotive, and defense. The research developments in polymer nanocomposites for industrial applications are increasing rapidly both in scientific advancement and industrial innovations due to the concern of eco-friendliness, recyclability, and sustainability. Thus it is necessary to focus on exploring the different aspects of polymer nanocomposites.

This book contains fundamental knowledge and recent advances in the area of science, technology, and applications of advanced polymer nanocomposites. Through contributions of eminent editors and recognized authors from around the world, this book should be vital source material for academics, practitioners, and researchers both in academia and industry. It covers a wide range of topics on properties of advanced polymer nanocomposites such as rheological, biological, electrical, optical, and thermal; it also covers versatile applications of advanced polymer nanocomposites, for example, automotive, building, biomedical, packaging, defense, drug distribution, microelectronic devices, adhesives and coatings, energy, and textiles. Lastly, it concludes with the scopes, challenges, and recycling of the advanced polymer nanocomposites.

The editors are sincerely grateful to the authors worldwide including Australia, Bangladesh, India, Italy, Lithuania, Malaysia, Morocco, New Zealand, Saudi Arabia, Thailand, and United States for their scholarly contribution. Last but not least, the editors like to thank the Elsevier team for their persistent assistance and cooperation at every stage of this book production.

**Md Enamul Hoque**
**Kumar Ramar**
**Ahmed Sharif**
**Editors**

# Section 1:
# Fundamentals, processing and properties

# Fundamentals of polymer nanocomposites

1

*Vineet Tirth*[1,2], *Syed Waheedullah Ghori*[1] *and Parul Gupta*[3]
[1]Mechanical Engineering Department, College of Engineering, King Khalid University, Abha, Asir, Saudi Arabia
[2]Research Center for Advanced Materials Science (RCAMS), King Khalid University, Abha, Asir, Saudi Arabia
[3]Global Institute of Technology & Management, Gurgoan, Haryana, India

## 1.1 Introduction

### *1.1.1 Polymers*

Polymers are the organic materials favored by researchers and industries due to their low-energy processing, ease of handling, high strength-to-weight ratio, and potential recycling. The term "polymer" originated from a combination of "poly" meaning many and "mer" meaning bonds. Hence, the organic compounds comprising a large number of bonds centered around carbon atoms emerged as polymers. Based on their structure, the polymers may be classified into three broad classes: linear, branched, and cross-linked, depicted in Fig. 1.1.

The linear polymer, shown in Fig. 1.2A, consists of a long chain of linear bonds between carbon atoms and the hydrogen and oxygen atoms or the methyl ($CH_3$) group primarily attached to the C-atoms. Branched polymers, shown in Fig. 1.2B, have transverse branches of C-atoms in addition to the linear ones. The structure expands in two dimensions. Cross-linked polymers, shown in Fig. 1.2C, form bonds in three dimensions, primarily the $C_6H_5$ group.

Polymers are broadly classified into three classes, depicted in Fig. 1.3, i.e., thermoplastics (TP), elastomers, and thermosets (TS). The TP have a linear or branched structure. The word "thermo" means heat, and "plastic" indicates the permanent deformation under heat. Examples of TP include day-to-day plastic materials such as bottles, polybags, disposable bags, and packing sheets. They have a low tolerance to temperature, and plastic deformation (flow) initiates as the temperature is

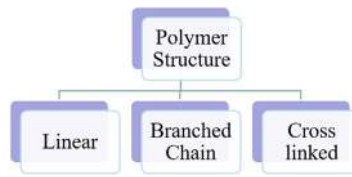


**Figure 1.1** Classification of polymers based on molecular structure.

**Advanced Polymer Nanocomposites. DOI: https://doi.org/10.1016/B978-0-12-824492-0.00017-9**

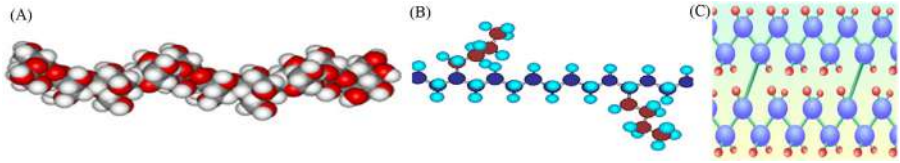


**Figure 1.2** Structure of polymers: (A) linear, (B) branched, (C) cross-linked (open source).

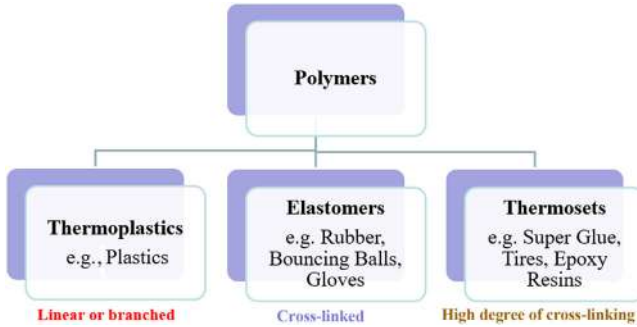


**Figure 1.3** Types of polymers.

increased. The elastomers are branched and have some degree of cross-linked structures, which makes them highly elastic and stretchable; examples include bouncing balls, surgical gloves, and rubber. The third class of polymers is TS. As the name suggests, "thermo" means heat, and "set" means settlement or hardness.

Contrary to TP, the TS start polymerization and a high degree of cross-linking in response to the heat, making them harder and stiffer. A few examples of TS include superglue, epoxy resins, and tires. The TP are completely recyclable while the TS are not. The recyclability of elastomers lies in between the two.

Fig. 1.4 summarizes the most common manufacturing processes for polymers and raw materials. Extrusion requires TP or TS as raw materials, and long and continuous products are manufactured from this process, for example, rods, bars, and channels of the different cross sections. Primarily, TP are the widely used raw materials for extrusion. The injection molding process employs both TP and elastomers as raw materials in a closed mold process. It is suitable for the mass production of limited-sized products, for example, plastic parts such as electric plugs, pens, bottle caps, mobile and laptop, parts of appliances, etc. The blow molding produces hollow products and has a large volume and surface area by inflating air during molding, hence, the term "blow molding" comes. Examples of blow-molded products include tanks, plastic bottles, and jars. The casting process provides for the production of complex shapes and profiles in open or closed molds. The parts for machines, housings, casings, etc. which contain seats, sockets, fixtures, and assembly with other components are produced by casting. Thermoforming is a secondary manufacturing process that shapes the products from a plastic sheet by heating it and giving it shape by the pressure of air or vacuum. Products such as cups, glasses, and plates are produced by thermoforming.

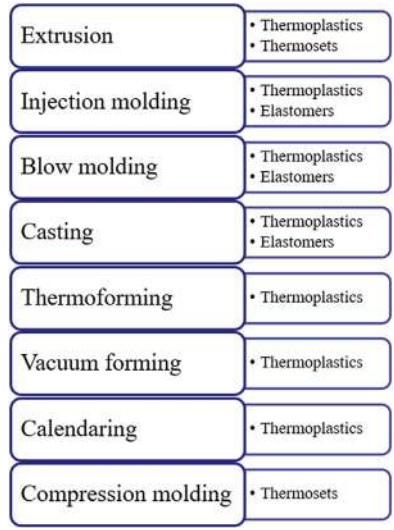


**Figure 1.4** Manufacturing processes of polymers and raw materials used.

This process provides an option to engrave text, images, grooves, etc. into the product using a preform over which the heated plastic sheet takes shape. Thermoforming includes a great deal of wastage as some part of the sheet has to be clamped and cut away during finishing. The vacuum forming process is also a secondary forming process where a plastic sheet is given the desired shape by heating it and then creating a vacuum to provide it with the desired shape using a preform. Vacuum forming is used to produce very thin cross-sectional products such as packing materials for machine parts. Calendaring is a continuous manufacturing process in which a continuous supply of semisolid plastic is maintained through extrusion or injection molding. This semisolid plastic material is rolled between rollers to produce sheet stock of desired thickness and size, for example, curtains, polyvinyl chloride flooring, sheets for inflatable toys, etc. The compression molding process employs TS materials in the form of powder or resin. The raw material is given a shape using a closed die, and then it is compressed under pressure and heated simultaneously until it becomes stiff. High-strength components such as automobile bumpers, bonnets, machine parts, and fixtures are made by compression molding.

### *1.1.2 Polymer matrix composites*

To enhance the properties of the materials and impart contrasting features to a material, composites are made. Polymer matrix composites (PMCs) include a more extensive constituent called base or polymer added with reinforcements in the form of particles, fibers, and whiskers in relatively smaller concentrations. A typical example of PMC is fiber-reinforced plastic, a commonly used material for making lightweight and high-strength structural and storage products. PMC exhibits

enhancement of tensile strength, corrosion resistance, fracture toughness, coefficient of thermal expansion, and thermal resistance. Several factors that affect the properties of PMC include interfacial adhesion, which should be strong irrespective of the shape and size of the reinforcement. The shape, size, and orientation of the reinforcements play a significant role in the isotropy and homogeneity of the PMC. The shape of the reinforcement may be angular, cubic, spherical, platelet, or random. The orientation may be aligned, longitudinal, transverse, inclined at a specific angle, and arbitrary. The size may vary from microns to several centimeters. The next important aspect is the property of the matrix itself. The matrix is expected to accommodate the reinforcement favorably, providing appropriate space and adhesion. TP and TS are two primary matrix materials out of which TS are easy to process. The matrix's significant properties that affect the overall properties of the PMC include cost, chemical resistance, and stability, ease of handling and processing, low specific gravity, high strength, high elastic modulus, and high thermal stability and operating temperature.

The TP exhibit strong intramolecular bonds but weak intermolecular bonds. They have low thermal stability and low tolerance to temperature and pressure. TS exhibit strong intermolecular covalent bonds with a network or cross-linking. Fig. 1.5 summarizes the standard processes used for making PMC. Large products such as boat hulls, domes, tanks, and containers are made by the open mold processes. Hand lay-up is a primitive unmechanized process where polymer and reinforcement layers are layered up in an open mold. This process can be mechanized

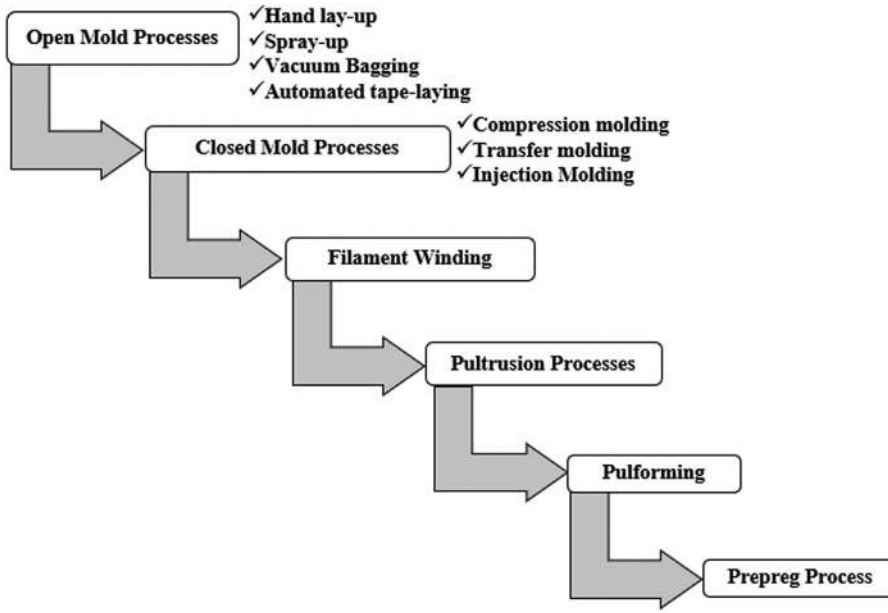


**Figure 1.5** Manufacturing processes of polymer matrix composites.

to reduce variability and increase speed by using the spray-up method. Vacuum bagging is used to develop laminates. The automated tape-laying process is used to produce large flat parts such as the wings of an aircraft [1].

Closed mold processes produce distinct components of restricted size. The compression molding is used to develop high-strength parts by compressing a mixture of polymer matrix and reinforcement, called charge, in a closed mold. The transfer molding is a process executed in two steps. The uncured polymer is forced from one part of the mold (pot) into the other part (cavity) under pressure. This is done by indirectly applying the pressure and filling the cavity to preserve the intrinsic and complex shape or profile of the product. The injection molding process to develop polymers is extended and modified to develop the PMC by mixing the reinforcement during the melt supply for the injector or forcing the melt from the injector into a preform of reinforcement placed in a closed mold. The filament winding process is widely preferred and more reliable in developing PMC with TS resin as matrix and fibers are reinforcement. The products made from filament winding have high strength, and the process can be accurately controlled. The pultrusion process is similar to extrusion as it is a continuous process, while it is different from extrusion as 'protrusion is made from two words: "pull," which means the reinforcement impregnated with polymer is pulled rather than pushed as in the case of extrusion, and "trusion" indicates a continuous process. This process is used for developing PMC products of uniform cross section. The performing process is a replica of pultrusion in which the reinforcement impregnated with polymer is pulled out from one mold and put in a heated mold, where it is given shape and cured. Contrary to pultrusion, pulforming is a semicontinuous process. High-strength products of variable cross sections, for example, leaf springs, are made by pulforming.

### 1.1.3 Types of fiber reinforcements for polymer matrix composite

The reinforcements used in PMC include fibers, particulates, and whiskers. The particulates may be spherical or angular, usually derived from metals, alloys, or ceramics. The fibers offer a great variety, given in Fig. 1.6. Two broad classes of fiber reinforcement include natural and synthetic fibers. Natural fibers may be derived from animals or minerals, while synthetic fibers may be organic or inorganic [2].

Fibers are often cut into a specific size to obtain whickers. Whisker-reinforced PMC enables the designers to develop functionalized PMC.

### 1.1.4 Properties of materials: a comparison

The PMC, in comparison to polymers, metals, alloys, and metal matrix composites (MMCs), is given in Fig. 1.7. The fracture toughness increases with Young's modulus almost linearly. The properties of PMC are higher than the polymers and lower than metal, alloys, and MMCs [3]. The ceramic matrix composites (CMCs) exhibit lower fracture toughness. Young's modulus-to-density ratio of the PMCs is higher than the MMCs

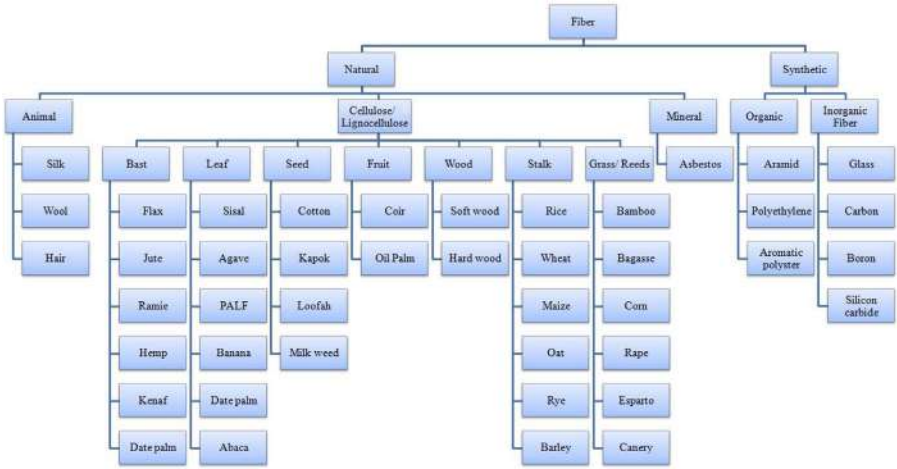


**Figure 1.6** Types of fiber reinforcements used in PMC [2]. *PMC*, polymer matrix composite.

and CMCs, making them the most preferred choice for lightweight applications [4]. The MMC dominates other composites in creep resistance. Fig. 1.7 gives useful information for the selection of materials and the design of composite systems.

### 1.1.5 Polymer nanocomposites

In order to enhance and refine the properties further, nanocomposites are developed. Here the size of the reinforcement is reduced to the nanoscale, and its concentration is reduced. In very small fractions, the nanoreinforcements produce a better result than the macro- or microreinforcement. The nanoreinforcements increase the interface between the polymer (matrix) and the reinforcement, enhancing mechanical and tribological properties such as toughness and wear resistance [5]. Moreover, nanofillers that exhibit good electrical and thermal conductivity, such as carbon nanotubes (CNT) and nanoalumina particles, develop electrically conductive and thermally stable polymers. Fig. 1.8 gives the general classification of PNC. Four types of PNC are popular among researchers due to nanofillers' compatibility with the polymer matrix. These are CNTs, silver, silica, and clay-based PNCs.

### 1.1.6 Advantages of adding nanofillers to a polymer matrix

The structural advantages of adding nanofillers to the polymer matrix are depicted in Fig. 1.9. Due to the nanofillers' small size, they have a large surface area but comparatively small volume, resetting the surface phenomenon such as van der Waals forces and surface tension to supersede density and gravitational force. Nanofillers' surface energy increases, resulting in a significant improvement in the mechanical and thermal properties of the nanocomposite despite small loading. The nanofillers with a loading fraction of

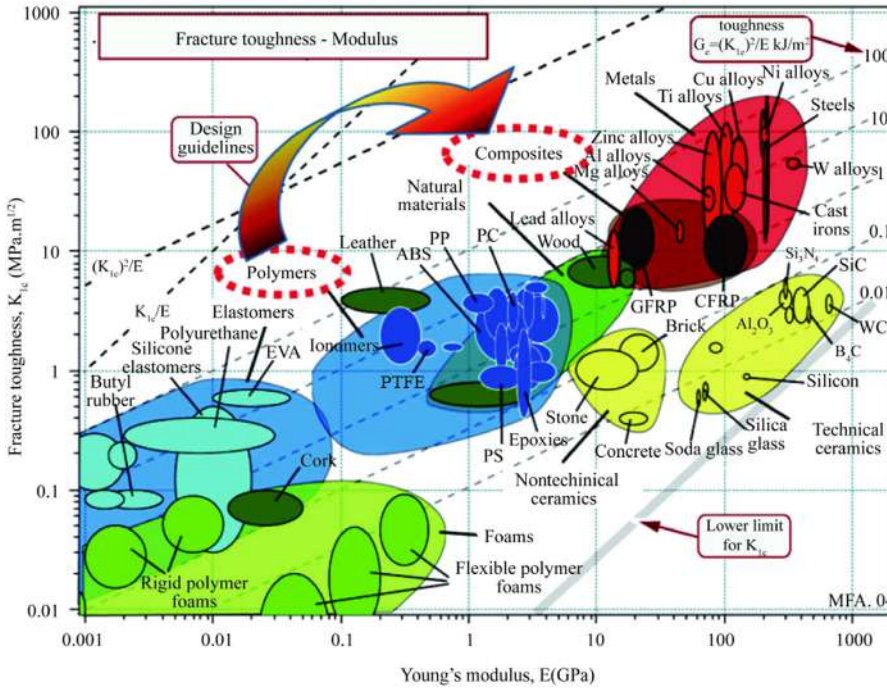


**Figure 1.7** Comparison of properties of Young's modulus and fracture toughness of PMC with other materials [4]. *PMC*, polymer matrix composite.

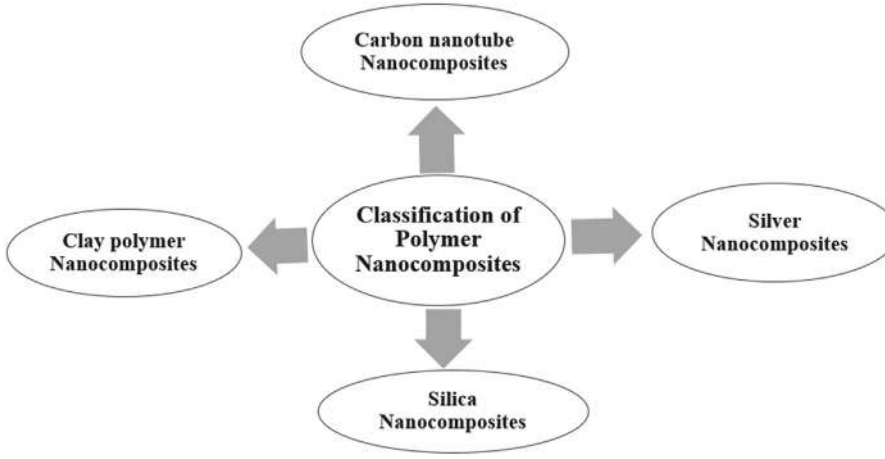


**Figure 1.8** Classification of PNC. *PNC*, polymer nanocomposite.

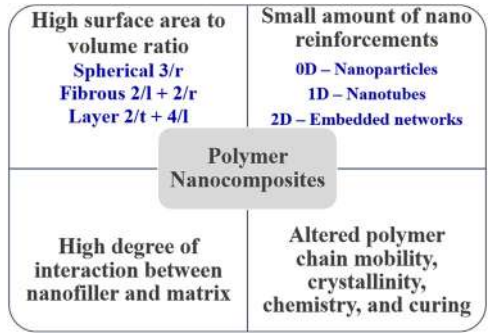


**Figure 1.9** Advantages of nanofillers in a polymer matrix; *r* is the radius, *l* is length, and *t* is thickness.

less than 5% may render superior properties to the composites than what 20%−50% fraction of macro- or microfillers. The polymer chain's mobility, crystallinity, curing response, and general chemistry are profoundly altered due to excellent interaction between the nanofillers and the polymer matrix [6,7].

### 1.1.7 Problems associated with the addition of nanofillers

The nanofillers' integration to the polymer matrix includes specific processing difficulties and significant challenges such as agglomeration and density difference. Due to the large surface area-to-volume ratio, the nanofillers have a large number of surface charges resulting in agglomerations of the nanofillers in the polymer matrix, leading to chunks' formation at several places in the matrix and some areas devoid of nanofillers. Agglomeration results in nonhomogeneity and nonuniform distribution of the functional properties throughout the matrix. To address the issue of agglomeration, the nanofillers are functionally coated to suppress the surface charges before their addition to the polymer matrix to keep them away from each other. The density of the nanofillers is minimal compared to the matrix material. As a result, the nanofillers float or tend to move toward the top in the matrix resulting in failed or uneven dispersion. Ideally, the nanofillers should be uniformly dispersed in the polymer matrix before curing. The surface and interface properties, such as frictional and adhesive forces, are incredibly critical at the reinforcements' smaller size. The problems associated with the polymer matrix include incomplete melting of pellets leading to the formation of blebs during extrusion and injection molding processes [8].

## 1.2 Materials

### 1.2.1 Matrix of polymer nanocomposites

The matrix material is a crucial choice to develop a more robust and reliable polymer nanocomposite (PNC). The option of selecting appropriate matrix material includes TP, TS, elastomer, or a blend of these [9]. The selection of the matrix materials or their blend

depends on the desirable properties, processing priorities, and nanofillers' type and amount. A few examples of the widely used TP polymer matrices include polythene (PE), high-density polyethylene (HDPE), low-density polyethylene (LDPE), polypropylene (PP), polyetherimide, polylactic acid (PLA), polyether, polyacetal (PA), polyphenylene sulfide, polysulfone (PS), polyoxymethylene (POM), acrylonitrile butadiene styrene (ABS), ethylene−propylene−diene−monomer (EPDM), polyvinylalcohol (PVA), and ultrahigh-molecular-weight polyethylene (UHMWPE. [10]. The commonly used TS polymer matrices are epoxy resins, urea, silicone, polyamide, melamine, phenolics, polyesters, acetal polyamide 6 (PA6), epoxy resin DER 331 [11], hydroxyapatite ($Ca_5(OH)(PO_4)_3$), known as HA, epoxy resin and hardener (Jointmine 905−3 S) [12], rigid polyurethane RPU60, flexible polyurethane FPU50 [13], Nylon 6 by FDM (3DP) [14], recycled polyethylene terephthalate (PETr), etc. TS polymers decompose on heating instead of softening or melting.

### 1.2.2 Nanofillers for polymer matrix

Several nanofillers used to reinforce the TP and TS polymer matrix include multilayer graphene nanoplatelets (MLNGPs), multiwalled CNTs (MWCNTs), single-walled CNTs (SWCNTs) or CNTs [15−17], graphene oxide (GO) [18−20], nitrogen-doped graphitic carbon (NC), graphene nanosheets (GN), nanoalumina, and nanoclay [21]. Fig. 1.10A presents a typical scanning electron microscopic (SEM) pictures of nanoalumina [22], Fig. 1.10B illustrates a transmission electron microscopic picture of MWCNTs produced using chemical vapor deposition [23], and Fig. 1.10C gives the SEM picture of GN [24]. The CNT may be functionalized or nonfunctionalized [25]. Nonfunctionalized CNTs refer to a single graphite sheet with stacks of numerous SWCNTs, one in the other. Such CNTs exhibit inferior interfacial collaboration with the matrix, limiting their reinforcement potential.

### 1.2.3 Exceptional properties of nanofillers

Fig. 1.11 presents the exceptional properties imparted to the polymer matrix by the nanofillers. The small size of the nanofillers enables their loading in relatively small

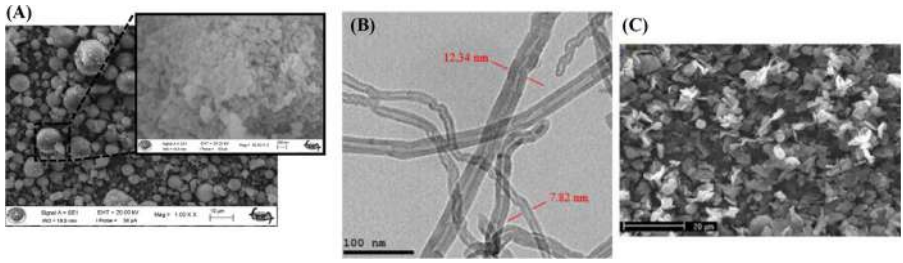


**Figure 1.10** Images of a few nanofillers. (A) SEM picture of nanoalumina [22]. (B) TEM image of MWCNT [23]. (C) SEM image of graphene nanosheets [24]. *MWCNT*, multiwalled carbon nanotube; *SEM*, scanning electron microscopic; *TEM*, transmission electron microscopic.

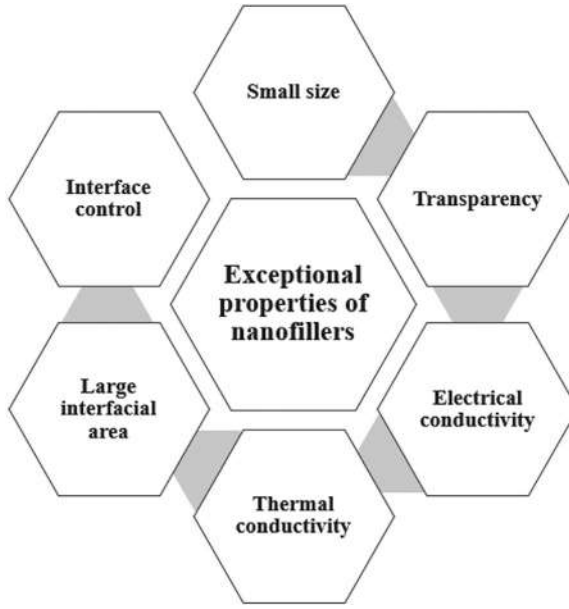


**Figure 1.11** Exceptional properties of nanofillers.

quantities. Due to the small size, they hardly affect the optical clarity and hence boost the electrical and thermal conductivity without affecting the transparency. This enables the applications of PNC in optical, electrical, thermal, and mechanical applications. They control the interface and offer a large interface area. They offer a very large surface area-to-volume ratio in small loading fractions, providing large interface junctions among the constituent phases. When there is a crack or a dislocation front propagation, they get arrested at this large interface area, preventing or prolonging the failure [26].

## 1.3 Fabrication of polymer nanocomposites

Several processes have been established to fabricate the PNC successfully. The most simple process is wet dispersion, as shown in Fig. 1.12. The polymer is first dissolved in a volatile solvent, for example, toluene, acetone, ethyl-acetate, n-hexane, chloroform, etc. The polymer solution is agitated using a mechanical or ultrasonic stirrer. The use of an ultrasonic stirrer for mixing is called ultrasonication. A typical ultrasonic tool vibrates at a very high frequency, of the order of 20 kHz and small amplitude. As the ultrasonic probe or tool vibrates in the polymer solution, it creates many cavity bubbles, which move from bottom to top in the polymer solution. At this moment, the nanofillers are introduced. A mechanical stirrer initiates a vortex, and the nanofillers are introduced along its walls for good

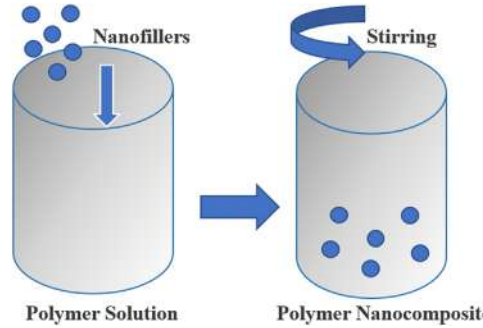


**Figure 1.12** Fabrication of PNC by a solution method. *PNC*, polymer nanocomposite.

reception by the polymer solution. The nanofillers are then introduced into the polymer solution, and the agitation is continued until a uniform dispersion on the nanofillers is achieved. Gradually, the solvent evaporates, leaving behind the PNC as a thin sheet. The solvent aids in the mobility of the polymer chains to enable their intercalation with nanofillers. A controlled supply of heat may expedite the evaporation of the solvent and curing of the TP polymer, whereas in TS polymers, the temperature rises during ultrasonication, which may be controlled using an ice bath surrounding the polymer–nanofiller container. An extension of the solution method is solution casting in which the polymer [most common is a polyurethane (PU)] is melted in a container and stirred with a solvent. The nanofillers are introduced into the agitated solution, and the solvent is evaporated. The process may be executed in an inert gas environment to avoid porosity. The solvent gradually evaporates, and the slurry is either cast in a mold if a particular shape of PNC is desired or introduced on a spinning disk if a thin film or sheet is required.

Fig. 1.13 shows the melt extrusion process [27,28]. The granules of polymer (TP) are mixed with the nanofillers by milling and fed into an extrusion machine's hopper. The polymer is melted with the heat inside the barrel, and the rotating screw mixes the molten TP polymer with the nanoparticles. A typical temperature of 240°C and an extruder speed of 100 rpm are used [27]. The mobility of the polymer is due to thermal energy. The PNC is then extruded through a nozzle continuously and given the desired shape using a die. An adapter is used to couple the die with the extruder. This process is also called melt blending. In case a fixed shape is required, in place of a continuous process, the extruded polymer–nanofiller mix is introduced in a compression molding die, where it is frozen under compression. The advantages of the melt blending process over solution casting include higher gas barrier formation, restricting pinholes, the exfoliated structure of PNC instead of intercalated structure, and high creep resistance. Moreover, melt blending is an environment-friendly technique. In melt extrusion, it is better to employ an intermeshing twin-screw extruder instead of a single-screw extruder (Brabender) to enable smooth addition of nanofillers and their uniform mixing with the polymer matrix [29].

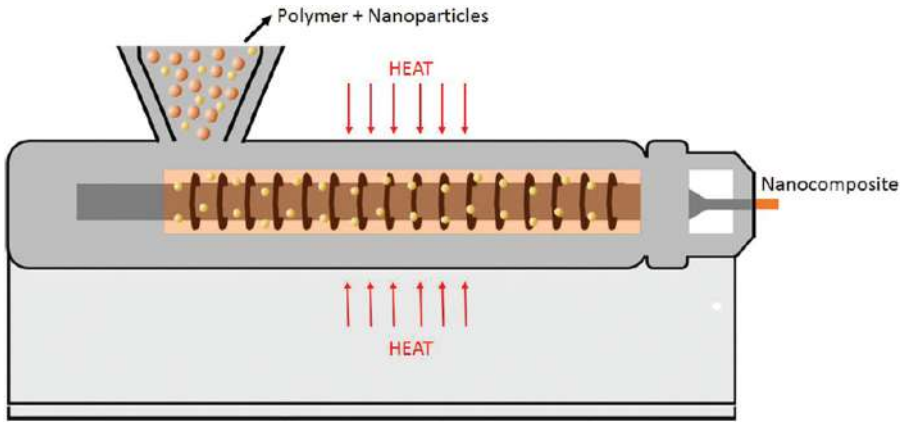


**Figure 1.13** Fabrication of PNC by melt extrusion [27]. *PNC*, polymer nanocomposite.

Fig. 1.14 presents a schematic diagram of the spray drying process to fabricate PNC [27]. The polymer is dissolved in a solvent, and the nanofillers are dispersed. The polymer−nanofiller solution is then sprayed in a drying chamber in which the solvent starts evaporating. A cyclone is created at the exit chamber, attached to the drying chamber, to mix the nanofillers with the polymer thoroughly. The dried PNC is finally collected in a collection chamber. Fig. 1.15 presents the fabrication of HDPE/MWCNT PNC using a high-energy ball milling (HEBM) process [10]. The HDPE polymer granules and MWCNT nanofillers are introduced in an HEBM. The granules of the matrix and the nanofillers are thoroughly mixed in the mill at high speed. The mixture is then compacted using a mechanical press, or the mixture may be supplied to an injection molding or extrusion machine to develop the desired PNC.

The nanofillers can be particulates (0D), nanotubes or nanowires (1D), and thin-film coating on quantum wells, nanosheets, or embedded networks (2D). To avoid the problem of agglomeration, the nanofillers may be coated or impregnated before adding to the polymer matrix, as shown in Fig. 1.16 [30,31]. The modified nanofillers are then mixed with the polymer solution to develop the PNC using hot pressing, vacuum filtration, shearing, laminates, or electrophoretic deposition. A sol−gel method may also be used to develop the PNC.

Fig. 1.17 gives alternative methods to develop PNC [30]. The nanowires are impregnated with the TS resin and rolled over a rotating mandrel to develop PNC, and the method is called spray winding. It is an extension of the filament winding process. In shear pressing, an array or preform is made from the nanofillers, typically, CNT, in which the TS resin infiltrates to develop the PNC. Fig. 1.18 presents the spinning process to develop PNC. Here, the nanofiller wire of CNT is impregnated by a TS resin and stretched to get the fibrous nanocomposite. Another way to fabricate the PNC during spinning is to wet the nanofiller wire with a solvent such as PVA solution. The polymer is deposited layer by layer on the nanofiller wire

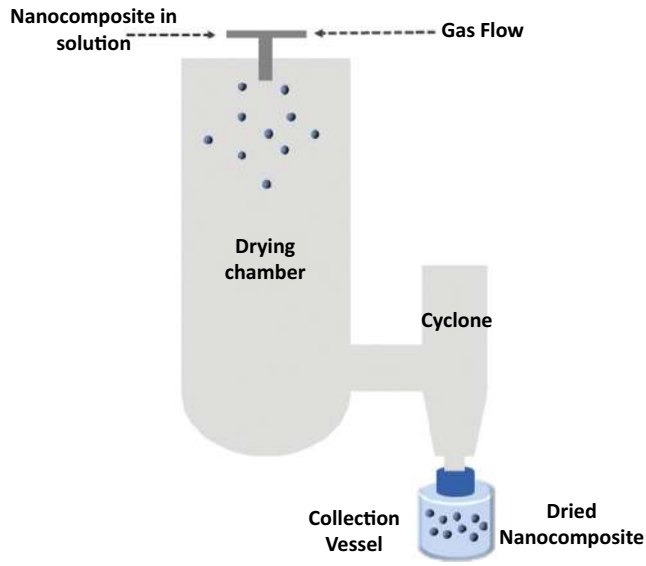


**Figure 1.14** Fabrication of PNC by spray drying [27]. *PNC*, polymer nanocomposite.

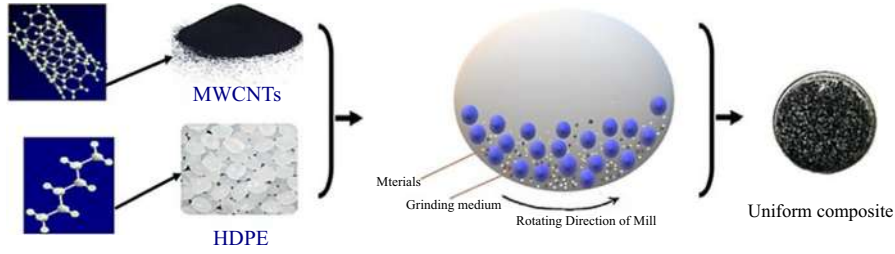


**Figure 1.15** Fabrication of hybrid PNC by high-energy ball milling [8]. *PNC*, polymer nanocomposite.

substrate as the spinning is continued. In situ polymerization includes both intercalation and exfoliation. In PNC, there are a lot of charges responsible for agglomeration. To separate the nanofillers, functionalization is done by intercalation and exfoliation.

Intercalation includes the insertion of an ion or molecule between the nanofiller layers expanding the van der Waals gaps. The energy required to create these gaps is derived from charge transfer between the host and guest molecules. Exfoliation includes complete separation of the nanofiller layers, an extreme case of intercalation. Aggressive polar solvents and reagents carry out exfoliation. A simple analogy is to put spacers between the nanolayers to separate them. First, a nanofiller solution is prepared by dispersing the nanofillers in a low-viscosity monomer, a prepolymer, and letting them swell by adsorbing the monomer on the surface. As the

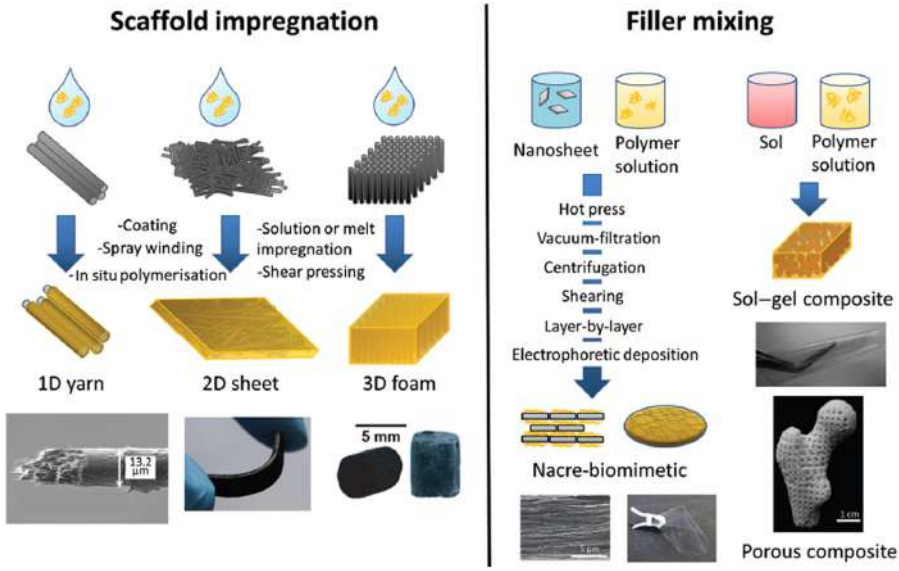


**Figure 1.16** Scaffold impregnation combined with filler mixing methods to develop PNC [30]. *PNC*, polymer nanocomposite.

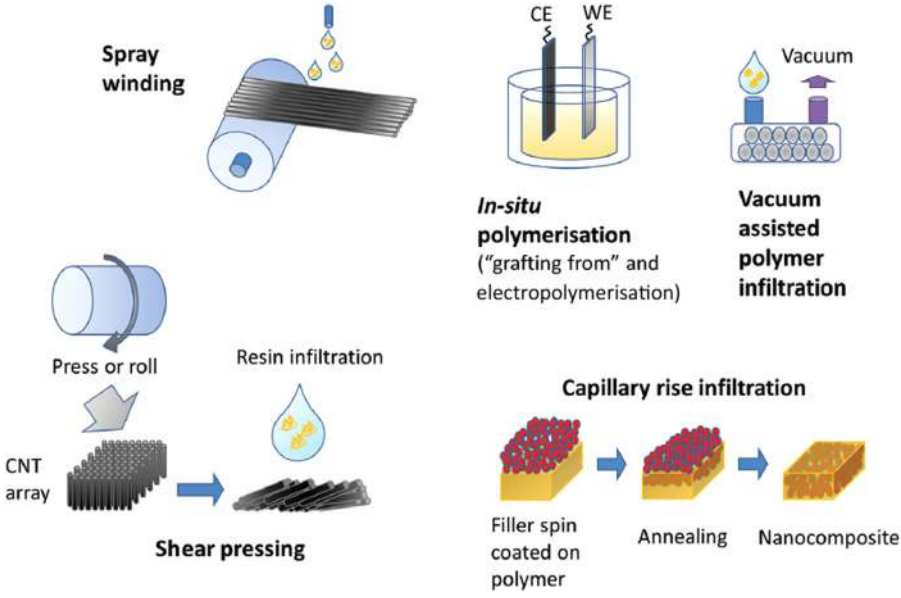


**Figure 1.17** Alternative methods for fabrication of PNC [30]. *PNC*, polymer nanocomposite.

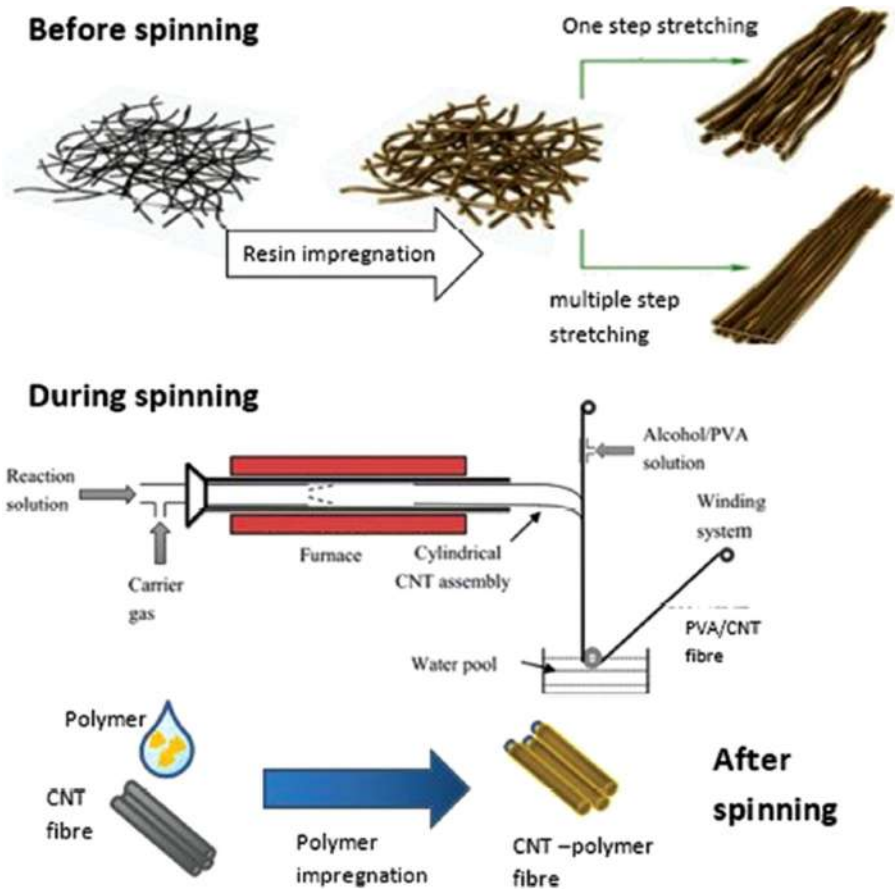


**Figure 1.18** Fabrication of PNC by spinning [30]. *PNC*, polymer nanocomposite.

polymerization is initiated, the polymer chains facilitate the unbundling or delamination of these swollen nanofillers. Fig. 1.19 describes a typical in situ fabrication of PU-carbon dot PNC in which the emulsion polymerization technique is used as the medium is water [32]. A waterborne PU emulsion is functionalized with 2-methyl-propionamide-dihydrochloride-functionalized clay, where clay acts as nanofillers and an initiator for functionalization influencing polymerization as cross-linking in TS polymers [33]. The monomer transforms into the polymer by emulsion polymerization, and the coagulation of the polymer−nanoclay emulsion acquires the PNC. Due to the monomer's lower viscosity than polymer, the interactions between the nanofillers and polymer chains are stronger and interfacial interactions are stronger in in situ fabrication than the solution method yielding a uniform dispersion of the nanofillers in the polymer matrix. In situ polymerization excludes solvents and high energy requirements, so considered as an eco-friendly technique.

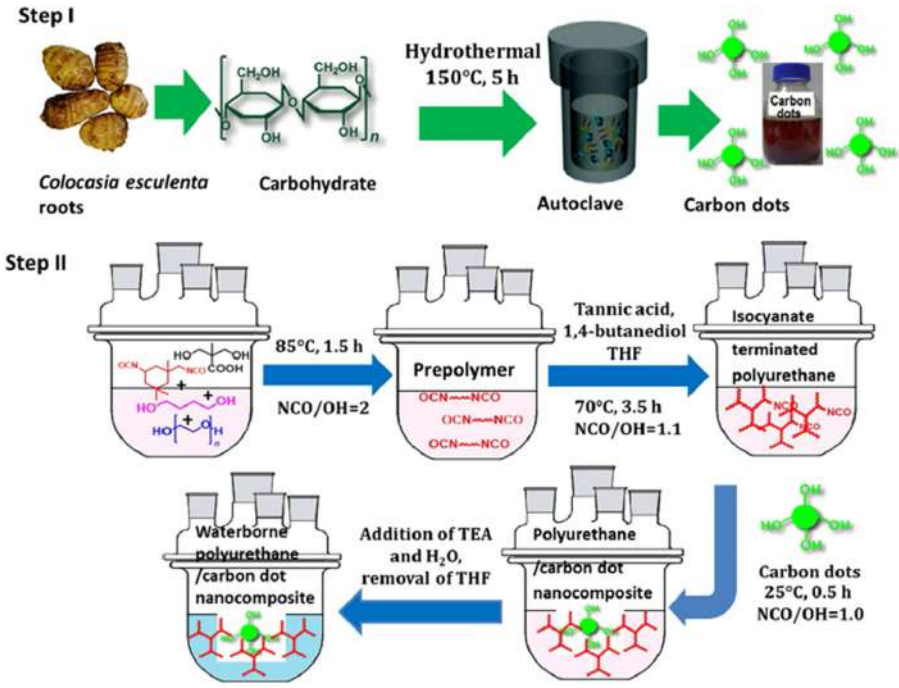


**Figure 1.19** In situ fabrication of PNC [33,34]. *PNC*, polymer nanocomposite.

The nanofillers such as particulates (0D); wires, ribbons, tubes, fibers, or threads (1D); and nanoplatelets or nanosheets (3D) are coated on the outer surface by polymers as shown in the middle column of Fig. 1.20 by adsorption, grafting, sol−gel, and hydrothermal methods. The coated nanofillers are then transformed into the PNC by choosing methods such as casting and hot pressing. Such PNCs are suitable for energy storage applications such as batteries and panels.

Researchers have explored several innovations in the fabrication of PNC by combining two or more methods, called hybrid processing. More than one nanofillers have also been introduced to achieve the benefits of both to develop hybrid nanocomposites.

Fig. 1.21 presents one such example in which a combination of solution and HEBM process has been employed together. The HDPE polymer is first dissolved in a solvent, and hybrid nanofillers (MWCNT and nanoalumina) were dispersed in the polymer solution. The solvent evaporated due to heating at 90°C leaving behind a coagulated mix of hybrid nanofillers and HDPE polymer, which were hot-pressed in a die to develop the desired PNC. Such PNC was evaluated for biomedical applications with promising results. 3D printing (3DP) offers immense opportunities to innovate with the matrix and nanofiller compositions [36]. The polymer/nanofiller wires may be produced using melt extrusion, and the wires may be used as filament in 3DP equipment to develop the desired shapes [13].

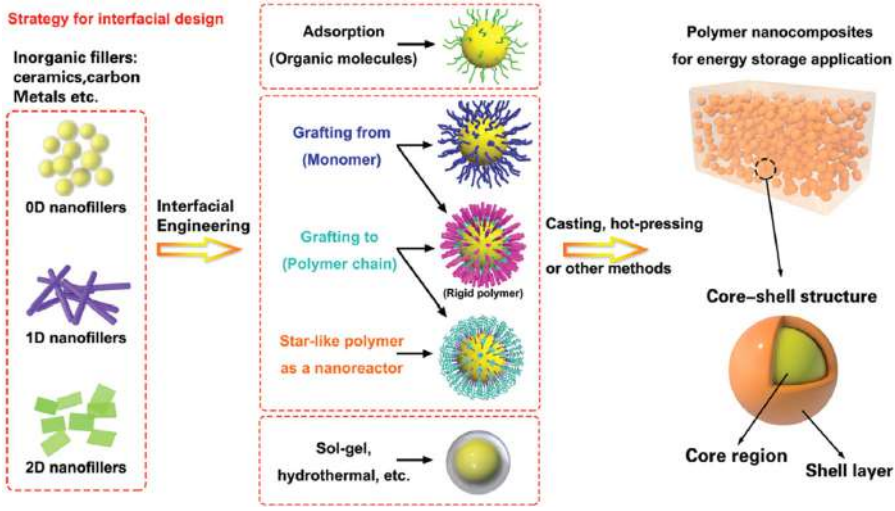


**Figure 1.20** The interface design of PNC [35]. *PNC*, polymer nanocomposite.

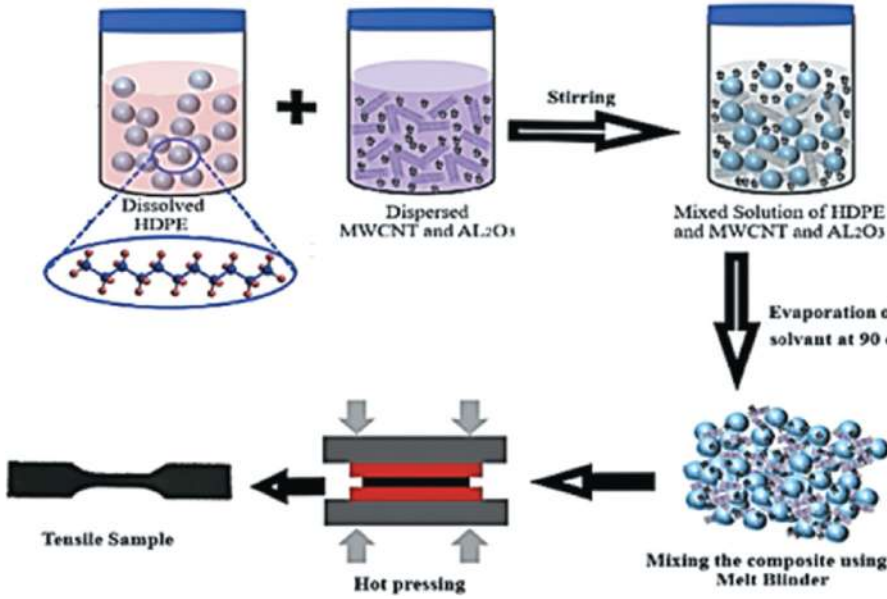


**Figure 1.21** Fabrication of hybrid PNC by solution−milling−hot pressing [29]. *PNC*, polymer nanocomposite.

Fig. 1.22 depicts a model to describe the interactions between the ceramic nanoparticles and polymer in three layers, namely, loose, bound, and bonded, shown in Fig. 1.22A. The layer binds the inorganic ceramic nanoparticles and organic

polymer by hybrid bonding, including covalent, electrostatic, van der Waals, and hydrogen. The bonding largely depends on the polymer chains, which interact with the nanoparticles. The thickness of each layer is of the order of 1−10 nm. As shown in Fig. 1.22B, the nanoparticles get electrostatically charged due to the electric potential difference with the polymers. The surrounding layers screen these electronic charges. A double layer develops containing a positively charged Gouy−Chapman and a negatively charged Stern layer. The charge distribution across this layer depends on the electrical potential $\Psi(r)$ at the interface where $r$ is the layer's distance from the particle surface. $\Psi$s represent the positively charged layer, and $\Psi$ represents the electrical potential [35].

## 1.4 Characterization of polymer nanocomposites

Characterization of PNC gives detailed information about the key parameters, which govern the properties and performance of the PNC. Fig. 1.23 presents primary characterization techniques employed to analyze the composition, structure, and defects in the PNC. Spectroscopes give surface and subsurface properties, nanofillers' distribution, and defects such as agglomerations, porosity, and interface properties. Depending on the magnification, a suitable spectroscope is selected.

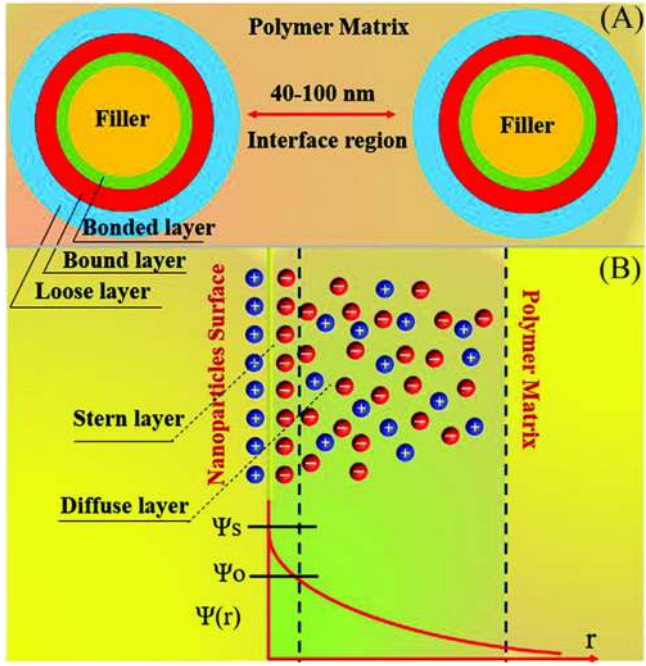


**Figure 1.22** (A) A model for PNC. (B) Distribution of electrical charge of the diffused double layer [35]. *PNC*, polymer nanocomposite.

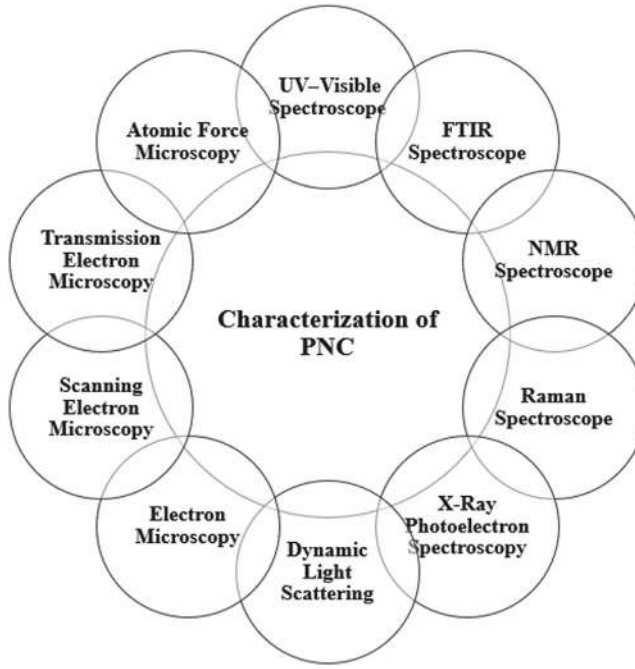


**Figure 1.23** Characterization techniques of PNC. *PNC*, polymer nanocomposite.

## 1.5 Degradation of polymer nanocomposites

Polymers have low creep resistance, and they deteriorate when exposed to the Sun, chemicals, extreme temperatures, and changing weather conditions. Due to the polymer matrix being the bulk of the material, degradation also affects PNS. Fig. 1.24 gives the common degradation mechanisms of PNC. Exposure to oxygen at high temperatures results in oxy-degradation and exposure to sunlight results in photodegradation, and the combined exposure to oxygen and sunlight results in photo-oxy degradation. Exposure to excessive heat and chemicals results in thermal and chemical degradation, while cytotoxic activity results in biodegradation. Coating and using hybrid nanofillers are effective means to prevent degradation mechanisms.

## 1.6 Applications of polymer nanocomposites

The scope of the applications of the PNC is wide open. Fig. 1.25 highlights significant fields in which the applications of PNC have been well established. The primary reason to select a PNC is less weight and more strength. Proven applications of PNC are in energy storage [37], sensors and actuators, structural components and

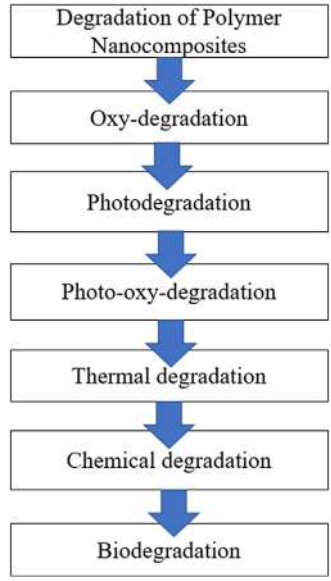


**Figure 1.24** Degradation of PNC. *PNC*, polymer nanocomposite.

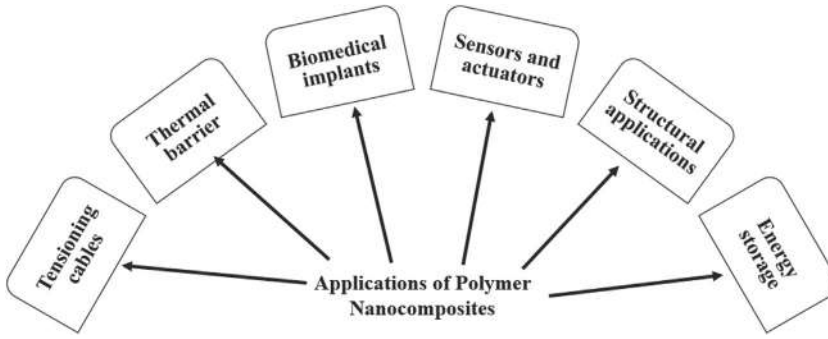


**Figure 1.25** Applications of PNC. *PNC*, polymer nanocomposite.

tensioning cables, biomedical implants, thermal barrier applications [38], filtration (functionalized PNC), biochemical separation, gas separation, catalysts, fast charge and slow discharge capacitors, and low-friction and high-strength components [39–41].

The lightweight and superior properties such as elastic modulus, strength, fracture toughness, electrical and thermal conductivity, high surface area-to-volume ratio, and good tribological performance make PNC the most preferred material. Biocompatibility, resistance to impact and corrosion, and tailored stiffness are crucial for compatibility with human tissues. Hence, prosthetic implants are one of the

brightest applications of PNC. Their lightweight makes them highly preferred organic implant material.

## 1.7 Conclusion

Polymers are easy to process and offer high strength-to-weight options at the lesser expense of energy. Three primary types of polymer are TP, TS, and elastomers. All these polymers may be used as matrix materials to develop macro-, micro-, and nanocomposites. Proven techniques to process polymers include extrusion, injection molding, blow molding, casting, thermoforming, vacuum forming, calendaring, and compression molding. In contrast, those to process macro- and microcomposites include open and closed mold processes, filament winding, pultrusion, pulforming, and prepreg processes. All these techniques offer opportunities for innovation and exploration to develop PNC using nano-sized reinforcements. A comparison of properties of polymers, metals, ceramics, and their composites reveals that the PMCs offer the highest Young's modulus-to-density ratio. These properties may be further enhanced by using nanofillers instead of micro- or macrofillers. In very small fractions, the nanoreinforcements produce a better result than the macro- or microreinforcement. Due to the nanofillers' small size, they have a large surface area but comparatively small volume, resetting the surface phenomenon such as van der waals forces and surface tension to supersede density and gravitational force. Nanofillers' surface energy increases, resulting in a significant improvement in the mechanical and thermal properties of the nanocomposite despite small loading. The nanofillers with a loading fraction of less than 5% may render superior properties to the composites than what 20%−50% fraction of macro or microfillers.

The polymer chain's mobility, crystallinity, curing response, and general chemistry are profoundly altered due to excellent interaction between the nanofillers and the polymer matrix. The nanofillers' integration to the polymer matrix includes specific processing difficulties and significant challenges such as agglomeration and density difference. To address the issue, the nanofillers are functionally coated to suppress the surface charges before their addition to the polymer matrix to keep them away from each other. A few examples of the widely used polymer matrices include PE, HDPE, LDPE, PP, polyetherimide, PLA, PA, polyphenylene sulfide, PS, POM, ABS, EPDM, PVA, UHMWPE, epoxy resins, urea, silicone, polyamide, melamine, phenolics, polyesters, PA6, HA, RPU, FPU, and PETr, etc. Examples of popular nanofillers for polymer matrices include MLNGPs, MWCNT, SWCNT, GO, NC, GN, nanoalumina, and nanoclay. The techniques used to develop PNC have conventional methods such as solution method, wet dispersion, solution casting, melt extrusion, spray drying, and HEBM and alternative methods such as scaffold impregnation, spray winding, in situ polymerization, vacuum filtration, spinning, and hybrid processing, for example, solution−milling−hot pressing. PNCs exhibit exceptional mechanical, thermal, electrical, optical, and biocompatible properties making them suitable for energy storage, sensors and actuators,

structural components and tensioning cables, biomedical implants, thermal barrier applications, filtration, biochemical separation, gas separation, catalysts, fast charge, and slow discharge capacitors, and low-friction and high-strength applications.

## 1.8 Scope for future work

PNCs include the integration of reinforcements of nanosize into the matrix of the polymers. The conventional fabrication processes offer a limited choice of TP and TS matrices and a short range of nanofillers to choose from. The scope of future research is unlimited in the areas of development, characterization, and applications of PNC. With the future perspective, the innovations in selecting materials and the processes both offer great opportunities. Researchers may explore hybrid matrix materials and newer combinations of hybrid nanofillers. The innovations and integration of processing techniques also open new avenues by combining two or more processes together to achieve a more uniform PNC. The opportunities in the nanofillers' functionalization to avoid defects and inhomogeneity may be further explored as well. To summarize, research know-how on the PNC is far from saturation, and this thrust area of research has great potential for innovation in materials, methods, and applications.

## Acknowledgments

The authors gratefully acknowledge the resources and facilities given by the Mechanical Engineering Department, College of Engineering, and the financial support by the Deanship of Scientific Research at King Khalid University, Abha, Kingdom of Saudi Arabia to conduct the study.

## References

[1] S.W. Ghori, R. Siakeng, M. Rasheed, N. Saba, M. Jawaid, The role of advanced polymer materials in aerospace, Sustainable Composites for Aerospace Applications, Elsevier Ltd., 2018. Available from: https://doi.org/10.1016/B978-0-08-102131-6.00002-5.

[2] W. Ghori, N. Saba, M. Jawaid, M. Asim, A review on date palm (*Phoenix dactylifera*) fibers and its polymer composites, IOP Conference Series: Materials Science and Engineering 368 (1) (2018). Available from: https://doi.org/10.1088/1757-899X/368/1/012009.

[3] G.M.S. Ahmed, I.A. Badruddin, V. Tirth, A. Algahtani, M.A. Ali, Wear resistance of maraging steel developed by direct metal laser sintering, Mater. Express 10 (7) (2020) 1079−1090. Available from: https://doi.org/10.1166/mex.2020.1715.

[4] R. Atif, F. Inam, Modeling and simulation of graphene based polymer nanocomposites: advances in the last decade, Graphene 05 (02) (2016) 96−142. Available from: https://doi.org/10.4236/graphene.2016.52011.

[5] M. Zboncak, F. Ondreas, V. Uhlir, P. Lepcio, J. Michalicka, J. Jancar, Translation of segment scale stiffening into macroscale reinforcement in polymer nanocomposites, Polym. Eng. Sci. 60 (3) (2020) 587−596. Available from: https://doi.org/10.1002/pen.25317.

[6] Dalton, A.B., Collins, S., Razal, J.M., & Howard, V. (2002). Super-tough carbon-nanotube fibres. 886, 2002.
[7] Y. Han, X. Zhang, X. Yu, J. Zhao, S. Li, F. Liu, et al., Bio-inspired aggregation control of carbon nanotubes for ultra-strong composites, Sci. Rep. 5 (2015) 1−9. Available from: https://doi.org/10.1038/srep11533.
[8] S. Dabees, V. Tirth, A. Mohamed, B.M. Kamel, Wear performance and mechanical properties of MWCNT/HDPE nanocomposites for gearing applications, J. Mater. Res. Technol (2020). Available from: https://doi.org/10.1016/j.jmrt.2020.09.129.
[9] N. Salah, A.M. Alfawzan, A. Saeed, A. Alshahrie, W. Allafi, Effective reinforcements for thermoplastics based on carbon nanotubes of oil fly ash, Sci. Rep. 9 (1) (2019) 1−13. Available from: https://doi.org/10.1038/s41598-019-56777-1.
[10] S. Dabees, V. Tirth, A. Mohamed, B.M. Kamel, Wear performance and mechanical properties of MWCNT/HDPE nanocomposites for gearing applications, J. Mater. Res. Technol (2020). Available from: https://doi.org/10.1016/j.jmrt.2020.09.129.
[11] N. Saba, O.Y. Alothman, Z. Almutairi, M. Jawaid, W. Ghori, Date palm reinforced epoxy composites: tensile, impact and morphological properties, J. Mater. Res. Technol 8 (5) (2019) 3959−3969. Available from: https://doi.org/10.1016/j.jmrt.2019.07.004.
[12] M.H. Gheith, M.A. Aziz, W. Ghori, N. Saba, M. Asim, M. Jawaid, et al., Flexural, thermal and dynamic mechanical properties of date palm fibres reinforced epoxy composites, J. Mater. Res. Technol 8 (1) (2019) 853−860. Available from: https://doi.org/10.1016/j.jmrt.2018.06.013.
[13] S. Begum, G.M.S. Ahmed, I.A. Badruddin, V. Tirth, A. Algahtani, Analysis of digital light synthesis based flexible and rigid polyurethane for applications in automobile bumpers, Mater. Express 9 (8) (2019) 839−850. Available from: https://doi.org/10.1166/mex.2019.1578.
[14] I.A. Badruddin, A.N. Saquib, A.E. Anqi, V. Tirth, M.F. Addas, F.O. Mahroogi, et al., Finite element analysis of nylon based 3D printed autonomous underwater vehicle propeller, Mater. Res. 23 (5) (2020).
[15] K. Yusupov, D. Hedman, A.P. Tsapenko, A. Ishteev, S. You, V. Khovaylo, et al., Enhancing the thermoelectric performance of single-walled carbon nanotube-conducting polymer nanocomposites, J. Alloys Compd. 845 (2020) 156354. Available from: https://doi.org/10.1016/j.jallcom.2020.156354.
[16] M.B. Bryning, D.E. Milkie, M.F. Islam, L.A. Hough, J.M. Kikkawa, A.G. Yodh, Carbon nanotube aerogels, Adv. Mater. 19 (5) (2007) 661−664. Available from: https://doi.org/10.1002/adma.200601748.
[17] J. Chen, L. Wang, X. Gui, Z. Lin, X. Ke, F. Hao, et al., Strong anisotropy in thermoelectric properties of CNT/PANI composites, Carbon N. Y. 114 (2017) 1−7. Available from: https://doi.org/10.1016/j.carbon.2016.11.074.
[18] N. Faisal, Mechanical behavior of nano-scaled graphene oxide reinforced high-density polymer ethylene for orthopedic implants, Biointerface Res. Appl. Chem 10 (6) (2020) 7223−7233. Available from: https://doi.org/10.33263/BRIAC106.72237233.
[19] S. Ploychompoo, Q. Liang, X. Zhou, C. Wei, H. Luo, Fabrication of Zn-MOF-74/polyacrylamide coated with reduced graphene oxide (Zn-MOF-74/rGO/PAM) for As(III) removal, Physica E Low Dimens. Syst. Nanostruct. 125 (July 2020) (2021) 114377. Available from: https://doi.org/10.1016/j.physe.2020.114377.
[20] R. Badry, S.H. Radwan, D. Ezzat, H. Ezzat, H. Elhaes, M. Ibrahim, Study of the electronic properties of graphene oxide/(Pani/teflon), Biointerface Res. Appl. Chem 10 (6) (2020) 6926−6935. Available from: https://doi.org/10.33263/BRIAC106.69266935.

[21] P. Das, J.M. Malho, K. Rahimi, F.H. Schacher, B. Wang, D.E. Demco, et al., Nacre-mimetics with synthetic nanoclays up to ultrahigh aspect ratios, Nat. Commun. 6 (2015) 1–14. Available from: https://doi.org/10.1038/ncomms6967.

[22] H.B. Kaybal, H. Ulus, O. Demir, Ö.S. Şahin, A. Avcı, Effects of alumina nanoparticles on dynamic impact responses of carbon fiber reinforced epoxy matrix nanocomposites, Int. J. Eng. Sci. Technol. 21 (3) (2018) 399–407. Available from: https://doi.org/10.1016/j.jestch.2018.03.011.

[23] A. Mohamed, V. Tirth, B.M. Kamel, Tribological characterization and rheology of hybrid calcium grease with graphene nanosheets and multi-walled carbon nanotubes as additives, J. Mater. Res. Technol. 9 (3) (2020) 6178–6185. Available from: https://doi.org/10.1016/j.jmrt.2020.04.020.

[24] B.M. Kamel, V. Tirth, A. Algahtani, M.S. Shiba, A. Mobasher, H.A. Hashish, S. Dabees, Optimization of the rheological properties and tribological performance of Sae 5w-30 base oil with added MWCNTs, Lubricants 9 (9) (2021) 1–13. Available from: https://doi.org/10.3390/lubricants9090094.

[25] S. Qiu, Y. Zhou, X. Ren, B. Zou, W. Guo, L. Song, et al., Construction of hierarchical functionalized black phosphorus with polydopamine: a novel strategy for enhancing flame retardancy and mechanical properties of polyvinyl alcohol, Chem. Eng. J. 402 (March) (2020) 126212. Available from: https://doi.org/10.1016/j.cej.2020.126212.

[26] G.S. Liou, P.H. Lin, H.J. Yen, Y.Y. Yu, T.W. Tsai, W.C. Chen, Highly flexible and optical transparent 6F-PI/TiO2 optical hybrid films with tunable refractive index and excellent thermal stability, J. Mater. Chem. 20 (3) (2010) 531–536. Available from: https://doi.org/10.1039/b916758g.

[27] M.I.B. Tavares, E.O. da Silva, P.R.C. da Silva, L.R. de Menezes, Polymer Nanocomposites Chapter 7, Nanostructured Materials - Fabrication to Applications, IntechOpen, 2017, pp. 135–151. Available from: http://doi.org/10.5772/intechopen.68142.

[28] O. Manero, A. Sanchez-Solis, Polymer nanocomposites. *Handbook of Polymer*, Synthesis, Characterization, and Processing, Wiley, 2013, pp. 585–604. Available from: https://doi.org/10.1002/9781118480793.ch31.

[29] S. Dabees, B.M. Kamel, V. Tirth, A.B. Elshalakny, Experimental design of Al2O3/MWCNT/HDPE hybrid nanocomposites for hip joint replacement, Bioengineered 11 (1) (2020) 679–692. Available from: https://doi.org/10.1080/21655979.2020.1775943.

[30] C. Harito, D.V. Bavykin, B. Yuliarto, H.K. Dipojono, F.C. Walsh, Polymer nanocomposites having a high filler content: synthesis, structures, properties, and applications, Nanoscale 11 (11) (2019) 4653–4682. Available from: https://doi.org/10.1039/c9nr00117d.

[31] E. Mäder, J. Liu, J. Hiller, W. Lu, Q. Li, S. Zhandarov, et al., Coating of carbon nanotube fibers: variation of tensile properties, failure behavior, and adhesion strength, Front. Mater. Sci. 2 (July) (2015) 1–9. Available from: https://doi.org/10.3389/fmats.2015.00053.

[32] C. Gao, N. Li, C. Xue, H. Wang, H. Liu, Q. Chang, et al., Highly improved mechanical performances of polyvinyl butyral through fluorescent carbon dots, Mater. Lett. 280 (2020) 128537. Available from: https://doi.org/10.1016/j.matlet.2020.128537.

[33] D. Hazarika, N. Karak, Nanocomposite of waterborne hyperbranched polyester and clay@carbon dot as a robust photocatalyst for environmental remediation, Appl. Surf. Sci. 498 (September) (2019) 143832. Available from: https://doi.org/10.1016/j.apsusc.2019.143832.

[34] N. Karak, Fundamentals of nanomaterials and polymer nanocomposites, Nanomaterials and Polymer Nanocomposites: Raw Materials to Applications, Elsevier Inc, 2018. Available from: https://doi.org/10.1016/B978-0-12-814615-6.00001-1.

[35] H. Luo, X. Zhou, C. Ellingford, Y. Zhang, S. Chen, K. Zhou, et al., Interface design for high energy density polymer nanocomposites, Chem. Soc. Rev. 48 (16) (2019) 4424–4465. Available from: https://doi.org/10.1039/c9cs00043g.

[36] D.J. Horst, P.P. de Andrade Junior, C.A. Duvoisin, R.de A. Vieira, Fabrication of conductive filaments for 3d-printing: polymer nanocomposites, Biointerface Res. Appl. Chem. 10 (6) (2020) 6577–6586. Available from: https://doi.org/10.33263/BRIAC106.65776586.

[37] S. Nie, J. Mo, Y. Zhang, C. Xiong, S. Wang, Ultra-high thermal-conductive, reduced graphene oxide welded cellulose nanofibrils network for efficient thermal management, Carbohydr. Polym. 250 (May) (2020) 116971. Available from: https://doi.org/10.1016/j.carbpol.2020.116971.

[38] M. Tiwari, B.K. Billing, H.S. Bedi, P.K. Agnihotri, Quantification of carbon nanotube dispersion and its correlation with mechanical and thermal properties of epoxy nanocomposites, J. Appl. Polym. Sci. 137 (29) (2020) 1–11. Available from: https://doi.org/10.1002/app.48879.

[39] E. Manias, G. Polizos, H. Nakajima, M.J. Heidecker, Nanocomposite Technology, Flame Retardant Polymer Nanocomposites, Wiley, 2007, pp. 31–66.

[40] T. Tanaka, M. Kozako, N. Fuse, Y. Ohki, Proposal of a multi-core model for polymer nanocomposite dielectrics, IEEE Transactions on Dielectrics and Electrical Insulation 12 (4) (2005) 669–681. Available from: https://doi.org/10.1109/TDEI.2005.1511092.

[41] L. Zhang, G. Xie, S. Wu, S. Peng, X. Zhang, D. Guo, et al., Ultralow friction polymer composites incorporated with monodispersed oil microcapsules, Friction 9 (1) (2021) 29–40. Available from: https://doi.org/10.1007/s40544-019-0312-4.

# Rheology and crystallization of polymer nanocomposites

2

*Hamid Essabir*[1,2], *Marya Raji*[1], *Rachid Bouhfid*[1] *and Abou el kacem Qaiss*[1]

[1]Moroccan Foundation for Advanced Science, Innovation and Research (MAScIR), Institute of Nanomaterials and Nanotechnology (NANOTECH), Laboratory of Polymer Processing, Rabat, Morocco

[2]Mechanic Materials and Composites (MMC), Laboratory of Energy Engineering, Materials and Systems, National School of Applied Sciences of Agadir, Ibn Zohr University, Morocco

## 2.1 Introduction

Nanocomposites are a new type of composite material that has fillers that have at least one-nanometer dimension. Polymer nanocomposites are made up of a variety of inorganic nanomaterials that can be combined with polymer or monomer on a nanoscale scale [1–5]. They have sparked a lot of interest because they theoretically promise to improve a variety of properties; including thermal and acoustic isolation, as well as mechanical, electrical performances, and flame retardant properties, by adding a slight amount of nanofiller [6–9]. The nanofiller surface properties and the interfacial interaction of the nanofiller with the host polymer can be attributed to this improvement [10–12]. Oftentimes, the nature of application demands modifications of properties of polymer nanocomposites. The properties of mechanical, and electrical or thermal conductivity all improve dramatically when nanofillers are used in between 0.5 and 5 wt. % in the polymer matrix [13–16]. In contrast, the addition of nanofillers to polymer causes an increase in melt viscosity, which may cause processing issues. As a result, manufacturing these materials necessitates a thorough understanding of their rheological behavior. It was recently demonstrated that adding trace amounts of nanofiller to a polymer can reduce its viscosity [17–21].

According to theoretical assumptions, the foundation for polymer nanocomposites is thought to be a broad interface between nanosized heterogeneities and pure polymer macromolecules. In contrast to usual microfilled polymer composites, the broad interface between nanofillers and macromolecules is expected to provide novel properties. Nanofillers are frequently used in nanocomposites to provide substantial reinforcement while also improving other properties such as flammability and conductivity [22,23]. Montmorillonite (MMT) clay, for example, has been employed as a nanofiller in polymer nanocomposites [24], cellulose nanocrystals [25] or, carbon derivatives as carbon nanotubes (CNTs) [26] and grapheme [27,28]. The use of such nanofillers into polymer matrices has been shown to significantly

**Advanced Polymer Nanocomposites. DOI: https://doi.org/10.1016/B978-0-12-824492-0.00011-8**


improve the mechanical, thermal, and electrical characteristics of the polymer matrices [29,30]. However, the use of this kind of nanofillers for the manufacture of polymer nanocomposite materials comprising controlling the orientations and the dispersion of the nanofillers is a huge challenge due to the high manufacturing cost with the presence of some difficulties in the polymer matrix (isotropic) as like dispersion, dispersion and orientation [27,28,31].

Nanocomposites containing certain nanoparticles display a diversity of distinct properties, including electrical, optical, magnetic, thermal, mechanical, and surface wear. The huge surface area of the nanofillers is the major explanation because of its prediction to have a substantial influence on polymer crystallization behavior. The polymer processing (film blowing, injection molding, and extrusion) does not always involve isothermal crystallization conditions, knowing the factors driving crystallization is essential for improving processing conditions and ultimate product quality [32]. The crystallinity degree and the morphology (crystal sizes and crystalline structure) of semicrystalline polymers are heavily affected by crystallization circumstances. The most well-known crystallization effects include heterogeneous nucleation and transcrystallinity [33]. By lowering the required enthalpy of recrystallization at the melt solid interface, the surfaces of the nanofillers may induce the heterogeneous nucleation effect in a polymer at the melting state. Chain mobility at the particle surface may have a significant impact on crystallization because nanoparticles have such a large surface area [34]. The shape of the polymer chain is also affected by the interfacial adhesion and/ or polarity of the used nanoparticles and the chain of the polymer matrix.

This chapter describes recent developments in understanding the crystallization and rheological behavior of polymer nanocomposites. It all begins with the most popular nanofillers, then examines how the integration of nanofillers in polymer matrix impacts polymer chain topologies, and enhances the performances and functionalities of polymer nanocomposites, particularly rheological and crystallization characteristics [34,35]. Technical challenges and future perspectives are discussed at the end of this chapter.

## 2.2 Classification of nanofillers in polymer nanocomposites

Several publications on polymer nanocomposites have been published in recent years, covering a wide range of topics such as preparation, processing, and properties (physical and mechanical as well as thermal and mechanical properties and functional applications). There are three types of nanofillers: one-dimensional (1D; rod-like), two-dimensional (2D; sheetlike), and three-dimensional (3D; nanoparticles). There are three fundamental types of nanoreinforcements, as classified by Ramanathan et al. [36] and highlighted in Fig. 2.1:

1. *One-dimensional nanofillers* or fillers with cylinder or rod-like dimensions, such as MMT clay and nanographene platelets, as well as CNTs, are characterized with at least one dimension

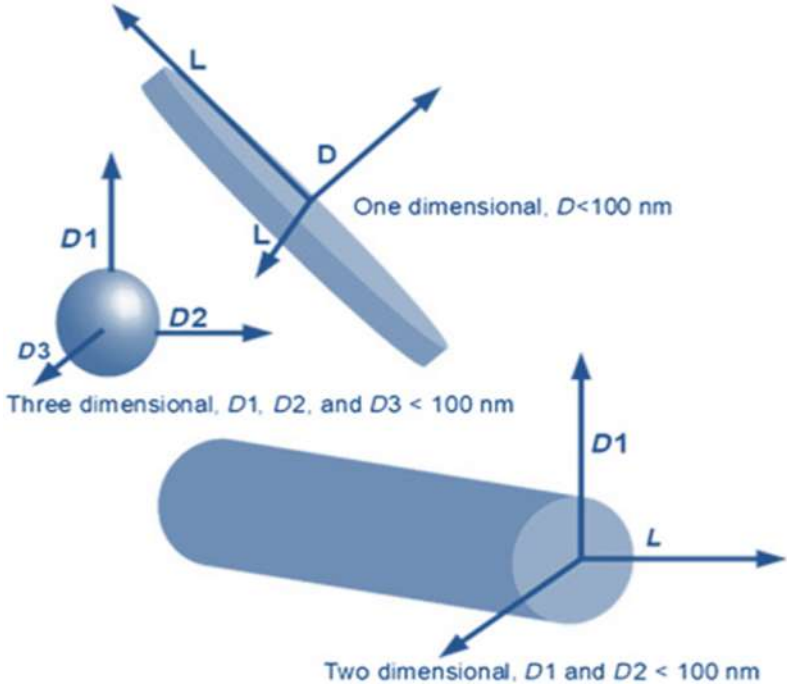


**Figure 2.1** Classification of Nanofillers[36].

sized lesser than 100 nm. They are frequently shaped as nanosized sheets with thicknesses around a few nanometers and with length may attain hundreds of thousands of nanometers in. One-dimensional nanofillers are available in a varied choice of forms and sizes.

2. *Two-dimensional nanofillers* or nanotubes and nanofibers which diameter is lower than 0.1 μm. Nanofillers with a size less than 100 nm in two dimensions are named two-dimensional nanofillers. They typically are tubes, fibers, or filaments in the shape.
3. *Three-dimensional nanofillers or nanoparticles*, despite their lengthy history, are not novel types of nanofiller. Spherical particles occur when all three dimensions of the particles are inside the nanometer range (100 nm). Because of their reduced size, these nanoparticles outperform 1D and 2D nanofillers.

## 2.3 Use of nanofillers in nanocomposite materials

The science of reinforced composites has revealed that filter materials' size and shape have a tremendous effect on the final composite qualities [7,37]. The size and form of a nanofiller influence its surface interactions with the matrix, as well as its adherence and filler movement. This is particularly true at the nanoscale, where many of these effects become more pronounced as the size of the nanofiller decreases [38,39]. To address the limitations of conventional micrometer−scale polymer composites, nanoscale filled polymer nanocomposites with filler smaller than 100 nm and an aspect

ratio of at least 100 were created. It is well known that there is a thin interphase layer around the fillers in polymer matrix composites, in which the polymer chains have a different conformation than their bulk counterparts [5,6]. The significance of nanocomposites materials stems from their multifunctionality and capacity to create new combinations of characteristics that are not achievable with traditional materials. The inclusion of nanomaterials in polymeric structures allows for the modification of mechanical, thermal, electrical, or barrier characteristics, thus broadening their application areas. As previously mentioned, the dispersion of the nanofiller and its interaction with the matrix are two of the controlling factors for the characteristics of nanocomposites. Both are affected by the use of chemical treatment on the filler's surface. This surface treatment applies to all types of nanofillers. Pretreatment is required for the usage of nanofillers in thermoplastics and thermoset resins to enhance the interfacial interactions between the filler and the matrix. Functionalization enhances the intercalation of polymer chains between layers by introducing suitable organic connections between the matrix and the filler. Nanofillers may be readily distributed in polymer matrices. Using the solution blending method, many polymer nanocomposites containing nanofillers such as graphene, clay, and CNT were created. To produce nanocomposites, nanofillers and water-soluble polymers such as poly(vinyl alcohol) (PVA) and chitosan were mixed. This technique of generating polymer nanocomposites via solution processing is efficient. However, the molten mixing technique is the most cost-effective and interesting approach for dispersing nanofillers in the polymer matrix. This technique is also suitable for compounding nanofillers with polymer matrices. Tiouitchi et al. [40] have developed, using a micro-twin-screw extruder, a nanocomposite based black phosphorus (BP) as nanofillers, and polyvinylidene fluoride (PVDF) matrix. The results (Fig. 2.2) indicated the BP nanofillers were altered without aggregation formation inside of the polymer chain matrix. The surfaces are generally level and smooth which may designate that BP nanofillers were dispersed uniformly inside PVDF. The nonappearance of the filler agglomeration on the nanocomposites'

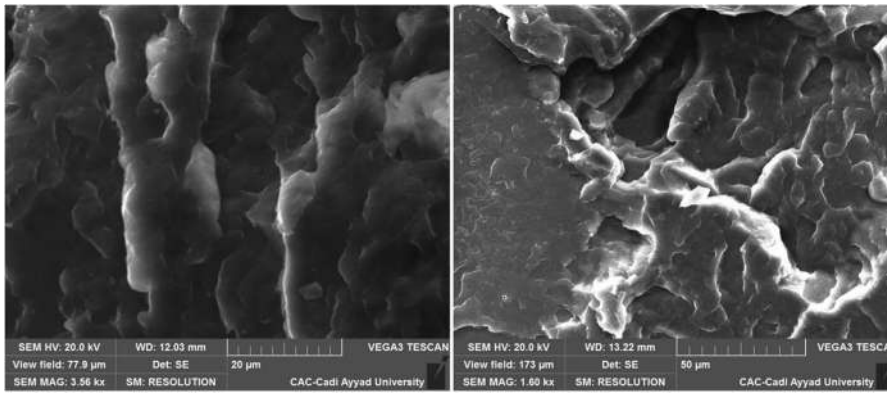


**Figure 2.2** SEM micrograph of nanocomposites based on 2.5 wt.% black phosphorus nanoparticles [40].

surfaces also confirms their good dispersion and distribution. This result shows that suitable processing conditions have been utilized to attain a uniform distribution as well as an excellent affinity of BP nanofillers to the PVDF matrix.

New nanofiller dispersion and distribution methods, on the other hand, are continuously being developed. To optimize their advantages as effective reinforcements in high-strength nanocomposites, nanofillers must not form aggregates and be dispersed properly to prevent slippage. Only a few strategies of improved nanofiller dispersion in polymer matrices include optimized physical mixing, in situ polymerization, or chemical functionalization. The easiest and best strategy to improve the scatter of nanofillers in the polymer matrix is to use optimal physical mixing techniques, such as ultrasonic and high-speed shearing, for high-energy dispersion. It is conceivable to function both covalent and noncovalent. Chemical bonds are created on nanofillers, whereas noncovalent functionality involves methods such as enveloping nanofillers via numerious electromagnetic interactions or adsorption forces like as van der Waal forces, hydrogen bonds, π-π interaction, and electrostatic interactions. Zhou et al. [41] synthesized silane-functionalized multiwalled CNTs and dispersed them in a suitable solvent such as ethanol using ultrasonication. The composites were then created using a melt mixing method with polypropylene. The effects of kaolinite bleaching and functionalization on the mechanical and thermal characteristics of polyamide 6 nanocomposites were studied by Raji et al. [42]. Using a displacement technique, bleached kaolinite was changed with dimethylsulfoxide and then methanol (MeOH) (Fig. 2.3). Thus triethoxy(octyl)silane and cetyltrimethyl ammonium bromide molecules were intercalated into kaolinite nanoplatelets. Using pure, bleached, or intercalated kaolinite, seven different kinds of nanocomposites were created. Results show that kaolinite intercalation improves distribution, improves interfacial adhesion, and increases kaolinite nanoparticle aspect ratio; this provides remarkable improvements to the nanocomposite properties, with a high Young's modulus value of 4.68 GPa with a maximum percentage growth of 80.6% in the silane grafted kaolinite nanoparticles at 8 wt.%.

The surfactant or polymer can thread or wrap around a CNT surface and impair the interaction between Van der Waals that causes nanotubes to aggregate into a group. The effects of different surfactants in natural rubber (NR)-based nanocomposites reiforced with single-walled carbon nanotubes (SWNTs) were investigated by Anand et al. [43]. They employed different surfactants including sodium dodecylbenzene (NaDDBS), sodium dodecyl sulfate, PVA, and sodium benzoate. Due to the presence of aryl groups and the comparatively lengthy alkyl chain, NaDDBS was discovered to be a very good surfactant. The homogeneous dispersion and adjustable matrix alignment of the CNTs are critical for mechanical properties enhancement.

## 2.4 Crystallization properties of polymer nanocomposites

Crystallization is the phase of transformation into a selected crystal structure, which generally is made at temperatures lower than the balance temperature of the melting

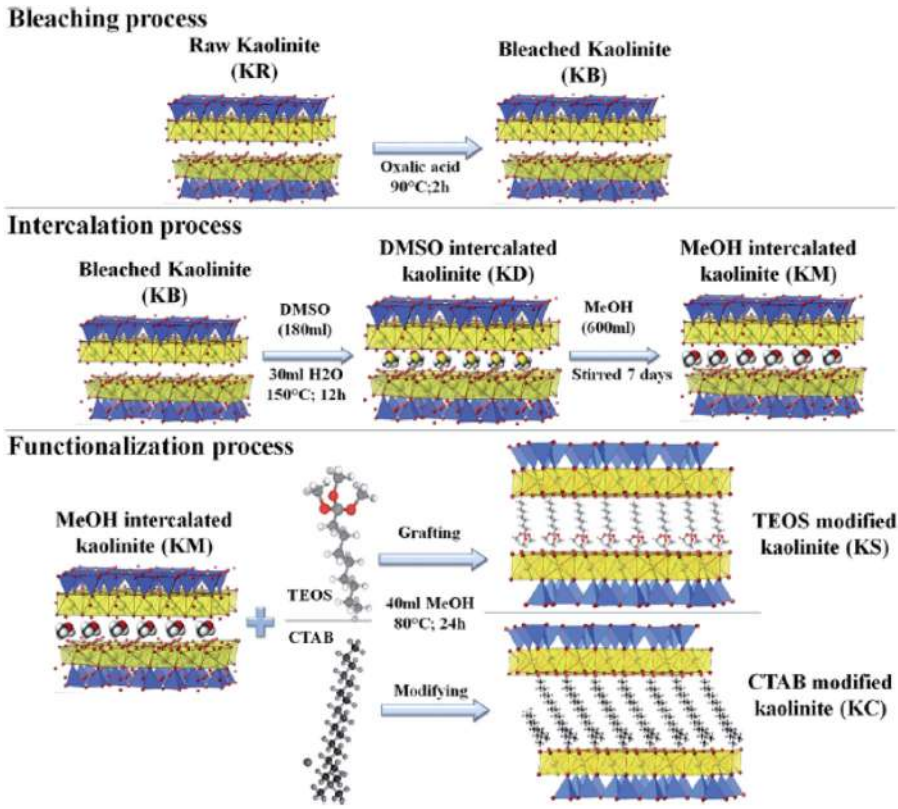


**Figure 2.3** Schematic of the chemical treatments of the kaolinite nanoparticles [42].

(Tm) [44,45]. The entire process can be detached into three phases: starting by nucleation phase, crystal growing, and secondly perfection/crystallization [46]. The process of creating a crystal nucleus in the melt state is known as primary nucleation. Nuclei can be formed homogeneously by the statistical fluctuation of chain segments in the melt, or heterogeneously by the presence of heterogeneities. Polymer nucleation is frequently heterogeneous, beginning on the surfaces, cavities, or fractures of insoluble impurities [47]. Following the formation of the nucleus, crystalline lamellae arise and can build a variety of superstructures. Spherulite is the most typical semicrystalline shape found during melt solidification [42].

The formation of bubbles from a liquid is an example of nucleation or the beginning of a phase transition in a small region. The existence of a second phase in the solution, such as a surface from an additional polymer or foreign particle, determines whether the nucleation is homogeneous or heterogeneous. The intermolecular interactions of parallel arrays of polymer chains first produce a stable nucleus [48,49]. When the temperature goes below the melting point (Tm), the molecules prefer to migrate to their lowermost energy conformation, which leads to a stiffer

chain segment. As a consequence, the development of a stable polymer chain, and therefore a stable nucleus, will be promoted. Small particles stimulate secondary nucleation and increase the stability of the nuclei formed. In polymer melts, nucleation is typically heterogeneous, with impurity surfaces, voids, or fissures serving as initiators. Homogeneous crystal nucleation is the formation of small aggregates from a few parallel chains known as nuclei, which are sufficiently stable if they have a supercritical size to begin the crystal growth of their surface [48]. The cryptographic temperature determines the minimal nucleus required for stability, which lowers as supercooling increases (Tc). Increased supercooling or lowered crystallization temperature allows for the crystallization of smaller nuclei. This corresponds to kinetic constraints such as an increase in the feature time of transit to the growth front of chain segments or a drop in the mobility scale. The assessment and management of crystallization behavior is a critical topic in polymer manufacturing. The crystallization rate can affect both the productivity of a manufacturing line and the product quality. Polymer crystallization speed may be adjusted by altering the material composition or formulation, as well as process parameters, depending on the kind of processing (e.g., extrusion, injection, or blow-molding) and the desired characteristics of the finished products. Crystallization can be accelerated by using nucleating or clarifying agents, for example. Similarly, crystallization rates may be influenced by changing processing temperatures. Material characteristics vary as a result of changes in material formulation and processing conditions, which influence crystallinity, crystal thickness and morphology, crystal structure, and other variables, all of which have an impact on bulk material attributes [50,51].

Analyzing polymer crystallization behavior is critical for identifying whether processing or formulation changes are necessary to adapt to crystallization circumstances. To monitor, measure, and simulate polymer crystallization, a variety of calorimetric techniques, including temperature-modulated differential scanning calorimetry, differential scanning calorimetry (DSC), and rapid scanning chip calorimetry, can be utilized. Calorimetry is most utilized for studying polymer crystallization. The overall crystallization processes are measured via the superposition of crystal nucleation and evolution of growth, which is most commonly measured using DSC [52−54]. This known method investigates the time requirement for enhancing the crystallinity at numerous crystallization temperatures. Optical methods are often employed to measure nucleation rates and densities, which allow for a quantitative assessment of the number of crystals formed per unit volume of nuclei. Differential scanning calorimetry is used to determine the polymer's degree of crystallinity as well as the temperatures of crystallization and melting. In general, the mechanical properties of semicrystalline thermoplastic polymers are directly linked to the microstructure and crystallinity of the polymer. To look into the effects of BP as nanofillers (for PVDF matrix) [37] on fusion characteristics and crystallization of neat polymer, heating/cooling/heating cycles at a rate of 10°C per minute were carried out. However, because nanocomposites hardened at ambient temperature after extrusion, the thermal history of the samples may be deleted before investigating by eliminating the first heating cycle. The first cooling cycle produced crystallization data, whereas the second heating cycle produced melting data [55].

Results of this study conducted by Tiouitchi et al. [40]. The crystallization enthalpy of the PVDF matrix varies as the concentration of BP nanoparticles grows from 1 to 5 wt.% (Fig. 2.4). Furthermore, compared to pristine PVDF, nanocomposites with 2.5 wt.% BP concentration have the maximum crystallization enthalpy; however, when the BP level (5 wt.%) is increased, the crystallization enthalpy drops. The PVDF crystallization influence of the reduction is related to the crystallization degree and the impact of the dispersed nanofillers acting as nucleating agents. Molecular polymers can crystallize either on their own (homogeneous nucleation) or with the help of a nucleating agent (heterogeneous nucleation). In our case, the nuclear impact is good at low concentrations (1% and 2.5), but at higher concentrations (5%), the high particle quantity cannot create nuclear power efficiently owing to nanofiller interactions and a limited area for crystal nucleation/growth. The temperature of crystallization, on the other hand, follows the same trend as the enthalpy. The temperature of crystallization peaks at a pure PVDF (137.8°C) concentration of BP at 2.5 wt.% (139.1°C). A greater temperature for crystallization indicates that germination/nucleation has begun, and the material crystallizes more quickly than at a lower temperature. Given the effect of BP on the crystallization rate of PVDF, the higher crystallization (Tc) at 2.5 wt.% concentration may be explained. Because of the heterogeneous nucleation influence in nanocomposite materials, BP plays a key role in the rapid crystallization of PVDF when it is cooled out of melt as a nanofiller.

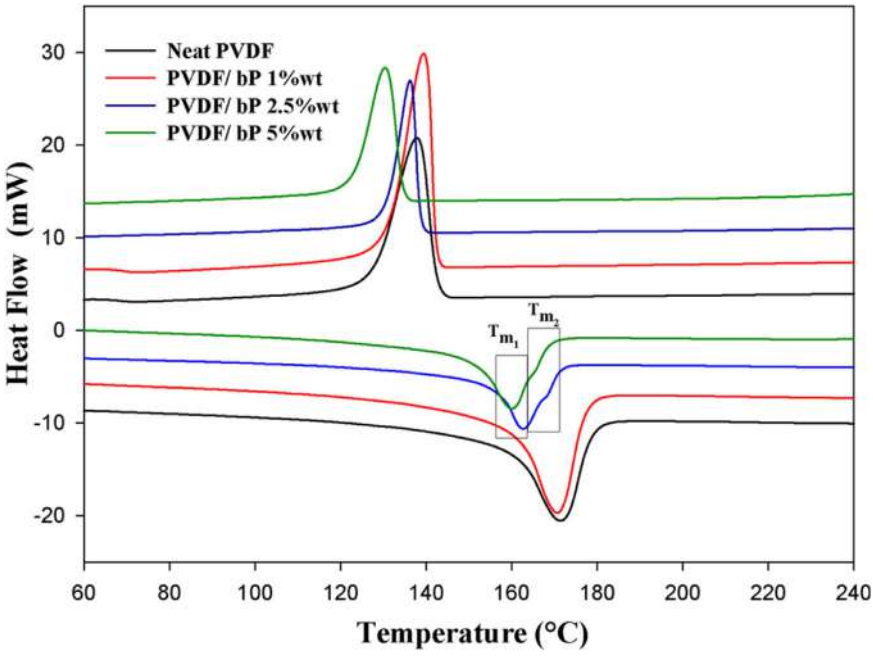


**Figure 2.4** Crystallization of nanocomposites based on black phosphorus as nanofiller and PVDF matrix [40]. *PVDF*, Polyvinylidene fluoride.

In this context, Bhadu et al. [56] have studied the impact of the state of dispersion of trisilanolphenyl (TSP)-polyhedral oligomeric silsesquioxane (POSS) melt blended with poly (trimethylene terephthalate) on the rheological, melting, and crystallization properties via the utilization of the corotating twin-screw extruder with three kneading zones. The inclusion of TSP-POSS increased the crystallization degree and led to producing a crystal with limited distribution−dispersion, according to DSC findings. TSP-POSS serves as a nucleating agent and a flow promoter at lower concentrations, according to the findings. The features of a polymer matrix influencing the characteristics of the nanocomposites with an emphasis on crystallization were examined by Kaur et al. [57]. Their results demonstrate the substantial relationship between the crystallization temperature and the loading and dispersion level of nanoparticles. This has been attributed to the unable to rearrange the polymer chains because of limited mobility in the fusion. In other words, as the quantity of additional nanoparticles increases the viscosity of the polymer melt. As a result, the larger the level of crystallinity in the material, the fewer nanoparticles have been loaded. El Achaby et al. [58] studied nanocomposites based on nanofillers of graphene and polypropylene (PP) matrices have been studied for their crystallization properties. Crystallization enthalpy (Hc) increases with increased graphene content. The crystallization enthalpy enhancement in the nanocomposites is associated with a greater degree of crystallization of neat PP matrix as the scattered filler works play the role of nuclear agent during PP crystallization. Graphene nanosheets (GNs) change the crystallization performances of PP, which is essential to understanding the mechanical characteristics of such nanocomposites. Adding GNs impacts the melting temperatures of neat PP by increasing the concentration of GNs. However, the impact of bleaching treatment and functionalization process of kaolinite on the mechanical and thermal properties of reinforced polyamide 6 nanocomposites was investigated by Raji et al. [42]. The nanofillers employed in this study did not play the role of nucleating agent, which is a substance that helps crystal nuclei form. In comparison to the conventional PA6 polymer, the crystallinity degrees (Xc) of the nanocomposites increased. This is because the kaolinite nanoparticles interacted with PA6 chains; this reduce the mobility of the PA6 chains, causing the crystallization procedure to be hindered. The addition of multi-walled carbon nanotubes (MWCNT) may alter the nonisothermal crystallization kinetics of PVDF, but it did not affect the polymer's crystalline polymorphs [59]. The inclusion of nanoparticles has been shown to affect the polymer's initial properties, either positively or negatively. Because all of these characteristics are crucial to material performance, the influence of such nanoparticles on the crystallization procedure, the types of morphology generated, and the crystalline structure formed is of significant interest. Understanding such processes, however, necessitates familiarization with mechanisms in the creation of a pure or single polymer in polymers including nanoparticles. Nucleation, development of spherulite, and subsequent growth were all described as crystallization stages. The nuclear procedure is used to explain the stage restricting the crystallization. The optimization of the nucleation process thus impacts kinetic crystallization. There is still a discussion on the usage of nanoscale components in polymer mixes. On the other hand, surface chemistry,

particle dimension, and the type of modifications to nanoparticles may all impact crystallization and kinetics.

## 2.5 Rheology of polymer nanocomposites

Studying the rheological properties of polymer nanocomposites in a molten state is fundamental to both their processing and the comprehension of their microstructure and dynamics. Processing of polymer nanocomposites requires, thus, information on the rheological properties which depend on the interactions between nanofiller and polymer chains [60–62]. Increasing the viscosity of the melt by adding nanofillers to the polymer causes processing issues. This necessitates a thorough understanding of their rheological behavior during the manufacturing process. The most challenging problem during the production of nanocomposites is the aggregation propensity of the nanofillers [63,64]. Because of their enormous specific surface area, nanoparticles can aggregate extremely fast, and the aggregation can be a defect center and occasionally cause a deterioration of the polymer's mechanical properties [38,65,66].

The type of the structure formed by the interactions between components, the amount of intercalation/exfoliation, the applied stresses, and the form of phase distribution and flow domain orientation all influence the rheology of a nanofiller-based nanocomposite. Intercalant attachment of macromolecules to nanofillers may result in "end-tethers," which resemble highly branched nanofillers and are significantly influenced by the external flow field. The interfacial strength of the filler and polymer is an important factor in the production of filler/polymer nanocomposites [67,68]. The absence of adherence between the filler and polymer might lead to the creation of nanocomposite aggregates that are tightly bound, or it can lead to an early interface defect, and therefore change the physical characteristics. To avoid nanofillers aggregation, it is important to know the kinetics of this process [69,70].

The linear viscoelastic behavior of polymer nanocomposites has recently been explored in the literature since it was revealed to be very sensitive to the microstructure of the nanofiller–polymer nanocomposite. Because of their exceptionally high aspect ratio (length-to-diameter ratio), nanofillers (1D, 2D, or 3D) can alter the rheological characteristics at very low loadings, with a significant rise in the storage modulus and the detection of apparent yield stress at low frequencies [71,72]. The higher viscoelasticity modulus, among other things, indicates the limited mobility of the nanofillers. The existence of a percolated network structure, which contributes to nanocomposite viscoelasticity, leads the polymer nanocomposites to transition from a viscous fluid to a solid-like behavior as the nanofiller content rises. In nanocomposites, the dispersion state, aspect ratio, and nanofiller alignment all affect the linear viscoelastic behavior [39].

A thermoplastic polymer's complex viscosity ($n^*$) often consists of two different behaviors: Newtonian behavior and resolidifying activity (shear thinning). The first characteristic is found at low frequencies and is defined by the viscosity's

independence from frequency. Rheofluidifying behavior, on the other hand, is observed at high frequencies and is characterized by a linear reduction in viscosity with increasing frequency. El Achaby et al. [58] The rheological properties of nanocomposites based on polypropylene reinforced with GNs at various concentrations were investigated (0.2, 0.5, 1, 1.5, 2, 3 wt.%). At 200°C and frequencies ranging from $10^{-2}$ to $10^{2}$ Hz, the nanocomposites were exposed to small-amplitude oscillatory shear flow. Fig. 2.5 depicts the measured dynamic viscosity. The complex viscosity was found to increase with increasing graphene content. The neat PP demonstrates Newtonian behavior at low frequencies (1 Hz) and shear-thinning behavior at high frequencies (1 Hz). The Newtonian plateau began to disappear at 1% GNs content, indicating that the nanosheets began to form a continuous network. And when GNs content is greater than 1.5%, the Newtonian behavior is completely disappeared. The development of a GN network in the PP matrix and the shift to a solid-like viscoelastic answer are all accompanied by this. The threshold of rheological percolation is around the GNs level of 1 wt.%. These measurements were carried out to characterize the quality of the dispersion GNs in the PP matrix, the degree of surface interaction among the GNs and the PP chains, and the structure of the rheological percolation threshold.

Numerous factors including the clay−matrix interactions and clay−clay network that may influence the viscoelasticity and the manufacturing process of the epoxy/clay (MMT) nanocomposite were investigated by Wang et al. [71]. The incorporation of clay nanofillers leads to a significant change in viscosity. The low shear region is a distinguishing of nanofiller, whereas the matrix's behavior dominates in the high shear region. In most cases, the neat polymer displays a Newtonian flow at all shear rates; (however, the use of clay as nanofillers may create predominant non-Newtonian comportment with a strong shear-thinning effect). Adding colloidal fillers (clay) of 1% weight to Newtonian fluid (epoxy) improves the medium's viscosity by exercising quadrupolar stress on the fluid. The reduction of the Melt Flow

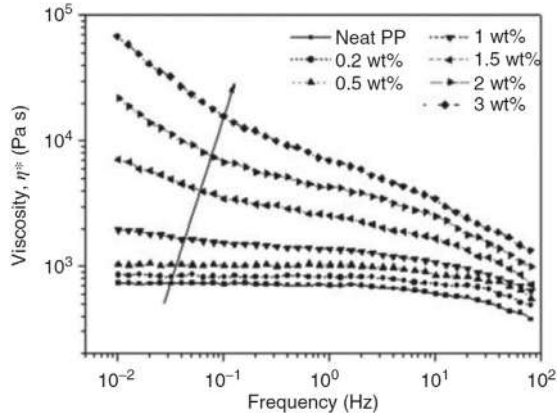


**Figure 2.5** Complexes viscosity measurement as a function of GNs content and frequency [58].

Index is due to changes in nanofillers or processing conditions indicates an increased degree of nanofiller dispersion. Viscosity control during thermoset processing is especially important because viscosity varies not only with temperature and flow conditions but also with time due to polymerization reactions.

The impact of maltaised propylene in the rheology of nanocomposite polypropylene based on organophilic MMT clay compatible with polypropylene maltaised (PP-g-MA) has been investigated by Wang et al. [73]. The results reveal that the $\eta^*$ range in all samples is much higher at a low frequency. The complicated viscosity of nanocomposites at low frequencies significantly change depending on the filler network, the behavior of $\eta^*$ shows the change from fluid to pseudosolid. The long-lasting characteristic is due to the existence of randomly oriented anisotropic stacks in silicate layers, which form a percolated network structure unable to fully relax. The distinctive structure of the network becomes more evident as the degree of clay dispersion increases.

For nanocomposite, dynamic shear flow, also known as nonterminal viscoelastic behavior, was often found. Furthermore, the initial slopes of the G' and G" moduli are entirely independent of the nanocomposite structure, that is, whether it is end-tethered or intercalated, but are mainly determined by the number of nanofillers loaded [74,75]. As the nanofiller loading rises, the dynamic moduli increase significantly, particularly in the low-frequency region. The slopes of G' and G" for nanocomposites, on the other hand, are much smaller than for traditional microcomposites and unfilled resin. The form and size of the filler, the filler loading, and the degree of any particle interactions are all critical factors to consider [74,75]. In addition to the filler network and the interaction of filler-matrices, the study group of Kalfus and Jancar [76] It was discovered that a stiff interface with restricted mobility of matrix chains could be addressed, causing the nanocomposite structure to be disrupted at high strain amplitudes. G' does not fall monotonically as frequency drops but rather exhibits a little plateau with the lowest frequencies. This apparent plateau, which might impede the molecular rearrangement of the epoxy matrix, could be justified by a percolated micronetwork of anisometric clay feuillets. The absence of this peak after the hardener mix could be related to the hardener's lubrication or plasticization effect on the clay and epoxy resin at lower temperatures. The activity of the clay network at higher temperatures compensated for this influence by reemerging at lower frequencies of the G' plateau.

This was also seen by El Achaby et al. [58] for the clear PP, whereas G' and G" begin to decline with frequency dropping and display a clear terminal area at low frequencies values (Fig. 2.6). However, the G' of PP-nanocomposite rises with increasing GNs content across all frequency ranges (0.01−100 Hz). At low frequencies, the PP chains are completely loosened and exhibit normal homopolymer behavior. G' has been somewhat enhanced in nanocomposites with 0.2% and 0.5% GNs content, but the material has the same viscoelastic behavior as PP, suggesting that 0.2−0.5 wt.% is inadequate to limit polymer chain relaxation. But at 0.5 wt.%, with rising GN content, storage increases and shows a low-frequency pseudo plateau. This nonterminal behavior showed at low frequencies is attributed to the formation of a 3D network of GNs with a variable density depending on the GNs

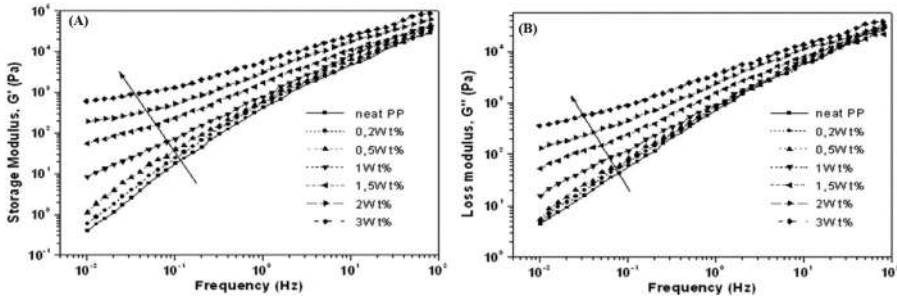


**Figure 2.6** The melt rheological results of the nanocomposites versus the GNs content and frequencies: (A) storage modulus (G'); (B) storage modulus (G") [58].

concentration, resulting in polymer chain restriction. This seems to happen at a percolation threshold attained between 0.5 and 1 wt.% particle content. Fig. 2.6, on the other hand, reveals that the G" follows a similar pattern to the G', where G" grows as the number of contents GNs increases.

In this respect, Prolongo et al. [77] conducted a comparative examination of the influence on rheological and electrical features of epoxy resins of carbon nanofibers (CNFs) and nanotubes CNTs, as well as the nanofiller content of epoxy adhesives. For the same amount of carbon nanofiller, the authors conclude that the viscosity of CNT is considerably larger than that of CNF. The viscosity at 0.5% of CNT content is showing a value greater than that at 1% CNF. This effect might be ascribed to CNTs having a higher specific surface area, which leads to better dispersion. The viscosity measurements are useful for establishing the appropriate amount of nanofillers, and the viscosity of the nanocomposites resin should be close to that of epoxy resin to ease the manufacturing process and give a high dispersion and distribution of nanofiller into the resin. In the case of CNT, the nanofiller content must be less than 0.25 wt.%, whereas the CNF percentage could attain a value close to 1 wt.% [77]. This difference in nanofiller content is due to the greater specific surface area of CNT (approximately 300 $gm^{-2}$) versus that of CNF ($150-200\ g\ m^{-2}$), which produces significant viscosity increases at lower nanofiller concentrations. The use of more nanofillers than is recommended may result in an increase in viscosity, which will make it harder to make excellent joins owing to a reduction in adhesive wettability.

## 2.6 Conclusion

This chapter has covered the rheology and crystallization of polymer composites. The linear viscoelastic of polymer−composites melt at low frequencies revealed that the polymer matrix still dominates the viscoelastic properties of the nanocomposites at low nanofillers contents, whereas increasing the nanofillers loading causes the nanocomposite to transition from liquid to solid-like behavior. Rheological measurements

are used to determine the "rheological percolation threshold," which is determined by polymer chain immobility in a mixed nanofiller−polymer network. The nanofillers' dispersion state was observed to impact the percolation threshold. However, the complex modulus was primarily influenced by the matrix's viscoelasticity in the high-frequency results. The crystallization conditions have a significant impact on the final structure and physical properties of polymeric nanocomposites. The crystallization kinetics of polymer nanocomposites has attracted the interest of researchers because nanofillers function as an effective nucleating agent in the polymer matrix. As nanotechnology advances, the emphasis is shifting toward understanding the crystalline features of materials in nanodimensions and, as a consequence, adjusting the properties for a variety of tailored applications.

## References

[1] A. Bhat, S. Budholiya, S.A. Raj, M.T.H. Sultan, D. Hui, A.U.M. Shah, et al., Review on nanocomposites based on aerospace applications, Nanotechnol. Rev. 10 (2021) 237−253. Available from: https://doi.org/10.1515/NTREV-2021-0018.

[2] H. Bai, G. Ge, X. He, B. Shen, J. Zhai, H. Pan, Ultrahigh breakdown strength and energy density of polymer nanocomposite containing surface insulated BCZT@BN nanofibers, Compos. Sci. Technol. 195 (2020) 108209. Available from: https://doi.org/10.1016/j.compscitech.2020.108209.

[3] M. Raji, M. El, M. Mekhzoum, A.el K. Qaiss, R. Bouhfid, Nanoclay modification and functionalization for nanocomposites development: effect on the structural, morphological, mechanical and rheological properties, Nanoclay Reinf. Polym. Compos. (2016) 1−34. Available from: https://doi.org/10.1007/978-981-10-0950-1.

[4] H. Bensalah, M. Raji, H. Abdellaoui, H. Essabir, R. Bouhfid, A. el kacem Qaiss, Thermo-mechanical properties of low-cost "green" phenolic resin composites reinforced with surface modified coir fiber, Int. J. Adv. Manuf. Technol. (2021) 1−14. Available from: https://doi.org/10.1007/s00170-020-06535-9.

[5] H. Essabir, M. Raji, E.M. Essassi, D. Rodrigue, R. Bouhfid, A. el kacem Qaiss, Morphological, thermal, mechanical, electrical and magnetic properties of ABS/PA6/SBR blends with Fe3O4 nano-particles, J. Mater. Sci. Mater. Electron. 28 (2017) 17120−17130. Available from: https://doi.org/10.1007/s10854-017-7639-2.

[6] H. Bensalah, K. Gueraoui, H. Essabir, D. Rodrigue, R. Bouhfid, A.E.K. Qaiss, Mechanical, thermal, and rheological properties of polypropylene hybrid composites based clay and graphite, J. Compos. Mater. 51 (2017) 3563−3576. Available from: https://doi.org/10.1177/0021998317690597.

[7] M. Malha, S. Nekhlaoui, H. Essabir, K. Benmoussa, M.O. Bensalah, F.E. Arrakhiz, et al., Mechanical and thermal properties of compatibilized polypropylene reinforced by woven doum, J. Appl. Polym. Sci. 130 (2013) 4347−4356. Available from: https://doi.org/10.1002/app.39619.

[8] C.A. Kakou, H. Essabir, M.-O. Bensalah, R. Bouhfid, D. Rodrigue, A. Qaiss, Hybrid composites based on polyethylene and coir/oil palm fibers, J. Reinf. Plast. Compos. 34 (2015) 1684−1697. Available from: https://doi.org/10.1177/0731684415596235.

[9] M.D. Arit, M.A. Rahman, M.M.H. Milu, A.B. Siddik, M.E. Hogue, Green nanomaterials: synthesis, properties and spectroscopic applications, Nanomater. Spectrosc. Appl. (2021) 213−272. Available from: https://doi.org/10.1201/9781003160335-8.

[10] H. Essabir, E. Hilali, A. Elgharad, H. El Minor, A. Imad, A. Elamraoui, et al., Gaoudi, Mechanical and thermal properties of bio-composites based on polypropylene reinforced with Nut-shells of Argan particles, Mater. Des. 49 (2013) 442–448. Available from: https://doi.org/10.1016/j.matdes.2013.01.025.

[11] F.Z. El Mechtali, H. Essabir, S. Nekhlaoui, M.O. Bensalah, M. Jawaid, R. Bouhfid, et al., Mechanical and thermal properties of polypropylene reinforced with almond shells particles: impact of chemical treatments, J. Bionic Eng. 12 (2015). Available from: https://doi.org/10.1016/S1672-6529(14)60139-6.

[12] E.D. Martínez, A. Prado, M. Gonzalez, S. Anguiano, L. Tosi, L. Salazar Alarcón, et al., Recent advances on nanocomposite resists with design functionality for lithographic microfabrication, Front. Mater. 0 (2021) 16. Available from: https://doi.org/10.3389/FMATS.2021.629792.

[13] Y.Y. Lin, Y. Chien, J.H. Chuang, C.C. Chang, Y.P. Yang, Y.H. Lai, et al., Development of a graphene oxide-incorporated polydimethylsiloxane membrane with hexagonal micropillars, Int. J. Mol. Sci. 19 (2018). Available from: https://doi.org/10.3390/ijms19092517.

[14] M. Raji, E. Essassi, H. Essabir, D. Rodrigue, A. El kacem Qaiss, R. Bouhfid, Properties of nano-composites based on different clays and polyamide 6/acrylonitrile butadiene styrene blends, Bio-based Polymers and Nanocomposites: Preparation, Processing, Properties & Performance, Springer International Publishing, 2019, pp. 107–128. Available from: https://doi.org/10.1007/978-3-030–05825-8_6.

[15] K. Yan, C. Mu, L. Meng, Z. Fei, P.J. Dyson, Recent advances in graphite carbon nitride-based nanocomposites: structure, antibacterial properties and synergies, Nanoscale Adv. 3 (2021) 3708–3729. Available from: https://doi.org/10.1039/D1NA00257K.

[16] M.C. Biswas, B. Jony, P.K. Nandy, R.A. Chowdhury, S. Halder, D. Kumar, et al., Recent advancement of biopolymers and their potential biomedical applications, J. Polym. Environ. 2021 (2021) 1–24. Available from: https://doi.org/10.1007/S10924-021-02199-Y.

[17] A. Tuteja, P.M. Duxbury, M.E. Mackay, Multifunctional nanocomposites with reduced viscosity, Macromolecules. 40 (2007) 9427–9434. Available from: https://doi.org/10.1021/ma071313i.

[18] M.E. Mackay, T.T. Dao, A. Tuteja, D.L. Ho, B. Van Horn, H.C. Kim, et al., Nanoscale effects leading to non-einstein-like decrease in viscosity, Nat. Mater. 2 (2003) 762–766. Available from: https://doi.org/10.1038/nmat999.

[19] R. Bouhfid, H. Essabir, A. El Kacem Qaiss, Graphene-based nanocomposites: mechanical, Therm Electric Rheol Prop. (2016). Available from: https://doi.org/10.1002/9781118969809.ch12.

[20] Fabrication of Hierarchical Nanocomposites through a Nature-Mimic Method: Depositing MoS2 Nanoparticles on Carbon Nitride Nanotubes by Polydopamine Coating, (n.d.). https://www.hindawi.com/journals/jnm/2021/6668393/ (accessed 08.08.21.).

[21] K.F. Amin, A. Asrafuzzaman, Sharif, Md. Enamul Hoque, Bamboo/bamboo fiber reinforced concrete composites and their applications in modern infrastructure, Bamboo Fiber Compos. (2021) 271–297. Available from: https://doi.org/10.1007/978-981-15-8489-3_15.

[22] A. Sharif, S. Mondal, M.E. Hoque, Polylactic acid (PLA)-based nanocomposites: processing and properties, Bio-Based Polym. Nanocomposites Prep. Process. Prop. Perform. (2019) 233–254. Available from: https://doi.org/10.1007/978-3-030-05825-8_11.

[23] J. Anita Lett, S. Sagadevan, I. Fatimah, M.E. Hoque, Y. Lokanathan, E. Léonard, et al., Recent advances in natural polymer-based hydroxyapatite scaffolds: properties and applications, Eur. Polym. J. 148 (2021) 110360. Available from: https://doi.org/10.1016/J.EURPOLYMJ.2021.110360.

[24] M.E.M. Mekhzoum, H. Essabir, D. Rodrigue, A.el K. Qaiss, R. Bouhfid, Graphene/montmorillonite hybrid nanocomposites based on polypropylene: morphological, mechanical, and rheological properties, Polym. Compos. 16 (2016) 101−113. Available from: https://doi.org/10.1002/pc.

[25] F. Ram, P. Kaviraj, R. Pramanik, A. Krishnan, K. Shanmuganathan, A. Arockiarajan, PVDF/BaTiO3 films with nanocellulose impregnation: investigation of structural, morphological and mechanical properties, J. Alloy. Compd. 823 (2020). Available from: https://doi.org/10.1016/j.jallcom.2020.153701.

[26] Y. Liu, A. Wilkinson, Rheological percolation behaviour and fracture properties of nanocomposites of MWCNTs and a highly crosslinked aerospace-grade epoxy resin system, Compos. Part. A Appl. Sci. Manuf. 105 (2018) 97−107. Available from: https://doi.org/10.1016/j.compositesa.2017.11.012.

[27] H. Essabir, M. Raji, R. Bouhfid, A.el kacem Qaiss, Rheological properties of functionalized graphene and polymeric matrices−based nanocomposites, Functionalized Graphene Nanocomposites and Their Derivatives, Elsevier, 2019, pp. 109−120. Available from: https://doi.org/10.1016/b978-0-12−814548-7.00006-4.

[28] M. Raji, H. Essabir, D. Rodrigue, R. Bouhfid, A. el kacem Qaiss, Influence of graphene oxide and graphene nanosheet on the properties of polyvinylidene fluoride nanocomposites, Polym. Compos. 39 (2018) 2932−2941. Available from: https://doi.org/10.1002/pc.24292.

[29] R. Bouhfid, H. Essabir, A. El Kacem Qaiss, Graphene-based nanocomposites: mechanical, thermal, electrical, and rheological properties, Rheology and Processing of Polymer Nanocomposites, Wiley, 2016, pp. 405−430. Available from: https://doi.org/10.1002/9781118969809.ch12.

[30] A.B. Asha, A. Sharif, M.E. Hoque, Interface interaction of jute fiber reinforced PLA biocomposites for potential applications, Green. Energy Technol. 0 (2017) 285−307. Available from: https://doi.org/10.1007/978-3-319-49382-4_13.

[31] H. Essabir, F.Z. El Mechtali, S. Nekhlaoui, M. Raji, M.O. Bensalah, D. Rodrigue, et al., Compatibilization of PA6/ABS blend by SEBS-g-MA: morphological, mechanical, thermal, and rheological properties, Int. J. Adv. Manuf. Technol. 110 (2020) 1095−1111. Available from: https://doi.org/10.1007/s00170-020-05888-5.

[32] V.P. Cyras, D.A. D'Amico, L.B. Manfredi, crystallization behavior of polymer nanocomposites, Cryst. Multiph. Polym. Syst. (2018) 269−311. Available from: https://doi.org/10.1016/B978-0-12-809453-2.00010-4.

[33] Kusmono, Z.A. Mohd Ishak, W.S. Chow, T. Takeichi, Rochmadi, Influence of SEBS-g-MA on morphology, mechanical, and thermal properties of PA6/PP/organoclay nanocomposites, Eur. Polym. J. 44 (2008) 1023−1039. Available from: https://doi.org/10.1016/j.eurpolymj.2008.01.019.

[34] X. Lu, W. Deng, J. Wei, Y. Wan, J. Zhang, L. Zhang, et al., Crystallization behaviors and related dielectric properties of semicrystalline matrix in polymer-ceramic nanocomposites, Compos. Part. B Eng. 224 (2021) 109195. Available from: https://doi.org/10.1016/J.COMPOSITESB.2021.109195.

[35] T.G. Gopakumar, J.A. Lee, M. Kontopoulou, J.S. Parent, Influence of clay exfoliation on the physical properties of montmorillonite/polyethylene composites, Polymer (Guildf.) 43 (2002) 5483−5491. Available from: https://doi.org/10.1016/S0032-3861(02)00403-2.

[36] T. Ramanathan, A.A. Abdala, S. Stankovich, D.A. Dikin, M. Herrera-Alonso, R.D. Piner, et al., Functionalized graphene sheets for polymer nanocomposites, Nat. Nanotechnol. 3 (2008) 327−331. Available from: https://doi.org/10.1038/nnano.2008.96.

[37] M. Raji, S. Nekhlaoui, I.E.E.A. El Hassani, E.M. Essassi, H. Essabir, D. Rodrigue, et al., Utilization of volcanic amorphous aluminosilicate rocks (perlite) as alternative materials in lightweight composites, Compos. Part. B Eng. 165 (2019) 47–54. Available from: https://doi.org/10.1016/j.compositesb.2018.11.098.

[38] H. Essabir, M. Raji, S.A. Laaziz, D. Rodrique, R. Bouhfid, A.E.K. Qaiss, Thermo-mechanical performances of polypropylene biocomposites based on untreated, treated and compatibilized spent coffee grounds, Compos. Part. B Eng. 149 (2018) 1–11. Available from: https://doi.org/10.1016/j.compositesb.2018.05.020.

[39] M. Raji, H. Essabir, D. Rodrigue, R. Bouhfid, Abou el kacem Qaiss, Influence of graphene oxide and graphene nanosheet on the properties of polyvinylidene fluoride nanocomposites, Polym. Polym. Compos. (2017). Available from: https://doi.org/10.1002/pc.

[40] G. Tiouitchi, M. Raji, O. Mounkachi, M.A. Ali, A. Mahmoud, F. Boschini, et al., Black phosphorus-based polyvinylidene fluoride nanocomposites: synthesis, processing and characterization, Compos. Part. B Eng. 175 (2019) 107165. Available from: https://doi.org/10.1016/j.compositesb.2019.107165.

[41] Z. Zhou, S. Wang, L. Lu, Y. Zhang, Y. Zhang, Functionalization of multi-wall carbon nanotubes with silane and its reinforcement on polypropylene composites, Compos. Sci. Technol. 68 (2008) 1727–1733. Available from: https://doi.org/10.1016/j.compscitech.2008.02.003.

[42] M. Raji, A.E.K. Qaiss, R. Bouhfid, Effects of bleaching and functionalization of kaolinite on the mechanical and thermal properties of polyamide 6 nanocomposites, RSC Adv. 10 (2020) 4916–4926. Available from: https://doi.org/10.1039/c9ra10579d.

[43] A. Anand, Polymer nanocomposites crystallization, reinforcement and conductivity through SWNTs Faculty of Technology, Cochin University of Science & Technology, 2006. http://cusat.ac.in/ (accessed 11.01.21.).

[44] S. Nekhlaoui, H. Essabir, D. Kunal, M. Sonakshi, M.O. Bensalah, R. Bouhfid, et al., Comparative study for the talc and two kinds of moroccan clay as reinforcements in polypropylene-SEBS-g-MA matrix, Polym. Compos. 36 (2015). Available from: https://doi.org/10.1002/pc.22986.

[45] Crystallization of Polymers: Volume 2, Kinetics and Mechanisms - Leo Mandelkern - Google Books, (n.d.). https://books.google.co.ma/books?hl = en&lr = &id = rlYRn4T_nFQC&oi = fnd&pg = PR9&ots = srHTK60EHx&sig = yyLo5qL6UQXNqJULf8CyNJbtaoM&redir_esc = y#v = onepage&q&f = false (accessed 11.01.21).

[46] Y. Ming, Z. Zhou, T. Hao, Y. Nie, Y. Wei, S. Zhang, et al., Insights into the crystallization of polymer nanocomposite systems blended with grafted and free chains studied by molecular simulation, Cryst. Growth Des. 21 (2021) 2243–2254. Available from: https://doi.org/10.1021/ACS.CGD.0C01674.

[47] Effect of Chitin Nanocrystals on Crystallization and Properties of Poly(lactic acid)-Based Nanocomposites. | Sigma-Aldrich, (n.d.). https://www.sigmaaldrich.com/MA/fr/tech-docs/paper/1366365 (accessed 08.08.21.).

[48] M.L. Di Lorenzo, R. Androsch, A.M. Rhoades, M.C. Righetti, Analysis of polymer crystallization by calorimetry, Handbook of Thermal Analysis and Calorimetry, Elsevier B.V, 2018, pp. 253–299. Available from: https://doi.org/10.1016/B978-0-444-64062-8.00007-3.

[49] H. Okamoto, M. Nakano, M. Ouchi, A. Usuki, Y. Kageyama, Improvement of crystallization and mechanical properties of PLA by means of clay nanocomposite, MRS Online Proc. Libr. 791 (2003) 399–404. Available from: https://doi.org/10.1557/PROC-791-Q11.10.

[50] J.L. Carvalho, K. Dalnoki-Veress, Homogeneous bulk, surface, and edge nucleation in crystalline nanodroplets, Phys. Rev. Lett. 105 (2010) 237801. Available from: https://doi.org/10.1103/PhysRevLett.105.237801.

[51] G. Groeninckx, M. Vanneste, V. Everaert, Crystallization, morphological structure, and melting of polymer blends, Polymer Blends Handbook, Springer, Netherlands, 2003, pp. 203−294. Available from: https://doi.org/10.1007/0-306-48244-4_3.
[52] P. Szymoniak, Z. Li, D.Y. Wang, A. Schönhals, Dielectric and flash DSC investigations on an epoxy based nanocomposite system with MgAl layered double hydroxide as nanofiller, Thermochim. Acta. 677 (2019) 151−161. Available from: https://doi.org/10.1016/j.tca.2019.01.010.
[53] I. Hammami, H. Hammami, J. Soulestin, M. Arous, A. Kallel, Thermal and dielectric behavior of polyamide-6/clay nanocomposites, Mater. Chem. Phys. 232 (2019) 99−108. Available from: https://doi.org/10.1016/j.matchemphys.2019.04.048.
[54] V. Tambrallimath, R. Keshavamurthy, S.D., P.G. Koppad, G.S.P. Kumar, Thermal behavior of PC-ABS based graphene filled polymer nanocomposite synthesized by FDM process, Compos. Commun. 15 (2019) 129−134. Available from: https://doi.org/10.1016/j.coco.2019.07.009.
[55] B. Wunderlich, Reversible crystallization and the rigid-amorphous phase in semicrystalline macromolecules, Prog. Polym. Sci. 28 (2003) 383−450. Available from: https://doi.org/10.1016/S0079-6700(02)00085-0.
[56] G.R. Bhadu, S. Kumar, V. Choudhary, Rheological, melting and crystallization behaviour of an open cage POSS/PTT nanocomposite prepared by melt blending, Int. J. Plast. Technol. 14 (2010) 7−23. Available from: https://doi.org/10.1007/s12588-010-0003-5.
[57] J. Kaur, J.H. Lee, M.L. Shofner, Influence of polymer matrix crystallinity on nanocomposite morphology and properties, Polymer (Guildf.) 52 (2011) 4337−4344. Available from: https://doi.org/10.1016/j.polymer.2011.07.020.
[58] M. El Achaby, F.E. Arrakhiz, S. Vaudreuil, A. El Kacem Qaiss, M. Bousmina, O. Fassi-Fehri, Mechanical, thermal, and rheological properties of graphene-based polypropylene nanocomposites prepared by melt mixing, Polym. Compos. 33 (2012) 733−744. Available from: https://doi.org/10.1002/pc.22198.
[59] J.Y. Lim, J. Kim, S. Kim, S. Kwak, Y. Lee, Y. Seo, Nonisothermal crystallization behaviors of nanocomposites of poly(vinylidene fluoride) and multiwalled carbon nanotubes, Polym. (Guildf.) 62 (2015) 11−18. Available from: https://doi.org/10.1016/j.polymer.2015.02.012.
[60] M.R. Nobile, M. Raimondo, K. Lafdi, L. Guadagno, Rheological and morphological properties of graphene-epoxy nanocomposites, in: AIP Conf. Proc., American Institute of Physics Inc., 2016: p. 020143. https://doi.org/10.1063/1.4949718.
[61] M. Ghaffari, R. Naderi, M. Ehsani, Effect of silane as surface modifier and coupling agent on rheological and protective performance of epoxy/nano-glassflake coating systems, Iran. Polym. J. (Engl. (Ed.) 23 (2014) 559−567. Available from: https://doi.org/10.1007/s13726-014-0250-y.
[62] R. Hsissou, A. Bekhta, O. Dagdag, A. El Bachiri, M. Rafik, A. Elharfi, Rheological properties of composite polymers and hybrid nanocomposites, Heliyon. 6 (2020) e04187. Available from: https://doi.org/10.1016/J.HELIYON.2020.E04187.
[63] I.O. Navas, M. Kamkar, M. Arjmand, U. Sundararaj, Morphology evolution, molecular simulation, electrical properties, and rheology of carbon nanotube/polypropylene/polystyrene blend nanocomposites: Effect of molecular interaction between styrene-butadiene block copolymer and carbon nanotube, Polym. (Basel) 13 (2021) 1−25. Available from: https://doi.org/10.3390/polym13020230.
[64] F.-Z. Semlali Aouragh Hassani, R. Bouhfid, A. el K. Qaiss, rheological properties of hybrid nanocomposites based on graphene and other nanoparticles (2021) 283−312. https://doi.org/10.1007/978-981-33-4988-9_11.

[65] H. Essabir, M.O. Bensalah, D. Rodrigue, R. Bouhfid, A.E.K. Qaiss, Biocomposites based on Argan nut shell and a polymer matrix: Effect of filler content and coupling agent, Carbohydr. Polym. 143 (2016) 70−83. Available from: https://doi.org/10.1016/j.carbpol.2016.02.002.

[66] S.A. Laaziz, M. Raji, E. Hilali, H. Essabir, D. Rodrigue, R. Bouhfid, et al., Biocomposites based on polylactic acid and argan nut shell: production and properties, Int. J. Biol. Macromol. 104 (2017) 30−42. Available from: https://doi.org/10.1016/j.ijbiomac.2017.05.184.

[67] M. Mojtaba, M.C. Heuzey, P.J. Carreau, A. Taguet, Morphological and rheological properties of PLA, PBAT, and PLA/PBAT blend nanocomposites containing CNCs, Nanomater. (Basel, Switz.) 11 (2021). Available from: https://doi.org/10.3390/NANO11040857.

[68] J.K. Palacios, A. Ben Fekih, C.Y. Argon, S. Irusta, S. Jestin, S. Dagréou, Tailoring the rheology and electrical properties of polyamide 66 nanocomposites with hybrid filler approach: graphene and carbon nanotubes, Polym. Int. 70 (2021) 1329−1343. Available from: https://doi.org/10.1002/PI.6204.

[69] M. Kracalik, Rheology of multiphase polymer systems using novel “melt rigidity” evaluation approach, in: AIP Conf. Proc., American Institute of Physics Inc., 2015: p. 040002. https://doi.org/10.1063/1.4918890.

[70] M.E.M. Mekhzoum, H. Essabir, D. Rodrigue, A.el K. Qaiss, R. Bouhfid, Graphene/montmorillonite hybrid nanocomposites based on polypropylene: morphological, mechanical, and rheological properties, Polym. Compos. 39 (2018) 2046−2053. Available from: https://doi.org/10.1002/pc.24166.

[71] M. Wang, X. Fan, W. Thitsartarn, C. He, Rheological and mechanical properties of epoxy/clay nanocomposites with enhanced tensile and fracture toughnesses, Polym. (Guildf.) 58 (2015) 43−52. Available from: https://doi.org/10.1016/j.polymer.2014.12.042.

[72] H. Essabir, M. Raji, R. Bouh, Nanoclay and natural fibers based hybrid composites: mechanical, morphological, thermal and rheological properties, Nanoclay Reinf. Polym. Compos. (2016) 29−49. Available from: https://doi.org/10.1007/978-981-10-0950-1.

[73] Y. Wang, K.C. Wu, J.Z. Wang, Effect of maleated propylene on rheology of polypropylene nanocomposites, J. Cent. South. Univ. Technol. (Engl. (Ed.) 14 (2007) 160−164. Available from: https://doi.org/10.1007/s11771-007-0236-4.

[74] S.O. Ilyin, T.V. Brantseva, I.Y. Gorbunova, S.V. Antonov, Y.M. Korolev, M.L. Kerber, Epoxy reinforcement with silicate particles: rheological and adhesive properties - Part I: characterization of composites with natural and organically modified montmorillonites, Int. J. Adhes. Adhes. 61 (2015) 127−136. Available from: https://doi.org/10.1016/j.ijadhadh.2015.05.008.

[75] A. Irekti, B. Bezzazi, Rheological study of composite materials based on thermosetting matrix and fillers mineral, Key Eng. Mats. 550 (2013) 79−84. Available from: https://doi.org/10.4028/http://www.scientific.net/kem.550.79.

[76] J. Kalfus, J. Jancar, Viscoelastic response of nanocomposite poly(vinyl acetate)-hydroxyapatite with varying particle shape—dynamic strain softening and modulus recovery, Polym. Compos. 28 (2007) 743−747. Available from: https://doi.org/10.1002/pc.20331.

[77] S.G. Prolongo, M.R. Gude, A. Ureña, Rheological behaviour of nanoreinforced epoxy adhesives of low electrical resistivity for joining carbon fiber/epoxy laminates, J. Adhes. Sci. Technol. 24 (2010) 1097−1112. Available from: https://doi.org/10.1163/016942409X12584625925060.

# Biological aspects of polymer nanocomposites

3

*Swapnita Patra and Sarat K. Swain*
Department of Chemistry, Veer Surendra Sai University of Technology, Burla, Sambalpur, Odisha, India

## 3.1 Introduction

The use of nanotechnology is increasing day by day, including its fabrication and uses in the preparation of various nano-sized devices. Nanotechnology plays a major role in biomedical areas as it helps in the prevention and cure of certain diseases. The polymer-based nanocomposites (PNCs) create much interest among the researcher for their great properties developed when a polymer is combined with the inorganic nanomaterials. The mixture of polymer and organic/inorganic fillers helps in the formation of PNCs at the nanometer scale. PNCs have remarkable properties such as reusability, high toughness, biodegradability, excellent biocompatibility, and certain biofunctionalities. Biomedical application comes into action via proper linking between the biomolecules and functional polymers. Polysaccharides such as starch, chitosan, alginates or the proteins such as fibrin gels and collagens are the natural polymers that can be used in biomedical applications [1]. Similarly, the synthetic polymers used in biomedical applications are mainly poly(lactic acid) (PLA), poly(glycolic acid) (PGA), poly(caprolactone), etc. The rate of degradation of PNCs is less as compared to other similar materials. The soluble polymers mainly used in this application are poly(acrylic acid), polyvinyl alcohol (PVC), polyethylene glycol (PEG) [2]. Some polymers which can conduct electricity (polyaniline, polypyrrole) can also be used for this purpose. There are also other polymers that show similar applications for biomedical uses are polyethylene (PE), polypropylene (PP), polyurethane (PU) [3]. Greater surface-to-volume ratio of nanoparticles (NPs) leads to excellent magnetic properties and is more effective than that of larger particles, which is the reason behind the wide use of NPs recently in different fields such as electronics, biology, and chemistry. Moreover, nanocomposites are increasingly used more in the field of science for their tunable properties [4,5]. As there are many advantages, there are also certain limitations of the NPs in certain fields such as the loss of the size of the nanocomposites due to aggregation and inadequate stabilities [6,7]. In some solvents, dissolution/dispersion takes place instead of aggregation due to stabilization of the metal nanocomposites. The metal NPs are embedded in polymer matrices by which aggregation of nanocomposites is avoided leading to many effective and efficient properties. So, in case of PNCs, the polymer phase behaves as a stabilizer or we may say

**Advanced Polymer Nanocomposites. DOI:** https://doi.org/10.1016/B978-0-12-824492-0.00003-9


it the protecting agent which shows many needed applications. The NPs can be used in different emerging fields such as sensing, dye removal, drug delivery, photoablation therapy, bioimaging, and so on. Among all the NPs, iron oxide has some more efficient applications in drug delivery, bioimaging, gene delivery, and cell labeling for its outstanding performance on stability, nontoxicity, great magnetic susceptibility, saturation magnetization, as well as biocompatibility. As the alternative to iron oxide, we may use other nanocomposites such as Cu−Ni, Mn−$Fe_2O_4$, Co−$Fe_2O_4$, and Fe−Ni for bioimaging, drug delivery, etc. [8].

The NPs used in biological applications improve the technologies and implementation of medical equipments and their designs. In this chapter, we targeted various utilization of the advanced PNCs in different biomedical fields such as antibacterial applications, drug delivery, gene therapy, tissue engineering, biosensing, bioimaging, and dental applications. The growth of microorganisms is prevented by the implementation of antibacterial agents. It also helps to reduce many harmful effects. We should develop new methods for the treatment of infections, as serious problems faced by the world recently due to the enhancement of antibiotic resistance of microorganisms [9]. Without affecting surrounding healthy cells, anticancer drugs can treat tumor cells, which is an important biomedical application of PNCs [10]. Among all the applications, gene therapy brings more interest in researchers. In this approach, genetic functions of the cytoplasm and nucleus of the cell are corrected by the transfer of nucleotide-based therapeutic agents into the cells [11]. The specific cellular behaviors are regulated by biomimetic scaffolds which are formed through controlled structures and certain properties. In cartilage tissue engineering, the specific cells that are present on the 3D matrix are separated and are implanted in the injury site [12]. In wound healing, the destroyed tissues are replaced by the newly regenerated tissue. In case of biosensing, the biosensor is a device that needs to analyze the biological sample. It changes a chemical, biological, or biochemical signal to an electrical signal. Magnetic resonance imaging (MRI), computed tomography (CT), and ultrasounds are the different bioimaging techniques used for the diagnosis of certain diseases. Some high-resolution images of the internal organs can also be produced from bioimaging devices.

## 3.2 Nanocomposites

In 1982−83 Roy et al. coined the term “nanocomposites” to understand the concept behind sol−gel processes [13]. Nanocomposites consist of continuous matrix phase and discontinuous reinforcement materials to obtain the best version of composite. Based on the size of reinforcement, composites are divided into three classes, that is, nanocomposites, microcomposites, and macrocomposites. Among all, nanocomposites are more efficient and have outstanding applications. The connection between the matrix and reinforcement is very high as it has a high surface-to-volume ratio [14]. Terms “nanocrystalline” and “nanophase” are different from the nanocomposites, which shows a single-phase in the nanometer range. In nanocomposites,

the solid phase is in a range between 1−20 nm. The solid phase we discussed here may be crystalline, semicrystalline, or amorphous. Similarly, these solid phases can be organic, inorganic, or both. For the past 20 years, PNCs are used in a vast amount in industries and also in research works. So, the rapid growth of PNCs is seen from the last 10 years. The great implementations of nanocomposites in engineering, plastics, rubber, adhesive, coating industries, etc. owes to its outstanding advantages. It also has certain disadvantages due to its late decomposition time. We can irradiate this problem by the use of nanocomposites prepared from biorenewable resources. We can obtain biorenewable resources by the utilization of vegetable oils, starch, cellulose, chitosan, natural rubber, and proteins etc. The nanocomposites, we got from biorenewable resources, have a great greener approach than petroleum-based composite, and they are specially used in food packaging, and in different biomedical industries. Based on the materials' functions, nanocomposites are grouped into sol−gel nanocomposites, intercalation-type nanocomposites, entrapment-type nanocomposites, electro ceramic nanocomposites, and structural ceramic nanocomposites [15]. The nanocomposites derived from polymers are formed by different methods. There are four routes for the preparation of nanocomposites such as melt intercalation, template synthesis, exfoliation, and adsorption. The nanocomposites are then characterized by different techniques such as UV−Vis, fourier-transform infrared spectroscopy (FTIR), X-ray powder diffraction (XRD), scanning electron microscopy (SEM), and transmission electron microscopy (TEM).

## 3.3 Biological aspects of nanocomposites

The self-assembly strategy helps in the construction of PNCs into nanostructures, which tend to create functional materials with great applications in biomedical sector. From the literature review (Fig. 3.1), it is found that the numbers of published

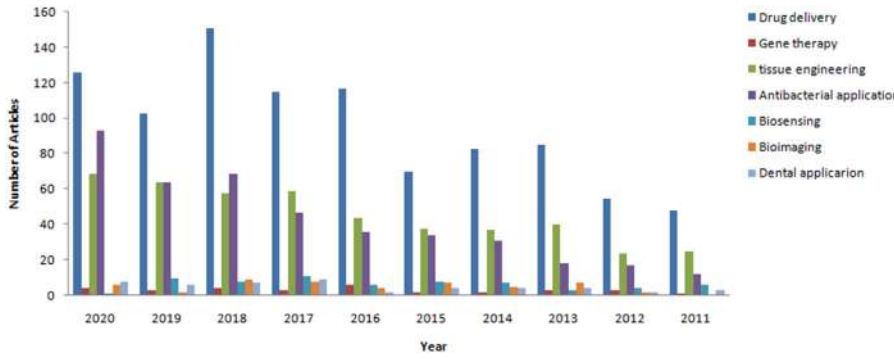


**Figure 3.1** Publication of articles in journals during one decade (2011−20) from "Web of Science" with searching different keywords mentioned in legends in the title.

articles are progressively increased in one decade which explores the applications of present work. Hence, this chapter may be an asset to the literature complying with biomedical applications.

The energy storage property of biomedicine is also an application of PNCs. The self-assembly of PNCs helps in the development of practical biomedical devices. There are certain techniques used in the fabrication of biomedical devices such as soft lithography, nanoimprinting, and hot embossing lithography. We can prepare a hydrogel with superior properties and with superior functions for applications in the biomedical and biotechnological area from the carbon-based ceramic, metallic, polymeric nanomaterials. Among nanocomposites, magnetic PNCs draw attention due to their outstanding magnetic properties, compatibility, and good stability. The formation of organic and inorganic magnetic nanocomposites can be done by certain techniques such as ex situ, in situ, coprecipitation, microwave reflux, melt blending, plasma polymerization, and ceramic−glass processing. These nanocomposites are used as drug carriers in several biomedical fields [16]. Other excellent nanocomposites are formed by combining the magnetic and fluorescent properties having multifunctional behavior, with outstanding biomedical applications in cell tracking, biological imaging, magnetic bioseparation, bio and chemosensoring, and nanomedicine [17]. Some smart biopolymers-based nanocomposites show some self-regeneration properties and can be implemented in different biomedical areas. Self-healing is a route that can repair or regenerate the degradation, damage, or failure of the tissue [18]. A comprehensive discussion is given found on the current progress reported in various biomedical fields such as antibacterial applications, drug delivery, gene therapy, tissue engineering, biosensing, bioimaging, and dental applications. Graphene-based PNCs due to their remarkable properties, such as superior mechanical properties, high thermal conductivity, and excellent electronic transport have prompted flexible emerging applications in many biomedical fields, particularly in antibacterial applications, drug delivery, tissue engineering, gene therapy, wound healing, biosensing, bioimaging, dental applications, etc. portrayed in Fig. 3.2 by representing graphene PNCs as a net, capturing all principal biomedical applications depicted as fishes for better understanding.

### 3.3.1 Antibacterial aspects

The enhancement in optical, electronic, mechanical, and antimicrobial properties is carried out by combining various properties of the polymer and NPs. By increasing the antibacterial applications of polymeric matrix or by including nanomaterials which have antibacterial properties, we can get nanocomposites with antibacterial properties. Owing to the synergistic effect of two components in composites, the increment of biocidal capacity takes place. Polymer provides antibacterial properties and the supporting matrix for NPs [19]. Cell wall, translational machinery, and DNA replication are the three major bacterial targets to which molecular antibiotics affect the bacteria. There are certain processes through which NPs react, that is, production of the reactive oxygen species (ROS), ion releases, electrostatic interaction with the cell membrane, and internalization. So, the NPs have a great influence

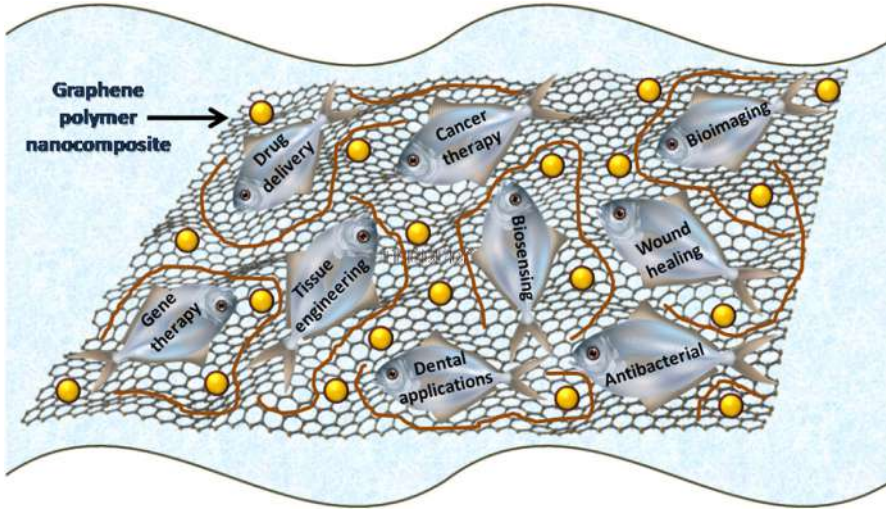


**Figure 3.2** Graphical representation showing biomedical applications of graphene-based PNCs. *PNCs*, Polymer-based nanocomposites.

on the antibacterial activity over molecular antibiotics, especially for the bacteria which can resist antibiotic. Against the pathogenic bacteria, noble NPs are found to have effective antibacterial activity for their prominent surface area to volume ratios and impressive physicochemical properties. Silver nanoparticles (AgNPs) are the most used NPs among all noble metal NPs for their better antibacterial activity. AgNPs are different kinds of NPs that can affect bacteria through all the antimicrobial mechanisms we discussed before. So, they can be treated as antimicrobial agents [20]. Human beings are affected by many diseases such as infections, allergies, and toxic reactions by airborne and waterborne pathogens. For the negligible formation of aerosol and hydrosols, the mechanical filtration by nano- and microfibers gives a cost-effective, chemical-free, and environmentally friendly approach to increase the performance and efficiency of filtration. As we discussed above, graphene-based nanocomposites such as graphene oxide (GO), reduced GO and porous graphene nanosheets have enormous antibacterial properties. Matharu et al. [21] demonstrated the antibacterial behavior of GO nanocomposite fibers. The contamination of bacteria on different surfaces of wound dressings, medical devices, industrial pipes, separation membranes, and food packages is a serious problem. So, the bacteria get attached to these places and grow at a faster rate under suitable conditions of the environment and form biofilms, the removal of which is difficult. So, an antibacterial coating is developed to kill the bacteria and to control the formation of the biofilms [22]. Alam et al. [23] designed a coating material named polyesteramide [LMPEA] nanocomposite by using *N*,*N*-bis (2-hydroxyethyl) fatty amide which is obtained from nonedible *Leucaena leucocephala* [LL] seed oil [LLO], and maleic anhydride, strengthened with the AgNPs, biosynthesized in *L. leucocephala* leaf extract, having outstanding antimicrobial efficiency. The

hydrogels which have large voids in the cross-linking networks act as a reservoir for the NPs and help in the growth of NPs and nucleation by the nanoreactor template. The synergetic effects produced by the insertion of the AgNPs between organic and inorganic components improve the applications via increment in mechanical toughness, swelling/deswelling rates, deformability, transparency, electrical conductivity, as well as antibacterial activity. Syed et al. [24] developed a nanocomposite having antibacterial applications, that is, almond gum-poly(acrylamide)/Ag hydrogel nanocomposites. Jayaramudu et al. [25] designed hydroxypropyl methylcellulose (HPMC) nanocomposite hydrogel films which got strengthened with HPMC capped copper nanoparticles (HCuNPs) for employment in antibacterial applications. The development of efficient antibacterial surfaces is important to achieve control on the arrangement of the biocides across the thickness of PNCs films. It is the way to increase the biocide quantity at the top of the surface of the film to ensure attachment with the bacteria. Martín-Fabiani and his co-workers used a method to control the vertical arrangement of the biocides in the polymer composite film formed from the zinc oxide (ZnO) nanoparticles and a colloidal blend of the polymer known as evaporation driven colloidal self-assembly [26]. To resist the release of substances into the environment, the mechanism may differ in the production of heat, pH variation, generation of ROS, photoinduced and/or photoexcitation acidification, photodynamic therapy, for which the researchers designed smart nanomaterials with significant antibacterial properties, which are activated by the light irradiation. Ballesteros et al. [27] designed a nanomaterial containing AgNPs on the surface of the biodegradable and biocompatible polycaprolactone (PCL) nanofiber mats prepared by electrospinning method and composed by a photoresponsive nanogel which shows some antibacterial behavior on the gram-negative *Escherichia coli* and gram-positive *Staphylococcus aureus*. Factori et al. [28] adopted microwave-assisted sol−gel synthesis method to design ZnO nanoparticle/poly(vinyl alcohol) nanocomposites which have potential application in the preparation of antibacterial films opposing gram-positive and gram-negative bacteria.

### 3.3.2 Drug delivery aspects

Because of the surface and rheological properties, drug delivery through nanocomposite systems becomes an emerging area of research interest not only in nanomedicine but also in material science research field. In the conventional way of drug delivery, there is no control over the release of therapeutic agent that results in a rapid increase of drug dosage in the bloodstream and then drops and the possibility of the desired amount of drug to reach predetermined site decreases. Because of the above fact, repeat administration of a drug is required to maintain the therapeutic level in the body avoiding which leads to life-threatening side effects. Therefore recent research works in drug delivery are based on the fabrication of controlled and targeted drug delivery systems. The drug carrier system should release the requisite amount of therapeutic agent at the targeted site without causing any harmful effect to other sites [10]. A nanostructured system can be a preferred choice for the controlled and sustainable release of drugs to reduce the lethal aftermath of taking

medicine. For anticancer therapeutic agents, drug delivery carriers should possess longer circulation period to target cancer cells and can release the therapeutic agent into the cytoplasm. The most advantageous carrier systems that are used as antitumor carriers are NPs, dendrimers, microspheres, and liposomes, whereas for anticancer drug delivery, nanomaterials are used as drug delivery carriers since nanomaterials can penetrate highly into tumor vasculatures and have multivalent effects [29]. Javanbakht et al. [30] prepared an anticancer nanostructured drug delivery carrier by incorporating doxorubicin (DOX) drug in carboxymethylcellulose/Zn-based metal−organic framework/GO bionanocomposite using green one-pot synthesis method. Currently, investigation related to nanocomposite drug delivery systems is not confined to the synthesis of drug delivery systems. Many aspects are now considered to prepare nanocomposite drug delivery, that is, capability to encapsulate therapeutics and to release them upon stimulus, ability to generate heat using external signals, and to produce highly oxidative species, for combinational therapies [31]. Graphene becomes a dominant nanocarrier material for drug administration application due to its two-dimensional structure, excellent stability, large surface area, easy surface modification, and high biocompatibility. Drug delivery application using nanoscale GO was first reported by, Sun et al. in 2008 [32]. They have successfully prepared a nanosystem drug delivery carrier by incorporating anticancer drug DOX onto PEG functionalized GO to kill cancer cells in vitro. Graphene can be a potential drug delivery carrier because the drug loading mass can reach 200% of the graphene-based drug nanocarrier [33]. Hydrogels are considered as one of the most significant biomaterials and have its dominance over other biomaterials in a variety of biomedical applications such as drug delivery because of their ability to encapsulate and protect therapeutic agents and most importantly the capability to release the drug in control and sustainable manner [34].

Unlike traditional chemotherapy, chemotherapy carried out using nanomaterials as a drug carrier system has excellent outcomes as drugs can reach the predetermined targeted site instead of even being distributed in the whole body and diffusing freely in the bloodstream. Chemotherapy using nanocarrier able to release therapeutic agents in a controlled way because of two types of stimuli: exogenous stimuli such as magnetic fields, temperature, ultrasound, electric fields; and light and endogenous stimuli such as enzyme concentration, pH, and redox. Drug administration carried out using these approaches helps to overcome a physical barrier, increase drug bioavailability, and minimize dosages of medicines that reduce the lethal aftermath of uptaking excessive drugs [35]. Nowadays various stimuli-responsive PNCs are used in drug delivery applications. The stimuli, light has several advantages that increase the efficacy of the drug delivery system, as it is cost-effective and can tune with wavelength and intensity along with spatiotemporal control. Huang et al. [36] engineered photoresponsive mesoporous silica PNCs using the atom transfer radical polymerization (ATRP) process for controlled drug delivery application. The most significant and typically used stimuli in the drug administration process is temperature because the physiological temperature has a great impact on thermoresponsive polymer. Poly(*N*-isopropylacrylamide) and Poly (*N*-vinylcaprolactam) (PNVCL) are the two most used temperature-responsive

polymer. The phase transition temperature of a polymer should consider while using it as a part of the drug carrier system. The phase transition temperature of PNVCL is close to the physiological temperature [37]. An in vivo drug release of a therapeutic agent from thermoresponsive polymeric matrix based on PPG, PEG, and tetraphenylethene with chromophore has been monitored using the aggregation-induced emission (AIE) concept [38]. Another exogenous stimulus is the electric field which allows drug release by deviating the binding force present between the drug model and nanodrug delivery carrier. Weaver and co-workers fabricated a drug administration carrier using GO nanosheets and conducting polymeric film. Drug delivery by using an electrically controlled system showed collinearity with time and voltage [39]. Mallakpour and Khodadadzadeh investigated the administration of zolpidem, a hydrophobic drug model from starch/multi-walled carbon nanotubes (MWCNT)−glucose nanocomposites carrier system using ultrasonic stimulation [40]. Magnetic-responsive drug delivery carrier plays a vital role in the treatment of cancer using the hyperthermia method. Paramagnetic materials such as superparamagnetic NPs are used in the preparation of composites to make the carrier system magnetically active. pH-responsive behavior of drug carrier system depends on the functional group present on the polymer that is used in composite preparation. Mdlovu et al. [41] have engineered a multiresponsive drug administration system by incorporating iron oxide nanoparticles (IONPs) into Pluronic F127 shell using DOX as a drug model, for neuroblastoma treatment. The in vitro drug release rate showed faster release of drug models in an acidic environment than others. Different concentrations and activities of enzymes can be employed for drugs delivery to tumor tissues [42]. Chen et al. [43] prepared a nanocomposite drug delivery system to release DOX in GSH-regulated environment using GO and AgNPs. This carrier system was redox stimulus responsive. Multiresponsive drug delivery system offers outstanding ability in multiple deliveries of different payloads and greater control over the release of drugs than a single responsive carrier system. It also provides sensing and imaging possibilities along with curative nature [44]. Song et al. [45] synthesized a dual-responsive, that is, pH and photoresponsive drug delivery carrier for the release of DOX using GO and gold nanorod. The prepared hybrid nanocomposite can release DOX in the near-infrared irradiation (NIR) region and acidic environment. Falcone et al. [46] engineered a peptide−polydopamine nanocomposite hydrogel for laser-induced drug delivery inhibiting the growth of gram-negative *E. coli* bacteria. Different PNCs reported having applications in drug delivery are summarized in Table 3.1, with their fabrication techniques and characterization methods adopted.

### 3.3.3 Gene therapy aspects

In past decades, researchers are more interested to do investigations on therapeutic approaches such as gene therapy. Gene therapy is a technique or process to treat or cure human disease by relocating genetic material into certain cells of the patient. The rectification of genetic functions in the cell nucleus or cytoplasm by administrating nucleotide-based therapeutic agents into the desired cells is an important

**Table 3.1** A summary of different PNCs reported for drug delivery with their fabrication techniques and characterization methods.

| No. | Polymer-based nanocomposites (PNCs) | Fabrication techniques | Characterization/properties | Applications | References | Ref. no. |
|---|---|---|---|---|---|---|
| 1 | Polyvinyl alcohol (PVC)/CuO nanocomposite hydrogel | Immersion Process | fourier-transform infrared spectroscopy (FTIR), X-ray, scanning electron microscopy (SEM) | Drug delivery agent | Ahmadian et al. | [47] |
| 2 | ZnS−cellulose nanocomposite | In situ method | X-ray powder diffraction (XRD), FTIR, SEM, transmission electron microscopy (TEM), EDX, UV−Vis | Drug delivery, antibacterial and photocatalytic activity | Pathania et al. | [48] |
| 3 | Gelatine-based biodegradable hydrogel nanocomposite | Immersion process | FTIR, XRD, energy dispersive X-ray spectroscopy, and SEM | Drug delivery agent | Bakravi et al. | [49] |
| 4 | Polymer nanocomposites-coated magnetic nanoparticles | In situ method | FTIR, VSM, TEM, SEM | Drug delivery | Prabha et al. | [50] |
| 5 | Carbon dots decorated carboxymethyl cellulose-hydroxyapatite nanocomposite | One-pot synthesis method | FTIR, XRD, TGA, FESEM, TEM, and DLS | Drug delivery, tissue engineering, and Fe3 + ion sensing | Sarkar et al. | [51] |
| 6 | Poly (2-hydroxyethyl methacrylate)/clay composites | In situ free-radical polymerization | FTIR, DSC, TGA, XRD | Drug delivery systems of paracetamol | Bounabi et al. | [52] |
| 7 | Chitosan-g-poly(acrylamide)/ZnS nanocomposite | Microwave radiations technique | FTIR, XRD, EDX, SEM, TEM, TGA | Drug delivery and antimicrobial activity | Gupta et al. | [53] |

(*Continued*)

**Table 3.1** (Continued)

| No. | Polymer-based nanocomposites (PNCs) | Fabrication techniques | Characterization/properties | Applications | References | Ref. no. |
|---|---|---|---|---|---|---|
| 8 | Structural nanocomposite consisted of tamoxifen citrate and polyvinylpyrrolidone as core and shellac as shell | Modified coaxial electrospraying process | SEM, TEM, XRD, FTIR | Colon-specific delayed drug delivery | Wang et al. | [54] |
| 9 | Doxorubicin loaded carboxymethyl cellulose/graphene quantum dot nanocomposite hydrogel films | Incorporation of graphene quantum dot | FTIR, UV−Vis, SEM | Potential anticancer drug delivery system | Javanbakht et al. | [55] |
| 10 | 5-Fluorouracil loaded chitosan/polyacrylic acid/$Fe_3O_4$ magnetic nanocomposite hydrogel | In situ method | FT-IR, XRD, VSM, TGA, and SEM analysis | Potential anticancer drug delivery system | Mohammadi et al. | [56] |

process in gene therapy [11]. In the last few decades, gene therapy technique has been significantly enriched by the development occur in nanotechnology-based applications such as medicine and consequently, nonviral gene therapy becomes an important factor in biomedicine [57]. The utilization of synthetic polymer as vectors in gene therapy has created opportunities in the research area related to gene therapy and in targeting oncogenes. Gene-based therapeutics technique uses synthetic polymers, such as polyethyleneimine (PEI) and poly(amidoamine) (PAMAM) dendrimers and poly(b-amino ester) as vectors. Numerous types of polymers have been fabricated to overcome the barriers and to get the desirable outcomes through gene therapy. The various designing criteria such as biocompatibility, DNA packaging and stability in vivo, and endosomal escape, must consider during the designing of polymers. The cationic polymer carrier has been used to create a range of drug delivery activities in the intracellular and extracellular transport of DNA vectors, for polyplex-mediated gene delivery [58]. The successful administration of in vitro nonviral gene delivery of primary amines [dithiobis(succinimidylpropionate) or dimethyl-3,30-dithiobispropionimidate. 2HCl] cross-linked PEI to Chinese hamster ovary (CHO) cells has been demonstrated by Gosselin et al [59]. By utilizing a luciferase reporter gene below cytomegalovirus promoter, the transfection efficiencies were evaluated in CHO cells. Zhong et al. [60] employed PAMAM dendrimers for gene delivery.

The integration of gene therapy with photodynamic therapy has shown an enhancement in therapeutic effectiveness. Lou and co-workers prepared a nanocomposite based on MnO2-DNAzyme-photosensitizer with AIE characteristics for cell imaging and photodynamic-gene therapy for combined treatment [61]. To overcome the challenges faced during targeted tumor imaging and to improve the efficacy of specific gene delivery in cancer-based gene therapy, many scientists have prepared nanovectors. Wang et al. [62] engineered multifunctional bioactive citric acid-based nanovectors for intrinsical targeted tumor imaging and specific administration of siRNA gene delivery which has applications in both in vitro and in vivo. The efficacy of gene delivery could be significantly enhanced by using magnetic nanostructures due to their distinctive properties than other nanostructures. Xu and his co-workers fabricated one-dimensional magnetic NPs based on IONPs and silicon oxide along with p-FS for the imaging-guided gene therapy without using any templates and magnetic stirrer [63]. The release of biomolecules from hydrogels is much more challenging and less effective because this may lead to rapid diffusion and degradation of biomolecules. Gene therapy offers an alternative medium for the sustainable production of proteins by transfected cells. Wang et al. [64] developed a nanocomposite-based system, which is capable of repairing tissues along with gene delivery, consisting of DNA-PEI-silica NP complexes coencapsulated with fibroblasts within collagen hydrogels.

### 3.3.4 Tissue engineering aspects

The replacement or the repair of damaged tissue can be done by tissue engineering. New tissue regenerates artificially by the applied methods of life science and

materials engineering by tissue engineering. The damaged or failing organs can also be repaired by tissue engineering. Cells are growing on scaffolds which act as temporary support for them during regeneration, without harming the 3D structures [65]. Tissue engineering deals with the combination of molecular biology and materials engineering. The scaffolds are mainly having high porosity, biocompatibility, biodegradability, proper size of the pore, and have a good degradation rate. [66]. There are also few more advantages of the scaffolds like it gives sufficient mechanical support to overcome stresses and the harm produced during in vitro or in vivo regeneration. The polymeric scaffolds play an important role in tissue engineering such as cell seeding, proliferation, regeneration of the new tissues in 3D. For bone tissue engineering, the designing of poly(propylene fumarate)-based nanocomposite with the PEG functionalized GO by sonication and thermal curing is one of the best preparation methods [67]. The synthetic biopolymer-based nanocomposites are the first choice of researchers to use in tissue engineering scaffolds for their biocompatibility and controllable biodegradation kinetics. Synthetic biopolymers can mostly be implemented for the treatment of patients having organ failure, or with damaged or lost tissue are mainly the saturated poly(α-hydroxy esters), PGA, PLA, poly(lactic acid-*co*-glycolic acid), and PCL [68−71]. A simplified representation for PNCs in tissue engineering is given in Fig. 3.3.

Other efficient bioscaffolds for tissue engineering are the stimuli-responsive hydrogels [72]. To develop a strong hydrogel for the treatment of patients by tissue engineering, Boere et al. [73] combined the temperature-induced physical cross-linking with native chemical ligation. Good biocompatible behavior is shown by the conducting polymers (polyaniline, polypyrrole, polythiophene, and their derivatives). An electric signal is stimulated due to its conducting nature which allows

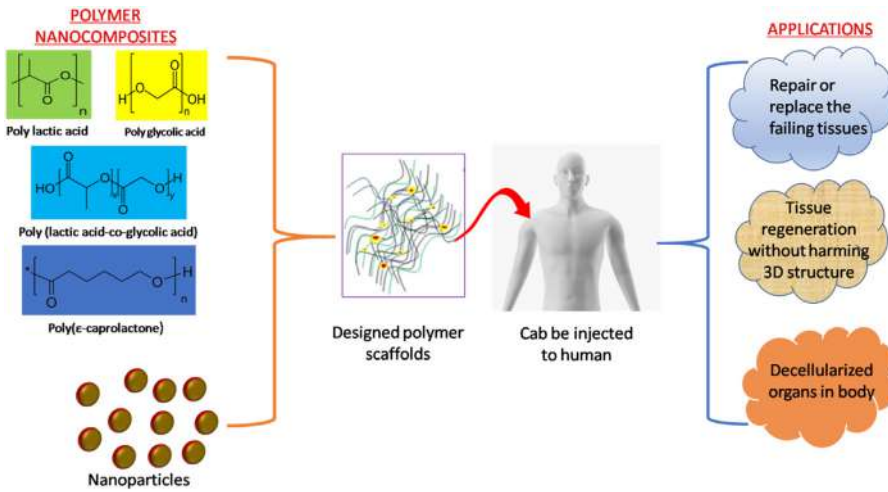


**Figure 3.3** Application of PNCs in tissue engineering. *PNCs*, Polymer-based nanocomposites.

cells or tissues cultured on them. There are also certain disadvantages that restrict their uses like their mechanical brittleness and low processability. So, the polymeric composites having good biocompatibility and biodegradability rate were developed using the conducting polymers [74]. PPY/PCL was prepared by first putting PCL film into polystyrene sulfonic acid and then mixing it with pyrrole DI water mixture. Then as an oxidant, the ferric chloride was added to it. Then there is the formation of the PPY-coated PCL conducting film. The resistivity of the film is found to be $1.0 \pm 0.4$ kΩ cm [75]. The reinforcement of nanomaterials in biopolymers leading to 3D structures shows great properties along with multifunctionality [76]. Different shaped structures, that is, hemisphere, cube, human nose, human ear, pyramid, and bundle, are designed from ternary PEG−alginate−nanoclay composite hydrogels, with great advantages like these are suitable for 3D printing and in long-lasting cell cultures [77]. Lalwani et al. [78] designed a polymeric nanocomposite that is biodegradable and reinforced by 2D nanostructure polypropylene fumarate for bone tissue engineering. Similarly, Zhang and co-workers prepared a well-structured cellulose nanocrystal piercing in an uniaxially alignment cellulose nanofiber by the spinning of an electron by a rotating drum which acts as a collector, for the application as a scaffold for tissue engineering [79].

### 3.3.5 Biosensing aspects

Because biosensor has advantageous qualities in terms of simplicity, time, and cost-efficiency, it emerges as an excellent technology in sundry types of applications. According to the sensing nature, sensors are typically categorized into two types: chemical sensor and physical sensor. Due to the overlapping of sensing methods, biosensors come under the chemical sensors category. Biological sensing elements can generate selective and sensitive analytical signals and these elements are used as a significant material to manufacture biosensors as analytical devices. The interactions between a target and the corresponding biorecognition element, such as enzymes, antibodies, and proteins, produce physiological changes and these changes are converted to an electrical signal by a transducer. The analyte concentration is responsible for the production amount of signals. Biosensors are employed in multivarious applications, mainly drug discovery, medical diagnosis, environmental monitoring, and food safety. Based on its limit of detection, sensitivity, selectivity, linear dynamic range, response to interferences, reproducibility, and other features the performance of a biosensor is evaluated [80]. Recently, biosensor research is attracting many important interests of researchers because of outstanding sensing capabilities, such as blood pressure, heart, body motions, pulse rate, blood glucose level, oxygen, antibodies, cholesterol, proteins, nucleic acids, cancer cells, heavy metals in drinking water and toxins in food products. Many types of biosensors including potentiometric biosensors, colorimetric biosensors, fluorescent biosensors, electrochemical biosensors, and Raman spectroscopy-based platforms have been reported [81]. Fig. 3.4 stands for various types of biosensors made from PNCs and their applications in different biomedical fields.

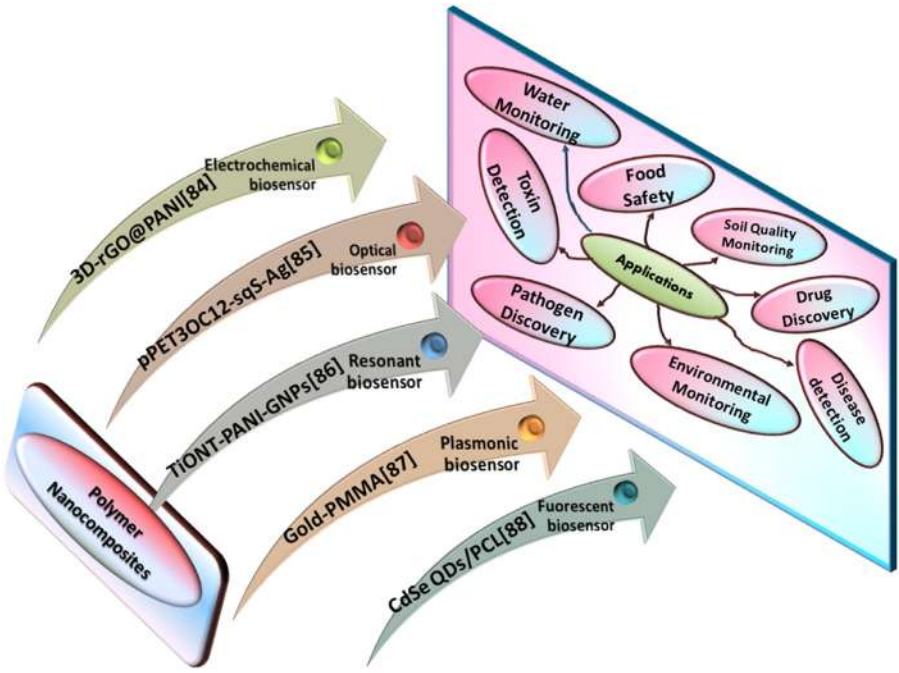


**Figure 3.4** Types of biosensors made from PNCs and their applications in different biomedical fields. *PNCs*, Polymer-based nanocomposites.

On account of enhanced biocompatibility, rapid electrode kinetics, excellent conducting properties, and environmental stability, PNCs can be a potential candidate in the electrochemical analysis process. Graphene-based materials, among several materials, are the prominent materials in the fabrication of biosensors and recent biosensors research-based studies. Graphene-based materials, which are synthesized by using biomolecules such as protein, peptide, DNA, and enzyme, play a significant role in improvising biosensing characteristics of graphene [82]. Graphene surfaces can be functionalized covalently, that is, chemically and noncovalently. A molecularly engineered graphene surface has been investigated by Liu et al. [83] for varieties of sensing applications such as electrochemical, electrical, and optical sensing. Electrochemical biosensors are superior to other biosensors, due to flexibly designed sensor architecture, easy operation, low cost, and high sensitivity. The poly(Lys) and hemoglobin functionalized graphene, for enzymatic detection of $H_2O_2$, has been fabricated by Wang et al. [84]. Due to rapid detection time, high sensitivity, and easy operation, fluorescence-based biosensors grow as a dominant material in the biological, biochemical, and medical research fields. The modified fluorescent biosensors offer direct recognition of molecular localization in various living cells and biological organisms. In addition to the above qualifications, the detection of several biological molecules, mainly $H_2O_2$, glucose, food toxins, dopamine, and metal ions by fluorescent biosensors, makes it a key element in medicinal

applications [81]. Chen et al. [85] fabricated a label-free fluorescent sensor for the detection of dopamine utilizing GO that is easily detectable in NIR region. For biosensing applications, chemiluminescence is a competent technology because of its outstanding sensitivity and insignificant interference by background scattering light. To detect bisphenol in water, a sensitive method was produced based on a system using luminal, KMnO4, and CuNCs (copper nanoclusters) [86]. Conducting polymer was first reported by Shirakawa et al. [87] in 1977. Considering the factors such as cost efficiency, easy processability, and immobilization through the stable and porous matrix, conducting polymers are widely used in electrochemical biosensors techniques. Conducting polymers like polypyrrole, polyaniline, polythiophene, and so on are extensively used in sensing applications [88]. Wang et al. [89] engineered poly(3,4-ethylenedioxythiophene)/hyaluronic acid (PEDOT/HA) nanocomposites with good antifouling activity and high porous microstructure by using a simple electrochemical method. An immunosensor was developed by immobilizing a carcinoembryonic antigen (CEA) antibody onto PEDOT/HA nanocomposites to detect tumor biomarker CEA. This combined effect uses to produce immunosensors with high sensitivity and low fouling activities. The excess glucose accumulation in human blood could lead to a life-threatening metabolic disease called diabetes mellitus. To reduce its unfavorable effect on people, real-time monitoring of glucose levels and quantitative detection is needed and is possible through sensing techniques. Xu et al. [90] fabricated a highly sensitive enzymatic glucose biosensor bionanocomposites using MWCNTs and glucose oxidase-loaded polymeric NPs. Mishra et al. [91] demonstrated the biosensing application of a plasmon-active polymer−NP composite triethylene glycol dimethacrylate-AuNPs.

### 3.3.6 Bioimaging aspects

Bioimaging is an excellent visualizing technique to create an image and to detect life activities in situ at a cellular or even subcellular level, and it also stands as a principal way for tumor monitoring and drug tracking in the biomedical area. Compared with other imaging techniques, biomedical optical imaging techniques give crucial data for the clinical and preclinical assessments of biochemical and biological processes [92]. Electromagnetic radiations have a significant contribution to bioimaging technology. For in vitro cell microscopic imaging, visible light is used. For in vivo small animal imaging, electromagnetic radiation with a greater wavelength than visible light is required for efficient penetration in tissue and lower autofluorescence. NIR light having a wavelength of $700 - 900$ nm is suitable for this purpose. The liaison of nanomaterials in imaging techniques has created more opportunities to generate various methods for imaging with enhancing features, than traditional materials, which include improved brightness, that is, inertness to their microenvironment, absorbance times quantum yield, and a more even distribution. Nanomaterials frequently used in bioimaging involve NPs prepared from organic hydrophilic and hydrophobic polymers, silica as well as organically modified silica, semiconducting organic polymers, carbonaceous nanomaterials including carbon nanotubes and nanoclusters, carbon (quantum) dots, upconversion materials,

nanodiamonds, metal oxides, metal particles, and others. Hybrid materials produced by cross-linking NPs with polymers are used in bioimaging applications. Polymers used in the preparation of hybrid materials include PUs, poly-(hydroxyethyl methacrylamide), polyacrylamide, certain PEGs or specialty polymers such as pluronic [a commercial poly(ethylene glycol)-*co*-poly-ethylene oxide] [93]. Bioimaging tools are prepared by using a certain type of contrast agents or functional components for specific imaging. Various substances, namely fluorescence components, X-ray absorbing agents, infrared absorbing agents, and paramagnetic components, are used in fluorescence imaging, CT imaging, photoacoustic imaging, and MRI, respectively. Jia et al. [94] prepared visible-light-induced clay-based lanthanide PNCs having excellent photoluminescence stability and high luminescence lifetime. Owing to their high suspension stability, outstanding luminescence, and low cytotoxicity in cell studies these PNCs acts as a potential candidate for biological cell imaging. Functionalized nanoscale graphene, as well as GO, has been employed in several molecular imaging techniques such as MRI, photoacoustic, optical, and radionuclide-based (e.g., positron emission tomography) imaging. Covalently functionalized nanoscale GO with PEG showed photoluminescence in the infrared and visible range [95]. GO having B-cell specific anti-CD20 antibody produce imaging in live lymphoma cells by using NIR radiation [96]. Wang et al. [97] designed nanoscale MOF@microporous fluorescent organic polymer composites for bioimaging along with improved intracellular uptake.

### 3.3.7 Dental aspects

Nowadays, the selection of suitable materials for the preparation of nanocomposite to mimic dental tissue and restoration of original dental esthetic is an arduous task for many dentists. The possibility to explore materials at the nanoscopic range has created several opportunities to investigate materials having pharmaceutical properties and to utilize these materials in the field of medicine. On account of their distinct physical and chemical properties, NPs are superior to larger-scale particles in terms of surface area which has gained attention in various dental applications [98]. Outstanding surface, biological and mechanical properties, cost-effective production, and simple processing makes polymeric films and polymeric materials highly promising to be employed in a wide range of medicinal and dental applications. Polymers generally used in dentistry are polymethyl methacrylate, PE, polycarbonate, polydimethylsiloxane, PEG, PU, PCL (poly(e-caprolactone)), polylactic acid, PPY (polypyrrole), etc [99]. Fig. 3.5 represents the application of PNCs in dental tissue regeneration. In recent times, GO has gained attention in the dental and restorative dentistry research area due to the biomechanical properties of GO. Given the above properties, Ramadas et al. [100] fabricated a biocompatible HAp−GO nanocomposite to utilize in drug delivery, orthopedic, and dental applications. Replication of columnar structure and analyzing the mechanical properties of enamel are the most investigated areas in dental applications. Yeom et al. [101] replicated enamel-inspired ZnO nanocomposites by reversing the sequence of enamel biosynthesis process.

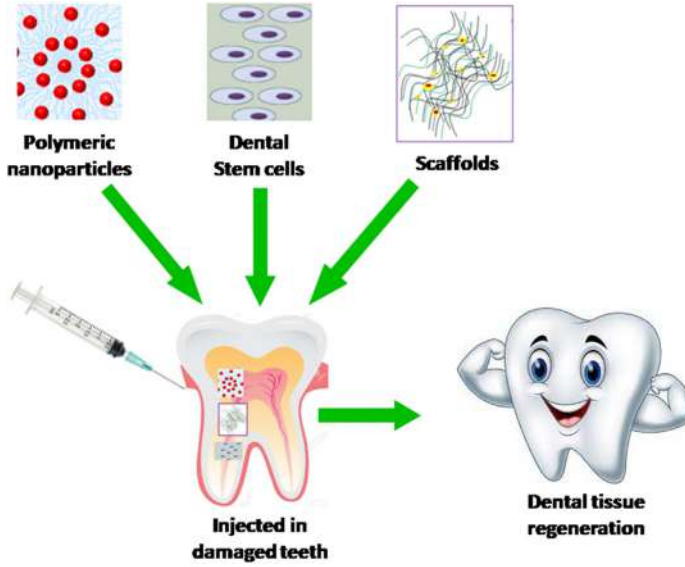


**Figure 3.5** A schematic representation showing the application of PNCs in dental tissue regeneration. *PNCs*, Polymer-based nanocomposites.

## 3.4 Conclusion

This chapter is a concise article summarizing the biological applications of different polymer nanocomposites. Biomedical applications such as drugs delivery, tissue engineering, gene therapy, and dental treatment are included in this chapter. The effects of nanostructured fillers are noticed as the key points for enabling the polymer towards biomedical applications. Although lots of methods have been adapted to design PNCs for biomedical applications, even now there are numerous challenges are required to be studied to reach their complete potential. The biodegradability and biocompatibility of the PNCs must be analyzed appropriately to elude false expectations. Efficient modification and functionalization of both nanomaterial and polymer drive novel prospects toward more impressive applications of PNCs. It will be very engrossing to see the swift maturing of this juvenile's extensively divergent research field in the next decade. This chapter can be a good asset for the readers having an interest in the biocompatibility of PNCs.

## References

[1] I. Shabani, V. Haddadi-Asl, M. Soleimani, E. Seyedjafari, S.M. Hashemi, Ion exchange polymer nanofibers for enhanced osteogenic differentiation of stem cells and ectopic bone formation, ACS Appl. Mater. Interfaces 6 (2013) 72−82.

[2] A. Gautam, S. Ram, Preparation and thermomechanical properties of Ag−PVA nanocomposite films, Mater. Chem. Phys. 119 (2010) 266−271.
[3] B.L. España-Sánchez, C.A. Ávila-Orta, F. Padilla-Vaca, M.G. Neira-Velázquez, P. González-Morones, J.A. Rodríguez-González, et al., Enhanced antibacterial activity of melt processed poly (propylene) Ag and Cu nanocomposites by argon plasma treatment, Plasma Process. Polym. 11 (2014) 353−365.
[4] J. Fei, W. Dou, G. Zhao, A sandwich electrochemical immunosensor for Salmonella pullorum and Salmonella gallinarum based on a screen-printed carbon electrode modified with an ionic liquid and electrodeposited gold nanoparticles, Microchim. Acta 182 (2015) 2267−2275.
[5] S. Nazir, T. Hussain, A. Ayub, U. Rashid, A.J. MacRobert, Nanomaterials in combating cancer: therapeutic applications and developments, Nanomed. Nanotechnol. Biol. Med. 10 (2014) 19−34.
[6] N.G. Patel, A. Kumar, V.N. Jayawardana, C.D. Woodworth, P.A. Yuya, Fabrication, nanomechanical characterization, and cytocompatibility of gold-reinforced chitosan bio-nanocomposites, Mater. Sci. Eng. C. 44 (2014) 336−344.
[7] L. Tamayo, P. Zapata, N. Vejar, M. Azócar, M. Gulppi, X. Zhou, et al., Release of silver and copper nanoparticles from polyethylene nanocomposites and their penetration into Listeria monocytogenes, Mater. Sci. Eng. C. 40 (2014) 24−31.
[8] K. McNamara, S.A.M. Tofail, Nanoparticles in biomedical applications, Adv. Phys. X 2 (1) (2017) 54−88.
[9] C. Xing, Q. Xu, H. Tang, L. Liu, S. Wang, Conjugated polymer/porphyrin complexes for efficient energy transfer and improving light-activated antibacterial activity, J. Am. Chem. Soc. 131 (2009) 13117−13124.
[10] H.H.P. Duong, L.-Y.L. Yung, Synergistic co-delivery of doxorubicin and paclitaxel using multi-functional micelles for cancer treatment, Int. J. Pharm. 454 (1) (2013) 486−495.
[11] D. Scherman, A. Rousseau, P. Bigey, V. Escriou, Genetic pharmacology: progresses in siRNA delivery and therapeutic applications, Gene Ther. 24 (2017) 151−156.
[12] E.A. Makris, A.H. Gomoll, K.N. Malizos, J.C. Hu, K.A. Athanasiou, Repair and tissue engineering techniques for articular cartilage, Nat. Rev. Rheumatol. 11 (1) (2014) 21−34.
[13] R. Roy, S. Komarneni, D.M. Roy, Multi-phasic ceramic composites made by sol-gel technique, MRS Online Proc. Library Archive 32 (1984) 347.
[14] B. Ates, S. Koytepe, A. Ulu, C. Gurses, V.K. Thakur, Chemistry, structures, and advanced applications of nanocomposites from biorenewable resources, Chem. Rev. 120 (2020) 9304−9362.
[15] S. Komarneni, Nanocornposites, J. Mater. Chem. 2 (12) (1992) 1219−1230.
[16] S. Kalia, S. Kango, A. Kumar, Y. Haldorai, B. Kumari, R. Kumar, Magnetic polymer nanocomposites for environmental and biomedical applications, Colloid Polym. Sci. 292 (2014) 2025−2052.
[17] S.A. Corr, Y.P. Rakovich, Y.K. Gun'ko, Multifunctional magnetic-fluorescent nanocomposites for biomedical applications, Nanoscale Res. Lett. 3 (2008) 87−104.
[18] N. Gendelberg, D. Bird, N.M. Ravindra, Nanocomposites for biomedical applicationsChapter 7 in Polymer-Based Multifunctional Nanocomposites and Their Applications, Elsevier, 2019pp. 175−199.
[19] L. Tamayo, M. Azócar, M. Kogan, A. Riveros, M. Páez, Copper-polymer nanocomposites: an excellent and cost-effective biocide for use on antibacterial surfaces, Mater. Sci. Eng. C. 69 (2016) 1391−1409.

[20] P.N. Tri, T.A. Nguyen, T.H. Nguyen, P. Carriere, Antibacterial behavior of hybrid nanoparticles. Chapter 7 in in: S. Mohapatra, T.A. Nguyen, P. Nguyen-Tri (Eds.), Noble Metal-Metal Oxide Hybrid Nanoparticles: Fundamentals and Applications, Elsevier, 2019, pp. 141–155.
[21] R.K. Matharu, T.A. Tabish, T. Trakoolwilaiwan, J. Mansfield, J. Moger, T. Wu, et al., Microstructure and antibacterial efficacy of graphene oxide nanocomposite fibres, J. Colloid Interface Sci. 571 (2020) 239–252.
[22] L. Guo, W. Yuan, Z. Lu, C.M. Li, Polymer/nanosilver composite coatings for antibacterial applications, Colloids Surf. A Physicochem. Eng. Asp. 439 (2013) 69–83.
[23] M. Alam, N.M. Alandis, E. Sharmin, N. Ahmad, F.M. Husain, A. Khan, Mechanically strong, hydrophobic, antimicrobial, and corrosion protective polyesteramide nanocomposite coatings from leucaena leucocephala oil: a sustainable resource, ACS Omega 5 (2020) 30383–30394.
[24] I. Syed, A. Hussain, V. Jaisankar, An eco-friendly synthesis, characterization and antibacterial applications of novel almond gum e poly(acrylamide) based hydrogel silver nanocomposite, Polym. Test. 62 (2017) 154–161.
[25] T. Jayaramudu, K. Varaprasad, R.D. Pyarasani, K.K. Reddy, A. Akbari-Fakhrabadi, V. Carrasco-Sánchez, et al., Hydroxypropyl methylcellulose-copper nanoparticle and its nanocomposite hydrogel films for antibacterial application, Carbohydr. Polym. 254 (2021) 117302.
[26] Y. Dong, M. Argaiz, B. He, R. Tomovska, T. Sun, I. Martín-Fabiani, Zinc oxide superstructures in colloidal polymer nanocomposite films: enhanced antibacterial activity through slow drying, ACS Appl. Polym. Mater. 2 (2020) 626–635.
[27] C.A.S. Ballesteros, D.S. Correa, V. Zucolotto, Polycaprolactone nanofiber mats decorated with photoresponsive nanogels and silver nanoparticles: slow release for antibacterial control, Mater. Sci. & Eng. C. 107 (2020) 110334.
[28] I.M. Factori, J.M. Amaral, P.H. Camani, D.S. Rosa, B.A. Lima, M. Brocchi, et al., ZnO nanoparticle/poly(vinyl alcohol) nanocomposites via microwave-assisted sol–gel synthesis for structural materials, UV shielding, and antimicrobial activity, ACS Appl. Nano Mater. 4 (2021) 7371–7383.
[29] Z. Shariatinia, Z. Zahraee, Controlled release of metformin from chitosan– based nanocomposite films containing mesoporous MCM-41 nanoparticles as novel drug delivery systems, J. Colloid Interface Sci. 501 (2017) 60–76.
[30] S. Javanbakht, M. Pooresmaeil, H. Namazi, Green one-pot synthesis of carboxymethylcellulose/Zn-based metal-organic framework/graphene oxide bio-nanocomposite as a nanocarrier for drug delivery system, Carbohydr. Polym. 208 (2019) 294–301.
[31] K. Liu, R.R. Xing, Q.L. Zou, G.H. Ma, H. Möhwald, X.H. Yan, Simple peptide-tuned selfassembly of photosensitizers towards anticancer photodynamic therapy, Angew. Chem. Int. (Ed.) 55 (2016) 3036.
[32] X.M. Sun, Z. Liu, K. Welsher, J.T. Robinson, A. Goodwin, S. Zaric, et al., Nanographene oxide for cellular imaging and drug delivery, Nano Res. 1 (2008) 203–212.
[33] Z. Liu, J.T. Robinson, X.M. Sun, H.J. Dai, PEGylated nanographene oxide for delivery of water-insoluble cancer drugs, J. Am. Chem. Soc. 130 (2008) 10876–10877.
[34] C.A. Dreiss, Hydrogel design strategies for drug delivery, Curr. Opin. Colloid Interface Sci. 48 (2020) 1–17.
[35] Z. Wang, L.C. Ciacchi, G. Wei, Recent advances in the synthesis of graphene-based nanomaterials for controlled drug delivery, Appl. Sci. 7 (2017) 1175.

[36] L. Huang, M. Liu, L. Mao, D. Xu, Q. Wan, G. Zeng, et al., Preparation and controlled drug delivery applications of mesoporous silica polymer nanocomposites through the visible light induced surface-initiated ATRP, Appl. Surf. Sci. 412 (2017) 571–577.
[37] M.N. Mohammed, K.B. Yusoh, J.H.B.H. Shariffuddin, Poly(N-vinyl caprolactam) thermoresponsive polymer in novel drug delivery systems: a review, Mater. Express 8 (2018) 21–34.
[38] S.S. Liow, Q. Dou, D. Kai, Z. Li, S. Sugiarto, C.Y.Y. Yu, Longterm real-time in vivo drug release monitoring with AIE thermogelling polymer, Small 13 (2017) 1–7.
[39] C.L. Weaver, J.M. LaRosa, X.L. Luo, X.T. Cui, Electrically controlled drug delivery from graphene oxide nanocomposite films, ACS Nano 8 (2014) 1834–1843.
[40] S. Mallakpour, L. Khodadadzadeh, Ultrasonic-assisted fabrication of starch/MWCNT-glucose nanocomposites for drug delivery, Ultrason. – Sonochem. 40 (2018) 402–409.
[41] N.V. Mdlovu, F.A. Mavuso, K. Lin, T. Chang, Y. Chen, S.S.-S. Wang, et al., Iron oxide-pluronic F127 polymer nanocomposites as carriers for a doxorubicin drug delivery system, Colloids Surf. A 562 (2019) 361–369.
[42] M.H. Xiong, Y. Bao, X.Z. Yang, Y.C. Wang, B.L. Sun, J. Wang, Lipase-sensitive polymeric triple-layered nanogel for "on-demand" drug delivery, J. Am. Chem. Soc. 134 (2012) 4355–4362.
[43] H. Chen, Z.Y. Wang, S.F. Zong, L. Wu, P. Chen, D. Zhu, et al., Sers-fluorescence monitored drug release of a redox-responsive nanocarrier based on graphene oxide in tumor cells, ACS Appl. Mater. Interfaces 6 (2014) 17526–17533.
[44] H. Wang, J. Yi, Y. Yu, S. Zhou, NIR upconversion fluorescence glucose sensing and glucose-responsive insulin release of carbon dot-immobilized hybrid microgels at physiological Ph, Nanoscale 9 (2017) 509–516.
[45] J.B. Song, X.Y. Yang, O. Jacobson, L.S. Lin, P. Huang, G. Niu, et al., Sequential drug release and enhanced photothermal and photoacoustic effect of hybrid reduced graphene oxide-loaded ultrasmall gold nanorod vesicles for cancer therapy, ACS Nano 9 (2015) 9199–9209.
[46] N. Falcone, N.M.O. Andoy, R.M.A. Sullan, H.-B. Kraatz, Peptide-polydopamine nanocomposite hydrogel for a laser-controlled hydrophobic drug delivery, ACS Appl. Bio Mater. (2021).
[47] Y. Ahmadian, A. Bakravi, H. Hashemi, H. Namazi, Synthesis of polyvinyl alcohol/CuO nanocomposite hydrogel and its application as drug delivery agent, Polym. Bull. 76 (2019) 1967–1983.
[48] D. Pathania, M. Kumari, V.K. Gupta, Fabrication of ZnS-cellulose nanocomposite for drug delivery, antibacterial and photocatalytic activity, Elsevier Mater. Des. 87 (2015) 1556–1564.
[49] A. Bakravi, Y. Ahamadian, H. Hashemi, H. Namazi, Synthesis of gelatin-based biodegradable hydrogel nanocomposite and their application as drug delivery agent, Adv. Polym. Technol. 37 (2018) 2625–2635.
[50] G. Prabha, V. Raj, Preparation and characterization of polymer nanocomposites coated magnetic nanoparticles for drug delivery applications, J. Magn. Magn. Mater. 408 (2016) 26–34.
[51] C. Sarkar, A.R. Chowdhuri, A. Kumar, D. Laha, S. Garai, J. Chakraborty, et al., One pot synthesis of carbon dots decorated carboxymethyl cellulosehydroxyapatite nanocomposite for drug delivery, tissue engineering and Fe3 + ion sensing, Carbohydr. Polym. 181 (2018) 710–718.

[52] L. Bounabi, N.B. Mokhanchi, N. Haddadine, F. Ouazib, R. Barille, Development of poly (2-hydroxyethyl methacrylate)/clay composites as drug delivery systems of paracetamol, J. Drug. Deliv. Sci. Technol. 33 (2016) 58−65.
[53] D. Pathania, D. Gupta, S. Agarwal, M. Asif, V.K. Gupta, Fabrication of chitosan-g-poly(acrylamide)/CuS nanocomposite for controlled drug delivery and antibacterial activity, Mater. Sci. Eng. C. 64 (2016) 428−435.
[54] K. Wang, H.F. Wen, D.G. Yu, Y. Yang, D.F. Zhang, Electrosprayed hydrophilic nanocomposites coated with shellac for colon-specific delayed drug delivery, Mater. Des. 143 (2018) 248−255.
[55] S. Javanbakht, H. Namazi, Doxorubicin loaded carboxymethyl cellulose/graphene quantum dot nanocomposite hydrogel films as a potential anticancer drug delivery system, Mater. Sci. Eng. C. 87 (2018) 50−59.
[56] M.S. Amini-Fazl, R. Mohammadi, K. Kheiri, 5-Fluorouracil loaded chitosan/polyacrylic acid/Fe3O4 magnetic nanocomposite hydrogel as a potential anticancer drug delivery system, Int. J. Biol. Macromol. 132 (2019) 506−513.
[57] V. Wagner, A. Dullaart, A.-K. Bock, A. Zweck, The emerging nanomedicine landscape, Nat. Biotechnol. 24 (2006) 1211.
[58] P.P. Kundu, V. Sharma, Synthetic polymeric vectors in gene therapy, Curr. Opin. Solid. State Mater. Sci. 12 (2008) 89−102.
[59] M.A. Gosselin, W. Guo, R.J. Lee, Efficient gene transfer using reversibly crosslinked low molecular weight polyethylenimine, Bioconjugate Chem. 12 (2001) 989−994.
[60] H. Zhong, Z.G. He, Z. Li, G.Y. Li, S.R. Shen, X.L. Li, Studies on polyamidoamine dendrimers as efficient gene delivery vector, J. Biomater. Appl. 22 (6) (2008).
[61] X. Wang, J. Dai, X. Wang, Q. Hu, K. Huang, Z. Zhao, et al., MnO2-DNAzyme-photosensitizer nanocomposite with AIE characteristic for cell imaging and photodynamic-gene therapy, Talanta 202 (2019) 591−599.
[62] M. Wang, Y. Guo, Y. Xue, W. Niu, M. Chen, P.X. Ma, et al., Engineering multifunctional bioactive citric acid-based nanovectors for intrinsical targeted tumor imaging and specific siRNA gene delivery in vitro/ in vivo, Biomaterials 199 (2019) 10−21.
[63] R. Wang, Y. Hu, N. Zhao, F. Xu, Well-defined peapod-like magnetic nanoparticles and their controlled modification for effective imaging guided gene therapy, ACS Appl. Mater. Interfaces 8 (2016) 11298−11308.
[64] X. Wang, C. Hélary, T. Coradin, Local and sustained gene delivery in silica-collagen nanocomposites, ACS Appl. Mater. Interfaces 7 (2015) 2503−2511.
[65] M. Okamoto, B. John, Synthetic biopolymer nanocomposites for tissue engineering Scaffolds, Prog. Polym. Sci. 38 (2013) 1487−1503.
[66] R.A. Quirk, R.M. France, K.M. Shakesheff, S.M. Howdle, Supercritical fluid technologies and tissue engineering scaffolds, Curr. Opin. Solid. State Mater. Sci. 8 (2004) 313−821.
[67] A.M. Díez-Pascual, A.L. Díez-Vicente, Poly(propylene fumarate)/polyethylene glycol-modified graphene oxide nanocomposites for tissue engineering, ACS Appl. Mater. Interfaces 8 (2016) 17902−17914.
[68] B.L. Seal, T.C. Otero, A. Panitch, Polymeric biomaterials for tissue and organ regeneration, Mater. Sci. Eng. Rep. 34 (2001) 147−230.
[69] P.X. Ma, Scaffolds for tissue fabrication, Mater. Today 7 (2004) 30−40.
[70] B.J.R.F. Bolland, J.M. Kanczler, P.J. Ginty, S.M. Howdle, K.M. Shakesheff, D.G. Dunlop, The application of human bone marrow stromal cells and poly(DL-lactic acid) as a biological bone graft extender in impaction bone grafting, Biomaterials 29 (2008) 3221−3227.

[71] R. Zhang, P.X. Ma, Processing of polymer scaffolds: phase separation, in: A. Atala, R. Lanza (Eds.), Methods of Tissue Engineering, Academic Press, San Diego, 2001, p. 715.
[72] N. Eslahi, M. Abdorahim, A. Simchi, Smart polymeric hydrogels for cartilage tissue engineering: a review on the chemistry and biological functions, Biomacromolecules 17 (2016) 3441−3463.
[73] K.W.M. Boere, B.G. Soliman, D.T.S. Rijkers, W.E. Hennink, T. Vermonden, Macromolecules 47 (7) (2014) 2430−2438.
[74] B. Guo, P.X. Ma, Conducting polymers for tissue engineering, Biomacromolecules 19 (2018) 1764−1782.
[75] B.S. Spearman, A.J. Hodge, J.L. Porter, J.G. Hardy, Z.D. Davis, T. Xu, et al., Conductive interpenetrating networks of polypyrrole and polycaprolactone encourage electrophysiological development of cardiac cells, Acta Biomater. 28 (2015) 109−120.
[76] M. Hassan, K. Dave, R. Chandrawati, F. Dehghani, V.G. Gomes, 3D printing of biopolymer nanocomposites for tissue engineering: nanomaterials, processing and structure-function relation, Eur. Polym. J. 121 (2019) 109340.
[77] S.M. Hong, D. Sycks, H.F. Chan, S.T. Lin, G.P. Lopez, F. Guilak, et al., 3D printing of highly stretchable and tough hydrogels into complex, cellularized structures, Adv. Mater. 27 (27) (2015) 4035−4040.
[78] G. Lalwani, A.M. Henslee, B. Farshid, L. Lin, F.K. Kasper, Y. Qin, et al., Two-dimensional nanostructure-reinforced biodegradable polymeric nanocomposites for bone tissue engineering, Biomacromolecules 14 (2013) 900−909.
[79] X. He, Q. Xiao, C. Lu, Y. Wang, X. Zhang, J. Zhao, et al., Uniaxially aligned electrospun all-cellulose nanocomposite nanofibers reinforced with cellulose nanocrystals: scaffold for tissue engineering, Biomacromolecules 15 (2014) 618−627.
[80] J. Moon, N. Thapliyal, K.K. Hussain, R.N. Goyal, Y. Shim, Conducting polymer-based electrochemical biosensors for neurotransmitters: a review, Biosens. Bioelectron. 102 (2018) 540−552.
[81] S.K. Krishnan, E. Singh, P. Singh, M. Meyyappan, H.S. Nalwa, A review on graphene-based nanocomposites for electrochemical and fluorescent biosensors, RSC Adv. 9 (2019) 8778−8881.
[82] L. Wang, Y. Zhang, A. Wu, G. Wei, Designed graphene-peptide nanocomposites for biosensor applications: a review, Analytica Chim. Acta 985 (2017) 24−40.
[83] J.Q. Liu, Z. Liu, C.J. Barrow, W.R. Yang, Molecularly engineered grapheme surfaces for sensing applications: a review, Anal. Chim. Acta 859 (2015) 1−19.
[84] J. Wang, Y. Zhao, F.X. Ma, K. Wang, F.B. Wang, X.H. Xia, Synthesis of a hydrophilic poly-l-lysine/graphene hybrid through multiple non-covalent interactions for biosensors, J. Mat. Chem. B 1 (2013) 1406−1413.
[85] J.-L. Chen, X.-P. Yan, K. Meng, S.-F. Wang, Graphene oxide based photoinduced charge transfer label-free near-infrared fluorescent biosensor for dopamine, Anal. Chem. 83 (2011) 8787−8793.
[86] S. Xu, M. Deng, Y. Sui, Y.Z. Chen, Ultrasensitive determination of bisphenol A in water by inhibition of copper nanoclusters enhanced chemiluminescence from the luminole KMnO4 system, RSC Adv. 4 (2014) 44644−44649.
[87] H. Shirakawa, E.J. Louis, A.G. MacDiarmid, C.K. Chiang, A.J. Heeger, Synthesis of electrically conducting organic polymers: halogen derivatives of polyacetylene, $(CH)_x$, J. Chem. Soc. Chem. Commun. (1977) 578−580.
[88] Z. Zhang, M. Liao, H. Lou, Y. Hu, X. Sun, H. Peng, Conjugated polymers for flexible energy harvesting and storage, Adv. Mater. 30 (2018) 1704261.

[89] W. Wang, M. Cui, Z. Song, X. Luo, An antifouling electrochemical immunosensor for carcinoembryonic antigen based on hyaluronic acid doped conducting polymer PEDOT, RSC Adv. 6 (2016) 88411–88416.
[90] S. Xu, Y. Zhang, Y. Zhu, J. Wu, K. Li, G. Lin, et al., Facile one-step fabrication of glucose oxidase loaded polymeric nanoparticles decorating MWCNTs for constructing glucose biosensing platform: structure matters, Biosens. Bioelectron. 135 (2019) 153–159.
[91] A. Mishra, A.R. Ferhan, C.M.B. Ho, J.H. Lee, D.-H. Kim, Y.-J. Kim, et al., Fabrication of plasmon-active polymer-nanoparticle composites for biosensing applications, Int. J. Precis. Eng. Manufacturing-Green Technol. 8 (2021) 945–954.
[92] S. Achilefu, Introduction to concepts and strategies for molecular imaging, Chem. Rev. 110 (2010) 2575–2578.
[93] O.S. Wolfbeis, An overview of nanoparticles commonly used in fluorescent bioimaging, Chem. Soc. Rev. 44 (2015) 4743.
[94] L. Jia, T. Zhou, J. Xu, Z. Xu, M. Zhang, Y. Wang, et al., Visible light-induced lanthanide polymer nanocomposites based on clays for bioimaging applications, J. Mater. Sci. 51 (2016) 1324–1332.
[95] M. Silva, N.M. Alves, M.C. Paiva, Graphene-polymer nanocomposites for biomedical applications, Polym. Adv. Technol. (2017) 1–14.
[96] Y. Zhang, T.R. Nayak, H. Hong, W. Cai, Graphene: a versatile nanoplatform for biomedical applications, Nanoscale 4 (2012) 3833–3842.
[97] L. Wang, W. Wang, X. Zheng, Z. Li, Z. Xie, Nanoscale fluorescent MOF@microporous organic polymers composites for enhanced intracellular uptake and bioimaging, Chem. Eur. J. 23 (6) (2017) 1379–1385.
[98] T. Barot, D. Rawtani, P. Kulkarni, Nanotechnology-based materials as emerging trends for dental applications, Rev. Adv. Mater. Sci. 60 (2021) 173–189.
[99] D. Rokaya, V. Srimaneepong, J. Sapkota, J. Qin, K. Siraleartmukul, V. Siriwongrungson, Polymeric materials and films in dentistry: an overview, J. Adv. Res. 14 (2018) 25–34.
[100] M. Ramadas, G. Bharath, N. Ponpandian, A.M. Ballamurugan, Investigation onbiophysical properties of hydroxyapatite/graphene oxide (HAp/GO) basedbinary nanocomposite for biomedical applications, Mater. Chem. Phys. 199 (2017) 179–184.
[101] B. Yeom, T. Sain, N. Lacevic, D. Bukharina, S.-H. Cha, A.M. Waas, et al., Abiotic Tooth Enamel, Nature 543 (2017) 95–98.

# Electrical properties of polymer nanocomposites

4

*B. Nivedha[1], H. Mohit[2], M.R. Sanjay[3], N.S. Suresh[4], Suchart Siengchin[3] and P. Ramesh[5]*

[1]Department of Physics, National Institute of Technology, Tiruchirappalli, Tamil Nadu, India
[2]Department of Mechanical Engineering, Alliance College of Engineering and Design, Alliance University, Karnataka, India
[3]Natural Composites Research Group, Department of Materials and Production Engineering, The Siridhorn International Thai German Graduate School of Engineering, King Mongkut's University of Technology North Bangkok, Bangkok, Thailand
[4]Department of Electrical and Electronics Engineering, St. Joseph Engineering College, Mangalore, Karnataka, India
[5]Department of Production Engineering, National Institute of Technology, Tiruchirappalli, Tamil Nadu, India

## 4.1 Introduction

The incrementing interest for biodegradable and environmentally friendly materials provokes the advancement of techniques to implement renewable feedstock from lignocellulosic components [1−5]. The vast quantities of lignocellulosic debris developed in the transformation of sugarcane in mills highlight the possibility of this component as feedstock to fascinate the developing interest for new bio-based ingredients [3,6−8]. Along with straw and sugarcane bagasse that is partly left in the sector for generation of bioenergy and soil protection [9], it could also be a possible feedstock for nanocellulose formation, where the fiber morphology and chemical constituents are similar to sugarcane plant [10−12]. The nanocellulosic components separated from plants consist of cellulose nanocrystals and cellulose nanofibrils that vary in their applications and characteristics. The cellulose nanofibril structure has widths and lengths of 5−60 nm and 0.1−2 μm, respectively, with disordered and crystalline phases and is generally collected by mechanical/chemical techniques.

In contrast, cellulose nanocrystals have cross-sections and lengths of 5−70 nm and 100−250 nm, respectively, extracted primarily from the acid hydrolysis technique [13]. The properties of these components are higher stiffness and strength, chemical functionalization/modification capacity, biodegradability, hydrophilicity, and lower weight [14,15]. The recent research advancement from nanocellulose has informed its possible applications in regions such as pharmaceutical and medical products [16,17], electronic devices [18], packaging, cosmetics [17], and composite fabrication [19]. The separation of nanocellulose from sugarcane bagasse has been formerly studied using different techniques containing a combination of enzymatic

**Advanced Polymer Nanocomposites. DOI: https://doi.org/10.1016/B978-0-12-824492-0.00006-4**


hydrolysis with mechanical modification [20], acid hydrolysis [21], and mechanical modification [22]. The chemical method utilizing strong acids such as sulfuric acid is the broadly applied technique for separating nanocellulose as cellulose nanocrystals.

Furthermore, the limitations of this technique have the complexity of the development of a vast quantity of salts during the process of neutralization, higher consumption of water during neutralization, corrosion of the hydrolysis reactor, and recovery of acid. Even though the hydrolysis technique to extract cellulose nanocrystals can be imposing, some industries are presenting creating kilograms to tons per day capacity of this component [23]. The cellulose nanocrystals emerging from sulfuric acid reaction provide shattered stability because of the appearance of sulfate components, whereas these constituents also decrease the thermal characteristics of the nanocellulose [24]. Hence, specific investigations have nominated the utilization of methods that target to create cellulose nanocrystals with more excellent thermal characteristics such as reaction from enzymes and phosphoric acid [17,25,26]. The fabrication of nanocellulose from enzymatic hydrolysis has the benefits of not producing hazardous waste, the potential of utilizing the soluble carbohydrates discharged in the reaction to collect other bio-based components, and decreased the utilization of water in the method [27]. In addition, the manufacturing of nanocellulose from the enzymatic reaction has been recorded to outcome in simple functionalized nanosized with higher aspect ratio and thermal characteristics [28]. Nonetheless, the utilization of enzymatic reaction as a surface to collect nanocellulose from the sugarcane biomass consisting of straw and bagasse prevails to be studied. However, a schematic comparison between possible renewable sources providing a similar examining procedure could help exemplify their potential utilization as feedstock for the fabrication of nanocellulose.

Presently, the hairy cellulose nanocrystals are produced from the periodate oxidation method to damage the C2−C3 strong bonds in the glucose restate [29−32], which has also achieved more attention. Furthermore, the periodate oxidation technique investigation is still in the inception stage and few published articles on regulating reaction cases for many raw materials [29]. For the different kinds of cellulose, the production of varying cellulose nanocrystals (crystallinity, functional groups, microstructures, etc.) to contact additional requirements still endures issues in the advancement of cellulose science and their respective sectors. In addition, the cellulose nanocrystals deficiencies such as lower thermal stability also restrict their more utilization. Hybrid conversion is one of the fundamental ways of altering cellulose. Hybrid components are a new type of matter that comprises physical or electrostatic interactions to produce materials possessing good characteristics and various components via solid covalent bonds [33−35]. The investigation on inorganic−organic hybrid component with cellulose nanocrystals as the organic region has been observed in recent decades. The inorganic materials contain gold nanoparticles, silicon dioxide, ferroferric oxide, cerium oxide, titanium carbide, alumina−zirconia, and graphene oxide [36−48]. These hybrid components comprise the superior characteristics of both constituents to present identical properties.

Furthermore, problems such as schematic investigations for various cellulose nanocrystals structures and the examination for novel hybrid components are imperatively required to be assigned. Differently, the polyhedral oligomeric silsesquioxane has been eliminated in producing cellulose nanocrystals mixed nano-based materials with good flame-retardant characteristics, higher mechanical and thermal features [49,50]. Furthermore, it has been applied to produce inorganic−organic elastomer with better self-healing and shape memory alloy [51−53]. However, comprehensively, it is still an issue to produce cellulose nanocrystals and hybrid schemes adequate for different sectors from a wide variety of biomass sources.

Here, we studied the usefulness of the nanocellulose fiber obtained from waste sugarcane bagasse using a mechanical milling process. The performance of the method assigned was determined using a wide variety of examining ways. The chemically treated and untreated sugarcane bagasse and aluminum silicon carbide (Al-SiC) [54−56] as a reinforcement material to epoxy polymer were analyzed in electrical and dielectric characteristics. The outcome signifies the possibility of applying the mechanical method as a surface to create cellulose nanocrystals with improved electrical and dielectric properties that are essential factors for utilization of this material in various applications such as printed circuit boards, insulating materials. The nanocellulose material collected fascinates the growing interest for new biomaterials and can share to free up a wide palette of valuable components within the feedstock.

## 4.2 Materials and method

### 4.2.1 Materials

The epoxy polymer (LY556) and hardener (HY951) were supplied from Sakthi Fiber Glass Inc. Chennai, India. The sugarcane bagasse was collected from the sugarcane manufacturing industry in the form of stalks. The aluminum powder (10 μm) and silicon carbide (150 μm) have been procured from Shri Ganapathy Colours Inc., Chennai, India and Carborundum Universal Ltd., Kochi, India.

### 4.2.2 Preparation of sugarcane nanocellulose fiber

The obtained sugarcane bagasse was cleaned with fresh tap water to remove the soil, dirt, and other foreign materials from the stalk fibers. After washing with fresh tap water, the stalk fiber was soaked in a salt solution for 2 days, as discussed in our previous investigation [57,58]. Then, the salt solution-treated sugarcane bagasse was shifted with 0.1 N NaOH solution at 100°C for the removal of lignin content from the structure of the bagasse fiber. After these chemical treatments, the sugarcane bagasse has been milled using an industrial grinder and transferred to the nanosieve of 70 nm (average size) to extract the nanocellulose particles as a reinforcement material.

### 4.2.3 Fabrication of Al-SiC nanoparticles

The supplied aluminum and silicon carbide particles were mixed in a horizontal type of high-energy ball mill, which drum is made up of aluminum−silicon carbide to avoid contamination with the milling material. The processing techniques were 10:1 as balls to powder weight ratio, 150 rpm as milling speed, and 3 hours as milling time with an interim period of 30 minutes per hour to avoid the overheating of the machine. After the milling process, the mixed powder is separated from a nanosieve of 55 nm (average size) and kept separately [59].

### 4.2.4 Production of sugarcane nanocellulose/Al-SiC epoxy hybrid composites

The 5 wt.% of chemically treated or untreated sugarcane nanocellulose and 5 wt.% of Al-SiC nanoparticles are combined using low energy planetary-type ball mill. In addition, silica gel was infused during the ball milling process in the mixture to produce strong bonding within the nanocellulose and inorganic fillers. Finally, the separated ball-milled sugarcane nanocellulose-Al-SiC particles were transferred into the epoxy polymer and homogeneously dispersed with an ultrasonicator probe under the frequency of 24 MHz and power of 20 kW, as discussed in our previous study. After the ultrasonication process, the 10 wt.% of hardener HY 951 has been combined with the resin mixture and mechanically stirred for 3 minutes. We then subjected it to poured into the die mold for the production of epoxy laminate. After 6 hours, the laminate has been removed from the die mold and placed in a heating furnace under $60 \pm 3^{\circ}C$ for 48 hours to remove the residual moisture content [45,60,61].

## 4.3 Epoxy polymer nanocomposite characterization

### 4.3.1 Electrical properties

The space charge characteristics were analyzed from the pulsed electro-acoustic technique under the 40 kV $mm^{-1}$ of direct current electric field and ambient temperature of $30 \pm 2^{\circ}C$. The specimen was nearly 400 μm thick and a 20 mm diameter of the aluminum electrode on both surfaces. Silicone oil was used between the specimen and electrode to reduce the outer interference.

The electric field versus current density graphs of the epoxy hybrid nanocomposites under ambient temperature were determined from a specimen of 250 μm thickness. Then, a three-electrode scheme was vapor-deposited in silver particles to collect guard and electrode on one surface and a higher-voltage electrode on another surface; this electrode scheme was placed in the oven and stored for 60 minutes under $50^{\circ}C$ before starting the circuit. Finally, the picoammeter (EST122) was applied to determine the direct current, and the charging current

60 minutes after starting the circuit was reported at 5−40 kV $mm^{-1}$ of an electric field.

The direct current breakdown for a specimen of 100 μm thickness was applied during the breakdown experiment and vapor-deposited in aluminum foil to produce 20 mm diameter of an aluminum electrode on both surfaces of the specimen. The specimen was sandwiched between two electrodes of 70 and 20 mm diameters. The dielectric breakdown was calculated under ambient temperature by increasing the voltage by 1 kV $s^{-1}$. The whole structure was soaked in silicone oil to avoid flashover. Weibull expression was analyzed from experimental outcomes to collect data discursiveness and breakdown.

The thermal stimulated current spectroscopy of the specimen was measured by setting in the vacuum chamber and polarized under an electric field of 30 kV $mm^{-1}$ at 60°C and half hours. Then, the specimens were rapidly cooled down below subzero temperature using nitrogen in liquid form. Furthermore, polarization voltage was eliminated, and the specimen was circuit-break for 600 seconds to remove the interface charge. Furthermore, the circuit break current was lower than one picoamemeter, and the thermally stimulated current was reported from 0°C to 90°C with 1°C $min^{-1}$ of heating rate.

### 4.3.2 Dielectric properties

The electrical conductivity and dielectric characteristics of a specimen with 1 $cm^2$ of the area were calculated from an impedance analyzer (Agilent 4294A) under the frequency ranges between 1 kHz and 10 MHz. Before the dielectric test, the thickness of the specimen was reported, and then the specimen was silver plate sputter coated. As a result, the loss parameter and dielectric permittivity of epoxy hybrid nanocomposites can be estimated.

## 4.4 Results and discussion

### 4.4.1 Space charge distribution

The electric field and distribution of space charge in chemically and untreated sugarcane nanocellulose fiber epoxy hybrid nanocomposites under ambient temperature was collected from the pulsed electroacoustic technique.

Fig. 4.1A and B presents the space charge in chemically and untreated epoxy hybrid nanocomposites within 1 hour at 40 kV $min^{-1}$ of an electric field. For untreated epoxy hybrid nanocomposites, apparent uniform charge injection around the cathode possessed, and both injection depth and amount of the aggregated constant charge increment with polarization period. The aggregated space charge tends to exaggeration of the electric region. Such critical electric region exaggeration is inadequate for insulation utilizations and postures crucial hazard to high voltage direct current wires. While comparing with untreated and chemically treated sugarcane nanocellulose, epoxy hybrid nanocomposites exhibit lower charge aggregation in the specimen.

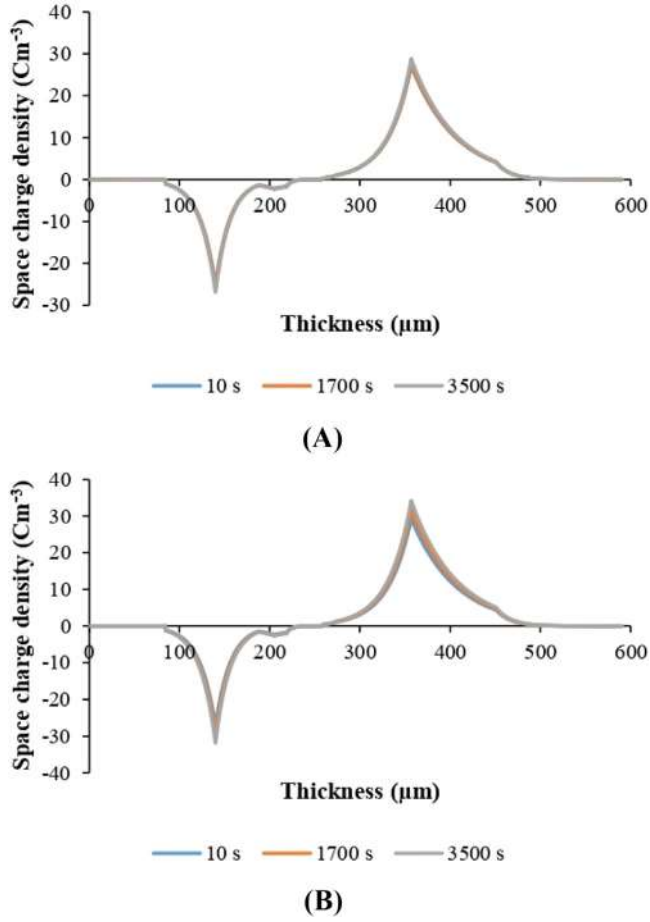


**Figure 4.1** Distribution of space charge of sugarcane nanocellulose/Al-SiC epoxy hybrid nanocomposites (A) untreated and (B) chemically treated.

A uniform charge injection is efficiently prohibited, and charge presents no proper validation with polarization period. Dispersion of charge after circuit breaker presents similar properties, as observed in Fig. 4.2A and B.

In this context, the amount of charge is decreased in chemically treated ones. Similarly, the deviation of charge with a period is correspondingly lower in chemically treated than the untreated epoxy hybrid nanocomposites [62].

### 4.4.2 Direct current conductance analysis

The electric field based on conduction current ($E-J$) properties was evaluated to discard ignite on the influence of the broad traps in chemically treated epoxy hybrid

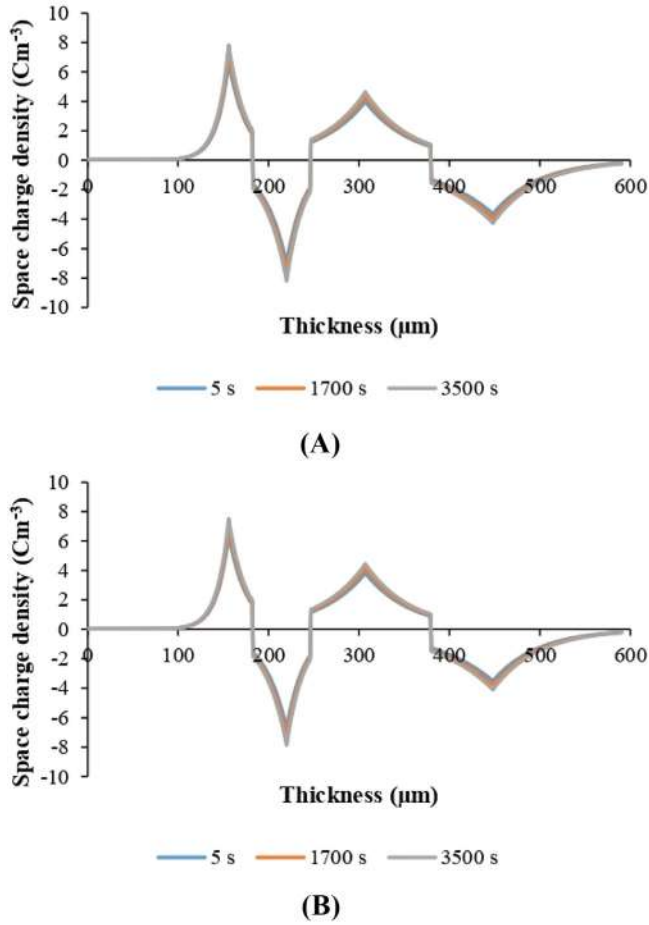


**Figure 4.2** Short circuit distribution of sugarcane nanocellulose/Al-SiC epoxy hybrid nanocomposites (A) untreated and (B) chemically treated.

nanocomposites on the transport properties and charge detrapping/trapping. In Fig. 4.3, the $E-J$ graphs of chemically and untreated epoxy hybrid nanocomposites are presented, and it was examined that both charts can be separated into two regions.

Under a lower temperature range in Fig. 4.3A, the current density improves continuously with the utilized electric field with ramps a bit greater than one at the lower electric field. This variation is assigned to improvement in carrier density with increment in electric field. Slopes for chemically and untreated sugarcane nanocellulose epoxy hybrid nanocomposites achieved greater in the higher electric field. The slopes at higher and lower electric field $m_1$, $m_2$, and the required electric field ($F_c$) are given in Table 4.1.

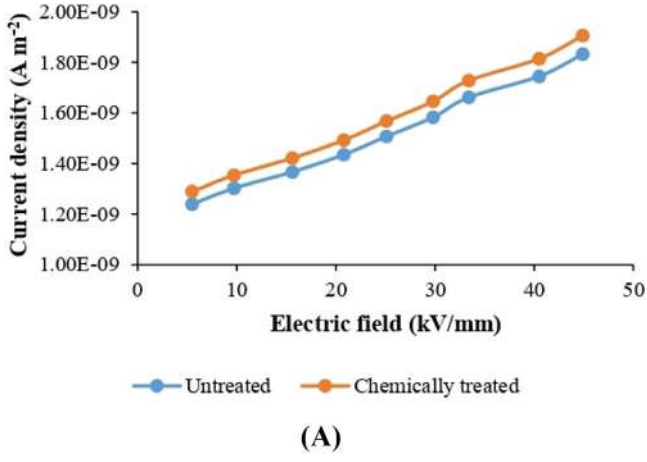


(A)

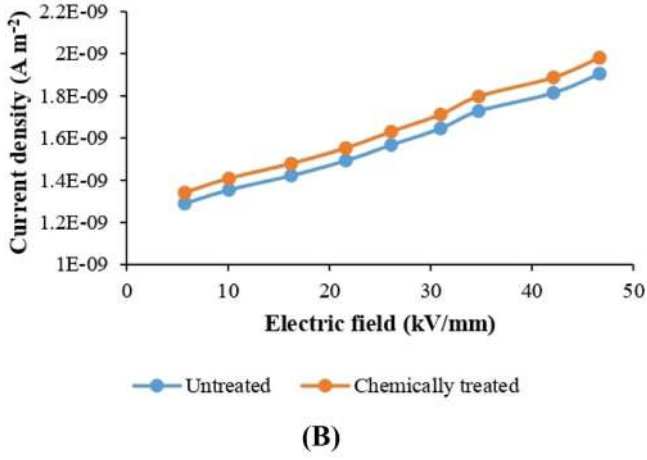


(B)

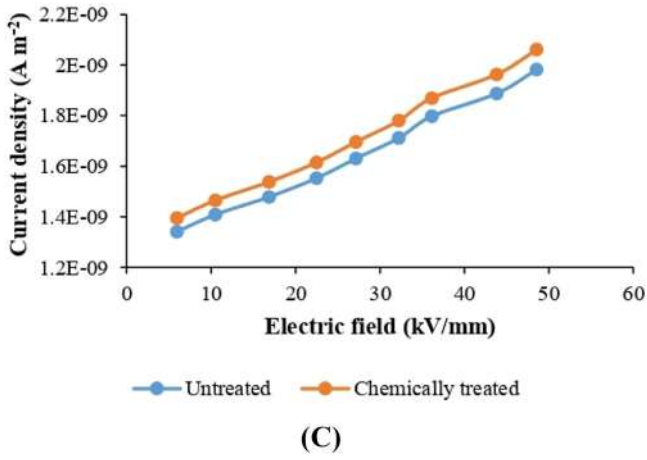


(C)

**Figure 4.3** Electric field versus current density graphs of untreated and chemically treated sugarcane nanocellulose and Al-SiC epoxy hybrid nanocomposites (A) 32°C, (B) 50°C, and (C) 60°C.

**Table 4.1** Slopes at higher and lower electric field $m_1$, $m_2$, and the required electric field $F_c$.

| Specimen | $m_1$ | $m_2$ | $F_c$ (kV mm$^{-1}$) |
|---|---|---|---|
| Untreated sugarcane nanocellulose/Al-SiC epoxy hybrid nanocomposite | 4.27 | 1.31 | 12.67 |
| Chemically treated sugarcane nanocellulose/Al-SiC epoxy hybrid nanocomposite | 5.29 | 1.35 | 18.96 |

The appearance of the necessary electric field is described from the restricted charge current principle [63]. The conduction current and required electric field pursue ohm's law, as shown in Eq. (4.1):

$$K = \frac{f_0 \mu l_0 V}{d} \tag{4.1}$$

where $f_0$, $V$, and $d$ are the charge of an element, applied field, and specimen thickness, respectively. $l_0$ is the equilibrium density of charge carrier. Carrier movement ($\mu$) is assigned to parameter of the field.

From the ohm's expression (1), the current density is directly proportional to the field. For illustration, m1 = one. When the electric field improves, carriers in broad traps capture dependent role and currently accept compared restricted space charge current expression, as given in Eq. (4.2) [64,65].

$$K = l_0 \mu f^{1-g}{}_0 \left(\frac{\beta g}{H(g+1)}\right)^g \left(\frac{2g+1}{g+1}\right)^{g+1} \left(\frac{V^{g+1}}{d^{2g+1}}\right) \tag{4.2}$$

where $l_0$, $\beta$, $H$, and $g$ are efficient density, permittivity of the sample, whole trap density, and consistent inverse to the temperature measured, respectively.

It may be forecasted that child's principle completely gratified if temperature or electric field is large. From Fig. 4.3B and C, the slopes of the conductivity graphs under more excellent electrical fields attain lower again and accept quantities nearly two. Chemically treated sugarcane nanocellulose/Al-SiC epoxy hybrid nanocomposites are higher than the untreated specimen, stating many traps in chemically treated composite samples that are persistent with the different density functional and thermally stimulated current principal evaluations.

The distribution of charge in a polymer is directly related to the movement of charge and detrapping/trapping. Thermally stimulated technique efficiently and broadly applied by analyzing trap regions of epoxy polymer. Regional trapping stages in epoxy have a drastic influence on composite's electrical characteristics. Thermal stimulated current properties of chemically and untreated epoxy hybrid nanocomposites are presented in Fig. 4.4A. Both untreated and chemically treated specimen are nonpolar epoxy polymers, and only the captured carrier is shared with

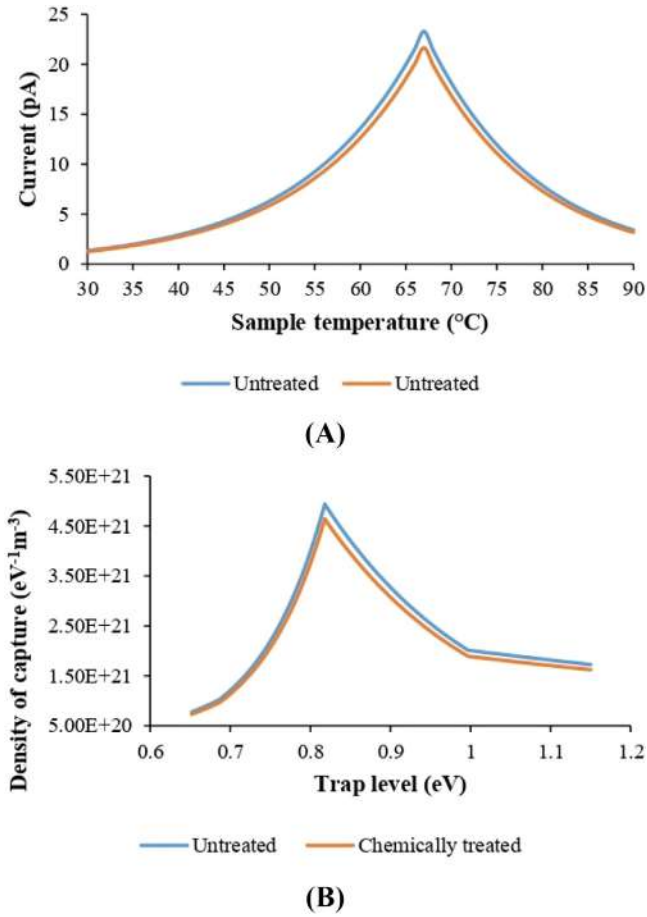


**Figure 4.4** Untreated or chemically treated sugarcane nanocellulose and Al-SiC epoxy hybrid nanocomposites (A) thermally stimulated current and (B) distribution of capture level.

the stimulated current. The thermally stimulated current properties found that there are higher captures in chemically treated than the untreated ones. The thermal stimulated current line of untreated attained its peak at nearly 55°C, exhibiting the discharge of a vast quantity of captured carriers. For the chemically treated specimen, two peaks were observed between 45°C and 75°C. When the temperature rises, the captured charge carriers collect sufficient energy for rescue trap regions. Larger thermal peak states broader carriers' captures in chemically treated samples. The broader traps would arrest the carrier charge nearly the insulator-electrode and hence increment the protection from injection charge. To highlight the trap stages in both untreated and chemically treated epoxy hybrid nanocomposites, the technology to observe the capture level depends on the hypothesis of linear trap level of dispersion and injection of electrons as discussed in a previous investigation [66].

The capture level density of untreated and chemically treated epoxy hybrid nanocomposites can be collected from Fig. 4.4B. The capture range density line of untreated specimen attains the peak at 0.93 eV, which is persistent with the outcome of the 0.922 eV collected from previous investigation [67].

While comparing the untreated epoxy hybrid nanocomposites, both broader and shallower carrier charge traps have been suggested from the polymer in the nanocomposites that is persistent with the previous investigation [62].

### 4.4.3 Direct current breakdown

Direct current breakdown was studied to determine insulation characteristics of chemically treated or untreated epoxy hybrid nanocomposites. The testing information was examined from the Weibull distribution that is comprehensively applied to resolve the insulating materials' breakdown properties. The following expression given in Eq. (4.3) is used:

$$R = 1 - e^{(-F/F_0)^{\gamma}} \tag{4.3}$$

where $R$ is the probability of breakdown, $F$ is breakdown evaluated, $F_0$ is breakdown under 64.5% of total probability, and $\gamma$ is shape factor corresponding to scatter characteristic. As per International Electro-technical Commission (Technical committee 56), the total probability of breakdown is collected from the expression given in Eq. (4.4) when the scheme has lower than 25 specimens were applied:

$$R_j = \left(\frac{j - 0.5}{o + 0.25}\right) \times 100\% \tag{4.4}$$

$J$ is the ordinal quantity of the specimen organized in incrementing step as per the strength of breakdown and $o$ is the cumulative number of the specimen that is 14 in the current investigation. The outcomes of the direct recent breakdown experiments of both chemically treated or untreated increments between 363.2 and 455.8 kV $mm^{-1}$ with the improvement by 25.5% still the shape factor reduces from 12.2 to 10.8.

### 4.4.4 Dielectric properties

The frequency based on the dielectric permittivity of chemically treated and untreated epoxy hybrid nanocomposites is shown in Fig. 4.5A. As predicted, both epoxy hybrid nanocomposites showed a significant reduction with frequency, signifying robust frequency confidence of dielectric permittivity. The required frequency dependency of dielectric permittivity is assigned from the influence of interfacial polarization of Al-SiC. Sugarcane nanocellulose is concluded by aggregating different carrier charges under the interior interfaces between the inorganic and inorganic natural fillers [68,69]. As a result, the dielectric permittivity of chemically treated

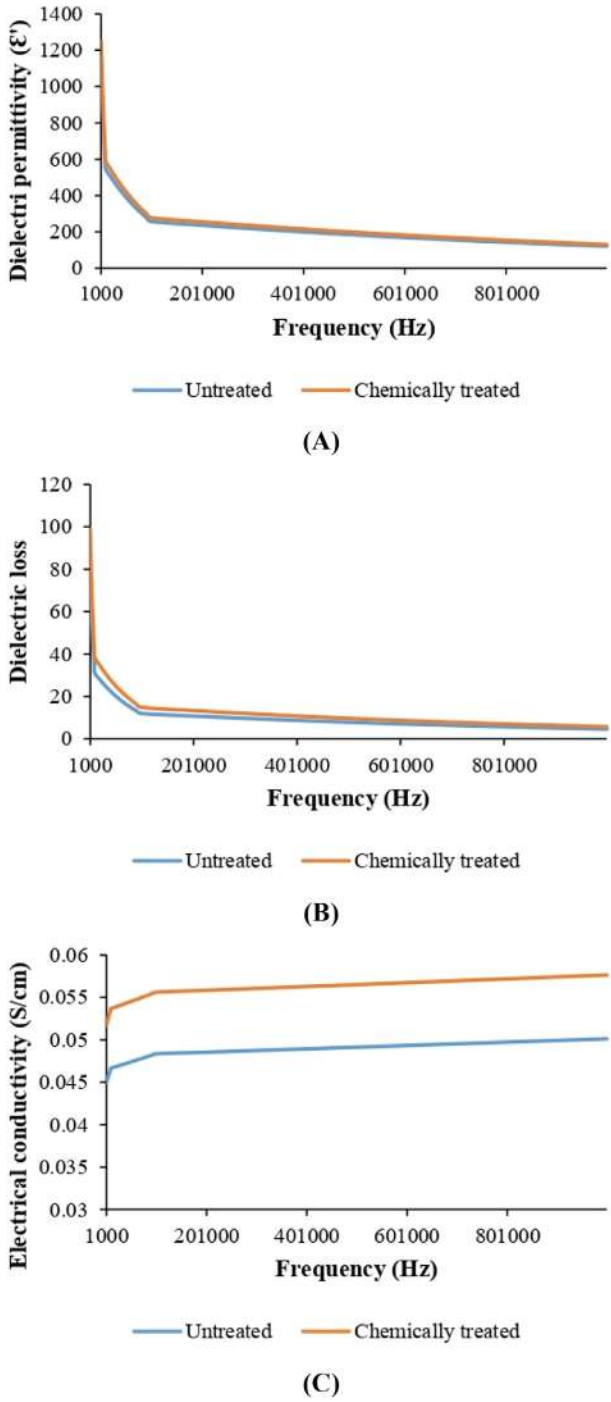


**Figure 4.5** Untreated or chemically treated sugarcane nanocellulose and Al-SiC epoxy hybrid nanocomposites (A) dielectric permittivity, (B) loss parameter, and (C) electrical conductivity.

epoxy hybrid nanocomposites starts to more significant improvement, signifying the development of a threshold of dielectric percolation that is followed by a region from an insulating to conducting medium. While comparing with untreated epoxy hybrid nanocomposites, the dielectric permittivity of the chemically treated one is improved to 170 under 1 kHz of frequency five times larger than the untreated one. The more significant improvement of dielectric permittivity around the threshold of percolation is affected by the influence of microcapacitor [70,71]. A burrowing percolation chain has been employed within the nanocomposites when the chemical treatment outstripped the percolation threshold. Hence, the injection of charge at the interfaces could not be eliminated combined with the interfacial polarization that decreases dielectric permittivity [72].

The loss parameter as the function of frequency for untreated and chemically treated epoxy hybrid nanocomposites is exhibited in Fig. 4.5B. It can be observed that the loss parameter of epoxy hybrid nanocomposites is considerably improved because of the addition of chemically treated sugarcane nanocellulose and conductive Al-SiC nanoparticles. The dielectric loss parameter of untreated epoxy hybrid nanocomposite is 0.004 under 1 kHz that is highly improved after reinforcing Al-SiC nanoparticles. The loss parameter of chemically treated epoxy hybrid nanocomposites attained up to 10.5 at 1 kHz. The high increment of loss parameter has emerged from the unavoidable improvement of electrical conductivity of chemically treated epoxy hybrid nanocomposites. Chemically treated epoxy hybrid nanocomposites are primarily affected by the leakage current. Higher conductive expressways can be established with the effect of the chemical treatment process. Subsequently, higher dielectric loss and more significant leakage current will be developed.

Fig. 4.5C exhibits the electrical conductivity as the function of the frequency of chemically treated and untreated epoxy hybrid nanocomposites. The electrical conductivity of untreated epoxy hybrid nanocomposites conceded a robust frequency dependency due to their insulating behavior [73]. The electrical conductivity of epoxy hybrid nanocomposites is improved with the rising frequency. A noticeable transition presented with the effect of chemical treatment. Then chemically treated epoxy hybrid nanocomposites suggest a conducting characteristic, and their respective conductive persists around the independence of frequency after enduring the chemical treatment. This signified that the interconnection between nanocellulose and inorganic fillers initiates to produce at this concentration, and the percolation threshold was also attained. This outcome is well established with the above dielectric characteristics of epoxy hybrid nanocomposites. When the untreated nanocellulose fiber is reinforced, the electrical conductivity is no longer improved. The potential logic is that the balance Al-SiC nanoparticles will be withdrawn from the surfaces of sugarcane nanocellulose, which tends to restrict the influence on developing conductive paths. As observed in system 1, encapsulation of Al-SiC on epoxy hybrid nanocomposites will tend to produce inorganic network-based epoxy nanocomposites after the hot-pressing process. The separated shape of Al-SiC in an epoxy matrix can advantage the higher electrical conductivity and dielectric constant.

## 4.5 Conclusion and future perspective

The conclusion exhibited that nanocellulose can be efficiently separated from the sugarcane bagasse using the mechanical milling process. The chemically treated and untreated sugarcane nanocellulose/Al-SiC epoxy hybrid nanocomposites have been fabricated using the ultrasonication-assisted wet layup method. The Al-SiC nanoparticles improved the space charge reticence capability. The direct current breakdown of epoxy nanocomposites is noticeably enhanced with the improvement by 25.5% while comparing untreated ones. Both the thermal and direct current conductivity properties exhibited increment of carrier charge captures. The quantum chemical evaluation examined that implanted epoxy molecules contain both broad and shallow trapping stages of both hole and electron kind. The trapping regions occur between 0.45−2.09 eV for hole and 0.04−0.62 eV 2.11−3.21 eV for the electron. Also, the apparent enhancement of the dielectric characteristics, the chemically treated epoxy hybrid nanocomposites, deceives nanoparticle accumulation, which tends to restrict the uniformly meshed percolating shield in the wire fabrication technique. The dielectric permittivity of chemically treated epoxy hybrid nanocomposites was improved up to 14.7 under 1 kHz of frequency. In this context, the dielectric loss parameter was regulated at a lower level. The production of Al-SiC-reinforced epoxy nanocomposites with lower dielectric loss and higher dielectric permittivity by reinforcing Al-SiC-encapsulated epoxy microsphere is an effortless technique to manufacture higher dielectric characteristics polymeric materials. From the research mentioned above, investigations and conclusions, the future perspective as it is essential to clarify the current techniques and compositions to expand customized electromagnetic interference shielding applications. Higher interest should be given to be hybrid nanoparticles and laminates with their more excellent interfaces, which can be applied for a broad region for shielding and protection purposes. Also, such laminates develop the considerable influence of polarization and dielectric assignments for higher electromagnetic energy absorption. Therefore it is more suitable to examine the synergy between laminate regions to interpret the potential change of various physical characteristics permissive enhanced application possibility. Also, the manufacturing of electromagnetic interference shielding materials on conducting inorganic fillers reinforced in polymers with different multifunctional applications can be fascinating.

## References

[1] H. Mohit, V.A.M. Selvan, A comprehensive review on surface modification, structure interface and bonding mechanism of plant cellulose fiber reinforced polymer based composites, Compos. Interf 25 (5−7) (2018) 629−667.

[2] R.S. Rana, et al., Mechanical properties of bamboo laminates with other composites, Mater. Today. Proc. 4 (2017) 3380−3386.

[3] M.R. Sanjay, et al., Wood Polymer Composites Recent Advancements and Applications, Springer, 2021.

[4] G.S. Sivagnanamani, et al., Fracture analysis of fused deposition modelling of biocomposite filaments, Fracture Failure Analysis of Fiber Reinforced Polymer Matrix Composites, Springer, 2021, pp. 71–84.
[5] S. Wang, et al., Recent advances in regenerated cellulose materials, Prog. Polym. Sci. 53 (2016) 169–206.
[6] P. Ramesh, et al., Environmental impact of wood based biocomposite using life cycle assessment methodology, Wood Polymer Composites Recent Advancements and Applications, Springer, 2021, pp. 255–268.
[7] P. Ramesh, et al., Environmental impact study on biobased composites using lifecycle methodology, Biobased Composites: Processing, Characterization, Properties, and Applications, John Wiley & Sons, Inc, 2021, pp. 213–222.
[8] R. Ruban, et al., Introduction to wood polymer composites, Wood Polymer Composites Recent Advancements and Applications, Springer, 2021, pp. 1–20.
[9] L.M.S. Menandro, et al., Comprehensive assessment of sugarcane straw: implications for biomass and bioenergy production, Biofuels. Bioprod. Biorefin. 11 (3) (2017) 488–504.
[10] H. Mohit, Selvan, Influence of chemical surface modification on micro-wear characteristics of sugarcane nanocellulose epoxy nanocomposites, Matter: Int. J. Sci. Technol. 4 (3) (2019) 157–158.
[11] H. Mohit, V.A.M. Selvan, Effect of a novel chemical treatment on the physico-thermal properties of sugarcane nanocellulose fiber reinforced epoxy nanocomposites, Int. Polym. Proc 35 (2) (2020) 211–220.
[12] S.C. Pereira, et al., 2G Ethanol from the Whole Sugarcane Lignocellulosic Biomass, Biotechnol. Biofuels. 8 (1) (2015) 44.
[13] D. Klemm, et al., Nanocellulose as a natural source for groundbreaking applications in materials science: today's state, Mater. Today. 21 (7) (2018) 720–748.
[14] N. Dubey, et al., Structure of wood fiber and factors affecting mechanical properties of wood polymer composites, Wood Polymer Composites Recent Advancements and Applications, Springer, 2021, pp. 137–160.
[15] K. Oksman, et al., Review of the recent developments in cellulose nanocomposite processing, Composites, Part A 83 (2016) 2–18.
[16] J. Li, et al., Nanocellulose/gelatin composite cryogels for controlled drug release, ACS Sustainable Chem. Eng 7 (6) (2019) 6381–6389.
[17] N. Lin, et al., Nanocellulose in biomedicine: current status and future prospect, Eur. Polym. J 59 (2014) 302–325.
[18] Jung, Y.H. et al., High-Performance Green Flexible Electronics Based on Biodegradable, 2015.
[19] L. Yue, et al., High performance biobased epoxy nanocomposite reinforced with a bacterial cellulose nanofiber network, ACS. Sustainable. Chem. Eng. 7 (6) (2019) 5986–5992.
[20] A. Campos, et al., Obtaining nanofibers from curaua and sugarcane bagasse fibers using enzymatic hydrolysis followed by sonication, Cellulose 20 (2013) 1491.
[21] F.B. Oliveira, et al., Production of cellulose nanocrystals from sugarcane bagasse fibers and pith, Ind. Crops Prod. 93 (2016) 48–57.
[22] Y.H. Feng, et al., Characteristics and environmentally friendly extraction of cellulose nanofibrils from sugarcane bagasse, Ind. Crops Prod. 111 (2018) 285–291.
[23] M.S. Reid, et al., Benchmarking cellulose nanocrystals: from the laboratory to industrial production, Langmuir. 33 (7) (2017) 1583–1598.
[24] L.P. Novo, et al., Subcritical water: a method for green production of cellulose nanocrystals, ACS. Sustain. Chem. Eng. 3 (11) (2015) 2839–2846.

[25] O.M. Vanderfleet, et al., Insight into thermal stability of cellulose nanocrystals from new hydrolysis methods with acid blends, Cellulose 26 (1) (2019) 507–528.
[26] S. Camarero Espinosa, et al., Isolation of thermally stable cellulose nanocrystals by phosphoric acid hydrolysis, Biomacromolecules 14 (4) (2013) 1223–1230.
[27] T.J. Bondancia, et al., A new approach to obtain cellulose nanocrystals and ethanol from eucalyptus cellulose pulp via the biochemical pathway, Biotechnol. Prog. 33 (4) (2017) 1085–1095.
[28] S.R. Anderson, et al., Enzymatic preparation of nanocrystalline and microcrystalline cellulose, Tappi J 13 (5) (2014) 35–42.
[29] F.F. Lu, et al., Spherical and rod-like dialdehyde cellulose nanocrystals by sodium periodate oxidation: optimization with double response surface model and templates for silver nanoparticles, Exp. Polym. Lett 10 (12) (2016) 965–976.
[30] T.G.M. van de Ven, A. Sheikhi, Hairy cellulose nanocrystalloids: a novel class of nanocellulose, Nanoscale 8 (33) (2016) 15101–15114.
[31] H. Yang, et al., Highly charged nanocrystalline cellulose and dicarboxylated cellulose from periodate and chlorite oxidized cellulose fibers, Cellulose 20 (4) (2013) 1865–1875.
[32] H. Yang, et al., Preparation and characterization of sterically stabilized nanocrystalline cellulose obtained by periodate oxidation of cellulose fibers, Cellulose 22 (3) (2015) 1743–1752.
[33] M.S. Islam, et al., Cellulose nanocrystals (CNC)–inorganic hybrid systems: Synthesis, properties and applications, J. Mater. Chem. B. 6 (6) (2018) 864–883.
[34] M. Jawaid, S. Siengchin, Hybrid composites: a versatile materials for future, Appl. Sci. Eng. Prog. 12 (4) (2019) 1.
[35] Q. Lu, et al., Controlled construction of nanostructured organic–inorganic hybrid material induced by nanocellulose, ACS. Sustain. Chem. Eng. 5 (9) (2017) 8456–8463.
[36] N. El Miri, et al., Synergistic effect of cellulose nanocrystals/graphene oxide nanosheets as functional hybrid nanofiller for enhancing properties of PVA nanocomposites, Carbohydr. Polym 137 (2016) 239–248.
[37] B. Huang, et al., Optimizing 3D printing performance of acrylonitrile-butadiene-styrene composites with cellulose nanocrystals/silica nanohybrids, Polym. Int. 68 (2019) 1351–1360.
[38] G.H. Kumar, H. Mohit, Wear testing of nano Alumina-Zirconia ceramic matrix composites, IEEE Xplore (2011) 223–227.
[39] Y. Li, H. He, B. Huang, L. Zhou, P. Yu, Z. Lv, In situ fabrication of cellulose nanocrystal-silica hybrids and its application in UHMWPE: rheological, thermal, and wear resistance properties, Polymer Compos. 39 (3) (2018) 1701–1713.
[40] M.N. Arshad, et al., Effect of coir fiber and TiC nanoparticles on basalt fiber reinforced epoxy hybrid composites: physico-mechanical characteristics, Cellulose 28 (2021) 3451–3471.
[41] B. Ashok, et al., Modification of waste leather trimming with in situ generated silver nanoparticles by one step method, Appl. Sci. Eng. Prog. 14 (2) (2021) 236–246.
[42] H. Mohit, et al., A comprehensive review on mechanical, electromagnetic radiation shielding, and thermal conductivity of fibers/inorganic fillers reinforced hybrid polymer composites, Polym. Compos. (2020) 3940–3965.
[43] H. Mohit, et al., Effect of TiC nanoparticles reinforcement in coir fiber based bio/synthetic epoxy hybrid composites: mechanical and thermal characteristics, J. Polym. Environ. (2021) 1–19.

[44] H. Mohit, et al., Nanoparticles addition in coir-basalt-innegra fibers reinforced bio-synthetic epoxy composites, J. Polym. Environ. (2021) 1–14.
[45] H. Mohit, et al., Effect of micro-dry-leaves-filler and Al-SiC reinforcement on the thermomechanical properties of epoxy composites, Mechanical and Dynamic Properties of Biocomposites, Wiley-VCH, 2021, pp. 191–206.
[46] S. Tiwari, et al., Investigation of structural, optical and electronic properties of (Co, Ni) codoped CeO2 nanoparticles, IOP Conf. Series 390 (2018) 1–7.
[47] S. Tiwari, et al., Effect of Co doping on structural and mechanical properties of CeO2, AIP Conf. Proc 1966 (2018) 020037.
[48] S. Tiwari, et al., Synthesis, structure and characterization of Co doped CeO2 nanoparticles, IOP Conf. Series 396 (2018) 1–7.
[49] D.B. Cordes, et al., Recent developments in the chemistry of cubic polyhedral oligosilsesquioxanes, Chem. Rev. 110 (4) (2010) 2081–2173.
[50] S.D. Jiang, et al., Surface functionalization of MoS2with POSS for enhancing thermal, flame-retardant and mechanical properties in PVA composites, RSC Adv 4 (7) (2014) 3253–3262.
[51] H. Mohit, et al., Future challenges and applications of polymer coatings, Polymer Coatings, CRC Press, 2020, pp. 325–337.
[52] H. Mohit, et al., Applications and drawbacks of bamboo fiber composites, Bamboo Fiber Composites, Springer, 2020, pp. 247–270.
[53] S. Xu, et al., Shape memory and self-healing properties of poly (acrylate amide) elastomers reinforced with polyhedral oligomeric silsesquioxanes, ACS. Appl. Polym. Mater 1 (2019) 359–368.
[54] G.H. Kumar, et al., The abrasive wear behaviour of Al-SiCpcomposites for automotive parts, IEEE Xplore (2010) 54–59.
[55] H. Mohit, et al., Effect of deep cryogenic treatment on composite material for automotive Ac system, Mater. Today. Proc 4 (2017) 3501–3505.
[56] H.B. Vishwanath, et al., Effect of chemically treated bamboo fiber reinforcement on the dielectric properties of epoxy composites, Bamboo Fiber Composites, Springer, 2020, pp. 111–126.
[57] H. Mohit, V.A.M. Selvan, Thermo-mechanical properties of sodium chloride and alkali-treated sugarcane bagasse fibre, Ind. J. Fiber. Tex. Res. 44 (3) (2019) 286–293.
[58] H. Mohit, V.A.M. Selvan, Effect of a novel chemical treatment on nanocellulose fibers for enhancement of mechanical, electrochemical and tribological characteristics of epoxy bio-nanocomposites, Fibers. Polym. 20 (2019) 1918–1944.
[59] H. Mohit, V.A.M. Selvan, Optimization of the tensile strength of sintered Al6061/SiC nanocomposites using response surface methodology, Mater. Today. Proc 27 (2020) 2801–2805.
[60] H. Mohit, V.A.M. Selvan, Physical and thermomechanical characterization of the novel aluminum silicon carbide-reinforced polymer nanocomposites, Iran. Polym. J 28 (2019) 823–837.
[61] H. Mohit, V.A.M. Selvan, Effect of Al-SiC nanoparticles and cellulose fiber dispersion on the thermomechanical and corrosion characteristics of polymer nanocomposites, Polym. Compos. 41 (5) (2020) 1878–1899.
[62] S. Song, et al., Enhanced electrical properties of polyethylene-graft-polystyrene/LDPE, Composites. 12 (124) (2020) 1–16.
[63] A. Rose, Space-charge-limited currents in solids, Phys. Rev. 97 (1955) 1538–1544.
[64] L. Lan, et al., Effect of temperature on space charge trapping and conduction in cross-linked polyethylene, IEEE Trans. Dielectr. Electr. Insul. 21 (2014) 1784–1791.

[65] Y. Zhou, et al., Mechanism of highly improved electrical properties in polypropylene by chemical modification of grafting maleic anhydride, J. Phys. D Appl. Phys. 49 (2016) 415301.
[66] F. Tian, et al., Theory of modified thermally stimulated current and direct determination of trap level distribution, J. Electrost. 2011 (69) (2011) 7−10.
[67] M. Ieda, Electrical conduction and carrier traps in polymeric materials, IEEE Trans. Dielectr. Electr. Insul. EI 19 (1984) 162−178.
[68] X. Jiang, et al., Enhancing the dielectric properties of polymethyl methacrylate by using low loading graphene encapsulated styrene-butyl acrylate copolymer microspheres, Synthetic. Metals. 259 (2020) 116229.
[69] W. Zhao, L. Duan, B. Zhang, X. Ren, G. Gao, et al., Tough and ultrastretchable hydrogels reinforced by poly(butyl acrylate-co-acrylonitrile) latex microspheres as crosslinking centers for hydrophobic association, Polymer 112 (2017) 333−341.
[70] E. Breckenfeld, et al., Effect of growth induced (Non)stoichiometry on the structure, dielectric response, and thermal conductivity of SrTiO3 thin films, Chem. Mater. 24 (2012) 331−337.
[71] M. Tian, et al., Graphene encapsulated rubber latex composites with high dielectric constant, low dielectric loss and low percolation threshold, J. Colloid. Interface. Sci. 430 (2014) 249−256.
[72] D. Wang, et al., Dielectric properties of reduced graphene oxide/polypropylene composites with ultralow percolation threshold, Polymer 54 (2013) 1916−1922.
[73] M. Arjmand, et al., Employing nitrogen doping as innovative technique to improve broadband dielectric properties of carbon nanotube/polymer nanocomposites, Macromol. Mater. Eng. 301 (2016) (2016) 555−565.

# Optical properties of polymer nanocomposites

5

*Pawan Kumar Rakesh*
Department of Mechanical Engineering, National Institute of Technology Uttarakhand, Srinagar Garhwal, Uttarakhand, India

## 5.1 Introduction

Nanotechnology has a probable impact on science and technology, such as nanomaterials, manufacturing processes, bioengineering, and the global economy. Nanoparticles, such as gold (Au), silver (Ag), copper (Cu), rhodium (Rh), titanium (Ti), lead (Pb), nanoclay, silica (Si), layered silicates (LS)—phyllosilicates, montmorillonite (MMT), hectorite, and saponite—carbon nanotubes (CNTs), and bionanoparticles like cellulose nanoparticles or nanowhiskers, may be available in pure form or consist of two or more different nanoparticles, having the particles size of 10−100 A or 1−100 nm [1−6]. The effectiveness of nanoreinforcements may be characterized by the ratio of surface area ($A$) to volume ($V$) ($>107{:}1$) of nanoparticles. In addition, the formation of oxides on nanoparticles, such as zirconium dioxide ($ZrO_2$), silicon dioxide ($SiO_2$), zinc oxide (ZnO), titanium dioxide ($TiO_2$), strontium zirconate ($SnZrO_3$), zinc titanate ($ZnTiO_3$), also improves the mechanical, electrical, and optical properties [7−10].

Polymers are rarely used in pure form for product development; it is generally reinforced with nanoparticles/additives/fibers to improve their mechanical and optical properties. The polymers are generally classified as thermoplastics, thermosets, and elastomers. The thermoplastic polymers, such as acrylonitrile-butadiene-styrene (ABS), polycarbonate, polyvinyl alcohol (PVA), polystyrene (PS), polymethyl methacrylate (PMMA), polyvinylidene fluoride, polyimides, polyaniline, and nylon, biodegradable polymers such as polycaprolactone, polylactic acid, polyhydroxybutyrate, polybutylene succinate (PBS), natural rubber, starch, cellulose, polyglycolic acid, poly(3-hydroxybutyrate), have unique properties, including excellent mechanical strength, high-impact strength, easy to process, chemical resistance, appearance, transparency, electrical properties, and dimensional stability [11−14]. However, one of the significant drawbacks of thermoplastic polymers is their lowest thermal stability and highest flammability. Recently, advanced techniques have been applied to modify the thermoplastic polymers that may offer improved mechanical properties, including scratch resistance and optical clarity.

The concept of polymer nanocomposites came into existence to manufacture intelligent devices such as medical catalepsy, windmills, electronic circuit boards, battery, microchips, single-electron transistors, optoelectronic devices, photonic

**Advanced Polymer Nanocomposites. DOI: https://doi.org/10.1016/B978-0-12-824492-0.00012-X**


crystals, depolarizes, scattering displays, compact disk, universal serial bus storage, windows with adjustable transparency, solar cells, light-emitting diodes, photodiodes, light-stable color filters; optical sensors, optical fibers, planar waveguide devices, and many more, due to their properties such as high strength, accuracy, precision, lightweight, good dimensional stability, and low cost [15−20]. The optical properties of polymer nanocomposites depend on particle size, shape, and chemical compositions. Polymer nanocomposites are usually transparent due to the nanometer length of reinforcement, which minimizes light scattering [21−24]. The properties and applications of different compositions of polymer nanocomposites, such as PVA/Argentum (PVA/Ag), PVA/silver nitrate ($PVA/AgNO_3$), polymethylmethacrylate/copper oxide (PMMA-CuO), PMMA/silicon dioxide ($PMMA/SiO_2$) [25], PVA/MMT [26], poly (*p*-phenylene vinylene)/$SiO_2$, polystyrene/strontium zirconate ($PS/SnZrO_3$) [27], are mentioned in Table 5.1. The hybrid polymer nanocomposites such as PP + PbS/CdS [2] have also been developed with improved mechanical and optical properties. The interfacial region between the polymer and nanoparticles are formed between 2− 50 nm. The critical parameters of the interfacial region are particle size distribution, interfacial interactions, manufacturing processes, melting temperature of nanoparticles, etc. The thermoset polymers such as epoxy resins, acrylic resin, polyurethane (PU) resin, and unsaturated polymers have been reinforced with clay, diamond, graphite, alumina, and oxides to make the thermoset nanocomposites for high strength and high-temperature applications [10]. The elastomer reinforced with silica nanoparticles, LS, carbon black, and CNTs has been used to make elastomer nanocomposites [28,29].

In this chapter, the fabrication method, characterization techniques, and optical properties of polymer nanocomposites have been reviewed. The optical parameters such as absorption, refractive index, and energy band gap, affecting the polymer nanocomposites, have also been described.

## 5.2 Production method

Various approaches, such as solution casting, melt intercalation, in situ, and ex situ polymerization, were used to prepare the polymer nanocomposites [19−21]. Solution casting is one of the oldest methods for the preparation of polymer nanocomposites. The polymer and the nanoparticles are mechanically mixed to fabricate polymer nanocomposites. It is difficult to disperse nanoparticles into the polymer homogeneously due to the stress-free agglomeration of nanoparticles. The fabrication process can be done at a low temperature; hence, it is processed very fast. For example, solution casting is used to prepare nanocomposite based on polystyrene (PS) and strontium zirconate ($SnZrO_3$) as filler. The polystyrene solution is prepared by adding 1.0 g weight of PS powder into 40 mL toluene and stirred via a magnetic stirrer for 3.0 hours to achieve a homogeneous solution. The solution casting process of PS:$SnZrO_3$ is performed in a different glass pot and then permitted to evaporate at ambient temperature for 2 weeks until nanocomposites were

**Table 5.1** Properties and applications of polymer nanocomposites.

| No. | Nanoparticles | Properties | Applications |
|---|---|---|---|
| 1 | HDPE/titanium dioxide ($TiO_2$) | Optical and electronic | Photocatalysis, solar cells, gas sensor, bone repair |
| 2 | LDPE/zinc oxide (ZnO)/ Ag | Optical, electrical, magnetic, and electronic | Medical filling materials, optoelectronic devices, orange juice packaging |
| 3 | Polyvinyl alcohol/silver nitrate ($PVA/AgNO_3$) | Optical and mechanical | Ceramic ultrafilters, fire-resistant |
| 4 | Polymethylmethacrylate/ silicon dioxide ($PMMA/SiO_2$) | Physicochemical, optical, luminescent | Tissue engineering, biosensing, optical devices |
| 5 | Polyvinyl alcohol/ Argentum (PVA/Ag) | Optical due to surface plasmon resonance | Biosensing, coating, temperature-sensitive transducers, spectrum, photo-resistors, and selective sensors |
| 6 | Polymethylmethacrylate/ copper oxide (PMMA-CuO) | Antimicrobial, anti-biotic, and anti-fungal agent | Thin-film, solar cells, optoelectronic devices |
| 7 | Polystyrene/strontium zirconate ($PS/SnZrO_3$) | Convert sunlight to electrical energy | Solar cells, photovoltaic |
| 8 | Nylon-6/nanoclays | Superior superhydrophobicity, improved wettability, chemicals resistance, abrasion resistance, impact, and scratch resistance properties | Fire-resistant, optoelectronic devices, films, and bottles - Honeywell |
| 9 | Shape memory polymers/SiC | High flexibility, low mass density, and a large aspect ratio | Medical devices for gripping |

prepared [16]. In another study, the PVA/Ag polymer nanocomposites were prepared by 3.0 g weight of PVA and dissolved in 100 mL of deionized water with stirring at 90°C. The freshly prepared $AgNO_3$ solution (0.1 M) is added dropwise in an aqueous PVA solution with continuous stirring for 2.0 hours to ensure the homogeneous solution. The solution is cast into a glass pot and left to dry at room temperature; then, the resulting nanocomposites are peeled off [17]. Next, polymer nanocomposites of PMMA/CuO are prepared by solution casting. Polymethylmethacrylate solution is prepared by dissolving it in chloroform using a magnetic stirrer. The copper oxide nanoparticles are added to polymethylmethacrylate with different concentrations for 20 minutes to get a homogenous solution [18].

The melt intercalation involves annealing the polymer with the filler at high temperatures and compressing the mixtures uniformly to cast polymer nanocomposites. The polymer inserted into the interlayer spacing between the LS is called intercalated polymer nanocomposites. In contrast, the silicate layers are entirely separated and dispersed in a polymer is called exfoliated polymer nanocomposites [8]. Nanoparticles are generally hydrophilic, and polymers are hydrophobic. Therefore interfacial adhesion needs to be very high to improve the polymer nanocomposites performance. The interfacial adhesion can be increased in two ways (1) to increase the space between the LS by adding intercalating agents and (2) organic molecules bonded to silicates to make it more miscible the polymer [8]. Quaternary ammonium surfactants are used to increase the intergallery spacing. The size of nanoparticles affects the dispersion morphology and emulsion stability during the preparation of ABS/LS nanocomposites.

The nanoparticles may also be coated with the oxide materials to improve their mechanical properties. The coating thickness of nanoparticles depends on process parameters, such as dipping time, temperature, nature of surfactant, and purity of nanoparticles [12–15].

Polymer nanocomposites are prepared by the in situ reduction of graphene oxide (GO) within the PVA solution, while a thermally reduced graphene oxide was used to prepare polymer nanocomposites using a polyester-based thermoplastic PU [19–22].

The optical properties of the polymer nanocomposites depend on the type of nanoparticles, the interlayer spacing, the interfacial strength between the polymer matrix and nanoparticles, the type and concentration of additives, and the viscosity of the resin [3–7].

## 5.3 Characterization techniques

The synthesis and characterization of polymer nanocomposites can be done by different techniques, namely, scanning electron microscope analysis, atomic force microscope, transmission electron microscopes/field emission scanning electron micrograph analysis, X-ray diffraction, dynamic mechanical analysis, differential thermal analysis, nuclear magnetic resonance, differential scanning calorimetry, thermogravimetric analysis, for detecting functional groups, molecular structure, elastic response to deformation, thermal stability, mechanical properties of a surface of nanocomposites; X-ray fluorescence, dynamic light scattering particle size analyzer, Ultraviolet (UV)-visible spectroscopy, Fourier transform infrared, polarized light optical microscopy may be used to study the effect of interfacial morphology, interparticle spacing and finite-size effects on optical properties of polymer nanocomposites.

The analysis of structure and morphology, degradation behavior of the dispersed nanoparticles, polymer phase, and the interface of the nanocomposites plays a major role in understanding the optical properties of nanocomposites.

## 5.4 Optical properties of polymer nanocomposites

The optical properties of polymer nanocomposites can be understood by two different theories: Maxwell Garnett and Bruggeman geometry. The Maxwell Garnett geometry has based on nanoparticles embedded in the matrix material. Two nanoparticles having different linear and nonlinear optical properties have been considered in the Bruggeman geometry. The polymer nanocomposites consist of two- or three-dimensional structures similar to the Maxwell Garnett structure. The optical properties of nanocomposites depend on their atomic structure, band structure, and electrical properties. The optical properties of the polymer nanocomposites can be determined by the following factors, that is, absorption, reflection, photoluminescence, and dichroism.

The absorption reflects the capacity for absorbing light by nanocomposites. It is the ratio of the decrease in the energy of the radiation to a unit of distance travel toward the propagation of the wave within the medium. It depends on the energy of the falling photons, the wavelength, the nature of the surfactant, the energy gap, and the type of electronic transitions between energy bands. The energy bandgap is measured from an electron jump in the absorption process called an absorption edge. The absorption edge is a region where an electron is induced to excite photons from the lowest energy level to the highest energy level. Thus the absorption coefficient of the nanoparticles is a powerful function of photon energy and bandgap energy [30].

PMMA is mostly used in the manufacturing of optical devices because of its high transmission at about 850 nm in a visible spectral region from 0.85 to 1.55 m in length. PMMA was filled with three different nanoparticles like ZnO, $SnO_2$, and $TiO_2$ to prepare the polymer nanocomposites via the solution casting method. Nanoparticles were varied from 1, 3, and 5 wt.% into the polymer matrix to study the effect of absorption and energy bandgap of the polymer nanocomposites. The optical properties of PMMA filled with ZnO, $SnO_2$, and $TiO_2$ polymer nanocomposites are measured using an UV-visible spectroscopic in the range of 200−800 nm wavelength at the ambient temperature. The constant parameters, that is, wavelength accuracy = 1 nm, and the scan speed = 600 nm per minute was used for all the samples in the ultraviolet-visible spectrophotometer. Fig. 5.1A shows the plot between the energy absorption and wavelength for all the polymer nanocomposites. Insignificant absorbance was observed in the case of pure PMMA in the entire visible range, while it increases at the lower wavelength. PMMA/ZnO polymer nanocomposites have a perceptible UV-blocking effect even at low concentrations of the ZnO fillers (0.017 wt.%) but retain high transparency in the visible range even at 1 cm thick. Moreover, the PMMA/ZnO nanocomposites show a much higher UV-blocking effect (approximately zero transmission in the range from 290 to 340 nm). The absorption was found significantly high for the PMMA/$TiO_2$ nanocomposites and comparatively low for the PMMA/$SnO_2$ nanocomposites compared to PMMA/ZnO nanocomposites. The absorption was enhanced in all the cases by increasing the concentration of nanoparticles into PMMA nanocomposites.

The energy bandgap of polymer nanocomposites can be calculated according to the Power-law. The photon energy versus energy bandgap plot is shown in

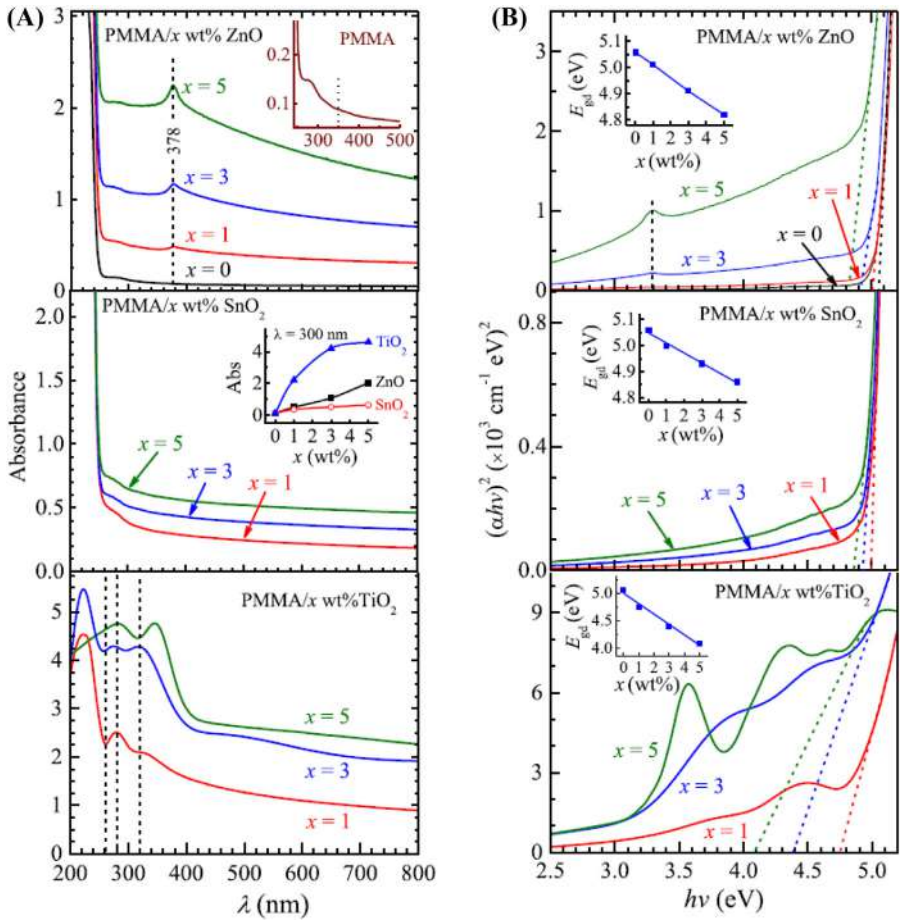


**Figure 5.1.** PMMA filled with ZnO, $SnO_2$, $TiO_2$-based nanocomposites (A) UV absorption versus wavelength $\lambda$ (B) photon energy $(\alpha h\nu)^2$ versus bandgap $(h\nu)$ [27].
*Source:* Optical Materials 113(2021) 110837.

Fig. 5.1B. It was observed that the photon energy decreases with an increased concentration of nanoparticles, which resulted in the creation of controlled conditions in the PMMA energy bandgap [32,33]. The refractive index of polymer nanocomposites can be controlled by the addition of nanoparticles into the polymer matrix.

## 5.5 Conclusion

The optical properties of polymer nanocomposites depend on the nature of the polymer and their concentration of nanoparticles reinforcement. In addition to other factors such as thickness, ambient temperature, angle of incidence, and polarization

also affect the optical properties of polymer nanocomposites. The absorbance of polymer nanocomposites increases with the increasing concentrations of nanoparticles, and the transmittance, energy bandgap of polymer nanocomposites decreases with increasing concentrations of the nanoparticles. Therefore the PMMA-reinforced nanoparticles-based polymer nanocomposites could be very useful for the product development of optical devices.

## References


[1] B.H. Rabee, B. Abd Al-Kareem, Study of optical properties of (PMMA-CuO) nanocomposites, Int. J. Sci. Res. 5 (4) (2016) 879–883.

[2] A.A. Novruzova, M.A. Ramazanov, A. Chianese, V.F. Hajiyeva, A.M. Maharramov, U. A. Hasanova, Synthesis structure and optical properties of PP + PbS/CdS hybrid Nanocomposites, Chem. Eng. Trans. 60 (2017).

[3] R.V. Kurahatti, A.O. Surendranathan, S.A. Kori, N.Singh, A.V.R. Kumar, S. Srivastava, Defence applications of polymer nanocomposites, Def. Sci. J., 60(5), 551–563.

[4] W.A. Shakir, S.H. Abdullah, F.I. Mustafa, K.K. Ateia, A.M. Ibraheem, Optical properties of ZnTiO3/epoxy nanocomposites thin films, Int. J. Sci. Res. Manag. 6 (10) (2018) 100–106.

[5] R.W. Boyd, R.J. Gehr, G.L. Fischer, J.E. Sipe, Nonlinear optical properties of Nanocomposites materials, Pure Appl. Opt. 5 (1996) 505–512.

[6] M. Safdari, M.S. Al-Haik, A review on polymeric nanocomposites: effect of hybridization and synergy on electrical properties, carbon-based polymer nanocomposites for environmental and energy applications, 2018, 113–146.

[7] P.H.C. Camargo, K.G. Satyanarayana, F. Wypych, Nanocomposites: synthesis, structure, properties and new application opportunities, Mater. Res. 12 (1) (2009) 1–39.

[8] R.S. Sinha, O. Masami, Polymer/layered silicate nanocomposites: a review from preparation to processing, Prog. Polym. Sci. 28 (11) (2003) 1539–1541.

[9] H. Farzana, H. Mehdi, O. Masami, G. Russell E, Review article: polymer-matrix nanocomposites, processing, manufacturing, and applications: an overview, J. Compos. Mater. 40 (17) (2006) 1511–1575.

[10] R. Kotsilkova, Thermoset nanocomposites for engineering applications, Smithers Rapra Technology Limited, UK, 2007, ISBN: 978-1-84735-062-6.

[11] D.G. Papageorgiou, I.A. Kinloch, R.J. Young, Graphene/elastomer nanocomposites, Carbon N. Y. 95 (2015) 460–484.

[12] M.N. Muralidharan, S. Mathew, A. Seema, Radhakrishnan, K. Thomas, Optical limiting properties of in situ reduced graphene oxide/polymer nanocomposites, Mater. Chem. Phys. 171 (2016) 367–373.

[13] M.A. Martins, S. Fateixa, A.V. Girao, S.S. Pereira, T. Trindade, Shaping gold nanocomposites with tunable optical properties, Langmuir 26 (13) (2010) 11407–11412.

[14] S.A. Hussen, Structural and optical characterization of pure and SnZrO3 doped PS based polymer nanocomposites, Materials Research Express, 7, 105302.

[15] H.M. Shanshool, M. Yahaya, W.M.M. Yunus, I.Y. Abdullah, Optical properties of PVDF/ZNO nanocomposites, Int. J. Tech. Res. Appl. 23 (2015) 51–58.


[16] J. Cuppoletti, 2011, Nanocomposites and polymers with analytical methods, InTech, ISBN 978-953-307−352-1.
[17] S. Srivastava, M. Haridas, J.K. Basu, Optical properties of polymer nanocomposites, Bull. Mater. Sci. 31 (3) (2008) 213−217.
[18] O. Sakhno, P. Yezhow, V. Hryn, V. Rudenko, T. Smirnova, Optical and nonlinear properties of photonic polymer nanocomposites and holographic gratings modified with noble metal nanoparticles, Polymers 12 (2020) 480.
[19] E. Sheha, H. Khoder, T.S. Shanap, M.G. Ei-Shaarawy, M.K. Mansy, Structure, dielectric and optical properties of p-type (PVA/CuI) nanocomposites polymer electrolyte for photovoltaic cells, Optik (2011). Available from: https://doi.org/10.1016/j.ijleo.2011.06.066.
[20] I.Y. Yaremchuk, V.M. Fitio, T.O. Bulavinets, Y.V. Bobitski, Optical properties of nanocomposites materials based on plasmon nanoparticles, Semicond. Phys. Quantum Electron. Optoelectron. 21 (2) (2018) 195−199.
[21] G. Qingchuan, et al., Comparison of in SITU AND EX SITU METHODS FOR SYNTHESIS OF TWO-PHOTON POLYMERIZATION POLYMER NANOCOMPosites, Polymers 6 (2014) 2037−2050.
[22] J. Fawaz, V. Mittal, Synthesis of polymer nanocomposites: review of various techniques, Synthesis techniques for polymer nanocomposites, Wiley-VCH Verlag GmbH & Co. KGaA, 2015. 1−30.
[23] A.M. Ibarra-Ruiz, D.C.R. Burbano, J.A. Capobianco, Photoluminescent nanoplatforms in biomedical applications, Adv. Phys. X 1 (2) (2016) 194−225.
[24] S. Kango, S. Kalia, A. Celli, J. Njuguna, Y. Habibi, R. Kumar, Surface modification of inorganic nanoparticles for development of organic-inorganic nanocomposites- a review, Prog. Polym. Sci. 38 (2013) 1232−1261.
[25] L.B. Ammar, S. Fakhfakh, Optical and dielectric properties of polypropylene/montmorillonite nanocomposites, Funct. Compos. Struct. 2 (2020) 045003.
[26] C. Etrich, S. Fahr, M.K. Hedayati, F. Faupel, M. Elbahri, C. Rockstuhl, Effective optical properties of plasmonic nanocomposites, Materials (Basel) 7 (2) (2014) 727−741.
[27] R.J. Sengwa, P. Dhatarwal, Polymer nanocomposites comprising PMMA matrix and ZnO, SnO2, and TiO2 nanofillers: a comparative study of structural, optical, and dielectric properties for multifunctional technological applications, Opt. Mater. 113 (2021) 110837.
[28] U. Ali, K.J.B. Abd Karim, N.A. Buang, A review of the properties and applications of poly (methyl methacrylate) (PMMA), Polym. Rev. 55 (2015) 678−705.
[29] A. Badhe Rashmi, A. Ansari, S.S. Garje, Study of optical properties of TiO2 nanoparticles and CdS@$TiO_2$ nanocomposites and their use for photocatalytic degradation of rhodamine B under natural light irradiation, Bull. Mater. Sci. 44 (2021) 1−11.
[30] P. Dhatarwal, S. Choudhary, R.J. Sengwa, Significantly enhanced dielectric properties and chain segmental dynamics of PEO/SnO2 nanocomposites, Polym. Bull. (2020). Available from: https://doi.org/10.1007/s00289-020-03215-2.
[31] C.I. Idumah, C.M. Obele, Understanding interfacial influence on properties of polymer nanocomposites, Surf. Interfaces 22 (2021) 100879.
[32] B. Kulyk, V. Kapustianyk, V. Tsybulskyy, O. Krupka, B. Sahraoui, Optical properties of ZnO/PMMA nanocomposite films, J. Alloys Compd. 502 (2010) 24−27.
[33] R. Y-Macias, E. H-Hernandez, C. Gallordo-Vega, L.-R. Raquel, F.Z. Ronald, M.-T. Y, et al., Covalent grafting of nonfunctionalized pristine MWCNT with Nylon-6 by microwave assist in-situ polymerization, Polymer (Guildf) 185 (2019) 121946.

# Thermal properties of polymer nanocomposites

6

*Ch. Sridhar Yesaswi*[1], *S. Krishna Satya*[1], *Santosh Kumar Sahu*[2], *Nitesh Dhar Badgayan*[3], *P. Sri Ram Murthy*[1], *V.M. Ravindra Kumar*[1] *and P.S. Rama Sreekanth*[1]

[1]Department of Mechanical Engineering, Vellore Institute of Technology - Andhra Pradesh (VIT-AP University), Amaravati, Andhra Pradesh, India

[2]Department of Mechanical Engineering, Amrita School of Engineering, Amrita Vishwa Vidyapeetham, Bengaluru, Karnataka, India

[3]Department of Mechanical Engineering, Centurion University of Technology and Management, Bhubaneswar, Odisha, India

## 6.1 Introduction

The thermal properties in very general terms aid in understanding the influence of heat on any material [1]. The case of polymeric materials is interesting as they are neither amorphous nor crystalline. In recent years, multifarious researchers have drawn attention to different thermal properties of polymers such as thermal stability, thermal conductivity, and thermal degradation [2,3]. Some polymeric materials exhibit in situ high tensile strength, flexural strength, superior wear and abrasion resistance, and low-temperature flexibility [4]. However, polymers, in general, have certain limitations like poor thermal stability and thermal conductivity. Many industries, such as automobiles, aerospace, electronics, and others, heavily depend on efficient thermal conductive and lightweight materials for their operations. In recent times, the digital revolution's generation led to the evolution of high-speed processors with their increased lifetime and reliability, calling for significant research in the field of thermal management materials. Applications of polymers were not utilized to the full extent due to their poor thermal stability. Polymers decomposition typically commences in the temperatures range from 150°C to 300°C [5].

As a consequence, degradation of polymeric material may already occur before processing it. Therefore in both cases, the material conductivity and degradation temperature play a crucial role in the longevity of polymers in various application areas. Improving thermal stability is the primary concern for developing polymers further. Owing to this, several researchers have attempted to improvise the thermal properties of polymers through the addition of various nanofillers. This chapter briefly discusses various research works allied with thermal properties of different polymeric nanocomposites such as thermoplastic polymer nanocomposites, epoxy and fiber-reinforced nanocomposites, recycled polymer nanocomposites, blend polymer nanocomposites, shape memory polymer (SMP) nanocomposites, and biopolymer nanocomposites.

**Advanced Polymer Nanocomposites. DOI:** https://doi.org/10.1016/B978-0-12-824492-0.00013-1

## 6.2 Thermal properties of polymers and polymer nanocomposites—terms, definitions, significance

A polymer material has multiple relevancies across various fields and works under varying temperatures. Thermal properties are as important as mechanical, chemical, and electrical properties since polymers are sensitive to minor changes in temperature. A sharp melting point is observed in semicrystalline polymers, unlike a gradual polymer softening polymer melt in amorphous materials. At higher temperatures, melt flow orientation, molecular weight affects the flexibility and the impact strength and also aids in the decrease of dimensional stability. Thermoplastics usually require higher temperatures to degrade due to the presence of tough covalent bonds completely. Thermosets, on the other hand, develop chemical bonds and also require elevated temperatures for complete degradation. However, these materials are considered less sensitive to higher temperatures than thermoplastics as there will not be a significant effect on the mechanical and thermal properties of these materials. When the polymers are exposed to higher temperatures for a long time in the presence of air, oxidation occurs, which gradually develops cracks in the layers of the materials and eventually leads to depletion of mechanical and thermal properties of the polymers.

Most polymeric materials are designed at melting temperatures. Initially, heat is utilized in melting the polymer and then to cure the product at room temperature. Curing involves cooling polymer products from relatively high temperatures, which often results in shrinkage and dimensional changes. In polymers, volume changes or dimensional changes concerning temperature are more when compared to metals and ceramics. Hence, shrinkage during the injection molding process is 1% in amorphous polymers, whereas for semicrystalline polymers it ranges from 3% to 4% [6]. When the polymers are blended with the fillers and stabilizers or composites, these dimensional changes need special attention, and also appropriate thermal data is required for molding or extrusion. If not, there will be more deviation in the dimension of the required samples.

### 6.2.1 Definitions and significance

The term thermal properties portray the phenomena of the polymers at a varied set of temperatures. These are key factors in deciding the behavior of the polymers at different temperatures. In this chapter, the transitional phenomena of polymers likewise glass transition temperatures ($T_g$) and melting temperatures ($T_m$) and thermophysical properties of polymers such as thermal conductivity, thermal diffusivity, specific heat capacity, linear thermal expansivity, and thermal stability are discussed.

#### 6.2.1.1 Melting point and glass transition temperature

The term transitional temperature refers to a change of mechanical/thermal properties by modifying the temperatures. Two typical thermal transitions are observed in

the polymers are referred are $T_g$ and $T_m$. Classically, glass transition temperature is known as the temperature at which there is molecular mobility in the amorphous/semicrystalline polymers, which results in significant changes in the properties of the material. At the glass transition temperature, material changes from solid state to the flowy or rubbery state in the amorphous materials. From Fig. 6.1, it can be seen that the molecular structure is at a certain gap at this temperature, which is in an increasing trend. When the temperature is below $T_g$, the molecular arrangement in the amorphous materials is more rigid. The molecules get the required energy to allow chain structures to move more freely in the glassy state. As the polymer is heated, molecules become flexible, and a rubbery state is observed. The temperature at which the rigid state changes to a flowy state is the glass transition temperature, $T_g$. Polymers with flexible chain structures show lesser $T_g$ values, whereas the materials whose chain structure is inflexible show higher $T_g$ values. As $T_g$ is associated with molecular motion, rotation about polymer chain links will also influence the $T_g$ of a polymer. Other factors include flexibility of chain structure, steric effects of molecular structure, molecular weight, branching, and cross-linking.

On the other hand, melting temperature is equally important as $T_g$ and the critical temperature lies above the crystalline regions in a polymer become flowy. A semicrystalline polymer starts to become rubbery after $T_g$, but it becomes liquid after melting temperature. Usually, in semicrystalline polymers, $T_m$ is higher than its $T_g$.

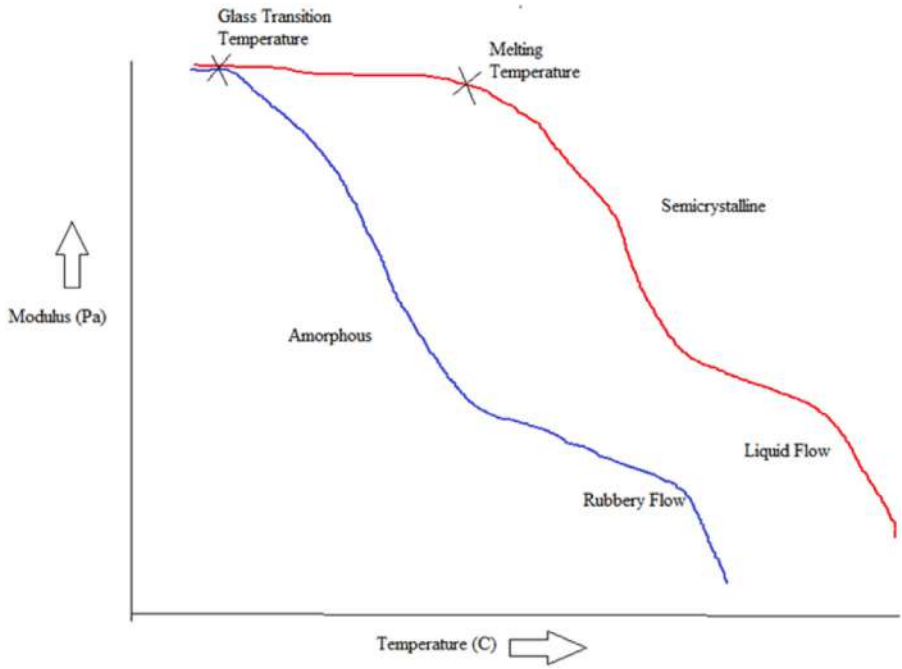


**Figure 6.1** Melting and glass transition temperature of semicrystalline and amorphous polymers.

The polymer exhibits larger elongations under lesser loads in the rubbery region at a temperature above $T_g$ and below $T_m$. Usually, in amorphous and semicrystalline polymers, their molecules require a different amount of energy to move randomly due to unequal chain lengths. Hence, $T_g$ or $T_m$ is not constant and varies with the temperature.

Fig. 6.1 shows the melting and rubbery nature of semicrystalline and amorphous polymers [7]. From the figure, it can be observed that in the semicrystalline polymers, at above the melting temperature, there is a phase change from solids to viscous liquids, which can be molded to the desired shape. The transition of amorphous layers into the rubbery region at glass transition temperature $T_g$ and continues to melt over a wide range of temperatures. In the amorphous materials, once the temperatures are above $T_g$, they tend to decrease in strength, whereas the semicrystalline materials proceed to exhibit stable nature, and also their mechanical properties remain unaffected till the temperature reaches the melting phase $T_m$. Also melting temperature of the polymer is affected by the molecular weight, chain flexibility, intermolecular bonding. The relation between melting and glass transition temperature is mathematically formulated [8] by data obtained from various research works and can be written as

$$\frac{\text{Glass transition temperature}(Tg)}{\text{Melting temperature}(Tm)} \approx \frac{2}{3}$$

where the units of the temperature are Kelvin.

### 6.2.1.2 Thermal conductivity

Thermal conductivity ($k$) is also important in the thermal analysis (TA) of polymers. This property signifies the energy transfer through the polymer structure from higher temperature regions to lower temperature regions. Thermal conductivity and resistance to the temperature of the respective plastic material need to be evaluated before proceeding to any application at higher temperatures. Thermal conductivity can be mathematically formulated as the following relation

$$k \approx C_P\, \rho u l$$

where $\rho$ is the density of the material, $u$ is the speed of sound, and $l$ *is* the separation of molecules [8]. In the amorphous polymers, there is an increasing trend in the thermal conductivity till $T_g$, and from thereon, there is a slowly decreasing trend as the temperatures further rise. Fig. 6.2 [9] presents the thermal conductivity concerning temperature for various polymers below the glass transition temperatures. Thermal conductivity in semicrystalline polymers is more in the solid state as the density is more and gradually reduces to the melt. In the case of polymer nanocomposites, the value of thermal conductivity depends on the properties of the fillers. If the fillers have higher thermal conductivity, then they will influence the conductivity of

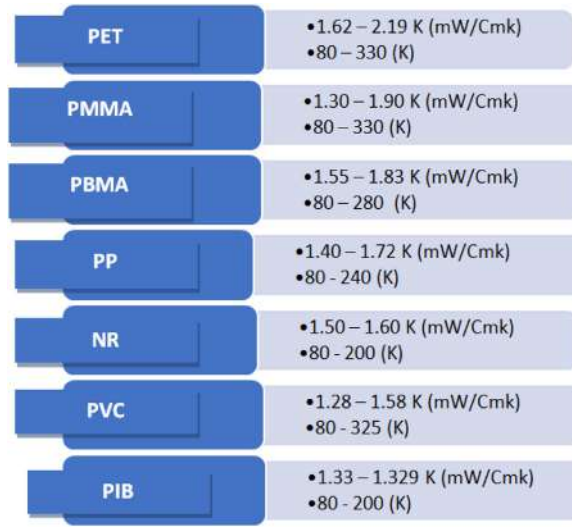


**Figure 6.2** Thermal conductivity of various thermoplastics.

the matrix material. Also, the fiber orientation in the organic fillers and gas content in the foamed or expanded fillers affects the thermal conductivity of the polymers.

In polymers, thermal conductivity depends on the degree of crystallinity; hence a polymer with a high crystalline structure will have higher conductivity than an amorphous polymer. Thermal conductivities of plastics are relatively low when compared to ceramic materials and are approximately around 0.0004 (cal-cm)/(°C-cm$^2$-s) [6]. Various thermal conductivities of the polymers and composites are shown in Table 6.1. Due to the lower thermal conductivities of the polymers, they are used in areas with higher heat transfer. Applications vary from usage in utensils holders to automobile parts, etc. One more important quality is that there will be a good feel of plastic parts and hence can enhance plastic usage in diverse areas.

### 6.2.1.3 Specific heat

The specific heat, $C$, often refers to the energy required for a unit mass of a polymer to change the temperature by one degree. Specific heat usually is considered to be the same in the case of constant volume and constant pressure but can change due to variation in processing or design temperatures of the polymers. In semicrystalline thermoplastics near the melting point of the polymers, the discontinued nature of specific heat is observed due to the formation of crystallites. To melt these crystallites, heat is required and is often defined as the heat *of fusion*. Values of the heat of fusion for polymers are shown in Table 6.2.

The function of temperature on the specific heat capacity of semicrystalline and amorphous polymers is illustrated schematically in Fig. 6.3 [10]. In semicrystalline plastics, a slight rise is observed at a $T_g$, and a peak is observed at $T_m$. This rise can

**Table 6.1** Thermal conductivity of polymers and their composites with respect to temperature.

| Type | Thermal conductivity W ($m^{-1} \cdot K^{-1}$) |
|---|---|
| PS | 0.16 |
| PMMA | 0.19 |
| PVC | 0.16 |
| Nylon 66 | 0.25 |
| PET | 0.14 |
| PU | 0.31 |
| PTFE | 0.24 |
| Polypropylene (PP) | 0.12 |
| 40% talc filled | 0.32 |
| 40% CaCO3 filled | 0.29 |
| 40% glass filled | 0.37 |
| LDPE | 0.35 |
| HDPE | 0.44 |

*HDPE*, High-density polyethylene; *LDPE*, low-density polyethylene; *PET*, polyethylene terephthalate, *PMMA*, polymethylmethacrylate; *PTFE*, polytetrafluoroethylene; *PVC*, polyvinyl chloride; *PU*, polyurethane.

**Table 6.2** Specific heat of polymers and polymer composites.

| Type | Specific heat J ($kg^{-1} \cdot K^{-1}$) |
|---|---|
| PS | 1190 |
| PMMA | 1270 |
| PVC | 1340 |
| Nylon 66 | 1310 |
| PET | 1030 |
| NR | 1800 |
| PU | 1775 |
| PTFE | 1045 |
| Polypropylene (PP) | 2350 |
| Polyethylene | 1550 |

*PVC*, polyvinyl chloride; *PU*, polyurethane.

be due to the heat of fusion of the crystallite structures present in the plastics. No peak is observed in the case of amorphous polymers. For a polymer, molecular weight and the history of the material have a significant effect on specific heat capacity. If the polymer is quenched at the temperature from the rubbery state to the rigid state, there will be an increase in the specific heat compared to annealing the sample at the same temperature. Generally, the specific heat value for the polymer materials (Cal/gm/°C) ranges between 0.3 and 0.4 for the polymers, and these values are much higher when compared to metals on a weight basis. Knowing the specific heat of a polymer helps in determining the amount of energy required for

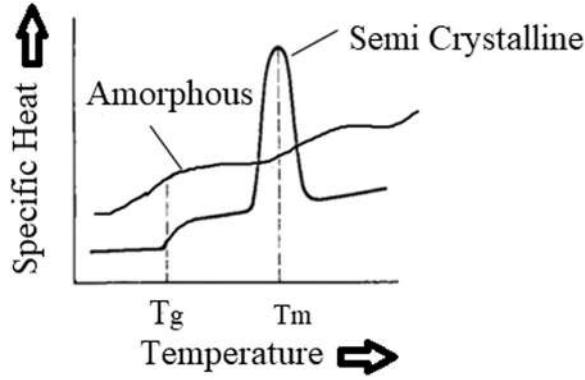


**Figure 6.3** Specific heat behavior of amorphous and semicrystalline polymers.

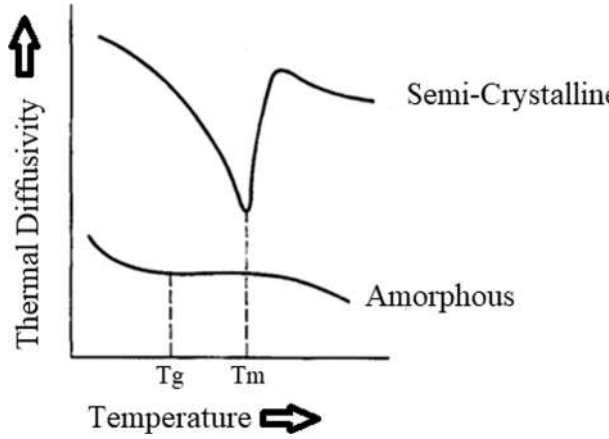


**Figure 6.4** Diffusivity across temperatures for amorphous and semicrystalline polymers.

the particular material, which will be further useful in compression and injection molding, and also, we can easily estimate the mold cooling requirements.

### *6.2.1.4 Thermal diffusivity*

Thermal diffusivity is termed as the property that manages the process of thermal diffusion across time. In the amorphous materials, the thermal diffusivity decreases with temperature but rises at the glass transition temperature due to decrement in heat region capacity and slows down later and the constant trend is maintained in elastic and slowly decrements in melt-flow, as shown in Fig. 6.4 [10].

In the case of semicrystalline materials, with the increase in temperature, there is a decrease in thermal diffusivity, and also relatively deep minimum value is observed at the melting point. On the other hand, with the increase in the degree of

crystallinity, one can observe that the thermal diffusivity increases. Thermal diffusivity ($\alpha$) can be explained with the help of the following relation in terms of thermal conductivity ($k$), heat capacity ($C_p$), and density of the polymer ($\rho$).

$$\alpha = k/\rho C\mathrm{p}$$

### 6.2.1.5 Coefficient of linear thermal expansion

The linear coefficient of thermal expansion (CTE) is related to volumetric changes in a polymer as the temperature changes. However, fibers and other fillers significantly reduce thermal expansion. In the general observation, expansivity depends on the orientation direction, the value increases in the directions parallel to the axis and decreases perpendicular to the axis. Table 6.3 shows the thermal expansion values of various polymers.

Due to weak bonds in the plastics, they usually exhibit higher thermal expansions and require less energy to expand the structure. Thermal cracking is rarely observed in polymers despite higher thermal expansion values due to the ability to take larger strain rates and less elasticity. Mold shrinkages in the polymers usually range from 1% to 2%, and in the case of polyethylene, there will be higher shrinkages also. Hence, it is difficult to produce the plastic parts with much closer tolerance values as it is tedious to maintain the shrinkages. In the practical scenario, plastic manufacturers usually use lower thermal expansion materials in higher temperature application areas because a higher thermal expansion plastic poses a severe threat to the life of the components when subjected to elevated temperatures. Phenolic and urea are typical examples of lower expansions but the use of filler material reduces the thermal expansion of polymers to a certain extent. In certain applications, the material with higher expansivity is required, especially in the

**Table 6.3** Coefficient of thermal expansion of polymers and polymer composite [10].

| Type | Thermal expansivity $10^{-6}$ m ($m^{-1} \cdot K^{-1}$) |
|---|---|
| PS | 65 |
| PVC | 190 |
| Nylon | 80 |
| PET | 59.4 |
| PU | 57.6 |
| PTFE | 95 |
| Polypropylene (PP) | 80 |
| 40% talc filled | 61 |
| 40% $CaCO_3$ | 40 |
| 40% glass filled | 30 |
| HDPE | 108 |

*HDPE*, High-density polyethylene; *PVC*, polyvinyl chloride; *PU*, polyurethane.

fitting of handles to the cutting pliers and other equipment and also has the potential use in mold design.

#### 6.2.1.6 Thermal stability

Polymer's thermal stability is the capacity of the material to overcome the heat and exhibit enhanced properties. It can be determined by a TA technique called thermogravimetric analysis (TGA) which will be discussed in detail in the next chapter. Many factors improve the thermal stability of polymer-like molecular weight of the polymer, structure, and crystallinity. On the other hand, various additives like aromatic compounds help from polymer backbone degradation and strengthen the cross-links, which will enhance the thermal stability of the polymer. However, polymers with more oxygen or double bonds are more prone to degrade at lower temperatures.

In the current research scenario, nanoparticles were found to outweigh any other fillers in improving the stability of the polymer matrix. This can be due to the presence of restricted chain mobility and multiple interactions [11]. Recently, nanofillers like hydroxyapatite, MMT, carbon nanotubes (CNTs), nanographene, or titanium dioxides have been found to increase in thermal stability nature of polymers by creating a railing to degrade to the supply of oxygen. Numerous other factors such as shape, structure, size of the nanofiller, dispersion rate, the dispersion medium, and the adhesion to the polymer surfaces define how much improvement is observed in thermal stability. Besides this, nanoparticles with modified structures also inherit new properties to the matrix resulting in new material behavior such as showing magnetic properties, exhibiting the catalytic nature, or improved antibacterial properties. Nanostabilizers can also be custom-made with the required properties using these fillers, which will further enhance the stability of the polymer along with the traditional stabilizers added to the polymer matrix.

## 6.3 Principal and techniques of thermal analysis

### 6.3.1 Introduction

Sample, reagent, and signal (treating heat as reagent source) are the three basic elements of a theoretical model of chemical analysis and can be utilized for TA [12]. A suggestion was given to extend the TA for rapid heating of workpiece for specific enhanced temperatures following the isothermal conditions for measuring the property with time. Fig. 6.5 represents the flow process in TA.

Generally, in TA instruments, working theory is very similar to one another. Based on the electric signals received from the transducers, the property or behavior of the sample is defined. Throughout the analysis as a function of temperature, results are drawn. The curve obtained from the analysis is called as TA curve, and curve attributes correspond to thermal events. Fig. 6.6 is the schematic representation of the TA instrument.

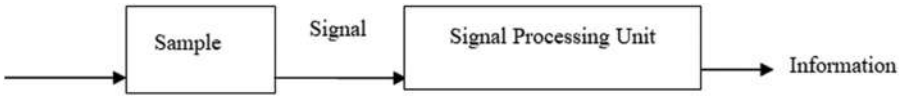


**Figure 6.5** Representation of the TA flow process in schematic diagram. *TA*, thermal analysis.

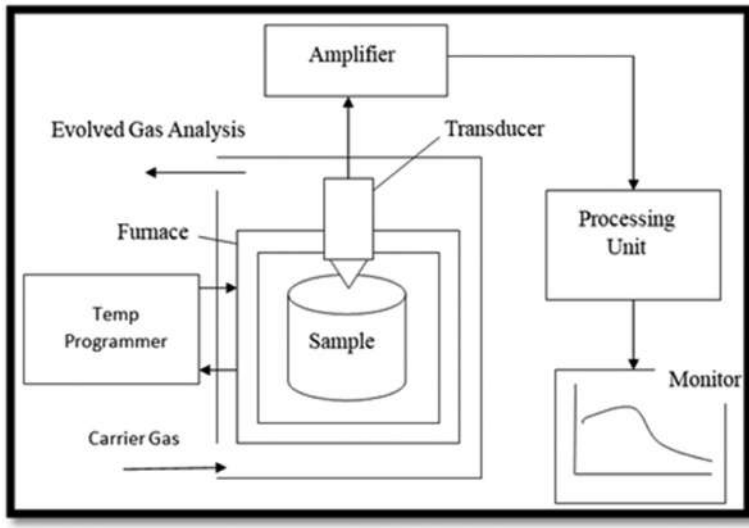


**Figure 6.6** Schematic diagram of the thermal analysis instrument.

From the curve, all the physical quantities concerning time or temperature are plotted. Derivative and differential are the most general terms that are used in TA. These terms explain the rate of change of physical quantity and temperature difference between the supporting sample and the specimen.

In these techniques, various parameters such as heat capacity, melting temperature, crystallization temperature, and other thermal parameters can be assessed at different heating or cooling rates. Fig. 6.7 shows the physical properties and its derived techniques for the analysis.

### 6.3.2 Differential scanning calorimetry/calorimeter

Power consumption differential scanning calorimetry (DSC) and heat flux DSC [also called differential thermal analysis (DTA)] are the two generic terms of DSC [13]. In this technique, under a controlled temperature program, the specimen and the supporting sample are heated to the required temperatures, and the heat flow

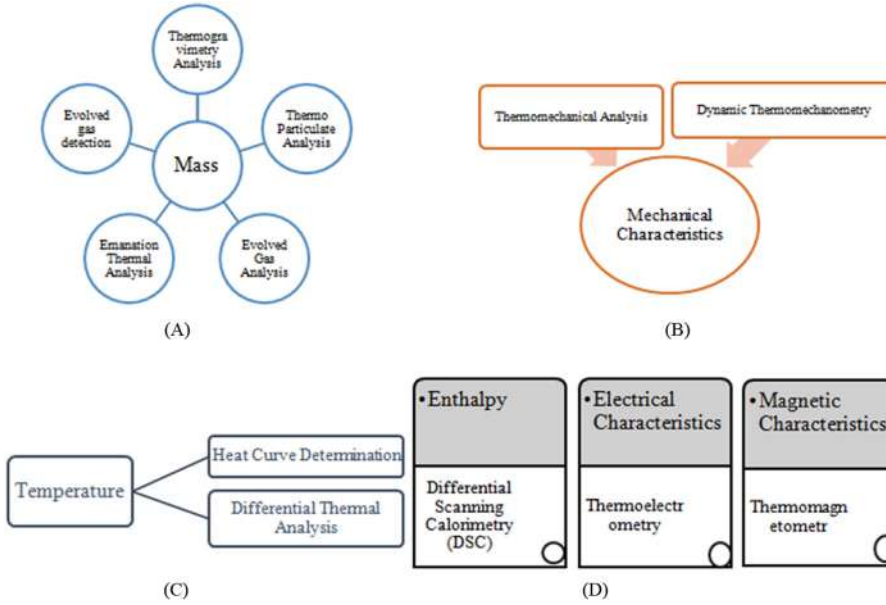


**Figure 6.7** (A, B, C and D) – Physical property and its derived techniques.

rate is calculated by taking the temperature difference between supporting material and specimen (as a function of temperature).

Its application is widened to different areas, majorly in pharmaceuticals, food industries, biotechnology, and polymers in identifying the glass transition temperature $T_g$, melting and crystallization points, in characterizing the thermosets, liquid crystal transitions, kinetic evaluation of chemical reactions, etc. The foremost advantage of DSC is that a sample with a smaller size (in milligrams) is enough to evaluate the material. In recent times, DSC has been upgraded with various techniques such as fast scan DSC, modulated temperature DSC, and so on. The main disadvantages are that preparation of the sample is difficult when samples contain solvent because it may be evaporative, and also interpreting the results is difficult. One more point to be considered for two-phase mixture DSC is not suitable [14].

### 6.3.3 Heat-flux differential scanning calorimetry

Both the specimen and the reference sample are sealed and placed in the pan and holder, as shown in Fig. 6.8. Sample vessels are made of gold, platinum, aluminum, steel, etc., and are of different shapes. From one side of the holder, inert supporting material is inserted. Then, using thermocouples, the temperature difference between the specimen and supporting material is measured as a function of temperature. At the same time, other thermocouples measure the furnace temperature and heat of the sensitive plate.

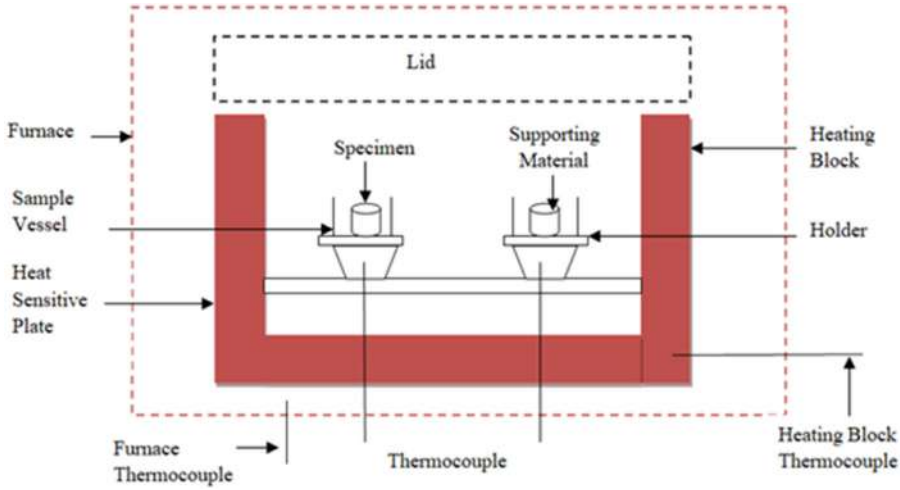


**Figure 6.8** Heat flux DSC – schematic diagram. *DSC*, Differential scanning calorimetry.

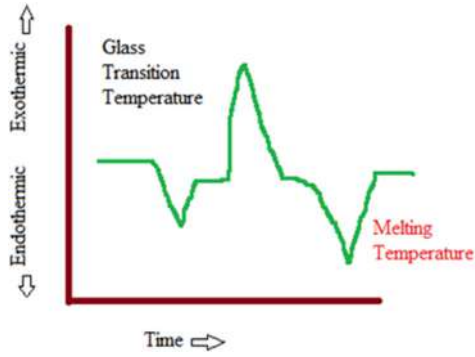


**Figure 6.9** Illustration of DTA curve. *DTA*, Differential thermal analysis.

When the furnace is heated, both the specimen and supporting material get heated. Due to this, energy is either liberated or absorbed by altering heat flux (from the heat-sensitive plate) and develops temperature difference during phase transformation, when the furnace is heated in a programmed manner. Curve from DTA plots the temperature difference as a time function, as shown in Fig. 6.9. In addition, transition enthalpy is measured through the DTA curve from the heat capacity of the sensitive plate as a function of temperature.

Using DTA, glass transition temperature ($T_g$) and transition enthalpy are measured accurately. In addition, a heat-sensitive plate's heat capacity is measured as a function of temperature.

### 6.3.4 Power compensation differential scanning calorimetry

In this system, holders of both specimen and supporting material are connected with resistance sensors individually. These sensors measure the temperature of the resistance heater as well as the holder base. Based on the specimen and supporting material temperature difference, electrical power will be supplied. The specimen's heat capacity and power input generate the curve, a function of programmed time or temperature. For this system, 35 mW is the maximum sensitivity. The major advantage of the power consumption DSC compared to heat flux DSC is its higher scanning rates (60,000 $min^{-1}$). Fig. 6.10 explains the process in DSC.

### 6.3.5 Thermogravimetric analysis

In this technique, changes in both the chemical and physical properties of the samples are evaluated as a function of time or temperature or both [15]. Along with the temperature programmer, electronic microbalance and furnace are associated. TG instruments are used for different investigations based on the applications and generally arranged for variable and vacuum atmospheres. Argon, chlorine, cobalt, hydrogen, nitrogen, hydrogen cyanide, sulfur dioxide gases analyze TG at various atmospheric conditions. Usually, dynamics conditions are preferable because the gas composition in and around the specimen changes due to the gas generating reactions. The point at which ferromagnetic material is turned into paramagnetic material by heating is called as Curie point. When a ferromagnetic material is brought to the Curie point, the mass of the magnet reaches zero, and the apparent mass loss is identified by balance, which helps in TG temperature calibration. Fig. 6.11 is the schematic presentation of the TGA. A refractory pan made of

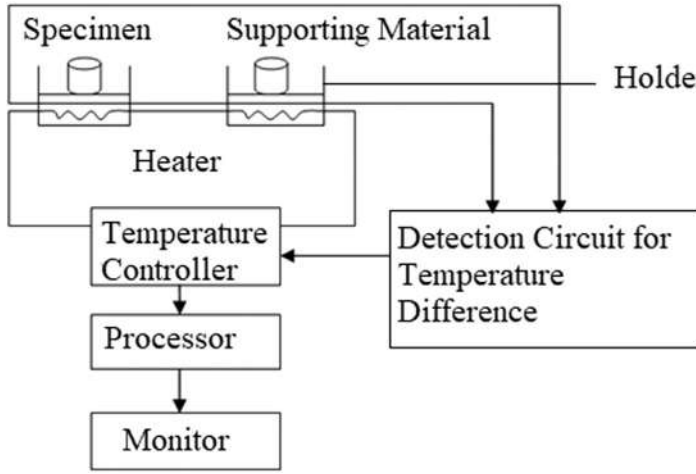


**Figure 6.10** Schematic diagram – power compensation DSC. *DSC*, Differential scanning calorimetry.

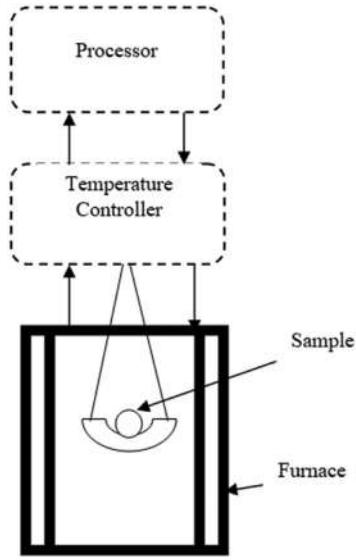


**Figure 6.11** TGA—schematic diagram. *TGA*, thermogravimetric analysis.

platinum or porcelain is suspended (which contains specimen powder) from high precision balance into the hot zone of the furnace. As this balance is electronically configured, it cannot tilt or move even after the specimen's weight loss or weight gain. To measure the temperature, thermocouples are arranged nearer to the specimen (noncontact).

In general, materials such as silicon carbide, platinum are used as heating coils in the furnace, whereas infrared ray heaters can heat the furnace to 1800K in minutes. Following are the different types of commercially available microbalance (Fig. 6.12).

Cahn's microbalance design is frictionless due to roller pins with a precision of 0.1 μg. Roller pins support the taut band to stay at its exact position. The taut band gets twisted, and the flag position changes when the current passes through the coil surrounding it. Servo mechanism is used in adjusting the current in the coil and parallelly to maintain continuous and constant illumination from photocell detectors. If the flag position gets changes, interference between infrared light propagation to the photocell detector changes. Weight gain or loss by the specimen will be balanced when the current is sent to the coil. From corrosive gases, electronic components, and chamber, get protected by inert gas and compressed air by developing positive pressure in the balance chamber. However, still, there are chances of gases from the specimen getting diffused into it. Exit port plays an important role by not diffusing inert gases back into the chamber. Through fluid, exit gas is bubbled out of the port and restricts the exit gad entering back into the chamber. When fluid does not bubble, it is an indication that there is a leak of gas fluid, whereas derivative thermogravimetric (DTG) curve discusses the mass loss of the sample. The

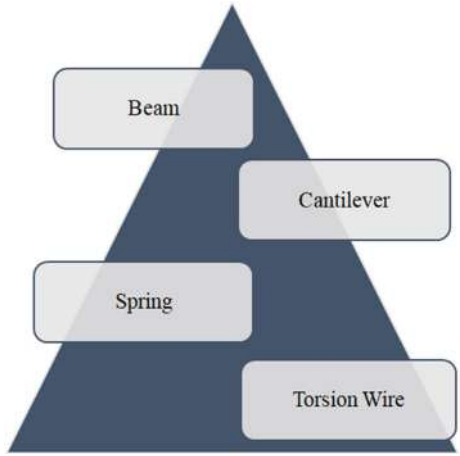


**Figure 6.12** Different types of microbalance.

main purpose of the DTG curve is to know about the temperature at which there is a maximum mass loss of the material. There are different types of TG and depend upon the arrangement of the sample holder. For TG-DTA, the above balance and parallel balance arrangements are followed, and for simple TG measurement, the below balance arrangement is followed.

### 6.3.6 Thermomechanical analysis

The technique in which load is applied in irregular intervals over the sample as a function of time or temperature in measuring the deformation under a defined atmosphere is known as thermomechanical analysis (TMA). Through the TMA curve, the thermal behavior of the sample is assessed, and in any mode (flexure, compression, tension and expansion), curve can be drawn between temperature and time on the *x*-axis and sample size variation on the *y*-axis. Even in thermodilatometry (TD), analysis can be performed. As a function of temperature, samples shrinkage and expansion are evaluated. Thermal expansion is measured from the analysis, which is expressed as the CTE. The major difference between TGA and TD is when minimal or negligible loads are applied to the sample TD measures the dimensional changes, whereas in TMA, a significant load is required [16]. Along with the determination of CTE, densification and kinetics, softening points, transition temperatures are determined [17,18]. From CTE records, blends and orientation of the crystals are differentiated, and also TMA provides CTE of various materials at the required temperatures. Furthermore, TMA gives results accurately compared to DSC due to its sensitivity in measuring composite materials' glass transition temperature ($T_g$).

Stress generator, furnace, deformation detector, temperature controller, programmer, and detector are the common and basic instruments used in the TMA. It measures bending, linear expansion, penetration, etc. of the samples which are of gel,

solid, or even in a liquid state. This indicates that at various atmospheric conditions and aqueous solutions, measurements can be performed. Figs. 6.13 and 6.14 represent types of probes being used along with the arrangement of TMA.

Before performing the analysis, probe weight and calibration of the instrument have to be carried out to get the results accurately. Of note, 1 mN to 10 N of load can be applied to the sample through a load cell with 0.001 N resolutions. Fig. 6.15 shows the TMA deformation modes. The selection of probe plays an important role in performing the analysis, and it generally depends on the dimensions of the sample, geometry, etc. During analysis, the sample expands, which results in the movement of the probe up and down. This helps in identifying the expansion of the sample.

In the compression mode, penetration, expansion, and volumetric expansion probes measure the coefficient of linear thermal expansion (CLTE), softening temperature, and glass transition temperature of the regular and irregular shaped samples. Along with creep measurement, properties such as CLTE, stress, and strain of

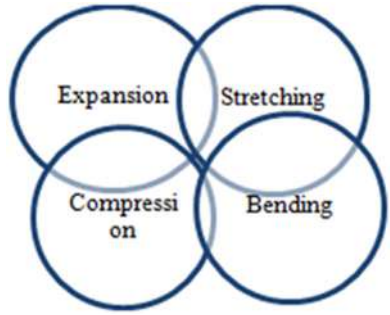


**Figure 6.13** TMA probes. *TMA*, Thermomechanical analysis.

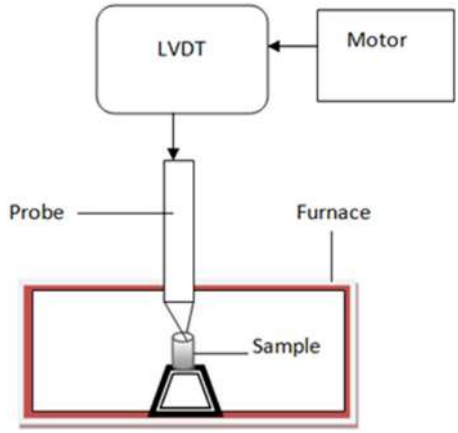


**Figure 6.14** Vertical TMA. *TMA*, Thermomechanical analysis.

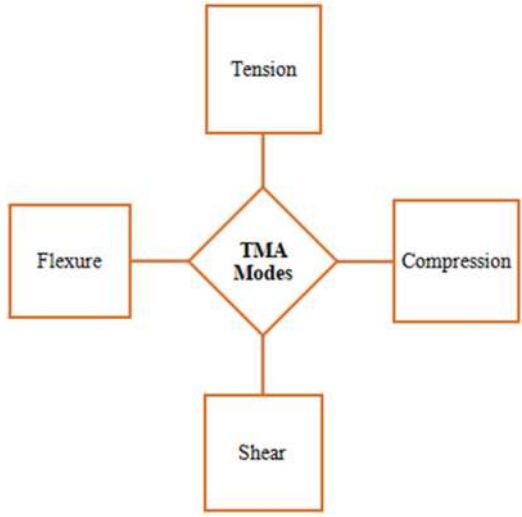


**Figure 6.15** TMA deformation modes. *TMA*, Thermomechanical analysis.

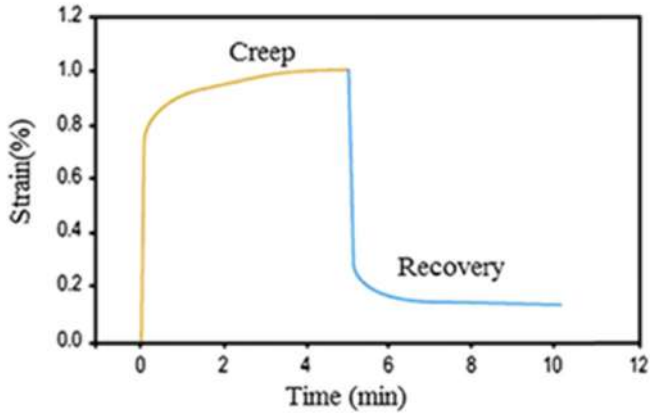


**Figure 6.16** Creep analysis in TMA. *TMA*, Thermomechanical analysis.

the material can be evaluated using tension probes. For thin films, a small amount of tensile load is applied to the sample to prevent it from twisting. Flexural and shear probes help identify the deflection properties and shear modulus (elastomers). Among these, an expansion probe is used most commonly. Always it is preferable to go with probes with more contact areas for identifying the CLTE. Fig. 6.16 represents the creep analysis performed in TMA, whereas Figs. 6.17 and 6.18 show the softening point of the polymer obtained with TMA.

Fig. 6.18 represents the material's expansion curve $T_g$ and softening point at constant applied force (temperature ramp).

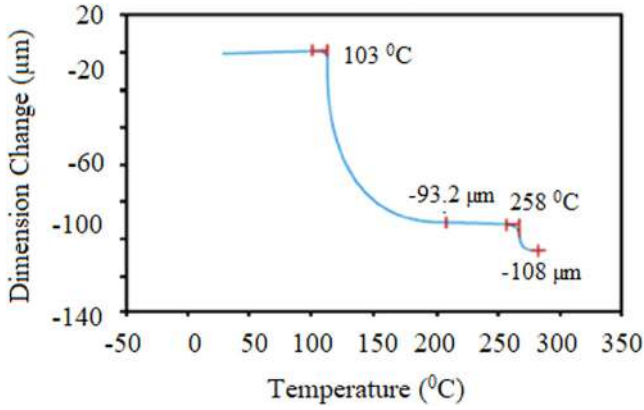


**Figure 6.17** Film (multilayer) analysis.

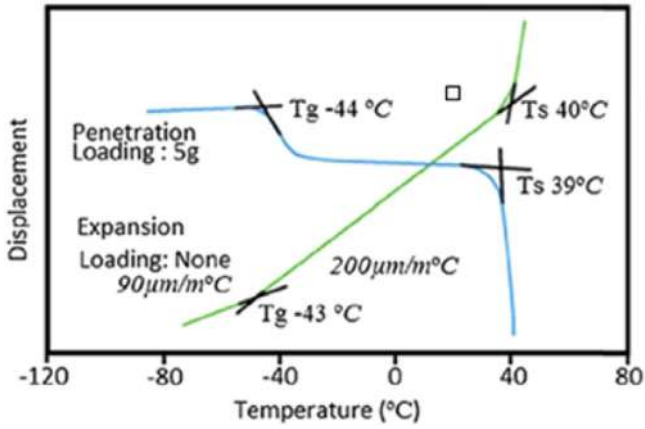


**Figure 6.18** The glass transition temperature ($T_g$) and softening point ($T_s$) of a polymer.

TMA rooted its applications in polymers and other materials such as ceramics, metals, glass, and so on. Even on ultrathin films, TMA is performed to analyze the thermal properties and to know whether phase transition temperature is independent or dependent on interactions between thin films and respective substrates [19] and it is suitable for the evaluation of the polymerization product [20]. Finally, it has the capability of finding the properties of innate and product or sample. Fig. 6.19 represents the application of TMA in the areas of polymers.

### 6.3.7 Dynamic mechanical analysis

In this method, the load is applied on the sample at rated temperature and at controlled frequencies to analyze the material's viscoelastic behavior. From the


**Figure 6.19** Applications of TMA in the area of polymers. *TMA*, Thermomechanical analysis.


**Figure 6.20** Types of forced resonance in DMA. *DMA*, Dynamic mechanical analysis.

analysis, glass transition temperature, storage modulus, and loss modulus are noted. One of the dynamic mechanical analysis (DMA's) major advantages is that DMA overcomes transitions that are not observed through side chain using DSC. In DMA, for the deformation of the sample, either stress (force) or strain (displacement) control load can be used. It is one of the ideal methods to analyze the behavior of the material at the smallest loadings. Nevertheless, testing fixture, loading mode, sample preparation, and plotting scale play a crucial role in repeatability and measurement accuracy [21]. In DMA, there are two types of analyzers, and both give the same results. In a strain type analyzer, the probe is made to touch the sample, and when it is heated to higher temperatures, stresses are measured with the help of a load cell or transducer. Its short and immediate response toward the load indicates the efficiency of the transducer, but there are chances of sensing less due to low signals or for continuous working conditions.

Similarly, in the stress-controlled analyzers, on a single shaft, all the parts are located on the single shaft. Short-time responses are its major disadvantage. Implementation of the force sensor and linear variable displacement transducer (LVDT) sensor, even at minimum or low signal resolution and viscosities, improves the system's efficiency. By choosing appropriate and proper fixtures to hold the sample and based on the selected sample geometry, both analyzers can perform a similar analysis. Fig. 6.20 represents the different types of forced resonance in DMA, and Table 6.4 tells about its factors.

Due to stiffness or relaxation time changes, there is a certain amount of release or absorption of heat in the sample (free volume, $V_f$). All these are monitored from its polymer volumetric change. Impact properties, aging, and penetration of the solvents are related to $V_f$ and describe different transitions in the polymer. When the

**Table 6.4** Types of analyzers.

| S. no | Analyzers | Factors | Test |
|---|---|---|---|
| 1 | Axial | Force-linear<br>Material-solid and semi-solid<br>Test higher modulus materials than Torsional analyzers | Flexure<br>Tensile<br>Compression<br>Creep recovery<br>Stress relaxation |
| 2 | Torsional | Force-twisting motion<br>Material-liquids and melts | Creep recovery<br>Stress relaxation<br>Stress<br>Strain<br>Shear and normal force measurements |

material is heated, internal molecules of the material have free movement in various directions due to high free volume, and this mobility results in the lower modulus of the molecule and side-chain movements. This approach is known as the crankshaft approach or crankshaft model [22–24].

As the material is heated from low temperatures to higher temperatures, a solid transition occurs initially, and subsequently, it develops some toughness due to the side chains and backbone atoms' movements. This is called gamma transition $T\gamma$ and beta transition $T\beta$ (related to toughness). The first curve falls or modulus reduces due to adjacent atoms or side-chain movements (gap between $T\gamma$ to $T\beta$) and further curve falls due to the change in the glass transition temperature $T_g$. Then due to the movements of the amorphous content in the main chain, it reduces drastically. There are chances of crystallites slipping over each other and at the end chain slippage at large scales occurs and finally material flows. This is known as melting temperature $T_m$.

Based on the $T_g$ values, one can assess the maximum working temperature range of the material (polymer). Fig. 6.21 shows the $T_g$ curve characteristics. $T_g$ is based on the degree of polymerization, and when the physical properties change, it tells at what temperature it turns to a rubbery state from glassy. The point to note is that finding $T_g$ is a little difficult for thin coatings and cured materials. Compared to DSC, DMA is more sensitive and accurate in identifying the $T_g$ values. It is difficult to identify the $T_g$ values in DSC compared to DMA when resins have high cross-linkages. In DMA and DSC and DTA, getting sudden peaks is most common in modulus graph due to stresses built in the material and to relieve these stresses, frozen rearrangement of the molecules takes place because of the free volume. When mobility is achieved, chains tend to move to low energy state. To achieve this condition, heat the material above $T_g$ (through annealing) and cool it.

TMA and DMA methods have the efficiency of finding the material's properties with clear and complete exploration. Below, DMA thermograms (Figs. 6.22 and 6.23) represent the storage modulus and glass transition temperature of Nafion [25].

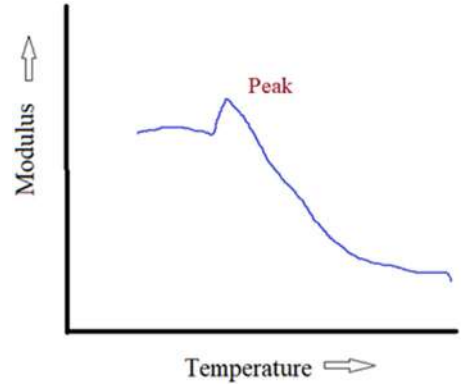


**Figure 6.21** Stress relief at $T_g$ in DMA. *DMA*, Dynamic mechanical analysis.

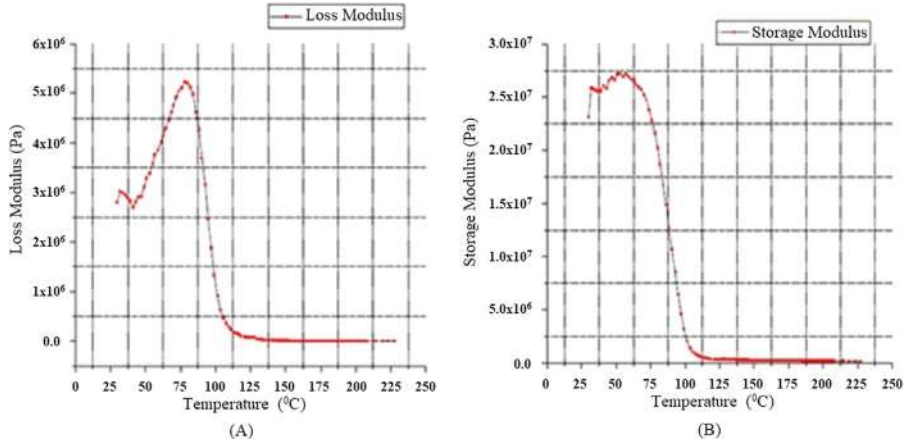


**Figure 6.22** (A) Loss modulus; (B) storage modulus of Nafion membrane.

Coming to the loss modulus graph, until 32°C it is raised and fallen to a smaller extent and increased to $5.2 \times 106$ Pa at 80°C. Storage modulus is high at 60°C with $2.9 \times 10^7$ Pa. This change is generally due to the main and side-chain lengthening. It indicates Nafion has very little energy storage capacity. In general, the storage modulus value can be enhanced by adding fillers. At the highest peak, $T_g$ values are identified as 105.6°C, and as temperature goes on, the increasing Tan delta value reached nearly 0.5°C. As this is a soft material, it has shown very little $T_g$ value. Many materials have shown higher as well as lower $T_g$ values when compared to Nafion. These values indicate that the Teflon fabric-reinforced Nafion membrane changes from rubbery to glass at minimum temperatures. Energy losses from molecular rearrangements can be explained based on the tan delta curve. The ratio of loss modulus to storage modulus is defined as the Tan delta curve.

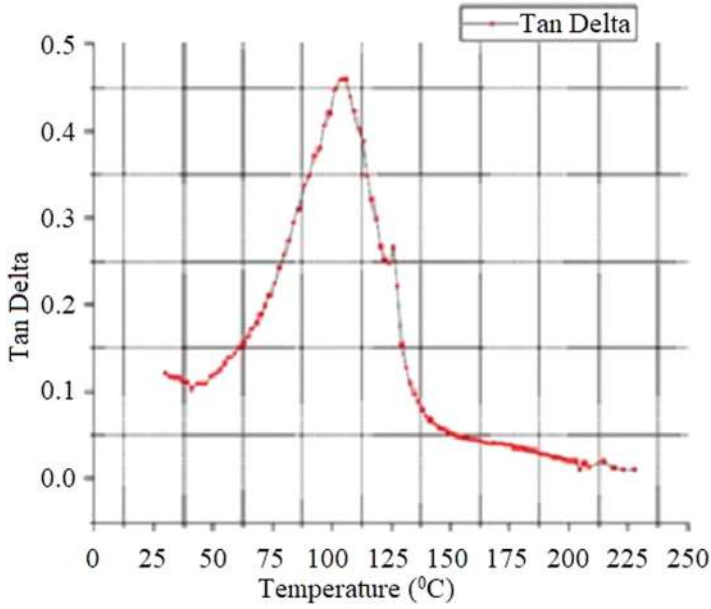


**Figure 6.23** Tan delta of Nafion.

### 6.3.8 Thermoptometry

To know the optical properties of the material, the thermoptometry technique is used. Under this technique, following subtechniques are involved (Fig. 6.24).

When the sample is heated at various conditions, to know its external appearance, thermos-microscopy is used. On the hot stage, the sample is placed in glass pans, and through the camera, foaming, sintering, creeping are observed/monitored in the display screen, and the recorder is used for recording observation [26]. These microscope lenses are heat resistant, and thin hot or cold stages are sustainable to very high temperatures (nearly 3000°C). To examine the sample even at sublimation, the movement of the sample holder should not be restricted, whereas in thermophotometry, intensity of the light is measured (transmitted or reflected). Defunct of light takes place after the formation of the isotropic structure. Fig. 6.25 is the schematic presentation of both thermomicroscopy and thermophotometry.

Thermoluminescence (TL) is a technique used to measure the light emitted from the sample (at isothermal or increasing temperatures). Due to the defects in the sample, TL takes place. High test peroxide and reducing ligands develop and join with the light emission. To absorb the excess heat and radiation, filters are incorporated. When TA is combined with the function of molecules and atoms spectrometry, the analysis is known as thermospectrometry. From the analysis, a specific wavelength of light can be measured. Atomic spectrometry is the basic principle for thermospectrometry. Sample deterioration happens due to the high temperatures in the furnace. The furnace can sustain to 1600°C−1700°C. Atomic spectrometry is

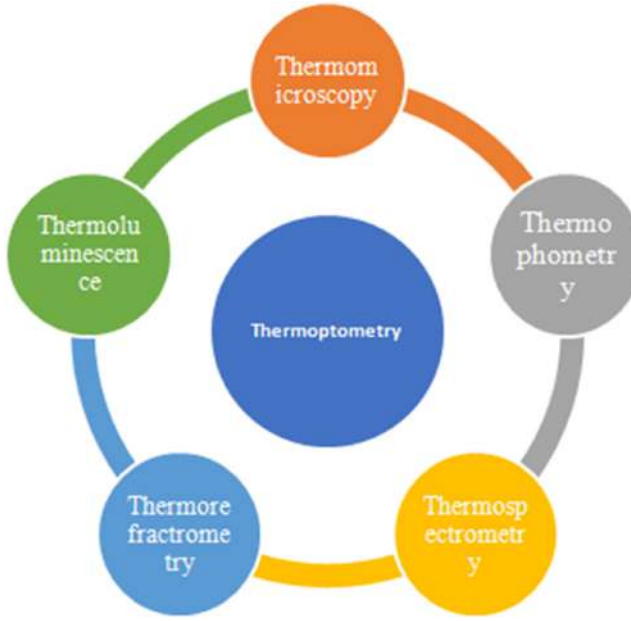


**Figure 6.24** Various techniques under thermoptometry.

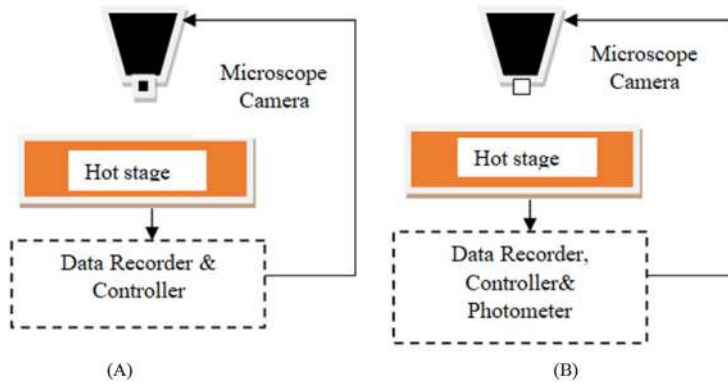


**Figure 6.25** (A) Schematic diagram of thermomicroscopy and (B) thermophotometry.

the basic principle for thermospectrometry. Sample deterioration happens due to the high temperatures in the furnace.

Along with the electric arc, inductively coupled plasma is used in the furnace. In the furnace, sample aerosols are removed due to high temperatures and reactive radicals in milliseconds. If argon gas is used as an aerosol carrier, thermal processes are not affected by any reactive materials. In the construction of the thermos-spectrometry, the furnace has two walls made of silicon carbide with windows.

There are three tubes of windows protector gas, sample inlet and cooling water tube. Based on the furnace height, the light source is arranged. The light beam is made to pass through the sample as well as the furnace. From the observation, absorption and emission of molecules, atoms, and ions, thermal changes occur in the sample and can be scrutinized in the furnace itself [27].

### 6.3.9 Evolved gas detection and evolved gas analysis

Whenever a material or sample is exposed to high temperatures, it releases some gases in the form of vapor. In the earlier techniques, neither TGA nor TG gives information about the evolved gases after heating. With complete information on the evolved gases, one can understand how it reacts concerning time as a function of temperature. It is always desirable to know the composition of the evolved gas. Using evolved gas detection (EGD) and evolved gas analysis (EGA) [28–30], one can predominantly analyze the gases in detail when the specimen is heated to various high temperatures. Fig. 6.26 shows the various analyses cover under EGA.

Evolved gasses are carried by purge gas to the detector. To minimize the reactions, condensation of vapors and time lag, the detector should the placed very close to the sample. Detectors such as thermal conductivity, ionization, and gas density are

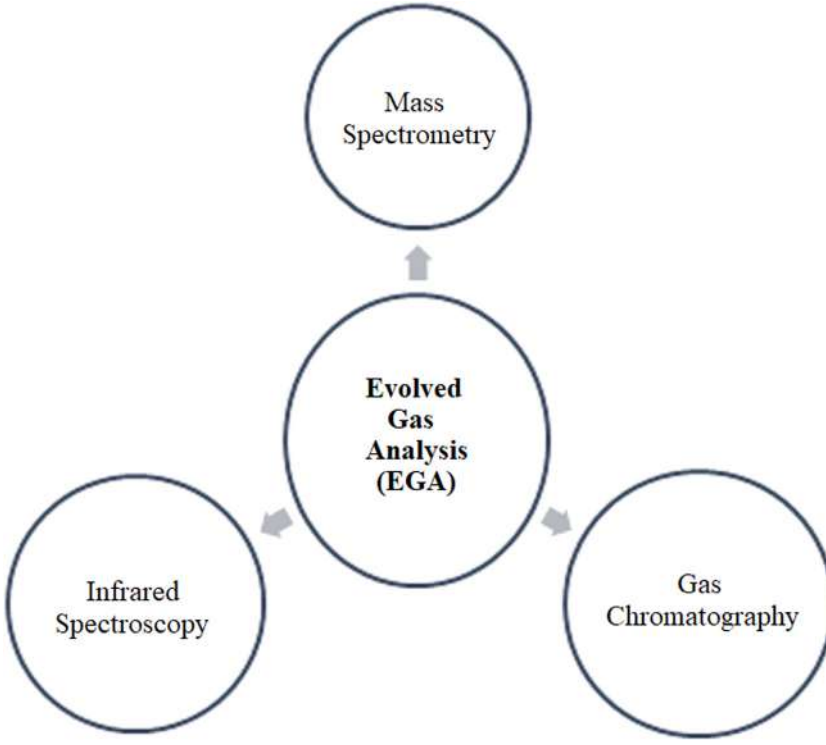


**Figure 6.26** Evolved gas analysis.


**Figure 6.27** Evolved gas detection.

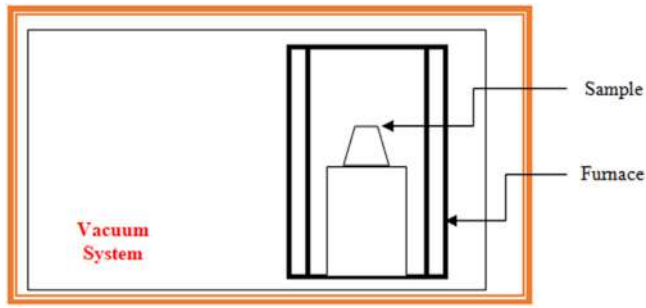


**Figure 6.28** Sample heated inside the vacuum system.

commonly used. Hydrogen, helium, and argon gases are the ideal carriers. Detectors such as flame ionization do not respond to water vapor, but they are highly tender towards organic compounds. With suitable absorbents or cold traps, separation of various gas amalgams is attainable. Fig. 6.27 shows the process in EGD.

In mass Spectrometry (Ms), there is no detector, and this technique is a repetitive gas analysis in identifying the gasses evolved from the thermal instruments. High vacuum pressure is used in this spectrometer (high cost), which is very costly, but the analysis is carried out in most thermal analyzers, just above atmospheric pressure. In Ms, even inside the vacuum system, TA can be carried out, but the results achieved after heating are difficult to analyze and to understand the behavior of the material. To enhance the output, some carrier gases are induced into the system for carrying the evolved gases from thermal instruments to mass spectrometry through an external port. One of the major issues is the chances of carrier gases with high concentrations minimizing the evolved gases response and vapor condensation. Fig. 6.28 is the simple and schematic representation of the sample in a vacuum system.

## 6.4 Polymeric nanocomposites and their mathematical models for reckoning the thermal conductivity

Thermal conductivity is an intrinsic property that explains how a material deals with heat. Polymer nanocomposites are filled with different fillers such as fibers or particles, and it becomes predominant to reckon this property which owes it to different application areas. The application area includes coatings, electronic

packaging, and thermoelectric devices. Applications to material design are based on measuring thermal results and modeling thermal conductivity. Based on particle size, distribution, volume fraction (based on adding fillers), topology, space and spatial distribution, etc., various models such as theoretical, empirical, and semiempirical models are developed. The objective of the following section is to discuss various models for the prediction of thermal conductivity which might help future researchers for further work. Fig. 6.29 depicts the schematic diagram of important models available for estimating thermal conductivity.

### 6.4.1 Series, parallel, and geometric model

Agarwal et al. [31] discussed some defining rules such as series, parallel and geometric models, and they are given as:

Series model is:

$$k = \left(1 - V_f\right)k_m + V_f K_f$$ Parallel model is:

$$\frac{1}{k} = \frac{\left(1 - V_f\right)}{k_m} + \frac{V_f}{K_f}$$

And the geometric model is

$$k = {k_m}^{1-V_f} {K_f}^{V_f}$$

where
"$k$: thermal conductivity of the composite;
$k_m$: thermal conductivity of polymer matrix;
$k_f$: thermal conductivity of filler material."

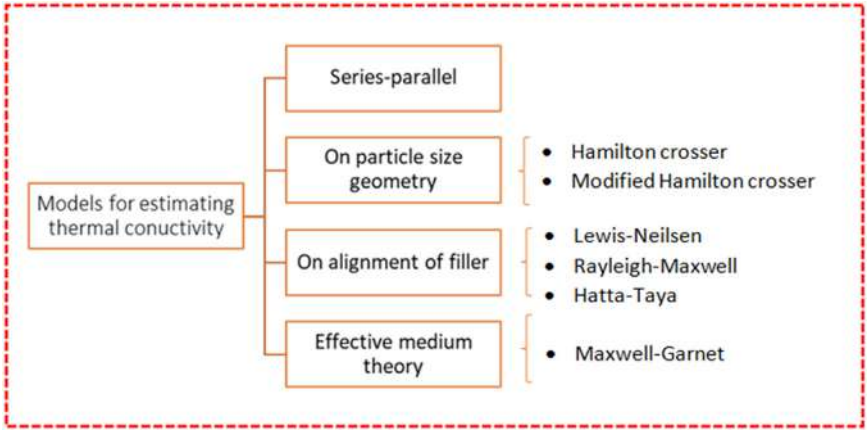


**Figure 6.29** Schematic diagram of different models for estimating thermal conductivity.

The limitation of the series and parallel models are

1. The estimation of thermal conductivity is overestimated by the series model.
2. The estimation of thermal conductivity is underestimated by the parallel model.

The cardinal reason for the same accounts for the overdependence of these models on the amount of filler loading. This is further reasoned to neglect the true geometry and correct size of the filler particles.

### 6.4.2 Models on geometrical particle size

The Hamilton−Crosser model is based on particle size, filler geometry, and the order of particle packing in the matrix [32]. This model is considered as casting away the limitations of series and parallel models.

The model based on Hamilton−Crosser is given by:

$$k = k_m \left[ \frac{k_f + (n-1)k_m - (n-1)V_f(k_m - k_f)}{k_f + (n-1)k_m + V_f(k_m - k_f)} \right]$$

where

"***$V_f$***: volume fraction of the filler material

***n***: geometric factor based on sphericity of the particles."

Modification of Hamilton−Crosser model:

The limitation of the Hamilton−Crosser model is restricted to predicting the thermal conductivity of particles reinforced nanocomposites when more than one nanofillers are present. Badgayan et al. [33] modified the Hamilton−Crosser model for prediction of thermal conductivity of HDPE-based composite and its hybrids, which predicts the thermal conductivity of hybrid nanocomposites, and it is given by

"The thermal conductivity of CNT composite,

$$K_{C_1} = K_m \left[ \frac{K_{CNT} + (n-1)K_m - (n-1)\varphi_{CNT}(K_m - K_{CNT})}{K_{CNT} + (n-1)K_m + \varphi_{CNT}(K_m - K_{CNT})} \right]$$

The thermal conductivity of h-boron nitride nanoplatelets (h-BNNP) composite,

$$K_{C_2} = K_m \left[ \frac{K_{BNNP} + (n-1)K_m - (n-1)\varphi_{BNNP}(K_m - K_{BNNP})}{K_{BNNP} + (n-1)K_m + \varphi_{BNNP}(K_m - K_{BNNP})} \right]$$

where

The volume fraction of CNT composite, $\varphi_{CNT} = \frac{\rho_m W_{CNT}}{\rho_m W_{CNT} + \rho_{CNT} W_m}$

The volume fraction of BNNP composite, $\varphi_{BNNP} = \frac{\rho_m W_{BNNP}}{\rho_m W_{BNNP} + \rho_{BNNP} W_m}$

$\rho_m$ is the density of polymer matrix, $\rho_f$ is the density of nanofiller, $W_f$ is the weight fraction of nanofiller, $W_m$ is the weight fraction of polymer matrix, $K_m$ is the thermal conductivity of polymer matrix, $K_f$ is the thermal conductivity of nanofiller, $n$ is empirical shape factor $= \frac{3}{\varphi}$, $\varphi$ is sphericity."

### 6.4.3 Model based on the alignment of filler

The limitation of Hamilton−Crosser model is that it is limited to predicting the thermal conductivity of particle reinforced nanocomposite and is unable to predict the thermal conductivity of fiber-reinforced composite. The Lewis−Nielsen model takes into account fiber geometry and alignment, and it is given by

"The Lewis−Nielsen model is given by [34,35]:

$$k = k_m\left[\frac{1 + ABV_f}{1 - B\psi V_f}\right]$$

where

$$B = \frac{k_f/k_m - 1}{k_f/k_m + A}$$

$$\psi = 1 + \left(\frac{1 - \varnothing_m}{\varnothing^2}\right)V_f;$$

$$k = k_m\left[\frac{1 + \sum_{i=1} A_i B_i V_{fi}}{1 - \sum_{i=1} B_i \psi_i V_{fi}}\right]$$

Thermal conductivity of a particulate composite based on Rayleigh−Maxwell's model is expressed by [36]:

$$k = \frac{k_m[2k_m + k_p - 2V_p(k_m - k_p)]}{2k_m + k_p + V_p(k_m - k_p)}$$

where

$k$:thermal conductivity,
$V$:volume fraction.

For a nanocomposite with spherical inclusions [37]

$$k = k_m\frac{\left(1 + 2V_d\frac{\left(1 - \frac{k_m}{k_d}\right)}{1 + \frac{2k_m}{k_d}}\right)}{\left(1 - \frac{V_d\left(1 - \frac{k_m}{k_d}\right)}{1 + \frac{2k_m}{k_d}}\right)}$$

where $k_d$ conductivity of dispersion matrix, respectively.

The thermal conductivity of the CNT-based nanocomposites is shown in Ref. [38]

$$k = k_m + \left\langle\cos^2\theta\right\rangle k_f V_f$$

For a well-aligned nanotube $<\cos^2\theta> = 1$, and for completely random nanotube $<\cos^2\theta> = 1/3$.

Hata and Taya [39] predict thermal conductivity of composite with MWNT filler which is described as:

$$k = k_m\left(1 + V_f\frac{\left[\left(k_f - k_m\right)\left(2S_{33} + S_{11}\right) + 3k_m\right]}{J}\right)$$

$$J = 3\frac{\left(1 - V_f\right)\left(k_f - k_m\right)S_{33}S_{11} + k_m\left[3\left(S_{11} + S_{33}\right) - V_f\left(2S_{11} + S_{33}\right)\right]}{k_f - k_m}$$

$$S_{11} = \frac{l/d}{2\left[\left(l/d\right)^2 - l\right]}\left\{\left(l/d\right)\left[\left(\frac{l}{d}\right)^2 - 1\right]^{0.5} - \cosh^{-1}\left(\frac{l}{d}\right)\right\}$$

$$S_{33} = 1 - 2S_{11}$$

where $k$, $k_m$, and $k_f$ are thermal conductivity of composite, matrix, and filler, respectively, in W $mK^{-1}$; $V_f$ is the absolute volume fraction; $l$ is the length of MWNT in meter; and $D$ is the diameter of MWNT in meter."

### 6.4.4 Effective medium theory

The thermal conductivity of composite materials is delineated in effective medium theory (ET). The typicality of ET is its ability to describe microstructural properties interdependence on materials such as heterogeneous [40,41]. The calculation proceeds with an assumption that an effective homogeneous and isotropic medium with property $k_0$ and a deviation in property $k_r$ depends on the presence of the filler. Heterogeneous medium properties at a position $r$ are expressed

$$``k(r) = k_0 + k'(r)$$

The effective result of composite property is given by Green's function and is read as

$$k_e = k_0 + \langle T\rangle\left(I + \langle GT\rangle\right)^{-1},,$$

where "$I$" is the unit tensor and denotes spatial averaging. Matrix $T$ is simplified by eliminating the interaction forces between filler units with respect to lower filler loading:

$$T \cong \sum\nolimits_n T_n = \sum\nolimits_n k_n'(1 - Gk_n')^{-1}$$

Lin et al. [42] presented the Maxwell−Garnett (MG) form, where effective thermal conductivity can be read as

$$``k_{e11} = k_{e12} = k_m \frac{2 + V_f\left[\beta_{11}(1 - L_{11})\left(1 + \left\langle \cos^2\theta \right\rangle\right) + \beta_{33}(1 - L_{33})\left(1 + \left\langle \cos^2\theta \right\rangle\right)\right]}{2 - V_f\left[\beta_{11}L_{11}\left(1 + \left\langle \cos^2\theta \right\rangle\right) + \beta_{33}L_{33}\left(1 - \left\langle \cos^2\theta \right\rangle\right)\right]}$$

$$k_{e33} = k_m \frac{1 + V_f\left[\beta_{11}(1 - L_{11})\left(1 - \left\langle \cos^2\theta \right\rangle\right) + \beta_{33}(1 - L_{33})\left(1 + \left\langle \cos^2\theta \right\rangle\right)\right]}{1 - V_f\left[\beta_{11}L_{11}\left(1 - \left\langle \cos^2\theta \right\rangle\right) + \beta_{33}L_{33}\left\langle \cos^2\theta \right\rangle\right]}$$

$$\beta_{11} = \frac{k_{fii} - k_m}{k_m + L_{ii}(k_{fii} - k_m)}$$

$$L_{11} = L_{22} = \frac{p^2}{2(p^2 - 1)} + \frac{p}{2(1-p^2)^{1.5}}\cos^{-1}p$$

$$L_{33} = 1 - 2L_{11}$$

where $k_{e11}$ $(=k_{e22})$ and $k_{e33}$ are the in-plane and the through-thickness effective thermal conductivities of the nanocomposite samples and $k_{f11}$ $(=k_{f22})$ *and* $k_{f33}$ in-plane and the through-thickness thermal conductivities of the filler unit respectively, and

$\boldsymbol{V_f}$**:** filler loading in volumetric terms

$\boldsymbol{k_m}$**:** isotropic thermal conductivity of the matrix.

$p$ = aspect ratio of the filler (the thickness over the in-plane diameter of a filler unit)."

MG models are the modified effective medium approaches or MG-ET approach (MG-EMA). Conventional EMA validates the rationality of thermal transport behavior in heterogeneous media. The typicality of MG-EMA is its ability to analyze the thermal conductivity of polymer nanocomposites by a very tiny filling ratio. The thermal conductivity of polymer/clay nanocomposites can be studied by the below equation [43]:

$$``k = k_{pol}(1 + f(\frac{2\left(k_c - k_{pol}\right)}{k_c + k_{pol}} + k_c - k_{pol}))$$

where $k$, $k_{pol}$, and $k_c$ are thermal conductivities of the nanocomposite, polymer matrix, and nanoclay, respectively, and $f$ is the volume fraction of nanoclay."

## 6.5 Thermal properties of various polymeric materials and their Nanocomposites

### 6.5.1 *Thermal properties of thermoplastic polymer nanocomposites*

Thermoplastics are the class of polymeric material that can soften or melt when heated, then shaped or formed when cooled. The repeated heating and cooling cycle

can be performed without severe damage, which has the countless advantage of reprocessing thermoplastic polymer. Thermoplastic materials are used in diverse areas, from automotive to aerospace, medical to nautical, and electronic to packaging applications. Thermop4lastic nanocomposite exhibits unique material properties than virgin, such as improved barrier properties, flame retardance, and mechanical properties, depending on the choice of filler. This section details the different work carried out by researchers on various thermoplastic nanocomposites.

Sonawane et al. [44] reported on TGA of polyamide-$CaCO_3$ nanocomposites at different sizes (11, 17, and 23 mm) of $CaCO_3$ and were processed by the in situ deposition process. Nano-$CaCO_3$ was added from 1 to 4 wt.% in the polyamide. It was observed that at 4 wt.% loadings, the decomposition temperature improved by 15% compared to commercially available $CaCO_3$. Cheval et al. [45] followed in situ sol/gel synthesis method to fabricate Polyamide 66/$WO_3$ nanocomposite. The TA of at various wt.% tungsten trioxide, that is, 0, 1, 3, 5, and 10 wt.% was performed and found that adding $WO_3$ filler within the polyamide PA66 matrix decreases the crystallization temperature. Additionally, the degree of crystallinity of PA66 decreases with the increase in wt. % of $WO_3$. Choi et al. [46] investigated polyacrylate composites with two different fillers, such as multiwalled carbon nanotubes (MWCNT) and aluminum flake (Al-flake). It was observed that thermal decomposition temperature increased by 64°C for 70 wt.% of polyacrylate/Al-flake composite than pure. The thermal conductivity of polyacrylate/Al−CNT composites augmented 0.50−1.67 W $mK^{-1}$ when Al−CNT content increased from 50 to 80 wt.%. It was due to the synergistic effect of two powders in the matrix.

Badgayan et al. [33] reported thermal property, and dynamic mechanical thermal analysis (DMTA) of HDPE reinforced with MWCNT/h-BNNP nanofiller. The results confirmed that 0.1 MWCNT exhibited the best damping properties, as shown in Fig. 6.30, whereas for 0.25 MWCNT/0.15 h-BNNP, there is a significant improvement in thermal stability. The same can be manifested due to their tubular and hexagonal morphology of individual nanofillers, which confirms from the TEM image as shown in Fig. 6.30A−C, and their synergistic effect from Fig. 6.30C. Fig. 6.30D−F shows the schematic view of the interaction of the filler system inside the HDPE matrix for better understanding.

Sahu et al. [47] investigated DMTA and thermal conductivity analysis of HDPE filled with 0.1% loading of MWCNT, graphene nanopowder (GNP), and nanodiamond (ND) nanofillers and its influence on contact pressure at temperature sweep from 30°C to 110°C. The result showed that the loss factor followed the trend pure $>$ 0.1 MWCNT $>$ 0.1 GNP $>$ 0.1 ND and highest exhibited by 0.1 GNP/ND as shown in Fig. 6.31A. Highest Tan $\delta$ and lowest contact pressure can be related by inducing 0.1 GNP/ND and is explained from the positive synergy between GNP, HDPE, and ND. Even though NDs are superhard materials, these are not sufficient to support the inherent. Fig. 6.31B shows the thermal conductivity result, elaborating high thermal conductivity for 0.1 ND/GNP by increasing 100% and 40% when compared to 0.1 ND pure composite. The reason for this great increment is the high thermal conductivity of individual filler and positive synergy. Badgayan et al. [48] carried out TMA of high-density polyethylene (HDPE) reinforced with

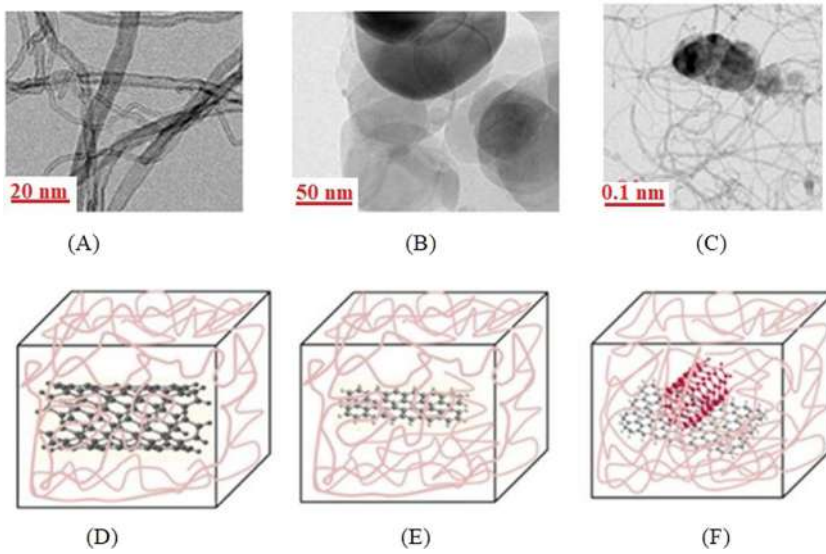


**Figure 6.30** TEM images of (A) 0.25 MWCNT; (B) 0.15 h-BNNP; (C) 0.25 MWCNT/0.15 h-BNNP; Schematic representation of (D) 0.25 MWCNT; (E) 0.15 h-BNNP; (F) 0.25MWCNT/0.15 h-BNNP.

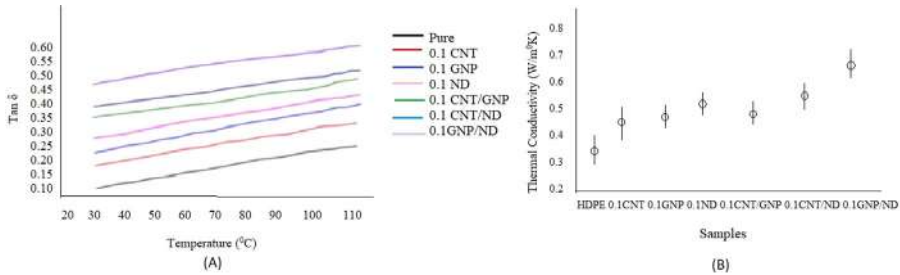


**Figure 6.31** (A) Tan δ versus sample and (B) thermal conductivity of sample.

1DMWCNTs and 2DBNNP nanofillers. The CTE result is shown in Fig. 6.32, which indicates that the pure sample is 138 mm $mK^{-1}$, which reduced to 16.6%, 24.6%, 40%, 52%, and 63% for 0.1 MWCNT/HDPE, 0.1 BNNP/HDPE, HDPE/0.25 MWCNT/0.1 BNNP, HDPE/0.25 MWCNT/0.15 BNNP, respectively. The reduced CTE leads to better dimensional stability for the polymer nanocomposites and their hybrids. Sahu et al. [49] reported thermal conductivity analysis of HDPE reinforced with alternate and possible combination MWCNT, GNP, ND nanocomposite at 0.1 wt.% to form nano and hybrid nanocomposite. The highest thermal conductivity is shown by 0.1 GNP/ND, which increased by 100% and 40% compared to pure and 0.1 ND composite. The actual reasons are the same as discussed

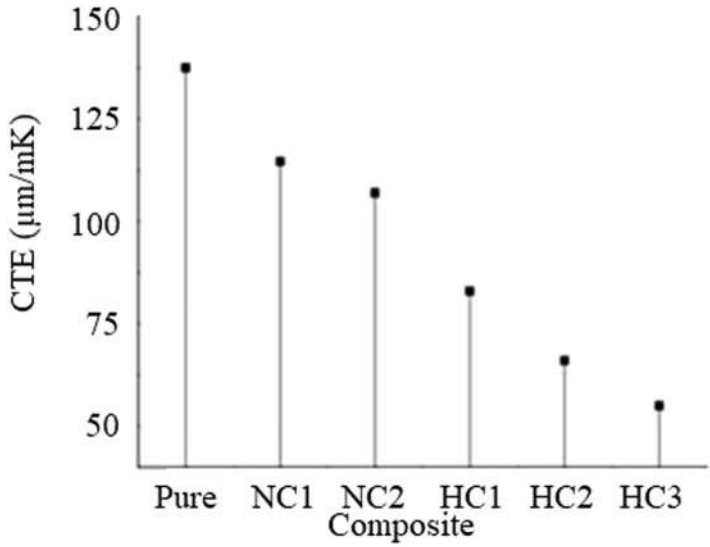


**Figure 6.32** Coefficient of thermal expansion of the sample.

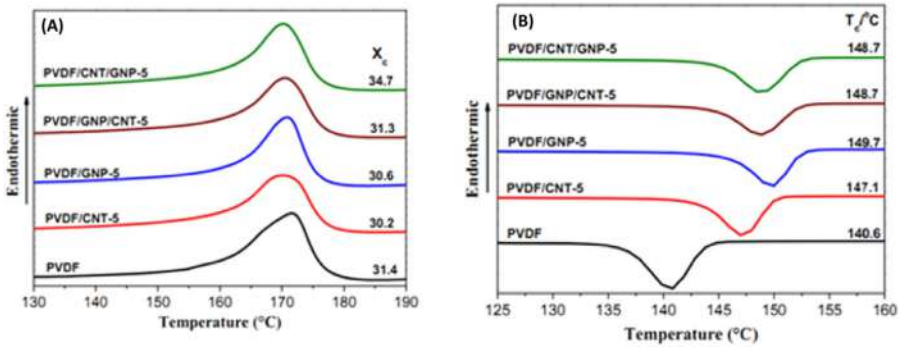


**Figure 6.33** DSC (A) heating and (B) cooling curves showing the melting and crystallization behavior of various samples. *DSC*, Differential scanning calorimetry.

above such as high thermal conductivity in individual layers and positive synergy in both materials. Yu et al. [50] reported on the evaluation of thermal conductivity of polycarbonate matrix reinforced with different weight fractions of MWCNT (0−2 wt.%) at an increment of 0.5 wt.% and GNP (0−20 wt.%) at an increment of 5 wt.%. At 18 wt.% GNP and 2 wt.% MWCNT, thermal conductivity was observed to increase by 479% compared to the thermal conductivity of neat polycarbonate. Xiao et al. [51] stated, by using DSC, that the crystallization temperature of nanocomposites based on poly(vinylidene fluoride) (PVDF) and hybrid composite reinforced with MWCNT and GNP were evaluated. Including pure PVDF, five samples

were prepared, two nanocomposites and two hybrids: PVDF/GNP, PVDF/CNT, PVDF/CNT/GNP, and PVDF/GNP/CNT. The crystallization temperature of PVDF/5 wt.% CNT, PVDF/5 wt.% GNP, PVDF/GNP/5 wt.% CNT, and PVDF/CNT/5 wt.% GNP was improved by 5%, 6%, 6%, and 6%, respectively in comparison to pure PVDF. The possible reason was addressed to the low lamellar thickness of the PVDF matrix in comparison with composites. The crystallization temperature of pure PVDF was noted as 141°C, which further increased for composite samples indicating excellent nucleation effects of GNPs and/or CNTs on the crystallization of the PVDF matrix. It is evident from Fig. 6.33A and B, all the composite samples exhibited a low melting point compared to the pure PVDF matrix.

### 6.5.2 Thermal properties of epoxy and fiber-reinforced nanocomposite

Thermosetting plastic is a polymer that, upon the addition of heat, becomes rigid irreversibly. The initial state of polymer is in a liquid or soft solid state. They begin in a malleable or liquid form, and after being cured, the material becomes hard and remains in that form. This means that once the material is cured, it cannot be reheated, reshaped, or recycled. The curing behavior also means that this material holds up well under elevated temperatures, expanding its range of applications. Thermosets are highly cross-linked, which gives them good mechanical properties, such as a high modulus and strength and good resistance to creep, but they have poor ductility due to their rigid behavior [52].

Polymers possess low thermal stability, high electrical resistivity, and low thermal conductivity [53]. Many thermoset polymers have been known for their excellent thermal performance, making them prime candidates for the primary base to develop further advancements with nanocomposites. Among many thermoset polymers, epoxy is known for its excellent chemical and corrosion resistance, good adhesive properties, low shrinkage, and low price [54]. As mentioned earlier, curing gives them a highly cross-linked microstructure, which results in a high modulus and strength, good resistance to creep, good performance at elevated temperature, but poor ductility [55]. Addressing different shortcomings, there were several attempts made to reinforce neat polymer with different nanofillers. Following are some important investigations carried out by different researchers in the area mentioned.

Chinnasamy et al. [56] reported thermal properties 2 wt.% of Cloisite 30B/hardener-modified epoxy hybrid composites reinforced with glass Kevlar/fiber at 35:65, 40:60, 45:55, and 50:50, respectively. It was observed that the hybridization of based composites with modified Kevlar/glass fiber improves the thermal properties and increases the glass transition temperature without affecting the thermal stability. Jani et al. [57] investigated properties of 7.5/10 wt.% NaOH treated Agave Americana/carbon fiber hybrid-reinforced epoxy composites. It was observed that 10 wt.% NaOH-treated fiber composites have superior thermal stability and thermal conductivity value due to the higher cellulose exposure, resulting in higher hydrogen bond density in the fibre-reinforced plastic system. Filho et al. [58] carried out

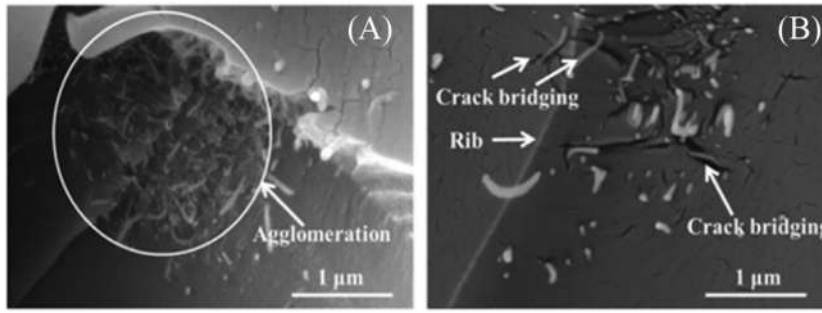


**Figure 6.34** Dispersion of (A) CNT and (B) FCNT in epoxy taken form SEM. *CNT*, Carbon nanotube; *FCNT*, functionalized CNT.

thermal properties of the piassava fiber-reinforced epoxy composite functionalized with graphene oxide (GO). Thermal properties were reported to improve owing to GO functionalization of the piassava fiber epoxy composite. Hiremath et al. [59] investigated the thermal performance of pure epoxy, discontinuous glass fiber/epoxy which is randomly oriented (RODGE) composite, CNT-reinforced RODGE (CNT-RODGE) composite, and functionalized CNT-reinforced RODGE (FCNT-RODGE) composite.

Fig. 6.34A shows the SEM image of CNT and FCNT. It was evident from Fig. 6.34A that the CNTs which were not functionalized tended to agglomerate, whereas functionalized CNTs were uniformly dispersed, as shown in Fig. 6.34B. In addition, the DSC curves revealed a drop in the $T_g$ value of 1.81%, 12.91%, and 6.13% for RODGE, CNT-RODGE, and FCNT- RODGE composites, respectively. The reason for this was attributed to functionalization and a decrease in the movement of the polymeric chain.

Gheith et al. [60] investigated thermal properties of date palm fibers-reinforced epoxy composites by dynamic mechanical and thermos-gravimetric analyzer at different loading of date palm fibers (DPF) (40%, 50%, and 60% by wt.). Fig. 6.35A and B depicts the TGA and DTG curve, and the analysis exposed that at 50% DPF loading, there was an improvement in the thermal stability. This was due to better compatibility and adhesion in which polymer acts as a barrier to prevent the degradation of fibers.

### 6.5.3 Recycled polymer nanocomposites

The extent of plastics consumed worldwide has been increasing drastically due to their exceptional attributes such as flexibility, easy fabrication and processing facilities, cost-effectiveness, and immense durability. Further reports warn that the number of waste plastics in oceans will be greater than fish in just 30 years unless radical action is taken. Recycling has been carried out on scraps and postconsumer plastics for several years because they can be easily gathered and reprocessed. In recent times, the recycling industry has been concentrating on the blend of plastics,

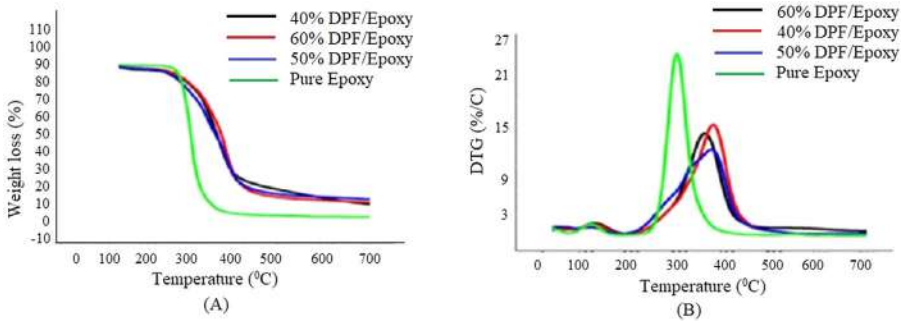


**Figure 6.35** (A) TGA (B) DTG curve of DPF/epoxy composites. *DTG*, Derivative thermogravimetric; *DPF*, date palm fibers; *TGA*, thermogravimetric analysis

and it is a challenge to many recyclers. New technologies related to the processing of heterogeneous plastics are growing at a fast pace. Solid waste plastics can be recycled in different stages, and there is a broad classification as follows [6].

Primary recycling is also referred to as re-extrusion. This type commonly applies to processing defective parts from injection molding or out-of-specification products by grinding and reintroducing them into the recycling loop. In this recycling technique, plastics with uniform composition and uncontaminated plastics are segregated and processed. Problems that occur in primary recycling are loss of properties, strength, and chemical resistance. Secondary recycling: often known as mechanical recycling, as there is no chemical alteration during the process. Waste plastics are made into pellets or flakes, or powders and reused in the fabrication of products. Examples of this type of plastics are polyethylene, polypropylene, polystyrene, polyurethane, PET, etc. Mechanical recycling is mostly used process in many applications as it is more easy and practical. Tertiary recycling is also called as chemical recycling, where the polymers are chemically cracked down to recover other by-products from the plastic waste. This process involves much time, and it is used mostly in the petrochemical industry. Examples of this tertiary recycling are pyrolysis, catalytic cracking, and gasification. Quaternary recycling: this is also termed energy recovery recycling; it refers to the recovery of energy from waste plastics by burning to produce energy. This process works for the waste plastic materials which fail in the recovery process.

Recycling plastics provides not only benefits the environment by reducing landfills but also improves the economy. Recycling helps keep waste plastics out of the earth and is one of the energy-efficient methods adopted to produce new materials instead of using renewable sources. Reprocessing/recycling of polymers may lead to thermal oxidation in the cross-links or chains, resulting in lesser properties than that of the pure polymers. To avoid degradation of the thermophysical properties, stabilizers that will improve the workability of the polymers are added to the recycled polymers. Furthermore, incorporating fillers, modifier agents, plasticizers, etc. further enhances the properties of recycled plastic and aids the performance of the polymers. Various fillers can be used with the plastics depending on the

application such as glass fillers, mineral, wood fillers, CNTs, graphene sheets/flakes/powder, etc. In this chapter, various thermal properties of recycled plastics and their nanocomposites are discussed.

### 6.5.4 Thermal properties of polymer blend nanocomposite

Polymer blends are mixtures of chemically different polymers and/or copolymers. They are primarily a mixture with the multiphase structure, which is obtained directly by the blending action. The major advantages of using polymer blends are (1) improved performance at an abridged price, (2) extension of the performance of specialty resins, (3) recycling of plastic, and (4) generation of high-class materials about process-ability and/or performance. Furthermore, compared with pure polymer, polymer blend nanocomposites can be attained with better thermal properties, stability, optical and electrical conductivity subject to the type of polymers and nanofillers. Followings are some important investigations carried out by different researchers in the area mentioned.

Paes et al. [61] reported on thermal properties of polymer blend nanocomposite with amorphous polyamide (aPA)styrene−ethylene−butylenestyrene (80/20 wt.%) matrix reinforced with CNT and MMT at 0.25 and 1 wt.%, respectively. It was observed that with both nanoparticle additions, there was no significant increase in thermal stability. However, a slight rise and fall of storage modulus were seen with MMT and CNT, respectively. Zare et al. [62] investigated thermal properties of poly (lactic acid) (PLA)/poly (ethylene oxide) (PEO) blends, that is, PLA/PEO reinforced with CNTs. The concentrations of PLA in the blends and nanocomposites were 60, 75, and 90 wt.% and CNTs contents of 1 and 2 wt.%. The test result revealed that the thermal decomposition of PEO was accelerated with CNTs due to enhanced heat transfer to the dispersed phase in nanocomposites.

Huang C et al. [63] reported thermal conductivity analysis of PVA/lignin and PVA/gelatin blend. The test result showed the thermal conductivity was 0.53 and 0.57 $W\ m^{-1}\ K^{-1}$ at 2 wt.% lignin loading and 5 wt.% gelatin loading, respectively. The reason for improvisation in thermal conductivity was attributed to the H-bond that induced enlargement of chain coils and the continuous microstructures in polymers. This greater thermal conductivity in H-bond networks is formed by three polymer blends (PVA, lignin, and gelatin) to supply more heat transfer pathways. This mechanism is illustrated in Fig. 6.36 [63].

Hussain et al. [64] reported thermal properties of polymer blends (thermoplastic polyether ester elastomer and polybutylene terephthalate). It was observed that the thermal properties were enhanced significantly by adding a small amount of nanoclay (NC), which was reasoned to the homogeneous dispersion. Bagotia et al. [65] carried out dynamic mechanical thermal properties of polycarbonate/ethylene methyl acrylate blend nanocomposite reinforced with MWCNT. The loss factor result is shown in Fig. 6.37A and B, which depicts that the tan $\delta$ max value of the PCE5 blend was higher than PC/EMA-MWCNT nanocomposites.

The reason for this was due to the immobilization effect of MWCNT on PCE chains leading to a significant decay in tan $\delta$ max value.

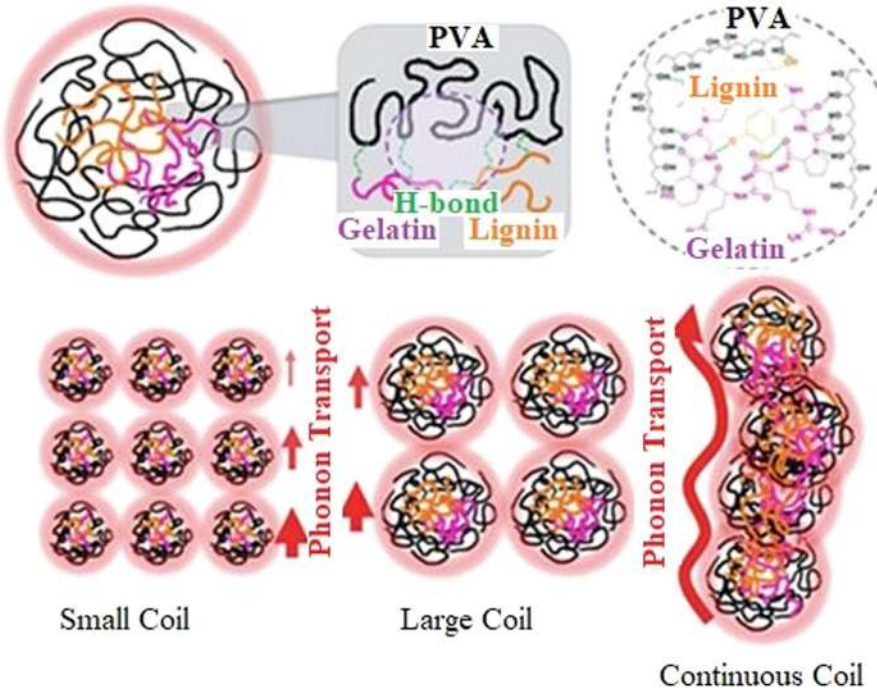


**Figure 6.36** H-bonds in polymer blends and phonon transport for small, large, and continuous coil structures.

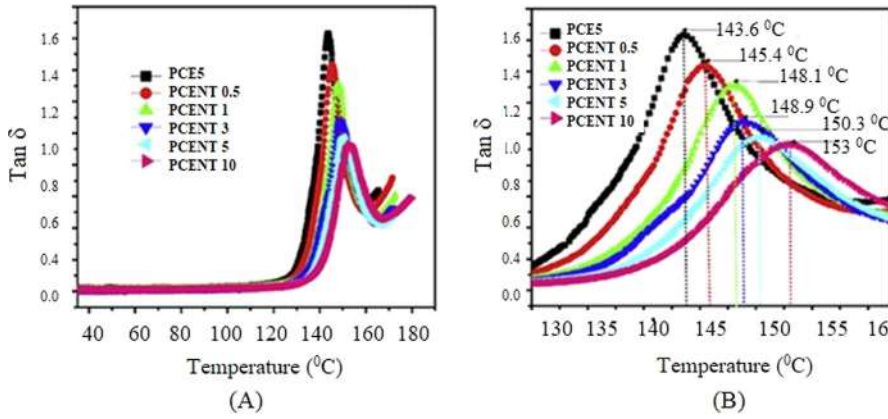


**Figure 6.37** (A) Tan $\delta$ versus temperature and (B) Tan $\delta$ in the temperature range of 130°C and 162°C.

### 6.5.5 Thermal properties of shape memory polymer nanocomposite

Shape memory materials (SMMs) are unique materials that can recover from a significant plastic deformation when a particular stimulus is applied [66]. Among the different SMMs, SMPs are increasingly attracting researchers' interest from academia and industry due to their specific advantages such as low mass density, low production cost, ease in processing, and noncorrosive features [67]. However, pure SMPs have drawbacks like low strength and stiffness and poor thermal stability, hindering the usage of structural and functional application materials [68]. Consequently, a few reinforcing strategies are required to improve the mechanical and thermal residences of shape memory epoxy polymer (SMEP) without changing the shape recovery effect of pure SMPs. Following are some important investigations carried out by different researchers in the area mentioned.

Hassanzadeh-Aghdam et al. [69] reported thermomechanical properties of SMEP reinforced with CNT nanofiller. A micromechanical model using a simplified unit cell model was adopted for the investigation. It was observed that CTEs decreased with the increase in CNT volume, and there was good agreement between the micromechanical model and experimental data. Cho et al. [70] investigated thermomechanical properties of polyurethane tetraethoxysilane (TEOS) SMPs hybrid at 5, 10, 20, and 30 wt.% of TEOS. The result showed a good shape retention ability of more than 80% for all the samples.

Gunes et al. [71] reported the influence of the CTE on the performance of shape memory polyurethane reinforced with organoclay, carbon nanofiber (CNF), silicon carbide (SiC), and carbon black (CB). The results indicated that organoclay and CNF are more effective in moderating CTE than SiC and CB. Liu et al. [72] investigated thermomechanical properties of SMPs reinforced with 0 and 20 wt.% of SiC.

It was observed that the glass transition temperature of pure SMP is 88°C, which increased to 98°C when 20 wt.% SiC nanoparticles are added. The reason for this was exonerated as possible chemical changes in the polymer near the polymer/particle interface. Barwood et al. [73] carried out the addition of organoclay on thermal properties of t-butylacrylate-*co*-poly(ethyleneglycol) dimethacrylateSMP reinforced with 1−5 mass% of benzyl tallow dimethylammonium-exchanged bentonite. It was observed that the addition of unit mass % in SMPs, accelerates the recovery rate of SMP nanocomposite than pure SMP.

### 6.5.6 Thermal properties of biopolymer nanocomposite

Biocomposite is a type of composite material formed by a biocompatible matrix/resin reinforced with biocompatible fillers. These kinds of materials often mimic the structure of living materials involved in keeping the strengthening properties of the matrix that was used by providing biocompatible properties. Among different biocomposites, polymer-based biocomposites are the keen interest due to inherent properties such as lightweight, good mechanical strength and stiffness, noncorrosive, stretch-ability, etc. The biopolymers used as matrices are primarily derived from renewable and

nonrenewable resources. The polymer matrix plays an important role in protecting the composite from environmental degradation and mechanical damage to hold the reinforcement together and transfer its load. Biopolymer nanocomposites are fabricated with biopolymers and bio-nanofillers that have improved mechanical and thermal properties. The interest in biopolymer nanocomposites is rapidly growing in medical industries such as prosthetics, dental implants, bone replacements, total heap replacement, heart stents, biocompatible screws, pins, etc. Following are some important investigations carried out by different researchers in the closed area of biopolymer nanocomposite thermal properties. Hareesh et al. [74] reported on the thermal properties of PLA/clay nanocomposite using TGA and DSC. The TGA results indicated that the pure PLA starts degrading at 180°C, and with clay nanofiller addition, it shifts to 465°C, which shows improvisation in the thermal stability of the nanocomposite. The DSC results showed an improvement in glass transition temperature with the addition of clay content. Al et al. [75] investigated thermal properties of polyhydroxybutyrate and PLA biopolymer nanocomposite reinforced with NC and cellulose nanofibrils, and the nanofiller content varied from 0.5−4 wt.% using TGA and DSC. It was observed that the addition of nanofiller improvised the thermal properties of biopolymer nanocomposite. Marras et al. [76] evaluated the role of NC reinforcement on the thermomechanical properties of poly(e-caprolactone) nanocomposite with the addition of 1−15 wt.% organoclay content. TGA curve depicted that the onset temperature of 1 wt.% of clay content increased the onset temperature from 330°C to 355°C, which showed improvisation in the thermal stability due to the presence of $N_2$ in the polymer/clay nanocomposite.

Badgayan et al. [33] reported DMTA of HDPE reinforced with MWCNT and hBNNP nanocomposite at various weight %. Tan delta results indicate that 0.1 MWCNT nanocomposites show the best damping properties at higher temperatures. This was justified due to the tubular morphology of CNT, and at a higher temperature, the polymer chain becomes more mobile and dissipates energy. Among all the composites, 0.25 MWCNT/0.1 BNNP showed superior results for crystallinity and thermal stability.

Sreekanth et al. [77] evaluated the influence of MWCNT and gamma irradiation on the thermal properties of UHMWPE. It was observed that the addition of MWCNT and performing gamma irradiation improvised the thermal stability and crystallinity of UHMWPE bionanocomposite. Narimissa et al. [78] carried out a thermal property investigation of polylactide (PLA)/nanographite platelets (NGP) with a variation of NGP content from 1 to 10 wt.%. The results depict that the highest degree of crystallinity and enthalpy of fusion is seen for 5 wt.% NGP nanocomposite. Heidarbeigi et al. [79] investigated thermal properties of biopolymer nanocomposite fabricated with low-density polyethylene matrix reinforced with cellulose nanocrystal (CNC). The DSC test was performed with reinforcement 0−5 wt.%. It was observed that at 5 wt. % PE/CNC biocomposite, the crystallinity value is superior due to the preferred orientation of the CNC.

Salehan et al. [80] worked on nanocomposite solid biopolymer electrolyte with different concentrations of aluminum oxide (nanosize) and studied the effects of aluminum oxide on electrolyte characteristics. DSC thermograms demonstrated the lowest $T_g$ and $T_m$ for the ideal conducting film which is due to ion migration.

Conventional food packages are hazardous to both environment and health due to toxic gases and infiltrating food webs [81]. Andini et al. [82] worked on biodegradable polymers in the application of food packaging to minimize the problems related to plastic sustainability and environmental problems. A biopolymer nanocomposite is developed with the help of two different types of biopolymer matrix, namely bioceta and materbi and nanoclay as reinforcement material with two different concentrations and observed improved thermal performance and gas barrier enhancement.

## 6.6 Summary

The overview of the recent technology in augmenting the thermal properties of thermoplastic polymer nanocomposites, epoxy and fiber-reinforced nanocomposites, recycled polymer nanocomposites, blend polymer nanocomposites, SMP nanocomposites, and biopolymer nanocomposites was analyzed in detail. The results suggested that the improvisation in the thermal properties of polymers can be enhanced through the addition of different nanofillers. The selection of nanoadditives may be based on size, aspect ratio, dimension, and geometry. Among the nanofillers, MWCNT and organoclay were the prime choices by different researchers due to their uniform dispersion, high thermal stability, and consistent performance. Thermal conductivity is an important parameter that interprets the thermal performance of polymer nanocomposites. Many theoretical models are available to predict the thermal conductivity of nanocomposites. The simplest of these are mixture rules such as series, parallel, and geometric models. However, it has the limitation that it neglects the true geometry and correct size of the filler particles. To overcome this, various models such as the Hamilton−Crosser model, Lewis−Neilsen, Rayleigh−Maxwell, and Hatta−Taya models are useful. However, all these models have their advantages and limitations. The limitations are overcome in some other improvised models like the modification of Hamilton and Crosser's model proposed by Badgayan et al. [33], and modified effective medium approaches proposed by Nejad et al. [43] are very much expedient. It was also observed that the performance of polymer is highly reliant on the functionalization of nanoparticles through surface treatment of nanoparticles along with specific processing techniques. Polymer nanocomposite with superior thermal performance is a promising material that led to significant advancements in recent years and remains in high demand in the relevant industry.

## References

[1] S.K. Sahu, P.S. Rama Sreekanth, Mechanical, thermal and rheological properties of thermoplastic polymer nanocomposite reinforced with nanodiamond, carbon nanotube and graphite nanoplatelets, Advances in Materials and Processing Technologie (2022). Available from: https://doi.org/10.1080/2374068X.2022.2034309 (Accepted 23 Jan 2022).

[2] S.K. Satya, P.S. Rama Sreekanth, Morphological, thermal and viscoelastic behavior of recycled high density polyethylene nanocomposite incorporated with 1D/2D nanofllers, Polymer Journal (2021). Available from: https://doi.org/10.1007/s13726-022-01023-1 (Accepted: 27 November 2021).

[3] C.S. Yesaswi, P.R. Sreekanth, Characterisation of Silver coated Tefon fabric reinforced Nafon ionic polymer metal composite with carbon nanotubes and graphene nanoparticles, Iranian Polymer Journal (2021). Available from: https://doi.org/10.1007/s13726-021-01015-7 (Accepted: 30 October 2021).
[4] K. Zhou, Z. Gui, Y. Hu, S. Jiang, G. Tang, The influence of cobalt oxide−graphene hybrids on thermal degradation, fire hazards and mechanical properties of thermoplastic polyurethane composites, Compos. Part. A Appl. Sci. Manuf. 88 (2016) 10−18.
[5] K. Krol-Morkisz, K. Pielichowska, Thermal decomposition of polymer nanocomposites with functionalized nanoparticles, Polym. Compos. Functionalized Nanopart. (2019) 405−435. Elsevier.
[6] M. Chanda, Plastics Technology Handbook, Plastics Engineering, CRC Press, 2017.
[7] A. Shrivastava, Introduction to Plastics Engineering, William Andrew Publishing, 2018.
[8] T.A. Osswald, G. Menges, Thermal Properties of Polymers, Material Science of Polymers for Engineers, Third Edition, Hanser, 2012.
[9] Yuli, K. Godovsky, Thermophysical Properties of Polymers, 1992. Springer-Verlag Berlin Heidelberg.
[10] E.V. Thompson, Thermal Properties, In Encyclopaedia of Polymer Science and Technology, Wiley, 2010.
[11] K.K. Morkisz, K. Pielichowska, 13 - Thermal Decomposition of Polymer Nanocomposites with Functionalized Nanoparticles, Elsevier, 2019, pp. 405−435.
[12] I. Meisel, T.Thermal Anal. 29 (1984) 1379.
[13] J D Menczel, R E Prime, "Thermal analysis of polymers-fundamentals and applications," Copyright © 2009 by John Wiley & Sons.
[14] M.S.H. Akash, K. Rehman, Differential scanning calorimetry, Essentials of Pharmaceutical Analysis, Springer, Singapore, 2020. https://doi.org/10.1007/978-981-15-1547-7_17.
[15] J. Riley, M. Marsh, Macro thermogravimetric analyzers: versatile and underutilized analytical instruments, J. Test. Eval. 49 (2021). Available from: https://doi.org/10.1520/JTE20200706. Published ahead of print, 05 April.
[16] D.M. Joseph, J. Michael, "5 - Thermomechanical analysis of fibers," Therm. Anal. Text. Fibers Text. Inst. Book. Ser. 2020, Pages 81−94
[17] Thermal Analysis of Polimers. Part 2: TGA, TMA and DMA of thermopastics, UserCom 32 (2010).
[18] Dilatometry. 2016; Available from: http://thermalanalysislabs.com/dilatometry/.
[19] Sun, W., Guen, E., Hamaoui, G., El Sachat, A., Alzina, F., Sotomayor-Torres, C. M., et al., Thermal and thermomechanical investigation of polymeric thin films on substrate, in: 2020 26th Int. Workshop Therm. Investigations ICs Systems(THERMINIC), 2020, pp. 226−231, https://doi.org/10.1109/THERMINIC49743.2020.9420489.
[20] A. Galukhin, R. Nosov, I. Nikolaev, E. Melnikova, D. Islamov, S. Vyazovkin, Synthesis and polymerization kinetics of rigid tricyanate ester, Polymers 13 (2021) 1686. Available from: https://doi.org/10.3390/polym13111686.
[21] J. Schalnat, D.G. Gómez, L. Daelemans, I.D. Baere, K.D. Clerck, W.V. Paepegem, Influencing parameters on measurement accuracy in dynamic mechanical analysis of thermoplastic polymers and their composites, Polmer Test. 91 (2020) 106799. November.
[22] N. McCrum, G. Williams, B. Read, Anelastic and Dielectric Eff. Polymeric Solids, Dover, New York, 1967. 39. R.F. Boyer, Polym. Eng. Sci, 8(3), 161 (1968).
[23] J.D. Vrentas, J.L. Duda, J.W. Huang, Macromolecules 19 (1986) 1718.
[24] W. Brostow, M.A. Macip, Macromolecules 22 (6) (1989) 2761.

[25] C.S. Yesaswi, P.R. Sreekanth, Evaluation of dynamic mechanical properties of teflon fabric reinforced artificial muscle material, Mater. Today: Proc. 27 (2020) Pages 936–939. Available from: https://doi.org/10.1016/j.matpr.2020.01.262. Part 2.
[26] P.K. Gallagher, in: E.A. Turi (Ed.), Thermal Characterisation of Polymeric Materials, end edition, Academic Press, NewYork, 1997. Ch.1.
[27] D. Nagy, C. Falussy, J. Posta, A new method to follow the thermal processes with spectrometric methods, J. Therm. Anal. Calorim., DOI: 10.1007/s10973-013-3254-5
[28] J. Mullens, Handbook of Thermal Analysis and Calorimetry, in: M.E. Brown (Ed.), Vol.1, Elsevier, Amsterdam, 1998. Ch.12.
[29] E. Kaiserberger (Ed.), Coupling thermal analysis and gas analysis methods, Special issue of Thermochim, Acta 295 (1997) 1–186.
[30] S.B. Warrington, in: E.L. Charsley, S.B. Warrington (Eds.), Thermal Analysis; Techniques and Applications, Royal Society of Chemistry, Cambridge, 1992, p. 84.
[31] S. Agarwal, M. Masud, K. Khan, R.K. Gupta, Polym. Eng. Sci. (2008) 2474.
[32] R.L. Hamilton, O.K. Crosser, Thermal conductivity of heterogeneous two-component systems, Ind. Eng. Chem. Fundam. 1 (1962) 187.
[33] N.D. Badgayan, S.K. Sahu, S. Samanta, P.R. Sreekanth, Evaluation of dynamic mechanical and thermal behavior of HDPE reinforced with MWCNT/h-BNNP: an attempt to find possible substitute for a metallic knee in transfemoral prosthesis, Int. J. Thermophys. 40 (10) (2019) 93.
[34] L.E. Nielsen, The thermal and electrical conductivity of two-phase systems, Ind. Eng. Chem. Fundam. 13 (1974) 17.
[35] R. Pal, On the Lewis–Nielsen model for thermal/electrical conductivity of composites, Compos. Part. A 39 (2008) 718–726.
[36] S. Maensiri, S.G. Roberts, J. Eur. Ceram. Soc. 22 (2002) 2945.
[37] T. Hirano, K. Niihara, Mater. Lett. 26 (1996) 285.
[38] C.W. Nan, Z. Shi, Y. Lin, Chem. Phys. Lett. 375 (2003) 666.
[39] H. Hata, M. Taya, Effective thermal conductivity of a misoriented short fiber composite, J. Appl. Phys. 58 (1985) 2478.
[40] M.B. Bryning, D.E. Milkie, M.F. Islam, J.M. Kikkawa, A.G. Yodh, Appl. Phys. Lett. 87 (2005) 161909.
[41] A. Balakrishnan, M.C. Saha, Mater. Sci. Eng. A 528 (2011) 906.
[42] W. Lin, R. Zhang, C.P. Wong, J. Electron. Mater. 39 (2010) 268.
[43] S.J.J. Nejad, A review on modeling of the thermal conductivity of polymeric nanocomposites, e-Polymers 12 (1) (2012).
[44] S.S. Sonawane, S. Mishra, N.G. Shimpi, Effect of nano-CaCO3 on mechanical and thermal properties of polyamide nanocomposites, Polym. Technol. Eng. 49 (1) (2009) 38–44.
[45] N. Cheval, F. Xu, N. Gindy, R. Brooks, Y. Zhu, A. Fahmi, Morphology, crystallinity, and thermal properties of polyamide 66/polyoxometalate nanocomposites synthesized via an in situ sol/gel process, Macromol. Chem. Phys. 212 (2) (2011) 180–190.
[46] S.W. Choi, K.H. Yoon, S.S. Jeong, Morphology and thermal conductivity of polyacrylate composites containing aluminum/multi-walled carbon nanotubes, Compos. Part. A: Appl. Sci. Manuf. 45 (2013) 1–5.
[47] S.K. Sahu, N.D. Badgayan, S. Samanta, P.S.R. Sreekanth, Dynamic mechanical thermal analysis of high density polyethylene reinforced with nanodiamond, carbon nanotube and graphite nanoplatelet, Mater. Sci. Forum 917 (2018) 27–31.
[48] N.D. Badgayan, S. Samanta, S.K. Sahu, S.V. Siva, K.K. Sadasivuni, D. Sahu, et al., Tribological behaviour of 1D and 2D nanofiller based high densitypoly-ethylene hybrid nanocomposites: a run-in and steady state phase analysis, Wear 376 (2017) 1379–1390.

[49] S.K. Sahu, N.D. Badgayan, P.R. Sreekanth, Understanding the influence of contact pressure on the wear performance of HDPE/multi-dimensional carbon filler based hybrid polymer nanocomposites, Wear (2019) 438.
[50] J. Yu, H.K. Choi, H.S. Kim, S.Y. Kim, Synergistic effect of hybrid graphene nanoplatelet and multi-walled carbon nanotube fillers on the thermal conductivity of polymer composites and theoretical modeling of the synergistic effect, Compos. Part. A Appl. Sci. Manuf. 88 (2016) 79−85.
[51] Y.J. Xiao, W. Wang, X. Chen, T. Lin, Y. Zhang, Y. Yang, et al., Hybrid network structure and thermal conductive properties in poly(vinylidene fluoride) composites based on carbon nanotubes and graphene nanoplatelets, Composites: Part. A 90 (2016) 614−625.
[52] A. Crosky, N. Soatthiyanon, D. Ruys, S. Meatherall, S. Potter, Thermoset matrix natural fibre-reinforced composites, Nat. Fibre Compos. (2014) 233−270. Woodhead Publishing.
[53] S.C. Tjong, Thermal properties of polymer nanocomposites, Polymer Composites with Carbonaceous Nanofillers, Wiley-VCH Verlag GmbH & Co. KGaA, Weinheim, 2012, pp. 103−141.
[54] S. Chatterjee, J.W. Wang, W.S. Kuo, N.H. Tai, C. Salzmann, W.L. Li, et al., Mechanical reinforcement and thermal conductivity in expanded graphene nanoplatelets reinforced epoxy composites, Chem. Phys. Lett. 531 (2012) 6−10.
[55] B. Debelak, K. Lafdi, Use of exfoliated graphite filler to enhance polymer physical properties, Carbon 45 (9) (2007) 1727−1734.
[56] V. Chinnasamy, S.P. Subramani, S.K. Palaniappan, B. Mylsamy, K. Aruchamy, Characterization on thermal properties of glass fiber and kevlar fiber with modified epoxy hybrid composites, J. Mater. Res. Technol. (2020).
[57] S.P. Jani, S. Sajith, C. Rajaganapathy, M.A. Khan, Mechanical and thermal insulation properties of surface-modified Agave Americana/carbon fibre hybrid reinforced epoxy composites, Mater. Today Proc. (2020).
[58] F. da Costa Garcia Filho, F.S. da Luz, M.S. Oliveira, A.C. Pereira, U.O. Costa, S.N. Monteiro, Thermal behavior of graphene oxide-coated piassava fiber and their epoxy composites, J. Mater. Res. Technol. (2020).
[59] M.M. Hiremath, R.K. Prusty, B.C., Ray, Mechanical and thermal performance of recycled glass fiber reinforced epoxy composites embedded with carbon nanotubes, Mater. Today Proc. (2020).
[60] M.H. Gheith, M.A. Aziz, W. Ghori, N. Saba, M. Asim, M. Jawaid, et al., Flexural, thermal and dynamic mechanical properties of date palm fibres reinforced epoxy composites, J. Mater. Res. Technol. 8 (1) (2019) 853−860.
[61] L.H.G. Paes, T.T. Steffen, D. Becker, Comparative performance of carbon nanotube and nanoclay on thermal properties and flammability behavior of amorphous polyamide/SEBS blend, Polym. Eng. Sci. (2020).
[62] Y. Zare, K.Y. Rhee, Following the morphological and thermal properties of PLA/PEO blends containing carbon nanotubes (CNTs) during hydrolytic degradation, Compos. Part. B Eng. 175 (2019) 107132.
[63] C. Huang, X. Qian, R. Yang, Thermal conductivity of polymers and polymer nanocomposites, Materials Science and Engineering: R: Reports 132 (2018) 1−22.
[64] M. Hussain, Y.H. Ko, Y.H. Choa, Significant enhancement of mechanical and thermal properties of thermoplastic polyester elastomer by polymer blending and nanoinclusion, J. Nanomater. (2016) 2016.
[65] N. Bagotia, D.K. Sharma, Systematic study of dynamic mechanical and thermal properties of multiwalled carbon nanotube reinforced polycarbonate/ethylene methyl acrylate nanocomposites, Polym. Test. 73 (2019) 425−432.

[66] W.M. Huang, Z. Ding, C.C. Wang, J. Wei, Y. Zhao, H. Purnawali, Shape memory materials, Mater. Today 13 (7–8) (2010) 54–61.
[67] Florence Pilate, Toncheva Antoniya, Dubois Philippe, Raquez Jean-Marie, Shape-memory polymers for multiple applications in the materials world, Eur. Polym. J. 80 (2016) 268–294.
[68] Qinghao Meng, Hu Jinlian, A review of shape memory polymer composites and blends, Compos. Part. A Appl. Sci. Manuf. 40 (11) (2009) 1661–1672.
[69] Mohammad Hassanzadeh-Aghdam, Reza Kazem, Ansari, Mohammad Javad Mahmoodi, Thermo-mechanical properties of shape memory polymer nanocomposites reinforced by carbon nanotubes, Mech. Mater. 129 (2019) 80–98.
[70] Jae Whan Cho, Sun Hwa Lee, Influence of silica on shape memory effect and mechanical properties of polyurethane–silica hybrids, Eur. Polym. J. 40 (7) (2004) 1343–1348.
[71] I. Gunes, Feina Sedat, Cao, Sadhan C. Jana, Effect of thermal expansion on shape memory behavior of polyurethane and its nanocomposites, J. Polym. Sci. Part. B: Polym. Phys. 46 (14) (2008) 1437–1449.
[72] Y. Liu, K. Gall, M.L. Dunn, P. McCluskey, Thermomechanics of shape memory polymer nanocomposites, Mech. Mater. 36 (10) (2004) 929–940.
[73] Michael J. Barwood, Chris Breen, Francis Clegg, Carol L. Hammond, The effect of organoclay addition on the properties of an acrylate based, thermally activated shape memory polymer, Appl. clay Sci. 102 (2014) 41–50.
[74] A. Hareesh, M.S. Muruli, A. Ramesha, Characterization of mechanical and thermal properties of biopolymer nanocomposites, Int. J. Eng. Res. Technol. 7 (2018) 89–96.
[75] G. Al, D. Aydemir, B. Kaygin, N. Ayrilmis, G. Gunduz, Preparation and characterization of biopolymer nanocomposites from cellulose nanofibrils and nanoclays, J. Composite Mater. 52 (5) (2018) 689–700.
[76] S.I. Marras, K.P. Kladi, I. Tsivintzelis, I. Zuburtikudis, C. Panayiotou, Biodegradable polymer nanocomposites: the role of nanoclays on the thermomechanical characteristics and the electrospun fibrous structure, Acta Biomater. 4 (3) (2008) 756–765.
[77] P.S.R. Sreekanth, S. Kanagaraj, Influence of MWCNTs and gamma irradiation on thermal characteristics of medical grade UHMWPE, Bull. Mater. Sci. 37 (2) (2014) 347–356.
[78] E. Narimissa, R.K. Gupta, H.J. Choi, N. Kao, M. Jollands, Morphological, mechanical, and thermal characterization of biopolymer composites based on polylactide and nanographite platelets, Polym. Compos. 33 (9) (2012) 1505–1515.
[79] J. Heidarbeigi, A.M. Borghei, H. Afshari, The mechanical and thermal properties of PE/CNC nanocomposite, Int. J. Nano Dimens. 10 (2) (2019) 209–216.
[80] S.S. Salehan, B.N. Nadirah, M.S.M. Saheed, et al., Conductivity, structural and thermal properties of corn starch-lithium iodide nanocomposite polymer electrolyte incorporated with $Al_2O_3$, J. Polym. Res. 28 (2021) 222. Available from: https://doi.org/10.1007/s10965-021-02586-y.
[81] R. Thiruchelvi, A. Das, E. Sikdar, Mater. Today Proc. 6 (2020).
[82] R. Andini, M.I. Sulaiman, Martunis, A.H. Umam, M. Olivia, H.J. Endres, Biopolymer nanocomposites: their mechanical, thermal, and gas barrier properties for food packaging, IOP Conf. Series Earth Environ. Sci. 667 (2021) 012067. Available from: https://doi.org/10.1088/1755-1315/667/1/012067.

# Life-cycle assessment of polymer nanocomposites

7

*Ayeman Mazdi Nahin*[1], *Asrafuzzaman*[1] *and Kazi Faiza Amin*[2]
[1]Department of Materials Science and Engineering, Rajshahi University of Engineering & Technology (RUET), Rajshahi, Bangladesh
[2]Department of Materials and Metallurgical Engineering, Bangladesh University of Engineering and Technology (BUET), Dhaka, Bangladesh

## 7.1 Introduction

Life-cycle assessment (LCA) is a very powerful tool to understand recyclability and to compute the sustainability of a product or a material. It is a wide-ranging and easy-to-understand methodology to presume all environmental impacts across the full life cycle of a product. The full life cycle of a product includes materials acquisition, manufacturing, use, transportation, and end-of-life treatment (i.e., disposal or recycling). LCA can model the environmental consequences of many systems that interact with each other to make an industrial product. An accurate LCA study yields valuable data that decision-makers can use to find greener routes of manufacturing.

This chapter focuses on the advantages, challenges, and versatility of the LCA of polymer nanocomposites (PNCs). It is beyond doubt that nanotechnology is one of the most promising technologies that humanity has ever got benefited from. But for any emerging technology, pointing out the issues related to health and the environment is very crucial, especially to know whether an engineered product is safe or not. However, in the early stage of research, modern system analysis like LCA poses unique challenges to researchers and designers and at the same time aids them to adopt suitable technologies. LCA helps researchers mark out long-term consequences of any product or material as well.

## 7.2 Life-cycle assessment for nanotechnology

The standard methodology of LCA is outlined by ISO 14000 and ISO 14040. According to the ISO guidelines, LCA has four basic phases:

1. goal definition and scope
2. inventory analysis
3. impact assessment
4. interpretation

**Advanced Polymer Nanocomposites. DOI:** https://doi.org/10.1016/B978-0-12-824492-0.00019-2


An illustrative representation of the four basic phases of LCA is depicted in Fig. 7.1. Each of the phases comprises different steps. The following sections will be explaining all these phases in brief.

### 7.2.1 Goal definition and scope

An LCA study can be a complete study when all the data related to the products' manufacturing, use, and disposal will be gathered. These include materials input, all processing parameters during its production, the energy used and wasted at the time of processing, waste treatment, environmental consequences when transporting, information on recycling, and many more. In a word, a farfetched amount of data, resources, and time are required to complete the task. Such an analysis is called "cradle-to-grave" in the field of LCA.

The "goal definition and scope" phase makes the task more manageable. In this phase, the purpose of an LCA study is defined clearly. This may involve comparing the preparation of a nanoproduct using different synthesis pathways or the use of a nanoproduct for a new application. System boundaries, functional units, and limits to the analysis are set to affix the beginning and the ending point of the life-cycle study. A *functional unit* is a basis for the study. It is a measurement of production or output against which impact indicator calculations are normalized. For example,

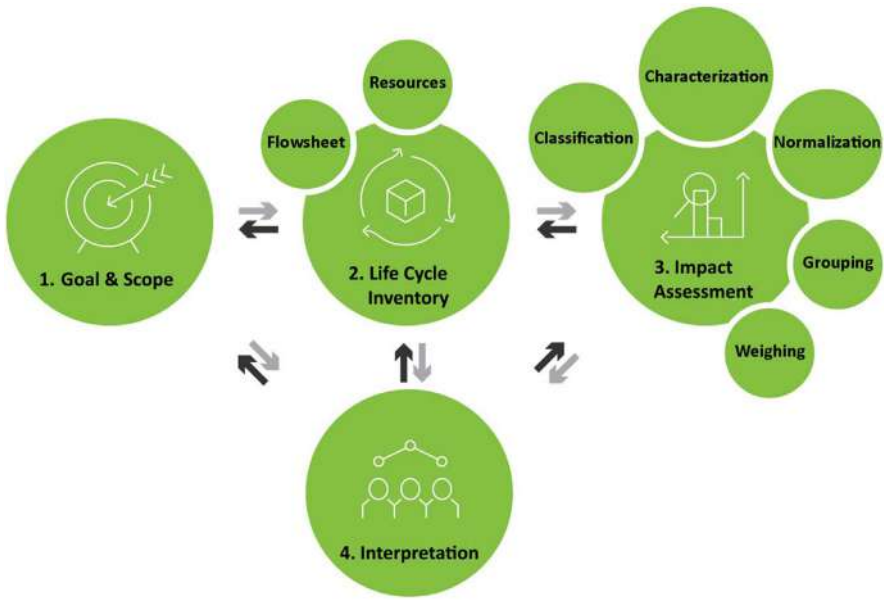


**Figure 7.1** Four basic phases of LCA according to ISO standard. *LCA*, Life-cycle assessment.
*Source*: Modified from https://www.rit.edu/sustainabilityinstitute/blog/what-life-cycle-assessment-lca

if we do a comparative LCA study between porcelain and disposable paper-made coffee mugs, we must consider the amount of hot beverages each of them can contain. A large porcelain mug may have a capacity of 400 mL, whereas a disposable cup may contain 200 mL. Thus the proper functional unit for our hypothetical case should be one porcelain mug versus two disposable paper-made cups.

Once the functional unit is defined, the *system boundary* should be specified clearly to define the scope of the LCA. The work of data collection and analysis can be very painstaking and even sometimes expensive. As a result, some researchers may get enticed to make the boundary too narrow, leading to invalid results. For example, making gold jewelry involves several steps such as metal forming, laser cutting, soldering, stone setting, enameling, and polishing. A researcher may face trouble in collecting data related to the stone-setting step. So, he should take proper care to describe the boundary limits and the purpose of his LCA study on gold jewelry. Otherwise, the results will be faulty. Business firms are more likely to prefer an LCA that is narrow in scope. But an in-depth study needs to use richer data to attract researchers and policymakers, as it can help them better understand real-world conditions.

### 7.2.2 Inventory analysis

The LCI phase (life-cycle inventory phase) is for collecting and sorting data for each of the processes that are laid down by the goal definition and scope phase. An LCA analyst may rely on experiments, different research papers, manufacturers of the product, and published databases for data collection. Data related to material and energy resources, equipment, packaging, and transportation are given as input. The output data consist of products, byproducts, wastes, emissions. Data related to the end of life of the product, that is, recycling, dumping, or incineration are also collected for a complete LCA. By the end of this phase, an inventory list with detailed input and output data is created.

There are a large number of LCI databases and Nifty software available in the field of LCA. These different methods often yield obvious differences in results. Some of the LCI compilation methods available are the *process flow diagram method, matrix inversion method*, and *input−output analysis* [1]. LCA practitioners love process flow diagrams as they show processes of a product system outlined in boxes and the interconnection with the commodity flows in arrows in an easily understandable way. From the flow charts, the LCI for the functional unit of the particular product can be obtained by simple multiplication of the value of environmental interventions with respective ratios.

To explain the use of process flowchart, we can take the LCA work done by Hervy et al. on nanocellulose-reinforced advanced fiber composites in a simplified manner [2]. Fig. 7.2 illustrates the life-cycle process in a very beginner's way. Hypothetically we assume that producing 1 kg of nanofiber cellulose (NFC) epoxy composite requires 1.3 MJ of electricity, 400 gm of NFC paper, 300 gm of epoxy resin, 200 gm porous medium, 70 gm hardener, and 30 gm of other consumables. Then we can calculate:

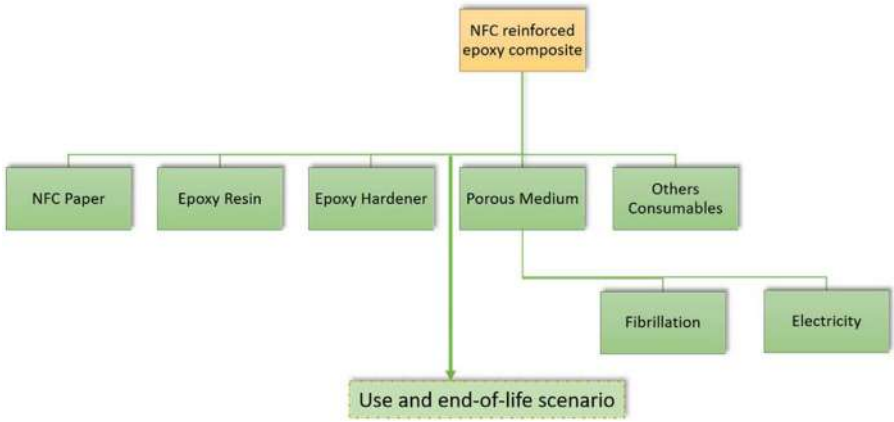


**Figure 7.2** A simplified flow diagram for NFC-reinforced epoxy composite. *NFC*, Nanofiber cellulose.

$$\left(\frac{6.5\text{kg}CO_2}{1\text{kgporous medium}} \times 0.2\text{kgporous medium}\right) + \left(\frac{96\text{kg}CO_2}{1\text{kg consumables}} \times 0.03\text{kg consumables}\right) + \left(\frac{-1.0\text{kg}CO_2}{1\text{kgNFC paper}} \times 0.4\text{kgNFC paper}\right) + \left(\frac{7.8\text{kg}CO_2}{1\text{kg resin}} \times 0.3\text{kg resin}\right) + \left(\frac{3\text{kg}CO_2}{1\text{kg hardener}} \times 0.07\text{kg hardener}\right) + \left(\frac{1.5\text{kg}CO_2}{1\text{MJ electricity}} \times 1.3\text{MJ electricity}\right) = 8.28\text{kg}CO_2;$$

for cradle-to-gate, that is, for raw materials to complete production of the composite.

But the above calculation will be valid only if (1) there is only one material or energy per production process, (2) there is only one type of waste per waste treatment process, (3) input and output of the current production system is not interrelated at all, and (4) material or energy flows between processes do not have a loop(s) [1].

For instance, if production of 1 kg epoxy resin requires 1.3 MJ of electricity and production of 1 MJ of electricity also needs 0.4 kg of epoxy then the inventory compilation is not that straightforward. This can be solved by remodeling the flow diagram in an iterative way or by adopting any other compilation method like matrix representation, etc. Further explanation of inventory analysis methods is


**Figure 7.3** An illustration of the necessity of normalization that straightaway summation does not reflect the actual scenario.

beyond the contents of this chapter. (For further reading please refer to Ref. [1].) (Fig. 7.3).

### 7.2.3 Impact assessment

After data collection, the life-cycle impact assessment (LCIA) phase is to make a meaningful context of potential damages to human and animal health and the environment. Results are characterized and quantified into several impact categories. Then the different impact categories are normalized and weighted to obtain a meaningful interpretation. For example, stating that a process emits 10 kg of carbon dioxide ($CO_2$) and 7 kg of sulfur dioxide ($SO_2$) is not an eloquent description of its contribution to climate change. An LCIA renders these raw data and gives relative potency of materials, emissions, or other factors. So, after a proper LCIA, in the case of $CO_2$ and $SO_2$, we will be able to say that one contributes 20−30 times (or whatever in reality) more to climate change than the other. Because the harm of 1 kg of $CO_2$ and 1 kg of $SO_2$ is not equal. Generally, all the impacts are normalized in terms of carbon dioxide equivalents to enumerate the potential for global warming. Several LCIA methods exist. The ReCiPe method, IMPACT 2002 +, Eco Invent 99, etc. are some of them. More often, the choice among the methodologies is made based on the goal of the study. Making comparisons between alternative ingredients of a product, or identifying an eco-friendly process, or contrasting between several end-of-life scenarios to improve recyclability may be some of the diverse goals of LCA studies. The calculation of impact potential can be easily understood from the following relation [3].

$$\text{Totalimpact potential} = \sum_{i=1}^{n} (\text{Characterization factor})_i \times (\text{Chemical emission})_i$$

Here, the characterization factor is different for different pollutants based on their impacts in various categories and is found in literatures. Common impact categories include global warming potential (GWP), terrestrial acidification, eutrophication, carcinogens, noncarcinogens, ozone layer depletion, freshwater ecotoxicity, and many more depending on the assessment method used.

Other terms to understand LCIAs are the *midpoint and endpoint modeling*. In midpoint impact assessment models, the relative potency of the stressors at a common midpoint is focused within the system boundary [e.g., greenhouse gas (GHG) is a stressor for global warming.] Analysis at a midpoint minimizes the amount of forecasting and therefore the modeling becomes less complex than the assessment based on an endpoint. A simple flowchart explains this in Fig. 7.4.

The United States Environmental Protection Agency splits an LCIA into seven steps [4]:

1. selection and definition of impact categories
2. classification
3. characterization
4. normalization

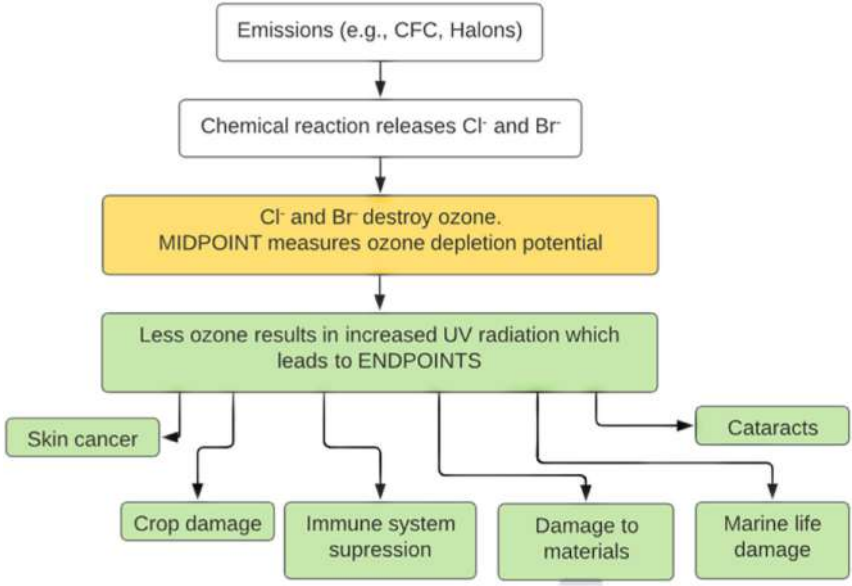


**Figure 7.4** Comparison of impact categories for midpoint versus endpoint modeling.
*Source*: Recreated form: https://nepis.epa.gov/Exe/ZyPDF.cgi/P1000L86.PDF?Dockey = P1000L86.PDF

5. grouping
6. weighting
7. evaluating and reporting LCIA results.

### 7.2.4 Interpretation

The last phase in an LCA study is interpretation. The data and results from the preceding phases are interpreted in this phase to deduct outcomes and make recommendations. Before interpretation, the validity of the results should be verified using sensitivity and uncertainty analysis. *Uncertainty analysis* means determining the inconsistency of the data and its impact on the results. The ultimate purpose of this phase is to reach the stated goals by detecting the significant factors. So, if the goal was to identify a healthier path of manufacturing, approaches to achieve it will be highlighted in this phase.

The ISO standards decree that LCA interpretation should

- identify the most significant issues from the study;
- make a way to evaluate the study itself. It should explain whether it is done sensitively and consistently or not, make uncertainty analysis; and
- provide conclusions, limitations, and recommendations to clarify the completeness of the study.

## 7.3 Expected benefits of LCA for PNCs

Nanotechnology is unquestionably an evolving technology. The doubled number of published papers in this field just within 1.6 years span in the late 1990s proves its convenience [5]. For any emerging technology, LCA can be a tool capable of reporting critical concerns such as material use, energy use, ecological impact, and toxicity. Implementation of LCA in nanotechnology and nanocomposites can develop the technology in a sustainable manner. Some of the expected benefits of LCA for PNCs are as follows:

1. Understanding each stage of a product's life cycle that which stage has how much impact on the environment.
2. Identification of most preferred end-of-life scenario(s) specific to a particular nanoproduct.
3. Selection of the right alternative from the various available processes in product design. LCA can even help decide the manufacture of partial items of a product. In the case of PNC, change in the choice or production of certain matrix materials may lessen the GWP to a great extent.
4. Evaluating the supremacy of nanoproducts in comparison to the others.
5. Marking out the hot spots and analyzing them to facilitate development.
6. In the early phases of a product design, LCA can be used as a screening tool for evaluating rival technologies.
7. LCA also assists in correcting any wrong value when low, high, or even no weighting value is allocated on any environmental aspect [6].

Without life cycle thinking, it is very likely to pay attention to issues of immediate attention and overlook issues that may lead to long-term environmental concerns.

## 7.4 Limitation and challenges on nanocomposites LCA

Though LCA methodology is standardized via the ISO series, databases and analytical software are available, the methodology has several challenges in all fields of nanotechnology.

- PNCs are specialized products. Today's available life-cycle inventory databases are not that versatile and are convenient only for evaluating typical products and common processes.
- Impact data of nanoproducts related to human and ecosystem health exposure are yet to be generated. In addition, some of the data are not publicly available for being proprietary.
- In many cases, a mismatch arises between the LCA approach and the goal of the assessment. For example, recycling neodymium−iron-boron magnets from hard disk drives can be a great way to reduce the environmental burden [7]. But these results would not be applicable in a comparison of secure digital (SD) cards, as they greatly differ in the construction process, weight, etc.
- In some instances, it may not be possible to mark a solution to be the best over the others due to the uncertainty of the final results. This ambiguity does not mean that LCA is not a practical tool for decision-makers.
- In some cases, LCA alone fails to provide a basis for decision-making without the involvement of other tools like risk assessment, cost assessment, etc.

As the LCA for nanoproducts has not yet reached a mature stage, we should focus on compiling a rich life-cycle inventory of engineered nanomaterials, which will help pave the way for LCA of specific nanoproducts such as nanocomposites. LCA practitioners cannot be able to overcome the gap on their own. But rather a multidisciplinary effort is needed for the task.

## 7.5 LCA of food packaging materials

Food packaging is essential for food processing businesses to increase shelf-life and to ensure fresh and undamaged food for their customers. Therefore this has become a major sector of material consumption. In a work done by Lorite et al., the environmental performance of polylactic acid (PLA)-based active packaging was studied by LCA, after adding nanoclays and surfactants in its formulation [8]. The PLA-based nanocomposites were made using Na-cloisite 20 and Na-cloisite 30B which are two nanoclays. Cloisite 20 is a bis (hydrogenated tallow alkyl) dimethyl salt with bentonite, and Cloisite 30B is an alkyl quaternary ammonium bentonite. They used Triton X-100 (Octyl phenol ethoxylate) as the surfactant [8].

LCA results showed that it is polyethylene terephthalate (PET) that has low environmental impact than PLA-based packaging with nanoclay and surfactant. But the latter one has a very competitive performance with PET. In the category of human health, PLA-based packaging is discovered to be more environmentally friendly. To briefly state the performance of both the food packaging considered, we can compare the single score results. It was 36.5 points for PLA nanocomposite and 35.9 for traditional PET. The most impactful phase of all the life cycle phases is the manufacturing of packaging phase (more than 20 points just in this single phase). The other part of the same study indicated that PLA-based packaging with additives can improve the shelf-life of foods. This may lead to a noteworthy reduction in food waste, reduce the digit of use of packaging and hence lessen the environmental impact. But the authors suggest further study regarding this to establish a broader conclusion [8].

Cinelli et al. have done an LCA study of food packaging made of PLA and chitin nanofibrils (NC) [9]. Their aim was to seek a sustainable technology to reuse the chitin found in crab, shrimp, and lobster shells discarded as waste all over the world. Chitin also has antioxidant and antimicrobial properties. [10] As the PLA and chitin nanofibrils made bionanocomposites are directly sourced from the nature, they are eco-friendly due to having compostability as a possible end-of-life scenario. Of all the impact categories, human toxicity is found to be the most vulnerable category here.

Both the above studies took 100% composting to be the preferable end-of-life scenario, though enough data is unavailable in the databases. The plastic packaging treatment of Europe for PLA is 20% composting, 40% incineration, 40% landfilling. For PET packaging, the current 60% incineration, 40% landfilling waste scenario resulted in a lower impact compared to the 100% incineration scenario. This was due to the typical database input of landfilling being more environmentally friendly than incineration [8].

In the food packaging industry, the use of silver nanoparticles (nAg) is another considerable option because of the antimicrobial property of nAg which lengthens the freshness period of the stored food. A study has been done by Westerband and Hicks on nanosilver containing polymer food storage composite material [11]. In this work, the TRACI midpoint analysis method was applied for LCA. They have made a comparison between nAg enabled polymer food storage containers and the conventional containers focusing on human health and the environmental impacts. The integration of nAg on food storage showed an increase of around 1.6% in the overall environmental impact compared to conventional food storage containers. This very small surplus impact from nAg addition can make it an option for advanced food packaging material. Summarized outcomes of the study are as follows:

- $AgNO_3$ contributes 77%−99% in total of all the impact categories. The consideration of mining and refining of the silver ore is the prime reason behind this. Recycling silver can be a suggestive way to lower this impact significantly. As nearly $4.24 \times 10^5$ kg of silver is released all over the world in a year [12].

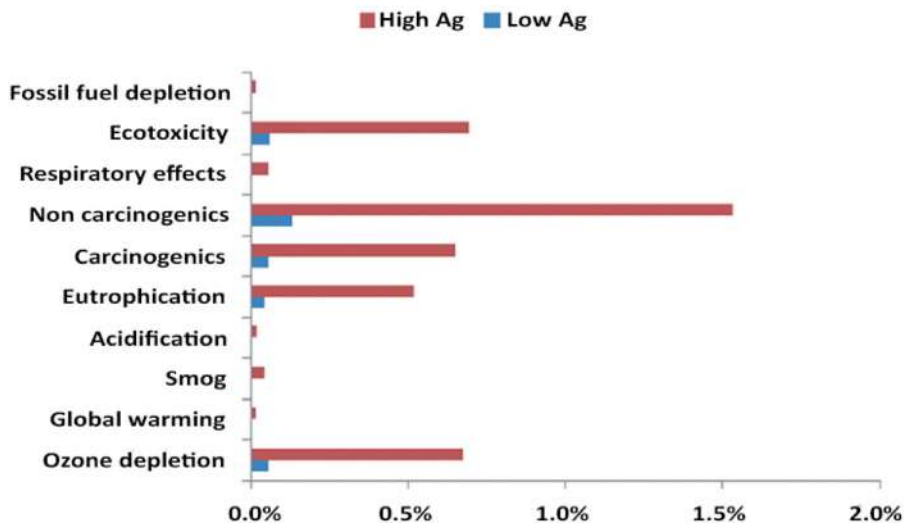


**Figure 7.5** Percentage of increase in impact categories after integrating nAg to the food containers [11].

- The impacts of ozone depletion, global warming, and ecotoxicity are increased for higher nAg content in raw materials processing and the production stages.
- Compared to conventional food containers the nAg−nanocomposite container shows an increase in every environmental impact category. But the highest increase is as high as 1.6% for the noncarcinogens category and the lowest is 0.001% for fossil fuel depletion and global warming.
- Unexpectedly, the electricity used during dishwashing has seriously affected the results for eight of the impact categories (Fig. 7.5).

More works and analyses are needed to assess the complete impacts of all these products and to innovate the most practical option. For example, the nAg PNC is susceptible to release from 0.1 to 31.5 ng $cm^{-2}$ of silver to the atmosphere, depending on the type of packaging [13−15]. Therefore other studies than LCA are required to establish a correct understanding of human health and animal life-related issues (Table 7.1).

## 7.6 LCA of polymer nanocomposites for automobiles

If we think about automobiles, steel and aluminum are being used in the body panels from a very early age. These conventional materials can be substituted by modern PNCs due to their improved mechanical properties, low density, good electrical conductivity, and other specific functionalities. Lloyd and Lave [16] have explored the benefits of using nanoclay−polypropylene (PP) composite instead of steel or aluminum in automobile body panels. The life-cycle analysis has shown

**Table 7.1** Summary of LCA on polymer nanocomposite for food packaging.

| Materials of the study | Functional unit | Environmental impact | Highlights | Ref. |
|---|---|---|---|---|
| Nanoclay-reinforced PLA nanocomposite | Packaging 100,000 kg of fresh fruits in 1 year | Single score results of PLA NC were 36.5 pt., whereas traditional PET has 35.9 pt. | PLA NC is a close competitor of PET. PLA-based packaging with additives has a lower impact in the human health category. | [8] |
| PLA and chitin nanofibrils (NC) composite | 1 kg of NC and one kg of PLA/NC/ PEG400 pellets | Human toxicity is found to be the worst impact category. | Composting is the most preferable end-of-life scenario. | [9] |
| Nanosilver polymer composite | One food container of 52 weeks lifetime; 1 kg nAg | Higher nAg content shows higher impact − $1.5 \times 10^{-10}$ kg CFC-11 eq., 0.124 kg $CO_2$ eq., 0.28 CTUe | Despite no recycling or recovery of the polymer or the nAg, only a 1.6% rise in the overall environmental impact is found | [11] |

LCA, Life-cycle assessment; PET, polyethylene terephthalate; nAg, silver nanoparticles.

potential benefits from PNCs in material processing and fuel economy by reducing energy consumption and pollutant discharges.

The study is based on vehicles' use in a span of 1 year within the United States. When steel in the automotive body panels is substituted by PNC, the amount of electricity used, energy used, the release of pollutants, release of GHGs, consumed fuel, utilized ores, generated hazardous waste, the release of toxic materials, use of water, and the number of highway fatalities—all the impact categories showed reduced values. For example, switching to a PNC automotive body panel would result in $7.2 \times 10^5$ to $16 \times 10^6$ tons of $CO_2$ eq. lesser GHG emissions and an energy saving of 51 to 240 thousand terajoules. Refining of petroleum, electric services, crude petroleum and natural gas, inorganic and organic chemicals, transportation of gas, etc. are the areas contributing the major portion of GWP [16].

The study was modeled using EIO-LCA (The Economic Input-Output Life Cycle Assessment) model. But the authors reported some certain drawbacks regarding the EIO model:

- The model allocates an equal quantity of energy use for recycled and primary materials.
- EIO model assumes a linear relationship between economic input and environmental effect and does not calculate any exception for mass production.

It was also assumed that 50% of both the steel and nanocomposite scrap would be reused and reprocessed. The practicality of manufacturing car body panels with PNC is only threatened due to its current higher market price. The researchers concluded that it would be a solution where everyone benefits if the cost gets reduced for PNC. Roes et al. [17] have done a study on a number of PNCs including glass-fiber-reinforced PP as internal panels of automobiles. In the study, glass fiber PP composite was considered as the traditional raw material for automotive internal body parts. This glass fiber/PP composite was compared with the clay/PP nanocomposite and it was found that the latter can yield only 1.25% lighter body panels. Most of the environmental impact categories such as climate change, nonrenewable energy use (NREU), eutrophication, acidification, and abiotic depletion have shown trivial improvements. Only photochemical oxidant formation and ozone layer depletion have shown improvement but are not that significant. The authors have commented on the fact that LCI data have high uncertainties for nanoclay production. This might have added some errors to the study. Otherwise, significant benefits would have been visible by the use of PP nanocomposites (Fig. 7.6).

Lloyd and Lave, and Roes et al.—both of the works utilized Ashby's material indices [18] to estimate the weight reduction of nanocomposite automotive panels. The same formula $M = \sqrt[3]{E}/\rho$ is used.

The traditional fiber-reinforced plastics have excellent in-plane mechanical properties. But they perform poorly at transverse and thickness directions because of the weaker polymer matrix. [19] Long-length carbon nanofibers (CNFs) can strengthen the polymer in these directions. Khanna and Bakshi [20] have analyzed the possibility of utilizing CNF PNC to manufacture internal panels of cars. They have carried out LCA on CNFs PNCs as well as on a hybrid PNC of carbon nanofiber-glass fiber (CNF-GF). In the study, PNCs and steel are considered to be equivalent on the basis

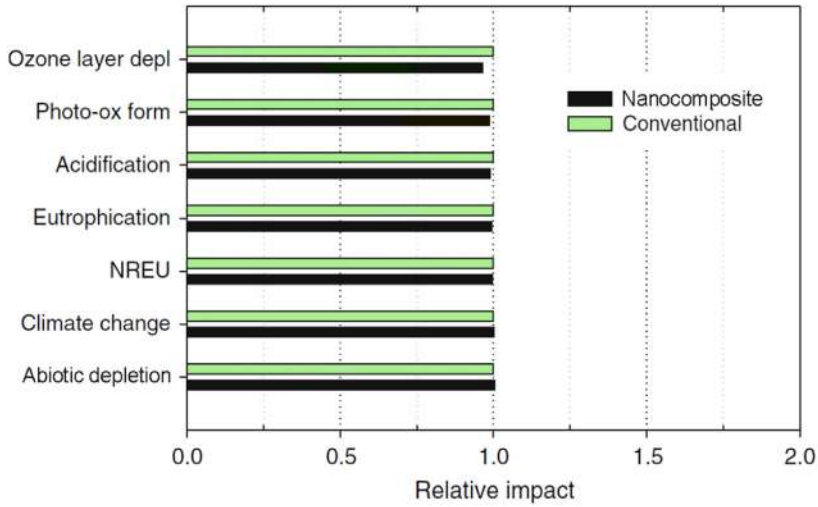


**Figure 7.6** Relative results of the impact assessment of conventional GF/PP composite versus PP nanocomposite [17]. *GF*, glass fiber; *PP*, polypropylene.

of equality in stiffness value. The result shows that, for an equal value of stiffness, the production energy required for CNF polymer composite is 1.6−12 times higher than that for steel [20] (Fig. 7.7).

But the CNF polymer composite gives net energy saving if the use phase is considered. When CNF PNC is used, the body panel becomes 18.9%−61.2% lighter. As the body panel comprises 10% of the total weight in a vehicle, less fuel is required during use. This fuel-saving leads to 18 GJ of energy saving for each car. For hybrid PNC of CNF-GF, this saving reaches as high as 65 GJ per car. If the unsaturated polyester resin is used instead of PP, the value of energy saving is lowered from 8 to 44 GJ/car [20]. The authors of this study have also focused on a design-related issue regarding PNC panels. To maintain equal stiffness, PNCs become 3.2−5.3 times thicker than steel-made panels. Such dimensional change may pose design limitations with respect to engineering and esthetic point of view.

The LCA of poly (3-hydroxybutyrate)-based (PHB) nanocomposites is studied by Pietrini et al. [21]. This study evaluated the application of nanoclay/biodegradable plastic and petrochemical polymers where sugar cane bagasse and nanosized organophilic montmorillonite are used as fillers. Only two impact categories are explored here—GWP, GWP100 (as the time prospect is 100 years), and NREU.

The problem regarding the use of PHB composite in substitution to GF/PP is its low stiffness, as stated earlier. So, to make a good quality automotive internal panel, 32%−36% more material is required by weight than GF/PP [21]. This high amount of PHB nanocomposite undoubtedly demands high energy and GHG emissions, and also an increase in the weight of the automobile results in higher energy or fuel usage during the operation stage. In the same study, the energy requirement and GHG emission are computed for the PHB nanocomposite to be used in the


**Figure 7.7** There is plenty of scope for polymer nanocomposites in automobiles and their LCA studies. *LCA*, Life-cycle assessment.

housing of the CRT monitors. This analysis has shown lower environmental impacts. But CRT monitors are obsolete in today's world and therefore the study needs further scrutinization (Table 7.2).

## 7.7 LCA of PNCs intended for different applications

### 7.7.1 Graphite nanoplatelets-filled epoxy-based composite

The versatility of polymers can be expanded many fold when they are reinforced with nanomaterials of superior properties. A study in 2014 was done by Pizza et al. [22] to assess the environmental impact of graphite nanoplatelets filled epoxy-based composite. The life-cycle phases that are taken into account in the study are raw materials extraction, nanoplatelets, and epoxy resin preparation, production of the nanocomposite, transportation, and the end of life. Most of the impacts come from the extraction of raw materials stage. Then comes the filler and epoxy matrix preparation stage. Of note, 50% of the primary energy is consumed by the matrix polymer, whereas the GnP production process contributes 36%. To produce 1 kg of epoxy composite, 0.058 kg of GnP (5.8% by weight) is required. This GnP demands 303 MJ of primary energy and the requirement for epoxy resin matrix is 187 MJ. The effect of composite production is very low compared to the others.

The motivation of adding graphite nanoplatelets to epoxy resin is to increase its intrinsic thermal conductivity so that it can be used in high-performance computer

**Table 7.2** Summary of LCA on polymer nanocomposite for automotive applications.

| Materials of the study | Functional unit | Environmental impact | Highlights | Ref. |
|---|---|---|---|---|
| Montmorillonite nanoclay-reinforced polypropylene composite | 16.9 million light-duty vehicles, 210 million vehicles on the road. Vehicle lifetime 150,000 miles, 10 years. | PNC can produce around 38% to 67% lighter body panels. This will lead to 49−87 million metric tons lesser emission of $CO_2$ and will save 5.7−10.1 billion gallons of petrol. | The estimated annual $CO_2$ reduction is 49−87 million tons. The current higher market price of PNC is the main hindrance to adopt its mass production. | [16] |
| Nanoclay silicate-reinforced polypropylene nanocomposite (PP NC) | Body panels of a lightweight family car of 150,000 km lifetime mileage. | Primary energy demand 8.23 GJ for conventional material and 8.21 GJ for PP NC. Greenhouse gas emissions 569 versus 570 kg $CO_2$-eq. | Only 1.25% lighter body panels from PP nanocomposite. No apparent environmental benefit is seen. | [17] |
| Carbon nanofiber (CNF)-reinforced polymer nanocomposites | Body panels of a midsize car that can travel 150,000 miles in its lifetime. | CNF-GF hybrid PNCs save around energy 65 GJ/car. Simple CNF PNCs save 18 GJ/car. Unsaturated polyester resin-based NC saves from 8 to 44 GJ/car. | PNC needs a higher amount of manufacturing energy. But the energy savings come from the 1.4%−10% fuel savings in the use phase of the vehicle's lifetime. | [20] |
| Poly (3-hydroxybutyrate) nanocomposites, with sugar cane bagasse and nano organophilic montmorillonite fillers | Total internal panels of one typical car with a lifespan of 10 years and 150,000 km mileage. | NREU of 10.6 and GWP100 of up to 722.8 are found for PHB nanocomposites. Whereas these values are 8.2 and 569.9 for conventional materials respectively. | PHB nanocomposite does not render any notable energy saving when used in internal body panels of cars. It is only applicable in CRT monitor casings. | [21] |

LCA, Life-cycle assessment; PET, polyethylene terephthalate; PHB, poly (3-hydroxybutyrate); PNC, polymer nanocomposites; nAg, silver nanoparticles.

processing units as thermal interface material. An optimized methodology is preset for LCA from metal depletion ReCiPe midpoint (H), IPCC 07, CML 2001, USEtox, and EDIP 2003. This practice has helped the authors evaluate energy consumption, metal, water, fossil, and ozone depletion, human toxicity, ecotoxicity, photochemical oxidant, freshwater, and marine eutrophication, acidification, and hazardous waste. The GWP (GWP100a) was 15.7 kg $CO_2$ eq [22].

### 7.7.2 Polyacrylic acid and polyethylenimine-coated magnetic nanoparticles

Magnetite ($Fe_3O_4$)-based magnetic nanoparticles (NPs) are used in wastewater treatment as heterogeneous Fenton or photo-Fenton catalysts. A study was done by Feijoo et al. in 2019 [23] to evaluate the environmental impacts related to the production of different magnetic NPs and to find out an environment-friendly option. The analysis of this study has concluded that the PNCs resulted from polyacrylic acid (PAA) and polyethylenimine (PEI)-coated magnetic NPs are the fittest option for their applications in heterogeneous Fenton processes.

Of all the materials studied, pure $Fe_3O_4$, $Fe_3O_4$/PEI, $Fe_3O_4$/PAA NPs, and $Fe_3O_4/SiO_2$ NPs, pure stabilized magnetite has shown the lowest impacts. On the other hand, silica-coated magnetic NPs have the highest impact. But using nanocomposites is a wiser decision because of their reactivity and transformation potential. Similarly, using the nanocomposites in photocatalysis proves to perform better due to faster reaction kinetics compared to Fenton [23].

Impact categories that are explored in this study are climate change, freshwater eutrophication, ozone depletion, fossil depletion, marine eutrophication, toxicity, and terrestrial acidification. If a quantitative comparison is done between PAA and PEI coating, the latter has performed somewhat well than the other one. For example, in ozone depletion, $Fe_3O_4$/PAA yielded $2.05 \times 10^{-8}$ kg CFC-11 eq. and $Fe_3O_4$/PEI yielded $1.29 \times 10^{-8}$ kg CFC-11 eq.

### 7.7.3 Silver-graphene oxide-reinforced polyvinylidene fluoride

Chan et al. in 2018 [24] have done an extensive LCA on polyvinylidene fluoride reinforced with Ag and graphene oxide (GO). The integration of Ag/GO nanohybrids into polyvinylidene fluoride (Ag/GO-PVDF) membrane fabrication showed a higher environmental impact than the stock PVDF membrane fabrication. However, the algal membrane photoreactor (A-MPR) system with the Ag/GO-PVDF membrane revealed a healthier environmental footprint as it allows a higher volume of permeate to pass through.

ReCiPe midpoint and endpoint analysis both are carried out in the study. Endpoint indicators are three—human health, ecosystem, and resources. The AMPR with the Ag/GO-PVDF membrane showed less harmful effects on all three impact categories compared with the A-MPR with PVDF membrane. The total environmental footprint of the A-MPR with PVDF membrane was 290 mPt per L permeate. On contrary, it is reduced by 15.9%, to 244 mPt per L permeate for A-MPR with the Ag/GO-PVDF

membrane. Some alternates to reduce energy demand are also sought out in the study. If renewable energy sources such as fuel cells, solar photovoltaic, hydropower can replace the use of electricity, impressive improvement is possible [24].

### 7.7.4 PNC in agricultural films

Schrijvers et al. [25] have conducted an ex-ante LCA of agricultural mulching films reinforced by nanoclays. A poly (butylene adipate-co-terephthalate) (PBAT)/layered double hydroxide (LDH) nanocomposite with PBAT and low-density polyethylene is studied in the work. A possible implementation of nanoclay surfactants and *p*-hydroxycinnamic acid is considered in LDH sheets. The study demonstrates that nonrenewable energy use and GHG generation are the lowest for LDPE films. As PBAT is biodegradable, it can be a good alternative to LDPE. Because recycling and incinerating is a typical end-of-life scenario for LDPE and recycling and energy recovery by incineration is not practical every time [25] (Table 7.3).

## 7.8 Narrowing the limitations of LCA for PNC

The absence of life-cycle analysis had led us to destructive engineering decisions in the past. For example, from the era of the 1930s, chlorofluorocarbons were thought to be an apparent magical aid in the refrigeration industry as they had substituted the use of toxic methyl chloride, carbon tetrachloride, etc. [26] But around 1974, researchers have started finding the other side of the coin. Soon it was realized that photodissociation of the CFCs produces significant amounts of chlorine atoms in the stratosphere and causes direct destruction of atmospheric ozone [27].

LCA can help decide any particular material before implementation. But in this modern era of today, newer technology like nanocomposite is emerging. At the same time, their real effect on the environment might be unknown to us. For example, the release of carbon nanotubes from nanocomposites [28], release of nanosilver into the environment are the outcomes of very recent researches. Such research work is very important to establish proper fruitful life-cycle analyses.

## 7.9 More research works to carry on

Composites have a very wide ground to play inside. There are numerous opportunities for LCA that are completely untouched in the field of polymer composite and PNC. Natural sources of fibers and nanoclays are another scope of newer works in this discipline. For example, Asrafuzzaman et al. [29] explained the bonding of bamboo fiber-reinforced composites. PNC can aid in property enhancement in this regard and an LCA study can help make the right decision from the environmental point of view. Natural fibers are finding their applications in heavy-duty structures like concretes [30]. But due to the lack of adequate LCA study, PNC is far behind that.

**Table 7.3** LCA studies of versatile PNCs.

| Materials of the study | Functional unit | Environmental impact | Highlights | Ref. |
|---|---|---|---|---|
| Graphite nanoplatelets (GnP)-filled epoxy-based composite | 1 kg of epoxy composite with 5.8 wt.% filler. Assumed thermal conductivity is 1 W $mK^{-1}$ and lifetime is 30 years. | 1 kg of GnP needs 1879 MJ of primary energy. 1 kg of epoxy composite contains 0.058 kg of GnP equivalent to 303 MJ, and the primary energy for epoxy resin is 187 MJ. | Thermal conductivity is considered a prime property in the study. The usability of the epoxy NC as a thermal interface material in high-performance computer processing units is considered here. | [22] |
| Polyacrylic acid and polyethyleni-mine-coated magnetic nanoparticles | The weight of magnetic nanoparticles produced in a batch | Pure has the lowest impact. For example, $8.21 \times 10^{-9}$ kg CFC-11 eq. ozone depletion of $Fe_3O_4$, whereas $Fe_3O_4$/PAA and $Fe_3O_4$/PEI have $2.05 \times 10^{-8}$ to $1.29 \times 10^{-8}$ kg CFC-11 eq. | Though PAA and PEI-coated nanoparticles show slightly higher impacts, they are better choices due to their good reactivity and transformation potential. | [23] |
| Ag-graphene oxide-reinforced polyvinylidene fluoride | 1 g of membrane; 1 L of permeate for algal membrane photoreactor | The single score of A-MPR with PVDF membrane was 290 mPt per L permeate. On contrary, the environmental footprint of A-MPR with the Ag/GO-PVDF membrane has lessened by 15.9%, to 244 mPt per L permeate. | Energy demand can be impressively reduced when the existing electricity mix will be replaced with renewable energy such as fuel cell, solar energy, windmill power, and hydropower. | [24] |

LCA, Life-cycle assessment; NC, nanofibrils; PAA, polyacrylic acid; PEI, polyethylenimine; PNC, polymer nanocomposites; PVDF, polyvinylidene fluoride.

One of the major impedances of the life-cycle analysis of PNC is the scarcity of a proper database. This can be partially overcome by studying the separate LCA of reinforcing nanomaterial and the polymer matrix material. For instance, many good scientific studies are available describing the LCA of only the matrix polymer material for food packaging [31]. Opting for an LCA of reinforcing materials and combining them would give an early assessment of complete LCA studies of PNC, though the results would lack accuracy. PLA is biodegradable material of lesser environmental pollution. [32] PLA-based nanocomposites may find their applications in the agriculture and packaging industries. Many LCA works have been done for PLA merely, excluding its nanocomposite form [33–37]. LCA research works of nanomaterials that are compatible with PLA can be adjoined with these studies to assess the results for PLA PNCs. Ex-ante LCA studies (forecasting analysis rather than actual results) can be conducted to fill up the existing gap in the life-cycle study of PNC. Ex-ante studies make comparison among different materials easier.

Many recent works of research works involve working on polymer composites and their LCA. Enriched literatures are available in nature-based scaffolds [38,39], fiber-reinforced composites [40,41], natural fiber-based composites [42–45], carbon fiber composites [46,47], polymer composites for home appliances [48], building construction purposes [49,50] and many others. LCA of composites made from recycled materials is also done so far [51,45]. But discussion of these studies is beyond the scope of this chapter, as they lack the involvement of any nanoscale reinforcements. An example in this context is the LCA of automotive materials [16] in this chapter. Despite more works are related to automobile materials [52], they are excluded, as they do not focus pointedly on PNCs.

## 7.10 Conclusion

Every production, consumption, and disposal activity greatly affect our environment. In this era of rampant technological improvements, advanced materials such as numerous PNCs are available as options and are even finding their applications in many engineered products. But the proper decision of material selection cannot be taken without a complete assessment of environmental impacts. LCA is an associative tool for material selection and even acts as a production process selector. For instance, any newly proposed manufacturing route, or modification within the process, or any decision regarding a material's recycling can be criticized or evaluated before implementation by the touchstone of LCA. Therefore laboratory research work and LCA collaboratively can pave the way to future comprehensive material study.

## References

[1] S. Suh, G. Huppes, Methods in the life cycle inventory of a product, in: S. Suh (Ed.), Handbook of Input-Output Economics in Industrial Ecology, Springer Netherlands, Dordrecht, 2009, pp. 263–282.

[2] M. Hervy, S. Evangelisti, P. Lettieri, K.Y. Lee, Life cycle assessment of nanocellulose-reinforced advanced fibre composites, Compos. Sci. Technol. 118 (2015) 154–162. Available from: https://doi.org/10.1016/j.compscitech.2015.08.024.
[3] V. Khanna, L. Merugula, B.R. Bakshi, Environmental Life-Cycle Assessment of Polymer Nanocomposites, Woodhead Publishing Limited, 2012.
[4] EPA, Life Cycle Assessment: Principles and Practice, Vasa, 2008. http://medcontent.metapress.com/index/A65RM03P4874243N.pdf (accessed 27.07.21.).
[5] P.H.C. Camargo, K.G. Satyanarayana, F. Wypych, Nanocomposites: synthesis, structure, properties and new application opportunities, Mater. Res. 12 (1) (2009) 1–39. Available from: https://doi.org/10.1590/S1516-14392009000100002.
[6] M.A. Curran, Strengths and limitations of life cycle assessment, in: W. Klöpffer (Ed.), Background and Future Prospects in Life Cycle Assessment, Springer Netherlands, Dordrecht, 2014, pp. 189–206.
[7] D.D. München, H.M. Veit, Neodymium as the main feature of permanent magnets from hard disk drives (HDDs), Waste Manag. 61 (2017) 372–376. Available from: https://doi.org/10.1016/J.WASMAN.2017.01.032.
[8] P. Saavalainen, G.S. Lorite, C.M.R. Rocha, G. Toth, LWT - Food Science and Technology Evaluation of physicochemical / microbial properties and life cycle assessment (LCA) of PLA-based nanocomposite active packaging € l a, 75, 2017.
[9] P. Cinelli, M.B. Coltelli, N. Mallegni, P. Morganti, A. Lazzeri, Degradability and sustainability of nanocomposites based on polylactic acid and chitin nano fibrils, Chem. Eng. Trans. 60 (2017) 115–120. Available from: https://doi.org/10.3303/CET1760020.
[10] F. Shahidi, J.K.V. Arachchi, Y.J. Jeon, Food applications of chitin and chitosans, Trends Food Sci. Technol. 10 (2) (1999) 37–51. Available from: https://doi.org/10.1016/S0924-2244(99)00017-5.
[11] E.I. Westerband, A.L. Hicks, Environmental Science Nano storage containers as a case study informed by literature review, Environ. Sci. Nano (2018) 8–10. Available from: https://doi.org/10.1039/C7EN01043E.
[12] M.J. Eckelman, T.E. Graedel, Silver emissions and their environmental impacts: a multilevel assessment, Environ. Sci. Technol. 41 (17) (2007) 6283–6289. Available from: https://doi.org/10.1021/es062970d.
[13] M. Cushen, J. Kerry, M. Morris, M. Cruz-Romero, E. Cummins, Evaluation and simulation of silver and copper nanoparticle migration from polyethylene nanocomposites to food and an associated exposure assessment, J. Agric. Food Chem. 62 (6) (2014) 1403–1411. Available from: https://doi.org/10.1021/jf404038y.
[14] Y. Huang, S. Chen, X. Bing, C. Gao, T. Wang, B. Yuan, Nanosilver migrated into food-simulating solutions from commercially available food fresh containers, Packag. Technol. Sci. 24 (5) (2011) 291–297. Available from: https://doi.org/10.1002/pts.938.
[15] Y. Echegoyen, C. Nerín, Nanoparticle release from nano-silver antimicrobial food containers, Food Chem. Toxicol. 62 (2013) 16–22. Available from: https://doi.org/10.1016/J.FCT.2013.08.014.
[16] S.M. Lloyd, L.B. Lave, Life cycle economic and environmental implications of using nanocomposites in automobiles, Environ. Sci. Technol. 37 (15) (2003) 3458–3466. Available from: https://doi.org/10.1021/es026023q.
[17] A.L. Roes, E. Marsili, E. Nieuwlaar, M.K. Patel, Environmental and cost assessment of a polypropylene nanocomposite, J. Polym. Environ. 15 (3) (2007) 212–226. Available from: https://doi.org/10.1007/s10924-007-0064-5.
[18] M.F. Ashby, Materials Selection in Mechanical Design, Fourth, Elsevier Ltd., Burlington, USA, 2011.

[19] P. Asokan, M. Osmani, A. Price, Improvement of the mechanical properties of glass fibre reinforced plastic waste powder filled concrete, Constr. Build. Mater. 24 (4) (2010) 448–460. Available from: https://doi.org/10.1016/j.conbuildmat.2009.10.017.
[20] V. Khanna, B.R. Bakshi, Carbon nanofiber polymer composites: evaluation of life cycle energy use, Environ. Sci. Technol. 43 (6) (2009) 2078–2084. Available from: https://doi.org/10.1021/es802101x.
[21] M. Pietrini, L. Roes, M.K. Patel, E. Chiellini, Comparative life cycle studies on poly(3-hydroxybutyrate)-based composites as potential replacement for conventional petrochemical plastics, Biomacromolecules 8 (7) (2007) 2210–2218. Available from: https://doi.org/10.1021/bm0700892.
[22] A. Pizza, R. Metz, M. Hassanzadeh, Life cycle assessment of nanocomposites made of thermally conductive graphite nanoplatelets, pp: 1226–1237, 2014, doi: 10.1007/s11367-014-0733-2.
[23] S. Feijoo, J. González-Rodríguez, L. Fernández, C. Vázquez-Vázquez, G. Feijoo, M.T. Moreira, Fenton and photo-fenton nanocatalysts revisited from the perspective of life cycle assessment, Catalysts 10 (1) (2020) 1–11. Available from: https://doi.org/10.3390/catal10010023.
[24] W. Chan, Y. Tao, Y. Haan, M. Zain, E. Mahmoudi, A. Wahab, Environmental impact of nanomaterials in composite membranes: life cycle assessment of algal membrane photoreactor using polyvinylidene fluoride e composite membrane, J. Clean. Prod. 202 (2018) 591–600. Available from: https://doi.org/10.1016/j.jclepro.2018.08.121.
[25] D.L. Schrijvers, F. Leroux, V. Verney, M.K. Patel, Nanocomposites using organo-modified layered, pp. 4969–4984, 2014, doi: 10.1039/c4gc00830h.
[26] T. Midgley, A.L. Henne, Organic fluorides as refrigerants, Ind. Eng. Chem. 22 (5) (1930) 542–545. Available from: https://doi.org/10.1021/ie50245a031.
[27] M.J. Molina, F.S. Rowland, 6' Evans, H.J., in How crops grow a century later (edit. Horsfa ll, Kennedy. I. R., Biochim. hio phys. Acta, 135(6), pp: 455–458, 1973.
[28] M. Kovochich, C.C.D. Fung, R. Avanasi, A.K. Madl, Review of techniques and studies characterizing the release of carbon nanotubes from nanocomposites: implications for exposure and human health risk assessment, J. Expo. Sci. Environ. Epidemiol. 28 (3) (2018) 203–215. Available from: https://doi.org/10.1038/jes.2017.6.
[29] Asrafuzzaman, K.F. Amin, A. Sharif, M.E. Hoque, Bonding mechanism and interface enhancement of bamboo fiber reinforced composites, in: M. Jawaid, S. Mavinkere Rangappa, S. Siengchin (Eds.), Bamboo Fiber Composites: Processing, Properties and Applications, Springer Singapore, Singapore, 2021, pp. 215–233.
[30] K.F. Amin, Asrafuzzaman, A. Sharif, M.E. Hoque, Bamboo/bamboo fiber reinforced concrete composites and their applications in modern infrastructure, in: M. Jawaid, S. Mavinkere Rangappa, S. Siengchin (Eds.), Bamboo Fiber Composites: Processing, Properties and Applications, Springer Singapore, Singapore, 2021, pp. 271–297.
[31] N. Kumar, P. Kaur, S. Bhatia, Advances in bio-nanocomposite materials for food packaging: a review, Nutr. Food Sci. 47 (4) (2017) 591–606. Available from: https://doi.org/10.1108/NFS-11-2016-0176.
[32] E. Rezvani Ghomi, et al., The life cycle assessment for polylactic acid (PLA) to make it a low-carbon material, Polymers (Basel). 13 (11) (2021). Available from: https://doi.org/10.3390/polym13111854.
[33] A. Morão, F. de Bie, Life cycle impact assessment of polylactic acid (PLA) produced from sugarcane in Thailand, J. Polym. Environ. 27 (11) (2019) 2523–2539. Available from: https://doi.org/10.1007/s10924-019-01525-9.

[34] D. Maga, M. Hiebel, N. Thonemann, Life cycle assessment of recycling options for polylactic acid, Resour. Conserv. Recycl. 149 (2019) 86−96. Available from: https://doi.org/10.1016/J.RESCONREC.2019.05.018.
[35] E.T.H. Vink, K.R. Rábago, D.A. Glassner, P.R. Gruber, Applications of life cycle assessment to NatureWorksTM polylactide (PLA) production, Polym. Degrad. Stab. 80 (3) (2003) 403−419. Available from: https://doi.org/10.1016/S0141-3910(02)00372-5.
[36] S. Nikoliae, F. Kiss, V. Mladenoviae, M. Bukurov, J. Stankoviae, Corn-based polylactide vs. PET bottles - cradle-to-gate LCA and implications, Mater. Plast. 52 (4) (2015) 517−521.
[37] V. Piemonte, Bioplastic wastes: the best final disposition for energy saving, J. Polym. Environ. 19 (4) (2011) 988−994. Available from: https://doi.org/10.1007/s10924-011-0343-z.
[38] T. Nuge, et al., Recent advances in scaffolding from natural-based polymers for volumetric muscle injury, Molecules 26 (3) (2021). Available from: https://doi.org/10.3390/molecules26030699.
[39] J. Anita Lett, et al., Recent advances in natural polymer-based hydroxyapatite scaffolds: properties and applications, Eur. Polym. J. 148 (2021) 110360. Available from: https://doi.org/10.1016/J.EURPOLYMJ.2021.110360.
[40] D. Ita-Nagy, et al., Life cycle assessment of bagasse fiber reinforced biocomposites, Sci. Total Environ. 720 (2020). Available from: https://doi.org/10.1016/j.scitotenv.2020.137586.
[41] Y. Wu, C. Xia, L. Cai, A.C. Garcia, S.Q. Shi, Development of natural fiber-reinforced composite with comparable mechanical properties and reduced energy consumption and environmental impacts for replacing automotive glass-fiber sheet molding compound, J. Clean. Prod. 184 (2018) 92−100. Available from: https://doi.org/10.1016/j.jclepro.2018.02.257.
[42] F. Gu et al., Industrial Crops & Products Can bamboo fi bres be an alternative to fl ax fi bres as materials for plastic reinforcement ? A comparative life cycle study on polypropylene / fl ax / bamboo laminates, 121, no. January, pp. 372−387, 2018, doi: 10.1016/j.indcrop.2018.05.025.
[43] L. El Foujji, K. El Bourakadi, A. El Kacem Qaiss, R. Bouhfid, Characterization and properties of biopolymer reinforced bamboo composites. 2021.
[44] R. Vidal, E. Moliner, P.P. Martin, S. Fita, M. Wonneberger, Life cycle assessment of novel aircraft interior panels made from renewable or recyclable polymers with natural fiber reinforcements and non-halogenated, 22(1), doi: 10.1111/jiec.12544.
[45] O. Väntsi, T. Kärki, Resources, Conservation and Recycling Environmental assessment of recycled mineral wool and polypropylene utilized in wood polymer composites, Resources, Conserv. Recycl. 104 (2015) 38−48. Available from: https://doi.org/10.1016/j.resconrec.2015.09.009.
[46] A. Van Grootel, J. Chang, B.L. Wardle, E. Olivetti, Manufacturing variability drives signi fi cant environmental and economic impact: rhe case of carbon fi ber reinforced polymer composites in the aerospace industry, J. Clean. Prod. 261 (2020) 121087. Available from: https://doi.org/10.1016/j.jclepro.2020.121087.
[47] A.D. La Rosa, D.R. Banatao, S.J. Pastine, A. Latteri, G. Cicala, Recycling treatment of carbon fi bre / epoxy composites: materials recovery and characterization and environmental impacts through life cycle assessment, Compos. Part B 104 (2016) 17−25. Available from: https://doi.org/10.1016/j.compositesb.2016.08.015.
[48] L.J. Rodríguez, S. Fabbri, C.E. Orrego, M. Owsianiak, Comparative life cycle assessment of coffee jar lids made from biocomposites containing poly(lactic acid) and

banana fiber, J. Environ. Manage. 266 (August) (2020). Available from: https://doi.org/10.1016/j.jenvman.2020.110493. 2019.

[49] M. Demertzi, J. Silvestre, M. Garrido, J.R. Correia, V. Durão, M. Proença, Life cycle assessment of alternative building floor rehabilitation systems, Structures 26 (2020) 237–246. Available from: https://doi.org/10.1016/j.istruc.2020.03.060.

[50] A. Daniela, L. Rosa, S.A Grammatikos, R.C. Ciobanu, C.M. Schreiner, Electromagnetic shielding for buildings using hybrid polymer composites: a life cycle assessment study, Key Eng. Mater. 827 (2020) 452–457. Available from: https://doi.org/10.4028/http://www.scientific.net/KEM.827.452.

[51] F. Hermansson, M. Janssen, M. Svanström, Prospective study of lignin-based and recycled carbon fibers in composites through meta-analysis of life cycle assessments, J. Clean. Prod. 223 (2019) 946–956. Available from: https://doi.org/10.1016/j.jclepro.2019.03.022.

[52] Y. Deng, Y. Guo, P. Wu, G. Ingarao, Optimal design of flax fiber reinforced polymer composite as a lightweight component for automobiles from a life cycle assessment perspective, pp. 1–12, 2020, doi: 10.1111/jiec.12836.

# Section 2: Advanced applications

# Polymer nanocomposites for biomedical applications

8

*Habibul Islam*[1], *Md Enamul Hoque*[1] *and Carlo Santulli*[2]
[1]Department of Biomedical Engineering, Military Institute of Science and Technology (MIST), Dhaka, Bangladesh
[2]School of Science and Technology, University of Camerino, Camerino, Italy

## 8.1 Introduction

With the introduction of newer and more sophisticated technology, the applications of the polymer have extended to such an extent that better modification and tailoring of these polymers are needed. Proper temperature exposure, treatment with various energy sources, and chemical modification have been performed on polymeric materials for the aforementioned purpose. Among these modification techniques, tailoring the chemical properties of polymers has been reported to be more effective than other modification techniques. One of the most common procedures of modifying polymer materials to be used in different applications is blending and mixing polymers with different reinforcement materials [1]. Nanomaterials due to their exceptional characteristics have been reported to improve different properties of polymer composite materials. With noticeable improvement in preparation procedures, polymer nanocomposites can surely replace conventional polymer materials in sophisticated applications such as biomedical applications. Polymer nanocomposites have been proved to possess significantly enhanced antibacterial and antifungal activities and many pieces of researches where antimicrobial activities of polymer nanocomposites against different kinds of microbes such as bacteria and fungus support this. Another important property that increases the effectiveness of polymer nanocomposites in biomedical applications is their controllable degradation rate. Bioelimination and controlled degradation are needed for materials used in tissue regeneration, tissue repair, scaffold formation, and various other medical applications. Also, the incorporation of various nanomaterials that include but are not limited to metallic nanoparticles, ceramic nanoparticles, and nanofiber from natural sources by different methods and with different additives has enhanced the properties of polymer-based nanocomposites significantly. The use of metallic and ceramic nanoparticles as incorporating materials increases mechanical and barrier properties where the use of nanofiber reinforcement into polymer matrices increases bioactivity and biocompatibility of the composites and due to these reasons often more than one type of nanofillers have been reported to be used in polymer matrices. Also, nanoparticles have shown a limited amount of toxicity which allows these nano-sized particles incorporated polymer materials to be used in biomedical applications where these materials would come into direct contact with the human body.

**Advanced Polymer Nanocomposites. DOI:** https://doi.org/10.1016/B978-0-12-824492-0.00016-7


## 8.2 Polymer nanocomposites and their preparation

Composites made from polymer or copolymer matrices and nanomaterials filler reinforcements where matrices and reinforcement materials have distinctive phases and properties. Polymer nanocomposites consist of polymer matrices and filler materials. For polymer matrices, synthetic polymers such as polyamide, polyethylene, polypropylene, polyurethane, epoxy-based polymers, polyelectrolyte, and rubber matrices [2,3]; biopolymers such as starch, chitosan, cellulose, lipid, collagen, gelatin, alginate, polyhydroxyalkanoates [4], polyisoprenes [5], peptides, and other polysaccharides [6]; and biopolymers derived materials like cellulose acetate are used. Some other synthetic biodegradable polymers such as polyglycolic acid, polyhydroxy butyrate, polycaprolactone, and nylon-2-nylon-6 can also be used as polymer matrices to form polymer nanocomposites [3,4]. Among the nano-reinforcements used as filler in polymer nanocomposites, some common ones include metal nanoparticles like silver, zinc, palladium, copper, gold, cobalt, and nickel nanoparticles [7]; nonmetal nanoparticles such as carbon nanotubes, nanodiamond, layered silicate, MXene [8]; graphene and nano-clay and natural fibers that include cellulose nanocrystal and other nanofibers [3,9,10]. Although the preparation of polymer nanocomposites seems fairly simple, many different synthesis processes have been developed to optimize the synthesizing process to keep the cost low as well as the process simple. Among various synthesis techniques in situ polymerization, solution casting technique, emulsion polymerization, solution intercalation, melt intercalation, and template synthesis are the most common polymer nanocomposite synthesis techniques [11–15]. Table 8.1 represents processing techniques and required conditions of polymer nanocomposites with different polymer matrices and nano-reinforcements.

## 8.3 Antimicrobial activities of polymer nanocomposites

The tailoring ability of polymer nanocomposites enables these materials to be biocompatible, biodegradable, and to show antibacterial and antifungal activities. By using a proper processing environment, doping materials, additives, and surfactants antimicrobial characteristics of polymer nanocomposites can be significantly enhanced. Many pieces of researches have shown the potential antimicrobial activities of polymer-based nanocomposites especially composites with metal nanoparticles as reinforcement materials as metal nanoparticles can exhibit selective toxicity against bacteria [38,39]. Also, green polymer composites with cellulose and chitosan nanofibers have shown excellent antimicrobial activities [40–43]. Polymer nanocomposites made from poly(vinyl alcohol) and graphene oxide incorporated with silver nanoparticles showed no antibacterial activity against different kinds of bacteria which includes *Escherichia coli* and *Staphylococcus aureus* but antimicrobial activity was reported to increase with the loading of reinforcement materials only within 24 hours when the composites were tested for antimicrobial activity by

**Table 8.1** The preparation techniques of various polymer nanocomposites.

| Polymer matrices | Filler materials | Processing techniques | Processing environments | Reference |
|---|---|---|---|---|
| Polystyrene | VISCOGEL S4 and VISCOGEL S7 MMT clay | Melt Intercalation | $150^{\circ}C-190^{\circ}C$ | [16] |
| Poly(ε-caprolactone) | Cloisite30B | Melt extrusion | $150^{\circ}C$, 25 rpm, and 3 kg $h^{-1}$ polymer flow | [17] |
| Eudragit RS | Cloisite Na, Cloisite 20 | Melt extrusion | $160^{\circ}C$, 100 rpm, and 0.3 kg $h^{-1}$ polymer flow | [18] |
| Polypropylene | Zirconium phosphate | Melt extrusion | 60 rpm | [19] |
| Poly(ethylene oxide) | Lithium montmorillonite | Melt intercalation | $90^{\circ}C$ for 8 h | [20] |
| Polycaprolactone | Layered double hydroxides (ca/al) | Melt blending | $120^{\circ}C$ for 10 min at 60 rpm | [21] |
| Polypropylene (pyrene-functionalized maleic anhydride-grafted) | Graphene nanoplatelet | Solvent-assisted melt blending | $200^{\circ}C$ for 10 min at 100 rpm | [22] |
| Polylactide | Silica nanoparticles | Melt blending | $175^{\circ}C$ for 3 min at 40 rpm | [23] |
| Nylon 6 | Graphene oxide | In situ polymerization | $80^{\circ}C$ for 30 min | [24] |
| Epoxy | Graphene oxide | In situ polymerization | $50^{\circ}C$ and *m*-phenylenediamine additive | [25] |
| Polyimide | Graphene oxide | In situ polymerization | $-5^{\circ}C$ to $0^{\circ}C$ for 10 h | [26] |
| Polyurethane | Graphene nanosheet | In situ polymerization | Hydrazine as reducer | [27] |
| Polyaniline | Montmorillonite clay | In situ polymerization | Stirring at $50^{\circ}C$ for 2 h | [28] |

(*Continued*)

**Table 8.1** (Continued)

| Polymer matrices | Filler materials | Processing techniques | Processing environments | Reference |
|---|---|---|---|---|
| Polyimide | Boron nitride nanotubes | In situ polymerization | Lead zirconate titanate, poly (vinylidene fluoride), and carbon nanotube | [29] |
| Polyaniline | Nano-fly ash | Inverted emulsion polymerization | 80°*C* for 24 h | [30] |
| Polystyrene and poly(butyl methacrylate) | Lignin nanoparticles | Pickering emulsion polymerization | Chitosan and glucose oxidase additives | [31] |
| Poly(vinyl acetate) | Cellulose nanocrystal | Emulsion polymerization | – | [32] |
| Polyvinyl acetate | Colloidal silica nanoparticles | Emulsion polymerization | Stirring at 450 rpm for 30 min | [33] |
| Poly(methyl methacrylate) | Holmium orthovanadate | Emulsion polymerization | Blending at room temperature | [34] |
| Polyacrylamide | Functionalized-multiwalled carbon nanotubes | Inverted emulsion polymerization | Sonication for 20 min | [35] |
| Poly(methyl methacrylate) | Cellulose nanofiber | Pickering emulsion polymerization | 25°*C* for 12 h | [36] |
| chitosan | Hydroxyapatite nanoparticle | Coprecipitation method | – | [37] |

a modified EUCAST dilution method [44]. Polymer nanocomposite prepared from cellulose and silver nanoparticles demonstrated exceptional antibacterial activity against *E. coli* and *S. aureus* when tested by disk diffusion method which is shown in Fig. 8.1 [45].

Polymer nanocomposites made from polyurethane, titanium nanoparticles, silver nanoparticles, and benzoic acid by solution casting method were tested for proof of antibacterial characteristics against *Pseudomonas aeruginosa* and *S. aureus* that are Gram-positive and Gram-negative bacteria, respectively. The result of the antimicrobial assessment showed no antibacterial activity for pure polyurethane but polyurethane and silver nanocomposites showed a 99% reduction in *S. aureus* with only 0.5 wt% reinforcement. Although titanium nanoparticles and benzoic acid have less antibacterial activity compared to silver nanoparticles, it was still a better result than pure polyurethane [46]. Composite films made from chitosan, glycerol monolaurate, titanium oxide nanoparticles also showed antibacterial characteristics by attacking bacterial cells with 1.5 wt% of filler loading [47]. A similar kind of results was observed by composites made from polyvinyl alcohol as polymer

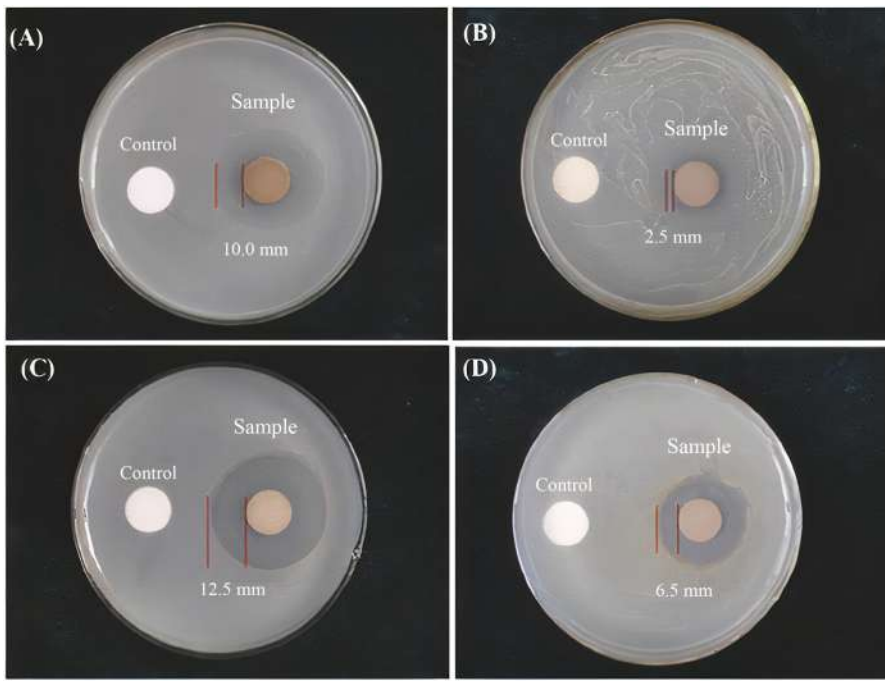


**Figure 8.1** Antibacterial activity of cellulose and silver nanocomposites against *Escherichia coli* (A and C) and *Staphylococcus aureus* (B and D).
*Source*: Reprinted with permission from S.M. Li, N. Jia, M.G. Ma, Z. Zhang, Q.H. Liu, R.C. Sun, Cellulose-silver nanocomposites: microwave-assisted synthesis, characterization, their thermal stability, and antimicrobial property, Carbohydr. Polym. 86 (2) (2011) 441−447, doi: 10.1016/j.carbpol.2011.04.060, Copyright (2011) Elsevier.

matrices, graphene oxide nanoparticles as reinforcement, and potassium chloride as a salt spacer by solvent casting that was assessed for antimicrobial activity against *P. aeruginosa*, *Campylobacter jejuni*, *E. coli* and *S. aureus* bacterial strains and *Candida albicans*, *Trichoderma harzianum*, and *Aspergillus niger* fungal strains [48]. Composites made from cotton and polyethylene terephthalate containing 3% silver ion-exchange zeolite also showed antibacterial and antifungal characteristics [49]. Natural rubber latex foam reinforced with silver nanoparticles prepared by Rathnayake and coworkers was assessed for antibacterial activity by agar diffusion method and was reported to show excellent inhibiting characteristics against Gram-negative bacteria *E. coli* which is shown in Fig. 8.2 [50].

Starch-based polymer nanocomposites were prepared where starch was used as thermoplastic polymer matrices with zinc oxide nanoparticles. The resultant composite material demonstrated better antimicrobial characteristics against *E. coli* and *S. aureus* compared to the antimicrobial properties of starch without reinforcements [51]. Bacterial growth inhibition of 55% against Gram-positive and Gram-negative bacteria was observed from piezoelectric polyvinylidene fluoride-based polymer

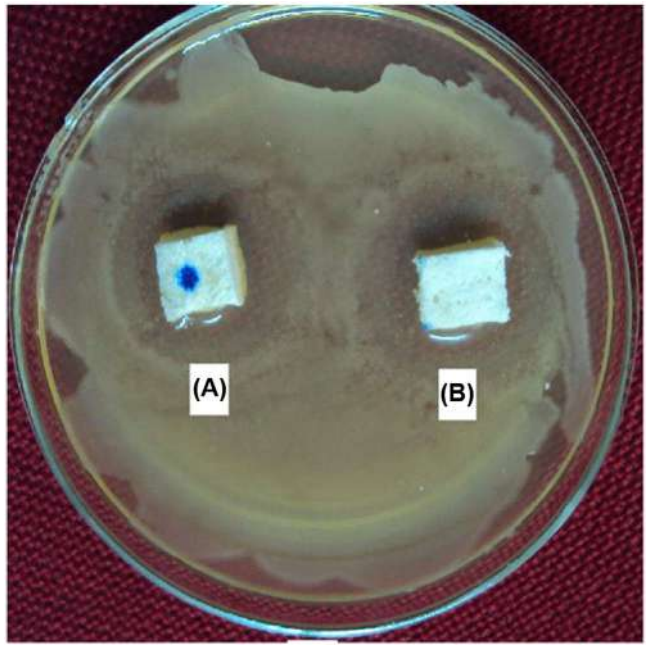


**Figure 8.2** Antimicrobial properties of (A) pure natural rubber latex foam and (B) natural rubber latex foam reinforced with silver nanoparticles.
*Source*: Reprinted with permission from W.G.I.U. Rathnayake, H. Ismail, A. Baharin, A.G. N.D. Darsanasiri, S. Rajapakse, Synthesis and characterization of nano silver based natural rubber latex foam for imparting antibacterial and anti-fungal properties, Polym. Test. 31 (5) (2012), 586−592, https://doi.org/10.1016/j.polymertesting.2012.01.010, Copyright (2012) Elsevier.

nanocomposites incorporated with nickel nanowires as fillers [52]. Composites made from polyacrylonitrile with incorporated silver nanoparticles showed excellent antibacterial characteristics against *E. coli*, *S. aureus*, and *Bacillus subtilis* and antifungal activity against *C. albicans* and *A. niger* by inhibition zone and reduction measurement [53]. Chlorosulfonated polyethersulfone-based nanocomposites were synthesized by preparing polymer matrices by sulfonation and chlorination and using zinc oxide nanoparticles as filler materials. This composite showed excellent microbial inhibition compared to unmodified composites along with better water permeability [54]. Polymer nanocomposite films from k-Carrageenan, hydroxyl ethyl cellulose, silicon dioxide, and silver nanoparticles were prepared by solvent evaporation method with different amounts of reinforcements. The composite was tested for antimicrobial activities against *S. aureus* and *Bacillus cereus* by well diffusion method and by assessment of their inhibition zone, these composites showed great promise to be used in biomedical applications as biocompatible and antimicrobial materials [55]. Cao et al. developed polyvinylpyrrolidone and polyvinyl alcohol-based polymer nanocomposites with the incorporation of titanium dioxide nanoparticles. The composites showed enhanced bacterial inhibition compared to neat polyvinylpyrrolidone and polyvinyl alcohol blend without any reinforced nanoparticles which is demonstrated in Fig. 8.3 [56].

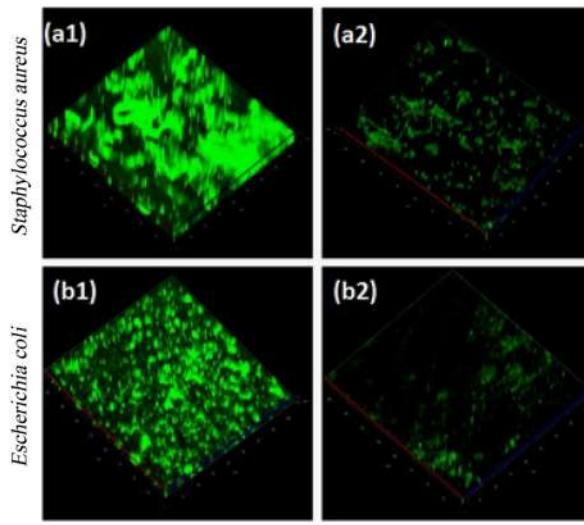


**Figure 8.3** Confocal laser scanning microscopic images of neat polyvinylpyrrolidone and polyvinyl alcohol blend (A1 and B1) and polyvinylpyrrolidone and polyvinyl alcohol polymer composites with incorporated titanium dioxide nanoparticles (A2 and B2).
*Source*: Reprinted with permission from L. Cao, X. Wu, Q. Wang, J. Wang, Biocompatible nanocomposite of $TiO_2$ incorporated bi-polymer for articular cartilage tissue regeneration: a facile material, J. Photochem. Photobiol. B Biol. 178 (2018) 440−446, https://doi.org/10.1016/j.jphotobiol.2017.10.026, Copyright (2018) Elsevier.

## 8.4 Biocompatibility and biodegradation of polymer nanocomposites

To be used in different medical applications a material should be biocompatible, bioactive, nontoxic, and susceptible to bioelimination. Usually, synthetic polymers are not biocompatible and biodegradable. Also, conventional polymers can break into microplastics which can directly play an active part as carcinogenic compounds. Many researchers have tried to find an alternative solution for these harmful materials that can be used in biomedical applications without any concern and recent studies have shown the potential of polymer nanocomposites in fulfilling these criteria [57]. Green polymer composites made from biopolymers such as starch, alginate, and chitosan and biopolymers derived polymers such as cellulose acetate as polymer matrices and nanofibers extracted from natural resources as fillers have already gained popularity in various medical applications. Various polymer nanocomposites based on natural and synthetic polymers are reported to have biocompatibility and biodegradability. For instance, natural polymers such as cellulose, silk, shellac, and gelatin and synthetic polymers like polycaprolactone, poly(lactic-*co*-glycolic acid), polylactic acid, and poly(glycerol-*co*-sebacate) act as biocompatible as well as biodegradable polymers where polyaniline, polypyrrole, poly(3,4-ethylene dioxythiophene), poly (vinyl alcohol), polydimethylsiloxane, etc. act as biocompatible polymers. By the addition of adequate additives and nanoparticles, the degradation properties and biocompatibility of these polymers can be enhanced along with significant improvement over other characteristics such as barrier properties, mechanical strength, and thermal properties [1], [58–61]. Polymer nanocomposites made from chitosan and montmorillonite nanoparticles were prepared, and cytotoxicity and cell proliferation were examined by WST-1 test and wound-healing measurements. Fig. 8.4 shows the cell viability percentage of different amounts of chitosan, montmorillonite, and chitosan/montmorillonite composites after 3 hours [62].

Biocompatible electrodes were developed from polymer nanocomposites made from thiadiazole moiety modified styrene-maleic anhydride copolymer with the incorporation of zinc oxide nanoparticles where biocompatibility of the developed electrodes was assessed by preliminary cell viability studies performed on 3T6 mouse fibroblast cells [63]. Cytotoxicity and cell viability test of composites of poly(acrylonitrile-butadiene-styrene) and silver nanoparticles were assessed on osteoblasts nor the fibroblast cells which showed a slight increase in cytotoxicity for osteoblast cells but that decreased within seven days of the culture [64]. Csarnovics and coworkers developed polyurethane-based polymer-metallic nanocomposites by incorporating gold, silica, zinc oxide, and titanium oxide nanoparticles into diurethane dimethacrylate which showed excellent biocompatibility when viability and activation level of human monocyte-derived dendritic cells were measured [65]. Cao et al. developed a biocompatible polymer hydrogel made by reinforcing titanium dioxide nanoparticles into polyvinylpyrrolidone and polyvinyl alcohol blend. The composites developed showed excellent biocompatibility results [56]. Prepared biocompatible polymer nanocomposites from high-density polyethylene, 1.8 wt % alumina nanoparticles, and 1.2 wt% multiwalled carbon nanotubes. Biocompatibility

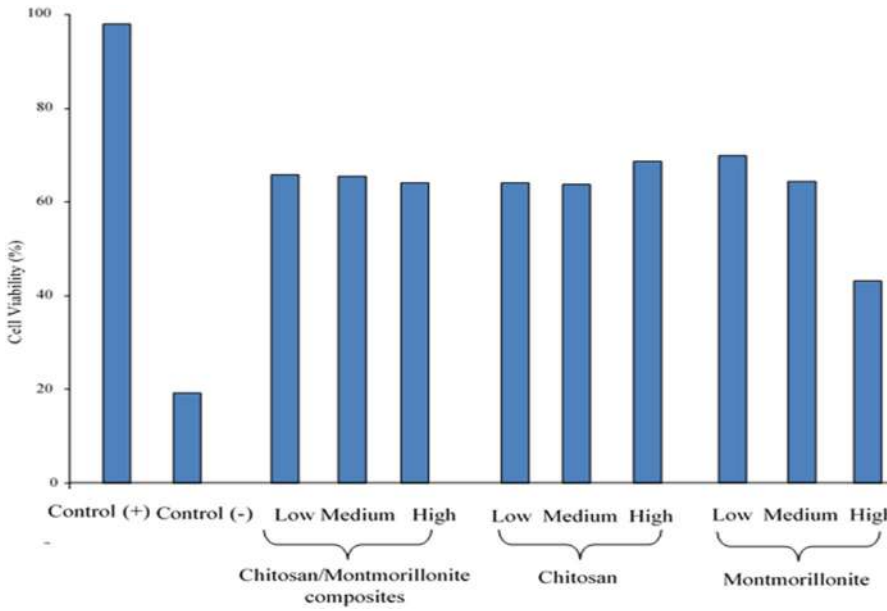


**Figure 8.4** Cell viability percentage of different amounts of chitosan, montmorillonite and chitosan/montmorillonite composites after 3 h.
*Source*: Reprinted with permission from I. Salcedo et al., In vitro biocompatibility and mucoadhesion of montmorillonite chitosan nanocomposite: a new drug delivery, Appl. Clay Sci. 55 (2012) 131−137, https://doi.org/10.1016/j.clay.2011.11.006, Copyright (2012) Elsevier.

of the mentioned material was assessed by cytotoxicity tests against normal skin fibroblast which is shown in Fig. 8.5 [66].

Biodegradation of materials used in biomedical applications is another concern along with biocompatibility and nontoxicity. Materials used in different medical applications are needed to be biologically eliminated after specific functions. By using nanocomposites within various biodegradable polymer biodegradation properties of a material can be tailored according to the specific need. Many pieces of researches reported the viability of nano-clay as nano-reinforcement in polymer matrices. Biodegradation of polymers can happen by depolymerization of the polymer either by nonenzymatic degradation through water, thermal treatment, and physical environments or enzymatic degradation by microbes. As water absorbed by a polymer material causes hydrolysis of polymer chains to be more hydrophilic the nature of reinforcements more susceptible the polymer is to biodegradation [67]. Also, many natural fillers used as reinforcement materials are susceptible to microbial attack which lead the material with porous structure ultimately better subjected to bio-disintegration [68]. Cellulose nanocrystals being hydrophilic and susceptible to microbial attack can enhance the biodegradation rate of polymer nanocomposites [69]. Poly(butylene adipate-*co*-terephthalate) polymer-based composites incorporated with cellulose nanocrystals showed enhanced biodegradation

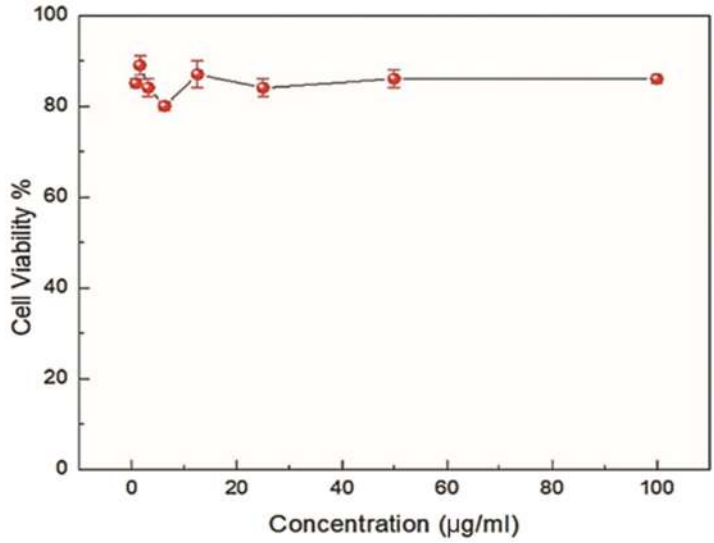


**Figure 8.5** Cell viability percentage of high-density polyethylene/multiwalled carbon nanotubes/$Al_2O_3$ nanocomposites over human cell lines.
*Source*: Reprinted with permission from S. Dabees, B.M. Kamel, V. Tirth, A.B. Elshalakny, Experimental design of $Al_2O_3$/MWCNT/HDPE hybrid nanocomposites for hip joint replacement, Bioengineered 11 (1) (2020) 679−692, doi: 10.1080/21655979.2020.1775943, Copyright (2020) Taylor and Francis.

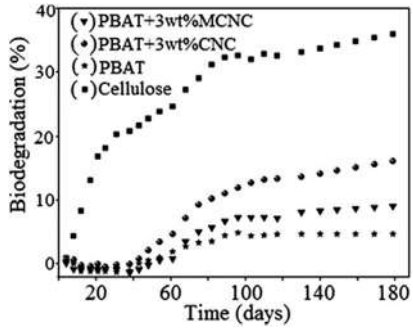


**Figure 8.6** Biodegradation rate of cellulose, poly(butylene adipate-*co*-terephthalate), and their composites.
*Source*: Reprinted with permission from I.F. Pinheiro et al., Mechanical, rheological and degradation properties of PBAT nanocomposites reinforced by functionalized cellulose nanocrystals, Eur. Polym. J. 97 (2017) 356−365, https://doi.org/10.1016/j.eurpolymj.2017.10.026, Copyright (2017) Elsevier.

as water absorbed by cellulose nanocrystals break the heterogenous chains of polyester. Fig. 8.6 shows biodegradation rate of cellulose and poly(butylene adipate-*co*-terephthalate)/cellulose nanocrystal composites [70].

Due to their hydrophilic nature, natural fibers can enhance the biodegradation rate of polymer nanocomposites when reinforced into polymer matrices. Metal oxides such as copper oxide have shown potential to enhance biodegradation properties of sodium alginate along with an increase in mechanical strength was reported by Padma et al. [71]. To use in applications where longer disintegration time is needed carbon nanotubes can replace natural fillers. Reported the synthesis of semibiodegradable nanocomposites based on polypropylene and poly(lactic acid) blend incorporated by carbon nanotubes [72]. Reinforcement of cellulose nanofibers into poly (butylene succinate) decreased biodegradation time from 80 days for poly(butylene succinate) without any reinforcements to 60 days [73].

## 8.5 Polymer nanocomposites for biomedical applications

Polymer nanocomposites have been reported to show great potential to be used in biomedical applications due to their excellent barrier properties, mechanical strength, thermal stability, biocompatibility, and nontoxicity. Better barrier properties of polymer nanocomposites enable these composites to be used in applications where an inert material is needed. Applications such as prosthetic devices, medical implants, and medical devices need materials to be mechanically strong and thermally stable. Also in vivo applications such as 3D bioprinting, drug delivery, biosensing, and tissue engineering need bioactive, biocompatible, and biodegradable materials. All of these criteria can be met by polymer nanocomposites due to their aforementioned properties.

### *8.5.1 Polymer nanocomposites in bioprinting*

Recent advancements in processing techniques and ease of property control have made polymer nanocomposites a prominent candidate for 3D bioprinting applications where a procedure based on additive manufacturing is used to imitate any biological tissues or organs. Bioinks used in 3D and 4D bioprinting need to be bioactive, biocompatible, and nontoxic. In addition to these properties, characteristics such as similar degradation kinetics as extracellular matrices, printability, biomimicking ability, and acceptable structural and mechanical properties are essential [74,75]. Due to these exceptional characteristics, various polymer nanocomposites have been reported to be used as bioinks for potential 3D and 4D bioprinting applications. Generally, polymer composites from natural sources show better biocompatibility and biodegradation characteristics. Also, the by-products of natural polymer-based nanocomposites are nontoxic which makes these materials ideal to be used in bioprinting applications. Also, the bioactivity of these materials allows a dynamic environment of the materials which is also known as 4D bioprinting. For example, any polymer composites with cellulose nanofibers as reinforcement material allow biodegradation of cellulose faster which results in porous inside the material to support better bio-disintegration. The construction of bioinks generally

depends on cross-linking and although using naturally or synthetically derived biodegradable polymers can solve the bioelimination issues the weakness of these polymers lies in inferior mechanical strength and their ability to uptake moisture from the environment [76–78].

Polymer nanocomposites made by incorporating $Ti_3C_2$ MXene nanosheets into hyaluronic acid and alginate blend have shown excellent printability as bioinks with relatively better biocompatibility in extrusion-based 3D bioprinting [79]. Markstedt and coworkers bioprinted human chondrocytes with nanocellulose-alginate biolink for cartilage tissue engineering applications. Fig. 8.7 demonstrates bioprinted human ears from the aforementioned bioink materials [80].

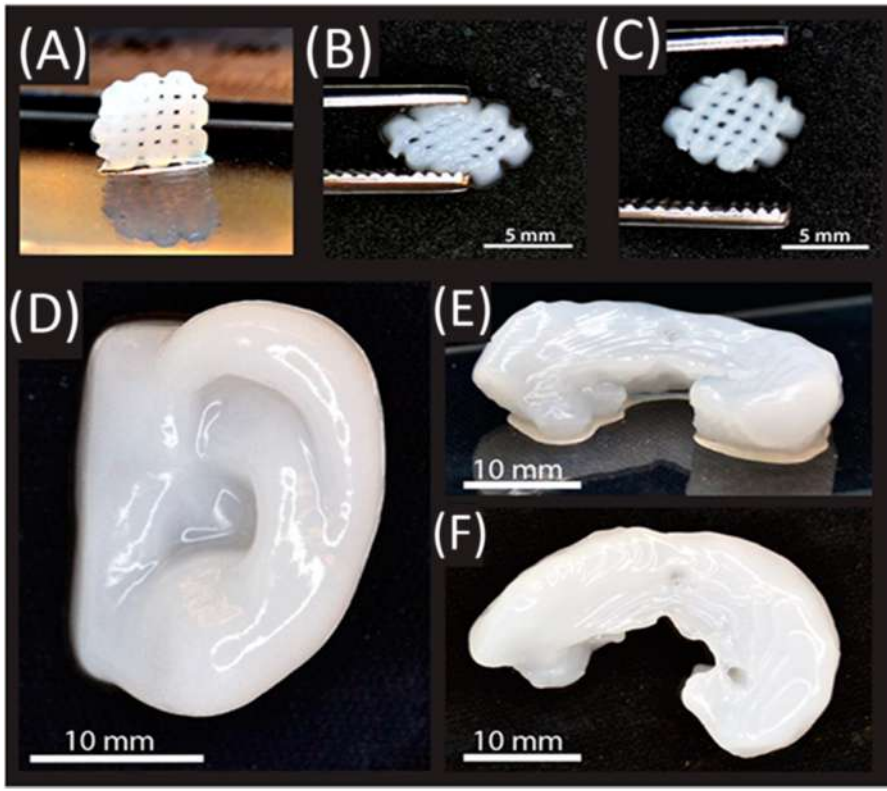


**Figure 8.7** (A) 3D printed small grids after cross-linking. (B and C) The shape of the grid deforms while squeezing, and after squeezing. (D) 3D printed human ear and (E) side view of sheep meniscus (F) top view of sheep meniscus.
*Source*: Reprinted with permission from K. Markstedt, A. Mantas, I. Tournier, H. Martínez Ávila, D. Hägg, P. Gatenholm, 3D bioprinting human chondrocytes with nanocellulose-alginate bioink for cartilage tissue engineering applications, Biomacromolecules 16 (5) (2015) 1489–1496, doi: 10.1021/acs.biomac.5b00188, Copyright (2012) American Chemical Society.

Besides cellulose and lignin-based natural fillers, nano-clay has also the potential to be used in bioprinting applications. Table 8.2 shows bioinks based on different nano-clay materials, their printing techniques, and biocompatibility assessment results.

### 8.5.2 Polymer nanocomposites in tissue engineering

Polymer nanocomposites based on different polymer matrices and nanofillers such as metal nanoparticles, clay nanoparticles, and nanofibers from natural sources have been studied extensively as potential materials in tissue engineering applications that include but are not limited to bone, ligament, and other types of tissue regeneration, scaffold designing, and simulation studies for research purpose. A porous scaffold model to heal femur fractures was made by Esmaeili and coworkers by reinforcing hydroxyapatite ceramic nanoparticles into polylactic acid [92]. 3D porous polymer nanocomposites made from thermoplastic starch and graphene oxide reinforcement materials by thermally induced phase separation technique showed no toxicity to cells and also took part in cell proliferation which ultimately ensured the possibility to be used in tissue engineering applications [93].

Hydroxyapatite nanoparticles, carbon nanotubes, metal nanoparticles, nano-clay, and nanofibers as nanofillers for polymer nanocomposites have shown prominent possibilities in tissue engineering applications.

Hydroxyapatite nanoparticles incorporated in polysaccharide and polypeptidic matrices such as chitosan, gelatin, and alginate or their blends have shown increased biocompatibility, bioactivity which allows better cell adhesion, proliferation, and expression of osteoblasts and other connective tissues ultimately showing great potential to be used in wound healing, pharmaceutical adhesives, hard tissue scaffolds, and other tissue engineering applications [94–98]. A scaffold for human umbilical cord blood-derived mesenchymal stem cells from hybrid material was developed by Huang and coworkers by doping gelatin with hydroxyapatite nanoparticles to by microextrusion 3D bioprinting and enzymatic cross-linking with properties that enable cell adhesion, proliferation, and division. Acute injury of the articular cartilage in a pig model was repaired by this scaffold when implanted [99]. Sun and coworkers prepared gelatin/hydroxyapatite fibers nanocomposites incorporated with metformin by electrospinning. Cytotoxicity, cell adhesion, cell differentiation, and quantitative osteogenic gene and protein expression analysis on bone marrow stem cells from rats showed the potential of the material to heal critical-size bone defects [100]. Khan and coworkers prepared a scaffold from arabinoxylan-*co*-acrylic acid, hydroxyapatite nanoparticles, aluminum oxide nanoparticles, and graphene oxide by freeze-drying technique to use in bone tissue regeneration application [101]. Polycaprolactone is a biodegradable polyester that has great potential to be used in various tissue engineering applications. Table 8.3 shows different cases of polycaprolactone-based nanocomposites, their fabrication techniques, and various applications.

Other synthetically prepared poly(propylene fumarate), polylactic acid, polyvinyl alcohol, and polyurethane-based nanocomposites have also been studied extensively for tissue regeneration and repair applications [111]. Carbon nanotubes incorporated

**Table 8.2** Bioinks based on different nano-clay materials and their various aspects.

| Polymer matrices | Filler materials | Printing technique | Biocompatibility | Reference |
|---|---|---|---|---|
| Alginate and carboxymethyl cellulose | Montmorillonite | Extrusion-based printing | 94% cell viability against human pancreatic cancer cells, | [81] |
| Poly(ethylene glycol) diacrylate | Laponite nanodisk | Extrusion-based printing | 96% cell viability murine preosteoblasts | [82] |
| Poly(ethylene glycol) diacrylate, alginate and gelatin | Laponite nanodisk | Extrusion-based printing for the cup and triple-walled tubular structures | Increased cell viability against NIH-3T3 mouse fibroblasts compared to copolymer blends | [83] |
| Poly(ethylene glycol)-b-poly (propylene glycol)-B-poly (ethylene glycol) and poly(*N*-isopropyl acrylamide) | Laponite clay | Extrusion type printing | More than 90% cell viability against L929 fibroblasts | [84] |
| Agarose | Laponite nanodisk | Extrusion-based printing | 50 times more cells spreading against HeLa and NIH/3T3 cells compared to neat agarose | [85] |

| | | | | |
|---|---|---|---|---|
| Poly(acrylamide) and agarose | Laponite clay | Melt extrusion printing | – | [86] |
| Poly(trimethylene carbonate)-*co*-poly(ethylene glycol)-*co*-poly (trimethylene carbonate)-methacrylic anhydride | Laponite nanodisk | Stereolithography | Cell viability against macrophages | [87] |
| Gelatin methacrylate | Laponite nanodisk | Extrusion-based printing | 60% cell viability against preosteoblast cell lines and NIH MC3T3 fibroblasts | [88] |
| Sodium alginate | Laponite disk | Extrusion-based printing | – | [89] |
| Sodium alginate and polyethylene glycol diacrylate | Laponite disk | Extrusion-based printing | 100% cell viability against bone marrow-derived human mesenchymal stem cells and human embryonic kidney 293 cells | [90] |
| Alginate and methylcellulose | Laponite disk | Extrusion-based printing | 70%−75% cell viability human mesenchymal stem cells | [91] |

**Table 8.3** Different polycaprolactone-based nanocomposites and their various aspects.

| Polymer blend | Reinforcement nanomaterials | Processing techniques | Applications | Reference |
|---|---|---|---|---|
| Polycaprolactone and gelatin blend | Nanohydroxyapatite | Electrospinning method | Scaffold for bone tissue engineering | [102] |
| Poly(ε-caprolactone) and chitosan blend | Hydroxyapatite nanoparticles | Electrospinning method | Scaffold for bone tissue engineering | [103] |
| Poly glycerol sebacate and polycaprolactone blend | Carbon quantum dots | Electrospinning method | Scaffold for cardiac tissue engineering | [104] |
| Polycaprolactone | Montmorillonite nanocomposite | Electrospinning method | Wound dressing application | [105] |
| Polycaprolactone | Folic acid modified zinc oxide nanoparticles | Sonochemical method | Bone tissue engineering | [106] |
| Polycaprolactone | Monolithic graphene foam | Inductive heating chemical vapor deposition growth process and | Nerve tissue engineering | [107] |
| Poly-ε-caprolactone | NaCl mixed with hydroxyapatite (HA) or aluminum oxide nanoparticles | Solvent casting or particulate leaching method | Osteogenesis promotion for bone tissue regeneration | [108] |
| Polycaprolactone nanofibers | Porous graphitic carbon nitride nanosheets | Electrospinning method | Bone tissue engineering | [109] |
| Cisplatin loaded polycaprolactone | Zeolite nanocomposite | Two-step particulate leaching-freeze-drying approach | Scaffolds for bone cancer treatment | [110] |

into natural and synthetic polymers have also drawn attention in biomedical applications. Carbon nanotubes/polyurethane nanocomposite was used to prepare scaffolds for cardiac tissue engineering applications where the prepared scaffolds showed cytocompatibility for H9c2 cells and human umbilical vein endothelial cells which ensured proper interactions between the scaffold and cardiomyoblasts [112]. A scaffold for bone tissue engineering was prepared from chitosan, bioactive glass, and carbon nanotubes hot press, and salt leaching process and cross-linked by hexamethylene diisocyanate. Cell adhesion and proliferation of MG63 osteoblast cell line for the prepared scaffolds were assessed by MTT assay and showed potential to be used in bone tissue engineering applications [113]. Multiwalled carbon nanotubes were incorporated into biocompatible poly(L-lactic acid) by Vicentini and coworkers to prepare a two-dimensional film for neural tissue engineering through electrospinning. The prepared scaffold showed excellent biocompatibility and bioactivity toward the human neuronal precursor cell line [114]. Wu et al. reported no neurotoxicity against Schwann cells for chitin and carbon nanotubes prepared by solution blending into a solution of $CH_4N_2O$ and NaOH [115]. Similar kinds of results were observed for graphene oxide acrylate/carbon nanotube/poly(ethylene glycol) acrylate composites against PC12 cell line [116], multiwalled carbon nanotubes/poly(2-hydroxyethyl methacrylate) against neuroblastoma cells [117], and polylactic acid/multiwalled carbon nanotubes/gelatin nanofibers against Schwann cells [118].

Metal and metal oxide nanoparticles due to their inert activities have been considered to be used in medical applications where antiinflammatory conditions must be met. Many pieces of researches have proved metal and metal oxide nanoparticles as potential reinforcement materials with polymer matrices to be used in tissue engineering applications. Balaji et al. prepared polymer nanocomposites from polypyrrole, reduced graphene oxide, and palladium nanoparticles. Limited cytotoxicity and enhanced antimicrobial properties made the composites a prime candidate for orthopedic tissue engineering [119]. Kolathupalayam Shanmugam et al. prepared composite by incorporating titanium oxide nanoparticles into chitosan and sodium alginate blend via solvent casting method which showed superior biocompatibility along with excellent biodegradation and mechanical properties suitable for bone tissue engineering applications [120]. Similar result was observed from polymer composites made from poly(lactic acid)/cellulose nanocrystals [121], polyvinyl alcohol/hydroxyapatite nanoparticles/folic acid/methotrexate [122], and poly(ε-caprolactone)/surface-oxidized cellulose nanocrystals [123].

### 8.5.3 Polymer nanocomposites for drug delivery

Polymer nanocomposites due to their exceptional biocompatibility, bioactivity, and nontoxic properties can be modified for controlled drug release to a specific location in the body by acting as drug carriers. Drug carriers from biocompatible polymer nanocomposites excite no inflammatory response when exposed to in vivo conditions which can successfully enable polymer nanocomposites to work in controlled drug release applications. Various polymer nanocomposites have been

considered as potential drug delivery capsules by optimizing the use of enzymes, pH sensing, temperature sensing, reducing agents, electrical field, and other parameters. Mallakpour et al. fabricated drug carrier polymer nanocomposites from starch as polymer matrices and D-glucose modified multiwalled carbon nanotube via the sonochemical method. Entrapment efficiency, loading capacity, and in vitro release study for zolpidem for the composites were assessed and the assessment showed the potential of the polymer nanocomposites to be used in drug delivery system as a hydrophobic drug model [124]. Drug carrying capabilities of halloysite nanotubes were ensured by assessing the entrapment ability of hydrophilic and lipophilic substances of halloysite nanotubes based polymer nanocomposites [125]. Chitosan acts as a positively charged material in an environment with low pH due to the protonation characteristics of the amino groups of chitosan which allows chitosan and chitosan-based composites suitable for pH-sensitive drug delivery systems [126–128]. Babu et al. utilized this property of chitosan to create novel drug delivery systems for lung cancer treatment by incorporating chitosan nanoparticles into polylactic acid-*co*-glycolic acid modified with RGD (arginine-glycine-aspartic acid) peptide. The prepared composites encapsulate and deliver cisplatin to lung cancer cells which attacks the integrin $\alpha v\beta 3$ receptor of lung cancer and also shows limited cytotoxicity toward normal cells around the target site [129]. Gerami and coworkers prepared a pH-sensitive drug delivery system using the protonation behavior of chitosan by preparing polymer composites made from chitosan/polyvinylpyrrolidone/hematite nanoparticles by an oil-in-water emulsification method to encapsulate and deliver doxorubicin to the target site [130].

Due to their large $sp^2$ hybridized carbon area, graphene and graphene-based material can also be potentially used in drug and gene delivery applications. Stable $\pi-\pi$ stacking interactions between the aromatic rings and the graphene surface makes drugs with planar aromatic domains like a chemotherapy drug doxorubicin [131,132]. Zhang and coworkers prepared such a system for delivering anticancer drug doxorubicin along with Bcl-2-targeted short interfering RNA by loading and delivering these into polymer nanocomposites made from polyethylenimine and conjugated graphene oxide. The drug delivery system showed significant enhancement in chemotherapy efficacy [133]. A chemotherapy drug, 5-fluorouracil, and an antiinflammatory drug, Ibuprofen was delivered by a composite prepared by Rana et al. from chitosan and functionalized graphene oxides where the drug release was controlled by the solubility of the polymer composite [134]. Ibuprofen is an antiinflammatory drug with poor solubility performance in water which can also be solved by loading ibuprofen into polyvinylpyrrolidone nanofibers which showed faster dissolution of the drug [135]. Iron oxide-doped silica nanoparticles were incorporated into polymer brushes consisting of poly(NIPAM-*co*-GMA) by surface-initiated reversible addition-fragmentation chain transfer polymerization by Pourjavadi and coworkers. The composites prepared were then modified with hydrazine groups to provide the composites with binding sites for doxorubicin which is a drug used for cancer treatment [136]. Graphene oxide/poly(2-hydroxyethyl methacrylate)-*g*-poly(lactide)-b-polyethyleneglycol-b-poly(2-hydroxyethyl methacrylate)-g-poly(lactide) composites prepared by reversible addition-

fragmentation chain and ring open polymerization also showed limited cytotoxicity with an encapsulation efficiency of around 82% when used as a carrier for doxorubicin [137]. Doxorubicin was also reported to be encapsulated within polymer nanocomposites made from graphene and *N*-phthaloylchitosan−graft-poly(methylmethacrylate-block-(polyethylene glycol methacrylate -random-dimethyl aminoethyl methacrylate)) via reversible addition-fragmentation chain transfer polymerization [138]. A novel polymer composite for targeted cancer drug delivery was prepared from chitosan and graphene oxide blend with reinforcement of iron oxide nanoparticles [139]. Nikfarjam and Kokabi reported a polymer composite nanogel made from nanometric chitosan/laponite nanocomposite by ionic gelation method using tripolyphosphate for drug delivery system [140]. Lei and coworkers prepared a pH-sensitive drug release system by preparing polymer nanocomposites from poly(ε-caprolactone)-block-poly(quaternized vinyl benzyl chloride/bipyridine) and zeolitic imidazolate framework-8. The developed composites showed excellent biocompatibility and nontoxicity toward MCF-7 cells ultimately proving the potential to be used in cancer drug delivery systems [141]. A novel drug delivery system for the controlled release of meloxicam, a nonsteroidal antiinflammatory drug for osteoarthritis was prepared from alginate, chitosan, and pluronic nanoparticles via the ionotropic gelation method. The release profile of meloxicam through the developed composites showed a sustained release profile following a burst release [142]. Jia et al. prepared a polymer nanocomposite drug delivery system using poly(lactic-*co*-glycolic acid) and titanium dioxide nanotubes for pH-controlled delivery of lidocaine and carprofen. The release of these two drugs depended on the solubility of lidocaine and carprofen, the degree of degradation of poly(lactic-*co*-glycolic acid) and titanium dioxide nanocomposites, and the electrostatic force between the composites and model drugs [143]. A temperature-sensitive controlled drug release system was prepared by Zhu et al. from soybean agglutinin-15/poly(*N*-isopropyl acrylamide)/$\gamma$-$Fe_2O_3$ magnetic nanoparticles where the release profile of gentamicin was assessed as a model drug [144]. Solubility and dissolution rate of irbesartan, a drug with poor solubility, were increased by encapsulating the drug with polymer nanocomposites from polyvinylpyrrolidone and nanofibers using solid dispersion preparation method [145].

Polymer nanocomposites based on synthetic polymers and biopolymers have gained attraction to be used in cancer drug delivery systems to assist in chemotherapy because of their better properties compared to conventional drug carrier materials. Table 8.4 shows different polymer nanocomposites and their application targeted drug delivery applications for cancer treatment.

### 8.5.4 Polymer nanocomposites in biosensing applications

Exceptional barrier and mechanical properties, thermal stability, and conductive characteristics of polymer matrices-based nanocomposites have opened new possibilities in the field of biosensing applications. These exceptional properties of polymer nanocomposites allow these materials to be used in electrochemical sensors, DNA biosensors, immunosensors, and aptamer sensors [154]. Polymer

**Table 8.4** Polymer nanocomposites for cancer treatment.

| Polymer base | Nano-reinforcement | Drug | Application | Reference |
|---|---|---|---|---|
| Polyethyleneimine | Paramagnetic iron nanoparticles | Doxorubicin | Breast cancer | [146] |
| Poly(ethylene Adipate) | Poly(vinyl pyrrolidone) nanofibers | Artemisinin | Prostatic cancer | [147] |
| Poly(ethylene glycol)-*co*-poly (vinyl pyridine) | Silica nanoparticles | Doxorubicin | Breast cancer | [148] |
| Poly(N-isopropyl acrylamide) | Silica nanoparticles | β-Cyclodextrin | Tumor therapy | [149] |
| Poly methacrylic acid | Mcm-41 (mesoporous nanostructured silica) | Naproxen | Rheumatoid arthritis | [150] |
| Chitosan and poly (methacrylic acid) blend | $Fe_3O_4$ nanoparticles | Doxorubicin hydrochloride | Breast cancer | [151] |
| Poly(D,L,-lactic-*co*-glycolic acid) | Platinum nanoparticles | Carboplatin | Antitumor drug | [152] |
| Poly(ethylene glycol) methacrylate | Chitosan nanoparticles | Bevacizumab | Ophthalmic cancer | [153] |

nanocomposites can detect biomarkers such as temperature, pH, urea, and glucose and by tracking these specific biomarkers polymer nanocomposites can detect any specific biological response in the human body. Although biocompatibility, bioactivity, and limited toxicity of polymer-based nanocomposites have been discussed earlier to perform as a biosensing material, polymer nanocomposites must be tailored to contain specific binding sites. German et al. developed a glucose biosensing polymer-based system by using polymer nanocomposites made from polyaniline and polypyrrole polymer blend and glucose oxidase and gold nanoparticles reinforcements on graphite rod electrodes. The prepared sensors showed high sensitivity, low limit of detection, wide linear range, good repeatability, appropriate stability, and excellent antiinterference ability to ascorbic and uric acids. These properties utilize the sensors developed to be used in glucose measurement systems effectively than other sensors [155]. Devi et al. created an electrochemical sensing system to measure xanthine in fish meat. The prepared sensor was developed by electropolymerizing polymer nanocomposite films of polypyrrole and zinc oxide nanoparticles onto platinum electrodes. The sensor showed pH-controlled detection of xanthine effectively [156]. Table 8.5 demonstrates various target analytes for

**Table 8.5** Different conductive polymer-based nanocomposites and their biosensing applications.

| Conductive polymers | Nanomaterials | Target analytes | Detection limit | Application | Reference |
|---|---|---|---|---|---|
| Polypyrrole | Nickel oxide | Glucose | 0.33 μM | Biosensor | [157] |
| Polyaniline | Nickel cobaltite | Glucose | 0.38 μM | Biosensor | [158] |
| Poly(3, 4-ethylene dioxythiophene) | Titanium dioxide | Ascorbic acid, Diclofenac | 20 nM for Ascorbic acid and 30 nM for diclofenac | Biosensor | [159] |
| Poly(3,4-ethylene dioxythiophene) | Zirconia nanoparticles | Vitamin B2, B6, C | 0.012 μM for Vitamin B2, 0.2 μM for Vitamin B6, 0.45 μM for Vitamin C | Biosensor | [160] |
| Polypyrrole | Tungsten trioxide | Nitrogen dioxide | 5 ppm | Gas sensor | [161] |
| Polyaniline | Palladium nanoparticles | Hydrazine | 0.06 μM | Electrochemical sensor | [162] |
| Polyaniline | Gold nanoparticles | Melamine | $1.39 \times 10^{-6}$ μM | Biosensor | [163] |
| Polypyrrole | Gold nanoparticles | Carcinoembryonic antigen | $1.6 \times 10^{-7}$ ng $mL^{-1}$ | Immunosensor | [164] |
| Poly(3,4-ethylene dioxythiophene) | Palladium nanoparticles | $H_2O_2$ | 2.84 μM | Electrochemical sensor | [165] |
| Poly(3,4-ethylene dioxythiophene) | Multiwalled carbon nanotubes | Magnolo | 3 nM | Biosensor | [166] |

biosensors and electrochemical sensors based on different conductive polymer-based nanocomposites and their limit of detection.

Along with conductive polymer-based nanocomposites, biopolymers have been also studied to be used as polymer blends in biosensing systems with appropriate nano-reinforcement. Polymer nanocomposites based on chitosan biopolymer matrices and gold nanoparticles, molybdenum disulfide nanosheets, and gold−carbon dot nanoconjugates as filler materials were reported to detect glucose effectively [167,168].

## 8.6 Conclusion and future aspects

Because of their exceptional barrier properties, mechanical strength, thermal stability, and controllable degradation rate polymer nanocomposites have been considered in applications where these materials can conveniently replace traditional polymer and polymer composites. Recent development in biocompatible, biodegradable, bioactive, and nontoxic polymer nanocomposites along with the aforementioned properties have given an edge to these materials over conventional polymer composites used in biomedical applications. This chapter comes up with a concise outline of recent studies where the properties of different polymer nanocomposites are needed for biomedical applications which include antimicrobial activities against different kinds of microbes that include different bacteria and fungus and biodegradation properties. Polymer nanocomposites on different medical field-related implications like bone and soft tissue engineering, tissue damage repair, tissue regeneration, scaffold preparation for research purposes, drug delivery, targeted chemotherapy drug release, 3D and 4D bioprinting, and biosensing of different biomarkers are also discussed briefly in this chapter. Complicated biomedical applications such as cancer imaging, gene delivery, and other medical imaging techniques can also be improved by using these polymer nanocomposites due to their tailorable half-life and active sites. Despite the research being undertaken to prove eligibility of polymer nanocomposites to be used in these sophisticated areas are limited, properties and controllability of these materials can surely insinuate the potential of these materials to be used in these complicated and involved biomedical applications.

Although many research works have been conducted to report the properties and potential applications of polymer nanocomposites in biomedical fields, the preparation of these materials at the industrial level still hasn't met any significant success. The preparation of polymer nanocomposites is still more expensive than conventional petroleum-based polymers and their composites. But some recent studies have reported reduced cost of production. With advances in technology, the production cost will steep lower than the present cost which will instigate the replacement of conventional polymer by these composite materials in various applications, particularly in biomedical fields.

## References


[1] M. Rahman, F. Zahin, M.A.S.R. Saadi, A. Sharif, M.E. Hoque, Surface modification of advanced and polymer nanocomposites, in: N. Dasgupta, S. Ranjan, E. Lichtfouse (Eds.), Environmental Nanotechnology: Volume 1, Springer International Publishing, Cham, 2018, pp. 187–209.

[2] A.A. Shamsuri, S.N. Md. Jamil, A short review on the effect of surfactants on the mechanico-thermal properties of polymer nanocomposites, Appl. Sci. 10 (14) (2020). Available from: https://doi.org/10.3390/app10144867.

[3] S.H. Zaferani, Introduction of Polymer-Based Nanocomposites, Elsevier Ltd., 2018.

[4] S. Sharma, S. Shekhar, A. Sarkar, A. Kumar, Surface functionalization of graphene based polyhydroxyalkanoates nanocomposites and their applications, in: B. Sharma, P. Jain (Eds.), Graphene Based Biopolymer Nanocomposites, Springer Singapore, Singapore, 2021, pp. 191–202.

[5] D. Dhara, A. Jimenez, Z. Abbas, M. Denn, B. Benicewicz, S. Kumar, Polyisoprene silica nanocomposites and its structure property relationship, Bull. Am. Phys. Soc. 65 (2020).

[6] H. Bai, et al., Biopolymer nanocomposites with customized mechanical property and exceptionally antibacterial performance, Compos. Sci. Technol. 199 (2020) 108338. Available from: https://doi.org/10.1016/j.compscitech.2020.108338.

[7] T.S. Motsoeneng, M.J. Mochane, T.C. Mokhena, E. Rotimi Sadiku, Chapter 8—Recent progress on antibiotic polymer/metal nanocomposites for health applications, Antibiotic Materials in Healthcare, Academic Press, 2020, pp. 129–139.

[8] X. Chen, et al., MXene/polymer nanocomposites: preparation, properties, and applications, Polym. Rev. 61 (1) (2021) 80–115. Available from: https://doi.org/10.1080/15583724.2020.1729179.

[9] A. Amari, F. Mohammed Alzahrani, K. Mohammedsaleh Katubi, N. Salem Alsaiari, M. A. Tahoon, F. Ben Rebah, Clay-polymer nanocomposites: preparations and utilization for pollutants removal, Materials 14 (6) (2021). Available from: https://doi.org/10.3390/ma14061365.

[10] S. Sagadevan, et al., A facile hydrothermal approach for catalytic and optical behavior of tin oxide- graphene (SnO2/G) nanocomposite, PLoS One 13 (10) (2018) 1–15. Available from: https://doi.org/10.1371/journal.pone.0202694.

[11] J. Fawaz, V. Mittal, Synthesis of polymer nanocomposites: nanocomposite method, Synth. Tech. Polym. Nanocomposite (2015) 1–30 [Online]. Available. Available from: https://application.wiley-vch.de/books/sample/3527334556_c01.pdf.

[12] O. Agboola, et al., A review on polymer nanocomposites and their effective applications in membranes and adsorbents for water treatment and gas separation, Membranes 11 (2) (2021). Available from: https://doi.org/10.3390/membranes11020139.

[13] F.M. Alzahrani, N.S. Alsaiari, K.M. Katubi, A. Amari, F. Ben Rebah, M.A. Tahoon, Synthesis of polymer-based magnetic nanocomposite for multi-pollutants removal from water, Polymers 13 (11) (2021). Available from: https://doi.org/10.3390/polym13111742.

[14] M.I.B. Tavares, in: E.O. da Silva (Ed.), Polymer Nanocomposites, IntechOpen, Rijeka, 2017. p. Ch. 7.

[15] I. Das, S. Sagadevan, Z.Z. Chowdhury, M.E. Hoque, Development, optimization and characterization of a two step sol–gel synthesis route for ZnO/$SnO_2$ nanocomposite, J. Mater. Sci. Mater. Electron. 29 (5) (2018) 4128–4135. Available from: https://doi.org/10.1007/s10854-017-8357-5.


[16] J.P. Chimanowsky Junior, I.L. Soares, L. Luetkmeyer, M.I.B. Tavares, Preparation of high-impact polystyrene nanocomposites with organoclay by melt intercalation and characterization by low-field nuclear magnetic resonance, Chem. Eng. Process. Process Intensif. 77 (2014) 66–76. Available from: https://doi.org/10.1016/j.cep.2013.11.012.

[17] S. Labidi, N. Azéma, D. Perrin, J.-M. Lopez-Cuesta, Organo-modified montmorillonite/poly(ε-caprolactone) nanocomposites prepared by melt intercalation in a twin-screw extruder, Polym. Degrad. Stab. 95 (3) (2010) 382–388. Available from: https://doi.org/10.1016/j.polymdegradstab.2009.11.013.

[18] X. Liu, X. Lu, Y. Su, E. Kun, F. Zhang, Clay-polymer nanocomposites prepared by reactive melt extrusion for sustained drug release, Pharmaceutics 12 (1) (2020). Available from: https://doi.org/10.3390/pharmaceutics12010051.

[19] D. de, M. Mariano, D. de, F. da, S. Freitas, L.C. Mendes, Nano lamellar zirconium phosphate and screw speed changing properties of melt extrusion polypropylene nanocomposites, J. Compos. Mater. 55 (18) (2021) 2443–2458. Available from: https://doi.org/10.1177/0021998320988758.

[20] M. Erceg, D. Jozić, I. Banovac, S. Perinović, S. Bernstorff, Preparation and characterization of melt intercalated poly(ethylene oxide)/lithium montmorillonite nanocomposites, Thermochim. Acta 579 (2014) 86–92. Available from: https://doi.org/10.1016/j.tca.2014.01.024.

[21] S. Bujok, J. Hodan, H. Beneš, Effects of immobilized ionic liquid on properties of biodegradable polycaprolactone/LDH nanocomposites prepared by in situ polymerization and melt-blending techniques, Nanomaterials 10 (5) (2020). Available from: https://doi.org/10.3390/nano10050969.

[22] M.G. Lee, S. Lee, J. Cho, J.Y. Jho, Improving dispersion and mechanical properties of polypropylene/graphene nanoplatelet composites by mixed solvent-assisted melt blending, Macromol. Res. 28 (12) (2020) 1166–1173. Available from: https://doi.org/10.1007/s13233-020-8144-7.

[23] N. Régibeau, R.G. Tilkin, C. Grandfils, B. Heinrichs, Preparation of poly-D,L-lactide based nanocomposites with polymer-grafted silica by melt blending: Study of molecular, morphological, and mechanical properties, Polym. Compos. 42 (2) (2021) 955–972. Available from: https://doi.org/10.1002/pc.25878.

[24] A. O'Neill, E. Archer, A. McIlhagger, P. Lemoine, D. Dixon, Polymer nanocomposites: in situ polymerization of polyamide 6 in the presence of graphene oxide, Polym. Compos. 38 (3) (2017) 528–537. Available from: https://doi.org/10.1002/pc.23612.

[25] Y. Guo, C. Bao, L. Song, B. Yuan, Y. Hu, In situ polymerization of graphene, graphite oxide, and functionalized graphite oxide into epoxy resin and comparison study of on-the-flame behavior, Ind. Eng. Chem. Res. 50 (13) (2011) 7772–7783. Available from: https://doi.org/10.1021/ie200152x.

[26] X. Zhou, et al., Mechanical and thermal properties of electrospun polyimide/rGO composite nanofibers via in-situ polymerization and in-situ thermal conversion, Eur. Polym. J. 141 (2020) 110083. Available from: https://doi.org/10.1016/j.eurpolymj.2020.110083.

[27] X. Wang, Y. Hu, L. Song, H. Yang, W. Xing, H. Lu, In situ polymerization of graphene nanosheets and polyurethane with enhanced mechanical and thermal properties, J. Mater. Chem. 21 (12) (2011) 4222–4227. Available from: https://doi.org/10.1039/C0JM03710A.

[28] S. Kalotra, R. Mehta, Synthesis of polyaniline/clay nanocomposites by in situ polymerization and its application for the removal of Acid Green 25 dye from wastewater, Polym. Bull. 78 (5) (2021) 2439–2463. Available from: https://doi.org/10.1007/s00289-020-03222-3.

[29] J.H. Kang, et al., Multifunctional electroactive nanocomposites based on piezoelectric boron nitride nanotubes, ACS Nano 9 (12) (2015) 11942−11950. Available from: https://doi.org/10.1021/acsnano.5b04526.

[30] R. Prabhu, T. Jeevananda, K.R. Reddy, A.V. Raghu, Polyaniline-fly ash nanocomposites synthesized via emulsion polymerization: Physicochemical, thermal and dielectric properties, Mater. Sci. Energy Technol. 4 (2021) 107−112. Available from: https://doi.org/10.1016/j.mset.2021.02.001.

[31] A. Moreno, M. Morsali, J. Liu, M.H. Sipponen, Access to tough and transparent nanocomposites via Pickering emulsion polymerization using biocatalytic hybrid lignin nanoparticles as functional surfactants, Green Chem. 23 (8) (2021) 3001−3014. Available from: https://doi.org/10.1039/D1GC00103E.

[32] A.P.M. Nozaki, L.M.F. Lona, Comparison between cellulose nanocrystal and microfibrillated cellulose as reinforcement of poly(vinyl acetate) composites obtained by either in situ emulsion polymerization or a simple mixing technique, Cellulose 28 (4) (2021) 2273−2286. Available from: https://doi.org/10.1007/s10570-021-03691-3.

[33] M. Azamian Jazi, A. Ramezani S.A., S.A. Haddadi, S. Ghaderi, F. Azamian, In situ emulsion polymerization and characterization of PVAc nanocomposites including colloidal silica nanoparticles for wood specimens bonding, J. Appl. Polym. Sci. 137 (15) (2020) 48570. Available from: https://doi.org/10.1002/app.48570.

[34] B. Bulbul, E.Y. Pekcaliskan, S. Beyaz, Synthesis of PMMA-HoVO4 nanocomposites by emulsifier-free emulsion polymerization: radical effects, Mater. Sci. 38 (1) (2020) 143−150. Available from: https://doi.org/10.2478/msp-2019-0091.

[35] M.A.M. Ali, A.M. Alsabagh, M.W. Sabaa, R.A. El-Salamony, R.R. Mohamed, R.E. Morsi, Polyacrylamide hybrid nanocomposites hydrogels for efficient water treatment, Iran. Polym. J. 29 (6) (2020) 455−466. Available from: https://doi.org/10.1007/s13726-020-00810-y.

[36] D.W. Kim, J. Shin, S.Q. Choi, Nano-dispersed cellulose nanofibrils-PMMA composite from Pickering emulsion with tunable interfacial tensions, Carbohydr. Polym. 247 (2020) 116762. Available from: https://doi.org/10.1016/j.carbpol.2020.116762.

[37] I. Yamaguchi, et al., Preparation and microstructure analysis of chitosan/hydroxyapatite nanocomposites, J. Biomed. Mater. Res. 55 (1) (2001) 20−27. https://doi.org/10.1002/1097-4636(200104)55:1 < 20:AID-JBM30 > 3.0.CO;2-F.

[38] K. Gold, B. Slay, M. Knackstedt, A.K. Gaharwar, Antimicrobial activity of metal and metal-oxide based nanoparticles, Adv. Ther. 1 (3) (2018) 1700033. Available from: https://doi.org/10.1002/adtp.201700033.

[39] M.A. Wahab, N. Islam, M.E. Hoque, D.J. Young, Recent advances in silver nanoparticle containing biopolymer nanocomposites for infectious disease control − a mini review, Curr. Anal. Chem. 14 (3) (2018) 198−202. Available from: 10.2174/1573411013666171009163829.

[40] A.D. Kramar, B.M. Obradović, S. Schiehser, A. Potthast, M.M. Kuraica, M.M. Kostić, Enhanced antimicrobial activity of atmospheric pressure plasma treated and aged cotton fibers, J. Nat. Fibers (2021) 1−15. Available from: https://doi.org/10.1080/15440478.2021.1946883.

[41] V. Guna, et al., Antimicrobial natural cellulose fibers from *Hyptis suaveolens* for potential biomedical and textiles applications, J. Nat. Fibers 18 (6) (2021) 867−876. Available from: https://doi.org/10.1080/15440478.2019.1658258.

[42] L.G. Confederat, C.G. Tuchilus, M. Dragan, M. Sha'at, O.M. Dragostin, Preparation and antimicrobial activity of chitosan and its derivatives: a concise review, Molecules 26 (12) (2021). Available from: https://doi.org/10.3390/molecules26123694.

[43] M. Sadeghi-Kiakhani, E. Hashemi, K. Gharanjig, Treating wool fibers with chitosan-based nano-composites for enhancing the antimicrobial properties, Appl. Nanosci. 10 (4) (2020) 1219−1229. Available from: https://doi.org/10.1007/s13204-019-01203-1.

[44] M. Cobos, I. De-La-Pinta, G. Quindós, M.J. Fernández, M.D. Fernández, Synthesis, physical, mechanical and antibacterial properties of nanocomposites based on poly (vinyl alcohol)/graphene oxide-silver nanoparticles, Polymers (Basel). 12 (3) (2020) 723. Available from: https://doi.org/10.3390/polym12030723.

[45] S.M. Li, N. Jia, M.G. Ma, Z. Zhang, Q.H. Liu, R.C. Sun, Cellulose-silver nanocomposites: Microwave-assisted synthesis, characterization, their thermal stability, and antimicrobial property, Carbohydr. Polym. 86 (2) (2011) 441−447. Available from: https://doi.org/10.1016/j.carbpol.2011.04.060.

[46] E. Anancharoenwong, W. Chueangchayaphan, N. Rakkapao, S. Marthosa, B. Chaisrikhwun, Thermo-mechanical and antimicrobial properties of natural rubber-based polyurethane nanocomposites for biomedical applications, Polym. Bull. 78 (2) (2021) 833−848. Available from: https://doi.org/10.1007/s00289-020-03137-z.

[47] X. Chang, et al., Physicochemical and antimicrobial properties of chitosan composite films incorporated with glycerol monolaurate and nano-TiO2, Food Hydrocoll. 119 (2021) 106846. Available from: https://doi.org/10.1016/j.foodhyd.2021.106846.

[48] K.S. Prashanth, V. Revathi, Antimicrobial and antifungal studies of polymer nanocomposites with 2D nanomaterials, Mater. Today Proc. (2021). Available from: https://doi.org/10.1016/j.matpr.2021.04.510.

[49] Y. Jeon, Y. Park, Antibacterial properties of knits made from PET and ion-exchanged zeolite nanocomposite yarns, J. Korean Soc. Dye. Process. Technol. 33 (1) (2021) 24−30. Available from: https://doi.org/10.5764/TCF.2021.33.1.24.

[50] W.G.I.U. Rathnayake, H. Ismail, A. Baharin, A.G.N.D. Darsanasiri, S. Rajapakse, Synthesis and characterization of nano silver based natural rubber latex foam for imparting antibacterial and anti-fungal properties, Polym. Test. 31 (5) (2012) 586−592. Available from: https://doi.org/10.1016/j.polymertesting.2012.01.010.

[51] M. Naushad, T. Ahamad, K.M. Al-Sheetan, Development of a polymeric nanocomposite as a high performance adsorbent for Pb(II) removal from water medium: Equilibrium, kinetic and antimicrobial activity, J. Hazard. Mater. 407 (2021) 124816. Available from: https://doi.org/10.1016/j.jhazmat.2020.124816.

[52] M.M. Fernandes, et al., Magnetoelectric polymer-based nanocomposites with magnetically controlled antimicrobial activity, ACS Appl. Bio Mater 4 (1) (2021) 559−570. Available from: https://doi.org/10.1021/acsabm.0c01125.

[53] M. Rehan, A.A. Nada, T.A. Khattab, N.A.M. Abdelwahed, A.A.A. El-Kheir, Development of multifunctional polyacrylonitrile/silver nanocomposite films: antimicrobial activity, catalytic activity, electrical conductivity, UV protection and SERS-active sensor, J. Mater. Res. Technol. 9 (4) (2020) 9380−9394. Available from: https://doi.org/10.1016/j.jmrt.2020.05.079.

[54] Z. Gončuková, M. Řezanka, J. Dolina, L. Dvořák, Sulfonated polyethersulfone membrane doped with ZnO-APTES nanoparticles with antimicrobial properties, React. Funct. Polym. 162 (2021) 104872. Available from: https://doi.org/10.1016/j.reactfunctpolym.2021.104872.

[55] B. Rukmanikrishnan, S. Ramalingam, S.S. Kim, J. Lee, Rheological and antimicrobial properties of silica and silver nanoparticles-reinforced K-carrageenan/hydroxyethyl cellulose composites for food packaging applications, Cellulose (2021). Available from: https://doi.org/10.21203/rs.3.rs-223398/v1.

[56] L. Cao, X. Wu, Q. Wang, J. Wang, Biocompatible nanocomposite of $TiO_2$ incorporated bi-polymer for articular cartilage tissue regeneration: a facile material, J. Photochem. Photobiol. B Biol. 178 (2018) 440–446. Available from: https://doi.org/10.1016/j.jphotobiol.2017.10.026.
[57] P.W. Brandt-Rauf, Y. Li, C. Long, R. Monaco, G. Kovvali, M.-J. Marion, Plastics and carcinogenesis: The example of vinyl chloride, J. Carcinog. 11 (2012) 5. Available from: https://doi.org/10.4103/1477-3163.93700.
[58] H. Liu, et al., Application of biodegradable and biocompatible nanocomposites in electronics: current status and future directions, Nanomaterials 9 (2019) 950. Available from: https://doi.org/10.3390/nano9070950.
[59] A. Sharif, S. Mondal, M.E. Hoque, Polylactic acid (PLA)-based nanocomposites: processing and properties, in: M.L. Sanyang, M. Jawaid (Eds.), Bio-Based Polymers and Nanocomposites: Preparation, Processing, Properties & Performance, Springer International Publishing, Cham, 2019, pp. 233–254.
[60] M. Khalid, C.T. Ratnam, R. Walvekar, M.R. Ketabchi, M.E. Hoque, Reinforced natural rubber nanocomposites: next generation advanced material, in: M. Jawaid, M.S. Salit, O.Y. Alothman (Eds.), Green Biocomposites: Design and Applications, Springer International Publishing, Cham, 2017, pp. 309–345.
[61] A. Sharif, M.E. Hoque, Renewable resource-based polymers, in: M.L. Sanyang, M. Jawaid (Eds.), Bio-based Polymers and Nanocomposites: Preparation, Processing, Properties & Performance, Springer International Publishing, Cham, 2019, pp. 1–28.
[62] I. Salcedo, et al., In vitro biocompatibility and mucoadhesion of montmorillonite chitosan nanocomposite: a new drug delivery, Appl. Clay Sci. 55 (2012) 131–137. Available from: https://doi.org/10.1016/j.clay.2011.11.006.
[63] S. Chakraborty, R.M. A., N.L. Mary, Biocompatible supercapacitor electrodes using green synthesised ZnO/Polymer nanocomposites for efficient energy storage applications, J. Energy Storage 28 (2020) 101275. Available from: https://doi.org/10.1016/j.est.2020.101275.
[64] M. Ziąbka, M. Dziadek, E. Menaszek, Biocompatibility of poly(acrylonitrile-butadiene-styrene) nanocomposites modified with silver nanoparticles, Polymers (Basel) 10 (11) (2018). Available from: https://doi.org/10.3390/polym10111257.
[65] I. Csarnovics, et al., Development and study of biocompatible polyurethane-based polymer-metallic nanocomposites, Nanotechnol. Sci. Appl. 13 (2020) 11–22. Available from: https://doi.org/10.2147/NSA.S245071.
[66] S. Dabees, B.M. Kamel, V. Tirth, A.B. Elshalakny, Experimental design of $Al_2O_3$/MWCNT/HDPE hybrid nanocomposites for hip joint replacement, Bioengineered 11 (1) (2020) 679–692. Available from: https://doi.org/10.1080/21655979.2020.1775943.
[67] A.A. Shah, F. Hasan, A. Hameed, S. Ahmed, Biological degradation of plastics: a comprehensive review, Biotechnol. Adv. 26 (3) (2008) 246–265. Available from: https://doi.org/10.1016/j.biotechadv.2007.12.005.
[68] C. Campbell, Soil microbiology, ecology, and biochemistry, Eur. J. Soil Sci. 59 (5) (2008) 1008–1009. Available from: https://doi.org/10.1111/j.1365-2389.2008.01052_2.x.
[69] F.V. Ferreira, et al., How do cellulose nanocrystals affect the overall properties of biodegradable polymer nanocomposites: a comprehensive review, Eur. Polym. J. 108 (2018) 274–285. Available from: https://doi.org/10.1016/j.eurpolymj.2018.08.045.
[70] I.F. Pinheiro, et al., Mechanical, rheological and degradation properties of PBAT nanocomposites reinforced by functionalized cellulose nanocrystals, Eur. Polym. J. 97 (2017) 356–365. Available from: https://doi.org/10.1016/j.eurpolymj.2017.10.026.

[71] G.T. Padma, T.S. Rao, V.R. Mudinepalli, Effect of copper oxide on biodegradable polymer nanocomposite thin films, Int. J. Eng. Res. Technol. 10 (01) (2021) [Online]. Available. Available from: https://www.ijert.org/effect-of-copper-oxide-on-biodegradable-polymer-nanocomposite-thin-films.

[72] E. Cordeiro, E.C. Lopes Pereira, A.A. Silva, B.G. Soares, Polypropylene/poly(lactic acid)/carbon nanotube semi-biodegradable nanocomposites: the effect of sequential mixing approach and compatibilization on morphology, rheology and electrical conductivity, J. Appl. Polym. Sci. 138 (40) (2021) 51195. Available from: https://doi.org/10.1002/app.51195.

[73] O. Platnieks, et al., Adding value to poly(butylene succinate) and nanofibrillated cellulose-based sustainable nanocomposites by applying masterbatch process, Ind. Crops Prod. 169 (2021) 113669. Available from: https://doi.org/10.1016/j.indcrop.2021.113669.

[74] S.V. Murphy, A. Atala, 3D bioprinting of tissues and organs, Nat. Biotechnol. 32 (8) (2014) 773−785. Available from: https://doi.org/10.1038/nbt.2958.

[75] A. Schwab, R. Levato, M. D'Este, S. Piluso, D. Eglin, J. Malda, Printability and shape fidelity of bioinks in 3D bioprinting, Chem. Rev. 120 (19) (2020) 11028−11055. Available from: https://doi.org/10.1021/acs.chemrev.0c00084.

[76] Y.S. Zhang, et al., 3D bioprinting for tissue and organ fabrication, Ann. Biomed. Eng. 45 (1) (2017) 148−163. Available from: https://doi.org/10.1007/s10439-016-1612-8.

[77] F.A. Kucherov, E.G. Gordeev, A.S. Kashin, V.P. Ananikov, Three-dimensional printing with biomass-derived PEF for carbon-neutral manufacturing, Angew. Chem. Int. Ed Engl. 56 (50) (2017) 15931−15935. Available from: https://doi.org/10.1002/anie.201708528.

[78] X. Yu, T. Zhang, Y. Li, 3D printing and bioprinting nerve conduits for neural tissue engineering, Polymers (Basel). 12 (8) (2020) 1637. Available from: https://doi.org/10.3390/polym12081637.

[79] H. Rastin, et al., 3D bioprinting of cell-laden electroconductive MXene nanocomposite bioinks, Nanoscale 12 (30) (2020) 16069−16080. Available from: https://doi.org/10.1039/D0NR02581J.

[80] K. Markstedt, A. Mantas, I. Tournier, H. Martínez Ávila, D. Hägg, P. Gatenholm, 3D bioprinting human chondrocytes with nanocellulose-alginate bioink for cartilage tissue engineering applications, Biomacromolecules 16 (5) (2015) 1489−1496. Available from: https://doi.org/10.1021/acs.biomac.5b00188.

[81] A. Habib, B. Khoda, Development of clay based novel hybrid bio-ink for 3D bioprinting process, J. Manuf. Process. 38 (2019) 76−87. Available from: https://doi.org/10.1016/j.jmapro.2018.12.034.

[82] C.W. Peak, J. Stein, K.A. Gold, A.K. Gaharwar, Nanoengineered colloidal inks for 3D bioprinting, Langmuir 34 (3) (2018) 917−925. Available from: https://doi.org/10.1021/acs.langmuir.7b02540.

[83] Y. Jin, A. Compaan, W. Chai, Y. Huang, Functional nanoclay suspension for printing-then-solidification of liquid materials, ACS Appl. Mater. Interfaces 9 (23) (2017) 20057−20066. Available from: https://doi.org/10.1021/acsami.7b02398.

[84] Z. Deng, T. Hu, Q. Lei, J. He, P.X. Ma, B. Guo, Stimuli-responsive conductive nanocomposite hydrogels with high stretchability, self-healing, adhesiveness, and 3D printability for human motion sensing, ACS Appl. Mater. Interfaces 11 (7) (2019) 6796−6808. Available from: https://doi.org/10.1021/acsami.8b20178.

[85] A. Nadernezhad, O.S. Caliskan, F. Topuz, F. Afghah, B. Erman, B. Koc, Nanocomposite bioinks based on agarose and 2D nanosilicates with tunable flow properties and bioactivity for 3D bioprinting, ACS Appl. Bio Mater. 2 (2) (2019) 796−806. Available from: https://doi.org/10.1021/acsabm.8b00665.

[86] J. Guo, R. Zhang, L. Zhang, X. Cao, 4D printing of robust hydrogels consisted of agarose nanofibers and polyacrylamide, ACS Macro Lett. 7 (4) (2018) 442−446. Available from: https://doi.org/10.1021/acsmacrolett.7b00957.
[87] S. Sharifi, S.B.G. Blanquer, T.G. van Kooten, D.W. Grijpma, Biodegradable nanocomposite hydrogel structures with enhanced mechanical properties prepared by photocrosslinking solutions of poly(trimethylene carbonate)−poly(ethylene glycol)−poly(trimethylene carbonate) macromonomers and nanoclay particles, Acta Biomater. 8 (12) (2012) 4233−4243. Available from: https://doi.org/10.1016/j.actbio.2012.09.014.
[88] J.R. Xavier, et al., Bioactive nanoengineered hydrogels for bone tissue engineering: a growth-factor-free approach, ACS Nano 9 (3) (2015) 3109−3118. Available from: https://doi.org/10.1021/nn507488s.
[89] J.L. Dávila, M.A. d'Ávila, Rheological evaluation of laponite/alginate inks for 3D extrusion-based printing, Int. J. Adv. Manuf. Technol. 101 (1) (2019) 675−686. Available from: https://doi.org/10.1007/s00170-018-2876-y.
[90] S. Hong, et al., 3D printing of highly stretchable and tough hydrogels into complex, cellularized structures, Adv. Mater. 27 (27) (2015) 4035−4040. Available from: https://doi.org/10.1002/adma.201501099.
[91] T. Ahlfeld, et al., Development of a clay based bioink for 3D cell printing for skeletal application, Biofabrication 9 (3) (2017) 34103. Available from: https://doi.org/10.1088/1758-5090/aa7e96.
[92] S. Esmaeili, et al., A porous polymeric−hydroxyapatite scaffold used for femur fractures treatment: fabrication, analysis, and simulation, Eur. J. Orthop. Surg. Traumatol. 30 (1) (2020) 123−131. Available from: https://doi.org/10.1007/s00590-019-02530-3.
[93] R. Geetha Bai, K. Muthoosamy, S. Manickam, A. Hilal-Alnaqbi, Graphene-based 3D scaffolds in tissue engineering: fabrication, applications, and future scope in liver tissue engineering, Int. J. Nanomedicine 14 (2019) 5753−5783. Available from: https://doi.org/10.2147/IJN.S192779.
[94] R.A. Hule, D.J. Pochan, Polymer nanocomposites for biomedical applications, MRS Bull. 32 (4) (2007) 354−358. Available from: https://doi.org/10.1557/mrs2007.235.
[95] H. Zhao, J. Liao, F. Wu, J. Shi, Mechanical strength improvement of chitosan/hydroxyapatite scaffolds by coating and cross-linking, J. Mech. Behav. Biomed. Mater. 114 (2021) 104169. Available from: https://doi.org/10.1016/j.jmbbm.2020.104169.
[96] N.K. Nga, L.T. Thanh Tam, N.T. Ha, P. Hung Viet, T.Q. Huy, Enhanced biomineralization and protein adsorption capacity of 3D chitosan/hydroxyapatite biomimetic scaffolds applied for bone-tissue engineering, RSC Adv. 10 (70) (2020) 43045−43057. Available from: https://doi.org/10.1039/D0RA09432C.
[97] H. Hwangbo, et al., Bone tissue engineering via application of a collagen/hydroxyapatite 4D-printed biomimetic scaffold for spinal fusion, Appl. Phys. Rev. 8 (2) (2021) 21403. Available from: https://doi.org/10.1063/5.0035601.
[98] I.V. Antoniac, et al., In vitro characterization of novel nanostructured collagen-hydroxyapatite composite scaffolds doped with magnesium with improved biodegradation rate for hard tissue regeneration, Bioact. Mater. 6 (10) (2021) 3383−3395. Available from: https://doi.org/10.1016/j.bioactmat.2021.02.030.
[99] J. Huang, et al., 3D printed gelatin/hydroxyapatite scaffolds for stem cell chondrogenic differentiation and articular cartilage repair, Biomater. Sci. 9 (7) (2021) 2620−2630. Available from: https://doi.org/10.1039/D0BM02103B.
[100] C.-K. Sun, et al., Metformin-incorporated gelatin/hydroxyapatite nanofiber scaffold for bone regeneration, Tissue Eng. Part A (2021). Available from: https://doi.org/10.1089/ten.tea.2021.0038.

[101] M.U.A. Khan, et al., Synthesis and characterization of silver-coated polymeric scaffolds for bone tissue engineering: antibacterial and in vitro evaluation of cytotoxicity and biocompatibility, ACS Omega 6 (6) (2021) 4335−4346. Available from: https://doi.org/10.1021/acsomega.0c05596.

[102] S. Gautam, et al., Gelatin-polycaprolactone-nanohydroxyapatite electrospun nanocomposite scaffold for bone tissue engineering, Mater. Sci. Eng. C 119 (2021) 111588. Available from: https://doi.org/10.1016/j.msec.2020.111588.

[103] I. Shirzaei Sani, M. Rezaei, A. Baradar Khoshfetrat, D. Razzaghi, Preparation and characterization of polycaprolactone/chitosan-g-polycaprolactone/hydroxyapatite electrospun nanocomposite scaffolds for bone tissue engineering, Int. J. Biol. Macromol. 182 (2021) 1638−1649. Available from: https://doi.org/10.1016/j.ijbiomac.2021.05.163.

[104] S. Rastegar, M. Mehdikhani, A. Bigham, E. Poorazizi, M. Rafienia, Poly glycerol sebacate/polycaprolactone/carbon quantum dots fibrous scaffold as a multifunctional platform for cardiac tissue engineering, Mater. Chem. Phys. 266 (2021) 124543. Available from: https://doi.org/10.1016/j.matchemphys.2021.124543.

[105] A. Sadeghianmaryan, Z. Yazdanpanah, Y.A. Soltani, H.A. Sardroud, M.H. Nasirtabrizi, X. Chen, Curcumin-loaded electrospun polycaprolactone/montmorillonite nanocomposite: wound dressing application with anti-bacterial and low cell toxicity properties, J. Biomater. Sci. Polym. (Ed.) 31 (2) (2020) 169−187. Available from: https://doi.org/10.1080/09205063.2019.1680928.

[106] S. Mallakpour, M. Lormahdiabadi, Polycaprolactone/ZnO-folic acid nanocomposite films: Fabrication, characterization, in-vitro bioactivity, and antibacterial assessment, Mater. Chem. Phys. 263 (2021) 124378. Available from: https://doi.org/10.1016/j.matchemphys.2021.124378.

[107] N. Bahremandi Tolou, et al., Fabrication of 3D monolithic graphene foam/polycaprolactone porous nanocomposites for bioapplications, J. Mater. Sci. 56 (9) (2021) 5581−5594. Available from: 10.1007/s10853-020-05596-1.

[108] M.-J. Chern, L.-Y. Yang, Y.-K. Shen, J.-H. Hung, 3D scaffold with PCL combined biomedical ceramic materials for bone tissue regeneration, Int. J. Precis. Eng. Manuf. 14 (12) (2013) 2201−2207. Available from: https://doi.org/10.1007/s12541-013-0298-1.

[109] G.P. Awasthi, et al., Assembly of porous graphitic carbon nitride nanosheets into electrospun polycaprolactone nanofibers for bone tissue engineering, Colloids Surfaces A Physicochem. Eng. Asp. 622 (2021) 126584. Available from: https://doi.org/10.1016/j.colsurfa.2021.126584.

[110] N. Zakeri, H.R. Rezaie, J. Javadpour, M. Kharaziha, Cisplatin loaded polycaprolactone − zeolite nanocomposite scaffolds for bone cancer treatment, J. Sci. Adv. Mater. Devices (2021). Available from: https://doi.org/10.1016/j.jsamd.2021.06.006.

[111] P.N. Christy, et al., Biopolymeric nanocomposite scaffolds for bone tissue engineering applications − a review, J. Drug Deliv. Sci. Technol. 55 (2020) 101452. Available from: https://doi.org/10.1016/j.jddst.2019.101452.

[112] N. Shokraei, S. Asadpour, S. Shokraei, M. Nasrollahzadeh Sabet, R. Faridi-Majidi, H. Ghanbari, Development of electrically conductive hybrid nanofibers based on CNT-polyurethane nanocomposite for cardiac tissue engineering, Microsc. Res. Tech. 82 (8) (2019) 1316−1325. Available from: https://doi.org/10.1002/jemt.23282.

[113] S. Shokri, B. Movahedi, M. Rafieinia, H. Salehi, A new approach to fabrication of Cs/BG/CNT nanocomposite scaffold towards bone tissue engineering and evaluation of its properties, Appl. Surf. Sci. 357 (2015) 1758−1764. Available from: https://doi.org/10.1016/j.apsusc.2015.10.048.

[114] H. Shao, et al., Carbon nanotube multilayered nanocomposites as multifunctional substrates for actuating neuronal differentiation and functions of neural stem cells, Biomaterials 175 (2018) 93–109. Available from: https://doi.org/10.1016/j.biomaterials.2018.05.028.
[115] S. Wu, B. Duan, A. Lu, Y. Wang, Q. Ye, L. Zhang, Biocompatible chitin/carbon nanotubes composite hydrogels as neuronal growth substrates, Carbohydr. Polym. 174 (2017) 830–840. Available from: https://doi.org/10.1016/j.carbpol.2017.06.101.
[116] X. Liu, et al., Covalent crosslinking of graphene oxide and carbon nanotube into hydrogels enhances nerve cell responses, J. Mater. Chem. B 4 (43)) (2016) 6930–6941. Available from: https://doi.org/10.1039/C6TB01722C.
[117] D. Arslantunali, G. Budak, V. Hasirci, Multiwalled CNT-pHEMA composite conduit for peripheral nerve repair, J. Biomed. Mater. Res. Part A 102 (3) (2014) 828–841. Available from: https://doi.org/10.1002/jbm.a.34727.
[118] M. Salehi, et al., Sciatic nerve regeneration by transplantation of Schwann cells via erythropoietin controlled-releasing polylactic acid/multiwalled carbon nanotubes/gelatin nanofibrils neural guidance conduit, J. Biomed. Mater. Res. Part B Appl. Biomater. 106 (4) (2018) 1463–1476. Available from: https://doi.org/10.1002/jbm.b.33952.
[119] B. Murugesan, et al., Fabrication of palladium nanoparticles anchored polypyrrole functionalized reduced graphene oxide nanocomposite for antibiofilm associated orthopedic tissue engineering, Appl. Surf. Sci. 510 (2020) 145403. Available from: https://doi.org/10.1016/j.apsusc.2020.145403.
[120] B. Kolathupalayam Shanmugam, S. Rangaraj, K. Subramani, S. Srinivasan, W.K. Aicher, R. Venkatachalam, Biomimetic $TiO_2$-chitosan/sodium alginate blended nanocomposite scaffolds for tissue engineering applications, Mater. Sci. Eng. C 110 (2020) 110710. Available from: https://doi.org/10.1016/j.msec.2020.110710.
[121] D.K. Patel, S.D. Dutta, J. Hexiu, K. Ganguly, K.-T. Lim, Bioactive electrospun nanocomposite scaffolds of poly(lactic acid)/cellulose nanocrystals for bone tissue engineering, Int. J. Biol. Macromol. 162 (2020) 1429–1441. Available from: https://doi.org/10.1016/j.ijbiomac.2020.07.246.
[122] W. Jing, et al., Polymer-ceramic fiber nanocomposite coatings on titanium metal implant devices for diseased bone tissue regeneration, J. Sci. Adv. Mater. Devices (2021). Available from: https://doi.org/10.1016/j.jsamd.2021.04.001.
[123] J.K. Hong, S.L. Cooke, A.R. Whittington, M. Roman, Bioactive cellulose nanocrystal-poly(ε-caprolactone) nanocomposites for bone tissue engineering applications, Front. Bioeng. Biotechnol. 9 (2021) 7. Available from: https://doi.org/10.3389/fbioe.2021.605924.
[124] S. Mallakpour, L. Khodadadzadeh, Ultrasonic-assisted fabrication of starch/MWCNT-glucose nanocomposites for drug delivery, Ultrason. Sonochem. 40 (2018) 402–409. Available from: https://doi.org/10.1016/j.ultsonch.2017.07.033.
[125] P.C. Ferrari, F.F. Araujo, S.A. Pianaro, Halloysite nanotubes-polymeric nanocomposites: characteristics, modifications and controlled drug delivery approaches, Cerâmica 63 (368) (2017). Available from: https://doi.org/10.1590/0366-69132017633682167.
[126] M.A. Islam, et al., Mucoadhesive chitosan derivatives as novel drug carriers, Curr. Pharm. Des. 21 (29) (2015) 4285–4309. Available from: 10.2174/1381612821666150901103819.
[127] Q.-X. Wu, D.-Q. Lin, S.-J. Yao, Design of chitosan and its water soluble derivatives-based drug carriers with polyelectrolyte complexes, Mar. Drugs 12 (12) (2014) 6236–6253. Available from: https://doi.org/10.3390/md12126236.

[128] J. Yang, J. Chen, D. Pan, Y. Wan, Z. Wang, pH-sensitive interpenetrating network hydrogels based on chitosan derivatives and alginate for oral drug delivery, Carbohydr. Polym. 92 (1) (2013) 719−725. Available from: https://doi.org/10.1016/j.carbpol.2012.09.036.

[129] A. Babu, et al., Chemodrug delivery using integrin-targeted PLGA-Chitosan nanoparticle for lung cancer therapy, Sci. Rep. 7 (1) (2017) 14674. Available from: https://doi.org/10.1038/s41598-017-15012-5.

[130] S.E. Gerami, M. Pourmadadi, H. Fatoorehchi, F. Yazdian, H. Rashedi, M.N. Nigjeh, Preparation of pH-sensitive chitosan/polyvinylpyrrolidone/$\alpha$-$Fe_2O_3$ nanocomposite for drug delivery application: emphasis on ameliorating restrictions, Int. J. Biol. Macromol. 173 (2021) 409−420. Available from: https://doi.org/10.1016/j.ijbiomac.2021.01.067.

[131] Y. Zhang, T.R. Nayak, H. Hong, W. Cai, Graphene: a versatile nanoplatform for biomedical applications, Nanoscale 4 (13) (2012) 3833−3842. Available from: https://doi.org/10.1039/c2nr31040f.

[132] B. Lu, et al., Graphene-based composite materials beneficial to wound healing, Nanoscale 4 (9) (2012) 2978−2982. Available from: https://doi.org/10.1039/c2nr11958g.

[133] L. Zhang, Z. Lu, Q. Zhao, J. Huang, H. Shen, Z. Zhang, Enhanced chemotherapy efficacy by sequential delivery of siRNA and anticancer drugs using PEI-grafted graphene oxide, Small 7 (4) (2011) 460−464. Available from: https://doi.org/10.1002/smll.201001522.

[134] V.K. Rana, et al., Synthesis and drug-delivery behavior of chitosan-functionalized graphene oxide hybrid nanosheets, Macromol. Mater. Eng. 296 (2) (2011) 131−140. Available from: https://doi.org/10.1002/mame.201000307.

[135] Y. Bai, et al., Testing of fast dissolution of ibuprofen from its electrospun hydrophilic polymer nanocomposites, Polym. Test. 93 (2021) 106872. Available from: https://doi.org/10.1016/j.polymertesting.2020.106872.

[136] A. Pourjavadi, M. Kohestanian, C. Streb, pH and thermal dual-responsive poly (NIPAM-co-GMA)-coated magnetic nanoparticles via surface-initiated RAFT polymerization for controlled drug delivery, Mater. Sci. Eng. C 108 (2020) 110418. Available from: https://doi.org/10.1016/j.msec.2019.110418.

[137] A. Ghamkhari, S. Abbaspour-Ravasjani, M. Talebi, H. Hamishehkar, M.R. Hamblin, Development of a graphene oxide-poly lactide nanocomposite as a smart drug delivery system, Int. J. Biol. Macromol. 169 (2021) 521−531. Available from: https://doi.org/10.1016/j.ijbiomac.2020.12.084.

[138] S.M. Mousavi, M. Babazadeh, M. Nemati, M. Es'haghi, Doxorubicin-loaded biodegradable chitosan−graphene nanosheets for drug delivery applications, Polym. Bull. (2021). Available from: https://doi.org/10.1007/s00289-021-03783-x.

[139] V. Karthika, M.S. AlSalhi, S. Devanesan, K. Gopinath, A. Arumugam, M. Govindarajan, Chitosan overlaid $Fe_3O_4$/rGO nanocomposite for targeted drug delivery, imaging, and biomedical applications, Sci. Rep. 10 (1) (2020) 18912. Available from: https://doi.org/10.1038/s41598-020-76015-3.

[140] M. Nikfarjam, M. Kokabi, Chitosan/laponite nanocomposite nanogels as a potential drug delivery system, Polym. Bull. 78 (8) (2021) 4593−4607. Available from: https://doi.org/10.1007/s00289-020-03335-9.

[141] Z. Lei, et al., Block copolymer@ZIF-8 nanocomposites as a pH-responsive multi-steps release system for controlled drug delivery, J. Biomater. Sci. Polym. (Ed.) 31 (6) (2020) 695−711. Available from: https://doi.org/10.1080/09205063.2020.1713451.

[142] S. Fattahpour, M. Shamanian, N. Tavakoli, M. Fathi, S.R. Sheykhi, S. Fattahpour, Design and optimization of alginate − chitosan − pluronic nanoparticles as a novel

meloxicam drug delivery system, J. Appl. Polym. Sci. 132 (28) (2015). Available from: https://doi.org/10.1002/app.42241.

[143] H. Jia, L.L. Kerr, Kinetics of drug release from drug carrier of polymer/$TiO_2$ nanotubes composite—pH dependent study, J. Appl. Polym. Sci. 132 (7) (2015). Available from: https://doi.org/10.1002/app.41570.

[144] Y. Zhu, S. Kaskel, T. Ikoma, N. Hanagata, Magnetic SBA-15/poly(N-isopropylacrylamide) composite: preparation, characterization and temperature-responsive drug release property, Microporous Mesoporous Mater. 123 (1) (2009) 107−112. Available from: https://doi.org/10.1016/j.micromeso.2009.03.031.

[145] E. Adeli, Irbesartan-loaded electrospun nanofibers-based PVP K90 for the drug dissolution improvement: fabrication, in vitro performance assessment, and in vivo evaluation, J. Appl. Polym. Sci. 132 (27) (2015). Available from: https://doi.org/10.1002/app.42212.

[146] F. Zaaeri, M. Khoobi, M. Rouini, H. Akbari Javar, pH-responsive polymer in a core−-shell magnetic structure as an efficient carrier for delivery of doxorubicin to tumor cells, Int. J. Polym. Mater. Polym. Biomater. 67 (16) (2018) 967−977. Available from: https://doi.org/10.1080/00914037.2017.1405348.

[147] I. Bonadies, et al., Electrospun core/shell nanofibers as designed devices for efficient Artemisinin delivery, Eur. Polym. J. 89 (2017) 211−220. Available from: https://doi.org/10.1016/j.eurpolymj.2017.02.015.

[148] A. Pourjavadi, Z.M. Tehrani, C. Bennett, PEG-co-polyvinyl pyridine coated magnetic mesoporous silica nanoparticles for pH-responsive controlled release of doxorubicin, Int. J. Polym. Mater. Polym. Biomater. 64 (11) (2015) 570−577. Available from: https://doi.org/10.1080/00914037.2014.996706.

[149] A. Pourjavadi, Z.M. Tehrani, Poly(*N*-isopropylacrylamide)-coated β-cyclodextrin−capped magnetic mesoporous silica nanoparticles exhibiting thermal and pH dual response for triggered anticancer drug delivery, Int. J. Polym. Mater. Polym. Biomater. 66 (7) (2017) 336−348. Available from: https://doi.org/10.1080/00914037.2016.1217531.

[150] A. Abbaszad Rafi, F. Fakheri, M. Mahkam, Synthesis and preparation of new pH-sensitive nanocomposite and nanocapsule based on 'MCM-41/poly methacrylic acid' as drug carriers, Polym. Bull. 73 (10) (2016) 2649−2659. Available from: https://doi.org/10.1007/s00289-016-1627-1.

[151] M. Zarouni, et al., Biocompatible polymer coated paramagnetic nanoparticles for doxorubicin delivery: synthesis and anticancer effects against human breast cancer cells, Int. J. Polym. Mater. Polym. Biomater. 64 (14) (2015) 718−726. Available from: https://doi.org/10.1080/00914037.2014.1002129.

[152] D. de Moraes Profirio, F.B.T. Pessine, Formulation of functionalized PLGA nanoparticles with folic acid-conjugated chitosan for carboplatin encapsulation, Eur. Polym. J. 108 (2018) 311−321. Available from: https://doi.org/10.1016/j.eurpolymj.2018.09.011.

[153] C.-L. Savin, M. Popa, C. Delaite, M. Costuleanu, D. Costin, C.A. Peptu, Chitosan grafted-poly(ethylene glycol) methacrylate nanoparticles as carrier for controlled release of bevacizumab, Mater. Sci. Eng. C 98 (2019) 843−860. Available from: https://doi.org/10.1016/j.msec.2019.01.036.

[154] S. Shrivastava, N. Jadon, R. Jain, Next-generation polymer nanocomposite-based electrochemical sensors and biosensors: a review, TrAC Trends Anal. Chem. 82 (2016) 55−67. Available from: https://doi.org/10.1016/j.trac.2016.04.005.

[155] N. German, A. Ramanaviciene, A. Ramanavicius, Dispersed conducting polymer nanocomposites with glucose oxidase and gold nanoparticles for the design of enzymatic glucose biosensors, Polymers 13 (13) (2021). Available from: https://doi.org/10.3390/polym13132173.

[156] R. Devi, M. Thakur, C.S. Pundir, Construction and application of an amperometric xanthine biosensor based on zinc oxide nanoparticles-polypyrrole composite film, Biosens. Bioelectron. 26 (8) (2011) 3420−3426. Available from: https://doi.org/10.1016/j.bios.2011.01.014.

[157] T. Marimuthu, S. Mohamad, Y. Alias, Needle-like polypyrrole−NiO composite for non-enzymatic detection of glucose, Synth. Met. 207 (2015) 35−41. Available from: https://doi.org/10.1016/j.synthmet.2015.06.007.

[158] Z. Yu, et al., Facile synthesis of $NiCo_2O_4$@polyaniline core−shell nanocomposite for sensitive determination of glucose, Biosens. Bioelectron. 75 (2016) 161−165. Available from: https://doi.org/10.1016/j.bios.2015.08.024.

[159] T. Soundappan, R. Muniyandi, S.-M. Chen, Nano TiOTi$O_2$-PEDOT film for the simultaneous detection of ascorbic acid and diclofenac, Int. J. Electrochem. Sci. 7 (2012) 2109−2122.

[160] T. Nie, K. Zhang, J. Xu, L. Lu, L. Bai, A facile one-pot strategy for the electrochemical synthesis of poly(3,4-ethylenedioxythiophene)/zirconia nanocomposite as an effective sensing platform for vitamins B2, B6 and C, J. Electroanal. Chem. 717−718 (2014) 1−9. Available from: https://doi.org/10.1016/j.jelechem.2014.01.006.

[161] A.T. Mane, S.T. Navale, S. Sen, D.K. Aswal, S.K. Gupta, V.B. Patil, Nitrogen dioxide ($NO_2$) sensing performance of p-polypyrrole/n-tungsten oxide hybrid nanocomposites at room temperature, Org. Electron. 16 (2015) 195−204. Available from: https://doi.org/10.1016/j.orgel.2014.10.045.

[162] S. Ivanov, U. Lange, V. Tsakova, V.M. Mirsky, Electrocatalytically active nanocomposite from palladium nanoparticles and polyaniline: oxidation of hydrazine, Sensors Actuators B Chem. 150 (1) (2010) 271−278. Available from: https://doi.org/10.1016/j.snb.2010.07.004.

[163] H. Rao, et al., A novel electrochemical sensor based on Au@PANI composites film modified glassy carbon electrode binding molecular imprinting technique for the determination of melamine, Biosens. Bioelectron. 87 (2017) 1029−1035. Available from: https://doi.org/10.1016/j.bios.2016.09.074.

[164] Q. Rong, H. Han, F. Feng, Z. Ma, Network nanostructured polypyrrole hydrogel/Au composites as enhanced electrochemical biosensing platform, Sci. Rep. 5 (1) (2015) 11440. Available from: https://doi.org/10.1038/srep11440.

[165] F. Jiang, R. Yue, Y. Du, J. Xu, P. Yang, A one-pot 'green' synthesis of Pd-decorated PEDOT nanospheres for nonenzymatic hydrogen peroxide sensing, Biosens. Bioelectron. 44 (2013) 127−131. Available from: https://doi.org/10.1016/j.bios.2013.01.003.

[166] K. Zhang, et al., Controllable synthesis of multi-walled carbon nanotubes/poly(3,4-ethylenedioxythiophene) core-shell nanofibers with enhanced electrocatalytic activity, Electrochim. Acta 137 (2014) 518−525. Available from: https://doi.org/10.1016/j.electacta.2014.06.053.

[167] S. Tajik, et al., Carbon and graphene quantum dots: a review on syntheses, characterization, biological and sensing applications for neurotransmitter determination, RSC Adv. 10 (26) (2020) 15406−15429. Available from: https://doi.org/10.1039/D0RA00799D.

[168] S. Su, H. Sun, F. Xu, L. Yuwen, C. Fan, L. Wang, Direct electrochemistry of glucose oxidase and a biosensor for glucose based on a glass carbon electrode modified with $MoS_2$ nanosheets decorated with gold nanoparticles, Microchim. Acta 181 (13) (2014) 1497−1503. Available from: https://doi.org/10.1007/s00604-014-1178-9.

# Polymer nanocomposites for microelectronic devices and biosensors

9

*Mamun Rabbani*[1], *Md. Sharjis Ibne Wadud*[2] *and Md Enamul Hoque*[2]
[1]Department of Biomedical Physics and Technology, University of Dhaka, Dhaka, Bangladesh
[2]Department of Biomedical Engineering, Military Institute of Science and Technology (MIST), Dhaka, Bangladesh

## 9.1 Introduction

In this era of digitization, the demand for electronic devices is ever on the rise. Nowadays, most of the electronic devices and sensors preferred are getting miniaturized for versatile applications in embedded and wearable systems. Shrinking dimensions in electronic devices based on semiconductor materials come along with various problems. Again, the increasing need for wearable devices demands materials that have more flexibility and less brittleness. Also, these devices are needed to be low power consuming and having a long run time. As the designing processes and fabrication methodologies are trying to keep up with the pace, a new dimension has been added to microelectronic devices by using polymer nanocomposites. Nanocomposites are referred to as a class of materials that have one of their dimensions in the nanoscale range. To be precise, a nanocomposite material should have a hybrid property apart from the parent material, which is the result of the submicron dimension of the component.

A subcategory of nanocomposites suitable for fabricating electronic devices is conducting polymer nanocomposites. These nanocomposites have conductive nanofillers embedded in the polymer matrices, which support the conduction of electrons. The nanofillers are usually made of carbon nanotube (CNT), metal nanoparticles, graphene-based compounds, etc. Nanocomposites demonstrate low density, flexibility, resistance to oxidation, ease of fabrication, tunable mechanical, electrical and optical properties. Due to versatile properties, polymer-based composites particularly nanocomposites have wider advanced applications such as sensors, wearable flexible electronics, thermoelectric devices, energy-storage devices, biomedical applications, and so on [1−8].

Some of the widely used polymer nanocomposites in designing microelectronic devices and sensors are polyaniline (PANI), poly(3,4-ethylenedioxythiophene) (PEDOT), polypyrrole (PPy), and poly(*p*-phenylene vinylene) (PPV) (Fig. 9.1). These polymers are used as matrices to embed conducting nanofillers. Widely used

**Advanced Polymer Nanocomposites. DOI:** https://doi.org/10.1016/B978-0-12-824492-0.00002-7


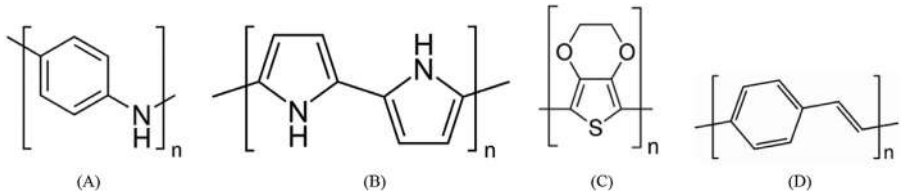


**Figure 9.1** Chemical symbols of (A) polyaniline, (B) polypyrrole, (C) poly(3,4-ethylenedioxythiophene), and (D) poly(*p*-phenylene vinylene).

conducting nanofillers include metal nanoparticles, metal nanowires, and various metallic nanostructures. Apart from metal, nanostructured metal oxides are also used as nanofillers. Carbon-based nanofillers are one of the most promising materials, which include CNTs, graphene, and oxides of graphene. The focus of this article is on the implementation of conducting polymer nanocomposites in fabricating microelectronic devices and sensing applications. The application of nanocomposites in optical devices brings out improvement in performance and stability. Energy-storing supercapacitors is another device that is enriched by the use of nanocomposites. Different sorts of sensors like strain sensors, electrochemical sensors, gas sensors, temperature sensors and their improvement by using polymer nanocomposites are discussed in this chapter.

## 9.2 Optical devices

Organic–inorganic polymer composite materials possess excellent optical properties, which are widely used in various optical applications. These composites exhibit a wide range of bandgap values, hence covering the entire visible bandwidth. The dimension of the inorganic nanoparticles in the composite has a significant role in the operation of the nanocomposite. A study shows that the size of the particles should be a decade less than visible light to avoid loss due to optical scattering [9]. The addition of inorganic nanoparticles to organic polymers also increases the stability of the overall device. The applications of polymer nanocomposites in optical device designing can be mainly divided into two groups, light-emitting diodes used in display technology and photovoltaic cells used in energy conversions.

### *9.2.1 Organic light-emitting diodes*

The use of organic thin films for diodes was first introduced in 1987 by Tang and VanSlyke [10]. Since then, organic light-emitting diodes (OLEDs) have been extensively used in many applications. In general, an OLED has four layers. The first layer is the anode which is supposed to be transparent hence deposited on a

substrate like plastic or glass. In most cases, indium tin oxide (ITO) is used for anode due to its transparency towards the light. Then comes the hole injection layer, which helps in injecting holes in the active layer from the anode. PEDOT: poly(styrene sulfonate) (PSS) is usually preferred in this layer due to its efficiency and easiness. A small potential barrier exists between PEDOT:PSS and ITO, which enables high injection of charge carriers in the anode. The active layer in the third layer is encapsulated by the fourth layer, which serves as the cathode. The work function in between the metal used as cathode and the active layer is chosen to be low so that electrons can be easily injected into the cathode. Polymer nanocomposites are preferred in designing OLEDs because they enhance the overall function of the device. Some of the aspects are discussed below.

#### 9.2.1.1 Improvement of efficiency

Recombination between electrons and holes occurs in the active layer of OLED. But due to the difference in mobility of electrons and holes, recombination does not occur as expected and decreases the efficiency of the device. One of the ways of increasing the efficiency of OLED is to increase the amount of recombination inside the active layer. Appropriate blocking layers can restrain the carriers inside the active region and influence them to recombine. Moreover, increasing the number of injected charges increase the possibility of recombination. Nanocomposites work a great deal in improving performance. During the preparation of the active layer, if nanoparticles are added with the polymer, it is expected that due to their weight, most of the particles will be in the vicinity of the anode. Due to this modified morphology, the surface of contact between the anode and active layer increases significantly increasing charge injection. Apart from this, the addition of nanoparticles in the polymer reduces the thickness of the film. Due to reduced film thickness, the applied electric field increases and, in turn, increases the charge transport and efficiency of the device.

Carter et al. reported the incorporation of insulating oxide to electroluminescent polymer materials enhanced the performance of OLEDs [11]. They fabricated the OLED from oxide nanoparticle/MEH−poly[2-methoxy-5-(2'-ethylhexyloxy)-1,4-phenylene vinylene (PPV) nanocomposite. They found that the inclusion of oxide nanoparticles enhanced the current densities by an order of magnitude with minimal loss. A radiance of 10,000 cd $m^{-2}$ was obtained by the OLED at 5 V. Various works show that the increase in the concentration of nanoparticles enhances the conductivity and performance of OLED. From the work of Prasad, it can be seen that the introduction of cadmium selenide (CdSe) nanoparticles in the matrix layers of polycarbazole polymer increases the mobility of the charge carrier [12]. This enhancement of charge carriers is strongly dependent on the electric field, indicating induced drift mobility. The nanoparticles absorb and accelerate the carriers, acting as a booster of conductivity. He also showed that the size of the nanoparticle plays a role in the electrical properties of the polymer. Small nanoparticles ($\sim$20 nm) produced disorder and hampered the carrier transport, whereas large particles ($\sim$100 nm) increased the conductivity.

#### 9.2.1.2 Improvement of color emission

Light emitted from OLED is related to the bandgap between the materials. Technically it is possible to get emissions of every color by modifying the bandgap values. However, it is pretty tough to get a wide range of wavelengths from one material. An approach to obtain a variety of colors from a single material is to deposit emitting layers of red, green, and blue and controlling the thickness of all three layers precisely to obtain e certain color. But this process, although technically sound, is not industrially feasible. A more feasible approach to reach the whole range of the visible spectrum is to use a blue-emitting copolymer with controlled amounts of red and green dyes. This was shown in the work of Kok et al. [13]. They used polyspirobifluorene as a blue-emitting copolymer in addition to red and green dye for preparing white OLEDs, which have color rendering indices greater than 80%. A different approach for improving color emission uses a combination of polymer chains, although the combination of polymer chains usually reduces light emission. But for certain materials, the combination of polymer chains enhances the emission. Hong et al. termed this as aggregation-induced emission [14]. Similar work was proposed by Tsai et al., where they displayed white light from anthracene-fused norbornadiene.

### 9.2.2 Organic photovoltaic cells

Organic photovoltaic cells (OPVs) are quite similar in structure, although the operating principle is quite different. OPVs convert the energy from light into usable electricity. This conversion process has three steps. First, an exciton (pair of electron−hole) having energy $E_x$ is generated on the absorption of a photon. Second, the exciton travels a length through the material known as exciton diffusion length. By the end of the diffusion length, charges in the exciton are separated. And finally, the separated charges are collected by their corresponding electrodes resulting in a voltage difference and current flow in the external circuit. The typical diffusion length in conjugated polymers is around 10 nm. This low value of exciton diffusion length creates a problem in carrier collection. All the carriers generated in the process are not collected; only the ones near the electrode interface get collected. Hence this degrades the performance of the OPVs. Moreover, the large bandgap value of polymer materials hinders the absorption of light in the infrared region. Many researchers have suggested that the incorporation of nanoparticles in the polymer results in enhanced performance of OPVs.

Two ways of incorporating nanoparticles in polymers for OPVs have been explored. The first process is fabricating a structure out of polymer substrate and blended polymer nanoparticles. This allows a good mixture of donor and acceptor atoms and an easy deposition of the thin film, as shown by Hoppe and Sariciftci [15]. One of the most widely used and efficient nanocomposites was designed by Dennler et al. [16]. Their nanocomposite was made from regioregular poly(3-hexylthiophene-2,5-diyl (P3HT) and phenyl-C61 butyric acid methyl ester, which is a derivative of fullerene. Efficiencies of more than 4% for this material have been

reported by Reyes et al. [17]. The second process of fabricating devices is the inorganic−organic approach. The conjugated polymer solution is used with a nanoporous metal oxide substrate. The inorganic metal oxide network enhances the transport of electrons towards the electrodes [18].

A way to enhance the photonic absorbance in the photoactive layer of OPVs is to incorporate dyes. Wang and Wang used a perylene derivative with P3HT and $TiO_2$ to fabricate OPVs [19]. The perylene derivative has a wide absorbance spectrum and enhances the efficiency of OPVs. Narrow bandgap nanoparticles have been used to harvest current from low-energy photons and thus extend the photovoltaic response to the near-infrared region. Such a work has been reported by Cui et al. [20]. They introduced PbS nanoparticles in a matrix of PPV to enhance infrared absorptions. Carrier transport improvement can be achieved by adding inorganic semiconductors having high mobility. This was proposed by Huynh et al., who devised a nanocomposite from P3HT and CdSe nanoparticles [21]. Their material showed high conductivity due to fast charge separation and recorded a conversion efficiency of nearly 1.7%.

A different method to enhance the performance of OPVs is to add nanowires and nanorods to the polymer substrate as the electric properties of nanorods and nanowires are better than that of nanoparticles. Using nanorods and nanowires in photovoltaic cells increases the absorption of photons by decreasing the optical reflectance of the material significantly. This was reported by Bouclé et al., where they used $TiO_2$ nanorods blended in hybrid P3HT and used as the active layer of photovoltaic cells [22]. ZnO nanorods have also proven to be efficient in charge transport when combined with a polymer to create nanocomposites for solar cells [23,24]. Liu et al. constructed a solar cell using P3HT and vertically grown ZnO in ITO/ZnO:P3HT/Ag structures [25]. Their cells recorded a short circuit current of 2.2 mA $cm^{-2}$, an open circuit voltage of 440 mV, 0.56 infill factor, and the power efficiency was found at 0.53%.

## 9.3 Supercapacitors

Capacitors are widely used as energy-storage devices. The capacitance of the capacitor varies depending on the type of dielectric material used. In recent times, a new type of capacitor is gaining popularity, which is known as supercapacitors. They exhibit high power density, long charging−discharging cycle, and ultrahigh capacitance. The material preferred for designing supercapacitors usually requires mechanical and chemical constancy, high specific area, and low cost of production. Conducting polymers can play a vital role in fulfilling all the requirements. Apart from being conducted, these conducting polymers show a fast redox reaction with electrolytes. PPy, PANI, and PEDOT are widely preferred conducting polymers used in supercapacitance applications [26]. Although these polymers possess unique qualities like high charging−discharging, high conductivity, and high capacitance [27], they face stability issues when used for supercapacitance application over

long periods. The redox reactions of conducting polymers give rise to mechanical stress, which results in loss of material and ultimately the breakdown of capacitance. A way around this demerit is to compound the conducting polymers with various forms of carbon. Graphene, which is a conducting form of carbon, has some intrinsic properties which give it an upper hand in energy-storage facilities. Incorporating conducting polymers with graphene gives rise to enhanced properties for energy-storing supercapacitors. Compounds of graphene and conducting polymers for supercapacitor applications are discussed here.

### 9.3.1 Graphene and polyaniline composites

PANI has high conductivity, high electroactivity, and high specific capacitance, along with good stability, hence PANI has been broadly studied in fabricating supercapacitors. Nanocomposites of graphene and PANI can be made through in situ polymerization of aniline with graphene suspension in an acidic medium. Zhang et al. prepared a nanocomposite with PANI and graphene oxide (GO) for electrochemical analysis [28]. They reported that different concentrations of GO resulted in a unique GO/PANI nanocomposite morphology, thus affecting the characteristics of the supercapacitance electrode. The specific capacitance of the nanocomposite decreases with the increasing concentration of GO. This was evident as pure PANI nanofibers exhibit a specific capacitance of 420 $Fg^{-1}$, whereas the specific capacitance of GO/PANI nanocomposite with 10 wt.% GO is 320 $Fg^{-1}$, with 50 wt.% GO is 207 $Fg^{-1}$, and with 80 wt.% GO is 158 $Fg^{-1}$. On the other hand, the capacitance retention of the nanocomposites is improved over long cycles due to the incorporation of GO. Pure PANI shows very poor cycling stability with specific capacitance decreasing to nearly 60% after five cycles due to the volumetric change in PANI. GO nanoparticles compensate for this volumetric change and provide more stability over the charging−discharging cycles.

In GO/PANI nanocomposites, the GO nanoparticles provide very little contribution to the specific capacitance due to the insulating nature of GO. The developed capacitance of the nanocomposite is mainly due to the pseudo-capacitance from PANI nanofibers. Many researchers have proposed using reduced graphene oxide (rGO) instead of GO in the nanocomposites [29,30]. rGO has a higher specific capacitance, and for its high conductivity, it can substantially reduce the equivalent series resistance of the supercapacitor electrode. Wang et al. proposed a way of synthesizing rGO/PANI nanocomposites [31,32]. Their nanocomposites have a thickness of 30−40 nm with a size of a few micrometers, hence having a large surface area. The highest specific capacitance was reported to be 1129 $Fg^{-1}$. The cyclic retention of rGO/PANI nanocomposites also showed significant improvement.

### 9.3.2 Graphene and polypyrrole composites

PPy has good conductivity and thermal stability for which is an attractive conducting polymer material for supercapacitor applications. However, unlike PANI, there are submicron particles in a thin film of PPy. These particles combine into

cauliflower-like structures due to increased polymerization and incline to increase the thickness of the film. These thick films tend to reduce the surface area and show a probability of blocking the electrolyte ions. Additionally, these structures tend to collapse under stress caused by the charging−discharging cycles of the supercapacitor. The performance of PPy nanocomposites for supercapacitor application is not as promising as PANI nanocomposites.

Bose et al. synthesized graphene nanosheets (GNS) by reducing GO to prepare a GNS/PPy nanocomposite [33]. They observed that the specific capacitance of the GNS/PPy nanocomposite was almost double than that of pure PPy. The charging−discharging cycle performance also improved significantly. The introduction of graphene in PPy facilitates the electrochemical utilization of PPy and also provides structural stability by providing mechanical support to PPy during the charging−discharging cycles.

### 9.3.3 Graphene and poly(3,4-ethylenedioxythiophene) composites

PEDOT is one of the most widely used polymers in making nanocomposites. An easy to fabricate polymer, PEDOT shows excellent electrical conductivity topping at 500 S $cm^{-1}$ [34]. It also possesses good chemical and thermal stability. Due to its outstanding cycling stability of holding 80% capacitance over 70,000 cycles, it is highly preferred in supercapacitor applications [35]. However, PEDOT shows a low specific capacitance due to its large molecular weight, which tends to be a disadvantage in supercapacitor application [36].

Graphene/PEDOT nanocomposites show better performances in supercapacitor applications. Choi et al. stated that the electrical conductivity of graphene/PEDOT nanocomposites doubled compared to pure PEDOT and the nanocomposite also showed a sixfold improvement in mechanical strength [37]. The overall behavior of charge transport of PEDOT improves on the incorporation of graphene is for the fact that graphene creates pathways for percolation and propagation of charge in the nanocomposite [38]. The introduction of graphene in PEDOT reduces the structural damages to PEDOT due to volumetric changes as graphene creates a heterogeneous structure with PEDOT [39]. The electrical conductivity of graphene is also superior to that of PEDOT, making the nanocomposite more conductive [39]. The incorporation of graphene makes a three-dimensional morphology of the nanocomposite, increasing the surface area and hence improving the specific capacitance [39].

Depending on the method of polymerization, pure PEDOT supercapacitors have shown specific capacitances of 70−130 $Fg^{-1}$ [35,39]. An improvement in cycling stability and specific capacitance has been reported on adding graphene to PEDOT. Graphene/PEDOT nanocomposites showing a specific capacitance of 304 $Fg^{-1}$ in HCl electrolyte and 261 $Fg^{-1}$ in $H_2SO_4$ have been reported by Alvi et al. [40]. Research work by Wen et al. showed a specific capacitance of 136 $Fg^{-1}$ for GO/PEDOT nanocomposites and 209 $Fg^{-1}$ for rGO/PEDOT nanocomposites. They also reported 87% retention of capacitance over 2000 cycles [41].

## 9.4 Strain sensor

In recent times, the demand for wearable devices and gazettes has been on the rise in the healthcare and medical sectors, prosthetics, robotics, professional sports, etc. An important application of wearable sensing technology is strain sensing. Various sorts of strain sensors have been developed over time which include the physics of Raman shift, fiber Bragg grating, liquid metal, piezoelectricity, and triboelectricity [42,43]. Although fabrication complexity, low resolution, unsatisfactory dynamic performance puts a limitation to their applications. A more popular and practical strain-sensing mechanisms are the resistive-type and capacitive-type strain sensors. These sensors have high flexibility, high sensitivity, and are easy to fabricate and integrate [44,45]. Although inexpensive, traditional strain sensors have very limited performance parameters. Sensors made from silicon and semiconductor films are rigid and brittle in nature and pose complexities in incorporating flexible wearable applications. Polymer nanocomposites are the choice of material for making flexible wearable strain sensors. A strain sensor from polymer nanocomposite has two parts, one part provides pathways for signal production, and the other part is an elastomeric polymer which provides protection, stretchability, and flexibility for the conductive part [46]. Various sorts of polymer nanocomposites are used in developing strain sensors. Some of the recent types are discussed here.

### 9.4.1 Silver nanoparticle–based strain sensor

A highly stretchable resistive strain sensor is designed by adding silver nanoparticles (Ag NPs) with rubber fibers. This composite is compatible with any substrate and can be scaled up for large-area implementation. Ag NP precursor is absorbed in electrospun poly (styrene-block-butadiene-block-styrene) (SBS) rubber fibers, which are then transformed into Ag NPs in the fiber mat [47,48]. The percolation of Ag NP within the SBS fibers leads to an increased conductivity at large deformation due to strain. Park et al. reported stress of 2200 S $cm^{-1}$ at a strain of 100% for a fiber mat of 150 μm thickness.

Another nanocomposite of Ag NP in designing strain sensors is the composite films of Ag NP and CNTs in the pattern of high aspect ratio fibers [49]. The composite has a high conductive network due to CNT with high bendability. Ag NP loading increasing the conductivity giving the composite high sensitivity to strain. The composites show resistance that is high sensitivity to strain along with pressure sensitivity of 8% $Pa^{-1}$. Both the resistivity and sensitivity of the nanocomposite can be altered by a few orders by altering the composition ratio of the constituents, making this material highly preferred for strain sensing.

### 9.4.2 Silver nanowire–based strain sensor

Silver nanowire (AgNW)–based composites have excellent electrical and mechanical properties, making them an appropriate candidate for strain sensors. A nanocomposite

of AgNW and polydimethylsiloxane (PDMS) elastomer has been explored for making highly flexible, sensitive, and stretchable strain sensors [50,51]. Amjadi et al. designed a sandwich structure of nanocomposite where AgNW thin film is implanted between two layers of PDMS. Sensors designed from such nanocomposites showed strong piezoelectricity along with adjustable gauge factors (2−14) and increased stretchability (∼70%). A similar sensor designed by Yao and Zhu [50] can detect strain up to 50% and pressure up to almost 1.2 MPa. Although quite efficient and robust, these proposed sensors detect strain in one direction. So such designs fail in applications where multiaxial, multidimensional, complex strain is involved. A novel scheme to counter this problem has been proposed by Kim et al. [52]. They have used prestrained AgNW percolation networks to design a highly stretchable and sensitive multidimensional strain sensor, which is capable of detecting multidimensional strain loadings in real time. The design is based on two intersecting prestrained percolation networks having decoupled electrical resistances. Electrical resistances are detected in both the major axis and perpendicular direction of the principal strain, thus detecting strain in both axes of surface strains. This design has demonstrated a gauge factor of nearly 20, strain measurements greater than 35%, and dynamic load performance with very little hysteresis. AgNW of lengths greater than 80 μm are used to provide electrical and mechanical stability in the percolation network.

Another promising application of AgNW was proposed by Lee et al. [53]. They developed very long AgNW and applied them as a recent type of highly conductive and highly stretchable metal electrode. The high aspect ratio of the AgNW served in favor of the high conductance and mechanical compliance. Very long AgNW were formed and percolated on hydrogel substrate. Such composite gave a strain of more than 460% with low sheet resistance.

### 9.4.3 Silver nanoflower fiber–based strain sensor

Flower-shaped Ag NPs having petals in the shape of nanodisks, also known as Ag nanoflowers, dispersed in polyurethane, provides a nanocomposite with high conductivity due to the enhanced surface area. Such materials are used in designing highly conductive stretchable fibers. These fibers present a conductivity of 41,245 S $cm^{-1}$, which is two times higher compared to fibers synthesized with Ag NPs [54]. The highest rupture strain of this fiber was found to be 776%, Young's modulus of 731.5 MPa, and a strength of 39.6 MPa. These highly conductive, stretchable fibers are an excellent choice for wearable strain sensors.

### 9.4.4 Graphene-based strain sensor

Graphene is one of the most preferred materials in terms of flexibility. Being a two-dimensional (2D) material, graphene composites are used in various sorts of strain sensors. Hempel et al. proposed a new design of strain sensor using graphene thin films [55]. Thin films of overlapping flakes were made by spray deposition. A tunable gauge factor exceeding 150 was observed.

A different type of graphene-based nanocomposites is the graphene woven fabrics (GWF) [56]. GWF has a behavior quite different from thin films. Due to their polycrystalline structures, GWFs experience significant changes when mechanically deformed. They also show high-density crack formation. GWFs have an electrical resistance that is exponentially correlated with tensile strain. Gauge factors of nearly $10^3$ are observed under 2%−6% strains which goes as high as $10^6$ under higher strains [56].

Another graphene derivative for strain sensors is the graphene−nanocellulose composite nanopaper. Crumpled graphene and nanocellulose are embedded in PDMS elastomer, which gives the composite stretchability up to 100% [57]. This novel technique provides a gauge factor of 7.1 and is effectively used in human motion detecting applications.

### 9.4.5 Gold nanowire−based strain sensor

A novel technique for fabricating strain sensors using gold nanowires (AuNWs) has been proposed by Gong et al. [58]. Ultrathin AuNW is quite different from other metal nanowires and possesses high conductivity along with mechanical flexibility. AuNWs can be fabricated to 2 nm thin and tens of micrometers long [59,60]. Gong et al. fabricated 1.64-μm-thin black-gold films on latex rubber using a drop-casting approach to create a highly stretchable strain sensor. The sensors could detect strains from 0.01% to 350%, having a gauge factor of 6.9−9.9. The AuNW thin films withstood 300% stretching without any apparent detachment or cracking. A smooth, positive correlation between electrical resistance and applied strain is also seen. A unique characteristic of this sensor is that it is fully reversible between 0% and 100% strain with no notable hysteresis.

## 9.5 Electrochemical sensor

An interesting and booming application of polymer nanocomposites is in detecting several chemical and biochemical analytes. Due to their high stability, simple synthesis techniques, low operating temperature, economic behavior, and lightweight, conducting polymer nanocomposites have been the material of choice for various electrochemical sensors [61]. Out of the various polymer nanocomposite used, composites of PANI, PPy, and PEDOT have unique qualities in favor of sensor applications [62,63]. Some widely researched conducting polymer nanocomposites in combination with different materials such as carbon and its derivatives and metals and their oxides are discussed here.

### 9.5.1 Conducting polymers/carbon nanoparticle−based sensors

Carbon nanomaterials are playing a leading role in designing sensors nowadays. Various sorts of carbon nanomaterials include single-walled carbon nanotubes

(SWCNTs), multiwalled carbon nanotubes (MWCNTs), carbon nanospheres, and carbon nanofibers. The incorporation of these nanomaterials in conducting polymers results in nanocomposites having improved thermal stability, electrical sensitivity, chemical properties, and mechanical strength [64,65]. Carbon polymer nanocomposites possess high corrosion resistance, low density, ease of molding, and varying electrical conductivities compared to their metallic conductor counterparts. Synthesizing nanocomposites with CNTs and nanofibers yields in conducting polymer nanocomposites having high charge transfer capacities and high surface area.

CNTs, an allotropic form of fundamental carbon having a single, double, or multilayered cylindrical shape, have been impacting the field of polymer nanocomposites since their early days. CNTs possess many unique mechanical and thermal properties, for which it is widely explored in electronics [66,67]. Using CNT nanofillers in conducting polymer matrix helps in modifying the electronic behavior of the components. Electrochemical polymerization was utilized to make thin films of PANI nanocomposite with functional SWCNT (f-SWCNT) doping to detect the presence of $H_2S$ [68]. To make the nanocomposite, a thin film with the best sensitivity, 0.01% f-SWCNT was added to the PANI matrix. Along with excellent sensitivity, the sensor displayed good recovery and response time for $H_2S$ at 50°C. Another work by Srivastava et al. described the process of using both SWCNTs and MWCNTs with PANI composites to prepare a resistive-type sensor for $H_2$ detection [69]. They found a better response of SWCNT/PANI and MWCNT/PANI nanocomposites compared to pure PANI; the response for pure PANI was 1.033 improved to 1.071 for SWCNT/PANI and 1.062 for MWCNT. In some sensing applications, it is needed to use materials that are tolerant to high temperatures. Sharma et al. observed the thermal qualities of PANI and PEDOT:PSS with MWCNTs in developing high-temperature-resistant sensors for $NH_3$ detection [70]. They found that although both sensors had very impressive sensitivity, they had degraded recovery time for $NH_3$ gas. But PEDOT:PSS was concluded to be superior in terms of sensitivity ($\sim$16%) and response time ($\sim$15 minutes) than PANI nanocomposite. The PEDOT:PSS nanocomposite showed better thermal stability in detecting $NH_3$ of concentration 1−50 ppm.

PPy is another extensively used conducting polymer, which has superior electrical properties and is highly used in electronic and chemical sensor fabrication. Sadrolhosseini et al. used designed plasmon resonance technique to detect minute amounts of mercury, lead, and iron using a PPy nanocomposite with MWCNT [71]. The incorporation of MWCNT enhanced the sensitivity of the sensor, giving it a lower detection limit of 0.1 ppm. A PPy-based biosensor for detecting glucose was proposed by Teh and Lin [72]. They designed an MWCNT/PPy nanocomposite laden in glucose oxidase to deter the presence of glucose. Their results showed a sensitivity of up to 20 mM, which is quite an important range for diabetic patients. Another work using PPy was developing a sensor to detect the presence of $NO_2$. An et al. synthesized the PPy polymer with functionalized SWCNT in the presence of oxalic acid as a dopant [73]. Their work measured the resistivity of the sensor at different temperatures to detect the presence of $NO_2$.

### 9.5.2 Conducting polymers/graphene-based sensors

Graphene, another allotrope of carbon, is widely used in various applications. The incorporation of graphene and its derivatives, namely GO and rGO, into nanocomposites have proven to improve the parameters of sensors in various applications. Although GO behaves mostly as an insulator, it can be reduced to graphene and acquire high electrical conductivity with the help of strong reducing agents like sodium tetrahydroborate ($NaBH_4$) or hydrazine ($NH_2NH_2$) [74]. So, GO is also widely used in preparing polymer nanocomposites/graphene-based sensors. A common conducting polymer PEDOT incorporated with GO is used to detect the presence of dopamine (DA) [75,76]. The sensor has a wide range of detection from 0.1 to 175 μM, with the lowest detection level of 39 nM. The detection was also linear and free of distortion from other components such as ascorbic acid and uric acid.

A popular polymer for designing electrochemical sensors is PANI. Knower et al. designed a sensor using PANI nanocomposites and GO for the detection of methanol vapor [77]. They synthesized the nanocomposite using a chemical synthetic route and considered the conductivity of direct electric current as a parameter for sensing. According to their work, the conductivity of the sensor was found 241 S $m^{-1}$, which is quite impressive compared to pure PANI, which has a conductivity of 7.5 S $m^{-1}$. rGO incorporated with PANI is used to detect heavy metal ions. Yang et al. reported a work where fabricated rGO/PANI nanocomposites were used for chemical oxidative polymerization to detect $Hg^{2+}$ ions [78]. Their designed nanocomposite showed good sensitivity and selectivity of $Hg^{2+}$ ions within the concentration range of 0.1−100 nM. The lowest limit of detection was reported to be 0.035 nM. Ruecha et al. prepared a PANI nanocomposite modified by graphene for sensing heavy ions like zinc, lead, and cadmium [79]. The graphene/PANI sensor was found to detect the lowest level of 1.0 μg $L^{-1}$ of zinc, 0.1 μg $L^{-1}$ of lead, and 0.1 μg $L^{-1}$ of cadmium.

### 9.5.3 Conducting polymers/metal nanoparticle−based sensors

The inclusion of metal nanoparticles in conducting polymers has resulted in nanocomposites with superior electrical and mechanical qualities along with performance upgradation. Some of the commonly used metal nanoparticles used to make polymer/metal nanocomposites like Ag NPs, palladium nanoparticles (Pd NPs), platinum nanoparticles (Pt NPs), and gold nanoparticles (Au NPs) are discussed.

#### 9.5.3.1 Silver nanoparticles

Ag NPs are quite largely preferred due to their modifiable chemical, thermal, physical, and electrical properties [80,81]. These properties can be modified more by using Ag NP with conducting polymers like PPy and PANI in preparing nanocomposites. Nia et al. designed a nonenzymatic sensor to detect $H_2O_2$. Their sensor had a linear range of detection from 0.1 to 5 mM with a lowest detection level of 0.115

μmol $L^{-1}$. The sensor also had great selectivity, repeatability, stability, and reproducibility in detecting $H_2O_2$.

A few researchers focused on detecting ammonia gas using Ag NP with conducting polymers. Nia et al. prepared Ag/PPy composite nanotubes in the presence of polyvinylpyrrolidone (PVP) to sense the presence of $NH_3$ vapor [82]. The introduction of Ag in the polymer caused an improvement in the chemical-resistor response of the sensor compared to pure PPy. Quite the same work was done by Nerkar, where they fabricated Ag/PPy nanocomposite sensors for $NH_3$ detection at room temperature [83]. Their design showed a quick response of 58−153 seconds and a recovery time of 347−746 seconds. The sensitivity was found to be high for 50−500 ppm $NH_3$. Although the amount of Ag NP contributes to the enhancement of sensor quality in conducting polymers, there is always a threshold of adding the nanoparticles in polymers. After that, the performance of the sensor starts to degrade. This was shown by the works of Park et al., where they synthesized PEDOT nanotubes with Ag NP to detect $NH_3$ [47,48]. They found that after a certain amount, the Ag NP starts to aggregate and diminish the performance of the sensor.

An excellent electrochemical sensor was designed using Ag NP and PANI nanoparticles to analyze the anticancer drug 5-fluorouracil (5-FU) [84]. Differential pulse voltammetry was utilized in measuring the electrochemical qualities of the sensor. It was found that the sensor gave a wide linear relation in detection 5-FU concentration. The maximum sensitivity was found at 1.0−300 μM with the lowest detection of 0.06 μM. The sensor displayed superior selectivity in the presence of other interfering compounds and drugs. It was concluded to be an effective, rapid, and simple device for detecting 5-FU.

### 9.5.3.2 Palladium nanoparticles

Pd NPs have unique catalytic, optical, and electrical properties, which help in various organic and inorganic reactions [85,86]. Incorporating Pd NPs in conducting polymers enhances both the electrical and catalytical characteristics of the nanocomposite, and such materials are widely used in electrochemical sensor designing.

Pd/PANI nanocomposites were synthesized to detect the presence of $H_2$ and humidity by Sandaruwan et al. [87]. They found that the Pd/PANI films showed a good response by having a decreasing impedance in contact with humidity compared to pure PANI films. Moreover, Pd NP-incorporated PANI films showed outstanding response towards $H_2$, although interestingly, pure PANI did not respond to $H_2$.

A sensor to detect glucose and $H_2O_2$ was designed by Hosseini et al. They synthesized Pd NP in PEDOT nanofibers to prepare the nanocomposite for the sensor. The sensor showed −0.3 V against Ag/AgCl electrode in the presence of $H_2O_2$. Chronoamperometric measurements showed that the peak currents in the anode are linear, with the concentration of $H_2O_2$ within the range of 0.2−25 μM and having the lowest limit of detection as 0.05 μM. Again, the same sensor showed excellent performance in detecting glucose, sensing −0.1 V against Ag/AgCl electrode. The peak current at the anode was shown to be linear, with a concentration within the

range of 0.04−9 mM and having a minimum limit of 1.6 μM. The sensor was capable of detecting glucose in the manifestation of interfering agents like ascorbic acid and uric acid, making it a good candidate for implementation in human trials. For high sensitivity and selectivity, good stability, and reproducibility, sensors made from Pd/PEDOT nanocomposite can be considered inexpensive amperometric glucose biosensors.

### 9.5.3.3 Platinum nanoparticles

Sensing biomolecules (DNA, proteins, antibodies, enzymes) and macromolecules are efficiently done by Pt NPs [88]. Conducting polymers like PPy and PANI have been synthesized with Pt NP to form nanocomposites in structures of nanotubes and nanofibers for various applications in sensing. A biosensor was developed by Mishra et al. using Pt NP and PPy nanocomposites to detect human C-reactive protein [89]. Both the Pt NP and PPy contribute separately in the transducing action. PPy has a long chain that offers space between the transducer and the biomolecule. Whereas Pt NP works in reducing the steric hindrance and preserving native conformity, thus contributing to accessibility of biomolecules to the analyte. The sensor is reported to have a large surface area and good performance. The sensor exhibited a linear detection range of 10 ng $mL^{-1}$ to 10 μg $mL^{-1}$. Another application of Pt NP/PPy nanocomposite as a biosensor was proposed by Adeloju and Hussain for sensing sulfite [90]. They used a potentiometric detection technique to measure sulfite in samples of beer and wine. They found the sensor to be linear within the range of 0.75−65.50 μM with a minimum sensing limit of 12.4 nM. The sensor also showed a response time of 3−5 seconds. A different nanocomposite comprising Pt NP and PANI was used in sensing glucose. Zhai et al. constructed the Pt/PANI hydrogel heterostructures for the enzymatic detection of glucose [91]. Their model showed excellent sensitivity of as high as 96.1 μA $mM^{-1}$ $cm^{-2}$. The response time of the sensor was as fast as 3 seconds. The sensor exhibited a linear range of 0.01−8 mM with a minimum detection level of 0.7 μM.

### 9.5.3.4 Gold nanoparticles

Au NPs incorporated with different conducting polymers construct nanocomposites, which are widely used in sensing $H_2O_2$, $NH_3$, DA, glucose, uric acid, ascorbic acid, nitrite, and heavy metals. Hung et al. synthesized PANI nanocomposites with Au NP to detect $H_2O_2$ [92]. Their sensor showed a quick response time of 3 seconds and high sensitivity of $H_2O_2$ with the lowest sensing limit of 0.1 μM. A glucose biosensor using a three-component nanocomposite was proposed by Miao et al. [93]. They fabricated an Au/PANI/PVP system by electrodepositing Au NP on glassy carbon having the two polymers. The sensor gave a large linear range of detection from 0.05 to 2.25 mM with the lowest detection level of $10^{-5}$ M. A high sensitivity of 9.62 μA $mM^{-1}$ $cm^{-2}$ was also recorded. The sensor showed satisfactory results in detecting glucose in human serum samples. Sadanandhan and Devaki devised an electrochemical sensor to simultaneously detect uric acid, serotonin,

ascorbic acid, and DA [94]. They fabricated a glassy carbon electrode with PANI using electrochemical polymerization and added Au NP by the chronoamperometric method. Their sensor was tested on blood serum and was suggested to be an excellent choice for sensing neurotransmitters. Another versatile electrochemical sensor fabricated from Au NP/PANI nanowires was put forth by Chaudhury et al. They fabricated the nanocomposites with three separate biomolecules, glucose oxidase, for detecting the presence of glucose, single-stranded DNA protein for detecting complementary DNA, and lamin A antibody for detecting lamin A protein. In glucose sensing, the sensor exhibited good stability and specificity. It gave a sensitivity of 14.63 $\mu A\ mM^{-1}\ cm^{-2}$ with the least detection of 1 μM. The sensor was capable of detecting complementary and noncomplementary DNA in analyte concentrations as low as 1 μM. A nearly similar result was found in protein detection. This portrays the effectiveness of Au NP/PANI nanocomposites as a general sensor platform. A nitrite-sensing electrochemical sensor was proposed by Lin et al. [95]. They synthesized PEDOT nanocomposites doped with Au NP to sense nitrite in tap water. Their sensor successfully detected nitrite in the range of 0.2−1400 μM, having the lowest sensing limit of 60 nM.

### 9.5.4 Conducting polymers/metal oxide nanoparticle−based sensors

The incorporation of metal oxides in conductive polymers improves the electrochemical properties of the nanocomposites, which gives an advantage in sensing applications. Various works in electrochemical sensing have been reported by different research groups.

A common polymer used in different applications is PPy. Suri et al. reported the synthesize of $Fe_3O_4$/PPy nanocomposites for the detection of humidity and $CO_2$, $CH_4$, and $N_2$ [96]. Their nanocomposite showed higher conductivity than pure PPy. Sensitivity towards humidity was found to be increasing with the concentration of PPy. A linear relation was also found between sensitivity and pressure in $CO_2$, $CH_4$, and $N_2$ sensing, with $CO_2$ showing the highest sensitivity. Another application of PPy was proposed in the design of the xanthine biosensor. Devi et al. constructed ZnO/PPy nanocomposite films through electropolymerization on platinum electrodes and immobilized xanthine oxidase on the surface through physisorption [97]. Their design worked as an amperometric sensor with a response of 5 seconds at a temperature of 35°C and pH 7.0. A linear characteristic was recorded from 0.8 to 40 μM of xanthine with the lowest sensing limit of 0.8 μM. The Michaelis−Menten constant was 13.51 μM for xanthine oxidase with a maximum current ($I_{max}$) of 0.071 μA.

Another favorable polymer for fabricating sensors is PANI. PANI-based sensors have been widely demonstrated in electrochemical and biosensing applications. A $TiO_2$/PANI nanocomposite-based sensor to detect the presence of blood glucose has been proposed by Zhu et al. [98]. They implemented aniline on $TiO_2$ nanotubes and used oxidative polymerization to form $TiO_2$/PANI nanocomposites. On the surface, they immobilized glucose oxidase for sensing glucose. Their sensor showed a

sensitivity of 11.4 μA and the lowest detection limit of 0.5 μM. A ternary nanocomposite comprising NiO−CuO and PANI was fabricated for electrochemical sensing of glucose by Ghanbari and Babaei [99]. This Amperometric sensor displayed a quick response, fair selectivity, and superior sensitivity for nonenzymatic detection of glucose in alkaline solution. The detection was in a broad linear range of 20−2500 μM with the lowest detection range of 2.0 μM. Their sensor is capable of detecting glucose in human serum samples avoiding unwanted interferences compared to $NiO_2$/PANI and CuO/PANI binary nanocomposites.

Jain et al. implemented a $Bi_2O_3$/PANI nanocomposite for analyzing pramipexole, which is an anti-Parkinson drug [100]. The electrochemical performance, high electroactive surface area, and easy fabrication make this nanocomposite a promising sensor material. Pang et al. fabricated a ternary nanocomposite of $TiO_2$−$SiO_2$/PANI in the form of nanofibers to detect the presence of $NH_3$ [101]. The nanocomposite showed ideal selectivity, repeatability, and response values for sensing $NH_3$ at room temperature. They also observed that the $NH_3$-sensing capability of the material improved with increasing concentration of $TiO_2$.

## 9.6 Gas sensor

Conducting polymer-based nanocomposites has seen rapid development over the recent years and has proven to be a potential aspirant for gas-sensing applications at room temperature. This advantage is for the fact that the electrical conductivity of polymer nanocomposites can be altered when subjected to oxidative or reductive gas molecules [102,103]. Various sorts of conducting polymers used for gas sensing include polyacetylene (PA), PPy, PEDOT, polythiophene (PT), PANI, PPV, and their derivatives. These conducting polymers show insulated or semiconductor-like nature in the undoped state. Doping processes such as protonic acid doping or redox doping enhance the conductivity of the polymers. This unique doping characteristic enables conducting polymers to be an ideal candidate for room-temperature gas-sensing schemes. Here we will see some of the popular gas sensors built on conducting polymer nanocomposite.

### 9.6.1 Metal oxide−conducting polymer-based gas sensors

Conducting polymers have very good electrochemical and electrical properties along with the added advantage of being stable, low cost, and easy to synthesize. However, slow response, low sensitivity, poor thermal stability, and sensitivity add to their disadvantages and hinders their application as gas sensors. Luckily, nanocomposites of conducting polymer and metal oxides have been shown to improve the demerits and thus paves the path for use in gas-sensing applications. Metal oxide−conducting polymer nanocomposites of various forms such as thin films [104], short rods [105], flowers [106], fibers [107], particles [108], sheets [109] have been successfully applied as gas sensors.

Various metal oxide nanocomposites with PANI were explored over the years. A nanocomposite of $TiO_2$−PANI was successfully implemented by Jiang et al. [104]. They implemented this sensor for sensing ammonia at room temperature. Their work showed a higher performance of hybrid nanocomposites considering sensitivity, responsivity, stability, and recovery time compared to monophase PANI-based sensors. Gong et al. also proposed a similar $TiO_2$−PANI-based gas sensor to detect diluted ammonia [110]. Their sensors detected 50 ppt of ammonia successfully. In this sensor, the PANI nanoparticles were implanted on the surface of $TiO_2$ microfibers acting as switches. These switches get activated or deactivated depending on the adsorption of ammonia particles on the nanocomposite. Wang et al. reported another type of gas sensor based on the core−shell $CeO_2$@PANI structure [75,76]. Their sensor was also based on detecting ammonia which should have a reliable response of 6.5−50 ppm along with long-term stability. A nanorod like $\alpha$-$MoO_3$/PANI-based triethylamine (TEA) sensor was put forward by Bai et al. [105]. The sensor was made on an elastic polyethylene terephthalate substrate with the PANI film enclosed onto the $MoO_3$ nanorod structure. This sensor showed good sensitivity and high selectivity of 5.5−10 ppm TEA at room temperature. The enhanced response of the sensor was due to the inclusion of $MoO_3$ nanorods into PANI as the nanorods provided a network of $\alpha$-$MoO_3$/PANI interfaces enhancing the adsorption of molecules of gas.

Another conducting polymer of choice for detecting volatile organic compounds is PPy. A tube-in-tube $SnO_2$@PPy structure was constructed by Jamalabadi et al. to detect dimethyl methylphosphonate (DMMP) [111]. Their proposed design could detect extremely low concentrations of DMMP. A similar gas sensor based on $Zn_2SnO_4$−PPy nanocomposite to detect ammonia was designed by Ly et al. [112]. They combined PPy nanospheres and $Zn_2SnO_4$ hollow spheres in an alternative layer-by-layer deposition. This design was proved to be extremely sensitive in detecting ammonia.

### 9.6.2 Metal-conducting polymer-based gas sensors

Metal-embedded nanostructures have been extensively used in gas-sensing applications. They have good stability with high electrolytic activity and can drastically improve the conductivity, adsorption, and thermal stability of gas sensors. In general, in a metal-conducting polymer system, metals occur in the form of nanoparticles, whereas the conducting polymers exist as the framework of thin films. Conducting polymers experiences an improvement in sensing properties due to the inclusion of metal nanoparticles for three reasons. First, metal nanoparticles change the conductivity of the polymers. Second, specific metal nanoparticles show chemical affinity towards certain gas substances, enhancing the selectivity of the sensors. Third, the inclusion of metal nanoparticles in conducting polymers increases the effective surface area of the nanocomposite.

In the early days of 2005, a study by Athawale et al. proposed the use of metal-conducting polymer nanocomposite in gas-sensing applications [113]. Their work stated the use of PANI/Pd nanocomposites in detecting various aliphatic alcohol

vapors, which included methanol, ethanol, and isopropanol. They found the nanocomposite to be highly sensitive and selective to methanol vapors with good reversibility and response time. This work paved the way for a further look into the field of metal-conducting polymer nanocomposites for gas detection. Later in 2009, Hong et al. came up with a nanocomposite of PPy with Pd for the detection of $NH_3$ gases [114]. The nanocomposite showed 13%−58% responsivity for detecting $NH_3$ at room temperature with a concentration of 50−2000 ppm. The sensor produced a fast, reproducible, and responsive output with a response time of 14 seconds and recovery time of 148 seconds for $NH_3$ at a concentration of 1000 ppm. They have added PVP to the nanocomposite to reduce the size of Pd NPs to less than 10 nm and give a uniform distribution of the particles. Sensors made from this nanocomposite showed superior gas-sensing qualities as the active surface reaction sites were increased due to the small-sized Pd NPs. A similar $NH_3$-sensing nanocomposite was designed by Zhang et al., where they prepared PPy/Au nanocomposite and introduced lysine to reduce the size of Au NPs [115]. The Au NPs were smaller than 5 nm which made them very active in detecting $NH_3$. The reported sensitivity of PPy/Au nanocomposites for $NH_3$ at room temperature was 1.47 for 300 ppm. From these works, it is evident that the size of metal nanoparticles plays a key factor in the sensitivity of the gas sensor.

Apart from the size, the metal nanoparticle concentration in the nanocomposite also plays a vital role. This effect of concentration was explored by Choudhury [116]. He prepared PANI/Ag nanocomposites of 0.5, 1.5, and 2.5 mol% Ag concentration. In comparison to pure PANI, the PANI/Ag nanocomposite-based sensor showed improved dielectric and conductivity while the conductivity of AC was increased by nearly 100 times. He used the sensors to detect the presence of ethanol. At a 2.5 mol% concentration of Ag, the sensor showed the best sensing capacity and stability along with faster and reversible performance. Quite a close study was conducted by Park et al., where they developed a nanocomposite of PEDOT nanotubes with Ag NPs to detect $NH_3$. They varied the concentration of Ag NPs from 5% to 40% and found that a concentration of 5% produced the best sensitivity and minimum detection limit for $NH_3$.

### 9.6.3 Carbon nanotube−conducting polymer-based gas sensors

CNTs are widely used for sensing chemicals, their unique quality of adjustable conductivity, high environmental stability, and excellent mechanical properties [117,118]. Nevertheless, CNTs show poor selectivity and sensitivity in gas sensing. On the other hand, gas-sensing polymers have good selectivity and sensitivity but low stability and conductivity. Hence a nanocomposite from combining CNT with polymers proves to be a better option for gas-sensing applications.

A nanocomposite of PANI and SWCNT for detecting $N_2H_2$ was proposed by Ding et al. [119]. They reported that due to the nominal interaction among the PANI shell and SWCNT core, the transfer of electrons was much easily achieved in redox reactions. This ease of electron transfer improves the detection of $N_2H_2$ and also makes it reversible.

In nanocomposite formation, the combination between CNT and polymer plays a vital role in sensing performance. Many research works have reported the use of secondary influence in the bonding approach between CNT and polymers to enhance the gas-sensing capability. For instance, Liao et al. fabricated PANI/SWCNT in the presence of *N*-phenyl-*p*-phenylenediamine, which worked as an initiator [120]. Such nanocomposites displayed conductivities variable from $10^{-4}$ to $10^{2}$ S $cm^{-1}$. Another similar work by Wu et al. showed the fabrication of ultrafast PANI/MWCNT in the presence of tetra-β-carboxyphthalocyanine cobalt (II) (TcPcCo) [121]. The addition of TcPcCo enhanced the polymerization of MWCNT and PANI and improved the conduction of PANI. It also performed like a sensitive accelerator for the sensing mechanism of gas. The synergistic effects of TcPcCo, MWCNT, and PANI made the hybrid nanocomposite highly sensitive, which results portrayed as 140.99% to 100 ppm $NH_3$ with a detection level as low as 36 ppb. The response time and recovery time to 100 ppm $NH_3$ were recorded to be 5.0 seconds and 12.0 seconds, respectively.

A unique advantage of CNT is the high transmittance to light, which reveals the scope to fabricate flexible transparent gas sensors from hybrid nanocomposites. Wan et al. used nanostructured PANI nanorods with transparent functional MWCNT networked conductive films to prepare a chemical gas sensor [122]. The gas sensors showed a transmittance of 85% at a concentration of 550 nm with high sensitivity at room temperature. The structural integrity was also found to be good as there was no significant degradation after 500 stretch cycles. They reported that in this hybrid nanocomposite, CNT provided the efficiency for conduction while the structure of the composite provided the increased ratio between surface area and volume, making the sensors more reliable and improving sensing performances.

### 9.6.4 Graphene-conducting polymer-based gas sensors

Graphene is an allotrope of carbon that is 2D in structure. In graphene, the carbon atoms are $sp^2$ bonded and form a honeycomb formation. Graphene has superior mechanical strength, increased thermal conductivity, and sizable surface area, making it an excellent choice for gas-sensing applications. Graphene-based sensors have shown good sensitivity in detecting $H_2$, $NO_2$, $NH_3$, $H_2O$, CO, and similar gases. This superior gas-sensing property of graphene is due to two reasons. First, all the carbon atoms in the 2D honeycomb structure are exposed to the environment providing a large surface area to interact with gas molecules. Second, the structure of graphene lattice makes it more susceptible to electrical noise and shield charge fluctuations. Hence, polymer/graphene nanocomposites have been the topic of research for many scientists.

A PANI/graphene nanocomposite-based gas sensor for detecting $H_2$ was proposed by Al-Mashat et al. [123]. Ultrasonic treatment was used to form PANI nanofibers on the surface of graphene. They reported that the sensor displayed a sensitivity of 16.57% in detecting 1% $H_2$ gas, which is quite remarkable. Quite the same work was done by Wu et al., where they used PANI/graphene nanocomposites to detect $NH_3$. They synthesized the nanocomposites by chemical oxidative

polymerization. Their design of $NH_3$-detecting sensor gave a nearly linear correlation with a concentration within the range of 1−6400 ppm. It also had a sensitivity that was about five times greater than pure PANI. The minimum detection level of this hybrid nanocomposite is also 10 times a minute than pure PANI.

rGO, which is an alternative to graphene, comes in with a low cost of fabrication, and high surface area is also explored in developing hybrid nanocomposite gas sensors. A PANI/rGO nanocomposite-based gas sensor to detect $NH_3$ was proposed by Guo et al. [124]. They modified PANI nanoparticles on rGO and incorporated them on PANI nanofibers, which formed a hierarchical network film. The sensor detected $NH_3$ within the concentration range of 100 ppb−100 ppm along with a recovery time of 18 seconds and a response time of 36 seconds. The film showed transparency of 90.3% at 550 nm. It had very dependable flexibility showing no noticeable lack of performance after 1000 bend−extension cycles.

## 9.7 Temperature sensor

The measurement of temperature is one of the basic needs in many industries like medical applications, air conditioning, food storage, etc. Some applications need high accuracy temperature measuring systems. Although various temperature measuring schemes like thermocouples, resistance-dependent sensors, thermistors exist, there are some limitations in their application. One of the prominent limitations is the presence of electromagnetic disturbances in the industrial environment. A comparatively widely accepted scheme for temperature measurement is conducting polymer nanocomposite-based temperature sensors [125]. Various sorts of interferometric schemes for measuring temperature using polymer nanocomposite have been proposed by Mach-Zehnder [31,32] and Fabry-Perot [126]. Other types of optical temperature measurement schemes include attenuation of light [127], controlled mode coupling [128], total internal reflection [129,130], fluorescence [131], and fiber Bragg grating wavelength shifts [132,133]. A well-used approach for temperature measurement is using polymer optical fiber (POF) [134]. Temperature-varying stress is introduced on the POF, which alters the index of refraction of the fiber and, in turn, changes the output power of the fiber. This property is used to measure temperature.

Metal nanoparticles are used as conducting fillers in polymer to synthesize conducting polymers. The resistivity of polymers varies with temperature [135]. The sensitivity of the polymer is evaluated by calculating the voltage with varying temperatures. Both negative temperature coefficient and positive temperature coefficient (PTC) are available [136]. The variation of resistivity with temperature is due to the insulating phase and conducting phase of nanocomposites in a conducting polymer. At a low temperature, the conducting fillers are separated, which does not allow any flow of electrical current resulting in a high resistivity. This is known as the insulating phase. As the temperature rises, the polymer reaches a semimolten state where the conducting fillers get close enough to allow electrical conduction, causing a low resistivity. This state is known as the conducting phase. The type of the polymers and

conducting fillers attribute to the temperature measuring limit of the sensor. Polymer ceramics are used in case of sensing temperatures up to 850°C [137].

### 9.7.1 Gas-filled cellular structures

A differential structure for sensing temperature using conducting polymers was proposed by Wang et al. [136]. The sensor shows an enhanced sensitivity in this structure. The introduction of a gas-filled cellular structure in the nanocomposite brings an alteration in the electrical resistance with the variation of temperature. The measured temperature is converted to electrical forms by placing the sensor in an electrical bridge.

### 9.7.2 Cellulose–PPy nanocomposite

Cellulose is used as a brilliant material for temperature sensing. Nano-scaled PPy, acting as a sensitive layer for temperature and humidity detection, is introduced on cellulose surface through in situ polymerization and is referred to as cellulose–PPy nanocomposite. Cellulose–PPy nanocomposite provides a unique blend between the properties of cellulose and the electrical properties of PPy. The work of Mahadeva et al. shows the use of cellulose–PPy nanocomposites for detecting humidity and temperature [138]. Capacitive sensor constructed from cellulose–PPy nanocomposite with 16 hours of polymerization time shows a linear relation with increasing temperature.

### 9.7.3 Carbon nanotubes

Temperature-sensing materials should be capable of performing under harsh temperatures. Many PCT materials undergo poor reproducibility and low intensity, which limits their performance. High-density polyethylene (HDPE) composites having multidimensional carbon fillers serve to improve the performance of temperature sensors. Zha et al. worked on improving the performance of HDPE by introducing both functionalized MWCNTs and carbon black (CB) as fillers in the nanocomposite matrix [139]. They have shown that the addition of a small amount of MWCNT (0.7 wt.%) together with 18 wt.% CB in HDPE composites shows significant improvement in the PCT behavior. Sensing devices made from such materials offer high current-bearing capacity and are very responsive [140].

### 9.7.4 Nanowires

Polyvinylidene fluoride (PVDF) nanocomposites along with thermally reduced graphene oxide (TRG) as fillers show poor electrical conductivity and very little percolation. A hybrid between TRG and AgNWs leads to remarkable improvement in the electrical conduction property of the nanocomposite [141]. The synergistic effect of AgNW leads to the improvement in electrical conductivity. Moreover, a positive correlation between the resistivity and temperature has been found, which attributes

to the PCT coefficient effect of the nanocomposite at the melting point of PVDF. Such properties make this composite an effective material for thermal sensors.

### 9.7.5 Graphite-mixed nanocomposites

Graphite−PDMS composite dispensed on flexible polyimide films is used to make flexible temperature sensors [142]. As per the finding of Shih et al., higher stability and temperature sensitivity in PDMS nanocomposite are observed when mixed with powdered graphite compared to other carbon fillers. The resistivity of the composite decreases significantly as the volume fraction of powdered graphite reaches the onset of percolation.

## 9.8 Conclusions

Since the past decade, the demand for embedded microelectronic devices has been on the rise. The need for minute sensing is ever increasing with increasing automation and adaptive applications. The incorporation of nanocomposites in designing sensors and devices has integrated a new aspect to the growth of the industry. Polymers such as PANI, PEDOT, and PPy have added structural and thermal stability to devices. The inclusion of various metallic and carbon-based conducting nanofillers has increased the conductivity and responsivity of sensors by many folds. These have been evident from the discussion of different sensors and devices. It is expected that the ever-developing field of nanocomposites will be the cornerstone to enhanced sensing techniques and devices, which would pave the way for cheap, robust, tunable applications in environmental, healthcare, agricultural, and various other aspects of human life.

## References

[1] C. Tang, N. Chen, X. Hu, Conducting polymer nanocomposites: recent developments and future prospects, in: V. Kumar, S. Kalia, H. Swart (Eds.), Conducting Polymer Hybrids, Switzerland: Springer, Cham, 2017, pp. 1−44.

[2] T. Mahbub, M.E. Hoque, Introduction to nanomaterials and nanomanufacturing for nanosensors, in: K. Pal, F.G. de Souza (Eds.), Nanofabrication and Smart Nanosensor Applications, Elsevier, UK, 2020. Available from: https://doi.org/10.1016/B978-0-12-820702-4.00001-5.

[3] J. Anita Lett, S. Sagadevan, I. Fatimah, M.E. Hoque, Y. Lokanathan, E. Léonard, et al., Recent advances in natural polymer-based hydroxyapatite scaffolds: properties and applications, Eur. Polym. J. 148 (2021) 110360. Available from: https://doi.org/10.1016/j.eurpolymj.2021.110360.

[4] M.C. Biswas, B. Jony, P.K. Nandy, R.A. Chowdhury, S. Halder, D. Kumar, et al., Recent advancement of biopolymers and their potential biomedical applications, J. Polym. Environ. 51 (74) (2021). Available from: https://doi.org/10.1007/s10924-021-02199-y.

[5] T. Nuge, Z. Liu, X. Liu, B.C. Ang, A. Andriyana, H.S.C. Metselaar, et al., Recent advances in scaffolding from natural-based polymers for volumetric muscle injury, Molecules 26 (3) (2021) 699. Available from: https://doi.org/10.3390/molecules26030699.
[6] M. Rabbani, M.E. Hoque, Z.B. Mahbub, Chapter 7 - Nanosensors in biomedical and environmental applications: perspectives and prospects, in: K. Pal, F. Gomes (Eds.), Nanofabrication for Smart Nanosensor Applications, Elsevier, 2020, pp. 163–186. Available from: https://doi.org/10.1016/B978-0-12-820702-4.00007-6.
[7] S. Sagadevan, K. Pal, E. Hoque, Z.Z. Chowdhury, A chemical synthesized Al-doped PbS nanoparticles hybrid composite for optical and electrical response, J. Mater. Science: Mater. Electron. 28 (15) (2017) 10902–10908. Available from: https://doi.org/10.1007/s10854-017-6869-7.
[8] Z.B.Z. Shawon, M.E. Hoque, S.R. Chowdhury, Chapter 6 - Nanosensors and nanobiosensors: agricultural and food technology aspects, in: K. Pal, F. Gomes (Eds.), Nanofabrication for Smart Nanosensor Applications, Elsevier, 2020, pp. 135–161. Available from: https://doi.org/10.1016/B978-0-12-820702-4.00006-4.
[9] H. Althues, J. Henlea, S. Kaskel, Functional inorganic nanofillers for transparent polymers, Chem. Soc. Rev. 36 (9) (2007) 1454.
[10] C.W. Tang, S.A. VanSlyke, Organic electroluminescent diodes, Appl. Phys. Lett. 51 (12) (1987) 913.
[11] S.A. Carter, J.C. Scott, P.J. Brock, Enhanced luminance in polymer composite light emitting devices, Appl. Phys. Lett. 71 (1997) 1145.
[12] P.N. Prasad, Polymer science and technology for new generation photonics and biophotonics, Curr. Opin. Solid. State Mater. Sci. 8 (1) (2004) 11–19.
[13] M.d Kok, W. Sarfert, R. Paetzold, Tuning the colour of white polymer light emitting diodes, Thin Solid Films 518 (18) (2010) 5265–5271.
[14] Y. Hong, J.W.Y. Lam, B.Z. Tang, Aggregation-induced emission: phenomenon, mechanism and applications, Chem. Commun. 29 (2009) 4332–4353.
[15] H. Hoppe, N.S. Sariciftci, Organic solar cells: an overview, J. Mater. Sci. 14 (2004) 1924–1945.
[16] G. Dennler, M.C. Scharber, C.J. Brabec, Polymer-fullerene bulk-heterojunction solar cells, Adv. Mater. 14 (2009) 1323.
[17] M.R.- Reyes, K. Kim, D.L. Carroll, High-efficiency photovoltaic devices based on annealed poly(3-hexylthiophene) and 1-(3-methoxycarbonyl)-propyl-1- phenyl-(6,6) C61 blends, Appl. Phys. Lett. 87 (2005) 83506.
[18] K.M. Coakley, M.D. McGehee, Photovoltaic cells made from conjugated polymers infiltrated into mesoporous titania, Appl. Phys. Lett. 83 (16) (2003) 3380.
[19] M. Wang, X. Wang, P3HT/TiO2 bulk-heterojunction solar cell sensitized by a perylene derivative, Sol. Energy Mater. Sol. Cell (2007) 1782–1787.
[20] D. Cui, et al., Harvest of near infrared light in PbSe nanocrystal-polymer hybrid photovoltaic cells, Appl. Phys. Lett. (2006) 183111.
[21] W.U. Huynh, J.J. Dittmer, A.P. Alivisatos, Hybrid nanorod-polymer solar cells, Science (2002) 2425–2427.
[22] J. Bouclé, et al., Hybrid bulk heterojunction solar cells based on blends of TiO2 nanorods and P3HT, Comptes Rendus Phys. (2008) 110–118.
[23] Y. Hameş, Z.A. Kösemen, A. Kösemen, Y. Yerli, Electrochemically grown ZnO nanorods for hybrid solar cell applications, Sol. Energy (2010) 426.
[24] A.M. Peiró, et al., Hybrid polymer/metal oxide solar cells based on ZnO columnar structures, J. Mater. Chem. (2006) 2088–2096.

[25] J. Liu, et al., Organic/inorganic hybrid solar cells with vertically oriented ZnO nanowires, Appl. Phys. Lett. (2009) 173107.
[26] C. Peng, S. Zhang, D. Jewell, G.Z. Chen, Carbon nanotube and conducting polymer composites for supercapacitors, Prog. Nat. Science: Mater. Int. 18 (7) (2008) 777–788.
[27] S.K. Tripathi, A. Kumar, S.A. Hashmi, Electrochemical redox supercapacitors using PVdF-HFP based gel electrolytes and polypyrrole as conducting polymer electrode, Solid State Ion 177 (33) (2006) 2979–2985.
[28] K. Zhang, L.L. Zhang, X.S. Zhao, J. Wu, Graphene/polyaniline nanofiber composites as supercapacitor electrodes, Chem. Mater. 22 (4) (2010) 1392–1401.
[29] J. Zhang, X.S. Zhao, Conducting polymers directly coated on reduced graphene oxide sheets as high-performance supercapacitor electrodes, J. Phys. Chem. C 116 (9) (2012) 5420–5426.
[30] N.A. Kumar, et al., Polyaniline-grafted reduced graphene oxide for efficient electrochemical supercapacitors, ACS Nano 6 (2) (2012) 1715–1723.
[31] H. Wang, et al., A nanostructured graphene/polyaniline hybrid material for supercapacitors, Nanoscale 2 (10) (2010) 2164–2170.
[32] Y. Wang, et al., High-temperature sensing using miniaturized fiber in-line Mach–Zehnder interferometer, IEEE Photon. Technol. Lett. 22 (1) (2010) 39–41.
[33] S. Bose, et al., Electrochemical performance of a graphene-polypyrrole nanocomposite as a supercapacitor electrode, Nanotechnology 22 (29) (2011) 295202.
[34] L.A. Pettersson, F. Carlsson, O. Inganäs, H. Arwin, Spectroscopic ellipsometry studies of the optical properties of doped poly(3,4-ethylenedioxythiophene): an anisotropic metal, Thin Solid Films 313–314 (1998) 356–361.
[35] K. Liu, et al., Electropolymerization of high stable poly(3,4-ethylenedioxythiophene) in ionic liquids and its potential applications in electrochemical capacitor, J. Power Sources 179 (2) (2008) 858–862.
[36] G.A. Snook, P. Kao, A.S. Best, Conducting-polymer-based supercapacitor devices and electrodes, J. Power Sources 196 (1) (2011) 1–12.
[37] K.S. Choi, F. Liu, J.S. Choi, T.S. Seo, Fabrication of free-standing multilayered graphene and poly(3,4-ethylenedioxythiophene) composite films with enhanced conductive and mechanical properties, Langmuir 26 (15) (2010) 12902–12908.
[38] B.N. Reddy, M. Deepa, A.G. Joshi, A.K. Srivastava, Poly(3,4-ethylenedioxypyrrole) enwrapped by reduced graphene oxide: how conduction behavior at nanolevel leads to increased electrochemical activity, J. Phys. Chem. C 115 (37) (2011) 18354–18365.
[39] Z. Zhao, et al., PEDOT-based composites as electrode materials for supercapacitors, Nanotechnology 27 (4) (2016) 042001.
[40] F. Alvi, et al., Graphene–polyethylenedioxythiophene conducting polymer nanocomposite based supercapacitor, Electrochim. Acta 56 (25) (2011) 9406–9412.
[41] J. Wen, Y. Jiang, Y. Yang, S. Li, Conducting polymer and reduced graphene oxide Langmuir–Blodgett films: a hybrid nanostructure for high performance electrode applications, J. Mater. Sci. Mater. Electron. 25 (2013) 1063–1071.
[42] J.-B. Chossat, Y.-L. Park, R.J. Wood, V. Duchaine, A soft strain sensor based on ionic and metal liquids, IEEE Sens. J. 13 (9) (2013) 3405–3414.
[43] H. Gullapalli, et al., Flexible piezoelectric ZnO-paper nanocomposite strain sensor, Small 6 (15) (2010) 1641–1646.
[44] L. Cai, et al., Super-stretchable, transparent carbon nanotube-based capacitive strain sensors for human motion detection, Sci. Rep. 3 (2013) 3048.
[45] S.R. Larimi, et al., Low-cost ultra-stretchable strain sensors for monitoring human motion and bio-signals, Sens. Actuator. A Phys. 271 (2018) 182–191.

[46] S. Zhao, et al., Recent advancements in flexible and stretchable electrodes for electromechanical sensors: strategies, materials, and features, ACS Appl. Mater. Interfaces 9 (14) (2017) 12147−12164.
[47] E. Park, et al., One-pot synthesis of silver nanoparticles decorated poly(3,4-ethylenedioxythiophene) nanotubes for chemical sensor application, J. Mater. Chem. 22 (4) (2012) 1521−1526.
[48] M. Park, et al., Highly stretchable electric circuits from a composite material of silver nanoparticles and elastomeric fibres, Nat. Nanotechnol. 7 (12) (2012) 803−809.
[49] K. Takei, et al., Highly sensitive electronic whiskers based on patterned carbon nanotube and silver nanoparticle composite films, Proc. Natl Acad. Sci. U.S.A. 111 (5) (2014) 1703−1707.
[50] S. Yaoa, Y. Zhu, Wearable multifunctional sensors using printed stretchable conductors made of silver nanowires, Nanoscale 6 (2014) 2345−2352.
[51] M. Amjadi, et al., Highly stretchable and sensitive strain sensor based on silver nanowire-elastomer nanocomposite, ACS Nano 8 (5) (2014) 5154−5163.
[52] K.K. Kim, et al., Highly sensitive and stretchable multidimensional strain sensor, Nanoletters 15 (8) (2015) 5240−5247.
[53] P. Lee, et al., Highly stretchable and highly conductive metal electrode by very long metal nanowire percolation network, Adv. Mater. 24 (25) (2012) 3326−3332.
[54] R. Ma, et al., Extraordinarily high conductivity of stretchable fibers of polyurethane and silver nanoflowers, ACS Nano 9 (11) (2015) 10876−10886.
[55] M. Hempel, D. Nezich, J. Kong, H. M., A novel class of strain gauges based on layered percolative films of 2D materials, Nano Lett. 12 (11) (2012) 5714−5718.
[56] X. Li, et al., Stretchable and highly sensitive graphene-on-polymer strain sensors, Sci. Rep. 2 (2012) 870.
[57] C. Yan, et al., Highly stretchable piezoresistive graphene−nanocellulose nanopaper for strain sensors, Adv. Mater. 26 (13) (2014) 2022−2027.
[58] S. Gong, et al., Highly stretchy black gold E-skin nanopatches as highly sensitive wearable biomedical sensors, Adv. Electron. Mater. 1 (4) (2015) 1400063.
[59] H. Feng, et al., Simple and rapid synthesis of ultrathin gold nanowires, their self-assembly and application in surface-enhanced Raman scattering, Chem. Commun. 15 (2009) 1984−1986.
[60] X. Lu, et al., Ultrathin gold nanowires can be obtained by reducing polymeric strands of oleylamine-AuCl complexes formed via aurophilic interaction, J. Am. Chem. Soc. 130 (28) (2008) 8900−8901.
[61] D.W. Hatchett, M. Josowicz, Composites of intrinsically conducting polymers as sensing nanomaterials, Chem. Rev. 108 (2) (2008) 746−769.
[62] Z. Liu, L. Zhang, S. Poyraz, X. Zhang, Conducting polymer - metal nanocomposites synthesis and their sensory applications, Curr. Org. Chem. 17 (20) (2013) 2256−2267.
[63] M. Naseri, L. Fotouhi, A. Ehsani, Recent progress in the development of conducting polymer-based nanocomposites for electrochemical biosensors applications: a mini-review, Chem. Rec. 18 (6) (2018) 599−618.
[64] R. Abdel-Karim, Y. Reda, A. Abdel-Fattah, Review—nanostructured materials-based nanosensors, J. Electrochem. Soc. 167 (2020) 037554.
[65] R. Kour, et al., Review—recent advances in carbon nanomaterials as electrochemical biosensors, J. Electrochem. Soc. 167 (2020) 037555.
[66] N. Karousis, N. Tagmatarchis, D. Tasis, Current progress on the chemical modification of carbon nanotubes, Chem. Rev. 110 (9) (2010) 5366−5397.
[67] P. Kim, L. Shi, A. Majumdar, P.L. McEuen, Thermal transport measurements of individual multiwalled nanotubes, Phys. Rev. Lett. 87 (2001) 215502.

[68] M.H. Suhail, O.G. Abdullah, G.A. Kadhim, Hydrogen sulfide sensors based on PANI/f-SWCNT polymer nanocomposite thin films prepared by electrochemical polymerization, J. Sci. Adv. Mater. Devices 4 (2019) 143−149.
[69] S. Srivastava, et al., Study of chemiresistor type CNT doped polyaniline gas sensor, Synth. Met. 160 (2009) 529−534.
[70] S. Sharma, S. Hussain, S. Singh, S. Islam, MWCNT-conducting polymer composite based ammonia gas sensors: a new approach for complete recovery process, Sens. Actuator. B Chem. 194 (2014) 213−219.
[71] A.R. Sadrolhosseini, et al., Application of polypyrrole multi-walled carbon nanotube composite layer for detection of mercury, lead and iron ions using surface plasmon resonance technique, PLoS One 9 (4) (2014) e93962.
[72] K.-S. Teh, L. Lin, MEMS sensor material based on polypyrrole-carbon nanotube nanocomposite: film deposition and characterization, J. Micromech. Microeng. 15 (11) (2005) 2019−2027.
[73] K. An, S. Jeong, H. Hwang, Y. Lee, Enhanced sensitivity of a gas sensor incorporating single-walled carbon nanotube−polypyrrole nanocomposites, Adv. Mater. 16 (12) (2004) 1005−1009.
[74] D.R. Dreyer, S. Park, C.W. Bielawski, R.S.R. Ruoff*b, The chemistry of graphene oxide, Chem. Soc. Rev. 39 (1) (2010) 228−240.
[75] L. Wang, et al., Enhanced sensitivity and stability of room-temperature $NH_3$ sensors using core−shell $CeO_2$ nanoparticles@cross-linked PANI with p−n heterojunctions, ACS Appl. Mater. Interfaces 6 (16) (2014) 14131−14140.
[76] W. Wang, et al., Enhanced catalytic and dopamine sensing properties of electrochemically reduced conducting polymer nanocomposite doped with pure graphene oxide, Biosens. Bioelectron. 58 (2014) 153−156.
[77] S. Konwer, A. Begum, S. Bordoloi, R. Boruah, Expanded graphene-oxide encapsulated polyaniline composites as sensing material for volatile organic compounds, J. Polym. Res. 24 (2017) 37.
[78] Y. Yang, et al., Electrochemical biosensor based on three-dimensional reduced graphene oxide and polyaniline nanocomposite for selective detection of mercury ions, Sens. Actuator. B Chem. 214 (2015) 63−69.
[79] N. Ruecha, et al., Sensitive electrochemical sensor using a graphene-polyaniline nanocomposite for simultaneous detection of Zn(II), Cd(II), and Pb(II), Anal. Chim. Acta 874 (2015) 40−48.
[80] K.M.A. El-Nour, A. Eftaiha, A. Al-Warthan, R.A. Ammar, Synthesis and applications of silver nanoparticles, Arab. J. Chem. 3 (3) (2010) 135−140.
[81] A. Haider, I.-K. Kang, Preparation of silver nanoparticles and their industrial and biomedical applications: a comprehensive review, Adv. Mater. Sci. Eng. 3 (2015) 1−16.
[82] P.M. Nia, W.P. Meng, Y. Alias, Hydrogen peroxide sensor: uniformly decorated silver nanoparticles on polypyrrole for wide detection range, Appl. Surf. Sci. 357 (2015) 1565−1572.
[83] D.M. Nerkar, Selective and Sensitive room temperature detection of ammonia by PPy-Ag nanocomposite, Int. J. Res. Appl. Sci. Eng. Technol. 6 (3) (2018) 1241−1249.
[84] F.M. Zahed, B. Hatamluyi, F. Lorestani, Z. Es'haghi, Silver nanoparticles decorated polyaniline nanocomposite based electrochemical sensor for the determination of anticancer drug 5-fluorouracil, J. Pharm. Biomed. Anal. 161 (2018) 12−19.
[85] M. Hazarika, et al., Biogenic synthesis of palladium nanoparticles and their applications as catalyst and antimicrobial agent, PLoS One 12 (9) (2017) e0184936.
[86] I. Saldan, Y. Semenyuk, I. Marchuk, O. Reshetnyak, Chemical synthesis and application of palladium nanoparticles, J. Mater. Sci. 50 (6) (2015) 2337−2354.

[87] C. Sandaruwan, et al., Polyaniline/palladium nanohybrids for moisture and hydrogen detection, Chem. Cent. J. 12 (2018) 1−13.
[88] M. Jeyaraj, et al., A comprehensive review on the synthesis, characterization, and biomedical application of platinum nanoparticles, Nanomaterials (Basel) 9 (12) (2019) 1719.
[89] S.K. Mishra, et al., Protein functionalized Pt nanoparticles-conducting polymer nanocomposite film: characterization and immunosensor application, Polymer 55 (16) (2014) 4003−4011.
[90] S.B. Adeloju, S. Hussain, Potentiometric sulfite biosensor based on entrapment of sulfite oxidase in a polypyrrole film on a platinum electrode modified with platinum nanoparticles, Microchim. Acta 183 (4) (2016) 1341−1350.
[91] D. Zhai, et al., Highly sensitive glucose sensor based on pt nanoparticle/polyaniline hydrogel heterostructures, ACS Nano 7 (4) (2013) 3540−3546.
[92] C.-C. Hung, T.-C. Wen, Y. Wei, Site-selective deposition of ultra-fine Au nanoparticles on polyaniline nanofibers for H2O2 sensing, Mater. Chem. Phys. 122 (2010) 392−396.
[93] Z. Miao, et al., Development of a glucose biosensor based on electrodeposited gold nanoparticles-polyvinylpyrrolidone-polyaniline nanocomposites, J. Electroanal. Chem. 756 (2015) 153−160.
[94] N.K. Sadanandhan, S.J. Devaki, Gold nanoparticle patterned on PANI nanowire modified transducer for the simultaneous determination of neurotransmitters in presence of ascorbic acid and uric acid, Appl. Polym. Sci. 133 (2016) 44351.
[95] P. Lin, et al., Electrochemical synthesis of poly(3,4-ethylenedioxythiophene) doped with gold nanoparticles, and its application to nitrite sensing, Microchim. Acta 183 (2016) 1235−1241.
[96] K. Suri, A. Subramanian, A. Sarkar, R.P. Tandon, Gas and humidity sensors based on iron oxide−polypyrrole nanocomposites, Sens. Actuator. B Chem. 81 (2−3) (2002) 277−282.
[97] R. Devi, M. Thakur, C.S. Pundir, Construction and application of an amperometric xanthine biosensor based on zinc oxide nanoparticles-polypyrrole composite film, Biosens. Bioelectron. 26 (8) (2011) 3420−3426.
[98] JieZhu, et al., Preparation of polyaniline−$TiO_2$ nanotube composite for the development of electrochemical biosensors, Sens. Actuator. B Chem. 221 (2015) 450−457.
[99] K. Ghanbari, Z. Babaei, Fabrication and characterization of non-enzymatic glucose sensor based on ternary NiO/CuO/polyaniline nanocomposite, Anal. Biochem. 498 (2016) 37−46.
[100] R. Jain, D.C. Tiwari, S. Shrivastava, Polyaniline−bismuth oxide nanocomposite sensor for quantification of anti-Parkinson drug pramipexole in solubilized system, Mater. Sci. Eng. B 185 (2014) 53−59.
[101] Z. Pang, et al., Free-standing $TiO_2$−$SiO_2$/PANI composite nanofibers for ammonia sensors, J. Mater. Sci. Mater. Electron. 29 (2018) 3576−3583.
[102] W. Wu, Stretchable electronics: functional materials, fabrication strategies and applications, Sci. Technol. Adv. Mater. 20 (1) (2019) 187−224.
[103] J.G. Ibanez, et al., Conducting polymers in the fields of energy, environmental remediation, and chemical − chiral sensors, Chem. Rev. 118 (9) (2018) 4731−4816.
[104] H. Tai, et al., Fabrication and gas sensitivity of polyaniline−titanium dioxide nanocomposite thin film, Sens. Actuator. B Chem. 125 (2) (2007) 644−650.
[105] S. Bai, et al., Preparation of conducting films based on α-MoO3/PANI hybrids and their sensing properties to triethylamine at room temperature, Sens. Actuator. B Chem. 239 (C) (2017) 131−138.

[106] S. Li, et al., The room temperature gas sensor based on Polyaniline@flower-like $WO_3$ nanocomposites and flexible PET substrate for $NH_3$ detection, Sens. Actuator. B Chem. 259 (2017) 505–513.
[107] A. Beniwal, Sunny, Electrospun $SnO_2$/PPy nanocomposite for ultra-low ammonia concentration detection at room temperature, Sens. Actuator. B Chem. 296 (2019) 126660.
[108] J. Sun, et al., Preparation of polypyrrole@WO3 hybrids with p-n heterojunction and sensing performance to triethylamine at room temperature, Sens. Actuator. B Chem. 238 (2017) 510–517.
[109] M. Wang, et al., Fabrication of polypyrrole/graphene oxide hybrid nanocomposite for ultrasensitive humidity sensing with unprecedented sensitivity, J. Mater. Sci. Mater. Electron. 30 (2019) 4967–4976.
[110] J. Gong, et al., Ultrasensitive $NH_3$ gas sensor from polyaniline nanograin enchased $TiO_2$ fibers, J. Phys. Chem. C 114 (21) (2010) 9970–9974.
[111] H. Jamalabadi, A. Mani-Varnosfaderani, N. Alizadeh, Detection of alkyl amine vapors using PPy-ZnO hybrid nanocomposite sensor array and artificial neural network, Sens. Actuator. A Phys. 9 (1) (2018) 228–237.
[112] A. Ly, et al., Ammonia sensor based on vapor phase polymerized polypyrrole, Chemosensors 8 (2) (2020) 38.
[113] A.A. Athawale, S. Bhagwat, P.P. Katre, Nanocomposite of Pd–polyaniline as a selective methanol sensor, Sens. Actuator. B Chem. 114 (2005) 263–267.
[114] L. Hong, Y. Li, M. Yang, Fabrication and ammonia gas sensing of palladium/polypyrrole nanocomposite, Sens. Actuator. B Chem. 145 (1) (2010) 25–31.
[115] J. Zhang, et al., One-pot fabrication of uniform polypyrrole/Au nanocomposites and investigation for gas sensing, Sens. Actuator. B Chem. 186 (2013) 695–700.
[116] A. Choudhury, Polyaniline/silver nanocomposites: dielectric properties and ethanol vapour sensitivity, Sens. Actuator. B Chem. 138 (1) (2009) 318–325.
[117] S. Shen, et al., An LC passive wireless gas sensor based on PANI/CNT composite, Sensors 18 (9) (2018) 3022.
[118] F. Wang, H. Gu, T.M. Swager, Carbon nanotube/polythiophene chemiresistive sensors for chemical warfare agents, J. Am. Chem. Soc. 130 (16) (2008) 5392–5393.
[119] M. Ding, et al., Chemical sensing with polyaniline coated single-walled carbon nanotubes, Adv. Mater. 23 (4) (2010) 536–540.
[120] Y. Liao, et al., Carbon nanotube/polyaniline composite nanofibers: facile synthesis and chemosensors, Nano Lett. 11 (3) (2011) 954–959.
[121] H. Wu, et al., Phthalocyanine-mediated non-covalent coupling of carbon nanotubes with polyaniline for ultrafast NH3 gas sensors, J. Mater. Chem. A 5 (46) (2017) 24493–24501.
[122] P. Wan, et al., Flexible transparent films based on nanocomposite networks of polyaniline and carbon nanotubes for high-performance gas sensing, Small 11 (40) (2015) 5409–5415.
[123] L. Al-Mashat, et al., Graphene/polyaniline nanocomposite for hydrogen sensing, J. Phys. Chem. C 114 (39) (2010) 16168–16173.
[124] Y. Guo, et al., Hierarchical graphene–polyaniline nanocomposite films for high-performance flexible electronic gas sensors, Nanoscale 8 (23) (2016) 12073–12080.
[125] Tapetado, A. et al., Experimental test of polymer optical fiber temperature sensor on different surrounding media, 2013.
[126] H.Y. Choi, K.S. Park, S.J. Park, U.-C. Paek, B.H. Lee, E.S. Choi, Miniature fiber-optic high temperature sensor based on a hybrid structured Fabry–Perot interferometer, Opt. Lett. 33 (21) (2008) 2455–2457.

[127] K. Kyuma, S. Tai, T. Sawada, M. Nunoshita, Fiber-optic instrument for temperature measurement, IEEE Trans. Microw. Theory Tech. 30 (4) (1982) 522–525.
[128] D.S. Montero, et al., A self-referencing intensity based polymer optical fiber sensor for liquid detection, Sensors 9 (8) (2009) 6446–6455.
[129] D.S. Montero, P.C. Lallana, C. Vázquez, A polymer optical fiber fuel level sensor: application to paramotoring and powered paragliding, Sensors 12 (5) (2012) 6186–6197.
[130] G. Rajan, Y. Semenova, G. Farrell, All-fibre temperature sensor based on macro-bend singlemode fibre loop, Electron. Lett. 44 (19) (2008) 1123–1124.
[131] C.-S. Chu, Y.-L. Lo, A plastic optical fiber sensor for the dual sensing of temperature and oxygen, IEEE Photonics Technol. Lett. 20 (1) (2007) 63–65.
[132] Bowei Z., Kahrizi M., High temperature resistance temperature sensor based on the hydrogen loaded fiber Bragg grating. Irvine, CA, USA, 2005.
[133] Y. Rao, et al., Optical in-fiber bragg grating sensor systems for medical applications, J. Biomed. Opt. 3 (1) (1998) 38–44.
[134] C. Meng, et al., Highly flexible and all-solid-state paperlike polymer supercapacitors, Nano Lett. 10 (10) (2010) 4025–4031.
[135] X. Chen, et al., Temperature dependence of the conductivity in conducting polymer composites, Polymer 35 (24) (1994) 5256–5258.
[136] L. Wang, Differential structure for temperature sensing based on conductive polymer composites, IEEE Trans. Electron. Devices 62 (9) (2015) 3025–3028.
[137] D.N. Nguyen, H. Yoon, Recent advances in nanostructured conducting polymers: from synthesis to practical applications, Polymers 8 (4) (2016) 118.
[138] S.K. Mahadeva, S. Yun, J. Kim, Flexible humidity and temperature sensor based on cellulose–polypyrrole nanocomposite, Sens. Actuator. A Phys. 165 (2011) 194–199.
[139] J.-W. Zha, et al., Enhanced positive temperature coefficient behavior of the high-density polyethylene composites with multi-dimensional carbon fillers and their use for temperature-sensing resistors, RSC Adv. 7 (19) (2017) 11338–11344.
[140] Y. Zeng, et al., Positive temperature coefficient thermistors based on carbon nanotube/polymer composites, Sci. Rep. 4 (2014) 6684.
[141] L. He, S.-C. Tjong, Electrical behavior and positive temperature coefficient effect of graphene/polyvinylidene fluoride composites containing silver nanowires, Nanoscale Res. Lett. 9 (1) (2014) 375.
[142] W.-P. Shih, et al., Flexible temperature sensor array based on a graphite-polydimethylsiloxane composite, Sens. (Basel) 10 (4) (2010) 3597–3610.

# Polymer nanocomposites for adhesives and coatings

10

*Kazi Faiza Amin*[1], *Asrafuzzaman*[2], *Ayeman Mazdi Nahin*[2] *and Md Enamul Hoque*[3]

[1]Department of Materials and Metallurgical Engineering, Bangladesh University of Engineering and Technology (BUET), Dhaka, Bangladesh

[2]Department of Materials Science and Engineering, Rajshahi University of Engineering & Technology (RUET), Rajshahi, Bangladesh

[3]Department of Biomedical Engineering, Military Institute of Science and Technology (MIST), Dhaka, Bangladesh

## 10.1 Introduction

Nanocomposites can be identified as materials composed of two or more characteristically distinct phases separated by an interfacial phase where at least one of the component phases, usually the filler is modified at a nanometer ($10^{-9}$ m) scale. Fillers in the nanometer range hold a higher surface area to volume ratio. This factor plays a critical role in enhancing the interactions with matrix, consequently giving nanocomposites superiority over conventional composites [1,2]. Dispersion of nanosized fillers in polymeric matrix ensures enhanced interfacial interaction between them [3]. Polymeric nanocomposites consist of a polymer as a matrix containing a wide range of fillers. Polymer nanocomposites have emerged in the 21st century as one of the most versatile materials. A significant amount of interest has been given in the last two decades to ascertain the functionality of polymeric nanocomposites as coatings and adhesives. The basic property of both coating and adhesive is adhesion to the surface. But the fundamental difference between a coating and an adhesive is that the former adheres to a single surface, while the latter acts as a bond sandwiched between two surfaces [4]. Other differences between coating and adhesive are that coating protects the substrate against external conditions such as heat, abrasions, or moisture, whereas adhesive renders a high fracture strength during the pull-apart of two surfaces [5]. The inclusion of nanomaterials into the polymeric matrices has been shown to increase the viscoelasticity of polymers and requires higher energy for deformation [6]. Hence polymer nanocomposites are widely considered as suitable candidates for coatings and adhesives. Among the various types of polymers used as matrices for coating and adhesives, epoxy, polyurethane (PU), vinyl ether polymers, cyanoacrylate, polyester, etc. are the prevailing substances. The choice of reinforcements is also widespread including clay, nanostructured carbon, or graphene, and oxides. The techniques used to form the

**Advanced Polymer Nanocomposites. DOI:** https://doi.org/10.1016/B978-0-12-824492-0.00014-3


polymer nanocomposites are correspondingly varied in nature. Therefore the possible combinations of polymer nanocomposites to be applied as coatings and adhesives are great in number. Ongoing research is focused on determining the optimum composites for particular applications.

## 10.2 Polymer nanocomposite coatings

The role of coatings is diverse in many aspects. A coating has to provide the substrate with protection against corrosion from the surrounding environment, erosion along with improvement of other properties corresponding to the nature of the application. The coating on a particular surface can also act as an adhesive agent for other coating materials. For example, phenolic, epoxy, and styrenated coatings applied on bamboo fiber ensure satisfactory adhesion of further applied coating materials [7]. Polymer nanocomposites have successfully proved their suitability as coatings. Polymer nanocomposite coatings vary in the type of matrices and fillers. The polymers that are most popular as matrices in nanocomposite coatings are epoxy, PU, chitosan, polyethylene glycol (PEG), polyvinylidene fluoride, polyaniline (PANI), polypyrrole (PPy), polystyrene, polyamic acid and polyimide, rubber-modified polybenzoxazine, polymers containing reactive trimethoxysilane (TMOS), pullulan, fluoroacrylic polymer, ethylene tetrafluoroethylene (ETFE), polyacrylate, poly(*N*-vinyl carbazole), polycarbonate, fluorinated polysiloxane, polyester, polyacrylic, polyvinyl alcohol, polydimethylsiloxane, polyamide, and ultraviolet ray (UV)-curable polymers. The broad range of polymer nanocomposite coatings can be classified based on their type of fillers and fabrication techniques.

### *10.2.1 Fillers of polymer nanocomposite coatings*

#### *10.2.1.1 Inorganic fillers and clay-based polymer nanocomposite coatings*

Incorporation of inorganic nanoparticles such as clay in pristine polymer coatings reduces their permeability to corrosive species and ensures a longer service life of the coating and substrate [8]. In the bioengineering field, hydroxyapatite (HA) [9] and silver nanoparticles [10] are the popular choice of fillers owing to their unique microbial properties. Among clay-based nanocomposites, the use of organically treated montmorillonite (MMT) has been reported by several research groups. Japanese automobile giant Toyota pioneered the research on layered silicate-reinforced polymer nanocomposite coating by developing a nylon-6 composite interphase with MMT with enhanced mechanical properties in the late 1980s. The use of nanoferrites [3], $CaCO_3$ [11] has also been explored in recent years. Nanosized glass flakes in epoxy matrix coating have been reported to exhibit better corrosion resistance than MMT organoclay in epoxy [12] (Table 10.1).

**Table 10.1** List of recent research on clay-based polymer nanocomposite coatings.

| Polymer matrix | Reinforcement | Fabrication process | Result | Reference |
|---|---|---|---|---|
| Epoxy | Montmorillonite | Sonication followed by spray and drying | Improved corrosion resistance | Bagherzadeh and Mahdavi [13] |
| Epoxy | Nanoclay and zirconia nanoparticles | Slurry method | Better exfoliation of clay particles and enhanced corrosion performance | Behzadnasab et al. [14] |
| Polybenzoxazine−trimethoxysilane | Silica nanoparticles | Ultrasonication and dip coating | Enhanced interfacial interaction and corrosion resistance | Zhou et al. [15] |
| Epoxy | Vermiculite | Solution casting | Improved permeation | Mittal [16] |
| Polyimide | Dodecylamine−montmorillonite | Solution casting | Reduced oxygen permeability, improved electrical resistivity and adhesion | Khayankarn et al. [17] |
| Polyurethane | Organically modified montmorillonite | Ultrasonication | Improved corrosion protection | Heidarian et al. [18] |
| Polyurethane | Montmorillonite | Spray casting followed by thermosetting | Superhydrophobicity and high adhesion to substrate | Steele et al. [19] |
| Soya polyurethane | Silica nanonetwork | In situ polymerization | Improved mechanical properties and corrosion resistance | Ghosal et al. [20] |

### 10.2.2 Carbon-based polymer nanocomposite coatings

Carbon-based fillers include the present-day prominent materials carbon nanotubes (CNTs) and graphene along with their derivatives. Graphene is a carbon allotrope consisting of $sp^2$-bonded planar sheets densely packed in a honeycomb structure that acts as the building block of other allotropes [21]. Graphite is stacked graphene sheets with a distance of 3.37 Å; CNTs are one-dimensionally rolled graphene sheets; and fullerene are wrapped graphene sheets. Graphite sheets are often subjected to solution-assisted exfoliation to produce graphene oxide (GO) where the plane of carbon atoms contains a large amount of oxygen-containing groups [22]. All of these nanoscaled allotropes of carbon have gained significant interest as reinforcement of polymeric composites as they provide the coatings with improved mechanical strength and corrosion resistance. GO is generally employed as the precursor material during the fabrication of graphene-based polymer nanocomposites since its dispersion in the polymer matrix is easier owing to its decorating functional groups, which include hydroxyls, epoxides, and carboxyl [23]. In some cases, further functionalization of GO is performed to achieve better dispersion in the matrix (Figs. 10.1 and 10.2).

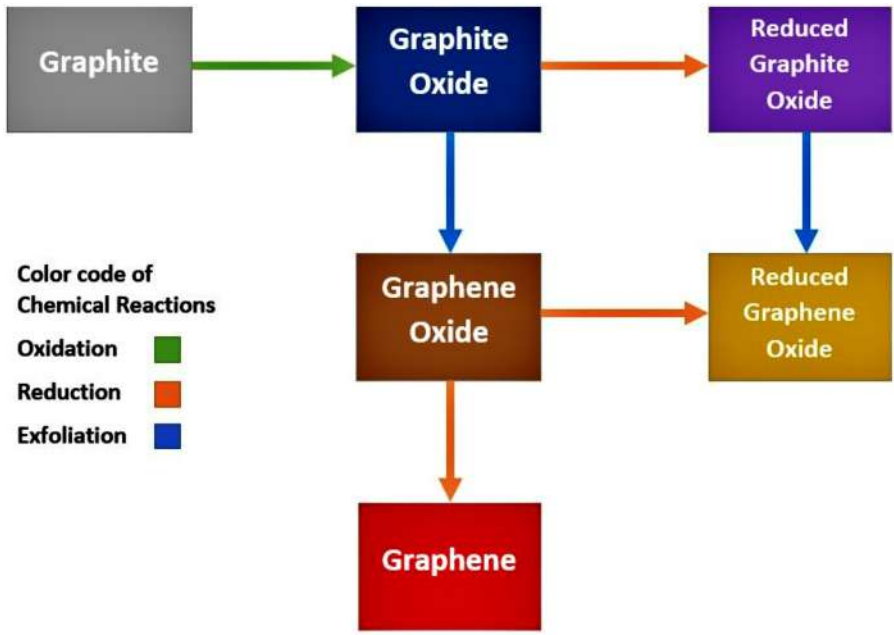


**Figure 10.1** Steps of graphene production and its derivatives.
*Source*: Modified from N.H. Othman, M. Che Ismail, M. Mustapha, N. Sallih, K.E. Kee, R. Ahmad Jaal, R, Graphene-based polymer nanocomposites as barrier coatings for corrosion protection, Prog. Org. Coat. 135 (2019) 82−99. https://doi.org/10.1016/j.porgcoat.2019.05.030.

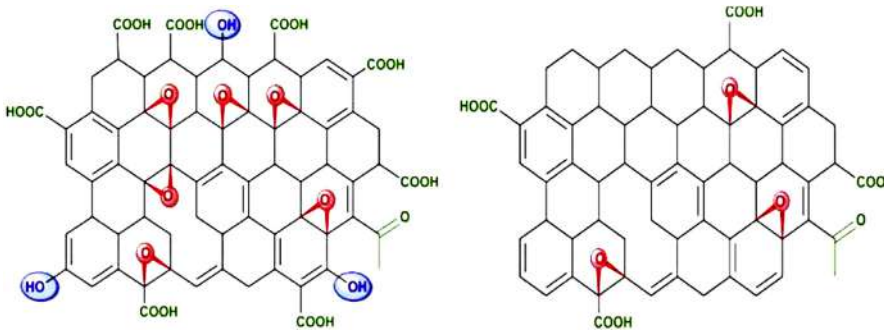


**Figure 10.2** The molecular arrangements of graphene oxide (GO) (*left*) and reduced graphene oxide (rGO) (*right*).
*Source*: From R. Aradhana, S. Mohanty, S.K. Nayak, Comparison of mechanical, electrical and thermal properties in graphene oxide and reduced graphene oxide filled epoxy nanocomposite adhesives, Polymer 141 (2018) 109−123. https://doi.org/10.1016/j.polymer.2018.03.005.

The arrangement of graphene fillers in the polymeric matrix can be in three formations: phase separated, intercalated, and exfoliated [22]. The agglomerated and intercalated formations influence the corrosion performance of the composite coating, while the exfoliated state provides better properties for barrier protection [24]. Fabrication methods of graphene-based nanocomposite coatings comprise solution mixing, melt mixing, and in situ polymerization. Solution mixing can be conducted by surface functionalization of graphene by macromolecules [25] or through the loading of inorganic particles on GO sheets [26]. CNTs have also been explored as potential fillers for polymer nanocomposites by several research groups. Epoxy/CNTs coating on glass fiber has been reported to improve the tensile strength of the fiber significantly [27]. In a different study, PANI/functionalized CNT composites and nanosilica integrated into ETFE matrix resulted in a superamphiphobic coating [28] (Fig. 10.3; Table 10.2).

### 10.2.3 Preparation methods of polymer nanocomposite coatings

The properties of polymeric nanocomposite coatings depend largely on fabrication methods. Preparation methods are crucial in imparting enhanced properties suitable for the desired service of the composite coating. The procedures generally utilized for developing polymer nanocomposite coatings are solution casting/blending, ex situ/in situ polymerization, mixed colloidal dispersion, and grafting [34]. The basic differences between these processes are the degree of interaction between the reinforcements and the matrices both chemically and physically [1,2]. Blending [35], casting [36], and colloidal dispersion [37] are preferable for achieving physical and electrostatic interactions between the fillers and the matrix. Meanwhile, the in situ polymerization method favors the formation of chemical bonding along with electrostatic bonding, hydrogen bonding, and physical boding resulting in better

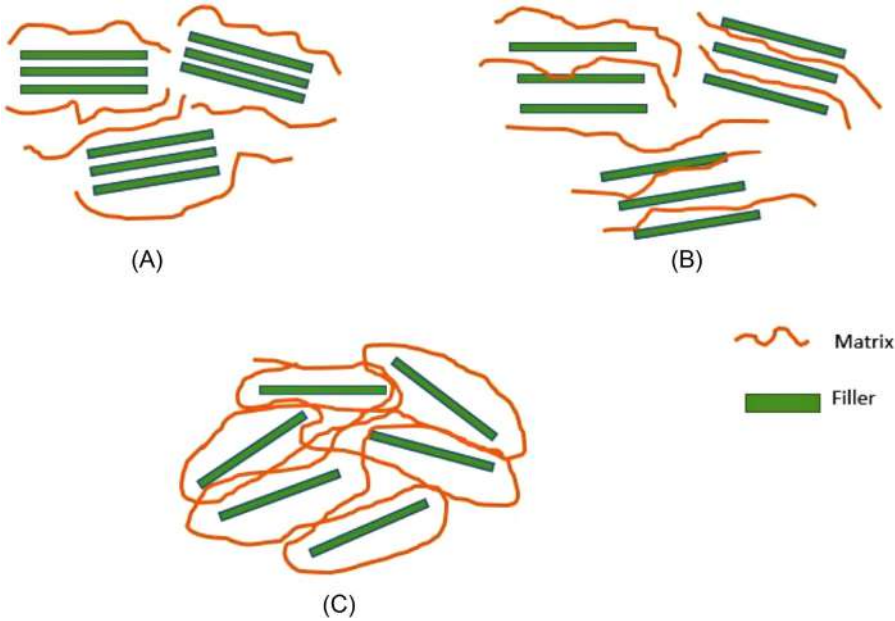


**Figure 10.3** Illustration of filler arrangement types in a polymer matrix: (A) phase separated, (B) intercalated, and (C) exfoliated.

dispersion [38]. A study comparing the effects of in situ process and grafting exhibited in situ process producing superior adhesion in hybrid silica/ PU nanocomposites while grafting rendered better mechanical properties [39].

Polymer nanocomposite coating can be further modified by chemical processes conducted on fillers and matrices in order to attain better mechanical, adhesion, thermal, and chemical resistance properties. These modifications include functionalization of carbon and silica-based fillers, polymer conduction with polar groups, hyperbranching, functionalization of polymeric chain end, etc. Hyperbranched polymers have heavily branched molecules with a spherical structure, low viscosity, and contain several functional groups on the chain end. Hyperbranched polyester filled with layered silicate $Na^+$ MMT has been reported to possess better hardness, adhesion, and flexibility [40] (Fig. 10.4).

### 10.2.4 Conductive polymer nanocomposite coatings

Modern-day nanocomposite coatings often contain electrically conductive polymers (ECPs) and conductive fillers. CNTs and graphene are the preferred choices among carbon-based conductive fillers. ECPs contain conjugation along the polymer chain backbone. Well-known ECPs are PANI, PPy, and polythiophene, etc. ECPs can transport electrons from the surrounding environment and thus provide excellent corrosion protection [41] (Fig. 10.5).

**Table 10.2** List of recent studies on graphene-based polymer nanocomposite coatings.

| Polymer matrix | Reinforcement | Fabrication process | Result | Reference |
|---|---|---|---|---|
| Solvent-based epoxy | Graphene oxide (GO) nanosheets | Addition of GO into polyamide hardener to be mixed with epoxy followed by spray coating | Improved barrier properties and corrosion protection | Pourhashem et al. [29] |
| Waterborne polyurethane (WPU) | GO−silica (GOSI) nanocomposites | Preparation of GOSI by surface functionalization of GO and $SiO_2$ followed by mixing into WPU | Enhanced interfacial cross-linking, tear and abrasion resistance, surface adhesiveness | Kale et al. [30] |
| Tannic acid−based hyperbranched epoxy resin | Reduced GO | Solution technique | Improved tensile strength, scratch hardness, impact strength, initial degradation temperature, and gloss | Boro and Karak [31] |
| WPU | Polydopamine functionalized GO | Solution blending | Uniform dispersion, enhanced corrosion protection, adhesion, and hydrophobicity | Zhao et al. [119] |
| Polyvinyl butyral | GO | Spin coating, surface modification by poly (methylhydrosiloxane) | Better corrosion resistance for aluminum | Zhu et al. [32] |
| Oleo-polyurethane | GO | The synergy of $\pi-\pi$ interaction and in situ polymerization | Improved filler dispersion, antimicrobial and anticorrosion properties | Ahmadi and Ahmad [33] |

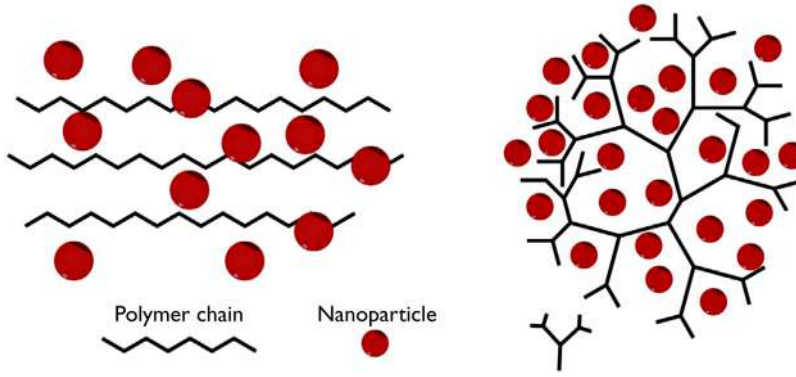


**Figure 10.4** Arrangement of nanoparticles in linear and hyperbranched polymer nanocomposites.
*Source*: From Y. Ahmadi, S. Ahmad, Chapter 19 - Polymeric nanocomposite coatings, in: S. Rajendran, T.A. Nguyen, S. Kakooei, M. Yeganeh, Y. Li (Eds.), Corrosion Protection at the Nanoscale, Elsevier, 2020, pp. 363−378. https://doi.org/10.1016/B978-0-12-819359-4.00019-2.

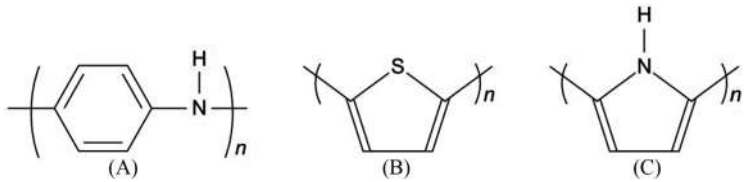


**Figure 10.5** Molecular structure of common ECPs: (A) polyaniline, (B) polythiophene, and (C) polypyrrole.
*Source*: From N.Y. Abu-Thabit, A.S.H. Makhlouf, Chapter 24 - Recent advances in nanocomposite coatings for corrosion protection applications, in: A.S.H. Makhlouf, D. Scharnweber (Eds.), Handbook of Nanoceramic and Nanocomposite Coatings and Materials, Butterworth-Heinemann, 2015, pp. 515−549. https://doi.org/10.1016/B978-0-12-799947-0.00024-9.

Corrosion protection by ECPs can be attained by three mechanisms. These are as follows:

1. Isolation of metal substrate by barrier protection [42];
2. Anodic protection by passive layer formation [43];
3. Providing the capacity to perform self-healing by the release of the doped corrosion blocker anions from the ECPs triggered by the electrochemical reduction [44].

For example, a dual-layer of PPy coating consisting of a molybdate-doped internal layer and dodecyl sulfate-doped external layer rendered outstandingly longer corrosion protection to steel than monolayer PPy coating where the outer layer prevented aggressive anion infiltration, while the inner layer exhibited a controlled release of the molybdate anions that ensured the self-healing capability [45]. In a separate study,

well-dispersed multiwalled carbon nanotubes (MWCNTs) in conducive PU expanded the diffusion route of corrosive ions and hindered their infiltration [46]. ECP nanocomposite coatings have been revolutionary for electrical energy storage systems as good corrosion resistance is a crucial factor in determining their service life.

### 10.2.5 Smart polymer nanocomposite coatings

Smart nanocomposite coatings can repair damage sustained during service and thus perform better than traditional coatings. Contrary to the practice of direct mixing of corrosion inhibitors into the matrix, smart coatings encompass the inhibitors in microcapsules, nanocontainers, and nanoreservoirs. Microencapsulation is the technique of packing solid, liquid, or gaseous active ingredients called core inside the shell of a second material to protect them from the surrounding environment. Microencapsulation prevents direct exposure of inhibitors to the coating and provides a constrained release thus ensuring lower consumption of inhibitors [42]. Microcapsule containing a poly(urea-formaldehyde) shell and hydrolyzable organic silane core used as fillers in epoxy coating imparted good corrosion resistance [47]. Generally utilized nanocontainers are halloysite nanotubes (HSNs), mesoporous silica nanocontainers, HA microparticles, and nanocrystalline-layered double hydroxides that provide deactivation, storage, and constrained release of inhibitors [42]. Some research groups have reported the use of ceramic-based nanocontainers such as cerium oxide [48] and cerium molybdenum [49].

### 10.2.6 UV-cured polymer nanocomposite coatings

UV-cured polymer nanocomposite coatings encompass photoinitiators which upon activation by radiation produce active free-radical species that interact with the unsaturated polymer matrix to give a polymerized solid film [50]. The photoinitiators utilize the high energy from UV-ray to go through photolysis. This phenomenon can produce either active radicals to cure acrylate monomers or yield cationic species that cure cycloaliphatic epoxy-based systems [51]. UV-cured nanocomposite coatings are economically sustainable alternatives to traditional coatings. UV-cured methacrylic−siloxane coating reinforced with boehmite nanoparticles have been reported to be an effective coating for wood elements [52]. Another research group focused on the effect of clay filler contents on UV curing behavior of urethane-acrylate/clay nanocomposite coating and reported that UV curing rate increased with increasing clay content [51].

### 10.2.7 Biocompatible and antimicrobial polymer nanocomposite coatings

In recent years, polymer nanocomposite coatings have gained significant acclamation as biocompatible and antimicrobial coatings for implants. Biocompatible coatings do not release any toxic substances into the human body and in some cases promote

tissue growth accelerating the healing process. Antimicrobial coatings hinder the growth of harmful microbes and prevent bacterial infections. Nanocomposite coatings developed recently have also exhibited promising results as drug reservoirs and drug deliverers. Poly(carboxybetaine methacrylate) coating embedded with a silver (Ag)−zwitterion nanocomposite synthesized through in situ reductions of $Ag^+$ precursor ions loaded on zwitterionic polymer brushes has been reported to possess satisfactory antimicrobial properties [35] (Fig. 10.6).

Hyperbranched poly(esteramide) with PANI nanofiber-modified MMT nanocomposite coating developed by separate research groups has exhibited potent microbial properties [53]. Another research group reported the fabrication of silver nanoparticle (AgNP)−embedded polymethyltrimethoxysilane composite coating through layer-by-layer assembly and siloxane self-condensation reaction where the self-healing polysiloxane provided better corrosion resistance while the AgNPs countered the susceptibility of polysiloxane to bacterial infection [54].

## 10.3 Polymer nanocomposite adhesives

The definition of adhesive according to Kinloch is a material that can join two surfaces when applied and resist separation [55]. Three basic qualities must be possessed by an adhesive to be effective: (1) surface wettability of the substrate by the adhesive, determined by pressure, time, viscosity, and surface energy; (2) proper curing to ensure a rigid mechanical bond between substrates; and (3) the ability of load transmission [56]. In general, the main ingredient of an adhesive is an organic polymer originally applied or produced from a chemical reaction of one or more components after application [4]. A prerequisite for polymer adhesives is that they must be in liquid form during application to wet the surface properly and eventually harden. Exceptions are pressure-sensitive adhesives (PSAs) that do not undergo any curing. Based on the curing process, adhesives can be classified into waterborne, solvent-borne, hot melt, hyperbranched, etc. Modification of polymer adhesives at the nanoscale has opened the door to the development of better adhesives with multifunctional properties. Similar to nanocomposite coatings, nanofillers used in adhesives also include carbon-based fillers such as graphene, CNTs, inorganic nanoclay, and oxides. In recent years, polyhedral oligomeric silsesquioxane nanocompounds having the general formula $RSiO_{1.5}$ (R is either a hydrogen atom or an organic functional group) have gained considerable attention as nanoreinforcement [57]. The next part of the chapter is dedicated to the discussion of different classes of polymer nanocomposite adhesives and their fabrication.

### *10.3.1 Epoxy-based high-performance nanocomposite adhesives*

Epoxy resins are thermosetting polymers with desirable properties, such as outstanding adhesion, high strength, low shrinkage, low creep, and good corrosion resistance [58]. Due to these critical properties, epoxy resins are the most widely

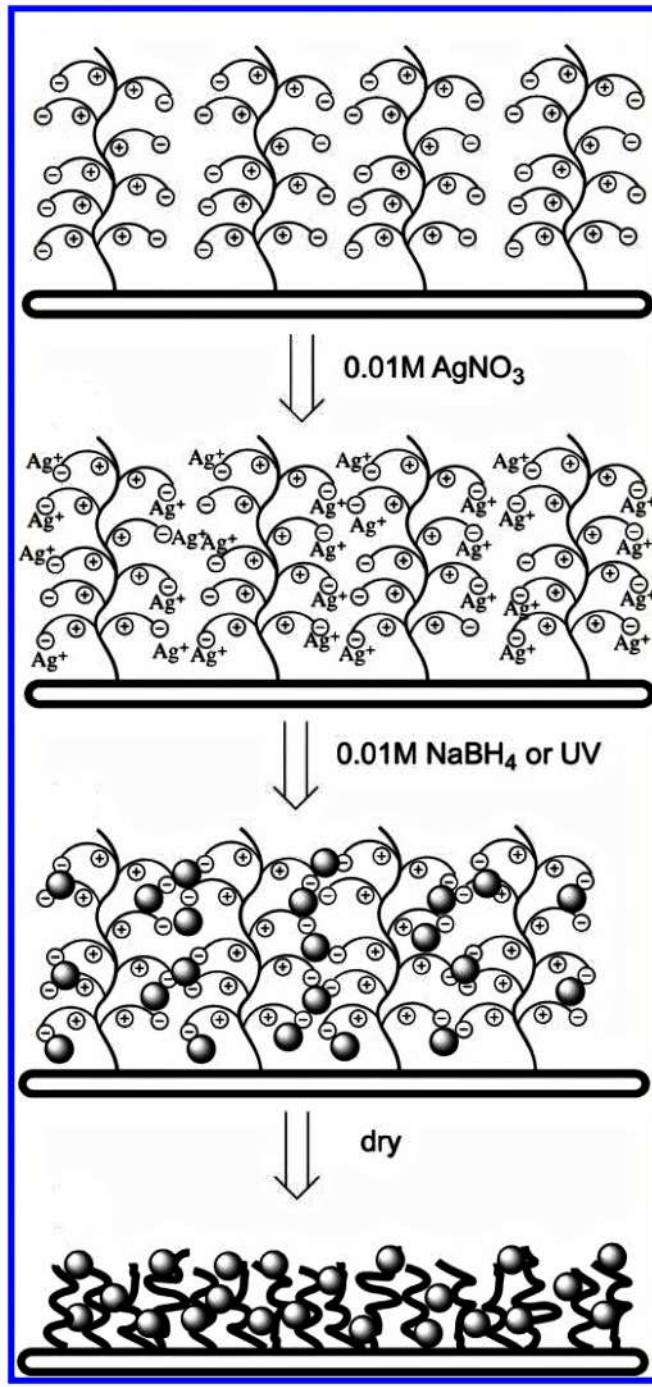


**Figure 10.6** Illustrative representation of the Ag ion-embedding process in zwitterionic polymer brush.
*Source*: From R. Hu, G. Li, Y. Jiang, Y. Zhang, J.-J. Zou, L. Wang, X. Zhang, Silver−zwitterion organic−inorganic nanocomposite with antimicrobial and antiadhesive capabilities, Langmuir 29 (11) (2013), 3773−3779. https://doi.org/10.1021/la304708b.

used matrices for high-performance or structural adhesives. Structural adhesives are capable of sustaining substantial loads. These are gradually replacing traditional joining techniques used in the building, mining, aerospace, and automotive sectors [59]. The dilemma that researchers face with epoxy resins is that the high cross-linking density which provides the epoxy its strength and corrosion resistance is also responsible for its brittleness and poor crack resistance. The introduction of nanoparticles in epoxy has allowed us to overcome its drawbacks without compromising other properties. The addition of nanofillers also improves favorable properties like wettability and adhesion [60]. Several mechanisms have been proposed by researchers about how nanoparticles render toughening of epoxy resins such as crack deflection, crack pinning, and plastic void growth [61]. However, the plastic void growth theory is more acceptable since nanoparticles are too small for crack deflection or pinning [62]. The degree of curing in epoxy nanocomposites is largely responsible for its end properties, and the addition of nanoparticles influences the curing of the epoxy [63]. The commonly used nanofillers in epoxies are various organic and inorganic particles such as CNTs, graphene nanoplatelets (GNPs), nanoclay, nanosilica, and nanoalumina [64]. The uniform dispersion of nanofillers in the epoxy matrix is vital as it ensures uniform stress distribution [65]. Ultrasonication, shear mixing, and calendaring methods are employed either individually or in combination to ensure the proper distribution of nanofillers in an epoxy matrix [64]. Epoxy adhesive reinforced with GNPs has been reported to follow a complex mechanism for moisture absorption, and their mechanical properties vary with the amount of water uptake which is controlled by the GNP content [66] (Table 10.3).

Aradhana et al. reported better mechanical properties in epoxy−GO adhesives than epoxy−reduced graphene oxide (rGO) adhesives which they ascribed to the existence of a greater number of oxygen functional groups in GO that favored reaction with epoxy resin and curing agent [67,68]. Han et al. studied the contrast between the effect of graphene platelets and CNTs on epoxy adhesives and concluded that GNPs and CNTs both enhance the mechanical properties and electrical conductivity of epoxy adhesives but CNTs provide the better structural reinforcement [75]. The scope of using recycled materials has also been explored by researchers to ensure sustainability in adhesive production. Epoxy adhesive filled with recycled poly(ethylene terephthalate) (PET), ground rubber tire, and GO nanoflakes possesses drastically improved tensile strength, and toughness [63]. A separate research group incorporated epoxy adhesive with microsized alumina fillers in combination with recycled tire particles and phenolic resin that resulted in an 80% rise in lap-shear strength [76] (Fig. 10.7).

### 10.3.2 Waterborne polyurethane nanocomposite adhesives

Waterborne polyurethanes (WPUs) are a special class of polymers that are synthesized by organic reactions between water and PU prepolymer in a water medium [77]. The reaction mechanism of WPU production is the introduction of hydrophilic groups into the hydrophobic PU by the addition of deionized water to emulsify and disperse the

**Table 10.3** Recently reported studies on epoxy-based structural nanocomposite adhesives.

| Reinforcement used | Result | Reference |
|---|---|---|
| Multiwalled carbon nanotube and a nanoclay | Improved thermal stability | Aradhana et al. [67,68] |
| Zirconia nanoparticles | Improved mechanical properties and interfacial wettability with an aluminum substrate | Dorigato et al. [60] |
| Untreated and calcined fumed alumina nanoparticles | Improved mechanical properties and interfacial wettability with an aluminum substrate | Dorigato and Pegoretti [69] |
| Glycidyloxypropyl trimethoxysilane-modified silica, alumina, and titania nanoparticles | Improved viscoelastic properties | Bauer et al. [70] |
| Acrylic rubber and montmorillonite | Increased glass transition temperatures $T_g$ and adhesive strength | Wang et al. [58] |
| Fullerene like tungsten disulfide and functionalized nano-polyhedral oligomeric silsesquioxane | Increased shear and peel strength of both low- and high-temperature cured epoxy | Shneider et al. [71] |
| Amine-functionalized and nonfunctionalized graphene nanoplatelets (GNPs) | Higher Young's modulus but lower tensile strength due to the aggregation of GNPs | Salom et al. [72] |
| Nanosilica particles | Increased toughness | Meng et al. [73] |
| Organo-modified nanoclay | Improved elastic modulus, tensile strength, and fracture toughness | Dorigato and Pegoretti [74] |

resultant hydrophilic WPU prepolymers along with the chain extension process [1]. The basic chemical components of WPUs are diisocyanates, polyols, amines, catalysts, and additives [78]. The main reactions that occur during the process are as follows:

1. Polyaddition reaction of excess isocyanates with polyols to produce PU polymers.
2. Reaction between remaining isocyanate groups and amines to form ureas.
3. Hydrolyzation of isocyanate groups by water medium to produce amines and ureas [78].

The synthesis methods of WPUs include prepolymer emulsification polymerization, ketamine−ketazine miniemulsion polymerization (MEP), homogeneous solution polymerization, acetone process, melt dispersion process, etc. [2]. WPU adhesives came into vogue when the use of solvent-borne polymers got restricted due to their harmful effects on the environment. Solvent-borne adhesives contain volatile organic content, which is hazardous to human health. Moreover, WPU adhesives are flame retardant and more cost-friendly [79]. WPU nanocomposite

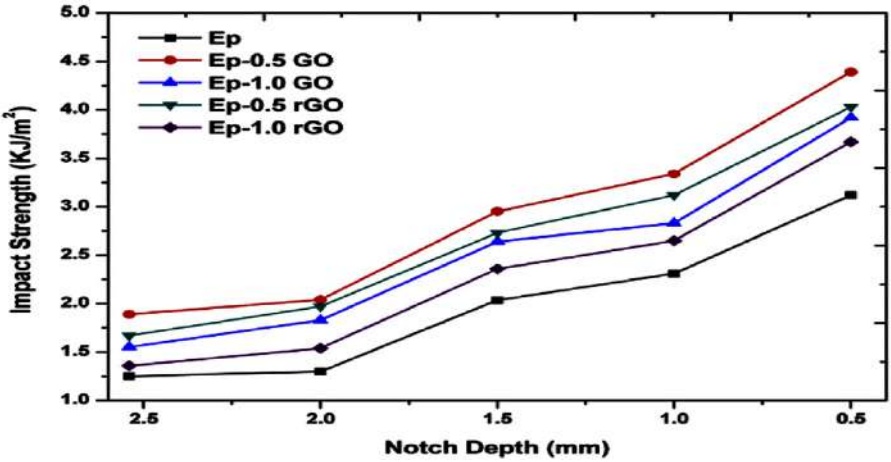


**Figure 10.7** Graphical representation of a comparison of impact strength against notch depth of pristine epoxy, epoxy−GO, and epoxy−rGO adhesive systems.
*Source*: From R. Aradhana, S. Mohanty, S.K. Nayak, Comparison of mechanical, electrical, and thermal properties in graphene oxide and reduced graphene oxide filled epoxy nanocomposite adhesives, Polymer 141, (2018) 109−123. https://doi.org/10.1016/j.polymer.2018.03.005.

adhesives exhibit a vast array of attractive properties. A superior level of interaction and dispersion occurs between nanofillers and WPU matrices owing to the existence of polar groups and ionic moieties in the WPU structure [2]. WPU/organoclay Cloisite 15A developed by Rahman et al. exhibited the highest level of thermal stability, mechanical property, and adhesive strength at optimum 2 wt.% clay content [80]. Huh et al. incorporated organically modified clays Cloisite 15A and Cloisite 30B into the WPU matrix and observed that Cloisite 30B rendered better dispersion stability, tensile strength, Young's modulus, and adhesive strength to the adhesive than Cloisite 15A [81]. Another research group developed a nano-$SiO_2$/fluorinated WPU nanocomposite adhesive for laminated films. The resultant adhesive showed improved adhesion strength owing to better wetting behavior, water resistance, and thermal stability [82] (Fig. 10.8).

Cakić et al. utilized (3-aminopropyl) triethoxysilane (APTES) as a chain extender to fabricate waterborne castor oil−recycled polyol-based PU−silica nanocomposite adhesive via the sol−gel method and observed that APTES can improve the thermal stability of WPU [83]. The effect of 2,2-dimethylol propionic acid (DMPA) on the dispersion in WPU/CNT nanocomposite adhesive was studied by another research group, and the results showed that the degree of homogeneous CNT dispersion increased with increasing DMPA content and the resultant adhesive displayed higher adhesive strength than pristine WPU at higher temperatures [84]. WPU reinforced with modified lignin amine reportedly exhibited increased adhesive strength and endured exposure to normal atmospheric weather conditions for 180 days making it a promising adhesive [80].

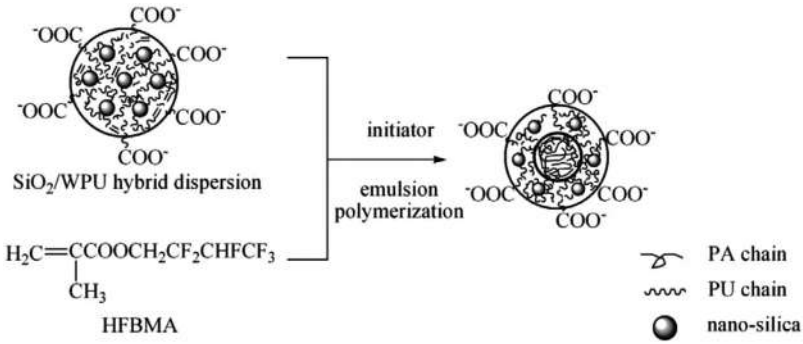


**Figure 10.8** Imaginative representation of formation process of nanosilica/fluorinated WPU nanocomposite adhesive. *PA*, polyamide; *PU*, polyurethane; *HFBMA*, 2,2,3,4,4,4-hexafluorobutyl methacrylate.
*Source*: From H. Fu, C. Yan, W. Zhou, H. Huang, Nano-$SiO_2$/fluorinated waterborne polyurethane nanocomposite adhesive for laminated films, J. Industr. Eng. Chem., 20 (4), (2014), 1623–1632. https://doi.org/10.1016/j.jiec.2013.08.009.

### 10.3.3 Pressure-sensitive adhesives

PSAs are adhesives that are permanently soft and deformable and adhere instantly to the substrate by basic contact with the slightest pressure without further curing or chemical bonding. The contact formed between the substrate and the adhesive is accredited to the weak van der Waals forces between the linear aliphatic polymeric chains with few polar functional groups [85]. Debonding of PSAs from substrates occurs by cavity formation that leads to cavity expansion that creates fibrils [86]. The requirements of an ideal PSA are an optimum viscosity and a significant amount of energy dissipation during deformation [58]. The most used polymers in PSAs are natural rubber, styrene-butadiene rubber, block copolymers, amorphous polyolefins, and acrylics [4]. Clay-based polymer nanocomposite adhesives have been observed to have better tack and shear resistance and peel strength than pristine polymeric ones [5].

Poly(lauryl acrylate) particles with Laponite clay armor were added to standard poly(butyl acrylate-co-acrylic acid) latex to develop waterborne PSA with a superior balance of viscoelasticity and tack energy [87]. Both modified and unmodified MMT clays dispersed in ethyl acrylate (EA)/2-ethylhexyl acrylate (2-EHA) monomer mixture polymerized via suspension polymerization technique resulted in an acrylic polymer/MMT PSA with an increased shear strength and storage modulus [88]. In a separate study, a solventless acrylic/modified MMT UV cross-linkable PSA was synthesized by bulk polymerization process of 2-EHA, acrylic acid (AA), and *t*-butylacrylate monomers, which exhibited satisfactory shear strength and storage modulus, but the addition of MMT adversely affected the UV cross-linking [89]. PU/(meth)acrylates matrix reinforced with exfoliated molybdenum disulfide ($MoS_2$) nanoplatelets possesses a superior balance of viscoelastic properties and tack adhesion energy with 0.25 wt.% $MoS_2$ [90]. Khalina et al. employed MEP of 2-EHA/AA/methyl methacrylate to produce latex that was later filled with

nanosilica, which located themselves in the shell of latex particles providing improvement in elastic and loss modulus, viscosity, and tack resistance [91]. Wang et al. dispersed single-walled CNTs functionalized with hydrophilic PVA in poly (butyl acrylate) latex to fabricate a PSA with high tack energy, optical transparency, and electrical conductivity [87]. Ouzas et al. successfully studied the potential effectivity of cellulose nanocrystals (CNCs) as a PSA property modifier by adding it to semibatch emulsion polymerization of 2-EHA)/*n*-butyl acrylate (BA)/methyl methacrylate (MMA) [92]. PSA developed from acrylic copolymers and terpolymers of EA, BA, and AA, and nanosilica via solution polymerization method also exhibited improved peel strength [93].

The application possibility of PSAs for transdermal drug delivery is a widely researched area. Poly(EHA-co-AA)/silicate nanocomposite prepared by the emulsion copolymerization of 2-EHA and AA with sodium silicate embedded with Cloxacillin sodium antibiotic exhibited satisfactory microorganism degradation [94]. Optimization of organosilicate content in polydimethylsiloxane (PDMS)/organoclay can provide enhanced control over drug release dynamics and improved adhesive properties [95]. Polyacrylamide and poly(acrylamide-hydroxyethyl methacrylate) hydrogel nanocomposites with monodisperse polystyrene nanoparticle fillers showed properties to be a promising PSA for dermatological patches [96].

### 10.3.4 Hydrogel and biomimetic adhesives

Polymer hydrogels are soft gel-like materials consisting of three-dimensional hydrophilic polymeric chain networks. These cross-linking networks are capable of absorbing and reserving water amounts up to 99 wt.% [97]. Hydrogels are considered to be a revolutionary innovation in wound healing technology due to their nontoxic and biodegradable characteristics [98]. This particular water-absorbing property of the cross-linked network makes hydrogels swell in aqueous solutions instead of dissolving [99]. The cross-linked network of the hydrogel can be formed either by a physical or a chemical process. Chemical cross-linking in hydrogels can be conducted via radical polymerization, reactions between complementary groups, energy irradiation, and enzymes [99]. Physical cross-linking processes include ionic interactions, crystallization, aqueous self-assembly of amphiphilic block and graft copolymers, hydrogen bonds, and protein interactions [99]. Hydrogels have structural similarities with natural soft tissue [75] and recovering capabilities after deformation [100]. Consequently, polymeric hydrogels have emerged as potential biomaterials. The main drawback of virgin polymer hydrogels is that they have a restricted elastic modulus range, rendering them unsuitable for load-bearing applications [97]. The application of nanotechnology in the hydrogel structure has immensely widened the scope of their implementation. Hydrogel nanocomposite adhesives encompass various types of particles ranging from organic to inorganic modified at the nano level dispersed among the cross-linked polymer chain network.

Research on nanocomposite hydrogel has gathered conspicuous momentum in the last decade. Wang et al. developed silane-modified sodium montmorillonite

(NaMMT)−reinforced hydrogel adhesive through free-radical polymerization of PEG methyl ether acrylate possessing the ability of dynamic restructuring- a potential material for self-healing and acoustic dampening [100]. A visual illustration of this fabrication process is depicted in Fig. 19.5. Skelton et al. prepared nanosilicate, Laponite-filled polyacrylamide (PAAm) nanocomposite hydrogels copolymerized with dopamine methacrylamide (DMA) [97]. The content of Laponite and DMA played a crucial role in determining the resultant nanocomposite adhesive's equilibrium water content, stiffness, and viscous dissipation properties. A separate research group used Laponite fillers poly(acrylic acid) (PAA) hydrogel nanocomposite adhesive produced via aqueous in situ free-radical polymerization [24]. This particular adhesive showed a tunable adhesive strength based on the Laponite content and could be considered as a suitable bioadhesive for dental, wound healing, and tissue engineering applications. Rajabi et al. developed an injectable hemostatic surgical adhesive consisting of thiolated gelatin (Gel-SH) and gelatin methacrylate (GelMA) matrix holding polydopamine functionalized Laponite (PD-LAP) nanoparticle by facilitating Michael reaction between Gel-SH and GelMA, and covalent interaction between PD-LAP and hydrogel [101]. The adhesive exhibited satisfactory recovery ability, tissue adhesiveness, cytocompatibility, and notably shorter blood clotting time. Hydrogel synthesized via polymerization of AA with $SiO_2$-g-polyacrylamide core−shell hybrid nanoparticles as cross-linking sites has been reported to possess outstanding skin mimetic, stretchability, and self-healing characteristics [102] (Figs. 10.9 and 10.10).

A special class of polymer nanocomposite adhesives can be labeled as mussel-inspired adhesives. Mussels are sea organisms that can rapidly attach themselves to solid surfaces by strong, durable adhesion. The adhesion mechanism of mussels in the aqueous environment has been the motivation for developing biomimetic adhesives. Essential strategies and technologies could be developed by mimicking the mussels' adhesion mechanism, which helped to overcome the high dielectric and solvation properties of water that hindered adhesive performance [51]. In order to replicate the catecholic functionality dihydroxyphenylalanine decorated mussel adhesive proteins, synthetic polymers have been modified with catechols to obtain improved adhesive, sealant, coating, and anchoring properties [103]. Shao et al. fabricated a mussel-inspired conductive self-healing adhesive through multiple coordination bonds among tannic acid-coated cellulose nanocrystals (TA@CNCs), PAA chains, and metal ions [104]. TA@CNCs were incorporated into chitosan/PAA double-network nanocomposite hydrogels via a salt soaking process in different research in order to prepare a conductive and strain-sensitive adhesive to be used as conformable biosensors [105]. Another research group incorporated Laponite into dopamine-modified four-armed PEG to develop a mussel mimicking injectable bioadhesive [106]. A tunable bone adhesive for sternal closure was developed by Zhang et al. [107] by introducing HA nanoparticles into hyperbranched poly-(β-amino ester) (polydopamine-co-acrylate) matrix. Polydopamine−clay−polyacrylamide hydrogel adhesive was prepared by Han et al. [108] by in situ polymerizations of acrylamide monomers resulting in increased adhesion, toughness, and biocompatibility.

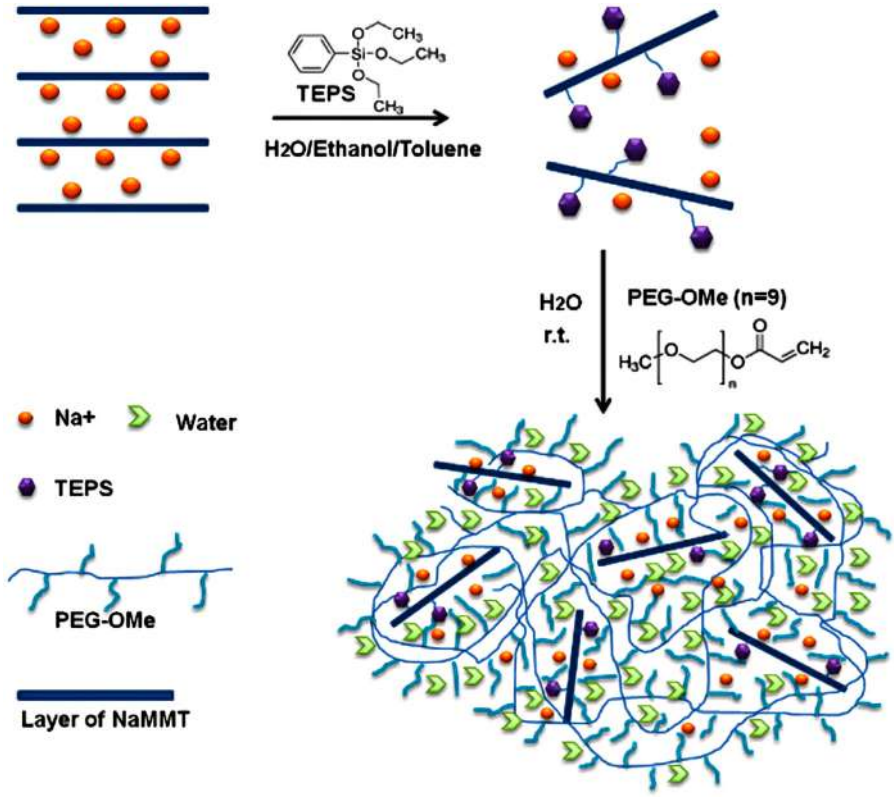


**Figure 10.9** Visual representation of the fabrication process of PEG/MMT nanocomposite hydrogel adhesive. *PEG-OMe*, poly(ethylene glycol) methyl etheracrylate; *TEPS*, triethoxyphenylsilane.
*Source*: From M. Wang, D. Yuan, X. Fan, N.G. Sahoo, C. He, Polymer nanocomposite hydrogels exhibiting both dynamic restructuring and unusual adhesive properties, Langmuir 29 (23) (2013) 7087−7095. https://doi.org/10.1021/la401269p.

### 10.3.5 Conductive polymer nanocomposite adhesives

Electrically conductive adhesives (ECAs) are primarily polymeric composites composed of a conductive filler dispersed in an insulating polymer matrix [109]. ECAs are used in electronic assemblies such as smart cards, liquid crystal displays, semiconductor packaging to provide shock resistance, vibration dampening, and inhibiting moisture and other corrosive constituents [5]. Based on the loading degree of conductive fillers, ECAs can be classified into three categories: isotropic conductive adhesives (ICAs), anisotropic conductive adhesives (ACAs), and nonconductive adhesives (NCAs) [109]. The difference between these three kinds is that ICAs can exceed the percolation threshold owing to the heavy filler load and conduct electricity in all directions, whereas ACAs and NCAs can only conduct electricity in one direction [109] (Fig. 10.11).

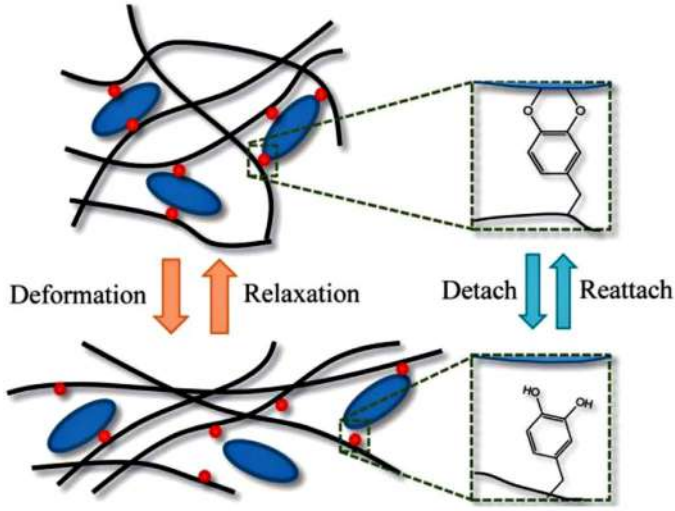


**Figure 10.10** Schematic representation of the recovery process of PAAm/Laponite/DMA nanocomposite adhesive.
*Source*: From S. Skelton, M. Bostwick, K. O'Connor, S. Konst, S. Casey, B.P. Lee, Biomimetic adhesive containing nanocomposite hydrogel with enhanced materials properties, Soft Matter 9 (14) (2013) 3825−3833. https://doi.org/10.1039/C3SM27352K.

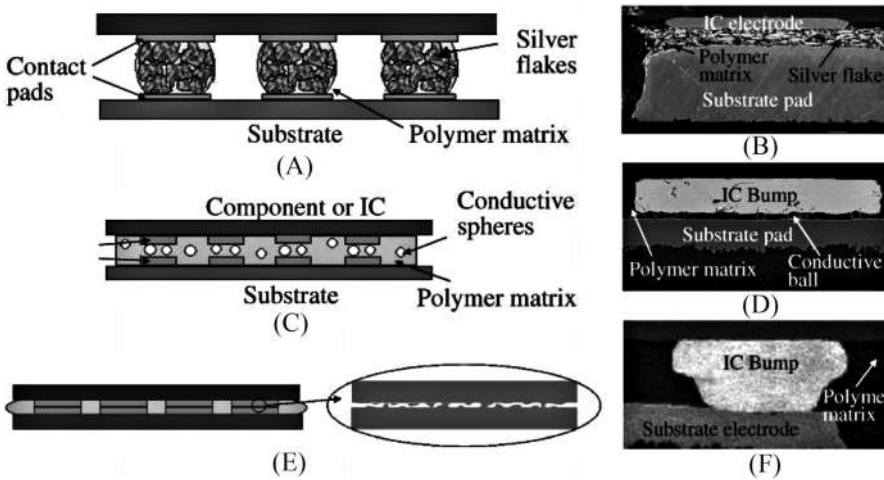


**Figure 10.11** Illustrative and scanning electron microscopic images of cross sections of ICA (A, B), ACA (C, D), and NCA (E, F) bonded flip-chip joints.
*Source*: From M.J. Yim, Y. Li, K. Moon, K.W. Paik, C.P. Wong, Review of recent advances in electrically conductive adhesive materials and technologies in electronic packaging, J. Adhes. Sci. Technol. 22 (14) (2008) 1593−1630. https://doi.org/10.1163/156856108X320519.

**Table 10.4** List of recently reported epoxy/CNT ECAs.

| Filler type | Result | Reference |
|---|---|---|
| CNTs | Maximum electrical conductivity $1.5 \times 10^5$ S/m with 3 wt.% CNTs, thermal diffusivity improved threefold | Li and Lumpp [111] |
| Ag and CNTs | Conductivity $10^5$ S/m with 66.5 wt.% Ag and 0.27% CNTs | Li et al. [112] |
| CNTs coated with Ag | Conductivity $4 \times 10^5$ S/m with 28 wt.% CNT−Ag | Wu et al. [113] |
| CNTs decorated with Ag | Conductivity $3 \times 10^3$ S/m with 0.5 wt.% CNT−Ag, improved flexural strength, and thermal conductivity | Ma et al. [114] |

*Source:* From A. Santamaria, M.E. Muñoz, M. Fernández, M. Landa, Electrically conductive adhesives with a focus on adhesives that contain carbon nanotubes, J. Appl. Polym. Sci. 129 (4) (2013) 1643−1652. https://doi.org/10.1002/app.39137.

The majority of the reported research works on ECAs is based on epoxy matrix reinforced with conductive metal fillers such as silver nanowires or carbon-based filler like graphene and CNTs [110]. Other polymer matrices used for ECAs are silicone, polyamide, PU, and PDMS. In recent years, the scope of using epoxy-based ECAs as an alternative to metallic solder has been widely explored by researchers due to its environmental safety and high-temperature usability. CNTs have an advantage over other ECAs fillers because of their outstanding electrical conductivity, suitable size, and high aspect ratio, which commends the foundation of the electron transport network [110] (Table 10.4).

Aromatic polyimides are potential ECAs for their dielectric property and thermal stability. However, the use of polyamides is restricted by high glass transition temperatures and insolubility in organic solvents [115]. Hatami filled the polyamide matrix with silver nanowires via the solution mixing method and concluded that the resultant nanocomposite adhesive exhibited optimum conductivity and thermal stability with 2 vol.% Ag nanowires [115]. Poly(methyl/vinyl)silsesquioxane (PMVS) nanospheres were produced by hydrolytic condensation method and added to PDMS before curing to develop a nanocomposite adhesive with improved tensile strength, conductivity, and thermal stability [116] (Fig. 10.12).

## 10.4 Application of polymer nanocomposite coatings and adhesives

Challenges of modern technologies demand the utilization of advanced composite materials [117]. The application of polymer nanocomposite coatings and adhesives can be observed in almost every industry and field of engineering nowadays. The exploitation of polymer nanocomposites as coatings and adhesives has revolutionized sectors such as automobiles, marine, biomedical, electronics, textile, and construction.

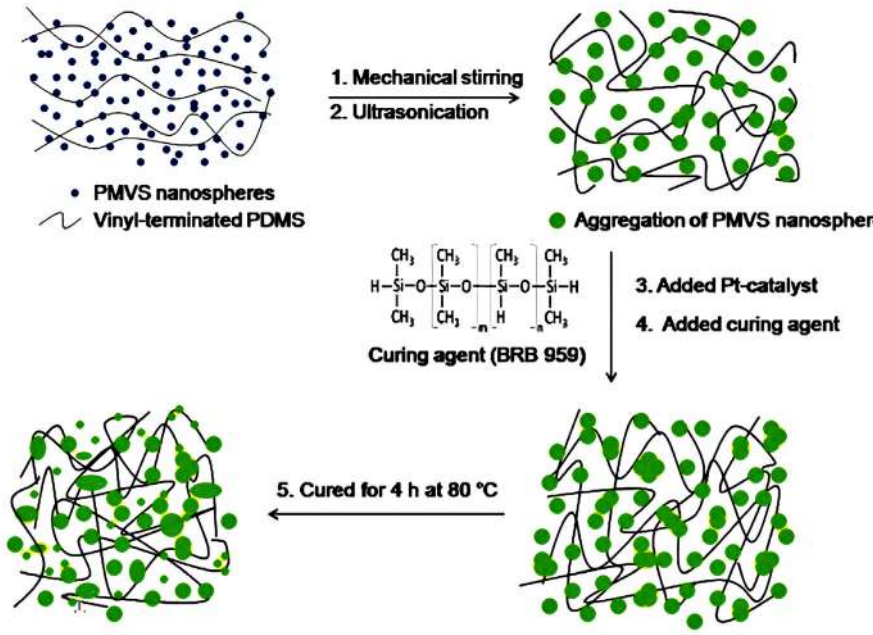


**Figure 10.12** Illustration of the fabrication process of PDMS/PMVS nanocomposite ECA. *Source*: From V. Anoop, S., Sankaraiah, N.L. Mary, Development of an optically transparent polysilsesquioxane/PDMS addition-cured nanocomposite adhesive for electronic applications. N. J. Chem. 43 (41) (2019) 16322−16330. https://doi.org/10.1039/C9NJ04092G.

Biomedical and bioengineering may have ripped the most benefits from the development of polymer nanocomposites. Polymer nanocomposites are probably the most explored materials for coating metallic and ceramic bioimplants. Polymer nanocomposite coatings are capable of protecting the bioimplant from corrosion in body fluids, act as drug reservoirs, and promote bioactivity. A porous nanocomposite coating of nanohydroxyapatite and poly(ε-caprolactone) on magnesium implants was reported to increase resistance to localized corrosion and improve bioactivity [118]. A separate research group developed a bionanocomposite of chitosan and gold nanoparticles through the electrodeposition method on titanium implants and successfully achieved a passive coating that inhibits bacteria [120].

The eligibility of nanocomposites to be used as surgical glue depends on three factors: resemblance to healthy tissue, nontoxicity, and minimal damage [5]. Antimicrobial property is another concern for developing nanocomposite for bioadhesives. A sunflower oil-based hyperbranched PU nanocomposite filled with iron-oxide nanoparticle-decorated MWCNTs was reported to be effective for wound dressing and controlled drug release [121]. A poly(methyl methacrylate)-grafted clay nanocomposite fabricated through free-radical polymerization has been reported to be a promising dental adhesive [122].

Polymer nanocomposite coatings are used in the automotive industry as engine enamel, decorative paint, etc., to provide durability. Self-healing carbon-based smart nanocomposites can be utilized as scratch-resistant coatings that can achieve recovery upon treatment such as heating [123]. Clay-based polymer nanocomposites are frequently used in the aerospace industry due to their thermal stability and flame retardancy [124]. Clay−epoxy nanocomposites are promising candidates for use in the marine environment because of their barrier properties and less moisture absorption [125].

Tan et al. reported the application of a flame retardant nanocomposite adhesive consisting of organo-modified HSNs and epoxidized natural rubber with 50% epoxidation level with increased hardness [126]. A PSA consisting of methacrylic nanoparticles in colloidal dispersion of soft acrylate copolymer particles has been reported to exhibit tunable tackiness via nanoparticle concentration distribution with potential application in sustainable disassembly and recycling of electronics [127].

## 10.5 Conclusion and future prospects

Exploration of polymer nanocomposite materials for the role of coatings and adhesives has emerged as one of the fastest-growing research areas of materials science. From the topics discussed in this chapter, it is evident that polymer nanocomposites can be utilized as coating and adhesives in many different aspects ranging from structural applications, corrosion protection to electronics, and smart material applications. The properties and performance of polymer nanocomposite coatings and adhesives depend on various factors including filler choice, filler modification, the synthesis process, and choice of matrix. Due to this diversity of options, the possibilities of polymer nanocomposite coatings and adhesives are endless. New and advanced coatings and adhesives nanocomposites are replacing traditional materials at a fast-growing pace. Advanced polymer nanocomposites have opened the door to a propitious future for coatings and adhesives in all branches of engineering and technology. However, the development of polymeric coatings and adhesives is yet to achieve its prime. At present, the most important goal in developing polymeric coatings and adhesives is to produce them via a cost-effective and environmentally sustainable method without compromising their superior properties and performance. The current research in this area is focused on developing the next generation of coatings and adhesive materials such as smart coatings and biomimetic adhesives. It can be presumed unequivocally that polymer nanocomposite coatings and adhesives will revolutionize all areas of modern technology in the near future.

## References

[1] Y. Ahmadi, S. Ahmad, Chapter 19 - Polymeric nanocomposite coatings, in: S. Rajendran, T. A. Nguyen, S. Kakooei, M. Yeganeh, Y. Li (Eds.), Corrosion Protection at the Nanoscale, Elsevier, 2020, pp. 363−378. https://doi.org/10.1016/B978-0-12-819359-4.00019-2.

[2] Y. Ahmadi, S. Ahmad, Recent progress in the synthesis and property enhancement of waterborne polyurethane nanocomposites: promising and versatile macromolecules for advanced applications, Polym. Rev. 60 (2) (2020) 226–266. Available from: https://doi.org/10.1080/15583724.2019.1673403.

[3] M. Rahman, F. Zahin, M.A.S.R. Saadi, A. Sharif, M.E. Hoque, Surface modification of advanced and polymer nanocomposites, Springer International Publisher Science, 2018, pp. 187–209. https://doi.org/10.1007/978-3-319-76090-2_6.

[4] J. Comyn, R.D. Adams, Chapter 2 - What are adhesives and sealants and how do they work? Woodhead Publishing Series in Welding and Other Joining Technologies. Woodhead Publishing, 2005, pp. 23–51. https://doi.org/10.1533/9781845690755.1.23

[5] S. Pramanik, N. Karak, Polymer nanocomposites for adhesive, coating, and paint applications, in: D.K. Tripathy, B.P. Sahoo (Eds.), Properties and Applications of Polymer Nanocomposites, Springer, Berlin, Heidelberg, 2017, pp. 173–204. https://doi.org/10.1007/978-3-662-53517-2_8.

[6] M.E. Mackay, T.T. Dao, A. Tuteja, D.L. Ho, B. Van Horn, H.-C. Kim, et al., Nanoscale effects leading to non-Einstein-like decrease in viscosity, Nat. Mater. 2 (11) (2003) 762–766. Available from: https://doi.org/10.1038/nmat999.

[7] K.F. Asrafuzzaman, Amin, A. Sharif, M.E. Hoque, Bonding mechanism and interface enhancement of bamboo fiber reinforced composites, Springer, Singapore, 2021, pp. 215–233. https://doi.org/10.1007/978-981-15-8489-3_12.

[8] N.Y. Abu-Thabit, A.S.H. Makhlouf, Chapter 17 - Recent advances in polyaniline (PANI)-based organic coatings for corrosion protection, in: A.S.H. Makhlouf (Ed.), Handbook of Smart Coatings for Materials Protection, Woodhead Publishing, 2014, pp. 459–486. https://doi.org/10.1533/9780857096883.2.459.

[9] G. Negroiu, R.M. Piticescu, G.C. Chitanu, I.N. Mihailescu, L. Zdrentu, M. Miroiu, Biocompatibility evaluation of a novel hydroxyapatite-polymer coating for medical implants (in vitro tests), J. Mater. Science: Mater. Med. 19 (4) (2008) 1537–1544. Available from: https://doi.org/10.1007/s10856-007-3300-6.

[10] L. Guo, W. Yuan, Z. Lu, C.M. Li, Polymer/nanosilver composite coatings for antibacterial applications, Nanoparticles Interfaces 439 (2013) 69–83. Available from: https://doi.org/10.1016/j.colsurfa.2012.12.029.

[11] B.A. Bhanvase, S.H. Sonawane, New approach for simultaneous enhancement of anticorrosive and mechanical properties of coatings: application of water repellent nano $CaCO_3$–PANI emulsion nanocomposite in alkyd resin, Chem. Eng. J. 156 (1) (2010) 177–183. Available from: https://doi.org/10.1016/j.cej.2009.10.013.

[12] M. Nematollahi, M. Heidarian, M. Peikari, S.M. Kassiriha, N. Arianpouya, M. Esmaeilpour, Comparison between the effect of nanoglass flake and montmorillonite organoclay on corrosion performance of epoxy coating, Corros. Sci. 52 (5) (2010) 1809–1817. Available from: https://doi.org/10.1016/j.corsci.2010.01.024.

[13] M.R. Bagherzadeh, F. Mahdavi, Preparation of epoxy–clay nanocomposite and investigation on its anti-corrosive behavior in epoxy coating, Prog. Org. Coat. 60 (2) (2007) 117–120. Available from: https://doi.org/10.1016/j.porgcoat.2007.07.011.

[14] M. Behzadnasab, S.M. Mirabedini, M. Esfandeh, Corrosion protection of steel by epoxy nanocomposite coatings containing various combinations of clay and nanoparticulate zirconia, Corros. Sci. 75 (2013) 134–141. Available from: https://doi.org/10.1016/j.corsci.2013.05.024.

[15] C. Zhou, X. Lu, Z. Xin, J. Liu, Y. Zhang, Polybenzoxazine/$SiO_2$ nanocomposite coatings for corrosion protection of mild steel, Corros. Sci. 80 (2014) 269–275. Available from: https://doi.org/10.1016/j.corsci.2013.11.042.

[16] V. Mittal, Epoxy—vermiculite nanocomposites as gas permeation barrier, J. Composite Mater. 42 (26) (2008) 2829−2839. Available from: https://doi.org/10.1177/0021998308096954.
[17] O. Khayankarn, R. Magaraphan, J.W. Schwank, Adhesion and permeability of polyimide−clay nanocomposite films for protective coatings, J. Appl. Polym. Sci. 89 (11) (2003) 2875−2881. Available from: https://doi.org/10.1002/app.12326.
[18] M. Heidarian, M.R. Shishesaz, S.M. Kassiriha, M. Nematollahi, Characterization of structure and corrosion resistivity of polyurethane/organoclay nanocomposite coatings prepared through an ultrasonication assisted process, Prog. Org. Coat. 68 (3) (2010) 180−188. Available from: https://doi.org/10.1016/j.porgcoat.2010.02.006.
[19] A. Steele, I. Bayer, E. Loth, Adhesion strength and superhydrophobicity of polyurethane/organoclay nanocomposite coatings, J. Appl. Polym. Sci. 125 (S1) (2012) E445−E452. Available from: https://doi.org/10.1002/app.36312.
[20] A. Ghosal, O.U. Rahman, S. Ahmad, High-performance soya polyurethane networked silica hybrid nanocomposite coatings, Ind. Eng. Chem. Res. 54 (51) (2015) 12770−12787. Available from: https://doi.org/10.1021/acs.iecr.5b02098.
[21] S. Eigler, Graphene. An introduction to the fundamentals and industrial applications Edited by Madhuri Sharon and Maheshwar Sharon, Angew. Chem. Int. (Ed.) 55 (17) (2016). Available from: https://doi.org/10.1002/anie.201602067. 5122-5122.
[22] N.H. Othman, M. Che Ismail, M. Mustapha, N. Sallih, K.E. Kee, R. Ahmad Jaal, Graphene-based polymer nanocomposites as barrier coatings for corrosion protection, Prog. Org. Coat. 135 (2019) 82−99. Available from: https://doi.org/10.1016/j.porgcoat.2019.05.030.
[23] X. Lin, X. Shen, Q. Zheng, N. Yousefi, L. Ye, Y.-W. Mai, et al., Fabrication of highly-aligned, conductive, and strong graphene papers using ultralarge graphene oxide sheets, ACS Nano 6 (12) (2012) 10708−10719. Available from: https://doi.org/10.1021/nn303904z.
[24] X.-J. Shen, X.-Q. Pei, S.-Y. Fu, K. Friedrich, Significantly modified tribological performance of epoxy nanocomposites at very low graphene oxide content, Polymer 54 (3) (2013) 1234−1242. Available from: https://doi.org/10.1016/j.polymer.2012.12.064.
[25] J. Li, J. Cui, J. Yang, Y. Ma, H. Qiu, J. Yang, Silanized graphene oxide reinforced organofunctional silane composite coatings for corrosion protection, Prog. Org. Coat. 99 (2016) 443−451. Available from: https://doi.org/10.1016/j.porgcoat.2016.07.008.
[26] Z. Yu, H. Di, Y. Ma, Y. He, L. Liang, L. Lv, et al., Preparation of graphene oxide modified by titanium dioxide to enhance the anti-corrosion performance of epoxy coatings, Surf. Coat. Technol. 276 (2015) 471−478. Available from: https://doi.org/10.1016/j.surfcoat.2015.06.027.
[27] N.A. Siddiqui, M.-L. Sham, B.Z. Tang, A. Munir, J.-K. Kim, Tensile strength of glass fibres with carbon nanotube−epoxy nanocomposite coating, Compos. Part A Appl. Sci. Manuf. 40 (10) (2009) 1606−1614. Available from: https://doi.org/10.1016/j.compositesa.2009.07.005.
[28] R. Yuan, S. Wu, P. Yu, B. Wang, L. Mu, X. Zhang, et al., Superamphiphobic and electroactive nanocomposite toward self-cleaning, antiwear, and anticorrosion coatings, ACS Appl. Mater. Interfaces 8 (19) (2016) 12481−12493. Available from: https://doi.org/10.1021/acsami.6b03961.
[29] S. Pourhashem, M.R. Vaezi, A. Rashidi, M.R. Bagherzadeh, Exploring corrosion protection properties of solvent based epoxy-graphene oxide nanocomposite coatings on mild steel, Corros. Sci. 115 (2017) 78−92. Available from: https://doi.org/10.1016/j.corsci.2016.11.008.

[30] M.B. Kale, Z. Luo, X. Zhang, D. Dhamodharan, N. Divakaran, S. Mubarak, et al., Waterborne polyurethane/graphene oxide-silica nanocomposites with improved mechanical and thermal properties for leather coatings using screen printing, Polymer 170 (2019) 43–53. Available from: https://doi.org/10.1016/j.polymer.2019.02.055.
[31] U. Boro, N. Karak, Tannic acid based hyperbranched epoxy/reduced graphene oxide nanocomposites as surface coating materials, Prog. Org. Coat. 104 (2017) 180–187. Available from: https://doi.org/10.1016/j.porgcoat.2016.10.039.
[32] G. Zhu, X. Cui, Y. Zhang, S. Chen, M. Dong, H. Liu, et al., Poly (vinyl butyral)/graphene oxide/poly (methylhydrosiloxane) nanocomposite coating for improved aluminum alloy anticorrosion, Polymer 172 (2019) 415–422. Available from: https://doi.org/10.1016/j.polymer.2019.03.056.
[33] Y. Ahmadi, S. Ahmad, Surface-active antimicrobial and anticorrosive oleo-polyurethane/graphene oxide nanocomposite coatings: synergistic effects of in-situ polymerization and π-π interaction, Prog. Org. Coat. 127 (2019) 168–180. Available from: https://doi.org/10.1016/j.porgcoat.2018.11.019.
[34] S. Bhat, Y. Ahmadi, S. Ahmad, Recent advances in structural modifications of hyperbranched polymers and their applications, Ind. Eng. Chem. Res. 57 (32) (2018) 10754–10785. Available from: https://doi.org/10.1021/acs.iecr.8b01969.
[35] J.W. Hu, M.W. Li, M.Q. Zhang, D.S. Xiao, G.S. Cheng, M.Z. Rong, Preparation of binary conductive polymer composites with very low percolation threshold by latex blending, Macromol. Rapid Commun. 24 (15) (2003) 889–893. Available from: https://doi.org/10.1002/marc.200300014.
[36] G. Mittal, K.Y. Rhee, S.J. Park, D. Hui, Generation of the pores on graphene surface and their reinforcement effects on the thermal and mechanical properties of chitosan-based composites, Compos. Part B Eng. 114 (2017) 348–355. Available from: https://doi.org/10.1016/j.compositesb.2017.02.018.
[37] C.-H. Yang, F.-J. Liu, Y.-P. Liu, W.-T. Liao, Hybrids of colloidal silica and waterborne polyurethane, J. Colloid Interface Sci. 302 (1) (2006) 123–132. Available from: https://doi.org/10.1016/j.jcis.2006.06.001.
[38] Y. Ahmadi, M. Yadav, S. Ahmad, Oleo-polyurethane-carbon nanocomposites: effects of in-situ polymerization and sustainable precursor on structure, mechanical, thermal, and antimicrobial surface-activity, Compos. Part B Eng. 164 (2019) 683–692. Available from: https://doi.org/10.1016/j.compositesb.2019.01.078.
[39] C.A. Heck, J.H.Z. dos Santos, C.R. Wolf, Hybrid silicas/waterborne polyurethane composite properties: in situ formation vs. grafting methods, J. Sol-Gel Sci. Technol. 81 (2) (2017) 505–513. Available from: https://doi.org/10.1007/s10971-016-4220-z.
[40] L. Fogelström, P. Antoni, E. Malmström, A. Hult, UV-curable hyperbranched nanocomposite coatings, Prog. Org. Coat. 55 (3) (2006) 284–290. Available from: https://doi.org/10.1016/j.porgcoat.2005.12.003.
[41] P.P. Deshpande, N.G. Jadhav, V.J. Gelling, D. Sazou, Conducting polymers for corrosion protection: a review, J. Coat. Technol. Res. 11 (4) (2014) 473–494. Available from: https://doi.org/10.1007/s11998-014-9586-7.
[42] N.Y. Abu-Thabit, A.S.H. Makhlouf, Chapter 24 - recent advances in nanocomposite coatings for corrosion protection applications, in: A.S.H. Makhlouf, D. Scharnweber (Eds.), Handbook of Nanoceramic and Nanocomposite Coatings and Materials, Butterworth-Heinemann, 2015, pp. 515–549. https://doi.org/10.1016/B978-0-12-799947-0.00024-9.
[43] B. Wessling, Passivation of metals by coating with polyaniline: corrosion potential shift and morphological changes, Adv. Mater. 6 (3) (1994) 226–228. Available from: https://doi.org/10.1002/adma.19940060309.

[44] D.G. Shchukin, H. Möhwald, Self-repairing coatings containing active nanoreservoirs, Small 3 (6) (2007) 926–943. Available from: https://doi.org/10.1002/smll.200700064.
[45] D. Kowalski, M. Ueda, T. Ohtsuka, The effect of ultrasonic irradiation during electropolymerization of polypyrrole on corrosion prevention of the coated steel, Corros. Sci. 50 (1) (2008) 286–291. Available from: https://doi.org/10.1016/j.corsci.2007.05.027.
[46] H. Wei, D. Ding, S. Wei, Z. Guo, Anticorrosive conductive polyurethane multiwalled carbon nanotube nanocomposites, J. Mater. Chem. A 1 (36) (2013) 10805–10813. Available from: https://doi.org/10.1039/C3TA11966A.
[47] M. Huang, H. Zhang, J. Yang, Synthesis of organic silane microcapsules for self-healing corrosion resistant polymer coatings, Corros. Sci. 65 (2012) 561–566. Available from: https://doi.org/10.1016/j.corsci.2012.08.020.
[48] I.A. Kartsonakis, E.P. Koumoulos, A.C. Balaskas, G.S. Pappas, C.A. Charitidis, G.C. Kordas, Hybrid organic–inorganic multilayer coatings including nanocontainers for corrosion protection of metal alloys, Corros. Sci. 57 (2012) 56–66. Available from: https://doi.org/10.1016/j.corsci.2011.12.034.
[49] A. Karatzas, P. Bilalis, I.A. Kartsonakis, G.C. Kordas, Reversible spherical organic water microtraps, J. Non-Crystalline Solids 358 (2) (2012) 443–445. Available from: https://doi.org/10.1016/j.jnoncrysol.2011.10.010.
[50] Chapter 14 - An introduction to rheology, in: R. Lambourne, T.A. Strivens, T.A. Strivens (Eds.), Metals and Surface Engineering, 2nd ed., Woodhead Publishing, 1999, pp. 550–574. https://doi.org/10.1533/9781855737006.550.
[51] J.M. Lee, D.S. Kim, Effect of clay content on the ultraviolet-curing and physical properties of urethane-acrylate/clay nanocomposites, Polym. Compos. 28 (2007) 325–330. Available from: https://doi.org/10.1002/pc.20252.
[52] C.E. Corcione, M. Frigione, UV-cured polymer-boehmite nanocomposite as protective coating for wood elements, Prog. Org. Coat. 74 (4) (2012) 781–787. Available from: https://doi.org/10.1016/j.porgcoat.2011.06.024.
[53] S. Pramanik, P. Bharali, B.K. Konwar, N. Karak, Antimicrobial hyperbranched poly (ester amide)/polyaniline nanofiber modified montmorillonite nanocomposites, Mater. Sci. Eng. C. 35 (2014) 61–69. Available from: https://doi.org/10.1016/j.msec.2013.10.021.
[54] Y. Zhao, L. Shi, X. Ji, J. Li, Z. Han, S. Li, et al., Corrosion resistance and antibacterial properties of polysiloxane modified layer-by-layer assembled self-healing coating on magnesium alloy, J. Colloid Interface Sci. 526 (2018) 43–50. Available from: https://doi.org/10.1016/j.jcis.2018.04.071.
[55] A. Kinloch, Adhesion and Adhesives-Science and Technology, 1st ed., Springer, Netherlands, 1987. https://doi.org/10.1007/978-94-015-7764-9.
[56] I. Skeist (Ed.), Handbook of Adhesives, 3rd ed., Springer US, 1990. https://doi.org/10.1007/978-1-4613-0671-9.
[57] H. Dodiuk-Kenig, Y. Maoz, K. Lizenboim, I. Eppelbaum, B. Zalsman, S. Kenig, The effect of grafted caged silica (polyhedral oligomeric silesquioxanes) on the properties of dental composites and adhesives, Null 20 (12) (2006) 1401–1412. Available from: https://doi.org/10.1163/156856106778456609.
[58] L. Wang, X. Shui, X. Zheng, J. You, Y. Li, Investigations on the morphologies and properties of epoxy/acrylic rubber/nanoclay nanocomposites for adhesive films, Compos. Sci. Technol. 93 (2014) 46–53. Available from: https://doi.org/10.1016/j.compscitech.2013.12.023.
[59] Q. Meng, S. Han, S. Araby, Y. Zhao, Z. Liu, S. Lu, Mechanically robust, electrically and thermally conductive graphene-based epoxy adhesives, J. Adhes. Sci. Technol.

33 (12) (2019) 1337–1356. Available from: https://doi.org/10.1080/01694243.2019.1595890.

[60] A. Dorigato, A. Pegoretti, F. Bondioli, M. Messori, Improving epoxy adhesives with zirconia nanoparticles, Compos. Interfaces 17 (9) (2010) 873–892. Available from: https://doi.org/10.1163/092764410X539253.

[61] A. Buchman, H. Dodiuk-Kenig, A. Dotan, R. Tenne, S. Kenig, Toughening of epoxy adhesives by nanoparticles, J. Adhes. Sci. Technol. 23 (5) (2009) 753–768. Available from: https://doi.org/10.1163/156856108X379209.

[62] B.B. Johnsen, A.J. Kinloch, R.D. Mohammed, A.C. Taylor, S. Sprenger, Toughening mechanisms of nanoparticle-modified epoxy polymers, Polymer 48 (2) (2007) 530–541. Available from: https://doi.org/10.1016/j.polymer.2006.11.038.

[63] S. Bayat, O. Moini Jazani, P. Molla-Abbasi, M. Jouyandeh, M.R. Saeb, Thin films of epoxy adhesives containing recycled polymers and graphene oxide nanoflakes for metal/polymer composite interface, Prog. Org. Coat. 136 (2019) 105201. Available from: https://doi.org/10.1016/j.porgcoat.2019.06.047.

[64] P. Jojibabu, Y.X. Zhang, B.G. Prusty, A review of research advances in epoxy-based nanocomposites as adhesive materials, Int. J. Adhes. Adhes. 96 (2020) 102454. Available from: https://doi.org/10.1016/j.ijadhadh.2019.102454.

[65] X. Gong, H. Kang, Y. Liu, S. Wu, Decomposition mechanisms and kinetics of amine/anhydride-cured DGEBA epoxy resin in near-critical water, RSC Adv. 5 (50) (2015) 40269–40282. Available from: https://doi.org/10.1039/C5RA03828F.

[66] N. Kong, N.Z. Khalil, H. Fricke, Moisture absorption behavior and adhesion properties of GNP/epoxy nanocomposite adhesives, Polymers 13 (11) (2021) 1850. Available from: https://doi.org/10.3390/polym13111850.

[67] R. Aradhana, S. Mohanty, S.K. Nayak, Comparison of mechanical, electrical and thermal properties in graphene oxide and reduced graphene oxide filled epoxy nanocomposite adhesives, Polymer 141 (2018) 109–123. Available from: https://doi.org/10.1016/j.polymer.2018.03.005.

[68] R. Aradhana, S. Mohanty, S.K. Nayak, High performance epoxy nanocomposite adhesive: Effect of nanofillers on adhesive strength, curing and degradation kinetics, Int. J. Adhes. Adhes. 84 (2018) 238–249. Available from: https://doi.org/10.1016/j.ijadhadh.2018.03.013.

[69] A. Dorigato, A. Pegoretti, Development and thermo-mechanical behavior of nanocomposite epoxy adhesives, Polym. Adv. Technol. 23 (3) (2012) 660–668. Available from: https://doi.org/10.1002/pat.1942.

[70] F. Bauer, U. Decker, H. Ernst, M. Findeisen, H. Langguth, R. Mehnert, et al., Functionalized inorganic/organic nanocomposites as new basic raw materials for adhesives and sealants: part 2, Int. J. Adhes. Adhes. 26 (7) (2006) 567–570. Available from: https://doi.org/10.1016/j.ijadhadh.2005.11.001.

[71] M. Shneider, H. Dodiuk, S. Kenig, R. Tenne, The effect of tungsten sulfide fullerene-like nanoparticles on the toughness of epoxy adhesives, Null 24 (6) (2010) 1083–1095. Available from: https://doi.org/10.1163/016942409X12584625925268.

[72] C. Salom, M.G. Prolongo, A. Toribio, A.J. Martínez-Martínez, I.A. de Cárcer, S.G. Prolongo, Mechanical properties and adhesive behavior of epoxy-graphene nanocomposites, Int. J. Adhes. Adhes. 84 (2018) 119–125. Available from: https://doi.org/10.1016/j.ijadhadh.2017.12.004.

[73] Q. Meng, C.H. Wang, N. Saber, H.-C. Kuan, J. Dai, K. Friedrich, et al., Nanosilica-toughened polymer adhesives, Mater. Des. 61 (2014) 75–86. Available from: https://doi.org/10.1016/j.matdes.2014.04.042.

[74] A. Dorigato, A. Pegoretti, The role of alumina nanoparticles in epoxy adhesives, J. Nanopart. Res. 13 (6) (2011) 2429–2441. Available from: https://doi.org/10.1007/s11051-010-0130-0.
[75] S. Han, Q. Meng, S. Araby, T. Liu, M. Demiral, Mechanical and electrical properties of graphene and carbon nanotube reinforced epoxy adhesives: experimental and numerical analysis, Compos. Part A Appl. Sci. Manuf. 120 (2019) 116–126. Available from: https://doi.org/10.1016/j.compositesa.2019.02.027.
[76] M. Aliakbari, O.M. Jazani, M. Sohrabian, M. Jouyandeh, M.R. Saeb, Multi-nationality epoxy adhesives on trial for future nanocomposite developments, Prog. Org. Coat. 133 (2019) 376–386. Available from: https://doi.org/10.1016/j.porgcoat.2019.04.076.
[77] H.T. Jeon, M.K. Jang, B.K. Kim, K.H. Kim, Synthesis and characterizations of waterborne polyurethane–silica hybrids using sol–gel process, Colloids Surf. A Physicochem. Eng. Asp. 302 (1) (2007) 559–567. Available from: https://doi.org/10.1016/j.colsurfa.2007.03.043.
[78] K.-L. Noble, Waterborne polyurethanes, Prog. Org. Coat. 32 (1) (1997) 131–136. Available from: https://doi.org/10.1016/S0300-9440(97)00071-4.
[79] A. Noreen, K.M. Zia, M. Zuber, S. Tabasum, M.J. Saif, Recent trends in environmentally friendly water-borne polyurethane coatings: a review, Korean J. Chem. Eng. 33 (2) (2016) 388–400. Available from: https://doi.org/10.1007/s11814-015-0241-5.
[80] M.M. Rahman, H.-J. Yoo, C.J. Mi, H.-D. Kim, Synthesis and characterization of waterborne polyurethane/clay nanocomposite – effect on adhesive strength, Macromol. Symposia 249–250 (1) (2007) 251–258. Available from: https://doi.org/10.1002/masy.200750341.
[81] J.H. Huh, M.M. Rahman, H.-D. Kim, Properties of waterborne polyurethane/clay nanocomposite adhesives, J. Adhes. Sci. Technol. 23 (5) (2009) 739–751. Available from: https://doi.org/10.1163/156856108X379191.
[82] H. Fu, C. Yan, W. Zhou, H. Huang, Nano-$SiO_2$/fluorinated waterborne polyurethane nanocomposite adhesive for laminated films, J. Ind. Eng. Chem. 20 (4) (2014) 1623–1632. Available from: https://doi.org/10.1016/j.jiec.2013.08.009.
[83] S.M. Cakić, M.D. Valcic, I.S. Ristić, T. Radusin, M.J. Cvetinov, J. Budinski-Simendić, Waterborne polyurethane-silica nanocomposite adhesives based on castor oil-recycled polyols: Effects of (3-aminopropyl)triethoxysilane (APTES) content on properties, Int. J. Adhes. Adhes. 90 (2019) 22–31. Available from: https://doi.org/10.1016/j.ijadhadh.2019.01.005.
[84] M.M. Rahman, E.Y. Kim, K.T. Lim, W.-K. Lee, Morphology and properties of waterborne polyurethane/CNT nanocomposite adhesives with various carboxyl acid salt groups, J. Adhes. Sci. Technol. 23 (6) (2009) 839–850. Available from: https://doi.org/10.1163/156856109X411210.
[85] Radiation-cured coatings, in: A.A. Tracton (Ed.), Coatings Materials and Surface Coatings, 1st ed., CRC Press, 2006. https://doi.org/10.1201/9781420044058.
[86] A. Zosel, The effect of fibrilation on the tack of pressure sensitive adhesives, Int. J. Adhes. Adhes. 18 (4) (1998) 265–271. Available from: https://doi.org/10.1016/S0143-7496(98)80060-2.
[87] T. Wang, C.-H. Lei, A.B. Dalton, C. Creton, Y. Lin, K.A.S. Fernando, et al., Waterborne, nanocomposite pressure-sensitive adhesives with high tack energy, optical transparency, and electrical conductivity, Adv. Mater. 18 (20) (2006) 2730–2734. Available from: https://doi.org/10.1002/adma.200601335.
[88] J. Kajtna, U. Šebenik, Microsphere pressure sensitive adhesives—acrylic polymer/montmorillonite clay nanocomposite materials, Int. J. Adhes. Adhes. 29 (5) (2009) 543–550. Available from: https://doi.org/10.1016/j.ijadhadh.2009.01.001.

[89] J. Kajtna, U. Šebenik, M. Krajnc, Synthesis and dynamic mechanical analysis of nanocomposite UV crosslinkable 100% solid acrylic pressure sensitive adhesives, Int. J. Adhes. Adhes. 49 (2014) 18–25. Available from: https://doi.org/10.1016/j.ijadhadh. 2013.12.010.

[90] V. Daniloska, J.L. Keddie, J.M. Asua, R. Tomovska, $MoS_2$ nanoplatelet fillers for enhancement of the properties of waterborne pressure-sensitive adhesives, ACS Appl. Mater. Interfaces 6 (24) (2014) 22640–22648. Available from: https://doi.org/10.1021/am506726f.

[91] M. Khalina, M. Sanei, H.S. Mobarakeh, A.R. Mahdavian, Preparation of acrylic/silica nanocomposites latexes with potential application in pressure sensitive adhesive, Int. J. Adhes. Adhes. 58 (2015) 21–27. Available from: https://doi.org/10.1016/j.ijadhadh.2014.12.007.

[92] A. Ouzas, E. Niinivaara, E.D. Cranston, M.A. Dubé, In situ semibatch emulsion polymerization of 2-ethyl hexyl acrylate/n-butyl acrylate/methyl methacrylate/cellulose nanocrystal nanocomposites for adhesive applications, Macromol. React. Eng. 12 (3) (2018) 1700068. Available from: https://doi.org/10.1002/mren.201700068.

[93] S. Patel, A. Bandyopadhyay, A. Ganguly, A.K. Bhowmick, Synthesis and properties of nanocomposite adhesives, J. Adhes. Sci. Technol. 20 (4) (2006) 371–385. Available from: https://doi.org/10.1163/156856106776381794.

[94] P.K. Rana, P.K. Sahoo, Synthesis and pressure sensitive adhesive performance of poly (EHA-co-AA)/silicate nanocomposite used in transdermal drug delivery, J. Appl. Polym. Sci. 106 (6) (2007) 3915–3921. Available from: https://doi.org/10.1002/app.27034.

[95] S. Shaikh, A. Birdi, S. Qutubuddin, E. Lakatosh, H. Baskaran, Controlled release in transdermal pressure sensitive adhesives using organosilicate nanocomposites, Ann. Biomed. Eng. 35 (12) (2007) 2130–2137. Available from: https://doi.org/10.1007/s10439-007-9369-8.

[96] N. Baït, B. Grassl, C. Derail, A. Benaboura, Hydrogel nanocomposites as pressure-sensitive adhesives for skin-contact applications, Soft Matter 7 (5) (2011) 2025–2032. Available from: https://doi.org/10.1039/C0SM01123A.

[97] S. Skelton, M. Bostwick, K. O'Connor, S. Konst, S. Casey, B.P. Lee, Biomimetic adhesive containing nanocomposite hydrogel with enhanced materials properties, Soft Matter 9 (14) (2013) 3825–3833. Available from: https://doi.org/10.1039/C3SM27352K.

[98] M.C. Biswas, B. Jony, P.K. Nandy, R.A. Chowdhury, S. Halder, D. Kumar, et al., Recent advancement of biopolymers and their potential biomedical applications, J. Polym. Environ. (2021). Available from: https://doi.org/10.1007/s10924-021-02199-y.

[99] W.E. Hennink, C.F. van Nostrum, Novel crosslinking methods to design hydrogels, Adv. Drug Deliv. Rev. 54 (1) (2002) 13–36. Available from: https://doi.org/10.1016/S0169-409X(01)00240-X.

[100] M. Wang, D. Yuan, X. Fan, N.G. Sahoo, C. He, Polymer nanocomposite hydrogels exhibiting both dynamic restructuring and unusual adhesive properties, Langmuir 29 (23) (2013) 7087–7095. Available from: https://doi.org/10.1021/la401269p.

[101] N. Rajabi, M. Kharaziha, R. Emadi, A. Zarrabi, H. Mokhtari, S. Salehi, An adhesive and injectable nanocomposite hydrogel of thiolated gelatin/gelatin methacrylate/Laponite® as a potential surgical sealant, J. Colloid Interface Sci. 564 (2020) 155–169. Available from: https://doi.org/10.1016/j.jcis.2019.12.048.

[102] X. Yu, Z. Yong, H. Zhang, Y. Wang, X. Fan, T. Liu, Fast-recoverable, self-healable, and adhesive nanocomposite hydrogel consisting of hybrid nanoparticles for ultrasensitive strain and pressure sensing, Chem. Mater. 33 (15) (2021) 6146–6157. Available from: https://doi.org/10.1021/acs.chemmater.1c01595.

[103] B.P. Lee, P.B. Messersmith, J.N. Israelachvili, J.H. Waite, Mussel-inspired adhesives and coatings, Annu. Rev. Mater. Res. 1 (41) (2011) 99–132. Available from: https://doi.org/10.1146/annurev-matsci-062910-100429.

[104] C. Shao, M. Wang, L. Meng, H. Chang, B. Wang, F. Xu, et al., Mussel-inspired cellulose nanocomposite tough hydrogels with synergistic self-healing, adhesive, and strain-sensitive properties, Chem. Mater. 30 (9) (2018) 3110–3121. Available from: https://doi.org/10.1021/acs.chemmater.8b01172.

[105] C. Cui, C. Shao, L. Meng, J. Yang, High-strength, self-adhesive, and strain-sensitive chitosan/poly(acrylic acid) double-network nanocomposite hydrogels fabricated by salt-soaking strategy for flexible sensors, ACS Appl. Mater. Interfaces 11 (42) (2019) 39228–39237. Available from: https://doi.org/10.1021/acsami.9b15817.

[106] Y. Liu, H. Meng, S. Konst, R. Sarmiento, R. Rajachar, B.P. Lee, Injectable dopamine-modified poly(ethylene glycol) nanocomposite hydrogel with enhanced adhesive property and bioactivity, ACS Appl. Mater. Interfaces 6 (19) (2014) 16982–16992. Available from: https://doi.org/10.1021/am504566v.

[107] H. Zhang, L. Bré, T. Zhao, B. Newland, M. Da Costa, W. Wang, A biomimetic hyperbranched poly(amino ester)-based nanocomposite as a tunable bone adhesive for sternal closure, J. Mater. Chem. B 2 (26) (2014) 4067–4071. Available from: https://doi.org/10.1039/C4TB00155A.

[108] L. Han, X. Lu, K. Liu, K. Wang, L. Fang, L.-T. Weng, et al., Mussel-inspired adhesive and tough hydrogel based on nanoclay confined dopamine polymerization, ACS Nano 11 (3) (2017) 2561–2574. Available from: https://doi.org/10.1021/acsnano. 6b05318.

[109] M.J. Yim, Y. Li, K. Moon, K.W. Paik, C.P. Wong, Review of recent advances in electrically conductive adhesive materials and technologies in electronic packaging, J. Adhes. Sci. Technol. 22 (14) (2008) 1593–1630. Available from: https://doi.org/10.1163/156856108X320519.

[110] A. Santamaria, M.E. Muñoz, M. Fernández, M. Landa, Electrically conductive adhesives with a focus on adhesives that contain carbon nanotubes, J. Appl. Polym. Sci. 129 (4) (2013) 1643–1652. Available from: https://doi.org/10.1002/app.39137.

[111] J. Li, J.K. Lumpp, Electrical and mechanical characterization of carbon nanotube filled conductive adhesive, in: Proceedings of the 2006 IEEE Aerosp. Conf., 2006, p. 6. https://doi.org/10.1109/AERO.2006.1655965

[112] Y. Li, D. Lu, C.P. Wong, Y. Li, D. Lu, C.P. Wong, Isotropically conductive adhesives (ICAs), Springer US, 2010, pp. 121–225. https://doi.org/10.1007/978-0-387-88783-8_4.

[113] H.P. Wu, X.J. Wu, M.Y. Ge, G.Q. Zhang, Y.W. Wang, J.Z. Jiang, Effect analysis of filler sizes on percolation threshold of isotropical conductive adhesives, Compos. Sci. Technol. 67 (6) (2007) 1116–1120. Available from: https://doi.org/10.1016/j.compscitech.2006.05.017.

[114] P.-C. Ma, N.A. Siddiqui, G. Marom, J.-K. Kim, Dispersion and functionalization of carbon nanotubes for polymer-based nanocomposites: a review, Compos. Part A Appl. Sci. Manuf. 41 (10) (2010) 1345–1367. Available from: https://doi.org/10.1016/j.compositesa.2010.07.003.

[115] M. Hatami, Production and morphological characterization of low resistance polyimide/silver nanowire nanocomposites: potential application in nanoconductive adhesives, J. Mater. Sci. Mater. Electron. 28 (4) (2017) 3897–3908. Available from: https://doi.org/10.1007/s10854-016-6003-2.

[116] V. Anoop, S. Sankaraiah, N.L. Mary, Development of an optically transparent polysilsesquioxane/PDMS addition cured nanocomposite adhesive for electronic applications,

N. J. Chem. 43 (41) (2019) 16322–16330. Available from: https://doi.org/10.1039/C9NJ04092G.

[117] K.F. Amin, Asrafuzzaman, A. Sharif, M.E. Hoque, Bamboo/Bamboo Fiber Reinforced Concrete Composites and Their Applications in Modern Infrastructure, Springer, Singapore, 2021, pp. 271–297. Available from: https://doi.org/10.1007/978-981-15-8489-3_15.

[118] A. Abdal-hay, T. Amna, J.K. Lim, Biocorrosion and osteoconductivity of PCL/nHAp composite porous film-based coating of magnesium alloy, Solid State Sci. 18 (2013) 131–140. Available from: https://doi.org/10.1016/j.solidstatesciences.2012.11.017.

[119] Z. Zhao, L. Guo, L. Feng, H. Lu, Y. Xu, J. Wang, B. Xiang, X. Zou, Polydopamine functionalized graphene oxide nanocomposites reinforced the corrosion protection and adhesion properties of waterborne polyurethane coatings, European Polymer Journal 120 (109249) (2019). Available from: https://doi.org/10.1016/j.eurpolymj.2019.109249. In this issue.

[120] R.A. Farghali, A.M. Fekry, R.A. Ahmed, H.K.A. Elhakim, Corrosion resistance of Ti modified by chitosan–gold nanoparticles for orthopedic implantation, Int. J. Biol. Macromolecules 79 (2015) 787–799. Available from: https://doi.org/10.1016/j.ijbiomac.2015.04.078.

[121] B. Das, P. Chattopadhyay, A. Upadhyay, K. Gupta, M. Mandal, N. Karak, Biophysico-chemical interfacial attributes of $Fe_3O_4$ decorated MWCNT nanohybrid/bio-based hyperbranched polyurethane nanocomposite: an antibacterial wound healing material with controlled drug release potential, N. J. Chem. 38 (9) (2014) 4300–4311. Available from: https://doi.org/10.1039/C4NJ00732H.

[122] M. Atai, L. Solhi, A. Nodehi, S.M. Mirabedini, S. Kasraei, K. Akbari, et al., PMMA-grafted nanoclay as novel filler for dental adhesives, Dental Mater. 25 (3) (2009) 339–347. Available from: https://doi.org/10.1016/j.dental.2008.08.005.

[123] J.R. Potts, D.R. Dreyer, C.W. Bielawski, R.S. Ruoff, Graphene-based polymer nanocomposites, Polymer 52 (1) (2011) 5–25. Available from: https://doi.org/10.1016/j.polymer.2010.11.042.

[124] K. Shree Meenakshi, E. Pradeep Jaya Sudhan, S. Ananda Kumar, M.J. Umapathy, Development and characterization of novel DOPO based phosphorus tetraglycidyl epoxy nanocomposites for aerospace applications, Prog. Org. Coat. 72 (3) (2011) 402–409. Available from: https://doi.org/10.1016/j.porgcoat.2011.05.013.

[125] S. Barua, P. Chattopadhyay, M.M. Phukan, B.K. Konwar, J. Islam, N. Karak, Biocompatible hyperbranched epoxy/silver–reduced graphene oxide–curcumin nanocomposite as an advanced antimicrobial material, RSC Adv. 4 (88) (2014) 47797–47805. Available from: https://doi.org/10.1039/C4RA07802K.

[126] W.L. Tan, A. Salehabadi, M.H. Mohd Isa, M. Abu Bakar, N.H.H. Abu Bakar, Synthesis and physicochemical characterization of organomodified halloysite/epoxidized natural rubber nanocomposites: a potential flame-resistant adhesive, J. Mater. Sci. 51 (2) (2016) 1121–1132. Available from: https://doi.org/10.1007/s10853-015-9443-9.

[127] R.S. Gurney, D. Dupin, J.S. Nunes, K. Ouzineb, E. Siband, J.M. Asua, et al., Switching off the tackiness of a nanocomposite adhesive in 30s via infrared sintering, ACS Appl. Mater. Interfaces 4 (10) (2012) 5442–5452. Available from: https://doi.org/10.1021/am3013642.

# Polymer nanocomposites for automotive applications

11

*Muhammad Ifaz Shahriar Chowdhury*[1], *Yashdi Saif Autul*[1], *Sazedur Rahman*[2] *and Md Enamul Hoque*[3]
[1]Department of Mechanical Engineering, Military Institute of Science and Technology (MIST), Dhaka, Bangladesh
[2]Department of Mechanical and Production Engineering, Ahsanullah University of Science and Technology (AUST), Dhaka, Bangladesh
[3]Department of Biomedical Engineering, Military Institute of Science and Technology (MIST), Dhaka, Bangladesh

## 11.1 Introduction

The United Nation forecasts that by 2030, the fleet of global vehicles is expected to double as much as 850 million by now to almost 1.5 billion. Nanotechnology is a fascinating field of scientific research that promises cheaper, quicker, and lighter automotive in the future. Companies and research institutions throughout the world are thus concentrating on their research and innovation increasingly to modify the reliability, convenience, and environmental efficiency of the automotive to fulfill consumers' increasing demands [1].

In many applications, nanotechnology research has been done, including enhanced tires; grains; cleaner energy fuel cells; lightweight and more solid engine and body-based materials; improved catalysts; nonporous filters; environmentally friendly corrosion-resistant, scratch-resistant, and self-healing coatings; self-cleaning windshield wipers; and changing colors [2–4].

Nanocomposites are a significant technology of polymeric material with outstanding material characteristics, increased modules and impact resistance, heat resistance, increased resistance to scratches and sea, superior heating and processing characteristics, reduced component warping, and improved dimensional stability that makes these composites ideal to be utilized in automobile applications [5]. It is thought to have a profound influence on the mechanophysical characteristics of nanocomposites due to the interactions between nanoparticles and the polymer matrices at the molecular level.

The marketing of nanocomposite polymers was initiated in 1991 when Toyota Motor Co., together with Ube industries, brought nylon-6/clue nanocomposites to the marketplace as part of manufacturing their engine. At around the same time, Unitika co. of Japan had launched a 20% reduced weight and an outstanding surface finish in nylon-6 nanocomposite for engine cover for Mitsubishi's GDI engines produced by injection molding. In 2002, General Motors introduced a 3% nanoclay-reinforced

**Advanced Polymer Nanocomposites. DOI: https://doi.org/10.1016/B978-0-12-824492-0.00010-6**


step-assist autocomponent for Chevrolet Astro and GM's Safari vans, supplemented using similar nanocomposites at the doors of Chevrolet Impalas in partnership with LyondellBasell Industries.

Natural fiber composites not only acquire great interest due to their beneficial environmental impact but mostly because of their economic advantages [6]. The most recent progress has been in the design and implementation of nanocomposite polymers as electrodes and electrolytes for supercapacitors, polymer electric membrane cells, and secondary batteries [7]. Poly-L-lactic acid (PLA) nanocomposites were a great material by making progress in the field of nanotechnology. These materials provide great potential for food packaging, medicinal uses, and tissue cultivation applications [8].

Another potential hybrid nanocomposite material in the automobile industry is the hybrid multiscale reinforcement because of its improved cargo transfer at the matrix/reinforcement interface, that is, by adapting its interface shearing strength, consisting of microsized carbon fiber and carbon-nanostructured fabrics. Excellent characteristics like structural rigidity, thermal protection, shock, compressive strength, and many more are needed for high-performance racing vehicles and high-end automobiles. Materials with increased thermal insular features, higher load capacity, increased threshold loads, and impact loads might be a good choice for polymer nanocomposite (PNC) foams.

The different players in an automobile value chain must notice the research and innovation of PNCs that are expanding internationally, but a deficiency that must also be solved is the higher cost of decomposition technique. This chapter describes how nanocomposite in the automobile industry progresses, prospects of goods, and how benefits and limits are achieved.

## 11.2 Composite and nanocomposite

A composite material consists of a basic matrix and a reinforcement agent. The matrix acts as a binder for the reinforcing agents and determines the material's overall form and surface characteristics. The reinforcing ingredient improves and contributes to the composite's desirable characteristics, such as strength and high-temperature resistance.

One method to categorize composites is by the kind of matrix material they include. Based on the matrix material, they can be categorized as follows [9]:

1. Metal matrix composite: The matrix is metallic in nature. For example, matrix of Al, Mg, etc.
2. Ceramic matrix composite: Ceramic is used to make the composite matrix, for example, alumina matrix.
3. Polymer matrix composite: Matrix made out of polymers, such as an epoxy matrix.

Another method to categorize composites is by the kind of reinforcement that has been added. Generally, particles, knitted and braided fiber bundles (continuous fiber-laminated composites, short fibers), and woven composites (braided and

knitted fiber form) are used to reinforce the composite matrix [10]. If a composite material is reinforced with particles or fibers which have at least one external dimension, which is less than 100 nm, then the composite is called nanocomposites. Therefore nanocomposites are materials made up of nanosized particles suspended in a matrix of standard material that does not dissolve in one another [1]. Nanocomposite can be classified into three major types according to their microstructure [11]:

1. Nanoparticulate composites: a combination of nanoscale particles and a matrix.
2. Nanofilamentary composites: a combination of nanoscale-diameter filaments and a matrix.
3. Nanolayered composites: a combination of alternating layers having nanoscale dimension.

## 11.3 Nano-advantage

Nanocomposites have been extensively documented in the published research during the past decades to offer significant property improvements, even at small nanoparticle concentrations. The improved properties are applicable to a wide range of purposes, including electronics, cosmetics, construction, energy, automotive, semiconductors, packaging, and aerospace [12]. Some distinct benefits provided by nanocomposites are improved tensile strength and mechanical properties; enhanced impermeability to liquid, vapor, and gases; lighter weight as a result of low filler loading; noise dampening; better wear properties; higher heat distortion temperature; higher electrical conductivity; enhanced flame retardancy; higher optical properties, etc. The smaller and more disorganized architecture of nanofillers resulting in more active, higher surface-energy areas is the key reason for the enhanced properties. Because of these active regions, polymers have a greater mechanical/physiochemical connection [1]. Some commercial usage of nanocomposites is shown in Table 11.1 [13].

## 11.4 Polymer nanocomposite

A PNC is essentially a composite in which a polymer matrix (matrix produced from elastomers, thermosets, or thermoplastics) is combined with a nanomaterial. As a result, PNCs can be defined as polymers having different-shaped fillers with one dimension less than 100 nm. These nanofillers can be categorized according to their morphologies as spherical particles [three dimensional (3D)], layered materials like clay (two dimensional), and fibers and nanotubes (one dimensional) [14,15]. Nanoparticles include polyhedral oligomeric silsesquioxanes (POSS), silica nanoparticles, and carbon black (CB), while fibrous materials include carbon nanotubes (CNTs) and cellulose nanofibers [15]. Layered nanomaterials are nanofillers with a nanoscale thickness, a plate-like structure, and a high aspect ratio (30−1000), such

**Table 11.1** Commercial usage of nanocomposite.

| Polymer matrix | Nanoparticle | Property improvement | Application | Company and/or product trade name |
|---|---|---|---|---|
| Polyamide 6 thermoplastic polyolefin | Exfoliated clay | Stiffness | Timing belt cover: automotive | Toyota/Ube |
| | Exfoliated clay | Stiffness/ strength | Exterior step assist | General Motors |
| Polyamides nylon-6, 66, 12 | Exfoliated clay | Barrier | Autofuel systems | Ube |
| Unknown | Silver | Antimicrobial | Wound care/ bandage | Curad Imperm: Nanocor Pirelli |
| Various | Silica | Viscosity control, thixotropic agent | Various | |
| Natural rubber | Silver | Antimicrobial | Latex gloves | |
| SBR rubber | Not disclosed | Improved tire in winter | Winter tires | |
| Nylon MXD6, PP | Exfoliated clay | Barrier | Beverage containers, film | |
| Epoxy | Carbon nanotubes | Strength/ stiffness | Tennis rackets | Babolat |
| Various | MWCNT | Electrical conductivity | Electrostatic dissipation | Hyperion |
| SBR, natural rubber, polybutadiene | Carbon black (20−100 nm: primary particles) | Strength, wear, and abrasion | Tires | Various |
| Polyisobutylene | Exfoliated clay | Permeability barrier | Tennis balls, tires, soccer balls | InMat LLC |
| Epoxy | Carbon nanotubes | Strength/ stiffness | Hockey sticks | Montreal: Nitro Hybtonite |

*Notes*: Information from company web pages and industry journal reviews. *MWCNT*, Multiwalled carbon nanotube; *PP*, polypropylene; *SBR*, styrene−butadiene rubber.

as graphite or montmorillonite (MMT) [16]. The reinforcing material is chosen depending on the application.

For the preparation of PNCs, various methods have been devised, such as sol−gel process, in situ polymerization, template synthesis, direct blend of particulate matters and polymer, melt intercalation, in situ intercalative polymerization, and intercalation of the polymer [17]. Due to its outstanding mechanical features, including high strength and elastic stiffness with a lower percentage of nanofiller, PNCs have received more interest from both industry and academics [18]. PNCs reinforced with 2%−6% of nanoparticles through in situ polymerization or melt compounding method are more electrically conductive, heat resistant, flame retardant, dimensionally stable, lightweight, and have improved thermomechanical characteristics [1].

Polymer nanocomposites are hybrid organic−inorganics in which inorganic phases such as nanoclay, nano-ZnO, and nanosilica are dispersed at the nanoscale inside an organic polymer matrix. Nanofillers with a larger surface area have a more robust interfacial polymer−nanofiller interaction. This improves mechanical and other characteristics, with applications in chemical, optical, electrical fields [1].

## 11.5 Advantageous properties of PNC

Some significant properties of nanocomposites are shown in Fig. 11.1 [19].

### *11.5.1 Mechanical strength and toughness*

Even at pretty low dosage levels (5 wt.%), mechanical properties, particularly the strength of a pure polymer, improve considerably when appropriate nanoparticles are included. The more nanoparticles interact with the polymeric matrix, the more mechanical strength is gained [20]. Impact strength rises when the nanomaterial is loaded up to a specific level in most PNCs. The interaction of nanoparticles with polymer matrix enhances the hardness. The inclusion of appropriate nanoparticles in the polymer matrix improves overall mechanical characteristics considerably. It is worth noting that combining appropriately functionalized nanoparticles with appropriate polymer matrices may also improve elongation at breaks while simultaneously increasing strength, making the resulting PNC a highly strong material. In situ functionalized Reduced Graphene Oxide (RGO)/hyperbranched polyurethane (PU) nanocomposites, for instance, demonstrated exceptional toughness by improving both elongations at break and tensile strength [21].

### *11.5.2 Thermal stability*

Because nanoparticles function as thermal insulators, operate as a mass transport barrier for volatiles produced during the decomposition, and modify the course of their breakdown, the integration of numerous nanomaterials improves thermal

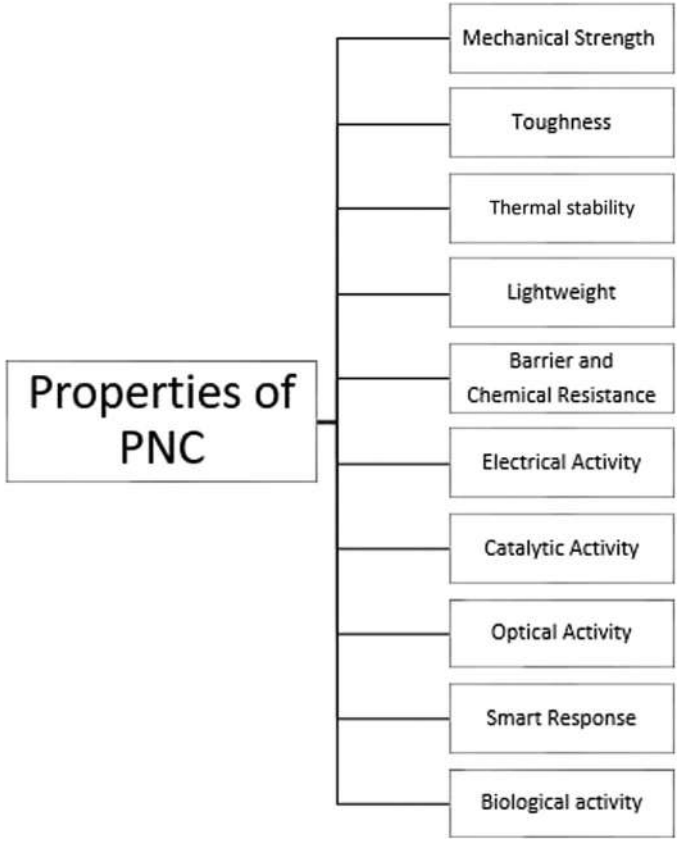


**Figure 11.1** Significant properties of PNC.

stability [22]. The limitation of polymeric chain mobility by stiff nanoparticles also raises the glass transition temperature ($T_g$). In addition, the creation of PNC may improve the total enthalpy of crystallization and crystalline melting temperature ($T_m$). Nanomaterials function as nucleating agents in these situations, promoting the crystallization of crystalline polymer matrices [19].

### *11.5.3 Chemical and barrier resistance*

The barrier properties and chemical resistance of pure polymers improve considerably when appropriate PNCs are formed. Because 2D nanomaterials' high aspect ratio significantly reduces gas permeability, the remarkable increase in barrier characteristics can be described using the zigzag or tortuous pathway concept. The tortuosity factor is calculated as the ratio of the actual distance that penetrants must travel to the shortest distance they would travel if barriers were not there. As diffusion becomes more complex, ions or chemical vapors created in various chemical settings have more difficulty interacting with PNCs, resulting in increased chemical resistance [19].

### 11.5.4 Electrical activity

With the exception of conducting polymers, most polymers function as insulators in their natural state, owing to their covalent composition and absence of ionic or electronic routes. PNCs with numerous conducting nanoparticles, on the other hand, have intriguing electrical characteristics. For example, adding 2% functionalized RGO to hyperbranched PU increased conductivity by $10^{10}$ times compared to pure PU [23].

### 11.5.5 Catalytic activity

Because of the increasing surface activity of nanomaterials, stability, and uniform dispersion in the polymer matrix, these catalysts with polymer support have been demonstrated to be more efficient than bare nanomaterials. Furthermore, "three-point anchoring" and cage effects allow the catalyst's access to the reactants due to the various functional groups and shape of the polymer. Similarly, photocatalytic effects in photoluminescence PNCs are shown to be more beneficial than bare nano-photocatalysts [19].

### 11.5.6 Optical activity

When nanocomposites are formed, the transparency of a transparent polymer is often preserved. PNCs can also show other intriguing optical characteristics, such as nonlinearity, luminescence, fluorescence, and so on, depending on the nanomaterials employed [19].

### 11.5.7 Smart response

Some PNCs also displayed unique and intelligent characteristics, such as stimulus-sensitive behaviors. The response characteristics of these polymeric materials were far better than those of pure systems. These intelligent behaviors are often bioinspired, making them suitable for complex applications. Some PNCs have smart features like self-cleaning, self-healing, and shape memory, to name a few [24].

### 11.5.8 Biological activity

By customizing the design and functionalization of PNCs, researchers have shown that they can achieve high biocompatibility. The most researched biocompatible materials include PU, polyamide, and polyester nanocomposites. While several metals and metal oxide nanoparticles were shown to be harmful to a variety of cell types when examined in vitro, those produced using a greener approach showed potential cell compatibility. Furthermore, following functionalization and integration of nanomaterials for instance, CNTs, graphene, and other materials into polymer matrices, their toxicity is significantly reduced. Furthermore, cell proliferation,

growth, and adhesion in PNCs have been proven to be advantageous for biocompatible materials [25].

## 11.6 Limitations of PNCs

Some of the limitations of PNCs are the following [26]:

1. Compatibility and uneven distribution problems.
2. Yields with high filler content and high viscosity.
3. Agglomeration and void formation.
4. Volume production consistency and dependability.
5. Nanoclays' oxidative and thermal instability.

## 11.7 Factors influencing the properties of polymer nanocomposites

PNCs' characteristics are impacted by a number of factors, including the following [27]:

1. Types of fillers and their orientation.
2. Nanofiller material's size and form.
3. At the matrix interface, the adhesion type.
4. Fabrication method for nanocomposites.
5. At the matrix interface, the characteristics of interphase evolved.
6. Characteristics of nanoparticles.
7. Nanoparticle's volume fraction.
8. The system's morphology.

The nanoparticles should be evenly distributed in the matrix material to achieve optimum properties. If nanoparticles are not dispersed and disseminated, they will clump together, which will degrade their characteristics. Nano-titanium oxide ($TiO_2$), nano-aluminum oxide ($Al_2O_3$), nanosilica (N-silica), single-walled CNTs (SWCNTs) and small-diameter nanotubes, CNTs (multiwalled CNTs [MWCNTs]), POSS, carbon nanofibers (CNFs), and MMT organoclays (OCs) are among the most commonly used nanoparticles. When the matrix/filler interface is well-bonded, the total characteristics of nanocomposites will be outstanding. Flame retardancy, thermal stability, fatigue, dielectric characteristics, shear strength, and corrosion resistance all benefit from good interface adhesion [27].

## 11.8 Types of nanoreinforcements

To understand the structure-property relationships of PNCs, the knowledge of the ratio of surface area to volume of nano-reinforcements plays an essential role.

At the nanoscale, material characteristics can be extremely size dependant, and the ratio of surface area and volume for nanoreinforcements is generally greater than threefold for micron-sized equivalents. As a result, as previously indicated, the nanoreinforcement's surface chemistry controls the characteristics of PNCs. Following types of nanoreinforcements may be distinguished [12].

1. Nanoparticles

   Micron-sized particles are commonly used as reinforcement in traditional polymer composites to enhance yield strength and elastic modulus. By reducing the size of these particle reinforcements to the nanoscale, on the other hand, can result in extraordinary new material characteristics. Gold nanoparticles, for example, are red, whereas silver nanoparticles (AgNPs) vary color based on form and size [28] as shown in Fig. 11.2.

2. Layered platelet materials

   For PNCs, layered platelet materials can be of three kinds. These are graphene, graphite, naturally occurring and synthetic clays—mica, MMT, saponite, etc.

   The unit and ratio of crystal types present in layered clay may be used to classify it. The following are the categories [1]:

   1. 1:1 type: consists of one silica tetrahedron crystal sheet coupled with one alumina tetrahedron crystal sheet, for example, illite, kaolinite, etc.
   2. 2:1 type: its unit crystal is made up of two silica tetrahedron crystal sheets and one alumina tetrahedron crystal sheet in the middle, for example, hectorite, bentonite, saponite, MMT, etc.
   3. 2:2 type: its constituent lamellar crystal is made up of four crystal sheets that alternately include silica tetrahedrons and alumina or magnesium octahedrons, for example, chlorite.

   Nanoclay nanocomposites have thermal stability, toughness, strength, and higher stiffness as well as decreased coefficient of thermal expansion and gas permeability [13]. The smectite group (2:1) clays, on the other hand, are the most often utilized

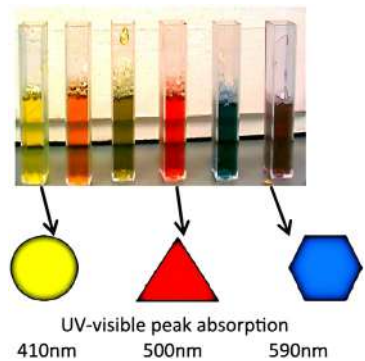


**Figure 11.2** Solutions with an average diameter of 50 nm silver nanoparticles; the colors of those nanoparticles vary based on their shapes, dictated by their circumstances of preparation.
*Source*: Reprinted with permission from G. Armstrong, An introduction to polymer nanocomposites, Eur. J. Phys. 36 (6) (2015) 063001 [12], Copyright 2015, IOP Science.

polymeric nanofillers. The most cost-effective nanomaterials are layered MMT clays made up of nanometer-thick platelets. A brief overview of MMT is given below:

**a.** Montmorillonite

MMT is the main constituent of bentonite mineral clay, which also includes minerals including zeolite, feldspar, mica, and quartz; depending on the source, bentonite is acquired via mining or quarrying. MMT is a phyllosilicate that belongs to the 2:1 group. $[(Na, Ca)_{0.33}(Al, Mg)_2(Si_4O_{10})(OH)_2\text{-}nH_2O]$ is the general formula of MMT. Two fused silica tetrahedral sheets sandwich an edge-shared octahedral alumina sheet to form one layer of MMT. When a certain crystal structure's atoms are substituted by atoms with differing valence electrons, this is called isomorphic replacement. Because of the large gap and flimsy binding between the layered sheets, MMT has the potential to absorb water between the charged layers, and it belongs to the smectites or smectite clays group of water-expandable clay minerals [1].

The layers of MMT are linked by a weak van der Waals force of attraction and organized in stacks with a space in between, which is commonly referred to as "interlayer" or "gallery spacing." The amount of negative charge produced by the isomorphic replacement of metal ions controls the characterization of the clay type, which is referred to as the cation exchange capacity (CEC) of the clay. The group I and II metal cations ($Ca^{++}$, $Na^{+}$, etc.) in their hydrated state balance this charge in natural MMT, which is why it is well-matched with hydrophilic polymers. However, dispersing this clay into a hydrophobic polymeric matrix is challenging. MMT may be organically changed to solve this issue by swapping inorganic cations like $K^{+}$, $Na^{+}$, and $Ca^{++}$ (which occur in the galleries of the silicate layer) with quaternary alkyl ammonium ions, resulting in improved silicate compatibility with the polymeric matrices [29–31].

Recently, graphene has gained a lot of attention as a potential nanomaterial. Graphene is made up of single sheets of graphite that have been exfoliated. These are comparable in thickness to exfoliated nanoclay, but they have much better characteristics than nanoclay platelets [12].

**3.** Nanotubes

CNTs, a key component of nanotechnology, have the potential to transform a number of areas in material science. CNTs, which are cylindrical carbon molecules, have become important components in high-strength composite materials, fuel cells and batteries, catalysts, optical devices, electrical devices, and sophisticated sensors because of their exceptional mechanical and electrical characteristics [32]. The percolation threshold of CNTs is considerably lower (i.e., a lower amount is needed for equivalent reinforcement). By incorporating a very tiny quantity of CNTs into the silica-filled material to produce electrical conductivity, it may be feasible to create a compound that has all the benefits of the "green" tire [33].

CNTs in their pristine form, single-walled CNTs (SWCNTs), are thought to have a unique set of characteristics that no other material can match, as shown in Table 11.2 [34].

Consider a piece of graphite, which is made up of layers of carbon atoms covalently linked in a honeycomb-shaped lattice, to see how CNTs, graphene, and graphite are connected. Imagine peeling a single layer of carbon atoms off a piece of pure graphite: this is a graphene sheet. Consider wrapping this graphene sheet into a tube—this is a CNT. It is referred to as an SWCNT since it only has one layer of graphene. A double-walled CNT is made by wrapping a second layer of graphene around it, while a MWCNT is made by wrapping three or more graphene sheets around each other. Fig. 11.3 shows the

**Table 11.2** Properties of SWCNTs.

| Property | SWCNT | Comparison value | Material |
|---|---|---|---|
| Thermal stability (°C) | 2800 (vacuum) 750 (air) | 600−1000 | Metal wires in microchips |
| Thermal conductivity at room temperature (W $m^{-1}$ $K^{-1}$) | 6000 | 3320 | Diamond |
| Electric current carrying capability (A $cm^{-2}$) | $1 \times 10^9$ | $1 \times 10^6$ | Copper wire |
| Tensile strength (MPa) | 2000 | 276−2000 | Steel |
| Elastic modulus (TPa) | 1.2 | 1.2 | Diamond |
| Density (g $cm^{-3}$) | 1.33−1.40 | 2.7 | Aluminum |

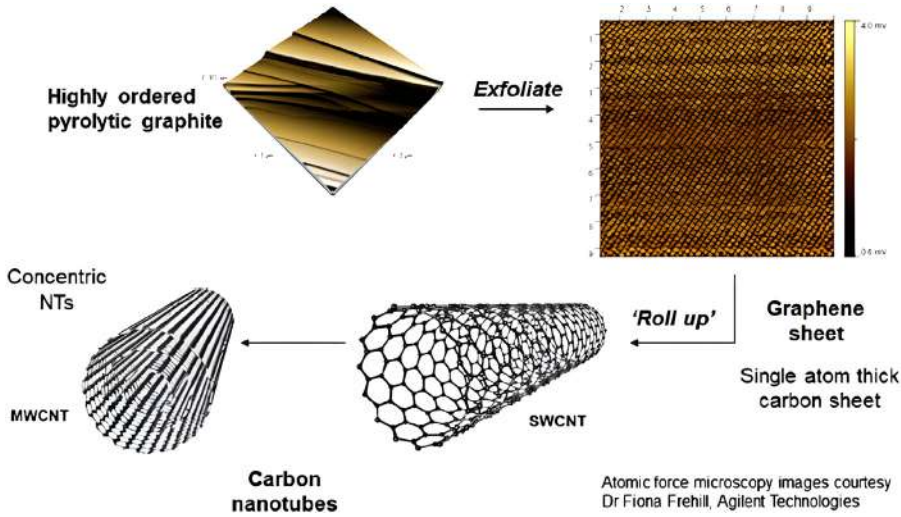


**Figure 11.3** The relationship between carbon nanotube, graphene, and graphite structures. *Source*: Reprinted with permission from G. Armstrong, An introduction to polymer nanocomposites, Eur. J. Phys. 36 (6) (2015) 063001 [12], Copyright 2015, IOP Science.

connection between these materials. Each graphene layer may be rolled up to create various atomic configurations, each of which gives the nanotube varied properties—metallic or semiconductor. CNTs, graphene, and graphite are not produced in this manner in reality. In fact, there are a variety of methods to create each of them, and each technique yields material of varying purity and properties [12].

4. Nanowires and nanofibers

Nanowires, like nanotubes, have diameters in the range of 10 nm, but length varies from microns to submillimeters. An archetypal CNF has a diameter greater than

a nanotube—diameters usually vary from 50 to 200 nm—and topologies that are diverse [35]. Various nanofiber morphologies result in different material characteristics, as we observed with CNTs. Many polymers, such as epoxy, acrylonitrile−butadiene−styrene (ABS), poly(phenylene sulfide), poly(ethylene terephthalate), poly(ether sulfone), nylon, polycarbonate (PC), and polypropylene (PP) have been reinforced with CNFs produced via vaporization. Many of the manufacturing, characterization, and modeling difficulties faced by CNF composites, for example, adhesion and dispersion, are comparable to those faced by nanoclay, nanoparticle, and nanotube-reinforced composites [12].

## 11.9 Most commonly used polymer matrices and nanoparticles

### 11.9.1 Polymer matrices [26]

1. Styrene−butadiene rubber (SBR)
2. Polyolefin
3. Polyamides (nylons)
4. Polyethylene terephthalate
5. PUs
6. Polyimides
7. Epoxy resins
8. Polystyrene
9. Ethylene-vinyl acetate copolymer
10. Conducting polymer.

### 11.9.2 Nanoparticles [26]

1. MMT OCs
2. Magnetic nanoparticles
3. Nano- $TiO_2$
4. Nano- $Al_2O_3$
5. POSS
6. Graphene
7. Nanosilica
8. CNTs
9. CNFs.

#### 11.9.2.1 Polyhedral oligomeric silsesquioxane

POSS has been utilized to make PNCs over the last decade. It stands out from other nanofillers such as CNFs, CNTs, and nanoclays because of its flexible chemistry, which allows for nearly unlimited chemical customization. Pendant-type, bead, or 3D network POSS-based PNCs may be produced depending on their functionality. These composites may be used to make goods with particular nanostructures for certain end-use applications.

## 11.10 Applications of PNC in automotive sector

PNCs are a novel kind of polymer with better thermal, mechanical, and processing characteristics, decreased warpage of components, and increased impact resistance, making them ideal for replacing metals in automotive applications. As a result, PNCs have the prospect of enhancing the quality of current technologies in areas including paints, catalytic converters, exhaust systems, transmissions, and engines [36]. Examples of successful nanocomposites with improved mechanical characteristics are shown in Fig. 11.4.

PNCs are widely used in the automobile sector because of their low cost and lightweight. The mechanical characteristics of PNCs are vital in vehicle design to fulfill some of the most urgent needs, such as reducing total vehicle weight [41]. The rationale is that decreasing vehicle weight improves fuel economy and reduces exhaust emissions, lowering pollution [42]. Several automakers have used PNCs to produce various parts of automobiles. Table 11.3 lists PNC-using automakers, models, and components [42,43].

### *11.10.1 Coatings*

Esthetic attractiveness and visual smoothness are vital to car purchasers. Not all paints have good adherence to a wide range of surfaces and are long-lasting. If the parts are constructed of PNCs that are electrically conductive, then electrostatic painting may be used instead of priming. This method improves paint consistency and control. Paint droplets are drawn to the back of the component during electrostatic painting. Controlling paint emission of volatile organic compounds lowers the environmental effect. This may save money and weight by replacing primer with PNC-enabled electrically conductive coatings on the outside of cars. Metal-free conductive PNCs are a possible cost-saving solution. Metal flakes, carbon fibers, and metal fibers are used in conjunction with a polymer matrix to create an electrically conductive network that serves as a Faraday cage [26].

With minimal coating, PNC coating may provide good shielding efficiency and electrical conductivity in high-volume manufacturing environments. PNC coating is a durable and cost-effective alternative to conventional paint processes. It also comes in brushed metal and chrome finishes. Aside from improved characteristics, PNC coatings save 10%−12% on costs by eliminating conventional painting.

#### *11.10.1.1 Clear coatings*

The inclusion of nanoparticles such as $TiO_2$, $ZrO_2$, $Al_2O_3$, and $SiO_2$ into a clear coat matrix has been discovered to improve scratch resistance substantially [44−47]. Ceramic nanoparticles have been shown to substantially enhance clear coat hardness and scratch resistance when used as hardening agents. Poor particle dispersion prevents easy improvement. They have no inherent affinity for the organic phase. These factors result in phase separation and aggregate formation. Clear coating features, particularly optical clarity, are degraded by aggregated

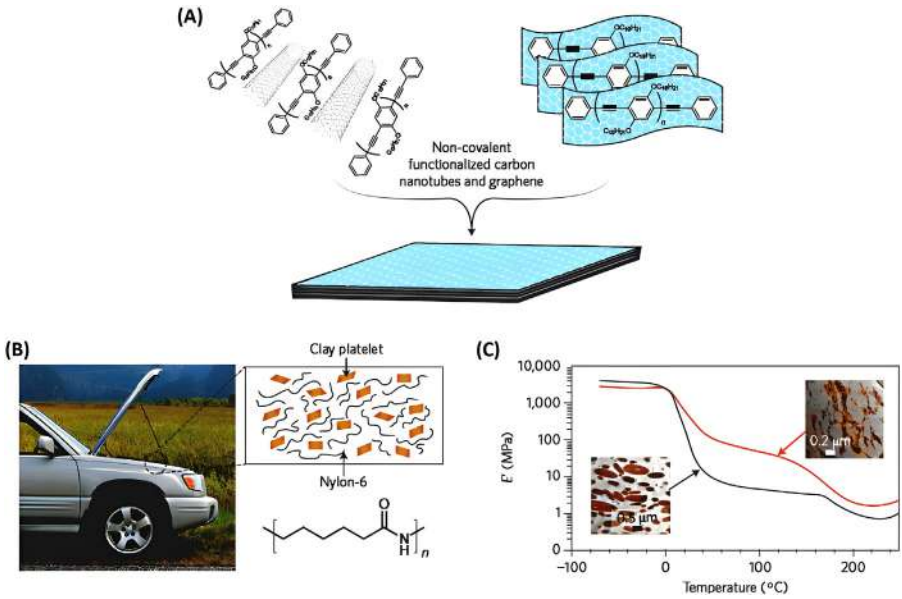


**Figure 11.4** Examples of successful nanocomposites with improved mechanical characteristics. (A) Carbon nanotubes or graphene platelets are dispersed in a hard conjugated polymer to create nanocomposites with structural properties of better toughness and high mechanical stiffness [37]. (B) Nylon-6 intercalated layered clay platelets are used in under-the-hood parts and engine covers in automobiles [38]. Car image: Noel Hendrickson/DigitalVision/Getty Images. (C) When compared to its discontinuous counterpart, a micrometer-scale agglomerated lignin phase, a co-continuous network of stiff biomacromolecules (lignin) in a nitrile rubber matrix exhibits a 10-fold upgrading in rubbery storage modulus (E). The discernible lignin network phase had lamellae with a thickness of 100 nm, revealing a strong yield point with yield stress as high as 40 MPa in tensile stress−strain curves. Without a clearly defined yield point and a low initial modulus, the discontinuous lignin agglomerates show elastomeric stress−strain behavior [39].
*Source*: Reprinted by permission from A.K. Naskar, J.K. Keum, R.G. Boeman, Polymer matrix nanocomposites for automotive structural components, Nat. Nanotechnol. 11 (12) (2016) 1026−1030 [40], Copyright 2016, Springer Nature Customer Service Centre GmbH.

particles ($>100$ nm). In order to make fillers more hydrophobic and therefore more dispersible in polymeric matrixes, surface modification using organosilanes has been attempted. As a consequence of surface alteration, particles and matrix may adhere more physically and chemically [47]. Specific nanofiller characteristics like surface modification, particle shape, size, and chemistry may influence scratch resistance. Nanoparticles have been shown to enhance clear coat characteristics. The hardness and elastic modulus of inorganic nanoparticles exceeds organic polymers. More hardness does not ensure scratch resistance in a clear coat. It is not all good news. The excessive force causes fracture-type scratches. As hardness

**Table 11.3** Automobile manufacturers and components made of polymer matrix composites.

| Automakers | Models | Components |
|---|---|---|
| Volkswagen | Passat Variant, Golf, Bora, | Boot-lid finish, panel boot liner, door panel, seatback |
| BMW | 3,5,7 series | Boot lining, seatback, door lining panel |
| Opel | Vectra, Zafira, Astra | Instrument panel, headliner panel, door panel |
| Fiat | Marea, Brava, Punto | Door panel, boot liner |
| Audi | A2, A3, A4, A6, A8 | Seatback, boot lining, hat rack, door panel, spare tire lining |
| Toyota | ES3, Brevis, Celsior, Raum | Door panel, floor mat, seatback, spare tire lining |
| Volvo | V70, C70 | Seat padding, natural foam |
| Mercedes-Benz | A, E, and S class | Roof cover, engine cover, windshield, dashboard, cover panel, door panel, seatback |
| Mitsubishi | Outlander and Eclipse cross | Door panel, cargo area floor, the instrument panel |
| Daimler Chrysler | A, C, E, and S class | Pillar cover panel, car windshield, dashboard, door panels |
| Peugeot | 406 | Parcel shelves, seatbacks, door panels (front and rear) |
| General Motors | Cadilac De Ville, Chevrolet, Trial Blazer | Cargo area floor mat, seatbacks |
| Ford | Mondeo CD 162, Focus | Floor trays door inserts, boot liner, door panels |
| Renault | Twingo and Clio | Rear parcel shelf |

*Note*: Various applications of PNCs in the field of automotive are discussed broadly in the following sections.

increases, so does brittleness, reducing other characteristics like as flexibility. To solve this issue, nanoparticles have been used to create a durable transparent layer. Recent study shows that nanoparticles may alter the clear coat's cross-linking density by influencing the curing process. Organosilane nanoparticles have functional groups capable of interacting with resin functional groups. Some chemical linkages between hardener (curing agent) and resin will be substituted by particle/resin or particle/hardener bonds. The transparent coat's cross-linking density decreases. Nanofillers, on the contrary, increase flexibility and hardness. Clear coat toughness is enhanced by these two effects when nanoparticles are present. A strong transparent coat resists abrasion and shows less breakage [45–48].

Clear coatings with nanofiller incorporated are more scratch and wear-resistant. The agglomeration of nanoparticles will affect the clear coat transparency. Obtaining suitable dispersion requires surface modification and several dispersing methods. The in situ synthesis of inorganic phases within an organic matrix utilizing the sol–gel method was explored [3,49,50]. Organic/inorganic precursors may

generate in situ silica networks. Adding these precursors to the main polymeric film-forming, either as network formers or as network modifiers, allows for the formation of hybrid nanocomposite films to be formed. This includes the hydrolysis of precursors as well as self-condensation. Hydrolyzed precursors may be cross-linked with the organic coating matrix utilizing polyol and other curing cross-links such as amino or isocyanate molecules, or they may be coated directly on the organic coating matrix. As shown in Fig. 11.5, this results in a hybrid nanocomposite that contains both organic and inorganic phases. The inorganic phase may help coatings resist mechanical damage, while the organic phase can help coatings adhere to surfaces and be more flexible [51].

Ahmadi et al. studied [53] the impact of nanolayers of silicates on the characteristics of a clear coat made of PU. Different weight percents of synthetic nanolayered silicates were distributed in a matrix of PU. The X-ray diffraction (XRD) findings revealed that the distance between the layers of the silicates increased partly, indicating that the nanocomposite is intercalated partially. Mar and scratch resistance testing revealed that nano-filled coating characteristics had improved significantly. Nobel et al. [54] used MMT, Boehmite, and Laponite particles to make

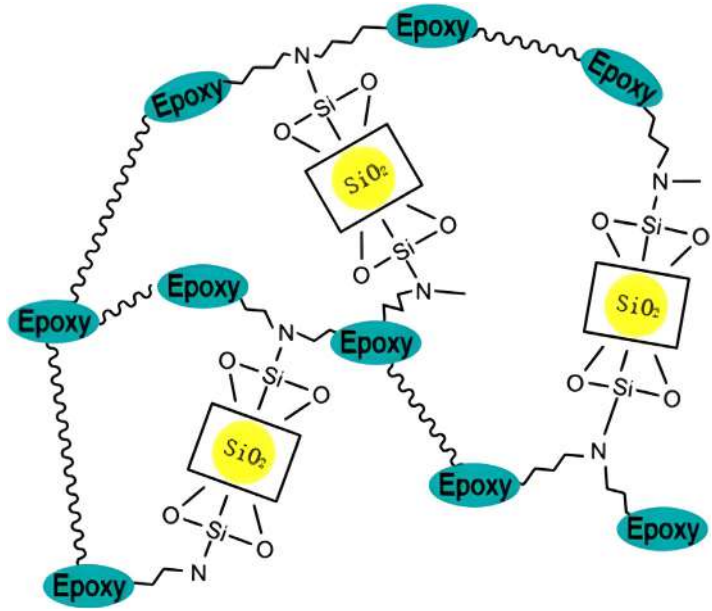


**Figure 11.5** Structure of organic/inorganic hybrid structure.
*Source*: Reprinted by permission from J. Jiao, P. Liu, L. Wang, Y. Cai, One-step synthesis of improved silica/epoxy nanocomposites with inorganic-organic hybrid network, J. Polym. Res. 20 (8) (2013), 202 [52] copyright 2013, Springer Nature Customer Service Centre GmbH.

acrylic PNC resins and films. Based on PNC liquid suspension versus cured film condition and added nanoparticle concentration, overall nanosized dispersion by a combination of transmission electron microscope (TEM) and XRD exhibits a heterogeneous morphology (zones of both intercalated and exfoliated nanostructures). The Halpin Tsai model predicts a degree of exfoliation that is consistent with experimental findings from TEM and wide angle x-ray scattering (WAXS) tests. Shielding nanoparticles with resin or organomodification surface coating is beneficial due to increased contact with the polymer matrix and decreased interactions between individual nanoparticles. Nobel et al. [54] and Verma et al. [55] investigated the physical and chemical interaction between the continuous polymeric matrix (PU coatings) and the dispersed nanofiller (OCs). Contact angle investigations, fourier transform infrared spectroscopy (FTIR)/attenuated total reflectance (ATR), and atomic force microscopy (AFM) offer visual and spectral evidence of such interactions. The chemical examination of these coatings confirmed the images of nanoplatelets of OC in hard segments of PU. Changing key bands like N−H, O−H, C−N, and C = O revealed the chemical interaction between PU functional groups and clay modifiers. The affinity is determined by two factors: (1) the quantity of OCs and (2) the kind of modifier employed to make the clay compatible with the PU formulation. These conclusions may assist material and polymer nanotechnologists design coating nanostructures, allowing them to control desired properties and applications better.

#### *11.10.1.2 Weather-resistant coatings*

The use of nanoparticles to polymeric coatings to enhance ultraviolet (UV) protection has received much interest. Nanoparticles such as silica, titanium oxide, cerium oxide, zinc oxide, and iron oxide have all been utilized. Nanoparticles, with a large surface area for absorbing UV radiation, protect coatings against deterioration. They are inorganic and nonmigratory as they are particles. So they are more effective and protect longer [1].

$TiO_2$ nanoparticles can protect the coating against UV radiation and degradation. However, these nanoparticles may generate extremely reactive free radicals, degrading the coating in which they are embedded. $TiO_2$ nanoparticles' photocatalytic activity must be regulated. Treatment of nanoparticles with silane agents, for example, decreases the photocatalytic activity of $TiO_2$ nanoparticles while providing obvious benefits such as simplicity, low price, and low processing temperatures. $TiO_2$ nanoparticles with aminopropyltrimethoxysilane surface modification decreased photocatalytic activity and increased weathering resilience of coating of PU [56]. Zinc oxide nanoparticles have been proven in different studies to be an excellent alternative for almost fully blocking UV radiation and protecting the coating [50,57]. Nano-ZnO particles were utilized to enhance the UV resistance of an aromatic PU-based automobile electrocoating. The findings demonstrated that the inclusion of nano-ZnO particles might reduce the film's photodegradation propensity and preserve it from deterioration [58].

#### 11.10.1.3 Self-healing nanocomposites for automotive coatings

Recently, there has been considerable interest in the study and development of self-healing anticorrosive coatings. It protects the material by immediately repairing any damage. The use of self-repairing materials is expected to spread quickly across all industries, including the automotive sector [59–67].

For multidimensional applications, smart high-performance materials are essential. In order to verify this hypothesis, aliphatic hyperbranched polyurethane nanocomposites (HPU/Si-GO) derived from bioresources were synthesized in situ utilizing different weight percents of 3 aminopropyltriethoxysilane-treated GO sheets (Si-GO). The addition of a very small quantity of Si-GO in the HPU matrix caused substantial increases in mechanical characteristics, including tensile strength, elongation at break, and toughness. Under microwave and sunshine irradiation, the nanocomposites showed efficient self-mending with high efficiency. Without any further surface treatment, the surface of the nanocomposite showed naturally hydrophobicity. As a result, the development of high-performance polymeric materials with intrinsic smart properties, including self-cleaning and self-healing materials, is beneficial for a variety of applications [68]. It has become more common in recent years to see graphene and its derivatives integrated into many types of polymeric materials. Because of the outstanding characteristics of graphene and graphene-based materials, graphene-filled polymeric materials are well suited for use in coatings, biological systems, conductive devices, and pharmaceuticals, among other applications [69]. Mendability is an essential factor in polymeric materials. As a result, research has been performed on the mendability efficacy of thermoplastic polyurethane (TPU) filled with graphene–CNTs and induced by microwave actions. The findings show that graphene/CNT synergy caused the creation of a combined structure of graphene/CNT. This graphene–CNTs combination has a synergistic impact on microwave-graphene–CNTs interface interaction and improves overall composite repair [70].

### 11.10.2 Tire

A tire is the most rubbery component of a vehicle. It is a toroidal high-performance composite having the qualities of a flexible membrane capable of holding pressurized gases while also bearing load, providing cushioning and traction. Modern tires are radial, with carcass cords running transversely from bead to bead. An inextensible restraining belt consisting of multiple layers is put above the carcass plies and beneath the tread to restrict radial expansion. The key components of a tire are shown in Fig. 11.6 [71].

The incorporation of clay mineral polymer nanocomposites (CPNs) into tire compounds aims to achieve the following qualities: (1) reduction in weight; (2) decrease in the dissipation of energy by the compounds; (3) increase in the balance of rolling resistance, wet traction, and wear—the so-called “magic triangle” of tire tread performances (as shown in Fig. 11.7); (4) reduction in heat build-up, resulting in fewer tire failures; (5) improvement in air retention; (6) improvement in colorability; and (7) improvement in electrical conductivity [71].

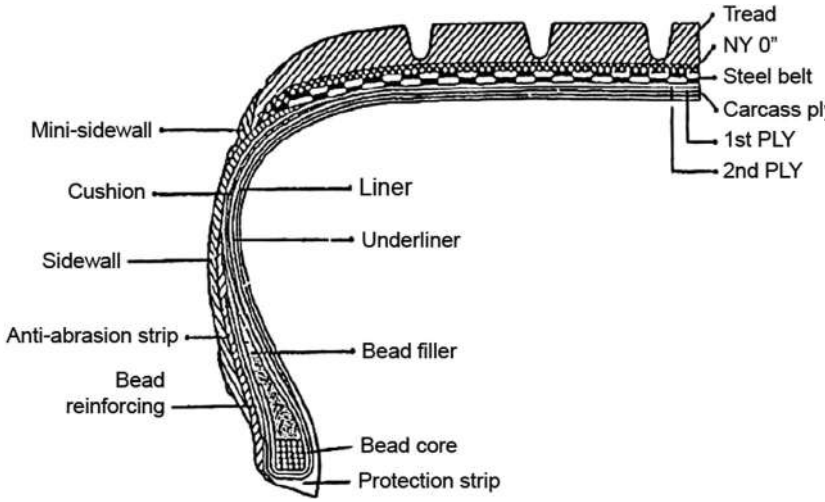


**Figure 11.6** Key components of tire.
*Source*: Reprinted from M. Galimberti, V.R. Cipolletti, M. Coombs (2013). Chapter 4.4—Applications of clay–polymer nanocomposites, in F. Bergaya, G. Lagaly (Eds.), Developments in Clay Science, vol. 5, Elsevier, 2013, pp. 539–586. https://doi.org/10.1016/B978-0-08-098259-5.00020-2 [71], with permission from Elsevier.

Low cost-to-performance, superior gas barrier property, outstanding antifatigue properties, improved flame-retardant property, increased traction, tread for lower rolling resistance, and increased flexibility with excellent tensile strength are some of the enhanced properties of polymer-layered silicate nanocomposites/clays that have sparked a tremendous amount of interest in the tire industry. Tire inner tubes, inner tire liners, off-the-road tire tread, and conveyer belts are all examples of PNC uses. Experts believe that there are eight distinct polymer kinds utilized in the tire business, although halogenated butyl rubber, isoprene rubber, butadiene rubber (BR), SBR, and natural rubber (NR) is the most widely used. Out of all of these polymers, SBR is the one that is most prevalent in tire manufacturing today [26]. Properties of some of these polymers are discussed below.

### *11.10.2.1 SBR/clay nanocomposite*

SBR/clay nanocomposites were created to achieve substantial nanoclay dispersion in a polymer matrix, which can be measured by XRD. It has been discovered that SBR may be strengthened in tension up to 40% by adding 10 parts nanofillers. It also enhances the compound's dynamic characteristics considerably. However, the impact of nanoclay on SBR is largely reliant on the concentration of nanoclay present, with up to 6 parts per hundred resin (phr) of nanoclay providing substantial mechanical and dynamical improvements. By incorporating CB with SBR, the impact of nanoclay may be substantially increased. It has been discovered that adding CB to an SBR/clay nanocomposite improves the mechanical characteristics

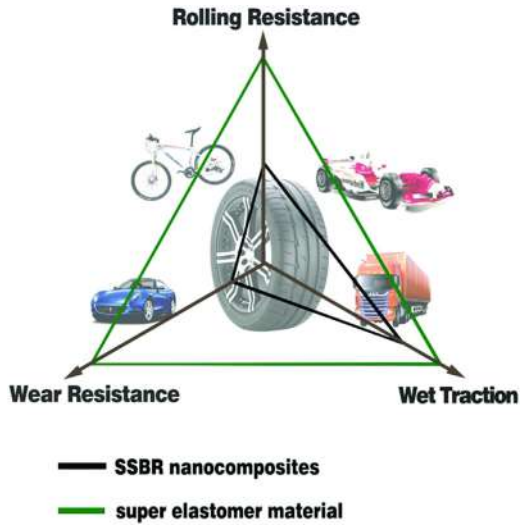


**Figure 11.7** Magic triangle of tire tread performance (comparison of performance of tire made of solution SBR nanocomposite and super elastomer material).
*Source*: Reprinted with permission from X. Qin, J. Wang, B. Han, B. Wang, L. Mao, L. Zhang, Novel design of eco-friendly super elastomer materials with optimized hard segments micro-structure: toward next-generation high-performance tires, Front. Chem. 6 (2018) 240 [72], an Open Access article distributed under the terms of the Creative Commons Attribution License.

dramatically. In passenger vehicle tread based on SBR/BR, nanoclay in conjunction with CB demonstrates a significant decrease in abrasion loss [1,73].

### *11.10.2.2 Epoxidized natural rubber/organoclay nanocomposite*

Epoxidized natural rubber (ENR) is rubber with characteristics of both natural and polar rubbers. To make nanocomposites, ENR (50%) was combined with nanoclay (10A, 15A, 20A) grades. Nanoclay is a lightweight alternative for polyamide (PA) + 30% glass beads that is as robust as PA filled with 7% glass and has a density of 1.14 g $cm^{-1}$. In a 3:1 ratio, nanoclay replaces conventional fillers [17]. Compared to traditional ENR compound, nanoclay reduces scorch time and increases maximum torque. ENR/clay nanocomposites exhibit greater storage modulus, indicating improved polymer−filler interaction and therefore superior physical characteristics.

At high temperatures, the composites' tan delta values were found to be substantially decreased, indicating that the ENR/clay nanocomposites had lower rolling resistance and improved fuel efficiency. As a result, ENR/OC nanocomposite may be utilized as a tread composition for high-performance tires in the future [74]. Temperature-dependent variation in storage modulus is shown in Fig. 11.8.

When it comes to the orientation of the particles of clay mineral, which is important in the construction of an inner tire liner, a number of factors are involved, including filler particle blockages, processing energy, and OC alkyl ammonium ion breakdown at high temperatures [76].

### 11.10.2.3 Butyl/clay nanocomposite

Butyl (IIR)/halobutyl (XIIR) has a well-known good air retention characteristic in the tire industry. These rubbers are widely utilized in tube-type tire inner tubes (IIR) and tubeless tire inner lines (XIIR). Other elastomers, for instance, PU, polysulfide rubber, and epichlorohydrin rubber are not utilized in tire manufacturing yet have excellent air retention characteristics (PU). There are other elastomers with modest air retention characteristics, such as ethylene/acrylate copolymers and nitrile rubber. The air retention characteristics of butyl as an elastomer and clay as a filler with a high aspect ratio may be enhanced by 50 times over those of a standard butyl combination. As a result of using this filler, the inner liner gauge or inner tube gauge may be lowered while maintaining the same level of service. Because CB is spherical, it has better air barrier characteristics than other fillers. This is because the flat form of the nanocomposite needle filler slows down the air movement [1].

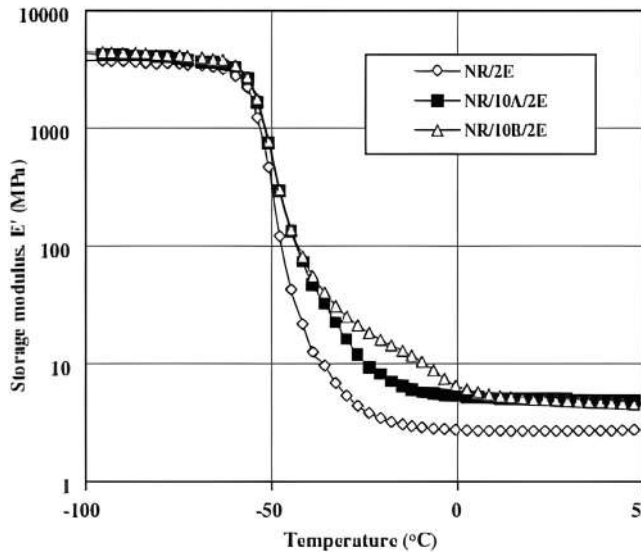


**Figure 11.8** Temperature-dependent variation in storage modulus.
*Source*: Reprinted from P.L. Teh, Z.A. Mohd Ishak, A.S. Hashim, J. Karger-Kocsis, U.S. Ishiaku, Effects of epoxidized natural rubber as a compatibilizer in melt compounded natural rubber–organoclay nanocomposites, Eur. Polym. J. 40 (11) (2004) 2513–2521 [75], with permission from Elsevier.

#### 11.10.2.4 Nanorubber

Drs Werner Obrecht and Lanxess worked together to make a number of patents on the manufacture and use of nanorubber. It is called nanorubber due to its chemical nanostructure and 40−65 nm rubber particles. High shear does not damage the nanorubber's particle morphology since it contains a cross-linked particle core. A strong cross-linking prevents accelerators, sulfur, and oil from being absorbed into the core. The $T_g$ is determined by the particle core's cross-link density and chemical composition. When dispersed in a conventional polymer matrix, they form a separate phase in the continuous phase of the polymer matrix, and as a result, they function just like filler. Nanorubber also has particle sizes similar to N550 and N660 CBs. Based on the observation that microgel at a high level and 70°C (158°F) in old SBR (E-SBR) emulsion and old polymerized BR emulsion gave high-rebound resilience to the resulting vulcanizates, which corresponds to low rolling resistance in tire treads, and low-rebound resilience at 23°C (73.4°F), ensuring high wet skid. While the microgel vulcanizates had excellent dynamic characteristics, they exhibited negative impacts on mechanical parameters, including wear resistance, tear resistance, and tensile strength [1].

### 11.10.3 Fuel cell and fuel tank

In recent years, increased government restrictions and environmental concerns have spurred research into fuel cell applications in cars. The following general fuel cell technologies are currently in development: polymer electrolyte fuel cells (PEFCs), phosphoric acid fuel cells, molten carbonate fuel cells, solid oxide fuel cells, alkaline fuel cells, and direct methanol fuel cells. However, due to its solid-state design, quick start-up features, and low operating temperature, PEFC development is getting significant attention in the automotive industry. PNCs that are electrically conductive may be utilized in PEFCs as bipolar plates, without the requirement for painting. Hyundai, Honda, Suzuki, Mitsubishi, Volkswagen, Peugeot, Fiat, GM, Ford, Renault, Nissan, Daimler Chrysler, and Toyota are among the world's major car manufacturers working on PEFCs [26].

Fuel cells of the present generation use catalysts based on platinum (Pt) for the fuel redox reaction process. These catalysts are nanoparticles of Pt-coated carbon that are extensively utilized in PEFCs nowadays (e.g., CB) [77]. Pt nanoparticle activity intensifies with the decrease in particle size down to −3 nm [78]. Gas-phase N-doping of CNTs resulted in a metal-free electrocatalyst, according to Dai's group [79]. Following that, many research showed excellent efficacy of N-doped carbon nanomaterials, including carbon quantum dots [80], mesoporous graphitic array (R [81]), graphene [82], and SWCNTs [83] as replacements for catalysts based on Pt [79,84,85]. Findings in Fe (or Co)/N/C systems and N-doped carbon nanomaterials may be integrated by utilizing graphene or CNTs as support in Fe (or Co)/N/C catalysts rather than CB. However, carbon nanoparticles seem to play a considerably larger role in next-generation fuel cell catalysts than they do in present

Pt/C commercial catalysts. The main problem would be the rational design of the nanostructure of the "upcoming catalyst" [1].

Although there is no longer any interest in fabricating solid-phase hydrogen reservoirs using CNTs, the discovery of the carbon-based thinnest materials, graphene, has reignited expectations for hydrogen storage tanks based on carbon [86–88]. In reality, since the hydrogen storage process in carbon nanostructures is based on physical absorption on the surface of graphene, hydrogen absorption is proportionate to the nanostructure's specific surface area with the greatest uptake occurring in graphene (2630 $m^2/g$) [87].

### 11.10.4 Battery and battery packaging

A "stretchy" polymer created by Stanford University and the US Department of Energy's SLAC National Accelerator Laboratory in Menlo Park, California, may pave the way for self-healing electrodes in future lithium-ion batteries. According to the researchers, a silicon electrode coated and bonded with the polymer repairs tiny fractures that occur during battery operation. Nanoparticles of carbon are mixed into the polymer to improve its electricity conduction ability. When ions flow into silicon electrodes during charging, they swell to three times their usual size, then shrink back to normal size when the ions are released during discharge. Because of the polymer coating, the electrodes saw a 10-fold increase in longevity, which "repaired any fractures in only a few hours," according to tests [89].

Yoo et al. [90] suggested a novel method for creating multifunctional hybrid nanocomposites by impregnating CB surfaces with nanosized MgO getter particles and then distributing the high-density polyethylene (HDPE) polymer matrix as shown in Fig. 11.9. For electric vehicle battery packaging, an effort was made to meet many criteria at the same time without causing trade-offs. This study also tested the characteristics of carbon-supported MgO polymer composites, including thermal conductivity, water-vapor transmission rate, and mechanical strength.

### 11.10.5 Mirror

Modern vehicle mirrors and headlights are made of high-quality glass and polymer components. Unique characteristics of nanotechnology are achieved. To do this, a tiny coating of aluminum oxide (less than 100 nm thick) is placed on the mirror surface or headlights. Thin coatings applied to mirrors may also make them more resistant to stains, grease, and moisture. Mirrors may be coated with nanometric oleophobic and hydrophobic layers using chemical vapor deposition. Fluoroorganic compounds may enhance surface hydrophobicity and oleophobicity at 5–10 nm thicknesses. The nanoscale layer may also create a surface smooth enough to wipe of waterdrops, dirt, grease, and fingerprints. This ultrathin coating is resistant to friction and may be used for extended periods. As shown in Fig. 11.10, the layer may be chemically attached to the mirror surface from the anchor group side. In the opposite direction, a hydrophobic surface is formed.

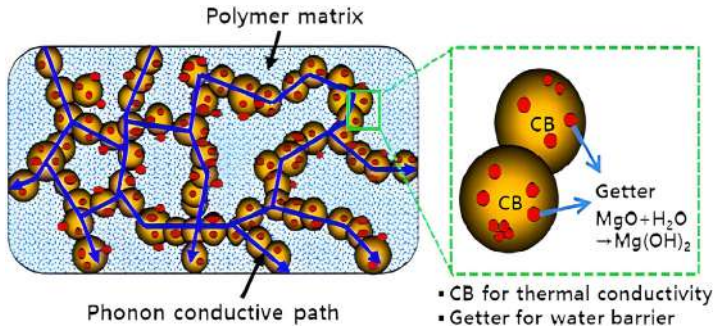


**Figure 11.9** Diagrams depicting a straightforward and practical method for fabricating multifunctional getter-impregnated CB polymer nanocomposites.
*Source*: Reprinted with permission from J.E. Yoo, V. Roev, J. Bae, D.-S. Yoon, S.-D. Kim, E.-S. Lee, Multifunctional hybrid polymer nanocomposites for automotive-battery packaging, J. Appl. Polym. Sci. 137 (36) (2020) 49059 [90], Copyright (2020) John Wiley and Sons.

Today's safety requirements for vehicle drivers have led to the development of rearview mirrors that provide an adequate vision at dusk and dawn. This may be accomplished by incorporating functional layer composites having electrochromic (EC) characteristics into glasses. When the intermediate layer, which transfers charges, is provided with a voltage, the glasses using this technology will have an alteration in their optical characteristics. Color centers generated by ions at the electrodes will absorb the incoming light. As a consequence, just a tiny amount of light is reflected. As the pole shifts, the glass may return to its previous characteristics, similar to how a vehicle battery charges and discharges. This glass, which was fitted with a rear sensor, could detect and regulate the glare from approaching cars. The mirror returns to its natural form as soon as the blazing light fades away [1].

### 11.10.6 Glasses

PC is a popular glass polymer because of its excellent toughness, impact strength, and lightweight. PCs have previously been utilized in the manufacture of light covers and lenses. PC, on the other hand, has poor scratch/abrasion and chemical resistance, as well as a propensity to yellow when exposed to UV radiation over an extended period of time. Glass is a tough substance that resists scratches well. When compared to polymeric glasses, it is heavier and has a lesser impact strength. Scratching PC glass components is caused by washing (both automated vehicle washes and manual washes) and sand/dust particles in the air. This may result in a substantial decrease in the transparency of the headlights and, as a consequence, light scattering. Attempts to address the issue have been made. For this aim, two approaches have been considered. One approach is to use nanoparticles embedded in PC polymeric glass parts and/or polysiloxane or acrylate paints over the headlight to create PC polymeric glass parts. In another approach, nanoparticles of aluminum oxide are also utilized in the coating's configuration to make it scratch and

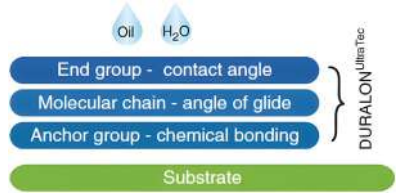


**Figure 11.10** Modern mirrors' ultrareflective layer composition.
*Source*: Reprinted with permission from M. Mohseni, B. Ramezanzadeh, H. Yari, M. Moazzami, M., The role of nanotechnology in automotive industries, in: J. Carmo (Ed.), New Advances in Vehicular Technology and Automotive Engineering, InTech, 2012. https://doi.org/10.5772/49939 [91], an Open Access article distributed under the terms of the Creative Commons Attribution License.

abrasion-resistant. Since the filler particles are so small, and because of their excellent dispersion, this coating has a high degree of transparency. The nano-embedded coating applied to PC has a thickness of around 1 mm on average. The UV stability of polycarbonate plastic glazing, antifogging, easy-to-clean, and antiscratch is achieved via the application of various nanocoating layers. Nanoparticles, for instance, $Al_2O_3$, $SiO_2$, and $TiO_2$ are utilized for $TiO_2$ for easy-to-clean characteristics, sol−gel-based TiO for antifogging behavior, UV protection, and abrasion resistance [92].

Using polymer and dichromic technologies, smart glasses can automatically regulate the transmission of solar radiation, improving the safety and comfort of passengers. EC smart glasses are among the most significant. In the presence of a voltage differential, nanotech EC materials change their optical properties (lightness/darkness). They may be used in displays, sunroofs, antiglare rearview mirrors, and energy-efficient windows [1].

### 11.10.7 Lightweight purpose

The automobile sector requires plastic parts with high dimensional precision and low weight, which pushes research into nonconventional manufacturing methods. The creation of lightweight automotive components is critical for increasing vehicle performance. By combining polymers with CNTs, glass fibers, and carbon fibers, polymer composites have been extensively used to decrease weight and enhance mechanical characteristics. To achieve even more weight reduction and water resistance, PP has been integrated into the carbon-fiber-reinforced nylon-6 (CF/PA6) composite. The inclusion of PP, on the other hand, decreased the mechanical characteristics. To compensate for the reduced mechanical characteristics caused by the addition of PP, MWCNTs were used by Nguyen-Tran et al. [93]. To assess the mechanical characteristics, tensile and bending tests were performed. CF/PA6/PP composites with a modest quantity of CNTs have better mechanical characteristics. The density of CF/PA6 was decreased from 1.214 to 1.131 g $cm^{-3}$ (6.8%) by adding 30 wt.% PP, and the tensile strength of the 30 wt.% PP composite was increased

from 168 to 173 MPa (3.0%) by adding 0.5 wt.% CNTs with a slight increase in density (1.135 g $cm^{-3}$) by adding 0.5 wt.% CNTs. The composite that has been created will be extensively utilized for lightweight automobile components with enhanced mechanical characteristics.

The influence of matrix materials, filler size, and filler type on the emission of particles during a low-velocity impact test was investigated by Sachse and the team using micro- and nanoreinforced glass fiber−polymer composites [94]. Extrusion in two stages, followed by final injection molding of the structures, yielded nano- and microsilica, as well as nanoclay-reinforced crash cones. The inclusion of secondary filler to glass-fiber-reinforced polymer composites has a substantial impact on both the material's mechanical behavior and particle emission.

Another study used glass-fiber-reinforced polyamide 66 (PA66), which has outstanding characteristics but is restricted in use due to its expensive cost. This study investigated the use of microcellular injection molding to decrease component costs while retaining material characteristics. The effect of processing factors on the performance and morphology of PA66 + 30% glass-fiber-foamed components was studied. An analysis of variance (ANOVA) was used to discover important variables influencing the shape of molded components. According to ANOVA, a 300°C injection temperature, a big part thickness, and a high gas injection pressure are required for homogeneous foamed components with excellent mechanical characteristics [95].

### 11.10.8 Gears

A few test rigs for PNC gears were constructed by Yousef et al. [96]. Yousef inspected the wear behavior of gears made of PNC with the help of the TS universal test rig [96,97]. The wear resistance of the CNT/acetal worm, bevel, helical, and spur gears increased by 47%, 44%, 35%, and 28%, respectively, according to the findings. The experimental parameters of PNC gear tests, such as the kind of test rig utilized in performing the test, PNC gear materials, and major findings, are listed in Table 11.4.

The heat produced by cumulative meshing in metallic gears may be dissipated in two ways: (1) by convection from the gear to the environment and (2) by conduction via the gear material. Because thermal conductivity is a determining factor in the conduction of heat transfer, and thermal conductivity of polymeric materials is very low, all heat generated is focused in the contact meshing area, causing higher wear rates. Adding nanofiller elements like CNT and graphene to polymeric polymers increased their heat conductivity, according to many studies. A further advantage of this component is that it can be tested with the TS universal test equipment, which provides an ideal setup for assessing thermal behavior in PNC gears, especially tooth surface temperatures [100].

During operation, the gearbox and other components often generate noise. Polymeric materials can reduce noise and can replace metallic materials to reduce acoustic emissions. According to Yousef et al. [96], adding nanomaterials may boost strength.

**Table 11.4** Gear materials, features, test settings and conditions, and tribological parameters of PNC.

| Gear material | Properties | Test rig | Test conditions | Results | Reference |
|---|---|---|---|---|---|
| CNT/POM (Polyoxymethylene) | Wear | TS universal test rig | No. of cycles = $200 \times 10^3$, speed = 1420 rpm, torque = 4 Nm | Improved percentage of average wear resistance of gears (CNT/acetal), worm = 47%, bevel = 44%, helical = 35%, spur = 28% | [97] |
| CNT/POM (Polyoxymethylene) | Wear | Simple test rig | No. of cycles = $200 \times 10^3$, speed = 1420 rpm, torque = 4 Nm | Improved percentage of average wear resistance of spur gear (CNT/acetal) with addition of 15 wt.% of CNT | [96] |
| Nanosize clay/PA | Transmission efficiency | Power absorption type | No. of cycles = $10^7$, speed = 1200 rpm, torque = 1.5, 2, 2.5 Nm | Improved power transmission efficiency of gears | [98] |
| Nanoclay/PA | Wear | Power absorption | No. of cycles = $9 \times 10^3$, speed = 800 rpm, torque = 1.5, 2, 2.5 Nm | Reduction in wear, heat generation and friction; increase in life | [99] |

### 11.10.9 Rear floor

Moulded Fiber Glass Companies (MFG, Ashtabula, Ohio) developed Nano-fill sheet Moulding Compound (SMC), a one-piece compression-molded nanocomposite for use in rear-floor applications in 2009. A density of about 1.5 g $cm^{-3}$ was obtained by mixing OC with a thermoset resin. The density was considerably lower than that of typical microsphere-filled SMC and resulted in increased fuel economy. General Motors used the composite material in the Pontiac Solace, as well as the Corvette ZO6 and Chevrolet Corvette Coupe [71].

### 11.10.10 Seatbacks

The structural seatbacks of the Honda Acura TL 2004 vehicle were manufactured using Noble Polymers' Forte PP nanocomposite, which replaced glass-filled PP and avoided issues including processing difficulties, esthetic flaws, and warping. CPN had a reduced density of 0.928 g $cm^{-3}$, better mechanical characteristics, and was recyclable. Honda Acura has produced clay mineral PP nanocomposites for structural seatbacks more recently [71].

### 11.10.11 Timing belt cover

A timing belt is an internal combustion engine component that controls the valve timing. Toyota and Ube collaborated in the early 1990s to create the first commercial CPN in automotive applications for Toyota Camry vehicles [101]. Exfoliated Mt was treated with *o*-trimethylammonium undecanoic acid to make the CPN. Only 4.2 mass% Mt caused a substantial increase in mechanical characteristics. The strength was raised by more than 50%, while the modulus was enhanced by a factor of 2. When compared to the virgin polymer, the heat distortion temperature was raised by 80°C [102]. The CPN was five times more resistant to gasoline penetration than the unloaded PA, according to Ube, with just 2% OC. Coextrusion of a multilayer nanocomposite composed of PA12/adhesive/PA6/66 nanocomposites based on PA6 was created as a product line with the Ecobesta brand name. The multilayer structure was claimed to provide cost savings, barrier properties, recyclability, adhesive properties, and high-speed extrusion [103].

### 11.10.12 Engine cover

The portion of a vehicle that provides access to the engine is known as an engine cover, sometimes known as a hood (in the United States) or a bonnet (in the United Kingdom). For the Mitsubishi GDI engine cover, Unitika Co. used Nylon-6 nanocomposites. This occurred about the same time as Toyota introduced CPN [103]. A 20% mass decrease in the CPN was achieved via injection molding, and the surface quality was reported to be excellent.

### 11.10.13 Miscellaneous

According to a study, Ethylene Propylene Diene monomer rubber (EPDM) and PP were used to make thermoplastic vulcanizates (TPVs) and thermoplastic vulcanizate nanocomposites (TPVNs). New-generation ultrahigh molecular weight EPDM (UHMW-EPDM) and nano-(nanosilica and nanoclay) filled PP have been thoroughly researched and described for applications in the automotive industry. This unique kind of UHM-EPDM-based TPV outperforms standard EPDM-based TPVs in terms of physicomechanical characteristics, and in the presence of nanofillers, they outperform them even more. The UHMW-EPDM/PP TPVNs may be utilized in a variety of automobile applications, including side panels, window seals, air bag covers, cooling air guides, roof trim, and dashboards [104].

Another study investigated the mechanical strength of polymer-based bumper beams reinforced with natural fiber. These materials were tested for tensile (strength and modulus), flexural (strength and modulus), and impact characteristics. The study showed that natural fiber could not provide the mechanical characteristics required in the automobile sector (as a bumper beam material). Despite its small weight, it has a low environmental impact due to its eco-friendliness, biodegradability, and carbon neutrality. The combination of natural (treated or untreated) and synthetic fibers improves the mechanical characteristics of the polymer composite compared to utilizing natural fiber alone as reinforcement. But it does not address the issue of insufficient impact attributes. Future studies should continue to optimize key factors for improved mechanical performance [105].

To replace an existing monoleaf metal leaf spring in a light commercial vehicle, composite-based monoleaf spring systems were developed and produced by Oztoprak et al. [106]. This research revealed that hybrid composite systems may be used to make composite-based leaf springs that have good mechanical performance. The findings showed that the kind and direction of the reinforcement had an important influence on the spring rate. With enhanced mechanical characteristics, the prototypes exhibited a substantial weight reduction of approximately 80%.

### 11.10.14 Green nanocomposite

In response to the demand for renewable, eco-friendly materials with better characteristics, researchers and industries have focused on natural filler composites (natural fibers, nanocrystalline cellulose, and nanofibrillated cellulose). Eco-friendly or green materials have been proposed as next-invention competitors for low-cost, lightweight, long-lasting, eco-friendly, and high-efficiency nanocomposites [107]. To create sustainable materials, several organic and manufactured green nanofillers and green polymers have been used. Natural fibers such as sisal (scientifically known as *Agave sisalana*), coconut (scientifically known as *Cocos nucifera*), jute (scientifically known as *Corchorus capsularis*), and curaua (scientifically known as *Ananas erectifolius*) have been utilized extensively in composite creation. Natural fibers also have been extensively used to produce cellulose nanofibrillated cellulose and nanocrystals, which are the crystalline parts of the cellulose. The natural fillers

have also been extensively utilized in a variety of polymer matrices, with noticeable enhancements in their mechanical and thermal characteristics [108].

### 11.10.14.1 Green composites in automotive sector

In various sectors, including the automobile industry [107,108], polymer composites strengthened with natural fillers have also been utilized to substitute widely used substances. The incorporation of natural fillers into polymer matrices is appealing for this sector for a variety of technical and environmental reasons. The tensile strength of the fibers, as well as their biodegradability, have prompted the development of polymer composites strengthened with organic fillers [109−111]. Another factor to consider is the fuel economy of lightweight vehicles constructed of polymer composites reinforced with natural fillers, such as automobiles, lorries, buses, and planes. Greenpeace, nongovernmental organizations in different countries, and the European Commission have published sustainability recommendations for companies [112]. These polymer composites are constantly being developed for these reasons, and their use in the automobile sector has been documented [113,114]. Wu et al. [115] produced organic fiber-structure composites along with good mechanical properties and low energy utilization, resulting in a more viable method.

Green materials like natural fiber and soy-based polymers were first used in the automobile sector in the 1950s [116]. As a result of the great expense of petroleum resources, hemp and jute biocomposites were used to create interior automobile components. In this sector, petrochemically manufactured polymers have been substituted with green composites. Seatbacks, door linens, the back door, shelving, and other vehicle interior components were developed using green composites [117,118]. Natural fibers have been used to restore glass fiber−strengthened composites in the automobile sector since they are more eco-friendly [119].

Several automobile firms have utilized polymer composites reinforced with natural fillers, particularly in interior vehicle components like door panels, dashboard trim pieces, parcel shelves, and so on [120,121]. In E-class cars, Mercedes-Benz utilized jute/epoxy door sheets [122], whereas the Audi A2 utilized PU filled with sisal/flax as door trim sections [123]. In the RAUM 2003 model, Toyota utilized various polymer composites coupled with organic fillers as additional tire wraps [124]. Mitsubishi Motors utilized poly(butylene succinate) strengthened with bamboo fibers designed for inner elements [124], whereas BMW applied a thermosetting acrylic copolymer packed with prepreg natural fiber matting for the bottom door panel [125]. Weather considerations, such as temperature and humidity, provide a barrier for the usage of composites strengthened along with natural fillers in external vehicle components [126]. As a result, there are only a few components manufactured specifically for this purpose [127,128].

### 11.10.14.2 Green nanofillers

Ecological nanofillers must be used to create a sustainable nanocomposite [129]. The demand for green reinforcement emerges as a result of nanocomposite's

nonhazardous and nontoxicological impacts on the environment [130,131]. Fig. 11.11 shows a few examples of green nanofillers. Green nanocomposites with silica nanoparticles have been developed. Nanosilica has been utilized in nanocomposites to improve their strength [132]. Green nanofiller halloysite nanotube (HNT) is a common kind [133]. Aluminosilicate nanoclay structure is seen in HNTs. HNTs have been utilized in nanocomposites to improve dispersion, surface hydrophobicity, and mechanical characteristics [134,135]. Green nanofillers such as cellulose nanofibers and cellulose nanoparticles are also common [136,137]. Using ultrasonic or chemical treatment techniques, cellulose nanofibers were extracted from plant extracts. To make the nanocomposites, starch nanocrystals were utilized as eco-friendly nanofillers [138,139]. In nanomaterials, starch reinforcement has been utilized in both its natural and chemically modified forms. Soy protein has been used to create effective green nanofillers [140]. Jute, zein, bamboo, and other natural fibers have also been utilized as green fillers. Nanocarbons are a kind of green nanofiller that is widely used [141]. As long-term fillers, graphene, graphene nanoplatelets (GNPs), and graphite have been utilized. These nanoparticles have been utilized to create nanocomposites that are lightweight, conductive, and durable. Several additional carbonaceous nanofillers, such as CNTs, nanofillers, and so on, were also studied [142–144].

### 11.10.14.3 Green polymeric nanocomposites

Waterborne PU, poly(ethylene oxide), poly(ethylene glycol), and poly(urethane-urea) are examples of well-known eco-efficient polymers [145–147]. Green


**Figure 11.11** Green nanofiller.
*Source*: Reprinted from A. Kausar, Progress in green nanocomposites for high-performance applications, Mater. Res. Innov. 25 (1) (2021), 53–65 [107], with permission from Taylor & Francis, Copyright 2020.

synthesis methods are often used to create these eco-polymers. MMT nanoclay is a mineral that belongs to the phyllosilicate family. MMT has long been regarded as an environmentally beneficial nanofiller. Due to its high surface area, aspect ratio, nanoclay, and minimal cost have been utilized as a nanocomposite strengthening. In PU and other green polymer matrices, charged nanoclay platelets may aid homogeneous dispersion [148]. Chemical stability, barrier characteristics, and thermal constancy of PU and nanoclay-based nanocomposites are all excellent. Green elastomeric PU nanocomposites with Cloisite nanoclay have been described [149]. For biodegradable PU, nanoclay may be used as a green-colored flame-retardant nanofiller. Nanofillers made of graphene oxide (GO) and graphene are also popular for their eco-friendly characteristics [150]. PLA is an aliphatic thermoplastic polyester created from sugarcane or starch that is biodegradable. PLA is a biodegradable polymer that may be utilized in a selection of applications. PLA is often treated along with poly(hydroxy acids) to inhibit enzymatic breakdown or hydrolysis [151].

### 11.10.15 Recent research reports

Longkullabutra et al. [152] have reported utilizing CNTs to increase the tensile strength of epoxy resin/hemp and epoxy resin composites (CNTs). Vibration milling was used to vibrate the CNTs after adding nanopowder for 6−48 hours. For epoxy resin/hemp composites, different percentages of CNTs were distributed. The findings show that milled CNTs can increase tensile strength. Liu and Erhan [153] synthesized epoxidized soybean oil-built composites along with flax fiber reinforcement and nanocomposites with OC reinforcement. The produced composites' tensile and flexural moduli increased proportionately along with the volume of epoxy resin, 1,1,1-tris(*p*-hydroxyphenyl)ethane triglycidyl ether.

Faruk and Matuana [154] investigated the best way to incorporate nanoclay into Wood-plastic composites (WPCs) in order to improve their mechanical characteristics. Nanoclays were introduced into HDPE-based WPCs using two distinct techniques. The experimental findings showed that by combining the nanoclay and the combination agent content in HDPE/wood−flour composites, the mechanical characteristics could be considerably enhanced.

Controlled synthesis of carbonate in an aqueous solution originated from a natural originator in the existence of wood cellulose fibers, and $CaCl_2$ has been used to create $CaCO_3$/wood cellulose nanocomposite materials. $CaCO_3$/cellulose nanocomposites may be used as strengthening fillers in polyethylene(PE) matrix-built composites, given that early dynamic mechanical analysis tests revealed that PE composites containing $CaCO_3$/cellulose fibers performed much better mechanically [155]. Once a proper scattering in the matrix is attained, the use of cellulose nanofibers as a replacement for microsized fibers is acknowledged as being more successful owing to contacts between the nanosized components that make it to a permeated group linked by hydrogen bonds or entanglements [156].

The mechanical characteristics of PLA-HNT nanocomposites are altered by adding a plasticizer [tributyl citrate (TBC)], with the goal of achieving mechanical qualities appropriate for automotive applications. A chosen plasticizer (TBC) was

co-combined with HNT into the PLA matrix to adjust the characteristics of PLA-HNT nanocomposites. Plasticization substantially enhanced the crystallization characteristics of PLA and PLA-HNT nanocomposites, permitting thermal classifications. The mechanical characteristics of the PLA-HNT-TBC ternary system have been investigated. The impact resistance and ductility of nanocomposites have been shown to be enhanced when increasing the plasticizer content. Despite this, a high TBC content (12.5−15 wt.%) developed in a reduction in tensile and flexural strength and stiffness. This research found that adding a plasticizer to PLA-HNT nanocomposites improves their strength and stiffness while also increasing other desirable characteristics, including impact resistance, ductility, crystallization speed, and crystallinity. Finally, a thorough examination showed that an improved PLA-HNT-TBC formulation (including 10 wt.% plasticizers) might be suggested as a bio-obtained substitute to automotive applications [157].

MMTs' influence on the morphological and tensile characteristics of PLA nanocomposites were also studied [158−160]. The optimal MMT concentration was determined to be 5 phr, or about 30 MPa, based on the tensile strength. In situ ring-opening polymerization was used by Sabatini et al. [161] to make PLA/MMT nanocomposites. 3-Glycidoxypropyltrimethoxysilane was used to treat the top of the MMT. Even extremely small quantities of MMT (0.1 wt.%) were shown to have a substantial influence on the characteristics of nanocomposites. MMT concentration of 0.1 wt.% was adequate to provide the same results as greater MMT levels (5 wt.% or more). Furthermore, when treated MMT was included in PLA nanocomposites, they were more thermally stable than plain PLA, while when untreated MMT was present in PLA matrix, the thermal stability of the nanocomposites was reduced.

Wu et al. [162] investigated the impact of aspect ratio on CNT characteristics. PLA nanocomposites with reinforcement PLA/CNT nanocomposites with a high aspect ratio CNT had a greater modulus than those with a minimal aspect ratio CNT, indicating that CNT dispersion is strongly dependent on its aspect ratio. Moon et al. [163] investigated mechanical and thermal characteristics as well as the electrical conductivity of PLA/CNT nanocomposites. The inclusion of CNT decreased the tensile strength and elongation at the break of PLA/CNT nanocomposites, whereas Young's modulus rose somewhat. Furthermore, PLA/thermal CNT's stability improved, while its electrical surface resistance was reduced. Moreover, PLA has been shown to be a suitable option for 3D printing and would reduce the requirement for spare parts storage [120].

MMT and GO-reinforced PU nanocomposites were developed by Vieira et al. [164]. These nanofillers were also combined with the poly(ethylene glycol) derivative polymer. GO has excellent mechanical and thermal characteristics, according to many experts, and is anticipated to become a key component in automotive purposes [165−168]. Because of their oxygenated surface functions, GO is anticipated to disperse easily in the PLA matrix, resulting in stable dispersibility through electrostatic repulsion and potential chemical interactions in PLA/GO nanocomposites [169,170]. Wang and Qiu [171] synthesized PLLA/GO nanocomposites with varying levels of GO (0.5, 1, and 2 wt.%). They discovered that PLLA/GO

nanocomposites' nonisothermal melt crystallization peak temperatures were somewhat higher than plain PLA. The addition of 1% GO to PLA raised the crystallization highest temperature from 95.1°C to 100.4°C. Furthermore, the addition of GO to the PLA matrix raised isothermal melt crystallization temperatures. The $T_g$ of neat PLA (61°C) and its nanocomposites also revealed that the addition of GO to PLLA did not affect the $T_g$ of PLA/GO nanocomposites when contrasted to simple PLA. The structural and rheological investigations were taken out in order to determine the capability of these eco-friendly materials. Singh and Dhaliwal [172] utilized an eco-polymer, poly (acrylic acid), to make nanocomposites containing AgNPs. The surface shape, crystallinity, and thermal characteristics of eco-materials were studied. Nanocomposites can hold/retain water and discharge a regulated quantity of water. The ability to retain water is critical to avoid environmental risks.

Recently, hybrid green nanocomposites have gotten a lot of interest because of their potential to make costly nanofillers more cost-effective by partly substituting them with a smaller amount of expensive ones. Furthermore, the characteristics of hybrid nanocomposites are dependent on the different nanofiller, with a balance of attributes achieved via nanofiller hybridization [173]. Studies reported the utilization of hybrid nanofillers in the PLA matrix to create PLA hybrid nanocomposites [174−177]. PLA/clay/CNT hybrid nanocomposites were produced and the impact of nanofillers content and UV radiation duration on the elastic moduli of the hybrid nanocomposites were studied by Gorrasi et al. [175]. Because of the strengthening action of the nanofillers, the PLA hybrid nanocomposites had a greater elastic modulus than clean PLA. Meng et al. [176] used melt blending to make PLA/MMT/wood nanocomposites. In comparison to clean PLA, the tensile modulus of PLA hybrid nanocomposites rose from 3.8 to 7.1 GPa. With the supplement of 5 wt.% MMT, however, the tensile strength dropped by approximately 20 MPa. In addition, as compared to PLA/wood composites, the thermal breakdown temperature of PLA hybrid nanocomposites rose by around 10°C. When contrasted to plain PLA, $T_g$ of PLA hybrid nanocomposites and melting temperature remained constant.

Poly(vinyl alcohol) (PVA) is a biopolymer that dissolves in water. PVA and carboxymethyl cellulose (CMC)-built eco-materials were developed by Morsi et al. [178]. Gold nanoparticles were used to strengthen the PVA/CMC (AuNP). Biosynthesis was used to extract AuNP from a green mint leaf extract.

Nylon 1010 was mixed with an aromatic polythioamide (PTA) that was synthesized. PA1010 (polyamide 1010)/PTA (PTA) (90:10) was chosen as the matrix material for the nanocomposite because it has the best molecular weight and rheological characteristics. GNP has been discovered to be an outstanding nanofiller with mechanical, morphological, and automotive characteristics. The findings also showed that adding GNP nanoparticles to processable blends and nanocomposites improved their thermal and flammability characteristics. As a result, original nylon 1010-built materials may be regarded as a potential option for the development of high-temperature-resistant automobile materials. PA1010/PTA/GNP3 nanocomposite along with appropriate flexural, tensile, and impact characteristics was injection-molded applying the appropriate method for automotive component

application. The waistline molding for automobiles was created successfully. Future study into the influence of greater GNP loading on the flexural, tensile, and impact characteristics of PA1010-based materials will lead to the development of a new class of nanoparticulate-packed polyamide nanocomposite intended for automotive products [179].

Irez et al. analyzed [180] fracture toughness of epoxy-recycled rubber-built composite strengthened with GNPs for structural applications in the automotive sector. Three-point bending tests were used to evaluate the composites' bending strength and fracture properties after they were manufactured. The use of GNPs as reinforcement improved the modulus of elasticity and fracture toughness of these new composites, according to mechanical tests.

For the earliest time, the decision-making model was used to choose the most suitable nonwoven organic fiber type built on a PP matrix for the internal components of an automobile. This decision was made after weighing several natural composites against a variety of factors at the same time. Coir, flax, date palm, kenaf, jute, and sisal fiber composites were examined. This would improve the natural fiber composite range process and minimize mistakes and bias in the choice process. The impact strength was discovered to be the most significant assessment criteria in assessing organic fiber composites for inner components in the automobile sector, while the tensile modulus was determined to be the least important. Determining the optimum kind of natural fiber composites for automobile production would not only improve the sector's sustainability and efficiency, but it would also help the environment by producing more apparent solutions that may decrease product weight and, therefore $CO_2$ emissions. In terms of the overall six assessment criteria, the treated flax/PP composite with 30 wt.% fiber loading has been determined to be the finest. PP/date palm has also been shown to be likely for use in automobiles [181].

## 11.11 Challenges

Reports have shown that there is a tremendous rivalry in the use of green materials in the automobile sector. The size and value of materials may be related. Recent efforts to develop hybrid composites combining plant fiber and aluminum to create lighter, more fuel-efficient vehicles have been made owing to persistent environmental pressures. However, the soaring cost of raw ingredients in the manufacturing process has been questioned in numerous published publications. Growth drivers and challenges of PNCs for the automobile industry are illustrated in Fig. 11.12.

Uniform dispersion, interfacial adhesion between components [182], and guided assembly of nanoparticles are all difficult to achieve in nanocomposites. The processing conditions have a large impact on flow-induced viscoelasticity [183]. Particle−particle interactions cause nanoparticles to agglomerate [184]. Heterarchical long-variety order in the polymer matrix may be formed by using stiff high aspect ratio rod-like nanoparticles [185]. Enhancing PNCs' mechanical


**Figure 11.12** PNCs' growth drivers and challenges for the automobile industry.
*Source*: Reprinted by permission from V. Patel, Y. Mahajan, Polymer nanocomposites: emerging growth driver for the global automotive industry, in: J.K. Pandey, K.R. Reddy, A.K. Mohanty, M. Misra (Eds.), Handbook of Polymer Nanocomposites. Processing, Performance and Application: Volume A: Layered Silicates, Springer, 2014, pp. 511−538, https://doi.org/10.1007/978-3-642-38649-7_23 [26], Springer Nature Customer Service Centre GmbH: Springer, Copyright 2014.

properties involves dispersing nanomaterials in the host polymer matrix, creating co-continuous structures of nanomaterial and polymer matrix held composed by irreversible adhesion among components, and directed fabrication of mesoscale constructions made of both. All these approaches are valid. Using a solvent-built nanoparticle diffusion approach resulting in solvent evaporation to maintain phase co-continuity without losing the directed character of the particle-matrix building is slow and expensive. Aerospace companies presently utilize these methods [186]. An overall idea of relative cost and performance profiles in the production of nanocomposites is shown in Fig. 11.13 [40].

To stay up with steel manufacturers' efforts to enhance alloying and processes, alternative materials like green composites should be developed, allowing for lighter, more eco-friendly future cars. Some of the issues with plant fibers should be addressed by this method. Green composites are troublesome, according to another opinion article, owing to their breakdown nature. When aiming for 100% bio-based composites, natural fiber biodegradability must be considered. Because of this, natural fibers cannot be used in the manufacture of car exterior panels. However, problems like repeatability and the life cycle of car components are still unresolved. Eco-friendly solutions may invert the value chain and place a fair price on existing efforts, according to some experts. Regarding the future, it is also important to consider how these materials may be blended in the most eco-friendly way feasible while maintaining comparable performance [187].

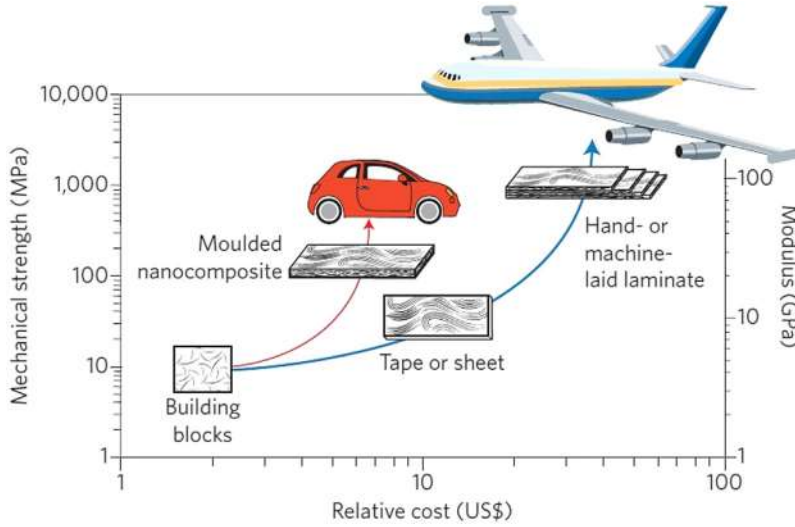


**Figure 11.13** Relative cost and performance profiles in the production of nanocomposites. *Source*: Reprinted by permission from A.K. Naskar, J.K. Keum, R.G. Boeman, Polymer matrix nanocomposites for automotive structural components, Nat. Nanotechnol. 11 (12) (2016) 1026−1030 [40]. Springer Nature Customer Service Centre GmbH, Copyright 2016.

## 11.12 Potential steps for quick commercialization

Several steps can be taken for faster commercialization of PNCs in the automotive industry [1]:

1. Develop quick, minimal-cost analytical processes for small trials that can deliver a point of exfoliation and direction, as TEM, XRD, and rheology are too costly and time-exhausting. For example, infrared can identify the silicon−oxygen bond in clay, which can aid in determining the degree of clay dispersion.
2. Develop low-cost, high-volume products to fulfill market demands quickly.
3. Create new nanoclay treatments to improve nanofiller adherence to polymers.
4. By combining nanofillers with traditional reinforcements like glass fiber, researchers can better understand the impact on performance.
5. Know how polymer composites behave in terms of rheology and chemorheology.
6. High rigidity without compromising impact resistance.
7. Cost/performance ratio of thermoplastic polyolefins (TPOs) against HIPS, PC/ABS, and PC (TPO).
8. Create online testing for nanocomposites.
9. Prediction of orientation and flow models.
10. Quantitative evaluation of changes in absorption and toxicity of chemically modified nanoparticles [188].
11. Fine dispersion, interfacial adhesion, and full exfoliation.

**12.** Life cycle analysis (LCA) exercises are critical for understanding the health impacts of nanotechnology, and LCA reports for various classes of nanoparticles and nanoproducts are required to anticipate the actual danger of nanowaste [188].

## 11.13 Conclusions

Over the past several years, tremendous technical breakthroughs have been witnessed in the automobile industry in PNCs, especially concerning the synthesis and commercialization of therapeutic polyolefin and polyamide nanocomposites. Nanocomposite products have achieved remarkable popularity in the automobile industry for exterior body parts, internal and sub-bonnet parts, fuel lines, coating, and fuel system component applications, by Original Equipment Manufacturers (OEMs) and molders. The pandemic of COVID-19 will undoubtedly impair the expansion of the sector to some extent. Major companies in the sector are apprehensive about the market's prospects and strive to rethink tactics in this challenging circumstance. By giving solutions for creating Personal Protective Equipment (PPE), they are attempting to help governments all around the world. The epidemic has had a serious impact on automotive manufacturing, and several major firms have been forced to halt production and other activities. This has entirely dropped the demand from these industries. There is a lack of workforce in various regions of the world owing to frequent lockdowns. The expansion of nanocomposite activity continues uninterrupted as further R&D funds are being provided by funding agencies, risk capitalists, and firms to utilize the wider variety of new characteristics that are being found. For example, the automobile sector invests more than 5% of its yearly gross revenue in research and development in Europe, and the emphasis is on improving coatings and paints and on strengthening end-use components for longer durability. In the next 10 years, the usage of PNCs in the car sector is therefore expected to grow.

## Acknowledgments

The authors thank the Military Institute of Science and Technology (MIST), Dhaka, for supporting this work.

## References

[1] A.K. Chandra, N.R. Kumar, Polymer nanocomposites for automobile engineering applications, in: D.K. Tripathy, B.P. Sahoo (Eds.), Properties and Applications of Polymer Nanocomposites: Clay and Carbon Based Polymer Nanocomposites, Springer, 2017, pp. 139–172. Available from: https://doi.org/10.1007/978-3-662-53517-2_7.

[2] A.K. Bhowmick (Ed.), Current Topics in Elastomers Research, CRC Press, 2008.

[3] G. Hernández-Padrón, F. Rojas, M. García-Garduño, M.A. Canseco, V.M. Castaño, Development of hybrid materials consisting of $SiO_2$ microparticles embedded in phenolic-formaldehydic resin polymer matrices, Mater. Sci. Eng. A 355 (1−2) (2003) 338−347. Available from: https://doi.org/10.1016/S0921-5093(03)00101-1.
[4] D.K. Tripathy, B.P. Sahoo (Eds.), Properties and Applications of Polymer Nanocomposites: Clay and Carbon Based Polymer Nanocomposites, Springer Berlin Heidelberg, 2017. Available from: https://doi.org/10.1007/978-3-662-53517-2.
[5] S. Komarneni, Feature article. Nanocomposites, J. Mater. Chem. 2 (12) (1992) 1219. Available from: https://doi.org/10.1039/jm9920201219.
[6] I. Kong, K.Y. Tshai, M.E. Hoque, Manufacturing of natural fibre-reinforced polymer composites by solvent casting method, in: M.S. Salit, M. Jawaid, N.B. Yusoff, M.E. Hoque (Eds.), Manufacturing of Natural Fibre Reinforced Polymer Composites, Springer International Publishing, 2015, pp. 331−349. Available from: https://doi.org/10.1007/978-3-319-07944-8_16.
[7] S.K.S. Hossain, M.E. Hoque, Polymer nanocomposite materials in energy storage: properties and applications, Polymer-based Nanocomposites for Energy and Environmental Applications, Elsevier, 2018, pp. 239−282. Available from: https://doi.org/10.1016/B978-0-08-102262-7.00009-X.
[8] A. Sharif, S. Mondal, M.E. Hoque, Polylactic acid (PLA)-based nanocomposites: processing and properties, in: M.L. Sanyang, M. Jawaid (Eds.), Bio-based Polymers and Nanocomposites, Springer International Publishing, 2019, pp. 233−254. Available from: https://doi.org/10.1007/978-3-030-05825-8_11.
[9] B. Stojanovic, M. Babic, S. Mitrovic, A. Vencl, N. Miloradovic, M. Pantic, Tribological characteristics of aluminium hybrid composites reinforced with silicon carbide and graphite. A review, 2013, p. 14.
[10] A. A.-K. Gazawi, Microstructure and mechanical properties of aluminium based nanocomposites strengthened with alumina and silicon carbide, Doctoral thesis, University of Waikato, 2014. https://hdl.handle.net/10289/8670.
[11] S. Pandya, Nanocomposites and it's application-review, 2015. https://doi.org/10.13140/RG.2.1.2798.9840.
[12] G. Armstrong, An introduction to polymer nanocomposites, Eur. J. Phys. 36 (6) (2015) 063001. Available from: https://doi.org/10.1088/0143-0807/36/6/063001.
[13] D.R. Paul, L.M. Robeson, Polymer nanotechnology: nanocomposites, Polymer 49 (15) (2008) 3187−3204. Available from: https://doi.org/10.1016/j.polymer.2008.04.017.
[14] J. Jancar, J.F. Douglas, F.W. Starr, S.K. Kumar, P. Cassagnau, A.J. Lesser, et al., Current issues in research on structure−property relationships in polymer nanocomposites, Polymer 51 (15) (2010) 3321−3343. Available from: https://doi.org/10.1016/j.polymer.2010.04.074.
[15] L.S. Schadler, L.C. Brinson, W.G. Sawyer, Polymer nanocomposites: a small part of the story, JOM 59 (3) (2007) 53−60. Available from: https://doi.org/10.1007/s11837-007-0040-5.
[16] F. Hussain, M. Hojjati, M. Okamoto, R.E. Gorga, Review article: polymer-matrix nanocomposites, processing, manufacturing, and application: an overview, J. Compos. Mater. 40 (17) (2006) 1511−1575. Available from: https://doi.org/10.1177/0021998306067321.
[17] K. Müller, E. Bugnicourt, M. Latorre, M. Jorda, Y. Echegoyen Sanz, J.M. Lagaron, et al., Review on the processing and properties of polymer nanocomposites and nanocoatings and their applications in the packaging, automotive and solar energy fields, Nanomaterials 7 (4) (2017) 74. Available from: https://doi.org/10.3390/nano7040074.

[18] I.Y. Shevtsov, V.L. Markine, C. Esveld, Optimal design of wheel profile for railway vehicles, Wear 258 (7) (2005) 1022–1030. Available from: https://doi.org/10.1016/j.wear.2004.03.051.
[19] N. Karak, Chapter 1—Fundamentals of nanomaterials and polymer nanocomposites, in: N. Karak (Ed.), Nanomaterials and Polymer Nanocomposites, Elsevier, 2019, pp. 1–45. Available from: https://doi.org/10.1016/B978-0-12-814615-6.00001-1.
[20] G. Lagaly, M. Ogawa, I. Dékány, Chapter 7.3 Clay mineral organic interactions, in: F. Bergaya, B.K.G. Theng, G. Lagaly (Eds.), Developments in Clay Science, vol. 1, Elsevier, 2006, pp. 309–377. Available from: https://doi.org/10.1016/S1572-4352(05)01010-X.
[21] S. Thakur, N. Karak, Alternative methods and nature-based reagents for the reduction of graphene oxide: a review, Carbon 94 (2015) 224–242. Available from: https://doi.org/10.1016/j.carbon.2015.06.030.
[22] J.W. Gilman, Flammability and thermal stability studies of polymer layered-silicate (clay) nanocomposites, Appl. Clay Sci. 15 (1) (1999) 31–49. Available from: https://doi.org/10.1016/S0169-1317(99)00019-8.
[23] S. Thakur, N. Karak, Multi-stimuli responsive smart elastomeric hyperbranched polyurethane/reduced graphene oxide nanocomposites, J. Mater. Chem. A 2 (36) (2014) 14867–14875. Available from: https://doi.org/10.1039/C4TA02497D.
[24] N. Karak, Biobased Smart Polyurethane Nanocomposites: From Synthesis to Applications, Royal Society of Chemistry, 2017.
[25] R. Duarah, Y.P. Singh, P. Gupta, B.B. Mandal, N. Karak, High performance bio-based hyperbranched polyurethane/carbon dot-silver nanocomposite: a rapid self-expandable stent, Biofabrication 8 (4) (2016) 045013. Available from: https://doi.org/10.1088/1758-5090/8/4/045013.
[26] V. Patel, Y. Mahajan, Polymer nanocomposites: emerging growth driver for the global automotive industry, in: J.K. Pandey, K.R. Reddy, A.K. Mohanty, M. Misra (Eds.), Handbook of Polymer Nanocomposites. Processing, Performance and Application: Volume A: Layered Silicates, Springer, 2014, pp. 511–538. Available from: https://doi.org/10.1007/978-3-642-38649-7_23.
[27] P. Senthil Kumar, E. Gunasundari, Nanocomposites: recent trends and engineering applications, Nano Hybrids Compos. 20 (2018) 65–80. Available from: https://doi.org/10.4028/http://www.scientific.net/NHC.20.65.
[28] D.M. Ledwith, A.M. Whelan, J.M. Kelly, A rapid, straight-forward method for controlling the morphology of stable silver nanoparticles, J. Mater. Chem. 17 (23) (2007) 2459–2464. Available from: https://doi.org/10.1039/B702141K.
[29] O. Becker, R. Varley, G. Simon, Morphology, thermal relaxations and mechanical properties of layered silicate nanocomposites based upon high-functionality epoxy resins, Polymer 43 (16) (2002) 4365–4373. Available from: https://doi.org/10.1016/S0032-3861(02)00269-0.
[30] W. Kim, B.-S. Kang, S.-G. Cho, C.-S. Ha, J.-W. Bae, Styrene butadiene rubber-clay nanocomposites using a latex method: morphology and mechanical properties, Composite Interfaces 14 (5–6) (2007) 409–425. Available from: https://doi.org/10.1163/156855407781291218.
[31] L. Le Pluart, J. Duchet, H. Sautereau, P. Halley, J.-F. Gerard, Rheological properties of organoclay suspensions in epoxy network precursors, Appl. Clay Sci. 25 (3) (2004) 207–219. Available from: https://doi.org/10.1016/j.clay.2003.11.004.
[32] J.N. Coleman, U. Khan, W.J. Blau, Y.K. Gun'ko, Small but strong: a review of the mechanical properties of carbon nanotube–polymer composites, Carbon 44 (9) (2006) 1624–1652. Available from: https://doi.org/10.1016/j.carbon.2006.02.038.

[33] A.K. Chandra, Tire technology—recent advances and future trends, Current Topics in Elastomers Research, CRC Press, 2008.
[34] C. Li, E. Thostenson, T.-W. Chou, Carbon-Nanotube-Based Compos. Damage Sens. (2010) 159−281. Available from: https://doi.org/10.1201/b10462-6.
[35] E.T. Thostenson, C. Li, T.-W. Chou, Nanocomposites in context, Compos. Sci. Technol. 65 (3) (2005) 491−516. Available from: https://doi.org/10.1016/j.compscitech.2004.11.003.
[36] S. Pavlidou, C.D. Papaspyrides, A review on polymer−layered silicate nanocomposites, Prog. Polym. Sci. 33 (12) (2008) 1119−1198. Available from: https://doi.org/10.1016/j.progpolymsci.2008.07.008.
[37] H. Kim, A.A. Abdala, C.W. Macosko, Graphene/polymer nanocomposites, Macromolecules 43 (16) (2010) 6515−6530. Available from: https://doi.org/10.1021/ma100572e.
[38] E. Munch, M.E. Launey, D.H. Alsem, E. Saiz, A.P. Tomsia, R.O. Ritchie, Tough, bio-inspired hybrid materials, Science 322 (5907) (2008) 1516−1520. Available from: https://doi.org/10.1126/science.1164865.
[39] C.D. Tran, J. Chen, J.K. Keum, A.K. Naskar, A new class of renewable thermoplastics with extraordinary performance from nanostructured lignin-elastomers, Adv. Funct. Mater. 26 (16) (2016) 2677−2685. Available from: https://doi.org/10.1002/adfm.201504990.
[40] A.K. Naskar, J.K. Keum, R.G. Boeman, Polymer matrix nanocomposites for automotive structural components, Nat. Nanotechnol. 11 (12) (2016) 1026−1030. Available from: https://doi.org/10.1038/nnano.2016.262.
[41] R.-M. Wang, S.-R. Zheng, Y.-P. Zheng, Introduction to polymer matrix composites, Polymer Matrix Composites and Technology, Elsevier, 2011, pp. 1−548. Available from: https://doi.org/10.1533/9780857092229.1.
[42] I.O. Oladele, T.F. Omotosho, A.A. Adediran, Polymer-based composites: an indispensable material for present and future applications, Int. J. Polym. Sci. 2020 (2020) e8834518. Available from: https://doi.org/10.1155/2020/8834518.
[43] L. Mohammed, M.N.M. Ansari, G. Pua, M. Jawaid, M.S. Islam, A review on natural fiber reinforced polymer composite and its applications, Int. J. Polym. Sci. 2015 (2015) e243947. Available from: https://doi.org/10.1155/2015/243947.
[44] Y. Bautista, J. Gonzalez, J. Gilabert, M.J. Ibañez, V. Sanz, Correlation between the wear resistance, and the scratch resistance, for nanocomposite coatings, Prog. Org. Coat. 70 (4) (2011) 178−185. Available from: https://doi.org/10.1016/j.porgcoat.2010.09.022.
[45] M. Groenewolt, Highly scratch resistant coatings for automotive applications, Prog. Org. Coat. 61 (2) (2008) 106−109. Available from: https://doi.org/10.1016/j.porgcoat.2007.07.036.
[46] M. Sangermano, M. Messori, Scratch resistance enhancement of polymer coatings, Macromol. Mater. Eng. 295 (7) (2010) 603−612. Available from: https://doi.org/10.1002/mame.201000025.
[47] N. Tahmassebi, S. Moradian, B. Ramezanzadeh, A. Khosravi, S. Behdad, Effect of addition of hydrophobic nano silica on viscoelastic properties and scratch resistance of an acrylic/melamine automotive clearcoat, Tribol. Int. 43 (3) (2010) 685−693. Available from: https://doi.org/10.1016/j.triboint.2009.10.008.
[48] E. Amerio, P. Fabbri, G. Malucelli, M. Messori, M. Sangermano, R. Taurino, Scratch resistance of nano-silica reinforced acrylic coatings, Prog. Org. Coat. 62 (2) (2008) 129−133. Available from: https://doi.org/10.1016/j.porgcoat.2007.10.003.

[49] H. Presting, U. König, Future nanotechnology developments for automotive applications, Mater. Sci. Eng. C 23 (6–8) (2003) 737–741. Available from: https://doi.org/10.1016/j.msec.2003.09.120.

[50] B. Ramezanzadeh, S. Moradian, N. Tahmasebi, A. Khosravi, Studying the role of polysiloxane additives and nano-$SiO_2$ on the mechanical properties of a typical acrylic/melamine clearcoat, Prog. Org. Coat. 72 (4) (2011) 621–631. Available from: https://doi.org/10.1016/j.porgcoat.2011.07.003.

[51] B. Ramezanzadeh, M. Mohseni, H. Yari, S. Sabbaghian, A study of thermal–mechanical properties of an automotive coating exposed to natural and simulated bird droppings, J. Therm. Anal. Calorim. 102 (1) (2010) 13–21. Available from: https://doi.org/10.1007/s10973-009-0442-4.

[52] J. Jiao, P. Liu, L. Wang, Y. Cai, One-step synthesis of improved silica/epoxy nanocomposites with inorganic-organic hybrid network, J. Polym. Res. 20 (8) (2013) 202. Available from: https://doi.org/10.1007/s10965-013-0202-9.

[53] B. Ahmadi, M. Kassiriha, K. Khodabakhshi, E.R. Mafi, Effect of nano layered silicates on automotive polyurethane refinish clear coat, Prog. Org. Coat. 60 (2) (2007) 99–104. Available from: https://doi.org/10.1016/j.porgcoat.2007.07.008.

[54] M.L. Nobel, S.J. Picken, E. Mendes, Waterborne nanocomposite resins for automotive coating applications, Prog. Org. Coat. 58 (2) (2007) 96–104. Available from: https://doi.org/10.1016/j.porgcoat.2006.08.017.

[55] G. Verma, A. Kaushik, A.K. Ghosh, Nano-interfaces between clay platelets and polyurethane hard segments in spray coated automotive nanocomposites, Prog. Org. Coat. 99 (2016) 282–294. Available from: https://doi.org/10.1016/j.porgcoat.2016.06.001.

[56] S.M. Mirabedini, M. Sabzi, J. Zohuriaan-Mehr, M. Atai, M. Behzadnasab, Weathering performance of the polyurethane nanocomposite coatings containing silane treated $TiO_2$ nanoparticles, Appl. Surf. Sci. 257 (9) (2011) 4196–4203. Available from: https://doi.org/10.1016/j.apsusc.2010.12.020.

[57] M.S. Lowry, D.R. Hubble, A.L. Wressell, M.S. Vratsanos, F.R. Pepe, C.R. Hegedus, Assessment of UV-permeability in nano-ZnO filled coatings via high throughput experimentation, J. Coat. Technol. Res. 5 (2) (2008) 233–239. Available from: https://doi.org/10.1007/s11998-007-9064-6.

[58] M. Rashvand, Z. Ranjbar, S. Rastegar, Nano zinc oxide as a UV-stabilizer for aromatic polyurethane coatings, Prog. Org. Coat. 71 (4) (2011) 362–368. Available from: https://doi.org/10.1016/j.porgcoat.2011.04.006.

[59] G. Chen, Z. Sun, Y. Wang, J. Zheng, S. Wen, J. Zhang, et al., Designed preparation of silicone protective materials with controlled self-healing and toughness properties, Prog. Org. Coat. 140 (2020) 105483. Available from: https://doi.org/10.1016/j.porgcoat.2019.105483.

[60] Z. Deng, H. Wang, P.X. Ma, B. Guo, Self-healing conductive hydrogels: preparation, properties and applications, Nanoscale 12 (3) (2020) 1224–1246. Available from: https://doi.org/10.1039/C9NR09283H.

[61] D. Gao, J. Zhang, B. Lyu, J. Ma, Z. Yang, Polyacrylate crosslinked with furyl alcohol grafting bismaleimide: a self-healing polymer coating, Prog. Org. Coat. 139 (2020) 105475. Available from: https://doi.org/10.1016/j.porgcoat.2019.105475.

[62] G. Lefever, D. Snoeck, D.G. Aggelis, N. De Belie, S. Van Vlierberghe, D. Van Hemelrijck, Evaluation of the self-healing ability of mortar mixtures containing superabsorbent polymers and nanosilica, Materials 13 (2) (2020) 380. Available from: https://doi.org/10.3390/ma13020380.

[63] S. Qiu, W. Li, W. Zheng, H. Zhao, L. Wang, Synergistic effect of polypyrrole-intercalated graphene for enhanced corrosion protection of aqueous coating in 3.5% NaCl solution, ACS Appl. Mater. Interfaces 9 (39) (2017) 34294−34304. Available from: https://doi.org/10.1021/acsami.7b08325.

[64] P. Wang, L. Yang, B. Dai, Z. Yang, S. Guo, G. Gao, et al., A self-healing transparent polydimethylsiloxane elastomer based on imine bonds, Eur. Polym. J. 123 (2020) 109382. Available from: https://doi.org/10.1016/j.eurpolymj.2019.109382.

[65] A. Yabuki, S. Tanabe, I.W. Fathona, Self-healing polymer coating with the microfibers of superabsorbent polymers provides corrosion inhibition in carbon steel, Surf. Coat. Technol. 341 (2018) 71−77. Available from: https://doi.org/10.1016/j.surfcoat.2017.08.030.

[66] D. Yuan, V.S. Bonab, A. Patel, I. Manas-Zloczower, Self-healing epoxy coatings with enhanced properties and facile processability, Polymer 147 (2018) 196−201. Available from: https://doi.org/10.1016/j.polymer.2018.06.017.

[67] D. Yuan, V. Solouki Bonab, A. Patel, T. Yilmaz, R.A. Gross, I. Manas-Zloczower, Design strategy for self-healing epoxy coatings, Coatings 10 (1) (2020) 50. Available from: https://doi.org/10.3390/coatings10010050.

[68] R. Bayan, N. Karak, Bio-derived aliphatic hyperbranched polyurethane nanocomposites with inherent self healing tendency and surface hydrophobicity: towards creating high performance smart materials, Compos. A Appl. Sci. Manuf. 110 (2018) 142−153. Available from: https://doi.org/10.1016/j.compositesa.2018.04.024.

[69] C.I. Idumah, S.R. Odera, Recent advancement in self-healing graphene polymer nanocomposites, shape memory, and coating materials, Polym. Technol. Mater. 59 (11) (2020) 1167−1190. Available from: https://doi.org/10.1080/25740881.2020.1725816.

[70] Q. Zhang, L. Liu, C. Pan, D. Li, G. Gai, Thermally sensitive, adhesive, injectable, multiwalled carbon nanotube covalently reinforced polymer conductors with self-healing capabilities, J. Mater. Chem. C. 6 (7) (2018) 1746−1752. Available from: https://doi.org/10.1039/C7TC05432G.

[71] M. Galimberti, V.R. Cipolletti, M. Coombs, Chapter 4.4—Applications of clay−polymer nanocomposites, in: F. Bergaya, G. Lagaly (Eds.), Developments in Clay Science, vol. 5, Elsevier, 2013, pp. 539−586. Available from: https://doi.org/10.1016/B978-0-08-098259-5.00020-2.

[72] X. Qin, J. Wang, B. Han, B. Wang, L. Mao, L. Zhang, Novel design of eco-friendly super elastomer materials with optimized hard segments micro-structure: toward next-generation high-performance tires, Front. Chem. 6 (2018) 240. Available from: https://doi.org/10.3389/fchem.2018.00240.

[73] J. Ayippadath Gopi, S.K. Patel, A.K. Chandra, D.K. Tripathy, SBR-clay-carbon black hybrid nanocomposites for tire tread application, J. Polym. Res. 18 (6) (2011) 1625−1634. Available from: https://doi.org/10.1007/s10965-011-9567-9.

[74] X. Wang, D. Jia, M. Chen, Structure and properties of epoxidized nature rubber/organoclay nanocomposites, in Proceedings of the 2008 Second IEEE International Nanoelectronics Conference, 2008, pp. 335−339. https://doi.org/10.1109/INEC.2008.4585499

[75] P.L. Teh, Z.A. Mohd Ishak, A.S. Hashim, J. Karger-Kocsis, U.S. Ishiaku, Effects of epoxidized natural rubber as a compatibilizer in melt compounded natural rubber−organoclay nanocomposites, Eur. Polym. J. 40 (11) (2004) 2513−2521. Available from: https://doi.org/10.1016/j.eurpolymj.2004.06.025.

[76] B. Rodgers, W. Weng, J. Soisson, D. Lohse, W. Waddell, R. Webb, Permeability of rubber compositions containing clay, Rubber-Clay Nanocomposites, John

Wiley & Sons, Ltd, 2011, pp. 343–365. Available from: https://doi.org/10.1002/9781118092866.ch11.

[77] J. Greeley, I.E.L. Stephens, A.S. Bondarenko, T.P. Johansson, H.A. Hansen, T.F. Jaramillo, et al., Alloys of platinum and early transition metals as oxygen reduction electrocatalysts, Nat. Chem. 1 (7) (2009) 552–556. Available from: https://doi.org/10.1038/nchem.367.

[78] A.S. Aricò, P. Bruce, B. Scrosati, J.-M. Tarascon, W. van Schalkwijk, Nanostructured materials for advanced energy conversion and storage devices, Nat. Mater. 4 (5) (2005) 366–377. Available from: https://doi.org/10.1038/nmat1368.

[79] K. Gong, F. Du, Z. Xia, M. Durstock, L. Dai, Nitrogen-doped carbon nanotube arrays with high electrocatalytic activity for oxygen reduction, Science 323 (5915) (2009) 760–764. Available from: https://doi.org/10.1126/science.1168049.

[80] Y. Li, Y. Zhao, H. Cheng, Y. Hu, G. Shi, L. Dai, et al., Nitrogen-doped graphene quantum dots with oxygen-rich functional groups, J. Am. Chem. Soc. 134 (1) (2012) 15–18. Available from: https://doi.org/10.1021/ja206030c.

[81] R. Liu, D. Wu, X. Feng, K. Müllen, Nitrogen-doped ordered mesoporous graphitic arrays with high electrocatalytic activity for oxygen reduction, Angew. Chem. Int. (Ed.) 49 (14) (2010) 2565–2569. Available from: https://doi.org/10.1002/anie.200907289.

[82] L. Qu, Y. Liu, J.-B. Baek, L. Dai, Nitrogen-doped graphene as efficient metal-free electrocatalyst for oxygen reduction in fuel cells, ACS Nano 4 (3) (2010) 1321–1326. Available from: https://doi.org/10.1021/nn901850u.

[83] M. Zhang, L. Dai, Carbon nanomaterials as metal-free catalysts in next generation fuel cells, Nano Energy 1 (4) (2012) 514–517. Available from: https://doi.org/10.1016/j.nanoen.2012.02.008.

[84] P. Chen, T.-Y. Xiao, H.-H. Li, J.-J. Yang, Z. Wang, H.-B. Yao, et al., Nitrogen-doped graphene/ZnSe nanocomposites: hydrothermal synthesis and their enhanced electrochemical and photocatalytic activities, ACS Nano 6 (1) (2012) 712–719. Available from: https://doi.org/10.1021/nn204191x.

[85] S. Wang, D. Yu, L. Dai, D.W. Chang, J.-B. Baek, Polyelectrolyte-functionalized graphene as metal-free electrocatalysts for oxygen reduction, ACS Nano 5 (8) (2011) 6202–6209. Available from: https://doi.org/10.1021/nn200879h.

[86] J.W. Burress, S. Gadipelli, J. Ford, J.M. Simmons, W. Zhou, T. Yildirim, Graphene oxide framework materials: theoretical predictions and experimental results, Angew. Chem. Int. (Ed.) 49 (47) (2010) 8902–8904. Available from: https://doi.org/10.1002/anie.201003328.

[87] G.K. Dimitrakakis, E. Tylianakis, G.E. Froudakis, Pillared graphene: a new 3-D network nanostructure for enhanced hydrogen storage, Nano Lett. 8 (10) (2008) 3166–3170. Available from: https://doi.org/10.1021/nl801417w.

[88] N. Park, S. Hong, G. Kim, S.-H. Jhi, Computational study of hydrogen storage characteristics of covalent-bonded graphenes, J. Am. Chem. Soc. 129 (29) (2007) 8999–9003. Available from: https://doi.org/10.1021/ja0703527.

[89] C. Wang, H. Wu, Z. Chen, M.T. McDowell, Y. Cui, Z. Bao, Self-healing chemistry enables the stable operation of silicon microparticle anodes for high-energy lithium-ion batteries, Nat. Chem. 5 (12) (2013) 1042–1048. Available from: https://doi.org/10.1038/nchem.1802.

[90] J.E. Yoo, V. Roev, J. Bae, D.-S. Yoon, S.-D. Kim, E.-S. Lee, Multifunctional hybrid polymer nanocomposites for automotive-battery packaging, J. Appl. Polym. Sci. 137 (36) (2020) 49059. Available from: https://doi.org/10.1002/app.49059.

[91] M. Mohseni, B. Ramezanzadeh, H. Yari, M. Moazzami, The role of nanotechnology in automotive industries, in: J. Carmo (Ed.), New Advances in Vehicular Technology and Automotive Engineering, InTech, 2012. Available from: https://doi.org/10.5772/49939.

[92] H. Yahyaei, M. Mohseni, S. Bastani, Using Taguchi experimental design to reveal the impact parameters affecting abrasiresistance sol−gel based UV curable nanocomposite films polycarbonate, J. Solgel Sci. Technol. 59 (1) (2011) 95−105. Available from: https://doi.org/10.1007/S10971-011-2466-Z.

[93] H.-D. Nguyen-Tran, V.-T. Hoang, V.-T. Do, D.-M. Chun, Y.-J. Yum, Effect of multi-walled carbon nanotubes on the mechanical properties of carbon fiber-reinforced polyamide-6/polypropylene composites for lightweight automotive parts, Materials 11 (3) (2018) 429. Available from: https://doi.org/10.3390/ma11030429.

[94] S. Sachse, L. Gendre, F. Silva, H. Zhu, A. Leszczyńska, K. Pielichowski, et al., On nanoparticles release from polymer nanocomposites for applications in lightweight automotive components, J. Physics Conf. Ser. 429 (2013) 012046. Available from: https://doi.org/10.1088/1742-6596/429/1/012046.

[95] V. Volpe, S. Lanzillo, G. Affinita, B. Villacci, I. Macchiarolo, R. Pantani, Lightweight high-performance polymer composite for automotive applications, Polymers 11 (2) (2019) 326. Available from: https://doi.org/10.3390/polym11020326.

[96] S. Yousef, A. Khattab, M. Zaki, T.A. Osman, Wear characterization of carbon nanotubes reinforced polymer gears, IEEE Trans. Nanotechnol. 12 (4) (2013) 616−620. Available from: https://doi.org/10.1109/TNANO.2013.2264902.

[97] S. Yousef, T.A. Osman, A.H. Abdalla, G.A. Zohdy, Wear characterization of carbon nanotubes reinforced acetal spur, helical, bevel and worm gears using a TS universal test rig, JOM 67 (12) (2015) 2892−2899. Available from: https://doi.org/10.1007/s11837-014-1268-5.

[98] S. Kirupasankar, C. Gurunathan, R. Gnanamoorthy, Transmission efficiency of polyamide nanocomposite spur gears, Mater. Des. 39 (2012) 338−343. Available from: https://doi.org/10.1016/j.matdes.2012.02.045.

[99] S. Kirupasankar, R. Gnanamoorthy, R. Velmurugan, Effect of apparent area, load, and filler content on sliding friction characteristics of polymer nanocomposites, Proc. Inst. Mech. Eng. J J. Eng. Tribol. 224 (2) (2010) 133−138. Available from: https://doi.org/10.1243/13506501JET648.

[100] S. Yousef, 16 - Polymer nanocomposite components: a case study on gears, in: J. Njuguna (Ed.), Lightweight Composite Structures in Transport, Woodhead Publishing, 2016, pp. 385−420. Available from: https://doi.org/10.1016/B978-1-78242-325-6.00016-5.

[101] M. Alexandre, P. Dubois, Polymer-layered silicate nanocomposites: preparation, properties and uses of a new class of materials, Mater. Sci. Eng. R Rep. 28 (1) (2000) 1−63. Available from: https://doi.org/10.1016/S0927-796X(00)00012-7.

[102] A. Okada, A. Usuki, The chemistry of polymer-clay hybrids, Mater. Sci. Eng. C 3 (2) (1995) 109−115. Available from: https://doi.org/10.1016/0928-4931(95)00110-7.

[103] F. Gao, Clay/polymer composites: the story, Mater. Today 7 (11) (2004) 50−55. Available from: https://doi.org/10.1016/S1369-7021(04)00509-7.

[104] A.B. Bhattacharya, A.T. Raju, T. Chatterjee, K. Naskar, Development and characterizations of ultra-high molecular weight EPDM/PP based TPV nanocomposites for automotive applications, Polym. Compos. 41 (12) (2020) 4950−4962. Available from: https://doi.org/10.1002/pc.25765.

[105] O.T. Adesina, T. Jamiru, E.R. Sadiku, O.F. Ogunbiyi, L.W. Beneke, Mechanical evaluation of hybrid natural fibre−reinforced polymeric composites for automotive bumper beam: a review, Int. J. Adv. Manuf. Technol. 103 (5) (2019) 1781−1797. Available from: https://doi.org/10.1007/s00170-019-03638-w.

[106] N. Oztoprak, M.D. Gunes, M. Tanoglu, E. Aktas, O.O. Egilmez, C. Senocak, et al., Developing polymer composite-based leaf spring systems for automotive industry, Sci. Eng. Composite Mater. 25 (6) (2018) 1167−1176. Available from: https://doi.org/10.1515/secm-2016-0335.

[107] A. Kausar, Progress in green nanocomposites for high-performance applications, Mater. Res. Innov. 25 (1) (2021) 53−65. Available from: https://doi.org/10.1080/14328917.2020.1728489.

[108] F.V. Ferreira, I.F. Pinheiro, S.F. de Souza, L.H.I. Mei, L.M.F. Lona, Polymer composites reinforced with natural fibers and nanocellulose in the automotive industry: a short review, J. Compos. Sci. 3 (2) (2019) 51. Available from: https://doi.org/10.3390/jcs3020051.

[109] D. Battegazzore, T. Abt, M.L. Maspoch, A. Frache, Multilayer cotton fabric biocomposites based on PLA and PHB copolymer for industrial load carrying applications, Compos. B Eng. 163 (2019) 761−768. Available from: https://doi.org/10.1016/j.compositesb.2019.01.057.

[110] A. Jiang, J. Xi, H. Wu, Effect of surface treatment on the morphology of sisal fibers in sisal/polylactic acid composites, J. Reinf. Plast. Compos. 31 (9) (2012) 621−630. Available from: https://doi.org/10.1177/0731684412441867.

[111] M.J. Mochane, T.C. Mokhena, T.H. Mokhothu, A. Mtibe, E. Sadiku, S. Ray, et al., Recent progress on natural fiber hybrid composites for advanced applications: a review, eXPRESS Polym. Lett. 13 (2) (2019) 159−198. Available from: https://doi.org/10.3144/EXPRESSPOLYMLETT.2019.15.

[112] D.S. Bajwa, S. Bhattacharjee, Current progress, trends and challenges in the application of biofiber composites by automotive industry, J. Nat. Fibers 13 (6) (2016) 660−669. Available from: https://doi.org/10.1080/15440478.2015.1102790.

[113] A.S. Herrmann, J. Nickel, U. Riedel, Construction materials based upon biologically renewable resources—from components to finished parts, Polym. Degrad. Stab. 59 (1) (1998) 251−261. Available from: https://doi.org/10.1016/S0141-3910(97)00169-9.

[114] K. Jayaraman, Manufacturing sisal−polypropylene composites with minimum fibre degradation, Compos. Sci. Technol. 63 (3) (2003) 367−374. Available from: https://doi.org/10.1016/S0266-3538(02)00217-8.

[115] Y. Wu, C. Xia, L. Cai, A.C. Garcia, S.Q. Shi, Development of natural fiber-reinforced composite with comparable mechanical properties and reduced energy consumption and environmental impacts for replacing automotive glass-fiber sheet molding compound, J. Clean. Prod. 184 (2018) 92−100. Available from: https://doi.org/10.1016/j.jclepro.2018.02.257.

[116] L.T. Drzal, A.K. Mohanty, M. Misra, Bio-composite materials as alternatives to petroleum-based composites for automotive applications, Magnesium 40 (60) (2001) 1−3.

[117] A. Ashori, Wood−plastic composites as promising green-composites for automotive industries!, Bioresour. Technol. 99 (11) (2008) 4661−4667. Available from: https://doi.org/10.1016/j.biortech.2007.09.043.

[118] D. Ray, State-of-the-art applications of natural fiber composites in the industry, Natural Fiber Composites. (2016) 319−340.

[119] O. Akampumuza, P.M. Wambua, A. Ahmed, W. Li, X.-H. Qin, Review of the applications of biocomposites in the automotive industry, Polym. Compos. 38 (11) (2017) 2553–2569. Available from: https://doi.org/10.1002/pc.23847.
[120] A. Bouzouita, D. Notta-Cuvier, J.-M. Raquez, F. Lauro, P. Dubois, Poly(lactic acid)-based materials for automotive applications, in: M.L. Di Lorenzo, R. Androsch (Eds.), Industrial Applications of Poly(lactic acid), Springer International Publishing, 2018, pp. 177–219. Available from: https://doi.org/10.1007/12_2017_10.
[121] J. Holbery, D. Houston, Natural-fiber-reinforced polymer composites in automotive applications, JOM 58 (11) (2006) 80–86. Available from: https://doi.org/10.1007/s11837-006-0234-2.
[122] C. Alves, P.M.C. Ferrão, A.J. Silva, L.G. Reis, M. Freitas, L.B. Rodrigues, et al., Ecodesign of automotive components making use of natural jute fiber composites, J. Clean. Prod. 18 (4) (2010) 313–327. Available from: https://doi.org/10.1016/j.jclepro.2009.10.022.
[123] A.K. Mohanty, M. Misra, L.T. Drzal (Eds.), Natural Fibers, Biopolymers, and Biocomposites, Routledge & CRC Press, 2005. Available from: https://www.routledge.com/Natural-Fibers-Biopolymers-and-Biocomposites/Mohanty-Misra-Drzal/p/book/9780849317415.
[124] G. Koronis, A. Silva, M. Fontul, Green composites: a review of adequate materials for automotive applications, Compos. B Eng. 44 (1) (2013) 120–127. Available from: https://doi.org/10.1016/j.compositesb.2012.07.004.
[125] R. Stewart, Automotive composites offer lighter solutions, Reinforced Plast. 54 (2) (2010) 22–28. Available from: https://doi.org/10.1016/S0034-3617(10)70061-8.
[126] S.P. Rawal, Metal-matrix composites for space applications, JOM 53 (4) (2001) 14–17. Available from: https://doi.org/10.1007/s11837-001-0139-z.
[127] A. Bismarck, A. Baltazar-Y-Jimenez, K. Sarikakis, Green composites as panacea? Socio-economic aspects of green materials, Environment, Dev. Sustain. 8 (3) (2006) 445–463. Available from: https://doi.org/10.1007/s10668-005-8506-5.
[128] M.J. John, S. Thomas, Biofibres and biocomposites, Carbohydr. Polym. 71 (3) (2008) 343–364. Available from: https://doi.org/10.1016/j.carbpol.2007.05.040.
[129] A. Llevot, P.-K. Dannecker, M. von Czapiewski, L.C. Over, Z. Söyler, M.A.R. Meier, Renewability is not enough: recent advances in the sustainable synthesis of biomass-derived monomers and polymers, Chem. Eur. J. 22 (33) (2016) 11510–11521. Available from: https://doi.org/10.1002/chem.201602068.
[130] J. Njuguna, K. Pielichowski, S. Desai, Nanofiller-reinforced polymer nanocomposites, Polym. Adv. Technol. 19 (8) (2008) 947–959. Available from: https://doi.org/10.1002/pat.1074.
[131] T. Tsujimoto, H. Uyama, S. Kobayashi, Green nanocomposites from renewable resources: biodegradable plant oil-silica hybrid coatings, Macromol. Rapid Commun. 24 (12) (2003) 711–714. Available from: https://doi.org/10.1002/marc.200350015.
[132] D. Akram, S. Ahmad, E. Sharmin, S. Ahmad, Silica reinforced organic–inorganic hybrid polyurethane nanocomposites from sustainable resource, Macromol. Chem. Phys. 211 (4) (2010) 412–419. Available from: https://doi.org/10.1002/macp.200900404.
[133] M. Du, B. Guo, D. Jia, Newly emerging applications of halloysite nanotubes: a review, Polym. Int. 59 (5) (2010) 574–582. Available from: https://doi.org/10.1002/pi.2754.
[134] G. Cavallaro, G. Lazzara, S. Milioto, F. Parisi, Halloysite nanotubes as sustainable nanofiller for paper consolidation and protection, J. Therm. Anal. Calorim. 117 (3) (2014) 1293–1298. Available from: https://doi.org/10.1007/s10973-014-3865-5.

[135] Y. Lvov, W. Wang, L. Zhang, R. Fakhrullin, Halloysite Clay Nanotubes for Loading and Sustained Release of Functional Compounds, Adv. Mater. 28 (6) (2016) 1227–1250. Available from: https://doi.org/10.1002/adma.201502341.

[136] M. Wang, S. Li, Y. Zhang, J. Huang, Hierarchical SnO2/carbon nanofibrous composite derived from cellulose substance as anode material for lithium-ion batteries, Chem. Eur. J. 21 (45) (2015) 16195–16202. Available from: https://doi.org/10.1002/chem.201502833.

[137] S. Zhou, M. Strømme, C. Xu, Highly transparent, flexible, and mechanically strong nanopapers of cellulose nanofibers @metal–organic frameworks, Chem. Eur. J. 25 (14) (2019) 3515–3520. Available from: https://doi.org/10.1002/chem.201806417.

[138] T. Baran, N.Y. Baran, A. Menteş, Sustainable chitosan/starch composite material for stabilization of palladium nanoparticles: synthesis, characterization and investigation of catalytic behaviour of Pd@chitosan/starch nanocomposite in Suzuki–Miyaura reaction, Appl. Organomet. Chem. 32 (2) (2018) e4075. Available from: https://doi.org/10.1002/aoc.4075.

[139] S.R. Beeren, S. Meier, O. Hindsgaul, Probing helical hydrophobic binding sites in branched starch polysaccharides using NMR spectroscopy, Chem. Eur. J. 19 (48) (2013) 16314–16320. Available from: https://doi.org/10.1002/chem.201302213.

[140] L. Jong, Natural rubber protein as interfacial enhancement for bio-based nano-fillers, J. Appl. Polym. Sci. 130 (3) (2013) 2188–2197. Available from: https://doi.org/10.1002/app.39277.

[141] L. Zhang, W. Liu, W. Shi, X. Xu, J. Mao, P. Li, et al., Boosting lithium storage properties of MOF derivatives through a wet-spinning assembled fiber strategy, Chem. Eur. J. 24 (52) (2018) 13792–13799. Available from: https://doi.org/10.1002/chem.201802826.

[142] C. Cho, M. Culebras, K.L. Wallace, Y. Song, K. Holder, J.-H. Hsu, et al., Stable n-type thermoelectric multilayer thin films with high power factor from carbonaceous nanofillers, Nano Energy 28 (2016) 426–432. Available from: https://doi.org/10.1016/j.nanoen.2016.08.063.

[143] J. Ding, O.u Rahman, Q. Wang, W. Peng, H. Yu, Sustainable graphene suspensions: a reactive diluent for epoxy composite valorization, ACS Sustain. Chem. Eng. 5 (9) (2017) 7792–7799. Available from: https://doi.org/10.1021/acssuschemeng.7b01282.

[144] L.A.-W. Ellingsen, C.R. Hung, G. Majeau-Bettez, B. Singh, Z. Chen, M.S. Whittingham, et al., Nanotechnology for environmentally sustainable electromobility, Nat. Nanotechnol. 11 (12) (2016) 1039–1051. Available from: https://doi.org/10.1038/nnano.2016.237.

[145] C.-F. Chow, W.-L. Wong, K.Y.-F. Ho, C.-S. Chan, C.-B. Gong, Combined chemical activation and Fenton degradation to convert waste polyethylene into high-value fine chemicals, Chem. Eur. J. 22 (28) (2016) 9513–9518. Available from: https://doi.org/10.1002/chem.201600856.

[146] Y. Fang, X. Du, Y. Jiang, Z. Du, P. Pan, X. Cheng, et al., Thermal-driven self-healing and recyclable waterborne polyurethane films based on reversible covalent interaction, ACS Sustain. Chem. Eng. 6 (11) (2018) 14490–14500. Available from: https://doi.org/10.1021/acssuschemeng.8b03151.

[147] I.R.S. Vieira, G.d S. Miranda, E. Ricci-Júnior, M.C. Delpech, Waterborne poly(urethane-urea)s films as a sustained release system for ketoconazole, E-Polymers 19 (1) (2019) 168–180. Available from: https://doi.org/10.1515/epoly-2019-0018.

[148] W. Fang, L. Liu, G. Guo, Tunable wettability of electrospun polyurethane/silica composite membranes for effective separation of water-in-oil and oil-in-water emulsions,

Chem. Eur. J. 23 (47) (2017) 11253–11260. Available from: https://doi.org/10.1002/chem.201701409.

[149] O.I.H. Dimitry, Z. Abdeen, E.A. Ismail, A.L.G. Saad, Studies of particle dispersion in elastomeric polyurethane/organically modified montmorillonite nanocomposites, Int. J. Green Nanotechnol. 3 (3) (2011) 197–212. Available from: https://doi.org/10.1080/19430892.2011.628585.

[150] A. Ambrosi, M. Pumera, Electrochemically exfoliated graphene and graphene oxide for energy storage and electrochemistry applications, Chem. Eur. J. 22 (1) (2016) 153–159. Available from: https://doi.org/10.1002/chem.201503110.

[151] Y. Shen, S. Zhang, H. Li, Y. Ren, H. Liu, Efficient synthesis of lactic acid by aerobic oxidation of glycerol on Au–Pt/$TiO_2$ catalysts, Chem. Eur. J. 16 (25) (2010) 7368–7371. Available from: https://doi.org/10.1002/chem.201000740.

[152] H. Longkullabutra, W. Thamjaree, W. Nhuapeng, Improvement in the tensile strength of epoxy resin and hemp/epoxy resin composites using carbon nanotubes, Adv. Mater. Res. 93–94 (2010) 497–500. Available from: https://doi.org/10.4028/http://www.scientific.net/AMR.93-94.497.

[153] Z. Liu, S.Z. Erhan, "Green" composites and nanocomposites from soybean oil, Mater. Sci. Eng. A 483–484 (2008) 708–711. Available from: https://doi.org/10.1016/j.msea.2006.12.186.

[154] O. Faruk, L.M. Matuana, Nanoclay reinforced HDPE as a matrix for wood-plastic composites, Compos. Sci. Technol. 68 (9) (2008) 2073–2077. Available from: https://doi.org/10.1016/j.compscitech.2008.03.004.

[155] C. Vilela, C.S.R. Freire, P.A.A.P. Marques, T. Trindade, C. Pascoal Neto, P. Fardim, Synthesis and characterization of new CaCO3/cellulose nanocomposites prepared by controlled hydrolysis of dimethylcarbonate, Carbohydr. Polym. 79 (4) (2010) 1150–1156. Available from: https://doi.org/10.1016/j.carbpol.2009.10.056.

[156] J. Njuguna, P. Wambua, K. Pielichowski, K. Kayvantash, Natural fibre-reinforced polymer composites and nanocomposites for automotive applications, in: S. Kalia, B.S. Kaith, I. Kaur (Eds.), Cellulose Fibers: Bio- and Nano-Polymer Composites, Springer Berlin Heidelberg, 2011, pp. 661–700. Available from: https://doi.org/10.1007/978-3-642-17370-7_23.

[157] D. Notta-Cuvier, M. Murariu, J. Odent, R. Delille, A. Bouzouita, J.-M. Raquez, et al., Tailoring polylactide properties for automotive applications: effects of co-addition of halloysite nanotubes and selected plasticizer, Macromol. Mater. Eng. 300 (7) (2015) 684–698. Available from: https://doi.org/10.1002/mame.201500032.

[158] R. Arjmandi, A. Hassan, S.J. Eichhorn, M.K. Mohamad Haafiz, Z. Zakaria, F.A. Tanjung, Enhanced ductility and tensile properties of hybrid montmorillonite/cellulose nanowhiskers reinforced polylactic acid nanocomposites, J. Mater. Sci. 50 (8) (2015) 3118–3130. Available from: https://doi.org/10.1007/s10853-015-8873-8.

[159] R. Arjmandi, A. Hassan, M.K.M. Haafiz, Z. Zakaria, Effect of microcrystalline cellulose on biodegradability, tensile and morphological properties of montmorillonite reinforced polylactic acid nanocomposites, Fibers Polym. 16 (10) (2015) 2284–2293. Available from: https://doi.org/10.1007/s12221-015-5507-3.

[160] R. Arjmandi, A. Hassan, M.K. Mohamad Haafiz, Z. Zakaria, Tensile and morphological properties of hybrid montmorillonite/microcrystalline cellulose filled polylactic acid composites: effect of filler ratio, Adv. Mater. Res. 1125 (2015) 271–275. Available from: https://doi.org/10.4028/http://www.scientific.net/AMR.1125.271.

[161] V. Sabatini, H. Farina, L. Basilissi, G. Di Silvestro, M.A. Ortenzi, The use of epoxy silanes on montmorillonite: an effective way to improve thermal and rheological

properties of PLA/MMT nanocomposites obtained via "in situ" polymerization, J. Nanomaterials 2015 (2015) e418418. Available from: https://doi.org/10.1155/2015/418418.

[162] C.-S. Wu, Renewable resource-based composites of recycled natural fibers and maleated polylactide bioplastic: characterization and biodegradability, Polym. Degrad. Stab. 94 (7) (2009) 1076−1084. Available from: https://doi.org/10.1016/j.polymdegradstab.2009.04.002.

[163] S.-I. Moon, F. Jin, C. Lee, S. Tsutsumi, S.-H. Hyon, Novel carbon nanotube/poly(L-lactic acid) nanocomposites; their modulus, thermal stability, and electrical conductivity, Macromol. Symposia 224 (1) (2005) 287−296. Available from: https://doi.org/10.1002/masy.200550625.

[164] I.R.S. Vieira, L.d F.d O. Costa, G.d S. Miranda, S. Nardecchia, M.S.d S.d B. Monteiro, E. Ricci-Júnior, et al., Waterborne poly(urethane-urea)s nanocomposites reinforced with clay, reduced graphene oxide and respective hybrids: synthesis, stability and structural characterization, J. Polym. Environ. 28 (1) (2020) 74−90. Available from: https://doi.org/10.1007/s10924-019-01584-y.

[165] P.K. Ang, M. Jaiswal, C.H.Y.X. Lim, Y. Wang, J. Sankaran, A. Li, et al., A bioelectronic platform using a graphene − lipid bilayer interface, ACS Nano 4 (12) (2010) 7387−7394. Available from: https://doi.org/10.1021/nn1022582.

[166] O.C. Compton, S.T. Nguyen, Graphene oxide, highly reduced graphene oxide, and graphene: versatile building blocks for carbon-based materials, Small 6 (6) (2010) 711−723. Available from: https://doi.org/10.1002/smll.200901934.

[167] S.-R. Ryoo, Y.-K. Kim, M.-H. Kim, D.-H. Min, Behaviors of NIH-3T3 fibroblasts on graphene/carbon nanotubes: proliferation, focal adhesion, and gene transfection studies, ACS Nano 4 (11) (2010) 6587−6598. Available from: https://doi.org/10.1021/nn1018279.

[168] Y. Zhu, S. Murali, W. Cai, X. Li, J.W. Suk, J.R. Potts, et al., Graphene and graphene oxide: synthesis, properties, and applications, Adv. Mater. 22 (35) (2010) 3906−3924. Available from: https://doi.org/10.1002/adma.201001068.

[169] J.I. Paredes, S. Villar-Rodil, A. Martínez-Alonso, J.M.D. Tascón, Graphene oxide dispersions in organic solvents, Langmuir 24 (19) (2008) 10560−10564. Available from: https://doi.org/10.1021/la801744a.

[170] X. Sun, Z. Liu, K. Welsher, J.T. Robinson, A. Goodwin, S. Zaric, et al., Nano-graphene oxide for cellular imaging and drug delivery, Nano Res. 1 (3) (2008) 203−212. Available from: https://doi.org/10.1007/s12274-008-8021-8.

[171] H. Wang, Z. Qiu, Crystallization behaviors of biodegradable poly(l-lactic acid)/graphene oxide nanocomposites from the amorphous state, Thermochim. Acta 526 (1) (2011) 229−236. Available from: https://doi.org/10.1016/j.tca.2011.10.006.

[172] J. Singh, A.S. Dhaliwal, Water retention and controlled release of KCl by using microwave-assisted green synthesis of xanthan gum-cl-poly (acrylic acid)/AgNPs hydrogel nanocomposite, Polym. Bull. 77 (9) (2020) 4867−4893. Available from: https://doi.org/10.1007/s00289-019-02990-x.

[173] R. Arjmandi, A. Hassan, Z. Zakaria, Polylactic acid green nanocomposites for automotive applications, in: M. Jawaid, M.S. Salit, O.Y. Alothman (Eds.), Green Biocomposites: Design and Applications, Springer International Publishing, 2017, pp. 193−208. Available from: https://doi.org/10.1007/978-3-319-49382-4_9.

[174] J.-H. Chang, Y.U. An, D. Cho, E.P. Giannelis, Poly(lactic acid) nanocomposites: comparison of their properties with montmorillonite and synthetic mica (II), Polymer 44 (13) (2003) 3715−3720. Available from: https://doi.org/10.1016/S0032-3861(03)00276-3.

[175] G. Gorrasi, C. Milone, E. Piperopoulos, M. Lanza, A. Sorrentino, Hybrid clay mineral-carbon nanotube-PLA nanocomposite films. Preparation and photodegradation effect on their mechanical, thermal and electrical properties, Appl. Clay Sci. 71 (2013) 49–54. Available from: https://doi.org/10.1016/j.clay.2012.11.004.

[176] Q.K. Meng, M. Hetzer, D. De Kee, PLA/clay/wood nanocomposites: nanoclay effects on mechanical and thermal properties, J. Composite Mater. 45 (10) (2011) 1145–1158. Available from: https://doi.org/10.1177/0021998310381541.

[177] S. Santangelo, G. Gorrasi, R.D. Lieto, S.D. Pasquale, G. Patimo, E. Piperopoulos, et al., Polylactide and carbon nanotubes/smectite-clay nanocomposites: preparation, characterization, sorptive and electrical properties, Appl. Clay Sci. 2 (53) (2011) 188–194. Available from: https://doi.org/10.1016/j.clay.2010.12.013.

[178] M.A. Morsi, A.H. Oraby, A.G. Elshahawy, R.M. Abd El-Hady, Preparation, structural analysis, morphological investigation and electrical properties of gold nanoparticles filled polyvinyl alcohol/carboxymethyl cellulose blend, J. Mater. Res. Technol. 8 (6) (2019) 5996–6010. Available from: https://doi.org/10.1016/j.jmrt.2019.09.074.

[179] A. Kausar, Polyamide 1010/polythioamide blend reinforced with graphene nanoplatelet for automotive part application, Adv. Mater. Sci. 17 (3) (2017) 24–36. Available from: https://doi.org/10.1515/adms-2017-0013.

[180] A.B. Irez, E. Bayraktar, I. Miskioglu, Fracture toughness analysis of epoxy-recycled rubber-based composite reinforced with graphene nanoplatelets for structural applications in automotive and aeronautics, Polymers 12 (2) (2020) 448. Available from: https://doi.org/10.3390/polym12020448.

[181] F.M. AL-Oqla, S.M. Sapuan, M.R. Ishak, A.A. Nuraini, A decision-making model for selecting the most appropriate natural fiber – polypropylene-based composites for automotive applications, J. Composite Mater. 50 (4) (2016) 543–556. Available from: https://doi.org/10.1177/0021998315577233.

[182] T. Ramanathan, A.A. Abdala, S. Stankovich, D.A. Dikin, M. Herrera-Alonso, R.D. Piner, et al., Functionalized graphene sheets for polymer nanocomposites, Nat. Nanotechnol. 3 (6) (2008) 327–331. Available from: https://doi.org/10.1038/nnano.2008.96.

[183] C. Wan, B. Chen, Reinforcement and interphase of polymer/graphene oxide nanocomposites, J. Mater. Chem. 22 (8) (2012) 3637–3646. Available from: https://doi.org/10.1039/C2JM15062J.

[184] D.W. Schaefer, R.S. Justice, How nano are nanocomposites? Macromolecules 40 (24) (2007) 8501–8517. Available from: https://doi.org/10.1021/ma070356w.

[185] X. Zheng, M.G. Forest, R. Vaia, M. Arlen, R. Zhou, A strategy for dimensional percolation in sheared nanorod dispersions, Adv. Mater. 19 (22) (2007) 4038–4043. Available from: https://doi.org/10.1002/adma.200700011.

[186] M. Yoonessi, Y. Shi, D.A. Scheiman, M. Lebron-Colon, D.M. Tigelaar, R.A. Weiss, et al., Graphene polyimide nanocomposites; thermal, mechanical, and high-temperature shape memory effects, ACS Nano 6 (9) (2012) 7644–7655. Available from: https://doi.org/10.1021/nn302871y.

[187] O. Adekomaya, Adaption of green composite in automotive part replacements: discussions on material modification and future patronage, Environ. Sci. Pollut. Res. 27 (8) (2020) 8807–8813. Available from: https://doi.org/10.1007/s11356-019-07557-x.

[188] M.C. Coelho, G. Torrão, N. Emami, J. Grćio, Nanotechnology in automotive industry: research strategy and trends for the future—small objects, big impacts, J. Nanosci. Nanotechnol. 12 (8) (2012) 6621–6630. Available from: https://doi.org/10.1166/jnn.2012.4573.

# Polymer nanocomposites for road construction: investigating the aging performance of polymer and carbon nanotube–modified asphalt binder

12

*Md Arifuzzaman*
Department of Civil and Environmental Engineering, King Faisal University, Al Hofuf, Saudi Arabia

## 12.1 Introduction

The aging of asphalt is a universal phenomenon that may occur anywhere in the world and could be related to internal chemical changes in the asphalt binder. Throughout the world, engineers and researchers work to explain the aging phenomenon of asphalt binder. The exact extent of damaged roadway/highway is not precisely known/reported in the open research literature, due to the very complex and highly nonlinear nature of aging in asphalt pavement [1]. Even the recently developed MEPDG software, which has been adopted in almost 48 states in the United States, does not incorporate aging phenomena in asphalt binder in the long service life of highways [2]. It is therefore necessary to carry out a study of the aging mechanism on asphalt roads. Many literatures found the use of nanocomposite to resist the aging effect [3–5].

It has been stated that aging happens because of oxidation inside the asphalt binder [6,7]. Oxidation in hot-mix asphalt concrete (HMAC) pavement makes it stiffer with oldness. As asphalt ages, subject to mainly the binder's chemical structure, composition as well as environmental factors, the asphalt pavement becomes more and more vulnerable to fracture under different stresses produced by different traffic loads [8]. Two types of aging are described in the research: long term and short term. Although long-term aging is thought to occur throughout long service life in the pavement structure, short-time aging occurs during transportation and storage. In the laboratory, both types can be simulated using rolling thin-film oven (RTFO) and pressure aging vessel (PAV) processing.

During the last few years, the demand for asphaltic materials in the Gulf region, particularly in Saudi Arabia, has increased markedly, due to the rehabilitation of existing highways and the construction of new highways to neighboring countries. The local refineries have been under pressure to meet this high demand in a short

**Advanced Polymer Nanocomposites. DOI: https://doi.org/10.1016/B978-0-12-824492-0.00004-0**


period. This has led to variation in the quality of asphalt produced by the local refineries. In addition, the local highway construction industry is currently facing problems in meeting the performance grade (PG) criteria for different regions of Saudi Arabia. As a result, the aging of asphalt is a significant factor in the region.

Hot-mix asphalt pavements subsequently turn out to be stiffer with age mainly due to oxidization. As they grow older, mainly subjected to asphalt chemistry and local ecology-related factors, asphalt made pavements befall vulnerable to malfunction under loads caused by heavy vehicles. Fresh samples of modified asphalts may pass the PG criteria, but aged (RTFO processed) asphalts may not satisfy them. This may be due to variations in the quality of asphalt being produced locally. Therefore the study of the asphalt aging process from both chemical and nanoscale points of view may help in addressing the issue.

This paper deals with aging in asphalt binder, which can direct to early and premature degradation of asphaltic pavements. In pavement engineering, asphalt aging has been described as the time-dependent performance depreciation of asphalt binder which occurs with time and is caused by several factors including oxidation, sunlight, heat, and moisture. Aging can be simulated in the laboratory using an air-convection oven. The current research focuses on the aging characterization of nanocomposites [carbon nanotubes (CNTs)] and polymer-modified asphalt binder with different additives using chemical force microscopy (CFM) tips.

## 12.2 Background of current study

The application of nano- to microlevel laboratory testing and technologies to the aging behavior in asphalt binder have been elaborated in various studies. For example, Adham and Arifuzzaman (2014) used CNT to investigate moisture damage in asphalt binder [9], and Hassan (2015) used CNT and artificial neural networks (ANNs) to model the damage due to moisture [10–14]. Tarefder et al. (2016) studied the aging of mica-modified asphalt binder without atomic force microscope (AFM) and ANN utilizations [15].

Zhang et al. considered the morphological change in asphalt utilizing AFM without further numerical and modeling work [16]. Rebeloa et al. (2014) investigated asphalt binder aging with AFM with rectangular silicon cantilevers. The study was questionable since silicon cantilevers only produce adhesion force [17].

Le Guern et al. (2010) employed IATROSCAN chromatography, FTIR (fourier transform infrared spectrometer) spectroscopy, and differential scanning calorimetry to identify the molecular organization and chemical species before and after artificial aging of asphalt binder [18]. Ouyang et al. (2006) evaluated the aging of base asphalt and styrene-butadiene-styrene (SBS)-modified asphalts using FTIR spectroscopy [19]. The X-ray diffraction (XRD) method was employed by Siddiqui et al. [20] to determine the aging pattern of asphalt fractions. Hesp et al. (2007) utilized XRD, mass spectrometry, and optical microscopy techniques to simplify the chemical and morphological features that are accountable for the reversible aging processes in asphalt binders [21]. XRD and nuclear magnetic resonance imaging were

employed by Siddiqui and Ali [22] to discover the likelihood of the occurrence of reaction mechanisms in laboratory aging, while Lamontagne et al. (2001) used FTIR [23] to expose the changes in the chemical structure of asphalt with aging. Lee et al. (2010) studied the thermal oxidation of SBS copolymer using a variety of analytical and spectroscopic methods, including dynamic mechanical analysis, thermal analysis, and FTIR spectroscopy. The experimental results indicated that the thermal oxidation of SBS is a free-radical self-catalyzing reaction including initiation, development, transfer, and expiry of the chain of four steps with both scission and cross-linking [24]. Wu et al. (2009) investigated the effect of aging on base bitumen and SBS-modified binders with the help of FTIR, dynamic shear rheometry and AFM. They used -$Si_3N_4$ AFM tips which derived the adhesion forces only [25].

Gandhi et al. (2009) considered the aging character of warm-mix asphalt (WMA) binders, which is not known in detail, using a pressure aging vessel and RTFO. The study found that the aging of WMA binders can be reduced by reducing the mixing temperatures, and the rutting resistance of the binders [26]. Cong et al. (2010) studied the effects of aging of asphalt binders modified with flame retardants (FRs) and SBS. RTFO and PAV were engaged to age asphalt binders in the laboratory. They concluded that the flame retardancy of the asphalt binder was increased after aging by RTFOT and PAV [27]. Banerjee et al. (2012) quantified the long-term aging consequences on the rheological possessions of WMA. In this study, the researchers used four types of WMA additives: Sasobit, Evotherm, Rediset, and Cecabase. The effect of aging on the rheological properties, specifically the complex shear modulus, of the binders in the laboratory environment was evaluated [28]. Ruan et al. (2003) studied the long-term aging of polymer-modified asphalt binders. They used diblock poly, triblock poly, and tire rubber as modifiers. The asphalt aging was conducted at 60°C in a controlled environmental chamber and at 100°C in PAV [29]. Cao and Ji (2011) studied the behavior of Sasobit-modified asphalt for aging. The 2%, 3%, 4%, and 5% Sasobit were used by the mass of asphalt binder. The PAV and RTFO methods simulated the long-term and short-term aging separately in the experiment [30]. Lins et al. (2008) considered photodegradation in asphalts pavements, especially in geographical regions where high-intensity solar radiation occurs [31]. Kim and Lee (2003) investigated the effect of oxidative aging of asphalt binders on the fatigue fracture properties and material characteristics during dynamic mechanical and controlled-strain testing. In the study, cylindrical sand asphalt samples were manufactured with two aged and an unaged binder [32].

Othman (2010) also studied the effect of the application of polypropylene on long-term aging in hot-mix asphalt. Three methods, namely the wet method, the dry method, and the coating method, were considered, and the aggregate surface was coated with polypropylene [33]. An investigation of the effect of customary aging laboratory-based methods on the rheological properties of asphalt binder was conducted by Molenaar et al. [34]. They compared laboratory outcomes with the results of field-aged binders. The results showed that laboratory methods for long-term aging are not able of simulating field aging. Zhang et al. (2011) considered the impact of long-term and short-term oxidative thermal aging on the thermal stability

and dynamic viscosity of SBS-mixed binder and storage-related stable SBS and sulfur-mixed binder. The outcomes showed that the sulfur addition consequences more changes in the binder's viscous performance owing to aging likened with sulfur-modified SBS binder [35].

Aging in asphalt pavement has been investigated by researchers for a long time. Most of the investigations have been based on macroscale testing, but the changes due to aging are chemical changes, which initiate from the molecular level. Hence, previous studies are questionable. Moreover, the current literature review found very few attempts to study the aging phenomena in asphalt binders using functionalized (asphalt chemical) CFM tips for CNT- and polymer-modified asphalt binders.

Hence the objectives of this research are to:

1. Find an appropriate relationship between asphalt chemistry changes and asphalt aging.
2. Compare polymer and CNT nanocomposite modification on aging based on CFM tests.
3. Determine the best percentages of polymer and CNT nanocomposites to resist aging in asphalt binder.

## 12.3 CFM test protocol

CFM machine was used to conduct laboratory experiments on all aged and unaged asphalt samples, and the schematic diagram is shown as in Fig. 12.1. Basically, CFM is the modified version of AFM. A detailed description of AFM also can be

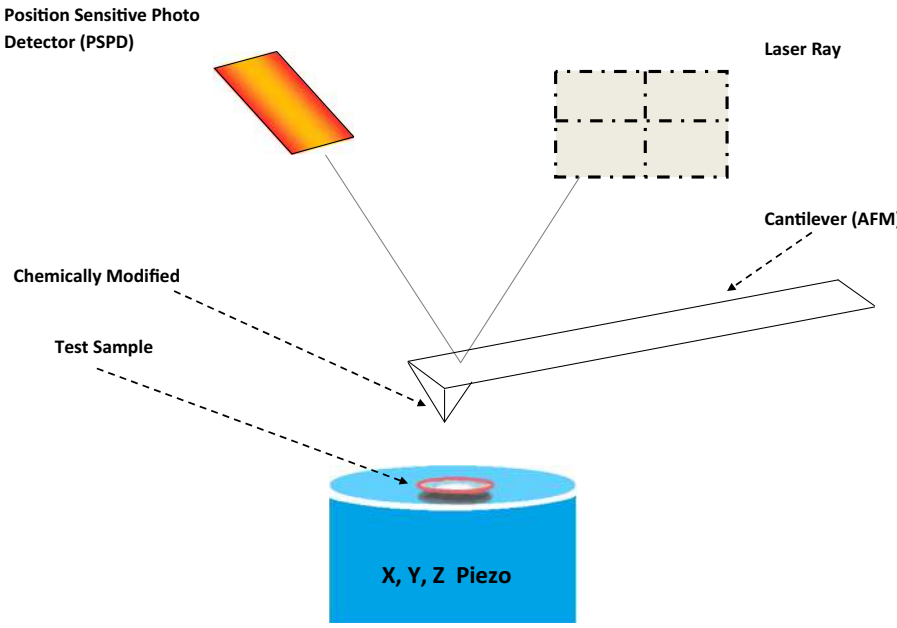


**Figure 12.1** Schematic diagram of CFM.

found in [11]. A thin asphalt binder film sample was placed in a glass substrate for AFM testing. Thin asphalt film was used for many reasons: pavements made of HMAC age more and more rapidly at the top surface due to elevated temperatures, with redundant oxygen, as well as the presence of moisture and sunlight.

Moreover, the binder portion at the surface of an asphalt-made road becomes brittle earlier than the binder, which is found even half an inch beneath the surface. In the study, very thin (around 1 mm height) samples with 4 mm long and 4 mm wide areas were tested under CFM.

### 12.3.1 CFM tip functionalization

The results of the chemical analysis of asphalts from several sources are presented in Table 12.1, which shows that the percentages of elements are not unique.

Based on the presence of major elements, to find the cohesion forces among similar elements, the current study found that the most common radicals are −COOH and −OH that match the similarities of asphalt binders when tested with CFM tips.

Furthermore, Fig. 12.2 shows the percentages of Saudi Arabian asphalt graphically.

Murgich et al. (1996) proposed the asphalt model, where the −OH functional group is also visible, as shown in Fig. 12.3. Hence this study proposes −OH functionalization of AFM probes so that the derived force value in terms of nano-Newtons can be assumed as the −OH (tip) to −OH (asphalt) interaction, which in terms defined as the cohesion forces in asphalt binder [36].

Therefore the current study selected −COOH and −OH functionals as the most suitable for acquiring cohesion forces in fresh and aged asphalt binder. Because −OH functional percentage in asphalt is the maximum and significant amount, this agent is used to modify all CFM tips for test and research work.

The base asphalt binder samples were firstly modified with 4% as well as 5% styrene-butadiene (SB) and SBS polymers. Later, the samples were mingled with 0.5%, 1.0%, and 1.5% of single-walled carbon nanotubes in an elevated temperature like the field mixing process.

**Table 12.1** Results from elementary analysis of representative refinery asphalts [6].

| Elements | Mexican blend | California | Arkansas-Louisiana | Boscan | Saudi Arabia (Riyadh) |
|---|---|---|---|---|---|
| Carbon, % | 83.77 | 86.77 | 85.78 | 82.90 | 84.25 |
| Hydrogen, % | 9.91 | 10.93 | 10.19 | 10.45 | 10.14 |
| Sulfur, % | 5.25 | 0.99 | 3.41 | 5.43 | 4.99 |
| Nitrogen, % | 0.28 | 0.26 | 0.78 | 1.10 | 0.41 |
| Oxygen, % | 0.77 | 0.20 | 0.36 | 0.29 | 0.21 |
| Nickel, ppm | 22 | 6 | 0.4 | 109 | 3.59 |
| Vanadium, ppm | 180 | 4 | 7 | 1380 | 97 |

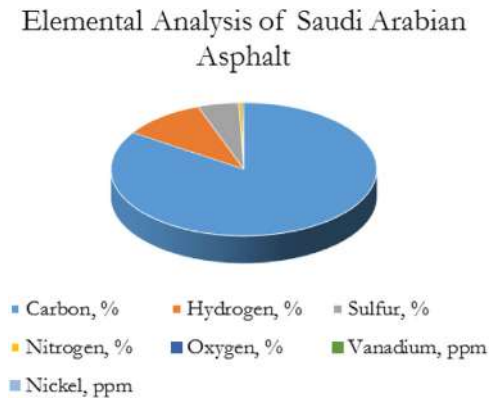


**Figure 12.2** Elemental analysis results of asphalt binder.

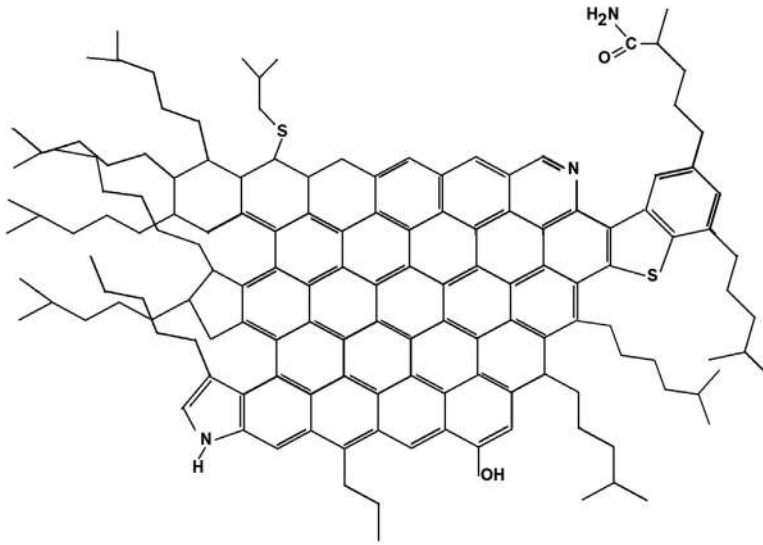


**Figure 12.3** Model of asphalt molecule: two-dimensional view [32].

All the samples were aged in a Superpave heavy-duty oven for a continuous 7 days at 60°C. The heating condition was forced-air convection to simulate accelerated field conditions [37].

### *12.3.1.1 Calibration of CFM tips*

To find the realistic CFM force adhesion values, understanding the real number of ($k$) values that represent the cantilever spring constant is required [38–40]. The task was done in the current study through the aid of the automated tip calibration

procedure, which is available with the CFM software. The cantilevers were calibrated by measuring the force−distance (F−D) curve on a platinum-coated and firm reference sample and using the suggested cantilever. The derived gradient of the force curve was defined as stiffness ($S$). Hence, $S_{ref}$ the deflection-related sensitivity of the reference cantilever and $S_{hard}$ the deflection-related sensitivity of the hard surface, were quantified. The procedure manual shows that the spring constant of the reference cantilever is $k_{ref}$. The final equation for calibrated $k$ value can be shown as:

$$k = \left(\frac{S\text{ref}}{S\text{hard}} - 1\right) k\text{ref} \tag{12.1}$$

### 12.3.1.2 Description of CNT

CNTs are molecular-level graphitic kind of carbon tubes that possess outstanding possessions. They are considered as one of the stiffest and strongest materials ever combined with the asphalt binders, and also partake noteworthy electronic chattels which may help AFM test conduction. Numerous academic and industrial interests have been served to these materials, and hundreds of journal and conference proceedings go on nanotubes are issued per annum. Nevertheless, the manufacturing price of the good quality CNT is rather extreme, which shrinks their use in commercial usages.

CNT configure into graphite matter resembles a carbon-made flat sheet atoms having hexagonally packed and bonded structure called graphene. The sheets of these graphenes are revolved at a specific angle, and then the effects of CNTs are completed by the amalgamation of the rolling angle and radius. Fig. 12.4A shows the basic components of the carbon tube sheets in two-dimensional (2D) view, and Fig. 12.4B shows the rolled tubes that create the tubes. The CNT is almost 10 times tougher than stainless steel and possesses one-fourth of its denseness; the hollow form of CNT provides a strong and additional structure which may form an antiaging agent between the aggregate and asphalt binder. Two types of carbon nanotubes are used for reinforcing asphalt binders and mixtures: single-walled nanotubes (SWNTs) and double-walled nanotubes. In this study, only SWNT was consumed to investigate the aging of asphalt binders.

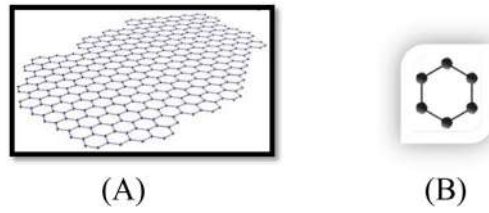


**Figure 12.4** (A) Graphene (2D view). (B) Graphite (2D view).

## 12.4 Results and discussion

The study accomplished laboratory testing of fresh and aged asphalt samples modified with polymers and CNTs using a CFM machine. The graphs of the CFM-derived force−distance (F−D) trend line for the aged and fresh asphalt samples modified with SB and CNT are presented in Fig. 12.5. This is the main output derived from laboratory testing. The horizontal axis shows the distance between the sample and the CFM tip (in nanometers), and the vertical axis shows the cohesion forces (in nanoNewtons) between the CFM tip and the asphalt samples. The cohesion forces are computed for the red line (the force difference between the axis to the lowest point).

The blue line represents the approach path towards the sample, whereas the red line shows the retraction path. Fig. 12.5A shows the F−D curve for a fresh (unaged) sample, and Fig. 12.5B shows the F−D curve for an aged sample. Both the asphalt samples were modified with 5% SB and 1.5% SWNT. The aged sample shows a noticeable and distinct shape, which is different from the fresh sample that seems to have been chemically distorted.

The results obtained from all the CFM testing are presented in Table 12.2 with the percentage variation for comparison purposes. The percentage variation was calculated based on the equation:

$$\text{Cohesion force change } (\%) = \frac{(\text{Aged sample force} - \text{Fresh sample force})}{\text{Fresh sample force}} \tag{12.2}$$

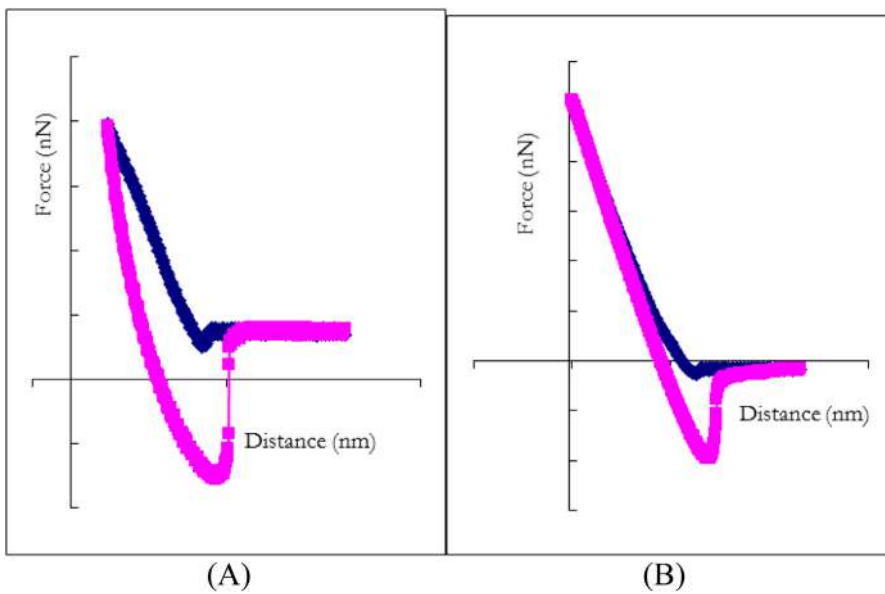


**Figure 12.5** Fresh sample (5% SB and 1.5% SWNT) and aged sample (5% SB and 1.5% SWNT) derived with −OH-modified CFM tips. (A) Fresh sample; (B) aged sample.

**Table 12.2** Cohesion forces (nN) as measured with −OH-modified CFM tips with the % variation for aged samples.

| CNT % | Fresh sample | | | | Aged sample | | | | % Variation | | | |
|---|---|---|---|---|---|---|---|---|---|---|---|---|
| | 4% SB | 5% SB | 4% SBS | 5% SBS | 4% SB | 5% SB | 4% SBS | 5% SBS | 4% SB | 5% SB | 4% SBS | 5% SBS |
| 0 | 128.58 | 125.63 | 123.34 | 73.26 | 164.61 | 149.70 | 130.98 | 79.79 | 28.03 | 19.16 | 6.20 | 8.91 |
| 0.5 | 84.80 | 104.89 | 80.12 | 98.25 | 120.69 | 135.97 | 97.44 | 98.10 | 42.32 | 29.64 | 21.61 | − 0.16 |
| 1 | 94.90 | 125.21 | 92.80 | 79.27 | 150.18 | 129.88 | 113.56 | 114.93 | 58.25 | 3.73 | 22.37 | 44.98 |
| 1.5 | 106.00 | 113.04 | 102.89 | 111.16 | 95.38 | 166.82 | 101.85 | 128.24 | − 10.02 | 47.57 | − 1.00 | 15.37 |

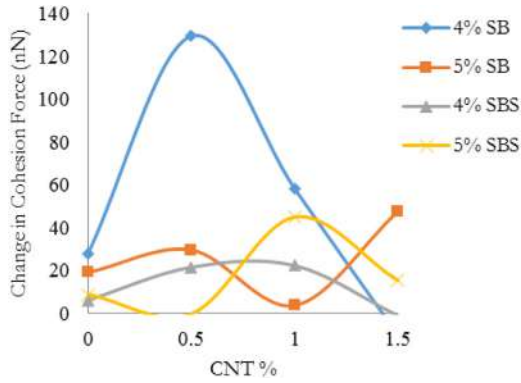


**Figure 12.6** Percentage variation in cohesion force due to CNT and polymer modification in asphalt binder.

Table 12.2 shows the cohesion forces between −OH-modified CFM tips for both fresh and aged asphalt binders, and their variations in terms of percentage. The variation appears to be higher for the cases of 4% SB and 0%, 0.5%, and 1% CNT-modified samples, which clearly suggests the vulnerability of this type of sample due to aging in asphalt binders compared with the other asphalt samples. All the variation data are plotted in Fig. 12.6 for analysis and investigation.

As explained earlier, most of the 4% SB samples modified with CNT were subjected to more deviation than those modified with other polymers (SB and SBS) and CNT.

The maximum variation in force can be seen in 4% SB and 0.5% CNT-modified samples. Other samples did not change significantly due to the aging effect. The samples modified with 4% SB polymer underwent a large amount of aging (maximum 130%−25%), which were initially mixed with the different percentages of CNT.

### 12.4.1 Comparative study between SB and SBS

Fig. 12.7 shows a comparison of 4% SB and SBS with −COOH functionalized CFM tips. The trend shows increasing adhesion force for 4% SB-modified samples with increased CNT mixing. However, the same effect was not observed when the same data were presented for 4% SBS and CNT-modified samples.

#### 12.4.1.1 Statistical analysis of CFM data for 4% SB and SBS (fresh and aged samples) with 0.5% CNT

Statistical analyses are fundamental measures for any laboratory testing data analysis, and the results are presented in Table 12.3 below for CFM-derived data for fresh and aged samples.

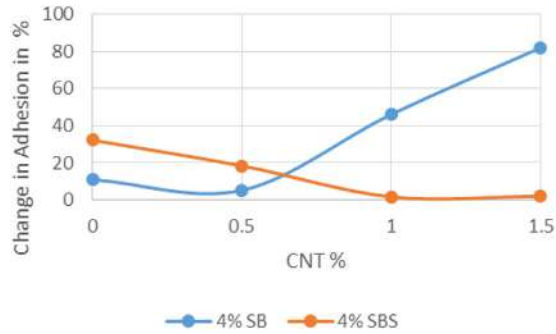


**Figure 12.7** Percentage variation in cohesion force based on SB and SBS effect in asphalt binder samples with −COOH tip.

Table 12.3 shows the statistical analysis for the laboratory-tested samples, which were modified with 0.5% CNT. Fig. 12.5 showed that 0.5% CNT mixed SB and SBS samples counterattack the aging effect, and samples with more than 0.5% CNT show some changes in CFM force values. Hence, the 0.5% CNT value can be taken as the control sample. The mean (the score which is exactly in the middle of all ordered scores) and median (the score which is exactly in the middle of all ordered scores) both describe the location (i.e., central tendency) of the laboratory-derived sample data. The mean and median values of the laboratory-generated CFM force values are sufficiently close to assume the analyzed data in this experiment are symmetrical.

Next, the standard deviations (SDs) for all the aged samples are computed and shown in Table 12.3 and found to be higher than those for the respective fresh samples. The value of SD is a quantity, which expresses by how much each one data item for a group may differ from the mean value for the whole data group. A similar trend can be noticed for the standard error (SE) values for almost all cases, since the SE values for aged samples are greater than those for the fresh samples, which may indicate some illogical chemical changes in the aged asphalt samples.

Skewness is a helpful statistical tool for the evaluation of experimental parameters and data. If a dataset looks the same to the left to the right compared with its central point, it gives the skewness, which is a perfect value (0 is the most preferable). It also describes qualitatively the gradation of asymmetry of a distribution in the vicinity of its computed mean value. Positive skewness directs a distribution with an asymmetric tail that extends to more positive values. Similarly, negative skewness designates a circulation with an asymmetric tail encompassing toward further negativity. Skewness values exceeding −1 to +1 are very rare. Our results show 4% SB and 5% SB are the most vulnerable to aging phenomena, since the values of skewness cross the limits. Hence, the aged samples for 4% SB and 5% SB are concluded to be highly skewed compared with the respective fresh samples.

Kurtosis is another statistical tool that measures the data, as well as the distribution pattern, whether they are heavily tailed or lightly tailed relative to a normal type of distribution. It represents and symbolizes the comparative flatness or peakedness

**Table 12.3** Statistical analysis of results for CFM test data.

| Statistical measurement parameters | Fresh 4% SB 0.5% CNT | Aged 4% SB 0.5% CNT | Fresh 4% SBS 0.5% CNT | Aged 4% SBS 0.5% CNT | Fresh 5% SB 0.5% CNT | Aged 5% SB 0.5% CNT | Fresh 5% SBS 0.5% CNT | Aged 5% SBS 0.5% CNT |
|---|---|---|---|---|---|---|---|---|
| Mean | 219.2 | 137.7 | 108.32 | 350.09 | 186.59 | 67.22 | 196.95 | 96.997 |
| Median | 219.15 | 128.22 | 107.66 | 364.43 | 184.91 | 66.777 | 197.63 | 97.542 |
| Standard deviation | 25.53 | 35.19 | 19.637 | 76.232 | 22.683 | 8.2794 | 7.2871 | 7.7623 |
| Standard error | 8.074 | 11.13 | 4.5051 | 24.106 | 7.1732 | 2.6181 | 1.67179 | 2.45465 |
| Skewness | 0.7353 | 2.342 | − 0.4061 | − 0.6001 | 1.0737 | 1.2244 | − 0.1034 | − 0.0819 |
| Kurtosis | 0.7589 | 6.5155 | − 0.7243 | − 0.8574 | 2.8181 | 2.9347 | 0.3785 | 0.38377 |

of a dataset related to the normal distribution. According to Sufian, the kurtosis value of a normally distributed curve is 3 [41]. Kurtosis is called leptokurtic when it has a more peaked (narrower) top than the normal curve with a value of more than 3. The current analysis found 4% SB-aged binder had a leptokurtic shape. The kurtosis value shows that the aged samples have higher values than all the fresh samples. Only 4% of SBS (both fresh and aged) have negative values, which indicates a flat type of distribution, although all others show a positive distribution. Hence, 4% SBS is not modified much by the aging consequences. Figs. 12.4 and 12.5 also support the research findings.

## 12.5 Conclusions

The laboratory CFM testing indicated that 4%, 5% SBS, and 5% SB doses resist the aging effect, although CNT appears to not have much effect on aging. Asphalt binders modified with 4% SB and CNT are not effective to protect against aging in the field.

The following conclusions can be drawn from the study:

- SB-modified samples achieved a higher skewed shape based on statistical analysis, which indicates more aging compared with SBS-modified samples.
- Statistical analyses (SD, SES (standard error), and skewness) showed that 4% SB has the maximum amount of distortion compared with fresh samples.
- Asphalt samples with 4% SBS mixed with 0.5% CNT are the best at resisting the aging effect.

## 12.6 Recommendation for future study

The nonlinear relationships among the data points could be further analyzed using ANN models. Moreover, the temperature variation effect can be further considered to gain more insights into aging in asphalt binders. The economical aspect/availability should be further investigated.

## Acknowledgment

The author thanks the King Faisal University for supporting this study. Special thanks are due to Engr. M. G. Baig from the Civil Engineering pavement laboratory, KFUPM, Saudi Arabia for help regarding samples preparation.

## References

[1] C. Glover, A. Martin, R. Han, N. Prapaitrakul, J. Zin, A. Chowdhury, et al., Evaluation of binder aging and its influence in aging of hot mix asphalt concrete: literature review

and experimental design, Report no 0-6009-1, Texas Transportation Institute, Texas, 2009.
[2] Research and Innovative Technology Administration, Asphalt surface aging prediction (ASAP) system, Final Report, Western Research Institute, Laramie, WY, USA, 2010.
[3] X. Sun, J. Yuan, Y. Zhang, Y. Yin, J. Lv, S. Jiang, Thermal aging behavior characteristics of asphalt binder modified by nano-stabilizer based on DSR and AFM, Nanotechnol. Rev. 10 (1) (2021) 1157−1182. Available from: https://doi.org/10.1515/ntrev-2021-0075.
[4] J. Xu, L. Sun, J. Pei, B. Xue, T. Liu, R. Li, Microstructural, chemical and rheological evaluation on oxidative aging effect of SBS polymer modified asphalt, Constr. Build. Mater. 267 (2021) 121028. Available from: https://doi.org/10.1016/j.conbuildmat.2020.121028. ISSN 0950-0618.
[5] M.A. Azadgoleh, A. Modarres, P. Ayar, Effect of polymer modified bitumen emulsion production method on the durability of recycled asphalt mixture in the presence of deicing agents,", Constr. Build. Mater. 307 (2021) 124958. Available from: https://doi.org/10.1016/j.conbuildmat.2021.124958ISSN 0950-0618. Available from: https://www.sciencedirect.com/science/article/pii/S0950061821027082.
[6] J. Petersen, J. Branthaver, R. Robertson, P. Harnsberger, J. Duvall, E. Ensley, Effects of physicochemical factors on asphalt oxidation kinetics, Transport. Res. Rec. 1391 (1993) 1−10.
[7] M. Liu, K. Lunsford, R. Davison, C. Glover, J. Bullin, The kinetics of carbonyl formation in asphalt, AIChE J. 42 (1996) 1069−1076.
[8] National Cooperative Highway Research Program (NCHRP) Guide for Mechanistic Empirical Design, NCHRP 1-37A.
[9] K.H. Al-Adham, M. Arifuzzaman, Moisture damage evaluation in carbon nanotubes reinforced asphalts, in: Proceedings of the Third International Conference on Transportation Infrastructures, University of Pisa-Hotel Tower Plaza, Pisa, 2014.
[10] M. Hassan, Modeling of moisture damage in carbon nano tube modified asphalt using hybrid of artificial neural network and other computational intelligence approaches, J. Comput. Theor. Nanosci. 12 (2015) 4927−4934.
[11] M. Arifuzzaman, M. Gul, K. Khan, S.M.Z. Hossain, Application of artificial intelligence (AI) for sustainable highway and road system, Symmetry 13 (2021) 60. Available from: https://doi.org/10.3390/sym13010060.
[12] M. Arifuzzaman, U. Gazder, M. Islam, A. Mamun, Prediction and sensitivity analysis of CNTs-modified asphalt's adhesion force using a radial basis neural network model, J. Adhes. Sci. Technol. 34 (2019) 10.
[13] M. Arifuzzaman, U. Gazder, M. Alam, O. Sirin, A. Mamun, Modelling of asphalt's adhesive behaviour using classification and regression tree (CART) analysis, Comput. Intell. Neurosci. 7 (2019) (ID 3183050).
[14] M. Hassan, A. Mamun, M. Hossain, M. Arifuzzaman, Moisture Damage Modeling in Lime and Chemically Modified Asphalt at Nanolevel Using Ensemble Computational Intelligence, Computat. Intell. Neurosci. 9 (2018) (Article ID 7525789).
[15] R. Tarefder, A. Mannan, M. Arifuzzaman, Evaluation of asphalt mastic containing mica due to aging, J. Transp. 169 (2016) 173−182.
[16] H. Zhang, J. Yu, Z. Feng, L. Xue, S. Wu, Effect of aging on the morphology of bitumen by atomic force microscopy, J. Microscopy 246 (2012) 11−19.
[17] L. Rebelo, J. de Sousa, A. Abreu, M. Baroni, A. Alencar, S. Soares, et al., Aging of asphaltic binders investigated with atomic force microscopy, Fuel 117 (A) (2014) 15−25.

[18] M. Le Guern, E. Chailleux, F. Farcas, S. Dreessen, I. Mabille, Physico-chemical analysis of five hard bitumens: identification of chemical species and molecular organization before and after artificial aging, Fuel 89 (2010) 3330–3339.
[19] C. Ouyang, S. Wang, Y. Zhang, Y. Zhang, Improving the aging resistance of the styrene-butadiene-styrene copolymer modified asphalt by addition of antioxidants, Polym. Degrad. Stab. 91 (2006) 795–804.
[20] M. Siddiqui, M. Ali, J. Shirokoff, Use of X-ray diffraction in assessing the aging pattern of asphalt fractions, Fuel 81 (2002) 51–58.
[21] S. Hesp, S. Iliuta, J. Shirokoff, Reversible aging in asphalt binders, Energy Fuel 21 (2007) 1112–1121.
[22] M. Siddiqui, M. Ali, Investigation of chemical transformations by NMR and GPC during the laboratory aging of Arabian asphalt, Fuel 78 (1999) 1407–1416.
[23] J. Lamontagne, P. Dumas, V. Mouillet, J. Kister, Comparison by FTIR spectroscopy of different ageing techniques: application to road bitumens, Fuel 80 (2001) 483–488.
[24] S.-J. Lee, S. Amirkhanian, K. Kim, Laboratory evaluation of the effects of short-term oven aging on asphalt binders in asphalt mixtures using HP-GPC, Constr. Build. Mater. 23 (2009) 3087–3093.
[25] S. Wu, L. Pang, L. Mo, Y. Chen, G. Zhu, Influence of aging on the evolution of structure, morphology and rheology of base and SBS modified bitumen, Constr. Build. Mater. 23 (2009) 1005–1010.
[26] T. Gandhi, C. Akisetty, S. Amirkhanian, Laboratory evaluation of warm asphalt binder aging characteristics, Int. J. Pavement Eng. 10 (2009) 353–359.
[27] P. Cong, S. Chen, J. Yu, S. Wub, Effects of aging on the properties of modified asphalt binder with flame retardants, J. Constr. Build. Mater. 24 (2010) 2554–2558.
[28] A. Banerjee, A. Smit, J. Prozzi, The effect of long-term aging on the rheology of warm mix asphalt binders, Fuel 97 (2012) 603–611.
[29] Y. Ruan, R. Davison, C. Glover, The effect of long-term oxidation on the rheological properties of polymer modified asphalts, Fuel 82 (2003) 1763–1773.
[30] D. Cao, J. Ji, Evaluation of the long-term properties of Sasobit modified asphalt, Int. J. Pavement Res. Technol. 4 (2011) 384–391.
[31] V. Lins, M. Araújo, M. Yoshida, V. Ferraz, D. Andrada, F. Lameiras, Photo degradation of hot-mix asphalt, Fuel 87 (2008) 3254–3261.
[32] Y. Kim, H. Lee, Evaluation of the effect of aging on mechanical and fatigue properties of sand asphalt mixtures, KSCE J. Civ. Eng. (Highw. Eng.) 7 (2003) 389–398.
[33] A. Othman, Impact of polypropylene application method on long-term aging of polypropylene-modified HMA, J. Mater. Civ. Eng. 22 (2010).
[34] A. Molenaar, E. Hagos, M. van de Ven, Effects of aging on the mechanical characteristics of bituminous binders in PAC, J. Mater. Civ. Eng. 22 (2010) 779–785.
[35] F. Zhang, J. Yu, S. Wu, Effect of aging on rheological properties of storage-stable, SBS/sulfur-modified asphalts, J. Hazard. Mater. 182 (2010) 507–517.
[36] J. Murgich, M. Jesus, A. Yosslen, Recognition and molecular mechanics of micelles of some model asphaltenes and resins, Energy Fuels 10 (1996) 68–76.
[37] O. Olabemiwo, G. Adediran, F. Adekola, A. Olajire, Aliphatic and polycyclic aromatic hydrocarbons profiles of photo-modified natural bitumen of Agbabu, southwestern Nigeria, Bull. Chem. Soc. Ethiopia 24 (2010) 461–466.
[38] B. Ohler, Cantilever spring constant calibration using laser Doppler vibrometry, Rev. Sci. Instrum. 78 (2007).

[39] M. Arifuzzaman, R. Tarefder, M. Islam, The behavior of carbon nano-tubes (CNTs) as a modifier to resist aging and moisture damage in asphalt, Nanosci. Nanotechnol.-Asia 11 (2) (2021). Available from: https://doi.org/10.2174/2210681210999200414113251.
[40] A. Mamun, M. Arifuzzaman, Nano-scale moisture damage evaluation of carbon nanotube-modified asphalt, Constr. Build. Mater. 193 (2018) 268–275.
[41] A. Sufian, Methods and Techniques of Social Research, second ed., The University Press Limited, Dhaka, 2009.

# Polymer nanocomposites for energy

13

*Asrafuzzaman*[1], *Kazi Faiza Amin*[2], *Aungkan Sen*[3] and *Md Enamul Hoque*[4]

[1]Department of Materials Science and Engineering, Rajshahi University of Engineering & Technology (RUET), Rajshahi, Bangladesh

[2]Department of Materials and Metallurgical Engineering, Bangladesh University of Engineering and Technology (BUET), Dhaka, Bangladesh

[3]Department of Chemical Engineering and Materials Science, Michigan State University, East Lansing, MI, United States

[4]Department of Biomedical Engineering, Military Institute of Science and Technology (MIST), Dhaka, Bangladesh

## 13.1 Introduction

One of the most daunting tasks that present-day scientists and researchers face is to raise social and environmental cognizance on suitable usage of natural resources [1] to develop renewable and clean energy technologies to meet the ever-growing need for energy that is both economic and eco-friendly [2]. Numerous materials are currently used for the application of energy storage such as high energy density capacitors, supercapacitors, batteries [3–5], energy conversion applications such as solar cells [6], fuel cells [7], as well as energy-saving applications such as carbon dioxide capture and electrochromic devices [8] to meet the rising demand associated with the advances in hybrid vehicles (electric), portable electronic devices, renewable power systems, and so on [9]. Specifically, compact and lightweight capacitor materials have caught the attention of researchers owing to their easy accumulation of energy and instantaneous energy delivery when required [5,10]. However, the energy density of dielectric materials that regulate these capacitors is comparatively low and thus fails to fulfill the increasing demand for advanced technologies [9]. Due to the possession of eco-friendly nature, the emergence of nanoparticle-reinforced composites showed promising aspects in this regard [11]. The addition of organic and inorganic nanoparticles into the polymer matrix has paved the way for the design and fabrication of polymer nanocomposites (PNCs). These polymers nanocomposites have proven to be a promising pathway to develop high energy density dielectric materials [3,12]. To develop flexible, processable, lightweight energy harvesting devices, researchers from both academia and industry tried to combine the dielectric properties of PNCs with better mechanical characteristics and thermal stability [13,14]. It has been proven that ceramic filler particles have a

**Advanced Polymer Nanocomposites. DOI: https://doi.org/10.1016/B978-0-12-824492-0.00007-6**


larger dielectric constant compared to the polymer matrix [15]. On the other hand, the polymer matrix possesses high energy density and high breakdown strength relative to the ceramic fillers [16]. Therefore the combination of the polymer matrix of high breakdown strength and the filler material of high dielectric constant may provide enhanced dielectric properties [5]. However, numerous variables such as nanofiller particle size and shape, innate properties of nanofillers, and matrix along with the interaction between them might affect the resulting characteristics of PNCs for dielectric energy application [17]. Moreover, the homogeneous dispersion of fillers throughout the matrix is quite difficult to attain because of the dissimilarity in their surface characteristics resulting in inhomogeneity between the components affecting the electrical performance of the PNCs [18,19]. Hence, to develop high energy density PNCs, improvement of the interface between polymer matrix and nanofillers is necessary [20]. In this chapter, we will briefly discuss the potential of PNCs in the field of energy applications, the ongoing research works regarding the use of different types of PNCs as energy materials along various challenges associated with this field.

## 13.2 Polymer nanocomposites as energy materials: terminology and annotations

In this section, we will discuss some basic terminologies and definitions associated with the dielectric properties of PNCs, for example, dielectric constant/relative permittivity, dielectric loss, dielectric nonlinearity, breakdown strength, and theory of percolation.

### *13.2.1 Dielectric constant/relative permittivity*

One of the important features of dielectric material is its permittivity ($\varepsilon$) that measures the material's ability to be polarized by an electric field. However, it is closely associated with capacitance ($C$). For a capacitor of capacitance $C$, the amount of charge $Q$ it can hold is directly proportional to the voltage $V$ applier across it [21]. Thus $Q = CV$, or $C = Q/V$. The unit of $C$ is the farad (coulomb per volt). The capacitance is dependent on the permittivity $\varepsilon$ of the dielectric layer, along with the area $A$ of the capacitor, and the separation distance $d$ between the two plates that are conductive in nature. The mathematical relation is as follows: $C = \varepsilon(A/d)$. When a vacuum is considered as a dielectric, then the capacitance $C_o = \varepsilon_o\ (A/d)$. $\varepsilon_o$ is known as the permittivity of vacuum ($8.85 \times 10^{-12}$ F m$^{-1}$).

Material's dielectric constant is expressed as "$k$." It is the ratio of its permittivity $\varepsilon$ to the permittivity of vacuum $\varepsilon_o$, so $k = \varepsilon/\varepsilon_o$. That is why it is also termed as the relative permittivity of materials. The dielectric constant value of the vacuum is considered 1. Any material is capable to polarize more than the vacuum, so the "$k$" value of a material is always $> 1$. In Fig. 13.1A, it is shown that for vacuum

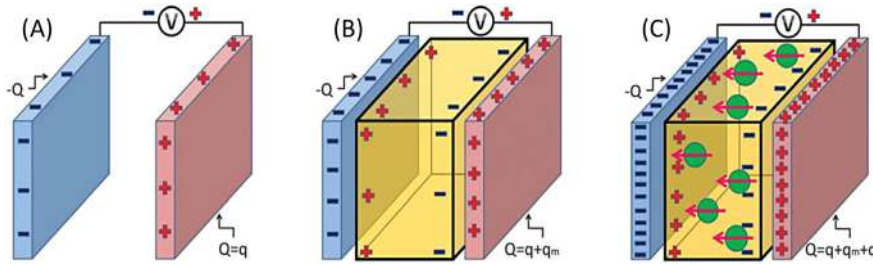


**Figure 13.1** Illustration of capacitor energy storage under applied voltage $V$ (A) A vacuum capacitor with a stored charge up to $q$; (B) A dielectric film capacitor with a stored charge up to $q + q_m$; (C) A high-$k$ particles filled dielectric film capacitor with storage charge up to $q + q_m + q_p$.
*Source*: From X. Huang, B. Sun, Y. Zhu, S. Li, P. Jiang, High-k polymer nanocomposites with 1D filler for dielectric and energy storage applications. Prog. Mater. Sci., 2019, 100, 187−225. https://doi.org/10.1016/j.pmatsci.2018.10.003.

dielectric the stored charge is $q$ due to applied voltage $V$. In Fig. 13.1B, the introduction of the dielectric film increased the stored charge amount by $q_m$ due to the energy for polarizing the film. Finally, Fig. 13.1C shows the addition of high-$k$ along with the dielectric film increased the stored charge amount by $q_p$ originated from the energy required to polarize the new particles and due to the dipole−dipole interaction energy among them [15].

### 13.2.2 Dielectric loss

Dielectric loss generally originates from conductional, interfacial, distortional losses. To ensure maximum energy storage, the dielectric loss of PNCs must be very low [22,23]. Power dissipation occurs in dielectrics due to the application of alternating voltage. One of the major sources of dielectric loss is the interfacial polarization resulting from interfacial charge procurement as a result of dielectric conductivity/constant mismatch [24,25]. Since dielectric loss is undesirable in energy storage applications, several parameters must be taken into account while fabricating PNCs including (1) polymer matrix and filler particles must show low loss, (2) reducing the presence of impurities, and (3) enhanced interfacial compatibility between matrix and filler [26]. It should be kept in mind that the dielectric loss of PNCs is dependent on the spatial orientation of filler particles.

### 13.2.3 Dielectric nonlinearity

In general, dielectric materials are classified as linear and nonlinear dielectrics [27]. In the case of linear dielectrics, no permanent dipole moments are observed and there is a linear relationship between dielectric displacement and electric field [28], whereas the nonlinear dielectrics show nonlinear relation with the electric field as the name implies [29]. For nonlinear dielectrics, discharge energy density, $U_e$ is

inversely related to the remnant polarization. The relation among $U_e$ and electric field $E$ and electric displacement $D$ is given by Eq. (13.1) [30].

$$U_e = \int E \quad dD \tag{13.1}$$

Though general-purpose ferroelectrics (FE) for energy density applications have a high dielectric constant, due to their large remnant polarization, they cannot be used as high energy density materials [10]. Better optimization between high dielectric constant and low remnant polarization (low energy loss) is obtained using relaxor ferroelectrics or antiferroelectric materials [29] (Fig. 13.2).

We are concerned with dielectric nonlinearity while discussing PNCs for energy application is because most of the filler materials for PNCs are ferroelectric in nature. Besides novel ferroelectric polymers such as poly(vinylidene fluoride) (PVDF) and PVDF-based copolymers are showing promising results in fabricating PNCs for energy appliances [8]. The discharge energy density, $U_e$, of dielectric PNCs is greatly dependent on the breakdown strength, $E_B$, of the dielectric materials [31]. Polymer matrix for this purpose such as biaxially oriented polypropylene shows high breakdown strength along with low dielectric loss. But the major limitation of such a polymer matrix is low dielectric constant/relative permittivity resulting in low energy density [32–34]. So, to fabricate efficient PNCs for energy application to gain maximum energy density, it is rational to assemble the low dielectric loss and high breakdown strength polymer with filler reinforcement (ceramics) of high dielectric constant keeping in mind the effect of dielectric nonlinearity [16,35] (Fig. 13.3).

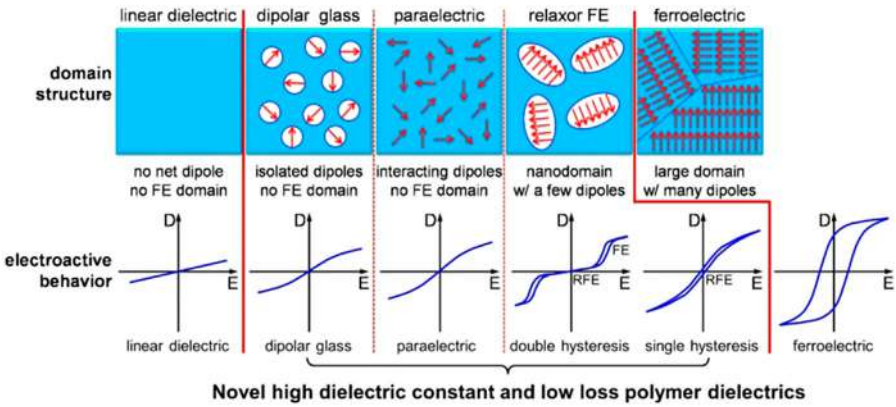


**Figure 13.2** Increasing domain size and cooperativeness with increased dielectric nonlinearity from left to right along with corresponding $D-E$ graphs.
*Source*: From V.K. Prateek, Thakur, R.K. Gupta, Recent progress on ferroelectric polymer-based nanocomposites for high energy density capacitors: synthesis, dielectric properties, and future aspects. Chem. Rev., 2016, 116(7), 4260–4317. https://doi.org/10.1021/acs.chemrev.5b00495.

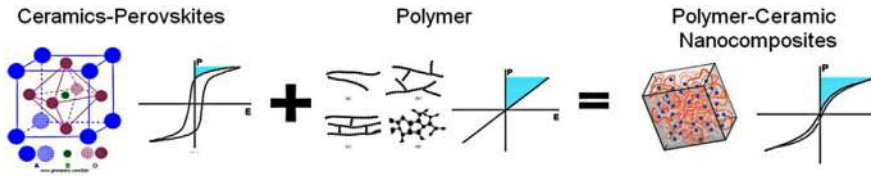


**Figure 13.3** Illustration of PNC fabrication for energy storage. *PNC*, Polymer nanocomposite.
*Source:* From B.C. Riggs, S. Adireddy, C.H. Rehm, V.S. Puli, R. Elupula, D.B. Chrisey, Polymer nanocomposites for energy storage applications in: The Selected Papers of 10th International Conference on Physics of Advanced Materials, ICPAM-10, 2015, 2(6), 3853−3863. https://doi.org/10.1016/j.matpr.2015.08.004.

### 13.2.4 Breakdown strength

Breakdown strength plays a pivotal role in assessing the energy density of PNCs. The maximum electric field a dielectric can endure without becoming conducting is termed as the breakdown strength. The is a square relationship between breakdown strength and energy density of linear dielectrics that is given by Eq. (13.2) where $\varepsilon_r$ and $\varepsilon_o$ are the dielectric permittivity of the material and vacuum ($8.85 \times 10^{-12}$ F m$^{-1}$), respectively, $E_b$ is the breakdown strength of the medium [36,37]. It is obvious from the equation that the higher breakdown strength of PNCs can ensure higher energy density.

$$\text{Energy density} = \frac{1}{2}\varepsilon_o \varepsilon_r {E_b}^2 \tag{13.2}$$

There are several types of breakdown that can occur in PNCs [38]:

- Intrinsic electronic breakdown: Due to the application of the electric field, electrons gain energy to jump across the forbidden energy gap from the valence band to the conduction band. This process is repetitive and as a result, the presence of an excess amount of electrons in the conduction band leads to the intrinsic electronic breakdown [39−41].
- Avalanche breakdown: Free electrons sometimes collide with bound electrons forming collision ionization resulting in more free electrons within the PNCs. Repetition of this process induces an avalanche effect resulting in the final breakdown [39−41].
- Thermal breakdown: High-frequency electric field can induce energy loss by heat energy dissipation. Due to the insulative nature of dielectric PNCs, they might get heated up and cause melting and thus cause a thermal breakdown [39−41].
- Defect breakdown: The presence of defects like pores, cracks, cavities is very common in PNCs. These spaces can be occupied with gas, air, or any other medium of low permittivity and strength causing this unusual type of breakdown [39−41].

### 13.2.5 Theory of percolation

Originally developed as a mathematical concept in the early 1950s [42], the percolation theory had later found its usage in materials science research to analyze the

physical properties of any heterogeneous materials [35,42]. Due to percolation phenomena, minor phase filler particles of PNCs come close to each other and form an interconnecting network resulting in tunneling [43]. Consequently, the charge accumulation ability of PNCs is extirpated and as a result, they become conductive under the applied electric field [27]. So, utilization of PNCs in energy storage applications becomes limited due to this phenomenon. Fig. 13.4 depicts a hypothetical PNC system showing percolation phenomena.

For a heterogeneous multicomponent material, the amount of volume fraction (critical point) of minor filler phase that contributes to insulator-metal transition by forming a continuous long-range network of minor constituents is known as "Percolation Threshold" [44]. A large difference between the attributes of filler (both conducting and nonconducting) and polymer matrix causes dramatic physical property change of PNCs near the percolation threshold [45]. The highly resistive filler-matrix interface of PNC inhibits tunneling among adjacent filler particles forming a percolative composite with high dielectric constant but low dielectric loss [45]. Filler size, shape, and orientation influence the percolation threshold [46]. Spherical-shaped filler shows a percolation threshold of $\sim 0.16$ (also known as Sher-Zallen invariant), whereas ellipsoidal-shaped fillers show a much lower percolation threshold since there is an easy connection among fillers to form a continuum [45,47]. It is proven that the percolation threshold is inversely related to the filler aspect ratio [48]. For instance, large-diameter (700 nm) $BaTiO_3$ nanoparticles showed a smaller percolation threshold than smaller diameter (100 nm) ones. Besides, shape change from nanoparticle to nanofibers shows a further reduction in percolation threshold, that is, graphene flakes exhibit 0.31 vol.% percolation

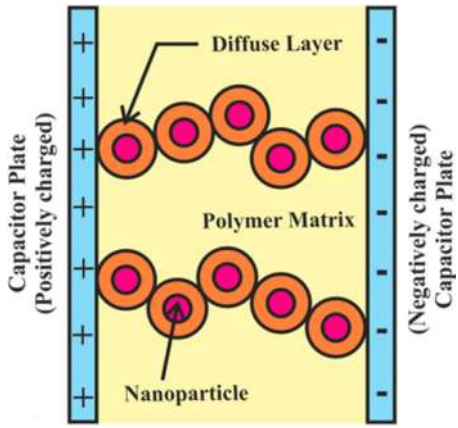


**Figure 13.4** Hypothetical polymer nanocomposite material showing conduction via diffuse layers due to percolation.
*Source:* From V.K. Prateek, Thakur, R.K. Gupta, Recent progress on ferroelectric polymer-based nanocomposites for high energy density capacitors: synthesis, dielectric properties, and future aspects. Chem. Rev., 2016, 116(7), 4260−4317. https://doi.org/10.1021/acs.chemrev.5b00495.

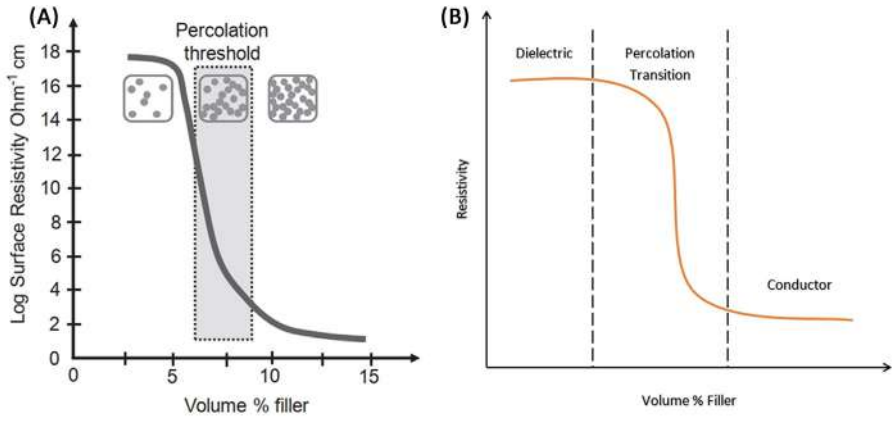


**Figure 13.5** (A) Schematics of percolation threshold. (B) Transition from dielectric to conductor due to percolation phenomena.
*Source*: From C. DeArmitt, M. Kutz, 23 - Functional Fillers for Plastics. In Plastics Design Library (pp. 517–532). William Andrew Publishing, 2017. https://doi.org/10.1016/B978-0-323-39040-8.00023-7.

threshold [49]. Not only filler shape but also PNC synthesis procedure as well as polymer matrix viscosity, polarity, and degree of crystallization have a major influence on the percolation threshold. Due to higher viscosity, higher polarity, and a lower degree of crystallization, uniform distribution of filler particles is not possible resulting in enhanced percolation threshold [50–52]. Therefore by controlling the percolation threshold, the optimum properties of PNCs can be achieved. Sometimes surface alteration of nanofillers is required to avoid percolation in PNCs used in the energy application [31,53–56] (Fig. 13.5).

## 13.3 Novel PNC energy materials: basic concepts

By definition, PNC dielectrics are composed of organic/inorganic fillers and dielectric polymer matrices utilizing the properties of both phases. It has already been stated earlier that the polymer phase has high dielectric energy density and high breakdown strength with low dielectric constant, while the filler phase (mostly ceramics) shows a high dielectric constant with low breakdown strength. So, utilization of PNCs as energy storage dielectrics is significantly dependent on the nature and types of fillers as well as polymer matrices [57].

### *13.3.1 Selection of matrix phase of PNCs for energy application*

The advent of conductive polyacetylene (PA) in the mid-to-late 1970s paved the way for the application of intrinsic conductive polymers (ICPs) the energy storage applications [23,58,59]. These conductive polymers consist primarily of organic

monomer groups with conjugated double bonds [60,61]. Compared to conventional polymers, the ICPs show a significant amount of electrical conductivity and they are of two types: (1) ionic conducting polymers and (2) electron-conducting polymers [62]. The most commonly used ICPs for energy storage purposes are polyaniline (PANI), polythiophene (PTh), PA, polypyrrole (PPy), poly(phenylenevinylene), poly(paraphenylene), and polyfuran [63]. Other than these, poly(methyl methacrylate) (PMMA) [64–66], epoxy [54–56,67–70], polydimethylsiloxane (PDMS) [71], polyimide (PI) [72–77], PVDF [34,78], poly(3,4-ethylene dioxythiophene) (PEDOT) [79] are also used in plethora to fabricate PNCs for energy applications. In addition to good dielectric properties, PMMA also possesses high strength and good optical properties [80,81]. Epoxy resins due to their insulative property as well as being lightweight and low cost are used in energy applications a lot [27]. However, due to their lower thermal conductivity ($0.17-0.21\ W\ m^{-1}\ K^{-1}$), heat-dissipating requirements, a major concern for energy storage applications, are not met [26]. Being transparent and biocompatible, silicon-based elastomers such as PDMS found their rightful position as matrix material of PNC [82]. Among thermoset polymers, polyimide is quite common to be used as matrices in PNC due to their chemical inertness, better thermal stability, and low moisture absorption index [27,83,84]. Nonpolar polymers such as polytetrafluoroethylene, low-density polyethylene, polyolefins, and so on are used sometimes but they exhibit a low dielectric constant. In contrast, polar polymers such as PVDF show high dielectric constant and greater breakdown strength [27]. Table 13.1 summarizes the dielectric properties of several polymers.

### 13.3.2 Selection of nanofillers of PNCs for energy applications

Enhanced dielectric properties of PNCs are dependent not only on the choice of proper matrices but also on the appropriate selection of fillers of different sizes, shapes, volume fraction, and state of dispersion [27,100]. Compared to polymer composites reinforced with micro-sized fillers, the PNCs show exceptional dielectric properties needed for energy application due to the synergistic interaction (also known as "nano-effect") between polymer and nanofillers [101].

Nanofillers of PNCs for energy application can be subdivided based on their conducting nature and dimensions. The nonconducting fillers are generally ceramic insulators. Having a very high bandgap, these fillers accumulate charge only if an electric field is applied [102,103]. The most common nonconducting ceramic nanofillers are strontium titanate ($SrTiO_3$) [104], barium titanate ($BaTiO_3$) [105–107], calcium titanate ($CaTiO_3$) [108], $Bi_2O_3-ZnO-Nb_2O_5$ [109], and so on. On the other hand, conducting fillers display a higher dielectric constant at low concentrations compared with nonconducting fillers [27]. However, a higher concentration of conducting filler causes percolation and dielectric properties to start to change unexpectedly near the percolation threshold [110]. Conducting fillers like carbon black [111–114], graphene [9,115,116], single-walled and multiwalled carbon nanotubes [117–120], graphite [121,122], fullerenes [123,124], nanodiamonds [53,125], etc. are used in a plethora of PNCs.

**Table 13.1** Dielectric characteristics of multifarious polymers.

| Polymers | Dielectric constant (1 kHz) | Breakdown strength (kV $cm^{-1}$) | Dielectric loss (loss tangent, 1 kHz) | Dielectric discharge energy density (J $cm^{-3}$) | References |
|---|---|---|---|---|---|
| Poly(vinylidene fluoride) | 10 | 1500–5000 | 0.04 | 2.8 (at 2400 kV $cm^{-1}$) | Song et al. [85–89] |
| Poly(methyl methacrylate) | 4.5 | 2500 | 0.05 | 1.5 (at ~3300 kV $cm^{-1}$) | Paniagua et al. [64,90–92] |
| Epoxy | 4.5 | 250–450 | 0.015 | – | Barber et al. [68,85–87,92–94] |
| Polyimide | 3.5 | 2380 | 0.04 | 1.4 | Chi et al. [95–97] |
| Polydimethylsiloxane | 2.6 | 660 | 0.01 | – | Molberg et al. [71,92] |
| Poly(ethylene terephthalate) | 3.6 | 2750–3000 | 0.01 | – | Huang et al. [92,94,98] |
| Polytetrafluoroethylene | 2 | 880–1760 | 0.0001 | – | Huang et al. [92,94] |
| Low-density polyethylene | 2.3 | 308.9 | 0.003 | – | Mohamed [92,94,99] |

Based on dimensionality, nanofillers can be of three types, namely, 1D nanofillers, 2D nanofillers, 3D nanofillers [100]. Fillers having at least one of their dimensions less than 100 nm are called 1D nanofillers [126]. Among various 1D nanofillers for energy applications ZnO nanoplatelets [127], ZnO nanosheets (Bai et al., 2000), ZnO nanodiscs [128], $Fe_3O_4$ nanodiscs [129] are the most prominent. When two dimensions of nanofillers are less than 100 nm, they are called 2D nanofillers. The most common 2D nanofillers are titanium dioxide [130], cerium dioxide [131,132], silica [133], $MoS_2$ [134], hexagonal boron nitride (h-BN) [135], and so forth. Usually known as nanospheres, nanogranules, and nanocrystals, 3D nanofillers are generally equiaxed particles having all their three-dimension on a nanoscopic scale [100]. Some 3D nanofillers used in PNC for energy applications are polyhedral oligomeric silsesquioxane [110], nano-alumina [100], nanotitanium oxide [100], quantum dots [136], etc. (Table 13.2).

## 13.4 Effect of interface on the dielectric properties of PNCs

Owing to the large surface area to volume ratio, a small portion of nanofiller loading displays enhanced dielectric characteristics in PNCs compared to micro-sized filler loading [9,93,142]. Interaction of nanofillers and polymer matrices is also controlled by parameters like chain mobility of polymers, their crystallinity, Coulombic potential, and so forth [57,143,144]. In an experiment, silica fillers (both nano and micron dimensions) were utilized in the epoxy polymeric matrix to comprehend the dielectric properties of the PNC [145]. The nanofiller composite showed an improved dielectric constant but a higher dielectric loss than the microfilter composite. The presence of contaminants accrued from the silica synthesis process was the main reason behind the unexpected increase in dielectric loss, they concluded [145]. Dielectric responses of dielectrics are dependent on two critical interface characteristics, namely their chemical formation mechanism and charge distribution across the interfacial region [31]. For further insight on the formation of the interface and its influence on the dielectric properties of PNCs, two important hypothetical models are known as "Tanaka's Model" and "Lewis's Model" are proposed.

### 13.4.1 Tanaka's theoretical model

A multi-core-shell model has been proposed by Tanaka et al. [144] for a spherical-shaped filler incorporated polymer matrix composite to form interfaces either by a chemical, physical, or electrical mechanism [27]. According to the model, the interface layer comprised three layers. The first layer, commonly known as, the bonded layer displays an intimate contact between nanofiller and polymer matrix due to van der Waals bonds, ionic bonds, hydrogen bonds, or covalent bonds [27]. The thickness of this layer is around 1 nm [144,146].

**Table 13.2** Dielectric properties of several nanofillers.

| Filler materials | Dielectric constant | Loss tangent | Dielectric strength (kV $cm^{-1}$) | References |
|---|---|---|---|---|
| Alumina (99% $Al_2O_3$) | 10.1 @ 1 MHz | 0.0002 @1 MHz | 135 | Yu et al. [92,94,137] |
| Boron nitride | 4.2 @ 1 MHz | 0.00034 @ 1 MHz | 140 | Raju [94] |
| Barium titanate, $BaTiO_3$ | 1235 @ 1 kHz | 0.012 @ 1 kHz | 150 | Huang et al. [92,138,139] |
| Quartz | 3.8 @ 1 MHz | 0.0038 @ MHz | – | Raju [94] |
| Silica (fused) | 3.2 @ 1 MHz | 45 @ 10 GHz | – | Raju [94] |
| $Ba_{0.7}Sr_{0.3}TiO_3$ | ~5000 @ 1 kHz | 0.03 @ 1 kHz | – | Hilton, Ricketts [140] |
| Strontium titanate, $SrTiO_3$ | 240 @ 10 kHz | 0.00076 | – | Muhamad et al. [141] |

The bound layer (the second layer), thickness ranging between 2 and 9 nm, corresponds to a strong interaction among the polymer chain and the bonded layer as well as the surface of nanofillers [27]. Reduction of dielectric permittivity due to this layer is reported in some scientific literature [144,146,147].

Due to loosely coupled with the bound layer, the third layer is known as the loose layer. Its thickness ranges from several tens of nanometer scale and due to this layer reduction in dielectric properties is observed. This layer also displays different polymer chain mobility, crystallinity, conformation, and free volume than bulk polymer [146,148,149].

The bound layer adversely affects the polar radical groups, and the loose layer causes free volume reduction. Both the layers thus lead to diminishing the dielectric constant. As a result, the choice of a proper coupling agent is essential for greater energy density PNCs [27].

### 13.4.2 Lewis's theoretical model

Charge distribution across the interface affects the morphologies of interface layers. Within the interfacial region, short-range electrostatic forces, mid-range van der Waals forces, and long-range Coulombic forces may exist that affect the interfacial layers [31]. Due to differences in chemical potential and Fermi levels of nanofiller and polymer matrix, the surface of the nanoparticles (sometimes partial) become charged [150]. To counter the effect, the adjacent polymer matrix phase establishes opposite charges near the surface of the nanoparticles [29,147]. Due to the migration of mobile ions in polymer, a diffuse electric double layer having high charge density is formed around the nanofillers. This layer is known as Stern Layer or Helmholtz double layer [27]. This double layer is formed due to motionless charged impurities, entrapped carriers, moving electrons, and holes in the nanoparticle. Adjacent to the Stern layer, the Gouy−Chapman diffused layer is formed due to the distribution of charges of opposite polarity [151]. This layer has a prevalent role in

ascertaining dielectric responses of PNCs [146]. Due to considering, electric potential and charge density within the interfacial region, this core−shell model promises excellent dielectric characteristics of PNC [152]. Fig. 13.6 depicts the above-mentioned hypothetical models.

## 13.5 Ferroelectric fluoropolymer-based PNCs as energy materials

Among the most frequently utilized PNCs for high-energy-density capacitor applications, fluoropolymer such as PVDF [153] based PNC shows the most promising result due to high breakdown strength [154], high dielectric constant, and large polarization [9]. The reasons behind those enhanced dielectric properties are the existence of strongly electronegative fluorine on the polymer chains as well as the spontaneous alignment of C-F dipoles in the crystalline phase [9]. Among various phases of PVDF, β-, γ-, and δ-phases exhibit high dielectric constant, in the range of 6−12 [155], compared to α-phase [156]. Numerical values of dielectric constant, breakdowns strength, dielectric loss are already stated in Table 13.1. Being ferroelectric in nature, β-PVDF-based polymer can be tailored to obtain desired dielectric properties by surface modification or blending [27]. Specific PVDF-based

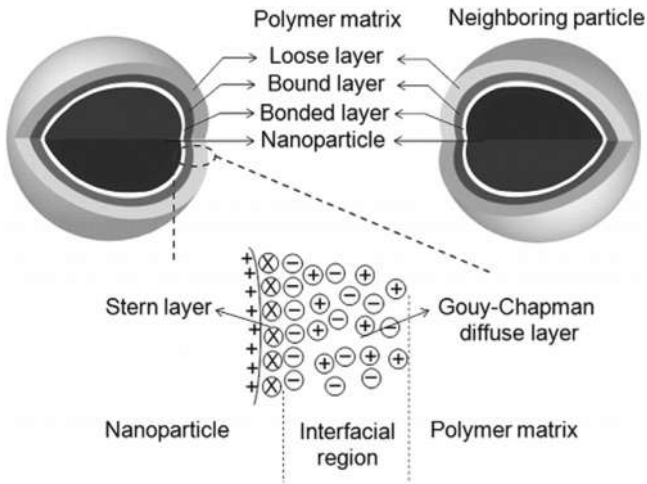


**Figure 13.6** Tanaka's model and Lewis's model showing the multi-core-shell structure of interfaces between polymer matrix and nanoparticles as well as the Stern and Gouy−Chapman diffusion layers within the interfacial region of a hypothetical polymer nanocomposite.
*Source*: From Z.-M. Dang, J.-K. Yuan, S.-H. Yao, R.-J. Liao,. Flexible nanodielectric materials with high permittivity for power energy storage. Adv. Mater., 2013, 25(44), 6334−6365. https://doi.org/10.1002/adma.201301752.

copolymers or terpolymers are used to modify the electrical characteristics of PNCs. Among them, poly(vinylidene fluoride-trifluoroethylene) (P(VDF-TrFE)), poly-(vinylidene fluoride-co-hexafluoropropene) (P(VDF-HFP)), poly(vinylidene fluoride-cochloride trifluoride ethylene) (P(VDF-CTFE)), poly-(vinylidene fluoride-trifluoroethylene-chlorofluoroethylene)(P(VDF-TrFE-CFE)), poly-(vinylidene fluoride-trifluoroethylene-hexafluoropropylene (P(VDF-TrFE-HFP)), poly-(vinylidene fluoride-trifluoroethylene-cochloride trifluoride ethylene) (P(VDF-TrFE-CTFE)) are utilized commonly [157,158].

Compared to PVDF, P(VDF-TrFE) shows a higher dielectric constant (approximately 18) with a loss tangent less than 0.1 at 1 kHz [159]. Analogous to that in P(VDF-TrFE), P(VDF-HFP) also exhibits a reduction in remnant polarization [149]. Dielectric constant and loss tangent of P(VDF-HFP) are 5.6 and 0.4 at 1 kHz, respectively [160]. But the most promising feature of P(VDF-HFP) is its higher energy density ($11-13.5\ \mathrm{J\ cm^{-3}}$ at $\sim 6000\ \mathrm{kV\ cm^{-1}}$) in comparison to PVDF and P(VDF-TrFE) [161]. For P(VDF-CTFE), loss tangent, dielectric constant, and energy density near breakdown field ($6000\ \mathrm{kV\ cm^{-1}}$) are consecutively 0.03 at 1 kHz, 13, and $\sim 25\ \mathrm{J\ cm^{-3}}$ [162].

Adding a third comonomer in P(VDF-TrFE)-based polymer is shown to increase the dielectric constant to a large amount. The dielectric constant values (based on the mole fraction of monomers) of P(VDF-TrFE-CFE), P(VDF-TrFE-CTFE), and P(VDF-TrFE-HFP) are 55 (at 56/36.5/7.5 mol%) [10,163], 47 (at 62.2/30.2/7.6 mol%) [164,165], and 30 (at 62/38/2.5 mol %) [166], respectively (Fig. 13.7).

PVDF and PVDF-based nanocomposites for energy application incorporate both conducting fillers like graphene, silver (Ag), zinc (Zn), copper (Cu), etc., and non-conducting fillers like $BaTiO_3$, $SrTiO_3$, $BiFeO_3$, etc. As stated earlier, filler size and shape have a substantial influence on the dielectric characteristics of PNCS. Though in terms of dielectric constant and energy density, PVDF-based PNCs provide a promising result, their lower dielectric breakdown strength still poses a severe problem. Modified fillers are proved to increase the dielectric properties of such PVDF-based PNCs for energy applications [167–169]. A summary of PVDF-based nanocomposites dielectric properties based on filler size, shape, modification, and conductivity are summarized in the following tables (Tables 13.3 and 13.4).

## 13.6 Graphene/graphene-based PNCs as energy materials

Since its discovery in 2004 [211], graphene has attracted remarkable attraction owing to its application in energy storage and energy conversion systems [2]. Owing to superior thermal and electrical conductivities, graphene/graphene-based PNCs have been utilized as nanoarchitectured electrode materials for electrochemical capacitors, also known as, supercapacitors [212–215]. PANI, PPy, PTh, poly(hexylthiophene) (PHTh), PEDOT, and poly(styrene sulfonate) (PSS) are among

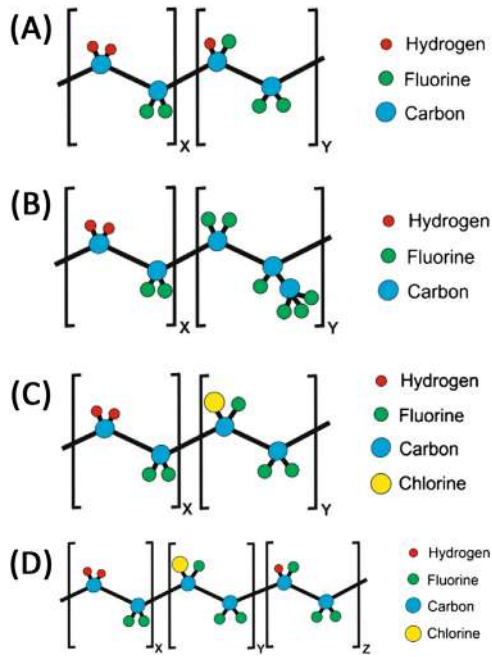


**Figure 13.7** Illustration of repeat units of (A) P(VDF − TrFE), (B) P(VDF − HFP), (C) P(VDF − CTFE), and (D) P(VDF − TrFE − CTFE). *P(VDF − TrFE)*, Poly(vinylidene fluoride-trifluoroethylene); *P(VDF − HFP)*, poly-(vinylidene fluoride-co-hexafluoropropene); *P(VDF − CTFE)*, poly(vinylidene fluoride-cochloride trifluoride ethylene); *P(VDF − TrFE − CTFE)*, poly-(vinylidene fluoride-trifluoroethylene-cochloride trifluoride ethylene) *Source:* From P. Martins, A.C. Lopes, S. Lanceros-Mendez, Electroactive phases of poly (vinylidene fluoride): determination, processing and applications. Top. Issue Electroactive Polym., 2014, 39(4), 683−706. https://doi.org/10.1016/j.progpolymsci.2013.07.006.

the common conducting polymers that are combined with graphene/graphene-based groups to enhance electrode performance of supercapacitors [7].

### 13.6.1 Graphene−PANI nanocomposites

Utilization of graphene/graphene-based PANI nanocomposites exhibited enhanced electrochemical properties of supercapacitor electrodes [194,216−218]. Interactions at the interface (between PANI and graphene) have a direct impact on the efficiency of the supercapacitor. Optimized ion-diffusion paths are obtained due to the larger interfacial area as a result of strong bonding [219]. In situ oxidation polymerization synthesized graphene−PANI nanocomposites exhibited a high specific capacitance of 863.6 F $g^{-1}$ at 0.2 A $g^{-1}$ which is very promising for supercapacitor application [72]. In another study, in situ polymerized graphene−PANI nanocomposites displayed higher specific capacitance of 1046 F $g^{-1}$ than pure PANI (115 F $g^{-1}$) [220]. A specific capacitance of 1126 F $g^{-1}$ with 84% capacitance retention (after 1000 cycles) has been

**Table 13.3** An overview of Nonconducting fillers and PVDF-based PNCs for capacitor application.

| Polymer matrix | Filler materials | Filler type | Dielectric constant (1 kHz) | Loss tangent (1 kHz) | Discharge energy density (J $cm^{-3}$) | Breakdown strength (kV $cm^{-1}$) | References |
|---|---|---|---|---|---|---|---|
| PVDF | $BaTiO_3$ | Spherical | 95 | 0.04 | – | 55 | Mao et al. [170] |
| | $BaTiO_3$ modified with polyvinylprrolidone | Spherical | 77 | 0.1 | 6.9 | ~1500 | Yu et al. [53–56] |
| | BaTiO3 modified with Ag grafting | Spherical | ~20 | 0.03 | 0.83 at (1000 kV $cm^{-1}$) | 881 | Xie et al. [90,91] |
| | $BaTiO_3$ modified with Ag coating | Spherical | 160 | 0.11 | – | ~200 | Luo et al. [171,172] |
| | $BaTiO_3$ modified with $SiO_2$ | Spherical | 14.7 | 0.02 | 6.28 | 3400 | Yu et al. [53–56] |
| | BaTiO3 modified with tertrafluorophthalic acid | Spherical | 40 | 0.04 | 5.1 | 1760 | Yu et al. [53–56] |
| | $BaTiO_3$ modified with $SnO_2$ | Spherical | 200 | 0.6 | – | – | Zha et al. [173] |
| | $BaTiO_3$ modified with Dopamine | Spherical | 56.8 | 0.04 | – | – | Lin et al. [17] |
| | BaTiO3 modified with tetradecylphosphonic acid | Spherical | 48 | 0.03 | – | – | Ye et al. [174] |
| | $K_2CO_3$ | Spherical | $2.9 \times 10^6$ | 27.5 | – | – | Wang et al. [175–177] |
| | $BiFeO_3$ | Spherical | ~1000 | 0.2 | – | – | Bhadra et al. [178] |
| | Calcium barium zirconate titanate ($Ba_{0.95}Ca_{0.05}Zr_{0.15}Ti_{0.85}O_3$) coated with dopamine | Spherical | ~100 | 0.05 | – | 679 | Luo et al. [171,172] |
| | $BaF_{12}O_{19}$ nanofibers | One-dimensional | 12.8 | 0.15 | – | – | Jing et al. [179] |
| | $V_2O_5$ nanobelts | One-dimensional | 80 | 0.45 | – | – | Quan et al. [180] |
| | $BaTiO_3$ nanofibers modified with dopamine | One-dimensional | 30 | 0.007 | – | ~2102 | Song et al. [85–87] |
| | $Ba_{0.6}Sr_{0.4}TiO_3$ nanofibers modified with dopamine | One-dimensional | 22.5 | 0.02 | 5.24 | 3088 | Song et al. [85–87] |
| | $TiO_2$ nanowires functionalized with aminopropyl triethoxysilane | One-dimensional | 16 | 0.08 | 12.4 | 4500 | Tang, Sodano [181] |
| | $BaTiO_3$ nanowires modified with aminopropyl triethoxysilane | One-dimensional | 24 | 0.018 | 3.36 (at 3300 kV $cm^{-1}$) | 2300 | Liu et al. [72,73] |

(*Continued*)

**Table 13.3** (Continued)

| Polymer matrix | Filler materials | Filler type | Dielectric constant (1 kHz) | Loss tangent (1 kHz) | Discharge energy density (J $cm^{-3}$) | Breakdown strength (kV $cm^{-1}$) | References |
|---|---|---|---|---|---|---|---|
| | $Ba_{0.6}Sr_{0.4}TiO_3$ nanofibers modified with aminopropyl triethoxysilane | One-dimensional | 21.78 | 0.015 | 4.2 (at 3800 kV $cm^{-1}$) | 2966 | Liu, Zhai [182] |
| P (VDF-HFP) | $BaTiO_3$ modified with pentafluorobenzyl phosphonic acid | Spherical | 31 | ~0.02 | – | 2150 | Kim et al. [183] |
| | $BaTiO_3$ coated with $TiO_2$ | Spherical | 110 | ~0.04 | 12.2 (at 3400 kV $cm^{-1}$) | ~1900 | Rahimabady et al. [16] |
| | $BaTiO_3$ coated with poly(1 H,1 H,2 H,2 H heptade cafluorodecyl acrylate) | Spherical | ~45 | ~0.02 | ~0.08 | ~1500 | Yang et al. [158, 184,185] |
| P (VDF-TrFE) | BaTiO3 | Spherical | 130 | 0.025 | – | – | Vacche et al. [186] |
| | $TiO_2$ decorated with Nickel | Spherical | 18.56 | 0.046 | – | – | Kuang et al. [187] |
| | $BaTiO_3$ nanowires modified with dopamine | One-dimensional | 30 | 0.02 | – | 2048 | Song et al. [85–87] |
| | $Ba_{0.3}Sr_{0.7}TiO_3 + Bi_2O_3$ nanofibers modified with dopamine | One-dimensional | 34 | 0.03 | 4.72 (at 1550 kV $cm^{-1}$) | ~1100 | Hu et al. [188] |
| P (VDF-CTFE) | Ba0.5Sr0.5TiO3 | Spherical | 54–70 | 0.07–0.1 | – | – | Zhang et al. [189] |
| | BaTiO3 modified with ethylenediamine | Spherical | ~24 | 0.05 | – | – | Li et al. [190] |
| | $TiO_2$ nanorods modified with Ba-OH | One-dimensional | 24 | 0.04 | – | ~1750 | Li et al. [191] |
| P (VDF-TrFE-CTFE) | $BaTiO_3$ modified with ethylenediamine | Spherical | ~55 | 0.07 | – | – | Li et al. [5] |
| | TiO2 nanorods modified with Ba-OH | One-dimensional | 40 | 0.05 | – | 2000 | Li et al. [191] |
| PVDF/PMMA | BaTiO3 | Spherical | 8–8.5 | ~0.045 | – | – | Mofokeng et al. [192] |
| PVDF | $BaTiO_3$ + polyacrylate elastomers | Spherical | 13 | 0.05 | 8.8 (at 4000 kV $cm^{-1}$) | – | Yu et al. [193] |

**Table 13.4** An overview of conducting fillers and PVDF-based PNCs for capacitor application.

| Polymer matrix | Filler materials | Filler type | Dielectric constant (1 kHz) | Loss tangent (1 kHz) | Breakdown strength (kV $cm^{-1}$) | References |
|---|---|---|---|---|---|---|
| PVDF | TiC | Spherical | 150 | – | – | Wang et al. [194] |
| | Carbon nanotube | One-dimensional | 16 | 0.01 | – | Baji et al. [195] |
| | Multiwalled carbon nanotube (MWCNT) | One-dimensional | 1000 | 1.5 | – | Yuan et al. [196,197] |
| | MWCNT coated with $TiO_2$ nano particles | One-dimensional | ~50 | ~0.25 | 1600 | Yang et al. [164,198] |
| | CNTs grown on SiC | One-dimensional | 8000 | 40 | – | Yuan et al. [196,197] |
| | $CaCu_3Ti_4O_{12}$ | Spherical | ~80 | ~0.11 | – | Thomas et al. [199] |
| | Polyaniline (PANI) | Spherical | 385 | 0.85 | 600 | Yuan et al. [200] |
| | PANI modified with dodecylbenzen-esulfonic acid | Spherical | ~95 | 0.55 | – | Shehzad et al. [201] |
| | Zinc flakes | Flakes shaped | 176 | 0.06 | – | Zhang et al. [202–204] |
| | ZnO | Flower shaped | ~180 | ~0.35 | 420 | Wu et al. [205] |
| | ZnO | Walnut shaped | ~ 80 | ~ 0.45 | 400 | |
| | Graphene nanosheets (GNs) | One-dimensional | 6000 | 4 | – | Fan et al. [76,77] |
| | Graphene oxide (GO) | One-dimensional | 35 | 0.64 | – | Ataur Rahman et al. [206] |
| | Reduced graphene oxide (RGO) | One-dimensional | 52 | 1.12 | – | |
| | $BaTiO_3$ + GO | – | 10 | 0.05 | 1500 | Shen et al. [207] |
| | BaTiO3 + RGO | – | 16 | 0.12 | – | |
| PVDF/polystyrene (PS) blend | Carbon black | – | 230 | 4 | – | Zhao et al. [208] |
| PVDF/PMMA | Hydroxylated MWCNT blend | – | 300 | 1 | – | Yang et al. [158,184,185] |

(*Continued*)

**Table 13.4** (Continued)

| Polymer matrix | Filler materials | Filler type | Dielectric constant (1 kHz) | Loss tangent (1 kHz) | Breakdown strength (kV $cm^{-1}$) | References |
|---|---|---|---|---|---|---|
| P (VDF-CTFE) | Ni | Spherical | ~800 | ~1 | – | Zhang et al. [209] |
| P (VDF-TrFE) | Ni | Spherical | ~970 | ~1 | – | |
| | MWCNT modified with nitro-sulfuric acid | One-dimensional | 900 | 0.9 | – | Wang et al. [175–177] |
| | GNs modified with APS | – | 74 | 0.08 | – | Wen et al. [167,168] |
| P (VDF-HFP) | RGO | – | 825 (spin-casting) | 233 (spin-casting) | – | Tong et al. [160] |
| PVDF/low-density polyethylene | MWCNT | One-dimensional | ~170 | ~5 | – | Yuan et al. [210] |

reported for graphene−PANI nanocomposites fabricated by in situ polymerization−reduction/dedoping−redoping method [157,221]. Hierarchical nanocomposite composed of 1D PANI nanowires physisorbed on 2D graphene oxide (GO) nanosheets showed specific capacitance of 555 F $g^{-1}$ at a low current density of 0.2 A $g^{-1}$ [159]. In another study, PANI nanowires were grown on 3D reduced graphene oxide (rGO). It showed a specific capacitance of 385 F $g^{-1}$ at a current density of 0.5 A $g^{-1}$ [222]. These hierarchical graphene−PANI nanocomposites showed a promising result to be used as electrode materials in flexible or rolling-up devices [203]. The graphene surface chemistry has an important role in the PANI growth as well as the final specific capacitance of supercapacitor electrodes. The amine-modified rGO integrated PANI composites displayed the highest increment in specific capacitance with a value as high as 500 F $g^{-1}$ [223]. Among other hybrid materials, graphene−PANI flakes [78], graphene−PANI nanofibers [135], hierarchical graphene@PANI@graphene sandwich containing hollow structures [224], etc. are utilized as promising materials for supercapacitors. In addition to supercapacitors, graphene-based PANI nanocomposites are also applied in fuel cells [225,226] as well as in dye-sensitized solar cells [6,175]. A graphical depiction of various synthesis processes of graphene−PANI nanocomposites is shown in Fig. 13.8.

### 13.6.2 Graphene−PPy nanocomposites

PPy is another emerging electrode material for supercapacitors. For the last few years, graphene/PPy nanocomposites have also been utilized as supercapacitors electrodes [24,227−229]. At a current density of 0.5 A $g^{-1}$, a specific capacitance of 482 F $g^{-1}$ is observed for polymerized PPy with graphene whereas sulfonated graphene (SG) and PPy composite exhibited a specific capacitance of 285 F $g^{-1}$ at a discharge rate of 0.5 A $g^{-1}$ [230]. A capacitance of 318.6 F $g^{-1}$ with 95% capacity retention after 1000 cycles is observed in hierarchical graphene−PPy nanosheet nanocomposites 279. PPy-wrapped graphene hydrogel nanocomposites showed a high specific capacitance of 375 F $g^{-1}$ along with excellent capacitance retention for more than 4000 cycles 281. Among other hybrid graphene−PPy nanostructures, graphene/bacterial cellulose/PPy composites [231], PPy/SG composite [227], freestanding $TiO_2$/graphene/PPy composite [232], and PPy/rGO-cetyltrimethylammonium bromide [76], etc. are commonly used as electrode materials in supercapacitor. A hypothetical schematics of the PPy−rGO nanocomposite synthesis process is shown in Fig. 13.9.

In addition, graphene-PEDOT [233], graphene-PEDOT: PSS [234], graphene-PTh [235], graphene-PHTh [2], etc. showed promising results to be utilized as supercapacitor materials.

## 13.7 Conclusion and prospects

To keep up with the constant rise of energy demand, researchers and scientists all over the globe are trying heart and soul every day to provide a solution that is both efficient and eco-friendly. The emergence of novel PNC materials caught researchers'

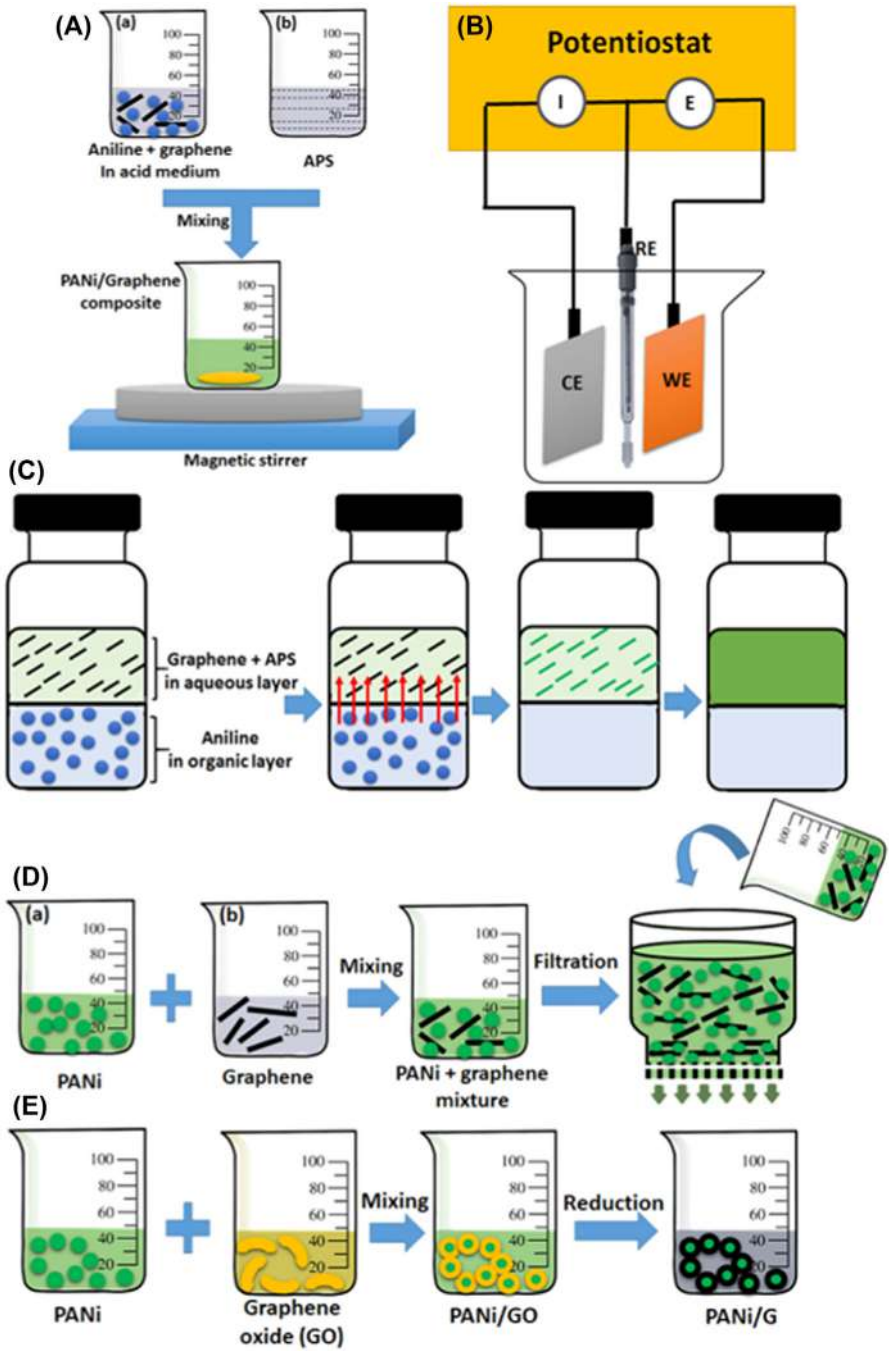


**Figure 13.8** Fabrication process of graphene−PANI nanocomposites by (A) in situ chemical oxidative polymerization, (B) in situ electro-polymerization, (C) interfacial polymerization, (D) solution mixing, and (E) self-assembly mechanism. *APS*, Ammonium persulphate; *CE*, counter electrode; *G*, graphene; *PANI*, polyaniline; *RE*, reference electrode; *WE*, working electrode. *Source*: From M. Moussa, M.F. El-Kady, Z. Zhao, P. Majewski, J. Ma, Recent progress and performance evaluation for polyaniline/graphene nanocomposites as supercapacitor electrodes. Nanotechnology, 2016, 27(44), 442001. https://doi.org/10.1088/0957-4484/27/44/442001.

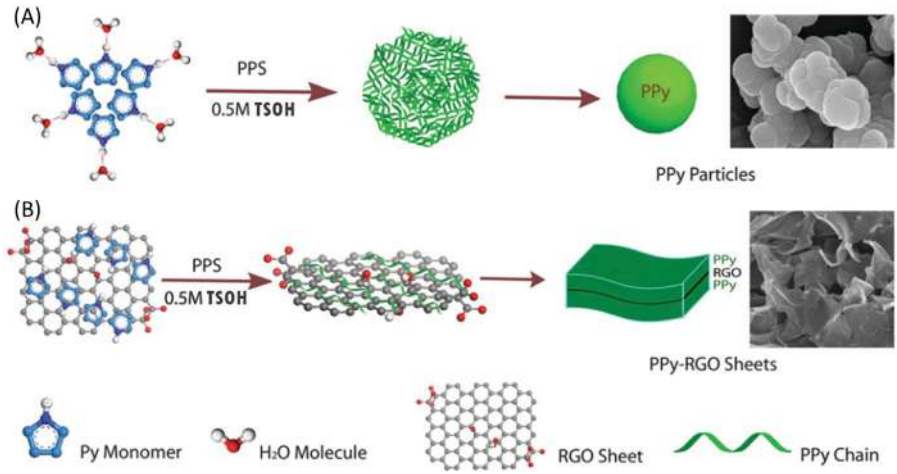


**Figure 13.9** Synthesis of PPy-rGO-based nanosheet composites.
*Source*: From J. Zhu, Y. Xu, J. Wang, J. Wang, Y. Bai, X. Du,. Morphology controllable nano-sheet polypyrrole−graphene composites for high-rate supercapacitor. Phys. Chem. Chem. Phys., 2015, 17(30), 19885−19894. https://doi.org/10.1039/C5CP02710A.

attention owing to their promising potential in energy-related applications. Till now multifarious polymer matrix combined with inorganic/organic nanofillers is investigated and studied to gain insight into the property, structure, processing, and performance of these PNCs. Among various combinations, fluoropolymer-based, and graphene-based PNCs exhibited outstanding possibilities. These PNCs have already found their place in energy storage devices like dielectrics, supercapacitors, as well as energy conversion devices such as fuel cells, solar cells, and so on. Judicious selection of matrix and fillers play a key role in controlling the energy properties of these PNC devices. Enhanced energy density, dielectric constant, breakdown strength, electric and ionic conductivity, etc. are observed from these polymer-based nanocomposites. However, there are plenty of challenges that are yet to be addressed. Though in most cases, higher filler loading enhances the energy (electrical) properties of these devices, it sometimes deteriorates mechanical properties that have a crucial effect on their fabrication process. In addition, the study of the matrix-filler interface of PNCs is still in its infancy. Moreover, the effect of the interface in multicomponent systems is still a puzzle. So, more detailed and meticulous studies are required to unveil the full capacity of PNC. It is certain that if these difficulties are overcome, polymer nanocomposites will open a new horizon in the field of energy application.

## References

[1] K.F. Amin, Asrafuzzaman, A. Sharif, M.E. Hoque, Bamboo/Bamboo Fiber Reinforced Concrete Composites and Their Applications in Modern Infrastructure, Springer, Singapore, 2021, pp. 271−297. Available from: https://doi.org/10.1007/978-981-15-8489-3_15.

[2] L. Ji, P. Meduri, V. Agubra, X. Xiao, M. Alcoutlabi, Graphene-based nanocomposites for energy storage, Adv. Energy Mater. 6 (16) (2016) 1502159. Available from: https://doi.org/10.1002/aenm.201502159.
[3] V.K. Thakur, G. Ding, J. Ma, P.S. Lee, X. Lu, Hybrid materials and polymer electrolytes for electrochromic device applications, Adv. Mater. 24 (30) (2012) 4071–4096. Available from: https://doi.org/10.1002/adma.201200213.
[4] V.K. Thakur, M.-F. Lin, E.J. Tan, P.S. Lee, Green aqueous modification of fluoropolymers for energy storage applications, J. Mater. Chem. 22 (13) (2012) 5951–5959. Available from: https://doi.org/10.1039/C2JM15665B.
[5] J.Y. Li, L. Zhang, S. Ducharme, Electric energy density of dielectric nanocomposites, Appl. Phys. Lett. 90 (13) (2007) 132901. Available from: https://doi.org/10.1063/1.2716847.
[6] Y.-C. Hsu, G.-L. Chen, R.-H. Lee, Graphene oxide sheet-polyaniline nanocomposite prepared through in-situ polymerization/deposition method for counter electrode of dye-sensitized solar cell, J. Polym. Res. 21 (5) (2014) 440. Available from: https://doi.org/10.1007/s10965-014-0440-5.
[7] D.J. Kim, M.J. Jo, S.Y. Nam, A review of polymer–nanocomposite electrolyte membranes for fuel cell application, J. Ind. Eng. Chem. 21 (2015) 36–52. Available from: https://doi.org/10.1016/j.jiec.2014.04.030.
[8] C. Yang, H. Wei, L. Guan, J. Guo, Y. Wang, X. Yan, et al., Polymer nanocomposites for energy storage, energy saving, and anticorrosion, J. Mater. Chem. A 3 (29) (2015) 14929–14941. Available from: https://doi.org/10.1039/C5TA02707A.
[9] Q. Wang, L. Zhu, Polymer nanocomposites for electrical energy storage, J. Polym. Sci. Part. B: Polym. Phys. 49 (20) (2011) 1421–1429. Available from: https://doi.org/10.1002/polb.22337.
[10] B. Chu, X. Zhou, K. Ren, B. Neese, M. Lin, Q. Wang, et al., A dielectric polymer with high electric energy density and fast discharge speed, Science 313 (5785) (2006) 334. Available from: https://doi.org/10.1126/science.1127798.
[11] K.F. Amin, Asrafuzzaman, A. Sharif, M.E. Hoque, Bonding Mechanism and Interface Enhancement of Bamboo Fiber Reinforced Composites, Springer, Singapore, 2021, pp. 215–233. Available from: https://doi.org/10.1007/978-981-15-8489-3_12.
[12] M.-F. Lin, V.K. Thakur, E.J. Tan, P.S. Lee, Surface functionalization of BaTiO3 nanoparticles and improved electrical properties of BaTiO3/polyvinylidene fluoride composite, RSC Adv. 1 (4) (2011) 576–578. Available from: https://doi.org/10.1039/C1RA00210D.
[13] M. Roy, J.K. Nelson, R.K. MacCrone, L.S. Schadler, C.W. Reed, R. Keefe, Polymer nanocomposite dielectrics-the role of the interface, IEEE Trans. Dielectr. Electr. Insulation 12 (4) (2005) 629–643. Available from: https://doi.org/10.1109/TDEI.2005.1511089.
[14] E. Tuncer, I. Sauers, D.R. James, A.R. Ellis, M.P. Paranthaman, T. Aytuğ, et al., Electrical properties of epoxy resin based nano-composites, Nanotechnology 18 (2) (2006) 025703. Available from: https://doi.org/10.1088/0957-4484/18/2/025703.
[15] C. Huang, Q.M. Zhang, J.Y. Li, M. Rabeony, Colossal dielectric and electromechanical responses in self-assembled polymeric nanocomposites, Appl. Phys. Lett. 87 (18) (2005) 182901. Available from: https://doi.org/10.1063/1.2105997.
[16] M. Rahimabady, M.S. Mirshekarloo, K. Yao, L. Lu, Dielectric behaviors and high energy storage density of nanocomposites with core–shell BaTiO3@TiO2 in poly (vinylidene fluoride-hexafluoropropylene), Phys. Chem. Chem. Phys. 15 (38) (2013) 16242–16248. Available from: https://doi.org/10.1039/C3CP52267A.

[17] D. Lin, W. Liu, Y. Liu, H.R. Lee, P.-C. Hsu, K. Liu, et al., High ionic conductivity of composite solid polymer electrolyte via in situ synthesis of monodispersed SiO2 nanospheres in poly(ethylene oxide), Nano Lett. 16 (1) (2016) 459−465. Available from: https://doi.org/10.1021/acs.nanolett.5b04117.

[18] C. Mao, Y. Zhu, W. Jiang, Design of electrical conductive composites: tuning the morphology to improve the electrical properties of graphene filled immiscible polymer blends, ACS Appl. Mater. Interfaces 4 (10) (2012) 5281−5286. Available from: https://doi.org/10.1021/am301230q.

[19] S. Siddabattuni, T.P. Schuman, F. Dogan, Dielectric properties of polymer−particle nanocomposites influenced by electronic nature of filler surfaces, ACS Appl. Mater. Interfaces 5 (6) (2013) 1917−1927. Available from: https://doi.org/10.1021/am3030239.

[20] T.P. Schuman, S. Siddabattuni, O. Cox, F. Dogan, Improved dielectric breakdown strength of covalently-bonded interface polymer−particle nanocomposites, Null 17 (8) (2010) 719−731. Available from: https://doi.org/10.1163/092764410X495315.

[21] V.K. Thakur, M.R. Kessler, Polymer nanocomposites: new advanced dielectric materials for energy storage applications, in: A. Tiwari, S. Valyukh (Eds.), Adv. Energy Mater, Scrivener Publishing LLC, 2014, pp. 207−258. Available from: https://doi.org/10.1002/9781118904923.ch5.

[22] R. Waser, Ceramic Materials for Electronics; Processing, Properties, and Applications, 2in: R.C. Buchanan (Ed.), Marcel Dekker Inc, New York, 1992. 1991; XII, 532 pp., hardcover, $ 166.75, ISBN 0-8247-8194-5. Advanced Materials, 4(4), 311−311. Available from: https://doi.org/10.1002/adma.19920040427.

[23] Q.M. Zhang, V. Bharti, X. Zhao, Giant electrostriction and relaxor ferroelectric behavior in electron-irradiated poly(vinylidene fluoride-trifluoroethylene) copolymer, Science 280 (5372) (1998) 2101−2104. Available from: http://www.jstor.org/stable/2896534.

[24] L. Zhu, Exploring strategies for high dielectric constant and low loss polymer dielectrics, J. Phys. Chem. Lett. 5 (21) (2014) 3677−3687. Available from: https://doi.org/10.1021/jz501831q.

[25] A. Fattoum, F. Gmati, N. Bohli, M. Arous, A. Belhadj Mohamed, Effects of the matrix molecular weight on conductivity and dielectric relaxation in plasticized polyaniline/polymethylmethacrylathe blends, J. Phys. D: Appl. Phys. 41 (9) (2008) 095407. Available from: https://doi.org/10.1088/0022-3727/41/9/095407.

[26] X. Huang, B. Sun, Y. Zhu, S. Li, P. Jiang, High-k polymer nanocomposites with 1D filler for dielectric and energy storage applications, Prog. Mater. Sci. 100 (2019) 187−225. Available from: https://doi.org/10.1016/j.pmatsci.2018.10.003.

[27] V.K. Prateek, Thakur, R.K. Gupta, Recent progress on ferroelectric polymer-based nanocomposites for high energy density capacitors: synthesis, dielectric properties, and future aspects, Chem. Rev. 116 (7) (2016) 4260−4317. Available from: https://doi.org/10.1021/acs.chemrev.5b00495.

[28] C.J.F. Böttcher, Chapter II - Some Concepts and Problems of Electrostatics, Theory of Electric Polarization, Elsevier, 1973, pp. 59−89. Available from: https://doi.org/10.1016/B978-0-444-41019-1.50008-0.

[29] C. Kittel, Dielectrics and Ferroelectrics, in: S. Johnson, P. McFadden (Eds.), Introduction to Solid State Physics, John Wiley & Sons, Inc, U.S.A, 2005, pp. 453−485.

[30] K. Yao, S. Chen, M. Rahimabady, M.S. Mirshekarloo, S. Yu, F.E.H. Tay, et al., Nonlinear dielectric thin films for high-power electric storage with energy density comparable with electrochemical supercapacitors, IEEE Trans. Ultrasonics Ferroelectrics

Frequency Control. 58 (9) (2011) 1968–1974. Available from: https://doi.org/10.1109/TUFFC.2011.2039.
[31] Y. Shen, Y. Lin, Q.M. Zhang, Polymer nanocomposites with high energy storage densities, MRS Bull. 40 (9) (2015) 753–759. Available from: https://doi.org/10.1557/mrs.2015.199.
[32] M. Rabuffi, G. Picci, Status quo and future prospects for metallized polypropylene energy storage capacitors, IEEE Trans. Plasma Sci. 30 (5) (2002) 1939–1942. Available from: https://doi.org/10.1109/TPS.2002.805318.
[33] C.W. Reed, S.W. Cichanowskil, The fundamentals of aging in HV polymer-film capacitors, IEEE Trans. Dielectr. Electr. Insulation 1 (5) (1994) 904–922. Available from: https://doi.org/10.1109/94.326658.
[34] W. Li, L. Jiang, X. Zhang, Y. Shen, C.W. Nan, High-energy-density dielectric films based on polyvinylidene fluoride and aromatic polythiourea for capacitors, J. Mater. Chem. A 2 (38) (2014) 15803–15807. Available from: https://doi.org/10.1039/C4TA03374D.
[35] C.-W. Nan, Physics of inhomogeneous inorganic materials, Prog. Mater. Sci. 37 (1) (1993) 1–116. Available from: https://doi.org/10.1016/0079-6425(93)90004-5.
[36] Z.-M. Dang, S.-C. Tjong, 9 - Polymer nanocomposites with high permittivity, Elsevier, 2014, pp. 305–333. Available from: https://doi.org/10.1016/B978-0-12-407796-6.00009-9.
[37] N. Guo, S.A. DiBenedetto, P. Tewari, M.T. Lanagan, M.A. Ratner, T.J. Marks, Nanoparticle, size, shape, and interfacial effects on leakage current density, permittivity, and breakdown strength of metal oxide − polyolefin nanocomposites: experiment and theory, Chem. Mater. 22 (4) (2010) 1567–1578. Available from: https://doi.org/10.1021/cm902852h.
[38] J.R. Laghari, W.J. Sarjeant, Energy-storage pulsed-power capacitor technology, IEEE Trans. Power Electron. 7 (1) (1992) 251–257. Available from: https://doi.org/10.1109/63.124597.
[39] N.H. Malik, A.A. Al-Arainy, M.I. Qureshi, Electrical insulation in power systems, Electr. Insulation Power Syst. (2018) 1–394. Available from: https://doi.org/10.1201/9780203758816.
[40] T.W. Dakin, Conduction and polarization mechanisms and trends in dielectric, IEEE Electr. Insulation Mag. 22 (5) (2006) 11–28. Available from: https://doi.org/10.1109/MEI.2006.1705854.
[41] L.A. Dissado, L.C. Fothergill, Electrical Degradation and Breakdown in Polymers, Peter Peregrins Ltd., London, UK, 1992. https://doi.org/10.1049/PBED009E.
[42] D. Stauffer, A. Aharony, Introduction to Percolation Theory, Taylor & Francis, 1992. Available from: https://doi.org/10.1201/9781315274386.
[43] R.P. Ortiz, A. Facchetti, T.J. Marks, High-k organic, inorganic, and hybrid dielectrics for low-voltage organic field-effect transistors, Chem. Rev. 110 (1) (2010) 205–239. Available from: https://doi.org/10.1021/cr9001275.
[44] D. Wilkinson, J.S. Langer, P.N. Sen, Enhancement of the dielectric constant near a percolation threshold, Phys. Rev. B 28 (2) (1983) 1081–1087. Available from: https://doi.org/10.1103/PhysRevB.28.1081.
[45] C.W. Nan, Y. Shen, J. Ma, Physical Properties of Composites Near Percolation, Annu. Rev. Mater. Res. 40 (2010) 131–151. Available from: https://doi.org/10.1146/annurev-matsci-070909-104529.
[46] K. Su, N. Nuraje, N.-L. Yang, Open-bench method for the preparation of BaTiO3, SrTiO3, and BaxSr1-xTiO3 nanocrystals at 80 °C, Langmuir 23 (23) (2007) 11369–11372. Available from: https://doi.org/10.1021/la701877d.

[47] Z.-M. Dang, J.-K. Yuan, S.-H. Yao, R.-J. Liao, Flexible nanodielectric materials with high permittivity for power energy storage, Adv. Mater. 25 (44) (2013) 6334–6365. Available from: https://doi.org/10.1002/adma.201301752.
[48] R.E. Hummel, Electrical Properties of Polymers, Ceramics, Dielectrics, and Amorphous Materials, Electron. Prop. Mater, Springer, Berlin Heidelberg, 2001, pp. 166–193. Available from: https://doi.org/10.1007/978-3-642-86538-1_9.
[49] L. He, S.C. Tjong, Low percolation threshold of graphene/polymer composites prepared by solvothermal reduction of graphene oxide in the polymer solution, Nanoscale Res. Lett. 8 (1) (2013) 132. Available from: https://doi.org/10.1186/1556-276X-8-132.
[50] K. Miyasaka, K. Watanabe, E. Jojima, H. Aida, M. Sumita, K. Ishikawa, Electrical conductivity of carbon-polymer composites as a function of carbon content, J. Mater. Sci. 17 (6) (1982) 1610–1616. Available from: https://doi.org/10.1007/BF00540785.
[51] M. Narkis, A. Vaxman, Resistivity behavior of filled electrically conductive crosslinked polyethylene, J. Appl. Polym. Sci. 29 (5) (1984) 1639–1652. Available from: https://doi.org/10.1002/app.1984.070290518.
[52] K.P. Sau, T.K. Chaki, D. Khastgir, Conductive rubber composites from different blends of ethylene-propylene-diene rubber and nitrile rubber, J. Mater. Sci. 32 (21) (1997) 5717–5724. Available from: https://doi.org/10.1023/A:1018613600169.
[53] J. Yu, R. Qian, P. Jiang, Enhanced thermal conductivity for PVDF composites with a hybrid functionalized graphene sheet-nanodiamond filler, Fibers Polym. 14 (8) (2013) 1317–1323. Available from: https://doi.org/10.1007/s12221-013-1317-7.
[54] K. Yu, Y. Niu, Y. Bai, Y. Zhou, H. Wang, Poly(vinylidene fluoride) polymer based nanocomposites with significantly reduced energy loss by filling with core-shell structured BaTiO3/SiO2 nanoparticles, Appl. Phys. Lett. 102 (10) (2013) 102903. Available from: https://doi.org/10.1063/1.4795017.
[55] K. Yu, Y. Niu, F. Xiang, Y. Zhou, Y. Bai, H. Wang, Enhanced electric breakdown strength and high energy density of barium titanate filled polymer nanocomposites, J. Appl. Phys. 114 (17) (2013) 174107. Available from: https://doi.org/10.1063/1.4829671.
[56] K. Yu, Y. Niu, Y. Zhou, Y. Bai, H. Wang, Nanocomposites of surface-modified BaTiO3 nanoparticles filled ferroelectric polymer with enhanced energy density, J. Am. Ceram. Soc. 96 (8) (2013) 2519–2524. Available from: https://doi.org/10.1111/jace.12338.
[57] Y. Li, T.M. Krentz, L. Wang, B.C. Benicewicz, L.S. Schadler, Ligand engineering of polymer nanocomposites: from the simple to the complex, ACS Appl. Mater. Interfaces 6 (9) (2014) 6005–6021. Available from: https://doi.org/10.1021/am405332a.
[58] H. Gu, Y. Huang, X. Zhang, Q. Wang, J. Zhu, L. Shao, et al., Magnetoresistive polyaniline-magnetite nanocomposites with negative dielectrical properties, Polymer 53 (3) (2012) 801–809. Available from: https://doi.org/10.1016/j.polymer.2011.12.033.
[59] H. Gu, S. Tadakamalla, Y. Huang, H.A. Colorado, Z. Luo, N. Haldolaarachchige, et al., Polyaniline stabilized magnetite nanoparticle reinforced epoxy nanocomposites, ACS Appl. Mater. Interfaces 4 (10) (2012) 5613–5624. Available from: https://doi.org/10.1021/am301529t.
[60] J. Yang, Y. Liu, S. Liu, L. Li, C. Zhang, T. Liu, Conducting polymer composites: material synthesis and applications in electrochemical capacitive energy storage, Mater. Chem. Front. 1 (2) (2017) 251–268. Available from: https://doi.org/10.1039/C6QM00150E.
[61] T.K. Das, S. Prusty, Review on conducting polymers and their applications, Polym. Technol. Eng. 51 (14) (2012) 1487–1500. Available from: https://doi.org/10.1080/03602559.2012.710697.

[62] S.K.S. Hossain, M.E. Hoque, 9 - Polymer nanocomposite materials in energy storage: properties and applications, in: M. Jawaid, M.M. Khan (Eds.), Woodhead Publishing Series in Composites Science and Engineering, Woodhead Publishing, 2018, pp. 239–282. Available from: https://doi.org/10.1016/B978-0-08-102262-7.00009-X.

[63] X. Lu, W. Zhang, C. Wang, T.-C. Wen, Y. Wei, One-dimensional conducting polymer nanocomposites: synthesis, properties and applications, Special Issue on Conducting Polymers 36 (5) (2011) 671–712. Available from: https://doi.org/10.1016/j.progpolymsci.2010.07.010.

[64] S.A. Paniagua, Y. Kim, K. Henry, R. Kumar, J.W. Perry, S.R. Marder, Surface-initiated polymerization from barium titanate nanoparticles for hybrid dielectric capacitors, ACS Appl. Mater. Interfaces 6 (5) (2014) 3477–3482. Available from: https://doi.org/10.1021/am4056276.

[65] V.K. Thakur, D. Vennerberg, S.A. Madbouly, M.R. Kessler, Bio-inspired green surface functionalization of PMMA for multifunctional capacitors, RSC Adv. 4 (13) (2014) 6677–6684. Available from: https://doi.org/10.1039/C3RA46592F.

[66] S. Gross, D. Camozzo, V. Di Noto, L. Armelao, E. Tondello, PMMA: a key macromolecular component for dielectric low-κ hybrid inorganic–organic polymer films, Eur. Polym. J. 43 (3) (2007) 673–696. Available from: https://doi.org/10.1016/j.eurpolymj.2006.12.012.

[67] M.A. Alam, M.H. Azarian, M.G. Pecht, Modeling the electrical conduction in epoxy–BaTiO3 nanocomposites, J. Electron. Mater. 42 (6) (2013) 1101–1107. Available from: https://doi.org/10.1007/s11664-013-2523-1.

[68] L. Fang, C. Wu, R. Qian, L. Xie, K. Yang, P. Jiang, Nano–micro structure of functionalized boron nitride and aluminum oxide for epoxy composites with enhanced thermal conductivity and breakdown strength, RSC Adv. 4 (40) (2014) 21010–21017. Available from: https://doi.org/10.1039/C4RA01194E.

[69] X. Huang, T. Iizuka, P. Jiang, Y. Ohki, T. Tanaka, Role of interface on the thermal conductivity of highly filled dielectric epoxy/AlN composites, J. Phys. Chem. C. 116 (25) (2012) 13629–13639. Available from: https://doi.org/10.1021/jp3026545.

[70] P. Kuzhir, A. Paddubskaya, A. Plyushch, N. Volynets, S. Maksimenko, J. Macutkevic, et al., Epoxy composites filled with high surface area-carbon fillers: optimization of electromagnetic shielding, electrical, mechanical, and thermal properties, J. Appl. Phys. 114 (16) (2013) 164304. Available from: https://doi.org/10.1063/1.4826529.

[71] M. Molberg, D. Crespy, P. Rupper, F. Nüesch, J.-A.E. Månson, C. Löwe, et al., High breakdown field dielectric elastomer actuators using encapsulated polyaniline as high dielectric constant filler, Adv. Funct. Mater. 20 (19) (2010) 3280–3291. Available from: https://doi.org/10.1002/adfm.201000486.

[72] J. Liu, G. Tian, S. Qi, Z. Wu, D. Wu, Enhanced dielectric permittivity of a flexible three-phase polyimide–graphene–BaTiO3 composite material, Mater. Lett. 124 (2014) 117–119. Available from: https://doi.org/10.1016/j.matlet.2014.02.105.

[73] S. Liu, S. Xue, W. Zhang, J. Zhai, Enhanced dielectric and energy storage density induced by surface-modified BaTiO3 nanofibers in poly(vinylidene fluoride) nanocomposites, Ceram. Int. 40 (10, Part A) (2014) 15633–15640. Available from: https://doi.org/10.1016/j.ceramint.2014.07.083.

[74] Y.-H. Zhang, Z.-M. Dang, J.H. Xin, W.A. Daoud, J.-H. Ji, Y. Liu, et al., Dielectric properties of polyimide-mica hybrid films, Macromol. Rapid Commun. 26 (18) (2005) 1473–1477. Available from: https://doi.org/10.1002/marc.200500310.

[75] F. Ding, W. Xu, G.L. Graff, J. Zhang, M.L. Sushko, X. Chen, et al., Dendrite-free lithium deposition via self-healing electrostatic shield mechanism, J. Am. Chem. Soc. 135 (11) (2013) 4450–4456. Available from: https://doi.org/10.1021/ja312241y.

[76] B.-H. Fan, J.-W. Zha, D.-R. Wang, J. Zhao, Z.-M. Dang, Experimental study and theoretical prediction of dielectric permittivity in BaTiO3/polyimide nanocomposite films, Appl. Phys. Lett. 100 (9) (2012) 092903. Available from: https://doi.org/10.1063/1.3691198.

[77] P. Fan, L. Wang, J. Yang, F. Chen, M. Zhong, Graphene/poly(vinylidene fluoride) composites with high dielectric constant and low percolation threshold, Nanotechnology 23 (36) (2012) 365702. Available from: https://doi.org/10.1088/0957-4484/23/36/365702.

[78] S. Chen, J. Hu, L. Gao, Y. Zhou, S. Peng, J. He, et al., Enhanced breakdown strength and energy density in PVDF nanocomposites with functionalized MgO nanoparticles, RSC Adv. 6 (40) (2016) 33599−33605. Available from: https://doi.org/10.1039/C6RA01869F.

[79] M. Taj, S.R. Manohara, S.M. Hanagodimath, L. Gerward, Novel conducting poly(3,4-ethylenedioxythiophene) − graphene nanocomposites with gigantic dielectric properties and narrow optical energy band gap, Polym. Test. 90 (2020) 106650. Available from: https://doi.org/10.1016/j.polymertesting.2020.106650.

[80] F. Namouchi, H. Smaoui, N. Fourati, C. Zerrouki, H. Guermazi, J.J. Bonnet, Investigation on electrical properties of thermally aged PMMA by combined use of FTIR and impedance spectroscopies, J. Alloy. Compd. 469 (1) (2009) 197−202. Available from: https://doi.org/10.1016/j.jallcom.2008.01.148.

[81] E.A. Stefanescu, X. Tan, Z. Lin, N. Bowler, M.R. Kessler, Multifunctional fiberglass-reinforced PMMA-BaTiO3 structural/dielectric composites, Polymer 52 (9) (2011) 2016−2024. Available from: https://doi.org/10.1016/j.polymer.2011.02.050.

[82] I. Sulym, P. Klonos, M. Borysenko, P. Pissis, V.M. Gun'ko, Dielectric and thermal studies of segmental dynamics in silica/PDMS and silica/titania/PDMS nanocomposites, J. Appl. Polym. Sci. 131 (23) (2014). Available from: https://doi.org/10.1002/app.41154.

[83] C.-K. Min, T.-B. Wu, W.-T. Yang, C.-L. Chen, Functionalized mesoporous silica/polyimide nanocomposite thin films with improved mechanical properties and low dielectric constant, Compos. Sci. Technol. 68 (6) (2008) 1570−1578. Available from: https://doi.org/10.1016/j.compscitech.2007.09.021.

[84] Y. Zhang, S. Ke, H. Huang, L. Zhao, L. Yu, H.L.W. Chan, Dielectric relaxation in polyimide nanofoamed films with low dielectric constant, Appl. Phys. Lett. 92 (5) (2008) 052910. Available from: https://doi.org/10.1063/1.2840715.

[85] Y. Song, Y. Shen, P. Hu, Y. Lin, M. Li, C.W. Nan, Significant enhancement in energy density of polymer composites induced by dopamine-modified Ba0.6Sr0.4TiO3 nanofibers, Appl. Phys. Lett. 101 (15) (2012) 152904. Available from: https://doi.org/10.1063/1.4760228.

[86] Y. Song, Y. Shen, H. Liu, Y. Lin, M. Li, C.-W. Nan, Enhanced dielectric and ferroelectric properties induced by dopamine-modified BaTiO3 nanofibers in flexible poly (vinylidene fluoride-trifluoroethylene) nanocomposites, J. Mater. Chem. 22 (16) (2012) 8063−8068. Available from: https://doi.org/10.1039/C2JM30297G.

[87] Y. Song, Y. Shen, H. Liu, Y. Lin, M. Li, C.-W. Nan, Improving the dielectric constants and breakdown strength of polymer composites: effects of the shape of the BaTiO3 nanoinclusions, surface modification and polymer matrix, J. Mater. Chem. 22 (32) (2012) 16491−16498. Available from: https://doi.org/10.1039/C2JM32579A.

[88] L. Gao, J. He, J. Hu, Y. Li, Large enhancement in polarization response and energy storage properties of poly(vinylidene fluoride) by improving the interface effect in

nanocomposites, J. Phys. Chem. C. 118 (2) (2014) 831–838. Available from: https://doi.org/10.1021/jp409474k.
[89] W. Li, Q. Meng, Y. Zheng, Z. Zhang, W. Xia, Z. Xu, Electric energy storage properties of poly(vinylidene fluoride), Appl. Phys. Lett. 96 (19) (2010) 192905. Available from: https://doi.org/10.1063/1.3428656.
[90] L. Xie, X. Huang, Y. Huang, K. Yang, P. Jiang, Core@Double-shell structured BaTiO3–polymer nanocomposites with high dielectric constant and low dielectric loss for energy storage application, J. Phys. Chem. C. 117 (44) (2013) 22525–22537. Available from: https://doi.org/10.1021/jp407340n.
[91] L. Xie, X. Huang, B.-W. Li, C. Zhi, T. Tanaka, P. Jiang, Core–satellite Ag@BaTiO3 nanoassemblies for fabrication of polymer nanocomposites with high discharged energy density, high breakdown strength and low dielectric loss, Phys. Chem. Chem. Phys. 15 (40) (2013) 17560–17569. Available from: https://doi.org/10.1039/C3CP52799A.
[92] X. Huang, P. Jiang, T. Tanaka, A review of dielectric polymer composites with high thermal conductivity, IEEE Electr. Insulation Mag. 27 (4) (2011) 8–16. Available from: https://doi.org/10.1109/MEI.2011.5954064.
[93] P. Barber, S. Balasubramanian, Y. Anguchamy, S. Gong, A. Wibowo, H. Gao, et al., Polymer composite and nanocomposite dielectric materials for pulse power energy storage, Materials 2 (4) (2009) 1697–1733. Available from: https://doi.org/10.3390/ma2041697.
[94] G.G. Raju, Appendix 3: Selected Properties of Insulating Materials, Dielectrics in Electric Fields, Marcel Dekker, Inc, 2003, pp. 561–566. Available from: https://doi.org/10.1201/9780203912270.
[95] C.W. Beier, J.M. Sanders, R.L. Brutchey, Improved breakdown strength and energy density in thin-film polyimide nanocomposites with small barium strontium titanate nanocrystal fillers, J. Phys. Chem. C. 117 (14) (2013) 6958–6965. Available from: https://doi.org/10.1021/jp312519r.
[96] Q. Chi, J. Sun, C. Zhang, G. Liu, J. Lin, Y. Wang, et al., Enhanced dielectric performance of amorphous calcium copper titanate/polyimide hybrid film, J. Mater. Chem. C. 2 (1) (2014) 172–177. Available from: https://doi.org/10.1039/C3TC31757A.
[97] Z.-M. Dang, Y.-Q. Lin, H.-P. Xu, C.-Y. Shi, S.-T. Li, J. Bai, Fabrication and dielectric characterization of advanced BaTiO3/polyimide nanocomposite films with high thermal stability, Adv. Funct. Mater. 18 (10) (2008) 1509–1517. Available from: https://doi.org/10.1002/adfm.200701077.
[98] J.C. Coburn, R.H. Boyd, Dielectric relaxation in poly(ethylene terephthalate), Macromolecules 19 (8) (1986) 2238–2245. Available from: https://doi.org/10.1021/ma00162a021.
[99] A.T. Mohamed, Experimental enhancement for dielectric strength of polyethylene insulation materials using cost-fewer nanoparticles, Int. J. Electr. Power Energy Syst. 64 (2015) 469–475. Available from: https://doi.org/10.1016/j.ijepes.2014.06.075.
[100] E.I. Akpan, X. Shen, B. Wetzel, K. Friedrich, K. Pielichowski, T.M. Majka, 2 - Design and Synthesis of Polymer Nanocomposites, Micro and Nano Technologies, Elsevier, 2019, pp. 47–83. Available from: https://doi.org/10.1016/B978-0-12-814064-2.00002-0.
[101] A.J. Crosby, J. Lee, Polymer nanocomposites: the "Nano" effect on mechanical properties, Null 47 (2) (2007) 217–229. Available from: https://doi.org/10.1080/15583720701271278.
[102] S. Piskunov, E. Heifets, R.I. Eglitis, G. Borstel, Bulk properties and electronic structure of SrTiO3, BaTiO3, PbTiO3 perovskites: an ab initio HF/DFT study, Comput.

Mater. Sci. 29 (2) (2004) 165–178. Available from: https://doi.org/10.1016/j.commatsci.2003.08.036.

[103] L.B. Kong, T.S. Zhang, J. Ma, F. Boey, Progress in synthesis of ferroelectric ceramic materials via high-energy mechanochemical technique, Prog. Mater. Sci. 53 (2) (2008) 207–322. Available from: https://doi.org/10.1016/j.pmatsci.2007.05.001.

[104] V.S. Nisa, S. Rajesh, K.P. Murali, V. Priyadarsini, S.N. Potty, R. Ratheesh, Preparation, characterization and dielectric properties of temperature stable SrTiO3/PEEK composites for microwave substrate applications, Compos. Sci. Technol. 68 (1) (2008) 106–112. Available from: https://doi.org/10.1016/j.compscitech.2007.05.024.

[105] D. Padalia, G. Bisht, U.C. Johri, K. Asokan, Fabrication and characterization of cerium doped barium titanate/PMMA nanocomposites, Solid. State Sci. 19 (2013) 122–129. Available from: https://doi.org/10.1016/j.solidstatesciences.2013.02.002.

[106] B. Schumacher, H. Geßwein, J. Haußelt, T. Hanemann, Temperature treatment of nano-scaled barium titanate filler to improve the dielectric properties of high-k polymer based composites, Microelectron. Eng. 87 (10) (2010) 1978–1983. Available from: https://doi.org/10.1016/j.mee.2009.12.018.

[107] T. Hoshina, Size effect of barium titanate fine particles and ceramics, J. Ceram. Soc. Jpn. 121 (1410) (2013) 156–161. Available from: https://doi.org/10.2109/jcersj2.121.156.

[108] Y. Hu, Y. Zhang, H. Liu, D. Zhou, Microwave dielectric properties of PTFE/CaTiO3 polymer ceramic composites, Ceram. Int. 37 (5) (2011) 1609–1613. Available from: https://doi.org/10.1016/j.ceramint.2011.01.039.

[109] F. Xiang, H. Wang, X. Yao, Preparation and dielectric properties of bismuth-based dielectric/PTFE microwave composites, in: Pap. Presented Third Int. Conf. Microw. Mater. Their Appl. - MMA2004 Inuyama, Jpn., 2006, 26 (10), 1999–2002. Available from: https://doi.org/10.1016/j.jeurceramsoc.2005.09.048.

[110] H. Deng, L. Lin, M. Ji, S. Zhang, M. Yang, Q. Fu, Progress on the morphological control of conductive network in conductive polymer composites and the use as electroactive multifunctional materials, Topical Issue Electroactive Polym. 39 (4) (2014) 627–655. Available from: https://doi.org/10.1016/j.progpolymsci.2013.07.007.

[111] R. Theravalappil, P. Svoboda, J. Vilcakova, S. Poongavalappil, P. Slobodian, D. Svobodova, A comparative study on the electrical, thermal and mechanical properties of ethylene–octene copolymer based composites with carbon fillers, Mater. Des. 60 (2014) 458–467. Available from: https://doi.org/10.1016/j.matdes.2014.04.029.

[112] G.G. Tibbetts, M.L. Lake, K.L. Strong, B.P. Rice, A review of the fabrication and properties of vapor-grown carbon nanofiber/polymer composites, Compos. Sci. Technol. 67 (7) (2007) 1709–1718. Available from: https://doi.org/10.1016/j.compscitech.2006.06.015.

[113] Y.W. Wong, K.L. Lo, F.G. Shin, Electrical and thermal properties of composite of liquid crystalline polymer filled with carbon black, J. Appl. Polym. Sci. 82 (6) (2001) 1549–1555. Available from: https://doi.org/10.1002/app.1993.

[114] M. El Hasnaoui, A. Triki, M.P.F. Graça, M.E. Achour, L.C. Costa, M. Arous, Electrical conductivity studies on carbon black loaded ethylene butylacrylate polymer composites, J. Non-Crystalline Solids 358 (20) (2012) 2810–2815. Available from: https://doi.org/10.1016/j.jnoncrysol.2012.07.008.

[115] V.G. Shevchenko, S.V. Polschikov, P.M. Nedorezova, A.N. Klyamkina, A.N. Shchegolikhin, A.M. Aladyshev, et al., In situ polymerized poly(propylene)/graphene nanoplatelets nanocomposites: dielectric and microwave properties, Polymer 53 (23) (2012) 5330–5335. Available from: https://doi.org/10.1016/j.polymer.2012.09.018.

[116] M. Tian, Z. Wei, X. Zan, L. Zhang, J. Zhang, Q. Ma, et al., Thermally expanded graphene nanoplates/polydimethylsiloxane composites with high dielectric constant, low dielectric loss and improved actuated strain, Compos. Sci. Technol. 99 (2014) 37–44. Available from: https://doi.org/10.1016/j.compscitech.2014.05.004.

[117] M. Moniruzzaman, K.I. Winey, Polymer nanocomposites containing carbon nanotubes, Macromolecules 39 (16) (2006) 5194–5205. Available from: https://doi.org/10.1021/ma060733p.

[118] S.C. Tjong, Electrical and dielectric behavior of carbon nanotube-filled polymer composites, in: S.C. Tjong, Y.-W. Mai (Eds.), Physical Properties and Applications of Polymer Nanocomposites, Woodhead Publishing Limited, 2010, pp. 495–528. Available from: https://doi.org/10.1533/9780857090249.3.495.

[119] H. Chang, G. Wang, A. Yang, X. Tao, X. Liu, Y. Shen, et al., A transparent, flexible, low-temperature, and solution-processible graphene composite electrode, Adv. Funct. Mater. 20 (17) (2010) 2893–2902. Available from: https://doi.org/10.1002/adfm.201000900.

[120] A.E. Daugaard, K. Jankova, J.M.R. Marín, J. Bøgelund, S. Hvilsted, Poly(ethylene-co-butylene) functionalized multi walled carbon nanotubes applied in polypropylene nanocomposites, Eur. Polym. J. 48 (4) (2012) 743–750. Available from: https://doi.org/10.1016/j.eurpolymj.2012.02.006.

[121] A. Yasmin, J.-J. Luo, I.M. Daniel, Processing of expanded graphite reinforced polymer nanocomposites, Nanocomposites 66 (9) (2006) 1182–1189. Available from: https://doi.org/10.1016/j.compscitech.2005.10.014.

[122] S. Ganguli, A.K. Roy, D.P. Anderson, Improved thermal conductivity for chemically functionalized exfoliated graphite/epoxy composites, Carbon 46 (5) (2008) 806–817. Available from: https://doi.org/10.1016/j.carbon.2008.02.008.

[123] A. Kausar, Advances in polymer/fullerene nanocomposite: a review on essential features and applications, Null 56 (6) (2017) 594–605. Available from: https://doi.org/10.1080/03602559.2016.1233278.

[124] E. Badamshina, M. Gafurova, Polymeric nanocomposites containing non-covalently bonded fullerene C60: properties and applications, J. Mater. Chem. 22 (19) (2012) 9427–9438. Available from: https://doi.org/10.1039/C2JM15472B.

[125] V.N. Mochalin, Y. Gogotsi, Nanodiamond–polymer composites, Diam. Relat. Mater. 58 (2015) 161–171. Available from: https://doi.org/10.1016/j.diamond.2015.07.003.

[126] R. Verdejo, M.M. Bernal, L.J. Romasanta, F.J. Tapiador, M.A. Lopez-Manchado, Reactive nanocomposite foams, Cell. Polym. 30 (2) (2011) 45–62. Available from: https://doi.org/10.1177/026248931103000201.

[127] G.K. Mani, J.B.B. Rayappan, A simple and template free synthesis of branched ZnO nanoarchitectures for sensor applications, RSC Adv. 4 (109) (2014) 64075–64084. Available from: https://doi.org/10.1039/C4RA09652E.

[128] A. Umar, Y.B. Hahn, ZnO nanosheet networks and hexagonal nanodiscs grown on silicon substrate: growth mechanism and structural and optical properties, Nanotechnology 17 (9) (2006) 2174–2180. Available from: https://doi.org/10.1088/0957-4484/17/9/016.

[129] H. Zou, S. Wu, J. Shen, Polymer/silica nanocomposites: preparation, characterization, properties, and applications, Chem. Rev. 108 (9) (2008) 3893–3957. Available from: https://doi.org/10.1021/cr068035q.

[130] S. Dhandapani, S.K. Nayak, S. Mohanty, Compatibility effect of titanium dioxide nanofiber on reinforced biobased nanocomposites: thermal, mechanical, and

morphology characterization, J. Vinyl Addit. Technol. 22 (4) (2016) 529–538. Available from: https://doi.org/10.1002/vnl.21475.
[131] S.R. Mohapatra, M.G. Nair, A.K. Thakur, Synergistic effect of nano-ceria dispersion on improvement of Li + ion conductivity in polymer nanocomposite electrolytes, Mater. Lett. 221 (2018) 232–235. Available from: https://doi.org/10.1016/j.matlet.2018.03.101.
[132] M.J. Parnian, S. Rowshanzamir, A.K. Prasad, S.G. Advani, High durability sulfonated poly (ether ether ketone)-ceria nanocomposite membranes for proton exchange membrane fuel cell applications, J. Membr. Sci. 556 (2018) 12–22. Available from: https://doi.org/10.1016/j.memsci.2018.03.083.
[133] W. Yuan, H. Zhao, H. Hu, S. Wang, G.L. Baker, Synthesis and characterization of the hole-conducting silica/polymer nanocomposites and application in solid-state dye-sensitized solar cell, ACS Appl. Mater. Interfaces 5 (10) (2013) 4155–4161. Available from: https://doi.org/10.1021/am4001858.
[134] T. Wang, S. Chen, H. Pang, H. Xue, Y. Yu, MoS2-based nanocomposites for electrochemical energy storage, Adv. Sci. 4 (2) (2017) 1600289. Available from: https://doi.org/10.1002/advs.201600289.
[135] K. Wu, Y. Li, R. Huang, S. Chai, F. Chen, Q. Fu, Constructing conductive multi-walled carbon nanotubes network inside hexagonal boron nitride network in polymer composites for significantly improved dielectric property and thermal conductivity, Compos. Sci. Technol. 151 (2017) 193–201. Available from: https://doi.org/10.1016/j.compscitech.2017.07.014.
[136] T. Tanaka, A quantum dot model for nanoparticles in polymer nanocomposites, IEEE Trans. Dielectr. Electr. Insulation 26 (1) (2019) 276–283. Available from: https://doi.org/10.1109/TDEI.2018.007599.
[137] J. Yu, R. Huo, C. Wu, X. Wu, G. Wang, P. Jiang, Influence of interface structure on dielectric properties of epoxy/alumina nanocomposites, Macromol. Res. 20 (8) (2012) 816–826. Available from: https://doi.org/10.1007/s13233-012-0122-2.
[138] H. Basantakumar Sharma, H.N.K. Sarma, A. Mansingh, Ferroelectric and dielectric properties of sol-gel processed barium titanate ceramics and thin films, J. Mater. Sci. 34 (6) (1999) 1385–1390. Available from: https://doi.org/10.1023/A:1004578905297.
[139] K.D. Schomann, Electric breakdown of barium titanate: a model, Appl. Phys. 6 (1) (1975) 89–92. Available from: https://doi.org/10.1007/BF00883554.
[140] A.D. Hilton, B.W. Ricketts, Dielectric properties of ceramics, J. Phys. D: Appl. Phys. 29 (5) (1996) 1321–1325. Available from: https://doi.org/10.1088/0022-3727/29/5/028.
[141] N.F. Muhamad, R.A. Maulat Osman, M.S. Idris, M.N. Mohd Yasin, Physical and electrical properties of SrTiO3 and SrZrO3, EPJ Web Conf. (2017) 162. Available from: https://doi.org/10.1051/epjconf/201716201052.
[142] Z.-M. Dang, J.-K. Yuan, J.-W. Zha, T. Zhou, S.-T. Li, G.-H. Hu, Fundamentals, processes and applications of high-permittivity polymer–matrix composites, Prog. Mater. Sci. 57 (4) (2012) 660–723. Available from: https://doi.org/10.1016/j.pmatsci.2011.08.001.
[143] T. Tanaka, G.C. Montanari, R. Mulhaupt, Polymer nanocomposites as dielectrics and electrical insulation-perspectives for processing technologies, material characterization and future applications, IEEE Trans. Dielectr. Electr. Insulation 11 (5) (2004) 763–784. Available from: https://doi.org/10.1109/TDEI.2004.1349782.
[144] T. Tanaka, M. Kozako, N. Fuse, Y. Ohki, Proposal of a multi-core model for polymer nanocomposite dielectrics, IEEE Trans. Dielectr. Electr. Insulation 12 (4) (2005) 669–681. Available from: https://doi.org/10.1109/TDEI.2005.1511092.

[145] X. Sun, M. Gan, L. Ma, H. Wang, T. Zhou, S. Wang, et al., Fabrication of PANI-coated honeycomb-like MnO2 nanospheres with enhanced electrochemical performance for energy storage, Electrochim. Acta 180 (2015) 977–982. Available from: https://doi.org/10.1016/j.electacta.2015.09.056.

[146] T.J. Lewis, Interfaces are the dominant feature of dielectrics at the nanometric level, IEEE Trans. Dielectr. Electr. Insulation 11 (5) (2004) 739–753. Available from: https://doi.org/10.1109/TDEI.2004.1349779.

[147] T.J. Lewis, Interfaces: nanometric dielectrics, J. Phys. D: Appl. Phys. 38 (2) (2005) 202–212. Available from: https://doi.org/10.1088/0022-3727/38/2/004.

[148] V. Ramani, H.R. Kunz, J.M. Fenton, Metal dioxide supported heteropolyacid/Nafion® composite membranes for elevated temperature/low relative humidity PEFC operation, J. Membr. Sci. 279 (1) (2006) 506–512. Available from: https://doi.org/10.1016/j.memsci.2005.12.044.

[149] T. Zhou, J.-W. Zha, R.-Y. Cui, B.-H. Fan, J.-K. Yuan, Z.-M. Dang, Improving dielectric properties of BaTiO3/ferroelectric polymer composites by employing surface hydroxylated BaTiO3 nanoparticles, ACS Appl. Mater. Interfaces 3 (7) (2011) 2184–2188. Available from: https://doi.org/10.1021/am200492q.

[150] K.C. Kao, Charge Carrier Injection from Electrical Contacts, Dielectric Phenomena in Solids, 1st edition, Academic Press, 2004, pp. 327–380. Available from: https://doi.org/10.1016/B978-012396561-5/50016-5.

[151] T.J. Lewis, Nanometric dielectrics, IEEE Trans. Dielectr. Electr. Insulation 1 (5) (1994) 812–825. Available from: https://doi.org/10.1109/94.326653.

[152] O. Lopez-Pamies, T. Goudarzi, A.B. Meddeb, Z. Ounaies, Extreme enhancement and reduction of the dielectric response of polymer nanoparticulate composites via interphasial charges, Appl. Phys. Lett. 104 (24) (2014) 242904. Available from: https://doi.org/10.1063/1.4884368.

[153] L. Zhu, Q. Wang, novel ferroelectric polymers for high energy density and low loss dielectrics, Macromolecules 45 (7) (2012) 2937–2954. Available from: https://doi.org/10.1021/ma2024057.

[154] J. Claude, Y. Lu, K. Li, Q. Wang, Electrical storage in poly(vinylidene fluoride) based ferroelectric polymers: correlating polymer structure to electrical breakdown strength, Chem. Mater. 20 (6) (2008) 2078–2080. Available from: https://doi.org/10.1021/cm800160r.

[155] P. Martins, J.S. Nunes, G. Hungerford, D. Miranda, A. Ferreira, V. Sencadas, et al., Local variation of the dielectric properties of poly(vinylidene fluoride) during the α- to β-phase transformation, Phys. Lett. A 373 (2) (2009) 177–180. Available from: https://doi.org/10.1016/j.physleta.2008.11.026.

[156] K. Tashiro, Crystal-Structure and Phase Transition of PVDF and Related Copolymers, in: H.S. Nalwa (Ed.), Ferroelectric Polymers: Chemistry, Physics, and Applications, Marcel Dekker, Inc., New York, 1995, pp. 63–181.

[157] Y. Wang, X. Zhou, Q. Chen, B. Chu, Q. Zhang, Recent development of high energy density polymers for dielectric capacitors, IEEE Trans. Dielectr. Electr. Insulation 17 (4) (2010) 1036–1042. Available from: https://doi.org/10.1109/TDEI.2010.5539672.

[158] L. Yang, X. Li, E. Allahyarov, P.L. Taylor, Q.M. Zhang, L. Zhu, Novel polymer ferroelectric behavior via crystal isomorphism and the nanoconfinement effect, Polymer 54 (7) (2013) 1709–1728. Available from: https://doi.org/10.1016/j.polymer.2013.01.035.

[159] H. Xu, Dielectric properties and ferroelectric behavior of poly(vinylidene fluoride-trifluoroethylene) 50/50 copolymer ultrathin films, J. Appl. Polym. Sci. 80 (12) (2001) 2259–2266. Available from: https://doi.org/10.1002/app.1330.

[160] W. Tong, Y. Zhang, L. Yu, X. Luan, Q. An, Q. Zhang, et al., Novel method for the fabrication of flexible film with oriented arrays of graphene in poly(vinylidene fluoride-co-hexafluoropropylene) with low dielectric loss, J. Phys. Chem. C. 118 (20) (2014) 10567−10573. Available from: https://doi.org/10.1021/jp411828e.

[161] F. Guan, J. Pan, J. Wang, Q. Wang, L. Zhu, Crystal orientation effect on electric energy storage in poly(vinylidene fluoride-co-hexafluoropropylene) copolymers, Macromolecules 43 (1) (2010) 384−392. Available from: https://doi.org/10.1021/ma901921h.

[162] X. Zhou, B. Chu, B. Neese, M. Lin, Q.M. Zhang, Electrical energy density and discharge characteristics of a poly(vinylidene fluoride-chlorotrifluoroethylene)copolymer, IEEE Trans. Dielectr. Electr. Insulation 14 (5) (2007) 1133−1138. Available from: https://doi.org/10.1109/TDEI.2007.4339472.

[163] G. Li, R. Zhu, Y. Yang, Polymer solar cells, Nat. Photon. 6 (3) (2012) 153−161. Available from: https://doi.org/10.1038/nphoton.2012.11.

[164] L. Yang, J. Qiu, H. Ji, K. Zhu, J. Wang, Enhanced dielectric and ferroelectric properties induced by TiO2@MWCNTs nanoparticles in flexible poly(vinylidene fluoride) composites, Compos. Part A Appl. Sci. Manuf. 65 (2014) 125−134. Available from: https://doi.org/10.1016/j.compositesa.2014.06.006.

[165] J. Li, Z. Sun, F. Yan, Solution processable low-voltage organic thin film transistors with high-k relaxor ferroelectric polymer as gate insulator, Adv. Mater. 24 (1) (2012) 88−93. Available from: https://doi.org/10.1002/adma.201103542.

[166] H. Xu, D. Shen, Q. Zhang, Structural and ferroelectric response in vinylidene fluoride/trifluoroethylene/hexafluoropropylene terpolymers, Polymer 48 (7) (2007) 2124−2129. Available from: https://doi.org/10.1016/j.polymer.2007.02.035.

[167] F. Wen, Z. Xu, S. Tan, W. Xia, X. Wei, Z. Zhang, Chemical bonding-induced low dielectric loss and low conductivity in high-K poly(vinylidenefluoride-trifluoroethylene)/graphene nanosheets nanocomposites, ACS Appl. Mater. Interfaces 5 (19) (2013) 9411−9420. Available from: https://doi.org/10.1021/am401784p.

[168] F. Wen, Z. Xu, W. Xia, X. Wei, Z. Zhang, High energy density nanocomposites based on poly(vinylidene fluoride-chlorotrifluoroethylene) and barium titanate, Polym. Eng. Sci. 53 (4) (2013) 897−904. Available from: https://doi.org/10.1002/pen.23312.

[169] S. Dalle Vacche, F. Oliveira, Y. Leterrier, V. Michaud, D. Damjanovic, J.-A.E. Månson, Effect of silane coupling agent on the morphology, structure, and properties of poly(vinylidene fluoride−trifluoroethylene)/BaTiO3 composites, J. Mater. Sci. 49 (13) (2014) 4552−4564. Available from: https://doi.org/10.1007/s10853-014-8155-x.

[170] Y.P. Mao, S.Y. Mao, Z.-G. Ye, Z.X. Xie, L.S. Zheng, Size-dependences of the dielectric and ferroelectric properties of BaTiO3/polyvinylidene fluoride nanocomposites, J. Appl. Phys. 108 (1) (2010) 014102. Available from: https://doi.org/10.1063/1.3443582.

[171] B. Luo, X. Wang, Y. Wang, L. Li, Fabrication, characterization, properties and theoretical analysis of ceramic/PVDF composite flexible films with high dielectric constant and low dielectric loss, J. Mater. Chem. A 2 (2) (2014) 510−519. Available from: https://doi.org/10.1039/C3TA14107A.

[172] S. Luo, S. Yu, R. Sun, C.-P. Wong, Nano Ag-deposited BaTiO3 hybrid particles as fillers for polymeric dielectric composites: toward high dielectric constant and suppressed loss, ACS Appl. Mater. Interfaces 6 (1) (2014) 176−182. Available from: https://doi.org/10.1021/am404556c.

[173] J.-W. Zha, X. Meng, D. Wang, Z.-M. Dang, R.K.Y. Li, Dielectric properties of poly(vinylidene fluoride) nanocomposites filled with surface coated BaTiO3 by SnO2

nanodots, Appl. Phys. Lett. 104 (7) (2014) 072906. Available from: https://doi.org/10.1063/1.4866269.

[174] H.-J. Ye, W.-Z. Shao, L. Zhen, Tetradecylphosphonic acid modified BaTiO3 nanoparticles and its nanocomposite, Colloids Surf. A Physicochem. Eng. Asp. 427 (2013) 19–25. Available from: https://doi.org/10.1016/j.colsurfa.2013.02.068.

[175] G. Wang, S. Zhuo, W. Xing, Graphene/polyaniline nanocomposite as counter electrode of dye-sensitized solar cells, Mater. Lett. 69 (2012) 27–29. Available from: https://doi.org/10.1016/j.matlet.2011.11.086.

[176] J. Wang, N. Wei, F. Wang, C. Wu, S. Li, Significantly enhanced dielectric response in composite of P(VDF-TrFE) and modified multi-walled carbon-nanotubes, E-Polymers 12 (1) (2012) 074. Available from: https://doi.org/10.1515/epoly.2012.12.1.869.

[177] M. Wang, J. Zhu, W. Zhu, B. Zhu, J. Liu, X. Zhu, et al., The formation of percolative composites with a high dielectric constant and high conductivity, Angew. Chem. Int. (Ed.) 51 (36) (2012) 9123–9127. Available from: https://doi.org/10.1002/anie.201203389.

[178] D. Bhadra, M.G. Masud, S. Sarkar, J. Sannigrahi, S.K. De, B.K. Chaudhuri, Synthesis of PVDF/BiFeO3 nanocomposite and observation of enhanced electrical conductivity and low-loss dielectric permittivity at percolation threshold, J. Polym. Sci. Part. B: Polym. Phys. 50 (8) (2012) 572–579. Available from: https://doi.org/10.1002/polb.23041.

[179] X. Jing, X. Shen, H. Song, F. Song, Magnetic and dielectric properties of barium ferrite fibers/poly(vinylidene fluoride) composite films, J. Polym. Res. 18 (6) (2011) 2017–2021. Available from: https://doi.org/10.1007/s10965-011-9610-x.

[180] H. Quan, D. Chen, X. Xie, H. Fan, Polyvinylidene fluoride/vanadium pentoxide composites with high dielectric constant and low dielectric loss, Phys. Status Solidi (a) 210 (12) (2013) 2706–2709. Available from: https://doi.org/10.1002/pssa.201330234.

[181] H. Tang, H.A. Sodano, High energy density nanocomposite capacitors using nonferroelectric nanowires, Appl. Phys. Lett. 102 (6) (2013) 063901. Available from: https://doi.org/10.1063/1.4792513.

[182] S. Liu, J. Zhai, A small loading of surface-modified Ba0.6Sr0.4TiO3 nanofiber-filled nanocomposites with enhanced dielectric constant and energy density, RSC Adv. 4 (77) (2014) 40973–40979. Available from: https://doi.org/10.1039/C4RA04369C.

[183] P. Kim, N.M. Doss, J.P. Tillotson, P.J. Hotchkiss, M.-J. Pan, S.R. Marder, et al., High energy density nanocomposites based on surface-modified BaTiO3 and a ferroelectric polymer, ACS Nano 3 (9) (2009) 2581–2592. Available from: https://doi.org/10.1021/nn9006412.

[184] D. Yang, H. Xu, Y. Wu, J. Wang, Z. Xu, W. Shi, Effect of hydroxylated multiwall carbon nanotubes on dielectric property of poly (vinylidene fluoride)/poly (methyl methacrylate)/hydroxylated multiwall carbon nanotubes blend, J. Polym. Res. 20 (9) (2013) 236. Available from: https://doi.org/10.1007/s10965-013-0236-z.

[185] K. Yang, X. Huang, Y. Huang, L. Xie, P. Jiang, Fluoro-polymer@BaTiO3 hybrid nanoparticles prepared via RAFT polymerization: toward ferroelectric polymer nanocomposites with high dielectric constant and low dielectric loss for energy storage application, Chem. Mater. 25 (11) (2013) 2327–2338. Available from: https://doi.org/10.1021/cm4010486.

[186] S.D. Vacche, F. Oliveira, Y. Leterrier, V. Michaud, D. Damjanovic, J.-A.E. Månson, The effect of processing conditions on the morphology, thermomechanical, dielectric, and piezoelectric properties of P(VDF-TrFE)/BaTiO3 composites, J. Mater. Sci. 47 (11) (2012) 4763–4774. Available from: https://doi.org/10.1007/s10853-012-6362-x.

[187] X. Kuang, S. Lin, H. Zhu, Synthesis and characterization of poly(vinylidene-trifluoroethylene)/Ni-TiO2, Phys. Status Solidi (a) 210 (3) (2013) 570−573. Available from: https://doi.org/10.1002/pssa.201228585.

[188] P. Hu, Y. Song, H. Liu, Y. Shen, Y. Lin, C.-W. Nan, Largely enhanced energy density in flexible P(VDF-TrFE) nanocomposites by surface-modified electrospun BaSrTiO3 fibers, J. Mater. Chem. A 1 (5) (2013) 1688−1693. Available from: https://doi.org/10.1039/C2TA00948J.

[189] L. Zhang, P. Wu, Y. Li, Z.-Y. Cheng, J.C. Brewer, Preparation process and dielectric properties of Ba0.5Sr0.5TiO3−P(VDF−CTFE) nanocomposites, Compos. Part. B: Eng. 56 (2014) 284−289. Available from: https://doi.org/10.1016/j.compositesb.2013.08.029.

[190] J. Li, J. Claude, L.E. Norena-Franco, S.I. Seok, Q. Wang, Electrical energy storage in ferroelectric polymer nanocomposites containing surface-functionalized BaTiO3 nanoparticles, Chem. Mater. 20 (20) (2008) 6304−6306. Available from: https://doi.org/10.1021/cm8021648.

[191] J. Li, S.I. Seok, B. Chu, F. Dogan, Q. Zhang, Q. Wang, Nanocomposites of ferroelectric polymers with TiO2 nanoparticles exhibiting significantly enhanced electrical energy density, Adv. Mater. 21 (2) (2009) 217−221. Available from: https://doi.org/10.1002/adma.200801106.

[192] T.G. Mofokeng, A.S. Luyt, V.P. Pavlović, V.B. Pavlović, D. Dudić, B. Vlahović, et al., Ferroelectric nanocomposites of polyvinylidene fluoride/polymethyl methacrylate blend and BaTiO3 particles: Fabrication of β-crystal polymorph rich matrix through mechanical activation of the filler, J. Appl. Phys. 115 (8) (2014) 084109. Available from: https://doi.org/10.1063/1.4866694.

[193] K. Yu, Y. Bai, Y. Zhou, Y. Niu, H. Wang, Poly(vinylidene fluoride) polymer based nanocomposites with enhanced energy density by filling with polyacrylate elastomers and BaTiO3 nanoparticles, Appl. Phys. Lett. 104 (8) (2014) 082904. Available from: https://doi.org/10.1063/1.4866585.

[194] D.-W. Wang, F. Li, J. Zhao, W. Ren, Z.-G. Chen, J. Tan, et al., Fabrication of graphene/polyaniline composite paper via in situ anodic electropolymerization for high-performance flexible electrode, ACS Nano 3 (7) (2009) 1745−1752. Available from: https://doi.org/10.1021/nn900297m.

[195] A. Baji, Y.-W. Mai, M. Abtahi, S.-C. Wong, Y. Liu, Q. Li, Microstructure development in electrospun carbon nanotube reinforced polyvinylidene fluoride fibers and its influence on tensile strength and dielectric permittivity, Compos. Sci. Technol. 88 (2013) 1−8. Available from: https://doi.org/10.1016/j.compscitech.2013.08.021.

[196] J.K. Yuan, W.L. Li, S.-H. Yao, Y.-Q. Lin, A. Sylvestre, J. Bai, High dielectric permittivity and low percolation threshold in polymer composites based on SiC-carbon nanotubes micro/nano hybrid, Appl. Phys. Lett. 98 (3) (2011) 032901. Available from: https://doi.org/10.1063/1.3544942.

[197] J.K. Yuan, S.-H. Yao, Z.-M. Dang, A. Sylvestre, M. Genestoux, J. Bail, Giant dielectric permittivity nanocomposites: realizing true potential of pristine carbon nanotubes in polyvinylidene fluoride matrix through an enhanced interfacial interaction, J. Phys. Chem. C. 115 (13) (2011) 5515−5521. Available from: https://doi.org/10.1021/jp1117163.

[198] L. Yang, B.A. Tyburski, F.D. Dos Santos, M.K. Endoh, T. Koga, D. Huang, et al., Relaxor ferroelectric behavior from strong physical pinning in a poly(vinylidene fluoride-co-trifluoroethylene-co-chlorotrifluoroethylene) random terpolymer, Macromolecules 47 (22) (2014) 8119−8125. Available from: https://doi.org/10.1021/ma501852x.

[199] P. Thomas, K.T. Varughese, K. Dwarakanath, K.B.R. Varma, Dielectric properties of Poly(vinylidene fluoride)/CaCu3Ti4O12 composites, Compos. Sci. Technol. 70 (3) (2010) 539–545. Available from: https://doi.org/10.1016/j.compscitech.2009.12.014.

[200] J.-K. Yuan, Z.-M. Dang, S.-H. Yao, J.-W. Zha, T. Zhou, S.-T. Li, et al., Fabrication and dielectric properties of advanced high permittivity polyaniline/poly(vinylidene fluoride) nanohybrid films with high energy storage density, J. Mater. Chem. 20 (12) (2010) 2441–2447. Available from: https://doi.org/10.1039/B923590F.

[201] K. Shehzad, A. Ul-Haq, S. Ahmad, M. Mumtaz, T. Hussain, A. Mujahid, et al., All-organic PANI–DBSA/PVDF dielectric composites with unique electrical properties, J. Mater. Sci. 48 (10) (2013) 3737–3744. Available from: https://doi.org/10.1007/s10853-013-7172-5.

[202] J. Zhang, D. Shu, T. Zhang, H. Chen, H. Zhao, Y. Wang, et al., Capacitive properties of PANI/MnO2 synthesized via simultaneous-oxidation route, J. Alloy. Compd. 532 (2012) 1–9. Available from: https://doi.org/10.1016/j.jallcom.2012.04.006.

[203] Xi Zhang, J. Zhu, N. Haldolaarachchige, J. Ryu, D.P. Young, S. Wei, et al., Synthetic process engineered polyaniline nanostructures with tunable morphology and physical properties, Polymer 53 (10) (2012) 2109–2120. Available from: https://doi.org/10.1016/j.polymer.2012.02.042.

[204] Y. Zhang, Y. Wang, Y. Deng, Y. Guo, W. Bi, M. Li, et al., Excellent dielectric properties of anisotropic polymer composites filled with parallel aligned zinc flakes, Appl. Phys. Lett. 101 (19) (2012) 192904. Available from: https://doi.org/10.1063/1.4766923.

[205] W. Wu, X. Huang, S. Li, P. Jiang, T. Toshikatsu, Novel three-dimensional zinc oxide superstructures for high dielectric constant polymer composites capable of withstanding high electric field, J. Phys. Chem. C. 116 (47) (2012) 24887–24895. Available from: https://doi.org/10.1021/jp3088644.

[206] M. Ataur Rahman, B.-C. Lee, D.-T. Phan, G.-S. Chung, Fabrication and characterization of highly efficient flexible energy harvesters using PVDF–graphene nanocomposites, Smart Mater. Struct. 22 (8) (2013) 085017. Available from: https://doi.org/10.1088/0964-1726/22/8/085017.

[207] Y. Shen, Y. Guan, Y. Hu, Y. Lei, Y. Song, Y. Lin, et al., Dielectric behavior of graphene/BaTiO3/polyvinylidene fluoride nanocomposite under high electric field, Appl. Phys. Lett. 103 (7) (2013) 072906. Available from: https://doi.org/10.1063/1.4818763.

[208] X. Zhao, J. Zhao, J.-P. Cao, X. Wang, M. Chen, Z.-M. Dang, Tuning the dielectric properties of polystyrene/poly(vinylidene fluoride) blends by selectively localizing carbon black nanoparticles, J. Phys. Chem. B 117 (8) (2013) 2505–2515. Available from: https://doi.org/10.1021/jp310021r.

[209] L. Zhang, W. Wang, X. Wang, P. Bass, Z.-Y. Cheng, Metal-polymer nanocomposites with high percolation threshold and high dielectric constant, Appl. Phys. Lett. 103 (23) (2013) 232903. Available from: https://doi.org/10.1063/1.4838237.

[210] J.-K. Yuan, S.-H. Yao, A. Sylvestre, J. Bai, Biphasic polymer blends containing carbon nanotubes: heterogeneous nanotube distribution and its influence on the dielectric properties, J. Phys. Chem. C. 116 (2) (2012) 2051–2058. Available from: https://doi.org/10.1021/jp210872w.

[211] K.S. Novoselov, A.K. Geim, S.V. Morozov, D. Jiang, Y. Zhang, S.V. Dubonos, et al., Electric field effect in atomically thin carbon films, Science 306 (5696) (2004) 666. Available from: https://doi.org/10.1126/science.1102896.

[212] N. Mahmood, C. Zhang, H. Yin, Y. Hou, Graphene-based nanocomposites for energy storage and conversion in lithium batteries, supercapacitors and fuel cells, J. Mater. Chem. A 2 (1) (2014) 15–32. Available from: https://doi.org/10.1039/C3TA13033A.

[213] R.R. Salunkhe, Y.-H. Lee, K.-H. Chang, J.-M. Li, P. Simon, J. Tang, et al., Nanoarchitectured graphene-based supercapacitors for next-generation energy-storage applications, Chem. – A Eur. J. 20 (43) (2014) 13838–13852. Available from: https://doi.org/10.1002/chem.201403649.

[214] H. Yan, W. Chen, X. Wu, Y. Li, Conducting polyaniline-wrapped lithium vanadium phosphate nanocomposite as high-rate and cycling stability cathode for lithium-ion batteries, Electrochim. Acta 146 (2014) 295–300. Available from: https://doi.org/10.1016/j.electacta.2014.09.040.

[215] B. Anasori, M. Beidaghi, Y. Gogotsi, Graphene – transition metal oxide hybrid materials, Mater. Today 17 (5) (2014) 253–254. Available from: https://doi.org/10.1016/j.mattod.2014.04.043.

[216] H.-P. Cong, X.-C. Ren, P. Wang, S.-H. Yu, Flexible graphene–polyaniline composite paper for high-performance supercapacitor, Energy Environ. Sci. 6 (4) (2013) 1185–1191. Available from: https://doi.org/10.1039/C2EE24203F.

[217] H. Gómez, M.K. Ram, Farah Alvi, P. Villalba, E.L. Stefanakos, A. Kumar, Graphene-conducting polymer nanocomposite as novel electrode for supercapacitors, J. Power Sources 196 (8) (2011) 4102–4108. Available from: https://doi.org/10.1016/j.jpowsour.2010.11.002.

[218] N.A. Kumar, H.-J. Choi, Y.R. Shin, D.W. Chang, L. Dai, J.-B. Baek, Polyaniline-grafted reduced graphene oxide for efficient electrochemical supercapacitors, ACS Nano 6 (2) (2012) 1715–1723. Available from: https://doi.org/10.1021/nn204688c.

[219] M. Moussa, M.F. El-Kady, Z. Zhao, P. Majewski, J. Ma, Recent progress and performance evaluation for polyaniline/graphene nanocomposites as supercapacitor electrodes, Nanotechnology 27 (44) (2016) 442001. Available from: https://doi.org/10.1088/0957-4484/27/44/442001.

[220] J. Yan, Z. Fan, T. Wei, W. Qian, M. Zhang, F. Wei, Fast and reversible surface redox reaction of graphene–MnO2 composites as supercapacitor electrodes, Carbon 48 (13) (2010) 3825–3833. Available from: https://doi.org/10.1016/j.carbon.2010.06.047.

[221] H. Wang, Q. Hao, X. Yang, L. Lu, X. Wang, A nanostructured graphene/polyaniline hybrid material for supercapacitors, Nanoscale 2 (10) (2010) 2164–2170. Available from: https://doi.org/10.1039/C0NR00224K.

[222] Y. Meng, K. Wang, Y. Zhang, Z. Wei, Hierarchical porous graphene/polyaniline composite film with superior rate performance for flexible supercapacitors, Adv. Mater. 25 (48) (2013) 6985–6990. Available from: https://doi.org/10.1002/adma.201303529.

[223] L. Lai, H. Yang, L. Wang, B.K. Teh, J. Zhong, H. Chou, et al., Preparation of supercapacitor electrodes through selection of graphene surface functionalities, ACS Nano 6 (7) (2012) 5941–5951. Available from: https://doi.org/10.1021/nn3008096. In this issue.

[224] X. Liu, Y. Zheng, X. Wang, Controllable preparation of polyaniline–graphene nanocomposites using functionalized graphene for supercapacitor electrodes, Chem. – A Eur. J. 21 (29) (2015) 10408–10415. Available from: https://doi.org/10.1002/chem.201501245.

[225] Y.-C. Yong, X.-C. Dong, M.B. Chan-Park, H. Song, P. Chen, Macroporous and monolithic anode based on polyaniline hybridized three-dimensional graphene for high-performance microbial fuel cells, ACS Nano 6 (3) (2012) 2394–2400. Available from: https://doi.org/10.1021/nn204656d.

[226] J. Hou, Z. Liu, P. Zhang, A new method for fabrication of graphene/polyaniline nanocomplex modified microbial fuel cell anodes, J. Power Sources 224 (2013) 139–144. Available from: https://doi.org/10.1016/j.jpowsour.2012.09.091.

[227] C. Bora, J. Sharma, S. Dolui, Polypyrrole/sulfonated graphene composite as electrode material for supercapacitor, J. Phys. Chem. C. 118 (51) (2014) 29688−29694. Available from: https://doi.org/10.1021/jp511095s.

[228] A. Davies, P. Audette, B. Farrow, F. Hassan, Z. Chen, J.-Y. Choi, et al., Graphene-based flexible supercapacitors: pulse-electropolymerization of polypyrrole on free-standing graphene films, J. Phys. Chem. C. 115 (35) (2011) 17612−17620. Available from: https://doi.org/10.1021/jp205568v.

[229] H. Kashani, L. Chen, Y. Ito, J. Han, A. Hirata, M. Chen, Bicontinuous nanotubular graphene−polypyrrole hybrid for high performance flexible supercapacitors, Nano Energy 19 (2016) 391−400. Available from: https://doi.org/10.1016/j.nanoen.2015.11.029.

[230] A. Liu, C. Li, H. Bai, G. Shi, Electrochemical deposition of polypyrrole/sulfonated graphene composite films, J. Phys. Chem. C. 114 (51) (2010) 22783−22789. Available from: https://doi.org/10.1021/jp108826e.

[231] Y. Liu, J. Zhou, J. Tang, W. Tang, Three-dimensional, chemically bonded polypyrrole/bacterial cellulose/graphene composites for high-performance supercapacitors, Chem. Mater. 27 (20) (2015) 7034−7041. Available from: https://doi.org/10.1021/acs.chemmater.5b03060.

[232] L.-L. Jiang, X. Lu, C.-M. Xie, G.-J. Wan, H.-P. Zhang, T. Youhong, Flexible, free-standing $TiO_2$ − graphene − polypyrrole composite films as electrodes for supercapacitors, The Journal of Physical Chemistry C 119 (8) (2015) 3903−3910. Available from: https://doi.org/10.1021/jp511022z. In this issue.

[233] F. Alvi, M.K. Ram, P.A. Basnayaka, E. Stefanakos, Y. Goswami, A. Kumar, Graphene−polyethylenedioxythiophene conducting polymer nanocomposite based supercapacitor, Electrochim. Acta 56 (25) (2011) 9406−9412. Available from: https://doi.org/10.1016/j.electacta.2011.08.024.

[234] G. Qu, J. Cheng, X. Li, D. Yuan, P. Chen, X. Chen, et al., A fiber supercapacitor with high energy density based on hollow graphene/conducting polymer fiber electrode, Adv. Mater. 28 (19) (2016) 3646−3652. Available from: https://doi.org/10.1002/adma.201600689.

[235] F. Alvi, M.K. Ram, P. Basnayaka, E. Stefanakos, Y. Goswami, A. Hoff, et al., Electrochemical supercapacitors based on graphene-conducting polythiophenes nanocomposite, ECS Trans. 35 (34) (2019) 167−174. Available from: https://doi.org/10.1149/1.3654215.

# Polymer nanocomposites for defense applications

14

*Adib Bin Rashid*[1] *and Md Enamul Hoque*[2]
[1]Department of Industrial and Production Engineering, Military Institute of Science and Technology, Dhaka, Bangladesh
[2]Department of Biomedical Engineering, Military Institute of Science and Technology (MIST), Dhaka, Bangladesh

## 14.1 Introduction

Modern military confrontations are characterized by asymmetry, or a considerable disparity in equipment, armament, technology, and resources between the combatants. Militaries with advanced technologies will invariably win the battle [1]. Hence, modern armed forces are attempting to gain a qualitative advantage over opponents by employing new technologies. Integrating several emerging technologies allows moving from "mass and mobility" to nontraditional techniques of increasing comparative fighting capability. Remote sensing, night vision, image processing, sensors, stealth technology, precision-guided missiles, and, most significantly, digital communications and computer networks force us to embrace novel warfare approaches.

The potential impact of nanotechnology on the defense sector spans a wide range of activities, including improving weapon mortality; securing communication and surveillance; protecting targets such as soldiers, strategic equipment, and assets; and developing lightweight ground, naval, and aerial platforms.

The importance of material science and technology may be seen in the evolution of defensive technologies from the Stone Age to the current day. Apart from the functionality, the selection of material for military applications depends on sustainability under harsh environments, such as changes in temperature, sandstorms, rainfalls, corrosion in humid and sea conditions, and structural stability under operational activities; furthermore, the material should have low density and be inexpensive. In addition, naval ships, submarines, airplanes, combat vehicles, sailors, pilots, military personnel, and mariners require advanced material constituents that allow for remarkable changes in maneuverability; protection from explosives through signature reduction and heavy armor; safety from nuclear, biological, and chemical weapons; and involvement with highly focused firepower and durable logistics.

Over the years, staggering growth in polymer nanocomposites (PNCs) has been observed in the defense and military sectors as it is significantly increasing the quality of military devices and enhancing personnel relaxation and safety [2]. PNCs are a type of polymer composite where nanomaterials are reinforced in the polymer matrix, giving them high fatigue and fracture resistance. Thus PNCs are utilized to

**Advanced Polymer Nanocomposites. DOI:** https://doi.org/10.1016/B978-0-12-824492-0.00015-5

make lightweight, relatively small, less expensive, more precise, inventive, and durable military gadgets and infrastructures [3].

The current chapter highlights the substantial opportunities of PNC in varied defense fields such as intelligent uniforms for soldiers, propellants and explosives, weaponry, camouflage, ultralight military vehicles, protective armors, thermal and radiation shielding, and other futuristic defense uses.

## 14.2 Defense applications of polymer nanocomposites

The defense industry is inextricably linked to the transportation sector since military and defense operations regularly need military-grade vehicles, aircraft, ships, and drones. The applications of PNCs have increased dramatically in numerous military divisions such as military automobiles, airplane, naval vessels, and drones; for sensing, intelligent textiles, structures, generating and storing of power, military medicine, weapons, etc. This gives rise to explicit requirements such as thermal insulation, vibration damping, radiation shielding, electrical energy storage, sensor systems, actuators, ballistic protection, and absorption of microwave in military automobiles, naval vessels, and military planes [4,5]. Various uses of PNC in the defense sectors are shown in Fig. 14.1.

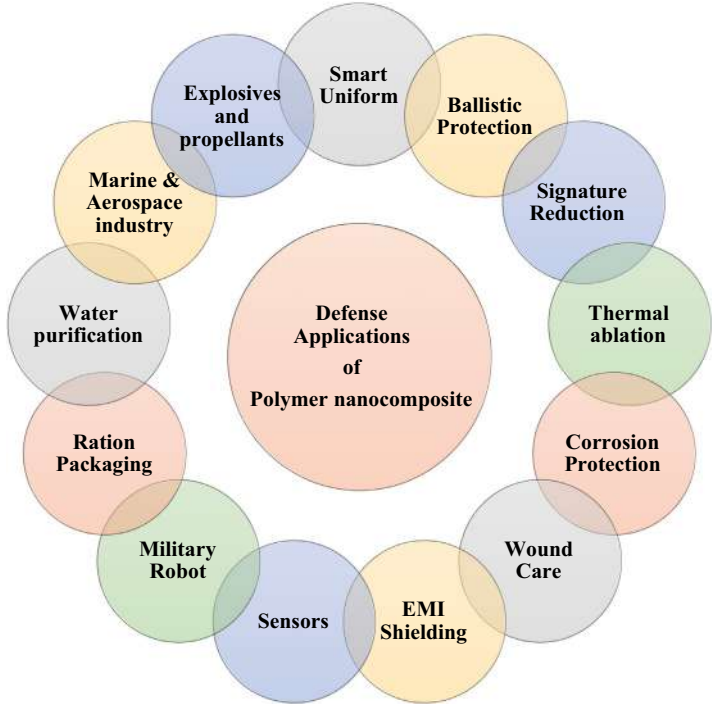


**Figure 14.1** Applications of polymer nanocomposite on the defense sector.

Any military's most valuable asset is its soldiers. Even on ordinary patrol duties, the role of soldiers is rising day by day in today's wartime situation, which includes the threat from nonstate actors, such as terrorists. As a result, it is essential to equip soldiers with technological innovations to make them prudent. Numerous aspects of nanotechnology, including body armor vests, smart fabrics capable of producing renewable electricity for the lightweight of power packs, communication systems, autonomous signature reduction, and so on, are relevant in this area.

Steel-made heavyweight military platforms constitute a significant issue regarding their excessive fuel consumption, speed, mobility, and heavy armors to protect against ballistic and explosive attacks in the battle effectiveness. As a result, polymer nanomaterials are the emerging choice for developing lightweight combat systems and armors due to their low weight and multiple capabilities.

### 14.2.1 Smart military uniforms

PNCs are utilized to make bulletproof vests, intelligent fabrics, helmets, gloves, and footwear for the protection of troops (Fig. 14.2). Polymer matrix enables the


**Figure 14.2** (A) Russian advanced high-tech armor [3]. (B) Chemical and biological protective suit (Saratoga) [6].

construction of incredibly strong, sophisticated, and ultralight high-tech combat suits when reinforced with nanomaterials [Kevlar, carbon nanotube (CNT), graphene, etc.]. The addition of shear thickening fluids containing silica nanopowder produces highly flexible, compact, and tougher body armors. These body armor vests let the wearer move more freely, defend against toxic poisons, withstand the high-speed bullets' impact, and protect from blunt weapons such as bars, stones, and sticks.

Nanosize warming and cooling systems, nonflammability, and wearable nanoelectronics/photonics are smart garment systems. Microencapsulated spun composite yarns are being used to create new thermal storage and controlled textiles. These materials have superior dynamic heat resistance, higher durability, flexibility, improved electrical conductivity and augmented tailoring abilities. A military uniform should include a load-carrying armor chassis, increased quickness, thermal controlling, signature management, ballistic armor plate, moisture-wicking undergarments, integrated knee and elbow pads, and assault leg panels,

Fig. 14.2A is a typical example from Russia's latest PNC-based fighting suit. The high-tech armor in "Star Wars" takes advantage of the distinctive features of graphene nanofillers, including outstanding strength, ultralight, great endurance, low wettability, good thermal and electrical conductivity, and ballistic effectiveness [3].

In today's battlefield, soldier's safety from hazardous chemical, biological, radiological, and nuclear (CBRN) weapons is crucial for successful mission execution. Therefore PNCs fabricated with clay, MgO, and $TiO_2$ are developed to provide the soldiers with outstanding protection and operational effectiveness.

Self-cleaning textile with $TiO_2$ nanoparticles has been produced according to their photocatalytic aptitude to oxidize dirt and other pollutants [7,8]. Military uniforms were coated with silver nanoparticles to make antimicrobial protective gear. These coatings also make the cloth self-healing as well as water and dirt resistant. CBRN shielding equipment with self-decontamination and drug-delivery properties is also being researched. For this purpose, decontaminants such as activated carbons, nanometal oxides (MgO, $Al_2O_3$), and antibiotics in the form of nanocoatings are being investigated [9]. Fig. 14.2B is a typical example of CBRN clothing fabricated by *Blücher, GmbH/Germany* under the trademark Saratoga, which ensures the utmost aptitude of adsorption and coziness under all-weather circumstances [6].

## 14.2.2 Impact and shock resistance/ballistic protection

### 14.2.2.1 Lightweight military platforms and armors

Soldiers on the battlefront require overhead cover while facing the enemy directly or indirectly. Bunkers and command posts, whether composed of stones, concrete, bricks, steel, or just plain soil, provide some protection but are not foolproof, crumbling at critical periods and incurring casualties and damage. Therefore high-strength nanocomposite material for bunkers and command posts is required to give protection. In addition, steel and polymer-based nanocomposites are helpful for

various protective systems such as helmets and body and vehicle armors against small arms ammunition.

Hybrid nanoparticles and fiber-reinforced composites have strong mechanical and fatigue characteristics and excellent scratch resistance and impact energy attenuation. In addition, reduced quantity of fiber-reinforced layers slackened weight and thickness. Furthermore, addition of conductive nanoparticles [carbon black (CB), graphene, graphite, CNTs, or metals] to composites allows them to conduct electricity. Because of these benefits, composites are primarily employed in the intelligent armament (Fig. 14.3) manufacturing industry.

Czech et al. [11], Clifton et al. (p. 1) [12], and Vijay Kumar et al. [13] have summarized the latest developments of polymer matrix composites for ballistic protection applications which are shown in Table 14.1.

### 14.2.3 Optically transparent armor

The optically transparent armor is designed to protect troops in various military vehicles (Fig. 14.4) from explosion or missile threats. Their use as a vehicle window or windshield extends from the ground to aerial, from naval warships to safety goggles, and from VIP safekeeping limousines to noncombat applications, such as tumult control and bomb disposal squads [19].

Because of the optical transparency, confrontation to fracture, and capability to soften and reseal around the projectile's path as it impacts the surface and passes through the bulk thermoset, and thermoplastic polymers such as acrylates, urethanes, and polycarbonate are the excellent candidates for invincible glass. When struck with a projectile, polyurethane (PU) demonstrates the capacity to remain translucent while encasing the projectile. PU reinforced with graphene has been displaying prospective properties of transparent composite laminate shield for window glass and windshield of military automobiles and those of other law implementation organizations. According to ballistics model tests, by adding graphene to


**Figure 14.3** (A) Military body armor systems. (B) Material groups used in an HAP [10]. *HAP*, hard armor plate.

**Table 14.1** Polymer matrix composites for ballistic protection.

| Reinforcement fiber type | Filler content | Effect | References |
|---|---|---|---|
| Glass fiber | 6, 7, and 8 wt.% $SiO_2$ | Enhanced tensile, flexural, and shear strengths | Tate et al. [14] |
| | 0.2, 0.6, and 1 wt. % GnP | Enhance impact energy absorption, tensile strength, and modulus<br>Improved adhesion between components and decrease the surface damage area | Vigneshwaran et al. [15] |
| Carbon fiber | 2 wt.% nanoclay + 0.1 wt.% GnP | Enhance flexural strength and higher stiffness with GnP<br>Superlative thermo-mechanical stability with nanoclay | Tareq et al. [16] |
| Aramid fiber | 0.15, 0.3, and 0.5 wt.% MWCNT | Enhance tensile, impact, and flexural strength,<br>Escalation of hardness | Suresha et al. [17] |

*MWCNT*, multiwalled carbon nanotube.


**Figure 14.4** Transparent armor window in (A) armored personnel carrier and (B) military aircraft [18].

PU (five layers of both), significant reduction of bullet's kinetic energy is observed (about 32%) compared to a similar thickness of single-layer PU [20].

### 14.2.4 Acoustics absorption

Acoustics damping is a significant component in designing military and aerospace vehicles for achieving comfort and structural stability. PU foams are broadly used as sound-absorbing materials that are now added with nanofillers such as silica,

barium sulfate, calcium carbonate, or fiberglass for further improvement of the level of acoustics absorbency. Sung et al. investigated the sound absorption capability of PU/nanosilica foams and found a significant reduction of acoustic waves [21]. Baferani et al. developed PU/CNT foam nanocomposites that can significantly absorb a widespread range (frequency 400−6300 Hz) of sound waves [22].

### 14.2.5 Signature reduction

The invisibility of soldiers and military infrastructure is astounding for the control over the battle with improvements in long-range armaments and pictorial recognition equipment. Colors (olive-green, brown, khaki, and black) of camouflage fabrics of military apparel, supple nets, garnishes, and coverings may vary based on the background. Present military materials must provide disguise and concealment under numerous ranges of wavelengths on the electromagnetic spectrum, especially the thermal or far-infrared region (3−5 and 8−14 μm), near-infrared region (NIR) (750−1200 nm), and visible region (400−800 nm) [23].

Karpagam et al. developed a camouflage printed fabric in a jungle motif using thermochromic colorants that exhibited a reversible color alteration with electrical power and temperature change (Fig. 14.5) [24].

Salehi et al. stated that addition of CB and activated carbon nanoparticles to viscose/polyester textiles considerably decreased the textile's IR reflectance for both black and green textures [25]. Mehrizi et al. produced nylon/cotton textiles with variable quantities of CB nanoparticles and pigments to tune the textiles' visibility and NIR disguise for a desert situation [26]. Mehrizi et al. also examined the addition of multiwalled CNT particles (MWCNTs) with a 50% nylon/50% cotton fabric which can slacken the NIR reflectance standards of the olive-green, light brown, and dark brown printed textiles [27]. Abbasipour and Mehrizi conducted another study on the reflectance performance of 35% polyester/65% cotton textiles produced with titanium dioxide ($TiO_2$) or CB powder-based pigment or vat dye [28].

Similarly, Siadat and Mokhtari showed the effect of zirconium dioxide ($ZrO_2$) nanoparticle- and cerium dioxide ($CeO_2$) nanoparticle-coated cotton/nylon textiles in desert and forest patterns, and $ZrO_2$- and magnesium oxide (MgO)-coated printed nylon/cotton textiles in desert and jungle pattern [29,30].

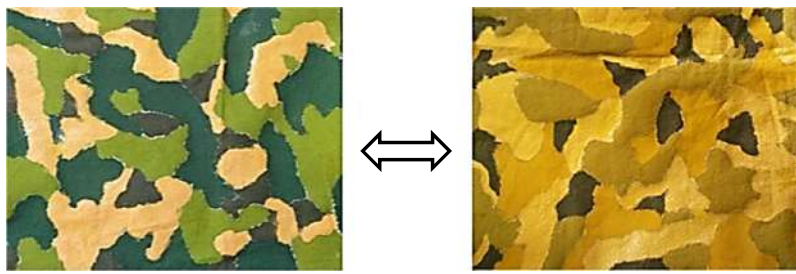


**Figure 14.5** Reversible color change of camouflage printed fabric [24].

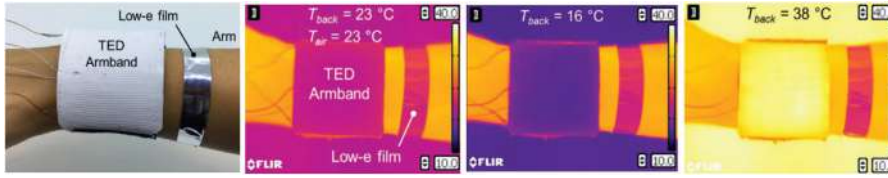


**Figure 14.6** TED armband for thermal camouflage on human skin [31]. *TED*, thermoelectric device.

Hong et al. suggested a stretchy wearable thermoelectric device (Fig. 14.6) that could replicate the ambient temperature around 16°C and 38°C and give thermal disguise to the users. Again, Xiao et al. created a thermal disguise scheme that consists of thin films of vanadium dioxide ($VO_2$), CNTs, and graphene stacked in a sandwich-like shape.

### 14.2.6 Thermal ablation/fire retardation

Thermal protection system (TPS) constituents are utilized to fabricate the thermal safeguard that guards aerodynamic surfaces and structures, missiles, probes, warheads, and payloads of planetary vehicles from widespread heating circumstances during the entrance flight through the terrestrial environment [32]. Constituents of aerospace shuttle such as sharp leading edges, nose caps, and rocket engines are exposed to a high-temperature condition in which temperatures can quickly rise to 3000°C from ambient temperature in a short time [33]. For the protection against extreme temperature conditions during hypersonic flight, NASA uses an ablative TPS on all of its planetary entry probes [34,35]. Polymeric ablative materials (PAMs) efficiently survive heat fluxes in the range of $\sim 30-30 \times 10^3$ W cm$^{-2}$. PAMs and carbon/carbon composites have been utilized to manufacture the heat safeguard of warheads (Fig. 14.7A) and the nozzle assembly of military solid rocket motors (SRMs) (Fig. 14.7B).

Manufacturing of chemical impulsion systems, such as SRMs for missiles, relies heavily on nanostructured PAMs (N-PAMs) [36,37]. This is due to N-PAMs' inherent advantages, including outstanding mechanical characteristics, low density, excellent shock resistance, and high thermal insulation. Thermal protection with ablative materials is also employed in similar technical applications such as a fire on military ground vehicles, naval ships, submarines, and airplanes that will have severe consequences. For example, Kumar et al. revealed that polymeric nanocomposite schemes for the armor of the battle tank (Fig. 14.8) exhibit reliable ablative qualities in various armor-piercing methods at extreme temperatures exceeding 3000°C [38].

As a result, flame retardant [39] polymeric nanocomposites have engrossed much consideration in current decades due to their exceptional flame retardancy and mechanical properties for various uses as exemplified in Fig. 14.9.

He et al. have recently reviewed PNCs used for flame retardant [40], and some of the recently used flame retardant polymeric nanocomposites are recorded in

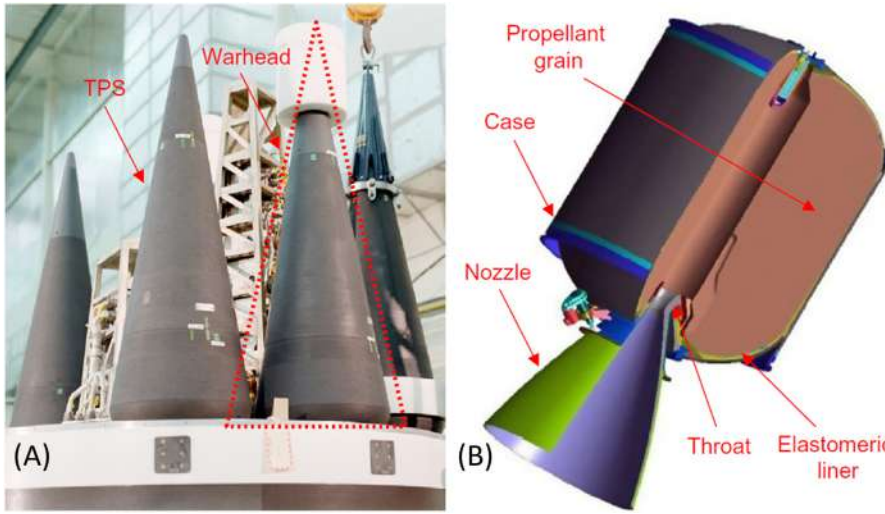


**Figure 14.7** Thermal protection system of (A) warheads (payload of the ballistic missile) and (B) SRM [18,36]. *SRM*, solid rocket motor.

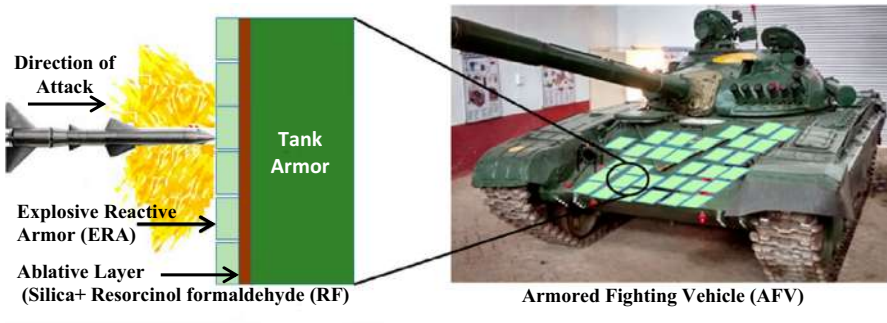


**Figure 14.8** Ablative armor protection in a combat tank [38].

Table 14.2. It has been observed that the addition of a shallow level (<5 wt.%) of nanomaterials can significantly decrease the burning tendency of the polymer by reducing the heat release rate and mass loss rate.

### 14.2.7 Corrosion protection

Metal corrosion has recently emerged as a major issue that has resulted in large financial losses for the military industry while also posing a considerable threat to the people. Since deterioration cannot be completely prevented, it is hindered and limited to reduce financial losses. Steel is also extensively used in various applications, including construction works, military automobiles, naval ships, and oil and

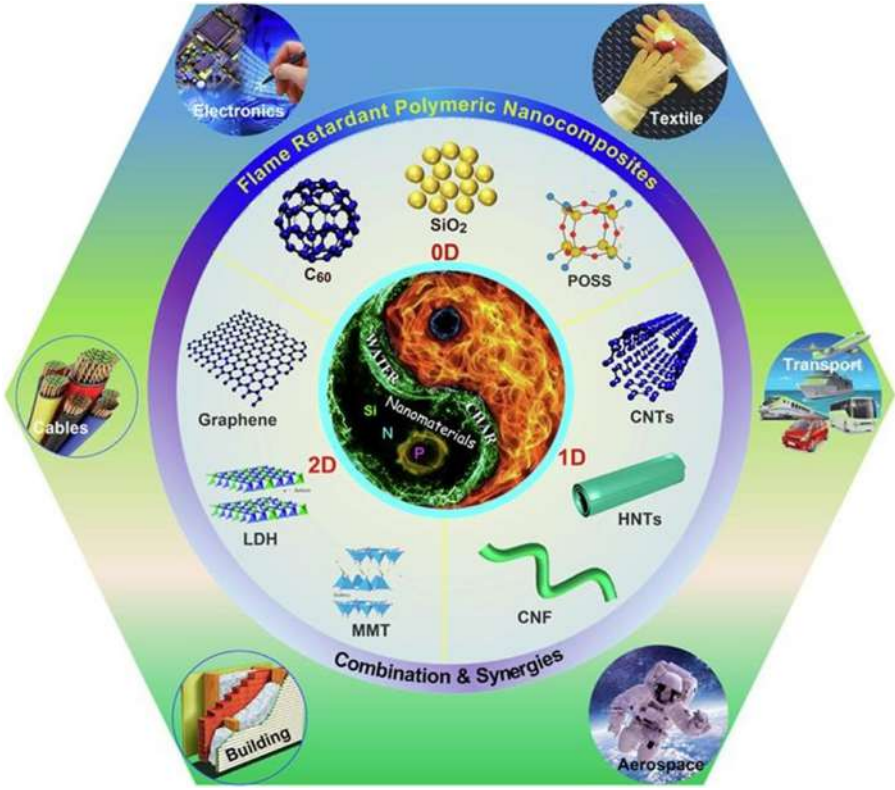


**Figure 14.9** Various applications of flame retardant polymeric nanocomposite [40].

gas pipelines due to its superior mechanical qualities and cost-effectiveness compared to modern alloys.

Nanocomposite coatings have sparked much attention recently, and researchers are promoting newer methods for designing and producing long-lasting corrosion protection surface coatings with exceptional qualities [54]. Owing to the nanoparticle's large surface area-to-volume ratio, $H_2O$ molecules cannot diffuse to the convoluted path, resulting in improved surface protection than bulk counterparts [55].

The development of PNC coating to preserve metal surfaces from corrosion appears to be an intriguing approach [56,57]. Numerous nanoparticles-based coatings have been discovered such as $TiO_2$, $Al_2O_3$, $SiO_2$, ZnO, and $Fe_2O_3$. Table 14.3 shows some of the recently developed PNCs for the protection of corrosion.

### 14.2.8 Explosives and propellants

In the military, large amounts of explosives and propellants are used in various weapons such as ammunitions, bombs, torpedoes, missiles, and rocket warheads. They are preserved and deported in massive amounts. However, they are always

**Table 14.2** Flame retardancy of different polymer nanocomposite.

| Polymer matrix | Flame retardancy additives | Flame retardancy properties | | References |
|---|---|---|---|---|
| | | Reduction of PHRR (%) | Reduction of THR (%) | |
| PET | 9 wt.% Exolit OP950 + 1 wt.% DP-POSS | 55 | 53 | Didane et al. [41] |
| PC | 3 wt.% BDP + 2 wt.% TPOSS[a] | 46 | 30 | He et al. [42] |
| ABS | 0.2 wt.% MWNT-PDSPB | 50 | 19 | Ma et al. [43] |
| | 18 wt.% PDSPB + 2 wt.% OMMT | 60 | 36 | Ma et al. [44] |
| TPU | 10 wt.% Br-$Sb_2O_3$@RGO (Br, Sb) | 72 | 15 | Huang et al. [45] |
| PP | 5 wt.% CNT-PDBPP | 60 | 6 | Yang et al. [46] |
| | 28 wt.% IFR + 1.8 wt.% OMMT | 64 | 48 | Du et al. [47] |
| | 1 wt.% CNT-graphene | 73 | – | Song et al. [48] |
| EVA | 5 wt.% LDH intercalated with DPHPA | 43 | 19 | Huang et al. [49] |
| | 1 wt.% GO-PPSPB (P, N) | 56 | 24 | Huang et al. [50] |
| | 5 wt.% CNT-clay | 36 | – | Beyer [51] |
| | 1 wt.% MWNT-PDPSPB | 33 | – | Xu et al. [52] |
| PVA | 2 wt.% Graphene-clay | 49 | 19 | Huang et al. [53] |

*ABS*, acrylonitrile butadiene styrene; *CNT*, carbon nanotube; *EVA*, ethylene-vinyl acetate; *GO*, graphene oxide; *PC*, polycarbonate; *PP*, polypropylene; *PET*, polyethylene terephthalate; *PHRR*, peak heat release rate; *PVA*, polyvinyl alcohol; *THR*, total heat release; *TPU*, thermoplastic polyurethane.
[a]POSS: polyhedral oligomeric silsesquioxanes, TPOSSa: trisilanolphenyl-POSSMWNT, multiwalled carbon nanotubes, PDSPB: poly(diaminodiphenyl methane spirocyclic pentaerythritol bisphosphonate, PDBPP:poly(4,4-diaminodiphenylmethane-O-bicyclicpentaerythritol phosphate-phosphate); OMMT: organically modified MMT (montmorillonite), BDP: bisphenyl A bis(diphenyl phosphate).

vulnerable to unintentional explosions, resulting in massive loss of life and property. Excessive heat, incautious handling, inadequate safety and security measures, as well as intentional sabotage by opponents may be the root causes of undesired explosions. As a result, effective control is critical to guarantee the safety and protection of high-energy ingredients [66].

Polymers have recently been used to regulate the sudden and unexpected ignition or burning of nanoscale explosive materials, resulting in the invention of a novel explosive known as polymer-bonded explosives (PBXs). Premature ignition is controlled using nano-Al and metal oxide nanoparticles in a hydroxyl-terminated polybutadiene binder matrix. A substantial rise in burning rate was also attained with a comparatively small amount of the novel nano-Al [67].

**Table 14.3** Corrosion protection properties of polymer nanocomposites.

| Polymer matrix | Filler material | Metal substrate | Processing method | Test condition/ NaCl solution (%) | Effect analysis | References |
|---|---|---|---|---|---|---|
| Polyamide adduct cured epoxy | $TiO_2$ NPs | Steel | Dispersion | – | Improved corrosion resistance<br>Polarization resistance 1000 times higher than naval steel | Mardareand Benea [58] |
| Epoxy | GO + $ZrO_2$ | – | Chemical route + ultrasonication + curing | 3.5 | Enhanced corrosion properties due to sheet-like structure,<br>Reduction of pores<br>Exfoliation of GO-$ZrO_2$ hybrid in the epoxy matrix | Di et al. [59] |
| Epoxy | CNT + Zn | Steel | Chemical route<br>Spray coating on steel | 3.0 | Corrosion resistance is due to the combined influence of Zn and C components | Valencia-Goujon et al. [60] |
| Epoxy | $SiO_2$-GO | Mild steel | Solution | 3.5 | Electrolyte diffusion has increased due to the hydrolysis reactions of silane agents | Pourhashem et al. [61] |
| PMMA | GO | Copper | In situ polymerization | 3.5 | The addition of GO to the metal electrolyte contact can effectively impede charge transmission | Qi et al. [62] |
| PU | MWCNT and Thermally expanded grapheme (1:1) | Cold-rolled steel | Solution | 3.5 | Graphene extended the diffusion pathways of corrosive ions | Tong et al. [63] |
| Polyaniline | Graphene nanosheets | 310 stainless steel | Electrochemical deposition | 3.5 | Polyaniline can passivate steel surfaces and graphene to improve the polymer coating's barrier characteristics | Jafari et al. [64] |
| Epoxy (zinc-rich) | GO-PANI, GO | Steel | Solution | 3.5 | The high specific surface area of GO sheets boosted the coating barrier characteristics<br>GO-PANI improves the electrical interaction between zinc particles and the steel substrate | Ramezanzadeh et al. [65] |

*CNT*, carbon nanotube; *GO*, graphene oxide; *MWCNT*, multiwalled carbon nanotube; *PMMA*, polymethyl methacrylate; *PU*, polyurethane.

In the PBX system, explosive elements are amalgamated with a polymeric binding medium. Flexible rubber-like thermosetting or thermoplastics-based composite will support in enthralling or extenuating shock and other impulses of explosives [68]. Common explosives such as RDX, TNT, and aluminum powders, bonded with polymer are also appealing for submerged ammo, with 50% more lethality. However, the confrontation to such superficial provocations will confide on the type of binder and its chemical bonding performance with explosive ingredients. Fig. 14.10 depicts some of the inert and energetic polymers utilized as combustible binders.

### 14.2.9 Wound care for soldiers

Military wounds are commonly caused by gunfire, numerous fragmentation injuries from grenades, improvised explosive devices, landmines, and suicide bombers. However, this is not always the case, as soldiers can be hurt in accidents even while on military operations [69].

War injuries are frequently heavily contaminated, and in the case of bomb attacks, contamination with foreign human material within the damage can complicate matters further. Because of their large size and exudate, combat wounds are difficult to dress. Antimicrobial agents are found in many dressings. Some dressings release the antimicrobial directly into the wound, while others trap wound exudate and use the antimicrobial within the dressing to control microbial growth [70,74].

Nanomaterial-coated dressings allow for controlled drug and protein release for a definite time [72,73]. In addition, the exciting prospects of regulating the levels of growth factors and other active ingredients to speed up wound healing are made possible by the unique characteristic of nanoparticle aggregate wound dressing [74]. Gobi et al. [75] have recently reviewed various biopolymer [76] and synthetic polymer-based nanocomposites used in wound dressing, and some are listed in Table 14.4.

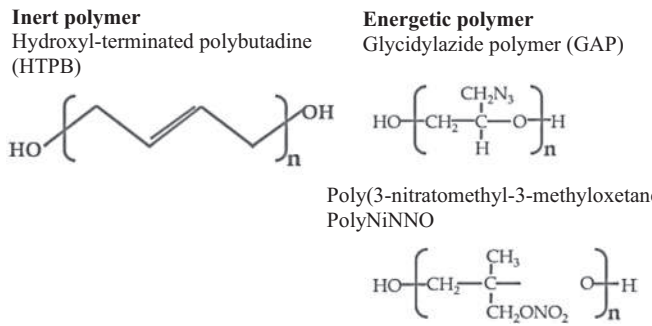


**Figure 14.10** Polymers (inert and energetic) used in PBX composites. *PBX*, polymer-bonded explosive.

**Table 14.4** Polymers and nanoparticles in wound dressing [75].

| Membrane composition | Method of preparation | Antibacterial strain | Cell line used | References |
|---|---|---|---|---|
| Heparinized ZnO/poly(vinyl alcohol)/carboxymethyl cellulose | Freeze-thaw | *Staphylococcus aureus* and *Escherichia coli* | L929 and Human dermal fibroblasts | Khorasani et al. [77] |
| Chitosan/poly(vinyl alcohol)/$AgNO_3$ and vitamin E | Solution Casting | *Salmonella typhimurium* | – | Nasef et al. [78] |
| Polyurethane/graphene oxide | Electrospun | *S. aureus and E. coli Human* | Dermal fibroblast | Sadeghianmaryan et al. [79] |
| Polyurethane/lavender oil/Ag | Electrospun | *S. aureus and E. coli* | – | Sofi et al. [80] |
| $CeO_2$/peppermint oil on polyethylene oxide/ graphene oxide | Electrospun | *S. aureus* and *E. coli* | – | Bharathi and Stalin [81] |
| Chitosan/poly(vinyl alcohol)/Ag | Freeze dryer | *Pseudomonas aeruginosa* and *S. aureus* | Fibroblast cells | Hiep et al. [82] |
| Polylactide/Ag | Electrospun | *S. aureus* and *E. coli* | Fibroblast cells | Alippilakkotte et al. [83] |
| Chitosan/poly (N-vinylpyrrolidone)/$TiO_2$ | Solution casting | *E. coli* *S. aureus* *Bacillus subtilis* and *P. aeruginosa* | NIH3T3 and L929 fibroblast cells | Archana et al. [84] |
| Chitosan/pectin/$TiO_2$ | Solution Casting | *E. coli* *S. aureus* *P. aeruginosa* *Aspergillus niger* *B. subtilis* | NIH3T3 and L929 fibroblast cells | Archana et al. [85] |
| Sodium alginate/graphene Oxide/poly(vinyl alcohol) | Freeze dryer | *S. aureus* and*E. coli* | NIH3T3 cells | Ma et al. [86] |
| Poly(vinyl alcohol)/chitosan/mGO | Solution casting | *S. aureus* and *E. coli* | Human keratinocyte cells | Chen et al. [87] |
| Cellulose/chitosan/polyethylene Oxide/graphene (HCPG) | Electrospun | *S. aureus* and *E. coli* | Human fetal skin fibroblast cells | Lin et al. [88] |

### 14.2.10 Electromagnetic interference shielding

The digital revolution occurs in the aerospace and defense sectors because of the proliferation of handy gadgets and embedded electronic devices. They contribute to a considerable increase in RF emissions, which may cause interference, data corruption, or device malfunction. All military platforms and vehicles, aircraft, naval ships, communication devices, missile systems, safety equipment, and rocket launchers require electromagnetic interference (EMI)/radio frequency interference shielding to work correctly [89,90].

Electronic warfare, in which electromagnetic radiations are utilized to interpose or interrupt military equipment, is a critical component of the battlespace [91]. Consequently, the requirements for EMI shielding in aerospace and defense applications will be severe, as the shielding structure and material must also withstand high-powered EM attacks such as electrostatic discharge and electromagnetic pulse, which can cause an electrical short or dielectric breakdown [92]. During the World War II, Germany created a carbonyl iron powder-loaded rubber sheet with a thickness of 0.3 in. and a resonance frequency of 3 GHz known as "Wesch" as a radar camouflage for submarines [93].

By the time the United States produced "HARP" (Halpern Anti-Radiation Paint). The airborne version (MX-410) comprises a base dielectric with a high permittivity of 150 due to the loading of highly orientated disk-shaped aluminum flakes suspended in a rubber matrix and CB. In the X band, this material reduced reflectance by 15−20 dB [90]. 20−35 dB shielding may be enough to defend low-power consumer devices from interference, but they are insufficient to encounter EMI shielding standards for aerospace and defense purposes (Fig. 14.11).

For aerospace and defense purposes, shielding of at least 50 dB is essential [91,94], and some of the PNCs used for EMI shielding are listed in Table 14.5.

### 14.2.11 Ultraviolet irradiation resistance

Under ultraviolet irradiation, common polymers are unstable and begin to break down after weeks to months. The polymer's mechanical qualities such as tensile strength and fracture toughness are significantly reduced, making it brittle. The space environment wreaks havoc on traditional carbon fiber/epoxy composites, which are often employed in space applications. Modifying the epoxy matrix, which is commonly utilized in space applications, has been explored by Jiang et al. [100].

It was discovered that by adding nanotitanium dioxide particles to the epoxy/carbon fiber composite, the confrontation to ultraviolet irradiation might be lowered by half, and mechanical qualities could be increased by 80%. If such materials are used, the material enhancements are anticipated to result in increased effective load, less outgassing, and a longer lifetime.

### 14.2.12 Refractive index tuning

Polymer optical fibers are highly appealing to regulate the refractive index (RI) of the linked optical fiber owing to their affluence of bulk manufacture and cost

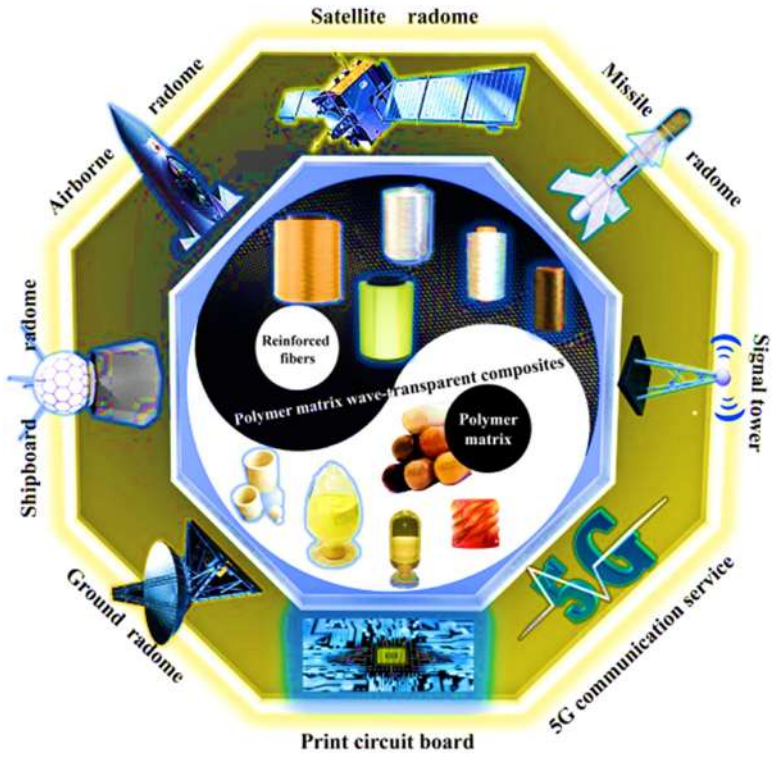


**Figure 14.11** Polymer nanocomposite and their wave-transparent applications [89].

**Table 14.5** EMI shielding polymer nanocomposites for the defense and aerospace industries.

| Ser. No | Polymer matrix | Filler material | Shielding effectiveness (dB) | Frequency (GHz) | References |
|---|---|---|---|---|---|
| 1 | Poly (vinyl chloride) | Graphite and nickel nanoparticles | 45−60 | 1−12 | Al-Ghamdi et al. [95] |
| 2 | Polyvinyl chloride | Graphite and copper nanoparticles | 22−70 | 1−20 | Al-Ghamdi and El-Tantawy [96] |
| 3 | UHMWPE | 10 wt.% CNT | 50 | 8−12 | Al-Saleh [97] |
| 4 | ABS copolymer | 15 wt.% MWCNT | 50 | 8.2 | Al-Saleh et al. [98] |
| 5 | Polyaniline | 5 wt.% graphene | 51−52 | 2−12 | Modak et al. [99] |

*ABS*, acrylonitrile butadiene styrene; *CNT*, carbon nanotube; *EMI*, electromagnetic interference; *MWCNT*, multiwalled carbon nanotube.

efficiency in many visual uses such as telecommunications and optical computing (connectors and switches). Shipboard communications, ship-to-shore communications, and deployable tactical communications are all examples of fiber optic devices that may give unrivaled security and stability. When every data item is valuable, the product that provides the highest and most consistent performance and that level can only be supplied by fiber-optics when it comes to data transmission.

Due to the outstanding optical characteristics such as high RI and noble transparency, they are convenient for a diversity of military uses [101], including optical waveguide [102] fabrication, antireflection coatings, ophthalmic lens [103], and glues for optical constituents.

So far, only a few polymers have been reported to have an RI value greater than 1.7, such as aromatic heterocyclic polymers [103], polythiophene [104], and conjugated polymers [105].

To minimize losses due to a mismatch between the RI of the optical fiber and semiconductor device or a silica optical fiber, it is essential to increase or decrease the RI of the polymer fiber, respectively. This can be accomplished by incorporating nanoparticles with different RI into the polymer. Modification of RI of poly (methyl methacrylate) (PMMA) could be possible by adding nanoparticles (zirconia, alumina, and silica), claimed by Böhm et al. [106]. By combining PMMA with varying amounts of two polyphosphate hybrid polymers with phosphorus in the main chain, Othayoth et al. [107] created promising optical materials with RI tunability.

### 14.2.13 Sensory applications

Innovative sensor technologies based on nanomaterials are being established to improve military information congregation by troops on the battlefield. For example, Nanosensors can identify dangerous chemicals [108] and biological weapons. Physical nanosensors could also detect cracks in military equipment, making them useful as damage detection devices. Manufacturing of military-grade active sensors for detecting damages (corrosion, substrate stability) as well as environmental circumstances (i.e., chemicals and explosives radiation, thermal condition, stress–strain, and toxic gases) is the blessing of nanotechnology, which has a significant impact on data and signal processing, automation, and intelligent schemes in the battlespace [109].

#### 14.2.13.1 Hazardous chemical detection

Conductive polymer and graphene composites have increased interest in chemical sensors and biosensors because of their exclusive electrical, mechanical, optical, chemical, and structural capabilities [110–112].

Salavagione et al. give a summary on chemical sensors constructed on polymer composites with graphene (G) and CNTs for investigation in a variety of uses, including biosensing, gas, and chemical sensing based on electrochemical and optical recognition approach [113].

Wei et al. fabricated chemical sensors with carbon nanocomposites such as poly (1,8-diaminonaphthalene)/functionalized MWCNTs sensor for the discerning of Hg2 + [114] and PPy/carbonaceous nanospheres for the discerning of Hg(II) and Pb(II) [115].

Numerous investigators have focused on creating ammonia gas sensors as determining the trace of ammonia is critical. Kong et al. established chemical sensors built on individual single-walled nano-tubes (SWNTs) [116]. They discovered that when a semiconducting SWNT was exposed to gas molecules such as $NO_2$ or $NH_3$, its electrical resistance altered drastically. Furthermore, conventional electrical sensor compounds, such as CB polymer composites, require high heat for significant responsiveness, but SWNT-based sensors had a rapid response and greater sensitivity at ambient temperature.

Huang et al. invented an $NH_3$ sensor constructed on polyaniline (PANI)/RGO nanocomposite, which has excellent sensitivity and selectivity to $NH_3$ gas [117]. Again, Jang et al. investigated that PPy/RGO nanocomposites have an upper response in noticing ammonia gas than PPy/graphite composites, PPy/graphene oxide (GO) composites, and only graphite [118].

### *14.2.13.2 Detection of explosives*

Terrorists may intend to use explosives, particularly at airports and border posts, and hence it is essential to determine explosives' constituents for assuring the protection of people and property. Therefore chemical detectors with extraordinary selectivity and sensitivity for the identification of main explosive constituents such as 2,4,6-trinirophenol [picric acid (P.A.)], 2,4,6-trinitrotoluene (TNT), and 1,3,5-trinitroperhydro-1,3,5-triazine (RDX) are used widely [108,119].

Nitroaromatic compounds (NACs) are the vital energetic ingredients used to prepare landmines [120,121]. These explosives can degrade the environment by polluting soil and water, posing a threat to humans and ecosystems [122,123]. In addition, P.A. is highly harmful to human health, causing kidney and liver impairment, respiratory difficulties, and hepatitis at large doses [124,125]. TNT is a cancerous element that acts as a severe skin and eye annoyance and can harm the liver, blood, reproductive, and immune system [126]. As a result, scientists worldwide are working to build highly effective chemical sensors that can detect nitroaromatic explosives selectively [127–129].

The conducting nanoparticles were used to boost the luminous polymer's electron density. The electron-rich nanocomposites will be exploited for extremely ultrasensitive and selective recognition of electron-deficient nitroaromatic explosives established on a fluorescence quenching approach. Dutta et al. used a single-step free radical polymerization procedure to make carbon and silver nanoparticle-infused poly (vinyl alcohol) and polythiophene for fluorescence sensing of nitroaromatic chemicals [130].

Förster resonance energy transfer (FRET) is a valuable mechanism for the sensitive discovery of NACs [131]. For instance, Xia et al. developed a FRET system based on Au nanorod and quantum dots to recognize TNT [132]. Again, Xu et al.

fabricated conjugated polymeric sensory systems for the sensitive and selective revealing of TNT and P.A. in an aqueous environment [133]. Again, Yang et al. applied poly(acrylic acid) films to design a unique sensing instrument to recognize TNT at a limit of 0.1 ppb in water [134]. Seena et al. also created a highly sensitive piezoresistive SU-8/CB nanocomposite-based nanomechanical cantilever sensors to identify TNT vapor [135].

### 14.2.13.3 Other sensors

Ajayan et al. devised a process for creating polymer matrix [e.g., poly (dimethylsiloxane) (PDMS)] nanocomposite film with freestanding nanotube that may be utilized to make nanosensors. This material can be utilized to identify the actual condition in real time, like the wing or chassis of an aircraft while the plane is flying [136].

Polymer nanocomposite-based sensors (Fig. 14.12) could also be used to measure temperature, humidity, pressure, etc., which are required to understand the environmental condition for the smooth conduct of the battle weapons, military, and aerospace vehicles [139,140].

CB and MWNT were instigated into the high-density polyethylene by Zha et al. for the measurement of temperature [141]. Wang et al. developed a silicone rubber composite filled with CB and PU composite filled with a carbon nanotube-based temperature sensor that shows a maximum measurement range of 75°C [142]. Majid et al. developed polyaniline/$Mn_3O_4$ composite [143], Shih et al. developed graphite/PDMS composite [138], and He et al. developed graphene/polyvinylidene fluoride (PVDF) composites [144] in the fabrication of temperature sensors [143].

Mahadeva et al. developed a cellulose−polypyrrole nanocomposite-based adjustable temperature and humidity sensor [137]. Patil et al. manufactured poly (o-anisidine)etin oxide (POA-$SnO_2$) nanocomposite for the measurement of humidity [145]. Again, Zhang et al. have developed a tricobalt tetroxide ($Co_3O_4$)/poly (sodium styrene sulfonate) composite base humidity sensor for the detection of humidity [146].

Ramalingame et al. established a susceptible capacitive pressure sensor built on MWCNT and PDMS, the maximum pressure sensing capacity of which is roughly

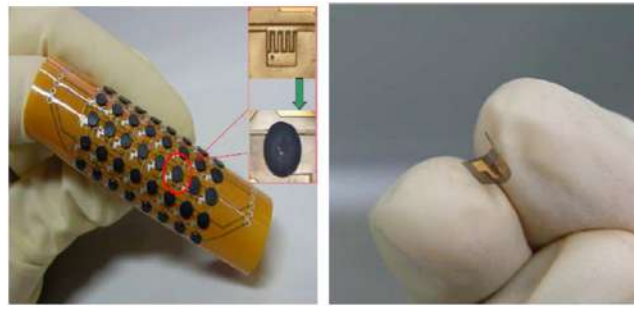

**Figure 14.12** Polymer nanocomposite-based temperature sensors [137,138].

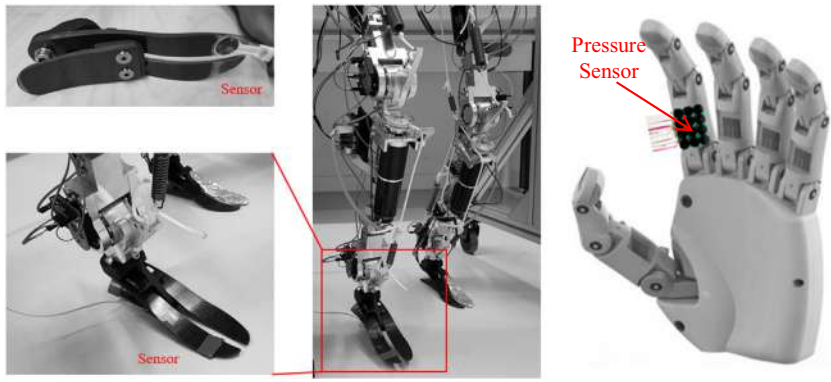


**Figure 14.13** Pressure sensor on foot and hand of the humanoid robot [147].

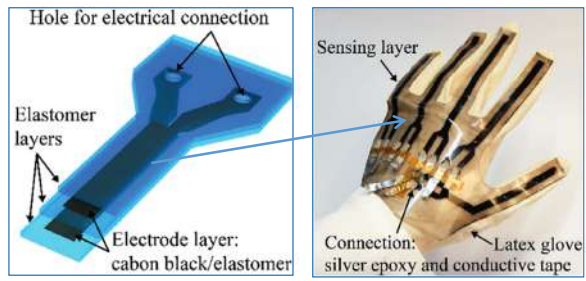


**Figure 14.14** Highly stretchable sensors with carbon black composite [158].

570 kPa [147]. This sensor could be implemented on the finger grip and gait analysis of humanoid military robots, as shown in Fig. 14.13.

Wearable strain sensors based on PNC for the soldiers' medical diagnosis and healthcare and various military robotic systems are intriguing. It can be connected onto military uniforms or directly worn on the soldier's skin by elastic straps or adhesive tapes for monitoring motions, physical and biochemical signals, etc. [148,149].

Seyedin et al. effectively invented a strain reactive PU/poly(3,4-ethylenedioxythiophene): polystyrene sulfonate (PEDOT:PSS) elastomeric composite [150] for monitoring strain on the human body. Lipomi et al. [151] also developed a strain sensor made of CNTs/PDMS. On the other hand, CB/Ecoflex elastomeric composites sensor for monitoring the strain has been fabricated by Shintake et al. [152] as shown in Fig. 14.14.

## 14.3 Actuators for military robots

As the usage of autonomous systems grows, the demand for actuators in defense systems is rapidly increasing. In military robotics, the required size of the actuators

is often tiny, which confines the usage of the traditional actuator for the electric motor. Electric motors may need high power levels. In addition, there is frequently a need to convert the rotary motion from an engine to a linear motion, which requires some form of the gearbox. Nanocomposite-based actuators are claimed to have various benefits, such as low power requirements and direct linear motion.

Koerner et al.[153] observed that dispersing a tiny amount (5%) of CNTs in a PU thermoplastic polymer (Morthane) allowed the nanocomposite to store (and release) 50% more strain energy than the unreinforced polymer. Furthermore, CNTs allowed either direct (Joule heating) or indirect (infrared) activation. Compared to traditional fillers (such as CB), significantly fewer CNT branches were required, resulting in a nanocomposite with better characteristics. Shape memory polymers are already on the market and in use in a variety of applications. They are, however, inadequately resilient to find broader applications. Gall et al. raised the recovery stress by up to 50% without compromising other features by introducing a mechanical restraint in inert silicon carbide nanoparticles to a profitable shape memory polymer [154].

Structural design of soft robots and muscle-like actuators [155–157] have been broadly studied for numerous potential uses (Fig. 14.15) in exploration and rescue operations, medical restoration, military investigation, etc. Liu et al. found that semicrystalline poly (ethylene-*co*-vinyl acetate) convoluted with silver nanowires (AgNWs) displays mutable light-trigged morphing behavior in the air or submerged [161].

## 14.4 Marine applications

Because of the superior engineering features, marine industry is extensively using advanced polymeric composites. The key reasons for using these constituents for diverse marine divisions are lightweight, cost savings, and ecological sustainability [162,163]. However, the widespread use of traditional materials and sophisticated composites in many marine sectors has sparked an outcry over the environmental consequences of these materials, which is aided even more by the harsh environments in which they operate, such as seawater [164].

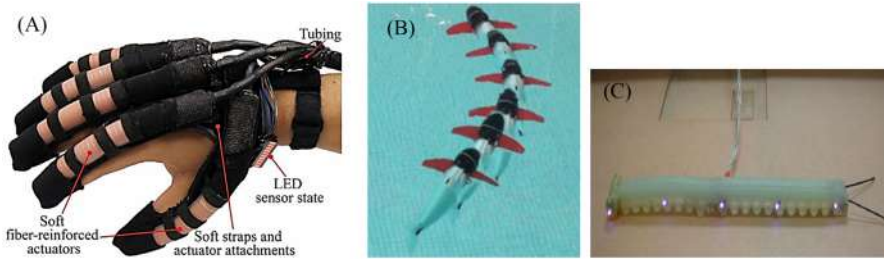


**Figure 14.15** (A) Soft robotic hand actuator [158]. (B) Autonomous soft robotic fish [159]. (C) Caterpillar-inspired soft robot (GoQBot) [160].

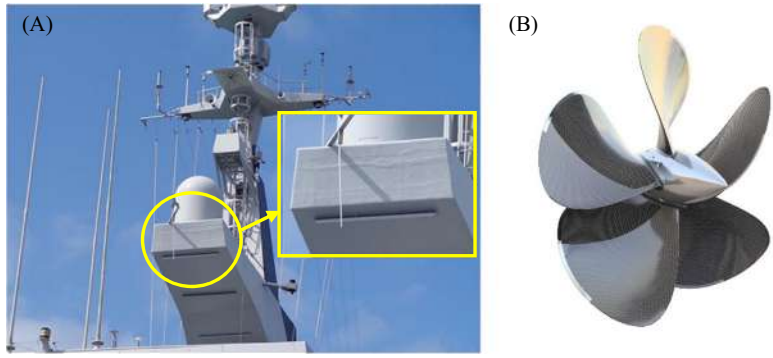


**Figure 14.16** (A) Naval ship topmast built up in fiberglass composite [165]. (B) Propeller blade made with carbon nanofiber.

High strength and durability, high load-bearing capacity, enhanced structural accuracy, flatness for stealth requirements, versatility, fuel efficiency, installation and maintenance expenses, and lower magnetic and electric signatures, high mobility, decreased friction and wear, low wettability, rusting, impact resistances, increased vibration damping, enhanced level of acoustic transparency, etc. are some of the excellent characteristics of advanced polymeric composites to proliferate their use in the marine sector (Fig. 14.16) [2,165].

Hence, many components of marine warships (destroyers, frigates, hovercraft, and corvettes) are fabricated with advanced polymer composites such as engine components, rotor blades, antenna, torpedo tubes, trunks, water, fuel, and lube oil storage tanks, various fittings, hulls, gas pipelines, floating platforms, and sonar domes [166,167].

The physical weight of a patrol boat constructed of glass-reinforced plastic composite material is 10% lighter than an aluminum boat and 36% lighter than a steel boat of equal size, according to Mouritz et al. [168]. In addition, nanocomposites such as hybrid glass carbon-reinforced polymer composite (GCG2C)s are the best at retaining the mechanical qualities that materials require for good functioning in the maritime industry over time. Hybrid (GCG2C)s also have an extraordinary flexural strength of 462 MPa and least susceptibility to absorb water.

Kim et al. developed basalt/CNT/epoxy multiscale composite, which could be used on marine structures such as a propeller and the ship's hulls. The composite sample's damping coefficient was augmented by 50%, and fracture toughness was reduced by 20% after immersion in seawater [169].

## 14.5 Military ration packaging (diffusion barrier)

Quality food and rations have long been critical to maintaining the health, morale, and discipline of the armed forces. As new technology has prepared the way for

future generations of military feeding systems, military rations and supplies have experienced several progressive adjustments throughout the years. PNC technology has significantly impacted the expansion and development of forthcoming packaging systems [170–172].

The next generation of MRE (Meal Ready-to-Eat) packaging materials are lighter, biodegradable, and outdo the present individual ration packaging systems by exploiting nanocomposite's enhanced thermal, mechanical, and barrier capability systems. The typical MRE Meal Bag comprises 280 μm thick low-density polyethylene (LDPE), which delivers a sound moisture barrier and can resist bugs, but it is relatively low in tensile strength and poor oxygen barrier [173].

In this regard, polymer nanocomposites can provide better gas-blocking characteristics of the Meal Bag to decrease the dispersion of aroma, water vapor, and oxygen through the matrix and preserve the quality of the food, thereby enhancing the shelf life [174,175].

Numerous experimental studies have confirmed substantial development in gas-blocking characteristics after integrating silicates in the polymer matrix. For example, de Abreu et al. stated that 5% addition of Cloisite 15A nanoparticles in P.P. and LDPE-based composites abridged the oxygen transmission rate from 480 to 374 cc $m^{-2}$ and from 240 to 210 cc $m^{-2}$ day, respectively [172].

Emamifar et al. fabricated Ag and ZnO nanoparticles dispersed LDPE films, found the antimicrobial activity of *Lactiplantibacillus plantarum*, and observed a decrease of *L. plantarum* ($P < .05$) in orange juice packet made of nanocomposite containing nanosilver and nano-ZnO [176].

In addition to increasing gas-blocking qualities, the addition of 1–5 wt.% nanoclay to polymer films has been demonstrated to increase mechanical properties [175,177].

Cho and Paul discovered that addition of 5% montmorillonite to nylon-6 improves composites' modulus and yield strength significantly [178]. Likewise, Ray et al. have exposed an escalation of 100% in Young's modulus of nylon-6 and LDPE-based nanocomposites [177].

Biopolymers such as polylactic acid (PLA) starch and poly-hydroxy-butyrate are auspicious constituents for green packaging. Many scientists reported that nanofillers could increase biopolymers' mechanical, thermal, and gas barrier properties though they usually have low mechanical characteristics, high wettability, and poor process ability. For example, Wu et al. [179] developed PLA-grafted $SiO_2$ nanocomposite and Li and Sun [180] developed a PLA-grafted MgO nanocomposite for packaging applications. Liu et al. [181] and Istrate and Chen [182] developed nanoclay-filled decomposable poly (e-caprolactone) (PCL) nanocomposite foam for packaging applications.

## 14.6 Water purification for defense

The military required ample clean water supplies in fast-moving operational environments as waterborne and other transmittable diseases could cause more fatalities

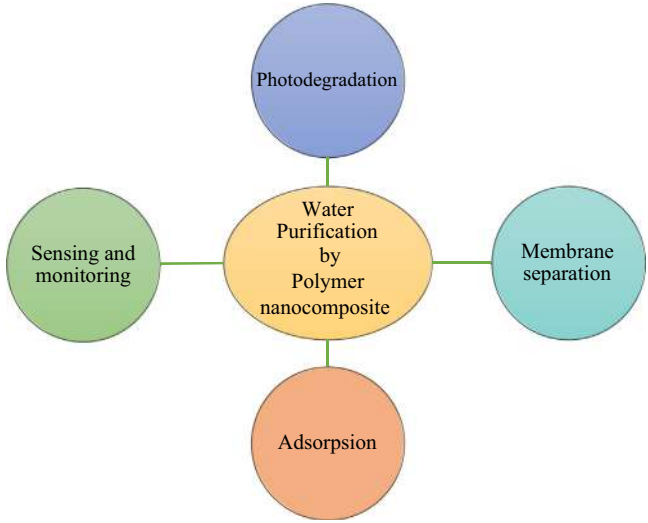


**Figure 14.17** Polymer nanocomposites for water decontamination.

than battlefield grievances [183]. PNCs of various sorts are now being investigated in the ideal military water purifier for use at the base or in the field. The primary reason for using PNCs in any application is because of their distinct features from their counterparts. Pandey et al. [184] have recently examined and tabulated several techniques utilized for water filtration, and different PNCs used for water decontaminations are shown in Fig. 14.17.

### 14.6.1 Removal of heavy metallic ions

Due to anthropogenic or geological origins, most surface and groundwater are polluted with heavy and radioactive metals. Heavy and radioactive metals accumulate in the environment and edible substances. They may move in the body through the food chain and are liable for biomagnification. Different and PNCs used as adsorbents of toxic heavy metal ions in the military water filtration systems are listed in Table 14.6.

### 14.6.2 Removal of dyes

PNCs' tunable surface and catalytic capabilities also have an excellent prospective for removing dyes, a severe contaminant. Exponential dye leakage into water bodies is causing severe water problems and waterborne diseases [195–197]. In addition, most dyes negatively impact the surroundings and aquatic living creatures and create allergies, dermatitis, skin irritation, and mutations in humans. For the removal of dyes, many researchers employ PNCs for efficient dye removal. In this regard, Table 14.7 lists some special dye adsorbing PNCs.

**Table 14.6** Suitable polymer nanocomposite adsorbents of metallic pollutants.

| Ser. No | Radioactive pollutants | Adsorbent | References |
|---|---|---|---|
| 1 | Uranium | Chitin/chitosan complex | [185] |
| | | PVA/TEOS/APTES hybrid nanofiber | Keshtkar et al. [186] |
| 2 | Thorium (IV) | Poly(methacrylic acid)-grafted chitosan/bentonite composite | Anirudhan et al. [187] |
| | | Polyacrylamide-aluminosilicate | Baybaş and Ulusoy [188] |
| | | Polyvinyl alcohol/titanium oxide | Abbasizadeh et al. [189] |
| 3 | Thorium | PAN/zeolite | Kaygun and Akyil [190] |
| 4 | Am (III) and Cm (III) | 2,6-Bistriazinylpyridine | Wei et al. [191] |
| 5 | Sr, Cd | Nafion 120 | Gasser and Nowier [192] |
| 6 | $UO_2^{2+}$, $Tl^{+}$, $Pb^{2+}$, $Ra^{2+}$, and $Ac^{3+}$ | Polyacrylamide−bentonite composite | Şimşek et al. [193] |
| 7 | Cesium, cobalt, and europium ions | $TiO_2$/poly (acrylamide−styrene sodium sulfonate) | Borai et al. [194] |

*APTES*, 3-aminopropyl)triethoxysilane; *PVA*, polyvinyl alcohol; *TEOS*, tetraethyl orthosilicate.

### 14.6.3 Desalination and removal of oil

Desalination is a procedure for removing minerals from seawater. Many polymer composites with considerable efficacy were proposed to achieve that goal. For instance, polyethylene glycol, cellulose acetate, and polyvinyl alcohol composite membrane were developed and reported for desalination of groundwater and saltwater [206−208].

The creation of polymer sponges with high oil/water selectivity, adsorption capacity, and mechanical durability is a successful technique for separating oil from oil-polluted water [209−211]. For example, Zhao et al. created a durable and recyclable sponge (Fig. 14.18) using a PDMS frame coated stereoscopically with GO, which has a good adsorption capacity for a diversity of oils and organic diluents [212].

In the current research, single-walled CNTs were introduced to a poly(N-isopropyl acrylamide)-*co*-(acrylamide) copolymer membrane to separate water−oil mixtures. Because of its oleophilic properties, CNT is employed for this purpose. The oil was removed from the constructed single-walled CNTs-based copolymer membrane at a rate of 99.99%. MWCNTs were inserted into a polysulfone (PS)/polyether blockcopolymer to create a CNTs-polymer membrane that may be utilized to extract oil from the oil−water mixture. The influence of the MWCNTs ratio on oil exclusion competence was demonstrated in this study. As can be seen, increasing the number of MWCNTs to 2.0 wt.% enhanced membrane oil denunciation from 91.4% to 99.79% [213].

**Table 14.7** Suitable polymer nanocomposite adsorbents for dyes removal.

| Ser. No | Dyes | Adsorbents | Adsorption capacity (mg $gm^{-1}$) | References |
|---|---|---|---|---|
| 1 | Methyl orange | γ-$Fe_2O_3$/CSCs | – | Zhu et al. [198] |
| 2 | Remazol Red 198 | L-Cht/γ-$Fe_2O_3$ | 267 | Debrassi et al. [199] |
| 3 | MO | γ-$Fe_2O_3$/$SiO_2$/chitosan composite | 3429 | Zhu et al. [200] |
| 4 | Basic violet 10 | CNTs/activated carbon fiber | 220 | Wang et al. [201] |
| 5 | Methyl orange | Chitosan/$Fe_2O_3$/MWCNTs | 66.90 | Zhu et al. [202] |
| 6 | Methylene Blue | Hydrolyzed nanosilica Incorporated polyacrylamide Grafted xanthan gum | 378.8 | Ghorai et al. [203] |
| 7 | Methyl Violet | Methyl violet onto poly (acrylic acid-*co*-acrylamide)/kaolin hydrogel | 908.0 | Tang et al. [204] |
| 8 | Alizarin Yellow | Polyaniline + MWCNTs | 884.80 | Wu et al. [205] |

*MWCNT*, multiwalled carbon nanotube.

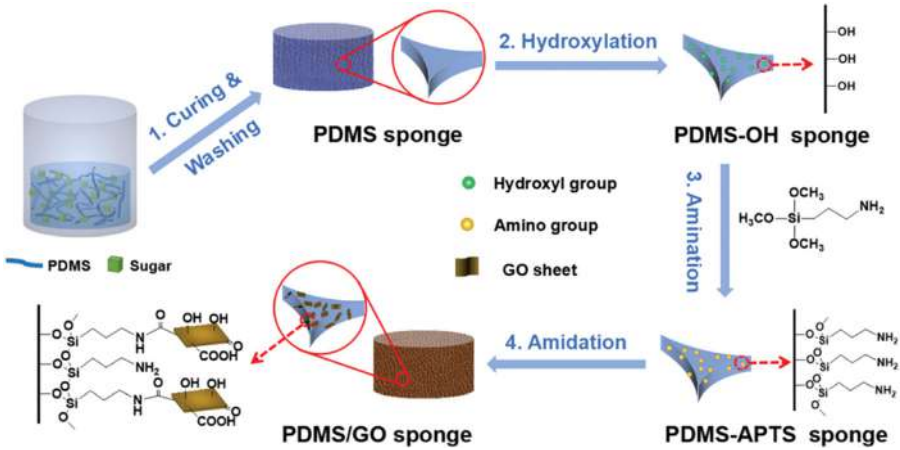


**Figure 14.18** The preparation of the porous PDMS/GO sponge [212]. *PDMS*, poly (dimethylsiloxane); *GO*, graphene oxide.

### 14.6.4 Removal of other pollutants

Microorganisms, insecticides, pathogens, and other organic elements are among the other essential water contaminants. The creation of decontamination by-products and multidrug-resistant bacterial species are two of their concerns, prompting new disinfection technologies. For example, Jain et al. found that Ag-coated PU foam (Fig. 14.19) can be utilized professionally for removing a broad spectrum of bacterial strains up to 99.9% [214].

Ag nanoparticles embedded with fibers of cellulose acetate were operative against bacteria. Aquatic purifiers made from PU foam with Ag-coated nanofibers show significant disinfecting against germs such as *Escherichia coli* [215].

Numerous composites embedded with activated carbon fibers and CNTs effectively eliminate pathogenic microorganisms [216,217]. Gunawan et al. have examined the AgNP/CNTs-coated hollow fiber membrane of polyacrylonitrile (PAN) for water cleansing [218]. The results exposed that AgNP/CNT coating has significantly enhanced the membranes' antifouling behaviors and antimicrobial activity.

### 14.6.5 Self-water purification system

In comparison to the regular military forces, Special Forces experience extraordinary challenges in guaranteeing the purity of their drinkable water. Conventional army's water purification system does not match the dimension, mobility, labor force, maintenance, or water supplies of army's special operational troops. For instance, logistic units support conventional armies that use material handling equipment to carry their water decontamination systems. In contrast, army special operational forces must frequently take all of their water purification system [219]. Army special operational forces use commercially available portable water purifying technologies such as "Lifestraw," shown in Fig. 14.20.

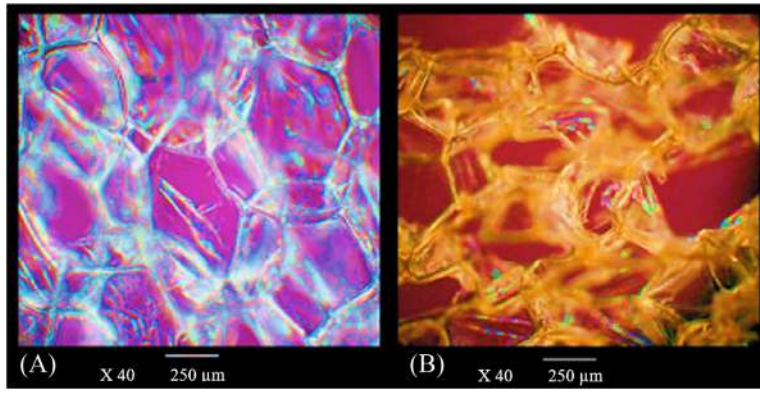


**Figure 14.19** Optical microscope image of (A) pure polyurethane foam and (B) Ag-coated polyurethane foam [214].

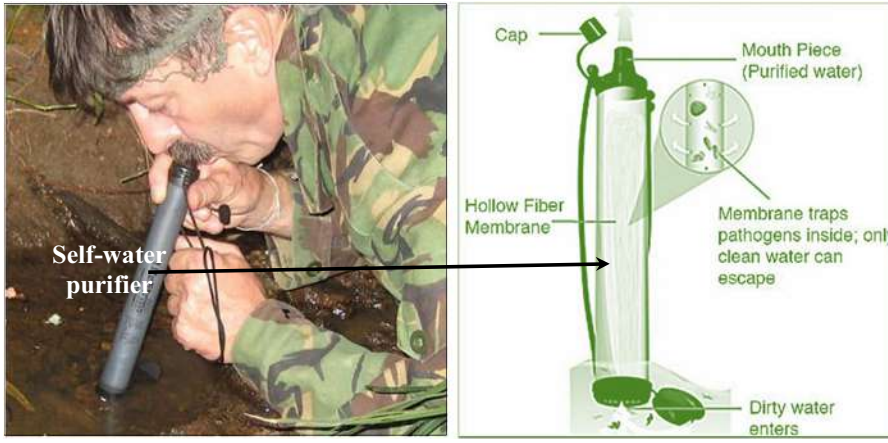


**Figure 14.20** Self-water purifier [220].

It is a simple straw that looks like a small tube with a filter inside and kills around 99.99% of bacteria in contaminated water. Self-water sucking purifying products use an ultrafiltration (UF) membrane [221,222]. UF can efficiently eliminate suspended matter, colloid, microbial pathogens, and macromolecular organic material [223,224]. Some of the standard commercial UF membranes materials are PS, polyvinyl chloride, PAN, PVDF, and polyethersulfone [225–227].

## 14.7 Conclusion

The 20th century, mainly after the World War II, has introduced a diversity of new materials that have a groundbreaking impact on all kinds of technologies related to defense industry. Today's warfare mostly depends on advanced technologies, and technologically advanced arm forces always lead on the combat. Hence, military researchers are always searching for new material which could be applicable to enhance the performance of modern armaments. Polymer matrix composites are widely used in various industries and defense sectors because of their superior qualities, which considerably boost the effectiveness and efficacy of materials in military disciplines. Based on current occurrences, future trends in the use of PNCs are expected to expand dramatically to meet the ever-changing and dynamic demands in tactical domains.

## References

[1] W. Chin, Technology, war and the state: past, present and future, Int. Aff. 95 (2019) 765–783.
[2] I.O. Oladele, T.F. Omotosho, A.A. Adediran, Polymer-based composites: an indispensable material for present and future applications, Int. J. Polym. Sci. 2020 (2020).

[3] N. Ramdani (Ed.), Polymer Nanocomposites for Advanced Engineering and Military Applications: Advances in Chemical and Materials Engineering, IGI Global, 2019. Available from: https://doi.org/10.4018/978-1-5225-7838-3.
[4] R. Kurahatti, A. Surendranathan, S. Kori, N. Singh, A. Kumar, S. Srivastava, Defence applications of polymer nanocomposites, Def. Sci. J. 60 (2010) 551–563. Available from: https://doi.org/10.14429/dsj.60.578.
[5] S.S. Godara, P.K. Mahato, Potential applications of hybrid nanocomposites, Mater. Today Proc. 18 (2019) 5327–5331. Available from: https://doi.org/10.1016/j.matpr.2019.07.557.
[6] R. Karkalić, V. Maslak, A. Nikolić, M. Kostić, D. Jovanović, Ž. Senić, et al., Application of permeable materials for CBRN protective equipment, Zastita Mater. 56 (2015) 239–242. Available from: https://doi.org/10.5937/ZasMat1502239K.
[7] T. Yuranova, R. Mosteo, J. Bandara, D. Laub, J. Kiwi, Self-cleaning cotton textiles surfaces modified by photoactive SiO2/TiO2 coating, J. Mol. Catal. Chem. 244 (2006) 160–167.
[8] A. Bozzi, T. Yuranova, J. Kiwi, Self-cleaning of wool-polyamide and polyester textiles by TiO2-rutile modification under daylight irradiation at ambient temperature, J. Photochem. Photobiol. Chem. 172 (2005) 27–34.
[9] M.M. Hussain, S. Ramkumar, Functionalized nanofibers for advanced applications, Indian J. Fibre Text Res. 31 (2006) 41–51.
[10] I.G. Crouch, Defence technology, 2019.
[11] K. Czech, R. Oliwa, D. Krajewski, K. Bulanda, M. Oleksy, G. Budzik, et al., Hybrid polymer composites used in the arms industry: a review, Mater. 14 (2021) 3047.
[12] S. Clifton, B.H.S. Thimmappa, R. Selvam, B. Shivamurthy, Polymer nanocomposites for high-velocity impact applications - a review, Compos. Commun. 17 (2020) 72–86. Available from: https://doi.org/10.1016/j.coco.2019.11.013.
[13] V. Vijay Kumar, G. Balaganesan, J.K.Y. Lee, R.E. Neisiany, S. Surendran, S. Ramakrishna, A review of recent advances in nanoengineered polymer composites, Polymers 11 (2019) 644.
[14] J.S. Tate, A.T. Akinola, S. Espinoza, S. Gaikwad, D.K. Kannabiran Vasudevan, S. Sprenger, et al., Tension–tension fatigue performance and stiffness degradation of nanosilica-modified glass fiber-reinforced composites, J. Compos. Mater. 52 (2018) 823–834.
[15] G. Vigneshwaran, B.P. Shanmugavel, R. Paskaramoorthy, S. Harish, Tensile, impact, and mode-I behaviour of glass fiber-reinforced polymer composite modified by graphene nanoplatelets, Arch. Civ. Mech. Eng. 20 (2020) 1–15.
[16] M.S. Tareq, S. Zainuddin, E. Woodside, F. Syed, Investigation of the flexural and thermomechanical properties of nanoclay/graphene reinforced carbon fiber epoxy composites, J. Mater. Res. 34 (2019) 3678–3687.
[17] B. Suresha, N. Indushekhara, C. Varun, D. Sachin, K. Pranao, Effect of carbon nanotubes reinforcement on mechanical properties of aramid/epoxy hybrid composites, Mater. Today Proc. 43 (2021) 1478–1484.
[18] N. Kumar, A. Dixit, Nanotechnology-Driven Explosives and Propellants, Nanotechnology for Defence Applications, Springer, 2019, pp. 81–115.
[19] R. Klement, S. Rolc, R. Mikulikova, J. Krestan, Transparent armour materials, J. Eur. Ceram. Soc. 28 (2008) 1091–1095.
[20] E. Carton, J. Broos, Innovative transparent armour concepts, in: The 26th International Symposium of Ballistics, Miami, USA, 2011.
[21] C.H. Sung, K.S. Lee, K.S. Lee, S.M. Oh, J.H. Kim, M.S. Kim, et al., Sound damping of a polyurethane foam nanocomposite, Macromol. Res. 15 (2007) 443–448.

[22] A.H. Baferani, A.A. Katbab, A.R. Ohadi, The role of sonication time upon acoustic wave absorption efficiency, microstructure, and viscoelastic behavior of flexible polyurethane/CNT nanocomposite foam, Eur. Polym. J. 90 (2017) 383–391.
[23] L.M. Degenstein, D. Sameoto, J.D. Hogan, A. Asad, P.I. Dolez, Smart textiles for visible and IR camouflage application: state-of-the-art and microfabrication path forward, Micromachines 12 (2021) 773.
[24] K. Karpagam, K. Saranya, J. Gopinathan, A. Bhattacharyya, Development of smart clothing for military applications using thermochromic colorants, J. Text. Inst. 108 (2017) 1122–1127.
[25] S.S. Salehi, M.K. Mehrizi, S.M. Bidoki, Z. Shahi, Comfort and reflectance properties of viscose/polyester blend fabric printed by vat/disperse dyes in visible/near-infrared region, Color. Res. Appl. 45 (2020) 477–484. Available from: https://doi.org/10.1002/col.22486.
[26] M.K. Mehrizi, S. Mortazavi, S. Mallakpour, S. Bidoki, M. Vik, M. Vikova, Effect of carbon black nanoparticles on reflective behavior of printed cotton/nylon fabrics in visible/near infrared regions, Fibers Polym. 13 (2012) 501–506.
[27] M. Khajeh Mehrizi, F. Bokaei, N. Jamshidi, Visible-near infrared concealment of cotton/nylon fabrics using colored pigments and multiwalled carbon nanotube particles (MWCNTs), Color. Res. Appl. 40 (2015) 93–98.
[28] M. Abbasipour, M.K. Mehrizi, Investigation of changes of reflective behavior of cotton/polyester fabric by TiO2 and carbon black nanoparticles, Sci. Iran. 19 (2012) 954–957.
[29] S.A. Siadat, J. Mokhtari, Diffuse reflectance behavior of the printed cotton/nylon blend fabrics treated with zirconium and cerium dioxide and citric acid in near-and short-wave IR radiation spectral ranges, Color. Res. Appl. 45 (2020) 55–64.
[30] S.A. Siadat, J. Mokhtari, Influence of ceramic nano-powders and cross-linker on diffuse reflectance behavior of printed cotton/nylon blend fabrics in near infrared and short-wave infrared spectral ranges, J. Text. Inst. (2020) 1–12.
[31] S. Hong, S. Shin, R. Chen, An adaptive and wearable thermal camouflage device, Adv. Funct. Mater. 30 (2020) 1909788.
[32] Y. Badhe, K. Balasubramanian, Novel hybrid ablative composites of resorcinol formaldehyde as thermal protection systems for re-entry vehicles, RSC Adv. 4 (2014) 28956–28963.
[33] C.V. Kumar, B. Kandasubramanian, Advances in ablative composites of carbon based materials: a review, Ind. Eng. Chem. Res. 58 (2019) 22663–22701.
[34] B. Laub, E. Venkatapathy, Thermal protection system technology and facility needs for demanding future planetary missions. in: Planetary probe atmospheric entry and descent trajectory analysis and science, 2004, pp. 239–247.
[35] I. Srikanth, N. Padmavathi, S. Kumar, P. Ghosal, A. Kumar, C. Subrahmanyam, Mechanical, thermal and ablative properties of zirconia, CNT modified carbon/phenolic composites, Compos. Sci. Technol. 80 (2013) 1–7.
[36] M. Natali, J.M. Kenny, L. Torre, Thermoset nanocomposites as ablative materials for rocket and military applications, Thermosets, Elsevier, 2018, pp. 477–509. Available from: https://doi.org/10.1016/B978-0-08-101021-1.00015-0.
[37] M. Natali, M. Rallini, J. Kenny, L. Torre, Effect of Wollastonite on the ablation resistance of EPDM based elastomeric heat shielding materials for solid rocket motors, Polym. Degrad. Stab. 130 (2016) 47–57.
[38] V. Kumar, S. Singh, B. Kandasubramanian, Thermal ablation and laser shielding characteristics of ionic liquid-microseeded functionalized nanoclay/resorcinol formaldehyde

nanocomposites for armor protection, Polym.-Plast. Technol. Eng. 56 (2017) 1542–1555.
[39] K. Tshai, H. Tan, P. Khiew, M. Hoque, C. Chia, Effects of aluminum trihydrate on the flame-retardant and smoke-suppressant properties of natural fibres filled composites, Polym. Res. J. 9 (2015) 181.
[40] W. He, P. Song, B. Yu, Z. Fang, H. Wang, Flame retardant polymeric nanocomposites through the combination of nanomaterials and conventional flame retardants, Prog. Mater. Sci. 114 (2020) 100687.
[41] N. Didane, S. Giraud, E. Devaux, G. Lemort, A comparative study of POSS as synergists with zinc phosphinates for PET fire retardancy, Polym. Degrad. Stab. 97 (2012) 383–391.
[42] Q. He, L. Song, Y. Hu, S. Zhou, Synergistic effects of polyhedral oligomeric silsesquioxane (POSS) and oligomeric bisphenyl A bis (diphenyl phosphate) (BDP) on thermal and flame retardant properties of polycarbonate, J. Mater. Sci. 44 (2009) 1308–1316.
[43] H.-Y. Ma, L. Tong, Z. Xu, Z. Fang, Functionalizing carbon nanotubes by grafting on intumescent flame retardant: nanocomposite synthesis, morphology, rheology, and flammability, Adv. Funct. Mater. 18 (2008) 414–421.
[44] H. Ma, L. Tong, Z. Xu, Z. Fang, Intumescent flame retardant-montmorillonite synergism in ABS nanocomposites, Appl. Clay Sci. 42 (2008) 238–245.
[45] G. Huang, P. Song, L. Liu, D. Han, C. Ge, R. Li, et al., Fabrication of multifunctional graphene decorated with bromine and nano-Sb2O3 towards high-performance polymer nanocomposites, Carbon 98 (2016) 689–701.
[46] H. Yang, L. Ye, J. Gong, M. Li, Z. Jiang, X. Wen, H. Chen, N. Tian, T. Tang, Simultaneously improving the mechanical properties and flame retardancy of polypropylene using functionalized carbon nanotubes by covalently wrapping flame retardants followed by linking polypropylene, Mater. Chem. Front. 1 (2017) 716–726.
[47] B. Du, Z. Guo, H. Liu, Z. Fang, Y. Wu, Flame retardant mechanism of organo-bentonite in polypropylene, Appl. Clay Sci. 45 (2009) 178–184.
[48] P. Song, L. Liu, S. Fu, Y. Yu, C. Jin, Q. Wu, et al., Striking multiple synergies created by combining reduced graphene oxides and carbon nanotubes for polymer nanocomposites, Nanotechnology 24 (2013) 125704.
[49] G. Huang, Z. Fei, X. Chen, F. Qiu, X. Wang, J. Gao, Functionalization of layered double hydroxides by intumescent flame retardant: preparation, characterization, and application in ethylene vinyl acetate copolymer, Appl. Surf. Sci. 258 (2012) 10115–10122.
[50] G. Huang, S. Chen, S. Tang, J. Gao, A novel intumescent flame retardant-functionalized graphene: nanocomposite synthesis, characterization, and flammability properties, Mater. Chem. Phys. 135 (2012) 938–947.
[51] G. Beyer, Carbon nanotubes as flame retardants for polymers, Fire Mater. 26 (2002) 291–293.
[52] G. Xu, J. Cheng, H. Wu, Z. Lin, Y. Zhang, H. Wang, Functionalized carbon nanotubes with oligomeric intumescent flame retardant for reducing the agglomeration and flammability of poly (ethylene vinyl acetate) nanocomposites, Polym. Compos. 34 (2013) 109–121.
[53] G. Huang, S. Chen, H. Liang, X. Wang, J. Gao, Combination of graphene and montmorillonite reduces the flammability of poly (vinyl alcohol) nanocomposites, Appl. Clay Sci. 80 (2013) 433–437.
[54] M.H. Nazari, X. Shi, Polymer-based nanocomposite coatings for anticorrosion applications, Industrial Applications for Intelligent Polymers and Coatings, Springer, 2016, pp. 373–398.

[55] A. Kausar, Corrosion prevention prospects of polymeric nanocomposites: a review, J. Plast. Film. Sheeting 35 (2019) 181–202.
[56] N.H. Othman, M.C. Ismail, M. Mustapha, N. Sallih, K.E. Kee, R.A. Jaal, Graphene-based polymer nanocomposites as barrier coatings for corrosion protection, Prog. Org. Coat. 135 (2019) 82–99.
[57] A. Radhamani, H.C. Lau, S. Ramakrishna, Nanocomposite coatings on steel for enhancing the corrosion resistance: a review, J. Compos. Mater. 54 (2020) 681–701.
[58] L. Mardare, L. Benea, Development of anticorrosive polymer nanocomposite coating for corrosion protection in marine environment, Presented at the IOP Conference Series: Materials Science and Engineering, IOP Publishing, 2017, p. 012056.
[59] H. Di, Z. Yu, Y. Ma, C. Zhang, F. Li, L. Lv, et al., Corrosion-resistant hybrid coatings based on graphene oxide–zirconia dioxide/epoxy system, J. Taiwan. Inst. Chem. Eng. 67 (2016) 511–520.
[60] V. Valencia-Goujon, T. Hawkins, E. Maya-Visuet, H. Castaneda, Electrochemical characterization in CO2 saturated environment of Zn-rich epoxy nanocoatings on API X52 pipeline grade steel substrate under flow conditions, Presented Corros. 2015 (2015). OnePetro.
[61] S. Pourhashem, M.R. Vaezi, A. Rashidi, Investigating the effect of SiO2-graphene oxide hybrid as inorganic nanofiller on corrosion protection properties of epoxy coatings, Surf. Coat. Technol. 311 (2017) 282–294. Available from: https://doi.org/10.1016/j.surfcoat.2017.01.013.
[62] K. Qi, Y. Sun, H. Duan, X. Guo, A corrosion-protective coating based on a solution-processable polymer-grafted graphene oxide nanocomposite, Corros. Sci. 98 (2015) 500–506. Available from: https://doi.org/10.1016/j.corsci.2015.05.056.
[63] Y. Tong, S. Bohm, M. Song, The capability of graphene on improving the electrical conductivity and anti-corrosion properties of Polyurethane coatings, Appl. Surf. Sci. 424 (2017) 72–81. Available from: https://doi.org/10.1016/j.apsusc.2017.02.081.
[64] Y. Jafari, S.M. Ghoreishi, M. Shabani-Nooshabadi, Electrochemical deposition and characterization of polyaniline-graphene nanocomposite films and its corrosion protection properties, J. Polym. Res. 23 (2016) 91.
[65] B. Ramezanzadeh, M.H. Mohamadzadeh Moghadam, N. Shohani, M. Mahdavian, Effects of highly crystalline and conductive polyaniline/graphene oxide composites on the corrosion protection performance of a zinc-rich epoxy coating, Chem. Eng. J. 320 (2017) 363–375. Available from: https://doi.org/10.1016/j.cej.2017.03.061.
[66] J.P. Agrawal, High Energy Materials: Propellants, Explosives and Pyrotechnics, John Wiley & Sons, 2010.
[67] T. Chen, W. Li, W. Jiang, G. Hao, L. Xiao, X. Ke, et al., Preparation and characterization of RDX/BAMO-THF energetic nanocomposites, J. Energ. Mater. 36 (2018) 424–434.
[68] H.G. Ang, S. Pisharath, Energetic Polymers: Binders and Plasticizers for Enhancing Performance, John Wiley & Sons, 2012.
[69] C. Taylor, S. Jeffery, Management of military wounds in the modern era, Wounds UK 5 (2009) 50–58.
[70] T. Nuge, K. Tshai, S. Lim, N. Nordin, M. Hoque, Preparation and characterization of CU-, FE-, AG-, ZN-and NI-doped gelatin nanofibers for possible applications in antibacterial nanomedicine, J. Eng. Sci. Technol. 12 (2017) 68–81.
[71] S.L. Jeffery, The management of combat wounds: the British Military Experience, Adv. Wound Care 5 (2016) 464–473.
[72] D. Chouhan, N. Dey, N. Bhardwaj, B.B. Mandal, Emerging and innovative approaches for wound healing and skin regeneration: Current status and advances, Biomaterials 216 (2019) 119267.

[73] S.K. Nethi, S. Das, C.R. Patra, S. Mukherjee, Recent advances in inorganic nanomaterials for wound-healing applications, Biomater. Sci. 7 (2019) 2652−2674.
[74] M.M. Mihai, M.B. Dima, B. Dima, A.M. Holban, Nanomaterials for wound healing and infection control, Materials 12 (2019) 2176.
[75] R. Gobi, P. Ravichandiran, R.S. Babu, D.J. Yoo, Biopolymer and synthetic polymer-based nanocomposites in wound dressing applications: a review, Polymers 13 (2021) 1962.
[76] M.C. Biswas, B. Jony, P.K. Nandy, R.A. Chowdhury, S. Halder, D. Kumar, et al., Recent advancement of biopolymers and their potential biomedical applications, J. Polym. Environ. (2021). Available from: https://doi.org/10.1007/s10924-021-02199-y.
[77] M.T. Khorasani, A. Joorabloo, A. Moghaddam, H. Shamsi, Z. MansooriMoghadam, Incorporation of ZnO nanoparticles into heparinised polyvinyl alcohol/chitosan hydrogels for wound dressing application, Int. J. Biol. Macromol. 114 (2018) 1203−1215.
[78] S.M. Nasef, E.E. Khozemy, E.A. Kamoun, H. El-Gendi, Gamma radiation-induced crosslinked composite membranes based on polyvinyl alcohol/chitosan/AgNO3/vitamin E for biomedical applications, Int. J. Biol. Macromol. 137 (2019) 878−885.
[79] A. Sadeghianmaryan, H.A. Sardroud, S. Allafasghari, Z. Yazdanpanah, S. Naghieh, M. Gorji, et al., Electrospinning of polyurethane/graphene oxide for skin wound dressing and its in vitro characterization, J. Biomater. Appl. 35 (2020) 135−145.
[80] H.S. Sofi, T. Akram, A.H. Tamboli, A. Majeed, N. Shabir, F.A. Sheikh, Novel lavender oil and silver nanoparticles simultaneously loaded onto polyurethane nanofibers for wound-healing applications, Int. J. Pharm. 569 (2019) 118590.
[81] B.S. Bharathi, T. Stalin, Cerium oxide and peppermint oil loaded polyethylene oxide/graphene oxide electrospun nanofibrous mats as antibacterial wound dressings, Mater. Today Commun. 21 (2019) 100664.
[82] N.T. Hiep, H.C. Khon, V.V.T. Niem, V.V. Toi, T. Ngoc Quyen, N.D. Hai, et al., Microwave-assisted synthesis of chitosan/polyvinyl alcohol silver nanoparticles gel for wound dressing applications, Int. J. Polym. Sci. 2016 (2016) e1584046. Available from: https://doi.org/10.1155/2016/1584046.
[83] S. Alippilakkotte, S. Kumar, L. Sreejith, Fabrication of PLA/Ag nanofibers by green synthesis method using *Momordica charantia* fruit extract for wound dressing applications, Colloids Surf. Physicochem. Eng. Asp. 529 (2017) 771−782.
[84] D. Archana, B.K. Singh, J. Dutta, P. Dutta, In vivo evaluation of chitosan−PVP−titanium dioxide nanocomposite as wound dressing material, Carbohydr. Polym. 95 (2013) 530−539.
[85] D. Archana, J. Dutta, P. Dutta, Evaluation of chitosan nano dressing for wound healing: Characterization, in vitro and in vivo studies, Int. J. Biol. Macromol. 57 (2013) 193−203.
[86] R. Ma, Y. Wang, H. Qi, C. Shi, G. Wei, L. Xiao, et al., Nanocomposite sponges of sodium alginate/graphene oxide/polyvinyl alcohol as potential wound dressing: In vitro and in vivo evaluation, Compos. Part. B Eng. 167 (2019) 396−405. Available from: https://doi.org/10.1016/j.compositesb.2019.03.006.
[87] S. Chen, H. Wang, Z. Jian, G. Fei, W. Qian, G. Luo, et al., Novel poly(vinyl alcohol)/chitosan/modified graphene oxide biocomposite for wound dressing application, Macromol. Biosci. 20 (2020) 1900385. Available from: https://doi.org/10.1002/mabi.201900385.
[88] C.-M. Lin, Y.-C. Chang, L.-C. Cheng, C.-H. Liu, S.C. Chang, T.-Y. Hsien, et al., Preparation of graphene-embedded hydroxypropyl cellulose/chitosan/polyethylene oxide nanofiber membranes as wound dressings with enhanced antibacterial properties, Cellulose 27 (2020) 2651−2667.

[89] L. Tang, J. Zhang, Y. Tang, J. Kong, T. Liu, J. Gu, Polymer matrix wave-transparent composites: a review, J. Mater. Sci. Technol. 75 (2021) 225−251. Available from: https://doi.org/10.1016/j.jmst.2020.09.017.
[90] J. Varghese, N. Joseph, H. Jantunen, S. Behera, H. Kim, M. Sebastian, Microwave materials for defense and aerospace applications, Handbook of Advanced Ceramics and Composites. Defence, Security, Aerospace and Energy Applications, Springer International Publishing, 2020, pp. 165−213.
[91] S.S. Chauhan, M. Abraham, V. Choudhary, Superior EMI shielding performance of thermally stable carbon nanofiber/poly (ether-ketone) composites in 26.5−40 GHz frequency range, J. Mater. Sci. 51 (2016) 9705−9715.
[92] B. Wen, M. Cao, M. Lu, W. Cao, H. Shi, J. Liu, et al., Reduced graphene oxides: light-weight and high-efficiency electromagnetic interference shielding at elevated temperatures, Adv. Mater. 26 (2014) 3484−3489.
[93] P. Saville, Review of radar absorbing materials, Defence Research and Development Atlantic Dartmouth (Canada), 2005.
[94] N. Joseph, S.K. Singh, R.K. Sirugudu, V.R.K. Murthy, S. Ananthakumar, M.T. Sebastian, Effect of silver incorporation into PVDF-barium titanate composites for EMI shielding applications, Mater. Res. Bull. 48 (2013) 1681−1687.
[95] A.A. Al-Ghamdi, F. El-Tantawy, N.A. Aal, E. El-Mossalamy, W.E. Mahmoud, Stability of new electrostatic discharge protection and electromagnetic wave shielding effectiveness from poly (vinyl chloride)/graphite/nickel nanoconducting composites, Polym. Degrad. Stab. 94 (2009) 980−986.
[96] A.A. Al-Ghamdi, F. El-Tantawy, New electromagnetic wave shielding effectiveness at microwave frequency of polyvinyl chloride reinforced graphite/copper nanoparticles, Compos. Part. Appl. Sci. Manuf. 41 (2010) 1693−1701.
[97] M.H. Al-Saleh, Influence of conductive network structure on the EMI shielding and electrical percolation of carbon nanotube/polymer nanocomposites, Synth. Met. 205 (2015) 78−84.
[98] M.H. Al-Saleh, W.H. Saadeh, U. Sundararaj, EMI shielding effectiveness of carbon based nanostructured polymeric materials: a comparative study, Carbon 60 (2013) 146−156.
[99] P. Modak, S.B. Kondawar, D.V. Nandanwar, Synthesis and characterization of conducting polyaniline/graphene nanocomposites for electromagnetic interference shielding, Procedia Mater. Sci. 10 (2015) 588−594. Available from: https://doi.org/10.1016/j.mspro.2015.06.010.
[100] L. Jiang, S. He, D. Yang, Resistance to vacuum ultraviolet irradiation of nano-TiO2 modified carbon/epoxy composites, J. Mater. Res. 18 (2003) 654−658.
[101] P.B. Ruffin, Review of fiber optics technology for military applications. Presented at the Novel Materials and Crystal Growth Techniques for Nonlinear Optical Devices: A Critical Review, International Society for Optics and Photonics (2000) p. 1029902.
[102] M. Yoshida, P.N. Prasad, Sol − gel-processed SiO2/TiO2/poly (vinylpyrrolidone) composite materials for optical waveguides, Chem. Mater. 8 (1996) 235−241.
[103] C.J. Yang, S.A. Jenekhe, Effects of structure on refractive index of conjugated polyimines, Chem. Mater. 6 (1994) 196−203.
[104] T. Sugiyama, T. Wada, H. Sasabe, Optical nonlinearity of conjugated polymers, Synth. Met., Proc. Int. Conf. Sci. Technol. Synth. Met. 28 (1989) 323−328. Available from: https://doi.org/10.1016/0379-6779(89)90541-9.
[105] C.-J. Yang, S.A. Jenekhe, Group contribution to molar refraction and refractive index of conjugated polymers, Chem. Mater. 7 (1995) 1276−1285.

[106] J. Böhm, J. Haußelt, P. Henzi, K. Litfin, T. Hanemann, Tuning the refractive index of polymers for polymer waveguides using nanoscaled ceramics or organic dyes, Adv. Eng. Mater. 6 (2004) 52−57. Available from: https://doi.org/10.1002/adem.200300542.
[107] A.K. Othayoth, B. Srinivas, K. Murugan, K. Muralidharan, Poly(methyl methacrylate)/polyphosphate blends with tunable refractive indices for optical applications, Opt. Mater. 104 (2020) 109841. Available from: https://doi.org/10.1016/j.optmat.2020.109841.
[108] S.W. Thomas, G.D. Joly, T.M. Swager, Chemical sensors based on amplifying fluorescent conjugated polymers, Chem. Rev. 107 (2007) 1339−1386.
[109] D.Y. Godovsky, Device applications of polymer-nanocomposites, Biopolymers · PVA Hydrogels, Anionic Polymerisation Nanocomposites, Advances in Polymer Science, Springer Berlin Heidelberg, Berlin, Heidelberg, 2000, pp. 163−205. Available from: https://doi.org/10.1007/3-540-46414-X_4.
[110] S. Kochmann, T. Hirsch, O.S. Wolfbeis, Graphenes in chemical sensors and biosensors, TrAC. Trends Anal. Chem. 39 (2012) 87−113.
[111] W. Lei, W. Si, Y. Xu, Z. Gu, Q. Hao, Conducting polymer composites with graphene for use in chemical sensors and biosensors, Microchim. Acta 181 (2014) 707−722. Available from: https://doi.org/10.1007/s00604-014-1160-6.
[112] S.M.C. Vieira, P. Beecher, I. Haneef, F. Udrea, W.I. Milne, M.A.G. Namboothiry, et al., Use of nanocomposites to increase electrical "gain" in chemical sensors, Appl. Phys. Lett. 91 (2007) 203111. Available from: https://doi.org/10.1063/1.2811716.
[113] H.J. Salavagione, A.M. Díez-Pascual, E. Lázaro, S. Vera, M.A. Gómez-Fatou, Chemical sensors based on polymer composites with carbon nanotubes and graphene: the role of the polymer, J. Mater. Chem. A 2 (2014) 14289−14328. Available from: https://doi.org/10.1039/C4TA02159B.
[114] D.T. Nguyen, L. Dai Tran, H. Le Nguyen, B.H. Nguyen, N. Van Hieu, Modified interdigitated arrays by novel poly (1, 8-diaminonaphthalene)/carbon nanotubes composite for selective detection of mercury (II), Talanta 85 (2011) 2445−2450.
[115] Y. Wei, R. Yang, J.-H. Liu, X.-J. Huang, Selective detection toward Hg (II) and Pb (II) using polypyrrole/carbonaceous nanospheres modified screen-printed electrode, Electrochim. Acta 105 (2013) 218−223.
[116] J. Kong, N.R. Franklin, C. Zhou, M.G. Chapline, S. Peng, K. Cho, et al., Nanotube molecular wires as chemical sensors, science 287 (2000) 622−625.
[117] X. Huang, N. Hu, R. Gao, Y. Yu, Y. Wang, Z. Yang, et al., Reduced graphene oxide−polyaniline hybrid: preparation, characterization and its applications for ammonia gas sensing, J. Mater. Chem. 22 (2012) 22488−22495.
[118] W.-K. Jang, J. Yun, H.-I. Kim, Y.-S. Lee, Improvement of ammonia sensing properties of polypyrrole by nanocomposite with graphitic materials, Colloid Polym. Sci. 291 (2013) 1095−1103.
[119] S. Hrapovic, E. Majid, Y. Liu, K. Male, J.H. Luong, Metallic nanoparticle − carbon nanotube composites for electrochemical determination of explosive nitroaromatic compounds, Anal. Chem. 78 (2006) 5504−5512.
[120] L.C. Shriver-Lake, B.L. Donner, F.S. Ligler, On-site detection of TNT with a portable fiber optic biosensor, Environ. Sci. Technol. 31 (1997) 837−841.
[121] A.W. Czarnik, A sense for landmines, Nature 394 (1998) 417−418.
[122] J.D. Rodgers, N.J. Bunce, Treatment methods for the remediation of nitroaromatic explosives, Water Res. 35 (2001) 2101−2111.
[123] R. Garg, D. Grasso, G. Hoag, Treatment of explosives contaminated lagoon sludge, Hazard. Waste Hazard. Mater. 8 (1991) 319−340.

[124] P. Ashbrook, T. Houts, Picric acid, Chem. Health Saf. 10 (2003) 27.
[125] P.C. Ashbrook, T.A. Houts, Targeting chemicals for waste minimization, Chem. Health Saf. 7 (2000) 41.
[126] A. Dorsey, C.S. Hodes, P. Richter-Torres, Toxicological profile for 2, 4, 6-trinitrotoluene, U.S. Department of Health and Human Services, Atlanta, Georgia, 1995.
[127] S. Zhang, F. Lü, L. Gao, L. Ding, Y. Fang, Fluorescent sensors for nitroaromatic compounds based on monolayer assembly of polycyclic aromatics, Langmuir 23 (2007) 1584−1590.
[128] E.S. Forzani, D. Lu, M.J. Leright, A.D. Aguilar, F. Tsow, R.A. Iglesias, et al., A hybrid electrochemical − colorimetric sensing platform for detection of explosives, J. Am. Chem. Soc. 131 (2009) 1390−1391.
[129] B. Gole, S. Shanmugaraju, A.K. Bar, P.S. Mukherjee, Supramolecular polymer for explosives sensing: role of H-bonding in enhancement of sensitivity in the solid state, Chem. Commun. 47 (2011) 10046−10048.
[130] P. Dutta, S. Chakravarty, N.S. Sarma, Detection of nitroaromatic explosives using π-electron rich luminescent polymeric nanocomposites, RSC Adv. 6 (2016) 3680−3689.
[131] S.S. Nagarkar, B. Joarder, A.K. Chaudhari, S. Mukherjee, S.K. Ghosh, Highly selective detection of nitro explosives by a luminescent metal−organic framework, Angew. Chem. 125 (2013) 2953−2957.
[132] Y. Xia, L. Song, C. Zhu, Turn-on and near-infrared fluorescent sensing for 2, 4, 6-trinitrotoluene based on hybrid (gold nanorod) − (quantum dots) assembly, Anal. Chem. 83 (2011) 1401−1407.
[133] B. Xu, X. Wu, H. Li, H. Tong, L. Wang, Selective detection of TNT and picric acid by conjugated polymer film sensors with donor−acceptor architecture, Macromolecules 44 (2011) 5089−5092.
[134] X. Yang, B. Shen, Y. Jiang, Z. Zhao, C. Wang, C. Ma, et al., A novel fluorescent polymer brushes film as a device for ultrasensitive detection of TNT, J. Mater. Chem. A 1 (2013) 1201−1206.
[135] V. Seena, A. Fernandes, P. Pant, S. Mukherji, V.R. Rao, Polymer nanocomposite nanomechanical cantilever sensors: material characterization, device development and application in explosive vapour detection, Nanotechnology 22 (2011) 295501.
[136] P. Ajayan, E. Lahiff, P. Stryjek, C.Y. Ryu, S. Curran, Embedded nanotube array sensor and method of making a nanotube polymer composite, 2010.
[137] S.K. Mahadeva, S. Yun, J. Kim, Flexible humidity and temperature sensor based on cellulose−polypyrrole nanocomposite, Sens. Actuators Phys. 165 (2011) 194−199.
[138] W.-P. Shih, L.-C. Tsao, C.-W. Lee, M.-Y. Cheng, C. Chang, Y.-J. Yang, et al., Flexible temperature sensor array based on a graphite-polydimethylsiloxane composite, Sensors 10 (2010) 3597−3610.
[139] R. Megha, F.A. Ali, Y. Ravikiran, C. Ramana, A.K. Kumar, D. Mishra, et al., Conducting polymer nanocomposite based temperature sensors: a review, Inorg. Chem. Commun. 98 (2018) 11−28.
[140] G. Wu, S. Li, J. Hu, M. Dong, K. Dong, X. Hou, et al., A capacitive sensor using resin thermoplastic elastomer and carbon fibers for monitoring pressure distribution, Pigment Resin Technol. 50 (2020) 437−443.
[141] J.-W. Zha, D.-H. Wu, Y. Yang, Y.-H. Wu, R.K. Li, Z.-M. Dang, Enhanced positive temperature coefficient behavior of the high-density polyethylene composites with multi-dimensional carbon fillers and their use for temperature-sensing resistors, RSC Adv. 7 (2017) 11338−11344.

[142] L. Wang, Differential structure for temperature sensing based on conductive polymer composites, IEEE Trans. Electron. Devices 62 (2015) 3025−3028.
[143] K. Majid, S. Awasthi, M. Singla, Low temperature sensing capability of polyaniline and Mn3O4 composite as NTC material, Sens. Actuators Phys. 135 (2007) 113−118.
[144] L. He, S.-C. Tjong, Electrical behavior and positive temperature coefficient effect of graphene/polyvinylidene fluoride composites containing silver nanowires, Nanoscale Res. Lett. 9 (2014) 1−8.
[145] D. Patil, P. Patil, Y.-K. Seo, Y.K. Hwang, Poly(o-anisidine)−tin oxide nanocomposite: Synthesis, characterization and application to humidity sensing, Sens. Actuators B Chem. 148 (2010) 41−48. Available from: https://doi.org/10.1016/j.snb.2010.04.046.
[146] D. Zhang, C. Jiang, Q. Zhou, Layer-by-layer self-assembly of tricobalt tetroxide-polymer nanocomposite toward high-performance humidity-sensing, J. Alloy. Compd. 711 (2017) 652−658.
[147] R. Ramalingame, A. Lakshmanan, F. Müller, U. Thomas, O. Kanoun, Highly sensitive capacitive pressure sensors for robotic applications based on carbon nanotubes and PDMS polymer nanocomposite, J. Sens. Sens. Syst. 8 (2019) 87−94.
[148] Y. Lu, M.C. Biswas, Z. Guo, J.-W. Jeon, E.K. Wujcik, Recent developments in bio-monitoring via advanced polymer nanocomposite-based wearable strain sensors, Biosens. Bioelectron. 123 (2019) 167−177.
[149] S. Park, K. Chung, S. Jayaraman, Wearables: fundamentals, advancements, and a roadmap for the future, Wearable Sensors, Academic Press, 2015.
[150] M.Z. Seyedin, J.M. Razal, P.C. Innis, G.G. Wallace, Strain-responsive polyurethane/PEDOT: PSS elastomeric composite fibers with high electrical conductivity, Adv. Funct. Mater. 24 (2014) 2957−2966.
[151] D.J. Lipomi, M. Vosgueritchian, B.C. Tee, S.L. Hellstrom, J.A. Lee, C.H. Fox, et al., Skin-like pressure and strain sensors based on transparent elastic films of carbon nanotubes, Nat. Nanotechnol. 6 (2011) 788−792.
[152] J. Shintake, E. Piskarev, S.H. Jeong, D. Floreano, Ultrastretchable strain sensors using carbon black-filled elastomer composites and comparison of capacitive vs resistive sensors, Adv. Mater. Technol. 3 (2018) 1700284.
[153] H. Koerner, W. Liu, M. Alexander, et al., Deformation−morphology correlations in electrically conductive carbon nanotube − thermoplastic polyurethane nanocomposites, Polymer 46 (2005) 4405−4420.
[154] K. Gall, M.L. Dunn, Y. Liu, D. Finch, M. Lake, N.A. Munshi, Shape memory polymer nanocomposites, Acta Mater. 50 (2002) 5115−5126.
[155] C. Lee, M. Kim, Y.J. Kim, N. Hong, S. Ryu, H.J. Kim, et al., Soft robot review, Int. J. Control. Autom. Syst. 15 (2017) 3−15. Available from: https://doi.org/10.1007/s12555-016-0462-3.
[156] R.F. Shepherd, F. Ilievski, W. Choi, S.A. Morin, A.A. Stokes, A.D. Mazzeo, et al., Multigait soft robot, Proc. Natl. Acad. Sci. 108 (2011) 20400−20403. Available from: https://doi.org/10.1073/pnas.1116564108.
[157] S. Kim, C. Laschi, B. Trimmer, Soft robotics: a bioinspired evolution in robotics, Trends Biotechnol. 31 (2013) 287−294. Available from: https://doi.org/10.1016/j.tibtech.2013.03.002.
[158] P. Polygerinos, Z. Wang, K.C. Galloway, R.J. Wood, C.J. Walsh, Soft robotic glove for combined assistance and at-home rehabilitation, Robot. Auton. Syst. 73 (2015) 135−143.
[159] R.K. Katzschmann, A.D. Marchese, D. Rus, Hydraulic autonomous soft robotic fish for 3D swimming, in: M.A. Hsieh, O. Khatib, V. Kumar (Eds.), Experimental

Robotics: The 14th International Symposium on Experimental Robotics, Springer Tracts in Advanced Robotics, Springer International Publishing, Cham, 2016, pp. 405–420. Available from: https://doi.org/10.1007/978-3-319-23778-7_27.
[160] H.-T. Lin, G.G. Leisk, B. Trimmer, GoQBot: a caterpillar-inspired soft-bodied rolling robot, Bioinspir. Biomim. 6 (2011) 026007.
[161] M. Liu, S. Zhu, Y. Huang, Z. Lin, W. Liu, L. Yang, et al., A self-healing composite actuator for multifunctional soft robot via photo-welding, Compos. Part. B Eng. 214 (2021) 108748. Available from: https://doi.org/10.1016/j.compositesb.2021.108748.
[162] R. Shenoi, J. Dulieu-Barton, S. Quinn, J. Blake, S. Boyd, Composite materials for marine applications: key challenges for the future, Composite Materials, Springer, 2011, pp. 69–89.
[163] P. Davies, Environmental degradation of composites for marine structures: new materials and new applications, Philos. Trans. R. Soc. Math. Phys. Eng. Sci. 374 (2016) 20150272.
[164] G. Neşer, Polymer based composites in marine use: history and future trends, Procedia Eng. 194 (2017) 19–24.
[165] B. Barsotti, M. Gaiotti, C.M. Rizzo, Recent industrial developments of marine composites limit states and design approaches on strength, J. Mar. Sci. Appl. 19 (2020) 553–566. Available from: https://doi.org/10.1007/s11804-020-00171-1.
[166] F. Rubino, A. Nisticò, F. Tucci, P. Carlone, Marine application of fiber reinforced composites: a review, J. Mar. Sci. Eng. 8 (2020) 26.
[167] M. Saravanan, D.B. Kumar, A review on navy ship parts by advanced composite material, Mater. Today Proc., Int. Conf. Mechanical, Electron. Computer Eng. 2020: Mater. Sci. 45 (2021) 6072–6077. Available from: https://doi.org/10.1016/j.matpr.2020.10.074.
[168] A.P. Mouritz, E. Gellert, P. Burchill, K. Challis, Review of advanced composite structures for naval ships and submarines, Compos. Struct. 53 (2001) 21–42.
[169] M.T. Kim, K.Y. Rhee, I. Jung, S.J. Park, D. Hui, Influence of seawater absorption on the vibration damping characteristics and fracture behaviors of basalt/CNT/epoxy multiscale composites, Compos. Part. B Eng. 63 (2014) 61–66. Available from: https://doi.org/10.1016/j.compositesb.2014.03.010.
[170] T. Saha, M.E. Hoque, T. Mahbub, Biopolymers for sustainable packaging in food, cosmetics, and pharmaceuticals, Advanced Processing, Properties, and Applications of Starch and Other Bio-Based Polymers, Elsevier, 2020, pp. 197–214. Available from: https://doi.org/10.1016/B978-0-12-819661-8.00013-5.
[171] A. Arora, G. Padua, Nanocomposites in food packaging, J. Food Sci. 75 (2010) R43–R49.
[172] D.P. de Abreu, P.P. Losada, I. Angulo, J. Cruz, Development of new polyolefin films with nanoclays for application in food packaging, Eur. Polym. J. 43 (2007) 2229–2243.
[173] C. Thellen, J. Ratto, D. Froio, J. Lucciarini, Development of a nanocomposite meal bag for individual military rations, Case Studies in Novel Food Processing Technologies, Elsevier, 2010, pp. 367–386.
[174] K. Bhunia, S. Dhawan, S.S. Sablani, Modeling the oxygen diffusion of nanocomposite-based food packaging films, J. Food Sci. 77 (2012) N29–N38.
[175] Q. Chaudhry, M. Scotter, J. Blackburn, B. Ross, A. Boxall, L. Castle, et al., Applications and implications of nanotechnologies for the food sector, Food Addit. Contam. 25 (2008) 241–258.
[176] A. Emamifar, M. Kadivar, M. Shahedi, S. Soleimanian-Zad, Effect of nanocomposite packaging containing Ag and ZnO on inactivation of *Lactobacillus plantarum* in orange juice, Food Control. 22 (2011) 408–413.

[177] S. Ray, S.Y. Quek, A. Easteal, X.D. Chen, The potential use of polymer-clay nanocomposites in food packaging, Int. J. Food Eng. 2 (2006).
[178] J. Cho, D. Paul, Nylon 6 nanocomposites by melt compounding, Polymer 42 (2001) 1083–1094.
[179] F. Wu, X. Lan, D. Ji, Z. Liu, W. Yang, M. Yang, Grafting polymerization of polylactic acid on the surface of nano-SiO2 and properties of PLA/PLA-grafted-SiO2 nanocomposites, J. Appl. Polym. Sci. 129 (2013) 3019–3027.
[180] Y. Li, X.S. Sun, Nanocomposites of poly (lactic acid) and surface-grafted MgO nanoparticles: preparation and characterization, J. Biobased Mater. Bioenergy 5 (2011) 452–459.
[181] H. Liu, C. Han, L. Dong, Study of the biodegradable poly (ε-caprolactone)/clay nanocomposite foams, J. Appl. Polym. Sci. 115 (2010) 3120–3129.
[182] O.M. Istrate, B. Chen, Porous exfoliated poly (ε-caprolactone)/clay nanocomposites: preparation, structure, and properties, J. Appl. Polym. Sci. 125 (2012) E102–E112.
[183] L.A. Koban, J. MacDonald Gibson, Small-unit water purifiers for remote military outposts: a new application of multicriteria decision analysis, J. Multi-Criteria Decis. Anal. 24 (2017) 146–161.
[184] N. Pandey, S. Shukla, N. Singh, Water purification by polymer nanocomposites: an overview, Nanocomposites 3 (2017) 47–66.
[185] R.A. Muzzarelli, Potential of chitin/chitosan-bearing materials for uranium recovery: an interdisciplinary review, Carbohydr. Polym. 84 (2011) 54–63.
[186] A.R. Keshtkar, M. Irani, M.A. Moosavian, Removal of uranium (VI) from aqueous solutions by adsorption using a novel electrospun PVA/TEOS/APTES hybrid nanofiber membrane: comparison with casting PVA/TEOS/APTES hybrid membrane, J. Radioanal. Nucl. Chem. 295 (2013) 563–571.
[187] T.S. Anirudhan, S. Rijith, A.R. Tharun, Adsorptive removal of thorium (IV) from aqueous solutions using poly (methacrylic acid)-grafted chitosan/bentonite composite matrix: process design and equilibrium studies, Colloids Surf. Physicochem. Eng. Asp. 368 (2010) 13–22.
[188] D. Baybaş, U. Ulusoy, The use of polyacrylamide-aluminosilicate composites for thorium adsorption, Appl. Clay Sci. 51 (2011) 138–146.
[189] S. Abbasizadeh, A.R. Keshtkar, M.A. Mousavian, Preparation of a novel electrospun polyvinyl alcohol/titanium oxide nanofiber adsorbent modified with mercapto groups for uranium (VI) and thorium (IV) removal from aqueous solution, Chem. Eng. J. 220 (2013) 161–171.
[190] A.K. Kaygun, S. Akyil, Study of the behaviour of thorium adsorption on PAN/zeolite composite adsorbent, J. Hazard. Mater. 147 (2007) 357–362.
[191] Y.-Z. Wei, H. Hoshi, M. Kumagai, T. Asakura, Y. Morita, Separation of Am (III) and Cm (III) from trivalent lanthanides by 2, 6-bistriazinylpyridine extraction chromatography for radioactive waste management, J. Alloy. Compd. 374 (2004) 447–450.
[192] M. Gasser, H. Nowier, Separation of strontium and cadmium ions from nitrate medium by ion-exchange membrane in an electrodialysis system, J. Chem. Technol. Biotechnol. Int. Res. Process. Environ. Clean. Technol. 79 (2004) 97–102.
[193] S. Şimşek, U. Ulusoy, Ö. Ceyhan, Adsorption of UO22 +, Tl +, Pb2 +, Ra2 + and Ac3 + onto polyacrylamide-bentonite composite, J. Radioanal. Nucl. Chem. 256 (2003) 315–321.
[194] E. Borai, M. Breky, M. Sayed, M. Abo-Aly, Synthesis, characterization and application of titanium oxide nanocomposites for removal of radioactive cesium, cobalt and europium ions, J. Colloid Interface Sci. 450 (2015) 17–25.

[195] G. Moussavi, M. Mahmoudi, Removal of azo and anthraquinone reactive dyes from industrial wastewaters using MgO nanoparticles, J. Hazard. Mater. 168 (2009) 806–812.
[196] M.T. Yagub, T.K. Sen, S. Afroze, H.M. Ang, Dye and its removal from aqueous solution by adsorption: a review, Adv. Colloid Interface Sci. 209 (2014) 172–184.
[197] A. Ahmad, S.H. Mohd-Setapar, C.S. Chuong, A. Khatoon, W.A. Wani, R. Kumar, et al., Recent advances in new generation dye removal technologies: novel search for approaches to reprocess wastewater, RSC Adv. 5 (2015) 30801–30818.
[198] H.-Y. Zhu, R. Jiang, L. Xiao, W. Li, A novel magnetically separable γ-Fe2O3/cross-linked chitosan adsorbent: preparation, characterization and adsorption application for removal of hazardous azo dye, J. Hazard. Mater. 179 (2010) 251–257.
[199] A. Debrassi, T. Baccarin, C.A. Demarchi, N. Nedelko, A. Ślawska-Waniewska, P. Dłużewski, et al., Adsorption of Remazol Red 198 onto magnetic N-lauryl chitosan particles: equilibrium, kinetics, reuse and factorial design, Environ. Sci. Pollut. Res. 19 (2012) 1594–1604.
[200] H. Zhu, R. Jiang, Y.-Q. Fu, J.-H. Jiang, L. Xiao, G.-M. Zeng, Preparation, characterization and dye adsorption properties of γ-Fe2O3/SiO2/chitosan composite, Appl. Surf. Sci. 258 (2011) 1337–1344.
[201] J.-P. Wang, H.-C. Yang, C.-T. Hsieh, Adsorption of phenol and basic dye on carbon nanotubes/carbon fabric composites from aqueous solution, Sep. Sci. Technol. 46 (2010) 340–348.
[202] H. Zhu, R. Jiang, L. Xiao, G. Zeng, Preparation, characterization, adsorption kinetics and thermodynamics of novel magnetic chitosan enwrapping nanosized γ-Fe2O3 and multi-walled carbon nanotubes with enhanced adsorption properties for methyl orange, Bioresour. Technol. 101 (2010) 5063–5069.
[203] S. Ghorai, A. Sarkar, M. Raoufi, A.B. Panda, H. Schönherr, S. Pal, Enhanced removal of methylene blue and methyl violet dyes from aqueous solution using a nanocomposite of hydrolyzed polyacrylamide grafted xanthan gum and incorporated nanosilica, ACS Appl. Mater. Interfaces 6 (2014) 4766–4777.
[204] Y. Tang, D. Ma, L. Zhu, Sorption behavior of methyl violet onto poly (acrylic acid-co-acrylamide)/kaolin hydrogel composite, Polym.-Plast. Technol. Eng. 53 (2014) 851–857.
[205] K. Wu, J. Yu, X. Jiang, Multi-walled carbon nanotubes modified by polyaniline for the removal of alizarin yellow R from aqueous solutions, Adsorpt. Sci. Technol. 36 (2018) 198–214.
[206] X. Lu, X. Feng, Y. Yang, J. Jiang, W. Cheng, C. Liu, et al., Tuning the permselectivity of polymeric desalination membranes via control of polymer crystallite size, Nat. Commun. 10 (2019) 2347. Available from: https://doi.org/10.1038/s41467-019-10132-0.
[207] M.A. Ashraf, M.J. Maah, A.K. Qureshi, M. Gharibreza, I. Yusoff, Synthetic polymer composite membrane for the desalination of saline water, Desalination Water Treat. 51 (2013) 3650–3661. Available from: https://doi.org/10.1080/19443994.2012.751152.
[208] S. Kim, X. Lin, R. Ou, H. Liu, X. Zhang, G.P. Simon, et al., Highly crosslinked, chlorine tolerant polymer network entwined graphene oxide membrane for water desalination, J. Mater. Chem. A 5 (2017) 1533–1540.
[209] N. Liu, M. Zhang, W. Zhang, Y. Cao, Y. Chen, X. Lin, et al., Ultralight free-standing reduced graphene oxide membranes for oil-in-water emulsion separation, J. Mater. Chem. A 3 (2015) 20113–20117.
[210] H.-Y. Mi, X. Jing, A.L. Politowicz, E. Chen, H.-X. Huang, L.-S. Turng, Highly compressible ultra-light anisotropic cellulose/graphene aerogel fabricated by bidirectional freeze drying for selective oil absorption, Carbon 132 (2018) 199–209.

[211] Y. Zhou, X. Tang, Y. Xu, J. Lu, Effect of quaternary ammonium surfactant modification on oil removal capability of polystyrene resin, Sep. Purif. Technol. 75 (2010) 266–272.
[212] J. Zhao, H. Chen, H. Ye, B. Zhang, L. Xu, Poly(dimethylsiloxane)/graphene oxide composite sponge: a robust and reusable adsorbent for efficient oil/water separation, Soft Matter 15 (2019) 9224–9232. Available from: https://doi.org/10.1039/C9SM01984G.
[213] J. Saadati, M. Pakizeh, Separation of oil/water emulsion using a new PSf/pebax/F-MWCNT nanocomposite membrane, J. Taiwan. Inst. Chem. Eng. 71 (2017) 265–276.
[214] P. Jain, T. Pradeep, Potential of silver nanoparticle-coated polyurethane foam as an antibacterial water filter, Biotechnol. Bioeng. 90 (2005) 59–63. Available from: https://doi.org/10.1002/bit.20368.
[215] K.A. Rieger, H.J. Cho, H.F. Yeung, W. Fan, J.D. Schiffman, Antimicrobial activity of silver ions released from zeolites immobilized on cellulose nanofiber mats, ACS Appl. Mater. Interfaces 8 (2016) 3032–3040.
[216] S.Y. Liu, X. Zheng, Y. Yang, J. Liu, J. Li, The removal and inhibitory effect of CNTs on model viruses. Presented at the Materials Science Forum, Trans Tech Publications, 2013, pp. 402–408.
[217] S.M. Al-Hakami, A.B. Khalil, T. Laoui, M.A. Atieh, Fast disinfection of *Escherichia coli* bacteria using carbon nanotubes interaction with microwave radiation, Bioinorg. Chem. Appl. (2013) 2013.
[218] P. Gunawan, C. Guan, X. Song, Q. Zhang, S.S.J. Leong, C. Tang, et al., Hollow fiber membrane decorated with Ag/MWNTs: toward effective water disinfection and biofouling control, Acs Nano 5 (2011) 10033–10040.
[219] A.H. Lundquist, G.H. White, A. Bonilla, T.E. Richards, S.C. Richards, Adapting military field water supplies to the asymmetric battlefield, US Army Med. Dep. J. (2011) 62–70.
[220] J. T, The LifeStraw. definearth. <https://definearth.com/2015/06/11/the-lifestraw/>, 2015 (accessed 8.26.21).
[221] S.-L. Loo, A.G. Fane, W.B. Krantz, T.-T. Lim, Emergency water supply: a review of potential technologies and selection criteria, Water Res. 46 (2012) 3125–3151.
[222] G. Fan, Z. Su, R. Lin, X. Lin, R. Xu, W. Chen, Influence of membrane materials and operational modes on the performance of ultrafiltration modules for drinking water treatment, Int. J. Polym. Sci. 2016 (2016) 1–8. Available from: https://doi.org/10.1155/2016/6895235.
[223] X. Du, F. Qu, H. Liang, K. Li, H. Yu, L. Bai, et al., Removal of antimony (III) from polluted surface water using a hybrid coagulation–flocculation–ultrafiltration (CF–UF) process, Chem. Eng. J. 254 (2014) 293–301.
[224] M.E. Hoque, A.M. Peiris, S.M. Atiqure Rahman, M. Abdul Wahab, New generation antibacterial nanofibrous membrane for potential water filtration, Curr. Anal. Chem. 14 (2018) 278–284. Available from: https://doi.org/10.2174/1573411013666171009162832.
[225] J. Catharina, A.-S. Jönsson, Influence of the membrane material on the adsorptive fouling of ultrafiltration membranes, J. Membr. Sci. 108 (1995) 79–87.
[226] A. Ahmad, A. Abdulkarim, B. Ooi, S. Ismail, Recent development in additives modifications of polyethersulfone membrane for flux enhancement, Chem. Eng. J. 223 (2013) 246–267.
[227] J. Gu, Y. Bai, L. Zhang, L. Deng, C. Zhang, Y. Sun, et al., VTOS cross-linked PDMS membranes for recovery of ethanol from aqueous solution by pervaporation, Int. J. Polym. Sci. (2013) 2013.

## Further reading

K. Kimura, Y. Hane, Y. Watanabe, G. Amy, N. Ohkuma, Irreversible membrane fouling during ultrafiltration of surface water, Water Res. 38 (2004) 3431–3441.

# Polymer nanocomposites for packaging

15

*Habibul Islam and Md Enamul Hoque*
Department of Biomedical Engineering, Military Institute of Science and Technology (MIST), Dhaka, Bangladesh

## 15.1 Introduction

The history of proper packaging dates back to ancient Egypt 3500 years ago as the first stepstone was set by developing nontransparent glass water pots. As the industrial revolution started, the need for better packaging materials increased by a huge margin. In 1810, the use of tin-coated iron cans instead of bottles to preserve food was invented by Napoleon's urge to find a solution for food preservation for the army in the midst of the war. The commercial invention of paper bags showed a big jump in the packaging industry in 1844, which took an even bigger loop with the creation of the paper the bag-making machine in 1852. The real development in packaging came with the invention of cellophane a transparent material that did not absorb liquids in 1908 and polyethylene terephthalate (PET) bottles in 1973 that were capable of containing carbonated drinks. It soon became a cheaper alternative to glass [1,2–4]. As the world keeps being united because of globalization, every nation depends on other countries. One report in 2017 showed that one in every six people in the world depends on the food imported. The United States alone imported food and food products worth $133 billion, where China comes second with a total of US$105.26 billion [5]. It is necessary to adequately package this massive amount of imported foods to guarantee the best quality for a better consumer experience. Conventional packaging polymers have an excellent barrier and insulating properties. Still, lack of mechanical strength and thermal properties can cause harmful effects for the packaged products especially during transportation as transportation can introduce the packaged food to extreme conditions.

With the continuous rise in the world economy, the use of packages has increased significantly. But a fair share of the package is disposed of immediately. These one-time-use plastics have a hard-hitting impact on the environment. The most amount of the plastics used in the packaging industry either ends up in the ocean or the soil as the recycling percentage is really small. Plastics decompose ever so slowly in the sea. Even in the presence of sufficient oxygen, plastic takes 500 years or more to get decayed. Upon degradation, they even release harmful gases. However, there are some talks to use biopolymers as packaging materials. But to ensure better-quality products with longer shelf life, a more appropriate and sustainable approach is needed. Numerous researches have taken place to prove the

**Advanced Polymer Nanocomposites. DOI:** https://doi.org/10.1016/B978-0-12-824492-0.00008-8


ability of polymer nanocomposites as superior to conventional materials in food and beverage packaging. Future technologies will only improve the packaging quality with the addition of nanofillers with conventional packaging polymers.

## 15.2 Issues with traditional packaging system

Plastics are the primary packaging materials used widely because of durability, low cost, ease to produce, light-weighted, and/or the abundance of production materials. In 2018, the production of plastics totaled over 350 million metric tons worldwide [6], where 39.7% of which are used in packaging applications [7]. But because of their nondegradable nature, they represent a serious global environmental problem. 50% of total plastics produced every year are for single-use purposes. These single-use purpose packaging plastics are used for just a few moments, but these plastics remain on the planet for at least several hundred years or more. Only 9% of those single-use purpose plastics are collected for recycling [8]. Every year our oceans are filled with 8 million tons of new plastic wastes. More than 500 billion plastic bags are disposed of in landfills, and less than 3% of these bags are being recycled [9]. These plastics are made of polyethylene and polystyrene and can take 500 or more years to degrade naturally and also release harmful greenhouse gases in the environment that increase global warming.

Besides the sustainable environment, mass consumers are also looking for better-quality products. The plastics used in packaging contain small molecules that can migrate from plastic to the product it is in contact with. Again, plastic can break down, releasing monomers [10]. For example, polycarbonate used to store food in containers and bottles can release Bisphenol A (BPA) [11]. An unwanted amount of BPA can cause many health problems like endocrine disruptions [12]. Biopolymers can solve the environmental problem caused by traditional packaging polymers and also can ensure a better quality of products. But biopolymers face limitation in different properties. The addition of nanoscale composites with polymers can allow better utilization of biodegradable and edible films. These will reduce the waste from the packaging of products and will ensure fresh foods with extended shelf life with the additional quality of desired mechanical strength and barrier properties.

Better thermal stability and heat resistance can also be achieved with polymer nanocomposites, which ensure a better quality of packaged foods. For packaging electronic components, thermal stability is a critical point. For packaging electronics, the ideal materials should have protection from dust, protection from mechanical hazards, protection from climatic hazards, protection from electrostatic discharge (ESD), protection from water [13]. Plastics are of low density. Though plastics have good chemical resistance, they lack thermal stability and have significant resistance to environmental degradation, which causes hazardous effects on the environment. Though ceramics have good thermal stability due to their brittle nature, they are not suitable for packaging. Polymer nanocomposites can solve all

the problems of these materials as polymer nanocomposites possess better barrier, mechanical, chemical, and thermal properties, and flame retardancy than conventional polymer materials [14]. Better optical and electrical properties were observed from cadmium ferrite nanoparticles [15]. To package electrical components, ESD bags are used to prevent the components to get static charged. Polymer nanocomposites can improve better insulation properties that can significantly increase the safety of both the components and the users.

## 15.3 Advantages of polymer nanocomposites in packaging

Composites that has one or more phase in the nanoscale range ($10^{-9}$ m) are classified as nanocomposites [16]. Studies showed that the material's properties at the nanoscale (less than 100 nm) could change by adequate means. With the reduction in size to the nanometer range, improvement in electrical and elastic properties, strength, better transparency, and various other new properties can be displayed by materials that are not observed at the macro- and microscale. For example:

1. Gold nanoparticles have a melting point that ranges from 615 to 1115 K, which depends on the nanoparticle size where bulk gold has a melting point of around 1400 K [17].
2. ZnO and $TiO_2$ are white on a microscale. But with the decrease in size, they become colorless. Below 12 nm, these particles become invisible to the human eye [18].
3. Spontaneous combustion of aluminum nanoparticles was observed, and this property has been utilized by using nanoscale aluminum as rocket fuel [19].

Enhancements in characteristics ensure better possibilities for polymer nanocomposites to solve the problems faced with traditional packaging [20–22].

### 15.3.1 Barrier properties

Barrier against $O_2$, $CO_2$, $H_2O$ vapor, aroma diffusion, and ultraviolet are the essential characteristics of nanoparticle-incorporated polymer matrices. Gases are absorbed by the surface of polymer nanocomposites and transported through matrices of the polymer but are hindered by nanocomposites inside the polymer matrices. In polymer nanocomposites, gases travel through a tortuous path where gases are trapped, and thus gas permeability is reduced [23,24]. The amount of gas blocked is dependent on the arrangements of the nanocomposites in the polymer matrices. Fig. 15.1 shows the straight travel path of gas molecules through polymer matrices, and Fig. 15.2 shows the sinuous path of any molecules through polymer nanocomposites [25,26].

Nanoparticles of improved aspect ratio and smaller volume fraction arranged in an exfoliated manner in the polymer matrices resulted in a reduction in oxygen transfer up to 97% [27]. Another study showed that nylon-6 nanocomposites have a four times lower oxygen transmission rate (OTR) than unfilled nylon-6 [23,24].

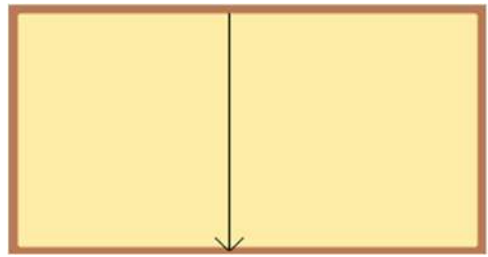

**Figure 15.1** Straight travel path of gas molecules through unfilled polymer matrices.
*Source:* Adapted with permission from Y. Cui, S.I. Kundalwal, S. Kumar, Gas barrier performance of graphene/polymer nanocomposites, Carbon N. Y. 98 (2016) 313−333 [25]. Copyright (2016) Elsevier.

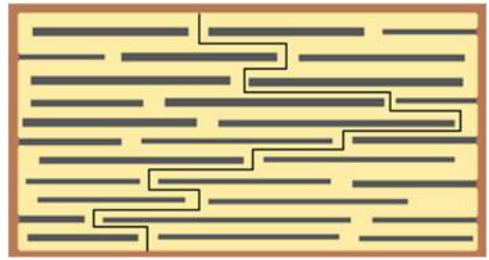

**Figure 15.2** Tortuous path model of polymer nanocomposites.
*Source:* Adapted with permission from J.R. Potts, D.R. Dreyer, C.W. Bielawski, R.S. Ruoff, Graphene-based polymer nanocomposites, Polym. (Guildf.). 52 (1) (2011) 5−25 [26]. Copyright (2011) Elsevier.

Mitsubishi Gas Chemical Company incorporated nanoscale clays into one type of nylon-6 resin to produce Imperm that can achieve significantly enhanced barrier properties than unfilled nylon-6. Nylon-6 nanoparticles itself if added with PET can decrease oxygen transmission rate from 8.172 to 7.594 g $m^{-2}$ $day^{-1}$ and water vapor transmission rate from 0.867 to 0.272 g $m^{-2}$ $day^{-1}$ [28,29]. Nylon-6 nanocomposites used with PET ensure three to four times better performance than traditional ethylene vinyl alcohol (EVOH) barrier as Nylon has 50°F more melting temperature than traditional EVOH barrier. Similarly, polylactide (PLA) with graphene oxide shows a significant amount of reduction in oxygen permeability [30]. The oxygen permeability coefficient of the starch/glycerol neat matrices is around 1.58. With the dispersion of silver and montmorillonite (MMT) in the matrices, the oxygen permeability reduced from 0.52 to 0.22 [31]. OTR of PLA reduced from 736 to 8 cc mm $m^{-2}$ $day^{-1}$ and water vapor transmission rate (WVTR) reduced from 556 to 431 g $m^{-2}$ $day^{-1}$ by adding chitosan/MMT clay nanocomposites [32]. Polymer matrices with less than 6% nanoclay concentration shows reduction of oxygen permeability and water vapor permeability by a significant amount. Cloisite

25A nanoclay added with low-density polyethylene by melt processing method shows a 79% reduction in water permeability [33]. MMT nanoclay added with different polymer matrices reduces water permeability. For example, 6 wt.% MMT added with polystyrene by solution casting reduces water permeability by 70%, 8 wt.% of MMT nanoclay added with polyimide showed 83% reduction of water permeability [34], and 15 wt.% of MMT added with polycaprolactone reduced water vapor permeability by 90% [35]. A meager amount of graphene and graphene oxide filler can significantly decrease water permeability. 0.1 wt.% of graphene added with polyimide reduces water permeability by 93%, and 0.1 wt.% of graphene oxide added with the same polymer reduces water permeability by 82% [36]. Low-density polyethylene (LDPE) has OTR of 134.9 $cm^3$ mm $m^{-2}$ $day^{-1}$ $atm^{-1}$. By addition of ethylene-co-vinyl acetate, OTR increases to 153.2 $cm^3$ mm m EVA $^2$/ day /atm. By adding up to 7 wt.% organic nanoclay the OTR value was reduced by 43.7% [37]. Polymer nanocomposites made from poly(propylene carbonate) (PPC), polyethylene glycol (PEG), and cellulose nanocrystal (CNC) showed a decrease in oxygen permeability with an increase in CNC contents compared to pure PPC and PPC/PEG composites. Fig. 15.3 shows the oxygen permeability ($\times 10^{-13} \cdot cm^3 \cdot m \cdot m^{-2} \cdot s^{-1} \cdot Pa^{-1}$) of the composite with different amounts of loading [38].

Oxygen barrier properties were examined for polymer nanocomposites made from polyacrylic acid, graphene oxide, and silver nanoparticles synthesized in an aqueous solution by in situ polymerization technique. Barrier properties were shown to be 11 times better when silver nanoparticles were incorporated with polyacrylic acid and graphene oxide composites. Also, better thermal resistance, antimicrobial properties, and excellent mechanical properties were observed by adding only

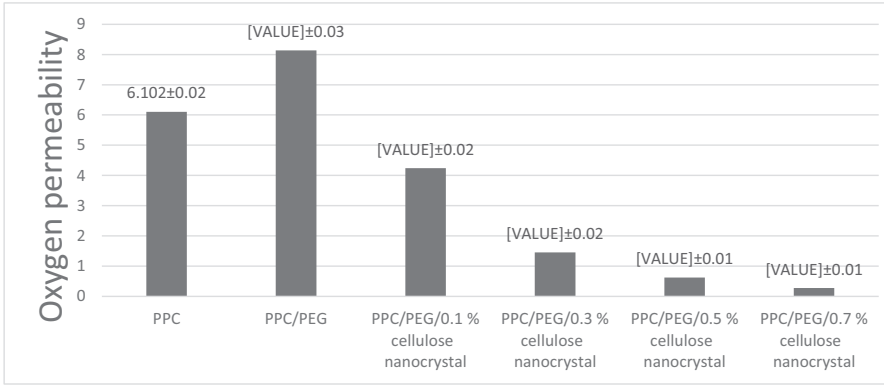


**Figure 15.3** Oxygen permeability of poly(propylene carbonate) and polyethylene glycol composites with different amounts of cellulose nanocrystal reinforcement.
*Source:* Reprinted with permission from G. Jiang, M. Zhang, J. Feng, S. Zhang, X. Wang, High oxygen barrier property of poly(propylene carbonate)/polyethylene glycol nanocomposites with low loading of cellulose nanocrystals, ACS Sustain. Chem. Eng. 5 (12) (2017), 11246−11254 [38]. Copyright (2017) American Chemical Society.

$27 \times 10^{-3}$ wt.% of silver nanoparticles in the composite matrices [39]. Bacterial cellulose extracted from *Komagataeibacter xylinus* by sulfuric acid hydrolysis was added with polymer matrices of gelatin and polyvinyl alcohol (PVA) to form a biodegradable polymer composite. The composite showed improvement in WVTR by 22% and water vapor permeability by 14% [40].

### 15.3.2 Mechanical properties

Polymer nanocomposites have a significant edge over normal packaging polymers and biopolymers in mechanical properties. Tensile strength, flexural strength, and tensile modulus were seen to be significantly increased by adding a very low amount of nanofillers. The tensile stress of polycaprolactam a composite derived from nylon was increased by 49% (1.11−2.25 GPa) by filling polycaprolactam with MMT, and Young's modulus was increased by 103% (68.6−102 MPa) [41,42]. The improvement in the mechanical strength of polymer nanocomposites is due to the high rigidity and aspect ratio of nanofillers together with better affinity through interfacial interaction between the polymer matrices and nanofillers [43]. Nanoclays in nylon increase tensile strength from 82 to 101 MPa (increase of 23%), tensile modulus from 2756 to 4657 MPa (increase of 69%), and flexural modulus from 2431 to 3780 MPa (increase of 56%) [28,44]. Neat agar film has tensile strength of around 29.7 MPa, whereas tensile strength of agar matrices reinforced with Cloisite $Na^+$ nanoparticles increased to 35 MPa [45]. By adding Ag nanoparticles with agar, tensile strength becomes around 53.44 MPa [46]. $TiO_2$ nanoparticles/poly(butylene adipate co-terephthalate) bionanocomposite films show a 46% and 70% improvement in tensile strength and Young's modulus, respectively [47]. Pure ethylene methyl acrylate copolymer has a tensile strength of 9.51 MPa, which increases by 36% with the dispersion of 2.5 wt.% multiwalled carbon nanotubes (MWCNTs) [48]. The advantages of nanocomposites in mechanical strengths were first demonstrated by a group in Toyota Research Centre in Japan with nylon/silicate nanocomposites [49−51]. Table 15.1 shows the mechanical properties of Nylon-6 and Nylon-6 filled with 4% silicate nanoclay. Tensile modulus and tensile

**Table 15.1** Mechanical properties of nylon-6 and nylon-6/clay nanocomposite [49].

| Property | Nylon-6 | Nylon-6/4 wt.% silicate nanocomposite |
|---|---|---|
| Tensile modulus (GPa) | 1.1 | 2.1 |
| Tensile strength (GPa) | 69 | 107 |
| Heat distortion temperature (°C) | 65 | 145 |
| Impact strength (kJ/m$^2$) | 2.3 | 2.8 |
| Water absorption (%) | 0.87 | 0.51 |
| Coefficient of thermal expansion | $1.3 \times 10^{-5}$ | $6.3 \times 10^{-5}$ |

strength increased by 91% and 55% by adding nanoclay fillers. A research packaged meal at the Defense Department of the United States and the Natick Soldier Centre showed that by adding nanoscale clay mechanical properties of LDPE were increased by twofold. Rubber nanocomposites are also reported to show better mechanical strengths [52].

Improved mechanical properties were observed from gelatin nanofibers from one experiment. An analysis with the integration of 1%−4% of Cloisite 30B nanoclay with high-density polyethylene demonstrated substantial increases in different mechanical properties and hardness values [53]. Polymer composites made from epoxy, 30 wt.% of palm fiber with different amounts of zinc oxide nanoparticles as additives showed tensile strength up to 39.44 MPa, flexural strength up to 40.64 MPa, and impact strength up to 3.082 J that were significantly greater than that of composites without any nanoadditives. Fig. 15.4 shows the tensile strength of the composite due to different amounts of ZnO nanoparticle reinforcements [54].

### 15.3.3 Thermal properties

Packaging materials for food, electronics, medical components, and cosmetics should be thermally stable and heat resistant. Especially a range of temperature for any specific food is needed to maintain. Temperature barrier properties of some polymer nanocomposites allow packages to maintain a suitable temperature. Also,

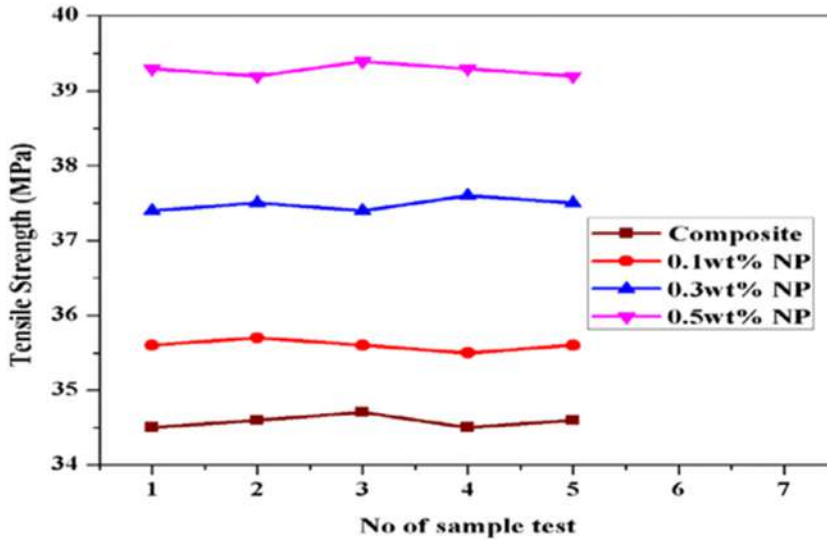


**Figure 15.4** Tensile strength of palm fiber and epoxy-based polymer composites incorporated with zinc oxide nanoparticles.
*Source:* Reprinted with permission from A. Devaraju, P. Sivasamy, G.B. Loganathan, Mechanical properties of polymer composites with ZnO nano-particle, Mater. Today Proc. 22 (2020) 531−534 [54]. Copyright (2020) Elsevier.

packaging materials should be stable at high temperatures and extreme conditions. For packaging of electronic and photonic components, packaging materials must be of low coefficients of thermal expansion (CTEs), high thermal conductivity, and low density. Traditional polymers used for packaging cannot solve all the thermal issues and transportation issues. Polymer nanocomposites can address the solution needed by providing better thermal properties than usual packaging polymers and metals.

Thermoplastic poly(vinyl chloride) (PVC) was among the first polymer produced for packaging applications because of strengths like low cost and high stiffness, intrinsic flame retardancy, good electrical insulation and vapor barrier properties, good dimensional stability at room temperature, and easy processing procedure. Nowadays PVC incorporated with polyethylenes is used in various kinds of packaging applications from blood bags to bottles, blister packs, transparent packs, and punnets. With exposure to flame and heat, PVC that is degraded can produce harmful hydrogen chloride gas that can cause harm to the environment. Also, extensive discoloration and reduction in mechanical properties are some of the consequences of problems with thermal deterioration [55]. Poly(methyl methacrylate) (PMMA) intercalated with 10 wt.% clay deteriorated at about 40°C−50°C higher than unfilled PMMA [56].

Studies showed that the thermal decomposition behavior of PVC could be improved significantly by the synthesis of recycled PVC/clay nanocomposites. CTEs were decreased by about three and a half times by incorporation of 5 wt.% organically modified clay Closite 30B [57]. Studies showed that incorporation of Cu nanoparticles under 5 wt.% in LDPE enhances thermal stability due to their higher heat capacity and thermal conductivity ($0.39\ kJ^{-1}\ g^{-1}$ compared to $0.18\ kJ^{-1}\ g^{-1}$). These properties allow more heat absorption, which results in LDPE degrading at a higher temperature than usual [58,59].

### 15.3.4 Flame retardancy

Polymer used for packaging has a significant demand for flame retardancy to ensure a more efficient and eco-friendly packaging system. Traditional packaging polymers have always suffered a lack of flame retardancy. Polymer nanocomposites have shown less combustion tendency than usual packaging polymers [60]. Polymer nanocomposites showed less flammability by producing a coproduct that has better thermal stability and works as a barrier between the flame and the surface [61]. Nanoclays are shown to increase flame retardancy according to some studies. For instance, only 5 wt.% nanoclay incorporation with nylon-6 has reduced flammability by 63% [19]. The heat release rate is considered an essential measurement to determine the flame retardancy of any material. The heat release rate of nylon-6 and maleic anhydride-grafted polypropylene (PP) nanocomposites was 50%−75% lower, showing that incorporation of nanoparticles with polymer reduces flammability [62]. The peak heat release rate of PP incorporated with 1 wt.% of MWCNT nanocomposites was 27% and of PP incorporated with 1 wt.% of MWCNT nanocomposites was 32% of unincorporated PP's heat release rate [63]. Delaminated

$Ti_3C_2T_x$ (MXene) nanoparticle−reinforced PVA nanocomposites showed less peak heat release rate and total heat release resulting in better flame retardancy. Table 15.2 shows the peak heat release rate and total heat release decrease by increasing MXene reinforcements in the polymer matrices.

### 15.3.5 Optical properties

The low-cost packaging of photonic components and modules can be improved by optically transparent materials. For packaging, photonic component materials need to have a controlled refractive index, low cure shrinkage, and a thermal expansion coefficient same as the packaged photonic components. Conventional polymer does not meet these requirements. Glasses can be used but can cause light transmittance issues [65]. Epoxy-based nanometer-order silica particle instead of micron-sized particles shows the reduction of coefficient of thermal expansion and an increase in fracture toughness, thus proving to be a better material for photonic component packaging [65]. Magadiite nanocomposites based on epoxy matrices are another material that can have a significant edge for photonic component packaging [66]. High transparency can also be achieved by smectite nanocomposites based on polyurethane matrices [67]. Polymer nanocomposites can achieve better transparency compared to polymer matrices filled with microscale composites. Nanocomposites allow passing light without deviation, which allows them to be transparent packaging materials. Figs. 15.5 and 15.6 show how light rays pass undeflected through the polymer matrices filled with nanoreinforcements [68,69]. Also improved optical properties and catalytic behavior were observed from graphene nanocomposites incorporated into tin oxide and silver-doped zinc oxide nanoparticles [70,71].

### 15.3.6 Degradation properties

To reduce plastic waste pressure on the environment, numerous researches were performed to find the possibility of degradable packaging materials. Biodegradable polymers can solve the waste problem faced by the environment. But biopolymers have significantly lesser mechanical strength and structural strength. That issue can be solved with organically modified nanoparticles incorporated with biopolymers [72−76]. Thermoplastic starch that is starchly pretreated with plasticizer was potential material for a degradable packaging solution, but it has low mechanical

**Table 15.2** Peak heat release rate and total heat release for PVA/MXene nanocomposites [64].

| Samples | Peak heat release rate (W/g) | Total heat release (kJ/g) |
|---|---|---|
| PVA | 258.9 | 28.6 |
| PVA−Mxene (0.5 wt.%) | 233.7 | 23 |
| PVA−Mxene (1 wt.%) | 192.3 | 21.3 |
| PVA−Mxene (2 wt.%) | 202.8 | 21.7 |

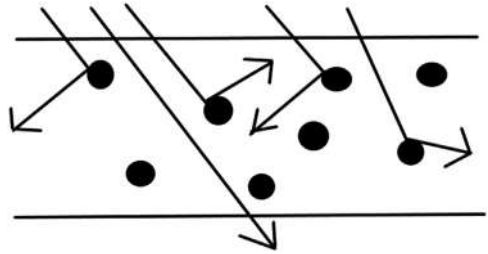

**Figure 15.5** Microscale particles in polymer matrices deflect light rays.
*Source:* Adapted with permission from A. Dang, S. Ojha, C.M. Hui, C. Mahoney, K. Matyjaszewski, M.R. Bockstaller, High-transparency polymer nanocomposites enabled by polymer-graft modification of particle fillers, Langmuir 30 (48) (2014) 14434−14442 [68]. Copyright (2014) American Chemical Society.

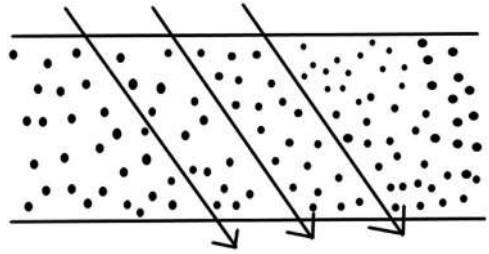

**Figure 15.6** Nanomaterials allow transmission of light without any deflection.
*Source:* Adapted with permission from A. Dang, S. Ojha, C.M. Hui, C. Mahoney, K. Matyjaszewski, M.R. Bockstaller, High-transparency polymer nanocomposites enabled by polymer-graft modification of particle fillers, Langmuir 30 (48) (2014) 14434−14442 [68]. Copyright (2014) American Chemical Society.

properties [77]. Adding 5 wt.% sodium MMT with thermoplastic starch increases tensile strength from 2.6 to 3.3 MPa [78]. After incorporating $C_3C_{18}$-MMT (trimethyloctadecyl ammonium-modified MMT) nanocomposites with neat PLA matrices enhanced biodegradability by significant amount [79,80]. Compared to untreated wood, the rate of degradation was lesser for wood treated with Melamine formaldehyde-furfuryl alcohol copolymer/1,3-dimethylol 4,5-dihydroxy ethylene urea/nanoclay [81]. CNCs used as nanofillers in biodegradable polymer matrices have enhanced biodegradability by a significant amount [82]. With recycling, the quality of plastic decreases.

Additional virgin materials are needed to incorporate with the recycled polymer to recycle without any loss in quality. Nanoadditives within recycled polymers can be used to upgrade recycled polymer [83,84]. Though nanocellulose has less mechanical strength than other nanocomposites like metal and clay nanoparticles, their low-cost production, biodegradability, and renewable production source [85] have made them a major

alternative to traditional plastics in packaging. Biodegradable composites made from gelatin films reinforced with CNC showed good barrier properties than other biopolymers, which prove their potential to be used in food packaging applications [86]. CNC was added as reinforcement materials in polyhydroxybutyrate and poly(hydroxybutyrate-co-hydroxyvalerate) to prepare biodegradable polymer composites by melt blending. The composite prepared showed excellent biodegradable properties with additional improvement in mechanical and thermal properties, which allow it to be used in packaging applications [87].

### 15.3.7 Antimicrobial and antibacterial properties

For the packaging of products like fruits, processed meat and fish, poultry items, bread, dairy products, and vegetables, antimicrobial activities of packaging materials are needed to be ensured to regulate the production of microorganisms. Nanomaterials can be used as killing agents, growing inhibitors, and antibiotic carriers with polymers [88–90]. Most of the polymer nanocomposites that are used as antimicrobial activities are based on metal oxide nanoparticles; specifically, silver nanoparticles as silver has high toxicity against many microorganisms. Different studies show that nanoclays have fewer inhibiting properties than silver nanoparticles. Nanosilver-incorporated nanocomposites showed significant inhibiting properties against Gram-positive as well as Gram-negative bacteria [91,92]. A Chinese fruit Jujube was preserved longer by using silver nanoparticles with polyethylene [93]. $TiO_2$ was reported to have the potential to inactive pathogenic food-related bacteria [94]. $TiO_2$ also has shown to prevent denaturation of protein [95]. Copper/polyaniline nanocomposite also can work as microbial inhibitors and can be used as copper nanoparticles which are cheaper than silver nanoparticles [96]. One study shows excellent antimicrobial and hemolytic properties observed from hydroxyapatite nanoparticles and lithium-substituted hydroxyapatite nanoparticles [97]. Polymer nanocomposites made from poly(L-lactic acid) reinforced with $SiO_2$ nanoparticles, mesoporous cellular foam, and Santa Barbara amorphous-15 showed good antimicrobial activity against *Escherichia coli* and *Staphylococcus aureus* bacterial strains as well as better mechanical strengths, thermal stability, and barrier properties compared to poly(L-lactic acid) without any reinforcements [98].

A novel biodegradable polymer composite was formed by incorporating silver nanoparticles and titanium dioxide nanoparticles into polyethylene oxide and chitosan polymer matrices. 0.3 wt.% of silver nanoparticles and 0.8% of titanium dioxide nanoparticles with the polymer blend showed antimicrobial activity of 32% against *E. coli*, 45.8% against *S. aureus*, 77.8% against *Candida albicans*, and 92% against *Aspergillus niger* [99]. Polymer composites prepared from regenerated cellulose and ZnO nanoparticles were reported to have excellent antimicrobial properties against Gam-negative bacteria, such as *Salmonella typhimurium*, *E. coli*, and *Vibrio parahaemolyticus* as well as Gram-positive bacteria, such as *Bacillus cereus*, *S. aureus*, and *Listeria monocytogenes* [100]. The antimicrobial activity assisted by improved mechanical properties was reported for composites made from PVA reinforced with zinc oxide–doped MWCNTs [101]. Various other biodegradable

polymer composites filled with nanoclay, nanocrystals, or nanoparticles have been reported to show antimicrobial activity against Gram-positive bacteria, Gram-negative bacteria, yeast, fungi, and other microbes [102−108].

## 15.4 Polymer nanocomposites for packaging foods and beverages

To ensure minimum food losses and ensure safe and food products, proper packaging materials and processes are needed to be confirmed. Conventional packaging is failing to meet the desire of the consumers for better-quality, fresh-like products, and the need for green packaging to ensure a sustainable environment. With the edge over conventional polymers in barrier properties, mechanical properties, thermal and chemical resistance, flame retardancy, optical properties, antimicrobial and antibacterial properties, and degradation properties, polymer nanocomposites are now thought to be the widespread material for food packaging [109−111,112,113]. Three main types of packaging that can be improved with polymer nanocomposites are the following:

- Improved packaging: Nanoparticles present in polymer nanocomposites can significantly improve packaging properties like a gas barrier, flexibility, transparency, temperature, and stable moisture content.
- Active packaging: Nanoparticles present in the matrices interact with the food and environment in order to play a more active role in food preservation [114].
- Intelligent packaging: Nanodevices present in the packaging materials detect the overall condition of the food and environment specifically during transportation and also creating a barrier against any imitation of the material [115−117].

For foods such as processed meat, dairy products, cheese, fish, boil-in-bag foods like noodles and ramen, fruit juice packets, and beverages need to have a long shelf life. Various polymer nanocomposites commercially developed by many companies, including Honeywell, Bayer, Ube America, and Mitsubishi Gas Chemical are already being used at industrial-level applications, such as:

- Nano-PA6: It was the first nanoclay−plastic nanocomposite developed by Nanopolymer Composites Corporation, Taiwan by in situ polymerization, which showed significant barrier and mechanical characteristic improvements compared to conventional packaging material [118].
- Imperm (Color Matrices Europe): It is used in multilayered PET bottles for beverage packaging and sheets for food packaging [119].
- Durethan KU 2-2601 (LANXESS Deutschland GmbH): It is a nanocomposite film used for juice packaging based on polyamide [120].
- Aegis OX (Honeywell Polymers): It is a nanocomposite-incorporated polymer film that contains nylon and nanocomposite clay particles to enhance barrier and mechanical properties. Three variants of nylon-6 nanocomposite: Aegis CDSE, OX, and HFX used for packaging applications of plastic PET beer bottles, hot-fill bottles, and carbonated soft drink bottles are produced by Honeywell. Among these three products, Aegis OX contains an oxygen-scavenging component that is intended for use in beer bottles and improves

shelf life up to 6−12 months. Aegis was used in a three-layered 1.6-L structure for a South Korean brewery in 2003 [119,121,122].

- A large-scale manufacturing process developed by Purdue University may change the storing processes of grocery items. CNCs were used in this process to improve barrier properties [123].
- M9 material developed by Nanocor used for layered ketchup bottles decreases bottle rejects by 71% compared to EVOH barrier [49].
- Southern Clay Products produced a nylon nanocomposite Cloisite, with a clay loading of 5%, which increases mechanical strength [44].

Waste reduction is a crucial issue for a sustainable environment and to work for waste reduction extensive research was undertaken by U.S. Army Natick Soldier Center to use polymer nanocomposites for packaged meals for military rations to lessen the waste in the packaging system and also to reduce costs. Due to the oxidation problem and flavor mixing problem, plastic bottles for the beer packaging industry cannot be used. Still, by introducing nanocomposites in polymer, these problems can be solved by incorporating nanocomposites with oxygen-scavenging quality with polymers and extended shelf life was achieved for beer bottles as well as soft drinks [124]. 70% market of polymer nanoparticles is based on polymer nanoclay materials. Nanoclays embedded with beverage containers improve packaging and decreasing OTR and WVTR to enhance the shelf life of bottles. A nanoclay polymer composite for paperboard cartons to keep the juice fresh was created by Bayer Polymers, which cost less than traditional juice packaging materials.

To ensure safe foods, better quality, and reduce environmental pollution, various kinds of active and smart packaging technologies have been developed. An example of active packaging is a programmable barrier that controls the atmosphere of the packaging [125]. Polymer nanocomposites prepared with polymer and $TiO_2$ nanoparticles possess oxygen scavenger quality and are used in oxygen-sensitive food products [126]. Packaged foods like meat and poultry products need to be high in carbon dioxide content to inhibit microbial growth to ensure longer shelf life. Ethylene is a plant hormone that works as a ripening agent; that is why packaging also needs to have ethylene-scavenging quality. The development of PP films coated with $TiO_2$ was reported to remove ethylene gas from packaged products [127]. Asahi Glass and Pilkington Glass are manufacturing self-cleaning glass prepared with $TiO_2$ nanoparticles, which in the presence of light react with dirt and grease to break down into a pool that will roll off from the glass [128]. Intelligent food packaging materials involve monitoring the packaging atmosphere [117]. Nanosensors can be used to monitor the packaging atmosphere to ensure the quality of food [129,130]. Various nanoparticles like gold nanoparticles, metal nanoparticles, carbon nanotubes, magnetic nanoparticles, and quantum dots are used to produce useful biosensors [131−133]. These biosensors incorporated with the polymer can detect pesticides, allergens, toxins, pathogens, temperature changes, residual oxygen, and leakages [134,135].

A time-temperature indicator (iStrip) based on gold nanoparticles was produced by Timestrip, which is red at temperatures above zero and irreversible color loss is caused by unintended freezing. Oxygen and carbon dioxide leak indicators that use $TiO_2$ nanoparticles are also being developed commercially [119,136]. To trace food

batches, Oxonica from California creates Nano barcodes from nanoparticles containing silver and gold bars ranging in diameter, length, and quantity, with the potential ability to brand each commodity with a billion variations [61,137,138]. $TiO_2$ nanowires were prepared to use as nanocursors [139]. Prospective implementations of bionanosensors in packaging include detection of bacteria in packaged fish and meat with the help of DNA biochips and detection of chemicals released during food deterioration [124,140−142]. There is a high demand for packaged orange juice due to its high nutritional value and availability. Because of increasing microbial spoilage, orange juice has a low shelf life [143]. LDPE filled with silver nanoparticles and ZnO nanoparticles used for Doypack packaging is commonly used for packaging fruit juice, which showed prolonged shelf life of packaged orange juice [144].

## 15.5 Polymer nanocomposites for packaging electronic components

In addition to enhanced barrier properties and mechanical efficiency, one specific challenge for packaging electronic components is enhancing the ability of the products used in packaging to work against gas particles and water vapor. Biopolymers can be used for the packaging of electronic devices because of their high crystallinity, high hydrophobicity, and fast handling. But better mechanical strength is needed to allow better shock absorbance. Using organophilic layered double hydroxides [145,146], nanosheets, MMT [147], and graphene oxide [148] with PLA can meet these requirements[149]. Polymer nanocomposites have advantages over unfilled polymers in electromagnetic shielding with the addition of nanofillers [150,151]. PLA/MWCNT nanocomposites foams were proved to have better electromagnetic shielding. The average specific electromagnetic interference shielding efficiency reaches 77 dB $g^{-1}$ $cm^3$, far exceeding those of metals like copper and similar density carbon-based composites [149]. The (Poly(butylene succinate)) (PBS)/MWCNT nanocomposites (MWCNT loading of 3 wt.%) have significant advantages compared with pure polymers in antistatic properties. The prepared PBS/MWCNT nanocomposites showed a surface resistivity of $7.30 \times 10^6$ Ω, which is $10^9$ times lower compared to the neat PBS sample [152]. Almost all electrical components come in plastic EST packages that prevent the components to get harmed by externally produced static charges. Although plastics have excellent electrical insulation, they also have very limited heat capacity. To solve this issue, better thermal properties of polymer nanocomposites can be utilized.

## 15.6 Toxicity of polymer nanocomposites

Consumers' safety for nanocomposite-incorporated polymer materials for packaging emphasizes the moment of exposure during ingestion [153,154]. Some reports show

that the toxicity of Ag nanoparticles is attributed to multiple organ groups, such as the liver. Also, various studies reported that nano-scaled Ag particles can have pernicious consequences on other species, such as zebrafish [155]. Silver nanoparticles have hazardous impacts on edible plants like zucchini [156] and have also shown cell wall degradation of onion plants [157]. Reduced shoot length and germination were observed in flax and ryegrass [158]. As most of the packaging materials end up in the environment, these hazardous effects can have harmful effects on the ecosystem. Migration of nanoparticles with a diameter of 1 nm from polymer matrices of packaging material to the food itself is reported. The health consequences of nanoparticles are still being studied, but when tested on a mice population, one study shows lung toxicity or inflammation. Related findings were found in the case of nanoparticles of copper [159]. Table 15.3 shows different diseases originated from human exposure to nanoparticles [160].

## 15.7 Conclusions and future prospects

To ensure sustainable development and better-quality products, the conventional plastic polymer has faced drawbacks in the barrier, mechanical, and thermal properties. While the pressure on the environment created by plastics from packaging can be

**Table 15.3** Associate diseases due to the exposure to nanoparticles through different organs.

| **Organs that absorb nanoparticles through ingestion and inhalation** | **Disease** |
|---|---|
| Gastrointestinal system | Crohn's disease |
| | Colon cancer |
| Orthopedic implant wear debris | Autoimmune diseases |
| | Dermatitis |
| | Urticaria |
| | Vasculitis |
| Brain | Parkinson's and Alzheimer's disease |
| Lungs | Asthma |
| | Bronchitis |
| | Emphysema |
| | Cancer |
| Heart | Arrhythmia |
| | Heart disease |
| | High blood pressure |
| Lymphatic system | Podoconiosis |
| | Kaposi's sarcoma |
| Skin | Autoimmune disease |
| | Dermatitis |

lessened by bio-based polymers, there are very few marine-grade biopolymers in the market. Cellulose, starch, and protein-based plastics are the main examples of biodegradable polymers, but these lack mechanical strength and barrier properties significantly. Polymer nanocomposites have the potential to be not only biodegradable but also with increasing packaging quality. Different edible chitosan, starch, and protein-based films that are modified with glycerol-like plasticizers and cellulose nanofillers are being developed to answer the question raised from plastic waste. Although there are not many pieces of research that prove that nanoparticles are nontoxic to the body, there is some nanoclay-like layered silicate, MMT that can be used. But due to environmental and technical barriers, complex manufacturing processes and high production costs make it hard to industrialize polymer nanocomposite packaging. Once technologies help researchers and markets to overcome those barriers, polymer nanocomposites can become the new future for packaging industries.

Because of excellent barrier properties, polymer nanocomposites have advantages over conventional packaging materials specifically for fruits, meats, fish, dairy products, confectionery items, and beverages and juices as it significantly improves the quality of these food items. Packaging and nanomaterial industries, academic institutes, and research laboratories are taking active projects to industrialize these materials for better performance. In 2018, the world market of polymer nanocomposites was around US$8 billion, which is estimated to become over US$30 billion, more than 15% of which is related to the packaging industry. Arkema Group, Evonik Industries AG, Nanocyl SA, DuPont, RTP Company, Inframat Corporation, Powdermet Inc., Nanocor Inc., Nanophase Technologies Corporation, Showa Denco KK are the companies that dominate the polymer nanocomposites industries with a lot of industrialized use of polymer nanocomposites [161–163]. In 2011, consumption was estimated to be more than 100 million pounds in which carbonated drinks and beers only were estimated to be more than 50 million pounds, which is a big jump from 3 million pounds in 2006 [28,41]. The compound annual growth rate of this market is estimated to increase by 18.5% by 2026 [164]. As of now, the production cost of polymer nanocomposites is higher than conventional packaging materials. But once the production and manufacturing costs are lower, polymer nanocomposites can be the only choice for packaging. Environmental and technical barriers are also essential factors that hamper the production of polymer nanocomposite packaging at a large scale. The defense and regulatory issues for the production and use of nanoparticles to package foods also inhibit mass production and usages. The advantages of nanocomposites outweigh the costs and problems, and the technique will be perfected over time and procedures will be highly evolved [165–169].

## References

[1] W. Rosse, A brief history of PNH, in: Neal S. young, Joel Moss (Eds.), PNH and the GPI-Linked Proteins, Academic Press, San Diego, 2000, pp. 1–20. Available from: http://doi.org/10.1016/b978-012772940-4/50002-5

[2] S.J. Risch, Food packaging history and innovations, J. Agric. Food Chem. 57 (18) (2009) 8089–8092. Available from: https://doi.org/10.1021/jf900040r.
[3] The history of packaging. https://www.digimarc.com/resources/history-of-packaging (accessed 24.11.20).
[4] The history of packaging crawford packaging blog. https://crawfordpackaging.com/automation-and-innovations/history-of-packaging (accessed 24.11.20).
[5] Countries most dependent on others for food - WorldAtlas. https://www.worldatlas.com/articles/the-countries-importing-the-most-food-in-the-world.html (accessed 24.11.20).
[6] H. Ritchie, M. Roser, Plastic pollution - our world in data, 2018. https://ourworldindata.org/plastic-pollution (accessed 15.11.20).
[7] PMERG, Plastics – The Facts, 2018, p. 38.
[8] R. Geyer, J.R. Jambeck, K.L. Law, Production, use, and fate of all plastics ever made, Sci. Adv. 3 (7) (2017) 25–29. Available from: https://doi.org/10.1126/sciadv.1700782.
[9] PlasticOcean, Facts. About plastic. Help - Plastic Oceans Foundation, 2020. https://plasticoceans.org/the-facts/ (accessed 15.11.20).
[10] L. Claudio, Our food: packaging & public health, Environ. Health Perspect. 120 (2012) A232–A237. Available from: https://doi.org/10.1289/ehp.120-a232.
[11] V. Krishnan, F. Permuth, P. Alto, Bisphenol-A: polycarbonate, May 2014.
[12] D. Zalko, C. Jacques, H. Duplan, S. Bruel, E. Perdu, Viable skin efficiently absorbs and metabolizes bisphenol A, Chemosphere 82 (3) (2011) 424–430. Available from: https://doi.org/10.1016/j.chemosphere.2010.09.058.
[13] S. Sikarwar, S.B. Yadaw, A.K. Yadav, B. Yadav, Nanocomposite material for packaging of electronic goods, Int. J. Sci. Innov. Res. 1 (2014) 93–108.
[14] R. Wever, C. Boks, A. Stevels, Packaging for consumer electronic products: the need for integrating design and engineering, in: Proceedings of the 16th IAPRI World Conference Package, Bangkok, Thailand, 8–12 June 2008, 2020.
[15] S. Sagadevan, K. Pal, Z.Z. Chowdhury, M.E. Hoque, Structural, optical and dielectric investigation of {CdFe}$2O_4$ nanoparticles, Mater. Res. Express 4 (7) (2017) 75025. Available from: https://doi.org/10.1088/2053-1591/aa77b5.
[16] R. Roy, R.A. Roy, D.M. Roy, Alternative perspectives on 'quasi-crystallinity': non-uniformity and nanocomposites, Mater. Lett. 4 (8–9) (1986) 323–328. Available from: https://doi.org/10.1016/0167-577X(86)90063-7.
[17] Z. Qiao, H. Feng, J. Zhou, Molecular dynamics simulations on the melting of gold nanoparticles, Phase Transit. 87 (1) (2014) 59–70. Available from: https://doi.org/10.1080/01411594.2013.798410.
[18] P. Mulvaney, Not all that's gold does glitter, MRS Bull. 26 (12) (2001) 1009–1014. Available from: https://doi.org/10.1557/mrs2001.258.
[19] S. Anandhan, S. Bandyopadhyay, Polymer nanocomposites: from synthesis to applications, Nanocompos. Polym. Anal. Methods (2011). Available from: https://doi.org/10.5772/17039.
[20] M.J. Mochane, S.I. Magagula, J.S. Sefadi, E.R. Sadiku, T.C. Mokhena, Morphology, thermal stability, and flammability properties of polymer-layered double hydroxide (LDH) nanocomposites: a review, Crystals 10 (7) (2020). Available from: https://doi.org/10.3390/cryst10070612.
[21] X. Sun, et al., Recent progress in graphene/polymer nanocomposites, Adv. Mater. 33 (6) (2021) 2001105. Available from: https://doi.org/10.1002/adma.202001105.
[22] X. Chen, et al., MXene/polymer nanocomposites: preparation, properties, and applications, Polym. Rev. 61 (1) (2021) 80–115. Available from: https://doi.org/10.1080/15583724.2020.1729179.

[23] T.V. Duncan, Applications of nanotechnology in food packaging and food safety: barrier materials, antimicrobials and sensors, J. Colloid Interface Sci. 363 (1) (2011) 1–24. Available from: https://doi.org/10.1016/j.jcis.2011.07.017.
[24] J. Luna, A. Vílchez, Polymer Nanocomposites for Food Packaging, Elsevier Inc, 2017.
[25] Y. Cui, S.I. Kundalwal, S. Kumar, Gas barrier performance of graphene/polymer nanocomposites, Carbon N. Y. 98 (2016) 313–333. Available from: https://doi.org/10.1016/j.carbon.2015.11.018.
[26] J.R. Potts, D.R. Dreyer, C.W. Bielawski, R.S. Ruoff, Graphene-based polymer nanocomposites, Polym. (Guildf.) 52 (1) (2011) 5–25. Available from: https://doi.org/10.1016/j.polymer.2010.11.042.
[27] K. Bhunia, S. Dhawan, S.S. Sablani, Modeling the oxygen diffusion of nanocomposite-based food packaging films, J. Food Sci. 77 (7) (2012) 29–38. Available from: https://doi.org/10.1111/j.1750-3841.2012.02768.x.
[28] A. Downing-Perrault, Polymer nanocomposites are the future [Online]. Univ. Wisconsin-Stout, Menomonie, Wisconsin, USA, 2005, pp. 1–13. Available at http://www.iopp.org/files/public/DowningPerraultAlyssaUWStroutNanoStructures.pdf.
[29] M.A. Mohsin, I. Ali, R.H. Elleithy, S.M. Al-Zahrani, Improvements in barrier properties of poly(ethylene terephthalate) films using commercially available high barrier masterbatch additives via melt blend technique, J. Plast. Film. Sheeting 29 (1) (2013) 21–38. Available from: https://doi.org/10.1177/8756087912438880.
[30] L. Fenfen, C. Zhang, Y. Weng, X. Diao, Y. Zhou, X. Song, Enhancement of gas barrier properties of graphene, 2020.
[31] P. Cheviron, F. Gouanvé, E. Espuche, Preparation, characterization and barrier properties of silver/montmorillonite/starch nanocomposite films, J. Memb. Sci. 497 (2016) 162–171. Available from: https://doi.org/10.1016/j.memsci.2015.09.039.
[32] K. Müller, et al., Review on the processing and properties of polymer nanocomposites and nanocoatings and their applications in the packaging, automotive and solar energy fields, Nanomaterials 7 (4) (2017). Available from: https://doi.org/10.3390/nano7040074.
[33] B. Tan, N.L. Thomas, A review of the water barrier properties of polymer/clay and polymer/graphene nanocomposites, J. Memb. Sci. 514 (2016) 595–612. Available from: https://doi.org/10.1016/j.memsci.2016.05.026.
[34] K. Yano, A. Usuki, A. Okada, Synthesis and properties of polyimide-clay hybrid films, J. Polym. Sci. A Polym. Chem. 35 (11) (1997) 2289–2294. 10.1002/(SICI)1099-0518(199708)35:11<2289::AID-POLA20>3.0.CO;2-9.
[35] B. Chen, J.R.G. Evans, Poly(ε-caprolactone) – clay nanocomposites: structure and mechanical properties, Macromolecules 39 (2) (2006) 747–754. Available from: https://doi.org/10.1021/ma052154a.
[36] M.-H. Tsai, C.-J. Chang, H.-H. Lu, Y.-F. Liao, I.-H. Tseng, Properties of magnetron-sputtered moisture barrier layer on transparent polyimide/graphene nanocomposite film, Thin Solid Films 544 (2013) 324–330. Available from: https://doi.org/10.1016/j.tsf.2013.02.105.
[37] H. Hosseinkhanli, A. Sharif, J. Aalaie, T. Khalkhali, S. Akhlaghi, Oxygen permeability and the mechanical and thermal properties of (low-density polyethylene)/poly (ethylene-co-vinyl acetate)/organoclay blown film nanocomposites, J. Vinyl Addit. Technol. 19 (2) (2013) 132–139. Available from: https://doi.org/10.1002/vnl.20329.
[38] G. Jiang, M. Zhang, J. Feng, S. Zhang, X. Wang, High oxygen barrier property of poly (propylene carbonate)/polyethylene glycol nanocomposites with low loading of cellulose nanocrystals, ACS Sustain. Chem. Eng. 5 (12) (2017) 11246–11254. Available from: https://doi.org/10.1021/acssuschemeng.7b01674.

[39] P.K. Sethy, P. Mohapatra, S. Patra, D. Bharatiya, S.K. Swain, Antimicrobial and barrier properties of polyacrylic acid/GO hybrid nanocomposites for packaging application, Nano-Struct. Nano-Objects 26 (2021) 100747. Available from: https://doi.org/10.1016/j.nanoso.2021.100747.
[40] H. Haghighi, et al., Characterization of bio-nanocomposite films based on gelatin/polyvinyl alcohol blend reinforced with bacterial cellulose nanowhiskers for food packaging applications, Food Hydrocoll. 113 (2021) 106454. Available from: https://doi.org/10.1016/j.foodhyd.2020.106454.
[41] S. Ray, S.Y. Quek, A. Easteal, X.D. Chen, The potential use of polymer-clay nanocomposites in food packaging, Int. J. Food Eng. 2 (4) (2006). Available from: https://doi.org/10.2202/1556-3758.1149.
[42] A. Usuki, Y. Kojima, M. Kawasumi, A. Okada, T. Kurauchi, O. Kamicaito, One-pot synthesis of nylon 6-clay hybrid, 1993.
[43] S. Shankar, J.W. Rhim, Polymer nanocomposites for food packaging applications, Funct. Phys. Prop. Polym. Nanocompos. (2016) 29−55. Available from: https://doi.org/10.1002/9781118542316.ch3.
[44] Y. Ling, S. Omachinski, J. Logsdon, J. Whan Cho, T. Lan, Nano-effects in in situ nylon-6 nanocomposites, 2004.
[45] J.W. Rhim, S. Bin Lee, S.I. Hong, Preparation and characterization of agar/clay nanocomposite films: the effect of clay type, J. Food Sci. 76 (3) (2011). Available from: https://doi.org/10.1111/j.1750-3841.2011.02049.x.
[46] J.W. Rhim, L.F. Wang, S.I. Hong, Preparation and characterization of agar/silver nanoparticles composite films with antimicrobial activity, Food Hydrocoll. 33 (2) (2013) 327−335. Available from: https://doi.org/10.1016/j.foodhyd.2013.04.002.
[47] R. Venkatesan, N. Rajeswari, $TiO_2$ nanoparticles/poly(butylene adipate-co-terephthalate) bionanocomposite films for packaging applications, Polym. Adv. Technol. 28 (12) (2017) 1699−1706. Available from: https://doi.org/10.1002/pat.4042.
[48] N.M. Barkoula, B. Alcock, N.O. Cabrera, T. Peijs, Flame-retardancy properties of intumescent ammonium poly(phosphate) and mineral filler magnesium hydroxide in combination with graphene, Polym. Polym. Compos. 16 (2) (2008) 101−113. Available from: http://doi.org/10.1002/pc.
[49] G. Asadi, S.M. Mousavi, Application of nanotechnology in food packaging. 2006, doi: 10.1051/iufost:20060739.
[50] E.P. Giannelis, Polymer-layered silicate nanocomposites: synthesis, properties and applications, Appl. Organomet. Chem. 12 (10−11) (1998) 675−680. 10.1002/(SICI)1099-0739(199810/11)12:10/11 < 675::AID-AOC779 > 3.0.CO;2-V.
[51] O. Kamigaito, et al., Synthesis of nylon 6-clay hybrid, J. Mater. Res. 8 (05) (1993) 1179.
[52] M. Khalid, R. Walvekar, M.R. Ketabchi, H. Siddiqui, M. Enamul Hoque, Rubber/nanoclay composites: towards advanced functional materials, in: M. Jawaid, A. Qaiss, R. Bouhfid (Eds.), Nanoclay Reinforced Polymer Composites, Springer, Singapore, 2016.
[53] N. Venkatesan, G.B. Bhaskar, S. Rajesh, K. Pazhanivel, S. Sagadevan, Effect of Cloisite 30B nanoclay on the mechanical properties of HDPE nanocomposites, Mater. Test. 59 (4) (2017) 355−360. Available from: https://doi.org/10.3139/120.111010.
[54] A. Devaraju, P. Sivasamy, G.B. Loganathan, Mechanical properties of polymer composites with ZnO nano-particle, Mater. Today Proc. 22 (2020) 531−534. Available from: https://doi.org/10.1016/j.matpr.2019.08.146.
[55] J. Brandsch, O. Piringer, Characteristics of plastic materials, in: O.G. Piringer, A.L. Baner (Eds.), Plastic Packaging, Interactions with Food and Pharmaceuticals, Second edition, 2000, pp. 39−41.

[56] Q.H. Zeng, A.B. Yu, G.Q. Lu, D.R. Paul, Clay-based polymer nanocomposites: Research and commercial development, J. Nanosci. Nanotechnol. 5 (10) (2005) 1574–1592. Available from: https://doi.org/10.1166/jnn.2005.411.

[57] Y. Yoo, S.-S. Kim, J. Won, K.-Y. Choi, J. Lee, Enhancement of the thermal stability, mechanical properties and morphologies of recycled PVC/clay nanocomposites, Polym. Bull. 52 (2004) 373–380. Available from: https://doi.org/10.1007/s00289-004-0296-7.

[58] F. Shen, Y. Wang, X. Yuan, W. Guo, C. Wu, Interfacial coordination reaction in copper sulfate particles filled styrene-acrylonitrile copolymer composites, J. Macromol. Sci. Part. B Phys. 47 (1) (2008) 76–86. Available from: https://doi.org/10.1080/15568310701744166.

[59] J.A. Molefi, A.S. Luyt, I. Krupa, Comparison of the influence of Cu micro- and nanoparticles on the thermal properties of polyethylene/Cu composites, Express Polym. Lett. 3 (10) (2009) 639–649. Available from: https://doi.org/10.3144/expresspolymlett.2009.80.

[60] J. W. Gilman, T. Kashiwagi, J. D. Lichtenhan, A revolutionary new flame retardant approach, 1997.

[61] A.M. Youssef, Polymer nanocomposites as a new trend for packaging applications, Polym. Plast. Technol. Eng. 52 (7) (2013) 635–660. Available from: https://doi.org/10.1080/03602559.2012.762673.

[62] J.W. Gilman, et al., Flammability properties of polymer - layered-silicate nanocomposites. Polypropylene and polystyrene nanocomposites, Chem. Mater. 12 (7) (2000) 1866–1873. Available from: https://doi.org/10.1021/cm0001760.

[63] T. Kashiwagi, E. Grulke, J. Hilding, R. Harris, W. Awad, J. Douglas, Thermal degradation and flammability properties of poly(propylene)/carbon nanotube composites, Macromol. Rapid Commun. 23 (13) (2002) 761–765. 10.1002/1521-3927(20020901)23:13 < 761::AID-MARC761 > 3.0.CO;2-K.

[64] Y. Pan, et al., Flammability, thermal stability and mechanical properties of polyvinyl alcohol nanocomposites reinforced with delaminated Ti3C2Tx (MXene), Polym. Compos. 41 (1) (2020) 210–218. Available from: https://doi.org/10.1002/pc.25361.

[65] Y. Zhou, F.G. Shi, Epoxy-based optically transparent nanocomposites for photonic packaging, in: Proc. Int. Symp. Exhib. Adv. Packag. Mater. Process. Prop. Interfaces, vol. 9, pp. 100–102, 2004. doi: 10.1109/isapm.2004.1287997.

[66] Z. Wang, T. Lan, T. Pinnavaia, Hybrid organic – inorganic nanocomposites formed from an epoxy polymer and a layered silicic acid (magadiite), Chem. Mater. 8 (1996). Available from: https://doi.org/10.1021/cm960263l.

[67] Z. Gao, W. Xie, J. Hwu, L. Wells, wei-ping Pan, The characterization of organic modified montmorillonite and its filled PMMA nanocomposite, J. Therm. Anal. Calorim. 64 (2001) 467–475. Available from: https://doi.org/10.1023/A:1011514110413.

[68] A. Dang, S. Ojha, C.M. Hui, C. Mahoney, K. Matyjaszewski, M.R. Bockstaller, High-transparency polymer nanocomposites enabled by polymer-graft modification of particle fillers, Langmuir 30 (48) (2014) 14434–14442. Available from: https://doi.org/10.1021/la5037037.

[69] M. Wilson, K. Kannangara, G. Smith, M. Simmons, B. Raguse, Nanotechnology: Basic Science and Emerging Technologies, first ed., CRC Press, Boca Raton, 2002.

[70] S. Sagadevan, et al., A facile hydrothermal approach for catalytic and optical behavior of tin oxide-graphene ($SnO_2$/G) nanocomposite, PLoS One 13 (10) (2018) 1–15. Available from: https://doi.org/10.1371/journal.pone.0202694.

[71] S. Sagadevan, K. Pal, Z.Z. Chowdhury, M.E. Hoque, Structural, dielectric and optical investigation of chemically synthesized Ag-doped ZnO nanoparticles composites, J. Sol-Gel Sci. Technol. 83 (2) (2017) 394–404. Available from: https://doi.org/10.1007/s10971-017-4418-8.

[72] R. Singh, R. Sharma, M. Shaqib, A. Sarkar, K.D. Chauhan, Chapter 10 - biodegradable polymers as packaging materials, in: S. Thomas, S. Gopi, A. Amalraj (Eds.), Biopolymers and Their Industrial Applications: From Plant, Animal, and Marine Sources, to Functional Products, Elsevier, 2021, pp. 245–259.
[73] F. Wu, M. Misra, A.K. Mohanty, Challenges and new opportunities on barrier performance of biodegradable polymers for sustainable packaging, Prog. Polym. Sci. 117 (2021) 101395. Available from: https://doi.org/10.1016/j.progpolymsci.2021.101395.
[74] G. Kaur, S. Sharma, S.A. Mir, B.N. Dar, Nanobiocomposite films: a 'greener alternate' for food packaging, Food Bioprocess. Technol. 14 (6) (2021) 1013–1027. Available from: https://doi.org/10.1007/s11947-021-02634-x.
[75] M.Z. Mulla, M.R.T. Rahman, B. Marcos, B. Tiwari, S. Pathania, Poly lactic acid (PLA) nanocomposites: effect of inorganic nanoparticles reinforcement on its performance and food packaging applications, Molecules 26 (7) (2021). Available from: https://doi.org/10.3390/molecules26071967.
[76] M. Heidari, M. Khomeiri, H. Yousefi, M. Rafieian, M. Kashiri, Chitin nanofiber-based nanocomposites containing biodegradable polymers for food packaging applications, J. Consum. Prot. Food Saf. (2021). Available from: https://doi.org/10.1007/s00003-021-01328-y.
[77] B. Chen, J.R.G. Evans, Thermoplastic starch-clay nanocomposites and their characteristics, Carbohydr. Polym. 61 (4) (2005) 455–463. Available from: https://doi.org/10.1016/j.carbpol.2005.06.020.
[78] H.-M. Park, W.-K. Lee, C.-Y. Park, W.-J. Cho, C.-S. Ha, Environmentally friendly polymer hybrids. Part I: mechanical, thermal, and barrier properties of thermoplastic starch/clay nanocomposites, J. Mater. Sci. 38 (2003) 909–915. Available from: https://doi.org/10.1023/A:1022308705231.
[79] S.S. Ray, K. Yamada, M. Okamoto, K. Ueda, Polylactide-layered silicate nanocomposite: a novel biodegradable material, Nano Lett. 2 (10) (2002) 1093–1096. Available from: https://doi.org/10.1021/nl0202152.
[80] S. Sinha Ray, K. Yamada, M. Okamoto, K. Ueda, New polylactide-layered silicate nanocomposites. 2. Concurrent improvements of material properties, biodegradability and melt rheology, Polym. (Guildf). 44 (3) (2002) 857–866. Available from: https://doi.org/10.1016/S0032-3861(02)00818-2.
[81] A. Hazarika, M. Mandal, T.K. Maji, Dynamic mechanical analysis, biodegradability and thermal stability of wood polymer nanocomposites, Compos. B Eng. 60 (2014) 568–576. Available from: https://doi.org/10.1016/j.compositesb.2013.12.046.
[82] F.V. Ferreira, I.F. Pinheiro, R.F. Gouveia, G.P. Thim, L.M.F. Lona, Functionalized cellulose nanocrystals as reinforcement in biodegradable polymer nanocomposites, Polym. Compos. 39 (2018) E9–E29. Available from: https://doi.org/10.1002/pc.24583.
[83] C. López de Dicastillo, E. Velásquez, A. Rojas, A. Guarda, M.J. Galotto, The use of nanoadditives within recycled polymers for food packaging: properties, recyclability, and safety, Compr. Rev. Food Sci. Food Saf. 19 (4) (2020) 1760–1776. Available from: https://doi.org/10.1111/1541-4337.12575.
[84] J. Zhu, et al., Comprehensive and sustainable recycling of polymer nanocomposites, J. Mater. Chem. 21 (2011) 16239–16246. Available from: https://doi.org/10.1039/c1jm13044g.
[85] J. Tusnim, M.E. Hoque, S.A. Hossain, A. Abdel-Wahab, A. Abdala, M.A. Wahab, F. inMohammad, H.A. Al-Lohedan, M.B.T.-S.N, in: N.N.S. from Jawaid (Ed.), Micro Nano Technol, Elsevier, 2020, pp. 81–113.
[86] L.S.F. Leite, F.K.V. Moreira, L.H.C. Mattoso, J. Bras, Electrostatic interactions regulate the physical properties of gelatin-cellulose nanocrystals nanocomposite films

intended for biodegradable packaging, Food Hydrocoll. 113 (2021) 106424. Available from: https://doi.org/10.1016/j.foodhyd.2020.106424.

[87] M. Pracella, C. Mura, G. Galli, Polyhydroxyalkanoate nanocomposites with cellulose nanocrystals as biodegradable coating and packaging materials, ACS Appl. Nano Mater. 4 (1) (2021) 260−270. Available from: https://doi.org/10.1021/acsanm.0c02585.

[88] N. Cioffi, et al., Copper nanoparticle/polymer composites with antifungal and bacteriostatic properties, Chem. Mater. 17 (21) (2005) 5255−5262. Available from: https://doi.org/10.1021/cm0505244.

[89] Z.X. Tang, B.F. Lv, MgO nanoparticles as antibacterial agent: preparation and activity, Braz. J. Chem. Eng. 31 (3) (2014) 591−601. Available from: https://doi.org/10.1590/0104-6632.20140313s00002813.

[90] M.A. Wahab, N. Islam, M.E. Hoque, D.J. Young, Recent advances in silver nanoparticle containing biopolymer nanocomposites for infectious disease control − a mini review, Curr. Anal. Chem. 14 (3) (2018) 198−202. Available from: https://doi.org/10.2174/1573411013666171009163829.

[91] J.W. Rhim, S.I. Hong, H.M. Park, P.K.W. Ng, Preparation and characterization of chitosan-based nanocomposite films with antimicrobial activity, J. Agric. Food Chem. 54 (16) (2006) 5814−5822. Available from: https://doi.org/10.1021/jf060658h.

[92] S. Gautam, S. Sharma, B. Sharma, P. Jain, Antibacterial efficacy of poly (vinyl alcohol) nanocomposites reinforced with graphene oxide and silver nanoparticles for packaging applications, Polym. Compos. 42 (6) (2021) 2829−2837. Available from: https://doi.org/10.1002/pc.26017.

[93] H. Li, et al., Effect of nano-packing on preservation quality of Chinese jujube (Ziziphus jujuba Mill. var. inermis (Bunge) Rehd), Food Chem. 114 (2) (2009) 547−552. Available from: https://doi.org/10.1016/j.foodchem.2008.09.085.

[94] S. Sébastien, Les soignants face à la mort, Rev. Infirm. 1 (180) (2012) 39−41.

[95] S. Sagadevan, et al., Investigation on optical, dielectric and invitro anti-inflammatory responses of titanium dioxide ($TiO_2$), Dig. J. Nanomater. Biostruct. 13 (3) (2018) 641−652.

[96] U. Bogdanović, et al., Nanomaterial with high antimicrobial efficacycopper/polyaniline nanocomposite, ACS Appl. Mater. Interfaces 7 (3) (2015) 1955−1966. Available from: https://doi.org/10.1021/am507746m.

[97] V.P. Padmanabhan, T.S.N. Sankara Narayanan, S. Sagadevan, M.E. Hoque, R. Kulandaivelu, Advanced lithium substituted hydroxyapatite nanoparticles for antimicrobial and hemolytic studies, N. J. Chem. 43 (47) (2019) 18484−18494. Available from: https://doi.org/10.1039/c9nj03735g.

[98] E. Psochia, et al., Bottom-up development of nanoimprinted PLLA composite films with enhanced antibacterial properties for smart packaging applications, Macromolecules 1 (1) (2021) 49−63. Available from: https://doi.org/10.3390/macromol1010005.

[99] M.M. Abutalib, A. Rajeh, Enhanced structural, electrical, mechanical properties and antibacterial activity of Cs/PEO doped mixed nanoparticles (Ag/TiO2) for food packaging applications, Polym. Test. 93 (2021) 107013. Available from: https://doi.org/10.1016/j.polymertesting.2020.107013.

[100] S. Saedi, M. Shokri, J.T. Kim, G.H. Shin, Semi-transparent regenerated cellulose/ZnONP nanocomposite film as a potential antimicrobial food packaging material, J. Food Eng. 307 (2021) 110665. Available from: https://doi.org/10.1016/j.jfoodeng.2021.110665.

[101] Y.-H. Wen, et al., Antibacterial nanocomposite films of poly(vinyl alcohol) modified with zinc oxide-doped multiwalled carbon nanotubes as food packaging, Polym. Bull. (2021). Available from: https://doi.org/10.1007/s00289-021-03666-1.
[102] M. Naushad, T. Ahamad, K.M. Al-Sheetan, Development of a polymeric nanocomposite as a high performance adsorbent for Pb(II) removal from water medium: equilibrium, kinetic and antimicrobial activity, J. Hazard. Mater. 407 (2021) 124816. Available from: https://doi.org/10.1016/j.jhazmat.2020.124816.
[103] M.M. Fernandes, et al., Magnetoelectric polymer-based nanocomposites with magnetically controlled antimicrobial activity, ACS Appl. Bio Mater. 4 (1) (2021) 559−570. Available from: https://doi.org/10.1021/acsabm.0c01125.
[104] I.M. Factori, et al., ZnO nanoparticle/poly(vinyl alcohol) nanocomposites via microwave-assisted sol−gel synthesis for structural materials, UV shielding, and antimicrobial activity, ACS Appl. Nano Mater. (2021). Available from: https://doi.org/10.1021/acsanm.1c01334.
[105] N.A. Sirotkin, et al., Experimental and computational investigation of polylactic acid/silver-NP nanocomposite with antimicrobial activity prepared by plasma in liquid, Plasma Process. Polym. 18 (2) (2021) 2000169. Available from: https://doi.org/10.1002/ppap.202000169.
[106] G. Sahu, et al., Ionic liquid-assisted fabrication of poly(vinyl alcohol)/nanosilver/graphene oxide composites and their cytotoxicity/antimicrobial activity, Mater. Chem. Phys. 266 (2021) 124524. Available from: https://doi.org/10.1016/j.matchemphys.2021.124524.
[107] S. Anandhi, M. Leo Edward, V. Jaisankar, Synthesis, characterization and antimicrobial activity of polyindole/$ZrO_2$ nanocomposites, Mater. Today Proc. 40 (2021) S93−S101. Available from: https://doi.org/10.1016/j.matpr.2020.04.068.
[108] S.S.P. Kanagaraj, et al., Antimicrobial activity of green synthesized biodegradable alginate−silver (Alg-Ag) nanocomposite films against selected foodborne pathogens, Appl. Nanosci. (2021). Available from: https://doi.org/10.1007/s13204-021-01882-9.
[109] J. Sarfraz, T. Gulin-Sarfraz, J. Nilsen-Nygaard, M.K. Pettersen, Nanocomposites for food packaging applications: an overview, Nanomaterials 11 (1) (2021). Available from: https://doi.org/10.3390/nano11010010.
[110] B.A. Kehinde, N. Chhikara, P. Sharma, M.K. Garg, A. Panghal, Chapter 6 - application of polymer nanocomposites in food and bioprocessing industries. C. M. B. T.-H. of P. N. for in: I.A. Hussain (Ed.), Micro and Nano Technologies, Elsevier, 2021, pp. 201−236.
[111] E. Velásquez, et al., Effect of organic modifier types on the physical−mechanical properties and overall migration of post-consumer polypropylene/clay nanocomposites for food packaging, Polym. (Basel) 13 (9) (2021). Available from: https://doi.org/10.3390/polym13091502.
[112] R. Shams, Q.H. Rizvi, A.H. Dar, I. Majid, S. Khan, Nanocomposite: Potential nanofiller for food packaging applications, in: S.M. Sapuan, R.A Ilyas (Eds.), Bio-based Packaging: Material, Environmental and Economic Aspects, John Wiley & Sons Ltd., 2021, pp. 119−131. Available from: https://doi.org/10.1002/9781119381228.ch7.
[113] H. Esmailzadeh, P. Sangpour, F. Shahraz, A. Eskandari, J. Hejazi, R. Khaksar, CuO/LDPE nanocomposite for active food packaging application: a comparative study of its antibacterial activities with ZnO/LDPE nanocomposite, Polym. Bull. 78 (3) (2021) 1671−1682. Available from: https://doi.org/10.1007/s00289-020-03175-7.
[114] A. Arora, G.W. Padua, Review: nanocomposites in food packaging, J. Food Sci. 75 (1) (2010) 43−49. Available from: https://doi.org/10.1111/j.1750-3841.2009.01456.x.

[115] D. Dainelli, N. Gontard, D. Spyropoulos, E. Zondervan-van den Beuken, P. Tobback, Active and intelligent food packaging: legal aspects and safety concerns, Trends Food Sci. Technol. 19 (2008) S103–S112. Available from: https://doi.org/10.1016/j.tifs.2008.09.011.
[116] C. Silvestre, D. Duraccio, S. Cimmino, Food packaging based on polymer nanomaterials, Prog. Polym. Sci. 36 (12) (2011) 1766–1782. Available from: https://doi.org/10.1016/j.progpolymsci.2011.02.003.
[117] K.L. Yam, P.T. Takhistov, J. Miltz, Intelligent packaging: concepts and applications, J. Food Sci. (2005). Available from: https://doi.org/10.1111/j.1365-2621.2001.tb16112.x.
[118] T. Lan, Nanocomposite materials for nanocomposite materials for packaging applications packaging applications, January 2007.
[119] A. Bratovcic, A. Odobasic, S. Catic, I. Sestan, Application of polymer nanocomposite materials in food packaging, Croat. J. Food Sci. Technol. 7 (2) (2015) 86–94. Available from: https://doi.org/10.17508/cjfst.2015.7.2.06.
[120] ZF Friedrichshafen AG, Technical information high performance materials case study, pp. 5–6, 2012.
[121] A. Brody, 'Nano, nano' food packaging technology, Food Technol. 57 (2003) 52–54.
[122] R. Leaversuch, How to properly maintain aluminum injection molds | Plastics Technology, 2001. https://www.ptonline.com/articles/how-to-properly-maintain-aluminum-injection-molds (accessed 15.11.20).
[123] Manufacturing process provides low-cost, sustainable option for food packaging - Purdue University News. https://www.purdue.edu/newsroom/releases/2018/Q2/changing-the-grocery-game-manufacturing-process-provides-low-cost,-sustainable-option-for-food-packaging.html (accessed 21.11.20).
[124] Z.B.Z. Shawon, M.E. Hoque, S.R. Chowdhury, Nanosensors and nanobiosensors: agricultural and food technology aspects, Elsevier Inc, 2020.
[125] M. Ozdemir, J.D. Floros, Active food packaging technologies, Crit. Rev. Food Sci. Nutr. 44 (3) (2004) 185–193. Available from: https://doi.org/10.1080/10408690490441578.
[126] L. Xiao-e, A.N.M. Green, S.A. Haque, A. Mills, J.R. Durrant, Light-driven oxygen scavenging by titania/polymer nanocomposite films, J. Photochem. Photobiol. A Chem. 162 (2–3) (2004) 253–259. Available from: https://doi.org/10.1016/j.nainr.2003.08.010.
[127] C. Maneerat, Y. Hayata, Gas-phase photocatalytic oxidation of ethylene with $TiO_2$-coated packaging film for horticultural products, Trans. ASABE 51 (1) (2008) 163–168.
[128] A. Karpilov, Nanomaterials in food packaging: promise and potential peril [Online], pp. 1–18, 2006. Available at: http://www.iopp.org/files/public/RITkarpilovIPTAsubmission.pdf.
[129] H. Bouwmeester, et al., Review of health safety aspects of nanotechnologies in food production, Regul. Toxicol. Pharmacol. 53 (1) (2009) 52–62. Available from: https://doi.org/10.1016/j.yrtph.2008.10.008.
[130] A.K. Srivastava, A. Dev, S. Karmakar, Nanosensors and nanobiosensors in food and agriculture, Environ. Chem. Lett. 16 (1) (2018) 161–182. Available from: https://doi.org/10.1007/s10311-017-0674-7.
[131] J. Fu, et al., An Au/Si hetero-nanorod-based biosensor for Salmonella detection, Nanotechnology 19 (15) (2008) 155502. Available from: https://doi.org/10.1088/0957-4484/19/15/155502.

[132] D. Cui, et al., Effects of antisense-myc-conjugated single-walled carbon nanotubes on HL-60 cells, J. Nanosci. Nanotechnol. 7 (4−5) (2007) 1639−1646. Available from: https://doi.org/10.1166/jnn.2007.348.
[133] P. Dallas, J. Tucek, D. Jancik, M. Kolar, A. Panacek, R. Zboril, Magnetically controllable silver nanocomposite with multifunctional phosphotriazine matrix and high antimicrobial activity, Adv. Funct. Mater. 20 (14) (2010) 2347−2354. Available from: https://doi.org/10.1002/adfm.200902370.
[134] D. Restuccia, et al., New EU regulation aspects and global market of active and intelligent packaging for food industry applications, Food Control. 21 (11) (2010) 1425−1435. Available from: https://doi.org/10.1016/j.foodcont.2010.04.028.
[135] M. Smolander, The use of freshness indicators in packaging, in: R. Ahvenainen (Ed.), Novel Food Packaging Techniques, Woodhead Publishing, United Kingdom, 2003, pp. 127−143.
[136] Smart packaging, packaging that communicates - food. https://www.interempresas.net/Alimentaria/Articulos/30555-Envases-inteligentes-envases-que-comunican.html (accessed 21.11.20).
[137] G. Miller, R. Senjen, Nanotechnology in food and agriculture, pp. 417−444, 2010.
[138] W. Stonas, L.J. Dietz, I.D. Walton, M.J. Natan, J.L. Winkler, Method of manufacture of colloidal rod particles as nanobarcodes, US 6,919,009 B2, 2005.
[139] A. Hebeish, M. Abdelhady, A. Youssef, $TiO_2$ nanowire and $TiO_2$ nanowire doped Ag-PVP nanocomposite for antimicrobial and self-cleaning cotton textile, Carbohydr. Polym. 91 (2013) 549−559. Available from: https://doi.org/10.1016/j.carbpol.2012.08.068.
[140] E. Omanović, M. Maksimović, Nanosensors applications in agriculture and food industry, Bull. Chem. Technol. Bosnia Herzeg. 47 (2016) 59−70.
[141] T. Mahbub, M.E. Hoque, Chapter 1 - Introduction to nanomaterials and nanomanufacturing for nanosensors, in: K. Pal, F.G. de Souza (Eds.), Micro and Nano Technologies, Elsevier, 2020, pp. 1−20.
[142] Z.B.Z. Shawon, M.E. Hoque, S.R. Chowdhury, Chapter 6 - Nanosensors and nanobiosensors: agricultural and food technology aspects, in: K. Pal, F.G. de Souza (Eds.), Micro and Nano Technologies, Elsevier, 2020, pp. 135−161.
[143] M.C. Corrêa De Souza, M. De Toledo Benassi, R.F. De Almeida Meneghel, R.S. Dos Santos Ferreira Da Silva, Stability of unpasteurized and refrigerated orange juice, Braz. Arch. Biol. Technol. 47 (3) (2004) 391−397. Available from: https://doi.org/10.1590/s1516-89132004000300009.
[144] A. Emamifar, M. Kadivar, M. Shahedi, S. Solimanian-Zad, Effect of nanocomposite packaging containing Ag and ZnO on reducing pasteurization temperature of orange juice, J. Food Process. Preserv. 36 (2) (2012) 104−112. Available from: https://doi.org/10.1111/j.1745-4549.2011.00558.x.
[145] J. Xie, et al., Biodegradable poly(vinyl alcohol)-based nanocomposite film reinforced with organophilic layered double hydroxides with potential packaging application, Iran. Polym. J. (Engl. Ed.) 26 (11) (2017) 811−819. Available from: https://doi.org/10.1007/s13726-017-0561-x.
[146] J. Xie, K. Zhang, J. Wu, G. Ren, H. Chen, J. Xu, Bio-nanocomposite films reinforced with organo-modified layered double hydroxides: preparation, morphology and properties, Appl. Clay Sci. 126 (2016) 72−80.
[147] S. Wang, Y. Jing, Effects of formation and penetration properties of biodegradable montmorillonite/chitosan nanocomposite film on the barrier of package paper, Appl. Clay Sci. 138 (2017) 74−80. Available from: https://doi.org/10.1016/j.clay.2016.12.037.

[148] L. Xu, et al., Hydrophobic graphene oxide as a promising barrier of water vapor for regenerated cellulose nanocomposite films, ACS Omega 4 (1) (2019) 509−517. Available from: https://doi.org/10.1021/acsomega.8b02866.
[149] H. Liu, et al., Application of biodegradable and biocompatible nanocomposites in electronics: current status and future directions, Nanomaterials 9 (7) (2019). Available from: https://doi.org/10.3390/nano9070950.
[150] T.K. Gupta, B.P. Singh, R.B. Mathur, S.R. Dhakate, Multi-walled carbon nanotube-graphene-polyaniline multiphase nanocomposite with superior electromagnetic shielding effectiveness, Nanoscale 6 (2) (2014) 842−851. Available from: https://doi.org/10.1039/c3nr04565j.
[151] S.P. Pawar, S. Kumar, A. Misra, S. Deshmukh, K. Chatterjee, S. Bose, Enzymatically degradable EMI shielding materials derived from PCL based nanocomposites, RSC Adv. 5 (23) (2015) 17716−17725. Available from: https://doi.org/10.1039/c4ra10364e.
[152] Y.F. Shih, L.S. Chen, R.J. Jeng, Preparation and properties of biodegradable PBS/multi-walled carbon nanotube nanocomposites, Polym. (Guildf.) 49 (21) (2008) 4602−4611. Available from: https://doi.org/10.1016/j.polymer.2008.08.015.
[153] J. Robbens, et al., Eco-, geno- and human toxicology of bio-active nanoparticles for biomedical applications, Toxicology 269 (2−3) (2010) 170−181. Available from: https://doi.org/10.1016/j.tox.2009.11.002.
[154] A. Cockburn, et al., Approaches to the safety assessment of engineered nanomaterials (ENM) in food, Food Chem. Toxicol. 50 (6) (2012) 2224−2242. Available from: https://doi.org/10.1016/j.fct.2011.12.029.
[155] P.V. Asharani, Y. Lianwu, Z. Gong, S. Valiyaveettil, Comparison of the toxicity of silver, gold and platinum nanoparticles in developing zebrafish embryos, Nanotoxicology 5 (1) (2011) 43−54. Available from: https://doi.org/10.3109/17435390.2010.489207.
[156] D. Stampoulis, S.K. Sinha, J.C. White, Assay-dependent phytotoxicity of nanoparticles to plants, Environ. Sci. Technol. 43 (24) (2009) 9473−9479. Available from: https://doi.org/10.1021/es901695c.
[157] M. Kumari, A. Mukherjee, N. Chandrasekaran, Genotoxicity of silver nanoparticles in Allium cepa, Sci. Total. Environ. 407 (19) (2009) 5243−5246. Available from: https://doi.org/10.1016/j.scitotenv.2009.06.024.
[158] Y.N. Sundukov, First record of the ground beetle Trechoblemus postilenatus (Coleoptera, Carabidae) in Primorskii krai, Far East. Entomol. 165 (2006) 16. Available from: https://doi.org/10.1002/tox.
[159] B. Schmidt, V. Katiyar, D. Plackett, E.H. Larsen, N. Gerds, C.B. Koch, J.H. Petersen. Migration of nanosized layered double hydroxide platelets from polylactide nanocomposite films. Food Addit Contam Part A Chem Anal Control Expo Risk Assess. 2011;28(7):956−966. https://doi.org/10.1080/19440049.2011.572927. Epub 2011 May 24. PMID: 21614708.
[160] C. Buzea, I.I. Pacheco, K. Robbie, Nanomaterials and nanoparticles: sources and toxicity, Biointerphases 2 (4) (2007) MR17−MR71. Available from: https://doi.org/10.1116/1.2815690.
[161] Polymer nanocomposites market size, share and industry analysis - 2025. https://www.gminsights.com/industry-analysis/polymer-nanocomposites-market (accessed 23.11.20).
[162] Polymer nanocomposite market | 2020-2027 | industry report | Covid insights. https://www.mordorintelligence.com/industry-reports/polymer-nanocomposite-market (accessed 23.11.20).

[163] Polymer nanocomposites market size | industry analysis - 2022. https://www.allied-marketresearch.com/polymer-nanocomposites-market (accessed 23.11.20).
[164] Polymer nanocomposites market size hit US$ 31.8 Bn by 2026. https://www.globe-newswire.com/news-release/2020/02/20/1988215/0/en/Polymer-Nanocomposites-Market-Size-Hit-US-31-8-Bn-By-2026.html (accessed 23.11.20).
[165] Nanotechnology information statement. https://www.ifst.org/resources/information-statements/nanotechnology (accessed 23.11.20).
[166] M.T. Takeuchi, M. Kojima, M. Luetzow, State of the art on the initiatives and activities relevant to risk assessment and risk management of nanotechnologies in the food and agriculture sectors, Food Res. Int. 64 (2014) 976−981. Available from: https://doi.org/10.1016/j.foodres.2014.03.022.
[167] T. Singh, S. Shukla, P. Kumar, V. Wahla, V.K. Bajpai, Application of nanotechnology in food science: perception and overview, Front. Microbiol. 8. (2017). Available from: https://doi.org/10.3389/fmicb.2017.01501. Frontiers Media S.A.
[168] L.F. Fraceto, R. Grillo, G.A. de Medeiros, V. Scognamiglio, G. Rea, C. Bartolucci, Nanotechnology in agriculture: which innovation potential does it have? Front. Environ. Sci. 4 (2016). Available from: https://doi.org/10.3389/fenvs.2016.00020.
[169] IFST, Information sheet on nanotechnology, 2006.

# Carbon-based polymer nanocomposites for electronic textiles (e-textiles)

16

*Md. Rubel Alam*[1], *Tarikul Islam*[2], *Md. Reazuddin Repon*[3,4,5] *and Md Enamul Hoque*[6]

[1]Department of Knitwear Manufacturing and Technology, BGMEA University of Fashion and Technology, Dhaka, Bangladesh
[2]Department of Textile Engineering, Jashore University of Science and Technology, Jashore, Bangladesh
[3]ZR Research Institute for Advanced Materials, Sherpur, Bangladesh
[4]Department of Textile Engineering, Khwaja Yunus Ali University, Sirajganj, Bangladesh
[5]Department of Production Engineering, Faculty of Mechanical Engineering and Design, Kaunas University of Technology, Kaunas, Lithuania
[6]Department of Biomedical Engineering, Military Institute of Science and Technology (MIST), Dhaka, Bangladesh

## 16.1 Introduction

Electronic textile (e-textile) is a complex structure that is made of textiles having electrical properties. Nowadays e-textiles are so much popular in flexible smart textiles. E-textiles are more flexible and stretchable than other textiles [1,2]. Wearable e-textile technologies are gaining popularity these days. It earns so much acceptance from people for medical instruments, surgical machinery, military instruments, athletics dresses for its flexibility, stretch-ability, ultralight advantages. Its composites from ultralight electrical fibers give shining looks to the dress in the dark. Electrically conducting textiles include the insertion of metallic wires inside yarns, the coating of the surface with metals, and the use of conductive fillers through the formation of polymer nanocomposites [3]. Like many other applications [4–10], nanoparticles/nanofillers such as graphene (GN), carbon nanotubes (CNTs), metal nanowires, metal nanoparticles, and so on also contribute to the e-textiles by enhancing the electrical conductivity. However, the employment of these nanoparticles sometimes makes the textile substrates less flexible for daily use. To overcome these obstacles, plastic substrates have been tried, but some applications require better mechanical properties and more flexibility. So, the idea of producing electrically conducting textile materials has become important. Conductive polymer composites are generally manufactured through soaking, dip coating, casting, paste brushing on fabric, and inkjet printing. In conjunction with conjugated and nonconjugated polymers, CNTs are used. Carbon-based nanoparticles make up the majority of nanocarbons. Chemical and physical

**Advanced Polymer Nanocomposites. DOI:** https://doi.org/10.1016/B978-0-12-824492-0.00020-9

vapor deposition, laser procedures, and plasma-related processes are the most feasible methods for producing nanocarbons. Nanocarbons are extremely tiny, with diameters in the nm range. CNTs, GN, nanodiamonds, and other nanocarbons can be generically classed. When compared to inorganic nanoparticles, nanocarbons have many advantages. E-textiles provide a lot of potential for innovation. Nanocarbon modification, processing, and biocompatibility are the most important aspects of nanocomposites production. Nanocarbons have remarkable physical features that make them appropriate for different applications. Nanocarbons resulted in various unique morphological, conducting, and sensing capabilities in nanocomposites [11]. Every day, new textiles with features like heat regulation, luminescence, touch, and sensitivity are introduced to the market. These capabilities are applied in a variety of industries, including healthcare, sports, space exploration, and gaming. Drug delivery, biological imaging, fluorescence imaging, biosensing, capacitance, and electronics have all used nanocarbon-based nanocomposites. The foundations and future prospects of nanocarbons, particularly nanocarbon-based textile materials, have gained researchers' curiosity. Because of their unique features, nanocarbons and hybrid materials have attracted the interest of textile researchers. The application of nanocarbon-based nanostructures to construct functional textiles, as well as the exploration of their structure-property correlations, must be the focus of future advancements. The downsizing of electric circuits allows for seamless integration of functionalities, reducing the risk of a bionic stigma and allowing for greater market penetration of wearable e-textiles. On the other hand, e-textiles are a special source of concern after their useable product life span as causing global environmental and societal concerns due to the huge volumes of electronic waste (e-waste) generated. Ibanez-Labiano et al. commented that a mixture of relatively short-lived mass-consumer items, electronics, and textiles would produce e-waste including contaminated used textiles [12]. Recycling and disposal issues are likely to occur if electronic textiles are designed and mass-produced without regard for their end-of-life fate. E-waste typically comprises several hazardous compounds or precursors that can affect human health and the environment [13]. In addition, e-discharge contains nonrenewable resources such as precious metals and rare earth components, which have a significant environmental impact even before being used in products. Due to current e-waste issues, it is now widely recognized that electrical high-tech devices should be built to minimize negative effects during the end-of-life stage. End-of-life treatment and recycling are considerably less beneficial than waste prevention by design [14]. However, these procedures normally cause nanofillers to poorly adhere to the polymers and can be rinsed away during the rinsing process. Thus it is impossible to wash the composites. E-textiles can be used for a long time with good washability. This can greatly save costs, be less harmful and ecologically sound.

## 16.2 Functions of e-textiles

E-textile has tremendous work in the textile industry with enormous functions. It shows some good impact on textiles [15]. It has become a common necessity in our

daily life [16]. E-textile's major function is to give ultra-flexible, scalable, ultra-light, highly conductive power to the textile material [15]. Due to this type of advantages, e-textile is involved in the processing of many biomedical, solar cells, electrical antennas, etc. It has a tremendous sensing capability so that it solves the biological factors of textiles. It is now thought to be used in the therapy for its stimulation strength. Wearable electronic fabrics that gather and utilize capacitive energy can be employed in customized electronics is another new field where e-textiles are heavily exploited for energy storage in personal electronics. Lab-on-fiber technology allows for the enhancement of efficient, independent, multifunctional, actuation, mechanical, and biosensing arrangements in textiles. It also works on light-emitting diodes. Experts are now using micro- and nanoparticles in e-textile, and it gives a comfortable, flexible, wound dressing. The e-textile fibers which are acceptable in drugs are now used in drug invention. Finally, e-textiles are very much suitable for wearable sensors [11,17,18]. After all, e-textile fiber is used in electronic, photonic, communicating instruments. Therapeutic drugs and biological factors are also used in e-textile. How many types of reflects, tattoos are used in textile by the e-textile method which cannot be washed or removed with damages to the dresses? The new material, fiber, is designed to make the raised issue solved by new conductive inks, reflected fiber, adhesive, printing procedure, and many other technologies to develop our e-textile world. It has an extended area of functions that includes electrocardiography (ECG), pressure sensor, radio frequency identification (RFID), entre bridge, sail panel, and box rail protector [19]. Nanocomposite also helps polymer barrier technology [20]. Recently, GN−silver was mixed with other materials and made composite for e-textiles, and it gives the garment a more conductive ultralight printing color on its surface which looks gorgeous on textile [19].

## 16.3 Carbon-based materials for e-textiles

The importance of electronic wearable devices has brought great attention to e-textiles. Conductive and capable of sensing are e-textiles, as opposed to ordinary textiles. Wearable electronic devices could be useful in a variety of fields, including robotics, healthcare monitoring, and sports activity monitoring. Because carbon material composite has outstanding characteristics, it received great attention from researchers, and they introduce carbon-based nanoparticles [21]. Some conductive materials are used in fabricating electronic textiles, Carbon-based electronic textiles detect human motion and monitor human health because of their properties of flexibility and stress ability [22]. Carbon derivatives such as activated carbon (AC), GN, graphene oxide (GO), CNT, carbon fiber (CF), and carbon black (GB) have recently been developed. Its superior mechanical and electrical properties have become more important in e-textile applications [21]. AC and CNTs have been intensively explored for supercapacitor applications due to their unique combination of features, such as high surface area, electrical conductivity, controlled pore size

distribution, and superior electrochemical capabilities [23]. Carbon-based nanoparticles are lightweight, comfortable, and flexible, and because of these features, carbon-based electronic composites in the textile are the most favorable ones [24].

### 16.3.1 Carbon derivatives

Economical manufacturing of functional materials is an important factor for the long-term development of wearable e-textiles [21]. To create electronics textiles, researchers have experimented with a variety of conductive materials. CNT yarns have sparked interest due to their outstanding electrical conductivity and ultralightweight, making them suited for future applications in a variety of sensing and energy domains [25].

#### 16.3.1.1 Activated carbon

Because of its low cost and ease of processing, AC has been widely used as an electroactive material in supercapacitors [23]. It has a large surface area but few pores [21]. The quality of AC is determined by its surface area, pore structure, and pore size distribution. It was possible to attain a surface area of 1000−2000 $m^2\ g^{-1}$ and a pore distribution of 2−5 nm [23]. AC is made up of natural raw materials that are both inexpensive and widely available, such as agricultural waste, municipal waste slurry, and industrial waste slurry [21]. It is less expensive than other competing electrode materials and the material produced by the process of carbonization in low vacuum yielded [26]. Poly (phenylene isophthalamide) (Nomex), polyacrylonitrile (PAN), and poly (amic acid) have all been effective in producing activated carbon fibers (ACFs) [23]. Nitric acid has also been used to modify AC, resulting in the formation of hydroxyl and carbonyl groups on the carbon surface [26]. Because of its decreased polarization, it was also changed with semiconducting material mixing, such as titanium oxide [22]. It has numerous exciting characteristics, but it has limited electricity storage due to its narrow pore structure and shorter path length, despite its excellent charge storage capability [27]. To make conductive fabrics, it is used in classic dip coating and screen-printing processes [23]. Different levels of activation of CF are shown in Fig. 16.1.

#### 16.3.1.2 Graphene

At present, GN has achieved great interest in carbon-based nanocomposite in e-textile. GN structure has excellent electrical and high thermal conductivity [21]. Its features include a large surface area, strong charge carrier ability, outstanding mechanical qualities, unique electromechanical stability, and exceptional flexibility [23]. GN fibers are produced from GO suspension [29]. A simple reduction of propylene carbonate at a high temperature (150°C) created GN [30]. Flexibility is one of the most significant characteristics of textiles since it allows the structure to be worn [31]. In terms of comfort, if the material is harsh, it is not suitable for clothes. It is strong due to its hydrophobic nature and strong contact between GN sheets

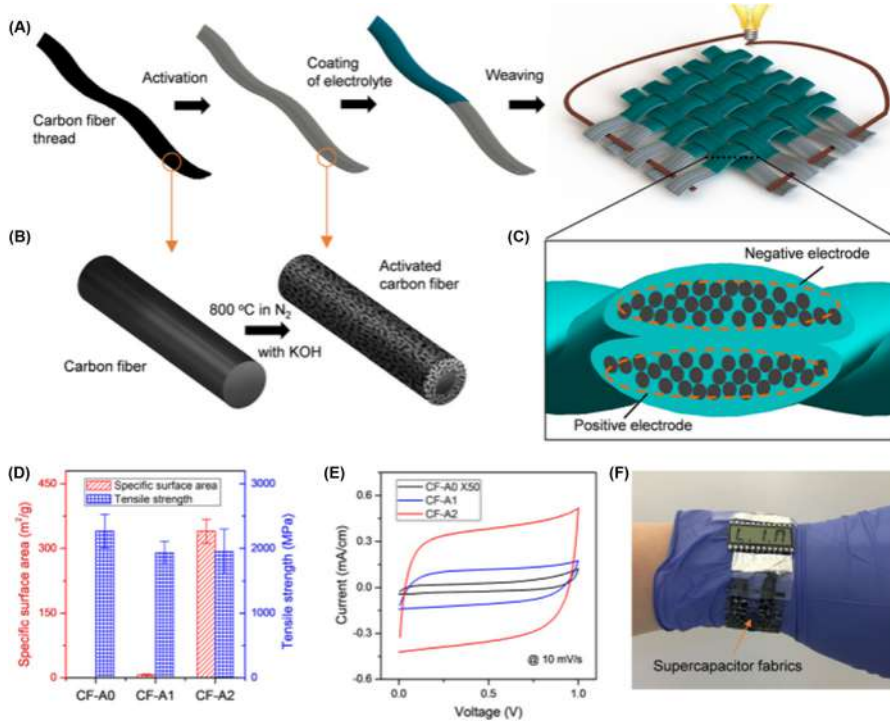


**Figure 16.1** (A) AC-based load-bearing supercapacitor fabrication; (B) activation of nanoporous carbon fiber; (C) cross-section of positive and negative electrode; (D) carbon fiber surface area and strength properties at different activation [28].

[23]. But due to its insoluble and nonmelting mechanical properties, GN has a low processing capability [32]. Creating high-performance flexible conduct in textile-like fiber, yarn 2D GN is used as a component [11]. Recently, due to its theoretical and practical advantages including high conductivity, huge surface areas, high mechanical strength, and cheap manufacturing costs, the focus has become GN-based material [26]. Flexible GN fibers, a new type of fiber-like material, have excellent strength, electrical and thermal conductivity [23].

### *16.3.1.3 Graphene oxide*

E-textiles with cotton, polyester (PES), nylon, and silk can be used for GO coating [31]. To apply GO to the textiles, vacuum filtration, simple dipping, screen printing, spraying, and blade coating were used [33]. The electrical conductivity of e-textiles is generated by the reduction of GO using heat treatment (HT), chemicals, or electrochemical methods. The use of GO in a range of applications, including electronic textiles, has grown in prominence. Liquid crystalline dispersions of GN were also used to make GN fibers and yarns [11]. The hydroxyl, carbonyl, and other oxygen functional groups of GO, as well as their numerous diminutions, are well

understood, allowing GO to display a wide range of behaviors [34]. A few examples are supercapacitors, membranes, sensors, and solar cells [23]. Because of the functional groups, GO can be coated on a variety of materials [35]. Electrical and thermal conductivity, mechanical strength, and electrochemical performance have all been enhanced by GN-conducting composites [26]. Polymers are conducting with large capacity and conductivities and are also quick to load and unload kinetics. The e-textile products are GO-coated commercial textiles, GO-coated cotton, GO-coated PES, and GO-coated nylon [36]. GO-coated cotton, PES, and nylon have demonstrated conduct [37]. Bovine serum albumin was used as an electrostatic adhesive between GO and commercial fabric for coating GO on nylon, PES, and cotton [35].

#### 16.3.1.4 Carbon nanotube

Due to their outstanding properties, CNTs have made a revolution in the application of supercapacitors of carbon-based materials [23]. Chemical and mechanical stability, larger volumetric currents, high heterogeneous transfer rates, and high conductivity are all characteristics of CNT. CNTs are incredibly light and are highly conductive, making them perfect for electronic textile uses [34]. With their great electric conductivity, exceptional thermal stability, high tensile strength, and low density, CNTs have recently proven to be appealing in electronic textiles [26]. A CNT-based supercapacitor showed unusual special capacitation of its original specific capacity after 1000 loading/discharge cycles [21]. Single-walled nanotubes (SWNT) and multi-walled nanotubes (MWNT) are the two fundamental structures of CNTs [38]. Wearable activity sensors built of CNTs are highly stretchy and flexible. The most prevalent methods for manufacturing CNTs are arc discharge, laser ablation, and chemical vapor deposition (CVD). CVD has grown in popularity in recent years because of the lower temperature (800°C) required compared to other methods [21]. Contrary to conductional carbon coatings, CNT fibers were found to be adequate temperature sensors as their strength remained unchanged substantially after repeated bending.

#### 16.3.1.5 Carbon black

CB is another all-embracing carbon-based conductor which has lately gained numerous advantages in e-textile production [23]. Due to its high energy conductivity, low prices, vast production potentials, improved chemical and thermal resistance, high flexibility, and easy chemical operation, CB has been widely used in wearable sensors [34]. Pure graphite, dried wood, sawdust, coconut shell, seashell high-density polyethylene, and benzene are some of the raw ingredients used to make CBs [22]. Metal nanoparticles could be used to separate the carbon sheets in the electrode, while also acting as a conductive channel for charge transport, improving specific capacitance and electrochemical stability [23]. Screen printing of CB is preferred to dip coating, according to the researchers [26]. In addition to

the flexibility of electrochemical processing, CB has a high load density per unit volume and is easier to synthesis [23].

#### 16.3.1.6 Carbon fiber

Using a pressure-sensitive capacitive sensor, CFs can be used to build arrays with a resolution defined by the distance between the strands [24]. High-temperature carbonization of acrylic fiber results in a very robust lightweight synthetic fabric [21]. CF is also fabricated using liquid crystalline dispersion [34]. Polypyrrole and polyaniline (PANI) are the most frequent leading CFs used in supercapacitors (PANI) [23]. CF is also manufactured using liquid crystal dispersion [37]. It is an appropriate blend of microspores and mesopores for quick ion mobility and high conductivity. CFs are extremely strong, thin fibers, whereas carbon crystals are honeycomb-shaped molecules made up of long chain-like molecules of pure carbon [24]. This can be used as a supercapacitor due to having high electrical conductivity. CFs having a diameter of 0.25 mm can also be effectively transformed to supercapacitors of 1−2 mm diameter by combined treatments of PVA (polyvinyl alcohol)/$H_3PO_4$ polymers.

## 16.4 Fabrication techniques

The incorporation of carbon compounds into textile materials via a variety of processes increases the use of conductive textiles in smart textiles. Textile circuits are built up of conductive channels, sensor elements, electrodes, and discrete components that are sewn or stitched together (e.g., resistors and capacitors). This is a common application for many textiles and yarns. These fantastic circuit elements can also be made using a variety of fabrication processes. The ideal material for sewing, bending, and wearing would have electric-charge properties that could be adjusted to any degree. Two fundamental methods are used to create conductive textiles (nonconductive substrate covered with conductive solution textiles available in fiber, yarn, and composite fabric form). Some examples of forming e-textiles are fiber, yarn or fabric extruding through carbon solution, carbon aerogel spinning, CVD, yarn wrapping on basic yarn, yarn twisting, etc. [39].

### 16.4.1 Fiber-based fabrication

A procedure of hummer is used for homogeneous graphic oxide in high concentration (18 mg $mL^{-1}$) (GO), which is then combined with CB under ultrasonic condition-controlled agitation. The solution was then injected down a glass tube at a specified boiling (90°C) temperature and speed, then dried in a furnace at 1000°C and cooled to produce conductive fibers [40]. Electrically producing textile fibers are often solution trimmed from semiconducting polymers, CNTs, and 2D materials quite GN and MXenes [41]. An existing physical or synthetic textile cloth shall be tinted, covered, or printed on an hourly basis with electrolytic material to form

a conductive textile [42]. Individual cotton fibers are equally coated with rGO and retain the equal porosity of cotton fabric on each side of the material during padding. The mechanical perversity of the three-dimensional conducting fibers controls the resistance change [43]. The carbon staple fiber yarn is embedded during a sheet of green wool, and continuous lengths of the CF current collectors are often knitted [38].

### 16.4.2 Yarn-based fabrication

The wet spinning method was used to create innovative stretchy composite fibers made of MWCNTs and thermoplastic polyurethane. This new class of highly mechanical embedded fibers could pave the way for smart textiles and artificial intelligence applications [44]. Melt spinning is not a possible approach for conducting fiber spinning [3]. Regardless of their diameter, conducting fibers can be formed by three different methods solution spinning with a stable homogeneous highly concentrated conducting polymer solution (10−30 wt.%), solution spinning with a heterogeneous less concentrated polymer solution in which an insulating polymer is used for better mechanical properties, and coating of conducting polymers on fibers from a dilute solution or interfacial polymerization [3]. CNTs and polyelectrolytes are coated on the cotton thread. To generate polymer-based conductive yarns, two practical ways are commonly employed: coating and spinning. The superior conductive powder is mixed with a suitable polymer in the melt of solution spinning to form conductive yarn. The carbon-based conductive yarn produced by spinning technology is depicted in Fig. 16.2.

### 16.4.3 Fabric and garment-based fabrication

Washed degummed Bombyx mori silk yarn immersed into an air-tight CNT/HEIP (Hexafluoro isopropanol) paint and dried at 70°C for the strong bond formation. The experiment was carried out using a chemical hood with additional alertness. This conductive fiber can be used in fabric preparation [45]. MWCNTs containing silk fabric were fabricated by a depositing and microdissolving method. An ultrasound bath was used for 30 minutes at room temperature to have a solution with sodium dodecyl benzenesulfonate (SDBS). The solution was then thinned to the silk fabric and sooner was immersed into ethanol-containing formic acid. Specific heat volatilizes the alcohol and resulting formic acid converts the silk fibroin toward natural adhesive. For applications in soft flexible e-materials, CSF had a high electrical conductivity (468-ohm $cm^{-1}$) and was long-lasting [46]. MWCNT-silk fabric (CSF) and patterned conductive MWCNTs@silk fabric were made effectively (shown in Fig. 16.3) for flexible and heating devices.

Fascinating material CNTs are applied through electrospinning processes and are also used to fabricate next-generation electronic textiles. All of the smart fabrics that use the piezopolymer fibers mat have membrane design, modified shape dispersed, and energy harvest. Piezoelectric poly (vinylidene difluoride) polymer solution mixed with CNTs solution at various percentages and then processed through

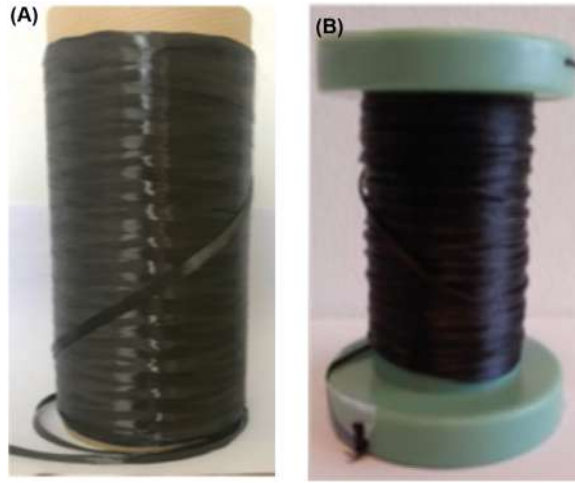


**Figure 16.2** Yarns conductive: (A) carbon fiber and (B) yarn containing carbon nanotubes [32].

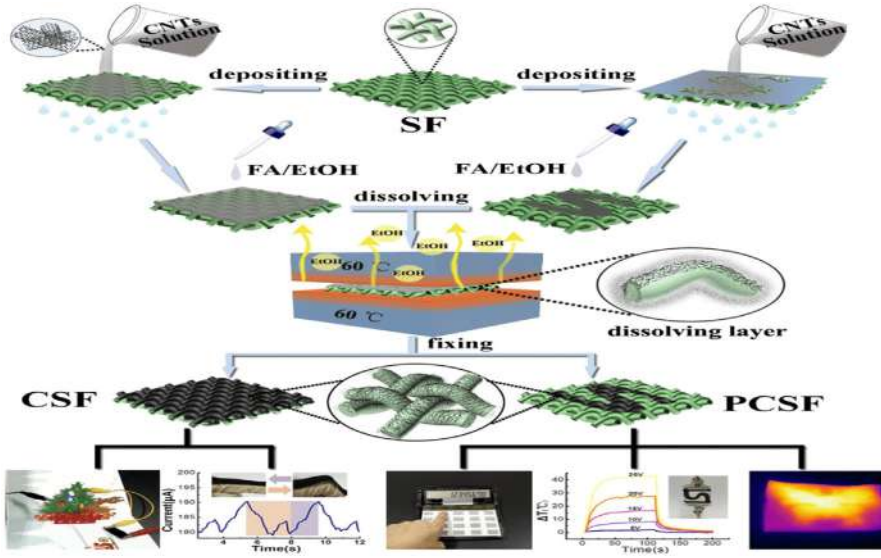


**Figure 16.3** Fabrication process and applications of CSF and PCSF [46]. *CSF*, MWCNT-silk fabric; *PCSF*, patterned conductive MWCNTs@silk fabric.

an electrospinning technique for the engineering applications [47]. Electrospinning of various CB rations with PAN demonstrates improved thermal and electrochemical activity [48]. Layer-by-layer CNTs are used by electrospinning techniques for

the manufacturing of flexible sensor-type materials without the use of any binder. The utility of porous structures in real-time detection is increased as a result of this approach [49]. The most common method for creating flexible and lightweight electronic textile is to use a low-cost dip coating method. Dip coating is the technology used to immerse and remove textiles from a liquid chemical so that a very thin layer can be applied on the surface of the material [50]. Recent research publications for applications like bending sensors and power storage have been published on the successful characterization of e-textiles created utilizing the dip-coating process [51]. The GN and MWCNT solution at a low speed was conveyed via a cotton fabric strip. Conductive textiles with a plate resistance of 33.2 ohms $Q^{-1}$ and 29.8 ohms $sq^{-1}$, respectively, were obtained from the MWCNT layer and GN. The resistance to fabric remained practically constant after the water and other organic solvents were washed and toned.

MWCNTs-SDBS solution with PVA mixture is stirred uniformly and applied by a pad-dry-cure technique. Briefly, toluene, ethanol, and water-washed cotton stripes are immersed and submitted to a padding process several times followed at 100°C drying for achieving good deposition. This approach will boost the high-tech application of e-textiles [52]. Pad-dry application of CB on cotton fabric for electrically conductive textile is scalable and simple. The coated cloth is flexible and washable, and it can monitor the human body, according to the findings [31]. Another work uses a pad-dry coating technique to apply SWCNTs to a polydopamine (PDA)-treated textile. Speaking, drinking, walking, bending of the finger and knee, and other actions have all been shown to be conceivable [53]. The reduced GO (rGO) of tea carbon has been consistently placed on the tightly woven fabric and then squished into a flexible wearable textile molding [54]. Figs. 16.4 and 16.5 show the facile fabrication of CNT-PDA-cotton composite fabrics provides a novel and simple framework for improving garment wearable electronics and heaters.

The above figures represent the synthesis of carbon dots from tea and fabrication with rGO for a pilot study. Under consistent high-speed striation, *N*-[3-(triethoxysilyl) propyl] ethylenediamine (EDAES68 L) and ethanol were mixed with a two distinct CNT solution (0.5 mg, 0.2 mg $mL^{-1}$) (132 L). The wetting agent Invadine PBN was then blended within using ultrasonication, and thickening was utilized under certain conditions. The paste was now applied to a cotton cloth using a knife-over-roll multilayer approach. The fabrics are excellent for biomedical signal processing, healthcare, sports, and military applications, according to the findings [55]. Fig. 16.6 shows that the knife over roll paste coating is an effective printing process.

The use of simple, economical, scalable approaches for mass manufacture of conductive natural fiber fabrics is examined with the graphene nanoplatelets and CB coatings for conducting cotton and conductive wool. The high-performance portable sensor tracks several movements of human beings including finger, wrist, and knee joints and acoustic identification [56]. Inkjet printing is a method of applying ink to a large area of textiles that is both automatic and regulated [57]. Without the use of masking or stencils, it is feasible to print practical patterns on textiles [51]. Inkjet printing is a multifaceted and cost-effective way to print thin

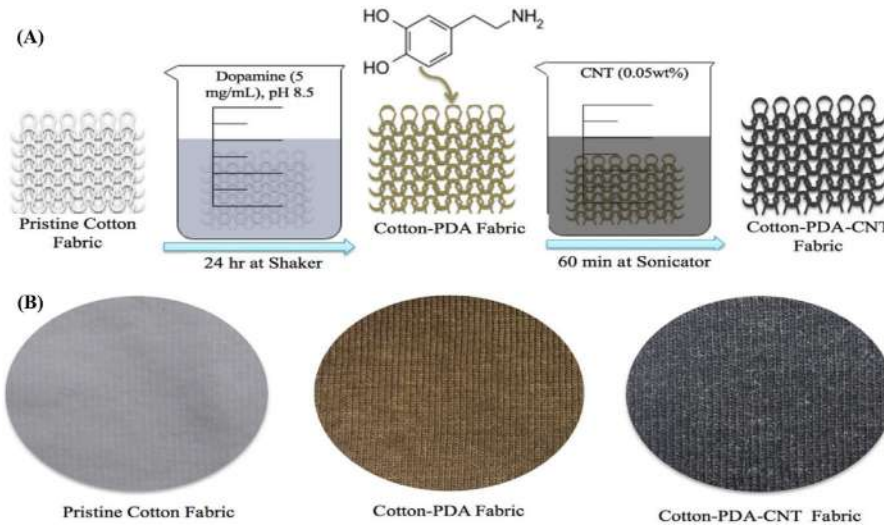


**Figure 16.4** (A and B) Dip-coating technique by CNT-PDA on cotton fabric [53]. *CNT*, Carbon nanotubes; *PDA*, polydopamine.

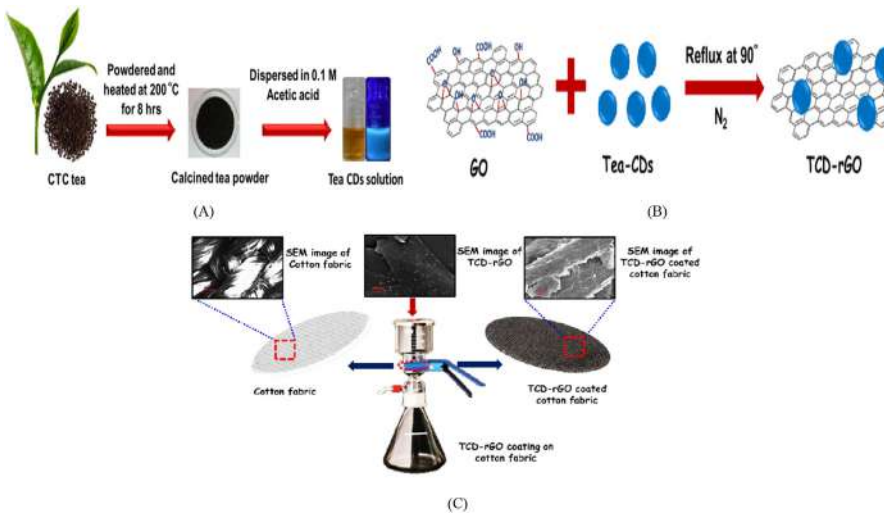


**Figure 16.5** (A) Carbon-dots synthesis from tea; (B) synergistic effect of TCD-rGO; (C) fabrication technique [54]. *TCD-rGO*, Reduced graphene oxide of tea carbon.

films with conductive carbon inks [58]. It has been used to print circuits in a large area with great success [59]. Inkjet-printed conductive materials are used to create wearable sensors, antennae, conductive channels, and energy equipment such as batteries, supercapacitors, ultracapacitors, and solar cells [60]. Further, because of

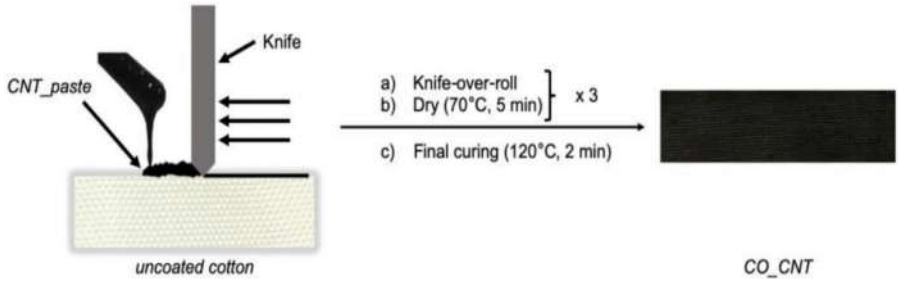


**Figure 16.6** Knife-over-roll coating findings [55].

the lesser inks waste, while printing, drop-on-demand may be a preferable choice for conductive ink printing [61]. Spray coating is a versatile, area-specific process that permits a precisely regulated amount of carbon to be uniformly sprayed on the cloth [62]. Pneumatic pressure and therefore lateral material movement concerning the fixed head are typically used to provide a uniform thickness of the film by use of spray-coating features [63]. The interface layer is needed to provide an adequate support layer with the following spray-coated active layer, and operating temperature can influence the functioning of the operating material [64]. The procedure of controlled spray coating was used to supply the material surface with a special amount of carbon solution [63]. Intriguingly, the diverse intrinsic mechanical characteristics of woven and knitted textiles are exploited to exhibit textile actuators to be used as artificial muscles with stiffness (woven fabric) [65]. The woven cotton fabric showed the minimum quantity of alternative within the electric resistance over an elaborate period of cyclic tensile tests [50]. Preliminary knitting of the welded cotton strands turned out to be just too breakable to face up to machine treatment. The knitting needles frequently cross the material even with slow speeds instead of forming knitting loops [66]. Yarn-based embroidered conductive materials have a lot more promise than weaving and knitting since they can combine numerous layers in one step. Because conductive yarn must follow physical location, there is a lack of homogeneity in resistance due to the imprecise gaps between the yarns, thus weaving and knitting are not suited for functional electrical stimulation [67]. However, the ES 65 Designer software embedded computerized embroidery machine (MEYAG model 912) was used to fabricate conductive material with a zigzag stitch and straight stitch pattern for integrating sensors, data processing, storage, and transmission circuitry in clothing, resulting in increased patient comfort, mobility, and privacy [68]. Stitching is a versatile and accurate method for producing leading fabrics or garments, which require careful management of the speed of stitching, length of the stitch, pretension thread, and direction of sticking [69]. The strands that carry electricity popular method of inclusion is to sew conductive strands into operable textile threads [70]. To achieve desirable electrical properties, electronic devices are frequently created out of the conductive thread by stitching thread fibers in designs with many crossings [11]. Electrodes are made by combining conducting yarns, which are silver-coated fibers, into a textile substrate using

an embroidery technique [71]. Because piecework is time-consuming and inaccurate, we have relied on the e-embroidery, or numerically controlled embroidery with conductive thread, as our principal method of circuit patterning. In the textile industry, the building of a state of art that precisely controls the planning, layout, and stitch pattern of circuits through computer-assisted design (CAD) processes, and used business stitch processes to sketch patterns that outline traces of a circuit, component connection pads, or sensing surfaces [72]. Embroidering electrical thread into textile surfaces is a typical method. This method stitches patterns that demarcate circuit lines, component connection pads, or sensor surfaces using CAD tools [73]. The lock stitch embroidered machine is the simplest procedure to incorporate conductive yarns in the fabric but it needs flexible thin yarn with sufficient strength to be withstand during process. So tailed fiber placement is another method for very stiff yarn concorporation with the help of zigzag stitch.

Screen printing is a cost-effective, flexible, and breathable technology that is also less cytotoxic and biocompatible. A four-layer carbon-loaded silicone rubber paste was applied to a poly/cotton blended fabric, then dried and cured for use in a variety of medical applications, including aid and rehabilitation in both clinical and home settings [67]. Screen-printing technology was employed in the creation of a textile condenser (nine samples of cloth) with conductive and dielectric inks. Criteria such as conductive dough type, viscosity, solids, and printing settings must be controlled based on the results to obtain maximum performance [74]. One of the most extensively utilized ways for generating practical designs on fabrics is screen printing [21]. Ink viscosity, binder, mesh no and mesh materials quality, such as surface ruggedness, porosities, and weight resistance, are dependent on the lifetime of the printed screen electronics [75]. On the other side, brush-paint is an adaptable, affordable pilot method and a fast technique in the manufacture of a carbon pack on a cloth. Ultra High Frequency passive RFID tags are fitted on a flexible elastic band with carbon-based stretch antennas. The RFID tags' wireless performance is similar to the silver expandable RFID tags. The results show that antennas with carbon tags and silver tags are not efficient but are sufficient for a range of built-in RFID textiles rating from 2 to 2.4 m [44].

## 16.5 Characterization techniques

The vastly expanding topic of textile-integrated conductive materials or electronics e-textiles is electronic goods with extra textile-specific needs as a result of integration into a textile foundation. In reality, these wearable e-textiles should be used on or near your body. Depending on the application, changes in their characteristics such as tensile, bending, shear, torsion, or compression stress must be observed. To assure the well-being of the users, suitable quality control procedures are used. The absence of standardization of e-textiles is regarded as a major impediment to industrial progress. Although the e-textile industry has always been eager to develop products with improved effectiveness and safety, its efforts could well have fallen

short of analyst estimates due to the lack of specialized standardized test techniques. There are now just a few standards defined expressly for e-textiles. The majority of the existing ones, including ISO/PRF TR 23383 and ASTM D 8248:2020, are concerned with language or definitions. Others, such as AATCC 76 for fabrics, AATCC 84 for yarns, and CSN EN 16812 for conductive tracks on textiles, give resistance measuring procedures for textile-based goods. IPC-8921 is a standard that specifies the language and provides options. There are additional efforts to address the lack of e-textile standards [54] (Table 16.1).

**Table 16.1** Current, proposed, and external e-textile standards [76].

| | Identification | Title | Year |
|---|---|---|---|
| Existing standard | DS/CEN/TR 16298 | Smart/intelligent textiles, categorization, applications, and standardization need | 2012 |
| | ASTM D 8248 | Standard terminology for smart textiles | 2020 |
| | AATCC 76 | Electrical resistivity of fabrics surface | 2018 |
| | AATCC 84 | Test method for electrical resistance of yarns | 2018 |
| | CSN EN 16812 | Electrical resistance of conductive materials | 2016 |
| | IPC-8921 | Prerequisites for conductive fibers, conductive yarns, and/or wires in woven and knitted electronic fabrics | 2019 |
| Upcoming standards | IEC 63203 204-1 | Resistance to washing for leisure and sportswear | 2022 |
| | IPC 8981 | Quality and reliability of e-textiles wearables | 2022 |
| | IPC 8952 | Design standard for printed electronics on coated or treated textiles and e-textiles | - |
| | IPC 8941 | Guideline on connections for e-textile | - |
| External standard for e-textiles wash testing | ISO 6330 | Home washing and drying procedures | 2012 |
| | ISO 105-C01 | C01: Color fastness to washing | 1989 |
| | ISO 15797 | Workwear washing and furnishing | 2017 |
| | DIN 54015 | Colorfastness assessment of dyeing and printing in the presence of peroxide | 2017 |
| | AATCC 6 | Fastness to acids and alkalis | 2016 |
| | AATCC 61 | Colorfastness to laundering: accelerated | 2013 |
| | AATCC 135 | Fabric dimensional alterations after home laundering | 2018 |

### 16.5.1 E-textile standardization

Standardization tests are performed on e-textiles to assess their electrical, mechanical, thermal, and optical properties (Table 16.3). The ASTM WK61479 test technique is used to assess the durability of an electroconductive textile exposed to sweat, whereas the ASTM WK61480 test method determines the durability of an e-textile exposed to washing and drying cycles [55,77]. AATCC RA111 has released new test methods AATCC TM210 and AATCC EP13 for measuring electrical resistance after several exposures to washing, perspiration, UV radiation, dry cleaning, wetness, seawater, and other factors in a single technique. The European Standard CEN EN 16812:2016 is used to determine the linear electric resistance and ohmic behavior of conductive tracks for textile constructions. IEC 63203-204-1 describes leisure and sports equipment testing techniques that have components and electrically conductive sensors that collect user data. To determine the electric resistance of conductive materials in garments in simulated microclimate IEC 63203-201-3 provides a test procedure. CEN EN 16806-1 is the method used to measure the heat storage and thermal release capacities of textile fibers, yarns, and textiles with PCM (phase change material), as well as the phase change temperature (phase change materials). Its test methodologies of Parts 2 and 3 shall be utilized to determine the heat transfer characteristics of textile fabrics and heat transfer of PCM-containing materials between the user and textile commodities. The accuracy of wearable glove-type motion sensors may be provided by adhering to the standard IEC 63203-402-1 without regard to device technology or size (Table 16.2).

Table 16.3 summarizes various research studies on the washing durability of carbon-based functionalized e-textiles. The application of international and US standards techniques to the laundry durability of carbon-based functionalized e-textiles is presented in Table 16.3.

## 16.6 Applications

Carbon-based e-textiles are widely used because of their remarkable performance in terms of flexibility and extensibility. Carbon-based materials that are suited for wearable applications have excellent electrical conductivity, lightweight, good chemical and thermal endurance, inherent and mechanical flexibility, facile chemical modification, low cost, and mass production possibilities. This section will cover the use of carbon-based materials in e-textiles.

### 16.6.1 Fiber-based applications

Fiber-based applications of carbon conductive materials are still in their early phases but research works are being conducted to enhance fiber-shaped wearable devices. To produce electrical energy, a fiber-shaped nanogenerator is used to store mechanical energy. A research group, Wang and co-workers exploited this approach to design a power generator using ZnO-coated CFs. Because of the continuous airflow, the power generator produces an AC output with an average current and voltage of 1.5 mV and 0.5 nA, respectively.

**Table 16.2** Standard test methods (existing and in development) for electrical, thermal, mechanical, optical, and physical properties of e-textile.

| E-textile properties | Test methods | Title | Ref. |
|---|---|---|---|
| Electrical | ASTM WK61479 | Durability of textile electrodes exposed to perspiration (in development) | [78] |
| | ASTM WK61480 | Durability of textile electrodes after laundering (in development) | [79] |
| | AATCC RA111(a) | Electrical resistance of electronically integrated textiles (in development) | [80] |
| | AATCC RA111(b) | Electrical resistance changes after home laundering (in development) | [81] |
| | CEN EN 16812:2016 | Linear electrical resistance of conductive tracks | [82] |
| | IEC 63203-204-1 | Washable durability for leisure and sportswear e-textile system (in development) | [83] |
| | IEC 63203-201-3 | Electrical resistance of conductive textiles under simulated microclimate (in development) | [84] |
| | IEC 63203-250-1 | Snap button connectors (in development) | [85] |
| | IEC 63203-201-1 | Basic properties of conductive yarns (in development) | [86] |
| | IEC 63203-201-2 | Basic properties of conductive fabric and insulation materials (in development) | [87] |
| Thermal | CEN EN 16806-1:2016 | PCM—heat storage and release capacity | [88] |
| | CEN EN 16806-2 | Heat transfer using a dynamic method (in development) | |
| | CEN EN 16806-3 | Determination of the heat transfer between the user and the product (in development) | |
| | IEC 63203-406-1 | Measuring skin contact temperature (in development) | [89] |
| Mechanical | IEC 63203-401-1 | Stretchable resistive strain sensor (in development) | [90] |
| | IEC 63203-402-1 | Finger movements in glove-type motion sensors (in development) | [91] |
| Physical | IEC 63203-402-2 | Fitness wearables—step counting (in development) | [92] |
| Optical | IEC 63203-301-1 | Electrochromic films for wearable equipment (in development) | [93] |

*PCM*, Phase change material.

**Table 16.3** Research papers investigating the durability of washing of carbon-based functionalized e-textile [37].

| Standard method | Fabric structure and fiber content | Methods | Results | Ref. |
|---|---|---|---|---|
| International | Woven, 100% cotton | ISO 105 C10:2006A; 5 g $L^{-1}$ soap at 40°C, for 30 min | Surface electrical resistivity increased following washing: 0.19 MΩ/square and 0.26 MΩ/square to 1.75 MΩ/square and 2.39 MΩ/square for knit and woven, respectively. | [94] |
| | Knit, 100% cotton | | | |
| | Dipped in graphene oxide, chemically reduced | | | |
| | 3/1 twill, 100% cotton treated with reduced graphene oxide | ISO BS EN 105 C06; 4 g $L^{-1}$ reference detergent, 10 stainless-steel balls at 40°C for 30 min | Electrical resistance increased from 36.94 to 70.32 KΩ/square after first wash; 139.09 KΩ/square after 10 washes | [50] |
| | Plain knit, 100% cotton spray-coating layer by layer of graphene solution | ISO 105-C03 | Surface resistance increased after wash | [95] |

(*Continued*)

**Table 16.3** (Continued)

| Standard method | Fabric structure and fiber content | Methods | Results | Ref. |
|---|---|---|---|---|
| United States | Plain woven, 100% polyester, treated with reduced graphene oxide | AATCC 61−2 A, 50°C for 30 min, liquor ratio 1:50 with AATCC soap, 5 cycles | Surface and volume resistivity increased | [96] |
| | Plain woven, 100% cotton, treated with graphene nanoplate and polyurethane dispersion | AATCC 61-2006; 500 mL (75 mm × 125 mm) stainless-steel lever lock canisters; 200 mL standard detergent with 10 steel balls | Surface electrical resistivity increased from $2.94 \times 10^{-11}$ Ω/m to $3.35 \times 10^{-11}$ Ω/m after 10 washes | [97] |

When this power generator is attached to the wrist, it may also be powered by the heartbeat [98]. In recent years, biofuel cells have gained popularity due to their sustainability and green environmental impacts, since they can harvest energy by employing biocatalysts such as enzymes or microorganisms derived from green and sustainable sources [99,100]. Mano and colleagues used amorphous microfibers as anodes when modified by glucose (GOx) or as a cathode when modified by bilirubin oxidase in the development of fiber-shaped biofuel cells [101]. Compared with the CF electrode, the CNTF electrode has oxygen reduction densities four times greater and a positive potential four times higher. The use of CNT-PEDOT discolored composite fiber in biofuel cells has increased fiber-shaped BFC's performance to 2.18 mW $cm^{-2}$ [102]. Any electronics device needs an energy storage unit to drive it. For wearable electronics with increased energy densities, wearable power storage units such as Li-ion batteries are essential. Ren et al. employed MnO2/CNT composite fiber twisted with lithium wire to prepare a fiber-shaped lithium-ion half-cells battery. The battery showed a special discharge current of 0.5 mAh of $<100$ mAh $cm^{-3}$ [103]. In another work, CNTF composite fiber was used to develop wearable batteries. When 38.1% of Si is deposited using a CNTF composite fiber battery, the performance has been improved to 1670 mAh $g^{-1}$ [104]. Different CNT-based composite fibers are produced for supercapacitors with a volumetric capacity of 25 to 48.5 F $cm^{-3}$ ([67,105]; Ren et al., [106]). The wound of elastic fiber aligned CNT sheets have also been created. This stretchy supercapacitor has a specific capacity of 18 f $g^{-1}$ and occurs after 100 washing cycles by 75% [107]. Wang and colleagues used a superfiber conveyor with a flexible triboelectric generator to collect mechanical energy. A bridge corrector has been used to load the supercapacitor to change the alternating current into a

direct current. In 5 seconds the supercapacitor may be loaded to 2.4 V and voltage can be increased by hand [108]. Hydrocarbon-fiber-shaped electrodes (CNTF), electrochemically inactive, organic, or inorganic are modified by glucose and used for glucose detection [109,110]. Various fiber-based applications are shown in Fig. 16.7.

### 16.6.2 Yarn-based applications

In the e-textile business, carbon-based conductive yarns are employed in many applications. The use of carbon-based conductive yarn for health monitoring sensors, power devices, actuators, and other applications has been the subject of numerous studies. Even though all of these studies are in their early stages, they will open up enormous opportunities for the e-textile sector. Dinh and colleagues created a CNT yarn-based thermal sensor as wearable electronics for humans in a research project [111]. To manufacture this device, extensible CNT yarns serve as very solid and lightweight thermal wire, as an electrode a graphite pencil, and as stretchable substrates pure and durable bioreusable paper. This sensor built on CNT yarn can monitor breath rates and assess respiratory disorders in real time. A temperature detector was also installed in the same device, which could detect the temperature of the human body without any contact with the body. Because they are lightweight, carbon-based wearable electronics are comfortable to use and are used to design a variety of healthcare devices. A strain sensor is used as a health monitoring device made of the textile composite where carbon filament yarns are used due to their lightweight and ability to be reinforced inside thermoplastic composite structures [112,113]. Zhang et al. created a fiber-based generator to fabricate power

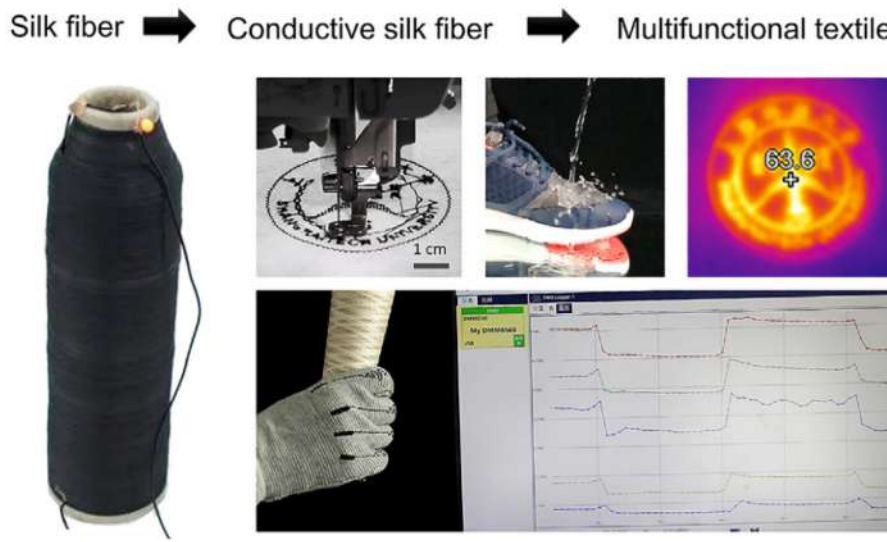


**Figure 16.7** Wearable appliances, human enhancement, health monitoring, and human−machine interface applications [45].

shirts that can be powered by a wireless body temperature system. CNT and polytetrafluoroethylene-coated cotton yarns are used to create an electrostatic induction effect capable of converting biomechanical vibration energy into electricity [114]. Photovoltaics make use of CNT yarns. CdSe nanowires are wrapped uniformly around a core metal wire, and the device is created by covering the top of the nanowires with a porous transparent electrode made of CNT and efficiency was recorded up to 3% [115]. Another unique application of CNT yarn is the construction of artificial muscles. Elastomer actuators based on CNTs that can be driven electrothermally are being developed [116,117]. CNT fiber components are then employed for the creation of hybrid-coiled yarn muscle covered by an elastomer−methanol composite. A small voltage that can be used to activate this hybrid-coiled yarn muscle composite is shown in Fig. 16.8 with SEM images [118].

### 16.6.3 Fabric-based applications

Self-encapsulation is a property of yarn-based devices, although they are costly to manufacture. Fabric-based e-textiles made of carbon materials are becoming increasingly popular in this regard. A solid-state, single-layer (SS-SL) fabric supercapacitor is a scalable, low-cost device that can be easily integrated into clothing and has capacitance comparable to comparable supercapacitors [62,119] created a supercapacitor with a maximum capacitance of 23.6 mF $cm^{-2}$ on cotton fabric using AC and CB as electrodes. Because of their flexibility, chemical resilience and enormous surface structure, carbon textiles manufactured from CFs are very promising applicants for supercapacitor applications. ACF can also be directly employed as an electrode in supercapacitor applications [120]. In the recent literature, a supercapacitor made by screen printing GO reduction by a process has also been mentioned. PVA-doped $H_2SO_4$ and hydrogel polymer electrolyte are used to print on the electrodes. A study found that GN mechanical stability results in high initial capacity and electrochemical excellency [121]. All mechanical actions to respond to carbon-based leads include bending and bending, distracting and untwisting, stretching and relaxing [43]. The rGO dip-coated cotton bend sensor and the

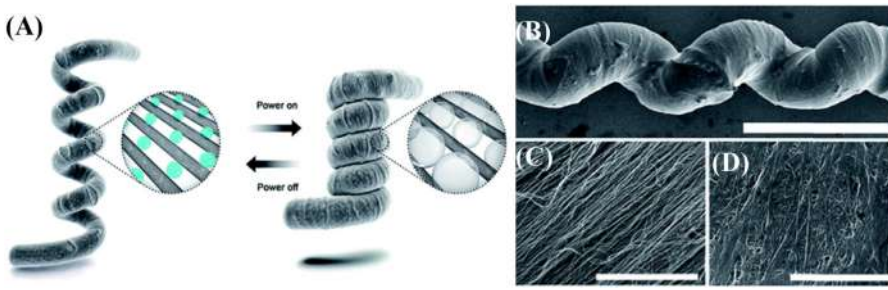


**Figure 16.8** (A) The hybrid CNT/elastomer composite's actuating mechanism; (B) SEM photograph; (C and D) surface morphology of the CNTs before and after elastomer-methanol composite infiltration [118]. *CNT*, Carbon nanotube.

expected and recurrent resistance changes during bending−unbending have been studied in the literature [50]. Wearable technologies for detecting human motions and athletic physical acts have also been created. Wang and Loh [122] developed wearable multifunctional sensors with a CNT-based fabric to detect commercial stress detecting capacities of sensors by monitoring human finger bending movements. In addition, a CNT-based sensor was put on a thoracic strap to assess human respiration. This CNT-made sensor has various advantages, including flexibility, ease of the synthetic process, low weight, low cost, and human consumption reliability. A dip-coating procedure is used to manufacture a graph enclosed textile electrode for the ECG monitoring sensor. Before the hydrazine vapor has decreased, nylon cloth has been soaked in GO suspension. The data show that the recording in high-time and frequency fields of EKG using textile electrodes is related to standard Ag/Ag Cl electrodes. ECG textile graphic electrodes offer advantages in addition to typical elements, as they remove gel needs, guarantee comfort, wearability and reusability, and are readily integrated with personal cleaning. The electric ECG textile material printed with electric rGO inkjet was the subject of a recent investigation [123]. The-rGO printed electrode collects high-grade ECGs with an estimated heart rate of less than 21 db when compared to a reference heart rate monitor with an estimated heart rate of fewer than 2.1 beats per minute (bpm). It has been described as a CNT-based dip-coated heating unit with good heating capability [124]. The CB screen printed wearable heater was also mentioned in a recent post. Screen printing on a 34 cm PES cloth was then done with the CB printing paste. Heating resistance decreases as the number of press layers grows, allowing Joule heating to perform better [125]. In Table 16.4, different applications of carbon-based functionalized fabrics in e-textile have been discussed.

### 16.6.4 Recent modifications in e-textiles

The cost-effectiveness of carbon-based total superconductors, the inherent safety qualities of the fabric, and the latest developments in carbon-based conductive textile production processes have stimulated interest in employing such substances in specific uses [148]. E-textiles composed of carbonaceous materials are used for a variety of reasons, including electromechanical properties, durability, and comfort (Kasaw et al., 2020). Wearable sensors (such as force sensors, stress−strain sensors, and chemical sensors), wearable and nonwearable heating pads, and textile-based healthcare monitoring systems are all examples of carbon-based e-textile applications [21]. A lipid bilayer-based coating for the CNT channel was presented as an alternative to biological molecules attached directly to the CNTs [149]. Carbonaceous materials with a high specific capacitance are also useful for making high-capacity storage devices like batteries and supercapacitors. The structures of electrical devices, heaters, and tissue-based sensors are presented in the next section of the study, along with a brief review of the qualities of the materials, manufacturing processes, and the corresponding electrical stability under various stimuli. Detection of hazardous gases and chemicals is essential both within the administrative center and as a precaution in unfamiliar environments [148]. Toxic gas sensors

**Table 16.4** Different applications of carbon-based functionalized fabrics [126]

| Carbon-based materials | Fabric structure and fiber content | Functionalization | Application | Ref. |
|---|---|---|---|---|
| CNTs | 100% cotton woven | Dipped in solution | Pressure sensor | [127] |
| | 100% wool twill woven washed with nonionic detergent washed wool 18 warp/ 10 mm, 16/10 mm | Impregnation | Electrically conductive textile | [128] |
| | 100% wool scoured, mass 67.6 g $m^{-2}$ 1/1 woven | Ultrasonic bath | Static dissipation, antispark, electromagnetic shielding, heating | [129] |
| | 100% cotton prepurified 1/1 woven | Padding | Electrically conductive superhydrophoic fabric | [130] |
| | 100% cotton twill woven | Screen printing with automatic squeegee, Ms-300FRO | Chemical vapor sensor | [131] |
| | 100% cotton 1/1 woven | Dip coating, screen printing | Energy storage | [51] |
| | 100% wool scoured; mass 350 g $m^{-2}$ twill woven | Impregnating bath | Electrically conductive fabric | [131] |
| | 100% cotton woven | Dipped in solution | Wearable electronic, energy storage | [133] |
| | Polyamide/Lycra | Coated | Stretch sensor | [134] |
| | Knit with flat-bed machine; two rows separated by two rows of nonconductive yarns | Activated carbon in swelled cellulose yarn of linen, bamboo, viscose | Supercapacitor | [66] |
| | Knit, 75% electroconductive yarn/ 25% Lycra 1/1 woven | Belltron | Piezoresistive sensor | [135] |

(*Continued*)

**Table 16.4** (Continued)

| Carbon-based materials | Fabric structure and fiber content | Functionalization | Application | Ref. |
|---|---|---|---|---|
| Reduced graphene oxide | 100% nylon, 100% cotton, 100% polyester 1/1 woven | Immersion in graphene oxide, reduction | Electrooculography | [136] |
| | 100% polyester woven | Immersion in graphene oxide, reduction | Plantar pressure sensor, gait analysis | [137] |
| | 100% cotton woven | Dipped in graphene nanoribbons | Potential for strain sensor | [138] |
| | 100% cotton woven | Graphene oxide with vacuum filtration, thermally reduced | Strain sensor | [43] |
| | Cotton fabric nickel nitrate treated | Immersion in graphene oxide | Energy storage | [139] |
| | 100% cotton (ISO 105/F standard fabric) woven | Immersion in graphene oxide, reduction | Counterelectrode | [140] |
| | 100% polyamide 1/1 woven | Immersion in graphene oxide | Electrocardiogram | [123] |
| | 100% wool 1/1 woven | Graphene oxide painted on fabric, reduction | E-textile (e.g., glove to operate smart devices) | [141] |
| | 100% cotton knit | GO coating, reduction | Motion sensor | [142] |
| | 90/10 nylon/10 spandex knit | GO coating, reduction | Strain sensor | [143] |
| | 100% polyester knit | rGO coating, polypyrrole variations | Energy storage | [144] |
| | 100% cotton knit | Ultrasonication coating | Strain sensor | [56] |
| | 100% wool knit | Ultrasonication coating | Strain sensor | [77] |
| | 100% polyamide Interlock weft knit | GO coating, reduction | Sensitive artificial skin | [145] |

(*Continued*)

**Table 16.4** (Continued)

| Carbon-based materials | Fabric structure and fiber content | Functionalization | Application | Ref. |
|---|---|---|---|---|
| | 100% viscose knit | Multicycle dipping-drying graphene oxide, reduction | Potential energy storage | [146] |
| | 100% nylon lycra knit | Immersion in graphene oxide, reduction, polypyrrole polymerization | Supercapacitor | [147] |

[150] thin polypyrene or polyaniline films are deposited onto PET or nylon threads, which are then woven into a fabric mesh. Although carbon particles have the inherent ability to adsorb gaseous molecules, very little research has been conducted on carbon-based fully textile sensors. The literature describes a carbon-based material sensing element capable of detective work dimethyl ketone and alkane vapor. This gas sensor was screen-written mistreatment GN pellets and a 3 wt.% liquid dispersion of MWNT during a carbon ink. CB printer ink is employed to make a screen-printed aerometric chemical sensor. As acetone and methane vapor are identified, the relative resistance adjusts. The rationale for this can be that the gas particles adhere to the fabric's surface, disrupting the MWNT's homogenized semiconductive channel [21]. ECG is a well-established scientific procedure that monitors the electrical activity of the guts and provides helpful info regarding coronary heart condition [151]. Using a dip-coating method, a GN-clad material conductor for a graph observance device is formed. In those artworks, nylon fabric is immersed in cross suspension and then reduced with the help of hydrazine vapor [152]. Conductive carbon-based fabrics are sensitive to mechanical movements such as bending and stretching, twisting and unwinding, stretching and relaxing [153]. They may be able to recognize human frame movements as well as wrist, elbow, and palm movements. The resistance variations of the RGO dip-coated cotton bend sensor during bending and unbending have been characterized in the literature in a repeatable and predictable manner [21].

Due to the high specific surface area and the inherent specific capacity of carbonaceous materials, current research is focused on scalable fabrication of flexible electrodes using carbon-based functional materials such as GN, rGO, GO, CNT, carbon onion, and alternating current [21,152]. Fabric and carbon textiles have this quality, making them acceptable for the use in an electric garage. Dip coating, screen printing, inkjet printing, and printing are all methods used to apply carbonaceous useful chemicals to fabrics. As per different studies, cotton material treated with GN, rGO, CNTs, and AC is then coated with an aluminous active material such $MnO_2$ nanoflakes, $RuO_2$, and $Co(OH)_2$ to enhance the particular capacitance [21]. According to current research, screen printing silk fabric using $MnO_2$-coated hollow carbon microspheres avoids the need for additional

coating [154]. It also has good electrochemical stability, with only 4% capacity loss after 2000 high-rate cycles, which is important in real-world scenarios. A recent study also disclosed inkjet-printed PVA gel/SWNT supercapacitor and $RuO_2$ nanowire/SWNT nanostructured supercapacitor [21]. Carbon-based materials, such as GN, CNTs, CF, and CB, have become one of the most widely used components in electromagnetic shielding due to their high electrical conductivity, good mechanical overall performance, lightweight, flexibility, and large aspect ratio. CB and CF applications arrived ahead of schedule. Because of its high specific strength and high conductivity, CF has become a popular shielding material. The conductive network of CB particles is stronger, but the absorption capacity of CF is weak. CNTs and GN have garnered a lot of attention in recent years due to their high-quality thing ratio and great overall transmission performance [155]. With 1286 retrieval effects in 2019, carbon-based electromagnetic shielding substance research far outnumbers metal and conductive polymer shielding substance research [156]. Numerous factors influence the response activities and kinetics of carbon-supported catalysts, including the nature of the carbon guide, catalytic particle size, and catalyst composition [157]. According to recent research, the physical properties of the carbon support can have a significant impact on the electrochemical activities of the Pt catalyst, thus improving the electrochemical efficiency of gas cellular devices [158]. CNTs have the advantage of having a large floor area and high porosity, which permits catalyst particles deposited on CNTs to be more easily accessed for desired catalyst use. Furthermore, CNTs have improved electrical conductivity, electrochemical sturdiness, and resistance [159]. Because of their high energy density, high operating voltage, and low self-discharge rate, lithium-ion batteries are becoming the dominant power source in today's portable digital devices and hybrid electric cars [160]. The commercialized lithium-ion batteries have a graphite anode and a cathode of steel oxide. Army utility of sweat sensors mounted on the pores and skin can actively analyze sweat for organic facts. The smart lifestyles era has advanced e-textiles by integrating knitted ECG electrodes, respiration sensors, and conductive pathways for interconnection and fitness monitoring. The capabilities of sensing, tracking, and data processing are networked collectively within a fabric. The protective apparel can detect the penetration of a projectile, screen the soldier's crucial signs, and alert medical triage units stationed near the battlefield. In the multilayer fabric, the internal apparel can be prepared from blends of excessive-performance fibers and cellulosic fibers (cotton/viscose) to provide both comfort and overall performance [157]. The outer garments need to offer the essential ballistic safety and could accommodate a unique set of sensors and other digital additives, together with temperature sensors, accelerometers, a GPS module, and a textile antenna.

## 16.7 Health aspects of e-textiles

E-textiles are a rapidly expanding body of materials in the world of fashion, and they have also been embellished in the military and medical sectors [161]. Nanomaterials, electrical components, and fibers are being combined in novel ways in e-textiles. In the medical realm, there are diverse sectors where e-textile is used

[162]. Personal health devices, fabric-based glucose sensors, breathing sensors, antimicrobial textiles, heated fabrics, textile-based drug-releasing items, and a variety of others are just a few examples. In general, e-textiles assist in the promotion of a healthy lifestyle [163]. There are various examples of health devices that monitor physical and mental well-being and provide benefits such as stimulating activities and sustaining functionality. E-textile technology can be used to analyze and treat a variety of age-related disorders [161]. There are electrocardiogram t-shirts for early detection of cardiovascular disease, electrode garments for stroke rehabilitation, shoes with embedded sensors for fall detection, and a variety of other products [164]. Notwithstanding the above statement, there is another side of e-textile on the heath. The chemicals, circuits, and other devices used on the fabric may severely affect health and sometimes can lead to diseases like cancer. E-textile may lead the fashion business to promising business opportunities, but its hazard to human life cannot be ignored. Hence, proper use of T-textile is crucial [165].

## 16.8 Environmental aspects of e-textiles

The environmental impact of e-textiles is linked to the entire life cycle of the product, which includes product design, material extraction, production, use phase, and finally end of life. As a result, we must consider the entire life cycle to provide an informed assessment. There is a new trend toward bio-based and nonmaterial solutions for e-textiles in the material extraction phase. Silver, for example, is a scarce metal with difficult mining circumstances and a larger environmental effect than CB. The environmental impact of textile manufacturing, particularly e-textile manufacturing, is mostly related to energy usage, as well as material and chemical consumption. Hazardous chemicals can form when e-waste is incorrectly disposed of or recycled. A variety of pollutants are released into the atmosphere as a result of chemical and thermal reactions, such as open burning. Corrosion can also occur as a result of improper disposal practices in the generation and discharge of contaminants (dumping). This is particularly problematic in nonsanitary landfills and dumpsites, which are frequently not just in developing countries but also in the European Union. As a result, toxic elements included in e-waste, as well as those created during improper disposal and recycling, endanger the environment and human health. E-textiles are fabrics or apparel products containing technologies that perceive and operate according to the circumstances they are inclined to, thus allowing the wearer to experience increased functionality [166]. Electronic items typically have a short lifespan. As a result, when their useful life is up, they will eventually be thrown away. Approximately 5−7 years following the mass-market introduction of e-textiles, significant amounts of trash develop. Textile products make up the majority of the waste stream in terms of weight [167]. There are various reasons to believe that future market diffusion of e-textiles will be at least as quick and ubiquitous as the previous market diffusion of mobile phones. There are

numerous similarities to electronic garbage, which is currently causing serious environmental issues. During the disposal process, there is a risk of harmful compounds being released. Furthermore, it is to be assumed that rare materials will be lost. This would hasten the depletion of natural resources [165]. Though e-textile has ushered in a new era in the textile industry, the e-waste it generates is costing our environment dearly. E-waste is one of the fastest-growing waste streams in the world, according to the OECD, and UNEP considers it a priority waste stream. As a result, we should pay close attention to the situation.

## 16.9 Recycle, reuse, and sustainability

Sustainability, recycling, and reuse are the globe's timely need toward proficient use and sustainability of the resources; these phrases are becoming increasingly important. The ongoing innovation process provides a window of opportunity to develop more sustainable e-textiles as well as a method to utilize e-textile waste, which contains limited raw materials such as valuable metals and textile fiber. Ecodesign ideas [such as design for recycling (DfR)] can be borrowed from the electronics and textiles industries, but they must be refined to meet the unique qualities of e-textiles [14]. In the case of product design, research on the toxicity and availability of basic materials, the projected influence of the manufacturing process involved, and the potential impact of unforeseen end-of-life stadiums should all be part of the design process. Electronic items typically have a short lifespan. Therefore it is critical to recycle and reuse these products. The fate of e-textiles is determined by the waste management plans in place at the point of disposal. They may differ significantly between countries. The recycling of e-textile goods is advanced in developed countries. Electronic devices are sometimes more difficult to recycle because they cannot be disposed of in the same way as other products. Metal recovery from incinerator bottom ash, for example, is only practicable for larger metal components in the centimeter range. Metallic components in e-textiles (such as silver-coated fibers) are significantly smaller, making the process more difficult to complete. E-textile goods can be recycled or disposed of by any of the following channels (Fig. 16.9).

Sustainable development is a complicated issue [168]. Today, there are a lot of things to think about when it comes to sustainable development [169]. Sustainability forbids resource consumption, the use of nonrenewable energy sources, and the loss of key natural capital [170]. As a result, sustainable development can be defined as a balance between man and the environment, with today's and future generations' lives and growth planned to meet and develop the expectations of future generations [171]. When producing e-textile products, sustainable terms and conditions should be taken into account. As a result, metal dispersion in e-textiles, as well as their dispersion among vast swaths of waste textiles, is a recycling concern. Metals will be lost at the end of the product life cycle since they are disseminated throughout textile materials. If e-textiles become commonplace,

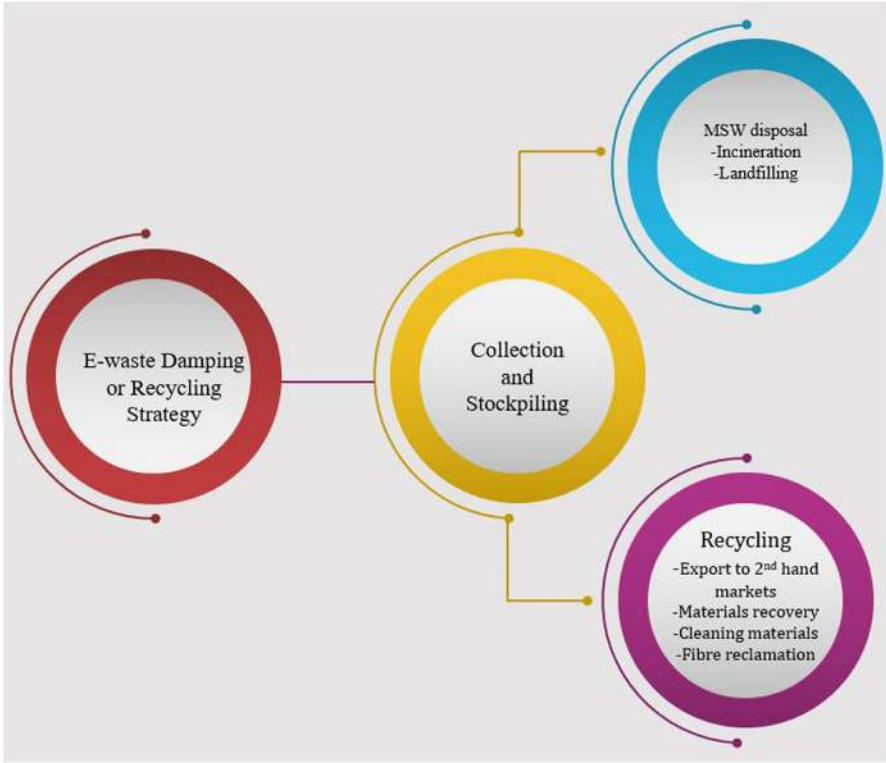


**Figure 16.9** Proposed scheme of e-textile damping and recycling [165]. *MSW*, Municipal solid waste.

resource scarcity will be exacerbated. Finally, the ultimate goal of e-textiles is to make them circular by extending the life of products and materials as much as feasible.

## 16.10 Conclusion and future stream

In this work, an attempt was made to explore the use of carbon nanocomposites in e-textile. From raw materials to design, production, consumer use, and finally disposal, a broader concept of e-textile has been discussed from what carbon composites suit and which properties they illustrate. Fabrication is one of the major portions of e-textile, from fiber to yarn to fabric using knitting or weaving. Dip coating, spray coating, embroidery, and stitching are all methods used to create nano-based e-textiles. Aside from it, scalable printing technologies such as inkjet and screen printing have been used. This chapter also describes the recent developments in e-textile and its use in different sectors, such as medical to military. It can

be predicted that in the future, the use of e-textile will rapidly expand. So, to give it fuel we need to focus on it because we believe that technology makes our life easier and efficient. But we need to keep in mind that technological development needs to be in a sustainable way. So, we need to also focus on the environmental aspect of e-textiles. In addition, ongoing research into the least harmful carbon nanoparticles, biodegradable and nontoxic electronic polymers, and materials for temporary electronics that decay over time could lead to breakthroughs in the development of a long-term e-textile. The continual innovation process offers an opportunity to develop more sustainable e-textiles as well as a means for repurposing e-textile waste, which comprises limited raw elements like valuable metals and textile fiber. When e-textiles approach the end of their useful lives, they will be disposed of. Eco-design concepts like DfR and extremely flexible and washable textile-based thermoelectrics can be borrowed from the electronics and textiles industries, but they must be further developed to fulfill the unique requirements of e-textiles. The use of heat generated by the human body to generate energy is a sustainable method as well as a type of waste utilization. Wearable and flexible platforms for combining multiple functionality, such as sensor-based devices and user-interface elements, have become a popular research issue in recent decades. Electrically integrated textiles that can communicate wirelessly have become a popular research area in recent years. E-textiles have recently changed their focus to more active and intelligent functionalities, pushing textile materials and structures with built-in electronic capabilities, such as piezoelectric yarns, photovoltaic fibers, and sensing fabrics. However, the nanofillers produced by these methods usually have weak adherence to the polymers and can be washed away during the rinse process. As a result, the composites are not washable. E-textiles that are easy to wash can be used for a long time. This has the potential to significantly reduce costs, is less hazardous to human health, and is environmentally benign. Washable e-textiles could be the next focused priority.

## References

[1] R. McLaren, F. Joseph, C. Baguley, D. Taylor, A review of e-textiles in neurological rehabilitation: how close are we? J. Neuroeng. Rehabilitation 13 (1) (2016). Available from: https://doi.org/10.1186/s12984-016-0167-0.

[2] E. Omanovi, A. Badnjevi, A. Kazlagi, M. Hajlovac, Nanocomposites: a brief review, 2019.

[3] O. Ala, Q. Fan, Applications of conducting polymers in electronic textiles, Res. J. Text. Appar. 13 (4) (2009) 51−68. Available from: https://doi.org/10.1108/RJTA-13-04-2009-B007.

[4] F.M. Michael, M. Khalid, R. Walvekar, C.T. Ratnam, S. Ramarad, H. Siddiqui, et al., Effect of nanofillers on the physico-mechanical properties of load bearing bone implants, Mater. Sci. Eng. C. 67 (2016) 792−806. Available from: https://doi.org/10.1016/j.msec.2016.05.037.

[5] T. Nuge, K.Y. Tshai, S.S. Lim, N. Nordin, M.E. Hoque, Preparation and characterization of Cu-, Fe-, Ag-, Zn- and Ni- doped gelatin nanofibers for possible applications in antibacterial nanomedicine, 2017, 3, 14.

[6] V.P. Padmanabhan, N.,S. N. T. S, S. Sagadevan, M.E. Hoque, R. Kulandaivelu, Advanced lithium substituted hydroxyapatite nanoparticles for antimicrobial and hemolytic studies, N. J. Chem. 43 (47) (2019) 18484−18494. Available from: https://doi.org/10.1039/C9NJ03735G.

[7] S. Sagadevan, Z.Z. Chowdhury, M.R.B. Johan, A.A. Khan, F.A. Aziz, R.F. Rafique, et al., A facile hydrothermal approach for catalytic and optical behavior of tin oxide-graphene (SnO2/G) nanocomposite, PLoS One 13 (10) (2018). Available from: https://doi.org/10.1371/journal.pone.0202694. e0202694.

[8] Md. A. Wahab, N. Islam, M.E. Hoque, D.J. Young, Recent advances in silver nanoparticle containing biopolymer nanocomposites for infectious disease control − a mini review, Curr. Anal. Chem. 14 (3) (2018) 198−202. Available from: https://doi.org/10.2174/1573411013666171009163829.

[9] M. Golieskardi, M. Satgunam, D. Ragurajan, M.E. Hoque, A.M.H. Ng, L. Shanmuganantha, Advanced 3Y-TZP bioceramic doped with Al2O3 and CeO2 potentially for biomedical implant applications, Mater. Technol. 34 (8) (2019) 480−489. Available from: https://doi.org/10.1080/10667857.2019.1578912.

[10] M.E. Ali, M.E. Hoque, S.K. Safdar Hossain, M.C. Biswas, Nanoadsorbents for wastewater treatment: next generation biotechnological solution, Int. J. Environ. Sci. Technol. 17 (9) (2020) 4095−4132. Available from: https://doi.org/10.1007/s13762-020-02755-4.

[11] C. Gonçalves, A.F. Da Silva, J. Gomes, R. Simoes, Wearable e-textile technologies: a review on sensors, actuators and control elements, Inventions 3 (1) (2018) 1−13. Available from: https://doi.org/10.3390/inventions3010014.

[12] I. Ibanez-Labiano, M.S. Ergoktas, C. Kocabas, A. Toomey, A. Alomainy, E. Ozden-Yenigun, Graphene-based soft wearable antennas, Appl. Mater. Today 20 (2020) 100727. Available from: https://doi.org/10.1016/j.apmt.2020.100727.

[13] P. Chancerel, C.E.M. Meskers, C. Hagelüken, V.S. Rotter, Assessment of precious metal flows during preprocessing of waste electrical and electronic equipment, J. Ind. Ecol. 13 (5) (2009) 791−810. Available from: https://doi.org/10.1111/j.1530-9290.2009.00171.x.

[14] A.R. Köhler, Challenges for eco-design of emerging technologies: the case of electronic textiles, Mater. Des. 51 (2013) 51−60. Available from: https://doi.org/10.1016/j.matdes.2013.04.012.

[15] S. Afroj, S. Tan, A.M. Abdelkader, K.S. Novoselov, N. Karim, Highly conductive, scalable, and machine washable graphene-based e-textiles for multifunctional wearable electronic applications, Adv. Funct. Mater. 30 (23) (2020). Available from: https://doi.org/10.1002/adfm.202000293.

[16] H.W. Zhu, H.L. Gao, H.Y. Zhao, J. Ge, B.C., Hu, J. Huang, et al., Printable elastic silver nanowire-based conductor for washable electronic textiles, Nano Res. 13 (10) (2020) 2879−2884. Available from: https://doi.org/10.1007/s12274-020-2947-x.

[17] J. Oladunni, J.H. Zain, A. Hai, F. Banat, G. Bharath, E. Alhseinat, A comprehensive review on recently developed carbon based nanocomposites for capacitive deionization: from theory to practice, Sep. Purif. Technol. 207 (2018) 291−320. Available from: https://doi.org/10.1016/j.seppur.2018.06.046.

[18] W. Zou, B. Gao, Y.S. Ok, L. Dong, Integrated adsorption and photocatalytic degradation of volatile organic compounds (VOCs) using carbon-based nanocomposites: a

critical review, Chemosphere 218 (2019) 845–859. Available from: https://doi.org/10.1016/j.chemosphere.2018.11.175.
[19] N. Karim, S. Afroj, S. Tan, K.S. Novoselov, S.G. Yeates, All inkjet-printed graphene-silver composite ink on textiles for highly conductive wearable electronics applications, Sci. Rep. 9 (1) (2019) 1–10. Available from: https://doi.org/10.1038/s41598-019-44420-y.
[20] R. Bogue, Nanocomposites: a review of technology and applications, Assembly Autom. 31 (2) (2011) 106–112. Available from: https://doi.org/10.1108/01445151111117683.
[21] N. Khair, R. Islam, H. Shahariar, Carbon-based electronic textiles: materials, fabrication processes and applications, J. Mater. Sci. (2019). Available from: https://doi.org/10.1007/s10853-019-03464-1.
[22] L. Zhong, R. Yu, X. Hong, Review of carbon-based electromagnetic shielding materials: film, composite, foam, textile, Text. Res. J. 91 (9–10) (2021) 1167–1183. Available from: https://doi.org/10.1177/0040517520968282.
[23] H.A.A. Bashid, H.N. Lim, S.M. Hafiz, Y. Andou, M. Altarawneh, Z.T. Jiang, et al., Modification of carbon-based electroactive materials for supercapacitor applications, Carbon-Based Polymer Nanocomposites for Environmental and Energy Applications, Elsevier Inc, 2018. Available from: https://doi.org/10.1016/B978-0-12-813574-7.00016-2.
[24] A. Lund, N.M. Van Der Velden, N.K. Persson, M.M. Hamedi, C. Müller, Electrically conducting fibres for e-textiles: an open playground for conjugated polymers and carbon nanomaterials, Materials Science and Engineering R: Reports, 126, Elsevier, 2018, pp. 393–413. Issue March. Available from: https://doi.org/10.1016/j.mser.2018.03.001.
[25] H. Lee, M.J. Glasper, X. Li, J.A. Nychka, J. Batcheller, H.J. Chung, et al., Preparation of fabric strain sensor based on graphene for human motion monitoring, J. Mater. Sci. 53 (12) (2018) 9026–9033. Available from: https://doi.org/10.1007/s10853-018-2194-7.
[26] A.S. Alshammari, Carbon-based polymer nanocomposites for sensing applications. In Carbon-Based Polymer Nanocomposites for Environmental and Energy Applications, Elsevier Inc, 2018. Available from: https://doi.org/10.1016/B978-0-12-813574-7.00014-9.
[27] M. Stoppa, A. Chiolerio, Wearable electronics and smart textiles: A critical review, Sens. (Switz.) 14 (7) (2014) 11957–11992. Available from: https://doi.org/10.3390/s140711957.
[28] C. Shen, Y. Xie, B. Zhu, M. Sanghadasa, Y. Tang, L. Lin, Wearable woven supercapacitor fabrics with high energy density and load-bearing capability, Sci. Rep. 7 (1) (2017) 1–8. Available from: https://doi.org/10.1038/s41598-017-14854-3.
[29] H. Ba, G. Giambastiani, C. Pham-Huu, L. Truong-Phuoc, V. Papaefthimiou, C. Sutter, et al., Cotton fabrics coated with few-layer graphene as highly responsive surface heaters and integrated lightweight electronic-textile circuits, ACS Appl. Nano Mater. 3 (10) (2020) 9771–9783. Available from: https://doi.org/10.1021/acsanm.0c01861.
[30] L. Zhi, J. Ning, Advances in flexible transparent conductive films based on carbon nanomaterials, Chin. Sci. Bull. 59 (33) (2014) 3313–3321. Available from: https://doi.org/10.1360/n972014-00591.
[31] R. Islam, N. Khair, D.M. Ahmed, H. Shahariar, Fabrication of low cost and scalable carbon-based conductive ink for E-textile applications, Mater. Today Commun. 19 (2019) 32–38. Available from: https://doi.org/10.1016/j.mtcomm.2018.12.009.
[32] E. Ismar, S. Kurşun Bahadir, F. Kalaoglu, V. Koncar, Futuristic clothes: electronic textiles and wearable technologies, Glob. Chall. 4 (7) (2020) 1900092. Available from: https://doi.org/10.1002/gch2.201900092.
[33] W. Weng, P. Chen, S. He, X. Sun, H. Peng, Smart electronic textiles, Angew. Chem. - Int. (Ed.) 55 (21) (2016) 6140–6169. Available from: https://doi.org/10.1002/anie.201507333.

[34] B.M. Li, O. Yildiz, A.C. Mills, T.J. Flewwellin, P.D. Bradford, J.S. Jur, Iron-on carbon nanotube (CNT) thin films for biosensing E-Textile applications, Carbon 168 (2020) 673–683. Available from: https://doi.org/10.1016/j.carbon.2020.06.057.
[35] H.S. Jang, M.S. Moon, B.H. Kim, Electronic textiles fabricated with graphene oxide-coated commercial textiles, Coatings 11 (5) (2021) 1–10. Available from: https://doi.org/10.3390/coatings11050489.
[36] X. Li, R. Wang, L. Wang, A. Li, X. Tang, J. Choi, et al., Scalable fabrication of carbon materials based silicon rubber for highly stretchable e-textile sensor, Nanotechnol. Rev. 9 (1) (2020) 1183–1191. Available from: https://doi.org/10.1515/ntrev-2020-0088.
[37] I. Kim, J.S. Heo, M.F. Hossain, Challenges in design and fabrication of flexible/stretchable carbon-and textile-based wearable sensors for health monitoring: a critical review, Sens. (Switz.) 20 (14) (2020) 1–29. Available from: https://doi.org/10.3390/s20143927.
[38] K. Jost, D. Stenger, C.R. Perez, J.K. McDonough, K. Lian, Y. Gogotsi, et al., Knitted and screen printed carbon-fiber supercapacitors for applications in wearable electronics, Energy Environ. Sci. 6 (9) (2013) 2698–2705. Available from: https://doi.org/10.1039/c3ee40515j.
[39] G. Ehrmann, A. Ehrmann, Electronic Textiles (2021) 115–130.
[40] Y. Jia, A. Ahmed, X. Jiang, L. Zhou, Q. Fan, J. Shao, Microfluidic fabrication of hierarchically porous superconductive carbon black/graphene hybrid fibers for wearable supercapacitor with high specific capacitance, Electrochim. Acta 354 (2020) 136731. Available from: https://doi.org/10.1016/j.electacta.2020.136731.
[41] A. Lund, Y. Tian, S. Darabi, C. Müller, A polymer-based textile thermoelectric generator for wearable energy harvesting, J. Power Sources 480 (August) (2020) 228836. Available from: https://doi.org/10.1016/j.jpowsour.2020.228836.
[42] L. Allison, S. Hoxie, T.L. Andrew, Towards seamlessly-integrated textile electronics: methods to coat fabrics and fibers with conducting polymers for electronic applications, Chem. Commun. 53 (53) (2017) 7182–7193. Available from: https://doi.org/10.1039/c7cc02592k.
[43] J. Ren, C. Wang, X. Zhang, T. Carey, K. Chen, Y. Yin, et al., Environmentally-friendly conductive cotton fabric as flexible strain sensor based on hot press reduced graphene oxide, Carbon 111 (2017) 622–630. Available from: https://doi.org/10.1016/j.carbon.2016.10.045.
[44] H. He, X. Chen, O. Mokhtari, H. Nishikawa, L. Ukkonen, J. Virkki, Fabrication and performance evaluation of carbon-based stretchable RFID tags on textile substrates, in: 2018 International Flexible Electronics Technology Conference, IFETC 2018, 1–5. https://doi.org/10.1109/IFETC.2018.8583938.
[45] C. Ye, J. Ren, Y. Wang, W. Zhang, C. Qian, J. Han, et al., Design and fabrication of silk templated electronic yarns and applications in multifunctional textiles, Matter 1 (5) (2019) 1411–1425. Available from: https://doi.org/10.1016/j.matt.2019.07.016.
[46] J. Zhou, Z. Zhao, R. Hu, J. Yang, H. Xiao, Y. Liu, et al., Multi-walled carbon nanotubes functionalized silk fabrics for mechanical sensors and heating materials, Mater. Des. 191 (2020) 108636. Available from: https://doi.org/10.1016/j.matdes.2020.108636.
[47] K. Laxminarayana, N. Jalili, Functional nanotube-based textiles: pathway to next generation fabrics with enhanced sensing capabilities, Text. Res. J. 75 (9) (2005) 670–680. Available from: https://doi.org/10.1177/0040517505059330.
[48] M. Maleki, G.A. El-Nagar, D. Bernsmeier, J. Schneider, C. Roth, Fabrication of an efficient vanadium redox flow battery electrode using a free-standing carbon-loaded electrospun nanofibrous composite, Sci. Rep. 10 (1) (2020) 1–14. Available from: https://doi.org/10.1038/s41598-020-67906-6.

[49] K. Saetia, J.M. Schnorr, M.M. Mannarino, S.Y. Kim, G.C. Rutledge, T.M. Swager, et al., Spray-layer-by-layer carbon nanotube/electrospun fiber electrodes for flexible chemiresistive sensor applications, Adv. Funct. Mater. 24 (4) (2014) 492–502. Available from: https://doi.org/10.1002/adfm.201302344.

[50] N. Karim, S. Afroj, S. Tan, P. He, A. Fernando, C. Carr, et al., Scalable production of graphene-based wearable e-textiles, ACS Nano 11 (12) (2017) 12266–12275. Available from: https://doi.org/10.1021/acsnano.7b05921.

[51] K. Jost, C.R. Perez, J.K. McDonough, V. Presser, M. Heon, G. Dion, et al., Carbon coated textiles for flexible energy storage, Energy Environ. Sci. 4 (12) (2011) 5060. Available from: https://doi.org/10.1039/c1ee02421c.

[52] R.S. Costa, A. Guedes, A.M. Pereira, C. Pereira, Fabrication of all-solid-state textile supercapacitors based on industrial-grade multi-walled carbon nanotubes for enhanced energy storage, J. Mater. Sci. 55 (23) (2020) 10121–10141. Available from: https://doi.org/10.1007/s10853-020-04709-0.

[53] M.S. Sadi, J. Pan, A. Xu, D. Cheng, G. Cai, X. Wang, Direct dip-coating of carbon nanotubes onto polydopamine-templated cotton fabrics for wearable applications, Cellulose 26 (12) (2019) 7569–7579. Available from: https://doi.org/10.1007/s10570-019-02628-1.

[54] A. Konwar, U. Baruah, M.J. Deka, A.A. Hussain, S.R. Haque, A.R. Pal, et al., Tea-carbon dots-reduced graphene oxide: an efficient conducting coating material for fabrication of an e-textile, ACS Sustain. Chem. Eng. 5 (12) (2017) 11645–11651. Available from: https://doi.org/10.1021/acssuschemeng.7b03021.

[55] V. Trovato, E. Teblum, Y. Kostikov, A. Pedrana, V. Re, G.D. Nessim, et al., Sol-gel approach to incorporate millimeter-long carbon nanotubes into fabrics for the development of electrical-conductive textiles, Mater. Chem. Phys. 240 (March 2019) (2020) 122218. Available from: https://doi.org/10.1016/j.matchemphys.2019.122218.

[56] H. Souri, D. Bhattacharyya, Highly stretchable multifunctional wearable devices based on conductive cotton and wool fabrics, ACS Appl. Mater. Interfaces 10 (24) (2018) 20845–20853. Available from: https://doi.org/10.1021/acsami.8b04775.

[57] F. Loffredo, A.D.G. Mauro, G. Del, Burrasca, V. La Ferrara, L. Quercia, E. Massera, et al., Ink-jet printing technique in polymer/carbon black sensing device fabrication, Sens. Actuators B: Chem. 143 (1) (2009) 421–429. Available from: https://doi.org/10.1016/j.snb.2009.09.024.

[58] P. Chen, H. Chen, J. Qiu, C. Zhou, Inkjet printing of single-walled carbon nanotube/RuO2 nanowire supercapacitors on cloth fabrics and flexible substrates, Nano Res. 3 (8) (2010) 594–603. Available from: https://doi.org/10.1007/s12274-010-0020-x.

[59] Y. Xu, I. Hennig, D. Freyberg, A. James Strudwick, M. Georg Schwab, T. Weitz, et al., Inkjet-printed energy storage device using graphene/polyaniline inks, J. Power Sources 248 (2014) 483–488. Available from: https://doi.org/10.1016/j.jpowsour.2013.09.096.

[60] X. Pu, L. Li, M. Liu, C. Jiang, C. Du, Z. Zhao, et al., Wearable self-charging power textile based on flexible yarn supercapacitors and fabric nanogenerators, Adv. Mater. 28 (1) (2016) 98–105. Available from: https://doi.org/10.1002/adma.201504403.

[61] S. Lawes, A. Riese, Q. Sun, N. Cheng, X. Sun, Printing nanostructured carbon for energy storage and conversion applications, Carbon 92 (April) (2015) 150–176. Available from: https://doi.org/10.1016/j.carbon.2015.04.008.

[62] S. Yong, J. Owen, S. Beeby, Solid-state supercapacitor fabricated in a single woven textile layer for e-textiles applications, Adv. Eng. Mater. 20 (5) (2018) 1700860. Available from: https://doi.org/10.1002/adem.201700860.

[63] S. Beeby, R. Torah, J. Tudor, N. Grabham, S. Yong, S. Arumugam, et al., Textiles (2019) 9–11.

[64] S. Arumugam, Y. Li, M. Glanc-Gostkiewicz, R.N. Torah, S.P. Beeby, Solution processed organic solar cells on textiles, IEEE J. Photovolt. 8 (6) (2018) 1710−1715. Available from: https://doi.org/10.1109/JPHOTOV.2018.2871334.

[65] A. Maziz, A. Concas, A. Khaldi, J. Stålhand, N.K. Persson, E.W.H. Jager, Knitting and weaving artificial muscles, Sci. Adv. 3 (1) (2017) 1−12. Available from: https://doi.org/10.1126/sciadv.1600327.

[66] K. Jost, D.P. Durkin, L.M. Haverhals, E.K. Brown, M. Langenstein, H.C. de Long, et al., Natural fiber welded electrode yarns for knittable textile supercapacitors, Adv. Energy Mater. 5 (4) (2014) 1401286. Available from: https://doi.org/10.1002/aenm.201401286.

[67] Z. Yang, J. Deng, X. Chen, J. Ren, H. Peng, A highly stretchable, fiber-shaped supercapacitor, Angew. Chem. Int. Ed. 52 (50) (2013) 13453−13457. Available from: https://doi.org/10.1002/anie.201307619.

[68] E.M. Swielam, S.M. Eltopshy, S.K. Sobhy, Z.M. Abdel-megied, A.M. Labeeb, Impact of the fabrication parameters on the performance of embroidered E-clothes, Egypt. J. Chem. 62 (1) (2019) 109−117. Available from: https://doi.org/10.21608/ejchem.2018.4555.1399.

[69] Y. Zheng, L. Jin, J. Qi, Z. Liu, L. Xu, S. Hayes, et al., Performance evaluation of conductive tracks in fabricating e-textiles by lock-stitch embroidery, J. Ind. Text. (2020) 1−20. Available from: https://doi.org/10.1177/1528083720937289.

[70] K.A. Shorter, G.F. Kogler, E. Loth, W.K. Durfee, E.T. Hsiao-Wecksler, A portable powered ankle-foot orthosis for rehabilitation, J. Rehabilitation Res. Dev. 48 (4) (2011) 459−472. Available from: https://doi.org/10.1682/JRRD.2010.04.0054.

[71] J. Cheng, S. Wille, B. Zhou, N. When, K. Kunze, J. Weppner, et al., Activity recognition and nutrition monitoring in everyday situations with a textile capacitive neckband, in: UbiComp 2013 Adjunct - Adjunct Publication of the 2013 ACM Conference on Ubiquitous Computing, 2013, 9(3), 155−158. https://doi.org/10.1145/2494091.2494143.

[72] P.R. Russo, N. Gershenfeld, E-broidery: Design and fabrication of textile-based computing, 2000, 39.

[73] C. Kallmayer, E. Simon, Large area sensor integration in textiles, in: International Multi-Conference on Systems, Signals and Devices, SSD 2012 - Summary Proceedings, m., 2012, https://doi.org/10.1109/SSD.2012.6198112.

[74] J. Ferri, R. Llinares Llopis, J. Moreno, J. Vicente Lidón-Roger, E. Garcia-Breijo, An investigation into the fabrication parameters of screen-printed capacitive sensors on e-textiles, Text. Res. J. 90 (15−16) (2020) 1749−1769. Available from: https://doi.org/10.1177/0040517519901016.

[75] M.I. Maksud, M.S. Yusof, Z. Embong, M.N. Nodin, N.A. Rejab, An investigation on printability of carbon nanotube (CNTs) inks by flexographic onto various substrates, Int. J. Mater. Sci. Eng. 2 (1) (2014) 49−55. Available from: https://doi.org/10.12720/ijmse.2.1.49-55.

[76] S. Rotzler, M. von Krshiwoblozki, M. Schneider-Ramelow, Washability of e-textiles: current testing practices and the need for standardization, Text. Res. J. (2021). Available from: https://doi.org/10.1177/0040517521996727.

[77] H. Souri, D. Bhattacharyya, Highly sensitive, stretchable and wearable strain sensors using fragmented conductive cotton fabric, J. Mater. Chem. C. 6 (39) (2018) 10524−10531. Available from: https://doi.org/10.1039/c8tc03702g.

[78] Draft ASTM WK61479 (2018). New Test Method for Durability of Smart Garment Textile Electrodes Exposed to Perspiration.

[79] Draft ASTM WK61480 (2018). New Test Method for Durability of Smart Garment Textile Electrodes after Laundering.
[80] Draft AATCC RA111 (2019a) Electrical Resistance of Electronically Integrated Textiles.
[81] Draft AATCC RA111 (2019b). Electrical Resistance Changes of Electronically-Integrated Textiles after Home Laundering.
[82] CEN EN 16812 (2016). Textiles and textile products - electrically conductive textiles - determination of the linear electrical resistance of conductive tracks.
[83] Draft IEC 63203-204-1 (2019). Wearable Electronic Devices and Technologies – Part 204-1: Electronic Textile – Washable Durability Test Method for Leisure and Sportswear E-Textile System.
[84] Draft IEC 63203-201-3 (2019). Wearable Electronic Devices and Technologies - Part 201-3: Electronic Textile - Determination of Electrical Resistance of Conductive Textiles Under Simulated Microclimate.
[85] Draft IEC 63203-250-1 (2018). Wearable Electronic Devices and Technologies – Part 250-1: Electronic Textile –Snap Button Connectors Between E-Textile and Detachable Electronic Devices.
[86] Draft IEC 63203-201-1 (2018). Wearable Electronic Devices and Technologies – Part 201-1: Electronic Textile – Measurement Methods for Basic Properties of Conductive Yarns.
[87] Draft IEC 63203-201-2 Wearable Electronic Devices and Technologies – Part 201-2: Electronic Textile – Measurement Methods for Basic Properties of Conductive Fabric And Insulation Materials.
[88] CEN EN 16806-1 (2016). Textiles and Textile Products - Textiles Containing Phase Change Materials (PCM) - Part 1: Determination of the Heat Storage and Release Capacity.
[89] Draft IEC 63203-406-1 (2019). Wearable Electronic Devices and Technologies - Part 406-1: Test Methods of on-Body Wearable Electronic Devices for Measuring Skin Contact Temperature.
[90] Draft IEC 63203-401-1 (2019). Wearable Electronic Devices and Technologies - Part 401-1: Devices and Systems – Functional Elements - Evaluation Method of the Stretchable Resistive Strain Sensor.
[91] Draft IEC 63203-402-1 (2019). Wearable Electronic Devices and Technologies – Part 402-1: Devices and Systems – Accessory – Test Methods of Glove-Type Motion Sensors for Measuring Finger Movements.
[92] Draft IEC 63203-402-2 (2019). Wearable Electronic Devices and Technologies – Part 402-2: Performance Measurement of Fitness Wearables – Step Counting.
[93] Draft IEC 63203-301-1 (2019). Wearable Electronic Devices and Technologies - Part 301-1: Test Method of Electrochromic Films for Wearable Equipment.
[94] A. Chatterjee, M. Nivas Kumar, S. Maity, Influence of graphene oxide concentration and dipping cycles on electrical conductivity of coated cotton textiles, J. Text. Inst. 108 (11) (2017) 1910–1916. Available from: https://doi.org/10.1080/00405000.2017.1300209.
[95] Z. Nooralian, M. Parvinzadeh Gashti, I. Ebrahimi, Fabrication of a multifunctional graphene/polyvinylphosphonic acid/cotton nanocomposite via facile spray layer-by-layer assembly, RSC Adv. 6 (28) (2016) 23288–23299. Available from: https://doi.org/10.1039/c6ra00296j.
[96] R.D. Kale, T. Potdar, P. Kane, R. Singh, Nanocomposite polyester fabric based on graphene/titanium dioxide for conducting and UV protection functionality, Graphene Technol. 3 (2–4) (2018) 35–46. Available from: https://doi.org/10.1007/s41127-018-0021-1.

[97] X. Hu, M. Tian, L. Qu, S. Zhu, G. Han, Multifunctional cotton fabrics with graphene/polyurethane coatings with far-infrared emission, electrical conductivity, and ultraviolet-blocking properties, Carbon 95 (2015) 625–633. Available from: https://doi.org/10.1016/j.carbon.2015.08.099.

[98] Z. Li, Z.L. Wang, Air/liquid-pressure and heartbeat-driven flexible fiber nanogenerators as a micro/nano-power source or diagnostic sensor, Adv. Mater. 23 (1) (2010) 84–89. Available from: https://doi.org/10.1002/adma.201003161.

[99] K.P. Prasad, Y. Chen, P. Chen, Three-dimensional graphene-carbon nanotube hybrid for high-performance enzymatic biofuel cells, ACS Appl. Mater. Interfaces 6 (5) (2014) 3387–3393. Available from: https://doi.org/10.1021/am405432b.

[100] Y. Chen, K.P. Prasad, X. Wang, H. Pang, R. Yan, A. Than, et al., Enzymeless multisugar fuel cells with high power output based on 3D graphene–Co3O4 hybrid electrodes, Phys. Chem. Chem. Phys. 15 (23) (2013) 9170. Available from: https://doi.org/10.1039/c3cp51410b.

[101] F. Gao, L. Viry, M. Maugey, P. Poulin, N. Mano, Engineering hybrid nanotube wires for high-power biofuel cells, Nat. Commun. 1 (1) (2010). Available from: https://doi.org/10.1038/ncomms1000.

[102] C.H. Kwon, S.H. Lee, Y.B. Choi, J.A. Lee, S.H. Kim, H.H. Kim, et al., High-power biofuel cell textiles from woven biscrolled carbon nanotube yarns, Nat. Commun. 5 (1) (2014). Available from: https://doi.org/10.1038/ncomms4928.

[103] J. Ren, L. Li, C. Chen, X. Chen, Z. Cai, L. Qiu, et al., Twisting carbon nanotube fibers for both wire-shaped micro-supercapacitor and micro-battery, Adv. Mater. 25 (8) (2012) 1155–1159. Available from: https://doi.org/10.1002/adma.201203445.

[104] H. Lin, W. Weng, J. Ren, L. Qiu, Z. Zhang, P. Chen, et al., Twisted aligned carbon nanotube/silicon composite fiber anode for flexible wire-shaped lithium-ion battery, Adv. Mater. 26 (8) (2013) 1217–1222. Available from: https://doi.org/10.1002/adma.201304319.

[105] Q. Meng, H. Wu, Y. Meng, K. Xie, Z. Wei, Z. Guo, High-performance all-carbon yarn micro-supercapacitor for an integrated energy system, Adv. Mater. 26 (24) (2014) 4100–4106. Available from: https://doi.org/10.1002/adma.201400399.

[106] J. Ren, W. Bai, G. Guan, Y. Zhang, H. Peng, Flexible and weaveable capacitor wire based on a carbon nanocomposite fiber, Adv. Mater. 25 (41) (2013) 5965–5970. Available from: https://doi.org/10.1002/adma.201302498.

[107] Z. Yang, J. Deng, X. Chen, J. Ren, H. Peng, A highly stretchable, fiber-shaped supercapacitor, Angew. Chem. Int. (Ed.) 52 (50) (2013) 13453–13457. Available from: https://doi.org/10.1002/anie.201307619.

[108] X. Xiao, T. Li, P. Yang, Y. Gao, H. Jin, W. Ni, et al., Fiber-based all-solid-state flexible supercapacitors for self-powered systems, ACS Nano 6 (10) (2012) 9200–9206. Available from: https://doi.org/10.1021/nn303530k.

[109] Z. Zhu, L. Garcia-Gancedo, A.J. Flewitt, F. Moussy, Y. Li, W.I. Milne, Design of carbon nanotube fiber microelectrode for glucose biosensing, J. Chem. Technol. Biotechnol. 87 (2) (2011) 256–262. Available from: https://doi.org/10.1002/jctb.2708.

[110] Z. Zhu, W. Song, K. Burugapalli, F. Moussy, Y.L. Li, X.H. Zhong, Nano-yarn carbon nanotube fiber based enzymatic glucose biosensor, Nanotechnology 21 (16) (2010) 165501. Available from: https://doi.org/10.1088/0957-4484/21/16/165501.

[111] T. Dinh, H.P. Phan, T.K. Nguyen, A. Qamar, A.R.M. Foisal, T. Nguyen Viet, et al., Environment-friendly carbon nanotube based flexible electronics for noninvasive and wearable healthcare, J. Mater. Chem. C. 4 (42) (2016) 10061–10068. Available from: https://doi.org/10.1039/c6tc02708c.

[112] E. Häntzsche, A. Matthes, A. Nocke, C. Cherif, Characteristics of carbon fiber based strain sensors for structural-health monitoring of textile-reinforced thermoplastic composites depending on the textile technological integration process, Sens. Actuators A Phys. 203 (2013) 189–203. Available from: https://doi.org/10.1016/j.sna.2013.08.045.
[113] M.M.B. Hasan, A. Matthes, P. Schneider, C. Cherif, Application of carbon filament (CF) for structural health monitoring of textile reinforced thermoplastic composites, Mater. Technol. 26 (3) (2011) 128–134. Available from: https://doi.org/10.1179/175355511x13007211258881.
[114] J. Zhong, Y. Zhang, Q. Zhong, Q. Hu, B. Hu, Z.L. Wang, et al., Fiber-based generator for wearable electronics and mobile medication, ACS Nano 8 (6) (2014) 6273–6280. Available from: https://doi.org/10.1021/nn501732z.
[115] L. Zhang, E. Shi, Z. Li, P. Li, Y. Jia, C. Ji, et al., Wire-supported CdSe nanowire array photoelectrochemical solar cells, Phys. Chem. Chem. Phys. 14 (10) (2012) 3583. Available from: https://doi.org/10.1039/c2cp00024e.
[116] Z. Zhou, Q. Li, L. Chen, C. Liu, S. Fan, A large-deformation phase transition electrothermal actuator based on carbon nanotube–elastomer composites, J. Mater. Chem. B 4 (7) (2016) 1228–1234. Available from: https://doi.org/10.1039/c5tb02715b.
[117] M.D. Lima, N. Li, M. Jung De Andrade, S. Fang, J. Oh, G.M. Spinks, et al., Electrically, chemically, and photonically powered torsional and tensile actuation of hybrid carbon nanotube yarn muscles, Science 338 (6109) (2012) 928–932. Available from: https://doi.org/10.1126/science.1226762.
[118] J.H. Jeong, T.J. Mun, H. Kim, J.H. Moon, D.W. Lee, R.H. Baughman, et al., Carbon nanotubes–elastomer actuator driven electrothermally by low-voltage, Nanoscale Adv. 1 (3) (2019) 965–968. Available from: https://doi.org/10.1039/c8na00204e.
[119] N. Hillier, S. Yong, S. Beeby, Optimization of carbon electrodes for solid-state e-textile supercapacitors, J. Phys. Conf. Ser. 1407 (2019) 012059. Available from: https://doi.org/10.1088/1742-6596/1407/1/012059.
[120] X. Cai, M. Peng, X. Yu, Y. Fu, D. Zou, Flexible planar/fiber-architectured supercapacitors for wearable energy storage, J. Mater. Chem. C. 2 (7) (2014) 1184–1200. Available from: https://doi.org/10.1039/c3tc31706d.
[121] A.M. Abdelkader, N. Karim, C. Vallés, S. Afroj, K.S. Novoselov, S.G. Yeates, Ultraflexible and robust graphene supercapacitors printed on textiles for wearable electronics applications, 2D Mater. 4 (3) (2017) 035016. Available from: https://doi.org/10.1088/2053-1583/aa7d71.
[122] L. Wang, K.J. Loh, Wearable carbon nanotube-based fabric sensors for monitoring human physiological performance, Smart Mater. Struct. 26 (5) (2017) 055018. Available from: https://doi.org/10.1088/1361-665x/aa6849.
[123] M.K. Yapici, T. Alkhidir, Y.A. Samad, K. Liao, Graphene-clad textile electrodes for electrocardiogram monitoring, Sens. Actuators B Chem. 221 (2015) 1469–1474. Available from: https://doi.org/10.1016/j.snb.2015.07.111.
[124] P. Ilanchezhiyan, A.S. Zakirov, G.M. Kumar, S.U. Yuldashev, H.D. Cho, T.W. Kang, et al., Highly efficient CNT functionalized cotton fabrics for flexible/wearable heating applications, RSC Adv. 5 (14) (2015) 10697–10702. Available from: https://doi.org/10.1039/c4ra10667a.
[125] L.R. Pahalagedara, I. Siriwardane, N.D. Tissera, R.N. Wijesena, K.M.N. de Silva, Carbon black functionalized stretchable conductive fabrics for wearable heating applications, RSC Adv. 7 (31) (2017) 19174–19180. Available from: https://doi.org/10.1039/c7ra02184d.
[126] Wilson, & Laing, Fabrics and garments as sensors: a research update, Sensors 19 (16) (2019) 3570. Available from: https://doi.org/10.3390/s19163570.

[127] M. Liu, X. Pu, C. Jiang, T. Liu, X. Huang, L. Chen, et al., Large-area all-textile pressure sensors for monitoring human motion and physiological signals, Adv. Mater. 29 (41) (2017) 1703700. Available from: https://doi.org/10.1002/adma.201703700. Available from: http://doi.org/10.1002/adma.201703700.
[128] N. Nafeie, M. Montazer, N.H. Nejad, T. Harifi, Electrical conductivity of different carbon nanotubes on wool fabric: an investigation on the effects of different dispersing agents and pretreatments, Colloids Surf. A Physicochem. Eng. Asp. 497 (2016) 81–89. Available from: https://doi.org/10.1016/j.colsurfa.2016.02.029.
[129] Z. Motaghi, S. Shahidi, Effect of single wall and carboxylated single wall carbon nanotube on conduction properties of wool fabrics, J. Nat. Fibers 12 (4) (2015) 388–398. Available from: https://doi.org/10.1080/15440478.2014.945225.
[130] T. Makowski, D. Kowalczyk, W. Fortuniak, D. Jeziorska, S. Brzezinski, A. Tracz, Superhydrophobic properties of cotton woven fabrics with conducting 3D networks of multiwall carbon nanotubes, MWCNTs, Cellulose 21 (6) (2014) 4659–4670. Available from: https://doi.org/10.1007/s10570-014-0422-0.
[131] E. Skrzetuska, M. Puchalski, I. Krucińska, Chemically driven printed textile sensors based on graphene and carbon nanotubes, Sensors 14 (9) (2014) 16816–16828. Available from: https://doi.org/10.3390/s140916816.
[132] M. Montazer, M. Samin, G. Asghari, and E. Pakdel, Electrical Conductivity of Single Walled and Multiwalled Carbon Nanotube Containing Wool Fibers, pp. 1–6, 2011, https://doi.org/10.1002/app.
[133] L. Hu, M. Pasta, F. La Mantia, L. Cui, S. Jeong, H.D. Deshazer, et al., Stretchable, porous, and conductive energy textiles, Nano Lett. 10 (2) (2010) 708–714. Available from: https://doi.org/10.1021/nl903949m.
[134] L. Guo, L. Berglin, Test and evaluation of textile based stretch sensors, in: Proceedings of the AUTEX World Textile Conference, Izmir, Turkey, p. 8. Hayward, J. (2020). A comprehensive review of materials, processes, components, products and the global market. E-textiles and Smart Clothing 2020–2030: Technologies, Markets and Players, 2009.
[135] M. Pacelli, L. Caldani, R. Paradiso, Performances evaluation of piezoresistive fabric sensors as function of yarn structure, in: 2013 35th Annual International Conference of the IEEE Engineering in Medicine and Biology Society (EMBC), 2013. Published. https://doi.org/10.1109/embc.2013.6611044.
[136] A.J. Golparvar, M.K. Yapici, Electrooculography by wearable graphene textiles, IEEE Sens. J. 18 (21) (2018) 8971–8978. Available from: https://doi.org/10.1109/jsen.2018.2868879.
[137] C. Lou, S. Wang, T. Liang, C. Pang, L. Huang, M. Run, et al., A graphene-based flexible pressure sensor with applications to plantar pressure measurement and gait analysis, Materials 10 (9) (2017) 1068. Available from: https://doi.org/10.3390/ma10091068.
[138] L. Gan, S. Shang, C.W.M. Yuen, S.X. Jiang, Graphene nanoribbon coated flexible and conductive cotton fabric, Compos. Sci. Technol. 117 (2015) 208–214. Available from: https://doi.org/10.1016/j.compscitech.2015.06.019.
[139] Z. Gao, N. Song, Y. Zhang, X. Li, Cotton-textile-enabled, flexible lithium-ion batteries with enhanced capacity and extended lifespan, Nano Lett. 15 (12) (2015) 8194–8203. Available from: https://doi.org/10.1021/acs.nanolett.5b03698.
[140] I.A. Sahito, K.C. Sun, A.A. Arbab, M.B. Qadir, S.H. Jeong, Graphene coated cotton fabric as textile structured counter electrode for DSSC, Electrochim. Acta 173 (2015) 164–171. Available from: https://doi.org/10.1016/j.electacta.2015.05.035.

[141] K. Javed, C. Galib, F. Yang, C.M. Chen, C. Wang, A new approach to fabricate graphene electro-conductive networks on natural fibers by ultraviolet curing method, Synth. Met. 193 (2014) 41–47. Available from: https://doi.org/10.1016/j.synthmet.2014.03.028.

[142] S.J. Kim, W. Song, Y. Yi, B.K. Min, S. Mondal, K.S. An, et al., High durability and waterproofing rGO/SWCNT-fabric-based multifunctional sensors for human-motion detection, ACS Appl. Mater. Interfaces 10 (4) (2018) 3921–3928. Available from: https://doi.org/10.1021/acsami.7b15386.

[143] Y.R. Lee, J. Park, Y. Jeong, J.S. Park, Improved mechanical and electrical properties of carbon nanotube yarns by wet impregnation and multi-ply twisting, Fibers Polym. 19 (12) (2018) 2478–2482. Available from: https://doi.org/10.1007/s12221-018-8140-0.

[144] X. Li, R. Liu, C. Xu, Y. Bai, X. Zhou, Y. Wang, et al., High-performance polypyrrole/graphene/SnCl2 modified polyester textile electrodes and yarn electrodes for wearable energy storage, Adv. Funct. Mater. 28 (22) (2018) 1800064. Available from: https://doi.org/10.1002/adfm.201800064.

[145] F. Yin, J. Yang, H. Peng, W. Yuan, Flexible and highly sensitive artificial electronic skin based on graphene/polyamide interlocking fabric, J. Mater. Chem. C. 6 (25) (2018) 6840–6846. Available from: https://doi.org/10.1039/c8tc00839f.

[146] W. Wu, H. Zhang, H. Ma, J. Cao, L. Jiang, G. Chen, Functional finishing of viscose knitted fabrics via graphene coating, J. Eng. Fibers Fabr. 12 (3) (2017). Available from: https://doi.org/10.1177/155892501701200301. 155892501701200.

[147] C. Zhao, K. Shu, C. Wang, S. Gambhir, G.G. Wallace, Reduced graphene oxide and polypyrrole/reduced graphene oxide composite coated stretchable fabric electrodes for supercapacitor application, Electrochim. Acta 172 (2015) 12–19. Available from: https://doi.org/10.1016/j.electacta.2015.05.019.

[148] S. Kumar, G. Saeed, L. Zhu, K.N. Hui, N.H. Kim, J.H. Lee, 0D to 3D carbon-based networks combined with pseudocapacitive electrode material for high energy density supercapacitor: a review, Chem. Eng. J. 403 (2021) 126352. Available from: https://doi.org/10.1016/j.cej.2020.126352.

[149] M.D. Angione, R. Pilolli, S. Cotrone, M. Magliulo, A. Mallardi, G. Palazzo, et al., Carbon based materials for electronic bio-sensing, Mater. Today 14 (9) (2011) 424–433. Available from: https://doi.org/10.1016/S1369-7021(11)70187-0.

[150] L.M. Castano, A.B. Flatau, Smart fabric sensors and e-textile technologies: a review, Smart Mater. Struct. 23 (5) (2014). Available from: https://doi.org/10.1088/0964-1726/23/5/053001.

[151] T.D. Fornes, D.R. Paul, Structure and properties of nanocomposites based on nylon-11 and -12 compared with those based on nylon-6, Macromolecules 37 (20) (2004) 7698–7709. Available from: https://doi.org/10.1021/ma048757o.

[152] J.S. Heo, J. Eom, Y.H. Kim, S.K. Park, Recent progress of textile-based wearable electronics: a comprehensive review of materials, devices, and applications, Small 14 (3) (2018) 1–16. Available from: https://doi.org/10.1002/smll.201703034.

[153] Z. Yang, H. Peng, W. Wang, T. Liu, Crystallization behavior of poly (ε-caprolactone)/layered double hydroxide nanocomposites, J. Appl. Polym. Sci. 116 (5) (2010) 2658–2667. Available from: https://doi.org/10.1002/app.

[154] M. Jamshidian, E.A. Tehrany, M. Imran, M. Jacquot, S. Desobry, Poly-lactic acid: production, applications, nanocomposites, and release studies, Compr. Rev. Food Sci. Food Saf. 9 (5) (2010) 552–571. Available from: https://doi.org/10.1111/j.1541-4337.2010.00126.x.

[155] B. Fan, X. Mei, K. Sun, J. Ouyang, Conducting polymer/carbon nanotube composite as counter electrode of dye-sensitized solar cells, Appl. Phys. Lett. 93 (14) (2008) 91−94. Available from: https://doi.org/10.1063/1.2996270.
[156] S. Yousef, Polymer nanocomposite components: a case study on gears. in lightweight composite structures in transport: design, manufacturing, Analysis and Performance, Elsevier Ltd, 2016. Available from: https://doi.org/10.1016/B978-1-78242-325-6.00016-5.
[157] R.J. Moon, A. Martini, J. Nairn, J. Simonsen, J. Youngblood, Cellulose nanomaterials review: Structure, properties and nanocomposites, Chem. Soc. Rev. 40 (7) (2011). Available from: https://doi.org/10.1039/c0cs00108b.
[158] S. Sharifi, S. Behzadi, S. Laurent, M.L. Forrest, P. Stroeve, M. Mahmoudi, Toxicity of nanomaterials, Chem. Soc. Rev. 41 (6) (2012) 2323−2343. Available from: https://doi.org/10.1039/c1cs15188f.
[159] S.M. Louie, R. Ma, G.V. Lowry, Transformations of nanomaterials in the environment, Front. Nanosci. 7 (2014) 55−87. Available from: https://doi.org/10.1016/B978-0-08-099408-6.00002-5.
[160] X. Xie, L. Hu, M. Pasta, G.F. Wells, D. Kong, C.S. Criddle, et al., Three-dimensional carbon nanotube-textile anode for high-performance microbial fuel cells, Nano Lett. 11 (1) (2011) 291−296. Available from: https://doi.org/10.1021/nl103905t.
[161] J. Saunders, Do e-textiles for fashion require specific legislation and developmental guidelines in order to avoid harmful waste? The International Conference on the Challenges, Opportunities, Innovations and Applications in Electronic Textile. UK, 2020.
[162] Yang, K., Isaia, B. (2019). E-Textiles for Healthy Ageing.
[163] S. Sim, H. Jeon, G. Chung, S. Kim, S. Kwon, W. Lee, et al., Fall Detection Algorithm for the Elderly Using Acceleration Sensors on the Shoes, 2011.
[164] K. Yang, K. Meadmore, C. Freeman, N. Grabham, A.-M. Hughes, Y. Wei, et al., Development of User-Friendly Wearable Electronic Textiles for Healthcare Applications, 2018.
[165] A. Köhler, End-of-life implications of electronic textiles assessment of a converging technology, Environ. Manag. IIIEE Thes (October) (2008) 1−88.
[166] P.V. Ilén, Review of the end-of-life solutions in electronics-based smart textiles. The Journal of the Textile Institute, 2020.
[167] S. Kind, M. Bovenschulte, Trends in micro system technology, 2006.
[168] M.A. Gardetti, S.S. Muthu, Handbook of Sustainable Luxury Textiles and Fashion, 2015.
[169] A.Y. Hoekstra, A.K. Chapagain, M.M. Aldaya, M.M. Mekonnen, The Water Footprint Assesment Manual, Earthscan, 2011.
[170] T. Wiedmann, J. Minx, A definition of 'carbon footprint', Ecol. Econ. Res. Trends 1 (2008) 1−11.
[171] D.V. Jaganathan, P. Cherurveettil, A. Chellasamy, D.M. Premapriya, Environmental Pollution Risk Analysis and Management in Textile Industry: A Preventive Mechanism. European Scientific Journal, 2014.

# Flame retardant nanofillers and its behavior in polymer nanocomposite

17

*M. Norkhairunnisa*[1,2,3], *B. Farid*[2] *and T. Chai Hua*[4]
[1]Institute of Nanoscience and Nanotechnology (ION2), Universiti Putra Malaysia, Serdang, Serdang, Selangor, Malaysia
[2]Department of Aerospace Engineering, Faculty of Engineering, Serdang, Selangor, Malaysia
[3]Aerospace Malaysia Research Center (AMRC), Universiti Putra Malaysia, Serdang, Selangor, Malaysia
[4]Institute of Tropical Forestry and Forest Products (INTROP), Serdang, Selangor, Malaysia

## 17.1 Introduction

Polymer materials can be extremely flammable and generate a great deal of heat when burned. Thermal degradation of polymer materials results in the formation of bubbles beneath the polymer's surface. By the diffusion of heat and oxygen, the number of bubbles produced increases as the burning time increases. When the bubble reaches the polymer's outer layer, the polymer melts and degrades [1]. Polymer materials have seen an increase in popularity over the years. Despite its high flammability, the polymer is still used in a wide variety of commercial products, ranging from textiles to molded items. This is a clear indication of consumer exposure to hazards. To compound matters, many polymeric materials are prone to melt flow and melt drip under elevated temperatures or fire conditions. This creates a significant secondary hazard, as melt flow and melt drip from polymeric materials (particularly the ceiling) can ignite flammable materials (especially of the lower area). This scenario's fire escalation is rapid, posing a greater risk to people [2].

The term "flame retardancy" is frequently used to refer to the property of the combustion process ceasing or the absence of afterglow when the ignition source is removed. The flame retardant is then referred to as the additive to the polymer that contributes to the polymer's increased flame retardancy [3]. However, ISO (2021) defines flame retardant as a substance added to or treatment applied to a material to suppress or delay the appearance of flame and/or reduce the rate of flame spread [4]. ASTM, on the other hand, provides a more detailed and descriptive definition of the subject. As a result, the term "flame retardant" has been deprecated and can only be used in conjunction with a defined compound to refer to a flame retardant chemical, flame retardant coating, or flame retardant treatment. A flame retardant

**Advanced Polymer Nanocomposites. DOI: https://doi.org/10.1016/B978-0-12-824492-0.00018-0**

chemical is a substance added to a combustible material to retard ignition and limit flame spread when the material is impinged by flames. A flame retardant coating is a fluid that is applied to the surface of a material to protect it from flame impingement [5]. Flame impingement occurs when material comes into contact with or is consumed by a flame [6]. Another ASTM-created term relating to flame retardants is flame retardant treatment. The term "flame retardant treatment" refers to the application of a flame retardant chemical or coating [5]. The published work successfully adapts the ASTM-recommended term for flame retardant chemicals [7].

While thermal stability is also a heat-related test and is frequently studied in conjunction with flame retardant behavior, it is important to understand that the thermal stability of polymers refers to the material's ability to resist action caused by heat [8]. Its data are derived from thermogravimetric analysis (TGA) measurements of weight loss as a function of temperature [9]. On the other hand, flame retardancy is not quantifiable. Rather than that, it can be quantified using characteristics such as ignitability, flame spread, and combustion rate [10]. Thus, to comprehend what makes a flame retardant chemical effective, one must first understand the combustion mechanism. When combined with sufficient heat, oxygen, and a suitable fuel, combustion becomes self-catalyzing and will continue until all of the components are depleted [11,12]. Thus, when polymeric materials are burned, the polymer serves as the fuel that sustains combustion in the presence of heat and oxygen.

The selection of flame retardant chemicals for incorporation into polymers is laborious, as different materials have varying compositions and characteristics. Additionally, the behavior of materials during combustion varies significantly, complicating the process of selecting an effective combination of polymer and flame retardant chemicals [13]. Thus, by incorporating the appropriate flame retardant fillers into the polymer, a protective or shielding function will be provided, limiting heat transfer to the internal substrate during combustion. Additionally, the nanoparticle acts as a physical barrier on the polymer substrate during polymer material thermal decomposition, forming a carbon layer [1]. As a result, it is expected that the addition of nanoparticles will reduce the flammability of polymers by delaying the formation of bubbles and the degradation process during combustion. Additionally, a high surface area or nanoparticles may improve the interaction with the polymer matrix.

By incorporating flame retardant nanoparticles, the specific characteristics of the polymer matrix can be altered, hence increasing flammability resistance. The performance of a nanocomposite is determined by the nanoparticles' dimensions, shape, specific surface area, volume, or concentration, as well as their compatibility with the matrix surface. Nanomaterials fall into two categories: nanostructured materials and nano-objects. Nanostructured materials have a nanoscale internal or external structure (1 −100 nm). At the nanoscale, nano-objects can have one or more external dimensions. Nanoparticles, nanofibers, and nanoplates are often used subcategories of nano-objects. Nanocoatings, nanofilms, and nanolayers are also termed nano-objects by ASTM [14]. Fig. 17.1 illustrates these nano-objects. As a result, flame-resistant nanoparticles must possess all three external dimensions at the nanoscale.

The two-dimensional (2D) nanofiller has a particle size of less than 100 nm and is more flame retardant than the 1D and three-dimensional (3D) nanofillers. This is

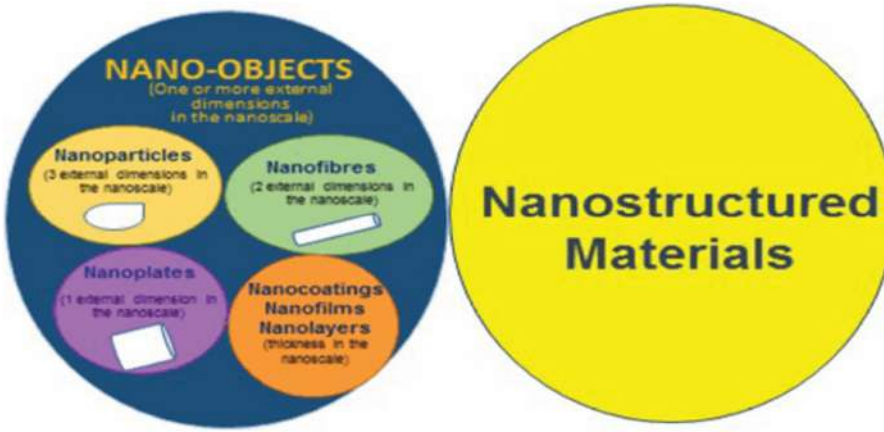


**Figure 17.1** The grouping of nanomaterials according to ISO [14].

because the 2D nanofiller has a layered structure that can act as a physical barrier, insulate, and boost the polymer matrix's thermal stability [15]. 2D nanofillers are frequently found as tubes, fibers, and filaments. The significant advantages of utilizing flame retardant nanoparticles are that they require a tiny amount of nanoparticles, less than 5% by weight, to increase the flame retardant qualities of polymer materials [16]. The effectiveness of nanoparticles in a polymer matrix in terms of flammability is dependent on their dispersion and interfacial coupling to the polymer matrix [17]. Due to agglomeration and a lack of interfacial adhesion with the polymer matrix, flame retardant nanofiller disperses poorly, reducing its flame retardancy [18].

On the other hand, the polymer nanocomposite's mechanical and physical properties will be harmed as a result of the nanofiller's weak bonding relationship with the polymer structure [19,20]. The tortuous pathway established by the 2D nanofiller can delay the release of pyrolysis gases during polymeric material combustion. Zhang et al. [21] have developed an organic−inorganic 3D nanostructured flame retardant material. $SiO_2$/PZM/Cu is a 3D core−shell nanostructure that was synthesized in a one-pot synthesis technique. As a result, it creates graphitized char during burning, which is more effective at inhibiting heat and mass transmission than disordered graphite is. The 3D core−shell nanostructure is extremely compact, which benefits fireproofing capabilities.

This chapter discussed the evolution of flame retardant polymer nanocomposites. There are numerous varieties of flame retardant nanoparticles, each with a unique active ingredient attached. Additionally, surface modification of nanoparticles has garnered attention, as dispersion of nanoparticles in the polymer environment is critical. Finally, several fire tests, such as UL-94, cone calorimeter, limiting oxygen index (LOI), smoke, and toxicity analysis, are described for numerous flame retardant nanocomposites.

## 17.2 Flame retardant nanomaterials

Through a chemophysical mechanism occurring below the ignition source, flame retardants can inhibit the ignition and propagation of the flame. Different forms and sizes of flame retardant nanoparticles were used in a variety of applications. Additionally, flame retardants can be classified into many broad classes based on their chemical constituents. Halogen-based, phosphorus-based, nitrogen-based, metal-based, and UV-curable are some examples. Historically, halogen materials containing flame retardants were used. However, public agencies expressed concern in the 1970s, and numerous restrictions limiting the use of brominated and chlorinated flame retardants were enacted. This is owing to the primary concern about the high levels of harmful chemicals emitted during burning, which can contaminate the environment and hurt human health, prompting the phase-out of the halogen-based substance. Later, due to the ecologically beneficial qualities of the halogen-free compound, it was regarded to be a viable alternative to the old halogen-based compounds [22].

Nanosized flame retardants are a group of modern materials that ride the wave of nanotechnology, leaving behind some traditional, toxic flame retardants containing halogen compounds. The advantage of being nanosized offers an innovative flame retarding mechanism that traditional flame retardants could not achieve. While conventional ways of flame retardation include the creation of free radicals in the gas phase, endothermic reaction, and char formation, nanosized flame retardants work by traditional and/or novel processes, such as increasing the thermal stability and viscosity of polymers [23–25]. Since the method in retarding flame depends on the type of compounds, this section will explain the mechanism based on different flame retardant nanomaterials.

Generally, flame retardant nanomaterials interact with polymers through van der Waals, hydrogen bonding, and electrostatic interaction. When the interaction is good, it is translated as good compatibility, which hugely contributes to retarding flame through well-dispersed nanomaterials in polymers [24].

### 17.2.1 Clay-based nanomaterials

Clay minerals are classified according to their layered structure as kaolinite, smectite, illite, and chlorite. Nanoclays are typically composed of 98% montmorillonite (MMT), a mineral that is a constituent of smectite [26]. The length of nanoclay can range between 1.5 μm and a few tenths of a micron [27], although the diameter (sometimes referred to as thickness or width) can be as small as 1 nm [26]. This classifies nanoclay as a type of flame retardant nanomaterial known as nanoplates. Nanoclay has a large surface area due to its size. This results in the aggregated and agglomerated nanoclay [28]. However, when dispersed properly, the high surface area of nanoclay contributes significantly to the flame retardant mechanism.

Nanoclay is made up of layered silicate layers that act as protection for the polymer substrate during the burning process. Nanoclay intercalated and exfoliated into a polymer matrix with a significant *d*-spacing indicates migration from the nanoclay platelet to the substrate surface [29,30]. Migration requires the formation of a

carbonization barrier that can retard the release of gas and heat transfer. At low temperatures, migration can occur due to the degradation of the organic modifier that binds to the nanoclay platelet. Additionally, the polymer may deteriorate when nanoclay is present in a restricted area. In this case, increased chain scission destroys the polymer into small molecules, resulting in the emergence of new degradation pathways [31]. Additionally, the catalytic action of nanoclay affects flammability. Degradation occurs at a different rate depending on the type of organic surfactant connected to the nanoclay structure [32]. According to Qin et al. [33], the polymer nanocomposite's shorter ignition time during combustion can be due to the acidic sites attached to the nanoclay degrading and the polymer matrix decomposing, which is catalyzed by the nanoclay (Fig. 17.2). Finally, the presence of nanoclay contributes to the reduction of combustion heat, gasification heat, and the nanocomposite's flaming state. Without the addition of nanoclay, the flame consumes the polymer skin, leaving no residue after flaming [34].

A varied level of dispersion of nanoclay as shown in Fig. 17.3, results in diverse nanoclay states in response to polymer mixing. Intercalated-flocculated nanoclays, exfoliated-intercalated nanoclays, or a combination of intercalated and exfoliated nanoclays are all possible. The effect of these four distinct nanoclay dispersion states in polylactide or polylactic acid (PLA) was investigated. The tortuous path formed by the nanoclays acts as a gas barrier, delaying the passage of gas molecules through the resin [36].

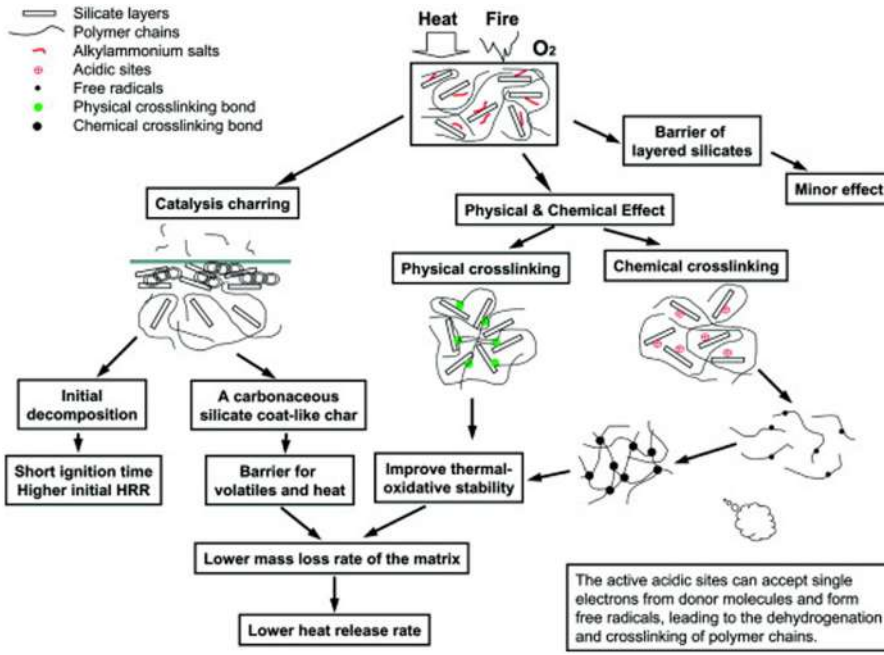


**Figure 17.2** Schematic diagram of combustion mechanism on nanocomposite filled with nanoclay silicate layers [33].

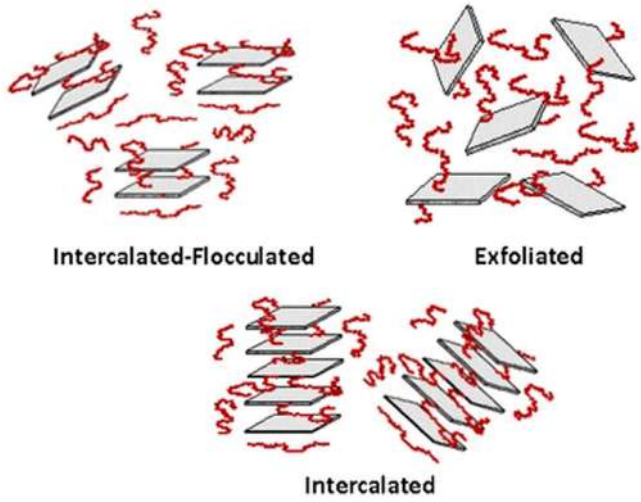


**Figure 17.3** Different structures of polymer-clay nanocomposites [35].

To obtain the desired dispersion form, the silicate surface of nanoclay can be changed by substituting cationic surfactants such as alkyl ammonium and alkyl imidazolium for the initial interlayer cations. This is accomplished by lowering the surface energy of nanoclay, increasing its wettability with polymers, and increasing the interlayer space in organo-modified nanoclays due to their long aliphatic tails [24].

Apart from nanoclay, there is another extensive clay class known as layered double hydroxide (LDH). This compound contains metallic cations that are divalent and trivalent [24]. Thus this flame retardant chemical takes use of the synergistic effect of combining two different types of flame retardant processes. It is reported that synergistic flame retardant systems are being developed to increase the effectiveness of flame retardants [37]. Endothermically, LDH decomposes, releasing water and carbon dioxide that cool and dilute the flammable components. The synergy between clay and metal compounds significantly reduces the peak heat release rate (PHRR) and mass loss rate values while increasing the LOI.

### 17.2.2 Metal-based nanomaterials

Inorganic nanoparticles that are flame retardants contain a metal-based chemical that is less poisonous and effective as a smoke suppressor. Inorganic nanoparticles containing a metal-based substance are less harmful and more efficient than organic nanoparticles as smoke suppressants [38]. Additionally, because metal-based compounds are good heat conductors, they can improve heat transfer within the material, hence delaying bubble migration. Simultaneously, it may lower the amount of heat released and the concentration of local oxygen caused by the oxides' oxidation−reduction reactions. Apart from that, these chemicals can operate as a heat and mass transfer barrier, altering the polymer degradation route and absorbing free

radicals. Additionally, because it is a nanomaterial, its presence can limit the mobility of polymer chains [24]. Apart from this, it has been suggested that metal-based nanomaterials release water molecules during decomposition, so creating an endothermic environment that self-extinguishes flames [25].

Metals with hydroxide groups [$Mg(OH)_2$, Al $(OH)_3$], metal-containing salts (carbonates, phosphates, borate), and metals with oxide groups (ZnO, $Sb_2O_3$, $Al_2O_3$) are all examples of metals with flame retardant properties [39]. Certain metal oxides, such as cuprous oxide ($Cu_2O$), can rapidly absorb or release oxygen from the surface lattice [40]. Due to its high thermal conductivity and heat capacity, zinc oxide (ZnO) is said to absorb heat from its surroundings and inhibit fires. The chemical is well-known as an inhibitor of flame propagation [25]. The synergistic effect of flame retardant metal oxides on graphene has been demonstrated to improve the polymer's flame retardant qualities via the generation of char [41].

### 17.2.3 Carbon-based nanomaterials

Nanocarbons such as carbon nanotubes (CNT), graphene oxide (GO), and fullerene (C60) are attractive nanofillers that have the potential to significantly increase the flame retardant properties of the polymeric composite. The primary mechanism by which CNT retards flame is by the creation of char layers. Char layers act as thermal insulators and heat barriers, re-emitting radiation into the gas phase. Ultimately, this retards polymer thermal breakdown. As with metallic components, CNT improve the heat conductivity of polymer nanocomposites. Not only that, CNT enhances the melt viscosity of polymers and works as a scavenger of free radicals [24]. Additionally, due to its highly elongated form, CNT have a high aspect ratio. This enables them to form a strong protective network of CNT around the polymer to shield it from heat. This reduces the amount of heat released and the rate of weight loss during burning. Interestingly, it has been found to have a low flame spread rate and antidripping characteristics as well. Finally, these benefits are contingent upon the dispersion and handling of CNT [25].

The addition of nanocarbons alone does not significantly improve the flame retardant properties due to their strong tendency for aggregation formation and minimal interfacial contact with the polymer matrix. The enhancement of nanocarbons' strength is related to their dispersibility in the polymer matrix. One way to enhance dispersion is to graft the nanocarbon surface with a compatibilizer. Wang et al. [42] grafted a phosphorus-nitrogen-containing polymer onto the surface of the CNT via strong-stacking interactions. The surface grafting improves the interfacial adherence of the CNT to the polymer's surface, resulting in enhanced flame retardant qualities. Unlike CNT, which have a tube-like structure, graphene has a platelet structure. Due to Van der Waals forces, graphene tends to restack, which may impair its effectiveness as a flame retardant nanomaterial. However, when properly disseminated, graphene improves the thermal stability of polymers due to graphene's heat-insulating properties. Additionally, its presence might act as a significant heat sink. To boost graphene's compatibility with polymers, it can be treated with metal oxide. On the other hand, C60 takes a different approach to flame retardance.

This chemical has a high level of reactivity toward free radicals. When in contact with polymers, C60 traps radicals created during burning, delaying their thermo-oxidative destruction [25]. Carbon-based flame retardants have been reported to be applied to polymers in conjunction with traditional flame retardants to increase their flame retardancy [43,44].

### 17.2.4 Silicone-based nanomaterials

Nanosilica has been shown to inhibit polymer chain mobility, hence delaying polymer dripping during combustion. The way it works is that when the viscosity of the polymer is increased due to the presence of nanosilica, a greater amount of energy is required for the polymer to drip. It has been demonstrated that the addition of nanosilica to polyethylene reduces the heat release rate (HRR). Polyhedral oligomeric silsesquioxane (POSS), a derivative of the substance, is an organic−inorganic hybrid chemical with a silicon-oxygen cage surrounded by organic groups. Copolymerization and grafting are two therapeutic options for POSS that modify the organic substituent groups chemically. When properly produced, POSS protects the underlying polymer by migrating to the surface and producing a ceramic layer after combustion. This results in a thermally stable silica material at elevated temperatures [24]. One of the most recent synergistic flame retardant processes involves the use of nanosilica in the synthesis of hybrid nanosilica/GO. The material is a porous sponge with exceptional flame retardancy [45].

### 17.2.5 Biobased nanomaterials

Environmental concerns have prompted the development of green additives or fillers. Lignin has the potential to generate char and retards the degradation process, making it an excellent biomass flame retardant filler [46−48]. To work effectively as a flame retardant material, lignin nanoparticles (LNPs) must be well disseminated in polymer media. The addition of around 5% grafted lignin with phosphorus increases the time to ignition (TTI) by approximately 23% and decreases the HRR of the PLA nanocomposite [46]. According to Sienkiewicz and Czub [49], functionalized CNT and expandable graphite can be incorporated into biocomposite to improve its flame retardant properties and to build a char layer to protect the beneath surface. With the inclusion of a flame retardant filler, flame retardants for biodegradable polymers such as PLA can be increased.

Apart from lignin, another bio-derived nanomaterial that can be employed as a flame retardant chemical is starch. The mechanism in retarding flame involves carbonization and char formation. The formation of char begins with the breakdown of starch. Starch is a type of polysaccharide composed of amylose and amylopectin. Starch dehydrates and releases stored moisture during heat decomposition. Immediately afterward, at elevated temperatures, hydroxyl groups undergo thermal condensation. Finally, at approximately 400°C, aromatic rings such as furan are created, contributing to the carbonization and char formation processes [25].

### 17.2.6 Nitrogen-based nanoparticle

Additionally, nitrogen-based flame retardant nanofillers were popular due to their environmentally acceptable features and their ability to enhance the flame retardant capabilities of polymeric materials. Nitrogen-based flame retardants such as melamine and ammonia are frequently employed and form salts to increase the thermal stability and volatility of polymers. Additionally, the phosphorus base exists in a variety of organic and inorganic compounds, including phosphonates of phosphine oxides, phosphites, phosphines, and phosphates. There are two types of phosphorus-based flame retardant materials: reactive and nonreactive. Red phosphorus, for example, is a nonreactive phosphorus flame retardant that is frequently employed in polymers. In comparison, reactive phosphorus is commonly employed in polymers as chain extenders or monomers.

The size of nanofillers can affect the performance of flame retardant properties. Sertsova et al. [39] reported that the particle size would affect the yield of char residue. The flame retardant efficiency of the polymer nanocomposite will be increased with the reduction in particle size. For smaller particles per weight, as for nanoparticles, the amount of particles in the same volume is higher than large particle size (microparticle). The presence of a high amount of nanoparticles increases the restriction sites on polymer chains, complicating the scission, and more thermal energy is desired [50]. Furthermore, the size of flame retardant particles also affects the amount of oxygen released during combustion [51].

## 17.3 Flame retardant polymer nanocomposite

The schematic diagram in Fig. 17.4A depicts the exfoliation of bulk molybdenum disulfate ($MoS_2$) nanosheets with tannic acid. The green tannic acid modifier generates a strong hydrogen bond with the polymer matrix, which accelerates the exfoliation of $MoS_2$ nanosheets and improves the mechanical characteristics of the polymer nanocomposite (Fig. 17.4B). Tannic acid, on the other hand, is a biobased flame retardant substance capable of generating intumescent char and forming a dense network with $MoS_2$ in the polyacrylonitrile (PAN).

The incorporation of pristine 2D graphene or the nanocarbon structure will not increase the polymer's fire retardant capabilities. Graphene or other nanocarbons have a strong agglomeration propensity and are poorly distributed in polymer

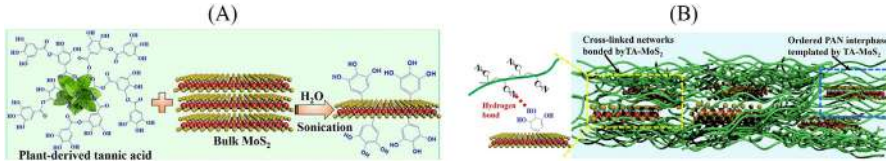


**Figure 17.4** Schematic diagram of (A) tannic acid-assisted exfoliation $MoS_2$ nanosheets and (B) cross-linked networks between tannic acid and $MoS_2$ nanosheets in PAN [52]. *PAN*, polyacrylonitrile.

matrixes. Additionally, the inserted nanocarbon's surface area will interact with the polymer chainless. Thus, by grafting a flame retardant component such as nitrogen or phosphorus onto the surface of the nanocarbon, the flame retardant capabilities of the polymer nanocomposite will be considerably improved [53].

The addition of a flame retardant filler to PLA had no discernible effect on the flame retardant properties of the PLA nanocomposite. The addition of an acid source, a carbonization agent, and a blowing agent to PLA results in the formation of an intumescent flame retardant (IFR) system, and approximately 30% by weight of nanoclay may have been added to the system [54]. Additionally, by protecting PLA, the addition of LNPs treated with diethyl chlorophosphate (diEtP) enhances the quantity of char produced following combustion.

The combination of two different nanofillers in polymer nanocomposites can be called hybrid flame retardant polymer nanocomposites. According to Wang et al. [55], adding 2.5 vol.% LNP to polyvinyl alcohol (PVA) loaded with hydroxyl boron nitride increases the flame retardant property (BN-OH). They discovered that the BN-OH/PVA/LNP flame did not propagate for roughly 5 seconds after ignition. Due to LNPs' capacity to generate char, they are an excellent contender for use as a flame retardant material.

The hybrid flame retardant nanofillers can be prepared in four ways: via covalent linkage, hydrogen bonding, π-π interaction, or an ionization process. The conventional approach is covalent coupling hybridization, which involves interacting an organic flame retardant chemical with active sites. For instance, several flame retardant chemicals have been covalently reacted with GO [56–59], black phosphorous [41], boron nitride [60,61], nanocellulose [62], and carbon black [63] for the purpose of forming hybrid flame retardant nanofillers. Due to the existence of flaws, the structure of the nanofiller is not retained during covalent bonding. The flawed structure can act as an anchor for the polymer chain, hence improving load transmission efficiency [53].

Hydrogen bonding is the simplest method for manufacturing hybrid flame retardant nanofillers without using harmful solvents. By immobilizing the hydrogen bonding contacts and increasing the graphene nanosheets' dispersibility in the polymer matrix, the strong van der Waals forces on graphene nanosheets can be minimized [64]. For instance, the polydopamine (PDA) combination in hexagonal boron nitride (h-BN) forms a hydrogen bond that aids in exfoliation and scatters the h-BN layers into the epoxy matrix. Furthermore, h-BN/PDA interacted favorably with $SnO_2$ and an epoxy matrix. This resulted in the formation of dangling bonds and external atoms between the nanofiller and the polymer matrix. The interaction will result in a high-efficiency catalytic performance, which will enhance the flame retardant qualities of the polymer nanocomposite [65].

Metal-based flame retardant nanoparticles can work synergistically with various forms of flame retardants. For example, polyvinyl chloride (PVC) filled with hybrid flame retardant nanoparticles such as ammonium polyphosphate (APP)/ZnO exhibits a drop in flame resistance compared to PVC filled with APP nanoparticles. Different flame retardants react differently, and the synergistic action of two different flame retardants may result in an increase in flammability [39]. Nitrogen-based flame retardants showed great synergy with phosphorus-based flame retardants.

The majority of salts based on nitrogen or nitrogen/phosphorus exhibit an IFR response. When the polymer nanocomposite burns at elevated temperatures, the phosphorous forms a char layer on the surface of the nanocomposite. Simultaneously, the nitrogen will release nonflammable gases into the flame zone, including $N_2$, $NH_3$, $CO_2$, and $H_2O$. Following that, the char layer will expand on the polymer's surface, acting as a heat and oxygen barrier.

## 17.4 Flammability of polymer nanocomposite

The ability of the sample to self-extinguish can be tested using the UL-94 vertical burning test, as specified in ASTM D 3801, as seen in Fig. 17.5. The materials shall be classed as V-0, V-1, or V-2 based on the results of the test. The drip of charred material on the cotton that ignited the fire suggests that the sample has low flammability but a significant potential for flame propagation. Generally, it has been observed that unreinforced polymers fail the burning test due to the lack of a protective ingredient for the polymer materials. By combining an acidic source, a carbonizing agent, and a blowing agent, an IFR system can be created. Because silica

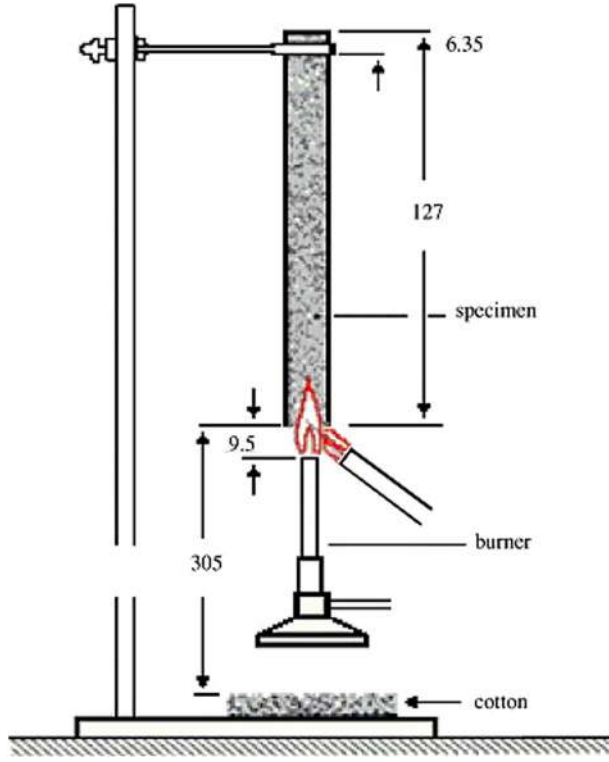


**Figure 17.5** Experimental setup for UL-94 vertical burning test [66].

($SiO_2$) has numerous acidic sites, it is an excellent source of acid for a catalytic breakdown of the polymer, particularly when paired with metal oxides [67]. When nanoclay is burned, the acidity of the hydroxyl groups (−OH) connected to the clay platelet's edge promotes char production [32].

Guo et al. [19] demonstrated that the addition of 17% melamine phosphate (MPP) to PLA with only 1% nanoclay achieved a V-0 rating. For 10 seconds, the sample self-extinguished without dripping. Melamine phosphate is nitrogen and phosphorus-based flame retardant. It absorbs a substantial amount of heat during the combustion process and releases nitrogen into the surrounding air, where it dissolves with oxygen. Additionally, the presence of nonhalogen polyphosphate accelerates the development of char and is also implicated in stimulating the polymer chains' dehydration [68]. The creation of char results in the formation of carbocation and C = C bonds during this stage. The layered silicate nanoclay was dispersed evenly with uneven and angular shapes, as illustrated in Fig. 17.6. The nanoclay structure in the composite system reduces the size of the MPP domains. However, adding around 2% nanoclay has no effect on the flammability property. It will alter the MPP domain's size by making the composite system more flexible and twistable throughout the manufacturing process.

It was discovered that adding 1%−3% nanosized NiO to PLA containing IFR components gradually improved the PLA's flame retardant capabilities (Gao et al., 2020). The UL-94 rating reached V-0 due to NiO's ability to build an effective barrier on the polymer surface, delaying the transfer of heat and oxygen. As illustrated in Fig. 17.7, two distinct char layers were formed on the sample using NiO. The initial char layer was formed by esterifying and crosslinking APP with a silicon-containing macromolecular charring agent (CSi-MCA). The finding indicates that given the UL-94 rating at V-1, degradation at this layer is unlikely to result in dripping. However, merely 1% enhances the flame retardant characteristics greatly, as the UL-94 achieved V-0 without dripping. The efficiency of the flame retardant was attributed to the catalytic carbonization process involving NiO, PLA, and CSi-MCA, which results in the formation of another char layer (char 2) with a high graphitic carbon content during combustion.

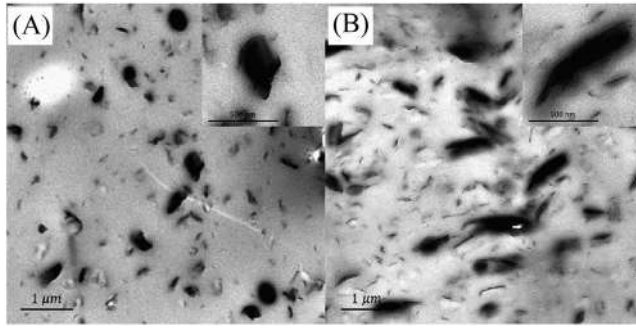


**Figure 17.6** TEM images of (A) 1% nanoclay/PLA/MPP and (B) 2% nanoclay/PLA/MPP [19]. *MPP*, melamine phosphate; *PLA*, polylactic acid.

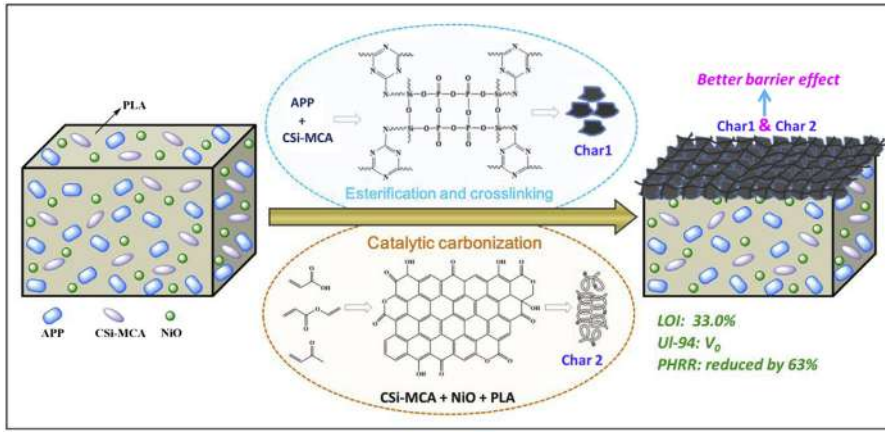


**Figure 17.7** Schematic diagram on the addition of NiO in PLA/APP/CSi-MCA [69]. *APP*, ammonium polyphosphate; *CSi-MCA*, silicon-containing macromolecular charring agent; *PLA*, polylactic acid.

According to Ref. [70], a hybrid graphene oxide nanoribbon (GONR)/MMT in polyethylene glycol (PEG) demonstrates favorable flame retardant capabilities. The hybrid nanocomposite was created using a low-temperature evaporation technique using only water as the solvent. The resultant solution was then applied to the polyurethane (PU) foam's surface. Fig. 17.8 depicts the uncoated and coated PU's reactivity to fire. The coating surface adheres extremely well to the PU foam. The hydroxyl groups in the PEG/montmorillonite/graphene (PMG) coating solution react with the N-H groups in the PU foam, delaying fire ignition. As illustrated in Fig. 17.8, increasing the coating solution concentration from 10% to 30% allows the structure to remain intact without dripping after the 20 seconds of combustion. The highly connected network of GONR/MMT prevents oxygen and heat from transferring to the PU foam, which is an outstanding flame retardant material.

## 17.5 Heat release rate of flame retardant polymer nanocomposite

A cone calorimeter can be used to determine the mass loss and gaseous release during the combustion of polymers (Fig. 17.9). The sample will be subjected to a heat flux of between 10 and 100 kW $m^{-2}$ during this study. The TTI is critical for determining the delay between fire start and ignition. By prolonging the TTI, additional time for escape is provided in the event of a fire. The HRR intensity is defined as the quantity of heat released per unit of time and the sample's surface area. If the materials are very flammable, the total heat release will be reduced.

Nanoclay dispersibility in polymers can be classified into three types: immiscible, intercalated, and exfoliated. Immiscibility, or the inability of nanoclay to

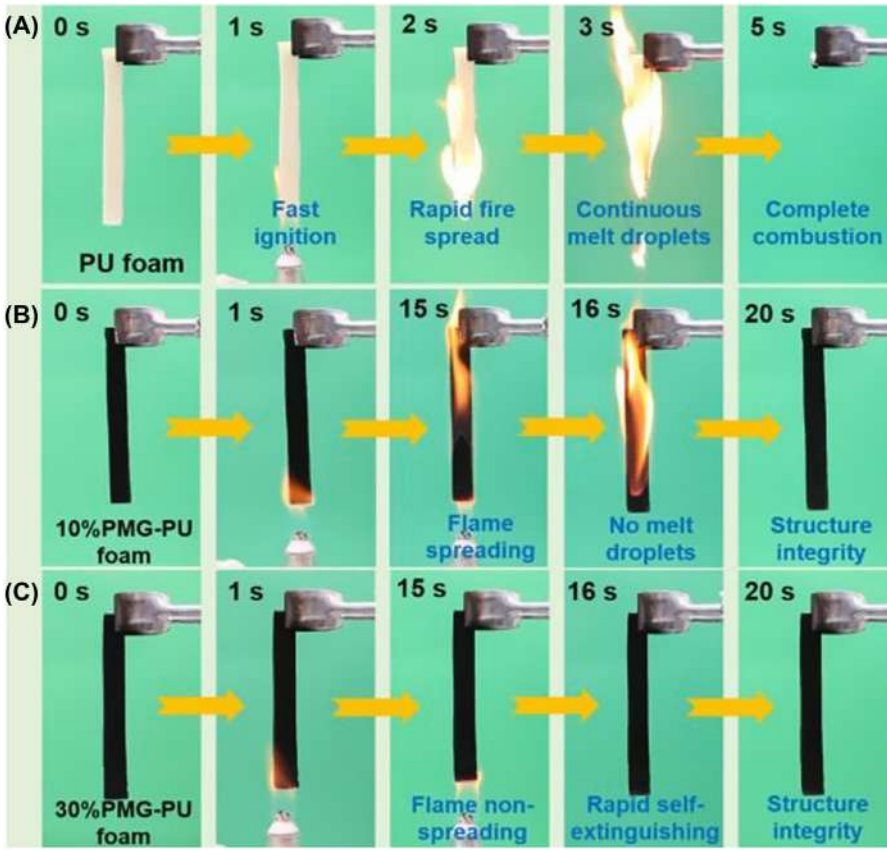


**Figure 17.8** Vertical burning test analysis of (A) PU foam, (B) 10% PMG-PU foam, and (C) 30% PMG-PU foam [58]. *PMG*, polyethylene glycol/montmorillonite/graphene; *PU*, polyurethane.

disperse in a polymer matrix, would not considerably affect the HRR value. However, for intercalated and exfoliated nanoclay, the high degree of dispersibility of the polymers has an effect on the HRR, which may be determined by cone-calorimetry. There are two mechanisms at work, both of which require nanoclay mixes in a polymer matrix at varying concentrations. Along with the low concentration of nanoclays, radical trapping occurs in the polymer nanocomposite. At elevated temperatures, as the amount of nanoclays added to the polymer matrix increases, a high carbonaceous char forms on the polymer surface. Expandable graphite disperses uniformly in PA-6 via the melt blending method, resulting in a significant reduction in HRR. Additionally, sulfuric acid was generated during this procedure, resulting in the nanocomposite's excellent flammability [72]. Additionally, it was discovered that the addition of nanocarbons such as CNT reduced the PHRR. The total heat release rate will not alter; however, because the CNT do not react in the vapor phase, interfering with the combustion process [73].

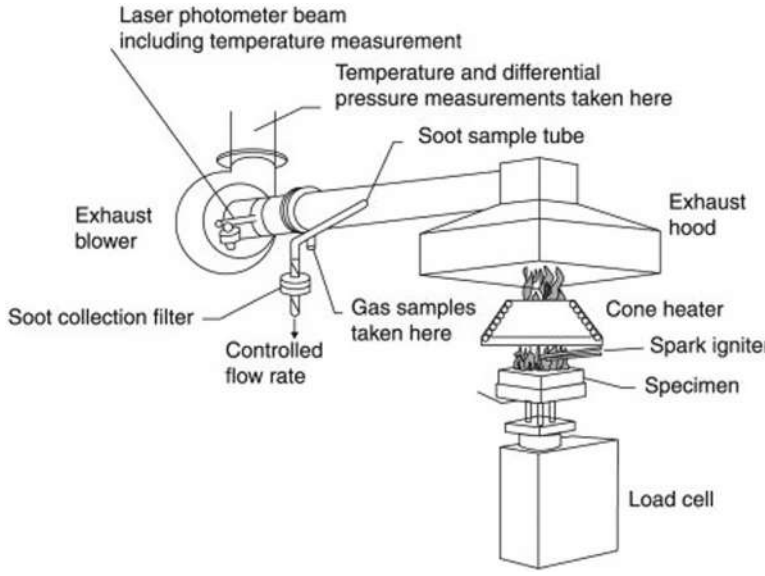


**Figure 17.9** Schematic diagram of cone calorimeter [71].

The dispersibility of N-doped modified graphene oxide (N-rGO) in acrylonitrile-butadiene-styrene copolymer (ABS) has been increased through grafting with 2,2-dimethyl-1,3-propanediol phosphoryl chloride and ammonium molybdate [$(NH_4)_2(MoO_4)$]. The interlayer gap of the grafted GO rises, indicating that the grafted GO layers are exfoliated and intercalated into the ABS matrix via strong interfacial interaction. Additionally, the inclusion of molybdate (Mo) increases the catalytic charring action by forming a physical flame retardant barrier on the underlying substrate materials. Furthermore, the layered GO structure can restrict the vitalization of minor degradation products [17].

## 17.6 Limiting oxygen index of flame retardant polymer nanocomposite materials

As illustrated in Fig. 17.10, the LOI of the polymer nanocomposite can be determined. The LOI analysis is used to determine the oxygen content of an oxygen/nitrogen mixture and the material's combustion capacity in 3 minutes, with the flame consuming approximately 5 cm of the sample length. It is the lowest oxygen concentration in a mixture of oxygen and nitrogen at which the samples will burn [74]. The following formula may be used to calculate the LOI: [24]:

$$LOI = 100 \times [O_2]/([O_2] + [N_2]) \quad (17.1)$$

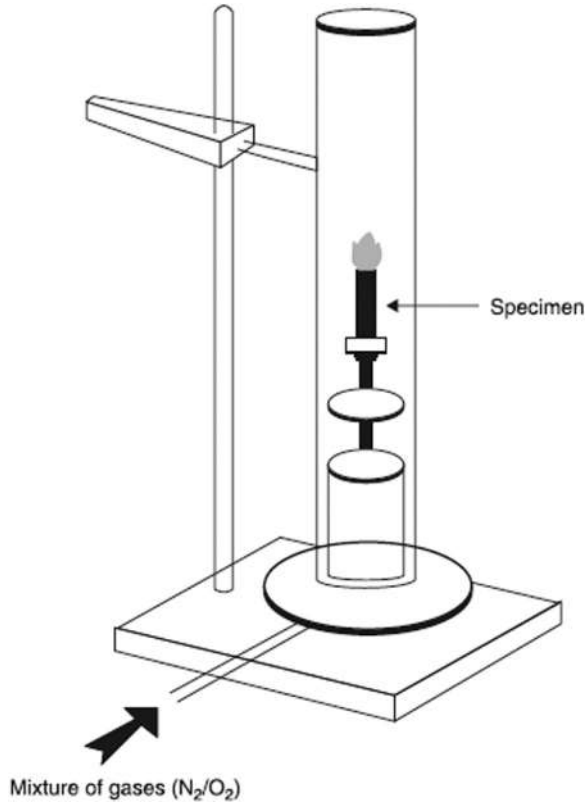


**Figure 17.10** Schematic diagram of limiting oxygen index (LOI) analysis [68].

where $[O_2]$ is an oxygen concentration and $[N_2]$ is a nitrogen concentration.

The LOI can be determined using ASTM 2863. The LOI indicator corresponds with the flame behavior of deteriorated materials, as shown in Table 17.1.

The adherence of the flame retardant nanofillers to the polymer matrix affects the LOI value. Compatibilizers can be used to improve interfacial interaction and produce a convoluted channel during high-temperature combustion, hence increasing flammability. The addition of 3phr $TiO_2$ to a wood polymer composite (WPC) along with the compatibilizer *N*-cetyl-*N*,*N*,*N*-trimethyl ammonium bromide (CTAB) increases the LOI. The presence of CTAB facilitates the formation of strong interfacial bonds between $TiO_2$ and WPC, forming a barrier to oxygen and heat transport [75]. When a sufficient amount of aluminum trihydrate (ATH) is included in a nanoclay polymer composite, a solid insulating layer is formed, increasing the LOI value during combustion [76].

Yang et al. [77] reported a relative difference in oxygen concentrations associated with combustion. They discovered that when oxygen concentrations are low enough, the surface of the polymer is sufficiently quenched to generate free radicals of O and −OH, which reduces the combustion intensity. The flame on the sample steadily dimmed and

**Table 17.1** LOI indicator on flame behavior of material.

| LOI indicator | Flame behavior of material |
|---|---|
| <21% | Combustible |
| >21% | Self-extinguish |
| >28% | Flame retardant |
| 21% < LOI < 28% | Slow burning |

eventually went out in this situation. Thus the char layer compacts the substrate and shields it from further degradation. On the other hand, as the oxygen concentration increased, the polymer's surface did not sufficiently cool. Due to a lack of O and −OH free radicals released, aggressive combustion occurred, resulting in the rapid breakdown of pyrolytic gases. As a result, the char layer takes on an intumescent appearance.

The LOI values for several nanocomposites are listed in Table 17.2. In general, increasing the graphene content increases the char residual, as well-dispersed filler produces continuous networks that act as heat sinks [75,76]. This indicates that the LOI value is directly proportional to the TGA value, which may be used to calculate the char residue [76]. Increased LOI results in decreased combustibility and improved flame retardant efficacy [78]. Certain endothermic decomposing materials, such as ATP (Attapulgite), release vaporized water and cool the combustion zone by diluting the concentration of combustible gases. This results in the formation of a dense isolation layer on the fibers' surface, which provides heat shielding, smoke suppression, oxygen penetration reduction, heat transfer inhibition, and degradation restraint [84,85,78]. Another possible explanation for how nanoparticle reinforcement raises the LOI is that oxygen root is released. Dheyaa et al. [79] explained that the release of oxygen roots from nanoparticles such as AnT (antimony trioxide) would promote the removal of active free radicals in the flame chain and impede the thermal fragmentation process that occurs during the initial stages of the flame due to its effect on the amount of heat generated by the flame. Because the HRR is also an LOI-dependent feature, a system with a greater LOI suggests that its flame produces less heat [76].

## 17.7 Smoke toxicity analysis

Smoke is produced during polymer combustion. The amount of smoke generated is determined by the chemical reaction that occurs during combustion. The emission of smoke can result in the production of hazardous gases that are potentially harmful when inhaled, lowering the survival rate. A smoke toxicity study can be performed following ISO TS 19700 by promoting air at a constant, increased temperature in a steady-state tube furnace [86]. The analysis can be measured by quantifying the harmful gases produced, including CO, $CO_2$, $NO_x$, and HCN [82].

With the high char residue observed in flame retardant polymer nanocomposites, the flammability of the nanocomposite can be reduced, whereas the smoke

**Table 17.2** LOI of various nanocomposites.

| Nanocomposites | LOI [%] | Source | Remarks |
|---|---|---|---|
| Epoxy/GNP (1.0 wt.%) | 24 | [78] | GNP (graphene nanoplatelets) |
| Epoxy/MMT (1.5 wt.%) | 23.5 | [79] | MMT (montmorillonite) |
| PDMS/NC (2.0 wt.%) | 23 | [80] | PDMS (polydimethylsiloxane) NC (nanoclay) |
| TOCN/LDH (20 wt.%) | 31 | [81] | TOCN (2,2,6,6-tetramethylpiperidine-1-oxyl radical-oxidized cellulose nanofibrils) LDH (layered double hydroxides) |
| Cotton/PAA/ ATP (1.0%.) | 22.7 | [82] | PAA (polyacrylic acid) ATP (Attapulgite) |
| Epoxy/AnT (10 wt.%) | 23.8 | [83] | AnT (antimony trioxide) |

production is high. However, an investigation by Huang et al. [17] indicates that modified grafted GO with Mo has improved the smoke suppression performance with high char yields. At low degradation temperature, which is about 470°C, incombustible gases such as $NH_3$ and $H_2O$ are released to dilute the fuel and oxygen in the gas phase to suppress the combustion process to some extent. Despite an increase in the degradation temperature, a high amount of styrene and its derivatives were observed in the gas phase, resulting in the release of CO and $CO_2$.

The schematic diagram in Fig. 17.11 illustrates how a graphene/black phosphorus (BP)/thermoplastic polyurethane (TPU) nanocomposite forms a protective char layer upon burning. Graphene is initially functionalized with melamine. BP was found to be extremely effectively integrated with functionalized graphene. The BP nanosheets react with the TPU and form a barrier that prevents the pyrolysis of the BP nanosheets and TPU. Exfoliated modified graphene nanosheets generate a protective char layer that shields the underlying substrate, hence reducing smoke particles.

## 17.8 Applications of flame retardant polymer nanocomposite materials

Polymer composites have found application in a wide range of applications. Polymer composites are used because of their lightweight nature, high durability, and cost-effectiveness. As illustrated in Fig. 17.12, different applications require varying degrees of fireproofing. Additionally, aeroplanes take a longer time to

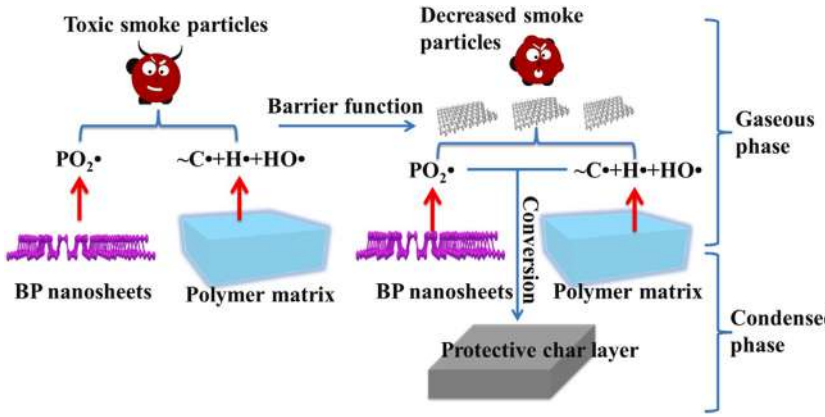


**Figure 17.11** Schematic diagram of graphene/BP/TPU nanocomposite as protective char layer [87]. *BP*, black phosphorus; *TPU*, thermoplastic polyurethane.

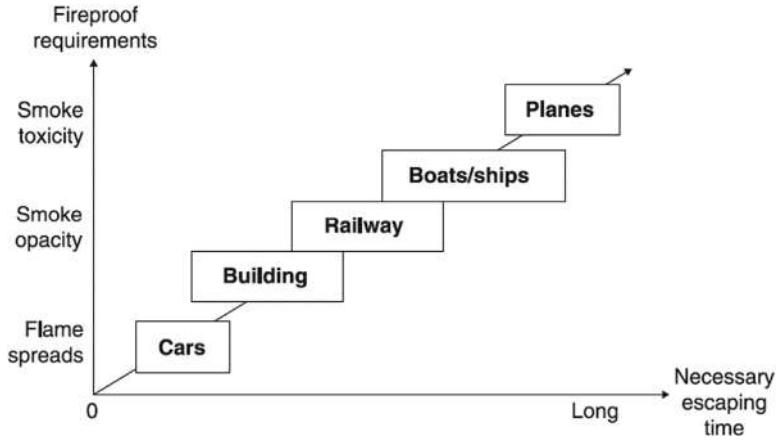


**Figure 17.12** Relationship between fireproofs requirement and time to escape for various applications [68].

evacuate during fire incidents. While driving on the road necessitates a quick response time, the flame spreads quickly in a car accident. As a result, the polymer composite's fire retardant qualities must be enhanced through the addition of flame retardant chemicals.

### 17.8.1 Aerospace

Safety and comfort for crew members, passengers, and valuables are essential to air vehicles. In the event of a fire, the use of flame retardant compounds in aircraft can

delay the generation of smoke and fire. In an aircraft, fire propagation can occur as a result of combustible objects in the cabin, fuel leaks, or technical failure during or after the crash. On an aircraft, the presence of combustion elements can generate tremendous heat. For instance, when 700 kg of polymer materials are contained within an aircraft, approximately 245 $\times$ 108 J of heat is generated [88]. Thus using nanofillers as reinforcement should improve the polymer composite's thermal and mechanical properties. This is consistent with the Aircraft Accident Records Board (ACOR) report by Bar et al. [89], which indicates that enhancements to the flame retardant qualities of the polymer composite may minimize the probability of an aircraft fire accident.

Raimondo et al. [90] investigated the possibility for aircraft lightning protection using a hybrid of 2D carboxylated partly exfoliated graphite (CpEG) and flame retardant glycidyl polyhedral oligomeric silsesquioxane (GPOSS) nanoparticles. They discovered that the flame retardant polymer nanocomposite they created did not degrade during degradation, which paved the way for industrial applications in aerospace. Additionally, Meenakshi et al. [91] synthesized POSS/nanoclay in epoxy and reported an increase in flame retardant characteristics. The improvement is due to Si−O−strong Si's thermal stability in POSS. Additionally, nanoclay silicate layers can migrate to the epoxy surface and produce a protective char layer. Another possible flame retardant material is a very porous 3D organic−inorganic PFR/$SiO_2$ aerogel embedded in a polymer nanocomposite. It is more insulating and has a lower PHRR value of 19 kW $m^{-2}$ than unfilled composite [92]. George et al. [93] examined phenolic covered with PBI and filled with calcium silicate. The LOI increased with the addition of calcium silicate, which resulted in a proportional increase in char proportional to the increase in oxygen percentage.

### 17.8.2 Automotive

Plastic is used in the design of several automotive components on purpose to minimize weight and fuel consumption. Due to the high flammability of plastics and the hazardous gases they generate, the addition of flame retardants is expected to reduce flammability. As a result, vehicle makers are required to conform to specific regulations, which include rules and limitations on the use of flammable materials. Among the flammable components found in an automobile are the car seat, boot liners, door liners, and door trim panel. It is critical to apply flame retardant compounds to the automobile to prevent vehicle components or parts from fire. Cogen et al. [94] created flame retardant materials for automobile wire by combining flame retardant nanoparticles and thermoplastic polymer crosslinking. According to Mathew et al. [95], nanoclay as a reinforcement for flame retardant nanofillers in a polymer is suitable for vehicle components located near the engine. This is because it possesses excellent thermal and flame retardant characteristics. [96] studied the potential for automotive uses of a hybrid $TiO_2$/CNT in polypropylene. They discovered that the presence of $TiO_2$/CNT tends to slow the HRR and spread of the flame during polymer combustion.

### 17.8.3 Textile

Flame retardant textiles are used in a variety of applications, including protective clothing for firefighters [97,98], smart textiles for health monitoring [99], mattresses [100,101], carpets [102,103], curtains [104] and many more. Flame retardant compounds are included into the fabric to retard ignition and contain the spread of fire during combustion.) The incorporation of nanoparticles into cotton fabrics can improve the thermal stability and flame retardant qualities of the textile polymer composite. According to Norouzi et al. [24], the addition of modified nanoclay to cotton resulted in a high char yield due to the nanoclay/cotton interfacial interaction with the polymer matrix. The schematic layout of the nanocomposite textile/halloysite (HNT) production in polypyrrole (PPY) is shown in Fig. 17.11. Attia et al. [105] used vapor phase polymerization to create a flame retardant textile nanocomposite. As illustrated in Fig. 17.13, the textile was first immersed in a solution of ferric chloride and hydrogen peroxide. It is then dried and exposed to pyrrole vapor. Finally, the polymerized textile nanocomposite was washed with methanol and deionized water to eliminate any remaining unreacted products and dried. Previously, degradation of the textile/HNT/PPY nanocomposite was attributed to PPY chain disintegration, which resulted in the formation of a nitrogen-rich char layer on the textile surface. In comparison, by filling the lumen cavity in the textile with HNT, the textile/HNT/PPY nanocomposite boosts its flame retardant properties.

### 17.8.4 Building

When exposed to fire, polymers produce heat, smoke, and hazardous fumes. The building's flammable materials include the roof, flooring, doors, and water supply insulation, among others. The addition of flame retardants improves the fire resistance of the polymer composite. Additionally, certain building materials, such as tiles, contain toxic elements and are not completely compostable when broken. Yildirim [106] developed biodegradable and more efficient nanocellulose ceiling tiles. To enhance the water repellent and flame retardant qualities of the nanocellulose, it was treated with *n*-octadecyltriethoxysilane and boric acid.

## 17.9 Future trend on flame retardant nanocomposite

Polymer materials are flammable and must be combined with flame retardant elements to mitigate their flammability and potential for flame spread, which results in the emission of heat, smoke, and hazardous fumes. At the moment, flame retardants are based on a nonhalogen chemical. Additionally, emphasis is placed on altering the surface of nanoparticles to enhance their surface area. Numerous studies have demonstrated that nanoparticles agglomerated in polymer composites reduce fire resistance, in contrast to a well-dispersed modified nanoparticle in the polymer matrix, which can lower flammability and increase the time required to ignite. However, as environmental awareness and concern rise, researchers and industry are becoming increasingly interested in developing green flame retardant materials

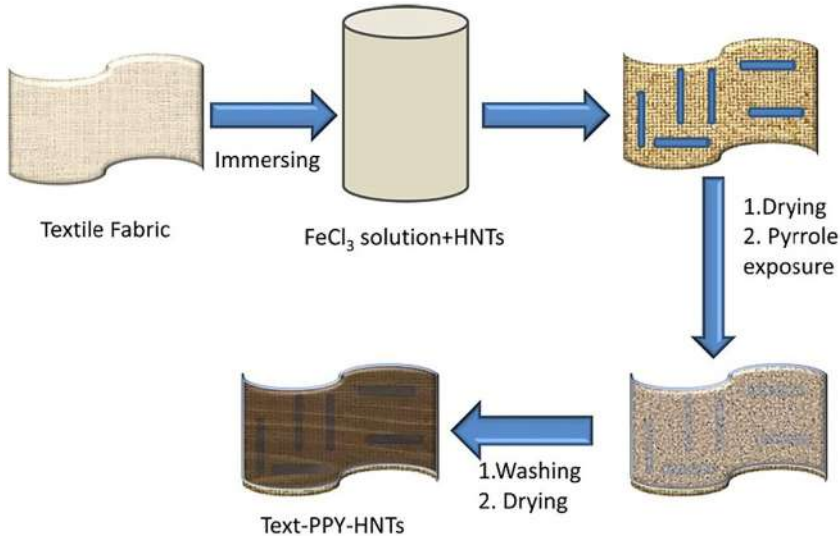


**Figure 17.13** Schematic presentation on the development of flame retardant textile fabrics/halloysite nanotube in polypyrrole [99].

that are acceptable for the required applications. As a result, it is critical to exploit and produce ecologically acceptable, highly effective, and compatible green and natural materials as flame retardants.

## 17.10 Summary and future directions

This chapter discussed recent advancements in the field of flame retardant nanoparticles and nanocomposites. A complete explanation of the polymer-modified nanoparticle interaction was offered to enhance the flame retardant capabilities. Additionally, the majority of research has demonstrated the usage of 2D nanofillers and their dispersibility in polymer media. Due to the strong interfacial adhesion between the nanoparticle surface and the polymer chain, the well-dispersed nanoparticles in the polymer matrix imply improved thermal performance. Additionally, the well-dispersed nanoparticle forms a char layer on the polymer surface, delaying the breakdown process and protecting the substrate layer beneath. However, the development of ecological and natural flame retardant materials is necessary for the future.

## Acknowledgments

The authors would like to thank Universiti Putra Malaysia (UPM), particularly the Institute of Nanoscience and Nanotechnology (ION2), Institute of Tropical Forestry and Forest

Products (INTROP), and Aerospace Malaysia Research Center (AMRC) for providing information and facilities to complete this chapter.

## References

[1] L. Ahmed, B. Zhang, L.C. Hatanaka, M.S. Mannan, Application of polymer nanocomposites in the flame retardancy study, J. Loss Prev. Process. Industries 55 (2018) 381–391.
[2] P. Joseph, S. Tretsiakova-McNally, Melt flow behaviours of thermoplastic materials under fire conditions: Recent experimental studies and some theoretical approaches, Materials. 8 (2015). 8973-8803.
[3] M. Niaounakis, Chapter 2: Properties, in: M. Niaounakis (Ed.), Biopolymers: Applications and Trends, Elsevier, Oxford, 2013.
[4] International Organization for Standardization. Fire Safety-Vocabulary (ISO 13943). (2021). Available from https://www.iso.org/obp/ui/#iso:std:iso:13943:ed-2:v1:en.
[5] ASTM International. Standard Terminology of Fire Standards (ASTM e 176). (2021). Available from https://www.nap.edu/read/1869/chapter/10.
[6] K. Vinayagam, Minimizing flame impingements in fired heaters, Chem. Eng. 114 (5) (2007) 70–73.
[7] J.G. Speight, Chapter 4: Sources and types of organic pollutants, in: J.G. Speight (Ed.), Environmental Organic Chemistry for Engineers, Elsevier, Oxford, 2017.
[8] R.G. Jones, J. Kahovec, R. Stepto, W.S. Wilks, M. Hess, T. Kitayama, et al., Terminology, 1. 13: Definitions of terms relating to degradation, aging, and related chemical transformations of polymers (1996), in: R.G. Jones, J. Kahovec, R. Stepto, W. S. Wilks, M. Hess, T. Kitayama, W.Val Metanomski (Eds.), Compendium of Polymer Terminology and Nomenclature. IUPAC Recommendations 2008, RSC Publishing, Cambridge, 2008.
[9] K. Król-Morkisz, K. Pielichowska, Chapter 13: Thermal decomposition of polymer nanocomposite with functionalized nanoparticles, in: K. Pielichowski, T.M. Majka (Eds.), Polymer Composites with Functionalized Nanoparticles. Synthesis, Properties and Applications, Elsevier, Poland, 2019.
[10] V. Babrauskas, R. Fuoco, A. Blum, Chapter 3: Flame retardant additives in polymers: when do the fire safety benefits outweigh the toxicity risks? in: C.D. Papaspyrides, P. Kiliaris (Eds.), Polymer Green Flame Retardants, Elsevier, Greece, 2014.
[11] R. Broughton, I. Cerkez, Chapter 2: Burning mechanisms of fibres, in: F.S. Kilinc (Ed.), Handbook of Fire Resistant Textiles, Woodhead Publishing, Cambridge, 2013.
[12] W.D. Schindler, P.J. Hauser, Chapter 8: Flame retardant finishes, in: W.D. Schindler, P.J. Hauser (Eds.), Chemical Finishing of Textiles, Woodhead Publishing Limited, Cambridge, 2004.
[13] A.B. Clariant, Flame retardants: frequently asked questions, Eur. Flame Retardants Assoc. 2007 (2007) 2–3.
[14] International Organization for Standardization. ISO/TR 18401:2017 (en) Nanotechnologies. (2017). Available from https://www.iso.org/obp/ui/#iso:std:iso:tr:18401:ed-1:v1:en.
[15] S. Lu, W. Hong, X. Chen, Nanoreinforcements of two-dimensional nanomaterials for flame retardant polymeric composites: an overview, Adv. Polym. Technol. (2019) 2019.

[16] J. Alongi, A. Frache, Flame retardancy properties of α-zirconium phosphate based composites, Polym. Degrad. Stab. 95 (9) (2010) 1928–1933.
[17] G. Huang, W. Chen, T. Wu, H. Guo, C. Fu, Y. Xue, et al., Multifunctional graphene-based nano-additives toward high-performance polymer nanocomposites with enhanced mechanical, thermal, flame retardancy and smoke suppressive properties, Chem. Eng. J. (2020) 127590.
[18] T. Kashiwagi, F. Du, J.F. Douglas, K.I. Winey, R.H. Harris, J.R. Shields, Nanoparticle networks reduce the flammability of polymer nanocomposites, Nat. Mater. 4 (12) (2005) 928–933.
[19] Y. Guo, C.C. Chang, G. Halada, M.A. Cuiffo, Y. Xue, X. Zuo, et al., Engineering flame retardant biodegradable polymer nanocomposites and their application in 3D printing, Polym. Degrad. Stab. 137 (2017) 205–215.
[20] Y. Han, T. Wang, X. Gao, T. Li, Q. Zhang, Preparation of thermally reduced graphene oxide and the influence of its reduction temperature on the thermal, mechanical, flame retardant performances of PS nanocomposites, Compos. Part. A: Appl. Sci. Manuf. 84 (2016) 336–343.
[21] H. Zhang, J. Mao, M. Li, Q. Cai, W. Li, C. Huang, et al., Design of h-BN@ boronate polymer core-shell nanoplates to simultaneously enhance the flame retardancy and mechanical properties of epoxy resin through the interficial regulation, Compos. Part. A: Appl. Sci. Manuf. 130 (2020) 105751.
[22] Y.L. Li, C.F. Kuan, S.W. Hsu, C.H. Chen, H.C. Kuan, F.M. Lee, et al., Preparation, thermal stability and flame-retardant properties of halogen-free polypropylene composites, High. Perform. Polym. 24 (6) (2012) 478–487.
[23] M. Norouzi, Y. Zare, P. Kiany, Nanoparticles as effective flame retardants for natural and synthetic textile polymers: application, mechanism, and optimization, Polym. Rev. 55 (2015) 1–30.
[24] M. Norouzi, Y. Zare, P. Kiany, Nanoparticles as effective flame retardants for natural and synthetic textile polymers: application, mechanism, and optimization, Polym. Rev. 55 (3) (2015) 531–560.
[25] G. Vahidi, D.S. Bajwa, J. Shojaeiarani, N. Stark, A. Darabi, Advancements in traditional and nanosized flame retardants for polymers: a review, J. Appl. Polym. Sci. (2020) 1–14.
[26] F. Uddin, Clays, manoclays, and montmorillonite minerals, Metall. Mater. Trans. A 39 (2008) 2804–2814.
[27] Nanocor, Technical Data, General Information about Nanocore Nanoclay. G-100 (12/04), Nanocor Inc, Illinois, 2021.
[28] M.A. Ashraf, W. Peng, Y. Zare, K.Y. Rhee, Effects of size and aggregation/agglomeration of nanoparticles on the interfacial/interphase properties and tensile strength of polymer nanocomposites, Nanoscale Res. Lett. 13 (2018) 214–221.
[29] O. Zabihi, H. Khayyam, B. Fox, M. Naebe, Enhanced thermal stability and lifetime of epoxy nanocomposites using covalently functionalized clay: experimental and modelling, N. J. Chem. 39 (3) (2015) 2269–2278.
[30] C.-W. Chiu, T.-K. Huang, Y.-C. Wang, B.G. Alamani, J.-J. Lin, Intercalation strategies in clay/polymer hybrids, Prog. Polym. Sci. 39 (3) (2014) 443–485.
[31] B.N. Jang, M. Costache, C.A. Wilkie, The relationship between thermal degradation behavior of polymer and the fire retardancy of polymer/clay nanocomposites, Polymer 46 (24) (2005) 10678–10687.
[32] A. Fina, G. Camino, S. Bocchini, Comprehensive approach to flame-retardancy evaluation of layered silicate nanocomposites, Polym. Green. Flame Retardants (2014) 441–459.

[33] H. Qin, S. Zhang, C. Zhao, G. Hu, M. Yang, Flame retardant mechanism of polymer/clay nanocomposites based on polypropylene, Polymer 46 (19) (2005) 8386–8395.
[34] A. Kausar, Chapter 7: Flame retardant potential of clay nanoparticles, in: G. Cavallaro, R. Fakhrullin, P. Pasbakhsh (Eds.), Clay Nanoparticles, Properties and Applications, Elsevier, Amsterdam, 2020.
[35] F.F. Azhar, A. Olad, A. Mirmohseni, Development of novel hybrid nanocomposites based on natural biodegradable polymer-montmorillonite/polyaniline: preparation and characterization, Polym. Bull. 71 (7) (2014) 1591–1610.
[36] S.S. Ray, K. Yamada, A. Ogami, M. Okamoto, K. Ueda, New polylactide/layered silicate nanocomposite: nanoscale control over multiple properties, Macromol. Rapid Commun. 23 (16) (2002) 943–947.
[37] Y. Xue, Y. Guo, M.H. Rafailovich, Chapter 3: Flame retardant polymer nanocomposites and interfaces, in: F. Zafar, E. Sharmin (Eds.), Flame Retardants, In techOpen, London, 2018. 2019.
[38] C.W. Li, M.W. Kanan, CO2 reduction at low overpotential on Cu electrodes resulting from the reduction of thick Cu2O films, J. Am. Chem. Soc. 134 (17) (2012) 7231–7234.
[39] A.A. Sertsova, S.I. Marakulin, E.V. Yurtov, Metal compound nanoparticles: flame retardants for polymer composites, Russian J. Gen. Chem. 87 (6) (2017) 1395–1402.
[40] T.J. Huang, D.H. Tsai, CO oxidation behavior of copper and copper oxides, Catal. Lett. 87 (3–4) (2003) 173–178.
[41] S. Qiu, B. Zou, T. Zhang, X. Ren, B. Yu, Y. Zhou, et al., Integrated effect of NH2-functionalized/triazine based covalent organic framework black phosphorus on reducing fire hazards of epoxy nanocomposites, Chem. Eng. J. 401 (2020) 126058.
[42] S. Wang, F. Xin, Y. Chen, L. Qian, Y. Chen, Phosphorus-nitrogen containing polymer wrapped carbon nanotubes and their flame-retardant effect on epoxy resin, Polym. Degrad. Stab. 129 (2016) 133–141.
[43] S. Araby, B. Philips, Q. Meng, J. Ma, T. Laoui, C.H. Wang, Recent advances in carbon-based nanomaterials for flame retardant polymers and composites, Compos. Part B: Eng. 212 (2021) 1–29.
[44] Y. Yang, J.L.D. Palencia, N. Wang, Y. Jiang, D.-Y. Wang, Nanocarbon-based flame retardant polymer nanocomposites, Molecules. 26 (2021) 1–32.
[45] M. Mao, H. Xu, K.-Y. Guo, J.-W. Zhang, Q.-Q. Xia, G.-D. Zhang, et al., Mechanically flexible, super-hydrophobic and flame-retardant hybrid nano-silica/graphene oxide wide ribbon decorated sponges for efficient oil/water separation and fire warning response, Compos. Part. A: Appl. Sci. Manuf. 140 (2021) 1–9.
[46] B. Chollet, J.M. Lopez-Cuesta, F. Laoutid, L. Ferry, Lignin nanoparticles as a promising way for enhancing lignin flame retardant effect in polylactide, Materials 12 (13) (2019) 2132.
[47] L. Costes, F. Laoutid, M. Aguedo, A. Richel, S. Brohez, C. Delvosalle, et al., Phosphorus and nitrogen derivatization as efficient route for improvement of lignin flame retardant action in PLA, Eur. Polym. J. 84 (2016) 652–667.
[48] P. Song, Z. Cao, S. Fu, Z. Fang, Q. Wu, J. Ye, Thermal degradation and flame retardancy properties of ABS/lignin: effects of lignin content and reactive compatibilization, Thermochim. Acta 518 (1–2) (2011) 59–65.
[49] A. Sienkiewicz, P. Czub, Flame retardancy of biobased composites—research development, Materials 13 (22) (2020) 5253.
[50] F. Yang, R. Yngard, G.L. Nelson, Flammability of polymer-clay and polymer-silica nanocomposites, J. Fire Sci. 23 (3) (2005) 209–226.

[51] M.A. Cárdenas, D. García-López, I. Gobernado-Mitre, J.C. Merino, J.M. Pastor, J.D.D. Martínez, et al., Mechanical and fire retardant properties of EVA/clay/ATH nanocomposites—effect of particle size and surface treatment of ATH filler, Polym. Degrad. Stab. 93 (11) (2008) 2032−2037.
[52] H. Peng, D. Wang, S. Fu, Tannic acid-assisted green exfoliation and functionalization of MoS2 nanosheets: Significantly improve the mechanical and flame-retardant properties of polyacrylonitrile composite fibers, Chem. Eng. J. 384 (2020) 123288.
[53] B. Yuan, Y. Hu, X. Chen, Y. Shi, Y. Niu, Y. Zhang, et al., Dual modification of graphene by polymeric flame retardant and Ni(OH) 2 nanosheets for improving flame retardancy of polypropylene, Compos. Part. A: Appl. Sci. Manuf. 100 (2017).
[54] X. Wang, S.L. Ji, X.Q. Wang, H.Y. Bian, L.R. Lin, H.Q. Dai, et al., Thermally conductive, super flexible and flame-retardant BN-OH/PVA composite film reinforced by lignin nanoparticles, J. Mater. Chem. C. 7 (45) (2019) 14159−14169.
[55] P. Li, Y. Zheng, M. Li, W. Fan, T. Shi, Y. Wang, et al., Enhanced flame-retardant property of epoxy composites filled with solvent-free and liquid-like graphene organic hybrid material decorated by zinc hydroxystannate boxes, Compos. Part. A: Appl. Sci. Manuf. 81 (2016) 172−181.
[56] Z. Li, A.J. González, V.B. Heeralal, D.Y. Wang, Covalent assembly of MCM-41 nanospheres on graphene oxide for improving fire retardancy and mechanical property of epoxy resin, Compos. Part. B: Eng. 138 (2018) 101−112.
[57] Y. Xiao, Z. Jin, L. He, S. Ma, C. Wang, X. Mu, et al., Synthesis of a novel graphene conjugated covalent organic framework nanohybrid for enhancing the flame retardancy and mechanical properties of epoxy resins through synergistic effect, Compos. Part. B: Eng. 182 (2020) 107616.
[58] B. Yu, Y. Shi, B. Yuan, S. Qiu, W. Xing, W. Hu, et al., Enhanced thermal and flame retardant properties of flame-retardant-wrapped graphene/epoxy resin nanocomposites, J. Mater. Chem. A 3 (15) (2015) 8034−8044.
[59] X. Li, Y. Feng, C. Chen, Y. Ye, H. Zeng, H. Qu, et al., Highly thermally conductive flame retardant epoxy nanocomposites with multifunctional ionic liquid flame retardant-functionalized boron nitride nanosheets, J. Mater. Chem. A 6 (41) (2018) 20500−20512.
[60] D. Wang, X. Mu, W. Cai, L. Song, C. Ma, Y. Hu, Constructing phosphorus, nitrogen, silicon-co-contained boron nitride nanosheets to reinforce flame retardant properties of unsaturated polyester resin, Compos. Part. A: Appl. Sci. Manuf. 109 (2018) 546−554.
[61] B. Yuan, Y. Sun, X. Chen, Y. Shi, H. Dai, S. He, Poorly-/well-dispersed graphene: abnormal influence on flammability and fire behavior of intumescent flame retardant, Compos. Part. A: Appl. Sci. Manuf. 109 (2018) 345−354.
[62] W. Cai, W. Guo, Y. Pan, J. Wang, X. Mu, X. Feng, et al., Polydopamine-bridged synthesis of ternary h-BN@ PDA@ SnO2 as nanoenhancers for flame retardant and smoke suppression of epoxy composites, Compos. Part. A: Appl. Sci. Manuf. 111 (2018) 94−105.
[63] F. Laoutid, L. Bonnaud, M. Alexandre, J.M. Lopez-Cuesta, P. Dubois, New prospects in flame retardant polymer materials: from fundamentals to nanocomposites, Mater. Sci. Eng.: R: Rep. 63 (3) (2009) 100−125.
[64] Y. Zuo, Y. Zhang, Y. Fu, Catalytic conversion of cellulose into levulinic acid by a sulfonated chloromethyl polystyrene solid acid catalyst, ChemCatChem 6 (3) (2014) 753−757.
[65] S.V. Levchik, E.D. Weil, A review of recent progress in phosphorus-based flame retardants, J. Fire Sci. 24 (5) (2006) 345−364.

[66] D. Gao, X. Wen, Y. Guan, W. Czerwonko, Y. Li, Y. Gao, et al., Flame retardant effect and mechanism of nanosized NiO as synergist in PLA/APP/CSi-MCA composites, Compos. Commun. 17 (2020) 170−176.
[67] Z.R. Yu, M. Mao, S.N. Li, Q.Q. Xia, C.F. Cao, L. Zhao, et al., Facile and green synthesis of mechanically flexible and flame-retardant clay/graphene oxide nanoribbon interconnected networks for fire safety and prevention, Chem. Eng. J., 405, 2020, p. 126620.
[68] C. Dewaghe, C.Y. Lew, M. Claes, P. Dubois, Fire-retardant applications of polymer−carbon nanotubes composites: improved barrier effect and synergism, Polymer−Carbon Nanotube Composites, Woodhead Publishing, 2011, pp. 718−745.
[69] F.M. Uhl, Q. Yao, H. Nakajima, E. Manias, C.A. Wilkie, Expandable graphite/polyamide-6 nanocomposites, Polym. Degrad. Stab. 89 (1) (2005) 70−84.
[70] Y. Arao, Flame retardancy of polymer nanocomposite, Flame Retardants, Springer, Cham, 2015, pp. 15−44.
[71] J.J. Willard, R.E. Wondra, Quantitative evaluation of flame-retardant cotton finishes by the limiting-oxygen index (LOI) technique, Text. Res. J. 40 (3) (1970) 203−210.
[72] B.K. Deka, T.K. Maji, Effect of TiO2 and nanoclay on the properties of wood polymer nanocomposite, Compos. Part. A: Appl. Sci. Manuf. 42 (12) (2011) 2117−2125.
[73] K.C. Cheng, C.B. Yu, W. Guo, S.F. Wang, T.H. Chuang, Y.H. Lin, Thermal properties and flammability of polylactide nanocomposites with aluminum trihydrate and organoclay, Carbohydr. Polym. 87 (2) (2012) 1119−1123.
[74] S. Yang, J. Wang, S. Huo, M. Wang, J. Wang, Preparation and flame retardancy of a compounded epoxy resin system composed of phosphorus/nitrogen-containing active compounds, Polym. Degrad. Stab. 121 (2015) 398−406.
[75] S.M. Kabeb, A. Hassan, Z. Mohamad, Z. Sharer, M. Mokhtar, F. Ahmad, Exploring the effects of nanofillers of epoxy nanocomposite coating for sustainable corrosion protection, Chem. Eng. Trans. 72 (2019) 121.
[76] A.S. Alex, R.S. Rajeev, K. Krishnaraj, K. Sreenivas, S.K. Manu, C. Gouri, et al., Thermal protection characteristics of polydimethylsiloxane-organoclay nanocomposite, Polym. Degrad. Stab. 144 (2017) 281−291.
[77] T. Wu, B. Cai, J. Wang, C. Zhang, Z. Shi, Q. Yang, et al., TEMPO-oxidized cellulose nanofibril/layered double hydroxide nanocomposite films with improved hydrophobicity, flame retardancy and mechanical properties, Compos. Sci. Technol. 171 (2019) 111−117.
[78] D. Gao, Y. Zhang, B. Lyu, P. Wang, J. Ma, Nanocomposite based on poly(acrylic acid) / attapulgite towards flame retardant of cotton fabrics, Carbohydr. Polym. 206 (2019) 245−253.
[79] B.M. Dheyaa, W.H. Jassim, N.A. Hameed, Evaluation of the epoxy/antimony trioxide nanocomposites as flame retardant, J. Phys.: Conf. Ser. 1003 (2018) 012078.
[80] M. Ebadi, Z. Mirdamadian, D. Ghanbari, L. Moradi, The effect of aminated carbon nanotube and phosphorus pentoxide on the thermal stability and flame retardant properties of the acrylonitrile-butadiene-styrene, J. Clust. Sci. 25 (2) (2014) 541−548.
[81] D. Ghanbari, M. Salavati-Niasari, M. Ghasemi-Kooch, A sonochemical method for synthesis of Fe3O4, nanoparticles and thermal stable PVA-based magnetic nanocomposite, J. Ind. Eng. Chem. 20 (6) (2014) 3970−3974.
[82] Y. Yuan, W. Wang, Y. Shi, L. Song, C. Ma, Y. Hu, The influence of highly dispersed Cu2O-anchored MoS2 hybrids on reducing smoke toxicity and fire hazards for rigid polyurethane foam, J. Hazard. Mater. 382 (2020) 121028.

[83] W. Cai, Z. Li, X. Mu, L. He, X. Zhou, W. Guo, et al., Barrier function of graphene for suppressing the smoke toxicity of polymer/black phosphorous nanocomposites with mechanism change, J. Hazard. Mater. 404 (2021) 124106.
[84] F. Uddin, Flame-retardant fibrous materials in an aircraft, J. Ind. Text. 45 (5) (2016) 1128–1169.
[85] M. Bar, R. Alagirusamy, A. Das, Flame retardant polymer composites, Fibers Polym. 16 (4) (2015) 705–717.
[86] M. Raimondo, L. Guadagno, V. Speranza, L. Bonnaud, P. Dubois, K. Lafdi, Multifunctional graphene/POSS epoxy resin tailored for aircraft lightning strike protection, Compos. Part. B: Eng. 140 (2018) 44–56.
[87] K.S. Meenakshi, E.P.J. Sudhan, S.A. Kumar, M.J. Umapathy, Development of dimethylsiloxane based tetraglycidyl epoxy nanocomposites for high performance, aerospace and advanced engineering applications, Prog. Org. Coat. 74 (1) (2012) 19–24.
[88] Z.L. Yu, N. Yang, V. Apostolopoulou-Kalkavoura, B. Qin, Z.Y. Ma, W.Y. Xing, et al., Fire-retardant and thermally insulating phenolic-silica aerogels, Angew. Chem. Int. (Ed.) 57 (17) (2018) 4538–4542.
[89] P. George, S. Bhowmik, M. Abraham, P.K. Sriram, M.K. Pitchan, G. Ajeesh, High-performance fire-resistant polymeric nanocomposite for aerospace applications, Proc. Inst. Mech. Engineers, Part. L: J. Materials: Des. Appl. 233 (2) (2019) 97–108.
[90] J. M. Cogen, T. S. Lin, J. Klier, P. D. Whaley. U.S. Patent Application No. 11/659,579. (2008).
[91] J. Mathew, J. Joy, S.C. George, Potential applications of nanotechnology in transportation: a review, J. King Saud. University-Science 31 (4) (2019) 586–594.
[92] Z. Zheng, L. Ren, P. Huang, X. Zhao, Preparation and properties of silicone coated glass fiber fabrics destined for firefighters' protective clothing, Pigm. Resin. Technol. (2020).
[93] S.H.E.N. Deyao, H.O.U. Dongyu, Comparative analysis of the performance of flame retardant materials between polyimide and other fibers for firefighting clothing, Wool. Text. J. 48 (2020) 4.
[94] V. Koncar, Smart Textiles for In Situ Monitoring of Composites, Woodhead Publishing, 2018.
[95] B.E. Boor, Y. Liang, N.E. Crain, H. Järnström, A. Novoselac, Y. Xu, Identification of phthalate and alternative plasticizers, flame retardants, and unreacted isocyanates in infant crib mattress covers and foam, Environ. Sci. Technol. Lett. 2 (4) (2015) 89–94.
[96] W. Mio, S. Iwade, Y. Matsumoto, M. Mihoichi, S. Maruyama. U.S. Patent No. 7,858,542. Washington, DC: U.S. Patent and Trademark Office. (2010).
[97] K. Mishra, R. Vaidyanathan, The influence of nanoclay on the flame retardancy and mechanical performance of recycled carpet composites, Recycling 4 (2) (2019) 22.
[98] H. Müller, P. S. Wormald, P. Bavaj. U.S. Patent No. 9,624,622. Washington, DC: U. S. Patent and Trademark Office. (2017).
[99] N.F. Attia, A.A. El Ebissy, M.A. Hassan, Novel synthesis and characterization of conductive and flame retardant textile fabrics, Polym. Adv. Technol. 26 (12) (2015) 1551–1557.
[100] N. Yildirim, Design of Adhesive-free Bio-based Suspended Ceiling Tiles Using Nanocellulose, BioResources 13 (4) (2018) 7360–7370.
[101] S. Bourbigot, G. Fontaine, Flame retardancy of polylactide: an overview, Polymer Chemistry 1 (9) (2010) 1413–1422.

[102] S.M. Kabeb, A. Hassan, Z. Mohamad, Z. Sharer, M. Mokhtar, F. Ahmad, Exploring the effects of nanofillers of epoxy nanocomposite coating for sustainable corrosion protection, Chemical Engineering (2019) 72.
[103] C. Cabello-Alvarado, P. Reyes-Rodríguez, M. Andrade-Guel, G. Cadenas-Pliego, M. Pérez-Alvarez, V.J. Cruz-Delgado, L. Melo-López, Z.V. Quiñones-Jurado, C.A. Ávila-Orta, Melt-mixed thermoplastic nanocomposite containing carbon nanotubes and titanium dioxide for flame retardancy applications, Polymers 11 (7) (2019) 1204.
[104] M. Tokumura, S. Ogo, K. Kume, K. Muramatsu, Q. Wang, Y. Miyake, T. Amagai, M. Makino, Comparison of rates of direct and indirect migration of phosphorus flame retardants from flame-retardant-treated polyester curtains to indoor dust, Ecotoxicology and environmental safety 169 (2019) 464−469.
[105] X. Wen, Z. Liu, Z. Li, J. Zhang, D.Y. Wang, K. Szymańska, X. Chen, E. Mijowska, T. Tang, Constructing multifunctional nanofiller with reactive interface in PLA/CB-g-DOPO composites for simultaneously improving flame retardancy, electrical conductivity and mechanical properties, Composites Science and Technology 188 (2020) 107988.
[106] B. Wicklein, D. Kocjan, F. Carosio, G. Camino, L. Bergström, Tuning the nanocellulose–borate interaction to achieve highly flame retardant hybrid materials, Chemistry of Materials 28 (7) (2016) 1985−1989.

# Section 3:
# Scopes, challenges and recycling

# Innovativeness and sustainability of polymer nanocomposites

18

*M. Azam Ali and Maree L. Gould*
Centre for Bioengineering and Nanomedicine, Faculty of Dentistry, University of Otago, Dunedin, New Zealand

## 18.1 Introduction

Presently worldwide, we are dealing with finite supplies of progressively dirty petroleum, climate change resulting from carbon dioxide emission and lower socio-economic communities living amongst the pollution caused by disposable manufacturing. Our dependency upon petroleum-based polymers has increased exponentially and synthetic polymers from petroleum-based hydrocarbons include polypropylene, nylon, polyester and epoxy (generally known as plastic). As a positive solution to these problems, the subject of sustainability has arisen to become a matter for serious discussion, particularly in the plastic industry. An entirely new generation of plastics, particularly PNC, based on 100% renewable resources may offer a solution for environmental impact. There is a critical need for improved environmental sustainability through the development of environmentally benign PNC (Table 18.1). Significant pollution reduction could be attained if these environmentally benign materials are implemented in place of petroleum-based plastics. Novel polymer nanocomposites, based entirely on renewable sustainable resources will allow the continued progressive growth of the plastic industries without the deleterious effects in the environment with the added advantage of a variety of economic and environmental benefits.

Sustainability, by definition, is described as balancing our own needs without compromising the capability of future generations to balance their own needs in that they should not cause irreversible change to the environment, should be economically viable, and should in some way benefit society as a whole. Informally called; profit, people and planet, these principles cannot be isolated from one another due to the interplay between these three principles (Fig. 18.1).

PNC derived from products from natural resources and based on environmentally friendly materials have received attention because of their ability to maintain a natural sustainable environment. Biodegradable polymers generated from either waste or renewable sources are the eco-friendly key to the problem from plastic waste.

PNC are multiphasic heterogeneous polymers whereas the filler is a continuous phase (Fig. 18.2). Individual constituents in the resulting composites are merged together by physical or chemical means but retain their individual identities. Mechanical properties are governed by the matrix. Some of the problems include

**Advanced Polymer Nanocomposites. DOI:** https://doi.org/10.1016/B978-0-12-824492-0.00001-5


**Table 18.1** Advantages and disadvantages of natural and synthetic polymers [1–3].

| | **Advantages** | **Disadvantages** |
|---|---|---|
| Natural | Low toxicity<br>Biocompatibility<br>Biodegradable<br>Low cost<br>Recyclable<br>Renewable<br>Infinite supply<br>Cell-binding sites<br>No immunogenic response | Hydrophilic<br>Low thermal stability<br>Structurally more complex<br>More variability<br>Low mechanical properties<br>Extraction complicated and costly |
| Synthetic | Biocompatibility<br>Mass produced cheaply | Toxic<br>Not degradable<br>Synthetic process complicated and costly<br>Made from finite resources<br>Good mechanical strength<br>Local acidity from degradation products |


**Figure 18.1** The interplay between environmental, economic and social aspects of sustainability.

processing, interface between nanoparticles and matrix, homogeneous dispersal of the nanoparticles, the compatibility amongst the various phases, controlled size and preservation of the nanoparticles within the matrix. The nanoparticle size ranges from 1 to 50 nm dispersed within a polymer matrix [5]. Production of these suspensions requires controlled interspersing and stabilization of the dispersed phase.

Technologies, like computers and cell phones, have become smaller over the years, at the same time becoming faster and more powerful, the development of nanoscale polymers in the field of biotechnology seems the next logical step. Researchers have studied polymer-based nanocomposites for the past few decades but despite their obvious potential, it remains unclear why these products have not been released commercially.

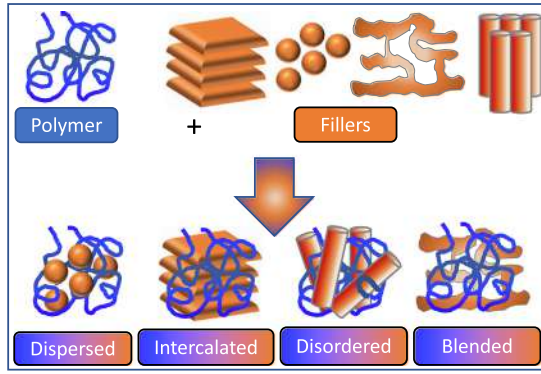


**Figure 18.2** Polymers combined with different fillers form a variety of nanocomposites [4,5].

Disposal of nanocomposites in that they are composed of more than one particle is challenging from both scientific and socio-economic perspectives due to the possibility of exerting a dramatic direct/indirect impact on our eco-system.

This chapter highlights various aspects of PNC including, chitosan, collagen and keratin functionalized with carbon nanotubes (CNT), graphene, nanoclay, and metal nanoparticles etc.

## 18.2 Chitosan

Chitosan is a hydrophilic bioactive linear polysaccharide acquired from the deacetylated form of chitin obtained from marine crustaceans' exoskeletons and shells, and a few species of fungi. Chitosan's rigid crystalline structure displays strong inter- and intra-molecular hydrogen bonding. From a biomedical viewpoint, chitosan displays antimicrobial, antiinflammatory, antioxidant properties, immune-stimulating effects, low toxicity. and high biodegradability. Despite availability and sustainability, chitosan is restricted by insolubility and poor processability in that it dissolves in weak acetic or formic acid.

Chitosan is composed of deacetylated and acetylated units, with N-acetyl-D-glucosamine in the acetylated units, whereas β-(1,4)-linked D-glucosamine is present in the deacetylated units, with the latter usually exceeding 80%. Each glycosidic unit contains a single −NH2 group and a pair of −OH groups (Fig. 18.3). The presence of these reactive groups delivers flexibility and provides features such as adhesivity, viscosity and film-forming characteristics. Although, the biological activity of chitosan depends on the molecular weight and the degree of deacetylation.

Often used in coatings, emulsions, drug release, gene delivery, and other biomedical applications. Owing to the regenerative effect of chitosan on living tissues Chitosan has been used extensively for tissue engineering [2,3].

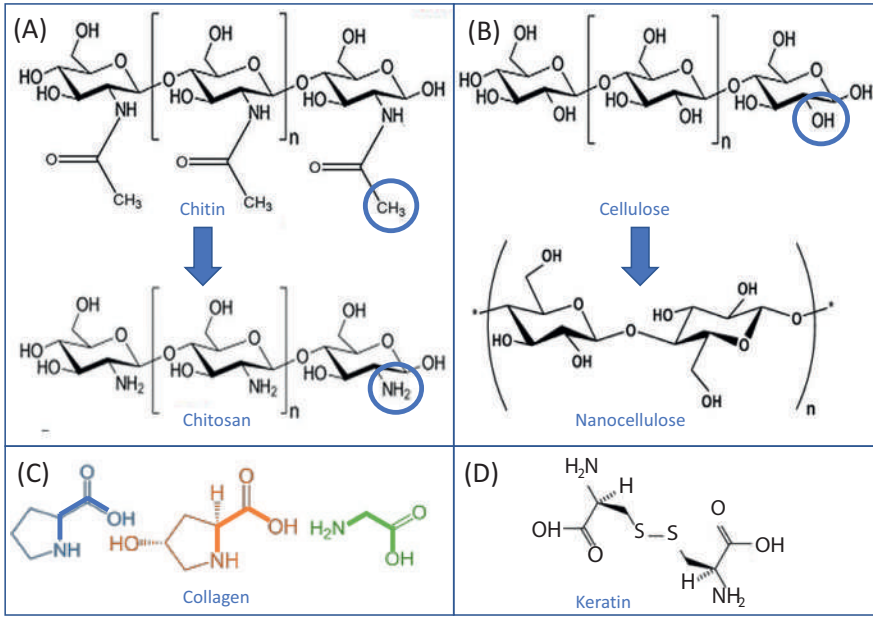


**Figure 18.3** The structure of (A) chitin, chitosan, and (B) cellulose differ by the group at position C2 [6]. (C) Collagen composed of proline (blue), hydroxyproline (orange), and glycine (green). (D) Keratin.
Adapted from PubChem.

### 18.2.1 Chitosan polymer nanocomposites

Chitosan can be blended with a variety of polymers including epoxy, polycarbonate, polystyrene, polysulfone, poly(methyl methacrylate), and polyaniline [7] including organic [8] and inorganic nanoparticles [9]. Furthermore, chitosan can be adapted utilizing CNTs, nanoclay, graphene, metallic and magnetic nanoparticles [10]. These modified chitosan composites have been adapted by using different polymers to form nanocomposites with superior properties such as increased surface area, increased porosity, tensile strength, photoluminescence, electrical conductivity, antibacterial, biocompatibility and thermal properties. The modification of chitosan-based nanocomposites requires further exploration to find applications in a variety of medical fields.

### 18.2.2 Polymer/chitosan/graphene nanocomposites

Graphene is single-layered $sp^2$-bonded carbon atoms organized into a honeycomb lattice. Graphene oxide (GO) is the oxidized form of graphene leading to a greater interlayer spacing of the graphite planes, whereas the reduced form (rGO) is processed, reducing the oxygen content. Graphene and GO are used as fillers in the polymeric nanocomposite [11]. fabricated chitosan-GO nanocomposite films with

the GO homogeneously dispersed throughout due to amide linkages forming between the GO carboxylic acid groups and chitosan amine groups. The Young's modulus glass transition temperature and tensile strength and of the nanocomposite were improved relative to pure chitosan [11]. Chitosan membranes were modified with GO and RGO from chemical exfoliation of graphite and postprocessing thermal reduction. The graphene materials formed small stacks of 6−8 sheets with a nanoscale thickness of 1−6 nm. Graphene dispersed within the chitosan matrix significantly reduced swelling by 460% but the hydrolytic degradation process and the membrane hydrophilicity was not diminished [12]. Furthermore, Yang et al., in 2010 fabricated chitosan and GO-based nanocomposites again showed GO dispersed homogeneously within the chitosan matrix owing to chitosan and GO interactions that increased tensile strength and Young's modulus [13]. The fabrication of chitosan-GO nanocomposite with tensile strength and are biocompatible may unlock innovative possibilities for these leading-edge biomaterials.

### 18.2.3 Polymer/chitosan/nanoclay nanocomposites

Polymer/nanoclay composites prepared by intercalation of the chitosan polymer into the layered silicate formed a superabsorbent chitosan-g-poly(acrylic acid)/montmorillonite (MMT) nanocomposite [14]. Electrospun nanofibrous nanocomposites from a chitosan/polyvinyl alcohol (PVA) blend and sodium montmorillonite (Na-MMT) nanoclays formed uniform bead-free nanofibers with the Na-MMT nanoclays inside the nanofibers. Amalgamation of the nanoclays into nanofibers increased the tensile strength and the glass transition temperature. The epidermal carcinoma A-431 cell line showed no cytotoxic effect on cell viability and the A-431 cells adhered to the surface of the fibers [15]. Poly(lactic acid) (PLA)/chitosan-modified MMT nanocomposites were synthesized using intercalation, with the aim of increasing the interlayer layout. The PLA improved the amorphous regions of the nanocomposites providing reduced degradation, indicating a reduction in crystallinity. Also, the expanded silicate layers were intercalated into the PLA matrix in a disorderedly manner [16].

### 18.2.4 Polymer/chitosan/metal nanocomposites

Metal-chitosan nanocomposites can be prepared using silver (Ag), gold, platinum or palladium. Metal nanoparticles can be fabricated using sodium tetrahydroborate ($NaBH_4$) that reduced the metal salts, however, this method suffered from a difference in particle size. A nanocomposite prepared using chitosan and colloidal silver nanoparticles showed increased thermal stability of the combined chitosan and silver nanoparticles when compared to pure chitosan. Such nanocomposites are aimed specifically at antibacterial applications for medical and biological purposes because both silver and chitosan have antimicrobial activities. Polycyclic aromatic hydrocarbons (PAHs) are categorized as high priority for the development of water quality standards and effluent restriction guidelines because they form toxic pollutants often present in wastewater that are mutagenic and persistent with proven

carcinogenicity hence, their total elimination is crucial. Chitosan iron oxide-nanocomposites trigger oxidative degradation of toxic PAHs such as phenanthrene (PHEN) and anthracene (ANTH). The highest photodegradation was observed for zinc ferrite ($ZnFe_2O_4$), followed by copper oxide-iron oxide ($CuO\text{-}Fe_2O_3$), nickel ferrite ($NiFe_2O_4$), copper oxide-iron oxide ($Co_2O_3\text{-}Fe_3O_4$) and iron chromite ($FeCr_2O_4$), respectively [17]. Palladium (Pd) nanoparticles embedded on a nanocomposite composed of chitosan, polyaniline (PANI), and magnetite ($Fe_3O_4$). Polymerization of the by-product ferrous chloride ($FeCl_2$), formed magnetite that formed a magnetic nanocomposite that may be used for the degradation of organic pollutants.

Consequently, there are many novel pioneering opportunities open to the use of modified chitosan-based nanomaterials. Therefore it can be expected that substantial developments in PNC may revolutionize a variety of scientific fields in the near future with adequate scientific developments.

## 18.3 Cellulose

Polymers can be biodegradable (natural i.e., animal or plant origin, or chemical) or nonbiodegradable to be combined with fillers of organic or nonorganic origin (Fig. 18.4). Globally, cellulose is abundant, natural and biodegradable providing strength, stiffness and toughness to the plant anatomy. The primary component in the rigid plant cell wall, cellulose is a linear polysaccharide composed of repeating β-D-glucopyranose rings covalently linked at C4 and C1 positions by glycosidic bonds and each repeating segment is a dimer of glucose [20]. Extensive inter- and intra-chain hydrogen bonding between the hydroxyl groups of the adjacent ring molecules results in the linear configuration of the cellulose chain stabilizing the

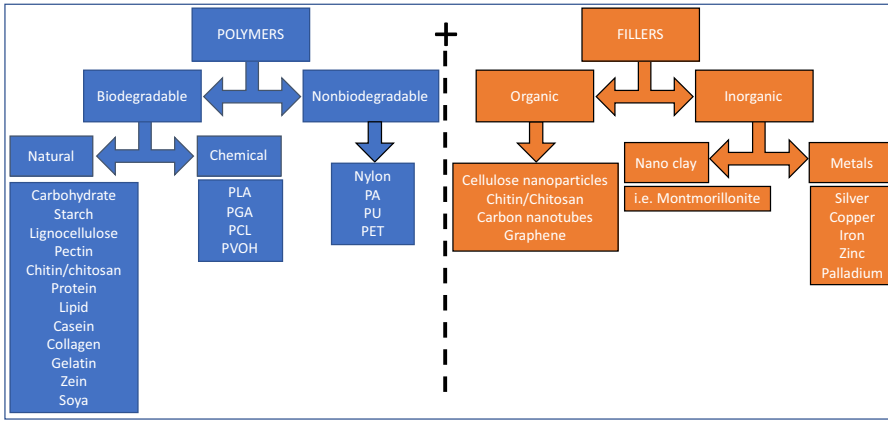


**Figure 18.4** Polymers can be biodegradable (natural i.e., animal or plant origin, or chemical) or nonbiodegradable to be combined with fillers of organic or nonorganic origin [3,18,19].

linkages [20,21]. The strong hydrogen bonds impart a high crystallinity thus limiting the ability of organic compounds to dissolve cellulose making it difficult to convert the short fibers from wood pulp. However, the high crystallinity gives rise to high mechanical properties [22] that allow cellulose fibers to compete with current engineering reinforcement materials, such as steel [23].

Nanocellulosic materials have the potential capacity as nanofillers due to them being inexpensive with a renewable sustainable nature, easy availability, high biocompatibility, and excellent physical properties. Plant fibers with natural resins are considered green composites because they are naturally biodegradable. Furthermore, cellulose-based PNC display exceptional properties that are an amalgamation of organic polymers and natural fillers.

### 18.3.1 Nanocellulose polymer nanocomposites

The mechanical properties of the nanocellulose PNC, can be improved by proper material dispersion within the polymer matrix. With the addition of a load, then the matrix effectively transfers the load to the enhanced nanocomposite. The nanocellulose-reinforced polymer nanocomposites mechanical properties are improved because of the rigidifying properties of the cellulosic nanomaterials mainly because of the large surface area interlocking the reinforcing materials together with the matrix, creating a strong interfacial adhesion. The surface area provides strong interfacial interactions between the polymer matrix and the nanocellulose as long as the nanofillers are homogeneously dispersed within the matrices.

### 18.3.2 Polymer/cellulose/graphene nanocomposites

On our planet, cellulose is the most plentiful biomaterial that potentially could serve as a solution to our limited fossil resources. Cellulose is blessed with nontoxicity, renewability, biocompatibility, biodegradability, high strength, high stiffness, excellent physicochemical properties, and environmental friendliness of cellulose derived from natural renewable resources; this product has attracted tremendous interest. The use of any organic nanomaterial in the preparation of nanocomposites is advantageous because these materials support the notion of environmental protection, thereby contributing to sustainability as the use of environmentally friendly products from renewable and biodegradable sources are more desirable than the chemical-based alternatives. The cellulose extracted from wood and wood-like materials is a polysaccharide consisting of β-1,4-linked anhydroglucopyranoside units with every monomer unit corkscrewed 180 degrees in comparison to its neighbors (Fig. 18.3). Furthermore, the development of cellulose nanocrystals (CNC) from cellulose after eliminating the more unstructured regions via acid hydrolysis [24,25] exhibit superior barrier properties, a larger surface area with ease of bioconjugation [26–28] further expanding the function of cellulose alone. The existence of reactive chemical groups on the surface of CNC provides modification by physical adsorption, surface grafting or covalent bonding [29].

The combination of CNC with other nanomaterials such as graphene has generated a novel series of hybridized materials. GO from the oxidation of graphite is rich in oxygen-containing functional groups including epoxy, hydroxyl, (present on the basal plane) and carboxyl, carbonyl, phenol, lactone, and quinone, (present at the sheet edges) and these change the van der Waals force of attraction.

Graphene loses aromaticity when oxidized due to the utilization of the π-electrons in the covalent bonding of the oxy groups to the graphene backbone. The carboxyl, carbonyl, and additional groups bound on the edge allow them to be homogeneously dispersed in organic solvents [30] and water [31]. The hydrophobicity of the aromatic frameworks and the hydrophilicity of the oxygen-containing groups transform GO allowing it to become more amphiphilic, giving it further interaction with organic and inorganic molecules.

Alternatively, rGO, with its eliminated oxygen atoms reduces the negative charge [32]. Whereas during reduction, rGO regains its graphic assembly by removing the oxygen-containing groups, which were introduced during oxidation reinstating its electronic properties [33,34]. Partial reduction along with chemical exposure permits the adaptation of the conductivity of the rGO [35,36].

### 18.3.3 Polymer/cellulose/nanoclay nanocomposites

Research that focuses on developing "green" composites uses natural fibers as a substitute for conventional inorganic fillers such as plastic. Natural fibers have intrinsic properties that transcend conventional reinforcing materials because of their renewable cheap properties. However, the evolution of the use of biodegradable polymers has been hampered due to low-performance characteristics, including heat distortion and brittleness. Biodegradable polymers can also come at a higher cost compared to other common polymers or plastics. The intrinsic shortfalls of biopolymers can be overcome by the incorporation of reinforcement materials, also at the nanoscale. Both silicate clay and cellulose are amongst the most common minerals and polymers in nature, so in some ways, it makes sense to combine them.

Nanocellulose (NC) with its high strength and stiffness, with low density, and significant mechanical properties, when formed into a composite displays enhanced overall properties when compared to nanocellulose alone. NC displays intrinsic flexibility when it comes to tailoring the design of the composites.

Nanoclay (NCl), on the other hand, is a natural industrial mineral chiefly used as fortification in composites due to being flame retardant and a mechanical barrier. Although not renewable, it is biodegradable and can augment the mechanical properties of other polymers. The clay mineral's structural unit is composed of silica tetrahedral sheets $[SiO_4]^{4-}$ and alumina octahedral sheets $[AlO_3(OH)_3]^6$. The silicon and oxygen tetrahedrons in the tetrahedral sheet link to the next-door tetrahedrons on three corners, while the fourth corner connects to the adjacent octahedral sheet. The octahedral sheet is formed from magnesium or aluminum in octahedral coordination between the oxygens from the hydroxyl group and the tetrahedral sheet. These sheets appear as a single layer and when many layers are combined together, they form clay crystallite. The layers are bound into stacks of

parallel lamellae via electrostatic and Van der Waals forces, and also hydrogen bonding. The gap between the neighboring layers can be lined with water or other liquids, causing the forces to weaken, resulting in the lattice expanding.

NCl fine-grained particles in stacked lamellar sheets are predominated by fine-grained aluminosilicates and phyllosilicates that are shaped from the weathering of silicate minerals on the earth surface [37]. NCl can be isolated away from the clay by procedures such as vigorous stirring with ultrasonication and cross-flow filtration [38]. The most common NCls used for reinforcement are halloysite and montmorillonite that have a robust influence on mechanical properties when combined in small quantities into the polymer matrix. Halloysite nanotubes are naturally tubular, with the structural formula of $Al_2(OH)_4Si_2O_5.nH_2O$. Crystalline layers are octahedral aluminum ($Al^{3+}$) and tetrahedral silicon ($Si^{4+}$) with water molecules in amongst the parallel layers. Montmorillonite is one of the most familiar smectites that undergoes reversible expansion on absorbing water. Having a dioctahedral structure, this NCl precipitates microscopic crystals from water, then when distributed in polymers undertakes a stiff maze structure that reduces its diffusion rate [39]. The morphology changes from platy to sponge-like to ribbons accentuating its practicality as a reinforcing filler, particularly useful in food packaging [40]. Each montmorillonite layer is $200 - 600$ nm thick and the crystal lattice has layers 1 nm thick, with a octahedral alumina sheet amid paired silica tetrahedral sheets [39]. Of note, montmorillonite when hydrated expands its hydrophilic behavior, but under those conditions, it is only miscible with hydrophilic polymers, such as poly(ethylene oxide) (PEO) and PVA [39]. Incorporation of the NCl prevents the polymer chains' free movement providing rigidity to soft polymeric composites thereby reducing internal flexibility providing increased mechanical properties, diffusion barrier features, fire retardant and ultraviolet light resistance properties [4].

Hybrid nanocellulose/NCl (Cloisite C30B) composites combined with PLA showed synergistically enhanced barrier properties, improving thermomechanical resistance and crystallization kinetics whilst upholding transparency aimed at food packaging applications [41]. The assemblage of two dissimilar hydrophilic products, namely, nanoclay platelets and nanocellulose fibrils increased the water contact angle of the surfaces of the composite films due to the high density of ionic groups on their surfaces. The two hydrophilic nanoelements exhibited a contact angle larger than the individual neat films [42]. Furthermore, cellulose from banana pseudo-stems combined with nanoclay enhanced the film tensile strengths but reduced the elasticity further improving the nanocellulose/nanoclay based bioplasticity [43]. NCl fibrils with montmorillonite dispersed homogeneously in the matrix showed that the optical transparency increased as the concentration of the montmorillonite increased alongside the mechanical moduli [18].

### 18.3.4 Polymer/cellulose/metal nanocomposites

A combination of inorganic and organic nanomaterials will provide a nanocomposite with features evolving from combining both materials. Cellulose is the most profuse biopolymer on earth, as detailed above. From the extensive range of

obtainable inorganic fillers, metal nanoparticles from silver (Ag), gold (Au), or copper (Cu) display properties that diverge from their original analogs due to a variety of size, distribution and surface effects. Accordingly, the final material properties could be fine-tuned by the addition of nanofillers and the interactions that occur with the cellulose fiber surfaces.

A simple blending of inorganic nanometals with cellulose as a matrix, frequently causes nanoparticle aggregates that reduce the advantages usually correlated with the presence of nanoparticles leading to poor durability and lower antibacterial efficiency [44]. Direct addition of Ag or Au nanoparticles onto filter papers leads to the heterogeneous distribution of nanoparticles and aggregate formation during the drying process [45–47]. However, the metal salts reduce in the cellulose aqueous suspensions in the presence of ether and hydroxyl groups in the cellulose fibers to securely bond the metal ions strongly onto the fibers via ion–dipole interactions that further stabilizes the metal nanoparticles through surface interactions [19,48].

Sodium borohydride ($NaBH_4$) and tri-sodium citrate ($Na_3C_6H_5O_7$) can reduce the metal ions in cellulose matrices [49]. Ascorbic acid combined with gelatin or polyvinylpyrrolidone worked as a colloidal stabilizer acting as a reducer for gelatin and $Ag+$ controlling particle size. The reducing agent triethanolamine reduced the Ag ions producing 8.5 nm spherical particles, homogeneously dispersed in the bacterial cellulose membranes [50]. Streaming hydrogen ($H_2$) gas over a preformed cellulose matrix formed Au salts nanoparticles with a variable thickness that could be adjusted by the addition of different halides [51].

## 18.4 Collagen

Collagen is the main insoluble structural protein of the extracellular matrix located within the connective tissue. As the most copious protein in the animal kingdom situated in the tendons, dermis, and bones renders collagen type I the ideal substrate for the culture of a variety of different cell lines. Collagen is, unsurprisingly, the most plentiful protein in the human body, it is an important component of the extracellular matrix imparting tensile strength and structural integrity to body tissues. Subsequent to injury tissue disruption requires collagen to restore normal function and structure [52].

### *18.4.1 Collagen polymer nanocomposites*

Although collagen has drawn awareness in the tissue engineering community because of the low mechanical properties, any application concerning mechanical loading or demanding structural integrity is inhibited. To overcome that weakness, organic collagen combined with a nanoscale inorganic bioactive material, like silica in a composite. Bioactive materials naturally contain hydroxyapatite (HA), calcium phosphate $Ca_3(PO_4)_2$ these include bioactive glasses. Bioactive materials are capable of promoting nucleation and consequently form calcium phosphate crystals, HA

crystals or other calcium phosphates on their surfaces [53,54]. Naturally organic materials are incapable of this ability, however, by supplementing these with nanoscale inorganic bioactive materials, the subsequent composites become bioactive and this is particularly useful for bone tissue. The incorporation of inorganic bioactive materials can offer cell adhesion sites that expedite incorporation with the adjacent tissue [55]. The composite materials provide a strong bond at the location of implantation and form a layer of HA upon their surface [53–55]. Organic composites combined with nanoscale inorganic bioactive materials have increased mechanical properties, compression strength and stiffness. In that respect, the particle size s will affect the composite properties. Nanosized inorganic particles deliver high surface area, by providing a high interaction area for the reaction may improve the bonding strength between the inorganic filler and consequently augment the overall mechanical properties of the composite [56,57].

### 18.4.2 Polymer/collagen/silica nanocomposites

Bone tissue engineering scaffolds ought to be biodegradable, biocompatible, osteoconductive and in particular, should exhibit sound structural properties [58,59]. Natural bone is compiled of collagen fibrils mineralized by calcium phosphate that is comparable to HA. Silica ($SiO_2$) itself is biocompatible and osteoconductive [60], and plays a critical role in promoting bone formation. Silica provides mineralization on the silica/collagen composites [60,61] as the surface silanol groups (Si-OH) of amorphous silica encourage the development of the biologically active bone-like apatite [62]. The collagen's carboxylate functional group binds to the calcium ions and simultaneously releases silicic acid from silica forming calcium silicate that provides nucleation sites for additional calcium phosphate deposits [61]. Electrostatic binding between the positive charges of the amine groups of collagens and the negative charges of the silica can increase the overall strength of the matrix [63].

A combination of a colloidal (sol) into an integrated network (gel) provides sol-gel-derived silica that has the ability to stimulate neoangiogenesis in the tissue surrounding the bone substitute [64], which is the ultimate goal for vascularized bone regeneration [65]. Human bone marrow stromal cells (hBMSCs) seeded onto nano silica-collagen scaffolds increased up to sixfold during 28 days of cultivation and alkaline phosphatase (ALP) activity of hBMSCs on hybrid scaffolds or pure collagen scaffolds proliferated at the same rate [63]. Human dermal fibroblasts adhered preferentially to a silicified collagen hydrogel when compared to the pure collagen hydrogel control [66].

Mouse osteoblast precursor (MC3T3) cells on a pure collagen membrane showed a rounded morphology, however, as the silica content increased in the collagen/silica membrane, the cells showed excellent adhesion and spreading characteristics. Furthermore, the collagen membranes containing a higher proportion of silica demonstrated twice the ALP activity of pure collagen [67].

Medicated dressings composed of core-shell collagen–silica nanocomposites showed prolonged release of two topical antibiotics, gentamicin sulfate and sodium

rifamycin. Antibiotics released from the nanocomposites showed sustained antibacterial properties against Staphylococcus aureus (S. aureus). Histological examination of the wound bed showed that M1 inflammatory macrophages were absent posttreatment and the biocomposite promoted cutaneous wound repair [68].

Specifically aimed at packing specific bone defects, the development of osteo regenerative silica/collagen composites capable of influencing the bone remodeling process and promoting particularly, neovascularization could be the gold standard in bone tissue engineering.

### 18.4.3 Polymer/collagen/hydroxyapatite nanocomposites

Bone is a hierarchical biological composite composed of minerals in the form of HA crystals and organic collagen molecules. A composite structure fabricated from a pair of outer layers of HA and an internal collagen layer in between showed that when HA aligned with the c-axis of the crystal parallel to the main axis of the collagen molecule, the H-bonds between collagen and HA increased resistance against catastrophic failure. The HA increased the mechanical properties of the composite and through the geometric confinement increased the mechanical performance. Certainly, the progressive breakage then the formation of the H-bonds acted as a toughening mechanism providing a realistic molecular model of bone [69].

### 18.4.4 Polymer/collagen/metal nanocomposites

Collagen scaffolds that incorporated gold nanoparticles (AuNPs) at $<20$ ppm with a size of $>20$ nm were biocompatible with HaCat keratinocytes and 3T3 fibroblasts. The inclusion of AuNPs into glutaraldehyde cross-linked scaffolds increased tensile strength and hydrolytic degradation. In vivo healing of full-thickness skin, wounds examined histopathologically showed that AuNPs repressed inflammation while elevating granulation, neovascularization and wound closure. AuNPs had the highest Young's modulus and tensile strength when used for wound healing treatments [70].

For centuries, silver has been utilized as an antimicrobial mediator for treating bacterial infections, particularly for treating antibiotic-resistant bacteria. These Ag nanoparticles are created at a smaller scale (hence increased surface area) because of their strong magnetic, chemical and plasmonic properties. In the production of silver particle nanosuspensions, chemical reduction is commonly used due to its large-scale production of aggregation-free nanoparticles with low formulation costs. However, the method of chemical reduction creates particles of variable dimensions and morphology [71]. *Escherichia coli* (*E. coli*) cells in the presence of Ag nanoparticles showed that the Ag accumulated causing pitting in the bacterial cell wall significantly increasing permeability resulting in cell apoptosis [72]. Yeast, *S. aureus* and *E. coli* were inhibited by Ag nanoparticles [73]. Additionally, Ag nanoparticles as a low concentration of 10 ppm exerted significant toxicity against bacterial Bacillus subtilis, causing significant chromosomal DNA degradation and increased membrane permeability [74].

Silver nanoparticles stabilized with type I collagen displayed antimicrobial activity specifically against *S. aureus* and *E. coli* but showed no identifiable cellular cytotoxicity [75]. In another study, collagen sponges achieved by cross-linking collagen gels with glutaraldehyde that was then plasma sputtered with Ag nanoparticles showed activity against E. coli [76]. Furthermore, a composite of titanium dioxide (TiO2)-Ag encapsulated in collagen increased both biocompatibility and skin regeneration with resistance towards *S. aureus* activity [77]. Electrospun Ag nanoparticles in collagen nanofibers on the incision of the skin of a Wistar rat showed that the wound healing rate of the composite appeared accelerated when compared to pure collagen nanofibers with an increased rate of reepithelialisation, collagen production, hemostatic properties and wound contraction [78].

## 18.5 Keratin

It is possible to add value to waste keratin-rich materials such as poultry feathers and sheep wool by partially substituting them with synthetic polymers producing biocomposites with improved mechanical properties. The strong intermolecular ionic keratin bonds of disulfide, and hydrogen (Fig. 18.3) generate a thermoset material that is not easily processed or blended with another polymer. Since the organic biodegradable fibers are agricultural waste products at greatly reduced cost, one thought-provoking possibility is to combine the organic with the inorganic. Each year, over 5 million tons of keratin-based waste products from "dirty" wool, horn, feathers and nails are created from slaughterhouses, butchery, farms and of course, the poultry business [79,80]. These organic proteins have underutilised positive characteristics such as biodegradability, biocompatibility, and fire retardant capability, and owing to the increased sulfur content (of around 3%−4%), landfill or incineration have an adverse environmental impact [81]. The function of these organic fibers reinforcing the polymer composites is an intriguing idea for the development of new commercial products that concurrently reduces and recycles these waste products [82].

### 18.5.1 Polymer/keratin/graphene nanocomposites

Carbon as the 6th element of the periodic table is capable of forming many allotropes including diamond, graphite, fullerenes, CNTs and the newly discovered graphene. Graphene is a flat monolayer of tightly packed carbon atoms in a two-dimensional (2D) honeycomb lattice. Graphene is used in the preparation of PNC as a substitute carbon-based nanofiller

Electronic devices are commonly formed from rigid, nondegradable materials, as they are designed to be long-lasting. But this characteristic, along with traces of rare and/or toxic elements generates additional problems for waste management [1]. Recently, researchers have been working on keratin in the form of feathers or waste wool incorporated into sensors or sustainable packaging. For example, a novel

approach using keratin combined with graphene produced protein-based electronic materials, including capacitors, resistors and inductors assembled together to form electrical circuits. Furthermore, a water-based ink of keratin and graphene produced flexible electrodes with electrical conductivity [83]. Composites of a keratin matrix with 1% GO or keratin with 1% carbon fibers fabricated composite film sensors with the latter exhibiting a higher degree of sensitivity, fast response/recovery times and greater ionic conductivity behavior [84]. Feather keratin/PVA/tris(hydroxymethyl)aminomethane (FK/PVA/Tris) bio-nanocomposite films containing GO or graphene prepared using a solvent casting method formed hydrogen bonds between the GO and the film matrix for use in the packaging field [85]. As our awareness of sustainability increases and our focus shifts from traditional plastic materials to more environmentally-friendly alternatives for a variety of applications such as food packaging.

Bio-based electrically conductive fibers polyacrylonitrile (PAN) combined with waste wool were fabricated using the wet spinning method then chemically reduced through hydrazine vapor exposure providing bonding between the carboxylic and hydroxyl groups of the amino groups of wool and the GO sheets. The GO nanosheets showed increased electrical conductivity when compared to the control. These GO/wool/PAN hybrid fibers may provide an application in smart textile products.

Keratin, in particular, has the potential to replace traditional petrochemical-derived polymers for use as a sustainable alternative in a variety of applications.

## 18.6 Conclusions and future directions

This chapter outlines the essential characteristics of PNC in various categories such as chemical modifications and chemical linking leading to the homogeneous dispersion of nanofillers throughout the polymer matrix. Further endeavors are required to pinpoint the optimal nanofiller loading required for peak thermal, electrical conductivity, sensing, and mechanical properties furthering novel prospects for the production of functional sustainable biomaterials.

Linking nanoclay, or graphene, or metals to chitosan or cellulose or even keratin produces nanocomposites that may fabricate advanced eco-friendly packaging with superior properties. The attachment of chitosan to metal nanoparticles for sensor applications, as the metallic particles may enhance sensitivity. The applications of these PNC in tissue engineering and implants, filters, dye removal, clothing, sensors, membrane technology, antimicrobial with biomedical relevance are endless (Fig. 18.5).

As the demand for PNC increases, a balance between the consumers' high expectations, government regulations, and industry will consequently enhance the available products as well as tackle the increasing worldwide concerns with packaging waste. PNC are gaining momentum and may hold the key, not only for today but also in the future. Once production costs are reduced, then companies will

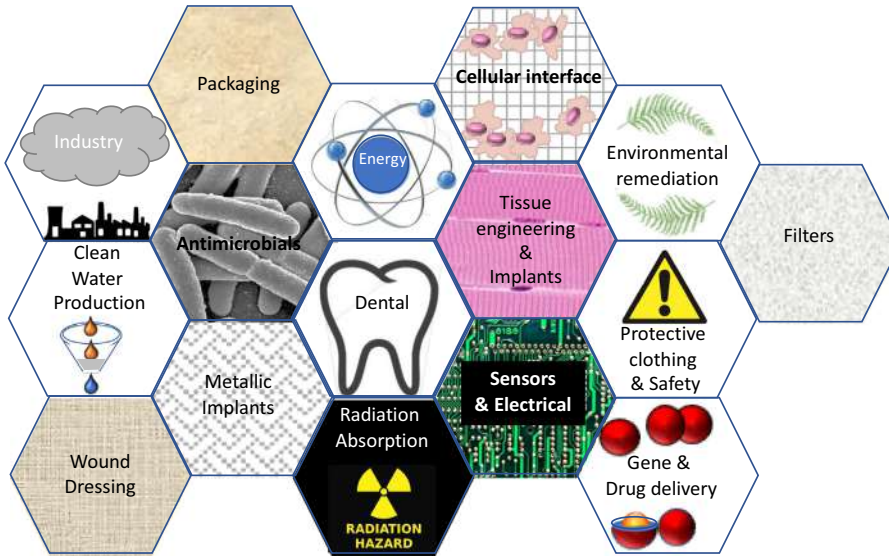


**Figure 18.5** The endless possibilities of polymer nanocomposite applications[1,3,30].

utilize this technology to change product sustainability delivering high quality products to the customers while saving money and making a profit. The benefits offered by PNC far outweigh the costs and in time will become further refined.

Declarations of interest: none.

Author contributions:

Azam Ali: review, conceptualization and correction

Maree Gould: writing

No specific grant from funding agencies in the commercial, public or not-for-profit areas was received for this research.

## References

[1] M.A. Ali, M.L. Gould, Untapped Potentials of Hazardous Nanoarchitectural Biopolymers, J. Hazard. Mater. 411 (2021). Available from: https://doi.org/10.1016/j.jhazmat.2020.124740.

[2] A. Ghosh, M. Azam Ali, R. Walls, Modification of Microstructural Morphology and Physical Performance of Chitosan Films, Int. J. Biol. Macromol. 46 (2) (2010) 179–186. Available from: https://doi.org/10.1016/j.ijbiomac.2009.11.006.

[3] A. Shavandi, D. Bekhit Ael, M.A. Ali, Z. Sun, M. Gould, Development and characterization of hydroxyapatite/beta-tcp/chitosan composites for tissue engineering applications, Mater. Sci. Eng. C. Mater Biol. Appl. 56 (2015) 481–493. Available from: https://doi.org/10.1016/j.msec.2015.07.004.

[4] R. Rafiee, R. Shahzadi, Mechanical properties of nanoclay and nanoclay reinforced polymers: a review, Polym. Compos. 40 (2) (2019) 431–445. Available from: https://doi.org/10.1002/pc.24725.

[5] A. Zielinska, F. Carreiro, A.M. Oliveira, A. Neves, B. Pires, D.N. Venkatesh, et al., Polymeric nanoparticles: production, characterization, toxicology and ecotoxicology, Molecules 25 (16) (2020) 3731. Available from: https://doi.org/10.3390/molecules25163731.
[6] M.H. Periayah, A.S. Halim, A.Z. Saad, Chitosan: a promising marine polysaccharide for biomedical research, Pharmacogn. Rev. 10 (19) (2016) 39–42. Available from: https://doi.org/10.4103/0973-7847.176545.
[7] A. Kausar, Scientific potential of chitosan blending with different polymeric materials: a review, J. Plastic Film. & Sheeting 33 (4) (2017) 384–412. Available from: https://doi.org/10.1177/8756087916679691.
[8] A. Shavandi, D. Bekhit Ael, Z. Sun, A. Ali, M. Gould, A novel squid pen chitosan/hydroxyapatite/beta-tricalcium phosphate composite for bone tissue engineering, Mater. Sci. Eng. C. Mater Biol. Appl. 55 (2015) 373–383. Available from: https://doi.org/10.1016/j.msec.2015.05.029.
[9] M. Li, A. Dopilka, A.N. Kraetz, H.K. Jing, C.K. Chan, Layered double hydroxide/chitosan nanocomposite beads as sorbents for selenium oxoanions, Ind. & Eng. Chem. Res. 57 (14) (2018) 4978–4987. Available from: https://doi.org/10.1021/acs.iecr.8b00466.
[10] G.A. Kloster, D. Muraca, O.M. Londono, M. Knobel, N.E. Marcovich, M.A. Mosiewicki, Structural analysis of magnetic nanocomposites based on chitosan, Polym. Test. 72 (2018) 202–213. Available from: https://doi.org/10.1016/j.polymertesting.2018.10.022.
[11] P.P. Zuo, H.F. Feng, Z.Z. Xu, L.F. Zhang, Y.L. Zhang, W. Xia, et al., Fabrication of biocompatible and mechanically reinforced graphene oxide-chitosan nanocomposite films, Chem. Cent. J. 7 (2013) 39. Available from: https://doi.org/10.1186/1752-153x-7-39.
[12] T.G. Maraschin, R.D. Correa, L.F. Rodrigues, N.M. Balzarettid, J.A. Malmonge, G.B. Galland, et al., Chitosan nanocomposites with graphene-based filler, Mater. Research-Ibero-American J. Mater. 22 (2019) e20180829. Available from: https://doi.org/10.1590/1980-5373-MR-2018-0829.
[13] X.M. Yang, Y.F. Tu, L.A. Li, S.M. Shang, X.M. Tao, Well-dispersed chitosan/graphene oxide nanocomposites, Acs Appl. Mater. & Interfaces 2 (6) (2010) 1707–1713. Available from: https://doi.org/10.1021/am100222m.
[14] J.P. Zhang, L. Wang, A.Q. Wang, Preparation and properties of chitosan-g-poly(acrylic acid)/montmorillonite superabsorbent nanocomposite via in situ intercalative polymerization, Ind. & Eng. Chem. Res. 46 (8) (2007) 2497–2502. Available from: https://doi.org/10.1021/ie061385i.
[15] M. Koosha, H. Mirzadeh, M.A. Shokrgozar, M. Farokhi, Nanoclay-reinforced electrospun chitosan/PVA nanocomposite nanofibers for biomedical applications, Rsc Adv. 5 (14) (2015) 10479–10487. Available from: https://doi.org/10.1039/c4ra13972k.
[16] T.M. Wu, C.Y. Wu, Biodegradable poly(lactic acid)/chitosan-modified montmorillonite nanocomposites: preparation and characterization, Polym. Degrad. Stab. 91 (9) (2006) 2198–2204. Available from: https://doi.org/10.1016/j.polymdegradstab.2006.01.004.
[17] M. Rani, Rachna, U. Shanker, Metal oxide-chitosan based nanocomposites for efficient degradation of carcinogenic PAHs, J. Environ. Chem. Eng. 8 (3) (2020) 103810. Available from: https://doi.org/10.1016/j.jece.2020.103810.
[18] Y.G. Jeong, J.H. Ryu, Nanoclay-reinforced nanocellulose composite films with improved heat resistance, gas barrier performance, and mechanical properties, TechConnect Briefs, 1, Adv. Mater. (2018) 167–168.
[19] T. Maneerung, S. Tokura, R. Rujiravanit, Impregnation of silver nanoparticles into bacterial cellulose for antimicrobial wound dressing, Carbohydr. Polym. 72 (1) (2008) 43–51. Available from: https://doi.org/10.1016/j.carbpol.2007.07.025.

[20] Krässig, H., Schurz, J., Steadman, R., Schliefer, K., Albrecht, W., Mohring, M., et al. (2004). Cellulose. Ullmann's Encyclopedia of Industrial Chemistry, 7, 279–330.
[21] D. Klemm, B. Heublein, H.P. Fink, A. Bohn, Cellulose: fascinating biopolymer and sustainable raw material, Angew. Chem. Int. (Ed.) Engl. 44 (22) (2005) 3358–3393. Available from: https://doi.org/10.1002/anie.200460587.
[22] A. Pinkert, K.N. Marsh, S. Pang, M.P. Staiger, Ionic liquids and their interaction with cellulose, Chem. Rev. 109 (12) (2009) 6712–6728. Available from: https://doi.org/10.1021/cr9001947.
[23] W.I. Thomas, G. Rowley, G. Doveston, An investigation of the influence of the core material properties on the compression and properties of dry-coated tablets, Drug. Dev. Ind. Pharm. 24 (10) (1998) 973–978. Available from: https://doi.org/10.3109/03639049809097277.
[24] H. Charreau, E. Cavallo, M.L. Foresti, Patents involving nanocellulose: analysis of their evolution since 2010, Carbohydr. Polym. 237 (2020) 116039. Available from: https://doi.org/10.1016/j.carbpol.2020.116039.
[25] F. Khili, J. Borges, P.L. Almeida, R. Boukherroub, A.D. Omrani, Extraction of cellulose nanocrystals with structure I and II and their applications for reduction of graphene oxide and nanocomposite elaboration, Waste Biomass Valoriz. 10 (7) (2019) 1913–1927. Available from: https://doi.org/10.1007/s12649-018-0202-4.
[26] Y. Chen, L. Gan, J. Huang, A. Dufresne, Reinforcing mechanism of cellulose nanocrystals in nanocomposites, in: A.D. Jin Huang, N. Lin (Eds.), Nanocellulose: From Fundamentals to Advanced Materials, Wiley, Milton QLD 4064 Australia, 2019.
[27] A. Dufresne, Nanocellulose processing properties and potential applications, Curr. Forestry Rep. 5 (2) (2019) 76–89. Available from: https://doi.org/10.1007/s40725-019-00088-1.
[28] D. Trache, M.H. Hussin, M.K.M. Haafiz, V.K. Thakur, Recent progress in cellulose nanocrystals: sources and production, Nanoscale 9 (5) (2017) 1763–1786. Available from: https://doi.org/10.1039/c6nr09494e.
[29] Q. Zhang, L. Zhang, W.B. Wu, H.N. Xiao, Methods and applications of nanocellulose loaded with inorganic nanomaterials: a review, Carbohydr. Polym. 229 (2020) 115454. Available from: https://doi.org/10.1016/j.carbpol.2019.115454.
[30] A.T. Lawal, Graphene-based nano composites and their applications. a review, Biosens. & Bioelectron. 141 (2019) 111384. Available from: https://doi.org/10.1016/j.bios.2019.111384.
[31] K. Thakur, B. Kandasubramanian, Graphene and graphene oxide-based composites for removal of organic pollutants: a review, J. Chem. Eng. Data 64 (3) (2019) 833–867. Available from: https://doi.org/10.1021/acs.jced.8b01057.
[32] A.T. Smith, A.M. LaChance, S.Z. Bin Liu, L. Sun, Synthesis, properties, and applications of graphene oxide/reduced graphene oxide and their nanocomposites, Nano Materials Science 1 (1) (2019) 31–47. Available from: https://doi.org/10.1016/j.nanoms.2019.02.004. ISSN 2589-9651.
[33] X.B. Cao, D.P. Qi, S.Y. Yin, J. Bu, F.J. Li, C.F. Goh, et al., Ambient fabrication of large-area graphene films via a synchronous reduction and assembly strategy, Adv. Mater. 25 (21) (2013) 2957–2962. Available from: https://doi.org/10.1002/adma.201300586.
[34] S.S. Siwal, Q.B. Zhang, N. Devi, V.K. Thakur, Carbon-based polymer nanocomposite for high-performance energy storage applications, Polymers 12 (3) (2020) 505. Available from: https://doi.org/10.3390/polym12030505.
[35] T. Rydzkowski, K. Reszka, M. Szczypinski, M.M. Szczypinski, E. Kopczynska, V.K. Thakur, Manufacturing and evaluation of mechanical, morphological, and thermal properties of reduced graphene oxide-reinforced expanded polystyrene (EPS) nanocomposites, Adv. Polym. Technol. 2020 (2020) 3053471. Available from: https://doi.org/10.1155/2020/3053471.

[36] S. Schoche, N. Hong, M. Khorasaninejad, A. Ambrosio, E. Orabona, P. Maddalena, et al., Optical properties of graphene oxide and reduced graphene oxide determined by spectroscopic ellipsometry, Appl. Surf. Sci. 421 (2017) 778–782. Available from: https://doi.org/10.1016/j.apsusc.2017.01.035.

[37] K. Majeed, M. Jawaid, A. Hassan, A. Abu Bakar, H.P.S.A. Khalil, A.A. Salema, et al., Potential materials for food packaging from nanoclay/natural fibres filled hybrid composites, Mater. & Des. 46 (2013) 391–410. Available from: https://doi.org/10.1016/j.matdes.2012.10.044.

[38] M.C. Floody, B.K.G. Theng, P. Reyes, M.L. Mora, Natural nanoclays: applications and future trends—a chilean perspective, Clay Miner. 44 (2) (2009) 161–176. Available from: https://doi.org/10.1180/claymin.2009.044.2.161.

[39] M.S. Nazir, M.H. Mohamad Kassim, L. Mohapatra, M.A. Gilani, M.R. Raza, K. Majeed, Characteristic properties of nanoclays and characterization of nanoparticulates and nanocomposites, in: Q.A. Jawaid M., R. Bouhfid (Eds.), Nanoclay Reinforced Polymer Composites. Engineering Materials, Springer, Singapore, 2016. Available from: https://doi.org/10.1007/978-981-10-1953-1_2.

[40] A. Arora, G.W. Padua, Review: nanocomposites in food packaging, J. Food Sci. 75 (1) (2010) R43–R49. Available from: https://doi.org/10.1111/j.1750-3841.2009.01456.x.

[41] J. Trifol, D. Plackett, C. Sillard, P. Szabo, J. Bras, A.E. Daugaard, Hybrid poly(lactic acid)/nanocellulose/nanoclay composites with synergistically enhanced barrier properties and improved thermomechanical resistance, Polym. Int. 65 (8) (2016) 988–995. Available from: https://doi.org/10.1002/pi.5154.

[42] C.N. Wu, T. Saito, Q.L. Yang, H. Fukuzumi, A. Isogai, Increase in the water contact angle of composite film surfaces caused by the assembly of hydrophilic nanocellulose fibrils and nanoclay platelets, Acs Appl. Mater. & Interfaces 6 (15) (2014) 12707–12712. Available from: https://doi.org/10.1021/am502701e.

[43] R.H.F. Faradilla, G. Lee, J. Roberts, P. Martens, M. Stenzel, J. Arcot, Effect of glycerol, nanoclay and graphene oxide on physicochemical properties of biodegradable nanocellulose plastic sourced from banana pseudo-stem, Cellulose 25 (1) (2018) 399–416. Available from: https://doi.org/10.1007/s10570-017-1537-x.

[44] T.A. Dankovich, D.G. Gray, Bactericidal Paper Impregnated with Silver Nanoparticles for Point-of-Use Water Treatment, Environ. Sci. Technol. 45 (5) (2011) 1992–1998.

[45] W.Q. Ma, Y. Fang, Experimental (Sers) and theoretical (Dft) studies on the adsorption of P-, M-, and O-nitroaniline on gold nanoparticles, J. Colloid Interface Sci. 303 (1) (2006) 1–8. Available from: https://doi.org/10.1016/j.jcis.2006.05.001.

[46] Y.H. Ngo, D. Li, G.P. Simon, G. Gamier, Paper surfaces functionalized by nanoparticles, Adv. Colloid Interface Sci. 163 (1) (2011) 23–38. Available from: https://doi.org/10.1016/j.cis.2011.01.004.

[47] D. Wu, Y. Fang, The adsorption behavior of p-hydroxybenzoic acid on a silver-coated filter paper by surface enhanced raman scattering, J. Colloid Interface Sci. 265 (2) (2003) 234–238. Available from: https://doi.org/10.1016/S0021-9797(03)00348-5.

[48] J.H. He, T. Kunitake, A. Nakao, Facile in situ synthesis of noble metal nanoparticles in porous cellulose fibers, Chem. Mater. 15 (23) (2003) 4401–4406. Available from: https://doi.org/10.1021/cm034720r.

[49] R. Tankhiwale, S.K. Bajpai, Graft copolymerization onto cellulose-based filter paper and its further development as silver nanoparticles loaded antibacterial food-packaging material, Colloids Surf. B-Biointerfaces 69 (2) (2009) 164–168. Available from: https://doi.org/10.1016/j.colsurfb.2008.11.004.

[50] H.S. Barud, C. Barrios, T. Regiani, R.F.C. Marques, M. Verelst, J. Dexpert-Ghys, et al., Self-supported silver nanoparticles containing bacterial cellulose membranes, Mater. Sci. & Eng. C-Biomimetic Supramolecular Syst. 28 (4) (2008) 515–518. Available from: https://doi.org/10.1016/j.msec.2007.05.001.
[51] T. Ishida, H. Watanabe, T. Bebeko, T. Akita, M. Haruta, Aerobic oxidation of glucose over gold nanoparticles deposited on cellulose, Appl. Catal. a-General 377 (1-2) (2010) 42–46. Available from: https://doi.org/10.1016/j.apcata.2010.01.017.
[52] G. Yang, B.B. Rothrauff, R.S. Tuan, Tendon and ligament regeneration and repair: clinical relevance and developmental paradigm, Birth Defects Res. C. Embryo Today 99 (3) (2013) 203–222. Available from: https://doi.org/10.1002/bdrc.21041.
[53] K. Gkioni, S.C.G. Leeuwenburgh, T.E.L. Douglas, A.G. Mikos, J.A. Jansen, Mineralization of hydrogels for bone regeneration, Tissue Eng. Part. B-Reviews 16 (6) (2010) 577–585. Available from: https://doi.org/10.1089/ten.teb.2010.0462.
[54] M.A. Lopez-Heredia, A. Lapa, A.C. Mendes, L. Balcaen, S.K. Samal, F. Chai, et al., Bioinspired, biomimetic, double-enzymatic mineralization of hydrogels for bone regeneration with calcium carbonate, Mater. Lett. 190 (2017) 13–16. Available from: https://doi.org/10.1016/j.matlet.2016.12.122.
[55] S.M. Rea, S.M. Best, W. Bonfield, Bioactivity of ceramic-polymer composites with varied composition and surface topography, J. Mater. Science-Materials Med. 15 (9) (2004) 997–1005. Available from: https://doi.org/10.1023/B:Jmsm.0000042685.63383.86.
[56] M. Ara, M. Watanabe, Y. Imai, Effect of blending calcium compounds on hydrolytic degradation of poly(DL-lactic acid-co-glycolic acid), Biomaterials 23 (12) (2002) 2479–2483. Available from: https://doi.org/10.1016/S0142-9612(01)00382-9.
[57] K. Rezwan, Q.Z. Chen, J.J. Blaker, A.R. Boccaccini, Biodegradable and bioactive porous polymer/inorganic composite scaffolds for bone tissue engineering, Biomaterials 27 (18) (2006) 3413–3431. Available from: https://doi.org/10.1016/j.biomaterials.2006.01.039.
[58] J.T. Ratnayake, E.D. Ross, G.J. Dias, K.M. Shanafelt, S.S. Taylor, M.L. Gould, et al., Preparation, characterisation and in vitro biocompatibility study of a bone graft developed from waste bovine teeth for bone regeneration, Mater. Today Commun. 22 (2020) 100732. Available from: https://doi.org/10.1016/j.mtcomm.2019.100732.
[59] J.T.B. Ratnayake, M.L. Gould, A. Shavandi, M. Mucalo, G.J. Dias, Development and characterization of a xenograft material from new zealand sourced bovine cancellous bone, J. Biomed. Mater. Res. Part. B-Applied Biomater. 105 (5) (2017) 1054–1062. Available from: https://doi.org/10.1002/jbm.b.33644.
[60] S. Heinemann, C. Heinemann, H. Ehrlich, M. Meyer, H. Baltzer, H. Worch, et al., A novel biomimetic hybrid material made of silicified collagen: perspectives for bone replacement, Adv. Eng. Mater. 9 (12) (2007) 1061–1068. Available from: https://doi.org/10.1002/adem.200700219.
[61] D. Eglin, S. Maalheem, J. Livage, T. Coradin, In vitro apatite forming ability of type i collagen hydrogels containing bioactive glass and silica sol-gel particles, J. Mater. Science-Materials Med. 17 (2) (2006) 161–167. Available from: https://doi.org/10.1007/s10856-006-6820-6.
[62] W. Lai, J. Garino, P. Ducheyne, Silicon excretion from bioactive glass implanted in rabbit bone, Biomaterials 23 (1) (2002) 213–217. Available from: https://doi.org/10.1016/S0142-9612(01)00097-7.
[63] S. Heinemann, C. Heinemann, M. Jager, J. Neunzehn, H.P. Wiesmann, T. Hanke, Effect of silica and hydroxyapatite mineralization on the mechanical properties and the biocompatibility of nanocomposite collagen scaffolds, Acs Appl. Mater. & Interfaces 3 (11) (2011) 4323–4331. Available from: https://doi.org/10.1021/am200993q.

[64] V. Alt, D.V. Kogelmaier, K.S. Lips, V. Witt, S. Pacholke, C. Heiss, et al., Assessment of angiogenesis in osseointegration of a silica-collagen biomaterial using 3d-nano-ct, Acta Biomaterialia 7 (10) (2011) 3773−3779. Available from: https://doi.org/10.1016/j.actbio.2011.06.024.

[65] A.R. Boccaccini, U. Kneser, A. Arkudas, Scaffolds for vascularized bone regeneration: advances and challenges, Expert. Rev. Med. Devices 9 (5) (2012) 457−460. Available from: https://doi.org/10.1586/Erd.12.49.

[66] M.F. Desimone, C. Helary, S. Quignard, I.B. Rietveld, I. Bataille, G.J. Copello, et al., In vitro studies and preliminary in vivo evaluation of silicified concentrated collagen hydrogels, Acs Appl. Mater. & Interfaces 3 (10) (2011) 3831−3838. Available from: https://doi.org/10.1021/am2009844.

[67] E.J. Lee, S.H. Jun, H.E. Kim, Y.H. Koh, Collagen-silica xerogel nanohybrid membrane for guided bone regeneration, J. Biomed. Mater. Res. Part. A 100a (4) (2012) 841−847. Available from: https://doi.org/10.1002/jbm.a.34019.

[68] A.M. Mebert, G.S. Alvarez, R. Peroni, C. Illoul, C. Helary, T. Coradin, et al., Collagen-silica nanocomposites as dermal dressings preventing infection in vivo, Mater. Sci. & Eng. C-Materials Biol. Appl. 93 (2018) 170−177. Available from: https://doi.org/10.1016/j.msec.2018.07.078.

[69] F. Libonati, A.K. Nair, L. Vergani, M.J. Buehler, Mechanics of collagen−hydroxyapatite model nanocomposites, Mech. Res. Commun. 58 (2014) 17−23. Available from: https://doi.org/10.1016/j.mechrescom.2013.08.008.

[70] O. Akturk, K. Kismet, A.C. Yasti, S. Kuru, M.E. Duymus, F. Kaya, et al., Collagen/gold nanoparticle nanocomposites: a potential skin wound healing biomaterial, J. Biomater. Appl. 31 (2) (2016) 283−301. Available from: https://doi.org/10.1177/0885328216644536.

[71] F. Ekiz-Kanik, D.D. Sevenler, N.L. Ünlü, M. Chiari, M.S. Ünlü, Surface chemistry and morphology in single particle optical imaging, Nanophotonics 6 (4) (2017) 713−730. Available from: https://doi.org/10.1515/nanoph-2016-0184.

[72] I. Sondi, B. Salopek-Sondi, Silver nanoparticles as antimicrobial agent: a case study on *E. coli* as a model for gram-negative bacteria, J. Colloid Interface Sci. 275 (1) (2004) 177−182. Available from: https://doi.org/10.1016/j.jcis.2004.02.012.

[73] J.S. Kim, E. Kuk, K.N. Yu, J.H. Kim, S.J. Park, H.J. Lee, et al., Antimicrobial effects of silver nanoparticles, Nanomedicine 3 (1) (2007) 95−101. Available from: https://doi.org/10.1016/j.nano.2006.12.001.

[74] Y.H. Hsueh, K.S. Lin, W.J. Ke, C.T. Hsieh, C.L. Chiang, D.Y. Tzou, et al., The antimicrobial properties of silver nanoparticles in bacillus subtilis are mediated by released Ag + ions, PLoS One 10 (12) (2015) e0144306. Available from: https://doi.org/10.1371/journal.pone.0144306.

[75] J. Gouyau, R.E. Duval, A. Boudier, E. Lamouroux, Investigation of Nanoparticle Metallic Core Antibacterial Activity: Gold and Silver Nanoparticles against Escherichia coli and Staphylococcus aureus, J. Int J Mol Sci 22 (4) (2021) 1905. Available from: https://doi.org/10.3390/ijms22041905.

[76] J.M. Patrascu, I.A. Nedelcu, M. Sonmez, D. Ficai, A. Ficai, B.S. Vasile, et al., Composite scaffolds based on silver nanoparticles for biomedical applications, J. Nanomaterials (2015) (Special Issue: Applications of Nanomaterials in Multifunctional Polymer Nanocomposites), Article ID 587989.

[77] A. Spoiala, G. Voicu, D. Ficai, C. Ungureanu, M.G. Albu, B.S. Vasile, et al., Collagen/Tio2-Ag composite nanomaterials for antimicrobial applications, Univ. Politehnica

Buchar. Sci. Bull. Ser. B-Chemistry Mater. Sci. 77 (4) (2015) 275–290. Retrieved from <Go to ISI>://WOS:000417047800025.

[78] G. Rath, T. Hussain, G. Chauhan, T. Garg, A.K. Goyal, Collagen nanofiber containing silver nanoparticles for improved wound-healing applications, J. Drug. Target. 24 (6) (2016) 520–529. Available from: https://doi.org/10.3109/1061186X.2015.1095922.

[79] A. Shavandi, A. Carne, A.A. Bekhit, A.E.A. Bekhit, An Improved Method for Solubilisation of Wool Keratin Using Peracetic Acid, Journal of Environmental Chemical Engineering 5 (2) (2017) 1977–1984. Available from: https://doi.org/10.1016/j.jece.2017.03.043.

[80] A. Shavandi, T.H. Silva, A.A. Bekhit, A.E. Bekhit, Keratin: Dissolution, Extraction and Biomedical Application, Biomaterials Science 5 (9) (2017) 1699–1735. Available from: https://doi.org/10.1039/c7bm00411g.

[81] A. Shavandi, M. Azam Ali, Keratin based thermoplastic biocomposites: a review, Reviews in Environmental Science and Bio/Technology 18 (2018) 299–316.

[82] L. Conzatti, F. Giunco, P. Stagnaro, A. Patrucco, C. Marano, M. Rink, E. Marsano, Composites Based on Polypropylene and Short Wool Fibres, Composites Part a-Applied Science and Manufacturing 47 (2013) 165–171. Available from: https://doi.org/10.1016/j.compositesa.2013.01.002.

[83] P. Cataldi, O. Condurache, D. Spirito, R. Krahne, I.S. Bayer, A. Athanassiou, et al., Keratin-graphene nanocomposite: transformation of waste wool in electronic devices, Acs Sustain. Chem. & Eng. 7 (14) (2019) 12544–12551. Available from: https://doi.org/10.1021/acssuschemeng.9b02415.

[84] H. Hammouche, H. Achour, S. Makhlouf, A. Chaouchi, M. Laghrouche, A Comparative Study of Capacitive Humidity Sensor Based on Keratin Film, Keratin/Graphene Oxide, and Keratin/Carbon Fibers, Sensors and Actuators a-Physical, 329 (2021). Available from: https://doi.org/10.1016/j.sna.2021.112805.

[85] S. Wu, X. Chen, T. Li, Y. Cui, M. Yi, J. Ge, G. Yin, X. Li, M. He, Improving the Performance of Feather Keratin/Polyvinyl Alcohol/Tris(Hydroxymethyl)Aminomethane Nanocomposite Films by Incorporating Graphene Oxide or Graphene, *Nanomaterials (Basel)* 10 (2) (2020). Available from: https://doi.org/10.3390/nano10020327.

# Industrial implementation of polymer-nanocomposites

19

*Oishy Roy and Ahmed Sharif*
Department of Materials and Metallurgical Engineering, Bangladesh University of Engineering and Technology, Dhaka, Bangladesh

## 19.1 Introduction

Polymer nanocomposite (PNC) is a class of multiphase material having polymer matrix and nanosized fillers. It can be referred to as 2D, 1D, or 0D depending on the dimension of filler dispersed in it [1]. Respectively, the fillers can have only one dimension in the nanorange, resulting in layered sheet structure; two dimensions in the nano range, having tube, fiber, wire shape; or all three dimensions in nano range like a sphere, particle shape. Nanofillers add multifunctionality to PNC. Sheets of clay, graphene, carbon nanotube (CNT), carbon nanofiber (CNF), metal nanowires, nanorods and spheres of silica, titania, $C_{60}$, quantum dots, barium titanate, indium tin oxide, zirconia, iron oxide, etc. are some of the filler materials used in PNC [2]. Polymers used as the matrix can be thermoplastic or thermoset. Polyolefins, polyamides, polystyrene, polyethylene terephthalate, epoxy resin, polyimides, conducting polymers, styrene-butadiene rubber, etc. are commonly used as a matrix [3].

PNC offers an excellent combination of properties which is way more exciting than conventional composites. These properties include superior mechanical, optical, thermal, magnetic, electrical, and other physicochemical properties in lower density and lower loading of filler. High specific strength, high specific modulus compared to even lighter metals or alloys result in lower fuel consumption, lower gas emission and make it a strong competitor in the structural part of an automotive application. Other than that, wear resistance, antiscratch property, and chemical resistance are utilized in paint and coating applications. Gas barrier properties, antimicrobial properties are being utilized in the packaging of meat, soft drink, beer bottles, medicine, pharmaceuticals, computers, and electronics. Enhanced electrical properties help to find its application in the energy sector which includes fuel cell membrane, supercapacitor, electrode of battery, semiconductors, hard disk storage, sensors, etc. Also, consumer goods like sporting tools, furniture, toys, home appliances; medical sectors including dental filling material, biosensors, body implants, medical devices; fire retardant foams, fire-resistant products, self-cleaning windows, etc. can utilize PNC. Properties of light transparency, UV light protection, optical clarity, noise damping, shielding of EM signal, etc. are being utilized or have the potential to be utilized in many more applications [4].

**Advanced Polymer Nanocomposites. DOI: https://doi.org/10.1016/B978-0-12-824492-0.00005-2**


Because of the nanoscale dimension of fillers, the interface area, that is, the surface area to volume ratio is increased dramatically in PNC. This interface effect leads to unique properties than the effect of micro-sized fillers in conventional composites.

## 19.2 Applications and challenges of PNC industry

The PNC-based applications which have been successfully commercialized with medium to high volume production include the tires and some structural parts (i.e., exterior and interior structural parts, under the hood) of an automotive system. Medium volume manufacturing of PNC products includes timing belt cover, inverter cover, door panel, etc. of an automobile. The applications which are commercialized with low volume production include conducting paints, coatings, engine, power train, under the hood components, suspension, braking system, diesel fuel tanks, battery cases, etc. and those which are not commercialized yet are sensors, fuel cells, and batteries [3]. PNC-based gas separation membrane and dielectrics for capacitors, insulations, etc. have great commercialization potential.

Challenges are confronted in optimization of enhanced property combination, in maintaining optimal conditions during the manufacturing process, and in scaling up laboratory innovations in the large-scale industry with quality products.

### *19.2.1 Innovation challenge*

Optimum conditions of variables are still not understood for many established or potential applications of PNC. Though in general, the interface effect causes the superior properties of PNC, the impact of this interface effect is not similar for different electrical or optical properties such as light transparency, permeability, dielectric breakdown, conductivity, etc. Again, its impact on the viscoelastic property and thermomechanical property is different for temperature above and below $T_g$ [2]. Another challenging factor is that the optimum morphology and distribution of the nanofiller are not the same for enhanced electrical, mechanical, or other properties. This is very complex and challenging to engineer the interface effect of PNC so that optimized thermal, mechanical, electrical, optical properties can be obtained simultaneously without making processing too difficult [2].

Among the established market of PNC, the tire industry is the one that requires focus on properties of rolling resistance, wear-resistance, and wet traction with reduced cost and weight. It uses carbon and silica nanofillers in a rubber matrix. Though it is referred to as an established industry because of high volume production, it faces certain uncertainty which demands more research. Those issues include not knowing the correct combination of size, shape, property, and dispersion state of nanofillers which would optimize required properties of the given application with lower cost and better processability in large-scale production [2]. Meeting all these requirements is complex and challenging. For adhesive or coating-related applications, nanofiller of copper oxide is used to increase the fracture toughness of epoxy

matrix with the challenge of degrading other properties; this problem was solved by using grafted nanoparticles in glassy un-crosslinked epoxy. But optimum processing conditions for crosslinked epoxy should also be studied [2].

### 19.2.2 Processing challenge

In the application of continuous fiber-reinforced composites, implementing optimum findings is tough in the industry due to processing issues of high viscosity, agglomeration of nanofillers, void formation, etc. Even though various automated and precise advanced fabrication techniques are available (such as injection molding, resin transfer molding, contact molding, compression molding), the fact that there are numerous parameters in the processing of PNC makes it difficult to automate. The property of the PNC product depends on parameters of the size and shape, loading of the filler, dispersion state of filler, aspect ratio of filler, adhesion, and compatibility of matrix and filler, viscosity of matrix, etc. So, choosing one optimum manufacturing procedure among many emerging suggestions in a certain application is difficult.

### 19.2.3 Scaling up challenge

On a laboratory scale, finding and maintaining optimum processing conditions is comparatively easier but implementing these on a mass scale is difficult. So, finding scalable, industrially feasible, lower production cost manufacturing techniques with available technology or innovating required technology is a common challenge for almost all applications at different stages of their growth. Advanced technology and costly infrastructure with control over the process through automation and simulation are some options to explore. So, to ensure reliable and consistent mass production, all the parameters affecting product property along with correct blending without deteriorating filler aspect ratio, controlling formation of void or agglomerate of filler, controlling viscosity of matrix with the loading of filler, etc. should be maintained.

## 19.3 Business ecosystem

### 19.3.1 Manufacturer

NYCOA, USA; BASF, Germany; UNITIKA Ltd., Japan; Goodyear Tire and Rubber Co., USA; InMat Inc., USA; and Continental AG, Germany are some of the leading manufacturers of PNC products used in an automotive application. Honeywell International Inc., USA; Plantic Technologies Ltd., Australia; Dai Dong Tien Corp., Vietnam; Fine Polymer Inc.; and Babydream Co. Ltd. are some of the food packaging and container manufacturing industries using PNC [5]. Developer or manufacturer of coating and painting of PNC includes Carbon Motor Corp., USA; GE Plastics and Hyperion Catalysis Int. Inc., USA, etc. [3]. To grow the market faster, the leading manufacturing companies should collaborate through sharing knowledge and technology.

The manufacturer of a PNC product depends on the supplier of nanofiller, polymer, and other additives. So, the cost and quality of the PNC product are dependent on the cost, quality, and processing of the resin and reinforcement. To lower the manufacturing cost of PNC, the price (i.e., the production cost) of nanofillers and matrix should be a concern. Among the nanofillers proved to enhance properties of composite with polymer, nanoclay has lower cost and consistent quality, which makes it easily accessible to both researchers and industrialists.

To increase control over the quality of the PNC product of already active manufacturing process or to decrease development time and cost of manufacturing trials, supervisory, interactive, or predictive digital twin of that process can be created using simulation [6]. Simulation can help to choose the correct manufacturing process. Then smart tools and augmented reality equipment (i.e., Microsoft HoloLens) can be used to train and guide technicians to inspect, trace, and control processes more successfully [6].

### 19.3.2 Research and development

Since the origination of PNC, there have been extensive research and numerous innovations. But finding optimum process conditions along with processes feasible for large-scale production needs more emphasis than exploring new materials. Also, more investment in the study of the toxicity effect of PNC on health and the environment is necessary which would push the development of safety regulations. So, industrial implementation and ensuring the safety of the growth of this industry should be the emphasis of further research.

### 19.3.3 Investor

The cost involved in the manufacturing and research of PNC is high, which means it demands significant funding to support the finance. Government-level investment in nanotechnology research and development has shown an increasing trend for several nations including the United States and European countries, whereas for Japan, it is consistently huge [4]. This huge sum of funding shows the promise to boost the PNC industry. Private companies should also be encouraged to invest and ignite this industry.

### 19.3.4 IP and consultancy

Organizations such as the WIPO (World Intellectual Property Organization) can help to protect and meaningfully use intellectual property (i.e., filing patent), to implement global policy issues related to IP, and to share knowledge across borders without risk of disputes.

Consultancy firm for a specific application (i.e., McKinsey & Company; The Boston Consulting Group, Inc., Bain & Company, etc. for automotive application) or specialized independent consultant group for an individual company is needed for strategic analysis and forecasting and development of the market, cost

performance balance, product optimization, resolving manufacturing problems, troubleshooting, regulatory advice, navigation of rules and requirements of the industry, and obtaining overall feedback of the development of PNC.

### 19.3.5 Infrastructure

PNC utilizes versatile materials, so the manufacturing process is difficult to automate. As the manufacturing process inherently has so many variables, it demands the infrastructure to be well planned, advanced, and sometimes expensive. The ability of collection and feedback of data should be increased through enhanced connectivity of equipment and database, use of intelligent vision systems such as sensors embedded in tools. This will facilitate enhanced monitoring of the progress of the process, reducing process time and if any deviation occurs, identifying root causes of it, and deciding the next step without stopping production [6]. Intelligent mixing, intelligent cure monitoring are examples that are being utilized in some composite industries [6]. Also, recycling facilities should be a concern during developing infrastructure.

### 19.3.6 Regulation

Safety regulation, strategy, policy or codes for manufacturing, handling, consumption, and disposal of PNC, which encompasses the whole PNC field should be developed by industry, academia, or government. The toxicity or safety issue should be considered when developing regulations, especially for food packaging, fire retardant, and medical-related applications. The nanomaterials of the PNC can be detached from the composite and have direct or secondary hazardous effects on health or the environment. As still there is a lack of knowledge about the effect of nanomaterials on the health and environment, extensive research is needed to understand the toxicity effect and only then well-defined regulations can be developed. To date, the effect on skin, lungs, respiratory system, absorbed by inhalation or drinking and effect on marine life have been studied [5]. Among the nanomaterials being used in PNC, titania, nanocarbon possibly can have a carcinogenic effect and cause respiratory disease on living animals [according to the National Institute of Occupational Safety and Health (NIOSH) and Occupational Safety and Health Administration (OSHA)] [7]. Nonbiodegradable polymer matrix, hazardous gases, and effluents of fire-retardant products can also cause a threat to damage the ecosystem.

Agencies like the US Environmental Protection Agency (USEPA), US Food and Drug Administration (USFDA), and OSHA are with the goal of regulating safe and toxic use of any product to the environment and human health [7]. Regulation related to reducing greenhouse gas emission is in favor of the automotive application of PNC but the safety of using PNC in food and medical applications is still uncertain. As delayed the generation of regulations and rules are, the more doubt will persist in investing in this field in fear of future unfavorable product market. So, solid statistical evidence and accurate method to find the response of these

nanomaterials intake on humans and the environment are needed to determine further well-planned steps of this industry.

### 19.3.7 Standardization

Standardization of products is a must to ensure consistency and uniformity of nature and quality of products available in different markets. Industries or organizations are supposed to follow guidelines while manufacturing products tested in nationally recognized testing laboratories following standard testing methods.

The obligations placed on the automobile manufacturer by national and international laws and regulations can be met using International Material Data System (IMDS). For packaging products, the standard testing method is provided by the American Safety for Testing and Materials (ASTM) or International Organization of Standardization (ISO); and regulations and guidelines developed by the FDA, US Department of Agriculture, EU (European Union) should be followed. The plastic regulations [8] of the EU for food contact material mentions overall and specific migration limits for plastics. Standardization for nanomaterials used in PNC and standardization of laboratory tests for biodegradability need more work [7].

## 19.4 PESTLE analysis

To anticipate the opportunities, influences, threats, and limitations of the PNC industry, the variables needed to be considered are as follows:

- steadiness of nanomaterial supply,
- production cost and price of nanomaterial,
- purity and consistency of quality of nanofillers,
- production of ecofriendly biodegradable polymer matrix,
- recyclability of nonbiodegradable polymer matrix,
- determination and complexity of optimum characteristics of matrix-filler system (i.e., matrix chemistry and chain length, filler chemistry and size, shape, functionalization, etc.),
- capital of PNC production,
- control over manufacturing process in large scale production,
- availability of technology and knowledge for mass production,
- awareness of technology,
- willingness to take risk of failure in creating a potential market,
- consistency of quality of produced PNC in mass production,
- environmental and health safety.

The external factors influencing the operation and growth of the PNC market are analyzed below in terms of political, economic, social, technological, legal, and environmental aspects.

### 19.4.1 Political variable

Several governments including the United States, Germany, China, India have stringent policies and regulations for automotive emission, which is supporting the growth of the PNC market; as the application of PNC in the automotive sector is simultaneously reducing fuel consumption, gas emission because of its reduced density. But the high cost of some nanofillers (CNT, graphene), high manufacturing cost, long lead time of production are making the growth slow.

The risk and toxicity impact of the PNC on human health and the environment is still not well defined. Most of the countries having leading PNC industries do not have regulations or legislations specific to nanomaterials in food application due to insufficient research [5]. The FDA or EU is under the expectation of developing regulations and guidelines for the industries. Currently, the use of nanofillers of PNC in food applications is going on without any strong guidelines. To prevent any detrimental effect of this unplanned growth of industry, specified regulations are necessary; on the other hand, if the harm is proved negligible, the path of other potential nanomaterials in similar applications will be smoothed once regulations are clearly defined.

### 19.4.2 Economic variable

Among the nanofillers, clay is the most used because of its lower price than multi-walled carbon nanotube (regular length \$6.5−\$14/g), single-walled carbon nanotube (SWCNT) (\$70−\$270/g), graphene (\$270/g), carbon nanofiber (CNF) (\$13.5/g), etc. [9]. As a result, clay-based PNC has found significant industrial application, while for CNT and graphene, high material cost and processing difficulty hinder full utilization of property enhancement.

Commercially, the potential of PNC has been showing an increasing trend. According to Allied Market Research Report, the global PNC market is projected to value USD 11.549 billion by 2022 [1]. The automotive and packaging industry has higher growth both in terms of volume and revenue. North America, Europe, and the Asia Pacific are regions with leading PNC markets. A report by Global Market Insights Inc. forecasted the PNC market to reach beyond 31 billion by 2025[10].

Among currently available equipment, attaining a feasible cost-effective synthesis method for PNC is difficult as the trade-off between the cost of processing technique and product property persists in all available cases. Undoubtedly processing methods and conditions have a significant effect on the properties of nanocomposite products. Techniques of solvent processing, electrospinning, layer by layer assembly are costly processes but offer better dispersion control than low-cost melt processing techniques [11]. For the processing of clay-based nanocomposites, melt intercalation is more compatible and environmentally friendly than solvent blending; in situ polymerization is also used [11]. So, the manufacturing cost is responsible for the higher cost of a product with better performance. Current technology is not enough to control all important process conditions.

### 19.4.3 Social variable

The superior performance offered by automotive using PNC attracts enthusiast consumers while high cost and long production lead time act otherwise. Doubts about food packages and containers also persist as the safety of these products has not been established yet. The main killer of the consumption is the higher cost of the product compared to alternative materials products.

### 19.4.4 Technological variable

Even though there are numerous innovative suggestions of the manufacturing process, scaling up the technology for high volume consistent quality production utilizing these suggestions is one of the biggest challenges. The suggested processes should be evaluated in terms of cost of developing infrastructure, cost of manufacturing, scalability, product quality, process condition, yield, recyclability, and effect of environment. Technologies to overcome challenges associated with current manufacturing processes (i.e., dispersion of fillers, compatibility with matrix, formation of void or agglomeration, degassing, controlling alignment of filler, etc.), to develop a real-time characterization method, tools, and instrumentation, to build affordable infrastructure with facilities, design tools, equipment, and skilled operators are necessary to move this industry forward [12]. Technology development should also focus on producing bio-resourced resin and lower cost CNT, graphene, CNF fillers, improving automation of PNC manufacturing through processing and structural simulation.

### 19.4.5 Legal variable

An effective method with less complexity and variation in the detection, characterization, quantification of nanomaterial migration from PNC package to food or drug needs to be developed to ensure the safety of the continuously growing packaging market. Specific new regulations for nanofillers of PNC are needed as current regulations cover only general substance in macroscopic size.

### 19.4.6 Environmental variable

To minimize the future problem of waste management of nonbiodegradable polymer-based PNC, research and investment in biodegradable polymer-based PNC are on growth. Governments of the United Kingdom, United Nations, and EU are interested in the growth of eco-friendly alternatives to conventional plastics [13–16]. Some of these eco-friendly polymers (i.e., polylactic acid, starch, cellulose, polycaprolactone, poly hydroxy alkanoates, polybutylene succinate, natural oils, polysaccharide derivatives, poly amino acid, polybutylene adipate) has renewable source and the properties are enhanced using additives or nanofillers [17]. But more research and funding are needed to add a biodegradability testing facility. Clear definition, validation, consistency, and standardization of testing method of

biodegradability should be developed to avoid confusion of different type of matrix, additive, test of a different laboratory. Testing of biodegradability on the final product is needed as the effect of nanofillers or nano additives can be either increase biodegradation rate or it can have a toxic effect on the environment [17].

Hazardous gases [i.e., asphyxiate gases (carbon monoxide, hydrogen cyanide), nitrogen dioxide, nitrogen oxide, hypoxia, hydrocarbon, organic species] released from fire retardant PNC during thermal degradation are also a concern for the environment and human health [7]. The fire hazards of those PNC need to be assessed.

## 19.5 Conclusion

Ultimately, the goal is to reduce the time frame for growth of the PNC market with high volume cost-effective high-performance products with lower investment risk, consumers' health, and environmental safety. No doubt, PNC offers lots of promising features, but significant challenges hamper the industrialization of the invented technology, ceasing the growth of the market for those potential applications. Poor learning, underfunded research, lack of guidance, lack of awareness of technology, scattered knowledge of processing technology, lack of proper design tools are limiting the widespread utilization of PNC. More fundamental studies from new processing strategies; an enhanced collaboration of information, knowledge, technology between industry, research institute, academia; adoption of intelligent digital infrastructure; with development of tools and technologies to collect and analyze relevant data are some of the proposed paths to obtain better understanding and growth of the market.

## References

[1] M.R. Mansor, M.Z. Akop, Polymer nanocomposites smart materials for energy applications, Polymer Nanocomposite-Based Smart Materials, Woodhead Publishing, 2020, pp. 157−176. Available from: https://doi.org/10.1016/b978-0-08-103013-4.00009-1.

[2] S.K. Kumar, B.C., Benicewicz, R.A. Vaia, K.I. Winey, 50th anniversary perspective: are polymer nanocomposites practical for applications? Macromolecules 50 (3) (2017) 714−731. Available from: https://doi.org/10.1021/acs.macromol.6b02330.

[3] V. Patel, Y. Mahajan, Polymer nanocomposites: emerging growth driver for the global automotive industry, Handbook of Polymernanocomposites. Processing, Performance and Application: Volume A: Layered Silicates, Springer Ltd, 2014, pp. 511−538. Available from: https://doi.org/10.1007/978-3-642-38649-7.

[4] J. Koo, J. Koo, Opportunities, trends, and challenges for polymer nanocomposites, Fundamentals, Properties, and Applications of Polymer Nanocomposites (2016) 648−692Issue May. Available from: https://doi.org/10.1017/cbo9781139342766.016.

[5] N. Bumbudsanpharoke, S. Ko, Nano-food packaging: an overview of market, migration research, and safety regulations, J. Food Sci. 80 (5) (2015) R910−R923. Available from: https://doi.org/10.1111/1750-3841.12861.

[6] J. Snudden, Progression to the next industrial revolution: industry 4.0 for composites, Reinforced Plast. 63 (3) (2019) 136–142. Available from: https://doi.org/10.1016/j.repl.2019.04.001.
[7] J. Koo, Environmental and health impacts for nanomaterials and polymer nanocomposites, Fundamentals, Properties, and Applications of Polymer Nanocomposites, Cambridge University Press, 2016, pp. 605–646. Available from: https://doi.org/10.1017/cbo9781139342766.015.
[8] European Union, Commission Regulation (EU) No 10/2011 of 14 January 2011, Off. J. Eur. Union, L 12 (2011) 1–89Retrieved from. Available from: https://eur-lex.europa.eu/LexUriServ/LexUriServ.do?uri = OJ:L:2011:012:0001:0089:EN:PDF.
[9] Nanostructured and Amorphous Materials, Incorporated. Retrieved from: http://www.nanoamor.com (assessed 01.01.21.).
[10] K. Pulidindi, H. Pandey, Polymer nanocomposites market size worth over $31 billion by 2025, Global Market Insights, 2019. Retrieved from: http://www.gminsights.com/pressrelease/polymer-nanocomposites-market/amp (accessed 12.12.20.).
[11] M. Bhattacharya, Polymer nanocomposites-a comparison between carbon nanotubes, graphene, and clay as nanofillers, Materials 9 (4) (2016) 1–35. Available from: https://doi.org/10.3390/ma9040262.
[12] F. Hussain, M. Hojjati, M. Okamoto, R.E. Gorga, Review article: polymer-matrix nanocomposites, processing, manufacturing, and application: an overview, J. Composite Mater. 40 (17) (2006) 1511–1575. Available from: https://doi.org/10.1177/0021998306067321.
[13] DEFRA, 25-Year-Environment-Plan., 2018, 1–151.
[14] United Nations, The State of Plastics: World Environment Day Outlook 2018. In UN Environment Programme, 2018. Retrieved from: https://wedocs.unep.org/bitstream/handle/20.500.11822/25513/state_plastics_WED.pdf?sequence = 1&isAllowed = y.
[15] C. Giacovelli, Single-use plastics: a roadmap for sustainability, 2018. Retrieved from: https://wedocs.unep.org/bitstream/handle/20.500.11822/25496/singleUsePlastic_sustainability.pdf?sequence = 1&isAllowed = y.
[16] EU European Commission, A European Strategy for Plastics in a Circular Economy, 2018, Retrieved from: https://eur-lex.europa.eu/resource.html?uri = cellar:2df5d1d2-fac7-11e7-b8f5-01aa75ed71a1.0001.02/DOC_1&format = PDF.
[17] A. Kjeldsen, M. Price, C. Lilley, E. Guzniczak, I. Archer, A Review of Standards for Biodegradable Plastics, in: Industrial Biotechnology Innovation Centre IbioIC, 2019. Retrieved from: https://assets.publishing.service.gov.uk/government/uploads/system/uploads/attachment_data/file/817684/review-standards-for-biodegradable-plastics-IBioIC.pdf.

# Environmental and health impacts of polymer nanocomposites

20

*Sitesh C. Bachar*[1] *and Kishor Mazumder*[2,3,4]
[1]Department of Pharmacy, Faculty of Pharmacy, University of Dhaka, Dhaka, Bangladesh
[2]Department of Pharmacy, Jashore University of Science and Technology, Jashore, Bangladesh
[3]School of Optometry and Vision Science, UNSW Medicine, University of New South Wales (UNSW), Sydney, NSW, Australia
[4]School of Biomedical Sciences and Graham Centre for Agricultural Innovation, Charles Sturt University, Wagga Wagga, NSW, Australia

## 20.1 Introduction

At present, nanotechnology is the most promising and versatile technology in the field of science and engineering. It refers to the discipline, method, and device that are used to control, restructure, and construct matter at the nanoscale for diverse purposes. This technology allows the creation of new materials by designing and developing new as well as desirable properties and structures, resulting in improved performance, lower maintenance costs, and increased functionality. Nanomaterials can be characterized as the materials containing filament, aggregate, or particle having a dimension of fewer than 100 nanometers (nm). The tiny particles are formed by nanoscale material modification and processing, which result in a great increase in the ratio of surface area in respect to volume. The outcome has enhanced the electrical, optical, functional, and mechanical properties of particles ensuing potential efficiency [1]. Development of nanoparticles, nanodispersion, nanowire, nanotube, nanolaminate, buckyball, quantum dot, nanocomposite, and other new structures and systems are the recent advancement of nanotechnology [2].

Nanocomposites are composite materials having a dimension in nanometer ranges existing in single or multiple phases and have unique properties. They are made up of two or more distinct elements or phases having distinct physicochemical characteristics, depending on the preparation techniques. In higher concentrations, nanocomposites contain a matrix, also known as nanofiller that helps to reinforce the mechanical properties [3]. Various types of reinforcement and matrix materials are used to formulate nanocomposites. Based on the varieties of matrix materials used, nanocomposites may be categorized into the polymer, ceramic, and metal matrix nanocomposites [4]. Polymer nanocomposites are the distinct types of nanocomposites in which naturally occurring or chemically synthesized biodegradable or nonbiodegradable polymers are used as matrices along with mineral, metallic, or organic nanofillers or reinforcement materials [5].

**Advanced Polymer Nanocomposites. DOI: https://doi.org/10.1016/B978-0-12-824492-0.00009-X**


Polymer nanocomposites have been acclaimed for their diverse health and environmental benefits. Polymer nanocomposites have been reported for a lot of advantageous applications in human health, including treating, diagnosing, and preventing diseases. It deals with the diagnosis and therapy of cancer, traumatic injury, inflammatory pain, and so others. A variety of applications of nanocomposites are observed in the pharmaceutical industry for drug development as well [6]. Besides, several environmental remedial effects of nanocomposites are demonstrated, involving water and air cleaning, toxic metal removal (such as arsenic, heavy metal cations), and organic and inorganic waste material treatments [7]. Along with these numerous advantages and wide range of applications, there have been reports that scientists and industrial researchers are exploiting the scheme which could have negative health and environmental implications [8]. For example, asbestos fiber exposure causes inflammation in the respiratory tract, which leads to fibrosis and carcinogenesis [9]. In this chapter, for better understanding, the environmental and health impacts of polymer nanocomposites are addressed through detrimental and beneficial perspectives.

## 20.2 Polymer nanocomposites: an overview

### *20.2.1 Definition and composition of polymer nanocomposites*

Polymeric nanocomposites are the greatest revolutionary replacement for traditionally filled polymers or polymer blends. Polymeric nanocomposites contain distinct components with 100 nm in as a minimum of one dimension. A polymer composite usually consists of a matrix along with filler. In polyamide, commonly used as reinforcement materials are thermoplastic polymers such as glass and carbon fibers. Lightweight, high endurance, corrosion resistance, versatility, fast processing, and low cost are the major advantages of polymers. Ceramics and metals are dense compared to polymers. They can be used as structural constituents as well as construction resources in vehicles having lightweight, aerospace engineering, defense department, and electronics due to their low coordination numbers and lightweight carbon and hydrogen atom backbone. The reinforcement material consists of elements (e.g., crystal, metallic nanoparticle, and carbon nanotube); sheet (exfoliated clay and graphene); or fibers (electrospun nanofiber). Clay is a type of nanofiller widely used to build polymer matrix nanocomposites [5,10]. Different types of nanofillers and the compounding of nanocomposites are schematically represented in Fig. 20.1.

Nanocomposites are distinguished from typical composites remarkably by their high aspect ratio. In certain respects, polymer nanocomposites are superior to typical composites. Polymer nanocomposites have the following advantages:

1. Preparation requires a small amount of nanofillers.
2. It is much lighter.

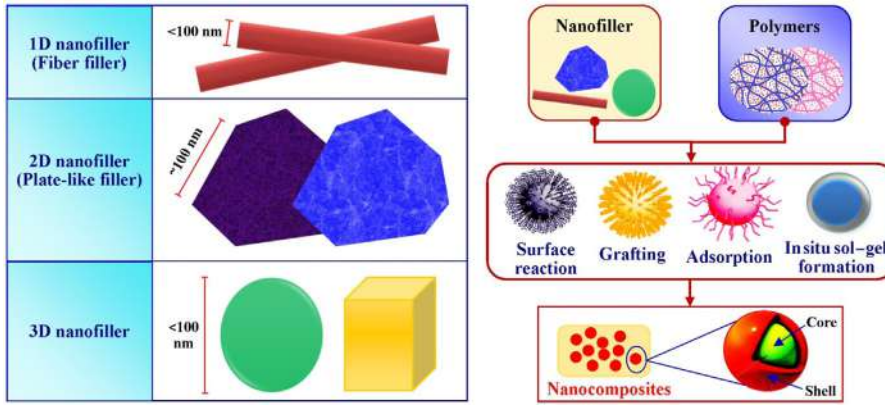


**Figure 20.1** Schematic representation of nanofillers used in the formulation of nanocomposites.

**3.** As opposed to traditional composites, it improves mechanical, chemical, thermal, electronic, optical, and magnetic features.

## *20.2.2 Types of polymer nanocomposites*

### *20.2.2.1 Nanoclay-reinforced composites*

Nanoclay-reinforced composites are made up of small inorganic particles that are less than 2 mm in size and have no defined compositions or crystallinity. Phyllosilicate is a layer-shaped fraction of hydrous silicate, magnesium silicate, and/or aluminum silicate found in clay minerals. Apart from this, montmorillonite ((Na,K,Ca)0.33(Al,Mg)2(Si4O10)(OH)2nH2O or (Na,K,Ca)0.33(Al,Mg)2(Si4O10)(OH)2nH2), hectorite (Na0.4,Si4(Mg2.7Li0.3)O10(OH)4), saponite ((Na,K,Ca)0.33,Si3.67Al0.33Mg3O10(OH)2), illite ((Al4)(Si7.5−6.8Al0.5−1.2)O20,(OH)4K0.5−1.5), and vermiculate have the highest acceptability in the polymer because of its higher surface area as well as the reactivity of surface [11].

### *20.2.2.2 Carbon nanotube-reinforced composites*

Nanoscale carbon tubes (CNTs) or near-perfect whiskers (dubbed nanotube) have a number of exciting developments in multiple industries [12]. The first nanotubes are composed of multiple concentric shells of graphene sheets with cylindrical shape and structured coaxially surrounding centrally a hollow core along with interlayer separation, similar to nanosized (0.34 nm) graphite. Single-shell nanotubes (SSNTs) and single-walled nanotubes are composed of single-layered graphene cylinders having narrow-ranged nanoscale size distribution (1.2 nm). Besides, huge numbers (10−1000) of SSNTs are aggregated to form larger cords [13,14].

As compared to other graphite fibers, CNTs have specialized properties. Traditional fibers of carbon have been utilized for reinforcement in aerospace and

airplane manufacturing, electronic batteries, and so others for years. Nanotubes are the most attractive, perfect, and ordered carbon fiber, with an atomic-level structure [15]. Carbon nanotubes have also improved the antimicrobial properties of nanosensors, which may be due to the fracturing microbial cell walls of nanotubes, causing permanent harm and cell death [16]. Keng et al. developed a carbon nanotube with a perfluorosulfonated polymer sensor that can easily detect *Escherichia coli* in food [17]. Similarly, a *Salmonella* infection in nutrient solution was discovered using an antibody-specific carbon nanotube sensor to monitor food safety. Cholesterol oxidase, a multiwalled carbon nanotube containing enzyme was designed by placing on a carbon electrode to detect cholesterol in high-fat foods [18,19].

#### 20.2.2.3 Carbon nanofiber-reinforced composites

Carbon nanofiber (CNF) composites are vapor-generated carbon fibers that bridge the gaps of conventional carbon fibers (5−10 mm) as well as carbon nanotubes (1−10 nm). Nanofibers have a smaller diameter, which means that they have a greater surface area with surface functionalities. Length of CNF can vary from 100 nm to several cm, and with an average aspect ratio of greater than 100. The diameter ranges from 100 to 200 nm. Truncated cones are the most common CNF structure, but there are several different morphologies (cone and stacked coins) [20].

#### 20.2.2.4 Inorganic particle-reinforced composites

The diameter of such inorganic nanoparticles is less than 100 nm [21]. Different organic−inorganic particles have been combined to produce nanometer-sized particles that improve the properties of composite materials [22]. Metals, polymers, and inorganic particles have been utilized to build polymer or inorganic particle-reinforced nanocomposites structures such as (1) pure metals (Al, Fe, Au, and Ag); (2) metal oxides (ZnO, $Al_2O_3$, $CaCO_3$, and $TiO_2$); (3) nonmetal oxides ($SiO_2$); and (4) other (SiC). The nanosized particles are chosen based on the preferred electrical, optical, mechanical, and thermal behaviors of the nanocomposites. For example, Al nanoparticles are frequently utilized for their high conductivity, whereas $CaCO_3$ nanoparticles are most commonly used for their cost-efficiency. All at once, SiC nanoparticles are used for their hardness, higher corrosion resistance, and strength [22].

### 20.2.3 Features of polymer nanocomposites

Polymer nanocomposites have recently gained a lot of attention in academics and industries because of their superior properties over traditional composites. The properties of various types of polymeric nanocomposites are determined by several parameters [23,24] in addition to the properties of individual components which involve:

1. nanocomposite fabrication process
2. types and orientations of filler materials

3. degree of mixing of two phases
4. type of matrix interface adhesion
5. nanoparticle volume fraction
6. characteristics of nanoparticle
7. characteristics of the interphase formed at the matrix interface
8. size and shape of nanofiller
9. morphology of the system

The nanoparticles must be adequately dispersed and sufficiently distributed in the matrix materials to achieve desired properties in nanocomposites. Otherwise, particles would clump together, resulting in the deterioration of the features of nanocomposites. These aggregates can serve as defects, limiting their strengthening capability. Thus nanoparticles should be homogeneously distributed in the matrix to attain desirable properties. In the matrix material, the different forms of nanoparticles could show four types of patterns due to good and/or poor distribution and dispersion [25]. Fig. 20.2 has shown the distribution as well as dispersion patterns schematically.

The properties of nanocomposites can be enhanced by the existence of the matrix−filler material interface. The foremost characteristics of polymer matrix nanocomposites are the matrix and filler materials' interphase boundary as well as formed interface layers. The interface differs from the matrix and the filler in terms of properties, composition, and microstructure. The major interphase properties are

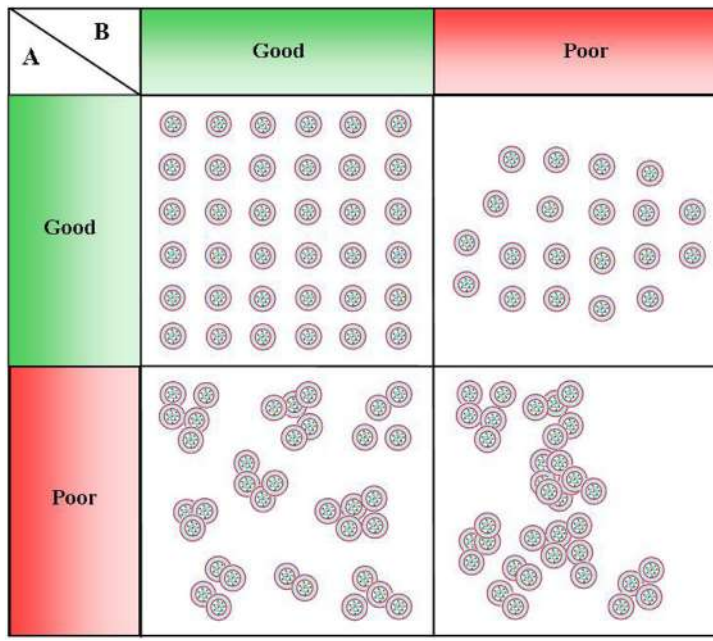


**Figure 20.2** Nanoparticles distributed and dispersed differently in the composite matrix. A: Dispersion and B: distribution.

described by the bound surface, thus nanocomposite characteristics can be modified by improving the interfacial bonds between the nanofiller and matrix. The nature of the interactions among the interconnecting phases is determined by the ratio of the filler and matrix surface energy. The extent of the interface phenomenon that contributes to the properties is defined by the average surface area of the nanocomposite [26,27].

## 20.3 Applications of polymer nanocomposites in human health

Polymer nanocomposites are used in varieties of platforms which are directly or indirectly associated with human health, including pharmaceuticals, nutraceuticals, agriculture, diagnosis, and hospitals. Human well-being has been associated not only with agriculture and food production but also with the preservation of natural lives. Reduced costs in the detection of disease and effective disease management practices are the major benefits of nanotechnology in the health industry. A summary of the applications of polymer nanocomposites in human health has been discussed in the following sections.

### *20.3.1 Polymer nanocomposites in pharmaceuticals*

Polymer nanocomposites have been used extensively in drug delivery. In conventional dosage form, the release of drugs from drug carriers can't be controlled which leads to short duration of therapeutic outcomes as well as generation of side effects. These unusual events can be controlled by designing an advanced delivery carrier that is capable of releasing drugs at a predetermined constant rate. Besides, this release kinetics can be programed by designing smart delivery approaches, such as stimuli-responsive drug carriers. Drug release from this carrier is mediated by internal stimuli, such as body temperature, pH, hypoxia, and biochemical ions or external stimuli, such as applied ultrasound, magnetic field, and an electric field [28]. Numerous nanocomposites have been reported to achieve controlled or sustained release of drugs. For example, pH-responsive nanocomposite microspheres have been formulated by using iron oxide nanoparticles of sorafenib, pH-responsive additive, and poly(lactic acid-*co*-glycolic acid) [29].

### *20.3.2 Polymer nanocomposites in diagnosis and treatment of diseases*

Nanocomposites have been reported to be used in numerous contexts of disease diagnosis and therapy [30]. Nanobiosensors and imaging have been using from the last decade for early diagnosis, therapy, and follow-up of life-threatening medical conditions, such as cancer, tumor, cardiovascular disorders, trauma, wound healing, orthopedics, ocular problems, and dental diseases. Targeted and site-specific

therapies have created an evolving progression of disease management. Recently, the nanothoranostic approach has achieved huge popularity to concurrent techniques of disease diagnosis and treatment by using nanocomposites [28,31]. The applications of polymer nanocomposites in the diagnosis and therapy of diseases have been discussed in the next sections.

#### 20.3.2.1 Diagnosis and treatment of tumor and cancer

The development of chemotherapeutic drugs, chemotherapy, and radiation therapy has progressed the diagnosis and treatment of various types of tumors and cancers remarkably. Due to severe adverse effects and the inability to attain targeted therapeutic drug concentration in the region of the tumor and/or cancer, the ultimate outcome can't meet the desired responses. Besides, the insufficient cellular concentration of drugs in the cancerous site may lead to the development of resistance or unresponsiveness of cancer cell to the chemotherapeutic drugs. Along with these, the accumulation of drugs in healthy tissues causes serious toxicities. Thus the search for effective delivery systems for chemotherapeutic drugs is an urgent global need. Nanocomposites designed for site-specific drug delivery to cancer/tumor region has provided an efficient delivery approach.

These nanocomposites have been formulated along with different types of receptors, proteins, or ligands of neoplastic cells, such as polysaccharides, monoclonal antibodies, transferrin, peptides, and folic acids [32]. For example, sorafenib-loaded albumin nanoshell and doxorubicin-loaded polyvinyl alcohol nanocore coated with transferrin-linked nanoparticles have significantly increased the cellular uptake of sorafenib and doxorubicin in hepatocellular carcinoma [33].

#### 20.3.2.2 Management of angioplasty

Polymer nanocomposites are extensively used in angioplasty procedure which is performed in a severe case of cardiovascular diseases such as myocardial infarction and cardiac artery blockage. A ring stent with a mounted balloon or blood-thinning medication is being placed into the cardiac artery to expand it. This stent made up of stainless steel or gold may provide adequate mechanical support to arteries, but after few days, the need to be removed. To avoid this critical removal procedure, stents are formulated by using nanocomposites containing biodegradable polymer which duplicates the operation cost and patient compliances [28].

#### 20.3.2.3 Tissue engineering

Tissue engineering refers to the utilization of a combination of cells to replace biological tissues by considering biochemical and physicochemical conditions. It is performed based on (1) 3D scaffold having biocompatibility, (2) suitable bioreactor conditions, and (3) similarity of biofunctional structure. In simple words, it is the replacement of extracellular matrix (ECM) surrounded whole tissues, known as "hierarchically organized nanofibers." The ECM nanocomposite offers a mechanical base for implanted cells along with facilitating the promotion and regulation of

cellular adhesion, migration, proliferation, differentiation, and morphogenesis. Different types of natural polymers (collagen, agarose, alginate, and chitosan) and synthetic polymers [poly(lactic acid)], poly(glycolic acid), poly(lactic acid-*co*-glycolic acid), poly(anhydride), poly(4-hydroxybutyrate), poly(urethane), and polyphosphoester have been used as biocompatible as well as biodegradable scaffolds in tissue engineering [28,34].

#### 20.3.2.4 Wound healing

Polymer nanocomposites have been reported for utilization in the wound healing process. Wound healing is the process of repairing the damages of the dermis and stratum epithelial layer of the injured tissues. Polymer nanocomposites containing Ag nanoparticles are reported to heal the wound, while other nanocomposites containing gold and chitosan have been used to heal injured tissues. Silver sulfadiazine and silver nitrate nanoparticles containing nanocomposites have been used as potential antimicrobial drugs and wound healers. Along with healing wound, these nanocomposites may provide protections against antibiotic-resistant microorganisms. Currently, methicillin-resistant *Staphylococcus aureus* (MRSA) is the most found resistant strain of bacteria. The infection caused by MRSA has been treated successfully by using poly(lactic-*co*-glycolic acid) and polyethyleneimine nanoparticles [35,36].

#### 20.3.2.5 Polymer nanocomposites in orthopedics

Polymer nanocomposites have been used in the therapy of the diseases of orthopedics. Collagen fibers, noncollagenous proteins, proteoglycans, lipids, peptides, and water comprise bone matrix. The loss of the bone matrix is the major cause of serious orthopedic diseases, such as osteoporosis and osteoarthritis. Nanocomposite containing carbonated calcium phosphate apatite nanocrystals is an excellent treatment option that works as filler by reinforcing itself into the bone matrix [28,37].

#### 20.3.2.6 Polymer nanocomposites in dentistry

Nanodentistry is the science of using nanotechnology in dental problems to ensure good oral health [38]. Recent studies have demonstrated that polymer nanocomposites are successfully used in dental implantation and diagnosis and treatment of dental neoplasm. Nanocomposites may help to develop the implant by releasing drugs [39]. Apart from this, nanopores (DNA sequencing), carbon nanotubes, and quantum dots are used in screening dental cancer [40]. Moreover, metal nanoshell containing nanocomposites can assimilate radiations with selective wavelengths leading to heat production and resultant damage of the neoplasm cells [41].

#### 20.3.2.7 Polymer nanocomposites in eye problems

Currently, ocular disorders, such as diabetic retinopathy, cataract, glaucoma, and retinal degeneration have become the leading causes of blindness due to the failure

of attaining therapeutic drug concentration in the eye. Therapy of glaucoma requires high drug concentrations which can be attained by using nanocomposites. For example, the therapeutic concentration of antiglaucoma drugs, timolol and brimonidine, is attained by hybrid polyamidoamine dendrimer hydrogel/poly(lactic-*co*-glycolic acid) polymeric nanoparticles. Moreover, excellent corneal bioavailability can be achieved by incorporating sustained-release nanocomposites into contact lenses [28].

### 20.3.3 Polymer nanocomposites in agriculture and nutraceuticals

The controlled release of nanofertilizers, herbicides, and encapsulated pesticides ensures the avoidance of large lumps or dumps of these chemicals into the soil. Currently, consumers place a priority on the protection of food quality. The creation of nanobiosensors in conjunction with intelligent packaging systems is a compassionate and fast method for detecting heavy metals, food pathogens, toxins, and maintaining food quality [42,43]. Moreover, nanotechnology-based formulation of nutraceuticals and functional foods has increased nutrient retention and absorption as well as provide better bioavailability in the body. Apart from the nutrient value and health benefits, nanotechnology helps scientists to adjust the structure, properties, and interactions between different components to produce consumer-friendly new foods with better taste, texture, flavor, freshness, and stability [44].

## 20.4 Applications of polymer nanocomposites on environment

A variety of polymer nanocomposites have been developed for remedial application in environment. These nanocomposites exhibit remedial impacts on wastewater, surface water, groundwater, contaminated air, sewage sludge, and soil. Nanocomposites containing metallic nanoparticles of antimicrobial agents can disinfect wastewater and surface water along with controlling microbial growth without generating any toxic by-products. Besides, the microbial solution can be reused after recovering from the matrix by applying an external magnetic field. For example, magnetic graphene carbon nanotube iron nanocomposites are capable of showing broad-spectrum activity against *Staphylococcus aureus* (Gram-negative) and *E. coli* (Gram-negative) [45]. Air cleanup is another remedial application of polymer nanocomposites. Recent studies have demonstrated that these nanocomposites function as adsorption interfaces for the simultaneous removal of benzene, toluene, ethylbenzene, m-xylene, and $SO_2$ from the air. $Fe_3O_4$, $Co_3O_4$, and $Ni(OH)_2$ nanoplates containing Pd nanoparticles as catalysts are used to oxidize carbon monooxide [46]. According to the conventional process, sewage sludge is stabilized by anaerobic digestion which ends up by the production of biogas. Advance researches reported that iron nanoparticles at a lower dose (0.5%) are capable of stabilizing sewage sludge with enhanced production of biogas compared to conventional

anaerobic digestion. Another nanocomposite, formulated as a biochar−mineral complex with $Fe_3O_4$ has shown efficiency as a soil improvement material, resulting in improvement of mycorrhizal colonization and nutrient uptake [7].

## 20.5 Toxicological insight of nanocomposites on human health

In the last few decades, the application and development of nanocomposites have been evolved surprisingly. Apart from the health benefits, a number of cytotoxic pieces of evidence have been reported. The nature of these toxicities on human body has been discussed in nanotoxicology. The special property of nanocomposites is that they have a higher surface area per unit volume. As a result, they behave rather differently than their bulk counterparts [47]. Nanocomposites have a greater chance of interacting with biological artifacts such as lipids and proteins, as well as whole cells. Nanocomposites have the potential to cross cell membranes and trigger inflammatory or immune responses in different organs [48,49]. Nanocomposites get exposed either deliberately by nanotherapeutics or inadvertently by natural/anthropogenic particles. The problem is an exacerbation of particle reactivity and several entry points (Fig. 20.3). Brownian movement allows these particles to travel long distances and are likely to be deposited in lung alveoli [50]. The entry of nanocomposites into the human body follows pharmacokinetic absorption, distribution, metabolism, and excretion processes. During these processes, they may interact

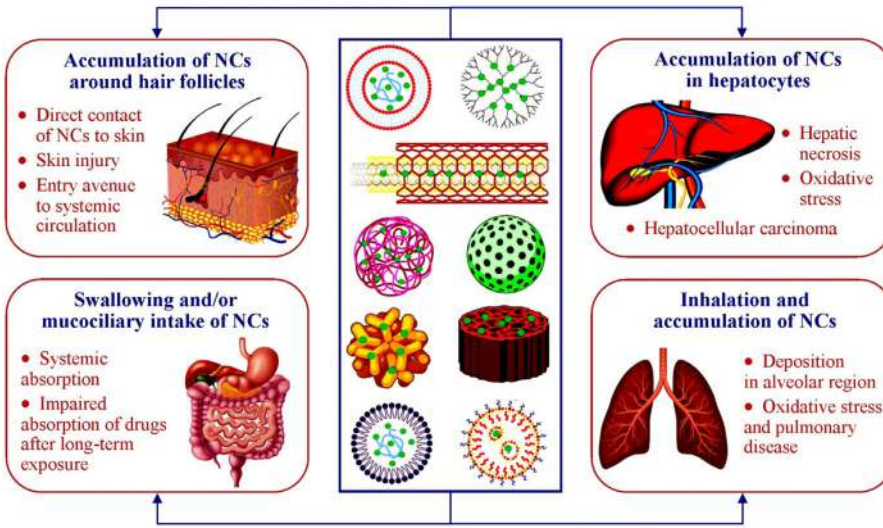


**Figure 20.3** Possible avenues to the entry of NCs into the human body and their impacts on major organs. *NCs*, nanocomposites.

with biological systems which result in cytotoxicity, such as allergy, fibrosis, organ failure, tissue damage, reactive oxygen species (ROS) generation, and DNA damage [51]. They can spread from the lungs to the bloodstream, central nervous system, and the cell nuclei, resulting in gastrointestinal irritation, Parkinson's disease, Alzheimer's disease, and DNA damages related disorders such as cancer, tumors, and hormonal issues. Moreover, another study reported that nanoparticles have a direct association with toxicities of kidneys, liver, and other vital organs after long-term exposure [52].

### 20.5.1 Potential causes of cytotoxicity

The ECM is crucial for cellular biochemical and biomechanical signals that mediate morphogenesis, differentiation, and homeostasis of tissues [53]. ECM also provides cellular scaffolding. During pathogenesis and progression of diseases, remodulation of ECM is occurred [54]. Therefore there is a greater possibility of interaction of nanocomposites with ECM. Several studies suggested that carbon nanotubes have interacted with the ECM in multiple mechanistic ways [55]. This type of interaction results in excess production of ROS followed by the progression of oxidative stress. This overproduction of ROS critically affects the remodulation process of ECM which leads to serious abnormalities such as tumor progression [56]. Another most common interaction of nanocomposites occurs with biological phospholipid membrane. The nanocomposites and biological phospholipid membrane interactions may be physical and/or chemical manners. Membranes and their functions, as well as the folding of proteins, aggregations, and other transportation processes, are disrupted as a result of physical interactions. Chemical interactions, on the other hand, produce ROS and cause oxidative damages in cells [57,58]. There are a lot of research works on carbon soot pollution particles and other nanosized pollutants that induce oxidative stress by generating ROS (Fig. 20.4).

The risk of toxicity in human health is higher in the case of agriculture and farming where nanoparticles are used as novel food ingredients and thus come to direct contact with food products. Table 20.1 lists the detrimental impacts of nanocomposites added to foods.

### 20.5.2 Factors influencing toxicity of nanocomposites

The interactions of engineered nanocomposites with different living organisms and the environment have yet to be thoroughly investigated. Nanomaterials can take on a range of physicochemical forms when they are released into the atmosphere due to their radically different properties from bulk equivalents. These novel physicochemical properties exhibit significant influences on their interaction behaviors with biological matters as well as their absorption, distribution, accumulation, and elimination from the body [74]. From the last decade, scientific studies on the adversative impacts of nanocomposites on human health as well as the environment have risen by 600%. The majority of these experiments were conducted in vitro,

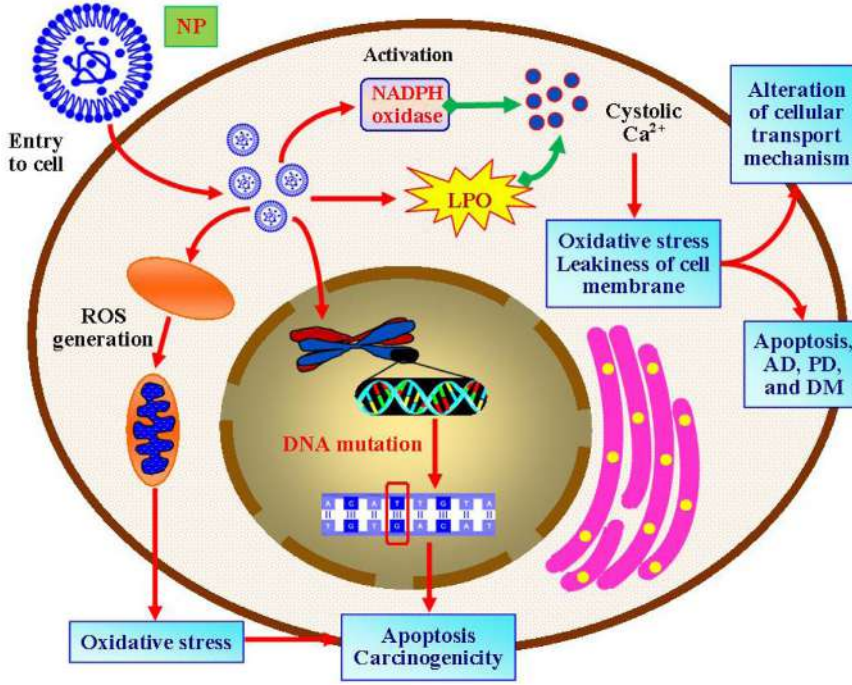


**Figure 20.4** Impacts of nanoparticle on the progression of oxidative stress and concurrent pathogenesis in the human cell. *AD*, Alzheimer's disease; *DM*, diabetes mellitus; *LPO*, lipid peroxidation; *NP*, nanoparticle; *PD*, Parkinson's disease; *ROS*, reactive oxygen species.

with cells being dosed with a particular amount of nanomaterial [75]. As shown in Fig. 20.5, the toxicity of nanoparticles is governed by a number of factors.

### 20.5.3 Toxicity assessment of nanocomposites: an overview

Nanotoxicological studies are essential to anticipate the uncertain effects of nanocomposite usages. Either cell lines or organs are exposed to a distinct dose of nanocomposites and their responses are monitored over time in a typical toxicity test. The dose–response relationship obtained from these tests which are used to assess the optimum dose and acceptable limits for nanoparticles in the form of chemicals. As compared to traditional chemicals and toxicology tests, nanoparticles have shapes, surface areas, and surface electrical charges that are entirely different from their bulk counterparts. These nanomaterials exhibit the efficiency to get dispersed, sediment, settle down, and alter the physicochemical features of the media in which they are produced. Traditional in vitro assays can misrepresent findings and dose–response curves, which is a remarkable conclusion. The peculiar actions of nanoparticles in the atmosphere and their cellular absorption are not taken into account in the traditional assays [76]. The assessment of the nanoparticle toxicity is

**Table 20.1** Toxicity bioassay of some reported nanocomposites as food components and their impacts on the test model.

| Nanocomposites | Assay tools | Toxicity | References |
|---|---|---|---|
| $TiO_2$ NPs | Anaerobic gut bacteria | Mild toxicity on bacteria | [59] |
| | Gastric epithelial cells | Oxidative stress DNA damage | [60] |
| | Human peripheral blood | ↓IDO activity and IFN production | [61] |
| Nanoclay | Alveolar epithelial cell | – | [62] |
| ZnO nanoparticles | Human pulmonary adenocarcinoma cell line (LTEP-a-2) | Carcinogenicity | [63] |
| | Human polymorphonuclear neutrophils | ↓Human neutrophil apoptosis | [64] |
| Silver nanoparticles | Colon carcinoma cells | Oxidative stress and cytotoxicity | [65] |
| | Human umbilical vein endothelial cells | Malfunction of endothelial cell | [66] |
| NiO NPs | Human pulmonary epithelial cell lines | ↑Inflammation and genotoxicity | [67] |
| FeO NPs | Human macrophages | ↓Cell viability | [68] |
| | Hepatocellular carcinoma cells | ↓Cell viability | [69] |
| Silica NPs | Human bronchoalveolar carcinoma cells | ↑ROS, LDH, and malondialdehyde | [70] |
| | Hepatocellular carcinoma cells (HepG2) | ↑ROS, oxidative stress, and mitochondrial damage | [71] |
| CuO NPs | Human lung epithelial cells | ↓Cell viability | [72] |
| $Al_2O_3$ NPs | Mixed lymphocyte culture test | DNA damage | [73] |

*IDO*, indole amine-pyrrole 2, 3-dioxygenase; *IFN*, interferons; *LDH*, lactate dehydrogenase; *ROS*, reactive oxygen species.

further complicated by environmental interactions [77]. Understanding the interactions between the nanocomposites and biological matters and the underlying mechanisms requires advanced investigations. These interactions predominantly involve biological macromolecules such as proteins, but some research suggests that they can be tracked in different ways. Wang et al. investigated the physical interactions of nanoparticles by discovering the influence of their lipid membrane phase structuring [78]. Phagocytosis, micropinocytosis, or pinocytosis mechanisms of lipid phospholipid membrane have been reported to be regulated by nanoparticles inserted into the cell. Investigation of the characteristic features of nanocomposites,

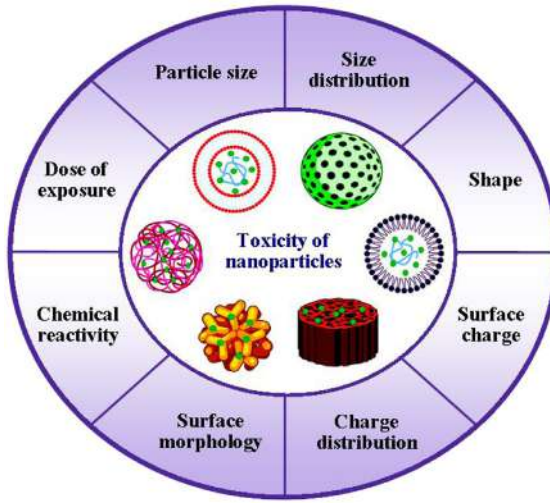


**Figure 20.5** Factors influencing the overall toxicity of nanoparticles.

their exposure directions, exposure time, correct dose, as well as the selection of appropriate study models can be complex, time-consuming, repetitive, and costly. Statistical methods and high-throughput screening techniques are the modern advances to cope with this situation. This can reduce the periods as well as workloads to develop a connection between material and biological activity by quickly screening and prioritizing nanoparticles for toxicology studies [79]. The cytotoxicity of many metal nanoparticles can be predicted easily by using a quantitative nanostructure−activity relationship [80,81]. Another important consideration is the requirement of detailed characterizations of the nanocomposites which may assist scientists in designing toxicology assays, correctly interpreting the findings, and ensuring that data can be reproductive.

Since the safety of hydrogel nanocomposite systems in biomedical applications is unknown, researchers looked into their biocompatibility and bioactivity. Protection issues with hydrogel nanocomposites arise as they are used in engineering and drug delivery. Traditional chemical compounds are regularly screened for toxicity before being released to the public, but nanomaterials lack such screening. Thus prescreening of nanomaterials will help greatly to assess their probable adverse effects on humans and the environment [82]. Despite these facts, numerous hydrogel nanocomposites have been evaluated for use in biomedical applications, such as biological tolerance and biocompatibility have yet to be established. This testing can be performed in vivo with animal models such as rats or in vitro using cell culture lines. The most common method for characterizing newly formed biomaterials is in vitro biocompatibility testing. Many of them are designed to induce and forecast biocompatibility to body tissues [83]. Preliminary screening tests can include cytocompatibility and hemocompatibility studies but are not limited to them.

The cytocompatibility research uses a cytotoxicity test which involves morphological assessments of cell lines to see if cells died or modified in any way as a result of interactions with biomaterials [84]. In order to determine hemocompatibility, the blood clotting cascade has been tested on biomaterials or devices that came into contact with blood. The most widely used cell lines are continuous cell lines, such as fibroblast or embryo cells, since they are typically inexpensive and simple to obtain. There are three types of cytocompatibility tests that should be performed: (1) direct contact testing involves evaluation of the impact of released matters when it interacts with cells; (2) indirect testing entails evaluating the effect of leachable substances in media that was in contact with the cells but did not touch them; and (3) elution or extract testing method for assessing the effect of the leachable substances. To determine the biocompatibility of blood-containing materials, a hemocompatibility test is needed.

Hemocompatibility testing is involved in five different areas, such as coagulation, thrombosis, platelet interactions, hematology, and immunology [85]. Platelets get activated when biomaterials interact with damaged tissue letting fibrin to get cross-linking to form platelet−fibrin thrombus, demonstrating a lack of hemocompatibility of the nanomaterials [86]. Nanocomposites should be tested for cytotoxicity and hemocompatibility due to various biomedical applications of the hydrogel. Based on these results, hydrogel nanocomposites are generally recognized as biocompatible and capable of being used in biomedical applications. When they are recognized as biocompatible, they are considered typically as least risky. In vitro and in vivo experiments have been conducted on a variety of hydrogels to determine their cytotoxicity and hemocompatibility. Because of their high biocompatibility, they are now used in many applications regarding pharmaceuticals as well as nutraceuticals.

Due to imparting interest in the green synthesis of nanoparticles by using natural matters, the ultimate aim of biomedical scientists is to develop “green nanomaterial” formulation methods for ensuing minimal health and environmental risks [87]. Essential aspects of nanocomposites involve revolutionizing many segments, including aerospace, communication, transportation, pharmaceuticals, nutraceuticals, cosmetics, agriculture, and environmental protection [87]. As a consequence of the betterment of the quality of future life, environmental as well as health risk assessments should be made mandatory to ensure safety as well as optimal usages of nanocomposites [88].

## 20.6 Toxicological insight of polymer nanocomposites on environment

In the 21st century, global environmental issues and energy concerns have become major problems which require the search for long-term and promising solutions. The introduction of nanocomposites in both laboratory research and industrial applications has become potential tools among the existing strategies to resolve

**Table 20.2** Environmental impacts of nanomaterials.

| Nanocomposites | Environmental elements | Effect or impact | References |
|---|---|---|---|
| Silver NPs | *Chlamydomonas reinhardtii* | Photosynthesis inhibition | [93] |
| | *Daphnia pulex* | Mortality | [94] |
| | *Danio rerio* | Modification of gene expression | [95] |
| | *Ceriodaphnia dubia* | Mortality | [96] |
| $TiO_2$ NPs | *D. rerio* | Modification of gene expression | [95] |
| | *Desmodesmus subspicatus* | Growth inhibition | [97] |
| | *Daphnia magna* | Mortality | [98] |
| | *Oncorhynchus mykiss* | Modification of gene expression | [95] |
| ZnO NPs | *Pseudokirchneriella subcapitata* | Growth inhibition | [97] |
| | *D. magna* | Mortality | [99] |
| | Zebrafish embryos | Development Hatching | [100] |
| $CeO_2$ NPs | *P. subcapitata* | Inhibition of growth Mortality | [101] |
| | *D. magna* | Reproduction problems | [94] |
| CuO NPs | *D. magna* | Mortality | [99] |
| | Zebrafish embryos | Development Hatching | [95] |
| | *C. dubia* | Mortality | [96] |
| $SiO_2$ NPs | *D. magna* | Mortality | [102] |
| Fullerene ($C_{60}$ NPs) | *D. magna* | Alteration of heart rate and behavior | [103,104] |
| | Zebrafish embryos | Brain and hatching mortality Edema and cardiac problems Development delay Modification of gene expression | [105,106] |
| Single-walled carbon NTs | *D. magna* | Mortality | [107] |
| | *O. mykiss* | Alteration of gill and behavior | [108] |
| Multiwalled carbon NTs | Zebrafish embryos | Hatching delay | [109] |
| Quantum dots | Zebrafish embryos | Mortality | [110] |
| | *C. dubia* | Mortality and lipid peroxidation | [111] |
| Zn NPs | Ryegrass | Reduction of germination rate | [112] |
| Al NPs | Ryegrass, lettuce, corn, cucumber | Inhibition of root length | [112] |
| $Al_2O_3$ NPs | Rape and corn | Inhibition of root length | [112] |
| | Radish and lettuce | Inhibition of root length | [112] |

*NPs*, nanoparticles.

environmental and energy issues [89,90]. The excessive application of nanocomposites in every aspect of science has created negative impacts on the environment. Formulation of nanocomposites requires the usage of organic solvents which are exposed to the environment as toxic gaseous products. Atmospheric and occupational discharges of nanocomposites are difficult to quantify precisely. The nanoparticles in the atmosphere don't exist as bare particles. The surfaces of nanoparticles have the characteristics of high reactivity, thus they can interact with other matters easily. The acquisition of a coronavirus protein by a nanoparticle surface has been discovered, revealing the mechanism for cell uptake, aggregation, and clearance [91].

When nanoparticles become more widely used, a significant number of them are released into the atmosphere, where they are most likely to end up in terrestrial and aquatic environments. Nanoparticles may release into the environment in one of three ways, such as naturally, inadvertently, or intentionally. Forest fires, volcanic eruptions, sea spray, winds, dust storms, and soil erosion all produce natural nanoparticles. Similarly, unintended nanoparticles are produced by smelting of metal, mining, welding, smoking, industrial waste generated by ignition of fossil fuel, and vehicle fumes. Natural and unintentional nanoparticles have a well-known environmental impact. Particle size, particle shape, size distribution, surface property, chemical composition, surface charge, crystal nature, agglomeration form, and porosity of nanocomposites are all physicochemical characteristics that influence their eco-toxicity [92]. The optical properties of nanoparticles cause some common issues such as atmospheric visibility and building soiling. Diesel particles contain a lot of black carbon, which absorbs a lot of light and leads to global warming. Engineered nanoparticles are nanocomposites designed for multiple applications. The nanoparticles may get exposed to the environment in many ways, depending on how they are used. Engineered nanocomposite's eco-toxicity, especially its effect on the aquatic environment, has been extensively researched (Table 20.2).

## 20.7 Concluding remarks and future directions

In summary, it can be concluded that the understanding of how nanocomposites interact physically or chemically with biological matters as well as environments is mandatory due to their direct association with human health and the environment. Various researches on the safety of nanocomposites have been conducted, with certain nanoparticles being found to have toxicity and adverse effects on humans and the environment. The most important criterion for distinguishing between toxic and nontoxic nanocomposites tends to be the perception and mechanism of oxidative stress and resulting physiological damages. The major toxicology tools used to assess toxicity are focused in animal studies with high concentrations or dose regimes. For years, these techniques have remained unchanged. In light of new knowledge and development, proven toxicological assays must be restored, and methods such as metabolomics, functional genomics, proteomics, and high-throughput

screening, and other advanced tools should be progressively integrated into these studies. The scientific community is under growing pressure to explain the protection of nanocomposites used in pharmaceuticals and nutraceuticals due to rising health consciousness and awareness. By integrating these advanced methods, many false positives will be eliminated, and the assessment of nanocomposites toxicity will be augmented and validated. Therefore the global introduction of such nanomaterials demands more researches, evaluation, risk assessment, as well as human health and environmental protection.

## References

[1] S. Neethirajan, D.S. Jayas, Nanotechnology for the food and bioprocessing industries, Food bioprocess. Technol. 4 (2011) 39−47.
[2] G. Scrinis, K. Lyons, The emerging nano-corporate paradigm: nanotechnology and the transformation of nature, food and agri-food systems, Int. J. Sociol. Agriculture Food 15 (2007) 22−44.
[3] R. Asmatulu, W.S. Khan, R.J. Reddy, M. Ceylan, Synthesis and analysis of injection-molded nanocomposites of recycled high-density polyethylene incorporated with graphene nanoflakes, Polym. Compos. 36 (2015) 1565−1573.
[4] D.D. Chung, Composite Materials: Functional Materials for Modern Technologies, Springer Science & Business Media, 2013.
[5] W.S. Khan, N.N. Hamadneh, W.A. Khan, Polymer nanocomposites−synthesis techniques, classification and properties, Sci. Appl. Tailored Nanostructures 50 (2016).
[6] D. Feldman, Polymer nanocomposites in medicine, J. Macromol. Science, Part. A 53 (2016) 55−62.
[7] C. Su, Environmental implications and applications of engineered nanoscale magnetite and its hybrid nanocomposites: a review of recent literature, J. Hazard. Mater. 322 (2017) 48−84.
[8] E.S. Michelson, D. Rejeski, Transnational nanotechnology governance: a comparison of the US and China, Nanotechnology & Society, Springer, 2009.
[9] B.T. Mossman, J. Bignon, M. Corn, A. Seaton, J.B. Gee, Asbestos: scientific developments and implications for public policy, Science, 247, 1990, pp. 294−301.
[10] E.T. Thostenson, C. Li, T.-W. Chou, Nanocomposites in context, Compos. Sci. Technol. 65 (2005) 491−516.
[11] S.M. Auerbach, K.A. Carrado, P.K. Dutta, Handbook of Layered Materials, CRC press, 2004.
[12] M. Alexandre, P. Dubois, Polymer-layered silicate nanocomposites: preparation, properties and uses of a new class of materials, Mater. Sci. Engineering: R: Rep. 28 (2000) 1−63.
[13] T.W. Ebbesen, Carbon Nanotubes: Preparation and Properties, CRC press, 1996.
[14] P. Ajayan, T. Ebbesen, Nanometre-size tubes of carbon, Rep. Prog. Phys. 60 (1997) 1025.
[15] D. Bethune, C.H. Kiang, M. D.E. Vries, G. Gorman, R. Savoy, J. Vazquez, et al., Cobalt-catalysed growth of carbon nanotubes with single-atomic-layer walls, Nature 363 (1993) 605−607.

[16] M. Dresselhaus, G. Dresselhaus, K. Sugihara, I. Spain, H. Goldberg, Graphite Fibers and Filaments, Springer-Verlag, *New York*, 1988, pp. 35–84.
[17] S. Kang, M. Pinault, L.D. Pfefferle, M. Elimelech, Single-walled carbon nanotubes exhibit strong antimicrobial activity, Langmuir 23 (2007) 8670–8673.
[18] Y. Cheng, Y. Liu, J. Huang, K. Li, Y. Xian, W. Zhang, et al., Amperometric tyrosinase biosensor based on Fe3O4 nanoparticles-coated carbon nanotubes nanocomposite for rapid detection of coliforms, Electrochim. acta 54 (2009) 2588–2594.
[19] M.B. Lerner, B.R. Goldsmith, R. Mcmillon, J. Dailey, S. Pillai, S.R. Singh, et al., A carbon nanotube immunosensor for *Salmonella*, Aip Adv. 1 (2011) 042127.
[20] M.M. Rahman, X.-B. Li, J. Kim, B.O. Lim, A.S. Ahammad, J.-J. Lee, A cholesterol biosensor based on a bi-enzyme immobilized on conducting poly (thionine) film, Sens. Actuators B: Chem. 202 (2014) 536–542.
[21] R. Kurahatti, A. Surendranathan, S. Kori, N. Singh, A.R. Kumar, S. Srivastava, Defence applications of polymer nanocomposites, Def. Sci. J. 60 (2010) 551–563.
[22] J. Tang, Y. Wang, H. Liu, Y. Xia, B. Schneider, Effect of processing on morphological structure of polyacrylonitrile matrix nano-ZnO composites, J. Appl. Polym. Sci. 90 (2003) 1053–1057.
[23] F. Hussain, M. Hojjati, M. Okamoto, R.E. Gorga, Polymer-matrix nanocomposites, processing, manufacturing, and application: an overview, J. composite Mater. 40 (2006) 1511–1575.
[24] J. Jordan, K.I. Jacob, R. Tannenbaum, M.A. Sharaf, I. Jasiuk, Experimental trends in polymer nanocomposites—a review, Mater. Sci. engineering: A 393 (2005) 1–11.
[25] I.-Y. Jeon, J.-B. Baek, Nanocomposites derived from polymers and inorganic nanoparticles, Materials 3 (2010) 3654–3674.
[26] D. Ciprari, K. Jacob, R. Tannenbaum, Characterization of polymer nanocomposite interphase and its impact on mechanical properties, Macromolecules 39 (2006) 6565–6573.
[27] L.S. Schadler, Polymer-based and polymer-filled nanocomposites, Nanocomposite Sci. Technol. (2003) 77–153.
[28] S. Mishra, S. Sharma, M.N. Javed, F.H. Pottoo, M.A. Barkat, M.S. Alam, et al., Bioinspired nanocomposites: applications in disease diagnosis and treatment, Pharm. Nanotechnol. 7 (2019) 206–219.
[29] W. Park, J. Chen, S. Cho, S.-J. Park, A.C. Larson, K. Na, et al., Acidic pH-triggered drug-eluting nanocomposites for magnetic resonance imaging-monitored intra-arterial drug delivery to hepatocellular carcinoma, ACS Appl. Mater. & interfaces 8 (2016) 12711–12719.
[30] Z. S Lu, C. M Li, Quantum dot-based nanocomposites for biomedical applications, Curr. medicinal Chem. 18 (2011) 3516–3528.
[31] N.D. Thorat, J. Bauer, Functional smart hybrid nanostructures based nanotheranostic approach for advanced cancer treatment, Appl. Surf. Sci. 527 (2020) 146809.
[32] M. Prasad, U.P. Lambe, B. Brar, I. Shah, J. Manimegalai, K. Ranjan, et al., Nanotherapeutics: an insight into healthcare and multi-dimensional applications in medical sector of the modern world, Biomedicine & Pharmacotherapy 97 (2018) 1521–1537.
[33] G.L. Malarvizhi, A.P. Retnakumari, S. Nair, M. Koyakutty, Transferrin targeted core-shell nanomedicine for combinatorial delivery of doxorubicin and sorafenib against hepatocellular carcinoma, Nanomedicine: Nanotechnology, Biol. Med. 10 (2014) 1649–1659.
[34] P.X. Ma, Scaffolds for tissue fabrication, Mater. today 7 (2004) 30–40.

[35] H. Brem, M.S. Golinko, O. Stojadinovic, A. Kodra, R.F. Diegelmann, S. Vukelic, et al., Primary cultured fibroblasts derived from patients with chronic wounds: a methodology to produce human cell lines and test putative growth factor therapy such as GMCSF, J. Transl. Med. 6 (2008) 1−9.
[36] H. Brem, M. Tomic-Canic, Cellular and molecular basis of wound healing in diabetes, J. Clin. investigation 117 (2007) 1219−1222.
[37] C. Rodrigues, P. Serricella, A. Linhares, R. Guerdes, R. Borojevic, M. Rossi, et al., Characterization of a bovine collagen−hydroxyapatite composite scaffold for bone tissue engineering, Biomaterials 24 (2003) 4987−4997.
[38] T. Kubik, K. Bogunia-Kubik, M. Sugisaka, Nanotechnology on duty in medical applications, Curr. Pharm. Biotechnol. 6 (2005) 17−33.
[39] S.R. Kumar, R. Vijayalakshmi, Nanotechnology in dentistry, Indian. J. Dent. Res. 17 (2006) 62−65.
[40] N. Dasilva, P. Díez, S. Matarraz, M. González-González, S. Paradinas, A. Orfao, et al., Biomarker discovery by novel sensors based on nanoproteomics approaches, Sensors 12 (2012) 2284−2308.
[41] M. Patil, D.S. Mehta, S. Guvva, Future impact of nanotechnology on medicine and dentistry, J. Indian. Soc. periodontology 12 (2008) 34.
[42] N. Duran, P.D. Marcato, Nanobiotechnology perspectives. Role of nanotechnology in the food industry: a review, Int. J. Food Sci. & Technol. 48 (2013) 1127−1134.
[43] B. Srilatha, Nanotechnology in agriculture, J. Nanomed. Nanotechnol. 2 (2011) 5.
[44] P. Sanguansri, M.A. Augustin, Nanoscale materials development−a food industry perspective, Trends Food Sci. & Technol. 17 (2006) 547−556.
[45] L. Wang, T.-F. Kang, L.-P. Lu, J.-G. Zhang, R. Xue, S.-Y. Cheng, Microcystin-(leucine-arginine) immunosensor based on iron (II, III) magnetic nanoparticles, Anal. Lett. 47 (2014) 2939−2949.
[46] H.A. Elazab, S. Moussa, B.F. Gupton, M.S. El-Shall, Microwave-assisted synthesis of Pd nanoparticles supported on Fe 3 O 4, Co 3 O 4, and Ni (OH) 2 nanoplates and catalysis application for CO oxidation, J. Nanopart. Res. 16 (2014) 1−11.
[47] D. Lin, B. Xing, Phytotoxicity of nanoparticles: inhibition of seed germination and root growth, Environ. Pollut. 150 (2007) 243−250.
[48] M.-C. Daniel, D. Astruc, Gold nanoparticles: assembly, supramolecular chemistry, quantum-size-related properties, and applications toward biology, catalysis, and nanotechnology, Chem. Rev. 104 (2004) 293−346.
[49] A. Gojova, B. Guo, R.S. Kota, J.C. Rutledge, I.M. Kennedy, A.I. Barakat, Induction of inflammation in vascular endothelial cells by metal oxide nanoparticles: effect of particle composition, Environ. health Perspect. 115 (2007) 403−409.
[50] T. Xia, M. Kovochich, J. Brant, M. Hotze, J. Sempf, T. Oberley, et al., Comparison of the abilities of ambient and manufactured nanoparticles to induce cellular toxicity according to an oxidative stress paradigm, Nano Lett. 6 (2006) 1794−1807.
[51] Z. Piperigkou, K. Karamanou, A.B. Engin, C. Gialeli, A.O. Docea, D.H. Vynios, et al., Emerging aspects of nanotoxicology in health and disease: from agriculture and food sector to cancer therapeutics, Food Chem. Toxicol. 91 (2016) 42−57.
[52] J.K. Momin, C. Jayakumar, J.B. Prajapati, Potential of nanotechnology in functional foods, Emirates J. food agriculture 25 (2013) 10−19.
[53] A.D. Theocharis, C. Gialeli, P. Bouris, E. Giannopoulou, S.S. Skandalis, A.J. Aletras, et al., Cell−matrix interactions: focus on proteoglycan−proteinase interplay and pharmacological targeting in cancer, FEBS J. 281 (2014) 5023−5042.

[54] D. Nikitovic, M. Tzardi, A. Berdiaki, A. Tsatsakis, G.N. Tzanakakis, Cancer microenvironment and inflammation: role of hyaluronan, Front. immunology 6 (2015) 169.
[55] X. Zhao, R. Liu, Recent progress and perspectives on the toxicity of carbon nanotubes at organism, organ, cell, and biomacromolecule levels, Environ. Int. 40 (2012) 244–255.
[56] D. Nikitovic, E. Corsini, D. Kouretas, A. Tsatsakis, G. Tzanakakis, ROS-major mediators of extracellular matrix remodeling during tumor progression, Food Chem. Toxicol. 61 (2013) 178–186.
[57] Z.J. Deng, M. Liang, M. Monteiro, I. Toth, R.F. Minchin, Nanoparticle-induced unfolding of fibrinogen promotes Mac-1 receptor activation and inflammation, Nat. Nanotechnol. 6 (2011) 39–44.
[58] J.G. Teeguarden, P.M. Hinderliter, G. Orr, B.D. Thrall, J.G. Pounds, Particokinetics in vitro: dosimetry considerations for in vitro nanoparticle toxicity assessments, Toxicological Sci. 95 (2007) 300–312.
[59] W. Dudefoi, K. Moniz, E. Allen-Vercoe, M.-H. Ropers, V.K. Walker, Impact of food grade and nano-TiO2 particles on a human intestinal community, Food Chem. Toxicol. 106 (2017) 242–249.
[60] M.C. Botelho, C. Costa, S. Silva, S. Costa, A. Dhawan, P.A. Oliveira, et al., Effects of titanium dioxide nanoparticles in human gastric epithelial cells in vitro, Biomedicine & Pharmacotherapy 68 (2014) 59–64.
[61] K. Becker, S. Schroecksnadel, S. Geisler, M. Carriere, J.M. Gostner, H. Schennach, et al., TiO2 nanoparticles and bulk material stimulate human peripheral blood mononuclear cells, Food Chem. Toxicol. 65 (2014) 63–69.
[62] C. Han, A. Zhao, E. Varughese, E. Sahle-Demessie, Evaluating weathering of food packaging polyethylene-nano-clay composites: Release of nanoparticles and their impacts, NanoImpact 9 (2018) 61–71.
[63] C. Wang, H. Wang, M. Lin, X. Hu, ZnO nanoparticles induced cytotoxicity on human pulmonary adenocarcinoma cell line LTEP-a-2, Process. Saf. Environ. Prot. 93 (2015) 265–273.
[64] D.M. Goncalves, D. Girard, Zinc oxide nanoparticles delay human neutrophil apoptosis by a de novo protein synthesis-dependent and reactive oxygen species-independent mechanism, Toxicol. Vitro 28 (2014) 926–931.
[65] R. Miethling-Graff, R. Rumpker, M. Richter, T. Verano-Braga, F. Kjeldsen, J. Brewer, et al., Exposure to silver nanoparticles induces size-and dose-dependent oxidative stress and cytotoxicity in human colon carcinoma cells, Toxicol. vitro 28 (2014) 1280–1289.
[66] J. Shi, X. Sun, Y. Lin, X. Zou, Z. Li, Y. Liao, et al., Endothelial cell injury and dysfunction induced by silver nanoparticles through oxidative stress via IKK/NF-κB pathways, Biomaterials 35 (2014) 6657–6666.
[67] L. Capasso, M. Camatini, M. Gualtieri, Nickel oxide nanoparticles induce inflammation and genotoxic effect in lung epithelial cells, Toxicol. Lett. 226 (2014) 28–34.
[68] H.A. Jeng, J. Swanson, Toxicity of metal oxide nanoparticles in mammalian cells, J. Environ. Sci. Health Part. A 41 (2006) 2699–2711.
[69] Y. Ge, Y. Zhang, S. He, F. Nie, G. Teng, N. Gu, Fluorescence modified chitosan-coated magnetic nanoparticles for high-efficient cellular imaging, Nanoscale Res. Lett. 4 (2009) 287–295.
[70] W. Lin, Y.-W. Huang, X.-D. Zhou, Y. Ma, In vitro toxicity of silica nanoparticles in human lung cancer cells, Toxicol. Appl. pharmacology 217 (2006) 252–259.
[71] L. Sun, Y. Li, X. Liu, M. Jin, L. Zhang, Z. Du, et al., Cytotoxicity and mitochondrial damage caused by silica nanoparticles, Toxicol. vitro 25 (2011) 1619–1629.

[72] M. Ahamed, M.A. Siddiqui, M.J. Akhtar, I. Ahmad, A.B. Pant, H.A. Alhadlaq, Genotoxic potential of copper oxide nanoparticles in human lung epithelial cells, Biochemical biophysical Res. Commun. 396 (2010) 578–583.
[73] Y.-J. Kim, H.-S. Choi, M.-K. Song, D.-Y. Youk, J.-H. Kim, J.-C. Ryu, Genotoxicity of aluminum oxide (Al1O3) nanoparticle in mammalian cell lines, Mol. & Cell. Toxicol. 5 (2009) 172–178.
[74] B. Naseer, G. Srivastava, O.S. Qadri, S.A. Faridi, R.U. Islam, K. Younis, Importance and health hazards of nanoparticles used in the food industry, Nanotechnol. Rev. 7 (2018) 623–641.
[75] C.D. Engeman, L. Baumgartner, B.M. Carr, A.M. Fish, J.D. Meyerhofer, T.A. Satterfield, et al., Governance implications of nanomaterials companies' inconsistent risk perceptions and safety practices, J. Nanopart. Res. 14 (2012) 1–12.
[76] M. Geiser, B. Rothen-Rutishauser, N. Kapp, S. Schürch, W. Kreyling, H. Schulz, et al., Ultrafine particles cross cellular membranes by nonphagocytic mechanisms in lungs and in cultured cells, Environ. health Perspect. 113 (2005) 1555–1560.
[77] G. Oberdörster, V. Stone, K. Donaldson, Toxicology of nanoparticles: a historical perspective, Nanotoxicology 1 (2007) 2–25.
[78] B. Wang, L. Zhang, S.C. Bae, S. Granick, Nanoparticle-induced surface reconstruction of phospholipid membranes, Proc. Natl Acad. Sci. 105 (2008) 18171–18175.
[79] A. Nel, T. Xia, H. Meng, X. Wang, S. Lin, Z. Ji, et al., Nanomaterial toxicity testing in the 21st century: use of a predictive toxicological approach and high-throughput screening, Acc. Chem. Res. 46 (2013) 607–621.
[80] D. Fourches, D. Pu, C. Tassa, R. Weissleder, S.Y. Shaw, R.J. Mumper, et al., Quantitative nanostructure – activity relationship modeling, ACS nano, 4, 2010, pp. 5703–5712.
[81] T. Puzyn, B. Rasulev, A. Gajewicz, X. Hu, T.P. Dasari, A. Michalkova, et al., Using nano-QSAR to predict the cytotoxicity of metal oxide nanoparticles, Nat. Nanotechnol. 6 (2011) 175–178.
[82] T.J. Brunner, P. Wick, P. Manser, P. Spohn, R.N. Grass, L.K. Limbach, et al., In vitro cytotoxicity of oxide nanoparticles: comparison to asbestos, silica, and the effect of particle solubility, Environ. Sci. & Technol. 40 (2006) 4374–4381.
[83] C.T. Hanks, J.C. Wataha, Z. Sun, In vitro models of biocompatibility: a review, Dental Mater. 12 (1996) 186–193.
[84] A. Pizzoferrato, G. Ciapetti, S. Stea, E. Cenni, C.R. Arciola, D. Granchi, Cell culture methods for testing biocompatibility, Clin. Mater. 15 (1994) 173–190.
[85] B.D. Ratner, A.S. Hoffman, F.J. Schoen, J.E. Lemons, Biomaterials Science: An Introduction to Materials in Medicine, Elsevier, 2004.
[86] L.P. Amarnath, A. Srinivas, A. Ramamurthi, In vitro hemocompatibility testing of UV-modified hyaluronan hydrogels, Biomaterials 27 (2006) 1416–1424.
[87] E. Omanović-Mikličanin, A. Badnjević, A. Kazlagić, M. Hajlovac, Nanocomposites: a brief review, Health Technol. 10 (2020) 51–59.
[88] R. Wen, L. Hu, G. Qu, Q. Zhou, G. Jiang, Exposure, tissue biodistribution, and biotransformation of nanosilver, NanoImpact 2 (2016) 18–28.
[89] W. Tu, Z. Bai, Z. Deng, H. Zhang, H. Tang, In-situ synthesized Si@ C materials for the lithium ion battery: a mini review, Nanomaterials 9 (2019) 432.
[90] P.S. Goh, A.F. Ismail, Nanocomposites for Environmental and Energy Applications, Multidisciplinary Digital Publishing Institute, 2021.
[91] R. Haggenmueller, W. Zhou, J. Fischer, K. Winey, Mechanical and structural investigation of highly aligned single-walled carbon nanotubes in polymer composites, J. Nanosci. Nanotechno 3 (2003) 105.

[92] I. Lynch, K.A. Dawson, Protein-nanoparticle interactions, Nano today 3 (2008) 40–47.
[93] V. Shah, Environmental Impacts of Engineered Nanoparticles, Wiley Online Library, 2010.
[94] K.V. Hoecke, J.T. Quik, J. Mankiewicz-Boczek, K.A.D. Schamphelaere, A. Elsaesser, P.V.D. Meeren, et al., Fate and effects of CeO2 nanoparticles in aquatic ecotoxicity tests, Environ. Sci. & Technol. 43 (2009) 4537–4546.
[95] A.P. Roberts, A.S. Mount, B. Seda, J. Souther, R. Qiao, S. Lin, et al., In vivo biomodification of lipid-coated carbon nanotubes by *Daphnia magna*, Environ. Sci. & Technol. 41 (2007) 3025–3029.
[96] C.J. Smith, B.J. Shaw, R.D. Handy, Toxicity of single walled carbon nanotubes to rainbow trout (*Oncorhynchus mykiss*): respiratory toxicity, organ pathologies, and other physiological effects, Aquat. Toxicol. 82 (2007) 94–109.
[97] K. Hund-Rinke, M. Simon, Ecotoxic effect of photocatalytic active nanoparticles (TiO2) on algae and daphnids (8 pp), Environ. Sci. Pollut. Res. 13 (2006) 225–232.
[98] E. Navarro, F. Piccapietra, B. Wagner, F. Marconi, R. Kaegi, N. Odzak, et al., Toxicity of silver nanoparticles to *Chlamydomonas reinhardtii*, Environ. Sci. & Technol. 42 (2008) 8959–8964.
[99] R.J. Griffitt, J. Luo, J. Gao, J.C. Bonzongo, D.S. Barber, Effects of particle composition and species on toxicity of metallic nanomaterials in aquatic organisms, Environ. Toxicol. Chemistry: An. Int. J. 27 (2008) 1972–1978.
[100] R.J. Griffitt, K. Hyndman, N.D. Denslow, D.S. Barber, Comparison of molecular and histological changes in zebrafish gills exposed to metallic nanoparticles, Toxicological Sci. 107 (2009) 404–415.
[101] N.M. Franklin, N.J. Rogers, S.C. Apte, G.E. Batley, G.E. Gadd, P.S. Casey, Comparative toxicity of nanoparticulate ZnO, bulk ZnO, and ZnCl2 to a freshwater microalga (*Pseudokirchneriella subcapitata*): the importance of particle solubility, Environ. Sci. & Technol. 41 (2007) 8484–8490.
[102] M. Heinlaan, A. Ivask, I. Blinova, H.-C. Dubourguier, A. Kahru, Toxicity of nanosized and bulk ZnO, CuO and TiO2 to bacteria *Vibrio fischeri* and crustaceans *Daphnia magna* and *Thamnocephalus platyurus*, Chemosphere 71 (2008) 1308–1316.
[103] L. Adams, D. Lyon, A. Mcintosh, P. Alvarez, Comparative toxicity of nano-scale TiO2, SiO2 and ZnO water suspensions, Water Sci. Technol. 54 (2006) 327–334.
[104] L.K. Adams, D.Y. Lyon, P.J. Alvarez, Comparative eco-toxicity of nanoscale TiO2, SiO2, and ZnO water suspensions, Water Res. 40 (2006) 3527–3532.
[105] X. Zhu, L. Zhu, Z. Duan, R. Qi, Y. Li, Y. Lang, Comparative toxicity of several metal oxide nanoparticle aqueous suspensions to Zebrafish (*Danio rerio*) early developmental stage, J. Environ. Sci. Health, Part. A 43 (2008) 278–284.
[106] X. Zhu, L. Zhu, Y. Li, Z. Duan, W. Chen, P.J. Alvarez, Developmental toxicity in zebrafish (*Danio rerio*) embryos after exposure to manufactured nanomaterials: buckminsterfullerene aggregates (nC60) and fullerol, Environmental Toxicology and Chemistry: An Int. J. 26 (2007) 976–979.
[107] E. Oberdörster, S. Zhu, T.M. Blickley, P. Mcclellan-Green, M.L. Haasch, Ecotoxicology of carbon-based engineered nanoparticles: effects of fullerene (C60) on aquatic organisms, Carbon 44 (2006) 1112–1120.
[108] T.C. King-Heiden, P.N. Wiecinski, A.N. Mangham, K.M. Metz, D. Nesbit, J.A. Pedersen, et al., Quantum dot nanotoxicity assessment using the zebrafish embryo, Environ. Sci. & Technol. 43 (2009) 1605–1611.
[109] C.Y. Usenko, S.L. Harper, R.L. Tanguay, Fullerene C60 exposure elicits an oxidative stress response in embryonic zebrafish, Toxicol. Appl. pharmacology 229 (2008) 44–55.

[110] J. Cheng, E. Flahaut, S.H. Cheng, Effect of carbon nanotubes on developing zebrafish (*Danio rerio*) embryos, Environ. Toxicol. Chemistry: An. Int. J. 26 (2007) 708−716.
[111] J. Gao, S. Youn, A. Hovsepyan, V.L. Llaneza, Y. Wang, G. Bitton, et al., Dispersion and toxicity of selected manufactured nanomaterials in natural river water samples: effects of water chemical composition, Environ. Sci. & Technol. 43 (2009) 3322−3328.
[112] J.L. Bouldin, T.M. Ingle, A. Sengupta, R. Alexander, R.E. Hannigan, R.A. Buchanan, Aqueous toxicity and food chain transfer of quantum dots™ in freshwater algae and *Ceriodaphnia dubia*, Environ. Toxicol. Chemistry: An. Int. J. 27 (2008) 1958−1963.

# Index

*Note*: Page numbers followed by "*f*" and "*t*" refer to figures and tables, respectively.